

PROCEEDINGS

of the Third
Mine Water Solutions Conference
2018

Vancouver, British Columbia, Canada
June 12–15



Proceedings of the Third Annual International Conference on Mine Water Solutions

June 12-15, 2018 • Vancouver, Canada

Editors
Joe Goodwill, Vancouver, Canada
Dirk Van Zyl, Norman B. Keevil Institute of Mining Engineering,
University of British Columbia, Canada

ORGANIZED BY:

THE UNIVERSITY OF BRITISH COLUMBIA

Norman B. Keevil Institute of Mining Engineering
and
UBC Conferences and Accommodation

C3 ALLIANCE CORP
Community, Commitment, Cooperation

Disclaimer

Any views and opinions expressed in the articles published in these proceedings are solely those of the authors and do not necessarily represent those of the University of British Columbia (UBC), or of the panel of editors. The authors take full and exclusive responsibility for technical content and accuracy of the information published herein. This information is not intended nor implied to be a substitute for professional advice. UBC and the panel of editors are not responsible for any damage to property or persons that may occur as a result of the use of the information contained in this volume.

CONTENTS

Organizers vii

Committees viii

Technical Reviewers x

Acknowledgements xi

Sponsors xii

Exhibitors xiii

Chapter 1: Characterization and Prediction 1

Characterizing the Geochemistry of Soil and Water Using Drone-Based Hyperspectral Analysis | Peter Kinghan and Jamie Robinson 3

Approaches to Water Quality Modeling Using Geochemical/ARD Test Data in Conjunction with Field Analog Data | Madhumitha Raghav and Erick Weiland 15

Dependence of Predicted Dewatering on Size of Hydraulic Stress Used for Groundwater Model Calibration Analysis | Vladimir Ugorets and Cristian Pereira 31

Base Mine Lake: The First End-Pit Lake for the Alberta Oil Sands | Dallas Heisler and Carla Wytrykush 45

Use of Adaptive Management Planning in Support of Environmental Monitoring and Permitting Process | Sheldon Smith, Michelle Fraser, Walter Sencza and Stephen Lines 51

Meteorological Time Series and Natural Runoff Model in a Cold Climate Environment | Joel W. Trubilowicz and Victor Muñoz Saavedra 65

Towards a Conservative Mine Design Practice through Probabilistic Calibration | John Markus Mayer 77

Novel Use of the Westbay System to Characterize Deep Hydrogeology for a Proposed Underground Coal Mine | Tyler Gale and Piotr Rzepecki 93

Groundwater Discharge into Tailings Facility during Intense Precipitation Events, Nyrstar Myra Falls | Christoph Wels, Andy Thomas and Nicole Pesonen 109

Estimating Operational Groundwater Inflows to a Proposed Underground Coal Mine on Vancouver Island | Laura-Lee Findlater, John Balfour, Bruce Mattson and Kathleen Russell 123

Predicted Post-Closure Contaminant Loads and Water Quality Conditions in Myra Creek, Nyrstar Myra Falls, Canada | Paul Ferguson, Christoph Wels, Alexander Trapp and Nicole Pesonen 139

A New Rapid Brine Release Extraction Method in Support of Lithium Brine Resource Estimation | Tzung-mow Yao, Michael Milczarek, Frits Reidel, Daniel Weber, Edward Peacock and Murray Brooker 153

A Comparison of Predicted Groundwater Impacts to Observed Effects at the Victor Diamond Mine, 11 Years after the Start of Dewatering | Simon Gautrey 163

Cold Desert Evapotranspiration Cover System Design Evaluation | Jason Keller, Chris Jim, Monisha Banerjee, Michael Milczarek, and Clay Self 181

The Role of Speciation for Selenium Treatment and Compliance with Site-Specific Aquatic Life Criteria | Ben Wozniak and Russ Gerads 195

Chapter 2: Operational Water Management 207

Is Water the Best Option? How to Evaluate which Fugitive Dust Management Practice is Right for Your Site | Jeff Ladderud 209

Dust Mitigation Using a Water Conservation Program | Steven R. Clark 223

Estimating the Wetting Time for Mine Waste Rock Piles | Mark Steinepreis 237

3D Deposition and Water Balance Modelling with Muk3D and GoldSim | Carlo Cooper, Jaco Grobler and Miguel Palape Reyes 245

Challenges in Containing Geochemical Risk at the Faro Mine Complex, Yukon | Dustin K. Rainey 259

Total Water Management: Canada's Contribution to Sustainable Mine Development | Jon Fennell 269

Multi-Parameter Time-Lapse Dam Seepage Investigation | Tomas C. Goode, Rachael Peavler and Hhan Olsen 283

Chapter 3: Regulatory and Social Challenges 297

Performance Review of a Passive Treatment System for Fe, As, and Mn at the Empire Mine State Historic Park | Neal Gallagher, Daniel Millsap, Steve Lofholm and Tom Rutkowski 299

Chapter 4: Water as a Valued Asset 311

New Tailings Encapsulation Methods Could Pave the Way toward Safe Long-Term Stacking of Filtered Tailings | Donald J. Lake and Lee A. Groat 313

Follow the Money (and the Water) – The Goldcorp Water Valuation Toolbox | Brendan O'Brien 323

A New Approach to Mitigation Banking | Eric McCleary 337

Mine Water: A Resource for the Circular Economy in South African Mining Communities | Dheepak Maharajh, Tamsyn Grewar, John Neale and Michelle van Rooyen 349

"Don't Make Waves:" Desalinated Water and the Social Licence to Operate in the Atacama Region, Chile | Cecilia Campero 363

From Water Management to Water Stewardship in Mining Regions | Nadja Kunz 377

Chapter 5: Water Management in Extreme Climates 387

Current PMP Estimation and Meteorological Parameter Development for Mining Facilities in Data Limited Regions | Bill Kappel 389

Hurricane Harvey Rainfall: Did It Exceed PMP, and What are the Implications? | Bill Kappel 401

Richmond Hill Mine Heap Leach Pad Soil Cover System Evaluation | Guosheng Zhan, Daniel Lattin, Jason Keller and Michael Milczarek 419

Investigation of Feed Water Treatment Options in an Arid Area | Mohsen Barkh 433

Application of SAGR Bioreactors for Ammonia Treatment in Mining Effluents | Michael Bratty, Alessandro Di Biase, Victor Wei, Martin Hildebrand and Jan A. Oleszkiewicz 449

Incorporating Climate Variability into Water Balance Modelling to Help Inform Water Management Design: The Pebble Mine Project | Alana Shewan and Jaime Cathcart 461

A Real Challenge in Mine Water Management in a High Precipitation Area: Grasberg Mine | Nanda Rinaldi, Iwan Setiawan, Vladimir Ugorets and Göktuğ Evin 473

Numerical Groundwater Flow and Thermal Transport Modelling in Cold Regions | Mundzir Basri and Niloofar Firoozy 487

Enhanced Reclamation of the Giant Nickel Tailings Storage Facilities in British Columbia, Canada | Allison Brown and Drummond "Dusty" Earley III 495

Implementing a Long-Term Closure Strategy for the Premier Gold Mine in Northwest British Columbia | Michael Dabiri, Charles Masala and Helena Lidhage 509

The Effect of Variability of Design Storms on the Galore Creek Project | Charles Masala, Andrew Thrift and Yapo Alle-Ando 519

Hydrogeology of the Coffee Gold Project: Groundwater Interactions in an Area of Discontinuous Permafrost | Laura-Lee Findlater, H. Jean Cho, David Flather, Jennie Gjertsen and James Scott 531

Planning Climate Change Adaptation Practices in Watershed Ecosystems: What is the Mining Sector Developing? | Gabriel Castillo Devoto 545

Chapter 6: Water Treatment 567

Removing Selenium from Very Low Concentration Mine Water | Mohsen Barkh 569

Synthetic Water Calibration for Water Quality Parameters and Water Treatment Program Validation | Lynda Smithard 583

Changing Effluent Regulations in Canada, Helping Mine Sites to Reach New Limits | Sean Miller and Terry Obal 597

Water Use, Quality and Treatment at Syncrude's Mineable Oilsands Operation in Northern Alberta | Warren Zubot 607

Water Treatment for Mine Closure: A Bioremediation Pilot-Scale Study | Leonard Santisteban, Ilsu Lee, Shane Hansen, Erick Weiland and Dan Ramey 609

Biochemical Cyanide Treatment of Gold Mine Tailings Supernatant: Pilot and Demonstration Trials | James Harrington, Monique Simair, Justin Bourne, Rachel Martz, Vanessa Friesen and Ben Ferris 623

Alkaline Flush Technology: An In-Situ Treatment Method for Mining Impacted Alluvial Aquifers | Olufunsho Ogungbade and Shane Hansen 635

The Development of a New Peat-Based Weak Anion Exchange Material that Removes Sulphate from Acidic Water | Liudmyla Kildyshova, Rami Hallak and Igor V. Kolomitsyn 649

Lime Treatment: Advantages of a Proven Technology and Competing Alternatives | Kristina Minchow, Bridgette Hendricks and Ryan Schipper 661

Electrocoagulation for the Removal of Silica in Reverse Osmosis Rejects from Acidic Rock Drainage Water Treatment | Zhong Xie, Marco Gomez Orzatti, Saviz Mortazavi, Eben Dy and Wei Qu 677

A New Zero Water Intake Technology for Chemical Treatment of Mining Tailings | Colin Klein, Morgan Tizzotti, Kirk Thomas and Trong Dang-Vu 691

Containerized Water Treatment for Remote Mine Sites | Veneil Sundar, Brent Baker and Alain Consigny 703

Mixing Zone Assessment for Mine Effluent Discharges in Receiving Waters: Challenges and Solutions through Best Practices | Mijanur R. Chowdhury, Cheryl Wiramanaden, Pierre Stecko and Kevin Martens 719

In-Situ Treatment of Arsenic in a Pit Lake – A Case History | Adam Whitman and Tom Patterson 733

Chapter 7: Miscellaneous | 745

Sea Water Intrusion at Abandoned Coal Mines in the Labin Region, Croatia | Mladen Kuhta and Željka Brkić 747

Chapter 8: Author Index 759

Author Index 761

ORGANIZERS

Norman B. Keevil Institute of Mining Engineering, University of British Columbia (UBC)

UBC's Department of Mining Engineering has faculty that teaches and mentors graduate students and staff to undertake research in all aspects of mining in order to study and improve the industry for future generations.

Known for being a small, close-knit family, the department is exemplified by the dedication of the faculty and staff who provide a dynamic, hands-on learning experience for both undergraduate and graduate students.

Gifts from alumni, corporations, foundations, students, parents and other friends assist the Keevil Institute in conducting leading edge research, providing outstanding education and contributing to social and economic development.

For more information, visit the website at http://mining.ubc.ca/

UBC Conferences and Accommodation

Hosting group events or conferences, UBC's conference venues are an impressive destination for attendees, esteemed visitors and event organizers from around the world.

UBC's Conference and Accommodation staff make every effort to help choose from impressive venues with breathtaking views of Vancouver's undeniable beauty. Their expert support services ensure a seamless event from start to finish.

For more information, visit the website at http://ubcconferences.com/

C3 Alliance Corp.

At **C3 Alliance Corp**. we understand that the sharing of information and ideas is vital to gaining insights and developing relationships which, in turn, leads to successful natural resource development. Community members, business people, and government representatives can all benefit from meeting to share stories and knowledge. C3 employs an expert team of event planners who specialize in conferences and networking opportunities. We benefit from a vast network of professional contacts to organize exciting events that connect people and knowledge across resources sectors, communities and government.

For more information, visit the website at http://www.c3alliancecorp.ca/

COMMITTEES

Organizing Committee

Chair
Dirk Van Zyl, Norman B. Keevil Institute of Mining Engineering, University of British Columbia

Co-Chair
Dan Ramey, Freeport-McMoRan Mining Company, USA

Co-Chair
Andrew Watson, Stantec

Resa Furey, Stantec
Sarah Weber, C3 Alliance Corp
Scott Broughton, Stantec
Amrita Budhwar, C3 Alliance Corp

Conference Committee

Dan Ramey, Freeport-McMoRan Mining Company, USA
Andrew Watson, Stantec
Geoff Beale, Piteau
Shannon Shaw, pHase Geochemistry Inc., Canada
Lisa Wade, Goldcorp
John Lupo, Newmont Mining Corporation

Technical Committees

Water as a Valued Asset
Briana Gunn, Newmont Mining Corporation
Brett Waterman, Freeport-McMoRan Inc.

Regulatory and Social Challenges
Luke Danielson, Sustainable Development Strategies Group

Operational Water Management
Mike Davies, Teck
Michael Geddis, KGHM

Water Treatment/Water Quality
Bob Kimball, Amec Foster Wheeler – Wood PLC
Jim Finley, Stantec

Climate Based Water Management
Wet – Sven Knutsson, Luleå University of Technology
Dry – John Rupp, Piteau
Cold –Jennie Gjertsen, Goldcorp
Alana Shewan, Knight Piésold

Characterization and Prediction
Shannon Shaw, pHase Geochemistry Inc., Canada
Madhumitha Raghav, Freeport-McMoRan Inc.
Jim Finley, Stantec

Alana Shewan, Knight Piesold
Sven Knutsson, Luleå University of Technology, Sweden
Hamish Weatherly, BGC Engineering
Daniel Mackie, SRK Consultingh

TECHNICAL REVIEWERS

The Organizing Committee expresses its appreciation and sincere gratitude to the following reviewers of the technical content, who helped to ensure the high quality of this publication.

Water as a Valued Asset

Briana Gunn	Newmont Mining Corporation
Brett Waterman	Freeport-McMoRan Inc.

Regulatory and Social Challenges

Luke Danielson	Sustainable Development Strategies Group
Daniel Dupon	Stantec

Operational Water Management

Mike Davies	Teck
Michael Geddis	KGHM

Water Treatment/Water Quality

Bob Kimball	Amec Foster Wheeler – Wood PLC
Jim Finley	Stantec

Climate Based Water Management

Wet – Sven Knutsson	Luleå University of Technology
Dry – John Rupp	Piteau
Cold – Jennie Gjertsen	Goldcorp

Characterization and Prediction

Shannon Shaw	pHase Geochemistry Inc., Canada
Madhumitha Raghav	Freeport-McMoRan Inc.
Jim Finley	Stantec
Alana Shewan	Knight Piésold
Hamish Weatherly	BGC Engineering
Daniel Mackie	SRK Consulting
David Luzi	Stantec

ACKNOWLEDGEMENTS

The Organizing Committee acknowledges with gratitude the authors' contributions of high quality, detailed and innovative papers. Their papers reflect ingenious and proactive solutions to challenging mining conditions around the world.

We would also like to thank the technical reviewers, the employees of UBC, and all those involved in the organization of this conference and the preparation and production of these proceedings. The support of the committees is greatly appreciated.

The Organizing Committee also wishes to thank all of our exhibitors, sponsors, institutional partners and media partners.

Finally, we would like to thank all the delegates who attended the conference to exchange their valuable knowledge and expertise, thus contributing to the great success of the Mine Water Solutions Conference. We look forward to seeing you all again at the next conference in this international series.

Organizing Committee
Mine Water Solutions 2018

THE ORGANIZERS PROUDLY ACKNOWLEDGE THE FOLLOWING CONFERENCE SPONSORS AND EXHIBITORS:

Sponsors

Patron

Stantec

Platinum Sponsor

GOLDCORP

Gold and Special Event Sponsors

BARRICK

Teck

FREEPORT-McMoRan

ECO MISTER EVAPORATOR

Silver Sponsor

wsp

Bronze Sponsors

CARL DATA SOLUTIONS

GOLDER

AWC WATER SOLUTIONS LTD.

Coffee Break Sponsor

Knight Piésold CONSULTING

Pen Sponsor

Klohn Crippen Berger

Exhibitors


AGAT Laboratories
Aquatic Life Ltd.
AWC WATER SOLUTIONS LTD.
BI Pure WATER
BOS SOLUTIONS
CARL DATA SOLUTIONS
DHI
ECO MISTER EVAPORATOR
Endress+Hauser People for Process Automation
ENVIROTECH SERVICES, INC.
TENCATE Geotube
GoldSim
McCUE ENGINEERING CONTRACTORS EST. 2000
Saltworks
sensemetrics
Stantec
VEOLIA
VISTACLARA NMR GEOPHYSICS
Westbay Instruments
wood.

Chapter 1:
Characterization and Prediction



Proceedings of Mine Water Solutions 2018
June 12–15, 2018, Vancouver, Canada
Published by the University of British Columbia 2018

Characterizing the Geochemistry of Soil and Water Using Drone-Based Hyperspectral Analysis

Peter Kinghan, SLR Consulting Ltd., Ireland
Jamie Robinson, SLR Consulting Ltd., UK

Abstract

Geochemical analysis through field samples and laboratory testing is a common method for understanding the composition of a soil and its contaminants. The limitation of this approach is in the spatial extrapolation of the diagnostic point-location samples. Over large areas such as operational and closed mine sites, sampling can be labour intensive; moreover, potential health, safety and environmental risks may be associated with the sampling. Hyperspectral image analysis has been shown to identify an object's spectral composition and discretize it from its surroundings. This has the potential to aid the interpretation of mine water chemistry by interrogating the source-pathway-target relationship.

SLR Consulting Limited (SLR) have been developing a methodology to assess the chemistry of soil and surface water using mounted hyperspectral sensors, and to combine these to provide greater accuracy and more precise insights across sites with known mine water contamination issues. Visible Near Infrared (VNIR) and Short-Wave Infrared (SWIR) sensors are mounted on unmanned aerial vehicles (UAVs). These deliver superior spatial and spectral resolution outcomes, compared to hyperspectral data acquired with multispectral satellites or manned fixed-wing airborne vehicles.

Using case studies in Ireland and the USA, SLR will seek to demonstrate the application of drone-based hyperspectral analysis, and also provide insights into the potential problems associated with the technique and how these can be overcome. The case studies present real data, which has been successfully correlated with ground-based analysis to such an extent that large areas can be surveyed. Preliminary studies compared trichromatic (RGB) data with hyperspectral data and demonstrated the differences, which can be seen beyond the variation in colour detection in normal light. In addition, interpretation of the data provided an initial assessment of elements that might be present in the waste rock and tailings, subject to the ground truthing.

The studies have shown that drone-based hyperspectral sensors have excellent potential for surveying mining land-use and mining legacy sites. The surveys provide benefits in investigating soil and water geochemistry at active and historic mining sites, both in data acquisition and in area coverage.

The application of change analysis to time variant surveys can also provide validation of mine closure plans, stability assessment and, in some cases, contaminant migration. The technique is also being considered for application in assessing closed landfill sites, radiation survey, and potential Unexploded Ordnance (UXO).

Introduction

The assessment of mining sites using geochemical and hydrochemical assessment is well established and can involve a variety of different analytical techniques. Similarly the use of multispectral and hyperspectral analysis of soil/rock has been undertaken for a number of years, using satellite and fixed wing aircraft to aid mineral exploration (e.g. Cudahy et al., 2001; McConachy et al., 2007; Rajendra et al., 2009) and in the interpretation of dominant geochemical regimes such as acidic and metalliferous mine drainage (e.g. Zabic et al., 2014 and Quental et al., 2013) and land contamination issues (e.g. Maya, 2014). It is a passive, non-intrusive analytical technique that can reveal alteration patterns that the human eye cannot detect.

SLR Consulting Limited (SLR) examined the information derived from multispectral and hyperspectral analysis and concluded that using drone technology could be a viable alternative when investigating mining sites. In particular it was seen as a useful method for assessing old and abandoned mine sites where acidic mine drainage is present. Furthermore, time variant studies were seen as a valuable addition to existing mine closure monitoring schemes. It is not the purpose of this paper to review the existing techniques for aerial hyperspectral analysis of soil and water, but rather to present the value-added application of using drone technology. This includes:

- Development of the approach;
- Brief presentation of Visible Near Infrared (VNIR) and Short-Wave Infrared (SWIR) technology and its use;
- Typical issues with using aerial assessment tools;
- Presentation of preliminary studies in Ireland and the USA that demonstrate successful use of the technology and value-added applications; and
- Next stages of assessment.

Study Hypothesis

There were two hypotheses addressed in the study. These involved considering hyperspectral surveys of areas where:

- The formation of minerals associated with pyrite oxidation is dominant. This presents opportunities to understand wider scale geochemical environments in areas of the mine; and
- Non-sulphidic mine areas, such as lead zinc mines in carbonate host rock.

The objective was to establish whether the drone-survey approach can integrate the geochemistry successfully, such that informed decisions regarding long-term sampling, monitoring, and management plans can be put in place.



Figure 1: Examples of field sampling to support hyperspectral analysis

Geochemical Environment

Recent studies have shown that by understanding certain mineral assemblages using the hyperspectral analysis, the likely dominant geochemical environment controlling the solubility of metals can be theorized. This is exemplified below, where other authors have successfully used hyperspectral imaging to understand the geochemical environment.

For example, review of such hyperspectral imaging demonstrates how identification of the different iron mineral assemblages can give an indication of acidity generation in an area, which has implications. Zabic et al. (2014) presented predicted pH maps for mining-impacted areas, based on the iron mineral assemblage, which showed a strong correlation to the measured soil pH.

The second consideration was those mine sites typically not involving sulphide ores, such as lead zinc ores in carbonate host rocks. In Ireland it was possible for the authors to assess preliminary metalloid concentrations in tailings, and these results are presented in Figure 3. This included consideration of a range of lead and zinc minerals, some of which are described in Table 1.

Table 1: Zinc minerals with associated spectral reflectance (after McConachy et al., 2007)

Name	Formula	Colour	Spectral reflectance
Common minerals			
Smithsonite	$ZnCO_3$	White	Red peak, broad depression at 800–1200 nm
Hydrozincite	$Zn_5(CO_3)_{2(}OH)_6$	White, grey, yellow	Peak at 600 nm
Cerusite	$PbCO_3$	White	Peak at 800 nm
Rare Minerals			
Adamite	$Zn_2(AsO_4)(OH)$	Clear – yellow if iron present	Peak at 650 nm (red)
Linarite	$PbCu(SO_4)(OH)_2$	Azure blue	Sharp peak at 450 nm (blue); broad depression at 550–1050 nm
Zinc melanterite	$(Zn,Cu,Fe)SO_4.7H_2O$	Yellow green	Peak at 515 nm; broad depression at 700–1100 nm with minimum at 790 nm
Tsumehite	$Pb_2Cu(PO_4)(SO_4)(OH)$	Green	Peak at 580 nm (green)

In addition, the risk posed by metalloids such as arsenic can be more fully appreciated by understanding the areal distribution in the soil over a wider area than that determined from soil sampling. An example of this is presented below.

A review of Table 1 and the literature shows:

- There are a number of lead and zinc compounds that might be present at such mine sites.
- Some of these may not be visible with the naked eye, but do have a spectral reflectance.
- Knowledge of the likely dominant metal form from the local geology and potential weathering assemblage is very important.
- A number of the reflectance spectra overlap, emphasizing the importance of ground truthing the surveys with relevant geochemical analysis (XRD, XRF etc.).

Notwithstanding the above, a hyperspectral survey can, depending on the mine site in question:

- aid in the understanding of the metal concentration across mine site areas;
- potentially provide information concerning the dominant geochemical environment; and

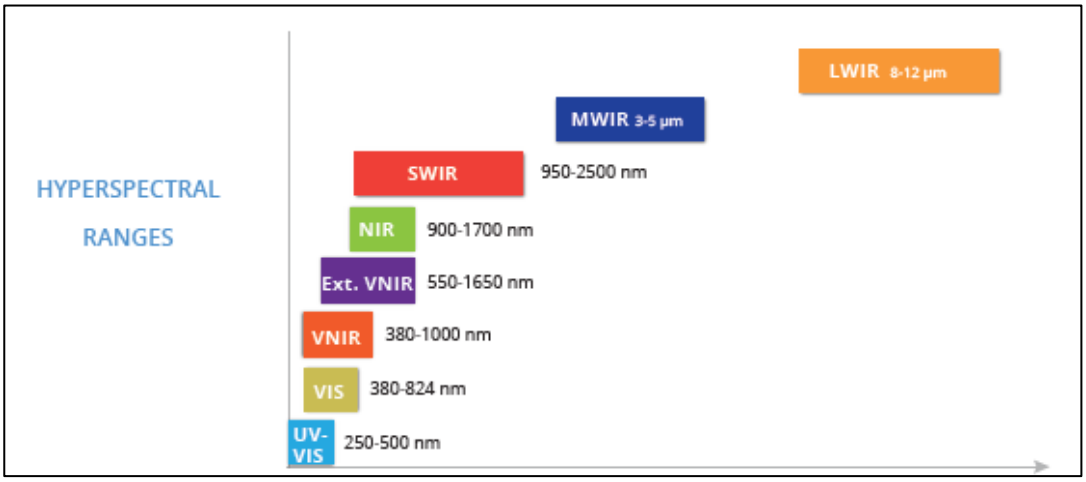
- consequently provide an enhanced interpretation of the risk posed by the metal presence, which can be theorized and applied though a source-pathway-target relationship.

The added benefit is that a drone-mounted hyperspectral sensor can cover a large area of the mine site, thereby accessing areas that might not be safe or accessible to sample by ground-based sampling teams.

Hyperspectral Imaging

Hyperspectral sensors collect hundreds of contiguous bands of reflected and emitted energy. Unique signatures or fingerprints are created by the collected wavelengths, where the reflectance is related to the composition of different materials in the ground. In the case of mine sites, the molecular structure of a minerals' surface generates the distribution of its reflectance and associated absorption; the resulting spectral signature serves as a unique fingerprint in the identification of its composition (ASD Inc. and Headwall Photonics Inc., 2016,).

Table 2: Hyperspectral ranges (Source: ASD Inc. and Headwall Photonics Inc., 2016)



The infrared region of light is considered a good mineral detection wavelength range because of the associated wide range of minerals that can be identified. As shown in Table 2, the infrared extends from:

- the visible and near-infrared (VNIR, 0.4–1 µm);
- through the short-wave infrared (SWIR, 1–2.5 µm); and
- mid-wave infrared (MWIR, 3–5 µm) to the long-wave infrared (LWIR, 7–13 µm).

The value of each infrared wavelength range to any application is determined by its detection capabilities of the targeted minerals. Electronic and vibrational ("exciting" of the elements) processes associated with bonded elements within minerals cause characteristic wavelengths in the infrared ranges,

which enable identification of mineral species and, in certain instances, mineral chemistries. As a result, the ability to identify mineral composition is significantly enhanced (Terracore Geo, 2017).

The detection capabilities of VNIR, SWIR, and LWIR are illustrated in the summary table of mineral classification (Table 3). These are the wavelength ranges where the most mineral detection capabilities are achieved.

Table 3: Detection capabilities of VNIR, SWIR and LWIR for minerals (Source: Terracore Geo, 2017)

	Structure	Mineral Group	Example	VNIR Response	SWIR Response	LWIR Response
Silicates	Inosilicates	Amphibole	Actinolite	Non-Diagnostic	Good	Moderate
		Pyroxene	Diopside	Good	Moderate	Good
	Cyclosilicates	Tourmaline	Elbaite	Non-Diagnostic	Good	Moderate
	Nesosilicates	Garnet	Grossular	Moderate	Non-Diagnostic	Good
		Olivine	Forsterite	Good	Non-Diagnostic	Good
	Sorosilicates	Epidote	Epidote	Non-Diagnostic	Good	Moderate
	Phyllosilicates	Mica	Muscovite	Non-Diagnostic	Good	Moderate
		Chlorite	Clinochlore	Non-Diagnostic	Good	Moderate
		Clay Minerals	Illite	Non-Diagnostic	Good	Moderate
			Kaolinite	Non-Diagnostic	Good	Moderate
	Tectosilicates	Feldspar	Orthoclase	Non-Diagnostic	Non-Diagnostic	Good
			Albite	Non-Diagnostic	Non-Diagnostic	Good
		Silica	Quartz	Non-Diagnostic	Non-Diagnostic	Good
Non-Silicates	Carbonates	Calcite	Calcite	Non-Diagnostic	Moderate	Good
		Dolomite	Dolomite	Non-Diagnostic	Moderate	Good
	Hydroxides		Gibbsite	Non-Diagnostic	Good	Moderate
	Sulphates	Alunite	Alunite	Moderate	Good	Moderate
			Gypsum	Non-Diagnostic	Good	Good
	Borates		Borax	Non-Diagnostic	Moderate	Uncertain
	Halides	Chlorides	Halite	Non-Diagnostic	Uncertain	Uncertain
	Phosphates	Apatite	Apatite	Moderate	Non-Diagnostic	Good
	Hydrocarbons		Bitumen	Uncertain	Moderate	Uncertain
	Oxides	Hematite	Hematite	Good	Non-Diagnostic	Non-Diagnostic
		Spinel	Chromite	Non-Diagnostic	Non-Diagnostic	Non-Diagnostic
	Sulphides		Pyrite	Non-Diagnostic	Non-Diagnostic	Non-Diagnostic

Case Study #1

Alaska Tundra Water Bodies

On behalf of our client, SLR supported collection of hyperspectral data using airborne hyperspectral cameras and ground-based spectrometers to evaluate metal concentrations in tundra water bodies in Alaska.

The characteristics of the hyperspectral sensor acquiring the data greatly influence the amount and quality of information available within each pixel. Consideration of the required scale of assessment

determines the resolution of the sensor used. For a large-scale assessment (over a large area) a resolution of 30 m, such as can be acquired from Landsat satellite data, is adequate. However, when a finer resolution is preferred, a more accurate, near ground assessment is needed. For the Alaska project, where some water bodies in the project area were significantly smaller than 30 m in diameter, a finer resolution was required. To achieve the project objectives, a hyperspectral camera was flown across the area at a flight height of about 1,500 m, by fixed wing manned aircraft at an elevation designed to achieve 2-meter pixel resolution. Concurrently, a ground-based crew was deployed to collect surface water samples and spectral readings from selected tundra water bodies along the flight lines. The SLR team in Anchorage designed an innovative method for simultaneously collecting water samples and spectral data safely from the shore. The Lake Sampling Device (LSD) designed by SLR eliminated the need to transport a boat across sensitive tundra and mitigated the risk of collecting samples from a boat in cold and windy conditions.

Using the water analysis results and ground-based spectral data, Satalytics, SLR's project team partner, developed algorithms for estimating dissolved phase metal concentrations. The algorithms were then used to process the airborne hyperspectral data and develop metal concentration maps (2 m resolution) for hundreds of tundra water bodies across the project area.

Traditional data collection methods involve sensors mounted on satellites (20 to 30 m resolution) and manned aircraft (2 to 10 m spatial: 10 – 20 nm spectral resolution). Sensors with medium to low resolution provide data adequate for regional and large-scale assessment, such as the tundra water body study in Alaska.

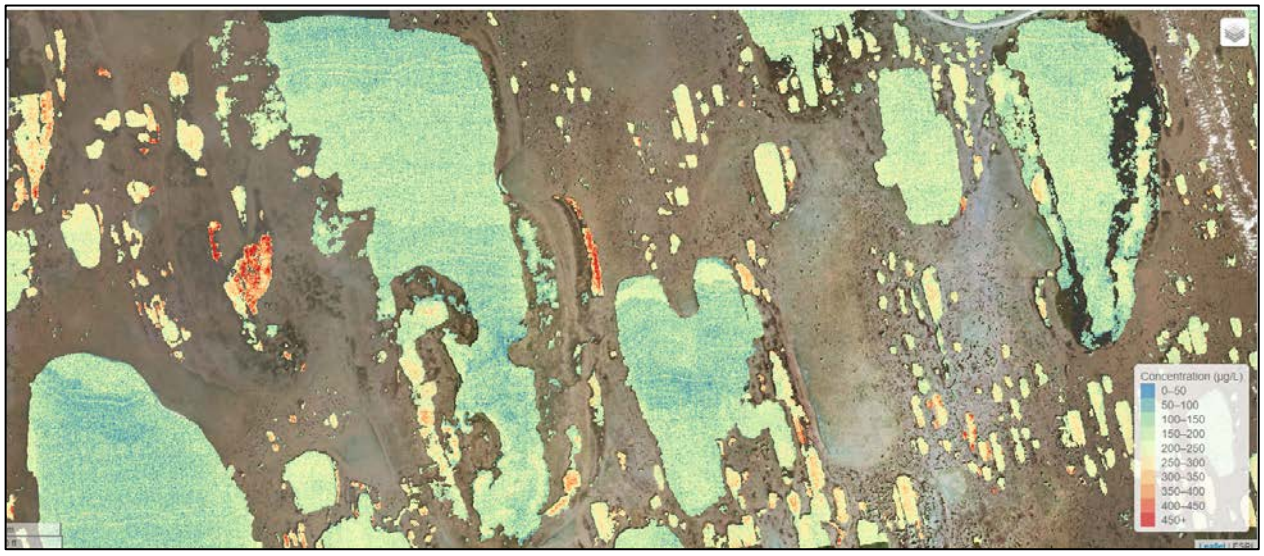


Figure 2: Barium concentration across survey area

However, large pixels produce spectral signatures that represent a mixing of many independent variables, rendering the image unreliable for most detailed land use or other thematic classification requirements. Sub-meter resolution is preferred when more accurate ground assessment is needed. Examples of the results for iron and barium are presented in Figures 2 and 3.

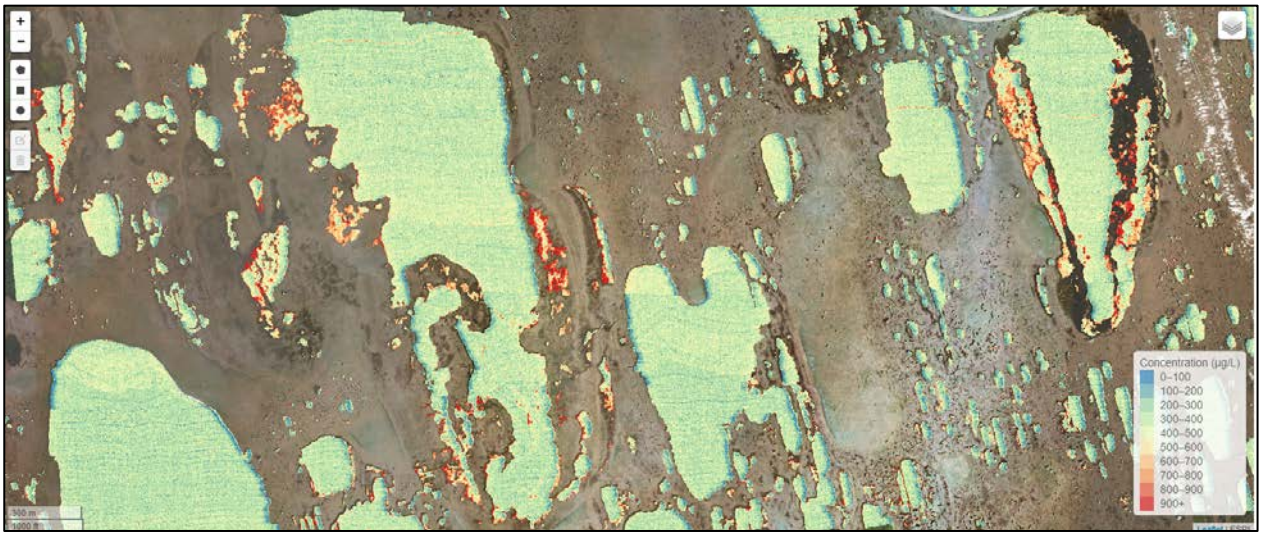


Figure 3: Iron concentration across survey area

Case Study #2

UAV-mounted Hyperspectral Survey – Irish Mine Investigation

Due to advances in technology, smaller and lighter hyperspectral sensors are being mounted on unmanned aircraft systems, allowing hyperspectral data to be collected at a higher temporal and spatial resolution. Following the Alaskan case study described above, and the limitations identified, SLR decided to explore the use of Unmanned Aircraft Vehicles (UAVs) for improving the data collection method to complement the use of more traditional methods.

Following a review of available systems at the time (summer of 2016) it was decided to use this system:

- 1 × Aibot X6 V2 and hyperspectral sensor (VNIR only)
  Sensor Specification: Headwall (VNIR) (Spectral bands: 272, Spectral Range: 400-1000 nm, Spatial Resolution (GSD): 5 cm, Spectral Resolution: 2 nm)

The fieldwork, consisting of the UAV-mounted sensor only (no ground truthing) was carried out in November 2016 at an active mine site in Europe. An area of about 2 hectares was covered at a flight height of 50 m, producing data of 5 cm resolution, with 1 battery. This 10-minute flight produced about

10 gigabytes of hyperspectral data collected across the full spectral range. The Alaska project produced data at about 2 m resolution using a manned aircraft, and was flown at about 1,500 m flight heights.



Figure 4: Drones used in the study

Interpretation of hyperspectral remote sensing requires specific algorithms able to manage larger amounts of dimensional data compared to multispectral data. The collected data was processed by Harris Geospatial using ENVI image analysis software and by Satelytics using their proprietary algorithms.

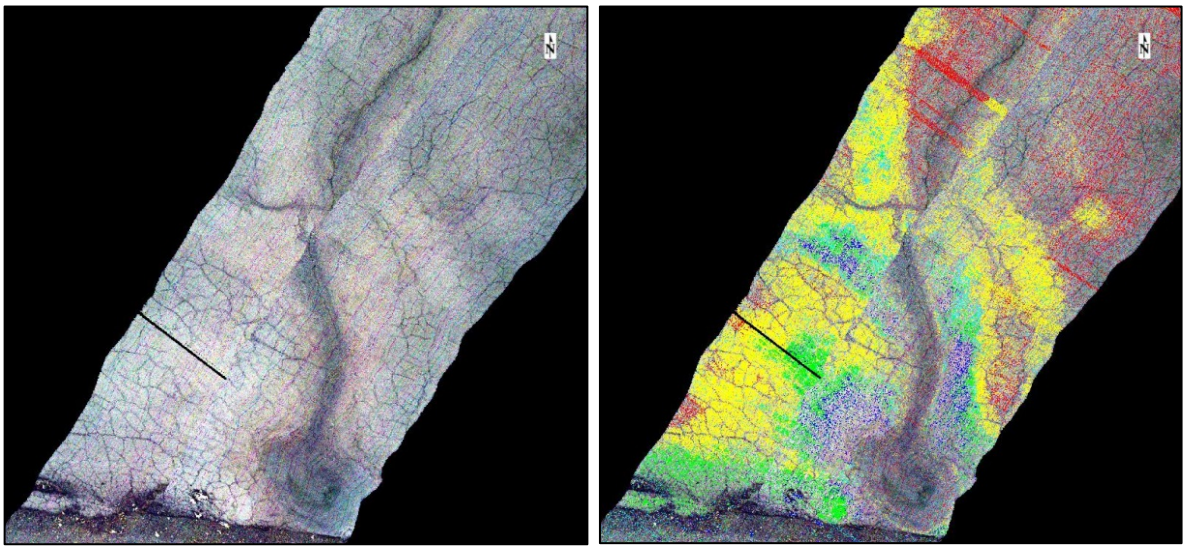


Figure 5: RGB Imagery compared to processed hyperspectral data

Results were processed to allow feature extraction for thematic purposes, using standard algorithms, leading to a spatial pattern and spectral identification pixels within the scene displayed as a map. Figure 5 shows the processed hyperspectral data compared to RGB imagery (i.e. visible to the human eye).

The area was a tailings dam that is approximately 5,000 m² in area. The information presented demonstrates that the hyperspectral survey picked up more than the naked eye; and with further preliminary interrogation, some elements in the soil are delineated. For example, the distribution of relative concentrations of arsenic is presented in Figure 6.

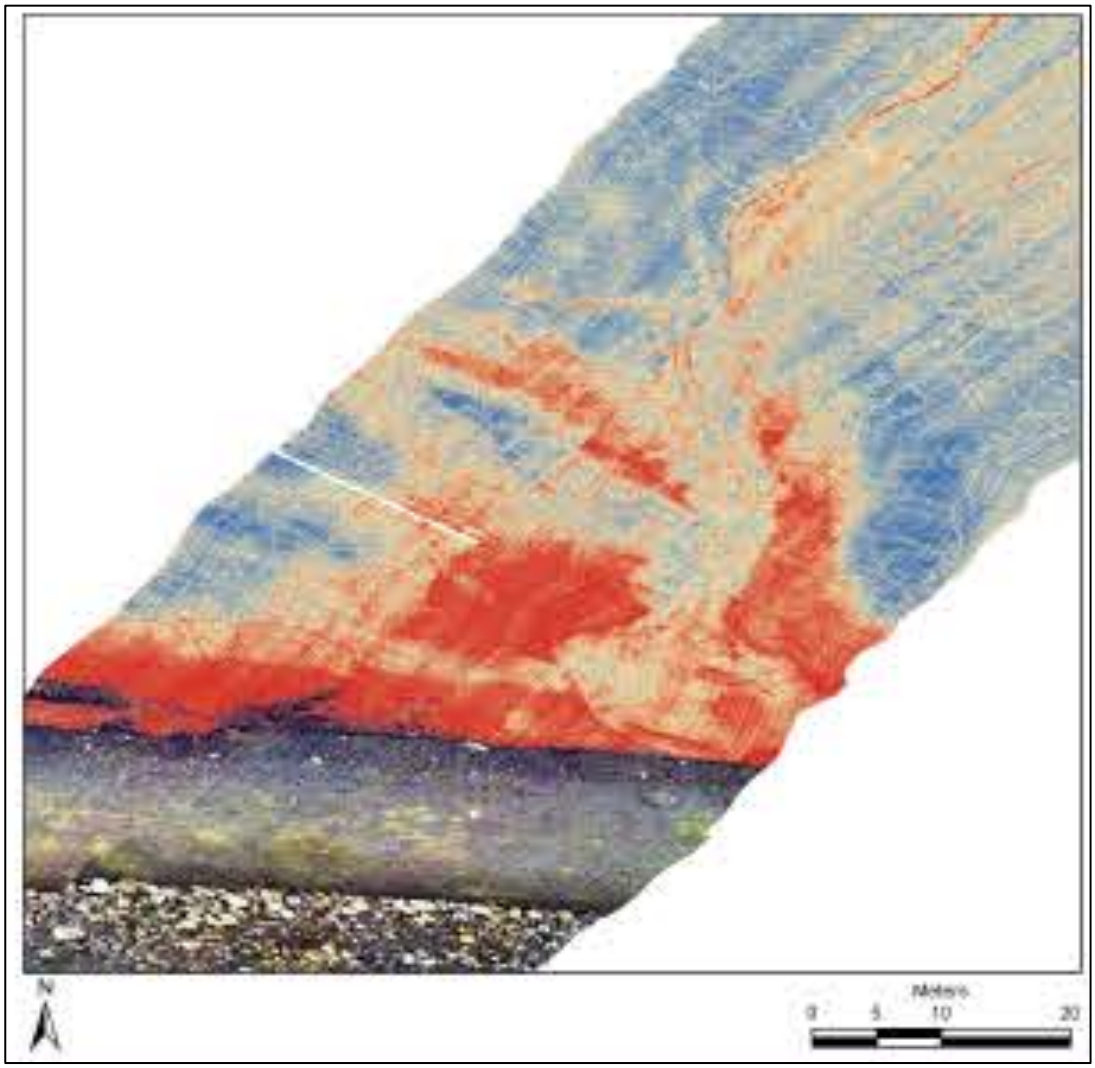


Figure 6: Relative concentration of arsenic in tailings dam (red: high concentration; blue: low)

The study indicates that the drone-based hyperspectral survey showed excellent potential to increase the understanding of elemental distribution at former mine sites in soil and water. In particular:

1. It provides areal distribution of metals and metalloids, which led to the interrogation of the conceptual site model for potential contamination migration at the site;
2. It allows relatively rapid assessments of areas to be undertaken (compared to field sampling and lab testing), albeit with a requirement to collect relatively large files of data;

3. Knowledge of the host geology is required such that key determinants can be optimized using the hyperspectral analyzer; and
4. Based on an understanding of the factors controlling metal and metalloid mobility at the site, informed decisions regarding optimum restoration can be made.

It was noted during the data collection stage that there were the usual issues with UAV's, including limited battery life allowing a limited flight time, variable wind speeds, and inconsistent lighting conditions. The data size of the captured spectrum was also a limitation factor due to the gigabyte size and associated transfer of data and associated storage. A number of challenges of working with the UAV collected hyperspectral data were identified by Harris Geospatial when processing the data, including systematic noise in the direction of acquisition, variable speed of acquisitions, and poor ortho-rectification. Awareness of these issues from the outset will dramatically improve the success of future surveys.

Next Stages of Assessment

The VNIR has limited mineral-detection capabilities on its own, but provides valuable undetected identification of minerals when measured across other wavelength ranges. The VNIR is especially important for iron-compound identification, which can be a useful area of study at sites producing acid mine drainage.

UAV systems are now available with VNIR and SWIR sensors, and SLR are currently developing methodologies to use these systems on a number of active and legacy mine sites in Europe. The combination of these sensors will improve the detection capabilities of the system for the required minerals/contaminants. The next field study will include additional ground-based sampling to enable calibration of the UAV collected data such that they make sense from a geochemical perspective, for example field spectral measurements, X-ray diffraction (XRD), and X-Ray Fluorescence (XRF), supported by laboratory mineralogical analysis.

Conclusions

UAV-mounted hyperspectral sensors have benefits for monitoring a range of environments, e.g. active and legacy mine sites, contaminated land, etc.

In the mining sector there are particular benefits in using this technology for mine closure monitoring and management (providing an invaluable tool for environmental evaluation and temporal/ spatial change analysis).

Hyperspectral data, when used in combination with other monitoring methodologies, and calibrated correctly, can assist in optimizing the time and cost required for long-term management and monitoring programmes.

Experience in data collection, complementary analysis methodologies, hyperspectral data processing, and geochemical interpretation are key to producing accurate and usable results.

Acknowledgements

We would like to thank the SLR Management Team for their support in advancing this applied research initiative. We also wish to thank Stan Flagel (SLR, Anchorage). We also greatly appreciate the help and technical skills of Julian Deeks, Aibotix, Headwall, Harris Geospatial, and Satelytics, which has enabled successful collaboration on these and other SLR projects.

References

ASD Inc. and Headwall Photonics Inc. 2016. Airborne hyperspectral and ground-truth technologies.

Cudahy, T.J., Hewson, R., Huntingdon, J.F, Quigley, M.A. and Barry, P.S. 2001 The performance of the satellite-borne Hyperion Hyperspectral VNIR-SWIR Imaging System from mineral mapping at Mount Fitton, South Australia, *IEEE Transaction on Geoscience and Remote Sensing,* 1(6): 314.

Maya, Mafuza. 2014. Application of hyperspectral remote sensing to assess contamination associated with gold mining in the Witwatersrand Gold Basin, South Africa. Ph.D. thesis, Johannesburg, South Africa.

McConachy, T.F., Yang, K., Boni, M. and Evans, N.J. 2007. Spectral reflectance: Preliminary data on a new technique with potential for non-sulphide base metal exploration, *Geochemistry: Exploration, Environment, Analysis,* 7: 139–151.

Quental, L., Sousa, A.J., Marsh, S. and Abreu, M.M. 2013. Identification of materials related to acid mine drainage using multi-source spectra at S. Domingos Mine, SE Portugal, *International Journal of Remote Sensing,* 34(6).

Rajendra, S., Aravindan, S., Rajakumar, T.J. and Murali Mohan, K.R. 2009. *Hyperspectral Remote Sensing and Spectral Signature Applications.* New Delhi: New India Publishing Agency.

Terracore Geo. 2017. Terracore geospectral imaging. Mineral detection in the infrared: Reflectance spectroscopy. Retrieved from http://terracoregeo.com/

Zabic, N., Revard, B., Ong, C. and Mueller, A. 2014. Using airborne hyperspectral data to characterize the surface pH and mineralogy of pyrite mine tailings, *International Journal of Applied Earth Observation and Geoinformation,* 32: 152–162.

Proceedings of Mine Water Solutions 2018
June 12–15, 2018, Vancouver, Canada
Published by the University of British Columbia, 2018

Approaches to Water Quality Modeling Using Geochemical/ARD Test Data in Conjunction with Field Analog Data

Madhumitha Raghav, Freeport-McMoRan, USA
Erick Weiland, Freeport-McMoRan, USA

Abstract

Prediction of long-term water quality at mining operations is a critical component of environmental liability management at any mine site. Acid rock drainage (ARD) alone is estimated to contribute over US$100 billion in total worldwide liability associated with current and future remediation, with neutral/alkaline metal impacted waters only driving these costs higher. The value that reliable water quality predictions can bring to a mining project beyond regulatory compliance (permitting and environmental impact assessments) is often under-appreciated. Water quality modeling can guide the early implementation of effective materials (overburden, development rock, tailings, and heap leach materials) and water management practices, as well as facilitate the design of water treatment plants at closure, thereby potentially reducing the overall project risks and future liabilities.

Various approaches to water quality predictions are viable depending on the mine lifecycle stage, site-specific conditions and risks, and the objectives of prediction. These include, among others, development of spreadsheet models to predict elemental mass loadings, geochemical models, and coupled water balance/water quality prediction models. Prediction models are developed based on available geochemical/ARD test data (Net Acid Generation test leachate data, humidity cell elemental release rates, mineralogy, elemental composition, etc.). The water quality predictions from these types of models generally need to be "scaled up" based on field data to provide estimates that are more representative of actual field conditions. Water quality data from field test pads provide excellent analog data to understand the scaling factors between the laboratory and field studies. However, these types of field-scale tests are time-, labour-, and cost-intensive, and may not be an option for a given mine site or stage of the project. Depending on what data are available for a given site or stage of a project, the objectives of water quality predictions and the overall conditions and risks associated with the project, other types of field analog data may be effectively applied. These may range from seepage water quality from an existing stockpile within the site, to mine water quality from another mine within the same mining district (similar

lithology, alteration, and mineralogy). It may be possible to start with scoping-level water quality predictions when limited data are available, and refine these initial estimates as additional field data become available. The authors demonstrate, through examples, a few approaches they have employed for water quality prediction using geochemical/ ARD characterization test data in conjunction with field analog data.

Introduction

Acid rock drainage (ARD) is estimated to contribute over US$100 billion in total worldwide liability associated with current and future remediation (Tremblay and Hogan, 2001). Typically, regulatory agencies, and financial corporations require acid rock drainage (ARD)/geochemical characterization work (e.g.; acid base accounting, net acid generation test, humidity cell test, and synthetic precipitation leaching procedure) to be completed by the mining companies as part of environmental impact assessment studies, discharge permit applications and project funding applications. However, the results from these tests can provide additional value in achieving reduction of long-term environmental liabilities by guiding the management of potentially acid generating materials and mine water management/treatment. The results from these tests can provide an early understanding of the environmental risks and allow the mines to proactively plan and implement strategies for effective ARD control/management (GARD, 2014). However, there are significant differences in laboratory humidity cells compared to rock piles in the field, such as temperature, particle size distribution, type and metabolic activity of microbial populations, air flow and movement of water within the, which influence the evolution and propagation of ARD and metal leaching (ML) processes (Kempton, 2012; Pearce et al., 2015). Additionally, due to the time and cost involved, the number of samples that can be tested is limited. This could lead to inadequate representation of the material heterogeneities present under field conditions. Hence, a scaling factor needs to be applied to the laboratory elemental release rates and mass fluxes to obtain a reasonable estimate of the field water quality (Kempton, 2012; Pearce et al., 2015).

Analog water quality data from another site or facility with similar geology, mineralogy, climatic conditions, hydrology, mining methods, etc., can be a powerful tool in the prediction of future water quality. For instance, the analog data could be from an existing facility within the same mine site or another mine site from the same mining district. The assumption here is that due to similarities in the type and extent of reactive minerals, climatic conditions and mining methods, the evolution of water quality can be expected to be reasonably similar. Analog water quality data have been previously used to estimate pre-mining water quality at sites that do not have sufficient baseline characterization data available (Runnells et al., 1992; Alpers and Nordstrom, 2000; Davis et al., 2000; Nordstrom, 2008).

In conjunction with data from ARD/geochemical tests, analog water quality can be quite useful for making scoping-level predictions of future mine water quality. Scoping-level predictions are generally adequate during the early stages of a project, when it is more valuable to identify the water quality constituents of concern and obtain a preliminary, ballpark estimate of the water quality. This paper will discuss a few approaches employed by the authors to use analog water quality in conjunction with ARD/geochemical characterization data to obtain scoping-level water quality estimates. The examples discussed here will demonstrate the value of this approach in water quality prediction during various stages of mining – exploration/pre-feasibility, operations, and closure.

Approach #1: Exploration/Pre-feasibility – Modeling of Future Mine Water Quality at an Underground Mine

Mine water quality predictions are generally based on kinetic test data such as humidity cell test results. However, during the early exploration and pre-feasibility stages of a project, data from these tests may be non-existent, or insufficient to estimate future water quality. Typically, a phased/tiered approach is used when selecting samples for ARD/geochemical characterization during the different stages of a project (GARD, 2014). During early project stages, more samples are characterized using static tests such as Acid Base Accounting (ABA), Net Acid Generation (NAG) test, Sequential Net Acid Generation test, and Synthetic Leaching Precipitation Procedure (SPLP), which are less time- and cost-intensive. The results from these tests are used at later project stages to select materials with uncertain/higher ARD/ML risk for more time-consuming and expensive kinetic tests. However, scoping-level predictions at early stages of a project may be required as part of environmental impact studies needed to permit the project. Scoping-level prediction of future mine water quality can also guide the design of future water treatment needs. Leachate quality data from static tests such as single NAG and Sequential NAG (AMIRA, 2002) can be used to develop a preliminary water quality prediction model. The single NAG test can underestimate water quality due to incomplete sulphide oxidation and mineral weathering during the test. The Sequential NAG test, which is a multi-stage test involving a series of single NAG tests, generally provides a better estimate of the total acid generating and metal leaching capacity of the material.

As part of the pre-feasibility study for an underground copper mine – Site A – a 9-year mining period was assumed for the Phase I operations (Direct Shipping Ore – DSO) for the purposes of obtaining a scoping-level mine water quality prediction. The results of the scoping-level water quality predictions presented here are based on two scenarios:

1. the entirety of the sulphides oxidized and metal mass leached, based on the single NAG testing, contained within the quantity of projected water across the 9-year mining period; and

2. the entirety of the sulphides oxidized and metal mass leached, based on Sequential NAG testing, generated over 5 oxidation cycles, and contained within the quantity of projected water across the 9 year mining period.

This approach results in a calculated average water quality across the 9-year mining period based on NAG and Sequential NAG test results.

The amount of material within each of the five potential source areas (decline, ramps, access tunnels, stopes in DSO, and sulphide storage facility) used in the water quality prediction modelling was calculated using information obtained from the mine plan available at the time of this evaluation. The exposed surface area for each of the five source areas was determined using the dimensions (tunnel length, circumference, etc.) provided by the mine planning team. Once the exposed surface area was determined, an estimated depth of oxidation/leachability was used to calculate the volume of material likely to be oxidized/leached in each source area. Preliminary estimates of the oxidation/leaching depth were based on the expected permeability of the rock within a particular source area. The total amount of material likely to be oxidized and leached for each source area was then determined by using the volume estimates and assumed densities for each rock type. NAG and Sequential NAG tests were performed on samples selected from 13 geological/analytical "bins" or rock types used for classification of the materials that will be mined in the future. Each of the 13 geological/analytical bins tested were given a weighting factor based on the amount of material expected from each of the bins to comprise each of the 6 different source areas (Figure 1). NAG and Sequential NAG leachate concentrations are generally reported in mg/L and were converted to mg of analyte per kg of source material for this evaluation using the rock to water ratio of 100 typically used in these tests (AMIRA, 2002). The mass of each analyte from the NAG and Sequential NAG leachate results for a given bin was multiplied by the weighting factor for the corresponding bin and then summed over all 13 bins.

The quantity of water for each of the sources was estimated based on preliminary analytical modelling completed by the site hydrologist. Finally, the overall mine water quality was predicted using the estimated mass release based on NAG leachate and Sequential NAG leachate data plus the volume of water in each source area (Table 1).

The modelled water quality based on the single NAG leachate chemistry is predicted to be less impacted than that based on the Sequential NAG leachate results, likely due to incomplete sulphide oxidation and mineral weathering during the single NAG test. The modelled iron, sulphate, and copper concentrations based on Sequential NAG test are reasonably similar to the water quality from Site B (an underground mine in the same mining district) when compared to the estimates based on the single NAG test. However, the modelled concentrations for aluminum, calcium, sodium and magnesium based on

Sequential NAG test are predicted to be lower than those observed at Site B. These elements are typically released from the slow weathering of silicate minerals.

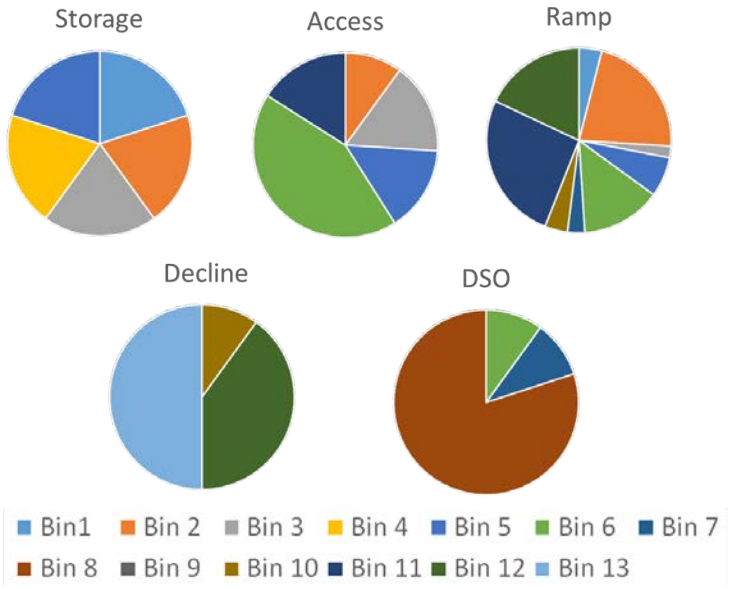


Figure 1: Bin weighting factor for different source areas in Site A

Table 1: Modelled water quality for Site A based on NAG and Sequential NAG results plus Site B analog water quality

Analyte	Concentration (mg/L)				
	NAG modeled	NAG Ion-balanced	Sequential NAG modeled	Sequential NAG ion-balanced	Site B
pH (su)	5.5	5.5	3.3	3.3	3.8
Iron (Fe)	83	83	340	340	280
Sulphate (SO4)	820	820	2,400	2,400	3,500
Aluminum (Al)	5.5	50	14	100	160
Calcium (Ca)	65	65	100	270	360
Magnesium (Mg)	2.1	50	3.7	130	180
Sodium (Na)	16	25	19	100	120
Potassium (K)	4.3	4.3	8.2	8.2	4.7
Copper (Cu)	76	76	140	140	170
Manganese (Mn)	0.93	0.93	1.7	1.7	NA
Arsenic (As)	0.25	0.25	0.36	0.36	0.0007
Cadmium (Cd)	0.0028	0.0028	0.0038	0.0038	–
Lead (Pb)	0.049	0.049	0.43	0.43	0.045
Selenium (Se)	0.026	0.026	0.081	0.081	NA
Zinc (Zn)	0.76	0.76	0.70	10	13

Due to the short duration of the NAG as well as Sequential NAG testing methods, it is unlikely that these elements were at their final equilibrium levels. The water quality from Site B has been used as an analog to adjust the Site A water quality estimates. Since the modelled water qualities derived from NAG and Sequential NAG leachate data are based on the mixing of multiple water sources, an ion-balance adjustment that is within the 10% variance was considered acceptable for this level of water quality modelling. These two scenarios ("NAG ion-balanced" and "Sequential NAG ion-balanced" in Table 1) potentially bracket the water quality likely to be observed when operations commence. The water quality predictions presented here based on static testing provided a reasonable scoping-level estimate that allowed for the early evaluation of potential water treatment requirements and costs as part of the pre-feasibility study. Humidity cell testing can help refine these predictions at later stages of the project.

Approach #2: Operations – Modeling of Seepage Water Quality from a Future Non-Mineralized Rock Stockpile as Part of an Expansion Project

Site C is an active mine that is in the planning stages of an expansion project. As part of the discharge permit application process, the future mined materials that would constitute the new non-mineralized rock stockpile have been characterized using static (ABA, NAG, SPLP) and kinetic (humidity cell) tests to understand their ARD/ML potential. The authors developed a reasonably simple spreadsheet model to obtain a scoping-level prediction of the future seepage water quality from the rock pile. The inputs to the model were:

1. tonnage distribution of different rock types based on the mine plan existing at the time of model development;
2. elemental mass release rate (mg/kg/week) from humidity cell tests;
3. annual precipitation and infiltration rates into the rock pile; and
4. total elemental mass available based on elemental assay of the material.

For the purposes of obtaining a scoping-level estimate, the following assumptions were made:

- elemental release rates based on laboratory humidity cell test results are representative of field conditions, and
- passivation due to build-up of secondary oxidation/weathering products on reactive mineral surfaces and limits on oxygen diffusion within a rock pile can be ignored.

Initial seepage water concentrations from rock stockpiles are typically elevated due to "first flush" of accumulated oxidation and weathering by-products. The concentrations generally decrease and stabilize over time, eventually reaching steady-state concentrations. These trends are usually observed in

the leachate from humidity cell tests as well. The "first flush" concentrations may guide short-term management strategies, but the steady-state concentrations represent long-term water quality and will thus drive the design of future water treatment plants and long-term water management strategies.

For the future rock stockpile at Site C, steady-state seepage water concentrations were calculated based on cumulative mass loading from the total rock mass deposited within the pile. The mass contribution of each rock type to the future rock stockpile was calculated based on the mine plan. Elemental release as a result of mineral reactions (oxidation/weathering) requires contact of rock with water. Hence, the calculated rock mass was multiplied by the fraction of rock contacted by water to estimate the mass of reactive rock within the rock pile. The fraction of rock contacted by water is a function of the porosity and moisture content within the rock pile. The total mass of each water quality constituent in the seepage was calculated by multiplying the release rate (mg/kg/week) with the mass of reactive rock. Release rate in mg/kg/week for each water quality constituent was calculated based on humidity cell leachate data according to the procedure in Price (2009). Mass released was calculated by assuming that the release rates stayed constant over time. This is expected to result in a conservative water quality estimate due to the fact that release rates in the field should decrease over time due to passivation of reactive mineral surfaces. The rock tonnage, weighted rock density, and the average annual precipitation at the site were used to estimate the total infiltration rate into the pile and subsequently, the volume of seepage. It was verified that the total mass released for each water quality constituent was less than the total mass available based on Whole Rock Assay data before estimating the overall seepage water quality from the rock pile.

Geochemical controls within the rock pile are an important consideration in the establishment of long-term seepage water quality. Hence, mineral solubility constraints were evaluated using the geochemical modelling software, PHREEQC. Based on mineral saturation indices – alunite, gypsum, calcite, ferrihydrite, K-Jarosite and calcium molybdate ($CaMoO_4$) were allowed to precipitate to account for mineral solubility controls on the steady-state seepage water quality. The Minteq.v4 thermodynamic database supplied with version v3.1.7 of PHREEQC was selected since it is a comprehensive database with thermodynamic constants for a range of elements and mineral phases. Table 2 shows the resulting steadystate seepage water quality. Similar approaches to seepage water quality prediction have been described in literature (Brown et al., 2006; Declercq et al., 2017).

Laboratory tests such as humidity cell tests may not be able to adequately represent field processes due to the differences in laboratory vs. field conditions such as temperature, particle size distribution, type and metabolic activity of microbial populations, and air flow and movement of water within the rock pile as compared to the humidity cell (Kempton, 2012; Pearce et al., 2015). Laboratory tests may also inadequately represent the material heterogeneities present under field conditions as a result of limited

number and small mass of samples. A more accurate estimate of the elemental release rates would be that obtained under field conditions, for instance, from an analog site or analog facility within the same mine site. Upon further investigation, it was determined that analog water quality data were not readily available for Site C. Because Site C is still under active operations, it has been determined that a field-scale test pile study could provide a rare but excellent opportunity to observe ARD/ML generation under field conditions. The results from these future test piles can be used to scale-up the laboratory-scale release rates to better represent field conditions and thereby, help refine the scoping-level predictions provided here.

Table 2: Estimated steady-state concentrations in future rock pile seepage at Site C

Element	Estimated steady-state concentrations (mg/L)
pH (su)	6.1
Al	4.7
As	0.22
Ba	1.3
Ca	580
Cd	0.022
Cr	2.2
Co	2.2
Cu	2.4
Fe	0.0036
Mg	150
Mn	1.4
Mo	0.63
Na	170
Ni	1.8
K	310
Se	0.15
Zn	2.2
SO4	1,300
Cl	170
F	19

Materials selection for the field test piles is based on three criteria:

1. tonnage contribution of rock type to the total tonnage in the rock pile according to the current mine plan;
2. amount of existing characterization available for the rock type; and
3. ARD/ML risk predicted from existing laboratory test data.

The annual precipitation volume on the test pads has been calculated using the catchment area for the test pads (top surface and partial side slopes) plus the average annual precipitation observed at the mine site. The annual precipitation volume was multiplied by a factor of ~10 to calculate the target water application rate to be used during the test. Depending on the mineralogy, sulphur content, and the site climatic conditions, ARD generation processes can take anywhere between decades to centuries to completely evolve. Based on Site C climatic conditions and results from static tests, a 10× factor was considered sufficient to accelerate the ARD/ML generating reactions and other associated reactions (e.g., weathering of carbonate/silicate minerals) in order to observe the resultant evolution of seepage water chemistry within a reasonable timeframe (<2 years). The seepage water quality from these test piles can then be used to refine the scoping-level predictions presented here. It has also been recommended to the site personnel to evaluate if there are any existing analog facilities at Site C or other sites that can provide water quality evolution data to adjust the scoping-level estimates presented here. Figure 2 shows a framework for the use of ARD/geochemical test data in conjunction with analog water quality data in scoping-level water quality predictions.

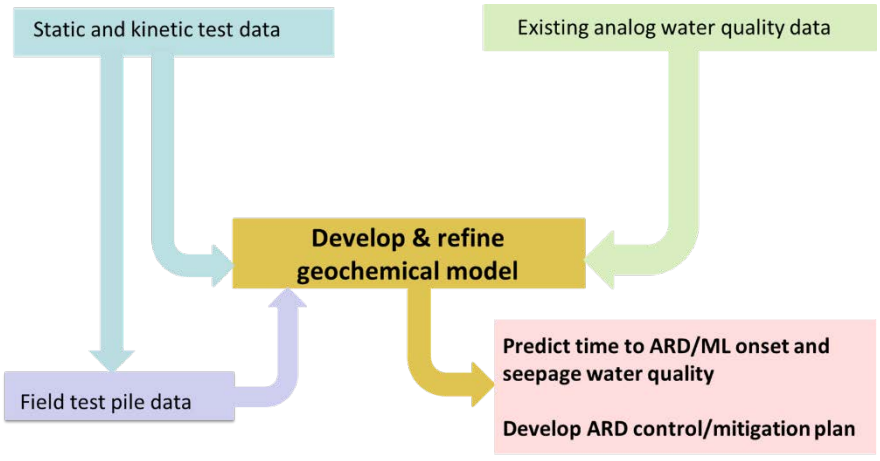


Figure 2: Framework for the use of ARD/geochemical test data in conjunction with analog water quality data in scoping-level water quality predictions

Approach #3: Closure – Modelling of Post-Closure Seepage Water Quality from a Tailings Facility

Site D's mill is entering final years of operation and the Tailings Storage Facility (TSF) will be placed into long-term care and maintenance. In order to evaluate the water treatment options for treatment of long-term, post-closure TSF seepage, it is critical to understand the current and likely future seepage water quality. This is especially important as the quality and quantity of TSF seepage water will change after closure measures have been implemented. Post-closure activities at TSFs are designed to control water infiltration and oxygen diffusion resulting in reduction of seepage flow as well as the mineral reaction rates that might otherwise increase the concentrations of constituents in the seepage. Figure 3 shows a conceptual matrix to broadly illustrate the post-closure evolutions of seepage flow and chemical mass flux that control the evolution of the seepage water quality. The post-closure geochemical evolution paths may vary for each water quality constituent depending on the geochemical mechanisms controlling the solid-aqueous phase distribution of that constituent. Drain-down modelling using FEFLOW allowed estimation of the post-closure TSF seepage flow rates. Reduction in chemical mass flux of reaction products from sulphide oxidation and mineral weathering is more challenging to estimate. Water and oxygen are two critical elements required for generation of ARD and associated mineral weathering/metal leaching. Hence, the reduction in chemical mass flux would depend on the effectiveness of the closure activities in reducing the extent of oxygen and water infiltration into the tailings.

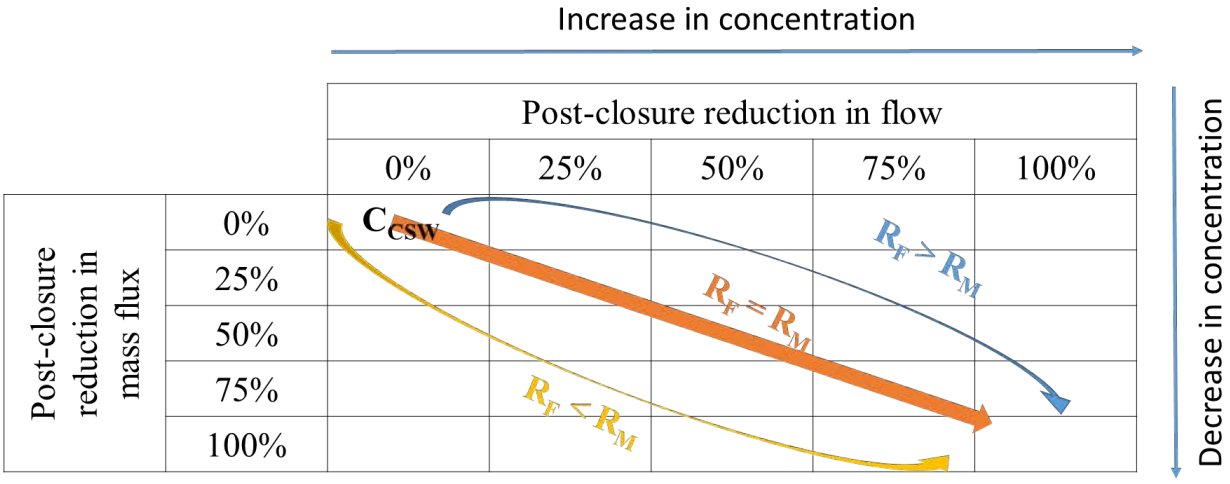


Figure 3: Conceptual matrix for the evolution of flow and mass flux after closure of Site D TSF. C_{CSW} = current seepage water quality, R_F = post-closure reduction in flow, R_M = post-closure reduction in mass flux

Two closed TSFs from Site E (closed 12 years) and Site F (closed 40 years), were considered as analogs to predict the post-closure TSF seepage water quality at Site D based on their similarities in

geology, mineralogy, hydrology, climatic conditions, and mining methods. As a result, it was reasonable to assume that evolution of TSF seepage water quality at Site D would be similar to that at the analog sites. For the purposes of obtaining a scoping-level water quality estimate, it was also assumed that the closure activities at the analog sites were similar to those planned at Site D in terms of their effectiveness in controlling ARD and ML. Mapping the geochemical changes observed in the Site E and Site F TSF seepages allowed evaluation of the potential geochemical paths for Site D seepage.

Using Year 1 and Year 10 Site E post-closure seepage water qualities (1 year and 10 years after closure, respectively; Table 3), the percent change (increase or decrease) from pre-closure concentrations was calculated for each water quality parameter. The percent change from pre-closure concentrations in the Site E seepage was applied to the corresponding water quality parameter in the Site D TSF pre-closure seepage to predict the Year 1 and Year 10 Site D post-closure water qualities. Since no two sites are exactly the same, this procedure accounts for the differences in the Site D and Site E pre-closure seepage water qualities, assuming that the geochemical evolution path would be similar at the two sites (similar % increase or decrease in concentrations during the same post-closure time period).

Percent change in seepage quality (Year 1) = $(C_{\text{Site E Pre-closure}} - C_{\text{Site E Year 1}})/C_{\text{Site E Pre-closure}}$

$C_{\text{Site D Year 1}} = C_{\text{Site D Pre-closure}} - (\text{Percent change}) \times (C_{\text{Site D Pre-closure}})$

Where,

$C_{\text{Site E Pre-closure}}$ = Concentration in Site E TSF pre-closure seepage

$C_{\text{Site E Year 1}}$ = Concentration in Site E TSF seepage 1 year after closure

$C_{\text{Site D Pre-closure}}$ = Concentration in Site D TSF pre-closure seepage

$C_{\text{Site D Year 1}}$ = Concentration in Site D TSF seepage 1 year after closure

In the case of Site F, pre-closure TSF seepage water quality data are not available and hence, there was no way to check and adjust for differences in pre-closure seepage water qualities between Site F and Site D. Site F Year 40 post-closure TSF seepage water quality (~40 years after closure) was considered as a reasonable estimate for the Site D TSF post-closure seepage water quality (without any adjustment) based on the similarity in the geology, mineralogy, hydrology and climatic conditions between the two sites. This was considered adequate to provide a reasonable scoping-level estimate for the Site D Year 40 post-closure seepage water quality (Table 4).

Table 3: Pre- and post-closure seepage water quality from Site E and Site F Tailings Storage Facilities

Water quality parameter	Pre-closure concentrations (mg/L)		Analog post-closure concentrations (mg/L)		
	Site E	Site F	Site E Year 1	Site E Year 10	Site F Year 40
Al	26.9		45.7	29.4	18.2
Fe	342		83.7	350	31.9
Mn	35.8		14.7	29.9	107
Zn	2.00		2.20	1.90	7.83
Ca	367		224	360	107
Mg	52.0	N/A	44.7	65.9	7.02
Na	67.2		21.5	40.6	13.9
K	123		38.7	N/A	19.5
Cl	13.0		N/A	9.00	5.52
F	62.5		31.7	72.0	26.6
SO_4	2,060		1,040	1,810	641

Based on historical reagent application data, sodium and chloride concentrations in Site E and Site F TSF seepages are likely to be controlled by mineral weathering; whereas in the case of Site D, mass accumulation within the TSF is controlled by the historical reagent application rates. Hence, for the estimation of post-closure sodium and chloride concentrations in Site D TSF seepage, neither Site E nor Site F TSF seepages were determined to be reasonable analogs. For the purposes of obtaining a scoping-level estimate for Site D seepage, it was reasonable to assume that all the sodium and chloride within the TSF (primarily from reagent application) are already in the aqueous phase and that the seepage concentrations were likely to be controlled by dilution with infiltrating rainwater. Based on "back-of-the-envelope" type mass and water balance calculations, the cumulative dilution over 40 years was estimated to be approximately 25%, resulting in a conservative estimate of the sodium and chloride concentrations in the Year 40 seepage. The effect of dilution was negligible (<5%) and hence, ignored when estimating the Year 10 concentrations.

Figure 4 shows the predicted geochemical evolution path for sulphate and calcium characterized by specific seepage flow and chemical mass flux decreases. Establishment of an effective cover during closure reduces the oxygen ingress and water infiltration into the TSF. After consumption of the oxygen existing within the TSF, the sulphide mineral oxidation rate can be expected to decrease. This explains the post-closure reduction in chemical mass flux that is predicted for sulphate. Calcium in the seepage is likely to be a result of dissolution of Ca-carbonate minerals and weathering of Ca-silicate minerals in

response to the acidity generated from sulphide mineral oxidation. This could explain why the post-closure geochemical path for calcium closely follows that for sulphate (Figure 4). An overall decrease in chemical mass flux was also predicted for the geochemical evolution paths of other water quality constituents during the 40-year post-closure period.

Table 4: Estimated post-closure Site D TSF seepage water quality

Water quality parameter	Pre-closure Site D water quality (mg/L)	Estimated Site D post-closure TSF seepage water quality (mg/L)					
		Year 1	Year 10	Year 40	Year 1 (corrected)	Year 10 (corrected)	Year 40 (corrected)
Al	21.9	37	24	19	37	24	20
Fe	220	54	230	32	54	230	30
Mn	190	78	160	110	78	160	110
Zn	7.95	8.8	7.6	7.9	8.8	7.6	10
Ca	410	250	400	110	250	400	110
Mg	36.0	31	46	7.0	31	46	7.0
Na	750	230	430	14	750	750	560
K	200	63	N/A	20	63	110	20
Cl	300	N/A	240	5.5	300	300	230
F	43.0	22	50	27	22	50	30
SO_4	3,300	1,700	2,900	640	2,400	3,100	1,500

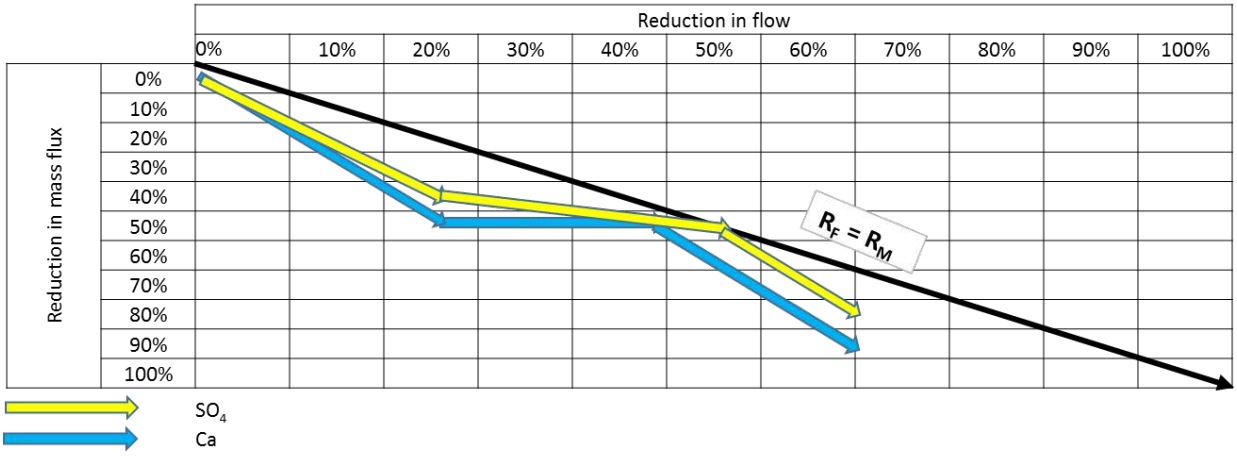


Figure 4: Estimated reduction in flow (based on FEFLOW modeling) vs. reduction in mass flux (based on analog water quality data) for sulphate and calcium in Site D TSF seepage

In addition to adjusting the sodium and chloride concentrations to account for the effect of reagent addition at Site D, ion-balance correction was applied to the seepage quality estimates based on the evolution of analog post-closure seepage water quality to obtain the scoping-level estimates reported in Table 4.

Conclusions

Scoping-level mine water quality predictions are generally adequate during the early planning stages of an exploration, operations expansion, or closure project, when it is valuable to identify the water quality constituents of concern and obtain back-of-the-envelope type estimates of water quality for planning purposes. Evolution of water quality at an existing site/facility can be used as a valuable analog for the prediction of future water quality at another site. Similarity in geology/mineralogy of deposits, mining methods, hydrology, and climatic conditions are the pre-requisites for establishing reasonable analogy between sites/facilities for the purposes of obtaining scoping-level water quality estimates. With this approach, the inherent assumption is that the reactions or mechanisms controlling water quality at analog sites are sufficiently similar to use as the basis for obtaining scoping-level water quality estimates. The biggest challenge with this approach is that no two sites are exactly the same. Variations in mineral type and quantity, mining methods, and climatic conditions as well as gaps/ inconsistencies in the analog water quality data are not uncommon. One needs to carefully evaluate whether an existing site is a reasonable analog for the purposes of obtaining a scoping-level water quality estimate. Collaborative efforts between various teams within your mine site or other potential analog sites to build a robust database of analog water quality data can go a long way towards improving scoping-level water quality prediction capabilities.

References

Alpers, C.N. and Nordstrom, D.K. 2000. Estimation of pre-mining conditions for trace metal mobility in mineralized areas: An overview, ICARD 2000, in *Proceedings from the Fifth International Conference on Acid Rock Drainage*, Denver, Colorado. Society for Mining, Metallurgy, and Exploration, Inc., Littleton, CO: 463-472.

AMIRA. 2002. ARD Test Handbook. Project P387A Prediction and Kinetic Control of Acid Mine Drainage, Ian Wark Research Institute and Environmental Geochemistry International Pty Ltd: 42.

Brown, D., Verburg, R., Letient, H. and Aranda, C. 2006. Geochemical characterization and water quality prediction at the Antamina Mine, in R.I. Barnhisel (ed.), ICARD 2006, *Proceedings of the 7th International Conference on Acid Rock Drainage*, St. Louis MO. American Society of Mining and Reclamation (ASMR), Lexington KY: 291–305.

Davis, A., Tisdale, A. and Byrns, C. 2000. Discriminating between background and mine-impacted waters, ICARD 2000, in *Proceedings of the Fifth International Conference on Acid Rock Drainage*; Denver, Colorado. Society for Mining, Metallurgy, and Exploration, Inc., Littleton, CO: 473–484.

Declercq, J., Charles, J., Bowell. R., Warrender. R. and Barnes, A. 2017. Comparison of thermodynamic equilibrium and kinetic approach in the predictive evaluation of waste rock seepage quality in Northern Finland, in C. Wolkersdorfer, L. Sartz, M. Sillanpää and A. Häkkinen (eds), IMWA 2017*, Proceedings of Mine Water and Circular Economy,* Vol. I, Lappeenranta, Finland: 664–672.

GARD (Global Acid Rock Drainage) Guide. 2014. The International Network for Acid Prevention (INAP).

Kempton, H. 2012. A review of scale factors for estimating waste rock weathering from laboratory tests, in W.A. Price, C. Hogan and G. Tremblay (eds), ICARD 2012, *Proceedings of the 9th International Conference on Acid Rock Drainage,* Vol. 1, Ottawa, Canada: 1026–1037.

Nordstrom, D.K. 2008. What was the groundwater quality before mining in a mineralized region? Lessons from the Questa project, *Geosci J.,* 12(2):139–149.

Pearce, S., Scott, P. and Webber, P. 2015. Waste rock dump geochemical evolution: Matching lab data, models and predictions with reality, in *Proceedings of the 10th International Conference on Acid Rock Drainage and IMWA 2015*, Santiago, Chile. Retrieved February 12, 2018, from: https://www.imwa.info/docs/imwa_2015/IMWA2015_Pearce_172.pdf

Price, W.A. 2009. Prediction manual for drainage chemistry from sulphidic geologic materials, MEND Report 1.20.1., CANMET Mining and Mineral Sciences Laboratories, British Columbia, Canada: 579.

Runnells, D.D., Shepard, T.A. and Angino, E.E. 1992. Metals in water: Determining natural background concentrations in mineralized areas, *Env. Sci. Technol.,* 26(12): 2316–2323.

Tremblay, G.A. and Hogan, C.M. 2001. Mine Environment Neutral Drainage (MEND) Manual 5.4.2d: Prevention and Control, Canada Centre for Mineral and Energy Technology, Natural Resources Canada, Ottawa: 352.

Proceedings of Mine Water Solutions 2018
June 12–15, 2018, Vancouver, Canada
Published by the University of British Columbia, 2018

Dependence of Predicted Dewatering on Size of Hydraulic Stress Used for Groundwater Model Calibration

Vladimir Ugorets, SRK Consulting (US), Inc., USA
Cristian Pereira, SRK Consulting (US), Inc., USA

Abstract

Accurate predictions of long-term dewatering requirements by groundwater models depend on the quality of calibrated hydraulic parameters and boundary conditions. The latter is very important for large-scale dewatering projects when drawdown propagates a significant distance away from the mine area and predicted mine inflow/dewatering rates predominantly depend on the hydrogeological behaviour of the model boundaries. This paper presents the results of a multiyear data collection and groundwater modeling study to define large-scale dewatering requirements for a mine project in a complex hydrogeological setting characterized by large bedrock transmissivity and groundwater storage, high recharge from precipitation, and the presence of leaky lateral and vertical boundaries. Over a period of 5 years, dewatering requirements were evaluated for scoping, pre-feasibility, and feasibility studies using a groundwater model calibrated to various hydraulic stresses, including short-term hydrogeological testing in geotechnical boreholes, 2 to 3 day airlift tests, 5 to 14 day pumping tests in prototype dewatering wells, one year of highly variable flow and water level data obtained during exploration decline (initial mine) dewatering, and observations of groundwater recovery once dewatering ceased.

Based on the size and length of the hydraulic stress applied to the groundwater system and observed responses, a series of conceptual and numerical models were developed for the project. When new data were obtained, an iterative approach was used to evaluate the robustness of the model calibration, assess the validity of the conceptual model, and revise to the predicted dewatering requirements. In total, the groundwater model was recalibrated five times to account for new data. The process required revising the conceptual model with regards to transmissivity, vertical hydraulic conductivity, groundwater storage, recharge from precipitation, and boundary conditions. Dewatering predictions were completed for two mining methods (block cave and open pit) and the high variation in predicted dewatering requirements highlights the importance of understanding vertical recharge to the groundwater system and the hydrogeological role of lateral model boundaries. In complex hydrogeological systems, these two factors

cannot be precisely evaluated based on short- to intermediate-term hydraulic testing; model calibration to long-term testing provided superior input to the conceptual models and resulted in more defensible mine dewatering predictions. Predictability of the final version of the model was verified by reproducing groundwater recovery observed during flooding of the exploration decline.

Introduction

Usually, the hydrogeological data collection effort is constrained to the areas near the ore body or mine footprint; however, in the case of large-scale and long-term dewatering projects, the hydrogeological boundaries play a decisive role in the conceptual model, and therefore in the dewatering predictions. Boundaries can be located several miles away from the mine area where hydrogeological data are sparse, yet boundaries are often the critical factor in the prediction of dewatering requirements for mine projects.

The size of the conceptual model and the distribution of field data must be balanced against the scale of the hydraulic stress (diameter and time) on the hydrogeological system to ultimately answer the question illustrated in Figure 1: "What amount of hydraulic stress (i.e., pumping rate and duration) is sufficient to calibrate a model in order to reliably predict long-term mine dewatering requirements in a highly permeable groundwater system with unknown lateral boundaries?"

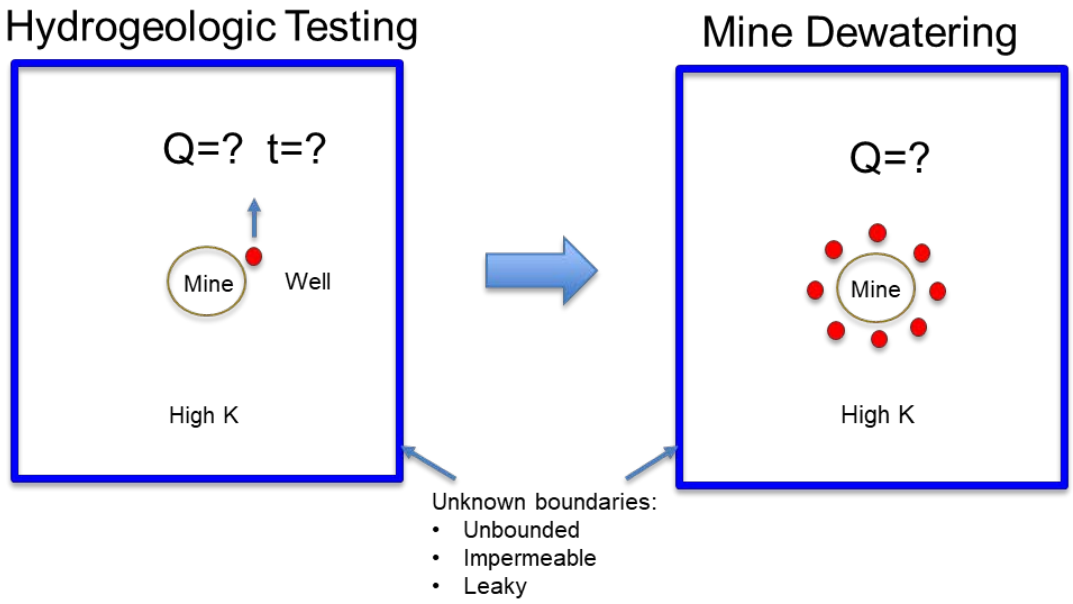


Figure 1: Problem description

This paper presents the results of a multiyear data collection and groundwater modeling study to define large scale dewatering requirements for a mine project in a complex hydrogeological setting. Over

a period of six years, dewatering requirements were evaluated for scoping, pre-feasibility, and feasibility studies using different conceptual and numerical models based on a long-term data collection effort.

Hydrogeological Studies

The confidential origin of the projects does not allow the presentation of a detailed description of the site; therefore, the data collection campaigns and hydrogeological studies are described in general terms.

The specific hydrogeological studies were developed over six years and included field campaigns and dewatering prediction for different proposed mine extraction methods. The authors as part of a larger team participated in the hydrogeological studies as follows:

- 2010 to 2011 – Scoping study for two block cave operations;
- 2013 to 2014 – Pre-feasibility study for one block cave; and
- 2014 to 2015 – Feasibility studies for an open pit.

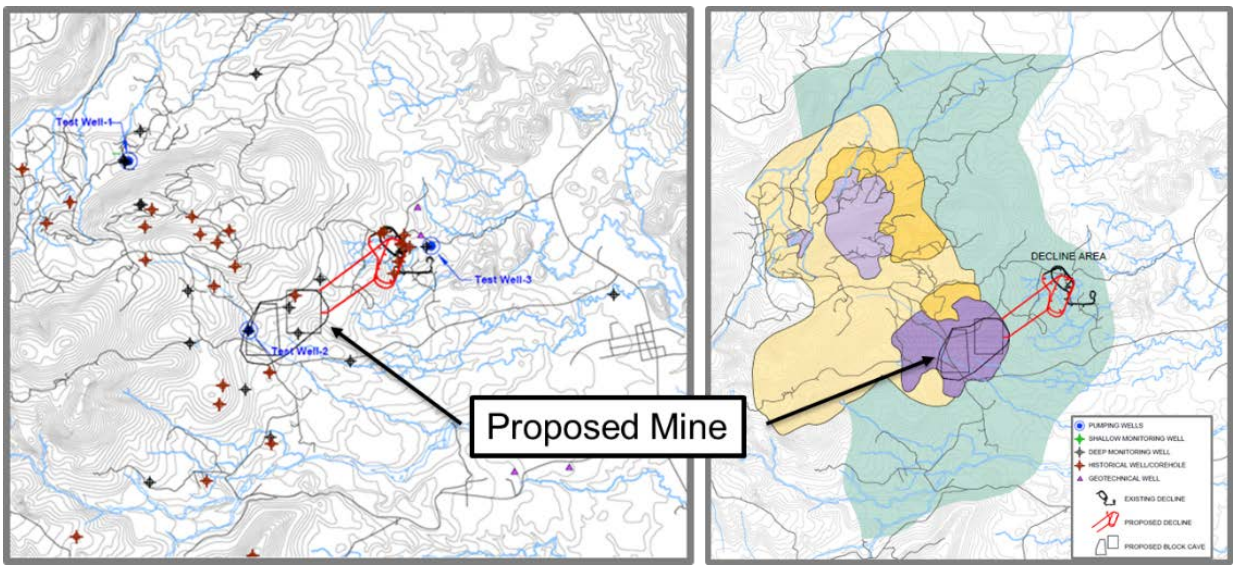
The field data collected during this time is summarized below:

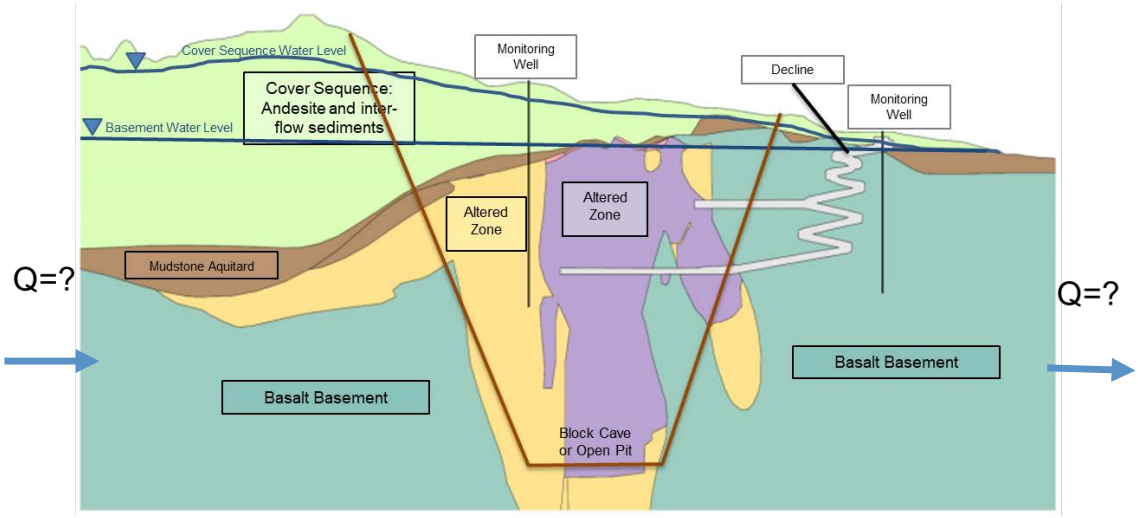
- Over 70 monitoring wells (27 shallow, 11 intermediate, and 36 deep) were constructed at the project area to a maximum depth of 621 m. The majority of monitoring wells were located within 1.5 km of the site.
- Short-term testing included 11 pumping or injection packer tests, and 95 falling/rising head tests.
- Additionally, 3 pumping tests were conducted in the proximity of the ore body in large diameter wells; the test duration was from 5 to 14 days with pumping rates spanning 5 to 60 L/s. These pumping tests were conducted during excavation of the exploration decline.
- The exploration decline started before hydrogeological studies began, and significant groundwater inflow was intercepted by the decline. Flow rates and water level data were collected for one year during the excavation of the exploration decline, and for one year after they ceased.

Location of pumping wells, monitoring wells, the exploration decline, and proposed mines are shown schematically in Figure 2.

Description of Hydrogeological Study Area

The hydrogeological study area (HSA) is comprised of shallow and deep groundwater systems with limited vertical hydraulic connection between the two systems. The shallow sequence is formed by about 50 to 100 m thick hill slope colluvium (HSC) with a large covering of andesitic and interflow sediments with thicknesses up to 300 m, getting significant recharge from precipitation. The deep system is formed by a basalt basement with altered and mineralized zones. A mudstone aquitard located between the shallow and deep systems acts as a barrier to vertical groundwater flow (Figure 2).





Notes: 1: Q represents regional groundwater flow

2: Water levels and direction of groundwater flow are shown for pre-mining conditions

Figure 2: Conceptual hydrogeological model

The HSA is characterized by high precipitation; approximately 5 m of rain falls on the project area annually. The heaviest precipitation generally occurs from November to March (from 500 to 850 mm/month), but an actual dry season is rarely seen – the rainfall during the remaining months varies from 130 to 300 mm/month. Meteoric recharge results in relatively high water levels in the HSC, with limited seasonal variation.

The data are interpreted as two separate water tables: a shallow system within HSC and andesite/interflow sediments below, and a deep system in the basement rocks.

The initial stages of the field campaign identified a low K cover sequence (except the first 50 to 100 m of HSC), a high hydraulic conductivity (K) fractured basement rock (K=0.3 to 1.5 m/d), and an

intermediate to high K ore body (K=0.1 to 1.5 m/d). The hydraulic role of lateral boundaries was unknown.

Long-Term Stress to Groundwater System Used for Model Calibration and Dewatering Predictions

The preliminary test results indicated the need for large-scale active dewatering due to high water table elevation (significantly exceeding the bottom elevation of the proposed mine) and the presence of high K Basalt Basement and ore body. Various hydrogeological conceptual models have been developed since 2010, the complexity and accuracy of each driven by field data available at each phase of the hydrogeological study. Consequently, several numerical groundwater flow models were developed to evaluate the dewatering requirements using predictive simulations.

The hydrogeological phases used in each numerical model are summarized below:

- Phase 1: Short-term testing prior to installation of an exploration decline within Basalt Basement
- Phase 2: Three pumping tests and 10 days of active decline dewatering (maximum dewatering rate up to 100 L/s)
- Phase 3: 120 days of active decline dewatering (maximum dewatering rate up to 220 L/s)
- Phase 4: 200 days of active decline dewatering (maximum dewatering rate up to 350 L/s)
- Phase 5: 365 days of active decline dewatering (maximum dewatering rate up to 125 L/s)

Figure 3 shows the applied stress to the groundwater system during Phases 2 through 5.

Phase 1

During the very early exploration stage, a limited set of hydrogeological field tests was performed consisting of only a few packer tests completed in two deep geotechnical boreholes near the ore body. A preliminary hydrogeological model was built assuming a very permeable cover unit and a basement with minimum groundwater flow. A numerical model was developed as an initial tool for estimating the groundwater inflow into the two proposed block cave mines. A steady-state model was calibrated to the water levels measured in the shallow piezometers screened within HSC representing the pre-mining conditions. The predicted dewatering requirements for two block caves were about 300 L/s (4,800 gpm). Figure 4 shows the extent of the groundwater numerical model used for Phase 1. The model had limited lateral extent with general head boundaries assigning at the model boundaries. Dewatering predictions were made under a passive inflow scenario to the two block caves and their results vs. ultimate mine bottom elevation and their results are shown in Figure 4. Inflow was simulated by drains at the draw point level and a block cave was modeled by the increase of K in space and time.

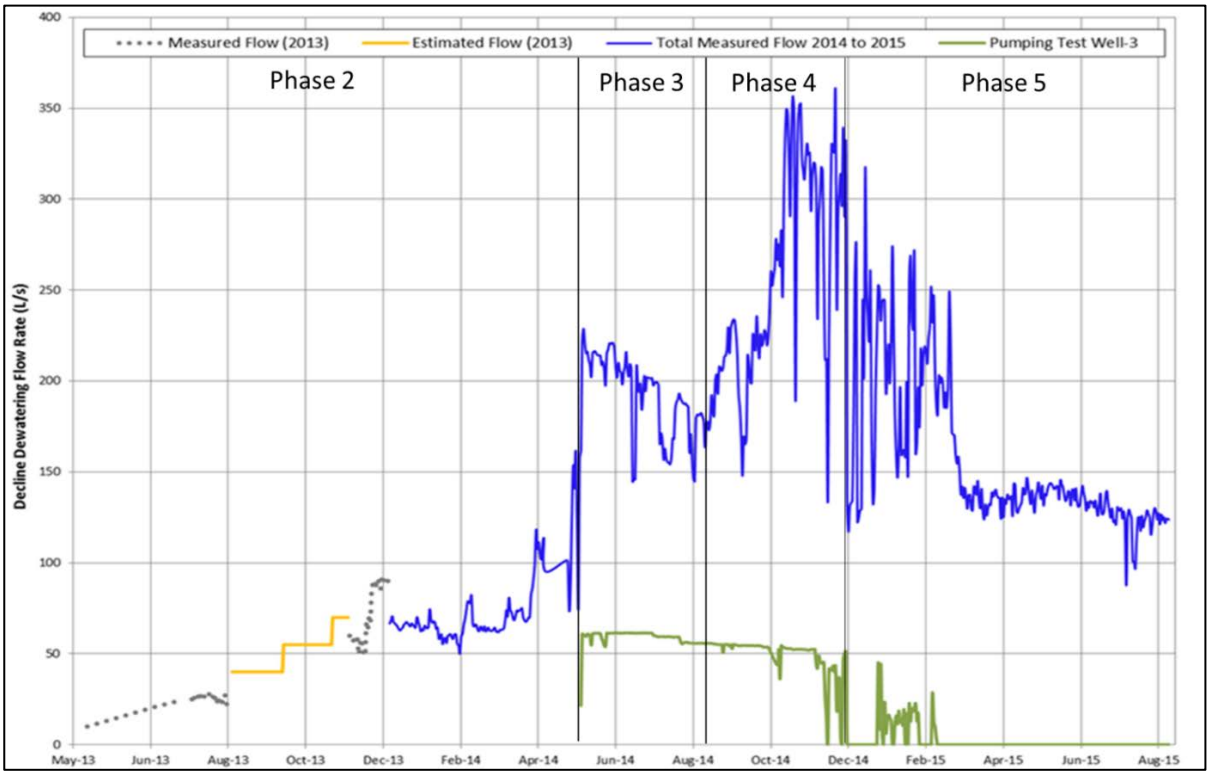


Figure 3: Stress applied to groundwater system during Phases 2 through 5

Phase 2

During the initial stage of decline installation, it was recognized that basement fractured rock around the ore bodies was permeable, because significant groundwater inflows were measured as soon as the decline advanced below the water table. The model was calibrated to measured water levels and the results of three pumping tests. Conceptual and numerical models were assumed to be unbounded (with no physical boundaries nearby so distant GHBs were used to represent the heads in the regional groundwater system), as shown in Figure 5a.

The numerical model was calibrated to changes in water levels (as shown in Figure 5b) and dewatering predictions were made for two block caves considered at that time. The maximum dewatering rate from the perimeter ring of the dewatering wells screened within Basalt Basement was estimated to be 1,500 L/s (Figure 5c) or 1,200 L/s larger than the Phase 1 prediction.

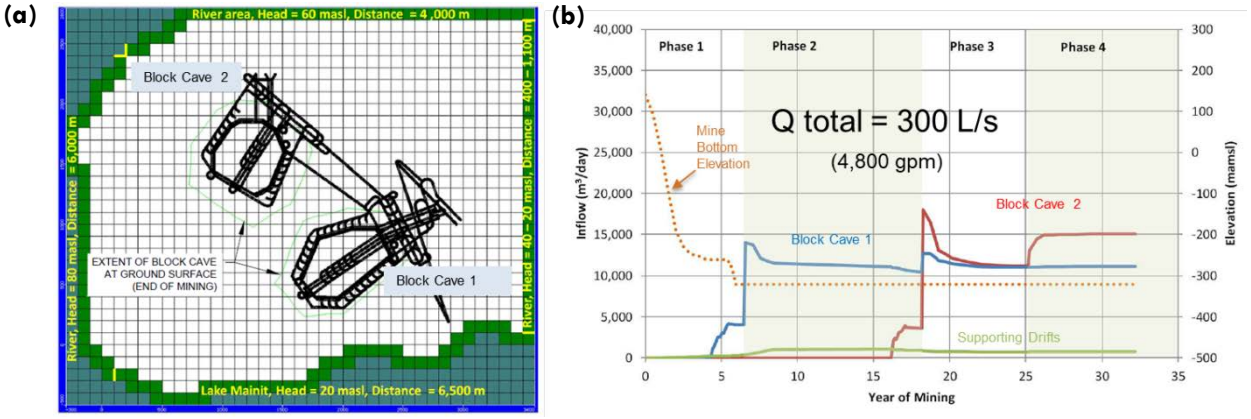


Figure 4: Phase 1 Scoping study model setup showing location of simulated general head boundaries (a) and dewatering predictions (b)

Phase 3

Pumping from the decline simulated by a combination of drain and pumping cells was increased to 220 L/s (including pumping from one surface dewatering well, both discharging water from the Basalt Basement) and the groundwater model was recalibrated after 120 days. Water levels in monitoring wells within the Basalt Basement started to decline, indicating the presence of a Halo Zone around the ore body (or permeable "bucket" with K about 3 orders of magnitude higher than basalt rocks outside of the "bucket"). The conceptual model was updated accordingly and the numerical groundwater model was transferred into a leaky horizontally bounded model, as shown in Figure 6a.

The model calibration to declining water levels was significantly improved compared to the unbounded model, as shown in Figure 6b, and prediction of the dewatering rate for a block cave scenario was updated accordingly. The predicted maximum dewatering rate (active pumping from the basalt basement and passive inflow from the Cover plus direst precipitation) was decreased by 800 L/s from 1,500 to 700 L/s (Figure 6c).

Phase 4

The pumping rate from the decline continued to increase due to the installation of additional drain holes, and reached about 330 L/s after 200 days of active dewatering. Water levels continued to decline indicating that the bucket of fractured basement rock was being successfully dewatered. Considering the uncertainties in the estimates of lateral groundwater inflow to the bucket (monitoring wells outside of the bucket were not available), two alternative conceptual models were adopted: "Leaky Bucket" and "Non-leaky Bucket" (simulating depletion of groundwater storage only), as shown in Figure 7a. Both models were able to reproduce changes in the water levels observed at that time, as shown in Figure 7b. However, the dewatering prediction for block cave by using two models were quite different – 800 L/s and 500 L/s.

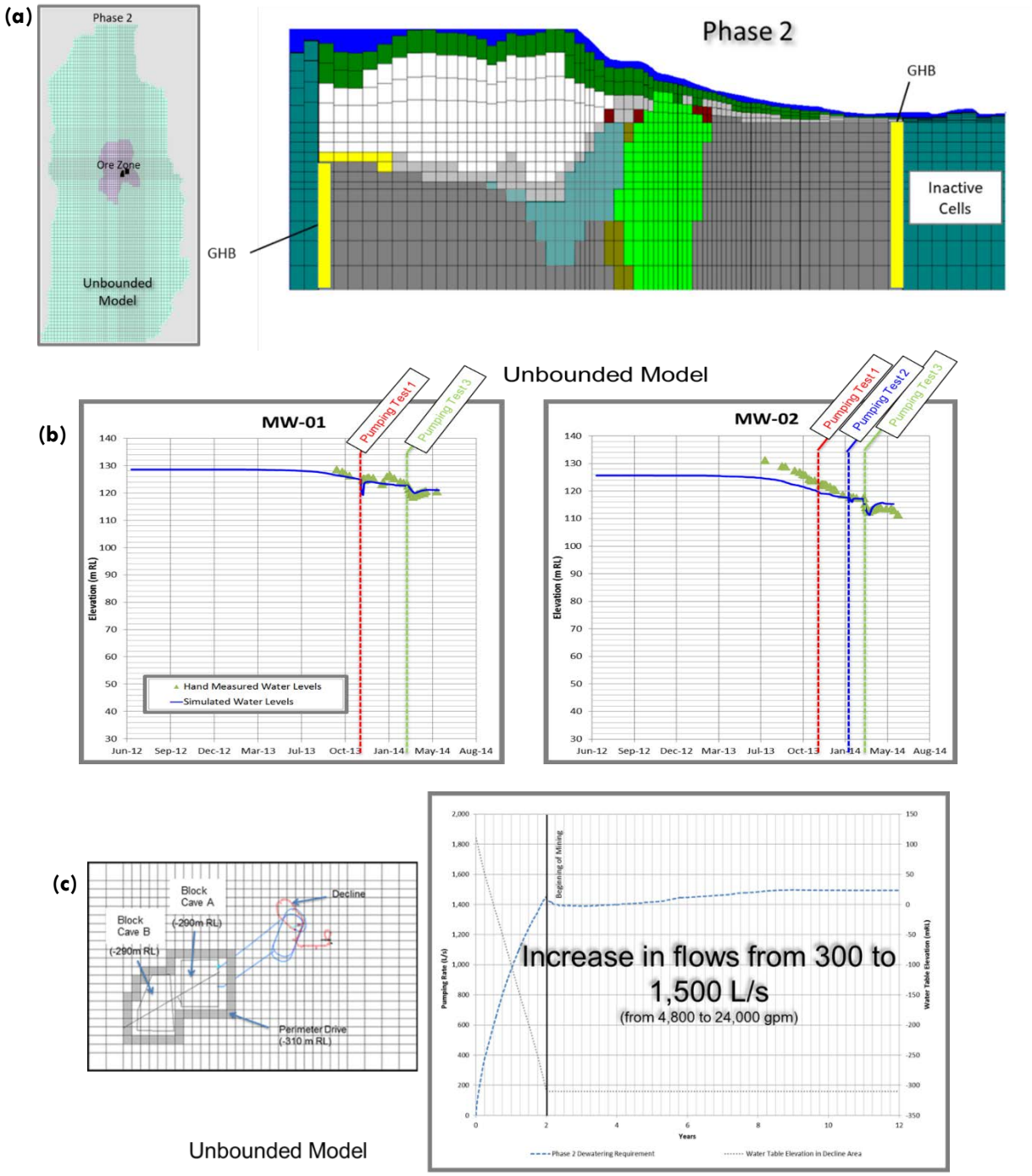


Figure 5: Phase 2 model setup (a), calibration (b), and prediction (c) used for block cave pre-feasibility study

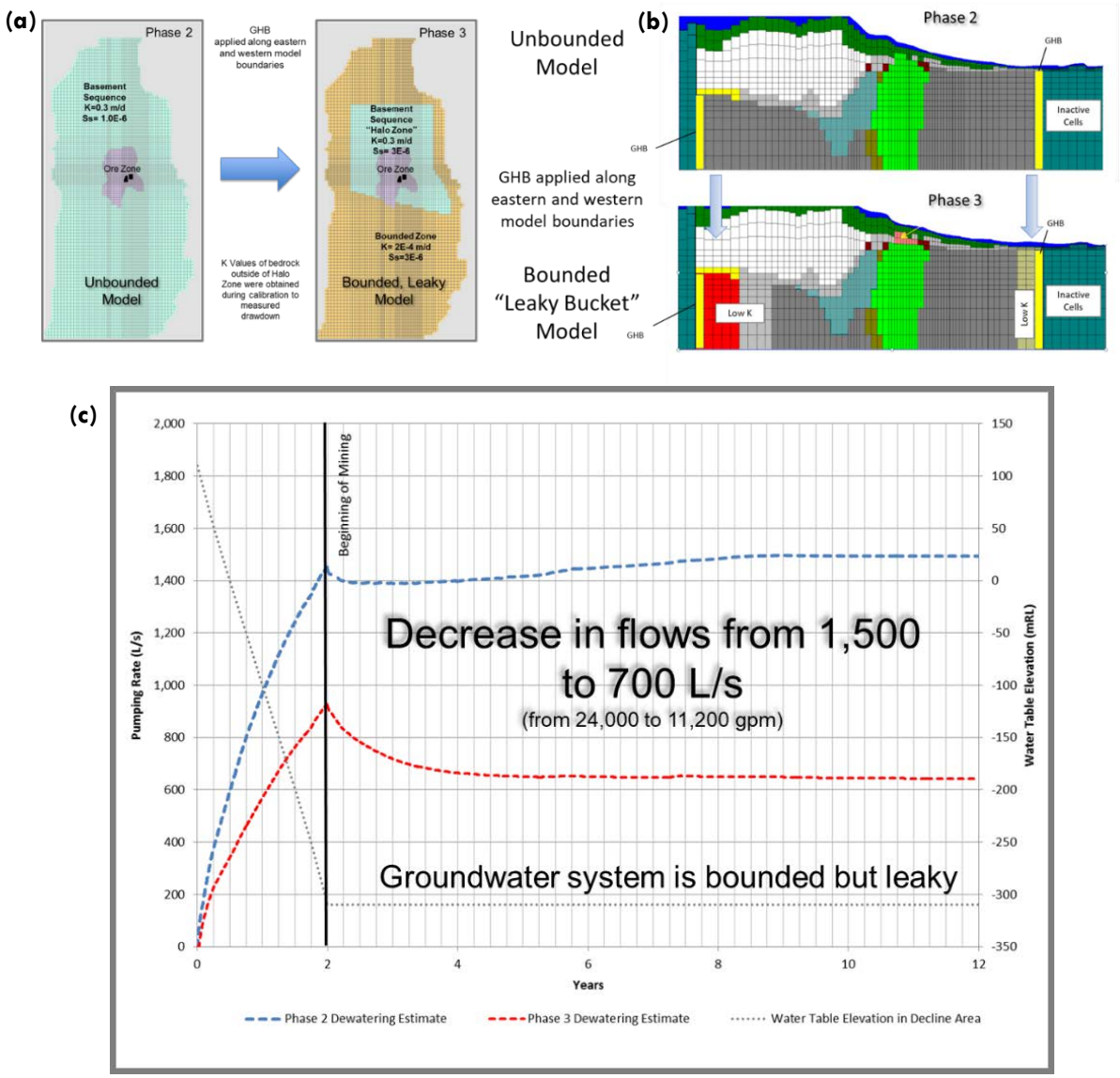


Figure 6: Phase 3 changes in model setup (a), model calibration (b), and prediction (c) used for block cave dewatering

Phase 5

Considering the majority of the dewatering equipment was taken offline, the pumping from the decline decreased to approximately 200 L/s after 320 days of active dewatering. Subsequently, discharge rates averaged between 120 and 140 L/s until completion of one year of total dewatering. The water in the deep system started to recover consistently with the reduction in the dewatering rates. At this time, it was apparent that an additional source of water, other than the groundwater storage, was contributing to the recovery of the groundwater system. The conceptual model was updated considering a "Leaky Bucket" model consisting of a high-K fractured rock bounded at an intermediate distance by low-K basaltic rocks (gradational decreasing away from ore body) and graben low-K fault to the south barriers and receiving

limited vertical recharge from the overlying andesite aquifer (Figure 8a).

The new transient calibration (Figure 8b) indicated that the model:

- Reproduces decreasing water levels in the basement to elevations of 50 to 70 mamsl and reasonably matches the slopes of the measured drawdown.
- Simulates observed recovery in groundwater levels when the decline dewatering rates significantly dropped from 250 L/s to 125 L/s – 135 L/s.
- Simulates no changes in water table within the cover groundwater system, which is consistent with measured data.
- Simulates 40 m and 50 m of drawdown reaching the western and eastern model boundaries, respectively, and no drawdown at the northern and the southern model boundaries simulated as no-flow at the end of transient calibration.

The predicted simulation shows an increment in the total dewatering rate from the proposed open pit up to 940 L/s (Figure 8c). Dewatering for Phase 5 was simulated by using 15 pumping wells installed both within Cover (11 wells) and Basalt Basement (4 wells). Active dewatering from Basalt Basement and passive inflow from the Cover were considered during Phases 3 and 4 for the block cave scenario described above.

Model Verification (Phase 6)

Once the pumping equipment was shut down after one year of operations, the water levels started to recover and their changes were recorded for about 250 days. The last conceptual and numerical groundwater models (used for Phase 5 and representing the "Leaky Bucket") were verified using the recovery data. The model could simulate the measured recovery trend in the deep groundwater system, as shown in Figure 9.

Conclusions

During five phases of data collection and model calibration, the predicted dewatering rates ranged from 300 to 1,500 L/s (as shown in Figure 10 and Table 1). Only after applying a large stress to the groundwater system and observing water level changes during the process of groundwater recovery could reliable conceptual and numerical models (Phase 5) be revised to arrive at the most defendable predicted dewatering rates (up to 940 L/s).

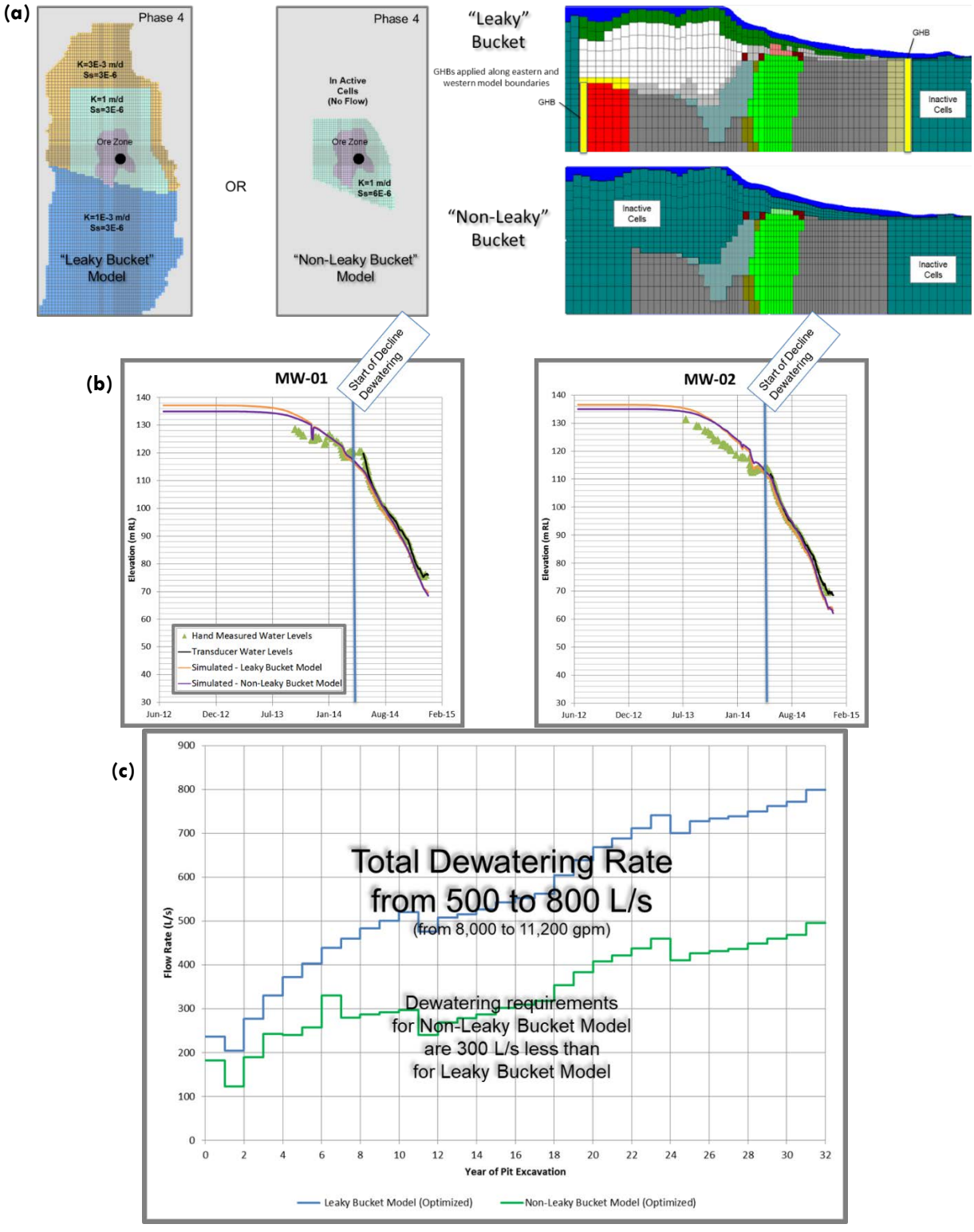


Figure 7: Phase 4 model setup (a), calibration (b), and prediction (c) used for block cave dewatering

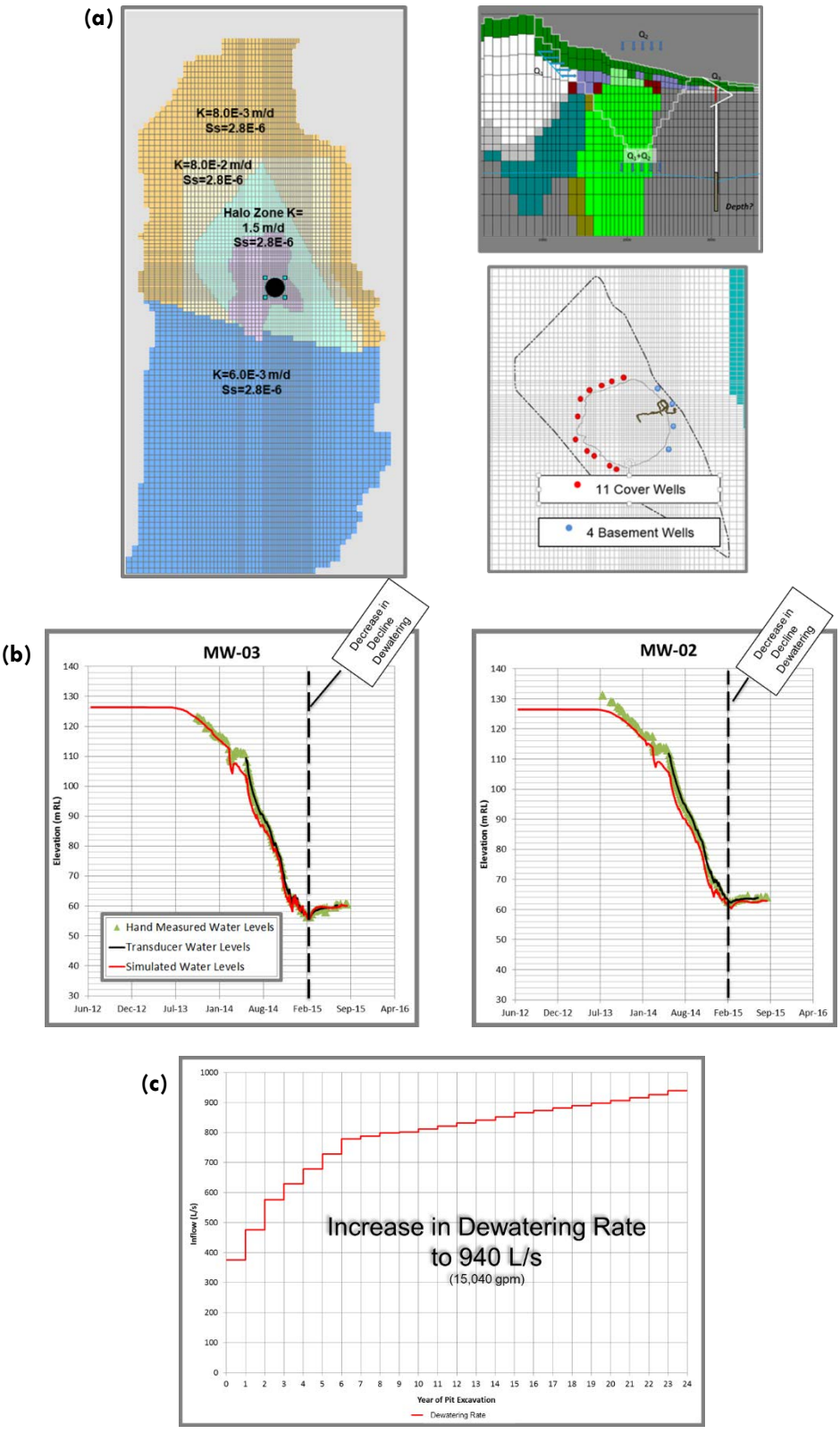


Figure 8: Phase 5 model setup (a), calibration (b), and prediction (c) used for open pit feasibility study

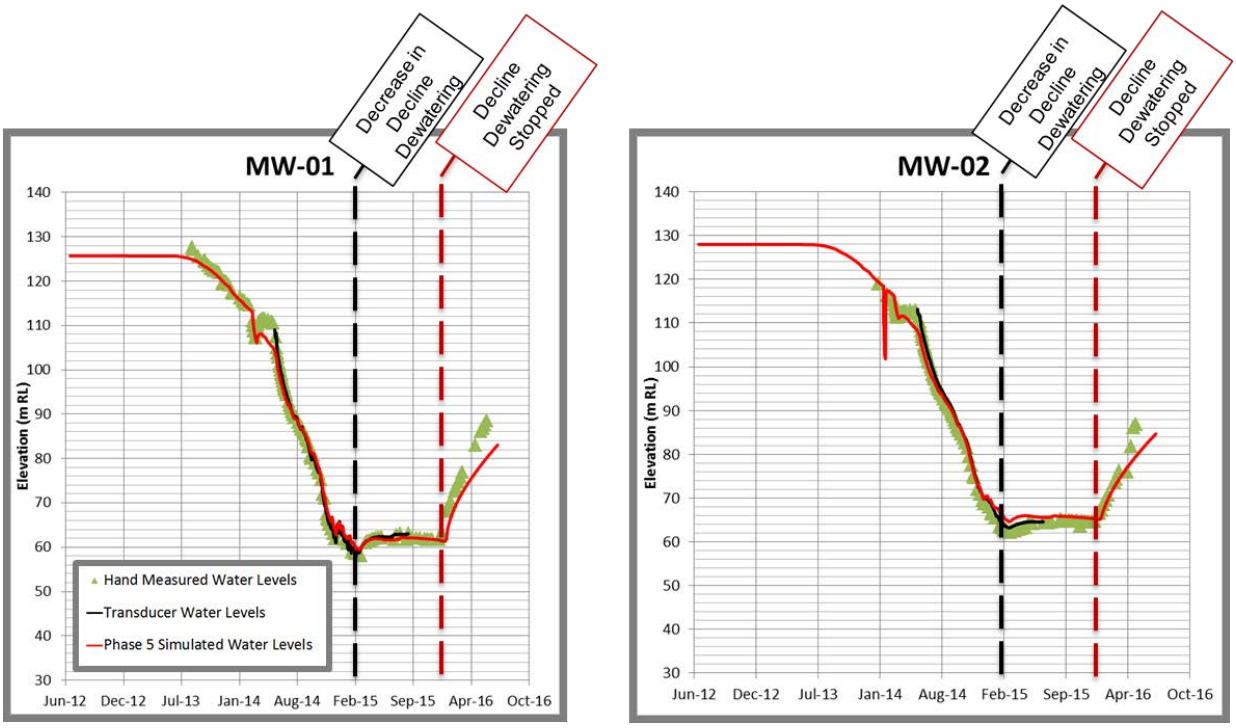


Figure 9: Phase 6 model verification to groundwater recovery

The results of the completed study allowed the authors to draw conclusions as follows:

- Dewatering predictions significantly depend on the hydrogeological role of lateral boundaries of the deep groundwater system and vertical recharge from the shallow groundwater system.
- These two factors cannot be precisely evaluated during short to intermediate-term hydraulic testing in the case of a highly permeable “bucket” groundwater system and horizontal “leaky" conditions.
- Long-term test data provides superior evidence to support conceptual models and defensible mine dewatering predictions.
- Groundwater level recovery data enables researchers to improve/confirm model predictability in the case of “horizontally leaky bucket” groundwater system.
- Water level monitoring data outside of a highly permeable “bucket” can significantly help in defining horizontal “leaky/non-leaky” conditions, but are not usually available during the initial stage of the mining project.

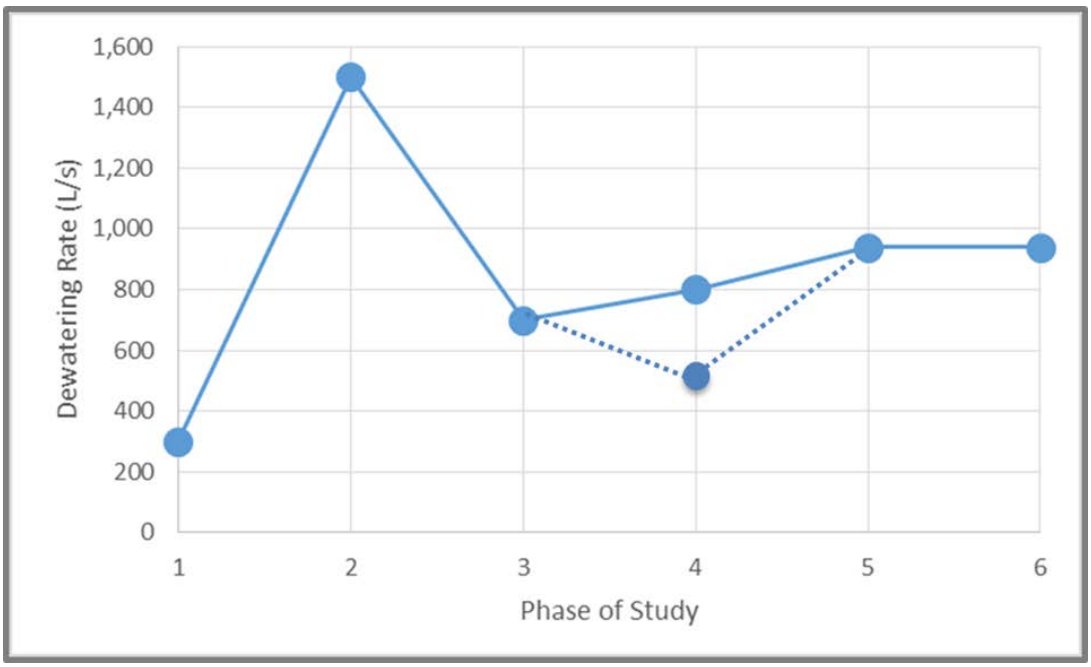


Figure 10: Predicted dewatering rates vs. phase of study

Table 1: Summary of conceptual models and predicted dewatering rates

Phase of Study	Days Since Active Mine Dewatering Began	Predicted Dewatering Rate (L/s)	Conceptual Model	Type of Dewatering
1	0	300	Unbounded, Low K	Passive inflow to two block caves
2	10	1,500	Unbounded, High K	Active dewatering of block cave
3	120	700	"Leaky Bucket"	Active dewatering of block cave
4	200	500 to 800	"Leaky Bucket"/Bounded	Active dewatering of block cave
5	365	940	"Leaky Bucket"	Active dewatering of open pit
6	730	940		

Proceedings of Mine Water Solutions 2018
June 12–15, 2018, Vancouver, Canada
Published by the University of British Columbia, 2018

Base Mine Lake: The First End-Pit Lake for the Alberta Oil Sands

Dallas Heisler, Syncrude Canada Ltd, Canada
Carla Wytrykush, Syncrude Canada Ltd, Canada

Introduction

Alberta's oil sands are among the largest petroleum deposits in the world, containing 300 billion barrels of proven reserves. Extraction of bitumen from surface mined oil sands generates significant quantities of fluid fine tailings (FFT) and oil sands process water (OSPW). Managing the inventory is critical to the sustainability of the surface mineable oil sands industry, and has been subject to escalating focus by industry, regulators and stakeholders. One technology for managing both FFT and OSPW involves placing these materials into an end pit lake, which is an area where overburden and oil sand has been removed and is then filled with fluids prior to closure. An end pit lake contains water (from the process of oil sands extraction or freshwater, or both) and may or may not contain FFT, treated fluid tailings, or other solids (for example, coarse tailings sand, or overburden). More than 20 years of research, small-scale piloting in the Syncrude Test Ponds, and input from external experts has been used to design Syncrude's Base Mine Lake (BML).

BML is the first commercial-scale demonstration of the end pit lake technology in the oil sands industry, initially containing 186 Mm^3 of FFT and 32 Mm^3 of OSPW in a 50 m deep, 7.7 km^2 mine pit. BML is located in the former West In-Pit of the Syncrude Mildred Lake (Base Lease) operation. It consists of a mined-out oil sands pit filled with fluid fine tailings (silt, clay, process-affected water, and residual bitumen) that sits below a combination of OSPW and fresh water. This pit lake configuration is often referred to as water capped tailings technology (WCTT). Based on previous research and modelling, the prediction for WCTT is that with time, end pit lake water quality will improve and the FFT (or other tailings) will remain sequestered below the water cap.

Infrastructure has been installed to pump water in from Beaver Creek Reservoir and pump water out to the tailings recycle water system until a more substantial upstream surface watershed is reclaimed and connected to BML, and outflow is established into the Athabasca River. This process will dilute the BML water cap over time.

BML Monitoring and Research program

The objective of the BML Monitoring and Research Program (MRP) is to validate WCTT for a FFT filled lake. The outcomes from the BML MRP will be useful for other pit lakes that may contain other tailings materials, including treated tailings. At the same time, the program establishes a baseline of biophysical data to assess the state of the lake at certification, including water quality and other lake processes. The monitoring program is designed to track trends in the lake both seasonally and annually, and to measure these trends against some key performance metrics. The research program focuses on key scientific questions designed to elucidate the mechanisms and processes that govern the current state of BML, and explain changes detected by the monitoring program. In other words, the monitoring program tracks the trends in the lake through time, and the research program investigates why those changes are occurring.

Syncrude recognizes three categories of monitoring: 1) Compliance 2) Adaptive Management/ Validation and 3) Continuous improvement research and monitoring. Components of the BML Monitoring Program fit into one or more of these categories. Each is described below.

1. *Compliance Monitoring*

   Compliance monitoring is data collection used to support compliance with regulatory approvals or other policy requirements (including certification assessments).

2. *Adaptive Management/Validation Monitoring*

   This refers to data collection to support plan stewardship and adaptive management actions, and is critical to support technology validation. It also tracks rates of progress towards certification criteria and permits early intervention when there are performance deviations.

3. *Continuous Improvement Research and Monitoring*

   Continuous improvement research and monitoring involves a combination of monitoring, assessments, and focused studies. This includes the lessons learned from results of compliance monitoring, plan stewardship, and adaptive management monitoring.

These three components are integrated, such that lessons learned from research would inform future monitoring programs, as well as support validation and corrective/preventive measures processes. Trends and information obtained from the compliance-monitoring program will guide priorities for the research program.

This integrated BML MRP supports the adaptive management of BML performance to ensure attainment of certification criteria. The BML MRP also provides knowledge and guidance valuable to the integration of other pit lakes in the region. The MRP is supported as a COSIA Joint Industry Project as

part of the Water Environmental Priority Area. Industry partners that contribute to the BML MRP include Suncor Energy Inc., Canadian Natural Resources Limited, and Imperial Oil.

Monitoring Program

The specific objective of the BML Monitoring Program is to provide information to support the validation of WCTT as a viable tailings management and reclamation option. In the early stages, the BML Monitoring program will demonstrate that fluid fine tailings are sequestered and that the water quality in the lake is improving. The monitoring program is designed to do this by tracking the physical, chemical, and biological changes in BML. The program captures these changes both temporally and spatially, and eventually in the context of regional climate cycles. The monitoring program supports regulatory compliance, but also informs adaptive management of BML. The physical, chemical, and biological components of the program are summarized in the following table:

Table 1: BML Monitoring program components

Physical	Chemical	Biological
FFT Assessment	Water Balance Assessment	Aquatic Biology Assessment
Shoreline Erosion Assessment	Surface Water Quality Assessment	
Physical Limnology Assessment	Groundwater Assessment	
Meteorological Monitoring		

Research Program

The BML Research Program follows Syncrude's Instrumented Watershed approach. The program uses a multi-university, multi- and inter- disciplinary approach that focuses on the analysis and interpretation of monitoring data, hypothesis-driven research activities, and integration and collaboration among and between research programs. Research results are integrated with monitoring results on an ongoing basis, with the ultimate goal of identification and quantification of the processes and properties in BML that are responsible for the trends observed in the Monitoring Program. The various components comprising the BML Monitoring and Research Program are closely linked.

The current focus of the Research Program is to support the demonstration of the WCTT. The program also provides supporting information about key processes fundamental to the progression of BML towards being a functional component of the closure landscape. The current research programs were focused on key parameters influencing early BML development.

The program has two overarching key themes. The first theme is validating the WCTT. Several research programs will determine the potential fluxes from the FFT to the water column, including

chemical, geochemical, mineral, gases and heat. Physical, biological and chemical mechanisms will be investigated. Further details of this research are provided below.

The second key (and related) theme relates to the oxygen dynamics in the lake. The programs focus on understanding the oxygen balance and process of oxygen consumption (e.g. metanotrophy) and oxygen production (photosynthesis). The research programs, associated researchers, and participating universities are summarized in Table 2. A list of peer-reviewed publications and theses from the research programs is provided in the Appendix to this paper.

Conclusion

This integrated BML MRP supports the adaptive management of BML performance to ensure attainment of certification criteria. The BML MRP also provides knowledge and guidance valuable to the integration of other pit lakes in the region. The MRP is supported as a COSIA Joint Industry Project (JIP) as part of the Water Environmental Priority Area (WEPA). Industry partners that contribute to the BML MRP include Suncor Energy Inc., Canadian Natural Resources Limited, and Imperial Oil.

Table 2: BML research programs

Research Component	University	Researchers (PIs)
Physical limnology of BML and the potential for meromixis	University of British Columbia	Greg Lawrence/Ted Tedford/Roger Pieters
Characterization of controls on mass loading to an oil sands end pit lake	University of Saskatchewan	Lee Barbour/ Matt Lindsay
Laboratory studies investigating chemical flux across tailings-cap water zones, simulating an end pit lake in the Athabasca oil sands region	University of Alberta	Ania Ulrich/Morris Flynn/Tariq Siddique
Field investigation of BML water cap oxygen concentrations, consumption rates and key BOD/COD constituents affecting oxic zone development.	University of Toronto/McMaster University	Lesley Warren/Greg Slater
Microbial communities and methane oxidation processes in Base Mine Lake	University of Calgary	Peter Dunfield
Understanding air-water exchanges and the long-term hydrological viability of Base Mine Lake (new project, will be initiated in 2017, details to be reported)	McMaster University/Carleton University	Sean Carey/Elyn Humphreys

Appendix

Peer-reviewed Publications Produced by BML Research Programs

Research Project: University
Physical limnology of BML and the potential for meromixis: University of British Columbia
Publications: Lawrence, G.A., Tedford E.A, and Pieters, R. 2016. Suspended solids in an end pit lake: potential mixing mechanisms, *Can. J. Civ. Eng.* 43:211–217
Characterization of controls on mass loading to an oil sands end pit lake: University of Saskatchewan
Publications: Dompierre, K.A., and Barbour, S.L. 2016. Characterization of physical mass transport through oil sands fluid fine tailings in and end pit lake: a multi-tracer study, *Journal of Contaminant Hydrology* 189:12–26. Dompierre, K.A., Lindsay, M.B.J., Cruz-Hernández, P., and Halferdahl, G.M. 2016. Initial geochemical characteristics of fluid fine tailings in an oil sands end pit lake, *Sci Tot Env* 556:196–206. Dompierre, K. and Barbour, S.L. 2017. Thermal properties of oil sands fluid fine tailings: Laboratory and in-situ testing methods, *Canadian Geotechnical Journal*, 2017, 54(3): 428–440. Dompierre, K., Barbour, L., North, R.L., Carey, S.K. and Lindsay, M.B. 2017. Chemical mass transport between fluid fine tailings and the overlying water cover of an oil sands end pit lake, submitted to: *Water Resources Res.,* Nov. 11. **Theses:** Dompierre, K. 2016. Controls on mass and thermal loading to an oil sands end pit lake from underlying fluid fine tailings. Ph.D. Thesis, University of Saskatchewan, December, 2016.
Microbial communities and methane oxidation processes in Base Mine Lake: University of Calgary
Publications: Aguilar, M., Richardson, E., Tan, B., Walker, G., Dunfield, P.F., Bass, D., Nesbø, C., Foght, J. and Dacks, J.B. 2016. Next-generation sequencing assessment of eukaryotic diversity in oil sands tailings ponds sediments and surface water, *J. Eukaryotic Microbiol.* 63:732–743. Rochman, F.F., Sheremet, A., Tamas, I., Saidi-Mehrabad, A., Kim, J.J., Dong, X., Sensen, C.W., Gieg, L.M. and Dunfield, P.F. Benzene and naphthalene degrading bacterial communities in an oilsands tailings pond, *Frontiers in Microbiology* 8: 1845. doi: 10.3389/fmicb.2017.01845. Rochman, F.F., Kim, J.J., Rijpstra, W.I.C., Sinninghe Damsté, J.S., Schumann, P. and Dunfield, P.F. *Oleiharenicola alkalitolerans gen. nov., sp. nov.,* a new member of the *Verrucomicrobia* isolated from an oilsands tailings pond. Accepted pending minor revisions, *International Journal of Systematic and Evolutionary Microbiology*. Saidi-Mehrabad, A., Kits, D.K., Kim, J.J., Tamas, I., Schumann, P., Khadka, R., Rijpstra, W.I.C., Sinninghe Damsté, J.S. and Dunfield, P.F. *Methylomicrobium oleiharenae* sp. nov., an aerobic methanotroph isolated from an oil sands tailings pond in Canada. Submitted to *International Journal of Systematic and Evolutionary Microbiology*. **Theses:** Haupt, Evan. 2016. Methanotrophic Bacteria and Biogeochemical Cycling in an Oil Sands End Pit Lake. MSc Thesis. University of Calgary. Rochman, Fauziah. 2016. Aerobic hydrocarbon-degrading microbial communities in oilsands tailings ponds. PhD Thesis. University of Calgary.
Field investigation of BML water cap oxygen concentrations, consumption rates and key BOD/COD constituents affecting oxic zone development: University of Toronto, McMaster University
Publications: Risacher, F.F., Morris, P.K., Arriaga, D., Goad, C., Colenbrander Nelson, T., Slater, G.F. and Warren, L.A. 2018. The interplay of methane and ammonia as key oxygen consuming constituents in early stage development of Base

Mine Lake, the first demonstration Oil Sands pit lake. Accepted by *Applied Geochemistry* Jan 18, 2018).

Bowman, D.T., McCarry, B.E., Warren, L.A. and Slater, G.F. 2017. Profiling of individual naphthenic acids at a composite tailings reclamation fen by comprehensive two-dimensional gas chromatography mass spectrometry. *Environmental Science & Technology*. (Revisions requested)

D.T. Bowman, Jobst, K.J., Ortiz, X., Reiner, E.J., Warren, L.A., McCarry, B.E. and Slater, G.F. 2017. Improved coverage of naphthenic acid fraction compounds by comprehensive two-dimensional gas chromatography coupled to a high resolution mass spectrometer, *Journal of Chromatography A*. 10.1016/j.chroma.2017.07.017

Theses:

Risacher, F.F. 2017. MSc. Biogeochemical development of the first oil sands pilot end pit lake. McMaster University.

Morris, P.K. 2017. MSc. The competitive impacts of methanotrophy and nitrification on oxygen status within Base Mine Lake. McMaster University.

Goad, C. 2017. MSc. Methane biogeochemical cycling over seasonal and annual scales in an oil sands tailings end pit lake. McMaster University.

Bowman, D. 2017. PhD. Chemical Fingerprinting of Naphthenic Acids by comprehensive two dimensional gas chromatography mass spectrometry at reclamation sites in the Alberta Oil Sands PhD. McMaster University.

Laboratory studies investigating chemical flux across tailings-cap water zones, simulating an end pit lake in the Athabasca oil sands region: University of Alberta

Publications:

Poon, H.Y., Brandon, J.T., Yu, X. and Ulrich, A. 2017. Turbidity mitigation in an oil sands pit lake through pH reduction and fresh water addition. Submitted to *Journal of Environmental Engineering* in November 17, 2017. Submission number: EMID:35369e758647869f.

Proceedings of Mine Water Solutions 2018
June 12–15, 2018, Vancouver, Canada
Published by the University of British Columbia, 2018

Use of Adaptive Management Planning in Support of Environmental Monitoring and Permitting Process

Sheldon Smith, Stantec Consulting Ltd., Canada
Michelle Fraser, Stantec Consulting Ltd., Canada
Walter Sencza, Newmont Canada Corporation, Canada
Stephen Lines, Greenstone Gold Mines, Canada

Abstract

An adaptive management plan (AMP) is an iterative decision-making process that includes assessing the problem, designing a management plan, implementing the plan and monitoring, followed by evaluating and adjusting the plan based on the results. Involving the use of an AMP early in the permitting process allows for the continuous re-evaluation of the monitoring program throughout the regulatory process and all phases of mine life in an effort to optimize the program by allocating resources to areas that are most informative.

In mining, it often takes time for environmental effects to be fully realized. During this time, scientific knowledge and economic conditions change and technical solutions that might not have been economically or scientifically feasible at the time of the Environmental Assessment may become practicable. Because of the uncertainties with changing economics and scientific knowledge, defining the triggers that require additional investigation and the decision-making process associated with trigger exceedances is critical for the protection of the environment. Subsequently, adaptive management planning can be used to determine the most effective contingency measures available at the time.

This paper will explain what an AMP is and how it can be used to provide flexible decision-making in the face of uncertainties. It will present the use of the AMP over nearly four decades at the Newmont Golden Giant Mine and how it was used to adapt to changing phases of mine life (operation to closure), emerging issues, and to mitigate potential environmental effects from dam seepage. It will highlight the content of a modern day AMP through examples of the Greenstone Gold Mines Hardrock Project.

Introduction

Over the past decades, the advancement of technology has allowed the extraction of commodities from lower-grade ore, resulting in larger mines and the redevelopment of historical mines. As the size and

complexities of these projects increase, assessing and permitting new mine sites is becoming more laborious to address. Adaptive management has proven to be a useful tool to address uncertainty, especially for sites where multiple potential receptors are involved.

An adaptive management plan consists of six steps: assessing the problem, designing a management plan, implementing the plan and monitoring, followed by evaluating and adjusting the plan based on the results (Figure 1). The adaptive portion of the adaptive management plan is taking what has been learned to date about the system and adapting the monitoring program accordingly to further reduce uncertainties and address knowledge gaps.

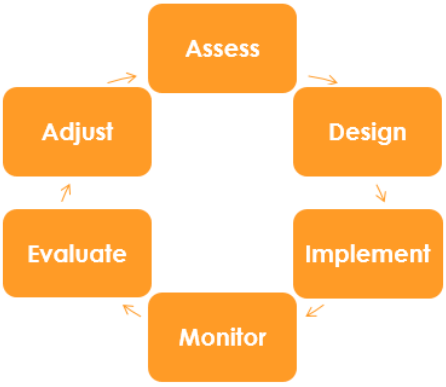


Figure 1: Adaptive management cycle

There are many benefits to adaptive management planning. The adaptive management cycle improves the extent of knowledge and understanding of key environmental indicators and action thresholds. Through this knowledge gained, the monitoring program can continuously be improved, allowing for the removal of some aspects that are no longer required or no longer providing added benefit to the program. Conversely, it is possible that a mitigation measure may not function as intended, and an adaptive management plan allows for the development of new mitigation measures in a timely manner. Adaptive management plans provide a forum for early stakeholder engagement, and public and/or stakeholder concerns about specific issues can be reduced through a commitment to an adaptive management approach.

The first step in an adaptive management plan is assessing potential for impacts from a project and the associated receptors. In the context of the life cycle of a mine, the initial knowledge is gained through baseline studies and an environmental effects assessment. Subsequently a monitoring program is developed to assess the potential impacts throughout the life of a project, as well as to confirm that implemented mitigation measures are effective. In order to develop an effective monitoring program, the key attributes that have the potential to directly impact the environment need to be clearly defined.

The establishment of impact triggers based on key ecosystem attributes, with the objective to sustain and protect the environmental conditions and to assess potential impacts resulting from the project, is a main component of an adaptive management plan. Triggers are intended to be used to manage potential impacts before they become serious.

The level of complexity of the resulting monitoring program and associated triggers will vary based on the degree of uncertainty and associated risk. If little information is known, then the monitoring program will likely be more detailed, complex, and costly, in order to mitigate the uncertainty and associated risk. As additional data is collected and knowledge gained, the complexity of the program may be reduced and mitigation measures refined as associated risk is reduced. An experienced consultant can provide good value and cost savings to a project with a well thought-out and executed field program, limiting the number of iterations needed to reach a conclusion through the adaptive management process.

This paper discusses the use of an adaptive management plan as it relates to mine water management. Two case studies are presented, the Newmont Golden Giant Mine and the Greenstone Gold Mines Hardrock Project. An adaptive management plan was used at the Newmont Golden Giant Mine to adapt to changing phases of mine life (operation to closure), emerging issues, and to mitigate potential environmental effects. The considerations for developing a modern-day AMP are highlighted through examples of the Greenstone Gold Mines Hardrock Project.

Newmont Golden Giant Mine

Adaptive management has been used at the Newmont Golden Giant Mine for over four decades. The Golden Giant mine is located in the Hemlo mining camp area, approximately 40 km west of Marathon, Ontario. The Golden Giant Mine started construction in 1983 and operation in 1985. It continued operation until 2006, primarily as an underground operation, mining over 6.7 million ounces of gold at a nominal production rate of 3,000 metric tonnes/day, with 15.3 million metric tonnes of tailings deposited into the Interlake Tailings Facility (ITF) with a crest height of 349.0 metres above sea level (masl). Noranda Mines Ltd was the original mine developer, and the mine was eventually acquired by Newmont in 2001.

The ITF started with conceptual designs in 1983 and was developed to have 4 phases with a capacity to hold 17 million metric tonnes of sloped tailings with a final tailings dam crest elevation of 351 masl. The ITF was ultimately built to 349.0 masl (but approved for 350.5 masl) with a flat tailings deposition plan applied in the final years of operation to sustain a water cover strategy for the long-term closure design. The ITF was originally proposed to have 4 dams as shown in Figure 2 (41being the main dam on the east side of ITF; 42 to the south, and dams 43 and 44 to the west). The ITF has a wet cover with at least 0.5 metres of water depth over 95% of the tailings deposited. Dam seepage was investigated through

geotechnical and hydrogeological investigations dating back to 1983. Original ITF designs included seepage mitigation features such as seepage interception ditches with downstream grout curtain, injection grouting into bedrock along dam alignments, and the use of a polymeric liner on the upstream face of the dams that was anchored/sealed to a concrete wall keyed into competent bedrock over the grouted dam alignments. As the main dam (dam 41) would be much higher than the 3 other dams, seepage collection was included in its design from the outset; however, seepage collection was not initially incorporated into the dam 42, dam 43, or dam 44 designs.

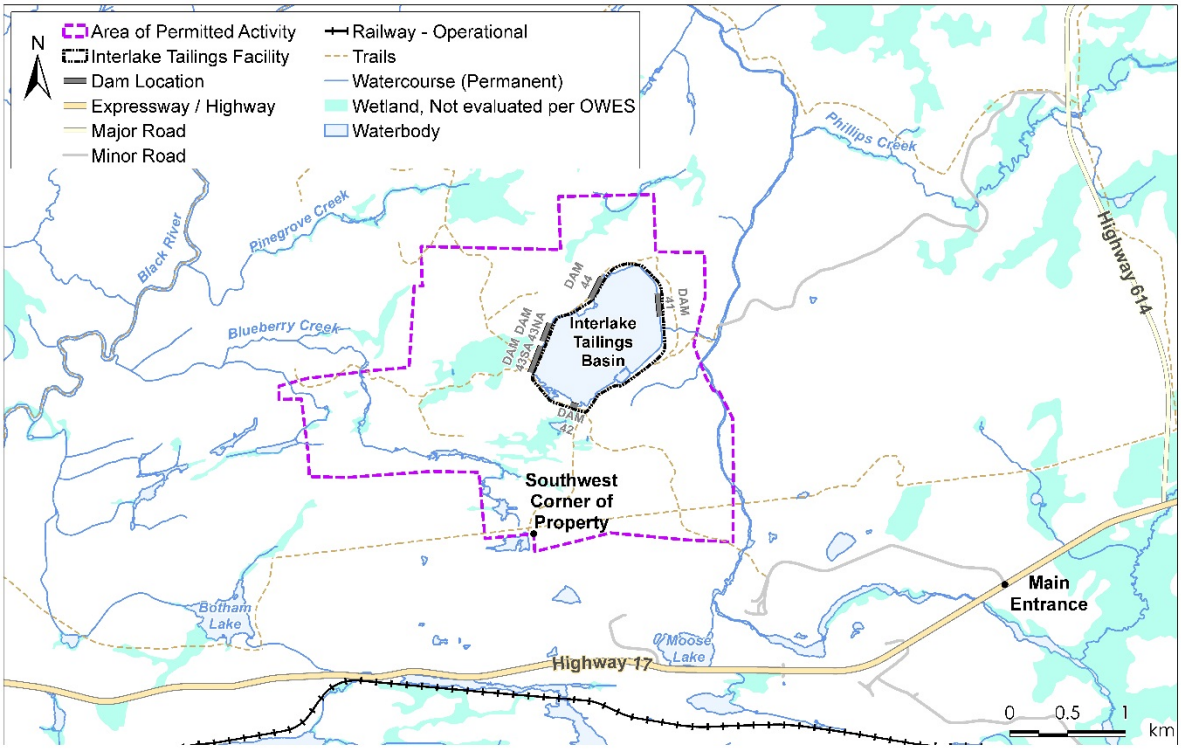


Figure 2: Newmont Interlake tailings facility site plan

As early as 1983, and well before the advent of the Ontario Mine Closure Regulations (O.Reg. 114/91 in 1991 and O.Reg. 240/00 in 2000), the Golden Giant mine was required to conduct an environmental impact assessment to consider the potential effects of ITF seepage to surrounding water bodies. The ITF is surrounded by Cedar Creek to the east and the Black River and its tributaries Pinegrove Creek and Blueberry Creeks to the west (Figure 2). These surrounding water bodies had excellent water quality and met Ontario Ministry of the Environment and Climate Change (MOECC) Policy 1 receiving water conditions (MOECC 2016a/b). Policy 1 receivers have water quality meeting or better than the Ontario MOECC Provincial Water Quality Objectives (PWQO) (MOECC 1994; MOECC 2016b) and are not allowed to be degraded beyond these standards. Pinegrove and Blueberry Creeks have

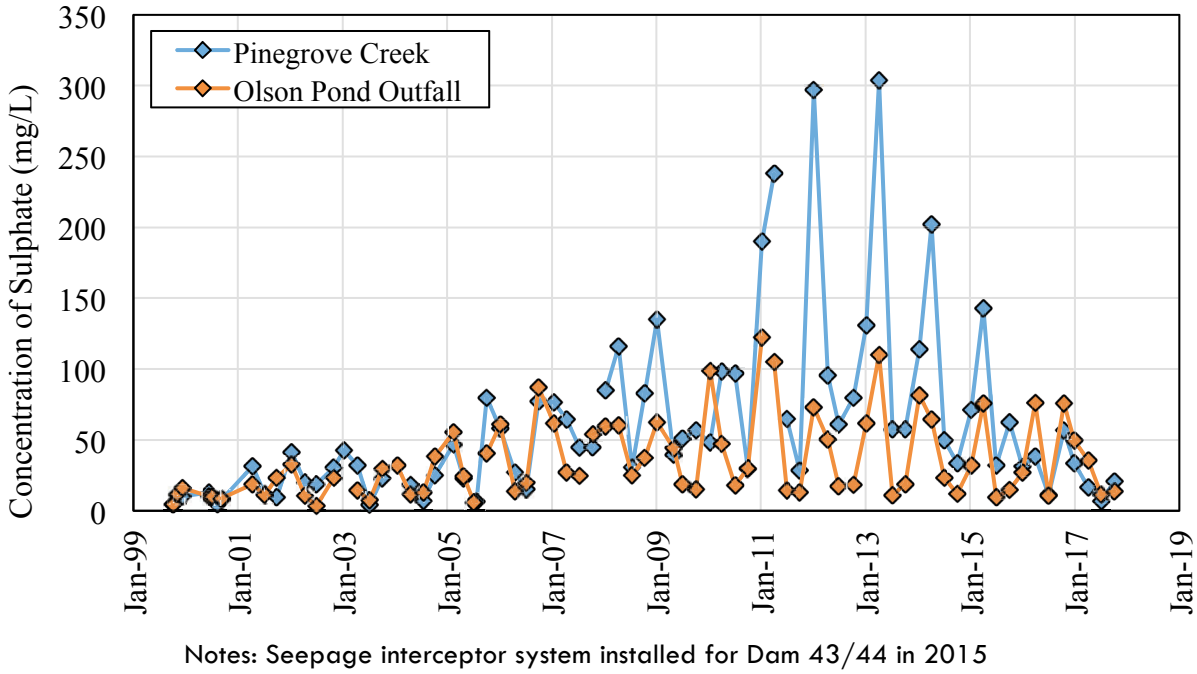
drainage areas of 5 km^2 and 6.65 km^2 before discharging into the Black River, and are 280 m and 520 m distant from Dam 43 and Dam 44 to their uppermost intermittent channel (Figure 2).

Seepage assessment studies were undertaken in the 1980s and 1990s to investigate the potential for ITF seepages to reach Pinegrove and Blueberry Creeks that would degrade water quality conditions (Geocon, 1984; AGRA, 1999). A network of groundwater monitoring wells and surface water sampling stations were established. The parameters of potential concern (PoPCs) were determined to be iron, lead, arsenic, cyanide, and molybdenum. Iron was considered elevated in surface water receivers due to persistent elevated suspended solids. Elevated concentrations of iron in groundwater samples were attributed to high iron content in monitoring well packing sands. Iron in ITF seepage was not assessed to have high potential to increase receiving water iron concentrations due to potential oxidizing conditions in the groundwater flow path from the ITF to the headwater channel reaches. Lead, being the most strongly adsorbed metal to soils in the Irving-Williams stability series (Irving and Williams, 1953), was thought to highly attenuate along the groundwater flow path. Arsenic in ITF seepage was thought to be oxidized over the groundwater flow path and upon surface discharge where oxidation would result in precipitation and deposition. Cyanide, a gold leaching reagent, was thought to be degraded through UV and oxidization breakdown along with bacterial consumption in the ITF pond during warm water conditions, with any cyanide bypassing the dam seepage reduction infrastructure being highly attenuated in down-gradient soils. Molybdenum was assessed as the only parameter of potential concern with potential to reach Pinegrove and Blueberry Creeks; however, due to soil attenuation and oxidation potential over the groundwater seepage flow path the risk of increasing molybdenum concentrations in receiving waters was considered low. As a result of these assessments, further seepage mitigation and/or collection for Dams 42/43/44 was not undertaken in the 1980s and 1990s.

However, the ITF effluent treatment system discharge permit (Certificate of Approval, now referred to as Environmental Compliance Approval) and the Closure Plan for the ITF retained requirements for Newmont to monitor down-gradient seepage in groundwater wells and receiving waters. The permit and closure plan also indicated that if water quality monitoring demonstrated an increasing trend in concentrations of PoPCs toward the PWQO, then further seepage mitigation/control would be required.

In the early 2000s, the British Columbia Ministry of the Environment (MOE) started considering development of a Provincial Water Quality Guideline (PWQG) for protection of aquatic life for sulphate. Previously, sulphate only had an aesthetic objective typical in drinking water standards or guidelines, and was thus not considered part of the PoPC group of parameters for the Golden Giant Mine. In 2013, the BC PWQG for sulphate was confirmed as 128 to 429 mg/L based on hardness (as $CaCO_3$) of 0 to 250 mg/L and determined site specifically when hardness is greater than 250 mg/L.

Newmont took a proactive approach on the potential that the Canadian Council of Ministers of the Environment (CCME) and/or the Ontario MOECC might adopt the BC MOE PWQG for sulphate, and evaluated the concentration of sulphate over time in the ITF seepage receiving waters. Figure 3 presents the concentration of sulphate in Pinegrove Creek and the Olson Pond Outfall location on Blueberry Creek.



Notes: Seepage interceptor system installed for Dam 43/44 in 2015

Figure 3: Concentration of sulphate (mg/L)

Based on historical groundwater monitoring data, Newmont had determined that tailings impacted groundwater was emanating from the ITF and migrating over time as a plume from the near- and middle-field monitoring wells, and recently into the far-field monitoring wells that are located within 300 m of Dam 43 and Dam 44 in the Blueberry Creek and Pinegrove Creek watersheds, respectively. As part of the final review of the mine Closure Plan by the Ministry of Northern Development and Mines (MNDM) on July 16 2010, the Ministry required Newmont to complete a detailed engineering study to assess mitigation alternatives and develop a preferred mitigation design to address elevated sulphate concentrations in Blueberry Creek and Pinegrove Creek.

Stantec was retained to investigate and design a sulphate seepage mitigation system (Stantec, 2012; 2013a, b, c). During the alternatives study and selection process, a number of source reduction, in-situ treatment and water collection designs were considered. The major alternatives considered were as follows:

- Increased ITF water depth;

- Tailings interface encapsulation;
- Dam grout curtain enhancement;
- External infiltration reduction;
- Permeable Reactive Barriers (PRB);
- A groundwater collection trench as an interceptor trench;
- A Horizontal Directional Drill (HDD) Collector; and,
- Vertical groundwater pumping wells.

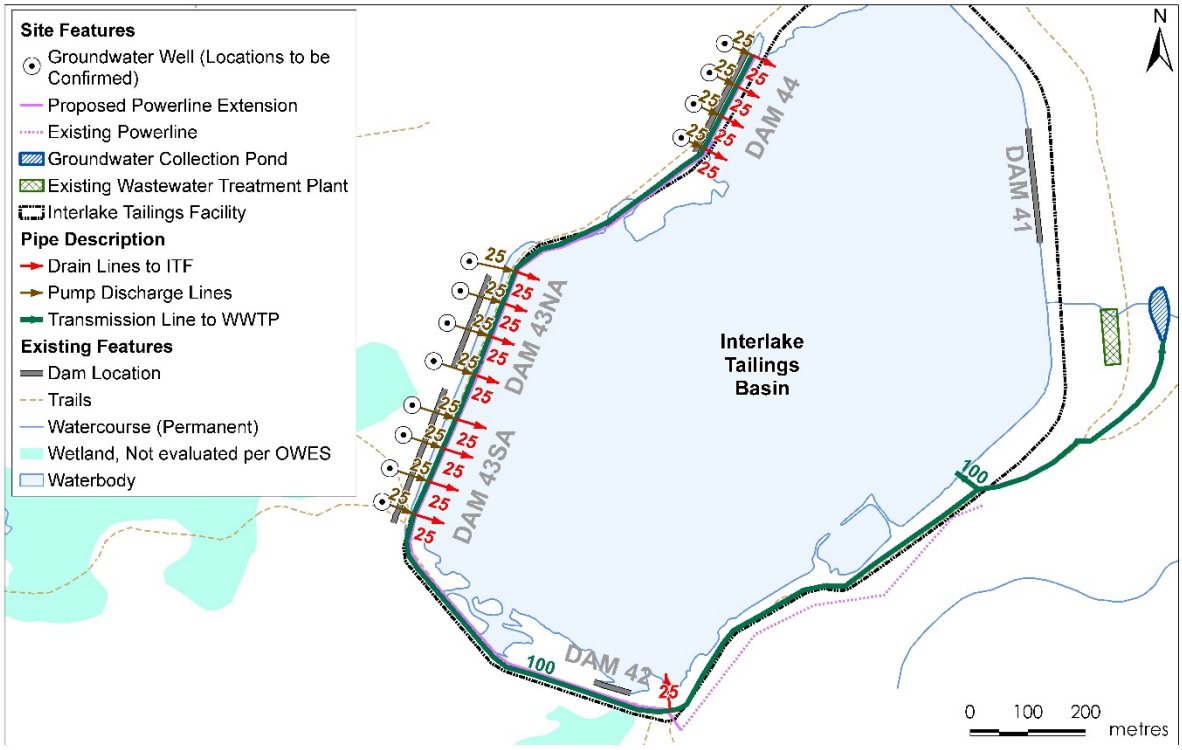


Figure 4: Interlake tailings facility interceptor well system design

The vertical groundwater pumping wells design was selected due to its technical effectiveness, constructability, reasonable operational and maintenance requirements, and cost-effectiveness. The design involved drilling groundwater interception wells down-gradient of the dam toes to collect shallow contaminated bedrock groundwater seeping from the ITF (Figure 4). The Interceptor Well System (IWS) is designed to operate at a rate that is slightly greater than the estimated ITF groundwater seepage and flow from beneath the dams to prevent migration of contaminated ITF seepage to the down-gradient surface watersheds. The collected seepage is pumped to the existing GCP (Groundwater Collection Pond) and subsequent treatment in an existing approved on site Wastewater Treatment Plant (WWTP). The IWS collected seepage is estimated to average 12 m^3/hr and can range up to 20 to 25 m^3/hr with seasonal high

groundwater conditions. The sulphate seepage mitigation target for the project was to maintain sulphate concentrations in receiving waters at less than 50 mg/L. After the seepage interceptor system was installed for Dam 43/44 in 2015, sulphate concentrations have successively declined in Blueberry and Pinegrove Creeks (Figure 3).

Adaptive Management at Golden Giant Mine

Original PoPCs and seepage predictions were generally confirmed throughout the life of mine operations and into the post-closure state of inactivity. Continued monitoring demonstrated increasing trends in sulphate concentrations. With the advent of a BC MOE Sulphate PWQG and the thought that this Guideline would eventually be adopted by CCME and Ontario MOECC, Newmont proceeded proactively (and with the agreement of Ontario Ministries) to develop a sulphate seepage mitigation plan. The key observations in this adaptive management case are:

- Meaningful and targeted monitoring must continue through and after operations as groundwater effects may take years to decades to emerge.
- The originally determined PoPCs may not always be the ultimate empirically observed PoPCs, thus it is important to monitor other parameters relevant to seepage quality characteristics.
- Sampling frequency should be adequate to characterize and filter out seasonal patterns in long-term assessment.
- Water quality trend analysis is the primary tool in confirmation of concentration change patterns.
- Definitive water quality targets/triggers in receiving waters aid in trend forecasting and determining when contingency actions should be undertaken.
- Commitment to take action based on sound science thus protecting the environment and saving the company from future downstream mitigation requirements.
- Changing regulatory parameter thresholds may cause a parameter not previously identified as a concern to emerge as a concern.

Greenstone Gold Mines Hardrock Project

Greenstone Gold Mines proposes to construct, operate, and ultimately decommission/close a new open pit gold mine known as the Hardrock Project (Project). The Project is located in north-western Ontario, approximately 275 km north-east of Thunder Bay, in the Municipality of Greenstone. The Project is situated in a rural area and partially within a historical mine site and has undergone extensive baseline studies and the submission of a provincial and federal environmental assessment (EA). A comprehensive set of fourteen (14) conceptual environmental management and monitoring plans (EMMP), which include an adaptive management framework, were submitted as part of the EA. The EMMPs will be further

defined through permitting incorporating the outcomes of both the EA and permit approvals to develop appropriate action triggers as applicable. Here we will discuss the conceptual EMMP for groundwater and considerations for further refinement under an adaptive management framework.

The first step in developing an adaptive management plan is understanding the potential effect of the Project and the associated receptors. The assessment of effects that was completed as part of the Project EA will form the basis for understanding the potential effects of the project and potential environmental receptors. The potential effect of the Project on groundwater quantity and quality is the potential for seepage from facilities such as the tailings management facility and waste rock storage areas and the change in groundwater levels and groundwater discharge as a result of dewatering and subsequent refilling of the open pit. Due to the rural location of the Project, the main receptor for a change in groundwater quantity and/or quality are the ecosystems associated with the receiving water bodies, predominantly Kenogamisis Lake.

Once the potential effect and associated receptors are defined through the EA, which in areas of historical tailings notably include positive effects related to enhanced reclamation and Project design mitigations, the key attributes that can be used to measure the effect are identified. The key attributes and associated triggers need to be measurable, interpretable, and statistically powerful for an effective adaptive management plan. For example, it is not effective to set triggers associated with concentrations that are not measurable or statistically different from seasonal variation and/or measurement accuracy. The key monitoring attributes for groundwater defined in the conceptual EMMP for the Project were groundwater levels and groundwater quality. For the EA, the PoPCs for groundwater were defined as those parameters predicted to exceed the Ontario MOECC Ontario Drinking Water Quality Standards (ODWQS) and MOECC O.Reg. 153/04 Aquatic Protection Values (APVs) at source seepage. The primary PoPC is arsenic associated with the historical tailings.

Once the key attributes are determined, triggers are set to alert for the potential of an effect before it becomes serious. One hurdle in developing triggers for an adaptive management plan is a lack of historical data to develop meaningful triggers and understand responses to natural variables. In the case of the Project, four years of groundwater level and groundwater quality data at 121 locations were captured under baseline conditions, allowing a robust understanding of seasonal variation.

Atkinson et al. (2004) suggest that a sound program acknowledges uncertainties at the beginning of the program and aims to reduce those uncertainties and any knowledge gaps while still fulfilling monitoring requirements. The Project baseline monitoring program has continued throughout the EA process, including during the post-submission regulatory review phase. This on-going data collection work, consistent with the intent of an adaptive management plan, will allow for additional data to be

collected, and evaluated prior to Project start-up to adjust the monitoring plans and associated triggers as needed, while providing effective feedback to stakeholders.

As noted, triggers are most reliably defined once the conditions of EA and permitting are known, and were not defined in the conceptual EMMP for the Project, but will be defined through the permitting process, which will include early stakeholder engagement. In the example of groundwater quality, the conceptual EMMP states that monitoring locations will be selected near the immediate source area to confirm the quality of water infiltrating the groundwater system and down-gradient of the seepage collection system. This monitoring will confirm the at-source seepage water quality and the groundwater quality discharging to the receiving environment. The monitoring locations immediately down-gradient of the Project component and seepage collection system will be used as trigger monitoring locations and considered as part of the adaptive management.

Triggers for groundwater quality require a parameter and a concentration to be defined. The parameter chosen for a trigger should be representative of both regulatory parameter thresholds and the quality of seepage from the Project. In choosing a parameter for a trigger, consideration needs to be given to mobility and background concentrations of the parameter. A parameter that is highly attenuated compared to other more mobile parameters associated with seepage from the project may not provide an early enough warning that additional investigation is warranted. A parameter that has substantial background variability may result in frequent trigger exceedances due to natural variation if the trigger is set too sensitively due to a lack of baseline data.

The triggers need to consider the predicted effect and the receiving environment of the site. Seepage concentrations from the tailings management facility and waste rock storage areas were predicted and PoPCs defined based on geochemical field bin testing and humidity cells. The receiving environment is surface water and the APVs were used in the Hardrock EA as a conservative approach for assessing potential groundwater quality effects to surface water as it assumes no attenuation during discharge, nor mixing and assimilation within the receiving water body. The trigger parameters and concentrations have yet to be defined for the Project. However, they are planned to consider the predicted at-source seepage concentration and the APVs, as well as receiving water quality and aquatic indicators, to allow for the detection of changes and trends for comparison against EA predictions. This will inform the adjustment of management actions in a timely manner, if required. Caution is required when developing triggers for adaptive management plans, which includes the potential for knowledge gaps and substantive uncertainty in the baseline data that may preclude the establishment of appropriate triggers or set overly sensitive or insensitive triggers. A trigger exceedance in and of itself does not necessarily equate to a corresponding negative effect on the ecosystem or mean that impacts may be occurring; just that further monitoring and/or investigation may be required to address a knowledge gap. Caution is also required at the

regulatory decision-making level so that conditions of approval are not overly prescriptive with respect to mitigation and monitoring details, so that adaptation and optionality of environmental management and monitoring approaches can be maintained and carried out in an efficient manner.

A trigger may not be limited to one parameter and/or a concentration. In some instances, it is useful to use multiple attributes while interpreting the data. For example, in the case of a closure-monitoring plan for a potash mine, a two-stage trigger was used. First, the trend line in concentration data was reviewed and if the linear trendline for a trigger parameter demonstrated an upward trend, then the data was compared to an applicable threshold value for each monitoring location, taken as the 95th percentile of baseline data. For a municipal well site assessing water taking, the two-stage trigger consisted of review of the vertical hydraulic gradient followed by water level. If the vertical hydraulic gradient at a nested monitoring well was downward and greater than that observed under the four years of baseline monitoring, then the absolute groundwater elevation was compared to the minimum observed groundwater elevation during baseline monitoring. At the Golden Giant Mine, trends in groundwater sulphate concentrations between near-, mid- and far-field field monitoring wells between the ITF and Pinegrove and Blueberry Creeks were set against the BC MOE sulphate PWQG concentrations. Subsequently that sulphate trend and PWQG end point assessment was used to conclude that further seepage mitigation was required, and to develop seepage mitigation performance targets.

For an adaptive management plan to be effective and efficient it requires early stakeholder engagement and building the mechanisms for change into the plan. Defining the adaptive management plan framework with regulators and acknowledging the framework in the permit process and decisions facilitate changes to the plan as appropriate, without requiring amendments to the permits. Figure 5 presents an example decision matrix for a groundwater monitoring program related to potential effects to groundwater quantity.

Adaptive Management at Greenstone Gold Mines Hardrock Project

In relation to groundwater, PoPCs, receptors, and regulatory criteria protective of these receptors have been conservatively defined as part of the EA for the Project. Conceptual EMMPs that include an adaptive management framework have been presented in the EA. The next stage in developing the EMMPs for the Project include defining triggers associated with the PoPCs. The groundwater triggers will need to consider the water quality and quantity predictions made as part of the EA, as well as the MOECC APVs, receiving water quality, and aquatic parameters. Early stakeholder engagement has occurred through the EA process and will continue through permitting towards the final EMMP and adaptive management framework for the Hardrock Project.

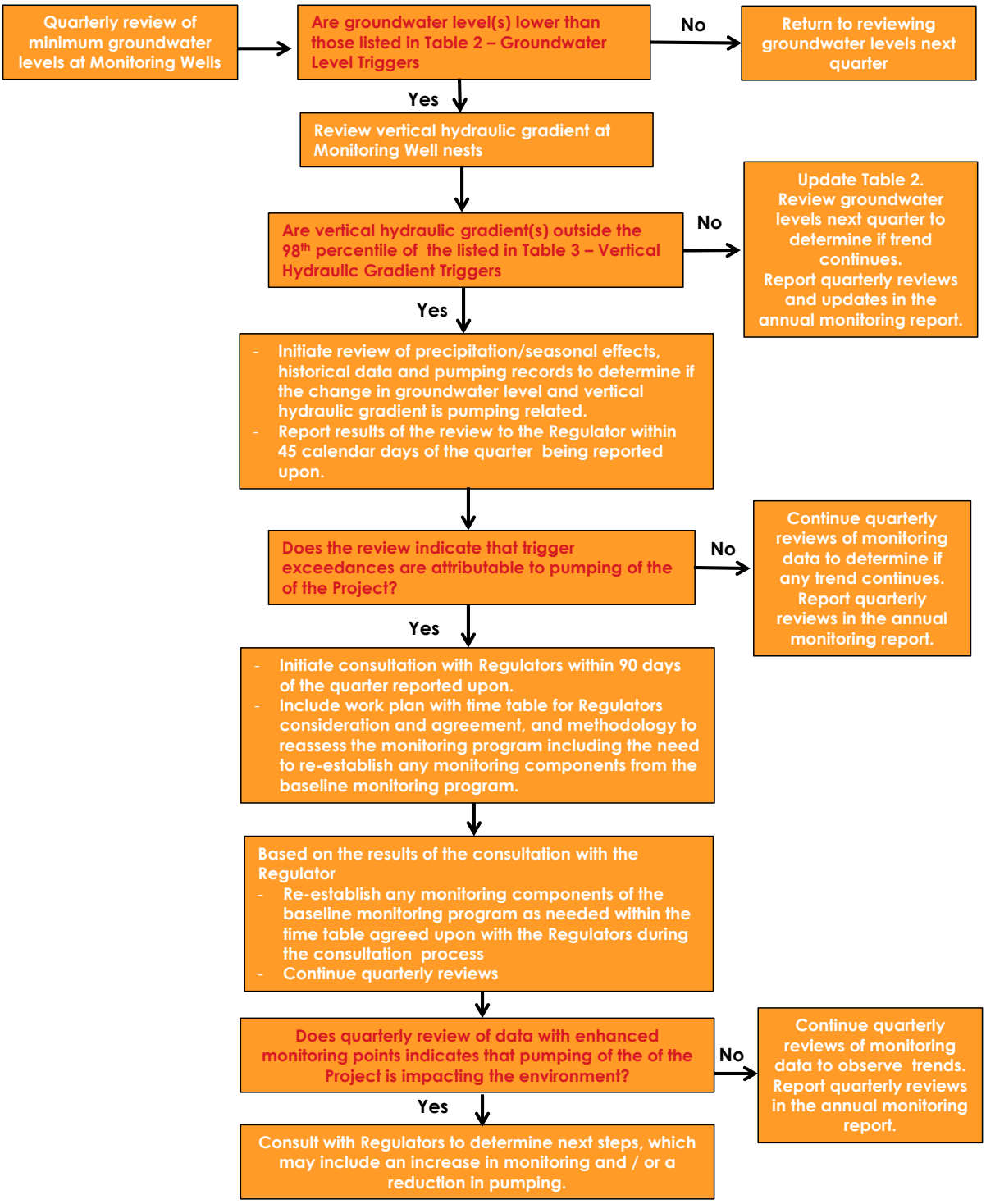


Figure 5: Example decision matrix

Conclusion

Adaptive management provides the opportunity for early and continued stakeholder engagement; furthers the understanding of the environmental indicators and action thresholds necessary to be protective of key receptors; provides flexible decision-making that can be adjusted if necessary based on the results of ongoing field monitoring; and allows the monitoring program to be focused on key areas and key parameters, allowing for efficient use of resources.

References

AGRA Earth and Environmental Limited. 1999. Preliminary Analysis of Tailings Seepage Effects on Pinegrove and Unnamed Creeks under Low Flow Conditions.

Atkinson, A.J., Trenham, P.C., Fisher, R.N., Hathaway, S.A., Johnson, B.S., Torres S.G. and Moore, Y.C. 2004. Designing Monitoring Programs in an Adaptive Management Context for Multiple Species Conservation Plans (US Geological Survey Technical Report). Sacramento, CA: US Geological Survey Western Ecological Research Center.

Geocon. 1984. Seepage Analysis – Interlake Tailings Area – Hemlo, Ontario.

Irving, H.M.N.H. and Williams, R.J.P. 1953. The stability of transition-metal complexes, *J. Chem. Soc*, 3192–3210.

Ministry of the Environment and Climate Change (MOECC). 2016a. B-1-5 Deriving Receiving Water Based Point Source Effluent Requirements for Ontario Waters. Retrieved from https://www.ontario.ca/page/b-1-5-deriving-receiving-water-based-point-source-effluent-requirements-ontario-waters.

Ministry of the Environment and Climate Change (MOECC). 2016b. Water Management: Policies, Guidelines, Provincial Water Quality Objectives. Retrieved from: https://www.ontario.ca/page/water-management-policies-guidelines-provincial-water-quality-objectives. Published September 2016. Updated January 2018.

Ministry of the Environment and Energy (MOEE). 1994. Water Management Policies, Guidelines, Provincial Water Quality Objectives of the Ministry of Environment and Energy. Queens Printer for Ontario. PIBS 3303E. July 1994.

Stantec, 2012. Newmont Golden Giant Mine – Interlake Tailings Facility Seepage Mitigation Project, ITF Water Balance and Dam Seepage Review. Prepared for Newmont Canada Corporation. January, 2012.

Stantec, 2013a. Newmont Golden Giant Mine – Interlake Tailings Facility Seepage Mitigation Project, Hydrogeological Investigation. Prepared for Newmont Canada Corporation. January, 2013.

Stantec, 2013b. Newmont Golden Giant Mine – Interlake Tailings Facility Seepage Mitigation Project, Remedial Alternatives Report. Prepared for Newmont Canada Corporation. February, 2013.

Stantec, 2013c. Newmont Golden Giant Mine – Interlake Tailings Facility Seepage Mitigation Project, Test Well Construction and Hydraulic Testing Report. Prepared for Newmont Canada Corporation. April, 2013.

Proceedings of Mine Water Solutions 2018
June 12–15, 2018, Vancouver, Canada
Published by the University of British Columbia, 2018

Meteorological Time Series and Natural Runoff Model in a Cold Climate Environment

Joel W. Trubilowicz, Northwest Hydraulic Consultants, Ltd., Canada
Victor Muñoz Saavedra, SRK Consulting, Inc., Canada

Abstract

Common issues with water supply estimation in remote mine sites, and with hydrology in general, are 1) a lack of observation data and 2) limited understanding of the uncertainty in results. These issues are addressed in a surface water runoff model at a mine site in central Yukon. Water management and water balance models require records of temperature and precipitation through local observations. The challenges faced in extreme weather environments often mean increased missing data in the observational record. To address this challenge, a model was developed to patch and extend local weather observations and estimate the vertical temperature and precipitation gradients, using regional weather stations combined with reanalysis sources. Seasonally-dependent temperature gradients provide dynamic changes to temperature and more accurately model the common mid-winter valley inversions in the Yukon. The improved meteorological time series were used to drive a semi-distributed, conceptual hydrologic model in the Raven platform to predict natural runoff to the mine site. The highly flexible Raven platform allowed for the selection of the most appropriate hydrologic processes for the mine site region.

Even with better certainty in the meteorological input data, there is considerable uncertainty in the output of hydrologic models. This is often due to an incomplete characterization of the subsurface processes, and inaccurate representation of spatial variability of meteorological datasets. One way to quantify these uncertainties is through the Generalized Likelihood Uncertainty Estimation (GLUE) method. The GLUE method was applied to the hydrologic model for the Yukon mine site to produce hydrologic outputs that can generate upper and lower bounds of potential natural runoff. This uncertainty-based framework provides greater confidence in the predicted hydrologic impacts of climate change and forest disturbance on natural runoff at the mine site.

Introduction

Mine water management and site water balances require a wide range of inputs from the area of hydrology. The quality and quantity of these hydrological inputs can vary based on the geographical

accessibility of the area. In central Yukon, the access is more limited during winter. In a cold climate, the historical records are mainly available during summer or open water season. In winter, climate measurements often contain substantial gaps, and typically snow accumulation or snowpack is not well characterized.

This paper implements a set of practical solutions for the meteorological time series and the runoff to address this uncertainty and complement the lack of quantity and quality of information within a cold climate environment such as central Yukon, Canada.

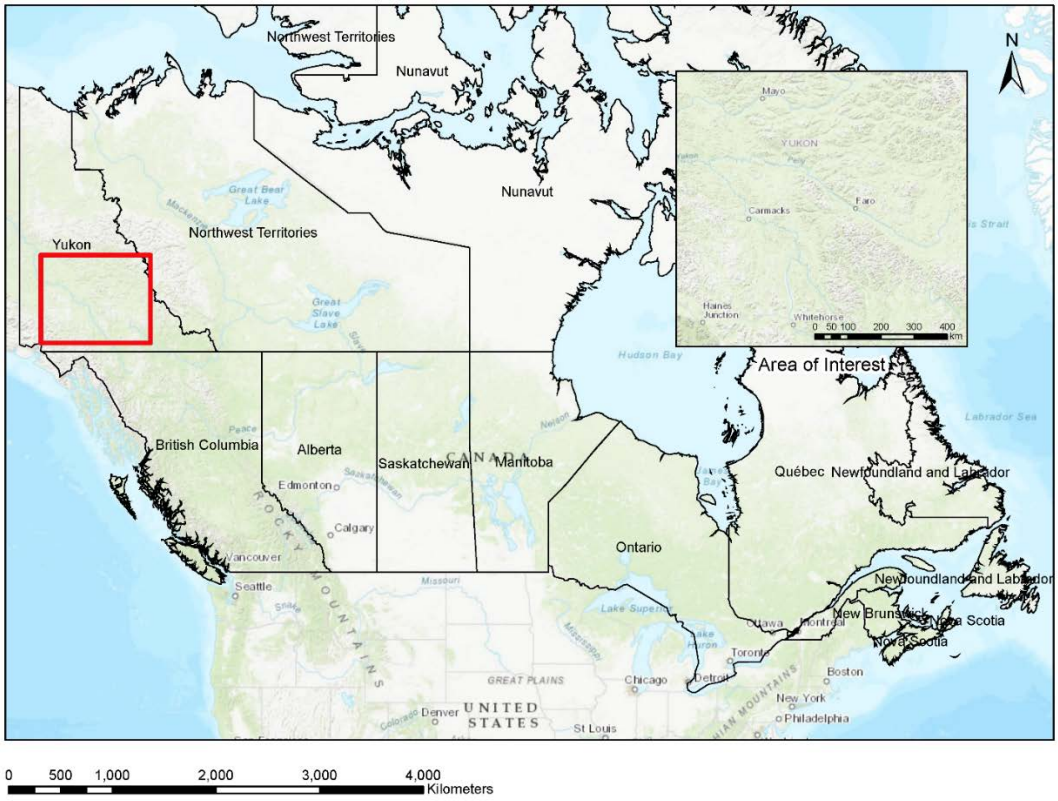


Figure 1: Area of interest – Central Yukon

Methodology

Precipitation and Temperature Records

The total precipitation and temperature in the region were recognized with the regional stations available from Environment and Climate Change Canada (2017). These regional precipitation and temperature records presented important gaps with several non-overlapping periods, which make them impossible to patch; further, if there is any time overlap, the limited extension of these gaps makes them difficult to process, and the results are uncertain.

Ideally, regional analysis requires that all the regional stations are available for the same period. In this review, the regional information was monthly patched as interpolation and extrapolation with reanalysis ERA Interim (ECMWF, 2017). ERA Interim is a reanalysis source that provides more than 120 meteorological parameters worldwide at the ground surface; this information is gridded and statistically downscaled to 0.125 by 0.125 degrees latitude and longitude (~14 by 14 km). ERA Interim provides the information every 8 hours from January 1, 1979 to the actual date.

Meteorological station patching was carried out in two steps with the goal of creating continuous daily records at the two local gauges, referred to as Sites 1 and 2. First, all regional meteorological stations were patched (infilled) on a monthly scale to confirm regional continuity. Second, the local Sites 1 and 2 were infilled on a daily scale using the surrounding regional meteorological stations and their respective cell from ERA-Interim. In the regional scale, the patched information presented Pearson correlation values higher than 0.75 for total precipitation and higher than 0.99 for temperature.

Undercatch

Nearly all precipitation gauges systematically record less precipitation than reaches the ground, due primarily to wind effects near the opening of the gauge. This is known as undercatch; gauge undercatch is greater for snowfall than rain (snow undercatch of more than 25% is common in windy conditions), and can be a significant source of error when computing the hydrologic water balance in a snow-dominant region. We found total annual undercatch in the region to be between 5% to 15%, with higher values associated with higher mean annual precipitation. Similarly, Mekis and Lucie (2011) found regional results of up to 10%. One approach to dealing with undercatch is to correct measured precipitation based on a simple model using wind speed. MacDonald and Pomeroy (2007) fit an empirical equation to field observations of the catch efficiency of a single alter gauge as compared to a "reference" snow gauge (a Canadian Nipher shielded gauge) as a function of wind speed on the Canadian Prairies. The resulting equation was as follows:

$$CE = 1.010e^{-0.09U} \qquad \text{Equation1}$$

where CE is catch efficiency and U is wind speed (m/s). We used this equation to correct daily snowfall at the site for input into the hydrologic model.

Raven Hydrologic Model

A hydrologic model for estimating natural inflows to the mine site was created using the Raven hydrologic model framework (Craig and Snowdon, 2010). The Raven platform is a highly flexible model that allows users to specify the most appropriate representation of each hydrologic process (e.g. snowmelt, groundwater flow, evapotranspiration, etc.) from a large library of equations. The Raven

platform is under active development, and intended as a long-term repository for hydrologic modelling in Canada via the Canadian Hydrologic Model Stewardship Program (CWRA, 2017).

Raven can emulate other hydrologic models, and the user can mix the best processes from different models to create the most appropriate model for a site. To model the Yukon watershed, we began with an emulation of the process-based HBV-EC model, which is an update of the original Swedish HBV model (Bergstrom, 1995) to include more process representations for mountainous cold regions of Canada (e.g. forest, slope, and aspect-dependent snowmelt and glacier processes) (Hamilton et al., 2002).

The HBV and HBV-EC models use a two-layer subsurface model, with a "fast"' reservoir to deliver rapid subsurface flow, and a "slow" reservoir to deliver baseflow. Both HBV-EC and Raven use a "semi-distributed" spatial representation of a watershed. Spatial units include sub-basins and hydrologic response units (HRUs). All HRUs are a member of a sub-basin, and sub-basins can either flow into other sub-basins or to the bottom of the catchment. HRUs have no physical position (i.e. water is not routed between HRUs, only between sub-basins). However, HRUS can have different land cover, soil, and terrain properties to represent the cumulative effect of these different properties on the surface mass and energy balance.

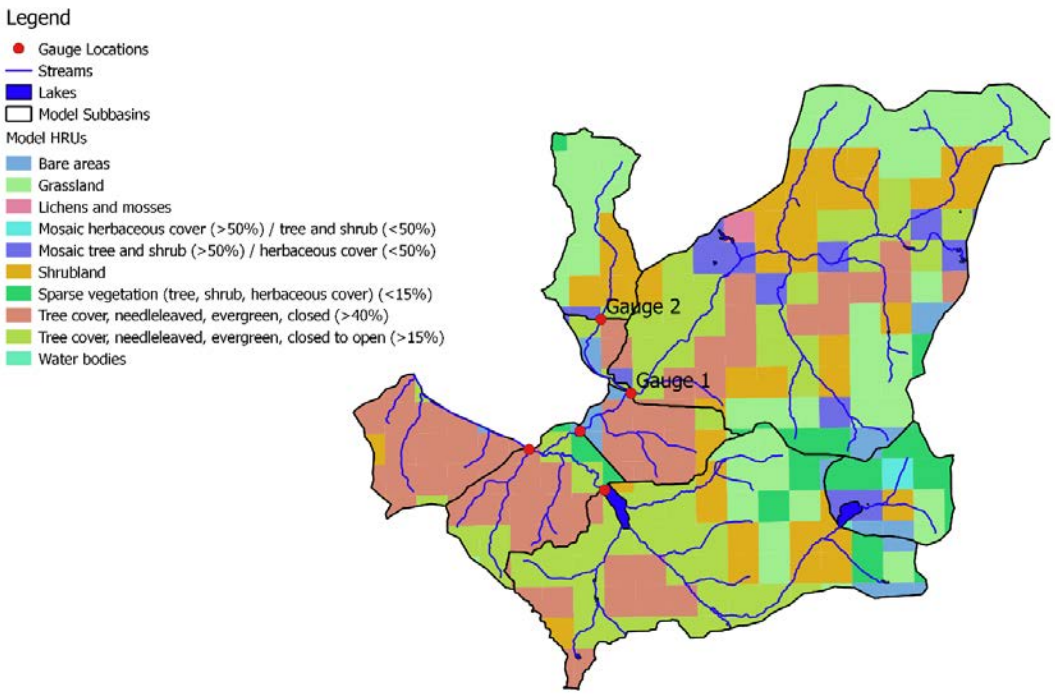


Figure 2: Hydrologic response units (HRUs) for the Faro mine model (1 km x 1 km grid cells)

The flexibility of Raven allows for HRUs of any size to be used within the model. We specified a quasi-distributed HRU setup for the site watershed, with 1 km grid cells representing a coarse view of the terrain, land cover and vegetation of the sub-basins (Figure 2). The discrete 1 km grid cells were overlaid upon the sub-basins (including surface water areas), and aggregate terrain (elevation and aspect) statistics were calculated for each of the resultant 331 HRUs. Land cover shown in (Figure 2) was obtained from the European Space Agency (ESA)'s global land cover dataset. Land cover and vegetation were lumped into 4 categories for the hydrologic model – Bare, Water, Shrubland and Forested.

The use of high resolution discrete HRUs allows for the future possibility of testing the impacts of changing land cover on the water balance of the watershed (and hence the mine) due to forest disturbance (e.g. disease, fire, forest harvesting) in future studies of the mine site.

Elevation and aspect were aggregated versions of the Canadian Digital Elevation Model (CDEM) to the resolution of the HRUs. Elevations range from 1,000 to 2,000 masl for the entire area.

Most of the hydrologic processes used in the model were based off the HBV-EC model, which allows for land cover and aspect corrections for snowmelt rate; however, some modifications were made for more appropriate modelling of the mine site:

- A cold content term was included in the snowpack model to allow for the build up of (parameterized) negative energy in the snowpack during extreme cold. Cold content slows the onset of spring melt, as the negative energy must first be erased, by bringing the internal temperature of the snow to 0^{o} C, before melt can occur.
- Vertical temperature and precipitation gradients were specified based on regional gradients (as described previously). A dynamic vertical temperature gradient was implemented to allow for different gradients for different seasons. The primary purpose of this was to better represent mid-winter valley inversions in the region.
- Snow sublimation was parameterized at open (non-vegetated) HRUs using the Kuzmin methodology (Kuzmin, 1957).

Data and Results

Precipitation

Based on the regional review, the most important regional predictor of total precipitation in the region was gauge elevation (Pearson correlation of 0.83). The local estimations were found to be consistent with the regional scale; the site information was found to be within the ranges expected, and these are presented as Site 1 and Site 2 in Figure 3. This figure suggests mean annual precipitation values within the regional values.

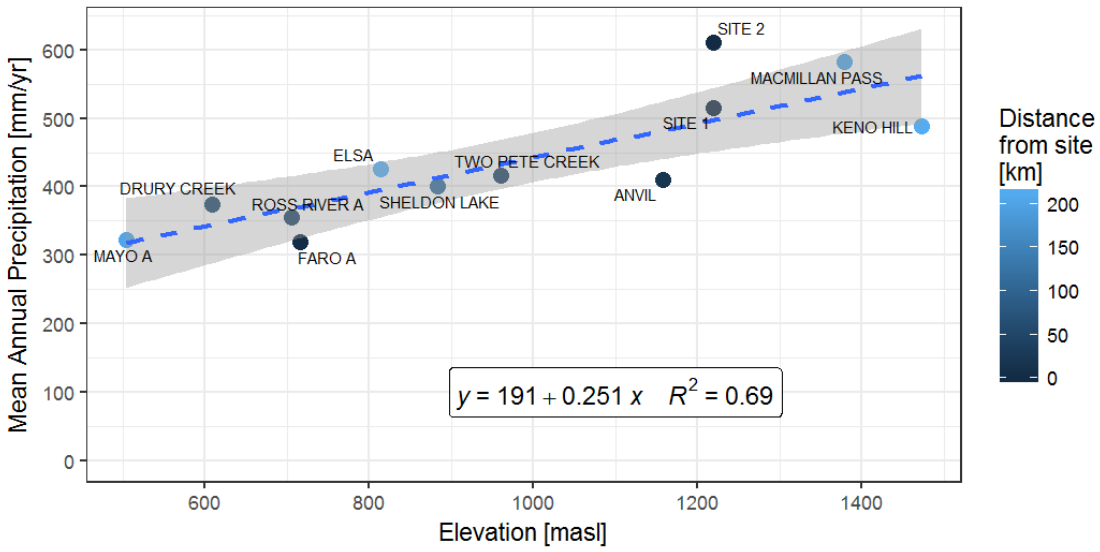


Figure 3: Total precipitation versus elevation

Temperature

A regional analysis of the mean annual air temperature (MAAT) did not show any important relationship between air temperature, latitude, longitude, and distance from the coast or elevation. Due to this lack of relevance between these variables, a monthly review was implemented, where strong correlations were observed between air temperature and elevation, with an average Pearson correlation by month of 0.71. Figure 4 presents a regression with the monthly relation between elevation and mean air temperature by month.

The local regional data during open water season (May to August) shows a typical adiabatical lapse with ranges from 4 to 7° C/1 km; during winter (November to February), this lapse is inverted, a thermal inversion existed where higher elevations were cooler. This inversion most likely is the result of cold air ponding during very cold, clear weather that can occur in the region. This phenomenon was also observed at our observation Sites 1 and 2.

Hydrologic Model Uncertainty Assessment

Precipitation and temperature from Site 1, and the regional precipitation and temperature gradients, were used to drive the Raven hydrological model.

The Raven hydrologic model created for the inflows to the site is considered a conceptual hydrologic model, where hydrologic processes are represented as parameters and functions within the model. The parameters dictating these processes are not physically measurable, and hence have some level of uncertainty. With this model and most hydrologic models in cold environments, the dominant

parameters controlling hydrologic response are those involved with snowmelt and subsurface flow of water.

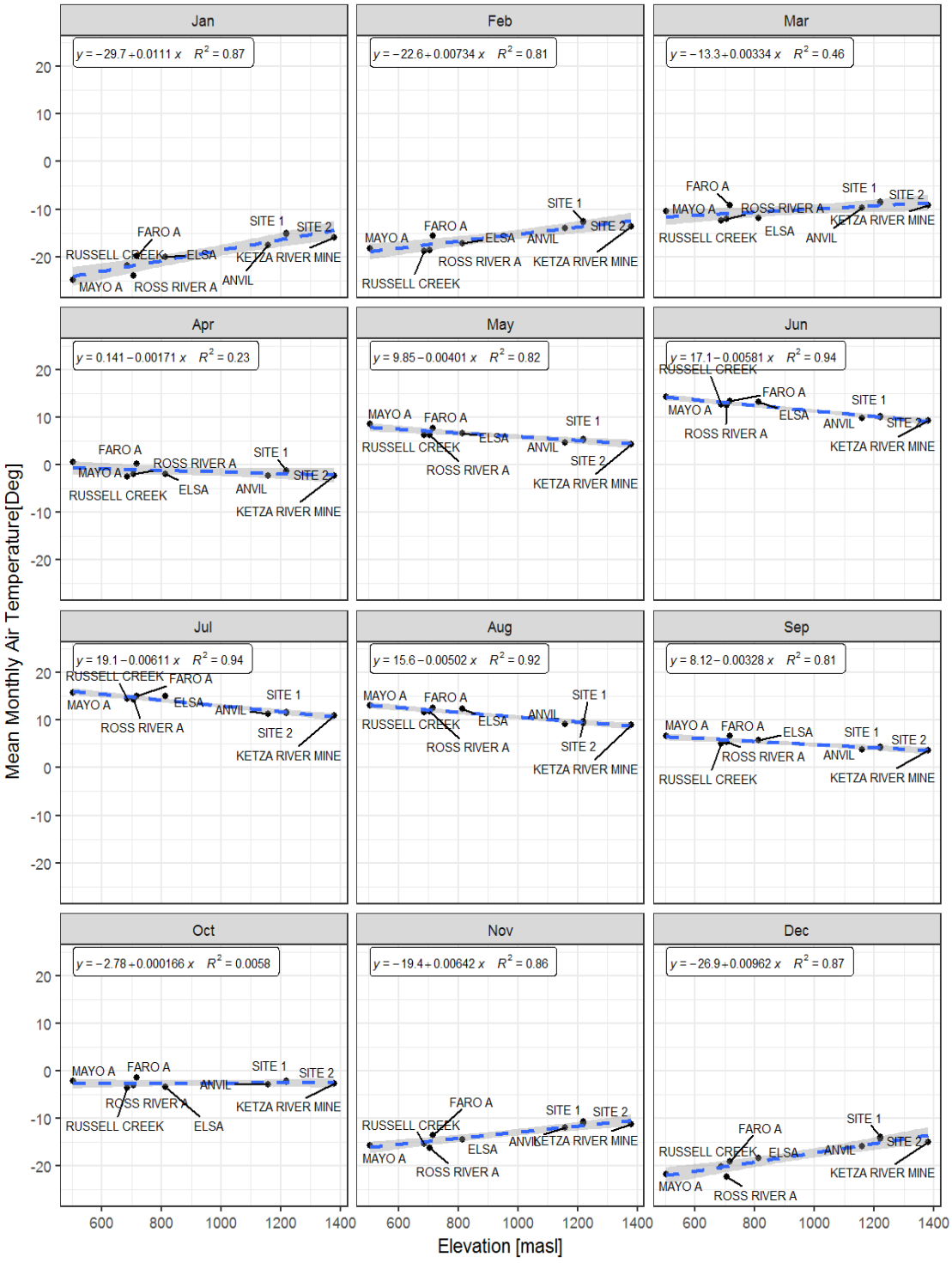


Figure 4: Mean air temperature by month versus elevation

An issue with all hydrologic models is the situation of "equifinality," in which multiple parameter combinations can result in the same, or virtually the same, model results at the calibration location. While results at the calibration location may be the same, model results at other locations, which have no calibration data, but are nevertheless important, could be different. This issue arises because there is almost always unknown information about how a watershed functions. In this model, we had 19 parameters that could vary. Thus, a vast number of parameter combinations are possible, and it is almost certain that more than one combination can produce acceptable results.

One of the best known methods for dealing with equifinality 'and assessing model uncertainty within a hydrologic model is known as the Generalized Likelihood Uncertainty Estimation (GLUE) methodology (Beven and Binley, 1992). The GLUE methodology assumes that multiple parameter sets will likely result in acceptable results (referred to as behavioural parameter sets). The user determines the statistical value that constitutes a behavioural parameter set, and then random parameter sets are drawn repeatedly from the n-dimensional parameter space until the requested number of behavioural parameter sets has been found.

We implemented the GLUE methodology using the Ostrich independent model calibration software (Matott, 2017). Ostrich is highly flexible software that allows the user to manipulate nearly any type of model, specifying:

- the parameters to be manipulated;
- allowable parameter ranges;
- the performance statistic to be used;
- optimization algorithm to be used (with dozens available); and
- desired level of convergence and maximum number of model runs that can be performed.

We quantified the performance of the hydrologic model primarily based on observations from two gauged sites within the model watershed (see Figure 2). The local site Gauge 1 had the longest period of record available within the watershed, approximately 12 full years between 1998 and 2012. The local site gauge 2 had two full years of data available as well, and was used as a secondary performance test. Ostrich was configured to manipulate 19 total parameters: 10 soil parameters, 5 snowmelt parameters, and 4 canopy interception parameters, during calibration.

We used the Nash-Sutcliffe model efficiency (NSE) (Nash and Sutcliffe, 1970) between simulations and observations as the primary metric of model performance. The NSE is one of the most commonly used general hydrologic model performance statistics. A perfect match between observations and simulations results in an NSE of 1. An NSE below 0 indicates that the mean of all observations provides more predictive power than the modelled data.

The primary reason that GLUE methods are not commonly employed in engineering is the significant computation time required, and the difficulty in dealing with multiple model results, as opposed to a single time series. In this analysis, we allowed Ostrich to perform up to 100,000 model runs to find 100 behavioural parameter sets at Gauge 1 based on random draws from the parameter space. A behavioural parameter set was considered a result with an NSE of greater than 0.5 at Gauge 1. After finding 100 behavioural sets for site gauge 1, we then subset those to only parameter sets that also had a NSE of greater than 0.5 at the site gauge 2.

Though it requires more computation time, the GLUE methodology was particularly suitable to this study, as the goal was to find an overall median inflow per year, based on the input mean annual precipitation, at an ungauged location. Thus, we could only partially rely on the performance statistics at Gauges 1 and 2 (i.e. the absolute highest NSE at site gauge 1 may not in fact give the most realistic results lower down in the watershed). Thus, an uncertainty framework for presenting the results was an appropriate choice at this site.

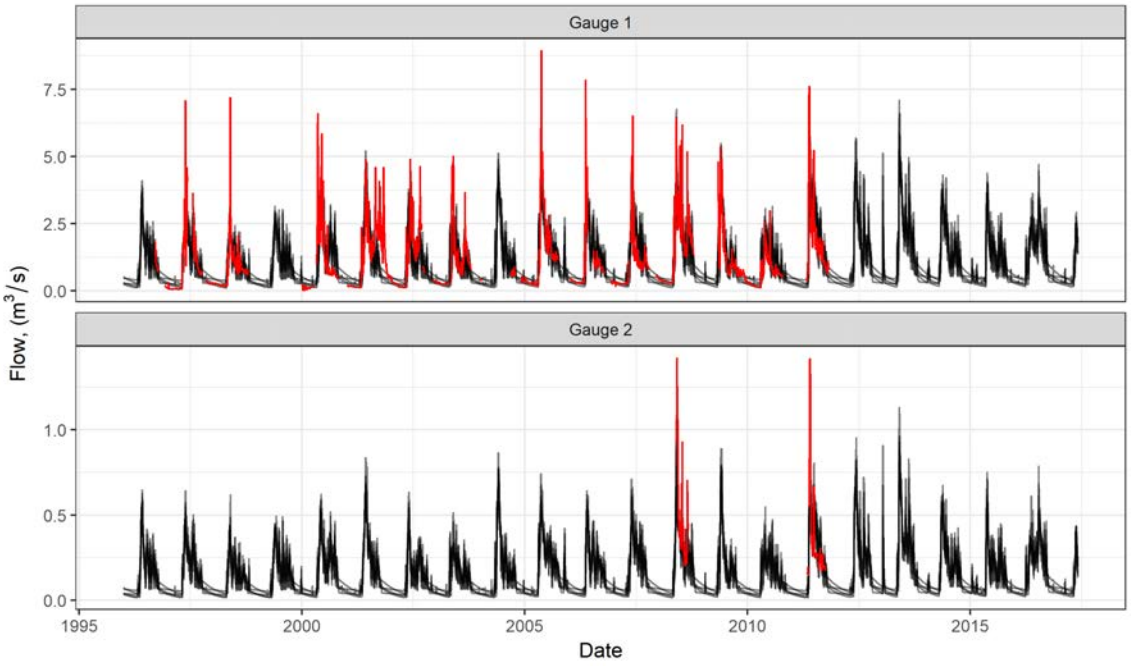


Figure 5: Ensemble output for Gauges 1 and 2.
Red indicates observations and black lines indicate the outputs from the five behavioural parameter sets

The GLUE procedure produced 100 parameter sets with an NSE > 0.5 for Gauge 1; of these, five sets also had an NSE greater than 0.5 for Gauge 2. These five sets represent a range of uncertainty within this model setup, and all five parameter sets should be considered equally likely "realities" (Figure 5). As the purpose of this model was to estimate the average watershed response, using 5 outputs has the effect of increasing the modelling period five-fold, and thus providing greater confidence in the model results.

Thus, we combined all years, and all model parameter sets to estimate a water balance at the lower outlet of the modelled watershed (the input to the mine site). Estimating this water balance as a range, presented as box plots in Figure 6, produces a simple bracketed index that can be used to estimate upper and lower confidence limits of monthly runoff within a watershed simply via knowing the mean annual precipitation at the site. As with all empirical models, however, confidence decreases when extrapolation goes beyond the fitted range. This relationship should remain strong when encountering future mean annual precipitation values within the same range as the 20 years modelled here, but for extremely wet or dry years, the confidence decreases.

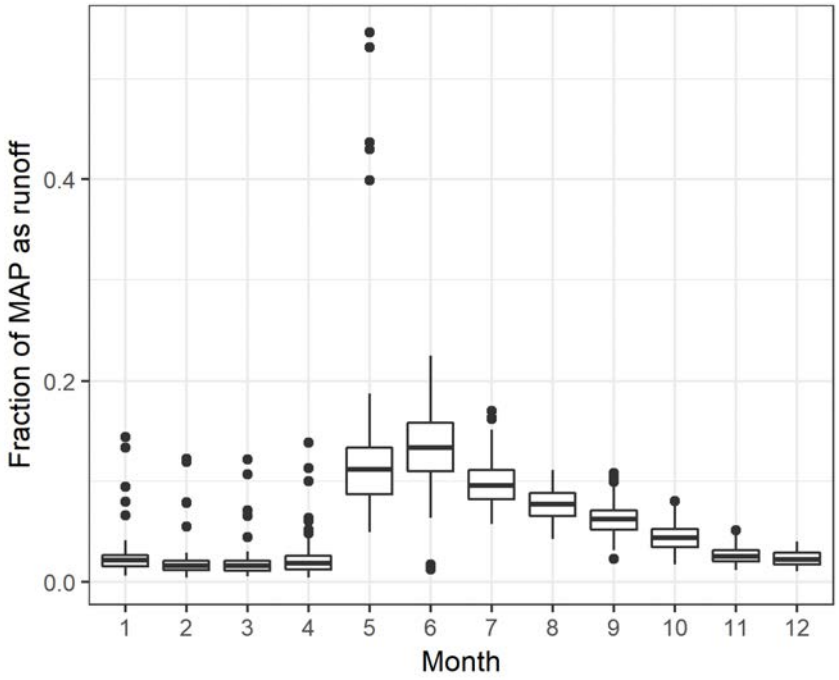


Figure 6: Boxplots showing the monthly fraction of mean annual precipitation that is expected to runoff at the lower outlet of the model catchment.
Middle values of each box indicate the median, and upper and lower box edges (hinges) are the 75th and 25th percentiles (the quartiles). Whiskers indicate the maximum and minimum ranges, with outliers (outside 1.5 times the inter-quartile range) shown as dots

Conclusions

This hydrologic analysis in a cold, data-sparse region has addressed several challenges facing practitioners in these regions. These can be summarized as follows:

- A combination of site weather observations, regional climate gauges and weather reanalysis models was successfully used to create a realistic, continuous, weather record at the mine site.
- Precipitation gauge undercatch was accounted for via a simple, wind based empirical model.

- The uncertainty of model results in a hydrologic model with little calibration data was accounted for using a formalized uncertainty assessment tool (Generalized Likelihood Uncertainty Estimation) that is commonly employed in scientific research, but rarely used by practitioners.

References

Bergstrom, S. 1995. The HBV Model, in V.P. Singh (ed.) *Models of Watershed Hydrology:* 443–76. Highlands Ranch, CO: Water Resources Publications.

Beven, K. and A. Binley. 1992. The future of distributed models: model calibration and uncertainty prediction, *Hydrological Processes*, 6(3): 279–298.

Craig, J. and Snowdon, A. 2010. Raven: A rigorously formalized modular hydrological model, *Environmental Modeling and Software* (Preprint Submitted) 2:20–21.

CWRA. 2017. Canadian Hydrological Model Stewardship. Retrieved from http://www.cwra.org/en/branches/affiliates/cshs-a/chyms

ECMWF. 2017. ERA Interim, Daily. Retrieved from http://apps.ecmwf.int/datasets/data/interim-full-daily/levtype=sfc/

Environment and Climate Change Canada. 2017. Historical Data. Retrieved from http://climate.weather.gc.ca/historical_data/search_historic_data_e.html

Hamilton, A.S., Hutchinson, D.G. and Moore, R.D. 2002. Estimating winter streamflow using a conceptual streamflow model, *Journal of Cold Regions Engineering,* 14(4): 158–75.

Kuzmin, P. 1957. Hydrophysical investigations of land waters, *Int. Assoc. Sci. Hydrol. Publ.,* 3: 468–478.

MacDonald, J. and Pomeroy, J.W. 2007. Gauge undercatch of two common snowfall gauges in a prairie environment, in *Proceedings of the 64th Eastern Snow Conference,* 29: 119–126.

Matott, L.S. 2017. *OSTRICH: an Optimization Software Tool, Documentation and User's Guide*, Version 17.12.19, University at Buffalo Center for Computational Research. Retrieved from www.eng.buffalo.edu/~lsmatott/Ostrich/OstrichMain.html.

Mekis, E. and Lucie, V. 2011. An overview of the second generation adjusted daily precipitation dataset for trend analysis in Canada, *Atmosphere-Ocean,* (2): 163–177.

Nash, J. and Sutcliffe, J. 1970. River flow forecasting through conceptual models Part 1 – A discussion of principles, *Journal of Hydrology,* 10(3): 282–90.

Proceedings of Mine Water Solutions 2018
June 12–15, 2018, Vancouver, Canada
Published by the University of British Columbia, 2018

Towards a Conservative Mine Design Practice through Probabilistic Calibration

John Markus Mayer, SRK Consulting (Canada) Inc., Canada

Abstract

Conventional groundwater model calibration is typically a deterministic process, whereby a set of unknown inputs is adjusted to minimize the difference between the measured and modelled outputs. The product is often a single, calibrated model used for subsequent decision analysis. However, such an approach can result in overfit models due to the stochastic nature of the inputs, and the state of incomplete information (i.e. limited number of hydraulic tests, variable recharge, etc.). To deal with this uncertainty, alternative Bayesian approaches are available that utilize stochastic learning techniques to find the probability distribution of both the inputs and outputs.

This paper explores the concept of probabilistic groundwater model calibration using the stochastic learning technique known as Markov Chain Monte Carlo (MCMC). Examples of the approach are presented for groundwater models at the preliminary economic assessment (PEA) and pre-feasibility study (PFS) levels, to predict both long-term inflow and drawdown trends. Results suggest that improved predictive abilities can be achieved using the proposed approach, with uncertainties explicitly quantified through the generation of multiple calibrated models. The broader implications of the Bayesian approach are then discussed, with the idea of ultimately applying it across the multiple disciplines involved in a mine design study.

Introduction

Hydrogeological studies often exist in a state of incomplete information, where design recommendations must be provided in the face of large uncertainties. Despite this, such studies often rely on a single "calibrated" model of the subsurface. However, this singular approach ignores one of the most important aspects of prediction: that it is not so much the estimate that matters, but the degree of confidence in the forecast (Taleb, 2005). Consider for instance inflow prediction to an underground mine. If a numerical model predicts an inflow rate of 300 ± 50 m^3/d, that might mean the installation of a few sumps; whereas, a prediction of 300 m^3/d ± an order of magnitude might require contingencies to be put in place for bulkheads, freeze walls, grout curtains, etc. Since hydrogeological uncertainties are often log-normal in

nature, prediction uncertainties often fall into the latter case as opposed to the former. In these cases, the brunt of the costs are often tied up in the contingencies required to deal with tail events, which are more often impacted by uncertainty on the estimates, as opposed to the estimates themselves.

This conclusion is vitally important, but often missed by professional engineers and scientists, whose work is often restricted to the left side of the risk equation, i.e.:

$$Risk = Probability \times Consequence \qquad \text{Equation 1}$$

This preoccupation with probability often causes scientists and engineers to equate it with the risks to a project; however, the maximum risk event only falls near the maximum likelihood event if the consequence is linear or quasi-linear. Unfortunately, this is often not the case. In reality the consequence of a mine design is often highly non-linear, causing the risk to be dominated by tail events (Taleb, 2010). These tail events end up driving the overall profitability of a mining project, as opposed to the highest likelihood scenarios (Figure 1).

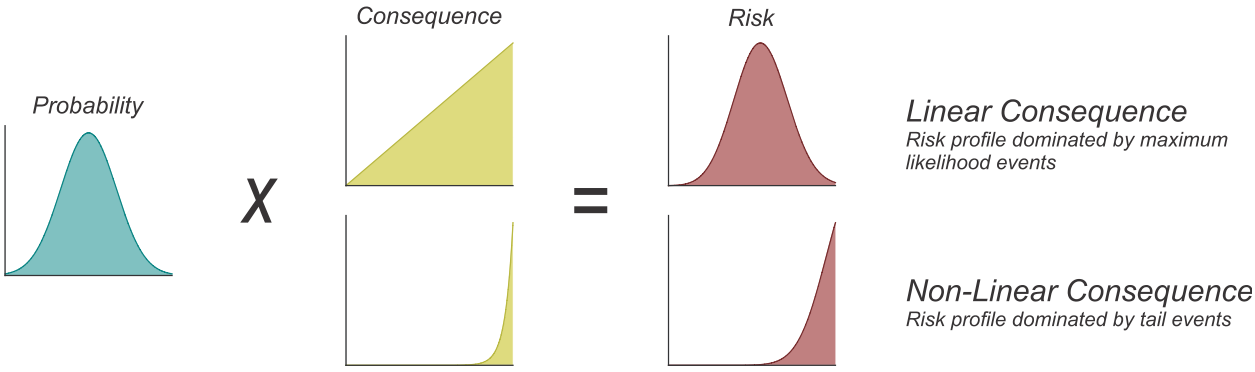


Figure 1: Effect of linear vs. non-linear consequence on the risk profile

The issue with the singular calibration approach is that it is unable to quantify these tail events, as it simplifies the probability side of the risk equation down to a single number close to the maximum likelihood event. Instead, a probabilistic viewpoint can be taken, whereby model parameters are treated as random variables, as opposed to fixed constants, and the model stochastically calibrated to the data. The term 'probabilistic calibration' is used throughout the text, as the proposed Bayesian viewpoint allows for both the calibration of the model during burn-in, and subsequent exploration of the uncertainty space using a single stochastic algorithm, in this case Markov Chain Monte Carlo (MCMC). The result is the generation of multiple calibrated realizations of the subsurface, which can be used to quantify both the mean forecast and degree of confidence in the estimate, through use of histograms or probability density functions (PDF). Results can then be incorporated into a formal risk framework, allowing for genuine conservative mine design which encompasses the influence of positive tail events.

Probabilistic Simulation

Bayesian Approach

Traditional probability theory, taught in introductory statistics courses, teaches a frequentist viewpoint; whereby, parameters are considered fixed, and approximated from the statistics of a sample. In essence, data are considered random variables, which can be used to approximate a parameter, based on the relative frequency of a large number of experimental trials. While this is an important application of probability theory, it is only one of the approaches. Another is the Bayesian viewpoint, which describes subjective states of information on a system (Mosegaard and Tarantola, 2002). In essence, data are considered fixed, and parameters treated as random variables. Probability distributions for the parameters are then constructed, using Bayes' theorem, which is generalized for inverse problems as:

$$\sigma(m) = k\rho(m)\mathcal{L}(m) \qquad \text{Equation 2}$$

where $\sigma(m)$ is the posteriori distribution of the model parameters (m) given the data and prior information, $\rho(m)$ is one's prior knowledge about the parameters, $\mathcal{L}(m)$ is the likelihood function which measures the degree of fit between the data and model, and k is a normalization constant (Tarantola, 1987). For a more complete primer on the Frequentist vs. Bayesian approach see Freedman (1995) or VanderPlas (2014).

An advantage of the Bayesian approach for geoscientists is that the method is not strictly confined by the data. Instead prior knowledge, or best-engineering judgement, can be formally incorporated into the analysis process. Although, sometimes cited as a disadvantage, this property is often a more organic interpretation of probability, as practitioners often unwittingly employ Bayes' rule on a daily basis. Take for example numerical modelling where it is not uncommon for a hydrogeologist to reject an unrealistic model, such as those having an effective porosity greater than 50%. This act of rejecting the model, or setting its probability to zero, is a direct use of Bayes' theorem, as the model is rejected based on one's prior knowledge of realistic porosity values. Formalizing this informal framework using the Bayesian approach allows for the explicit definition of both the data and prior knowledge within a rigorous decision framework. The key is to set realistic priors which encompass best-engineering judgement without overly restricting the problem.

Markov Chain Monte Carlo

A direct solution of the probabilistic inverse problem is often difficult in practice, as it requires a closed form solution for Equation 2. Instead, it is often easier to approximate the solution using a Monte Carlo approach, which pseudo-randomly generates a large collection of models to approximate the posterior probability distribution. Of the Monte Carlo methods one of the most important is Markov Chain Monte

Carlo (MCMC), first introduced by Metropolis et al. (1953). The algorithm is based on the use of a random walk, whose steps are assessed using a simple probabilistic rule that compares the relative likelihood of different Markov states.

In practice, the algorithm works as an unsupervised machine learning routine that can both calibrate a model during initial burn-in, and randomly explores the probability space to approximate the probability distributions of the unknown inputs. For a full description of the MCMC algorithm see Mosegaard and Tarantola (2005) or Shonkwiler and Mendivel (2009).

Likelihood Measure

Solution of a probabilistic inverse problem requires definition of a formal likelihood function, comparing the current model state with the observational data. This was conducted throughout the study by assuming independent, Gaussian data errors, resulting in the likelihood being defined by:

$$\mathcal{L}(m) = \exp\left(-\frac{\sum(\theta_{mod} - \theta_{obs})^2}{\sigma^2}\right) \quad \text{Equation 3}$$

where θ_{mod} and θ_{obs} are the calculated and measured response curves, and σ^2 is the standard deviation in the errors (Tarantola, 2005).

Case Study I: Steady-State Inflow Prediction

Groundwater models used for preliminary economic assessments (PEA) frequently involve a large degree of uncertainty due to the sparse nature of data on greenfield projects. In such cases, models are typically only calibrated to steady-state hydraulic head conditions; however, an underappreciated aspect is that without known fluxes, models are only calibrated for the hydraulic head (K) to recharge (R) ratio, as opposed to absolute values. This results in an inherently non-unique solution, with a wide range of K and R values capable of fitting the data with equal likelihood. To overcome this limitation, probabilistic techniques can be employed, which stochastically calibrate multiple groundwater models and integrate the results.

Such an approach, was utilized for a recent PEA study of an undisclosed exploration site. The study involved estimation of the expected inflow for a proposed open pit mine. Hydrostratigraphy at the site can be broken down into three primary units based on the regional geology (hanging wall, contact zone, and footwall). Based on these units, five parameters were designated as random variables for the stochastic simulation, namely:

- Hydraulic conductivity of the:
    - Hanging wall ($K_{hanging\ wall}$)
    - Contact zone ($K_{contact\ zone}$)
    - Footwall ($K_{footwall}$)
- Mean annual precipitation (MAP)
- Recharge as a percentage of the mean annual precipitation (%MAP)

Stochastic techniques were then utilized to both calibrate these parameters to the measured hydraulic head data and explore the uncertainty space.

Model Setup

The numerical groundwater model was setup using the FEFLOW v7.0 numerical simulation code (update 9) (DHI, November 2016). The model was constructed to encompass the potential surface catchment of the proposed mine, with external boundaries assigned as no-flow boundaries along catchments divides. Rivers and creeks were simulated using constant and constrained head boundaries, with the latter restricted based on total base flow measurements from local creeks. Recharge was applied as a constant source across the model, and calculated as a percentage of the mean annual precipitation (%MAP). The model size was set to 80,000 nodes, resulting in a 45s runtime using the preconditioned conjugate-gradient (PCG) solver.

Prior Information

Prior information was defined for five model input parameters, in order to quantify the current state of hydrogeological knowledge (Table 1). Datasets were assumed to be independent, making the total prior probability equal to the product of the marginal priors (i.e. $(m) = \prod \rho_i(m)$).

Table 1: Prior distributions used for Case Study I

Parameter		Distribution model	Mean / minimum	Std. dev. / maximum	Units
Hydraulic conductivity	Hanging wall	log-uniform	1×10^{-9}	1×10^{-5}	m/s
	Contact zone	log-normal	7×10^{-4}	0.25[i]	m/s
	Footwall	log-uniform	1×10^{-9}	1×10^{-5}	m/s
Percent recharge (%MAP)		log-normal	0.16	0.20[i]	%
Mean Annual Precipitation		normal	531	16	mm/a

[i] Log transformed standard deviation

[ii] Ranges were derived from published values for fractured rock (Beale and Reed, 2013) and global recharge variability (Jasechko et al., 2014).

Stochastic Calibration

Models were calibrated to match mean annual hydraulic head data collected at 44 locations, using the Metropolis algorithm (Metropolis et al., 1953). The algorithm was programed in pure Python and utilized the FEFLOW IFM kernel to interact with the groundwater model. This allowed for both unsupervised calibration of the groundwater model during burn-in and subsequent uncertainty estimation once the Markov chain reached the high probability space. In total, 20,000 groundwater models were constructed, with independent samples extracted every 25 Markov steps. This resulted in the generation of 800 uniquely calibrated models, with normalized root mean squared errors (NRMSE) varying between 14.9% and 15.9%.

Results

Mine inflow estimates were generated by running a forward simulation on each of the extracted samples, with the proposed open pit added as a seepage boundary. Results suggest an asymmetry in the probability functions, characterized by a positive skew (1.2), and average predicted inflow rate of 57,000 ± 20,000 m^3/d (Figure 2). Cumulative density (CDF), and associated probability density functions (PDF), were constructed from the results to provide a quantitative estimate of the forecast uncertainty. Functions were then provided to practitioners of the consequence side of the risk equation to allow for quantification of the total developmental risk to the mining project.

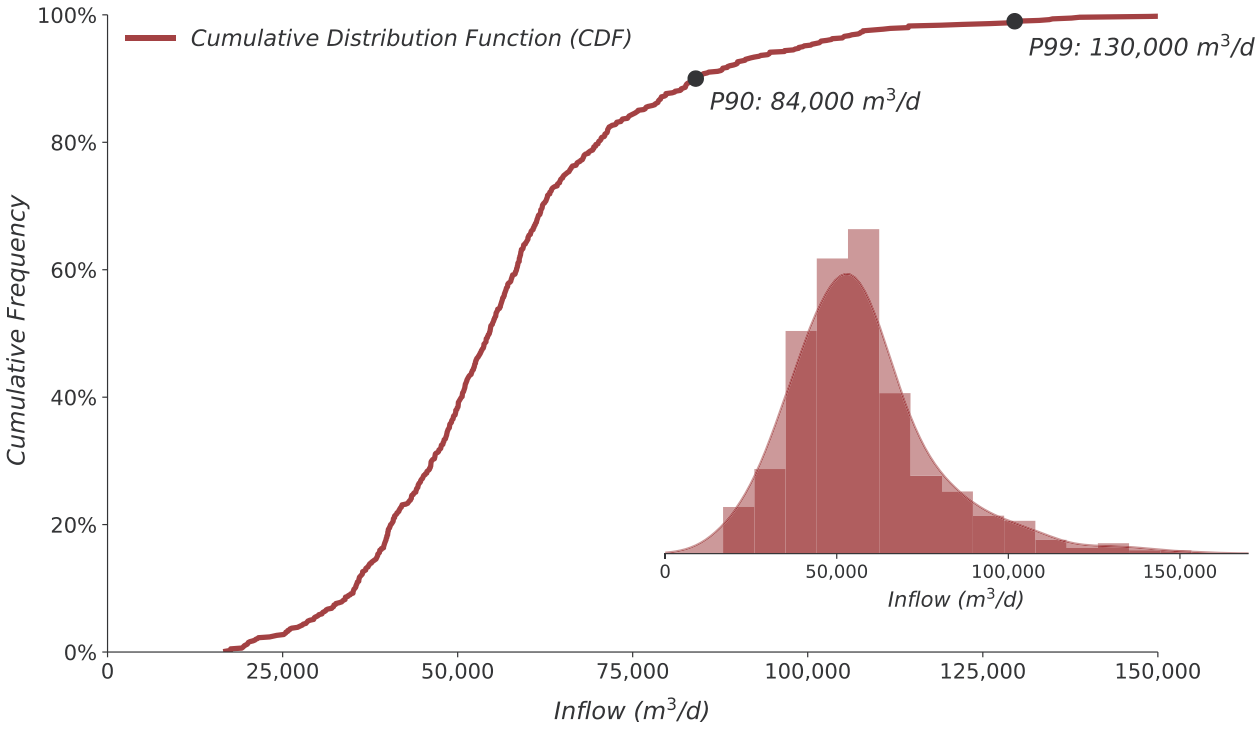


Figure 2: Uncertainty in predicted inflow for proposed open pit mine

Although risk quantification should be the ultimate goal of any mine design study, it is not always feasible to provide a CDF or PDF as output for a forecast due to the preferences and training of clients and/or regulators. In such a case, P90 or P99 statistics[1] can be extracted from the CDF to provide technical guidance on estimated inflows. Although not as rigorous as full risk quantification, use of non-exceedance statistics represents a more conservative approach to mine design as compared to singular forecasting methods. Such statistics are also often easier to incorporate into subsequent engineering design steps that do not fully characterize the forecast uncertainty, thus providing a compromise between full probabilistic simulation and traditional design. However, while more conservative, the use of non-exceedance statistics does not guarantee conservative design when the number of variables is large. This is due to the multiplication of probabilities, whereby the probability of a mine design remaining conservative for all variables tends to zero as the number of variables increase. This leads to Taleb's (2014) theory of fragility, where an inverse relation exists between the fragility of a design and its complexity. This law tends to explain the progressive increase in cost over-runs on major infrastructure projects as the complexity of design increases. Take for instance the 1999 Mars Climate Orbiter incident, where an output of pound-seconds was sent to the orbiter instead of the required newton-seconds. This caused the orbiter to pass through the upper atmosphere of Mars and disintegrate. The actual probability of this specific event was quite low, but the flaw resided in the sheer number of variables required to send an orbiter to Mars. This example presents an important consideration for mine design, as while the probability of any single parameter being above the non-exceedance statistic is low, the probability of at least one variable exceeding the criterion in an overall complex design is large. In essence, non-exceedance statistics should include a correction factor for the number of variables; however, this is rarely done in practice (i.e. the statistical threshold of non-exceedance should increase proportionally to the number of parameters). As a result, when the complexity of the design is large, conservative estimates derived from non-exceedance statistics should be viewed with caution.

Validation

Validation of the modeling process was conducted by comparing the predicted inflow with measured results from a flooding incident during development of a pilot shaft. Model predictions were constructed through forward simulation, with seepage nodes placed at the base of the shaft. Comparison of inflow indicates a good agreement between measured and P50 results, with a forecasted rate of 48,000 m^3/d compared to a measured rate of 55,000 m^3/d.

[1] P90 and P99 statistics represent the best estimate of the probability of inflow non-exceedance or rather that 90/99% of simulations estimated inflow rates are below this value.

Parameter Sensitivities

Inflow sensitivity to the five stochastic parameters was characterized by calculating correlation coefficients between the parameters and inflow (Table 2). Key parameters were then identified from the coefficients, and along with their uncertainty properties[2], used to guide future studies by focusing on the most sensitive parameters. In the case of the proposed open pit, the model was most sensitive to the hydraulic conductivity (K) of the hanging wall and the groundwater recharge as a proportion of precipitation (%MAP). Sensitivity to the former resulted from inflow between the proposed pit and the constant head boundary used to simulate a major river system to the north; while the latter resulted from the general recharge driven state of groundwater flow in a mountainous setting. Based on the sensitivity analysis, recommendations for a future PFS study were provided, that included an exploratory packer-testing program in the hanging wall, and a detailed, site-wide water balance.

Table 2: Summary of inflow sensitivity to stochastic parameters

Parameter		Pearson's r
Hydraulic conductivity	Hanging wall	0.94
	Contact zone	0.57
	Footwall	0.60
Percent recharge (%MAP)		0.96
Mean Annual Precipitation		0.49

Case Study II: Transient Calibration to Pumping Test

Pumping test analysis is typically conducted by matching type curves from idealized aquifer geometries to observational data (Kruseman and de Ridder, 1994). However, simplified analytical solutions are not always available when dealing with unconventional groundwater systems. In such a case numerical models can be utilized, which incorporate the unconventional geometry, and are calibrated to observational data

This alternative approach was used for one such test conducted within the waste rock of a backfilled pit. Flow within the system is restricted due to the fully bounded nature of the groundwater system. This has a large influence on its overall drawdown behavior, making it strongly dependent on the storage and recharge properties. Ambient flow within the system is generally northerly, with precipitation driven

[2] To minimize uncertainty in the output (inflow) it is often best practice to focus on the input parameters with the least uncertainty (Hogg et al., 2010). In the case of inflow predictions, this practice would dictate that it is often more efficient to spend resources characterizing the recharge (R), as even a poorly constrained R is likely to have orders of magnitude less uncertainty then a well constrained K, due to the log-normal behavior of the latter. Of course this assumes similar codependences exist between the inputs and output(s).

recharge percolating through approximately 150 to 180 m of waste rock before hitting the water table. Water then decants out of a low point at the north end of the pit.

Pump testing was conducted over a four-week interval that involved two weeks of active pumping followed by two weeks of recovery. Subsequent water extraction occurred over the following 72 days to support on-site dust suppression activity. Both phases of testing/extraction were monitored using downhole transducers and an inline flowmeter. The combined dataset allowed for a detailed calibration to the initial 28 days of testing, followed by validation to subsequent dust suppression activity.

Model Setup

Transient simulations were conducted using a two-dimensional groundwater model setup in FEFLOW v7.1 (update 4) (DHI, October 2017). The modelling domain was set to the boundaries of the backfilled pit, with decanting simulated using a constrained head (seepage) boundary. Recharge was set to the top and sides of the model using constant flux boundaries. Groundwater extraction was simulated using a variable rate, nodal flux boundary. Total runtimes were approximately 5s for a 1,000 node model.

Prior Information

Prior information was set based on published ranges for coarse gravel material and measured precipitation ranges at site (Table 3; Beale and Reed, 2013; Singhal and Gupta, 2010).

Table 3: Prior distributions used for Case Study II

Parameter	Minimum	Maximum	Units
Hydraulic conductivity	1×10^{-5}	1×10^{0}	m/d
Specific storage	1×10^{-6}	1×10^{-4}	s^{-1}
Specific yield	0.05	0.50	–
Recharge	37	3,700	mm/a

Stochastic Calibration

Stochastic calibration was conducted using the emcee 3.0.0 package available in Python (Foreman-Mackey et al., 2013). The library implements the affine-invariant ensemble sampler for MCMC proposed by Goodman and Weare (2010). The algorithm is advantageous over traditional MCMC approaches, as it requires hand-tuning of only a single parameter compared to N^2 for the traditional algorithm. Additionally, the emcee package facilitates parallel computing by simulating multiple walkers, or individual dependent Markov chains, speeding up overall runtimes by farming the expensive forward simulation setup to multiple cores and/or processors.

Stochastic calibration was set to match hydraulic head observations collected in two monitoring wells and the pumping well. This was done using 48 individual walkers, with progress monitored using the average integrated autocorrelation time (τ) across the ensemble. The integrated autocorrelation time is a measure of the number of steps required by a Markov chain to "forget" where it started (i.e. the number of steps required before an independent sample can be extracted from the chain). Sokal (1996) recommended that for traditional Markov chains, a minimum of 1,000 times the autocorrelation time be run. This is to minimize the statistical error in the MCMC analysis. In the case of the affine-invariant method this requirement can be reduced as multiple Markov chains, or walkers, are run in parallel. Foreman-Mackey (2017) found that for the emcee package, chains longer than 50 times the autocorrelation time were often sufficient. Results presented here-in used a 100 times cut-off to ensure minimal statistical error.

Results

Exploration of the uncertainty space indicates that model calibration to the four-week pumping test is highly dependent on the specific yield (S_Y) and recharge (R) parameters (Figure 3). This dependency allows for a reasonable level of statistical inference to be made on the underling populations, with a mean S_Y of 0.30 ± 0.08, and an R of 370 ± 130 mm/a (Table 4: Estimated). Extending the calibration for all 95 days of data (pumping test plus dust suppression activity) causes a 36% and 46% reduction in the R and S_Y uncertainty[3], respectively, with a S_Y of 0.30 ± 0.04, and an R of 370 ± 50 mm/a.

In comparison to R and S_Y, the model is found to be relatively independent of the simulated hydraulic conductivity (K) and specific storage (S_S). This suggests an overall poor statistical inference capacity, as indicated by the uniform distributions estimated for K and S_S (Figure 3). This secondary finding is counter intuitive to traditional pump testing, which typically aims to gain an understanding of the permeability of the groundwater system. The finding is also likely to be missed using traditional curve fitting which fails to fully explore the uncertainty space. This is demonstrated by the convergence of maximum likelihood estimates (MLE) in Figure 3 using the differential evolution algorithm in SciPy (Jones et al., 2014). While fits were obtained for the K and S_S using MLE, with the hindsight allowed by MCMC it can be seen that calibration is only to a local minimum. Without this hindsight, practitioners could easily be deceived by a false impression of calibration.

[3] Parameter uncertainty is measured using the standard deviation.

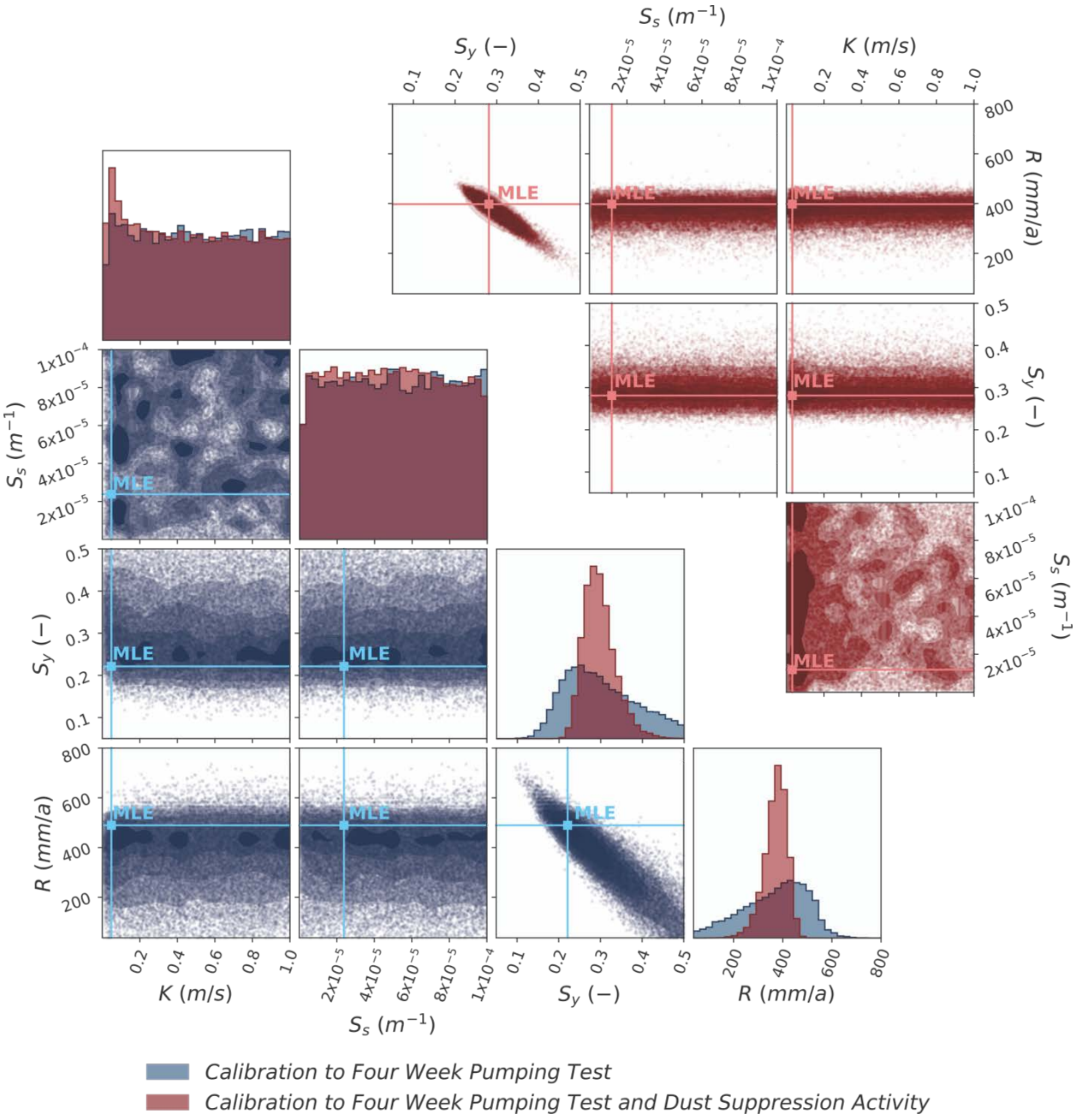


Figure 3: (Bottom-Left: Blue) Cross-plot of parameter uncertainty for calibration to four-week pumping test.
(Top Right: Purple) Extended calibration to four-week pumping test and subsequent dust suppression activity. Plots were generated using the corner.py library (Foreman-Mackey, 2016)

Table 4: Estimated parameter uncertainty in the specific yield and recharge

Statistic	Four week calibration		Three month calibration	
	Specific yield (–)	Recharge (mm/a)	Specific yield (–)	Recharge (mm/a)
Mean	0.30	367	0.30	371
Median	0.29	385	0.29	376
Maximum a posteriori	0.22	490	0.28	398
Standard deviation	0.08	129	0.04	47
Skewness	0.41	–0.42	0.81	–0.76
16th Percentile	0.21	223	0.26	327
84th Percentile	0.40	498	0.33	415

Validation

Validation of the transient calibration was conducted by comparing predictive forecasts with observed drawdown behaviour during subsequent groundwater extraction for dust suppression. The results demonstrate an overall good match between forecasts and actual drawdowns with long-term trends falling close to the mean simulation results (Figure 4).

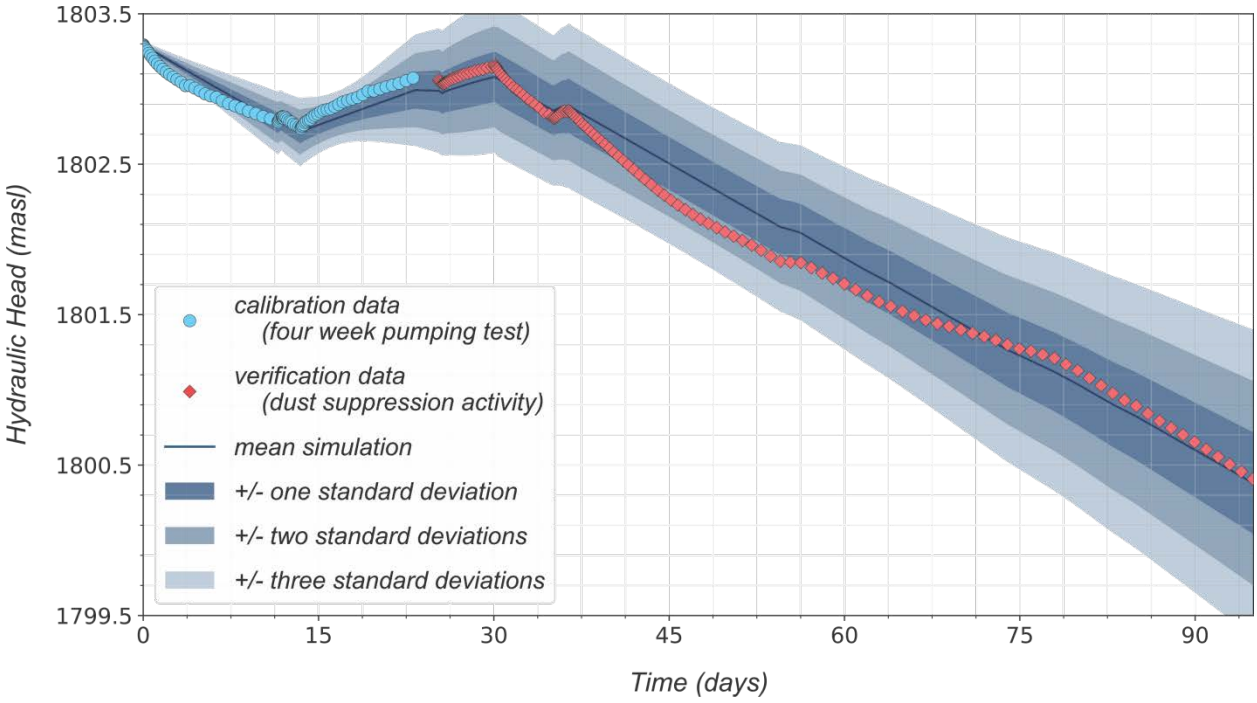


Figure 4: Comparison of predicted and actual drawdown following four-week pumping test

Discussion and Conclusions

Large uncertainties are an inherent property of mine designs, owing to the incomplete state of information. Despite this, decisions are often made based on singular "calibrated" models of the subsurface, close to the maximum likelihood event. However, as shown in Figure 1, if the consequences are non-linear the overall risk profile becomes dominated by tail events as opposed to the most likely event. To deal with this shortcoming, alternative Bayesian approaches are available, such as the MCMC techniques presented herein. The core of the approach is a move away from deterministic answers, and towards a probabilistic viewpoint, where both the inputs and outputs are treated as random variables described in terms of histograms and/or probability density functions (PDF) (Mosegaard and Tarantola, 2002).

This view requires a fundamental shift in the way problems are perceived by engineers and scientists. Instead of assuming that one plus one equals two, we should consider that uncertainty exists on our inputs, making the solution likely to be two, but also acknowledging the fact that it could be one or three, based on the concept that true values are random variables. This mode of thinking is often difficult for practitioners who like to think in terms of a base model, with sensitivities described by deviations from it. Unfortunately, this approach tends to cause us to assign too much weight to our base models, forgetting that they are simply interpretations of reality, and not reality itself. For example, it is not uncommon to have two geologists look at the same rocks, yet come to completely different interpretations. Instead of acknowledging that both interpretations may be equally likely and then subsequently moving forward with both models, we cling to our own base models and arbitrarily reject the possibility of the other. The alternative and more coherent approach is the probabilistic viewpoint, whereby we effectively assign a weight of near zero to any given model or hypothesis, and only after integrating the results of many interpretations can we begin to get a sense of the true behaviour of the system.

By integrating this probabilistic viewpoint with a Bayesian approach to science, we can begin to define a rigorous framework for mine design, which explicitly incorporates best engineering judgement through the use of prior distributions (Tarantola, 2005). For example, we can restrict the porosity of sand within our models using a uniform distribution to cover the published parameter range (Singhal and Gupta, 2010), or we can set priors based on the distribution of field test results, such as a log-normal distribution for hydraulic conductivity derived from packer tests. Although typically not formalized in mine design studies, use of best engineering judgement, or prior knowledge, is a common practice. For example, it is not uncommon for a hydrogeologist to expect to see a specific storage between 10^{-7} and 10^{-4} m^{-1} when reviewing a report, and to reject studies that deviate from this. The Bayesian approach simply aims to formalize these priors within a sound probabilistic framework (Savage, 1954).

The formalization and subsequent documentation of all components of the analysis is essential, as it improves the overall ability to review and critique a design report. This is critical, as probability estimates generated from Bayesian approaches are subjective assessments of the current state of information. The documentation therefore allows for an independent review of the assessment and decisions/judgements derived from it. Criticisms of the Bayesian approach often key in on the subjective interpretation of probability. While a fair critique, it is often difficult, if not impossible, to fully remove subjectivity from probability estimates (de Finetti, 1937 [1989]; de Finetti, 1970). This is due to the various assumptions and/or choices that need to be made during any scientific study or engineering design report (Freeman, 1995). For example, there is the choice of numerical model, applied error metric (Gaussian, Laplacian, etc.), key parameters to simulate/measure, underlying physics (Newtonian, special relativity), etc. While the goal of any study should be to minimize the subjectivity, and arrive at purely objective assessments of the probability, it must be acknowledged that limits exist in how much subjectivity can be removed[4]. Instead of outright rejection of probability measures because of this subjectivity, we should instead embrace it, and simply view probability estimates as models of our incomplete understanding of a problem. If this treatise is accepted then probability estimates become viewed in a new light, as simple decision tools used to ease the burden of risk managers, but fully fallible to irreducible modelling errors that must be considered.

Acknowledgements

This research was supported by SRK Consulting (Canada) Ltd. The author would like to thank Jennifer Mayer, Victor Munoz, Ray Yost, Neil Winkelmann, Aaron Fultz, and Nancy Snowden for their reviews of the abstract and/or manuscript. In addition, thanks to Michael Royle, Dan Mackie, Daryl Hockley, and Gregory Fagerlund for their support and guidance in the use of probabilistic methods to solve numerical modeling problems. Finally, the author would like to thank the anonymous reviewers for their helpful comments.

References

Beale, G. and Reed, J. 2013. *Guidelines for Evaluating Water in Pit Slope Stability.* Collingwood: Csiro Publishing.

De Finetti, B. 1937 [1989]. La Prévision: Ses Lois Logiques, Ses Sources Subjectives. *Annales Del'institut Henri Poincaré,* 7:1–68. Translated into English as Probabilism: A critical essay on the theory of probability and on the value of science, *Erkenntnis,* 31: 169–223.

[4] Purely objective probability estimates may be possible when a frequentist interpretation of probability can be applied (i.e. when a repeatable experiment can be conducted and its central tendency estimated). The problem arises when frequentist approaches are applied to non-repeatable experiments, such as one-off mining studies, which often require that subjective assumptions and/or choices be made during analysis.

De Finetti, B. 1970. *Theory of Probability.* New York: Wiley.

Freeman, D. 1995. Some issues in the foundation of statistics, *Found Sci.,* 1: 19–39.

Foreman-Mackey, D., Hogg, D.W., Lang, D. and Goodman, J. 2013. Emcee: The MCMC Hammer, *Publ Astron Soc Pac.,* 125(925): 306. Doi: 10.1086/670067.

Foreman-Mackey, D. 2016. Corner. Py: Scatterplot matrices in Python, *J Stat Softw.,* 1(2): 14.

Foreman-Mackey, D. 2017. Emcee documentation: Autocorrelation analysis and convergence. Retrieved January 9, 2018 from: Github.Com/Dfm/Emcee/Blob/Master/Docs/Tutorials/Autocorr.Rst

Goodman, J. and Weare, J. 2010. Ensemble samplers with affine invariance, *Comm App Math Com Sc.,* 5(1): 65–80.

Hogg, D.W., Bovy, J. and Dustin, L. 2010. Data analysis recipes: Fitting a model to data, Arxiv preprint. Arxiv:1008.4686

Jasechko, S., Birks, S.J., Gleeson, T., Wada, Y., Fawcett, P.J,. Sharp, Z.D., McDonnell, J.J. and Welker, J.M. 2014. The pronounced seasonality of global groundwater recharge, *Water Resour Res.,* 50: 8845–8867.

Jones, E., Oliphant, T. and Peterson, P. 2014. Scipy: Open source scientific tools for Python. Retrieved January 1, 2018 from: Www.Scipy.Org

Kruseman, G.P. and De Ridder, N.A. 1994. *Analysis and Evaluation of Pumping Test Data.* 2nd Ed. The Netherlands: International Institute for Land Reclamation and Improvement.

Metropolis, N., Rosenbluth, A.W., Rosenbluth, M.N., Teller, A.H. and Teller, E. 1953. Equation of state calculations by fast computing machines, *J Chem Phy.,* 21: 1087–1092.

Mosegaard, K. and Tarantola, A. 2002. Probabilistic Approach to Inverse Problems, *Int Geophys,* 81(A): 237–268.

Mosegaard, K. and Tarantola, A. 2005. Monte Carlo sampling of solutions to inverse problems, *J Geophys Res.,* 100(B7): 12431–12447. Doi:10.1029/94jb03097.

Savage, L.J. 1954. *The Foundations of Statistics.* New York: Wiley.

Shonkwiler, R.W. and Mendivil, F. 2009. *Explorations in Monte Carlo Methods*. New York: Springer.

Singhal, B.B.S. and Gupta, R.P. 2010. *Applied Hydrogeology of Fractured Rocks*. 2nd Ed. New York: Springer.

Sokal, A.D. 1996. *Monte Carlo Methods in Statistical Mechanics: Foundations and New Algorithms*. Cours De Troisi`Eme Cycle De La Physique En Suisse Romande.

Taleb, N. 2005. *Fooled by Randomness: The Hidden Role of Chance in Life and in the Markets.* 2nd Ed. New York: Random House.

Taleb, N. 2010. *The Black Swan: The Impact of Highly Improbable.* 2nd Ed. New York: Random House.

Taleb, N. 2014. *Antifragile: Things That Gain from Disorder.* New York: Random House.

Tarantola, A. 1987. *Inverse Problem Theory: Methods for Data Fitting and Model Parameter Estimation.* New York: Elsevier.

Tarantola, A. 2005. *Inverse Problem Theory and Methods for Model Parameter Estimation.* Philadelphia: Society for Industrial and Applied Mathematics.

Vanderplas, J. 2014. *Frequentism and Bayesianism: A Python-Driven Primer*. Arxiv preprint. Arxiv:1411.5018.

Proceedings of Mine Water Solutions 2018
June 12–15, 2018, Vancouver, Canada
Published by the University of British Columbia, 2018

Novel Use of the Westbay System to Characterize Deep Hydrogeology for a Proposed Underground Coal Mine

Tyler Gale, ERM Consultants Canada Inc., Canada
Piotr Rzepecki, ERM Consultants Canada Inc., Canada

Abstract

A deep hydrogeology site investigation was recently completed for a proposed underground coal mining project in north-eastern British Columbia. Central to the study was the installation and operation of two MP38 Westbay Multilevel Groundwater Monitoring System Completions (Westbay Systems™), one 980 m long and the other 716 m long. Innovative uses of the Westbay Systems provided for efficient hydraulic testing and collection of groundwater samples.

Shut-in methods were used to conduct hydraulic tests in lower hydraulic conductivity zones in the Westbay Systems. A theoretical foundation for shut-in testing has been established in the literature, and in this article we describe an adaption of this theory for use in the plastic Westbay System. Performing hydraulic tests under shut-in conductions allowed estimation of hydraulic conductivity over a range from 10^{-8} m/s to 10^{-12} m/s in a small fraction of the time required under open-water column conditions.

The primary challenge with the collection of groundwater samples in deep boreholes is the level of effort required to remove drilling circulation fluid first. In our study, we made use of the natural vertical hydraulic gradient to purge drilling fluid from borehole intervals near the depth of mining into a shallower "dump" zone. The purging process occurred without operational or maintenance needs for several weeks, followed by collection of depth-representative groundwater samples. The deep groundwater was shown to have elevated salinity, which resulted in mine inflow water quality being a significant consideration in discharge water quality predictions and site water-management planning.

Introduction

Characterizing the groundwater system deep underground represents a challenge for proposed mines. Measuring hydraulic conductivity and collecting representative groundwater samples may be time consuming, expensive, and prone to technical and logistical challenges. In this paper we present uses of the Westbay System that provide solutions to mitigate the challenges of collecting hydraulic conductivity measurements and groundwater samples at depths of 500 to 1000 m.

Problem #1: Collecting Accurate Low Hydraulic Conductivity Measurements

The common practice at mineral exploration and mining sites to collect hydraulic conductivity (K) measurements is to use packer systems with the support of a diamond drill. The use of packer systems to estimate K encounters practical limitations where K is low (less than about 1×10^{-9} m/s), for reasons such as the following:

- Packers sometimes cannot inflate to seal the zone properly (often referred to as hydro-locking);
- Slug tests in open drill rods take very long to attain recovery (e.g., several days at 10^{-9} m/s); and
- Injection (Lugeon) tests take very long to attain stabilized pressures and flow rates.

Where low K zones are encountered in a commercial setting, the practical alternative is to report K as the lower limit of measurability of the test equipment for a maximum test duration of a few hours (e.g., "$< 1 \times 10^{-9}$ m/s" might be reported if a 90% recovery cannot be attained within a 12-hour work shift).

Accurate measurements of K are often required below the practical lower limit of measurability of packer equipment. For example, calibration of a groundwater flow model used to predict mine inflow may require a defensible estimate of K for a tight bedrock formation that acts as an aquitard. Where investigators cannot quantify low K, they often make conservative assumptions, which in turn may lead to high mine inflow estimates and subsequently expensive infrastructure requirements to obtain permits and plan construction.

In this paper we present a method for estimating K of tight formations using shut-in tests with the Westbay System. The use of shut-in methods has been established in the literature as a means of obtaining K measurements in a fraction of the time required in an open standpipe column (e.g., Bredehoeft and Papadopulous, 1980). Although shut-in testing using the Westbay System has been in practice for some time, a detailed methodology has not been presented for review and discussion among the technical community (to the best of the authors' knowledge).

This paper does not attempt to present a complete rationale for installation of the Westbay system as an alternative to the use of packer equipment. There are many factors to consider in a planning-phase cost/benefit assessment.

Problem #2: Collecting Representative Groundwater Samples

Regulatory agencies are increasingly expecting robust groundwater quality datasets that include samples collected at the full range of depths planned for extraction for a proposed mine. This requirement is founded on the need for defensible predictions of discharge water quality. The quality of mine inflow groundwater should be an input to the site surface water quality model.

Groundwater tends to be more saline at greater depth. In many jurisdictions parameters tied to salinity (e.g. sodium, chloride, sulphate, barium, lithium) are assigned discharge water quality limits. As

such, deeper mines are more likely to be required to plan more involved management mechanisms for inflow water. These management mechanisms come with a cost that may be large enough to affect the findings of a feasibility study.

Groundwater samples are often not collected at proposed mine sites during the feasibility study process, largely because of the required level of effort and cost. Where samples are collected, diamond drill packer equipment is typically used.

The volume of water that must be purged from a drill-supported packer zone before a representative groundwater sample can be collected is typically large (see example in Table 1). In practical terms, at depths of 500 m to 1,000 m, collecting a representative sample is only possible in a reasonable amount of time (e.g., a few days) where hydraulic conductivity is high and the water level is close to ground surface. A diamond drill must be present on site to support the drill rod and packer assembly throughout the sample collection process.

Table 1: Estimated purge volumes for borehole depths of 500 m to 1,000 m

Hole Depth (m)	Estimated purge volume (L)	
	HQ	NQ
500	5,000	3,000
750	7,300	4,300
1,000	9,700	5,800

Estimated purge volume assumes two times the volume of: (1) the rod stem and (2) a 30 m long packer zone at the bottom of the hole

In this paper we present a case study in which the Westbay System was used to purge drill fluids using the natural vertical hydraulic gradient present in the formation. This approach can be applied to collect groundwater samples where K is lower (e.g., 10^{-7} to 10^{-9} m/s) and the vertical hydraulic gradient is relatively strong.

Background

Study Site

The study presented herein is a by-product of a project to support regulatory permitting for a proposed coal-mining site (the "Site"). The Site is located in north-eastern British Columbia, Canada, in the eastern foothills of the Rocky Mountains. Ridgetop elevations range as high as 1,800 m, while valley bottom elevations are as low as 650 m. The landscape is covered with coniferous forest, interrupted by clearcut logging, coal extraction, and natural gas development.

The extensive coal deposits in the region are often referred to collectively as the Peace River Coalfield. The stratigraphic column observed in core recovered during exploration drilling consists of formations belonging to the Lower Cretaceous Fort St. John Group (Figure 1). The rock has been subjected to folding and faulting, as characterized via exploration drilling and seismic refraction surveys (Figure 2). The coal deposits targeted for extraction are located at depths ranging from 500 to 1,100 m below ground surface (mbgs), corresponding with elevations ranging from 200 to 450 m (Canadian Geodetic Vertical Datum, 1928).

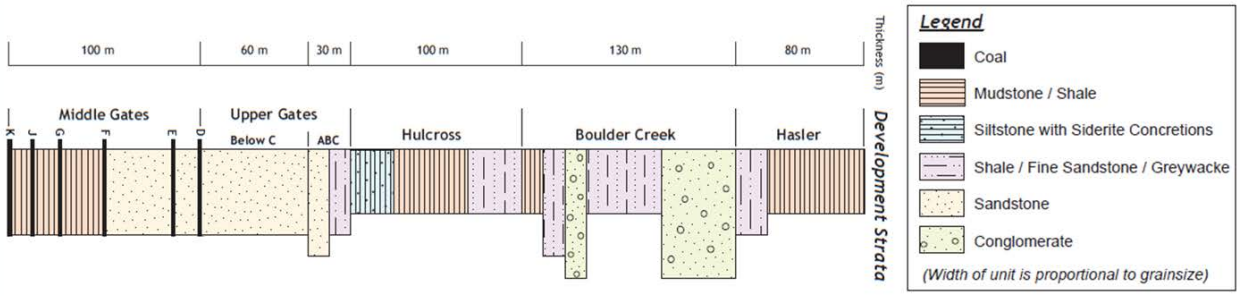


Figure 1: Typical stratigraphic column at the Site

Borehole Drilling and Hydrogeological Data Collection

Westbay systems were installed in two boreholes at the Site: DH-01 and DH-02 (Figure 2). Boreholes were drilled using diamond-drilling methods. Water for circulation was sourced from nearby surface water. Drilling water was re-circulated using a series of sumps. Commonly used polymer additives were mixed with the water. Core was recovered using a triple tube core barrel assembly.

Core logging was conducted at the drill site, with an emphasis on characterizing fracture properties. Wireline geophysical surveys were conducted following completion of drilling, including indicators of coal seam properties such as density, and indicators of fracture properties including dipmeter, calliper, and acoustic televiewer. The geophysical and rock core logs were used to inform design of the packer locations along the Westbay System Completions.

Static water levels observed as drilling advanced indicated a very large drop in hydraulic head with depth. In particular, a static water level of 385 mbgs was measured when circulation of drilling fluid was completely lost at a depth of 710 mbgs in DH-01. The decrease in hydraulic head with depth reflects the downward flow of groundwater expected in high elevation areas in mountainous terrain.

The difference in hydraulic head across a Westbay system installation must be less than 200 m to comply with pressure ratings of coupling seals at joints in the casing. Drill casing was grouted in to the upper 500 m of DH-01 and upper 300 m of DH-02, to seal off the higher-head shallow zones so that the Westbay systems could be installed and operated within allowable specifications with access to the lower half of the holes.

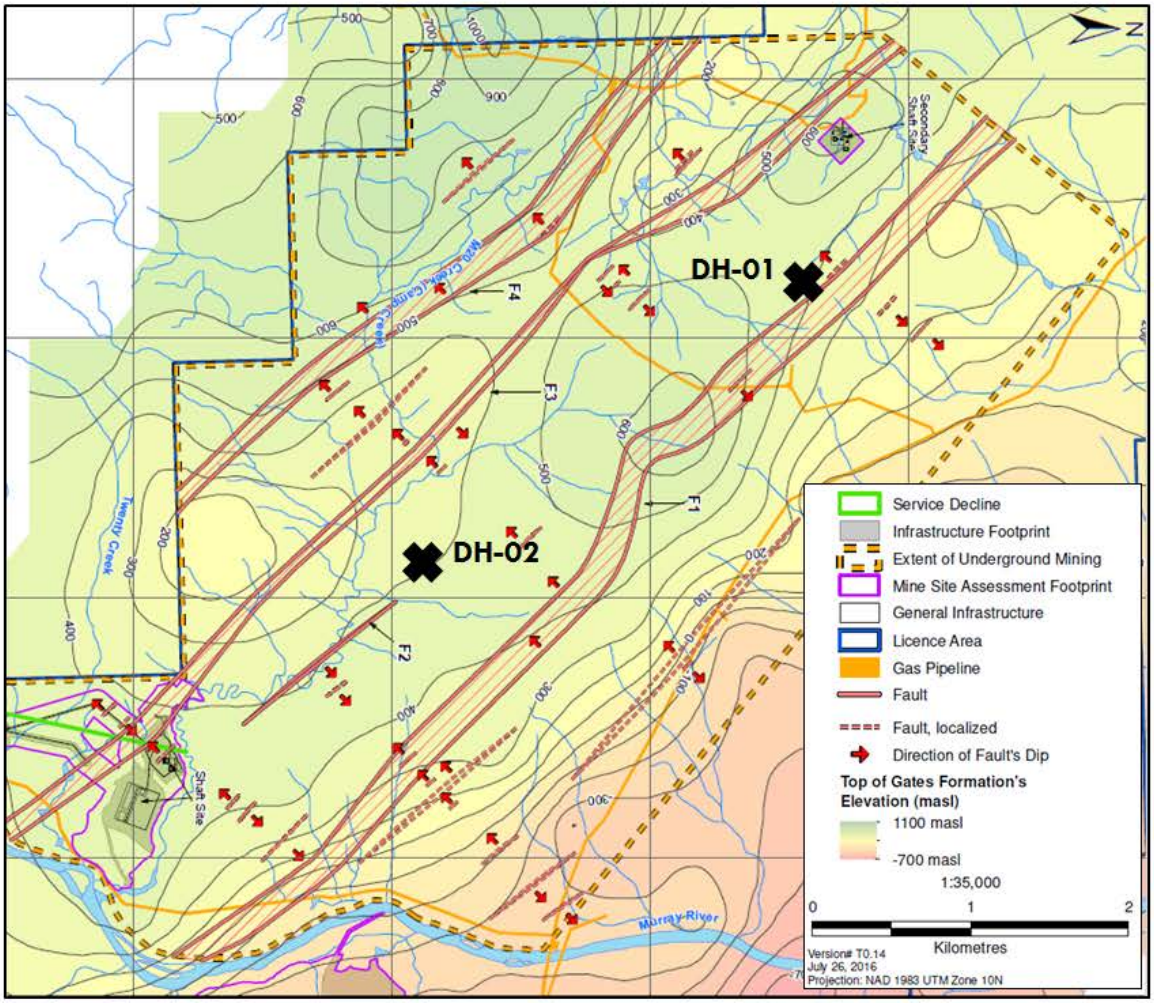


Figure 2: Locations of DH-01 and DH-02 Boreholes with geologic setting

Westbay System Installations

A complete description of the Westbay System is presented in Black et al. (1986).

MP38 Westbay System completions were installed in each of DH-01 (980 m long casing with 21 zones) and DH-02 (716 m casing, 16 zones). Target depths of Westbay System components (packers, measuring ports, and pumping ports) were designed based on the hydrogeological data collected from the boreholes. Intervals of the borehole with evidence of higher K were identified, and packer positions were selected along the intervals of competent rock nearest to these intervals. This approach created relatively short zones along intervals of inferred higher K. These shorter zones helped to minimize the purging volumes required to collect samples, and provided for a more accurate delineation of potential preferential flow pathways. The result was a series of short (about 5 to 15 m long) and long (about 30 to 100 m long) zones, whereby the shorter zones isolated inferred intervals of elevated K and the longer zones spanned the rock mass inferred to be tighter.

Shut-in Tests

The theoretical foundation for analysis of shut-in tests is documented in Bredehoeft and Papadopulos (1980), Neuzil (1982), and Hayashi et al. (1987). Bredehoeft and Papadopulos (1980) developed field and analytical methods to estimate K based on shut-in tests conducted in a packer-isolated interval. The packer zone is pressurized and rapidly shut in, and the pressure recovery is monitored. Analysis is conducted using the method of Cooper et al. (1967); however, the casing radius (the interval of standpipe in a slug test over which the water level response occurs) used in Cooper et al. (1967) is replaced with the right-hand side of equation 1. This approach simulates an imaginary casing, within which the hydraulic response occurs. This imaginary casing has a radius that is calculated using the volume of the test zone and the modulus of compressibility of the water, which governs its change in volume in response to changing pressure.

$$r_c^2 = V_w C_w \rho_w \mathrm{g}/\pi \qquad \text{Equation 1}$$

where:

r_c is the casing radius,

V_w is the volume of water in the shut-in zone,

C_w is the compressibility of water, and

ρ_w is the density of water.

Methods

Shut-in Testing

Shut-in tests were performed by extracting a volume of water from the test interval using the Westbay MOSDAX sampler probe. The test procedure included the following steps:

1. Assemble test equipment and lower it inside the Westbay casing. Down-well equipment includes a MOSDAX sampler probe connected to a 250 mL bottle with an interconnect hose, and a coil-tube flow restrictor upstream of the bottle.
2. Land the probe at the measuring port of the zone targeted for testing (the test zone).
3. Record the pressure inside the Westbay casing before beginning the test.
4. Seal the probe into the measuring port and record static pressure in the zone.
5. Begin recording pressures (one second intervals) with laptop connected to the MOSDAX controller.
6. Open the probe valve, allowing water to be directed from the test zone, through the sampler probe, and into a connected bottle (cause initial displacement).

7. Close the probe valve when measured pressure has dropped by up to 50 psi (typically a few seconds).
8. Continue recording pressure until it recovers 90% from initial displacement to static pressure.
9. Terminate recording, disconnect the probe from the port, record pressure inside Westbay casing.
10. Recover the down-well equipment at ground surface, measure volume of water in the bottle.

In the authors' experience, the pressure exerted on the Westbay casing when collecting water from deep, low-K zones using the MOSDAX sampler can exceed the operating pressure limit for coupling seals and possibly plastic casing. The result can be leakage from inside the Westbay casing into the test zone, and possibly plastic deformation of the Westbay casing. In our study, a coil tube flow restrictor (supplied by Westbay Instruments) connected in the fluid flow path served to prevent excessive stress on the Westbay casing and its sealed couplings. The flow restrictor acted to reduce the initial pressure drop in the test zone, which occurs in response to exposing the test zone to the initial atmospheric pressure in the bottle.

The approach we used to simulate the imaginary casing in a shut-in Westbay zone is founded on the method of Bredehoeft and Papadopulos (1980), with two adaptions.

First, the radius of the imaginary casing is determined empirically by observing the initial displacement in the zone and the volume of water withdrawn from the zone to cause the initial displacement (Equation 2). This empirical estimation is used because the Westbay System materials in contact with the water are expected to have moduli of compressibility that are not negligible. Developing a theoretical equation to assign a bulk modulus of compressibility for the plastic Westbay casing and urethane packers, in addition to the water, was assessed to be outside the scope of this study due to the complexity imposed by the irregular shapes of the solid components (perhaps a study for future consideration).

$$r_i^2 = \frac{V}{\pi \Delta H_i} \qquad \text{Equation 2}$$

where:
V is the volume of water recovered following the test,
ΔH_i is the observed initial displacement, and
r_i is the imaginary casing radius.

Second, analysis to estimate K was conducted using the methods of Hyder et al. (1994; often referred to as the Kansas Geological Survey Model, or KGS model) and Hvorslev (1951). The KGS model was used as an alternative to Cooper et al. (1967; used by Bredehoeft and Papadopulos, 1980) to

allow for partial penetration and non-radial flow. The method of Hvorslev (1951) was used to compare the results to one of the commonly used quasi-steady state solutions and examine its applicability.

Assumptions applicable to the analysis of slug tests in open water columns are applicable to shut-in tests as well. Specifically, the method of Hyder et al. (1994) assumes the tested zone represents a homogeneous medium with infinite aerial extents and a uniform thickness. Test initiation is assumed to be instantaneous. The method of Hvorslev (1951) makes an additional assumption that recovery is not influenced by change in storage.

The approach used to estimate the imaginary casing radius assumes the moduli of compressibility of the water and materials contacting it in the test zone are static over changing pressures. The calculated imaginary casing radius captures the compressibility of the water and contacted materials integrated over the pressure range from static to initial displacement.

Shut-in tests were performed at 16 Westbay zones: ten in DH-01 and six in DH-02. Most tests were allowed to proceed for up to two hours if 85% to 90% recovery was not achieved sooner. A few tests were set up to record overnight and allowed to proceed for as long as 24 hours.

Solutions to the Hvorslev (1951) and Hyder et al. (1994) models were obtained using the AQTSOLV™ software package.

DH-01 Groundwater Sampling

Collecting deep groundwater samples from Westbay Systems is often presented with the following challenges:

- K is low, resulting in rapid water level drawdown and pumping that cannot be sustained at a flow rate that would allow quick purging;
- Options available on the market to displace water from a 38 mm diameter pipe are limited; and
- Large volumes of water must be displaced to remove drilling fluid from the test zone.

Conditions at DH-01 were particular challenging for sample collection due to the very deep natural water level: the water level in DH-01 Westbay zones ranged from 280 to 378 mbgs.

To minimize the effort required to purge drilling fluid in DH-01, the natural vertical hydraulic gradient was used to move the fluid from zones targeted for sampling (Sample zones) to a “dump” zone (Figure 3). Two sample zones were identified, with depths of 943 mbgs (Zone 3) and 915 mbgs (Zone 6) near the coal seams. A suitable receiving zone (“dump zone”) was identified at a depth of 710 mbgs, characterized by lower water level (potentiometric elevation) than the sample zones and relatively high K.

The field procedure included the following steps:

1. Open pumping ports at sample and dump zones. Conduct diagnostics to confirm ports are open.

2. Remove MOSDAX equipment from the well. Return to site after a few weeks.
3. Close the pumping ports at the sample zone and the dump zone. Conduct standard diagnostic measurements to confirm pumping ports are closed.
4. Use the MOSDAX sampler to collect a sample from the measuring port at the sample zone.
5. Repeat steps 1 to 4 for another sample zone.

Water was allowed to flow under the introduced hydraulic gradient when pumping ports were open at both the dump and sample zone (Figure 3). The introduced hydraulic gradient directed water into the Westbay casing from the sample zone, upwards inside the Westbay casing, and out into the formation at the dump zone.

A series of control samples were collected to characterize the drilling fluid prior to commencing the purging effort. These included samples of the fluid circulated while drilling, and samples from the Westbay zones targeted for sampling after installation. Given that water was being re-circulated while drilling, the control samples contained unknown proportions of groundwater entrained in the borehole, polymers used in preparation of drilling fluid, constituents leached off cuttings, and the water trucked in from nearby sources. These samples were analyzed for anions and metals.

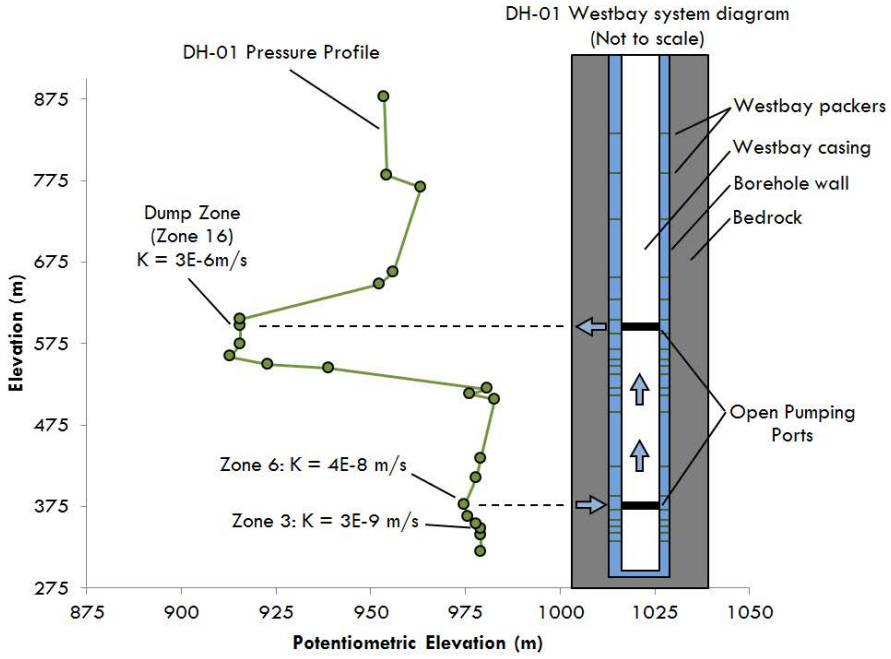


Figure 3: Illustration of method used to displace fluid from sample zones to dump zone

Samples were collected using the MOSDAX sampler probe and stainless steel Westbay bottles. Final groundwater samples were collected for analysis of anions, metals, nutrients, hydrocarbons, and

common hydrochemical tests. Water was transferred into sample bottles upon recovery at ground surface and preserved according to standard methods.

Results

Shut-in Tests

Adequate data for hydraulic conductivity analysis were collected from 13 of 16 shut-in tests (Table 2). The other three tests had very low hydraulic conductivity, and recovery did not progress adequately before the tests were terminated.

Table 2: Summary of shut-in test results

Westbay Zone	Depth (mbgs)	Δh_i (m H_2O)	Test Duration	Recovery	V (mL)	r_i (mm)	K (m/s)		K using eqn. 1 (m/s) [B]
							Hvorslev	KGS	
DH-01									
2	950.0 – 970.7	16.9	20 min	90%	150	1.68	2.E-10	2.E-10	5.E-11
3	942.7 – 949.4	13.2	12 min	90%	60	1.2	1.E-09	3.E-09	6.E-11
5	928.2 – 937.0	22.4	3 min	100%	101	1.2	1.E-08	1.E-08	2.E-10
7	866.0 – 913.4	32.6	2 hrs	85%	229	1.49	1.E-11	4.E-12	5.E-13
9	784.8 – 855.4	15.1	2 ½ hrs	40%	88	1.36	Note A	–	–
11	771.9 – 777.0	64.7	20 hrs	25%	64	0.56	Note A	–	–
12	746.0 – 770.9	46	24 hrs	55%	100	0.83	Note A	–	–
14	732.2 – 740.5	37.3	1 ½ hrs	85%	70	0.77	2.E-11	2.E-11	2.E-12
17	651.4 – 693.0	20.3	1 ½ hrs	85%	108	1.3	3.E-11	2.E-11	1.E-12
18	643.7 – 650.4	45.6	23 hrs	85%	51	0.6	2.E-12	1.E-12	2.E-13
DH-02									
3	654.4 – 661.7	92.9	1½ hrs	90%	196	0.82	3.E-09	2.E-09	9.E-11
5	632.3 – 639.6	35	2 hrs	90%	85	0.88	5.E-12	2.E-12	4.E-13
7	609.0 – 615.4	24.2	5 min	85%	80	1.03	9.E-09	8.E-09	2.E-10
10	523.8 – 532.7	55	30 min	85%	111	0.8	1.E-09	1.E-09	9.E-11
11	511.6 – 522.8	27.3	20 min	85%	130	1.23	1.E-11	9.E-10	3.E-11
15	350.9 – 391.1	27.2	50 min	85%	295	1.86	2.E-10	2.E-10	2.E-11

[A] Response data not adequate to estimate K

[B] Analyses conducted with KGS model

ΔH_i = initial displacement

V = volume of water removed from test zone to cause initial displacement

r_i = imaginary casing radius (equation 2)

The imaginary casing radii ranged from 0.5 mm to 2 mm, as calculated using the initial displacement and volume of water recovered (Equation 2). If we were to assume that water is the only

compressible material causing the observed response, the imaginary casing radii would be 0.17 mm to 0.73 mm (calculated with bulk modulus of 2.25 GPa at 1,000 psi and 20 °C, equation 1). The lower imaginary casing radii calculated using equation 1 indicate elastic deformation of the Westbay casing and packers is part of the response. Hydraulic conductivity values were analyzed using the radii calculated with equation 1, and gave values around one order of magnitude lower (units of m/s) than those calculated using equation 2.

Response data from shut-in tests tended to fit the type curves of Hyder et al. (1994) better than the Hvorslev (1951) solution (Figure 4); however, there was consistency in the estimated hydraulic conductivity between the two analysis methods. The greatest deviation of the K estimated between the two analysis methods was for DH-01 Zone 7, for which Hvorslev (1951) estimated a K about half an order of magnitude greater than the KGS model.

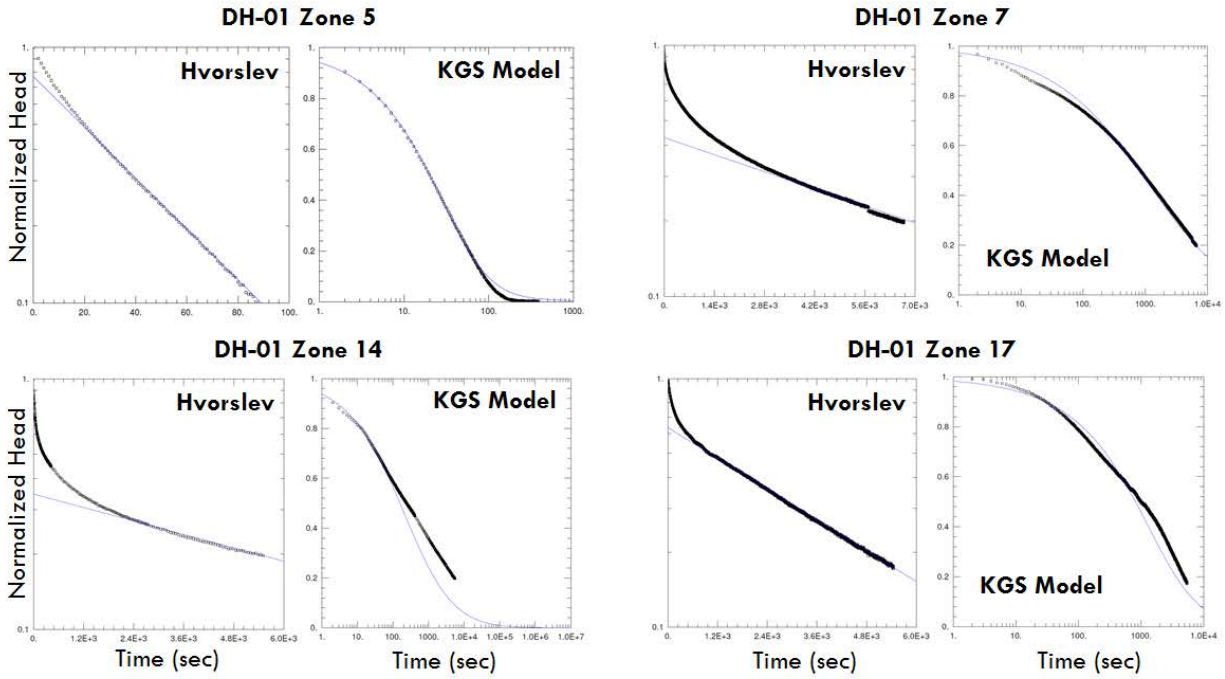


Figure 4: Response data analysis results for select shut-in tests

Response data have a distinct concave-up shape when plotted as log head vs. time. A concave-up response is typically expected due to elastic storage in the formation (Butler 1998). However, the concavity appears to be more pronounced than response data for slug tests conducted in open water columns. This additional concavity may be a result of pressure-dependent (variable) moduli of compressibility for the water and materials in contact with it.

We found a practical lower limit of measurability to be approximately 10^{-12} m/s, corresponding with a test duration of up to 24 hours. This is regarded as a "practical" lower limit due to the amount of time

required for the test to proceed to adequate recovery for estimation of K. The upper limit of measurability was found to be approximately 1×10^{-8} m/s. For hydraulic conductivity greater than 1×10^{-8} m/s, recovery proceeds too rapidly for the MOSDAX system response time to adequately capture early time data. An attempt to conduct a shut-in test in a zone with K of 1×10^{-7} m/s was aborted because water was not able to pass through the flow restrictor at a rate that generated a measurable initial displacement. This zone was later tested using the pumping port and the Westbay casing to conduct an open water column slug test.

Open water column slug tests conducted over the practical range of measurability we observed for the shut-in tests would have durations ranging 10 hours (1×10^{-8} m/s), to 3.5 days (1×10^{-9} m/s), to one month (1×10^{-10} m/s), and greater (assumed casing diameter of 1.5 inches).

Deep Groundwater Quality

Purging under the natural vertical hydraulic gradient successfully removed the drilling fluid from DH-01 Westbay zones 3 and 6. Inspection of a ternary diagram (Figure 5) shows a distinct contrast between control and groundwater samples, as well as groundwater samples collected six months apart (with continued purging) with consistent hydrochemistry. Samples from discrete seepage zones in an active decline were also collected, and had hydrochemistry consistent with the DH-01 samples where they were collected at similar depths.

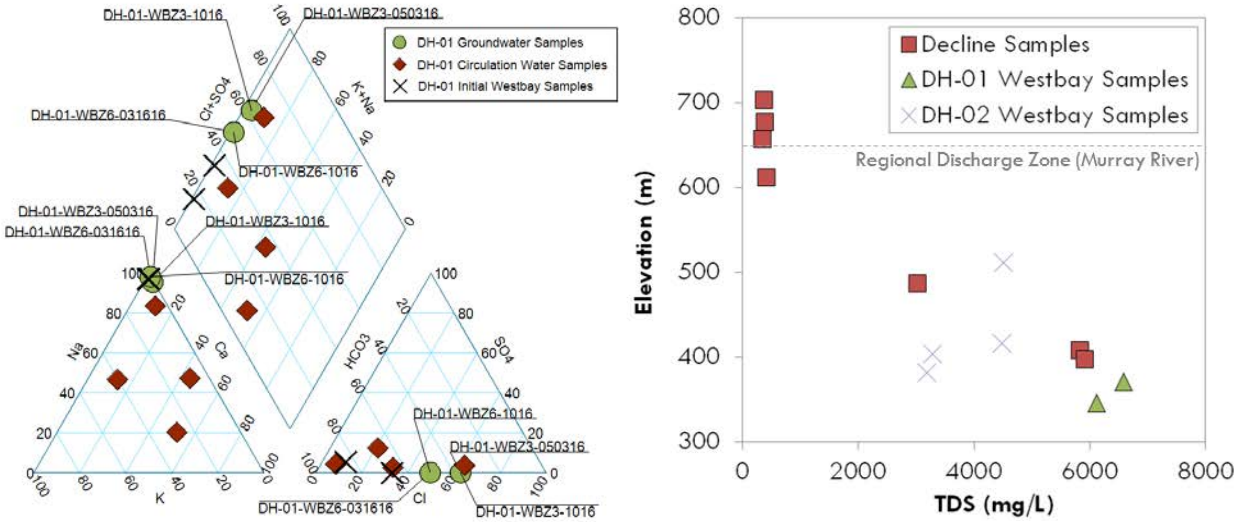


Figure 5: Deep groundwater quality. Left: Control and groundwater samples collected from DH-01 Zones 3 and 6. Right: Dissolved solids vs. elevation

Samples collected from the Westbay systems were used to characterize deep groundwater quality for the proposed mine (Table 3). A trend of increasing salinity with depth was identified, with total dissolved solids (TDS) ranging up to 6,600 mg/L over the depth of investigation (Figure 5). Tied to the elevated

salinity were concentrations of chloride and barium that exceeded the British Columbia Water Quality Guidelines for Freshwater Aquatic Life (BC Ministry of Environment 2017). Concentrations of chloride exceeded the guideline by multiples of 5 to 17, and concentrations of barium by multiples of 7 to 60. These findings have been used to examine the potential effects of mine inflow on discharge water quality, and to inform mine water management planning.

Table 3: Physical parameters, anions, and metals concentrations in deep groundwater samples

Analyte	No. (>DL)	Concentration Mean (Min–Max)	Analyte	No. (>DL)	Concentration Mean (Min – Max)
TDS	9 (9)	4,774 (3,030 – 6,590)	Cr	9 (5)	0.0015 (<0.00050 – 0.00301)
pH (field)	9 (9)	7.7 (7.27 – 8.22)	Co	9 (0)	(<0.00050 – <0.0010)
HCO_3 [A]	9 (9)	2,130 (1560 – 3015)	Cu	9 (0)	(<0.0010 – <0.0020)
NH_3 (as N)	9 (9)	2.0 (0.87 – 4.88)	Fe	9 (9)	3.7 (0.098 – 10.8)
Br	9 (6)	2.5 (<2.5 – 4.45)	Pb	9 (0)	(<0.00025 – <0.00050)
	9 (9)	1,520 (784 – 2555)	Li	9 (9)	2.5 (0.495 – 5.70)
F	9 (2)	0.63 (<1.0 – 1.33)	Mg	9 (9)	16 (4.85 – 26.3)
NO_3 (as N)	9 (0)	(<0.10 – <0.25)	Mn	9 (9)	0.022 (0.00128 – 0.0712)
NO_2 (as N)	9 (0)	(<0.020 – <0.050)	Hg	9 (1)	3.3E-06 (<5.0E-6 – 9.4E-6)
N, Total	9 (9)	6.2 (1.23 – 10.4)		9 (7)	0.0045 (<0.00025 – 0.0177)
PO_4 (as P)	8 (7)	0.047 (<0.010 – 0.0895)	Ni	9 (1)	0.0021 (<0.0025 – 0.0029)
P, Total		0.099 (<0.019 – 0204)	P	9 (0)	(<0.60 – <0.90)
SO_4	9 (0)	(<6.0 – <15)	K	9 (9)	16 (3.03 – 38.6)
S, Diss.	3 (3)	0.050 (0.023 – 0.075)	Se	9 (0)	(<0.00025 – <0.00050)
Al	9 (6)	0.073 (<0.0050 – 0.387)	Si		5.6 (3.42 – 8.88)
Sb	9 (2)	0.00071 (<0.00050 – 0.0029)	Ag	9 (0)	(<0.000050 – <0.00010)
As	9 (5)	0.0026 (<0.00050 – 0.0154)	Na	9 (9)	1757 (1080 – 2370)
Ba	9 (9)	28 (6.71 – 53.9)	Sr	9 (9)	7.44 (1.88 – 12.5)
Be	9 (0)	(<0.00050 – <0.0010)	Sn	9 (1)	0.00045 (<0.00050 – 0.00079)
Bi	9 (0)	(<0.00025 – <0.00050)	Ti	9 (0)	(<0.020 – <0.030)
B	9 (9)	0.38 (0.219 – 0.825)	U	9 (5)	0.00010 (<0.00005 – 0.00029)
Cd	9 (0)	(<0.000025 – <0.000050)	V	9 (0)	(<0.0025 – <0.0050)
Ca	9 (9)	42 (9.82 – 79.0)	Zn	7 (6)	0.060 (<0.0050 – 0.153)

No. = number of samples

DL = analytical detection limit

Mean calculated for analytes with one or more samples above detection limit, using half detection limit for samples below it.

"<" indicates concentration below analytical detection limit

All concentrations units of mg/L except pH

[A] HCO_3 concentration reported as $CaCO_3$

Conclusions

Hydrogeological data were collected from two MP38 Westbay systems using innovative methods that minimized the level of required effort.

Hydraulic conductivity estimates were obtained from 16 tight Westbay zones using a shut-in test methodology. These estimates provided a basis for assigning hydraulic conductivity of the deep mudstone, siltstone and sandstone bedrock materials with low joint densities in groundwater modelling analyses. The practical range of applicability of shut-in methods in the MP38 Westbay system is for hydraulic conductivity of 10^{-8} m/s to 10^{-12} m/s. Tests conducted over this range took a few minutes (1×10^{-8} m/s) to 24 hours (1×10^{-12} m/s) to complete, and would take an impractical amount of time to complete as open water column slug tests. The compressibility of the Westbay casing and packers should be incorporated into the analysis, as empirically-derived imaginary casing radii are greater than those calculated based on the bulk modulus of water alone, and result in hydraulic conductivity estimates about an order of magnitude greater.

Groundwater samples were collected from two Westbay zones by using the natural vertical hydraulic gradient presented along the borehole. The process of removing drilling fluid from the target zones was conducted unsupervised. The collected data were used to identify elevated salinity in the deep groundwater system, and were significant considerations in discharge water quality predictions and site water management planning.

Notes

"AQTSOLV" is a trade mark of HydroSOLVE, Inc.

"Westbay System" is a trade mark of Nova Metrix Ground Monitoring Canada Ltd., Westbay Instruments Division.

References

BC Ministry of Environment. 2017. Water quality guidelines. Retrieved January 2018 from: https://www2.gov.bc.ca/gov/content/environment/air-land-water/water/water-quality/water-quality-guidelines. British Columbia Ministry of Environment: Victoria, BC, Canada.

Black, W.H., Smith, H.R. and Patton, F.D. 1986. Multiple level groundwater monitoring with the MP System, in *Proceedings of NWWA-AGU Conference on Surface and Borehole Geophysical Methods and Groundwater Instrumentation,* Denver (CO): 41-61.

Bredehoeft, J.D. and Papadopulos, S.S. 1980. A method for determining the hydraulic properties of tight formations, *Water Resources Research,* 16(1): 233–238.

Butler, J.J., Jr. 1998. *The Design, Performance, and Analysis of Slug Tests*. Boca Raton: Lewis Publishers.

Cooper, H.H., Bredehoeft, J.D. and Papadopulos, S.S. 1967. Response of a finite-diameter well to an instantaneous charge of water, *Water Resources Research* 3(1): 263–269.

Hayashi, K., Ito, T. and Abe, H. 1987. A new method for the determination of in situ hydraulic properties by pressure pulse tests and application to the Hagashi Hachimantai geothermal field, *J Geophys Res,* 92: 9168–9174.

Hyder, Z., Butler, J.J., Jr., McElwee, C.D. and Liu, W. 1994. Slug tests in partially penetrating wells, *Water Resources Research*, 30(11): 2945–2957.

Hvorslev, M.J. 1951. Time lag and soil hydraulic conductivity in ground-water observations. Bull. No. 36, Waterways Exper. Sta. Corps of Engrs, US Army, Vicksburg, Mississippi: 1–50.

Neuzil, C.E. 1982. On conducting the modified "Slug test" in tight formations, *Water Resources Research,* 18(2): 439–441.

Proceedings of Mine Water Solutions 2018
June 12–15, 2018, Vancouver, Canada
Published by the University of British Columbia, 2018

Groundwater Discharge into Tailing Facility During Intense Precipitation Events, Nyrstar Myra Falls

Christoph Wels, Robertson GeoConsultants Inc., Canada
Andy Thomas, Robertson GeoConsultants Inc., Canada
Nicole Pesonen, Nyrstar Myra Falls, Canada

Abstract

Nyrstar Myra Falls (NMF) is an underground zinc mine on Vancouver Island, British Columbia, Canada. In 2014, groundwater discharge was observed at surface along the northeastern perimeter of the Old Tailings Disposal Facility (TDF). Flows of groundwater occurred at several discrete locations, including the so-called "Main Spring". Flows from the Main Spring flooded a portion of the Old TDF and were identified as a potential dam safety issue to be addressed for closure of the facility. A hydrogeological investigation was therefore conducted in 2015 to determine the factors controlling the discharge of impacted groundwater during periods of intense and prolonged rainfall.

The groundwater flow regime in the natural hillside along the northern perimeter of the Old TDF is highly transient due to steep gradients and rapid recharge from the upper catchment during high precipitation events. During high precipitation events (>50 mm), the capacity of the natural soils and mine waste on the northern hillside to transmit groundwater downslope is temporarily overwhelmed, and groundwater levels rise rapidly. When this occurs, mine waste materials are flooded after the storage capacity of natural soils has been reached. This effect is pronounced in areas where tailings, which have very low permeability and essentially no available storage, have been placed directly against the natural hillside, and therefore represent a hydraulic barrier. This rapid rise in groundwater levels behind the tailings deposit gives rise to significant discharge (up to 100 L/s) of groundwater impacted by contact with mine waste material. The findings of this study informed the design of improved operational water management and closure planning for the Old TDF.

Introduction

Nyrstar Myra Falls (NMF) is an underground zinc mine located in Strathcona Park on Vancouver Island, British Columbia, Canada. In 2014, groundwater discharge was observed at surface along the northeastern

perimeter of the Old Tailings Disposal Facility (TDF). Flows of groundwater occurred at several discrete locations, including the so-called "Main Spring". Flows from the Main Spring flooded a portion of the Old TDF and were identified as a potential dam safety issue to be addressed for closure of the facility. This paper presents key findings of a hydrogeological study conducted in 2015 to determine the factors controlling the discharge of impacted groundwater onto the Old TDF during periods of intense and prolonged rainfall.

Background

During high precipitation events in late November and early December 2014, numerous springs were observed emerging along the contact of the Old TDF with the waste rock and access road along the northeastern perimeter. Figure 1 shows the locations of the various seeps, which include:

- 8 seeps along the contact of the Amalgamated Paste Area (APA) beach with waste rock dump #6 to the north (Seeps #1 to #8 with elevations ranging from 3,397.6 m to 3,398.9 m mine elevation).
- 1 major seep at the northeastern abutment of the APA berm ("Main Spring" at elevation 3,387 m MD).
- 2 seeps at the northeastern abutment of the seismic berm of the Old TDF immediately upgradient of the pump house ("Pumphouse" seep at 3,359.2 m MD).

The APA seeps had estimated flows ranging from 5 to 30 L/min and were observed eroding the APA beach and contributed to ponding at the toe of the APA berm. The Main Spring reached peak flows up to and possibly exceeding 100 L/s and caused flooding of the "Strip Area," requiring emergency measures to maintain adequate freeboard (i.e. pumping into Reclaim Sand Area, RSA, and breaching of the RSA). The Pumphouse seeps showed intermediate flows (~5 to 10 L/s) and resulted in flooding of the immediate vicinity of the pump house area.

Sampling and water quality analysis of these seeps during the December 10, 2014 flooding event indicated that all seeps are impacted with acidic pH and elevated metal concentrations (including zinc, copper and cadmium). The observed seepage water quality exceeds the effluent limits for Myra Creek and will require collection and treatment prior to discharge to the environment. In December 2014, Robertson GeoConsultants Inc. (RGC) developed a hydrogeological field program to characterize the hydrogeological conditions near the observed seeps and springs (RGC, 2014). This scope was subsequently approved by NMF in January 2015, and fieldwork commenced in late February 2015.

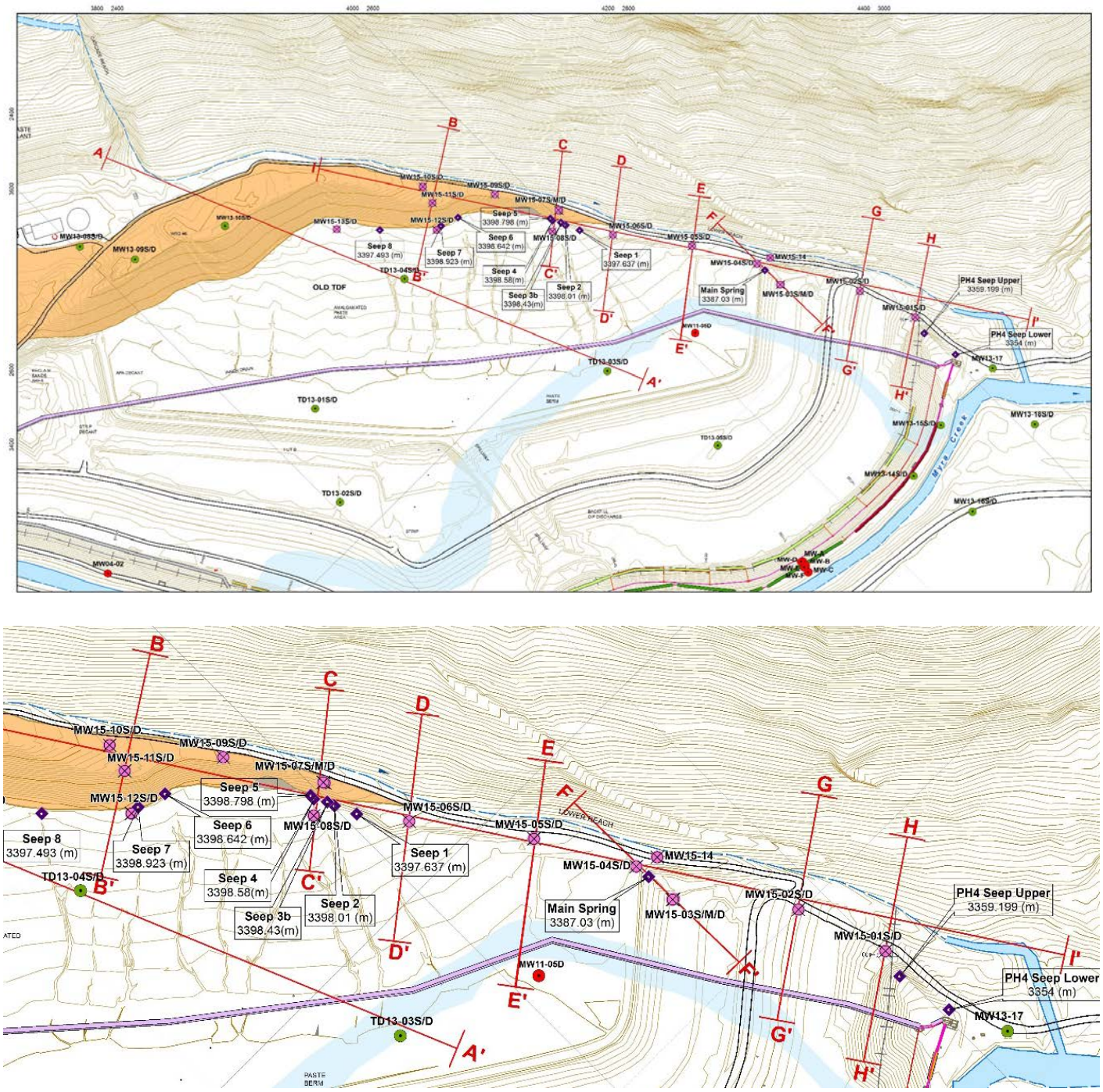


Figure 1: Site layout and conceptual model of Seeps/Springs for Old TDF, Myra Falls.
Lower graphic shows enlarged view of Seeps

Methods

The 2015 drilling program was conducted between February 23 and May 2, 2015. The program involved drilling eighteen boreholes (at 14 locations) with a SONIC drill rig and the installation of twenty-nine

(29) nested or paired monitoring wells ("MW15 series" of wells). Figure 1 shows the as-built locations of these newly completed monitoring wells.

Detailed monitoring of groundwater levels, spring flows and water quality was undertaken until January 2016. Two synoptic surveys of groundwater levels were completed in the newly installed 2015 series of wells and existing wells in the Old TDF area to determine the ground water flow field in this part of the site. In addition, detailed water level monitoring was completed in selected wells of the 2015 series to get a better understanding of the highly transient hydraulic regime in the northeastern portion of the Old TDF (APA) triggering seep and springs flows during high precipitation events ("event monitoring").

For event monitoring, selected monitoring wells of the 2015 series were equipped with Solinst Leveloggers for near-continuous monitoring of groundwater levels. Loggers were employed in up to 7 monitoring wells and synchronized to record water levels simultaneously. Water levels were typically recorded at 15-minute intervals and corrected for barometric pressure changes using a Solinst Barologger attached to one of the monitoring wells.

Groundwater samples were collected from each monitoring well that carried a sufficient depth of water using a downhole pump or bailer. Samples were submitted to MAXXAM in Vancouver for laboratory analysis of full water quality. For more details on the field methods see RGC (2016).

Results

Hillside Stratigraphy

Typical natural hillside stratigraphy encountered along the northern perimeter of the Old TDF includes (from top to bottom):

- Colluvium,
- Glacial Till (lateral and/or basal till),
- Bedrock.

The colluvial soils are typically comprised of coarse rockslide or talus material with high permeability while the underlying glacial till soils tend to be fine-grained and/or dense and exhibit much lower permeability. Shallow bedrock encountered in this study showed limited weathering and fracturing and is inferred to be of lower permeability than the overlying soils.

Along the northern perimeter of the Old TDF, the original soil profile was reworked to construct diversion ditches and access roads and then buried by waste rock and tailings. This has resulted in a complex sequence of mine waste materials overlying natural ground. Figure 2 and 3 show representative cross-sections of stratigraphy and observed groundwater levels in the Cascade Creek reach (section A-A') and in proximity of the Main Spring (section F-F', see Figure 1 for alignment).

Some key observations are summarized here:

- In the Cascade Creek area, historic waste rock was placed directly onto natural ground and later partially buried by conventional fine tailings (CFT) and paste tailings in the APA.
- Immediately to the east of WRD #6, some additional waste rock and/or fill was also placed onto tailings.
- In the eastern portion of the APA, both CFT and APA tailings were deposited directly against the natural hillside.
- Between the APA berm and the toe of the Old TDF, the natural hillside is overlain primarily by embankment fill (waste rock and sandy tailings) and road fill (reworked colluvium and waste rock).

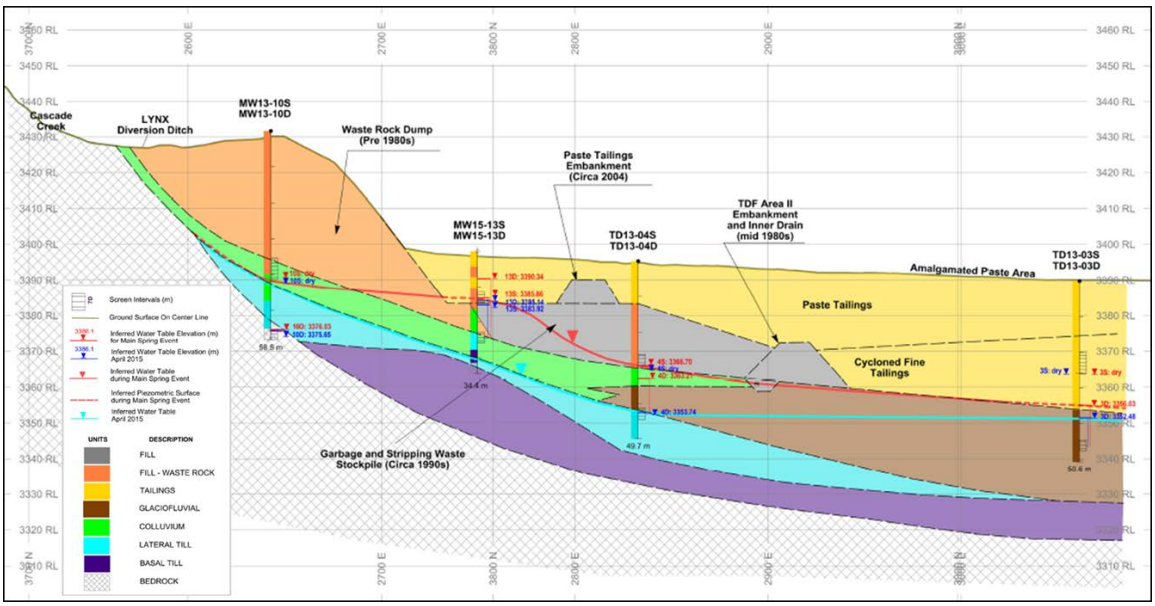


Figure 2: Hydrostratigraphic section and groundwater levels for Cascade Creek reach (A-A')

Groundwater Flow Regime

The groundwater flow regime in the natural hillside along the northern perimeter of the Old TDF is highly transient due to steep gradients and rapid recharge from the upper catchment during high precipitation events. Placement of mine waste (tailings and waste rock) against the natural hillside has significantly altered this transient flow regime.

During low flow periods and even moderate precipitation events (<20 mm), the principal direction of groundwater flow is in a southerly direction following the hillside topography ("downslope") (see Figure 4). During those periods, the transmissivity of the natural soils (and saturated waste rock and fill, where present) is sufficient to transmit all recharge from the hillside into the highly permeable glaciofluvial sediments of the Myra Valley Aquifer (MVA). Once the hillside recharge reaches the MVA, it flows in a southeasterly direction beneath the Old TDF towards the Outer Drain and Myra Creek.

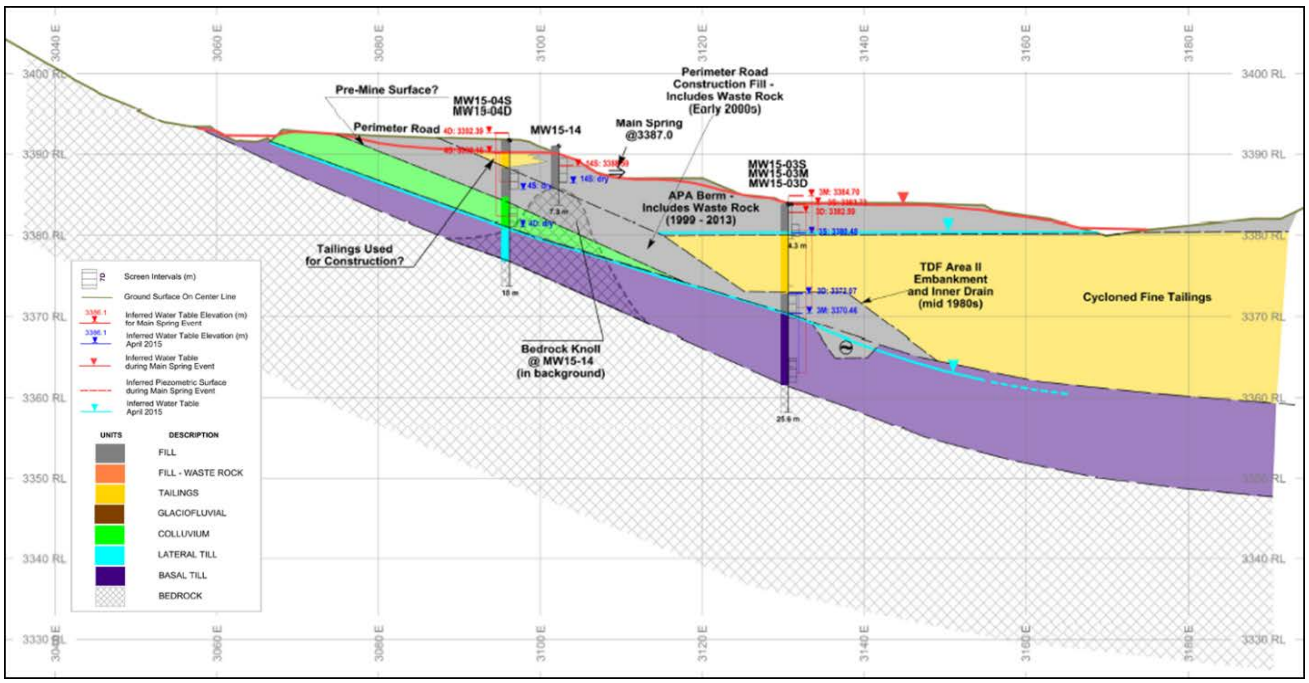


Figure 3: Hydrostratigraphic section and groundwater levels for Main Spring reach (F-F')

However, during high precipitation events (say >50 mm), the capacity of the natural soils and mine waste on the northern hillside to transmit groundwater downslope is temporarily overwhelmed and groundwater levels rise quickly. When this occurs, mine waste materials are flooded after the storage capacity of natural soils has been reached. This effect is pronounced in areas where tailings, which have very low permeability and essentially no available storage, were placed directly against the natural hillside, and therefore represent a hydraulic barrier (see Figure 3).

This rapid rise in groundwater levels behind the tailings deposit during high precipitation events gives rise to temporary seepage onto the APA ("APA seeps") and the larger, yet infrequent, spring flows at the northeastern abutment of the APA ("Main Spring") and near the northeastern abutment of the Old TDF embankment ("Pumphouse Seeps").

Event Monitoring

Between March 2015 and January 2016, hydraulic heads were monitored near-continuously in wells screened both in natural soils and overlying mine waste material along the northern perimeter of the Old TDF (APA). This automated monitoring was supplemented by manual monitoring of groundwater levels and spring flows during high precipitation events.

The monitoring period included four episodes when the "Main Spring" was flowing. Table 1 summarizes precipitation and Main Spring flow statistics for these high flow periods. Figure 5 shows

representative geodetic groundwater levels observed in selected monitoring wells located along the northern perimeter of the Old TDF during the March 29–31, 2015 event.

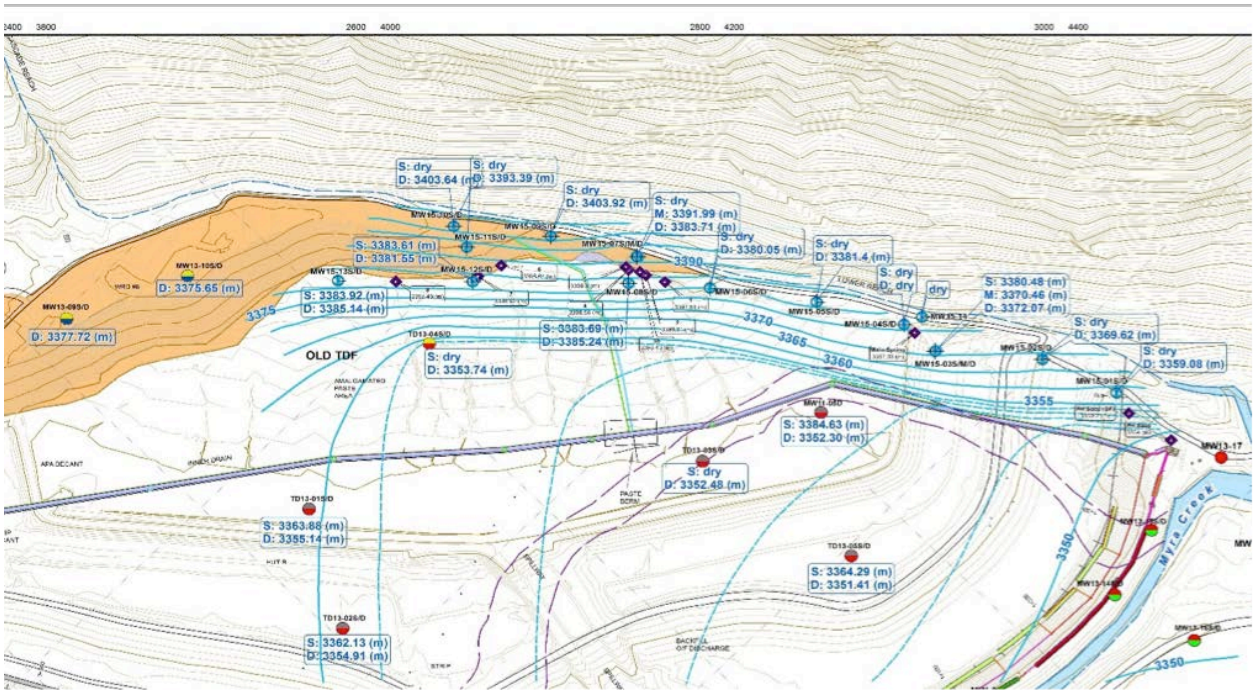


Figure 4: Groundwater flow field for low flow conditions (April 26, 2015)

Table 1: Summary of main spring events monitored between March 2015 and January 2016

Event	Precipitation		Duration of spring flow hours	Delay in spring flow hours	Estimated spring flow volume m³
	Total mm	Rate mm/hr			
March 20, 2015					
Event #1	96	4.6	1	26	<5
March 29–31, 2015					
Event #1	91	4.8	20	18	2,400–3,400
Event #2	56	2.5	14	25	50–200
December 3–8, 2015					
Event #1	117	4.2	21	20	2,800–3,900
Event #2	94	3.5	n/a	n/a	n/a
Event #3	73	3.0	15	19	900–1,500
Event #4	55	5.0	13	10	1,500–2,200
January 27–28, 2016					
Event #1	152	5.1	29	17	6,600–8600

The conclusions from this high flow monitoring can be summarized as follows:

- The hydrogeological regime along the northern perimeter of the Old TDF can be grouped into four different flow systems:

- *Cascade Creek Reach (west of MW15–13)* with limited hillside recharge, high storage in waste rock and good drainage into MVA (no seepage onto APA).
- *APA Seeps Reach (MW15-13 to MW15-7)* with diffuse hillside recharge and poor drainage into MVA resulting in seepage onto APA beach.
- *Main Spring Reach (MW15-6 to MW15-4)* with concentrated hillside recharge through colluvium (rockslide fan) and poor drainage into MVA resulting in lateral flow and concentrated discharge through NE abutment of APA berm ("Main Spring").
- *Pumphouse Seep Reach (east of MW15-14)* with local recharge from the Old TDF embankment and poor drainage into MVA resulting in seepage along buried access road ("Pumphouse Seeps").

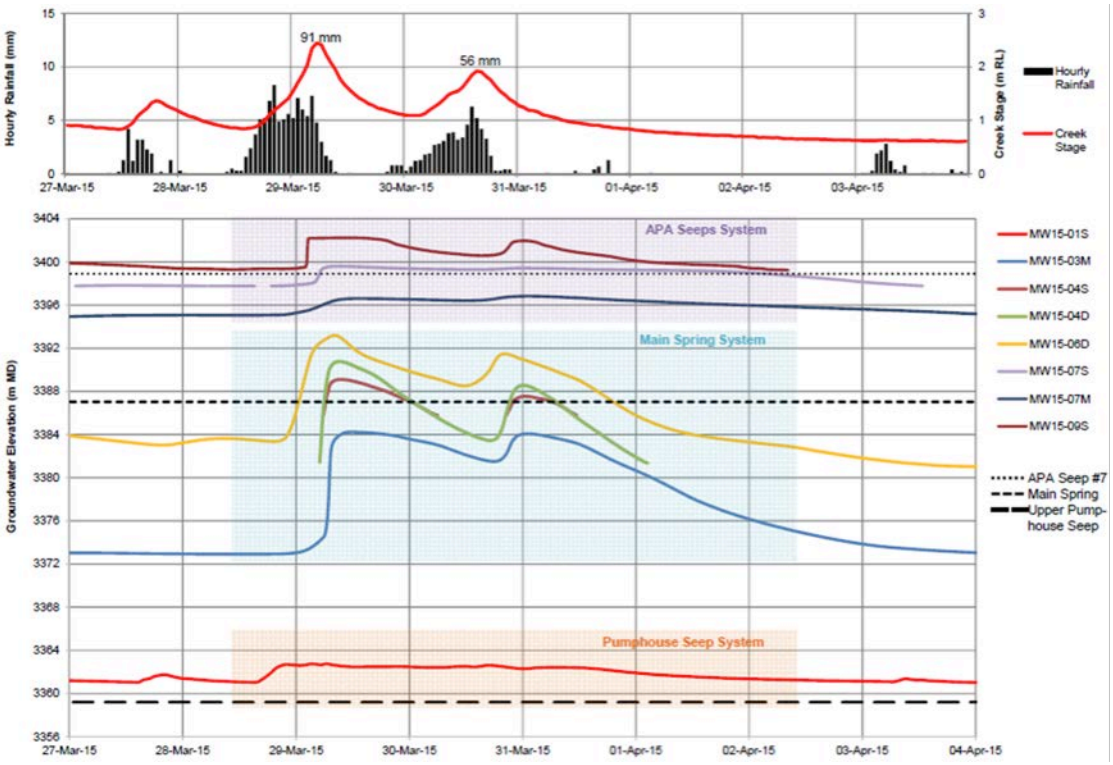


Figure 5: Representative groundwater levels responses for different seep/spring systems during high precipitation event (March 28–30, 2015)

- The Main Spring system shows a highly transient (or "flashy") response to precipitation with groundwater levels rising up to 10 m in only 6 hours. Discharge at the Main Spring was observed on eight occasions and lasted from less than 1 hour to about 25 hours, producing peak flows exceeding 100 L/s. The Main Spring typically starts flowing about 20 hours after onset of heavy precipitation and is triggered by precipitation events of 90 mm in 24 hours. However, this

precipitation threshold is significantly reduced (to as low as 50 mm in 24 hours) in the case of successive storm events and/or rain-on-snow.

- Groundwater levels in the APA seeps and Pumphouse seeps systems respond more quickly to precipitation but typically rise only 2 to 3 m and recover much slower suggesting poorer drainage. Consequently, those seeps flow significantly longer (several days) while peak discharge rates are lower (a combined ~5 to 10 L/s for APA seeps and 10 to 20 L/s for Pumphouse seeps).

Groundwater and Seep Water Quality

Groundwater and seep/spring flow samples were collected and submitted to Maxxam for water quality analysis. Tables 2 and 3 summarize water quality of different seeps and springs discharging onto the Old TDF.

The key findings of this water quality review can be summarized as follows:

- Groundwater and seep water quality showed significant spatial and temporal variations suggesting different contaminant sources in different reaches and significant "flushing" during high flow events.
- The highest contaminant concentrations were observed in groundwater beneath the potentially acid-generating (PAG) waste rock in the Cascade Creek reach (WRD#6) and seepage in the western APA reach (e.g. 30 to 50 mg/L Zn and 8 to 15 mg/L Cu in APA seeps #6 to #8).
- APA seeps #1 to #5 emerging further east onto the APA beach show consistently lower metal concentrations (1.0 to 5.3 mg/L Zn and 0.2 to 1.1 mg/L Cu) indicating less seepage from PAG waste rock (or lower leaching potential).
- Contaminant concentrations in the Main Spring tend to be significantly elevated during the onset of spring flow (up to 15 mg/L Zn and 4.8 mg/L Cu) but decline during peak flows and even subsequent events (down to 1.9 mg/L Zn and 0.4 mg/L Cu) indicating flushing during high flow events. Pyritic tailings used for berm construction in immediate proximity of the Main Spring may be the cause for the initial flush of highly impacted seepage. Once these accumulated oxidation products are flushed contaminant concentrations in the Main Spring are declining due to reduced residence time of groundwater recharging from the side hill in the sulphidic waste material.
- Seepage discharging at the Pumphouse seeps tend to show similar zinc concentrations (0.2 to 6.1 mg/L Zn) than the Main Spring and the APA seeps but typically lower copper concentrations (<0.01 to 0.8 mg/L Cu). The lower copper concentrations in the Pumphouse seep generally coincide with higher pH in the Pumphouse seep (5.5 to 7.5) suggesting potential solubility controls of copper. This seepage may be buffered by non acid-generating (NAG) material placed in this area

during the seismic berm upgrade work and/or mixing with well buffered groundwater discharging in this area.

Table 2: Seep water quality results Part 1 (2014–2016)

Spring and seep sampling events		Flow estimate at time of sample	Field data		Laboratory data					
			pH	EC[1]	pH	EC[2]	SO_4	Cd	Cu	Zn
		L/S	SU	µS/cm	SU	µS/cm	mg/L	mg/L	mg/L	mg/L
Main Spring										
27-Nov-14	–	–	–	–	2.8	1590	764	0.0684	4.76	15.0
10-Dec-14	–	–	–	–	3.4	354	90	0.0075	0.395	1.51
10-Dec-14	–	–	–	–	4.1	116	31	0.0016	0.092	0.33
6-Feb-15	10:45	100	3.3	468	3.2	462	129	0.0112	0.655	2.24
6-Feb-15	16:10	<20	2.9	430	3.3	441	135	0.0104	0.611	2.09
3-Dec-15	12:22	200	3.1	931	–	–	331	0.0299	1.40	5.65
7-Dec-15	~16:00	200	2.9	525	–	–	–	–	–	–
8-Dec-15	14:50	110	3.2	448	3.2	554	145	0.0106	0.573	2.54
9-Dec-15	10:40	dry	–	–	–	–	–	–	–	–
27-Jan-16	17:10	20-50	2.9	1053	–	–	399	0.0480	2.49	9.25
28-Jan-16	7:30	100	3.3	359	–	–	110	0.0085	0.433	1.87
28-Jan-16	14:30	30-40	3.3	376	–	–	118	0.0139	0.476	3.21
Pump House 4 Seep (upper)										
10-Dec-14	–	–	–	–	4.6	440	199	0.0145	0.583	3.87
6-Feb-15	11:07	20	6.4	249	7.6	246	79	0.0034	0.051	0.811
3-Dec-15	12:17	65	7.5	127	–	–	28	0.0008	0.009	0.182
8-Dec-15	14:45	50	5.4	261	7.5	238	83	0.0033	0.055	0.884
9-Dec-15	10:42	8	6.2	308	–	–	–	–	–	–
9-Dec-15	16:08	3	5.8	337	–	–	–	–	–	–
27-Jan-16	9:03	3-5	6.5	140	–	–	13	0.0002	0.002	0.0359
Pump House 4 Seep (lower)										
10-Dec-14	–	–	–	–	4.8	544	227	0.0262	0.773	6.12
27-Jan-16	9:11	1-2	5.5	130	–	–	32	0.0013	0.024	0.281

Notes:
1. Electrical Conductivity (µS/cm) at field temperature.
2. Electrical Conductivity (µS/cm) at laboratory temperature.
3. Field EC on 27-Jan-16 is specific conductance (SPC).

N.B: Metal and sulphate results are reported as dissolved concentrations.

Implications

All seeps and springs observed along the northeastern perimeter of the Old TDF (APA), including APA seeps, Main Spring and Pumphouse seeps currently exceed, at least during initial flushing, discharge permit limits and will require collection and treatment. The APA seeps and the Main Spring are currently collected and pumped together with surface run-on from the APA and strip area to the RSA and ultimately to the Super Pond for treatment. The Pumphouse seeps are currently not controlled and will require collection and treatment.

Table 3: Seep water quality results Part 2 (2014–2016)

Spring and seep sampling events		Flow estimate at time of sample	Field data		Laboratory data					
			pH	EC[1]	pH	EC[2]	SO_4	Cd	Cu	Zn
		L/S	SU	µS/cm	SU	uS/cm	mg/L	mg/L	mg/L	mg/L
APA 1										
6-Feb-15	13:00	<1	4.9	965	4.4	936	468	0.0227	1.15	5.33
APA 2										
6-Feb-15	13:00	<1	5.1	304	4.7	272	116	0.0088	0.192	1.03
APA 3										
6-Feb-15	13:00	<1	5.9	439	4.5	354	165	0.0111	0.194	1.21
APA 4										
10-Dec-14	–	–	–	–	3.5	354	125	0.0124	0.536	1.54
6-Feb-15	14:00	<1	3.3	617	–	–	–	–	–	–
APA 5										
10-Dec-14	–	–	–	–	3.7	306	104	0.0112	0.462	1.36
6-Feb-15	14:00	2	3.3	573	3.2	629	184	0.0328	0.593	4.21
APA 6										
10-Dec-14	–	–	–	–	4.0	219	77	0.0135	0.323	2.85
6-Feb-15	14:00	<1	4.0	1567	3.9	1570	–	0.1300	7.90	26.1
APA 7										
6-Feb-15	14:00	<1	3.3	2610	3.5	2200	1730	0.2310	13.3	51.5
3-Dec-15	12:30	5	3.3	2408	–	–	1560	0.2350	11.9	54.4
7-Dec-15	~16:00	5	3.3	2408	–	–	–	–	–	–
8-Dec-15	15:05	<1	3.3	2787	3.5	2540	1790	0.2530	13.9	59.0
9-Dec-15	10:45	3	3.3	2157	–	–	–	–	–	–
9-Dec-15	16:15	<1	3.5	2578	–	–	–	–	–	–
APA 8										
6-Feb-15	14:00	1	3.4	2960	3.5	2490	2080	0.2630	14.7	63.0
27-Jan-16	10:19	2	3.3	1975	–	–	1270	0.1700	9.34	38.9
Road Seep										
28-Jan-16	10:17	1-2	5.5	135	–	–	45	0.0002	0.001	0.036

Notes:
1. Electrical Conductivity (µS/cm) at field temperature.
2. Electrical Conductivity (µS/cm) at laboratory temperature.
3. Field EC on 27-Jan-16 is reported as specific conductance (SPC).

N.B: Metal and sulphate results are reported as dissolved concentrations.

An analysis of historic precipitation records for Myra Creek suggests that high precipitation events (>90 mm) triggering Main Spring flows are relatively frequent. For example, precipitation events with at least 90 mm in 24 hours were observed on 70 occasions during the last 35 years of record and occurred up to 7 times in a single year (1990).

The observed flows at the Main Spring were scaled up to estimate peak flows and volumes for the springs using design precipitation events provided by Amec Foster Wheeler. The peak flow rates in the Main Spring for a 1:200 and 1:1000 precipitation event are estimated to be about 235 and 263 L/s,

respectively. The total volume of Main Spring flow for a 1:200 and 1:1000 precipitation event is estimated to be about 20,000 m^3 and 24,000 m^3, respectively. The peak flow rate and total volume for the Probable Maximum Precipitation (PMP) event (635 mm) is estimated to be significantly higher (about 900 L/s and 76,000 m^3).

During Main Spring flow events significant upward pressures develop in the northeastern abutment of the APA berm (e.g. 2.2 m upward pressure over 4.5 m in MW15-4S/D for a vertical gradient of 0.49 m/m). Furthermore, a seepage face with visible seepage discharge has been observed to develop along the toe of the APA berm extending at least 50 m south of the Main Spring location. Implications of these hydraulic conditions for berm stability during such high flow events should be evaluated by a qualified engineer.

The existing Lower Lynx Diversion Ditch (LLDD) is undersized and requires an upgrade to carry the 1:200 year precipitation event. The implications of this hydrogeological study on the updated design of the LLDD are as follows:

- The LLDD will require lining to prevent leakage of clean diversion water into the groundwater system (contacting mine waste) during low flow periods and upwelling of potentially impacted groundwater into the LLDD.
- The LLDD will require under-drainage to prevent uplifting of the lined diversion channel due to seepage flows resulting in upward groundwater pressures.
- The larger capacity and new alignment of the LLDD will require partial excavation into native material and mine waste (waste rock and tailings). To the extent possible, the new alignment and invert of the LLDD should be constructed on native ground and/or clean fill to minimize contamination of groundwater collected in the under drain system.

Conclusions

The findings of this hydrogeological study informed the final design of the Updated Lower Lynx Diversion Ditch and associated Diversion Ditch Springs Drain (DDSD) designed to capture the Main Spring flow. Both of these structures were installed in the summer/fall of 2016. Initial monitoring of these new water management structures during the 2016/2017 winter season indicated that they are performing as intended.

More detailed monitoring of water quality in the discharge from the DDSD is planned for the 2017/2018 winter season to determine whether this water can be discharged or will have to be captured and treated (as currently done).

Acknowledgements

The authors wish to thank Nyrstar Myra Falls for permission to publish the findings of this study.

References

Robertson GeoConsultants Inc. 2014. Proposal – Old TDF seepage investigations, Myra Falls Mine Site. RGC Proposal submitted to Nyrstar Myra Falls, December 19, 2014.

Robertson GeoConsultants Inc. 2016. Old TDF (APA) Hydrogeological investigation, Nyrstar Myra Falls. RGC Report 212005/1. Report Submitted to Nyrstar Myra Falls, December 2016.

Proceedings of Mine Water Solutions 2018
June 12–15, 2018, Vancouver, Canada
Published by the University of British Columbia, 2018

Estimating Operational Groundwater Inflows to a Proposed Underground Coal Mine on Vancouver Island

Laura-Lee Findlater, Lorax Environmental Services Ltd., Canada
John Balfour, Enterprise Geosciences Ltd., Canada
Bruce Mattson, Lorax Environmental Services Ltd., Canada
Kathleen Russell, Quinsam Coal Corporation, Canada

Abstract

The Quinsam Coal Mine, located 20 km west of Campbell River on Vancouver Island, was operated as an open pit and underground thermal coal mine between 1998 and 2014. In 2013, the operator sought to expand the existing 7 South underground mine into a new area termed 7 South Area 5 (7SA5). The expansion proposed to mine the No. 4 Coal Zone within the Dunsmuir Member of the Comox Formation via conventional room-and-pillar mining methods. The proposed mine resides in the eastern limb of the Quinsam Syncline, the north and south extents of which are truncated by regional scale faults. Depth of cover over the mine ranges from 28 to 90 m. Exploration drilling logs indicated that a number of drill holes intercepted water-bearing features with airlift yields ranging from 0.1 to 3.8 litres per second (L/s). These features were found to occur above the No. 4 coal seam in the southern portion of the mine. This, along with initial slug tests on monitoring wells, raised concerns about potentially large groundwater inflows to the development. To facilitate estimates of potential mine inflows, a three-day 1.9 L/s pumping test was undertaken in the 7SA5 footprint, which created widespread drawdown (anisotropy at "fault scale" producing an elongated drawdown pattern). The drawdown data were analysed using AQTESOLV and found to be most accurately represented by the Gringarten-Witherspoon analytical solution for pumping tests in fractured bedrock. Fracture hydraulic conductivity was estimated at 2×10^{-6} m/s, while bulk rock hydraulic conductivity was estimated at 3×10^{-7} m/s. Given the relatively high permeability of bedrock in the 7SA5 area, it was considered probable that the hanging rock will dewater during mine development. As such, the approach taken for predicting potential groundwater inflows during mine development was to determine how much pumping would be required to lower the hydraulic head in the mining footprint to within +/–10 m of the No. 4 coal zone within 100 days. Drawdown from the 3-day pumping test was projected to 100 days and recontoured to simulate the effect of a single well pumping for 100 days. The 100-day drawdown cone was replicated over the mine domain, and through the

principle of superposition, used to estimate the effect of multiple pumping wells. Ultimately, it was found that 5 wells pumping 1.9 L/s for 100 days would be sufficient to dewater the area above the workings, for a total pumping rate of 8 to 10 L/s.

Introduction

The Quinsam Coal Mine is located on Vancouver Island, approximately 27 km southwest of Campbell River, BC. Since 1988, Quinsam Coal Corporation (QCC) has extracted coal from a number of underground mines on their coal leases located near Middle Quinsam Lake in the Quinsam River watershed. QCC is proposing an expansion of underground coal workings to the south of the existing 7 South mine area; this proposed underground mine is referred to as 7 South Area 5 (7SA5) (Figure 1). 7SA5 will mine the No. 4 Coal Zone, hosted in the middle Dunsmuir Member of the Comox Formation, via conventional room and pillar methods. The middle division of the Dunsmuir Member consists of siltstone and silty sandstones; the upper and lower divisions consist mainly of sandstone with minor interbeds of siltstone and occasional coals.

The proposed 7SA5 mine is in an area that is structurally more complex than previously mined areas on the mine lease. 7SA5 is positioned in the west-dipping, eastern limb of the Quinsam Syncline (Figure 1). Within the mining footprint, the beds generally dip gently at less than seven degrees, and flatten out to zero degrees along the axis of the syncline. At the eastern margins of the syncline (outside of the mining footprint), the beds dip more steeply at nearly 30 degrees. The syncline gently plunges to the south until it approaches the Iron River, where it is truncated by another regional scale fault. The sedimentary sequence hosting coal reserves is separated from an emergent ridge of basement rock to the east by the Boundary Fault, the principal fault within the property.

The entire Quinsam mine site is overlain by a variably thick cover of glacial, glaciofluvial, and glaciomarine sediments. In 7SA5, the thickness of this unit varies from 0 m to 39 m, with an average thickness of 12 m. The total depth of cover over 7SA5, including overburden and bedrock, ranges from 28 m to 90 m. Groundwater draining 7SA5 is inferred to go entirely to the Iron River under gentle to moderate gradients (3% to 8%). Water levels are generally within 30 m of ground surface. Head above the proposed 7SA5 workings ranges from 15 m at the north end to 75 m along the trough of the syncline (Figure 2).

In light of the structural complexity of the area, drilling logs for air rotary exploration drill holes were inspected for occurrences of water-bearing features. Of 21 exploration holes drilled in the footprint area or immediate perimeter of the proposed 7SA5 workings in 2011 to 2012, 11 of the holes intersected water-bearing features and had associated increases in airlift yield ranging from 0.1 to 3.8 litres per second (L/s). More than half of these boreholes encountered more than one water-bearing feature. The

spatial distribution of these water-bearing features is shown in Figure 1. In the northern portion of the proposed mine, most of the water-bearing features are below the No. 4 Coal Zone, while in the southern portion of the mine, these features tend to occur above the coal zone. This early data review suggested that 7SA5 could intersect water-bearing features and potentially intercept higher magnitude inflows than that observed in other mine areas. This prompted the undertaking of a multi-day pumping test to assist with the estimation of future underground inflows.

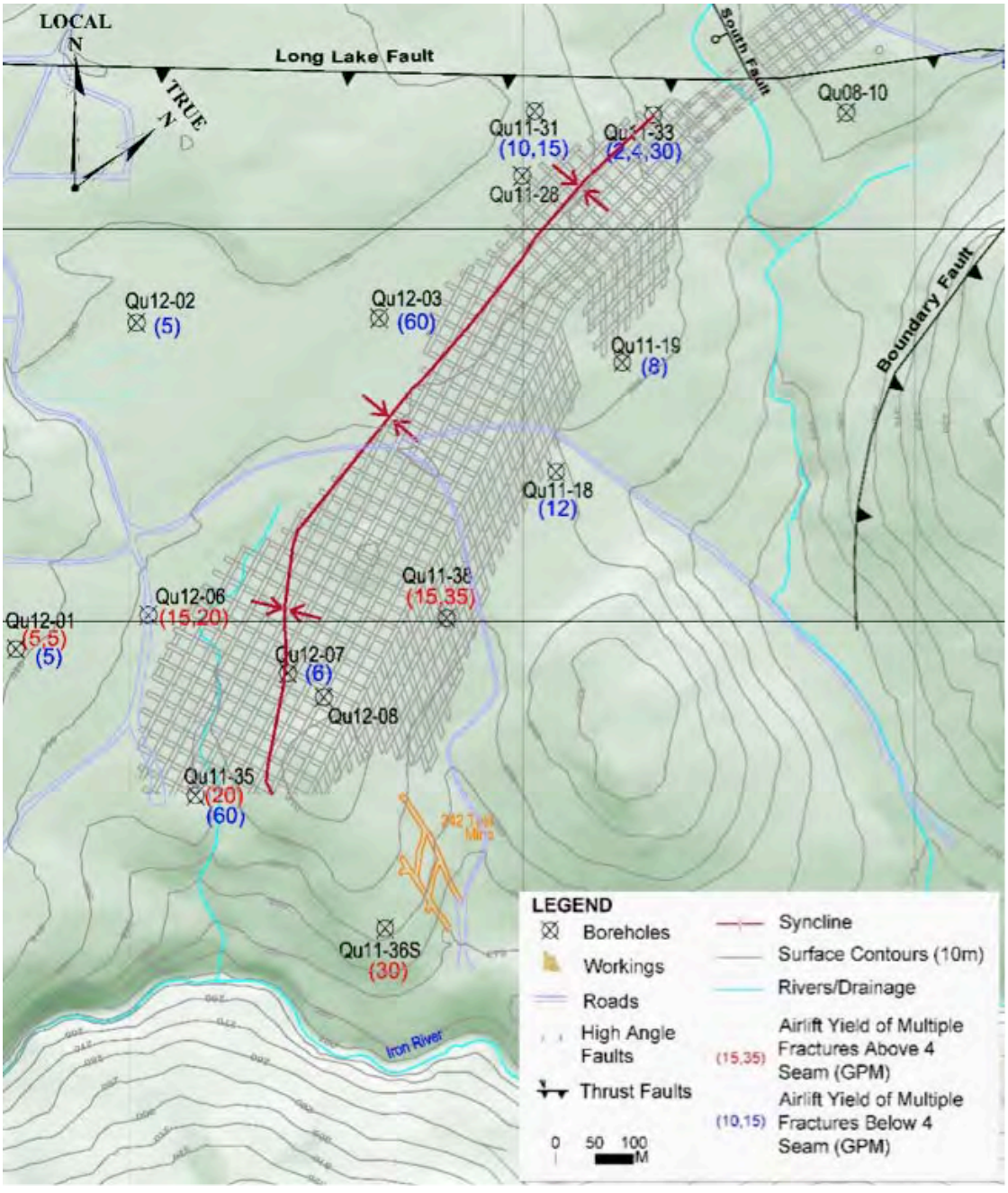


Figure 1: Proposed 7SA5 mine layout

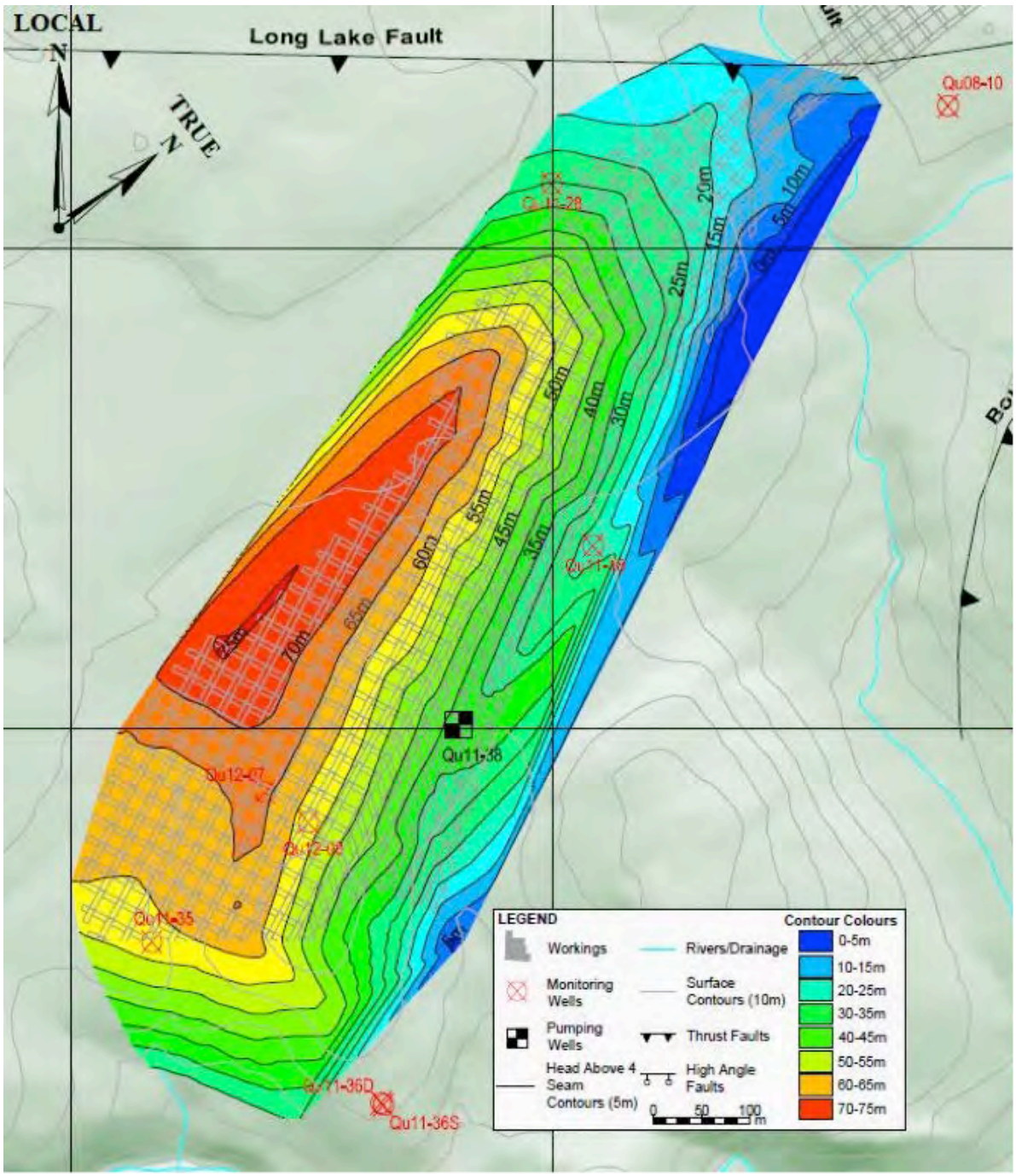


Figure 2: Head (m) above proposed 7SA5 mine workings

Field Methods and Data

Several conventional monitoring wells have been installed in and around the 7SA5 extents in support of baseline monitoring (QU11-18S/D, QU11-28 and QU11-36S/D) and pumping test monitoring (QU12-07, QU12-08, and QU11-35) (Figure 1, Table 1). The screening intervals for these wells were designed to

target either the No. 4 Seam and/or water-bearing features stratigraphically close to the No. 4 Seam.

Slug tests were performed on all monitoring wells; the results are summarized in Table 1. The average sedimentary bedrock hydraulic conductivity (K) in 7SA5 is approximately 7×10^{-6} m/s based on all results save that of QU08-10 (Figure 3), which is considered to be more reflective of bedrock conditions north of 7SA5. The average hydraulic conductivity for 7SA5 sedimentary bedrock is significantly higher than the unfractured, sedimentary bedrock K determined for other areas of the mine ($\sim8\times10^{-9}$ m/s), although the 7SA5 data set is considered biased high due to the purposeful screening of higher hydraulic conductivity features in slug-tested monitoring wells.

A constant rate pumping test was conducted in 7SA5 in October 2012, executed by Precision Services and Pumps of Abbotsford, BC. Exploration hole QU11-38 (Figure 1) was selected as the pumping location because (i) it intersected a high permeability feature, producing 2.2 L/s, immediately above the No. 4 Coal Zone; (ii) it is located in the southern portion of the proposed mine where these types of features are more likely to occur above the mined seam and present a water management issue; and (iii) it is at a significant distance (>500 m) from the Iron River, so that potential boundary effects from the Iron River would not completely mask the influence of the test. The pumping test used a Grundfos 460 Volt, 10 horsepower pump with 3-phase motor (Model 40S100-30). The constant rate test was preceded by a step test to identify an appropriate constant discharge-pumping rate. QU11-38 was pumped for 73 hours at a constant rate of 1.9 L/s.

Pumping Test Data Interpretation

In addition to the monitoring well network, several open exploration holes were also available for water-level monitoring during the pumping test. Maximum drawdown measured at all locations is listed in Table 1 and contoured in Figure 3. Drawdown was widespread across the study area with over 20 m of drawdown measured at the pumping well and 2 m of drawdown measured nearly 600 m away. The drawdown cone was asymmetrical and elongated along a line roughly parallel to the axis of the syncline.

Based on the drawdown measured at QU11-28, the drawdown cone is thought to widen at the northern end of the workings as it hits a no flow boundary formed by the impermeable bedrock north of the Long Lake fault, drawing water from the east and west instead. The drawdown cone appeared to be truncated at the southern extent of the workings due the presence of a positive (recharge) boundary, which could be the flooded 242 test mine and/or the Iron River. Groundwater quality was found to remain stable throughout the test as determined from multiple discharge samples and continuous monitoring of field parameters (pH, electrical conductivity, dissolved oxygen and oxidation-reduction potential).

Table 1: 7SA5 monitoring network

Well ID	Hole type[1]	Radius from PW[1] (m)	SWL (m bgs)	Depth/slotted interval (m bgs)		Screened lithology[3]	4 Seam interval[4] (m bgs)		Slug test hydraulic conductivity (m/s)	Pumping test drawdown (m)	Projected drawdown at 100 days (m)
QU11-38	PW	0	24.1	94.6		open hole	56.8	58.6	(–)	21.6	39
QU12-13	EXP	98	29.0	n/a		open hole	n/a	n/a	(–)	1.3	5.8
QU11-34	EXP	130	19.9	71.5		open hole	59.1	61.4	(–)	6.2	16.3
QU12-08	MW	186	44.4	93.1	96.2	No. 4/4L Coal	93.4	96.1	7E-07	2.1	8.4
QU11-37	EXP	210	31.7	157.4		open hole	95.4	98.0	(–)	3.6	11.8
QU12-07	MW	214	37.9	124.4	127.4	Fractured SLST/SST	95.1	97.7	2E-05	1.4	5.8
QU11-18S	MW	234	16.2	31	34.1	Till	41.2	43.2	1E-08	4.3	14.5
QU11-18D	MW	234	22.4	62	65	SST/SLST	41.2	43.2	1E-05	8.6	22.5
QU12-06	EXP	380	30.2	148.4		open hole	81.3	83.1	(–)	1.5	5.8
QU11-35	MW	391	28.0	70.7	73.8	Fractured SST	76.9	78.8	1E-06	1.5	6.7
QU11-28	MW	572	34.2	54.5	57.5	No. 4&4L/SST	54.5	57.9	1E-06	2.4	9.5
QU08-10	MW	821	26.2	19.7	27.1	No. 3 Coal	N/R	N/R	5E-09	0.1	0.3
QU11-36S	MW	402	20.4	38.9	41.9	Fractured SST	43.7	52.1	4E-06	0	0
QU11-36D	MW	402	30.7	63.9	66.9	Fractured SST	43.6	52	2E-05	0	0

Notes:

1. PW = pumping well, EXP = open exploration hole, MW = monitoring well
2. SWL = static water level
3. SST = sandstone, SLST = siltstone
4. N/R = not recovered, n/a = not available

The pumping test data were analysed using AQTESOLV Pro to determine aquifer parameters. AQTESOLV employs an automatic curve matching routine that performs nonlinear weighted least-squares parameter estimation. To assist in simulation convergence, only observation data from the pumping well and QU11-18D were used for curve matching.

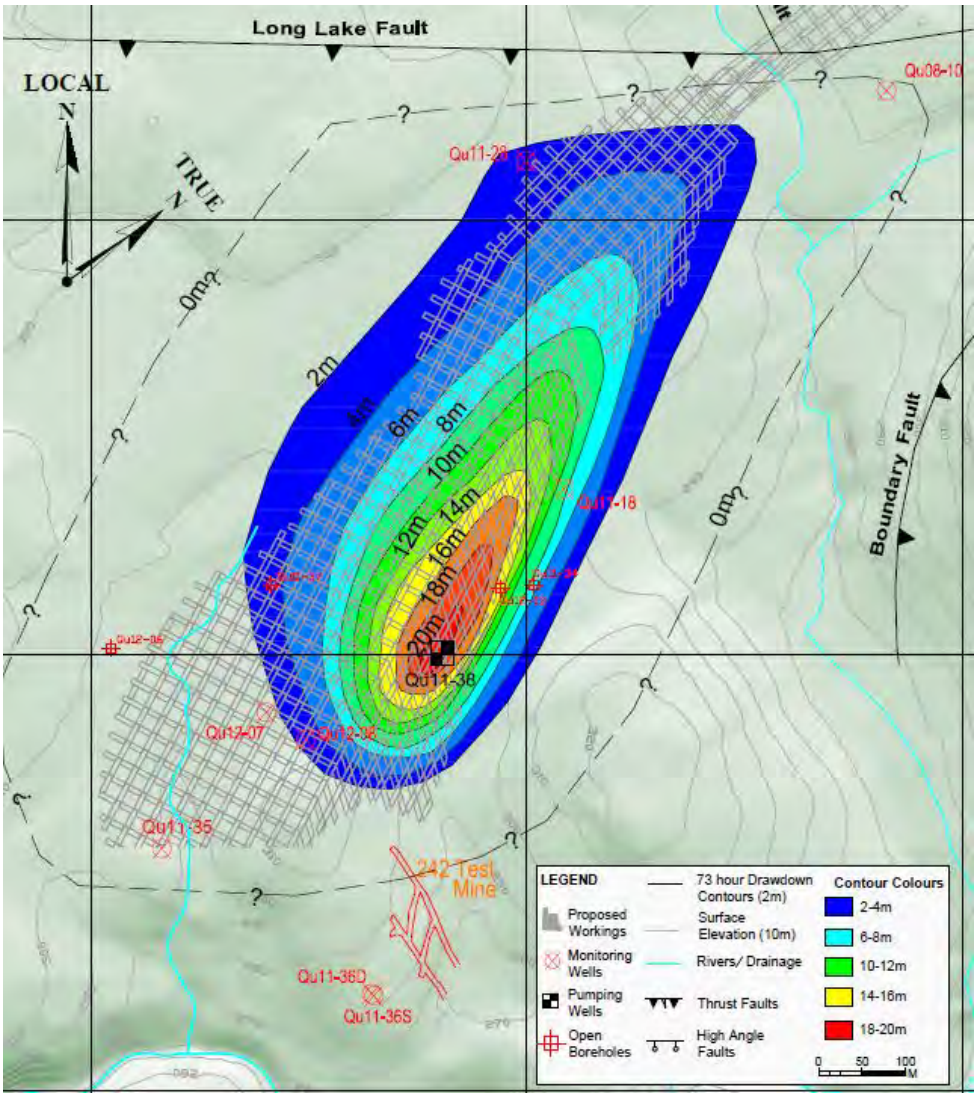


Figure 3: Drawdown at the end of the 73-hour pumping test

A composite plot of all observation well drawdown is provided in Figure 4. In an ideal confined aquifer, all observation well data should plot on the same line; deviations from this indicate that the aquifer is heterogeneous, there is a directionality to the aquifer parameters (i.e. anisotropy) and/or the aquifer is influenced by boundaries. The 7SA5 data indicate that one or all of these conditions are applicable to the observation well data from the QU11-38 pumping test. In light of these observations, it

was not surprising that the Theis method (1935) for confined, homogeneous, isotropic aquifers could not produce a reasonable match to the observed data, even with boundary conditions applied.

Ultimately, the Gringarten-Witherspoon method (1972) for confined aquifers with vertical, uniform fractures was found to produce the most reasonable match to the observed data (Figure 5). Computed hydraulic parameters are provided in Table 2. The regression improved with the application of boundary conditions. The model domain was simulated as a rectangle, with the average location of the Iron River at the southern limit of the domain as a constant head boundary along the y-axis and a no flow boundary at x=1180 m, representing Long Lake Fault at the north end of the domain.

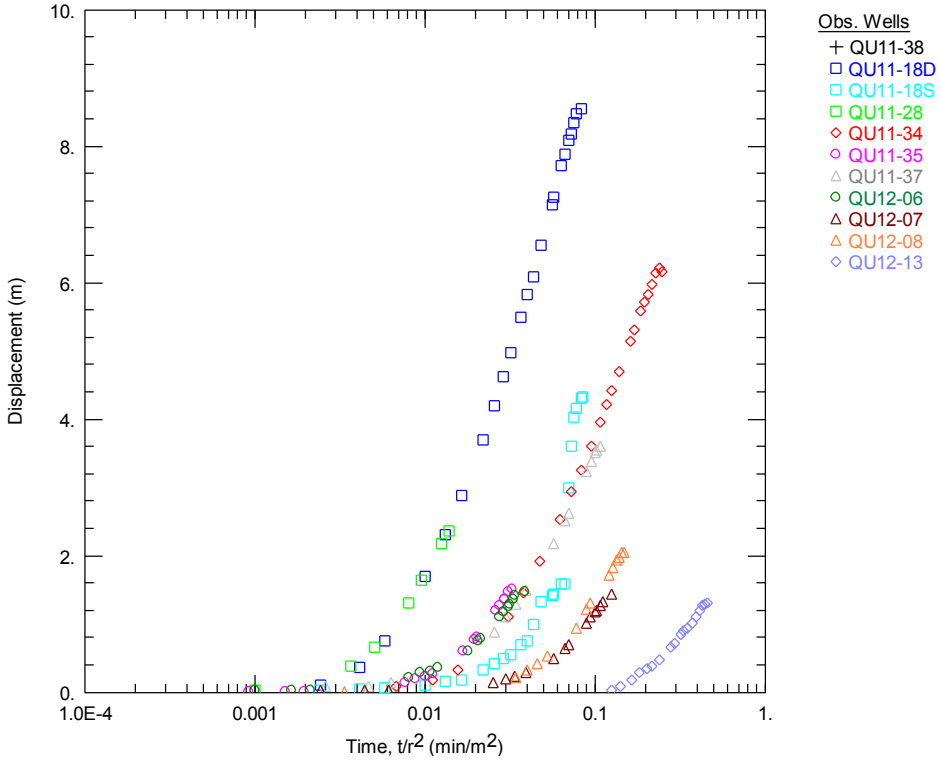


Figure 4: Composite plot of observation well drawdown data from the 73-hour pump test at QU11-38

Table 2: 7SA5 aquifer parameters simulated by AQTESOLV using the Gringarten-Witherspoon solution

Aquifer parameter	Description	Units	Computed value
K_x	Hydraulic conductivity of fracture	m/s	2×10^{-6}
K_y	Hydraulic conductivity of formation	m/s	3×10^{-7}
S_s	Specific storage	m^{-1}	2×10^{-6}
L_f	Fracture length	m	200

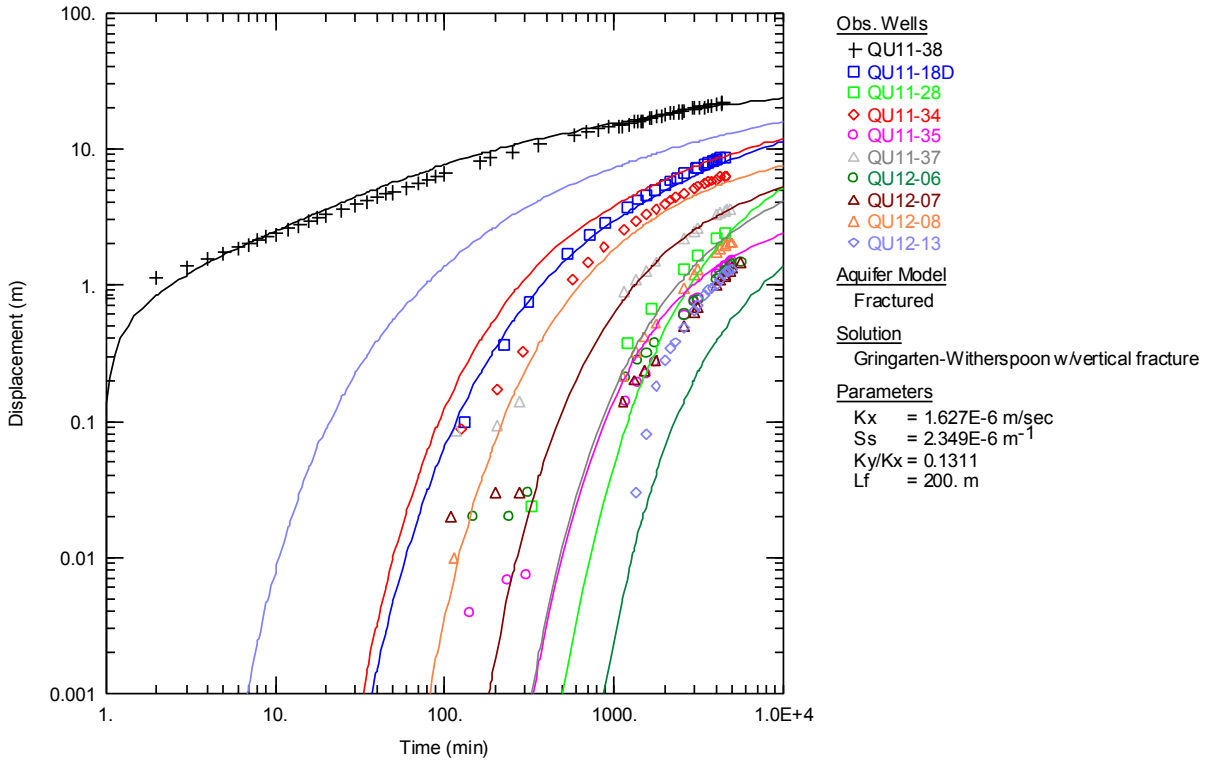


Figure 5: Time drawdown plot with the Gringarten-Witherspoon solution. Solution optimized to pumping well (QU11-38, black crosses) and QU11-18D (blue squares)

The use of the Gringarten-Witherspoon solution (1972) for fractured rock is supported for the following reasons: (i) the borehole log of QU11-38 indicated that the hole intercepted two water-bearing fracture zones, (ii) a log-log plot of drawdown versus time demonstrates an early straight line portion of slope approaching 0.5 indicating parallel, horizontal flow perpendicular to fracture (Figure 6) (Kruseman and de Ridder 1994), and (iii) the data demonstrate an early time constant difference between the derivative and drawdown curves corresponding to a multiplying factor of two which indicates that a fracture dominates the early flow regime (Figure 6) (Renard et al. 2009). The derivative is the change in drawdown at a well with respect to log time (Bourdet 1989). The data from the pumping well do not appear influenced by a constant head boundary condition as the drawdown data did not stabilize with an accompanying linear decrease in the drawdown derivative (Renard et al. 2009).

The computed hydraulic conductivity of the fracture (2×10^{-6} m/s) is of similar magnitude to the average hydraulic conductivity measured from slug tests on 7SA5 bedrock wells (~7×10^{-6} m/s), which were generally screened across higher permeability features. The hydraulic conductivity of the bulk formation (3×10^{-7} m/s) is about ten times higher than the average hydraulic conductivity of sedimentary rock determined from other mine areas (2×10^{-8} m/s), which is consistent with 7SA5 being a more structurally disturbed area. The computed specific storage of the formation is at the low end of values

reported for fractured rock (10^{-4} – 10^{-6} m^{-1}) (Walton, 1991). Overall, the solution was sensitive to the dimensions of the fracture and insensitive to boundary conditions on the east and west side of the model domain.

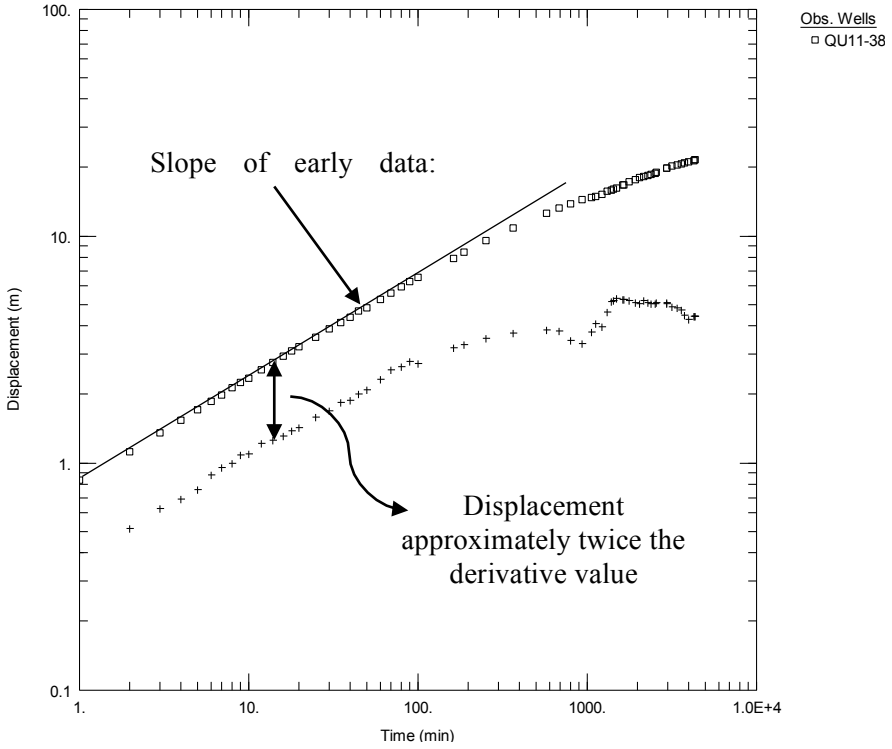


Figure 6: Log-log plot of drawdown (square) and drawdown derivative (cross) versus time at QU11-38

Prediction of Mine Dewatering Rates

Given the relatively high permeability of bedrock in the 7SA5 area, it was considered probable that the hanging rock would dewater during mine development. As such, the approach taken for predicting potential groundwater inflows during mine development was to determine how much pumping would be required to lower the hydraulic head in the mining footprint to within +/–10 m of the No. 4 coal seam. Figure 2 shows the head above the No. 4 seam. To compute this pumping rate, drawdown from the 73-hour pumping test was extrapolated to 100 days for all wells from log-linear plots of drawdown versus time. The extrapolation for the pumping well drawdown is shown in Figure 7; results for observation wells are provided in Table 1. One hundred days is considered to be a reasonable timeframe for preparation of the area in advance of mining, and assumes that the mining area would be fully or partially dewatered in advance of mining, as high inflows of nuisance water would be undesirable during operations.

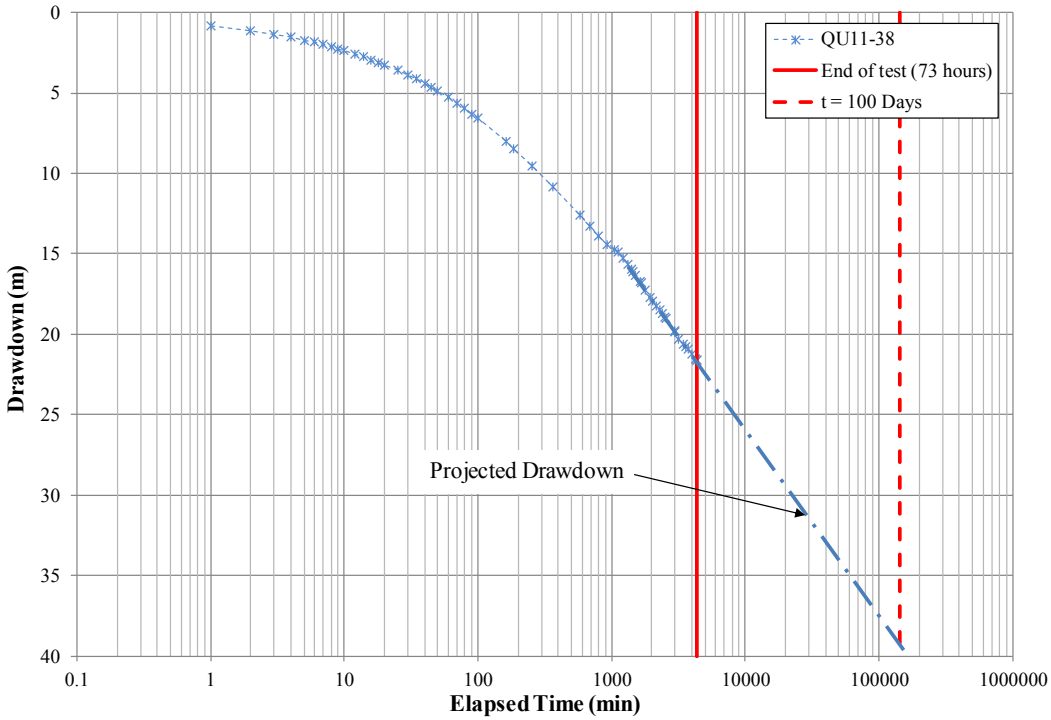


Figure 7: Drawdown at QU11-38 extrapolated to 100 days

The 100-day extrapolated drawdown was contoured in the same fashion as the 73-hour test; however, some of the peripheral aspects of the drawdown cone were modified to produce a more idealized drawdown pattern less influenced by boundary conditions (Figure 8). The idealized 100-day drawdown cone was replicated to additional pumping locations to simulate the effect of a multi-well groundwater interception system. The superimposed drawdown curves were then re-contoured to create an aggregate drawdown "surface" that approximates the effect of multiple pumping wells. This is based on the principle of superposition whereby drawdowns at a point in an aquifer from multiple pumping wells are additive. The drawdown produced from multiple pumping wells was then subtracted from the head above the No. 4 Coal Zone to produce a surface approximating the residual head above the No. 4 Coal Zone. The number and locations of the pumping wells were optimized by trial and error to provide sufficient drawdown in the footprint of the proposed workings without over-pumping (*i.e.* limiting drawdown to less than 10 m below the coal seam). Ultimately, it was found that 5 wells pumping 1.9 L/s for 100 days would be sufficient to dewater the area above the workings. The resultant drawdown surface created by this configuration of wells is shown in Figure 9; the residual head over the 7SA5 workings is shown in Figure 10. From this analysis, it is anticipated that operational groundwater inflows into the 7SA5 workings in the absence of dewatering wells would be in the range of 8 to 10 L/s.

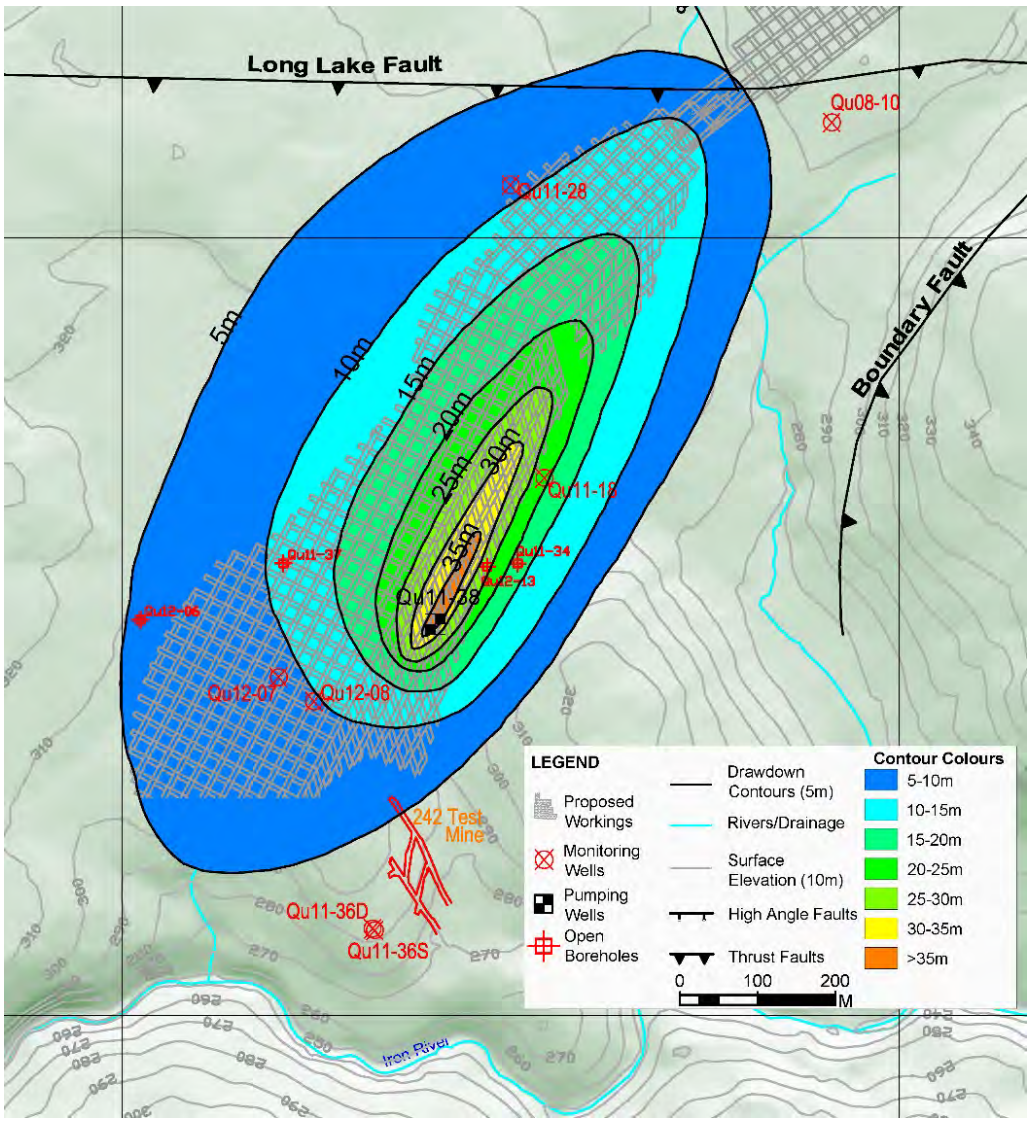


Figure 8: Idealized 100-day drawdown cone

This method for estimating groundwater inflows to the mine assumes that a similar drawdown pattern can be reproduced at any of the proposed pumping locations based on conditions encountered at QU11-38. This implies that each pumping location encounters a significant water-bearing fracture/fault and similar boundary conditions to QU11-38. According to Figure 1, two of the five theoretical pumping locations (QU11-38 and QU11-35) have encountered significant water near the No. 4 seam. Similar features have not been confirmed to exist at the other pumping locations. Should less permeable rock conditions prevail, the 1.9 L/s pump rate may not be sustainable, and the resultant drawdown cone would be steeper and of more limited extent. Additional pumping locations would be required to achieve the desired drawdown; however, total pumping rates may not change significantly.

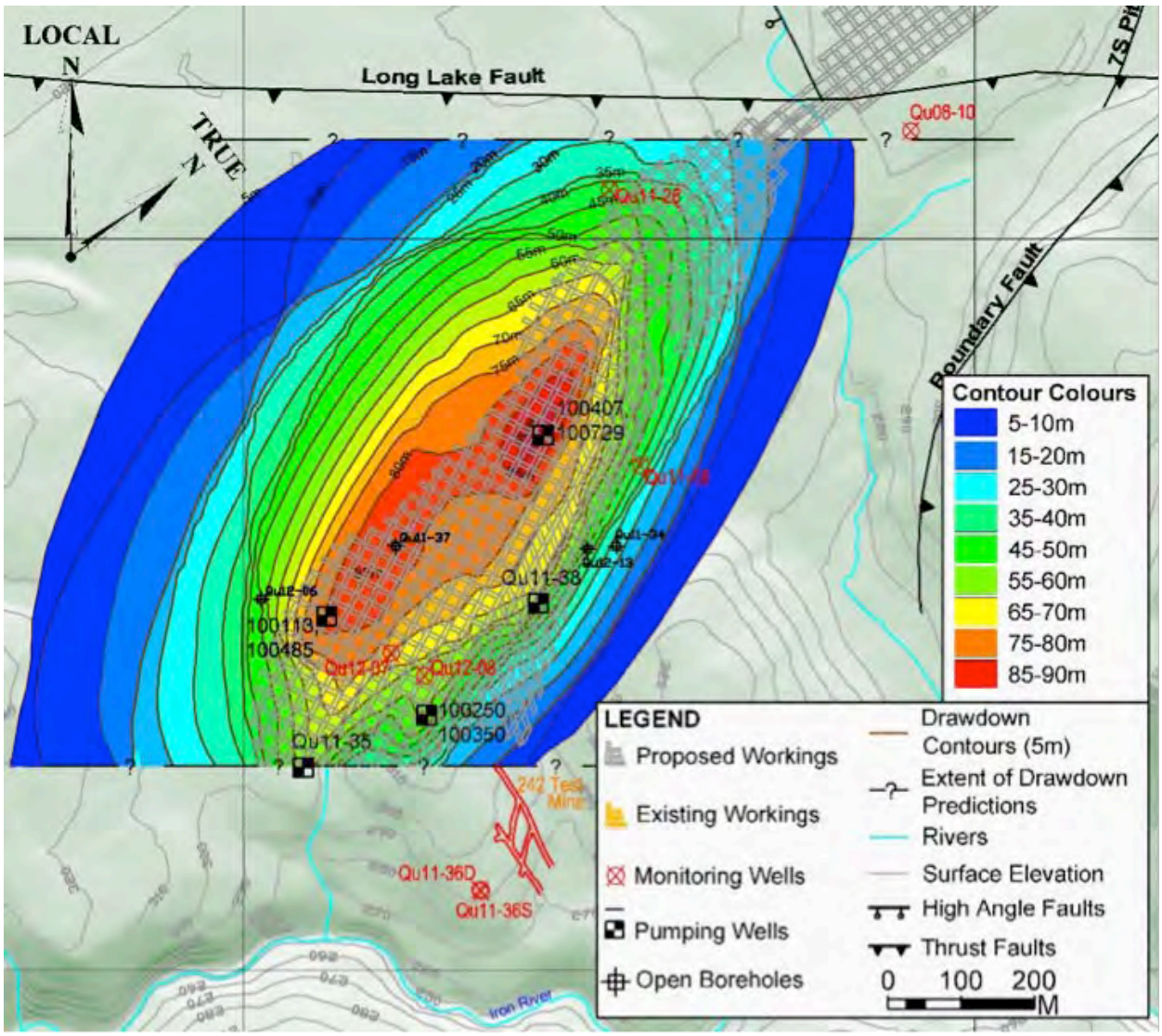


Figure 9: Extrapolated drawdown for 5 wells each pumping 1.9 L/s for 100 days

Unidentified boundary conditions may also influence the operational inflows. In general, no flow boundaries would amplify the effects of drawdown from nearby pumping wells, and thus operational inflows would be smaller (i.e. less pumping wells may be required to achieve target drawdown). A constant head/recharge boundary, however, would have the opposite effect. Negligible drawdown near the south end of the proposed mine suggests that the flooded 242 test mine or the Iron River is acting as a recharge boundary, but this was not definitively proven in the drawdown derivative plot. Due to the uncertainty over boundary conditions near the extreme southern portion of proposed workings, the 8 to 12 L/s operational inflow estimate is considered applicable to the mine area north of 100280 m Northing (mine grid) (lower dashed line in Figures 9 and 10).

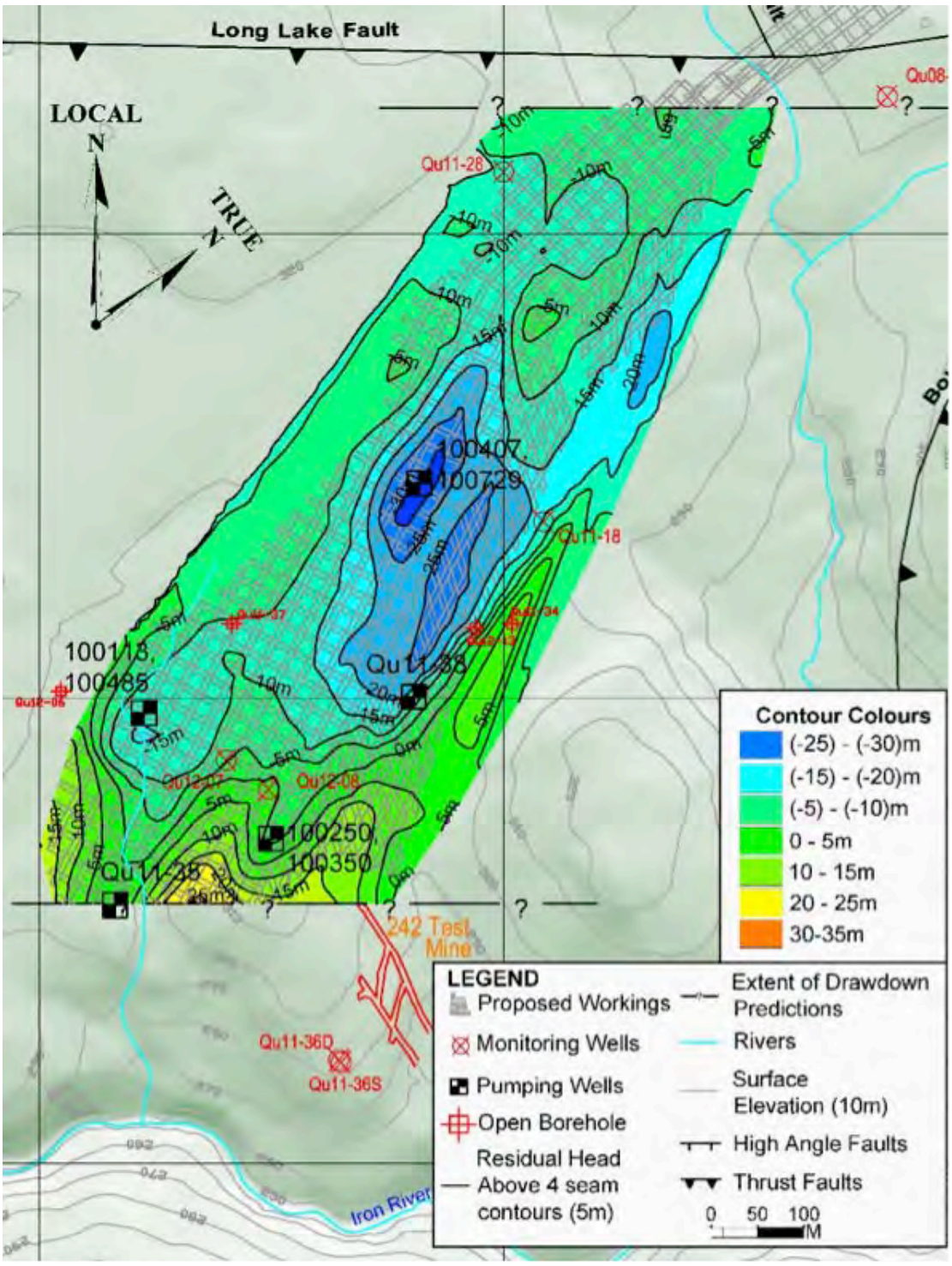


Figure 10: Residual head (m) above the No. 4 seam after 5 wells each pumping 1.9 L/s for 100 days

Conclusion

Quinsam Coal Corporation has proposed to expand its underground operations into a new area called 7SA5. The proposed expansion lies in an area that is more structurally disturbed than other areas of the mine lease. Through examination of exploration drilling records, it was noted about half of the drill holes intercepting the proposed working encountered water-bearing features with yields ranging from 0.1 to 3.8 L/s. In the southern portion of the mine, these features tend to occur above the proposed coal reserves. This data review prompted the undertaking of a 73-hour pumping test to assist with estimation of future underground inflows.

The 73-hour, 1.9 L/s constant rate pumping test created widespread drawdown across 7SA5, with drawdown at the southern extent muted by a suspected recharge boundary and drawdown in the north enhanced by a no flow boundary. A composite plot of the data revealed that the aquifer behaved in a non-ideal manner, which lead to use of the Gringarten-Witherspoon solution (1972) for a confined aquifer with vertical, uniform fractures. The solution computed a fracture hydraulic conductivity of 2×10^{-6} m/s and a formation hydraulic conductivity of 3×10^{-7} m/s. Given the relatively high permeability of bedrock in the 7SA5 area, it was considered probable that the hanging wall rock would dewater during mine development.

The approach taken for predicting potential groundwater inflows during mine development was to determine how much pumping would be required to lower the hydraulic head in the mining footprint to within +/–10 m of the No. 4 coal seam within 100 days. The drawdown created by the 73-hour pump test was extrapolated to 100 days and a generic "idealized" drawdown cone was produced. The 100-day drawdown cone was replicated to additional pumping locations to simulate the effect of a multi-well groundwater interception system, with locations and number of wells optimized to reduce head above the coal zone to less than 10 m. This was done by superimposing the drawdown curves to create an aggregate drawdown "surface" that approximates the effect of multiple pumping wells. This is based on the principle of superposition, whereby drawdowns at a point in an aquifer from multiple pumping wells are additive. Ultimately, it was found that 5 wells pumping 1.9 L/s each (or 8 to 12 L/s total) for 100 days would be sufficient to dewater the area above the workings.

The analysis above is considered applicable to an area north of mine grid 100280 m, as the 73-hour pumping test suggested that the southernmost tip of the mine may be under the influence of a recharge boundary condition – possibly the flooded 242 test mine or the nearby Iron River. Since receiving permits, the mine has elected not to mine south of 100280 m, thereby reducing the potential for connection to the Iron River. After a period of care and maintenance, the mine has resumed operations and expects to expand into 7SA5 in 2018.

This study has underscored the value of early collection of groundwater data at the exploration stage – namely airlift yields from air rotary holes. Observed yields were kept in a database, which facilitated the desktop review and allowed for early identification of potentially problematic groundwater conditions. This also facilitated the selection of pumping and monitoring well locations, thereby limiting drilling costs for the groundwater program. The incumbent analysis relied upon high quality field data and first principles to determine mine dewatering rates without the development of a costly 3-D numerical groundwater flow model.

Acknowledgements

The author would like to acknowledge Quinsam Coal Corporation for supporting this study and allowing the publication of its results.

References

Bourdet, D., Ayoub, J.A., and Pirard, Y.M. 1989. Use of pressure derivative in well-test interpretation, *SPE Formation Evaluation* 4(2): 293-302.

Gringarten, A.C. and Witherspoon, P.A. 1972. A method of analyzing pump test data from fractured aquifers, *Proceedings of Symposium on Rock Mechanics*, Stuttgart. Int. Soc. Rock Mechanics and Int. Assoc. Eng. Geol: (3-B): 1-9.

Kruseman, G.P. and de Ridder, N.A. 1994. *ILRI Publication 47: Analysis and Evaluation of Pumping Test Data* (Second Edition). Wageningen: International Institute for Land Reclamation and Improvement.

Renard, P., Glenz, D. and Mejias, M. 2009. Understanding diagnostic plots for well-test interpretation, *Hydrogeology Journal* 17(3): 589–600.

Theis, C.V. 1935. The relation between the lowering of the piezometric surface and the rate and duration of discharge of a well using groundwater storage, *Am. Geophys. Union Trans*. 16: 519–524.

Walton, W. 1991. *Principles of Groundwater Engineering*. Michigan: Lewis Publishers.

Proceedings of Mine Water Solutions 2018
June 12–15, 2018, Vancouver, Canada
Published by the University of British Columbia, 2018

Predicted Post-Closure Contaminant Loads and Water Quality Conditions in Myra Creek, Nyrstar Myra Falls, Canada

Paul Ferguson, Robertson GeoConsultants Inc., Vancouver, Canada
Christoph Wels, Robertson GeoConsultants Inc., Vancouver, Canada
Alexander Trapp, Robertson GeoConsultants Inc., Vancouver, Canada
Nicole Pesonen, Nyrstar Myra Falls, Campbell River, Canada

Abstract

Nyrstar Myra Falls (NMF) is an underground zinc mine on Vancouver Island, British Columbia, Canada. In 2016, Robertson GeoConsultants Inc. (RGC) developed a water and contaminant load balance model to support the closure planning for the Old Tailings Disposal Facility (TDF) and a closure cover design for the embankment berm of the active Lynx TDF. The model was used to (i) simulate current impacts to groundwater and Myra Creek by Metal Leaching (ML) and Acid Rock Drainage (ARD) and (ii) predict future, post-closure water quality conditions as closure and progressive reclamation proceeds.

This paper will describe RGC's conceptual load balance model and a numerical load balance model that was developed with the software GoldSim. The numerical model was calibrated to daily zinc (Zn) loads in Myra Creek from 2012 to mid-2016, and water quality data was collected from within the mine site. Once calibrated, the model was used to simulate the improvement in water quality conditions in Myra Creek during the future operation of the Lynx Seepage Interception System (SIS) and after the Old TDF has been closed and the Lynx TDF berm has been raised to its final height and covered.

Introduction

In 2016, Nyrstar Myra Falls (NMF) submitted a permit-level closure plan for the Old TDF, a closure cover design for the Lynx TDF embankment berm, and a conceptual design for the Lynx Seepage Interception System (SIS). Detailed closure engineering was completed by Amec Foster Wheeler, the Engineer of Record for the TDFs (see Amec Foster Wheeler, 2016a; 2016b).

Robertson GeoConsultants Inc. (RGC) developed and calibrated a numerical contaminant load balance in the software GoldSim. The model was then used to predict future Zn loads in groundwater and to Myra Creek once the Lynx SIS was operational and closure measures have been implemented.

Background

Site Location and Physical Setting

NMF is in the lower reaches of the Myra Valley about 90 km from the City of Campbell River within Strathcona Provincial Park. Myra Creek flows eastward through the site before discharging into Buttle Lake about 1.5 km downstream of the Old TDF. Mean annual precipitation (MAP) is 2480 mm and monthly average temperatures range from 2°C in January to 25°C in August.

Myra Valley contains sequences of glaciofluvial and glaciolacustrine sediments that were deposited during last glaciation. Rock slides, rock falls, and debris flows have produced local colluvial deposits that overlie these glacial sediments. Alluvial sediments have also been deposited more recently by Myra Creek and its tributaries. These glacial and alluvial sediments comprise the Myra Valley aquifer (MVA) that is the focus of this paper.

General Mine Arrangement

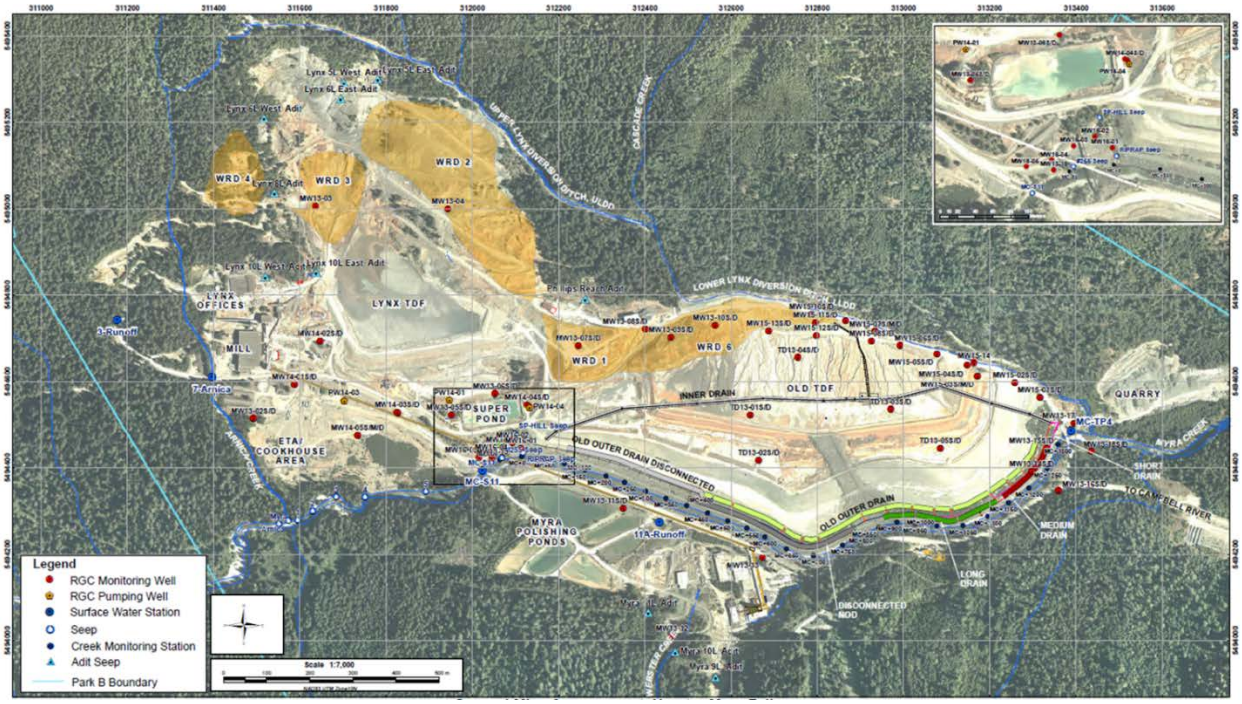


Figure 1: General mine arrangement and monitoring locations, Nyrstar Myra Falls

Key surface features at NMF are shown in Figure 1, including the Lynx TDF (around the former open pit), the Old TDF, Lower Lynx Diversion Ditch (LLDD), the historic WRDs, and the water treatment system (i.e. the Super Pond and Polishing Ponds). Underground workings (not shown) are extensive within Myra Valley and extend to Thelwood Valley. The Old TDF under-drain system near Myra Creek is shown in Figure 1 and described further below.

Groundwater and Surface Water Monitoring Network

There is a network of fifty-seven groundwater monitoring wells at NMF. Forty-one of these wells were installed in 2013 as part of RGC's environmental drilling program ("MW13" and "TD13" well series). Monitoring wells were also installed in 2014 and 2016 near the Lynx TDF to support the design of the Lynx SIS.

Surface water is routinely monitored at stations along Myra Creek. Daily composite samples are also collected using an auto-sampler at station MC-TP4. Monthly water quality surveys are also conducted at thirty locations along Myra Creek adjacent to the Old TDF (Figure 1). Flows in Myra Creek are recorded by a streamflow gauge underneath the carbridge. Zn and Cu concentrations in treated effluent are measured with an auto-sampler at station "Runoff 11A" near a Parshall flume.

Current Water Management and Treatment System

The Old TDF under-drains collect impacted groundwater near Myra Creek and direct it to Pumphouse #4. From Pumphouse #4, groundwater is pumped back to the Super Pond where it is treated. The Inner Drain and Area II Outer Drain are operational but it is the New Outer Drain (NOD) that is the most effective component of the Old TDF under-drain system and consists of a system of three separate drain sections referred to as (i) Short Drain, (ii) Medium Drain and (iii) Long Drain (see RGC, 2016c and Figure 1).

Flows of impacted groundwater, mine water, and surface water report to a Low-Density Sludge (LDS) water treatment system. Flows from the NOD account for about 50% of the total flow to the Super Pond.

Water Quality Guidelines (WQGs) and Objectives

Provincial WQGs for the protection of aquatic life in Myra Creek are discussed in Nautilus Environmental Inc. (2016). For Zn, the maximum and 30-day average WQGs at a water hardness of less than 90 mg/L as $CaCO_3$ are 0.033 mg/L Zn and 0.0075 mg/L Zn, respectively.

Water Quality Impacts

Groundwater at NMF is impacted by Acid Rock Drainage (ARD) from sulphidic, Potentially Acid Generating (PAG) waste rock and Neutral Mine Drainage (NMD) that flows from the upper levels of the Lynx and Myra mine workings. Most of the waste rock at surface is in the historic WRDs (i.e. WRD#1, #2, #3, and #4) and in the Lynx TDF embankment berm. The historic WRDs also contain Non-PAG waste rock and non-sulphidic waste rock.

Conceptual Site-Wide Load Balance

RGC developed a conceptual contaminant load balance model for groundwater in the MVA in 2014 (RGC, 2014). Mass loads of SO_4, Cd, Cu, and Zn were simulated in Excel using a monthly time step. The model was calibrated to the estimated Zn load (56.1 t Zn) to groundwater in the MVA in 2012. This Zn load is the sum of the Zn load recovered by the Old TDF under-drains via Pumphouse #4 (45.3 t Zn) and the Zn load in Myra Creek downstream of the site at MC-TP4 (10.8 t Zn).

For the TDFs and WRDs, loads were estimated as the product of monthly net percolation rates from O'Kane Consultants Inc. (2014) and constant Zn concentrations that were inferred from leach tests and historic groundwater quality data. Other Zn loads to groundwater in the MVA were estimated from mine water and surface water quality and measured flows (where available).

Key findings from that model are summarized here:

- Sources in the Old TDF Reach accounted for about two-thirds of the annual Zn load to groundwater in 2012. 65% of this Zn load is from WRD#1 and the other 35% was from WRD#6.
- Sources in the Lynx TDF Reach accounted for one-third of the annual Zn load to the MVA.
- Tailings are not currently a major source of Zn to groundwater in the MVA because tailings pore water at the base of the tailings profile consists of process water that is alkaline and characterized by low concentrations of metals.

In RGC (2016a), the conceptual load balance was updated as summarized below.

Hydrological Model for Myra Valley

A hydrological model was developed in GoldSim to simulate daily flows in Myra Creek from 2012 to mid-2016. Simulated flows from the model were used to estimate Zn loads in Myra Creek and Zn loads from un-gauged catchments in Myra Valley (namely, Arnica Creek, and Webster Creek). The hydrological model is a simplified version of the UBC Watershed Model that simulates the daily runoff hydrograph for Myra Creek. Simulated flows from the hydrological model are shown in Figure 2, with observed and simulated Zn concentrations in Myra Creek at MC+50 m, MC+800 m and MC-TP4, and provincial WQGs for Zn.

Zn Loads in Myra Creek

To estimate incremental Zn loads to Myra Creek from the major site reaches during low flow and high flow conditions, thirty-three sampling campaigns were undertaken from 2012 to mid-2016.

The following "reaches" of Myra Creek were identified from the monitoring data:

- Lynx Reach; extends from Arnica Creek (upstream of the Mill Reach) to station MC+50 m.

- Upper Old TDF Reach; extends from MC+100 m to the rock outcrop near MC+850 m.
- Lower Old TDF Reach; extends from MC+850 to MC+1350 m.

Daily Zn loads in Myra Creek during low flow and high flow periods are shown in Figure 2.

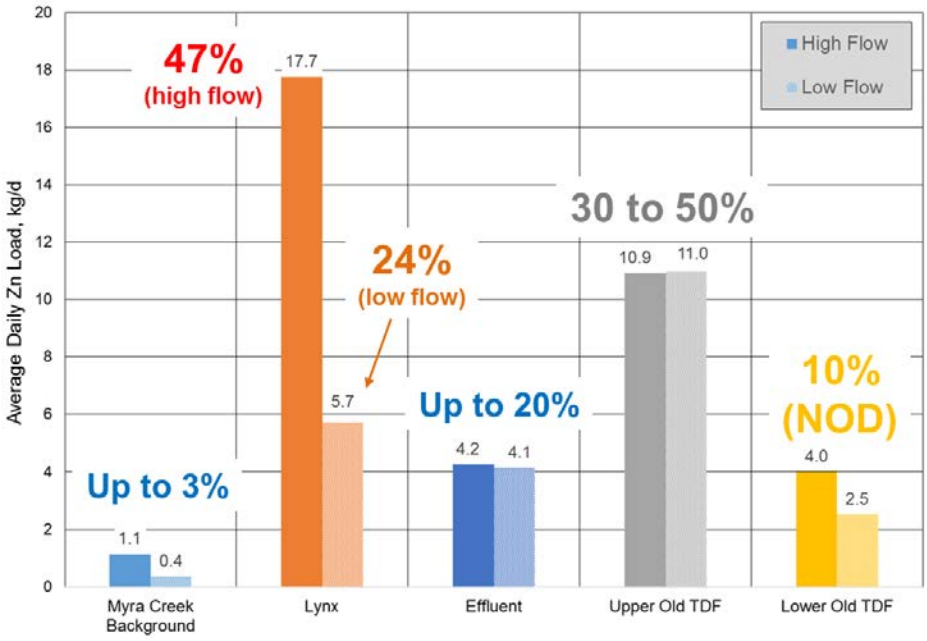


Figure 2: Average daily zinc loads in Myra Creek

Zn Load Captured by the Old TDF Under-Drains

From 2012 to 2016, the Old TDF under-drains recovered an estimated 43.7 t/year Zn from the local groundwater system. The average Zn load in Myra Creek at MC-TP4 from 2012 to 2016 is estimated to be 14.0 t/year Zn. The estimated Zn load to Myra Creek from the Lynx Reach, the Upper Old TDF Reach, and the Lower Old TDF Reach is estimated to be 11.8 t/year Zn after the 2.2 t/year Zn from treated effluent is accounted for. These Zn loads imply that the Old TDF under-drains capture about 80% of the Zn load that enters the groundwater system from various surface sources. NOD bypass is estimated to be ~10% of the load in Myra Creek, implying a substantial load to Myra Creek from the Lynx Reach and the Upper Old TDF Reach.

Zn Loads in Groundwater

Zn loads in groundwater within the Lynx Reach, Upper Old TDF Reach, and Lower Old TDF Reach were estimated to determine the contribution of source areas within these three study reaches. Zn loads in groundwater within each zone were estimated by multiplying groundwater flow in the aquifer by a representative Zn concentration in groundwater. Representative Zn concentrations for groundwater were selected by reviewing routine groundwater quality data collected since 2012.

Groundwater flows were estimated using the Darcy flow equation. Estimated Zn loads to Myra Creek were calibrated to observed Zn loads in Myra Creek during thirty-three sampling campaigns undertaken from 2012 to mid-2016.

Seven zones were delineated within the major site reaches:

- **Lynx Reach:** Zone I Mill and ETA/Cookhouse area and Zone II Lynx TDF and Super Pond area.
- **Upper Old TDF Reach:** Zone III Polishing Pond & HW area and Zone IV Upper Seismic Upgrade Berm.
- **Lower Old TDF Reach**: Zone V Upper Old TDF (upgradient of Inner Drain), Zone VI Lower Old TDF (downgradient of Inner Drain), and Zone VII downstream of NOD.

Loads in groundwater within the model zones are summarized in Figure 4. WRDs #1 and #6 (in Zone V and VI) and the Lynx TDF embankment berm (in Zone II) are the largest sources of Zn to groundwater. NOD bypass is estimated to be 1.4 t/year Zn. This is 12% of the annual Zn load in Myra Creek. The other 10.2 t/year Zn reports to the creek from areas upstream of the NOD (namely the Lynx Reach, mill area, and ETA/Cookhouse area).

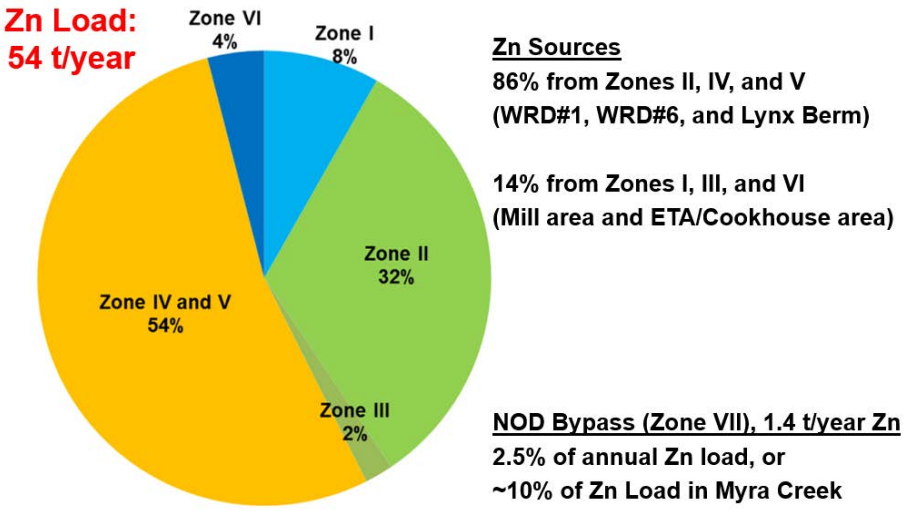


Figure 3: Estimated Zn loads in groundwater (by zone)

Numerical Contaminant Load Balance Model

RGC developed a numerical contaminant load balance model for NMF using the GoldSim platform. The model is a numerical representation of the conceptual site-wide contaminant load balance model that is summarized above. The model was developed to predict the performance of the Lynx SIS and assess proposed closure measures. Specific modeling objectives included simulating daily Zn loads within the groundwater system and to Myra Creek for current conditions (2012 to mid-2016). Further, Zn loads to

and from the MVA and Zn concentrations in Myra Creek were predicted for the following (future) conditions:

- Lynx SIS operational.
- Old TDF closed.
- Lynx TDF berm raised to its final height.
- Lynx TDF berm covered.
- Additional SIS options implemented.

Model Domain

The GoldSim model covers the entire catchment area of Myra Creek except for the small area that drains to Myra Creek downstream of MC-M2 between Myra Falls and Buttle Lake. The Myra Creek catchment was sub-divided into twenty-seven sub-catchments to estimate runoff components of the water balance. Sub-catchment boundaries were delineated based on footprint areas of Zn sources, boundaries of conceptual aquifer zones, outlines of diversion ditches, and locations of flow and/or water quality monitoring stations.

Model Structure

The numerical load balance model is a tool to track the movement and storage of water and associated Zn loads within the Myra Creek catchment. A flowline is established for each major source of water and/or Zn load to or from the MVA or Myra Creek. The load balance performs its computations for the MVA and Myra Creek from upstream to downstream. At any given point in Myra Creek, the model aggregates all flowlines and associated Zn loads that enter the stream at upstream locations, including discharges from the MVA.

The yield generated within the catchment of Arnica Creek has three potential destinations: the underground workings beneath the MVA, the MVA itself (i.e. recharge), or Myra Creek. The yield estimated by the hydrological model is partitioned based on user-defined fractions. The hydrological model represents the runoff process as comprising two components: one that responds quickly (overland flow and interflow) and one that responds slowly (groundwater), i.e. a "fast" and a "slow"' reservoir. The hydrological model was set up to simulate the delay and dispersion in the MVA by passing recharge flowlines through a linear reservoir.

Model Inputs (Zn Loads)

The following Zn loads report directly to Myra Creek within the boundaries of NMF:

- Zn loads from treated effluent.

- Zn loads from Arnica Creek and Webster Creek
- Zn loads from upstream areas of Myra Valley.

Zn loads in treated effluent were estimated from daily flow measurements from the Parshall flume and daily measurements of the total Zn concentration in effluent from the auto-sampler at station "Runoff 11A". The average daily effluent flow from 2012 to mid-2016 is 378 L/s (n = 1645). Daily flows ranged from 164 L/s to 1,529 L/s during this period. The average Zn load to Myra Creek via treated effluent from 2012 to 2016 is 2.4 t/year Zn.

Zn loads from Arnica Creek and Webster Creek (both un-gauged) were estimated from simulated daily flows from the hydrological model and average Zn concentrations in grab samples collected in 2011 and 2012. Estimated Zn loads to Myra Creek from Arnica Creek and Webster Creek are 0.6 t/year Zn and 0.1 t/year Zn, respectively. Zn loads in Myra Creek at MC-M1 (upstream of the mine site) were estimated as the product of the simulated daily flow and 0.004 mg/L Zn. This is the average Zn concentration in grab samples collected in 2011 and 2012. The Zn loads at MC-M1 represent natural loads from upstream sources. The annual Zn load in Myra Creek at MC-M1 was 0.7 t/year Zn from 2012 to 2016.

Daily Zn loads to groundwater from other sources to groundwater (i.e. WRDs, etc.) were estimated as the product of (i) daily recharge rates and (ii) a constant Zn concentration that is considered representative of seepage and/or tailings porewater. Initially, Zn concentrations from RGC (2014) were assigned to each source. Zn concentrations were then varied to reproduce Zn loads in groundwater within the model zones. For recharge, net percolation rates for waste rock from O-Kane Consultants Inc. (2014) were applied to WRD#1, WRD#6, the Lynx TDF embankment berm, and the Seismic Upgrade Berm. Monthly rates were re-distributed to match the daily time step in the GoldSim model. For other sources, daily recharge rates from the hydrological model were applied. Infiltration rates from the hydrological model were not assigned to the WRDs because these rates were not considered representative of waste rock.

Annually, the recharge rates for WRD#1, WRD#6, and the Lynx TDF embankment berm correspond to 74% of MAP. For tailings, a recharge rate of 300 mm/year from OKC (2014) was assigned. For the Seismic Upgrade Berm, the net percolation rate for waste rock covered with 1 m of vegetated till from OKC (2014) was applied. This rate corresponds to about 50% of MAP and is the same rate that was eventually assigned to the Lynx TDF embankment berm after it has been covered with till, rock, and soil. Lateral groundwater inflows to WRD#1 from the northern hillslope were assumed to represent an additional source of recharge to the model. Lateral groundwater inflows were varied to calibrate the numerical load balance model using the 50 mg/L Zn source term that was derived in RGC (2014). Lateral inflows of groundwater to WRD#1 were estimated to be 5.5 L/s during model calibration.

Model Calibration (Current Conditions)

The primary calibration targets for the load balance model were the observed daily Zn concentrations and inferred Zn loads in Myra Creek at MC-TP4 (n = 1644) and the observed zinc concentrations and inferred zinc loads from the thirty-three synoptic stream surveys at MC+50, MC+800 and MC-TP4 (i.e. at the end of each major site reach). The simulated concentrations at these MC stations were plotted against the observed zinc concentrations and these scatter plots evaluated visually and statistically. In addition, the incremental zinc loads simulated by the model for each model reach to Myra Creek and the total zinc load captured were compared to the inferred average zinc loads.

Initial model calibration involved varying flows to improve the fit of the scatter plots that compare simulated and observed daily Zn loads in Myra Creek. The model was also calibrated to groundwater flows and Zn loads to Pumphouse #4 during the initial stages of model calibration. Final calibration involved adjusting source terms to explain annual average Zn loads from 2012 to 2016 between model zones and to Myra Creek. Combined, these Zn loads represent 54.6 t/year Zn in groundwater each year.

Calibrated Results

Zn loads captured by the Old TDF under-drains range from 44.3 to 65.3 t/year Zn. The 4-year average for the calibration period is 55.3 t/year Zn. This represents about 86% of the average Zn load to groundwater after the Zn load from treated effluent is accounted for. Average annual flows from Pumphouse #4 range from 175 L/s (in 2014) to 241 L/s (in 2015). The 4-year average flow was 211 L/s. Calibrated Zn concentrations in Myra Creek are shown in Figure 2.

Some key observations regarding Zn concentration in Myra Creek are summarized here:

- The calibrated model suggests higher Zn concentrations in the creek often persist during lower flow periods (i.e. in the summer) when the dilution of Zn loads in the creek are lowest. Zn concentrations typically decrease in the fall and during the spring freshet due to the large flows of unimpacted water from upstream of the mine site. This variation is consistent with the observed pattern of Zn concentrations in Myra Creek. 85% of the simulated daily Zn concentrations in Myra Creek at MC-TP4 were higher than the provincial WQG.
- During high flow periods in 2012, 2013, and early 2014, simulated Zn concentrations in Myra Creek compare reasonably well to the Zn concentrations observed during sampling campaigns and with the auto-sampler at MC-TP4. During low flow periods, the model tends to over-estimate Zn concentrations by about 10 to 15%. This suggests that Zn loads to Myra Creek in 2012, 2013, and early 2014 are likely well-represented by the sources that were incorporated into the GoldSim model.

- From August 2014 to August 2015, the model tends to under-estimate Zn concentrations in Myra Creek during low flow and high flow periods. This could be related to more flushing of impacted groundwater from the MVA during the prolonged wet periods that characterized these years than during the drier years of 2012 and 2013. Alternatively, the number of sources represented in the GoldSim model could be insufficient to explain Zn loads to Myra Creek.

Model Predictions

To assess future conditions, RGC simulated loads and concentrations from 2012 to mid-2016 with the GoldSim model in "'post-closure mode". When this mode is specified, the model is run with the same climatological conditions that were applied during model calibration. This allowed future Zn loads and concentrations to be assessed as though the change to the model had been implemented during the calibration period. The effects of each closure measure are additive so there is a progressive decrease in simulated Zn concentrations over time as each measure is implemented. Predicted Zn loads and Zn concentrations are summarized in Table 1.

Table 1: Predicted flows and Zn loads for future conditions

Scenario	Input to Groundwater		Captured by Old TDF under-drains (Pumphouse #4)		Captured by Lynx SIS		Captured by Additional SIS	
	Load, t/year	Recharge L/s	Load, t/year	Flow, L/s	Load, t/year	Flow, L/s	Load, t/year	Flow, L/s
Current Conditions	62.1	48	55.3	211	-	-	-	-
Lynx SIS	60.0	46	39.8	167	16.6	57	-	-
Old TDF closure	48.4	42	28.9	163	16.6	57	-	-
Final Lynx TDF at closure	48.7	42	29.0	163	16.8	57	-	-
Covered Lynx TDF Berm								
Final Lynx TDF (rock and till cover)	43.7	41	27.5	162	13.3	57	-	-
Final Lynx TDF (geomembrane)	33.8	38	24.7	159	6.5	57	-	-
Additional SIS (assuming rock and till cover)								
Additional SIS (Zone IV only)	43.7	41	27.5	162	13.3	57	0.5	8
Additional SIS (Zone I only)	43.7	41	27.5	162	13.3	57	0.3	18
Additional SIS (Zones I and IV)	43.7	41	27.5	162	13.3	57	0.9	26

Lynx SIS Performance

Predicted Zn concentrations in Myra Creek are shown in Figure 4 with calibrated Zn concentrations (2012 to mid-2016). Key observations for this scenario are summarized here:

- The Lynx SIS is predicted to capture 16.6 t/year Zn or about 70% of the Zn load to groundwater from sources in Zones I and II.

- The Zn load to the Old TDF under-drains is predicted to be reduced by about 30% to 39.8 t/year Zn by seepage recovery upgradient. Flows to the Old TDF under-drains are reduced to 167 L/s. This represents a 20% reduction compared to the calibrated flows for current conditions.
- The average Zn concentration in Myra Creek at the carbridge (MC+50 m) is predicted to be 0.012 mg/L Zn once the Lynx SIS is operational. This represents a 60% reduction compared to the average annual Zn concentration that was simulated for current conditions.

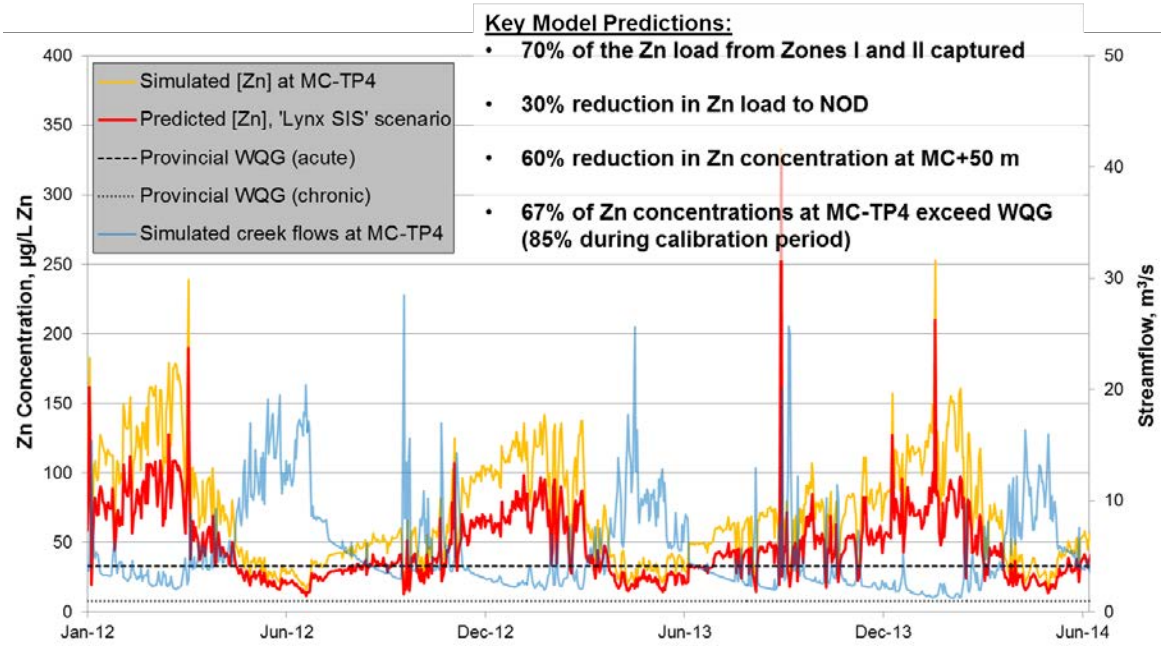


Figure 4: Predicted Zn concentrations in Myra Creek, Lynx SIS operational scenario

Old TDF Closure Performance

Predicted Zn concentrations in Myra Creek are shown in Figure 5 with predicted Zn concentrations from the "Lynx SIS Operational" scenario. Key observations for this scenario are summarized here:

- Reducing infiltration to WRD#6 to 2% of MAP (due to liner placement) is predicted to reduce Zn loads to groundwater by 11.6 t/year Zn. The model suggests that Zn concentrations in Myra Creek will not be substantially reduced by covering WRD#6 because the Zn load from WRD#6 (albeit smaller after Old TDF closure) will continue to be directed to the Lower Old TDF Reach where it will be mostly captured by the NOD.
- The annual Zn load to the Old TDF under-drains will be reduced to 28.9 t/year Zn by Old TDF closure and ongoing operation of the Lynx SIS. This is about 50% of the Zn load that reports to the Old TDF under-drains under current conditions. Old TDF closure is predicted to reduce Zn concentrations in Myra Creek by about 10%.

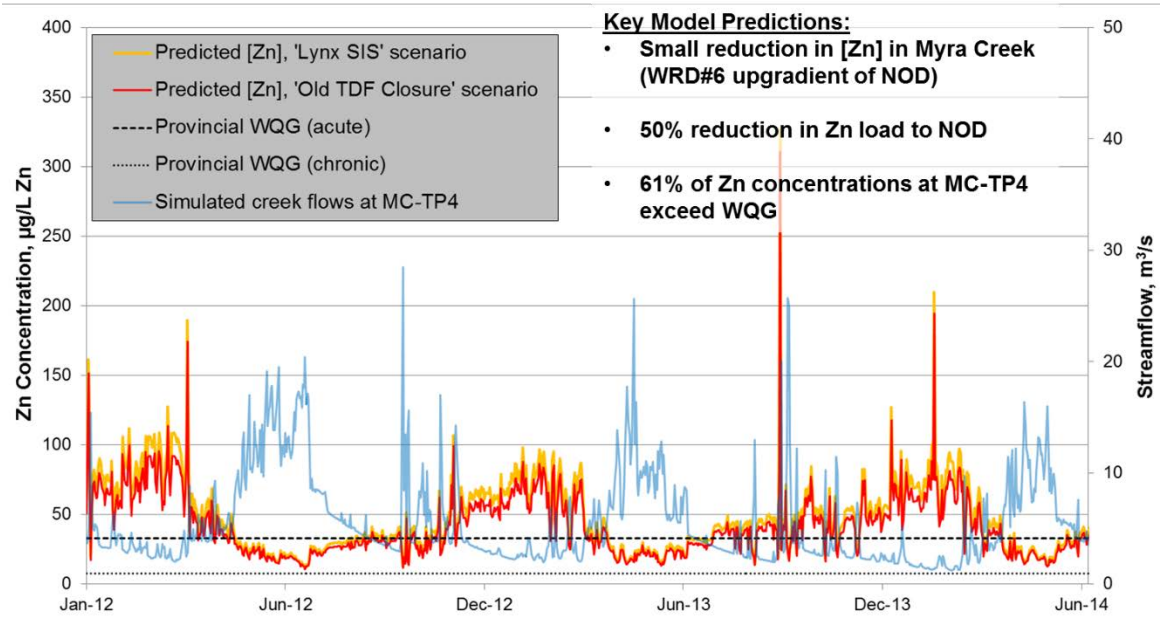


Figure 5: Predicted Zn concentrations in Myra Creek, Old TDF closure scenario

Final Lynx TDF Berm (No Cover)

Key observations for this scenario are summarized here (see Table 1):

- Zn loads to groundwater in Zone II are predicted to increase to 48.7 t/year Zn after the Lynx TDF berm is raised to its final height (or about 1% higher than the load after the Old TDF has been closed). This small increase is attributed to substantial Zn loads to groundwater that were simulated from surface waste within the future footprint of the berm under current conditions.
- The load to the Old TDF under-drains is predicted to be reduced to 29.0 t/year Zn. This is about the same Zn load as is predicted to be recovered from groundwater after the Old TDF is closed.
- Zn concentrations in Myra Creek will not be affected by raising the Lynx TDF embankment berm to its final height. This is because the Lynx SIS will continue to intercept most of the Zn load that is directed towards the creek in Zone II.

Performance of Lynx TDF Berm Cover

Key observations for this scenario are summarized here (see Table 3):

- For final closure, NMF plans to cover the Lynx TDF embankment berm with a mixture of rock, till, and soil that will be re-vegetated with trees (see Amec Foster Wheeler, 2016). Reducing recharge to the Lynx TDF embankment berm to 50% of MAP is predicted to reduce the Zn load to the groundwater system to 43.7 t/year Zn. This is 10% lower than the predicted Zn load to groundwater once the Lynx TDF berm has been raised to its final height.

- For comparison purposes, RGC simulated the effect of placing a geomembrane liner on the Lynx TDF embankment berm. Reducing recharge to 2% of MAP (representing a liner) is predicted to reduce the Zn load to groundwater by 30% but it is not predicted to affect simulated Zn concentrations in Myra Creek. This reflects the effectiveness of the Lynx SIS, which is assumed to operate in perpetuity to reduce Zn loads to Myra Creek.

Additional SIS Options

Zn concentrations in Myra Creek could be further reduced by additional seepage recovery in the Upper Old TDF Reach and in the ETA/Cookhouse area, by re-connecting the NOD in the Upper Old TDF Reach, or by the installation of additional pumping wells.

Should these measures be implemented, ~40% of the predicted Zn load to Myra Creek at MC-TP4 is related to treated effluent. 23% of the Zn load at MC-TP4 is related to Zn loads from upstream sources and Arnica Creek. Zn concentrations in Myra Creek could therefore only be further reduced by:

- Additional seepage recovery from the Lynx Reach.
- Improved performance of the NOD in the Upper and Lower Old TDF Reaches.
- Reducing Zn concentrations in treated effluent.

Of these options, reducing Zn concentrations in treated effluent by upgrading the water treatment system is likely the most feasible. Portions of Myra Creek could also be lined and/or raised to prevent groundwater discharge to the creek.

Conclusions

This paper has shown that future Zn loads and Zn concentrations in Myra Creek will be reduced most effectively by operating the Lynx SIS. NMF implemented the first phase of the Lynx SIS in 2017, and its hydraulic performance and effect on Myra Creek is currently being monitored. Performance monitoring will allow the interference between the Lynx SIS and NOD to be characterized, and will allow the operation of the Lynx SIS pumping wells (and the shallow drain component) to be optimized.

Neither the operation of the Lynx SIS, nor the subsequent closure of the Old TDF and Lynx TDF, are predicted to reduce Zn concentrations below provincial WQGs. To do so, one or more of the following measures could be implemented:

- Additional SIS pumping well(s) in the ETA/Cookhouse area.
- Western (upgradient) extension of the shallow component of the Lynx SIS.
- Shallow cut-off wall along northern side of Myra Creek stream channel in lower Lynx Reach.
- Lining and/or re-alignment of Myra Creek in the lower Lynx Reach.

NMF is also developing Science Based Environmental Benchmarks (SBEBs) in support of future closure planning. SBEBs for Cd, Cu, and Se are being developed. The SBEBs, when available, will determine whether any of the measures above will be implemented, or if alternative closure strategies should be further evaluated.

Acknowledgements

The authors wish to thank Nyrstar for their support and permission to publish this paper.

References

Amec Foster Wheeler. 2016a. NX14001K Nyrstar Myra Falls Mine Old TDF closure cover permit level design, Draft.

Amec Foster Wheeler. 2016b. NX14001K.2 Nyrstar Myra Falls Mine Lynx TDF dam face closure cover permit level design, Draft.

Nautilus Environmental Consulting Inc. 2016. Development of site-specific objectives for waterbodies associated with Nyrstar Myra Falls Mining Operations.

O'Kane Consultants Inc. 2014. Myra Falls closure planning – net percolation estimates for various TDF and WRD cover system alternatives.

Robertson GeoConsultants Inc. 2014. Site-wide contaminant load balance model for Nyrstar Myra Falls.

Robertson GeoConsultants Inc. 2016a. Contaminant load balance model for current and future conditions.

Robertson GeoConsultants Inc. 2016b. Old TDF (APA) hydrogeological investigation, Nyrstar Myra Falls.

Robertson GeoConsultants Inc. 2016c. Performance review of new outer drain, Nyrstar Myra Falls.

Wels, C., Thomas, A. and Pesonen, N. 2018. Groundwater discharge into tailings facility during intense precipitation events, Nyrstar Myra Falls, in *Proceedings of the Third Annual International Conference on Mine Water Solutions,* Vancouver, Canada.

Proceedings of Mine Water Solutions 2018
June 12–15, 2018, Vancouver, Canada
Published by the University of British Columbia, 2018

A New Rapid Brine Release Extraction Method in Support of Lithium Brine Resource Estimation

Tzung-mow Yao, GeoSystems Analysis, Inc., USA
Michael Milczarek, GeoSystems Analysis, Inc., USA
Frits Reidel, Flosolutions Chile, Chile
Daniel Weber, Montgomery & Associates, USA
Edward Peacock, Montgomery & Associates, USA
Murray Brooker, Hydrominex Geoscience, Australia

Abstract

Lithium brine mining via groundwater extraction and concentration in large evaporation ponds accounts for approximately half of the world's lithium production. Lithium brine mineral resources and reserves are typically located in large lacustrine evaporite closed basins (salt pans or salars) associated with high-angle faulting and hydrothermal fluids containing lithium migrating into the basins, where they are concentrated by up to 2 orders of magnitude. Lithium concentrations can vary laterally and vertically across a lithium deposit, and the host aquifers typically consist of highly heterogeneous layered sediments. Thus, knowledge of the relative lithium concentrations and the drainable porosity and potential flow contribution from the different lithological facies is essential for the resource estimation and to support groundwater modeling.

As a first step in determining economic viability, the lithium brine deposit is evaluated using statistically representative measurements of depth-specific brine sample lithium concentrations, as well as core samples to determine drainable porosity (specific yield) of the host aquifer materials. Whereas aquifer pumping tests can provide data on large-scale aquifer hydraulic characteristics, results typically cannot resolve explicit estimates of mineral grade and drainable porosity for multi-layer aquifer systems – such as lithium concentrations and specific yield of fine-grained hydrogeological units versus coarse-grained hydrogeological units. Consequently, brine mineral resource estimation requires supporting data from both field and laboratory testing programs to estimate the lithium concentrations associated with the various lithologies in concert with the ability to drain brine from the various lithological layers.

We present a rapid brine release (RBR) test based on a modified soil water characteristic curve (SWCC) method to determine specific yield characteristics of core samples collected during exploration drilling. The laboratory method takes less than one week and dozens of samples can be run

simultaneously using various core sample types (i.e., sonic, HQ, PQ wire line diamond drill core). To date this method has been used to determine specific yield characteristics on hundreds of samples from eight different brine deposits in North and South America. We present case studies from Clayton Valley Lithium Project, Nevada, USA (Pure Energy Minerals) and Minera Salar Blanco (Maricunga Joint Venture Project), Chile.

Background and Method

Specific yield (S_y) is assumed to be equivalent to the amount of brine solution that may be released under gravity drainage conditions from groundwater pumping of the brine deposit. The corresponding amount of water retained is referred to as specific retention (S_r) and the sum of the specific yield and specific retention is equal to the total porosity (P_t), which is the ratio of the volume of pores to the bulk test sample volume.

Laboratory methods to determine brine release/specific yield range from moisture retention characteristic (MRC/SWCC) methods (ASTM D6836-16, 2016), and centrifugal tests (ASTM D6836-16, 2016), to simple suction methods (Relative Brine Release Capacity, RBRC, Stormont et. al., 2011) to establish drainage, S_y and P_t. Traditional SWCC tests are time consuming and expensive; centrifugal and RBRC tests are rapid, but can result in significant errors due to unknown equilibrium times and/or uncontrolled boundary conditions. GeoSystems Analysis, Inc. (GSA) has developed a Rapid Brine Release (RBR) test based on a modified SWCC method and equipment (Figure 1) to determine the specific yield characteristics of core samples collected during exploration drilling. The laboratory method takes less than one week, and dozens of samples can be run simultaneously using various core sample types (i.e., sonic, HQ or PQ diamond core, Figure 2).

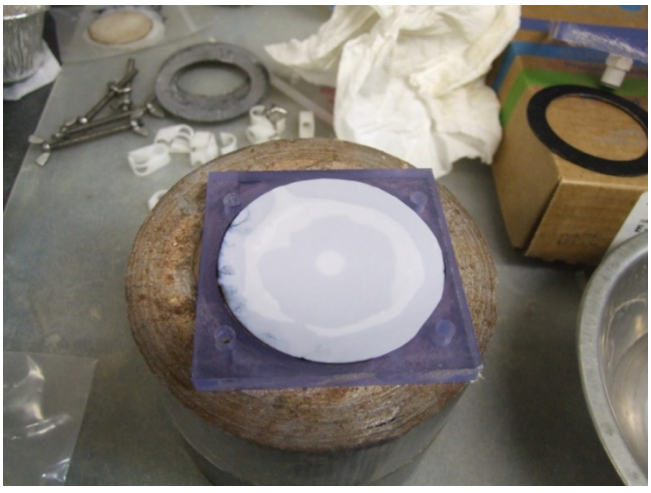


Figure 1: Test cell assembly with micropore filter paper at bottom



Figure 2: HQ core and test ring

The RBR method used by the GSA Laboratory is based on the SWCC method for direct measurement of total porosity (Flint and Flint, 2002; MOSA Part 4 Ch. 2, 2.3.2.1), specific retention (Romano and Santini, 2002; MOSA Part 4 Ch. 3, 3.3.3.5), and specific yield (Cassel and Nielson, 1986). A simplified Tempe cell design (Modified ASTM D6836-16) is used to test intact core samples (Figure 3). These cells can be arranged to handle large number of tests simultaneously (Figure 4). Brine release drainage is measured at –100 to –150 mbar and –330 mbar of soil water matric potential, where:

1. Brine release at –120 mbar is assumed to approximate drainable porosity from sandy sediments and macropores (–150 mbar suggested by Nwankwor et al., 1984; and –100 mbar suggested by Cassel and Nielsen, 1986)
2. Brine release at –330 mbar represents the S_y for intermediate to finer texture sediments (Cassel and Nielsen, 1986)

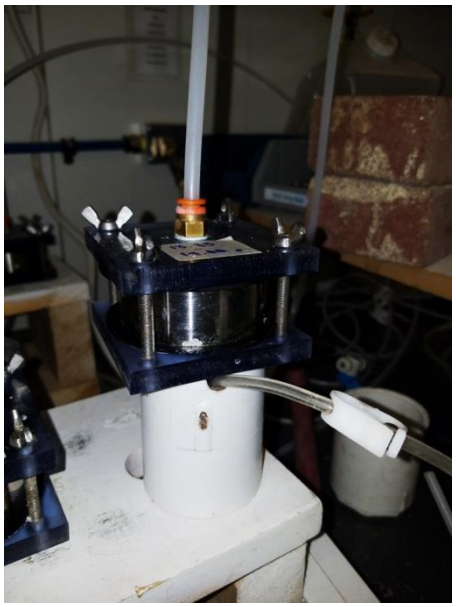


Figure 3: Simplified Tempe Cell



Figure 4: Simultaneous testing of forty cells

RBR Test Cells have a standard diameter of 6.35 cm by 2.5 cm length. HQ core samples can be tested directly or prepared by driving 6.35 cm diameter stainless steel liners into undisturbed sonic and HQ core samples using a hydraulic press in order to preserve the integrity of the core sample. PVC end caps are then placed on either side of the sample to create the RBR Test Cells. The PVC caps contain gaskets to provide an airtight test cell that maintains constant air pressure and allows continuous solution outflow through the membrane.

After sample preparation, the RBR Test Cell is then saturated with either a brine solution prepared to mimic the chemical composition of the brine solution found within the deposit, or native brine samples from the deposit. Saturation is achieved by repetitively applying brine solution from the bottom of the test cell and then applying a vacuum (–30 to –700 mbar) from the top of the test cell to assist the saturation. Any standing brine solution is carefully removed from the top of the test cell prior to starting the test.

Each saturated RBR Test Cell is transferred to a test rack for the pressure extraction procedure (Figure 4) for three pressure steps, as follows. Zero pressure is applied for a day and any free water due to core over-saturation is removed during this step. Two sequential pressure steps, at 120 mbar and 333 mbar (Romano and Santini, 2002; MOSA Part 4 Ch. 3, 3.3.3.2), are used to approximate brine solution release at –120 mbar and –333 mbar of matric potential.

The 120-mbar pressure step is maintained for two days and the 333-mbar step is continued until the sample reaches equilibrium (another two to four days). Test cells are weighed prior to saturation, after saturation, and then two to three times daily to determine brine solution loss over time. Samples are oven-dried after the final step to determine S_r, dry bulk density (ρ_b), and P_t (Flint and Flint, 2002; MOSA Part 4 Ch. 2, 2.3.2.1), where S_r is the volume of water retained by the sample under –333 mbar soil water matric potential.

Brine solution release volumes at the 120 mbar and at 333 mbar pressure steps are estimated as the difference of the brine weight divided by the brine solution specific gravity (i.e., 1.2 g/cm^3) between the initial cell assembly mass and the mass after each pressure plate step (Romano and Santini, 2002; MOSA Part 4 Ch. 3, 3.3.3.5). The S_y is assumed to approximate the volume of solution released between saturation to –333 mbar divided by the total sample volume. The S_y value is calculated as follows:

$$\boldsymbol{S_y = \frac{w_s - w_{333\,mbar}}{A * L * Bsg}} \qquad \text{Equation 1}$$

where w_s is the saturated weight,
w_{333} mbar is the weight at 333 mbar,
A is sample core area,
L is sample length, and
Bsg is the specific gravity of the brine solution.

Sample material from the test cell is then oven-dried at a low temperature for five days to determine the residual brine content and bulk density.

Particle density, (*PD*, volumetric mass of the solid) can also be estimated from the P_t and bulk density measurements since the volume of the test cell is known:

$$\boldsymbol{PD = \frac{\rho_b}{(1 - P_t)}} \qquad \text{Equation 2}$$

where *PD* is the particle density in g/cm^3.

Case Studies

Clayton Valley Lithium Project (Blois et. al., 2017)

GSA tested 48 HQ-size core samples from three boreholes at Clayton Valley using the RBR lab method. From this samples set, 10 duplicate samples were sent for RBRC testing by DBS&A (Albuquerque, NM) and 5 samples were sent to Vista Clara (Mukilteo, WA) for testing using a Nuclear Magnetic Resonance (NMR) laboratory method (Behroozman et. al., 2015). Lithologies ranged from fine sand to silt and ash deposits. Results from boreholes CV-7 (A) and CV-8 (B) shown in Figure 5 indicate:

- RBR values of total porosity were higher than the NMR Corona method, potentially due to initial brine content of the samples upon receipt and laboratory re-saturation methods used for the NMR laboratory method.
- Except for one anomalous measurement comprised of pellet ash, S_y measurements were in agreement. The anomaly may be related to the high proportion of ash in the sample and re-saturation conditions used by each of the labs.
- Coarser volcanic ash and fine sand material showed higher S_y and P_t, and lower particle density.
- RBR method results for all 48 samples showed a mean S_y of 6.9%.

Comparison of RBR and RBRC methods showed generally good agreement for S_y of volcanic ash sediments, and comparable results, though frequently lower S_y values were observed using the RBRC method for fine-grained, low specific yield sediments. This may be due to longer equilibrium times required for the finer grained materials.

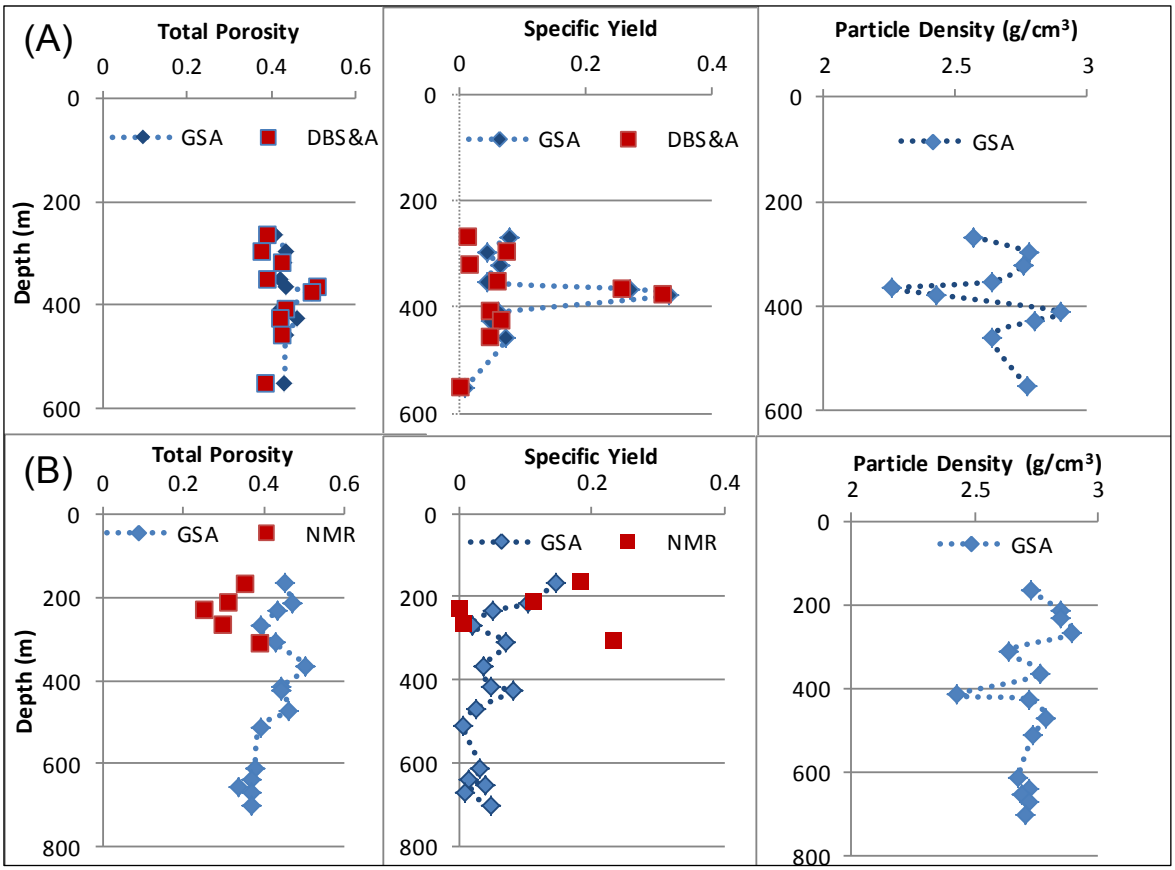


Figure 5: Comparison of RBR (GSA), RBRC (DBS&A) and NMR (Vista Clara) methods for total porosity and specific yield and GSA particle density estimates for (A) CV-7 and (B) CV-8

Minera Salar Blanco, Maricunga Lithium Project (Worley Parsons, 2017)

GSA tested 165 PQ samples from four boreholes drilled using sonic methods. From this samples set, 28 duplicate samples were sent for centrifuge testing by Core Laboratories (Houston, TX). Six different lithologies were identified as summarized in Table 1.

Table 1: Maricunga samples – total porosity and specific yield test results and summary

Material Classification	Core Lab P_t			GSA P_t			Core Lab S_y		GSA S_y	
	N	Mean	SD	N	Mean	SD	Mean	SD	Mean	SD
Clay dominated	6	0.53	0.05	58	0.44	0.08	0.02	0.03	0.03	0.04
Sand dominated	3	0.45	0.08	21	0.38	0.07	0.05	0.04	0.07	0.06
Gravel dominated	3	0.32	0.02	22	0.34	0.06	0.10	0.07	0.17	0.10
Volcaniclastic	13	0.46	0.05	41	0.45	0.06	0.13	0.05	0.15	0.06
Halite	2	0.35	0.08	17	0.33	0.13	0.07	0.05	0.09	0.09
Ulexite	1	0.49	N/A	4	0.35	0.09	0.04	N/A	0.06	0.04

Total porosity and specific yield values were profiled for four boreholes and statistically analyzed for five corresponding lithology types. The Ulexite sample is not shown in Figures 6, 7, and 8 because there were an insufficient number of samples from this lithology type. Figures 6 and 7 compare the values measured by the GSA RBR method and the Core Lab centrifuge method for P_t and S_y, respectively. Figure 8 shows the lithologically classified RBR P_t and S_y distributions and statistics assuming normal distribution.

- The RBR method showed acceptable agreement with the centrifuge test results, though higher S_y values on average were measured by the RBR method, possibly due to longer equilibrium times compared to the centrifuge test.
- Volcaniclastic and gravel materials showed higher S_y, values compared to clay, sand, and halite samples.
- Lower particle densities were also observed for volcaniclastic and halite samples (data not shown).

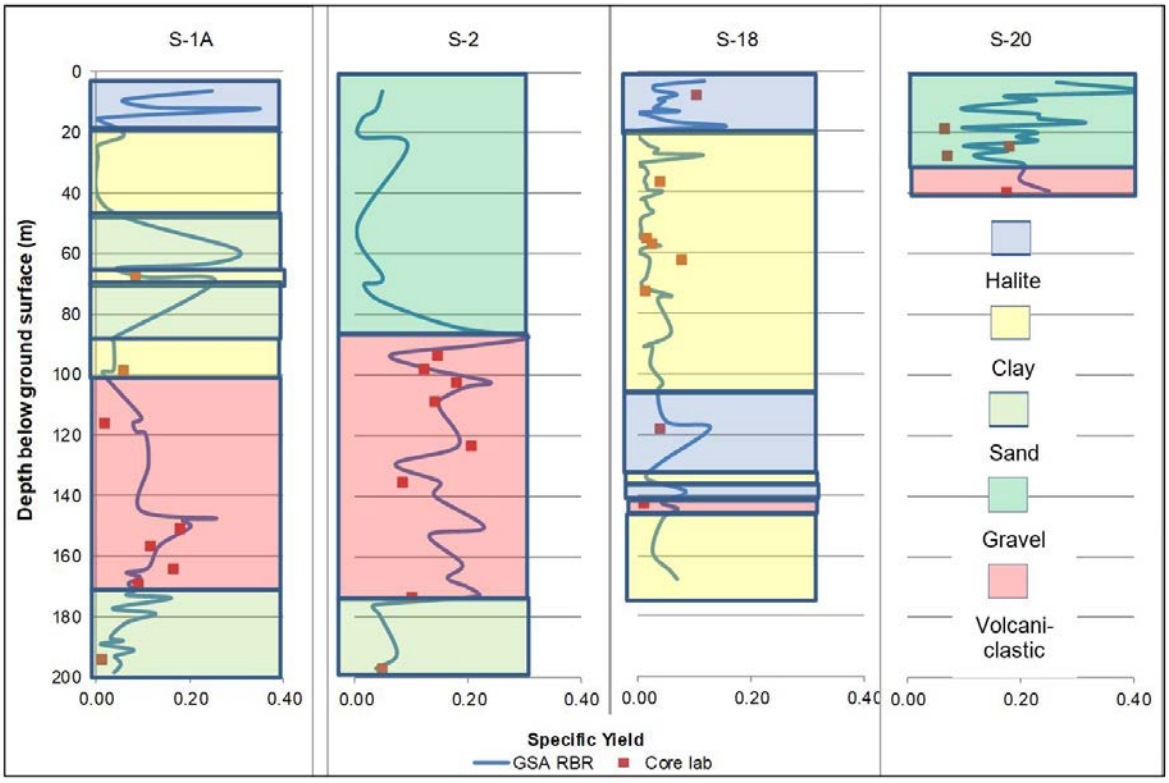


Figure 6: Comparison of GSA RBR and Core Lab measured *Sy* values

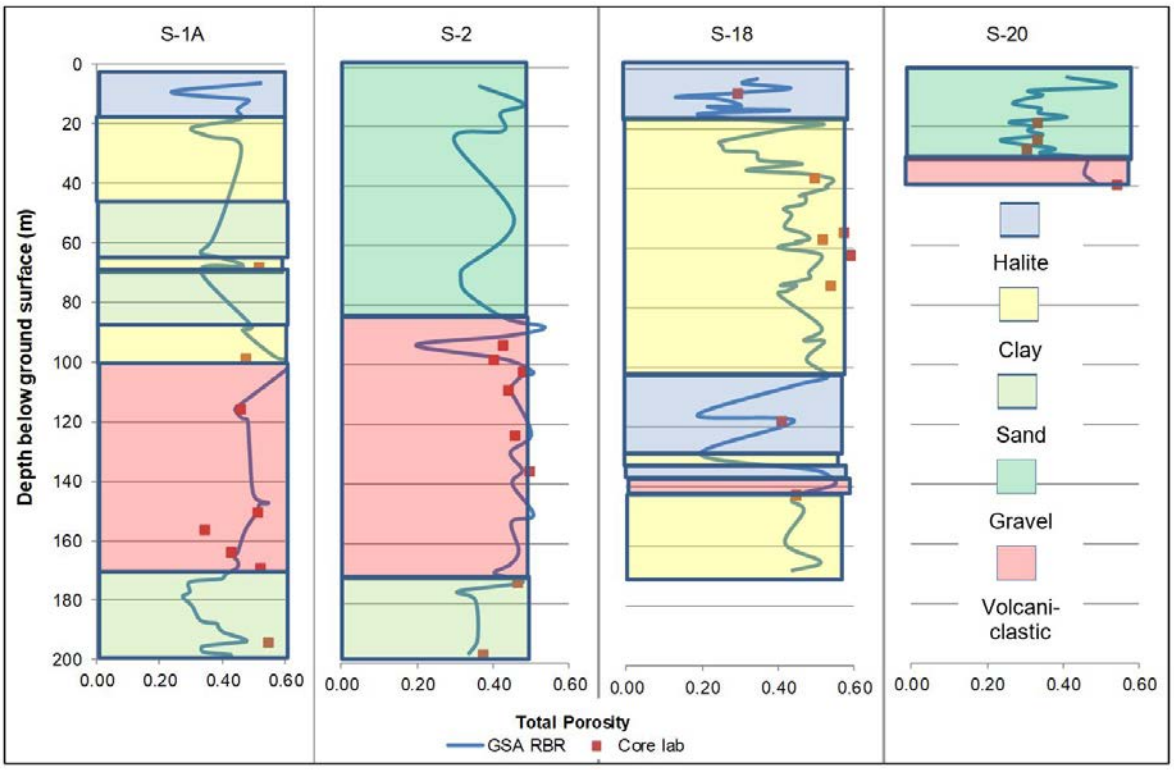


Figure 7: Comparison of GSA RBR and Core Lab measured *Pt* values

Conclusions

The Rapid Brine Release (RBR) method presented in this paper is an improvement over existing brine release laboratory test methods. It is based on proven and standard laboratory procedures that allow samples to be measured at equilibrium, and two drainage points can be measured. Duplicate sample testing indicates general agreement with other brine release methods, though the estimated drainable porosity values are slightly higher, possibly due to differences in equilibrium conditions. Benefits of this laboratory method include:

standard methodology is used to determine the specific yield, which results in higher accuracy and reproducibility;

the test is relatively rapid;

it is possible to test large quantities of samples and variable sample sizes/diameters, and;

it is possible to calculate/estimate particle density.

Acknowledgements

We thank Pure Energy Minerals Ltd. and Minera Salar Blanco for permission to use their data.

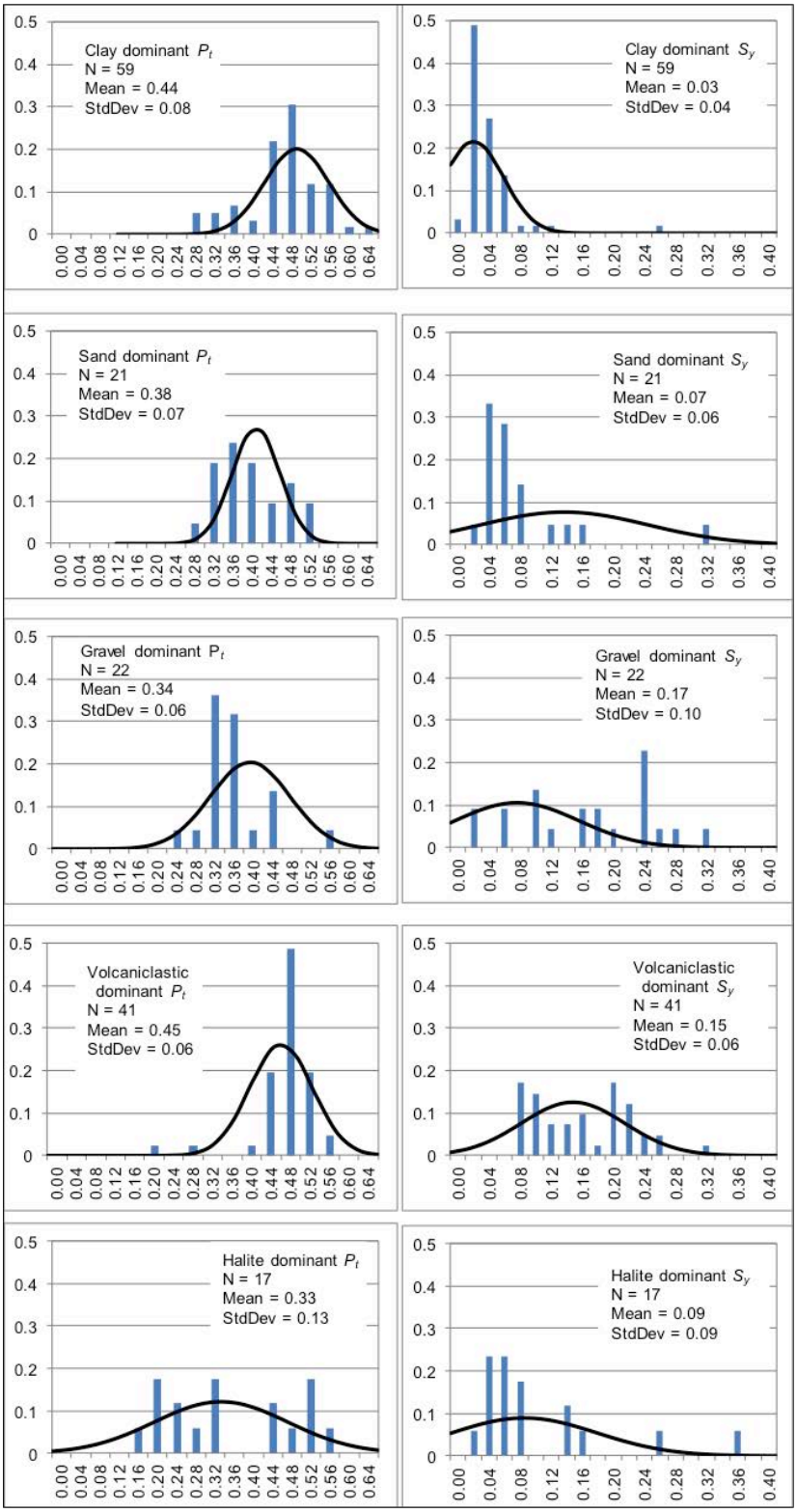


Figure 8: Lithologically classified Pt and Sy distributions and statistics (y-axis is fraction of samples). Curves in plots are the best-fit normal distribution

References

ASTM D6836-16. 2016. *Standard Test Methods for Determination of the Soil Water Characteristic Curve for Desorption Using Hanging Column, Pressure Extractor, Chilled Mirror Hygrometer, or Centrifuge.* West Conshohocken, PA: ASTM International.

Behroozman, A., Keating, K. and Auken, E. 2015. A review of the principles and applications of the NMR technique for near surface characterization, *Surveys in Geophysics,* 36(1): 27–85.

Blois, M.D.S., Weber, D.S., Burga, E. and Sawyer, V. 2017. *Clayton Valley Lithium Project,* Esmeralda County, NV, NI43-101 Technical Report, prepared for Pure Energy Minerals Ltd.

Bradley, D., Munk, L., Jochens, H., Hynek, S. and Labay, K. 2013. A preliminary deposit model for lithium brines: USGS Open-File Report 2013–1006.

Cassel, D.K. and Nielsen, D.R. 1986. Field capacity and available water capacity, in A. Klute (ed.), *Methods of Soil Analysis,* Part 1, Chap. 36. Madison, WI: American Society of Agronomy: 901–926.

Dane, J.H. and Topp, C.G. 2002. *Methods of Soil Analysis (MOSA),* Part 4, Physical Methods. Book Ser. 5.4. Madison, WI: Soil Science Society of America.

Flint, L.E. and Flint, A.L. 2002. Porosity, in J.H. Dane and C.G. Topp (eds), *Methods of Soil Analysis,* Part 4, Physical Methods. Book Ser. 5.4. Madison, WI: Soil Science Society of America.

MOSA (Methods of Soil Analysis). 2002. J.H. Dane and C.G. Topp (eds.), *Methods of Soil Analysis,* Part 4, Physical Methods. SSSA Book Ser. 5.4. Madison, WI: Soil Science Society of America.

Nwankwor, G.I., Cherry, J.A. and Gillham, R.W. 1984. A comparative study of specific yield determinations for a shallow sand aquifer, *Ground Water,* 22(6): 764–772.

Romano, N. and Santini, A. 2002. Water retention and storage – field, in J.H. Dane and C.G. Topp (eds), *Methods of Soil Analysis,* Part 4, Physical Methods. Book Ser. 5.4. Madison, WI: Soil Science Society of America.

Stormont, J.C., Hines, J.S., O'Dowd, D.N., Kelsey, J.A. and Eric Pease, R. 2011. A method to measure the relative brine release capacity of geologic material, *ASTM Geotechnical Testing Journal,* 34(5): 406–412.

Worley Parsons Resources & Energy. 2017. *Preliminary assessment and economic evaluation of the Salar Blanco Project Atacama Region, Chile,* NI 43-101 Technical Report, prepared for Minera Salar Blanco, Santiago, Chile.

Proceedings of Mine Water Solutions 2018
June 12–15, 2018, Vancouver, Canada
Published by the University of British Columbia, 2018

A Comparison of Predicted Groundwater Impacts to Observed Effects at the Victor Diamond Mine, 11 years after the Start of Dewatering

Simon Gautrey, Amec Foster Wheeler (Wood), Canada

Abstract

The Victor Diamond Mine is an open pit mine in Canada, located in the James Bay Lowlands, approximately 90 km west of the community of Attawapiskat and 120 km east of the Ring of Fire. Since early 2007, operation of the mine has been supported by dewatering of the limestone aquifers that surround the Victor kimberlites, but at the time of writing this paper, the mine is about to close. Monitoring throughout the period of active mining documented the response of the local groundwater system to mine dewatering, and can be compared to predictions of groundwater impacts made as part of the pre-mining Environmental Assessment process. This presentation will provide a summary of predicted groundwater impacts made prior to mining, and compare them to the observed effects towards the end of mine life. The comparison will be used to assess how well hydrogeological investigations completed between 2004 and 2007 predicted impacts to the groundwater environment.

Introduction

The Victor Diamond Mine is an open pit mine operated by De Beers Canada Inc. (De Beers) in Ontario, Canada. It is located in the James Bay Lowlands, approximately 90 km west of the community of Attawapiskat and 120 km east of the Ring of Fire (Figure 1). Mine dewatering began in 2007 and is slated to end in early 2019. The site is remote, and the mine is supplied via an airstrip and a winter road along the James Bay Coast from Moosonee. The main facilities at the mine consist of the open pit, rock and overburden storage areas, former quarries, fine processed kimberlite facilities, the airstrip, the processing plant, and office residential complex.

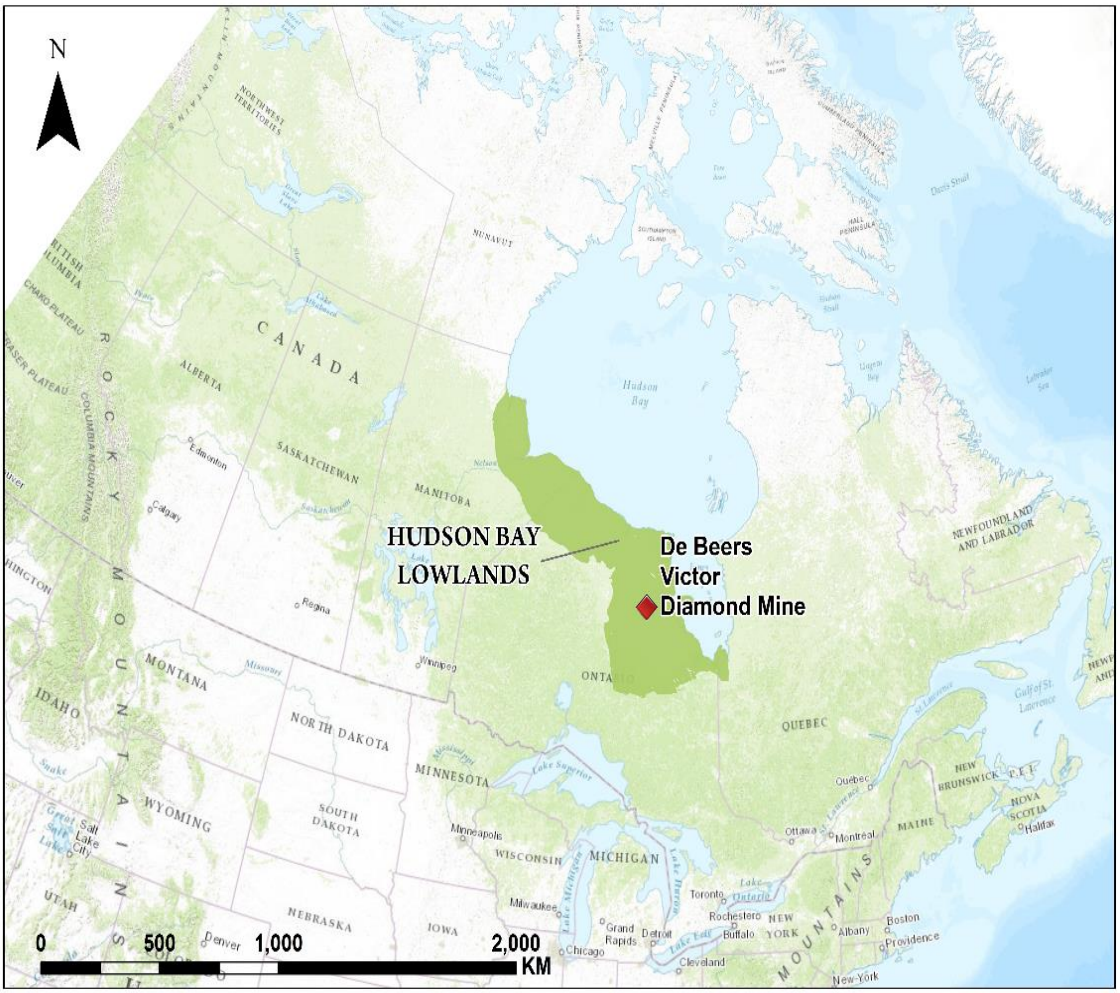


Figure 1: Site location map

The James Bay Lowlands are a vast peatland that is drained by numerous creeks and a few large rivers. Near the mine, the terrain is flat, except for small isolated bioherms, the occasional small pingos, and a few low relief former beach ridges, or where larger rivers have incised into peatlands. The area experiences cold winters (January has a mean temperature of –20.4ºC) and cool summers (July has a mean temperature of 16.2ºC), and is relatively dry, with an average annual precipitation of approximately 690 mm/year (AMEC, 2004).

The diamond-bearing kimberlite at the mine site consists of two intertwined kimberlite pipes that intrude through the country rock approximately 170 Ma (Kong et al., 1999). The country rock consists of up to approximately 260 m of Paleozoic sediment rock that overlies Precambrian crystalline bedrock of the Superior Craton (Figure 2).

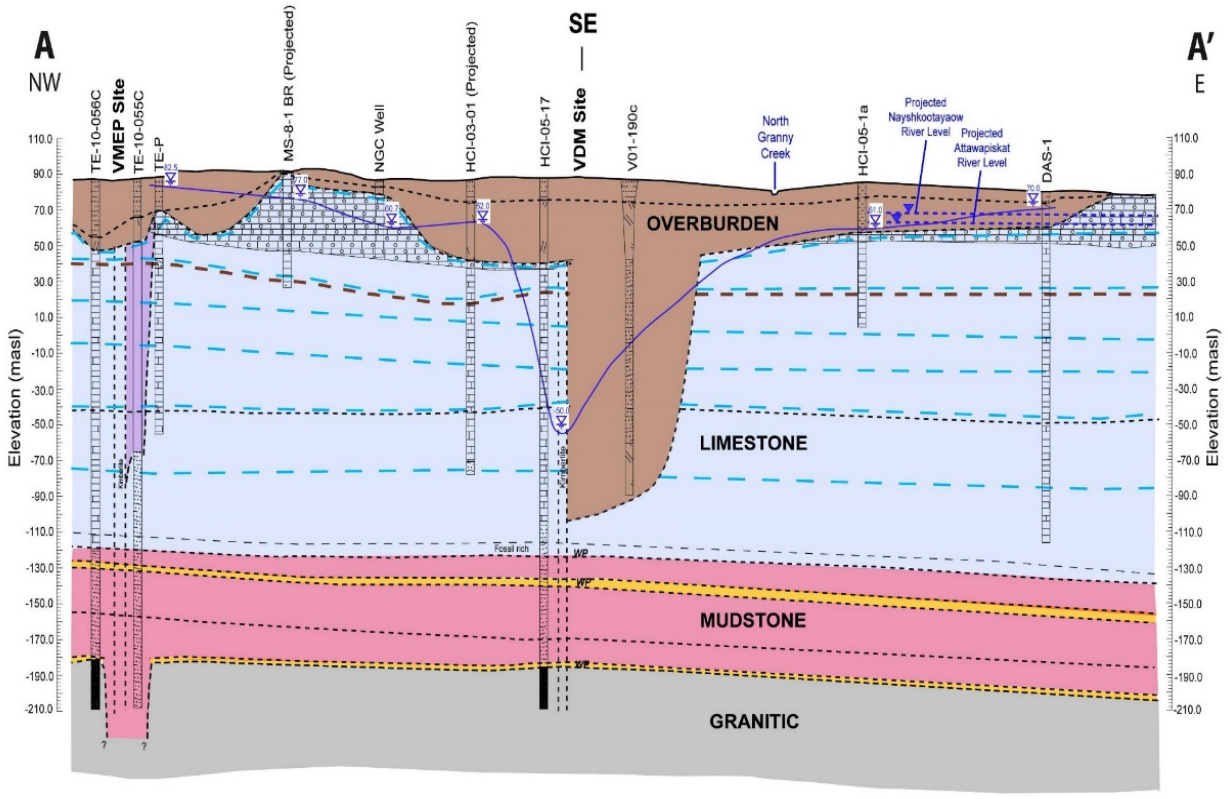


Figure 2: Hydrogeological cross section interpretation

The Paleozoic bedrock sequence is Ordovician and Silurian in age and part of the Hudson Platform, which formed within a large intracratonic basin centered in Hudson Bay. The upper, Silurian sequence consists of a capping layer of limestone bioherms over approximately 150 m of flat lying shallow marine limestones with increasing numbers of mudstone layers towards the base of sequence. The bioherms can be up to 50 m thick where they protrude through the overburden to surface, but may be absent where eroded. The Ordovician bedrock that underlies the Silurian sequence is approximately 60 m thick and composed of layered mudstone, with sandstone and evaporite layers.

The entire James Bay Lowlands was glaciated on several occasions, with the glaciers eroding the bedrock cover and leaving several clay- and silt-rich tills across the region. The presence of the glaciers also resulted in the isostatic depression of the ground surface, and after the departure of the glaciers, the James Bay Lowlands were submerged beneath the Tyrell Sea. Silt deposited within the Tyrell Sea covered almost all of the older glacial sediments and bedrock, filling in any depressions that remained after glaciation, and largely creating the flat topography of the area that is seen today. Subsequent to the retreat of the Tyrell Sea, the cool conditions and poor drainage have promoted the development of peatlands. Bedrock is only exposed where bioherms protrude through the Quaternary sediments, or where the larger rivers have incised through the overburden.

The sequence of geology contains several aquifers and aquitards. The aquifers consist of: a surficial peat aquifer; an upper limestone aquifer in a layer of bioherms; a lower limestone aquifer of thin karstic horizons within the intermediate to deep limestones; and deep sandstone layers between or beneath the Ordovician mudstones (Table 1). The silty overburden sediments, the mudstones, and the underlying crystalline basement form aquitards.

Table 1: Summary of main aquifers and aquitards at the Victor Diamond Mine

Unit	Description
Peat aquifer	The vast majority of the surface cover at the site is peat. The peat is typically several metres thick, with an upper, spongy, transmissive zone and a deeper, mucky, relatively non-transmissive zone.
Overburden aquitard	The overburden is composed of lower silty tills overlain by marine silt. The overburden thickness varies from absent where isolated bioherms protrude through the overburden and along some of the larger rivers, to greater than 50 m thick over former bedrock valleys. This unit is considered an aquitard.
Upper limestone aquifer	The upper limestone is composed of bioherms of the Attawapiskat Formation, and approximately 15 metres of the underlying limestone, located above a Blue-Green marker bed. The bioherms are highly porous, although this porosity is frequently filled with silt. The bioherms, along with an upper weathered zone, are considered an aquifer unit, while the underlying layered limestone has limited transmissivity. The bioherms occur frequently in the area of the mine, but they are not a continuous layer, and are separated from one another where the bedrock surface is eroded or intervening areas are filled with deeper marine limestones. Groundwater in this layer is usually fresh water.
Blue-green claystone aquitard	A several metre thick, blue-green claystone layer is an important regional aquitard and marker bed.
Lower limestone aquifer	The lower limestone consists of approximately 140 m of limestones from several formations. The bulk of the limestone is of low transmissivity, but significant groundwater movement can occur through several thin karstic horizons, which form the aquifer.
Mudstone aquitard	The majority of the 60 m thick Ordovician deposits at the site are mudstone, with some dolostone and limestone layers. These layers are interpreted to be aquitards.
Sandstone aquifers	There are several thin sandstone layers within and below the Ordovician mudstones. Two to three of these layers can be several metres thick and are considered aquifers. Higher hydraulic conductivities are found in those layers where associated evaporite layers have been subject to dissolution. The groundwater in these layers is moderately saline.
Crystalline basement	The crystalline basement is an aquitard, and is effectively a no-flow boundary at the base of the hydrogeological system. The groundwater within this unit is saline.

Prior to mining, regional groundwater flow in the area was west to east, with local components of flow towards the larger rivers, where the rivers incised into the bedrock. Vertical connections between the aquifers are limited by the large areal extent of the aquitards. Pre-mining groundwater quality consisted of fresh water in the peat and upper part of the limestone sequence and saline groundwater in the crystalline basement. The waters in the lower limestone aquifer and mudstones reflected mixtures of fresh water; relic Tyrell Sea water, water in contact with evaporites; and saline water found at depth.

Local surface water drainage in the area of the mine is from west to east. The main local surface water features are the Attawapiskat River to the north, the Nayshkootayaow River to the south, and the Granny Creek system, which has branches both north and south of the mine (Figure 3). Flow statistics for these creeks and rivers as available in 2007 are summarized in Table 2.

Table 2: Flow statistics of local creeks and rivers near the Victor Diamond Mine available prior to start of dewatering

Feature and flow station number	Watershed area (km²) above gauge	Mean annual flow (m³/day)	Calculated 7Q20 (m³/day)	Reference
Attawapiskat River (pro-rated from 04FC002)	49,000	41,500,000	5,310,000	CSR, 2005
Nayshkootayaow River (04FC001)	1,840	1,619,950	27,000	AMEC, 2007c
Granny Creek system (04FC011)	87	30,800	0[1]	AMEC, 2007c

[1] Periods of no measurable flow were observed in winters prior to the start of mine dewatering

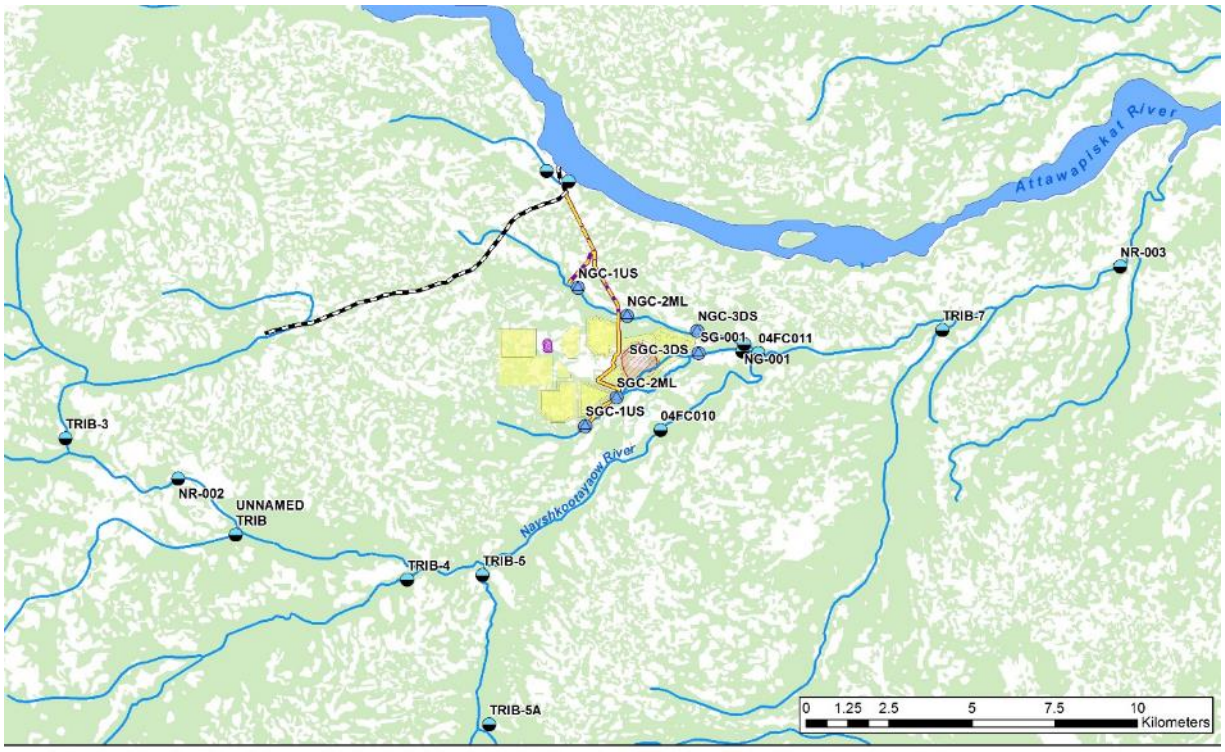


Figure 3: Local surface water features and the surface water monitoring network

Dewatering of the mine has evolved over the life of the mine. Initial dewatering began in 2007 from a single large diameter well located on the perimeter of the open pit. Over time, additional dewatering

wells have been added as required, initially around the perimeter of the open pit, but subsequently within the open pit. Until recently, all the water taken from the mine was withdrawn from these wells; however, in late 2017 small amounts of water were also collected from sumps within the pit. Discharge water from the mine is directed to the Attawapiskat River via pipelines.

Methodology

The objective of this paper is to evaluate how successful predictions made in 2007 and 2008 have been in anticipating changes in groundwater conditions as a result of mine dewatering. This objective will be accomplished by first reviewing the predictions of impacts from dewatering that were made in 2007 and 2008, and then comparing those predictions to observed changes in the groundwater system close to the end of mine life.

All mine developments result in changes to the local environment. The changes can have minor to significant impacts on the local environment. Where the changes are significant, mitigation of those effects can be required. The purpose of this paper is not to review all the mine related impacts. This paper will focus on the major groundwater quantity related issues identified at the time the mine was permitted in 2007 and 2008. These were: the amount of water to be pumped from the mine; the extent of the drawdown cone; and the anticipated effect of dewatering in the peatlands and local surface water features.

Groundwater Investigations and predicted impacts

The vast majority of the groundwater investigations made in the lead-up to the start of mining were made by Hydrologic Consultants Inc. (HCI), which subsequently became part of Itasca Denver Inc. (Itasca). AMEC (Amec Foster Wheeler), now known as Wood, completed the Environmental Assessment for the mine (AMEC, 2004), and supported HCI efforts with the collection of data for the environmental assessment, including hydrology data, and by completing scoped hydrogeological investigations. Because access to the site was along seasonal ice roads, the investigations tended to proceed on an annual basis.

Table 3 provides a short summary of the major phases of groundwater investigation at the site. The hydrogeological and hydrologic investigations were also supplemented with traditional ecological knowledge provided by Attawapiskat community elders.

Table 3: Summary of early groundwater related investigations at the Victor Diamond Mine

Time Frame	Description of investigation and main reference
2000 to 2008	Hydrologic monitoring of surface water features (AMEC, 2007a)
1999/2000	Packer testing and initial model development (ICCI, 2000a, b, & c)
2001	Test hole drilling in deep overburden feature. Update of groundwater model (HCI, 2000 and 2001)
2002	Overburden drilling and pumping test in deep overburden hole and in limestone country rock. Preparation of first three-dimensional groundwater model (HCI, 2002)
2003	Monitoring well drilling with air-lift testing, and 30-day pumping test to locate hydraulic boundaries, 10-day pumping test adjacent to Nayshkootayaow River to test vertical hydraulic conductivity (K) beneath river (HCI 2003)
2003/2004	Update of groundwater model (HCI, 2004a & b)
2005/2006	Monitoring well drilling with airlift testing, 60-day pumping test (HCI, 2006a and b). Monitoring of aquifer response to quarry dewatering (AMEC, 2007b).
2006/2007	Update of regional numerical model for the bedrock and preparation of localized overburden groundwater model, with small-scale models to simulate impacts to peat lands near bioherms and existing sinkholes (HCI, 2007a, b, c, d & e, and 2008c)
2007/2008	Observation of drawdown from ramp up pumping and update of groundwater in response to ramp up pumping (HCI, 2008a & b)

Pre-mining groundwater conditions

Prior to mining, groundwater levels in all the aquifers were generally at or close to the surface. Only on bioherms and in areas close to creeks and rivers, is the ground surface high enough or the water table low enough to allow for the growth of large trees. Locally, artesian conditions were found in some monitoring wells completed in deeper aquifers nearer to the rivers.

Hydraulic communication between the surficial peat aquifer and the bedrock is focussed on areas where bioherms protrude through the overburden. In the area between the Attawapiskat and Nayshkootayaow River, east of the mine, a karstic groundwater flow system with natural sinkholes has developed between the peat and the rivers (Cowell, 1983). Away from the rivers, in areas of higher bedrock groundwater levels or during high seasonal water table periods, groundwater could discharge from the bedrock to the peat through bioherms.

Prior to mining, regional groundwater flow in the bedrock was from east to west, with localized flow in the upper bedrock aquifers towards those sections of the Attawapiskat River and Nayshkootayaow River that incised into bedrock. Groundwater discharge to the rivers from the bedrock aquifers is concentrated in areas where there are bioherms along the river, and practically absent in areas where the rivers flow over overburden where the bedrock surface drops below the river level.

Groundwater flow in the peat is tied to the depth of the water table and seasonally variable. High water table conditions, like those reported in the spring and fall or following large rainfall events, raise the water table into the upper, sponge like section of peat. This effectively connects the many ponds in the

area through the high permeable upper section of peat, resulting in periods of high combined groundwater-overland flow. Conversely, there is relatively limited to almost no groundwater flow during drier periods and winter, when the water table declines into the mucky sections of peat. The episodic nature of the shallow groundwater-overland flow in the peat causes highly variable flow in local creeks – from flood-like conditions in the spring and fall, to no flow in smaller creeks during the winter.

The peat has an extremely high porosity and serves as a large seasonal reservoir of shallow groundwater across the entire region. The bioherms have some large cavities, which when not clay-filled, partake some storage capacity of the upper part of the limestone aquifers. Otherwise there is very limited storage capacity of the limestone units.

Prediction of Dewatering Effects on the Groundwater Flow System

The prediction of dewatering effects on the groundwater and surface water flow system was made using a series of numerical groundwater models, which included regional groundwater models and several small-scale models used to simulate the potential effect of drawdown on the peatlands near bioherms and pre-existing sinkholes (Table 3).

Separate regional groundwater models were developed for the bedrock system and for the overburden system for the area close to the mine, above the area of highest predicted drawdown in the upper bedrock aquifers. The purpose of the bedrock model was to predict required dewatering rate at the mine and the extent of drawdown in the bedrock aquifers. The purpose of the overburden model was to predict impacts to surface water flow in Granny Creek adjacent to the mine. The bedrock model developed over several years using data from drilling, monitoring wells, and testing, including 10 day and 30 day pumping tests. The 2007 version of the model was calibrated to a nominal "60 day" pumping test conducted at an average rate of approximately 16,000 m^3/day in 2006 (HCI, 2007a), with additional calibration made to the groundwater response from pumping during the first months of pit dewatering operations (HCI, 2008a).

Feasibility studies completed prior to mining determined that the most effective method to dewater the open pit would be through the use of dewatering wells installed in the bedrock around the perimeter of the open pit, with a sump within the pit only needed towards the end of mining (HCI, 2002, 2003, 2004a, 2004b and 2007a). Because of practical limitations, the dewatering systems was designed on the assumption that the number of dewatering wells would increase over time. By the end of mining, HCI (2008a) assumed that 17 dewatering wells would be in operation around the perimeter of the open pit.

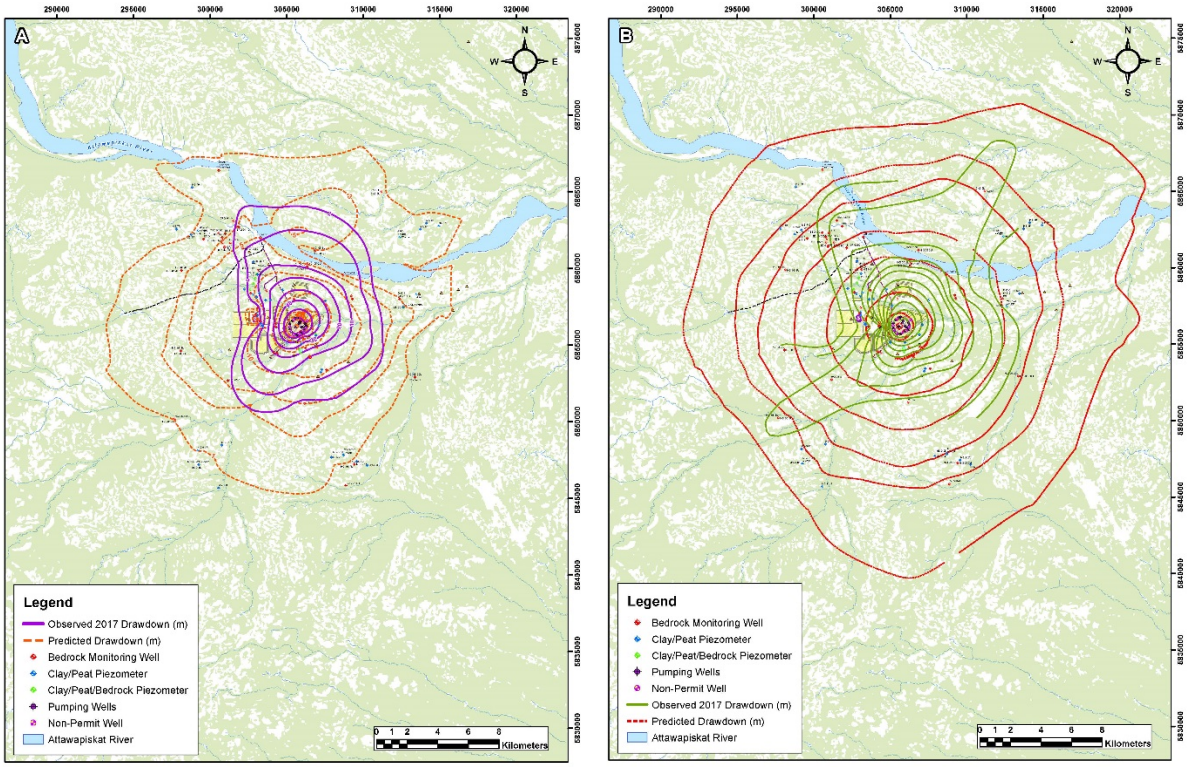
Predicted Dewatering Rate

The regional groundwater model developed in 2007 and refined in 2008 (HCI, 2008a) predicted that

dewatering of the open pit would require pumping at a long term average pumping of 130,000 m^3/day. The mining plan used as the basis of this model foresaw relatively aggressive downward progression of the mine, followed by widening of the mine.

Predicted Extent of Drawdown

The regional groundwater model was used to predict the extent of drawdown in both the upper and lower limestone aquifers. The drawdown cone was predicted to develop over time as water was removed from storage, with the drawdown cone beginning to stabilize around 2012. The groundwater model predicted that at the end of mining in late 2018/early 2019, drawdown attributable to mining would extend up to approximately 13 and 18 kilometres from the open pit in the upper and lower limestone aquifers, respectively (Figures 4a and 4b).



Figures 4a and b: Observed (2017) and predicted (2007) drawdown in the upper (a) and lower (b) limestone aquifers

Predicted Reductions in Surface Water Flows

Both the regional and overburden groundwater models predicted that the reductions in surface water flow as a result of mine dewatering would increase over time, as drawdown expanded out from the mine. For all the surface water features, the reductions in flow were expected to be at a result of interception of groundwater discharging to the features. For the Nayshkootayaow and the Attawapiskat River, the

maximum amount of groundwater intercepted was predicted to be approximately 17,400 and 30,600 m^3/day respectively (HCI, 2008a). In comparison to mean annual flows, the intercepted groundwater discharge to the Nayshkootayaow River and Attawapiskat River was estimated to represent 1.1 and 0.07 percent of the average annual flow, respectively.

The Granny Creek system was observed not to flow during some winters prior to mining, and as such the effects of mine dewatering on the creek flow are difficult to assess. The Granny Creek system is a watershed with significant storage capacity in the peat. It was considered likely that lowering of the water table in the peat as a result of dewatering, would open storage within the peat aquifer, which would be replenished during the spring and fall wet seasons. The net effect on creek flows were therefore expected to be a small reduction in peak flows in the spring freshette and fall, and only a limited impact on winter low flow conditions.

In the cases of the Nayshkootayaow River and Granny Creek system, the flow losses were considered high enough during low flow conditions or for there to be sufficient uncertainty in the predictions, to warrant flow supplementation of these features as a precaution against unacceptable flow loss during low flow conditions. The flow supplementation would occur through pipelines from the Attawapiskat River. Because any pipelines not in use during the winter would freeze, these supplementation flows are operated each winter to prevent line freezing, whether supplementation is required or not.

Predicted Impacts to Peatlands

The predicted impacts to peatlands were anticipated to be concentrated within the Granny Creek watershed, due to its proximity to the center of dewatering and general lack of pre-mining downward gradients. Other areas with high predicted drawdown located close to Nayshkootayaow and Attawapiskat Rivers, and between the rivers to the east of the mine, already experienced large, year-round downward gradients across the overburden. In these areas, ponds would periodically drain dry into long established sinkhole and karst features (Cowell, 1983) and the plant life reflected drier conditions. In these areas, the additional mine induced drawdown was not expected to impact peatlands already adapted to these conditions.

The mechanisms by which peatlands were anticipated to be effected by dewatering consisted of drainage of peat by increased infiltration through the overburden, and new, direct drainage of the peat lands to the bedrock through bioherms and sinkholes in areas where hydraulic gradients were reversed by mine dewatering.

A detailed overburden model was developed to assess the effects of increased downward gradients across the overburden in response to bedrock water level declines (HCI, 2008b). The peat system has

significant storage capacity, from which water can be drawn by evapotranspiration in the summer, and replenished each spring and fall during the wet seasons. A threshold for impact was developed where the increased infiltration exceeded average runoff in the watershed, such that the losses due to induced infiltration would not be offset by captured runoff. This model identified several areas where increased infiltration might exceed the surplus. All these areas were characterized by thin overburden. Because of the proximity to the open pit, a large portion of the identified area are locations of the mine infrastructure.

Detailed modelling of the peat and overburden in close proximity to existing bioherms and sinkholes predicted that direct drainage of peat to the bedrock through bioherms and sinkholes would be limited to the area immediately adjacent to the exposed bedrock (HCI, 2008c). This prediction was consistent with observations of drained ponds in naturally under-drained areas between the Nayshkootayaow and Attawapiskat Rivers prior to mining (AMEC, 2007c). This modelling did not identify any new areas of drainage not already identified in the overburden model.

Predicted Effect of Dewatering on Karst and Area of Natural and Scientific Interest

The mine site was located adjacent to an Area of Natural and Scientific Interest (ANSI) for karst features. These features were thought to be a minimum of thousands of years old (Cowell, 1983), having developed in the bedrock over thousands to millions of years. Given the short life span of the mine, there was no anticipated effect on these features as a result of mine dewatering (AMEC, 2005).

Prior to mining, there was concern that new sinkholes might develop as a result of overburden collapse into voids in pre-existing karst features, when the water within the voids was removed due to drawdown. Extensive work was done to ensure that mine infrastructure was not liable to collapse into sinkholes, and found nearly all of the near surface karst features to be tightly packed with overburden materials (AMEC, 2007b). As such, the probability of sinkhole development was considered low in areas of thin overburden, with no sinkholes anticipated in areas of thicker overburden. Where sinkholes were to develop, their primary effect was expected to be drainage of the peat immediately around the sinkhole, as discussed in a proceeding section.

Groundwater Observations during Mine Operations

Groundwater observations during mine operations are recorded by a comprehensive monitoring program at the site, which includes recording of pumping rates, observations of water levels in more than 150 monitoring wells, continuous flow monitoring in more than a dozen hydrometric stations, and periodic areal- and satellite-based surveys (Amec Foster Wheeler, 2017; Wood, 2018). The following sections describe the groundwater observations.

Observed Dewatering Rates

Observed pumping rates from the mine dewatering system have been much less than predicted prior to mining. After an initial ramp-up stage, the dewatering rate peaked in 2011 at approximately 93,000 m^3/day, and has slowly declined since then. The average dewatering rate in 2017 was approximately 73,000 m^3/day. This compares to a predicted dewatering rate of 130,000 m^3/day made in 2007 (HCI, 2007a), and more recent simulations made in 2016 of 80,000 m^3/day (Itasca, 2017).

Part of the difference between the predicted and observed pumping rates in the early stages of mining can be attributed to changes in the mine plan, shortly after the start of dewatering. The original mine plan called for initial aggressive construction of the mine to depth, followed by widening of the mine; however, the actual mine development proceeded with a wider, shallower mine. This difference in mine plan would result in lower initial pumping rates.

In addition to changing the mining plan, changes were also made in the arrangement of dewatering wells. Whereas in 2007, the plan was for dewatering wells to be placed just around the perimeter of the open pit, a number of dewatering wells have been installed inside the open pit. Furthermore, while it was originally envisioned that only 18 dewatering wells might be required, the mine has constructed 24 dewatering wells, a number of which have been drilled to replace wells that were taken out of service due to declining well efficiencies. During the mine life, a maximum of 22 wells have been in operation at any one time; however, in this configuration, several wells produce only very limited quantities of water.

Not all the groundwater is captured by the dewatering wells, and some groundwater enters the pit as passive inflow from the pit walls. Until late 2017, this inflow was able to re-infiltrate back into the pit floor and to be captured by the dewatering wells. Only in late 2017 has it been necessary to pump some of this pit sump water.

Observed Extent of Drawdown

In addition to the pumping rate being less than predicted, the observed extent of the drawdown cone has also been much smaller than predicted (Figures 4a and 4b). The extent of the observed drawdown cone in the upper aquifer is up to 8 km, compared to a predicted 13 km, while the extent of the observed drawdown in the lower aquifer is up to 12 km, compared to a predicted 18 km.

Observed Reductions in Surface Water Flows

Observed reductions in surface water flows are difficult to quantity due to the highly seasonal nature of flows; variable year-to-year conditions; and the addition of supplementation flows. To date, there have been no instances of flow loss along the Nayshkootayaow River or Granny Creek system that have been greater than the amount of supplementation water added. Furthermore, the water quality of the mine discharge water remains consistent with bedrock aquifer water chemistry and not surface water, indicating

the volume of captured surface water is relatively small.

The best estimate of the actual effect of mine dewatering on the Attawapiskat River and Nayshkootayaow River comes from the numerical groundwater model, which has been updated on a periodic basis throughout the mine life. An updated model (Itasca, 2015) estimated that the amount of groundwater discharge to these rivers intercepted by the mine dewatering system would peak at the end of mine life at 11,600 m^3/day and 6,700 m^3/day for the Attawapiskat River and Nayshkootayaow River, respectively. This equates to <0.03 and 0.4 percent of the average annual flows in these rivers.

Surface water flow losses in the Granny Creek have not been part of the regional groundwater model updates. Instead, flows in this system are compared to a reference watershed of similar characteristics located outside of the drawdown cone. Over the course of the mine life, this reference creek has stopped flowing during several winters, much like the Granny Creek system did prior to mining. Because of supplementation, however, since the start of mining, the Granny Creek system has continued to flow year round.

Observed Effects on Peatlands

The observed effects of drawdown on the peatlands are assessed by De Beers through a combination of piezometers installed in the peat, airborne observations, and routine satellite imagery analysis (Amec Foster Wheeler, 2017; Wood, 2018). Additional analysis of the effects of mine dewatering on the peatlands has also been made by university researchers (Whittington and Price, 2012; Whittington and Price, 2013; Leclaire et al., 2015).

The peatland ponds effectively serve as shallow groundwater level indicators for the peatland, and as they are shallow, small water level changes are readily observable from the air as dry patches around the ponds. There are thousands of ponds within the extent of the drawdown cone. As there are so many ponds, areas of significant water level declines in the peatlands can be confidently identified from the air.

The observed effects on peatlands in the airborne surveys has been spotty. Approximately 30 ponds located in areas of thin overburden have gone dry since the start of dewatering, while the vast majority of the thousands of ponds in the drawdown area remain water-filled throughout the year. Frequently, where a dry pond is located, it is adjacent to several water-filled ponds.

Monitoring of pond conditions is also assessed using satellite surveys of a nearby field area above the drawdown cone area and reference areas outside the drawdown cone made every five years. The changes in the pond sizes, for ponds greater than 100 m^2, are evaluated through an automated pixel recognition routine. A comparison of the results of these surveys from 2006 to 2012 indicates that the collective area of pond drying inside the drawdown cone at the near field site is 6.5 and 14 percent higher, respectively, for mid-field or far-field control sites, both located outside the drawdown cone. These

changes were concentrated in areas of thin overburden, and entirely consistent with the predictions made prior to start of mine operations (Amec Foster Wheeler, 2017).

The above observations are consistent with the conclusions of Whittington and Price (2012; 2013) and Leclaire et al. (2015), who examined the effects of dewatering on the hydrology of the peatlands at a research site within the drawdown cone of the mine. Whittington and Price (2012) concluded that the drawdown within bioherms resulted in only local effects on the peatlands, and Whittington and Price (2013) noted that infiltration was highest in areas of thin overburden. Leclaire et al. (2015) concluded that there were localized effects of dewatering on the peatland hydrology, but the effects were less than that of seasonal variation.

Observed Sinkhole Development

As of early 2017, 15 new sinkholes had been identified within the drawdown cone in thin overburden. The sinkholes that have appeared are generally less than two metres across and less than one metre deep, with a few sinkholes being approximately 10 metres across and less than three metres deep. They generally become apparent when the organic matt of woody materials of peat tears, revealing an absence of underlying materials. The appearance of the sinkholes suggest that the features have been created following the slumping of the water and muck at the base of the peat into pre-existing cavities in the bedrock.

Where the bedrock is visible and accessible in these sinkholes, the cavities in the bedrock appear to be small conduits, approximately 10 to 30 centimetres across. The bedrock appears to have experienced dissolution, likely from contact with the relatively low pH water in the peat, consistent with descriptions of organo-karst, noted by Cowell (1983) in areas east of the mine. All of the conduits appear to pre-date the mine by thousands or millions of years (Amec Foster Wheeler, 2015; Cowell et al., 2015).

The actual effect of the sinkholes on the peat is quite limited, as they are located in areas of thin overburden or bioherm outcrop, where the peat ponds were already prone to drainage, with or without the presence of sinkholes. In some cases, the sinkholes have re-flooded after the initial formation, much like the ephemeral ponds reported in the area documented by Cowell (1983) prior to mining. It is expected, following the rebound of groundwater levels after mining, that these features will revert to ponds.

Discussion

A comparison of the predicted and observed dewatering rate and drawdown cone sizes strongly suggests that the original predictions made in 2007 and 2008, prior to the start of mining, overestimated the potential environmental effect of mine dewatering operations on the local groundwater flow system. This subsequently decreased the expected area of potential impact and the expected effect of dewatering on

local surface water bodies.

The original predictions of impact were highly dependent on the numerical groundwater model(s) developed for the site. A review of periodic model updates made over the course of the mine life indicates that the overall transmissivity of the sedimentary bedrock sequence had to be reduced from approximately 500 m^2/day in 2007 to 293 m^2/day in 2016 (Itasca, 2017), with most of these decreases focused on the upper limestone and deeper limestone formation, leaving the middle sequence of limestone only slightly modified. Other important changes were:

- a reduction in the vertical hydraulic conductivity of most units by a factor of 10, with the exception of the bioherms in the upper limestone, which saw an increase in the vertical hydraulic conductivity by a factor of ten;
- refinement of the overburden geology to make it unnecessary to run separate overburden and bedrock models with the general effect of reducing the vertical hydraulic conductivity of the overburden; and
- a two order of magnitude decrease in the hydraulic conductivity of the deeper sandstones and crystalline basement rock.

The net effect of these changes was to generally decrease the horizontal and vertical hydraulic conductivity of all the aquifers, lowering the predicted pumping rates and the hydraulic connection between the aquifers and the groundwater and surface water/peat systems. These changes were entirely consistent with the observed effects of dewatering, which saw:

- no or very limited measurable impact of dewatering on nearby creeks and rivers;
- no evidence of large-scale capture of surface water in the mine dewatering system; and
- only isolated effects on the peatlands in areas of thin overburden.

Conclusion

Observations collected towards the end of mine life indicate that predictions of the effects of mining on the groundwater system made during the environmental assessment process overestimated the actual observed impacts. The predictions of effects made in 2007 and 2008 were highly dependent on the results of hydrogeological investigations and the numerical groundwater model developed at that time.

The tracking of refinements to the mine's numerical groundwater model shows that between 2007 and the most recent model, the estimated transmissivity of the bedrock has changed by less than a factor of two, which for a hydrogeological investigation should be considered a relatively minor difference. Despite the relatively minor differences in model parameters, the scale of the water takings means that the net effect on the predicted impacts is significant, with a large reduction in the size of the drawdown cone.

The sensitivity of the predicted impacts to the hydraulic parameters for projects with large-scale water takings strongly justifies the years of hydrogeological investigation conducted prior to mining.

Acknowledgements

The prediction of environmental effects and the monitoring of those effects requires an enormous amount of effort by a large number of people, all of whose efforts should be acknowledged. A list of those people who made significant contributions would be incomplete without including David Simms, Sheila Daniels, Mark Ruthven, Lesley Lorrimer, and Jason Dietrich of Wood (formerly AMEC and Amec Foster Wheeler); Dave Ott, Rob Patterson, Anne Boucher, Terry Ternes, Rubin Wallin, Charles Hookimaw, Andrew Sutherland, Jordan Edwards, Aline de Chevigny, and Brian Steinback from De Beers or formerly from De Beers; and Vladimir Ugorets, Roger Howell, Lee Atkinson, Jeff Wright, Houmao Liu and Steve Meyerhoff from or formerly from Itasca and its predecessors. In addition to those listed above, the project benefited from contributions from regulators and reviewers, as well as numerous students and researchers, who have studied the Victor Diamond Mine site. Last, and by no means least, De Beers should be recognized for its ongoing commitment and support of environmental monitoring at the site.

References

AGRA Earth & Environmental Limited. 1999. Environmental Baseline Study, Monopros Victor Kimberlite Project Advanced Exploration.

AMEC. 2004. Victor Diamond Project, Environmental assessment comprehensive study.

AMEC. 2005. Victor Diamond Project, Comprehensive study report. June 462. 462 pp.

AMEC. 2007a. Hydrology report.

AMEC. 2007b. Annual monitoring report for pumping at the Central Quarry as per Condition 4.8 of Permit to Take Water 2584-6UVMEK, MOE Reference 4460-6TDMLS

AMEC. 2007c. Victor Project, Request for permits to take water and a certificate of approval to allow full scale, well field dewatering of the bedrock aquifer for open pit mining. June 2007.

Amec Foster Wheeler. 2015. Investigation of sinkholes in the vicinity of the Victor Diamond Mine and potential effects on Muskeg.

Amec Foster Wheeler. 2017. Victor Diamond Mine follow up program agreement, Tenth annual report, 2016 reporting period.

Cowell, D.W. 1983. Karst hydrogeology within a subarctic peatland: Attawapiskat River, Hudson Bay Lowland Canada, *Journal of Hydrology,* 61: 169–175.

Cowell, D.W., Gautrey, S.J. and Steinback, B.J. 2015. Induced karst features in the drawdown zone of an open pit diamond mine in Ontario's James Bay Lowland, Canada. Presented at the International Conference on Groundwater in Karst, Birmingham, June 2015.

CSR (Comprehensive Study Report). 2005. Victor Diamond Project, Comprehensive study report.

HCI. 2000. Victor kimberlite geotechnical and hydrogeological assessment. Report prepared by Hydrologic Consultants, Inc., for AMEC, August.

HCI. 2001. Results of 2000−2001 hydrogeologic testing programme at Victor project. Technical memorandum prepared by Hydrologic Consultants, Inc., for SRK Consulting, 6 March.

HCI. 2002. Dewatering of Victor diamond project, predicted engineering, cost, and environmental factors. Report prepared by Hydrologic Consultants, Inc., for AMEC, August.

HCI. 2003. Dewatering of Victor diamond project, predicted engineering, cost, and environmental factors. Report prepared by Hydrologic Consultants, Inc., for SRK Consulting, December.

HCI. 2004a. Dewatering of Victor diamond project, predicted engineering, cost, and environmental factors. Report prepared by Hydrologic Consultants, Inc., for SRK Consulting, February.

HCI 2004b. Dewatering of Victor diamond project, predicted engineering, cost, and environmental factors, addendum I, update of groundwater flow model utilising new surface-water chemistry and flow data from Nayshkootayaow River and results of sensitivity analyses. Report prepared by Hydrologic Consultants, Inc., for SRK Consulting, September.

HCI. 2006. 2005−2006 hydrogeologic field programme, hydraulic testing and construction of monitoring wells, Victor diamond project, Ontario. Report prepared by Hydrologic Consultants, Inc., for SRK Consulting, October.

HCI. 2006b. Procedures and preliminary findings of 60-day pumping test, Victor diamond project, Ontario. Report prepared by Hydrologic Consultants, Inc., for SRK Consulting, February.

HCI. 2007a. Dewatering of Victor diamond mine, predicted engineering and environmental factors. Report prepared by Hydrologic Consultants, Inc., for SRK Consulting, June.

HCI. 2007b. Procedures and preliminary findings of a long-term pumping test, Victor diamond project, Ontario. Report prepared by Hydrologic Consultants, Inc., for SRK Consulting, 31 January.

HCI. 2007c. Predicted groundwater recharge through various representative bioherm areas at the Victor diamond project. Technical memorandum prepared by Hydrologic Consultants, Inc., 14 November.

HCI. 2007d. Predicted baseflow and recharge to underlying limestone in Granny Creek Basin. Report prepared by Hydrologic Consultants, Inc., for SRK Consulting, 7 December.

HCI. 2007e. Simulations with Victor regional groundwater flow model incorporating recharge derived from idealized bioherm and non-bioherm axisymmetric groundwater flow models. Technical memorandum prepared by Hydrologic Consultants, Inc., 19 December.

HCItasca. 2008a. Dewatering of Victor diamond project, predicted engineering, cost, and environmental factors, March 2008 update of June 2007 groundwater flow model based on data from 60,000 m^3/day ramp-up pumping. Report prepared by HCItasca Denver, Inc., for SRK Consulting, March.

HCItasca. 2008b. July 2008 Granny Creek overburden model – Responses to comments from NRCan in memorandum dated 15 May 2008. Technical memorandum prepared by HCItasca Denver, Inc., for SRK Consulting, 17 July.

HCItasca. 2008c. Response to comments on technical memorandum of 11 January 2008 entitled simulations with Victor regional groundwater flow model incorporating recharge derived from idealized bioherm and non-bioherm axisymmetric groundwater flow models. Technical memorandum prepared by Itasca Denver, Inc., for SRK Consulting, 4 February.

ICCI. 2000a. Preliminary hydrologic findings from geotechnical coreholes V-97-00 and V-98-00 at Victor kimberlite. Technical memorandum prepared by Itasca Consulting Canada, Inc., 18 February.

ICCI. 2000b. Updated hydrologic findings from geotechnical coreholes V-99-00 and V-100-00 at Victor kimberlite. Technical memorandum prepared by Itasca Consulting Canada, Inc., 13 March.

ICCI. 2000c. Evaluation of dewatering requirements and costs for Victor kimberlite. Report prepared by Itasca Consulting Canada, Inc., for Monopros Ltd., June.

Itasca, 2015. Dewatering of the Victor Diamond Mine: July 2015 update of the Victor integrated groundwater flow model. July.

Itasca, 2017. Update of the Victor groundwater flow model based on 2016 hydrogeologic data. February.

Kong J.M., Boucher D.R. and Scott Smith, B.H. 1999. Exploration and geology of the Attawapiskat kimberlites, James Bay Lowland, northern Ontario, Canada, in J.J. Gurney, J.L. Gurney, M.D. Pascoe and S.H. Richardson (eds), *Proceedings of the 7th International Kimberlite Conference.* Cape Town, South Africa: Red Roof Design, 1: 452–467.

Leclaire, M., Whittington, P. and Price, J. 2015. Hydrological functions of a mine-impacted and natural peatland-dominated watershed, James Bay Lowland, *Journal of Hydrology Regional Studies,* 4: 732–747.

Whittington, P. and Price, J. 2012. Effect of mine dewatering on the peatlands of the James Bay Lowland: The role of bioherms, *Hydrological processes,* 26: 1818–1826.

Whittington, P. and Price, J. 2013. Effect of mine dewatering on the peatlands of the James Bay Lowland: The role of marine sediments on mitigating peatland drainage, *Hydrological processes.* Published online.

Wood, 2018. Annual groundwater, subsidence and sinkhole report for 2017 period up to December 31 as per Conditions 4.2.4 and 4.2.6 of Permit to Take Water #1201-9HHJ5G, Victor Diamond Mine.

Proceedings of Mine Water Solutions 2018
June 12–15, 2018, Vancouver, Canada
Published by the University of British Columbia, 2018

Cold Desert Evapotranspiration Cover System Design Evaluation

Jason Keller, GeoSystems Analysis, Inc., USA
Chris Jim, Round Mountain Gold Corp., USA
Monisha Banerjee, GeoSystems Analysis, Inc., USA
Michael Milczarek, GeoSystems Analysis, Inc., USA
Clay Self, Round Mountain Gold Corp., USA

Abstract

Round Mountain Gold Corporation (RMGC) mine is located in central Nevada, USA at an elevation varying between 1,770 m and 2,070 m above mean sea level. The climate is characteristic of a cold desert climate, with cool winters and hot summers. Average annual precipitation is 16.1 cm, approximately 10 times less than the calculated average annual potential evapotranspiration (PET) of 160 cm. RMGC constructed evapotranspiration (ET) cover system test plots in 2012 to evaluate the effectiveness of 0.3 m, 0.9 m, and 1.5 m thick monolayer ET cover systems in minimizing net percolation of precipitation into underlying waste rock. Each test plot is approximately 200 m^2 and includes three cover system performance monitoring stations consisting of sensors placed at approximately 0.6 m intervals along a vertical profile in the cover and waste rock to a maximum depth of 2.4 m. The sensors measure soil matric potential, temperature, water content, and direct net percolation water flux. Soil water content and matric potential data are used to evaluate the cover systems' capacity to store infiltrated precipitation and to remove water via ET. Direct net percolation flux measurements are collected below the estimated depth of ET and these measurements provide a point estimate of net percolation flux into the waste rock. The site-specific seed mix applied to the test plots did not become established, thus test plot vegetation is primarily comprised of the invasive annuals Russian Thistle (*Salsola tragus*) and Halogeton (*Halogeton glomeratus*).

Annual precipitation from 2012 through 2017 was representative of long-term average precipitation conditions. Wetting was observed to a maximum depth of 1.2 m at the 0.3 m and 1.5 m ET cover system test plots. The deepest wetting (1.8 m) was observed in the 0.9 m ET cover system test plot due to focused run-on at the location of two of the three monitoring stations. At all test plots, drying of the soil profile occurred in late spring and early summer in response to decreased precipitation and increased ET. Net

percolation flux into the waste rock was calculated based on measured soil water matric potential data and also directly measured via water flux meters. The average annual calculated and measured net percolation flux over the monitoring period was zero for the 0.3 and 1.5 m ET cover systems and 0.8% and 0.2% of precipitation for the 0.9 m cover system, most likely due to run-on to the test plot. The establishment of native vegetation, particularly deeper rooting shrub type vegetation, is expected to decrease the amount of net percolation. Results to date indicate no difference in the effectiveness of 0.3 m, 0.9 m, and 1.5 m ET cover system thicknesses in minimizing net percolation of precipitation into underlying waste rock.

Introduction

Round Mountain Gold Corporation (RMGC) operates the Round Mountain gold mine located in central Nevada, USA, 72 km north of Tonopah, Nevada (Figure 1). Round Mountain uses conventional open-pit mining methods and processes ore by mill and heap leach. The current life of mine is through 2027, with 3.1 million oz of estimated proven and probable gold reserves. Mine site elevations vary between 1,770 m and 2,070 m above mean sea level, with the mine waste repositories located on the valley floor between the Toiyabe and Toquima mountain ranges.



Figure 1: Round Mountain Mine location map

The climate is characteristic of a cold desert climate, with cool winters and hot summers. Average monthly temperatures (1950 through 2017) ranged from –1°C in December to 22°C in July. Average annual precipitation (1950 through 2017) was 16.1 cm, approximately 10 times less than the Penman-Monteith method (Allen et al., 1998) calculated average annual potential evapotranspiration (PET) of 160 cm. On average, approximately half of precipitation falls during the fall/winter season (October through March) when 25% of PET is predicted to occur, and half of precipitation falls in the spring/summer season (April through September) when 75% of estimated PET is predicted. Snowfall at the site is negligible.

Evapotranspiration (ET) cover system trials have been initiated by RMGC in order to evaluate the efficacy of 0.3-, 0.9-, and 1.5-m mono-layer ET cover system thicknesses in minimizing net percolation of precipitation into potentially acid generating (PAG) waste repositories at Round Mountain. Large-scale test plots have been constructed over waste rock and instrumented with sensors to evaluate the cover systems' capacity to store infiltrated precipitation and to remove water via ET. In this paper we examine the performance of the ET cover systems in reducing net percolation.

Methods

Test Plot Monitoring

In December of 2012 RMGC constructed mono-layer ET cover system test plots consisting of 0.3-, 0.9-, and 1.5-m alluvium cover material over PAG waste rock. Each test plot is approximately 200 m^2 and includes three cover system performance monitoring stations spaced approximately 7 m apart and consisting of sensors placed at intervals along a vertical profile in the cover and waste rock to a maximum depth of 2.4 m (Figure 2). The cover material is on average 34% gravel (>4.75 mm), 52% sand (4.75 mm – 0.075 mm) and 14% fines (<0.75 mm). Waste rock particle size distribution is slightly finer textured than the cover material, on average containing 28% gravel, 50% sand, and 22% fines.

The three principle soil water parameters monitored are: 1) soil water potential, 2) water content, and 3) direct net percolation flux. Soil water potential and water content are used to evaluate the cover systems' water storage capacity, and observed hydraulic gradients determine the direction of soil water movement. Net percolation flux describes the rate of water movement beyond the ET depth (zero flux plane) that will eventually become groundwater recharge.

To monitor these three variables the following sensors are included at each monitoring station at various depth intervals (Figure 2):

- Four heat dissipation sensors to measure soil water potential and temperature under moderately wet to dry soil conditions and to provide data for the potential-based soil water net percolation flux model.
- Four capacitance sensors to measure water content.
- Two advanced tensiometers to measure soil water potential under wet soil conditions and to provide data for the potential-based soil water net percolation flux model.
- One passive capillary water flux meter (WFM) to directly measure net percolation flux.

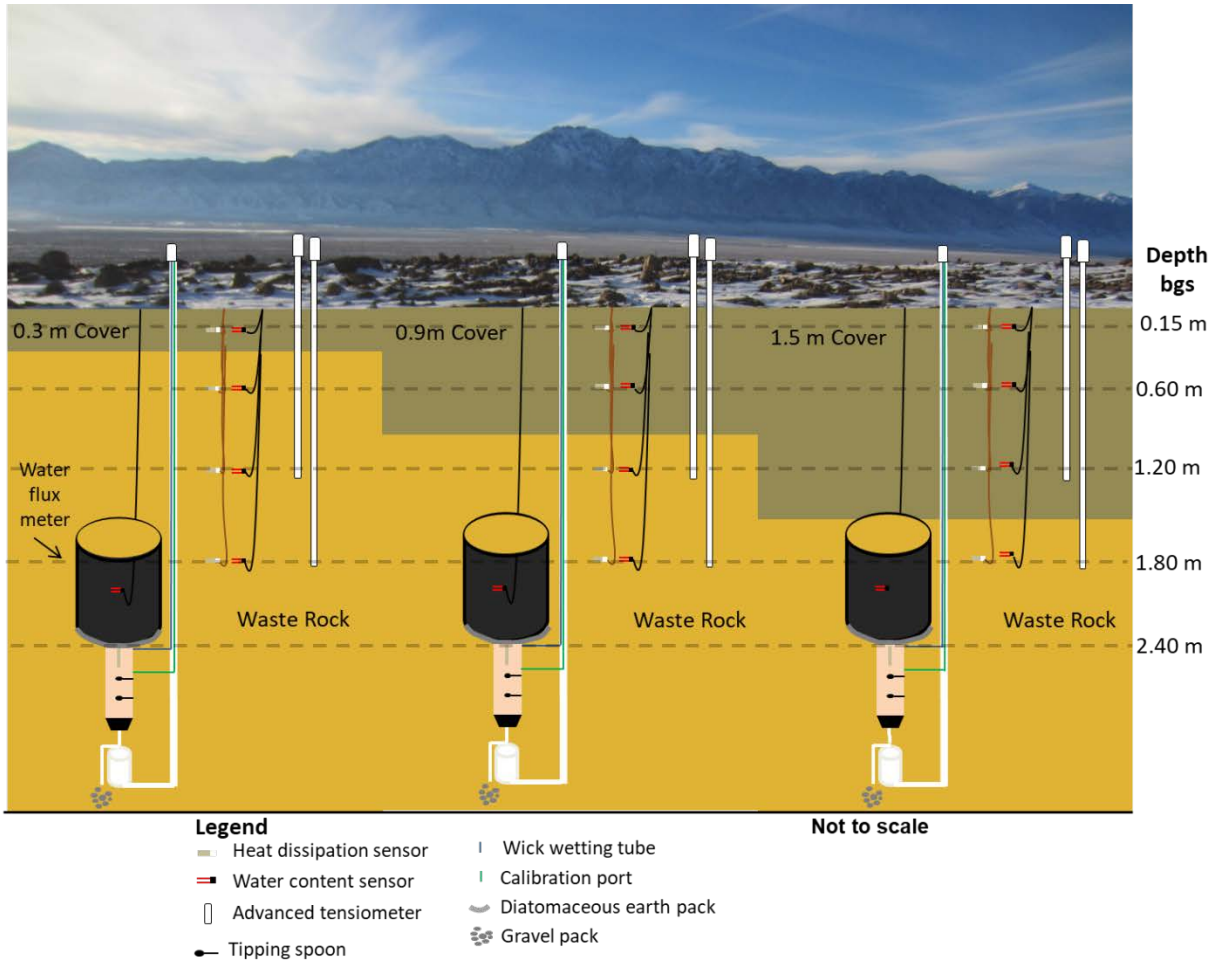


Figure 2: Cross-section of cover performance monitoring station with 0.3-, 0.9-, and 1.5-m cover thickness

Additionally, a precipitation gauge was installed to measure precipitation at the test plots. All sensors were connected to a datalogger that controls the sensors and stores sensor data for retrieval via telemetry.

In the spring of 2013 the ET cover system test plots were partially seeded using a site-specific seed mix; however, none of the seeded plants became established, and vegetation is primarily comprised of the invasive annuals Russian Thistle (*Salsola tragus*) and Halogeton (*Halogeton glomeratus*) (Figure 3).



Figure 3: Cover test plot surface conditions (July 2014)

Calculated Net Percolation Flux

Net percolation flux was calculated from sensor data at each monitoring station by calculating the one dimensional vertical flux from Darcy's Law for steady-state equilibrium as modified by Buckingham (1907) for unsaturated flow, and van Genuchten's (1980) analytical solution to Mualem's (1976) theoretical model of the relationship between unsaturated hydraulic conductivity and matric potential. Flux rates were calculated from soil water potential data and the measured hydraulic gradient between the two deepest soil water potential sensors located at each station, together with van Genuchten parameters determined from laboratory measurements of moisture-retention characteristics and in-situ measurements of saturated hydraulic conductivity using a Wooding's infiltrometer (Wooding, 1968) (Table 1). At the 0.3- and 0.9-m cover stations, these sensors are both installed in waste rock. At the 1.5-m cover stations, the sensor installed at 1.20 m bgs is in cover material and the sensor at 1.80 m bgs is in waste rock (Figure 2).

Results

Data are presented and analyzed by water year (WY), defined as the 12-month period from October 1 to September 30. For example, WY 2017 is the period from October 1, 2016 through September 30, 2017. The monitoring period reported here includes partial WY 2013 (December 21, 2012 through September 30, 2013) and complete WYs 2014 through 2017.

Table 1: Hydraulic properties used for calculated net percolation

Material	Saturated hydraulic conductivity[1]	van Genuchten Parameters[2]				
		Saturated water content	Residual water content	alpha	n	l
	(cm/sec)	(cm^3/cm^3)	(cm^3/cm^3)	(1/cm)	(–)	(–)
Waste rock	8.30E-04	0.459	0.005	0.086	1.252	–1
cover	3.03E-04	0.375	0.011	0.021	1.251	0.5

1 – waste rock n = 6; cover material n = 10

2 – waste rock n = 2; cover material n = 2

Precipitation

Long-term precipitation data (1950 to 2017) from the Smokey Valley-Carvers weather station located approximately 7 km west of the cover test plots were used to define WYs and seasons as average, wet, or dry. Average annual precipitation is 16.1 cm, with a standard deviation of 5.8 cm. A wet year is defined as one with a precipitation total greater than the annual mean plus the standard deviation (21.8 cm), and a dry year as one with a precipitation total less than the mean minus the standard deviation (10.3 cm). Fall/winter (October – March) and spring/summer (April – September) were similarly defined. By this definition, a wet year occurs approximately every 7 years and a dry year approximately every 8 years.

Table 2 provides cover test plot precipitation for the monitoring period by WY and season and designates these data as average, wet, or dry. Seventy percent or more of the WY precipitation occurred in spring/summer (April – September) in the 2014 and 2015 WYs; in WY 2016, more than 70% of the precipitation occurred in fall/winter (October – March). WY 2017 precipitation was similar between spring/summer and fall/winter. WYs 2014 through 2017 were average precipitation years based on the historic seasonal averages. Fall/winter precipitation in WY 2014 and WY 2015 was drier than average. All other seasonal precipitation was average.

Table 2: Cover test plot precipitation

Water year (October 1 – September 30)	Water year precipitation (cm)	Water year wet, dry, average[2]	Fall/winter (October – March) precipitation (cm)	Fall/winter season wet, dry, average[3]	Spring/summer (April – September) precipitation (cm)	Spring/ summer season wet, dry, average[4]
2013[1]	8.0	n/a	0.9	NA	7.1	Average
2014	11.9	Average	3.0	Dry	8.9	Average
2015	10.7	Average	3.2	Dry	7.5	Average
2016	16.9	Average	12.2	Average	4.7	Average
2017	13.1	Average	6.1	Average	7.0	Average

n/a: Not applicable due to being a partial water year of data;
[1]Partial water year: 12/22/2012 – 9/30/2012;
[2]Wet > mean + std dev (21.8 cm), Dry < mean – std dev (10.3 cm);
[3]Wet > mean + std dev (12.9 cm), Dry < mean – std dev (3.5 cm);
[4]Wet > mean + std dev (11.9 cm), Dry < mean – std dev (4.5 cm)

Soil Water Potential and Water Content

Measured soil water potential and water content for the 0.3-, 0.9-, and 1.5-m cover monitoring stations are presented in Figures 3 and Figure 4, respectively. Monitoring station data from one of the three stations in each test plot is presented; similar results were observed between the three monitoring stations within each test plot. Seasonal wetting and drying is generally observed, with wetting in the later fall, winter, and early spring when PET is low and drying during other times of the year. Soil/waste rock began drying slightly later at deeper depths as moisture was removed by ET starting from the soil surface and progressing down through the soil profile. For all WYs, wetting is observed in all test plots to a depth of 0.6 m bgs. Deeper wetting and longer wet conditions was observed in WY 2016 than other WYs due to increased precipitation relative to other years and specifically 12.2 cm of precipitation occurring in the fall/winter season (Table 2).

Wetting into the waste rock at the 0.3-m cover test plot was measured in all WYs; however measured wetting was limited to 1.2 m bgs and shallower depths. Wetting into the waste rock at the 0.9-m cover test plot was minor in WYs 2014 and 2015, with greater wetting observed to depths of 1.8 m bgs in WY 2016 and 1.2 m bgs in WY 2017. Minor wetting, though still dry conditions, was observed at the 1.8 m depth in the 1.5-m cover test plot in WYs 2014 through 2016, though no wetting was observed at this depth in WY 2017.

A topographic survey conducted in March 2015 identified settlement depressions around all stations that may create surface ponding and/or areas of focused infiltration. Cover material was added by RMGC in July 2015 to fill in these depressions. A November 2016 topographic survey indicated that major depressions near the stations had been alleviated; however, based on sensor response and visual observations, small depressions still exist in the 0.9 m cover. These depressions likely serve as locations of focused infiltration, resulting in greater wetting depth in the 0.9 m cover.

The zero-flux plane is a hypothetical depth that separates upward movement of soil water (due to ET) from downward movement to the water table. The depth of the zero-flux plane changes through the year, being shallower in the winter months and increasing in depth in the summer months as ET increases. Measured soil water potential gradients between the 1.2 m and 1.8 m bgs sensors, calculated as the difference in measured soil water potential divided by the difference in depth, indicates whether water is moving upward or downward over the 1.2 m to 1.8 m depth interval. In WY 2016, which observed the greatest wetting at the 0.9 m cover monitoring stations, the soil water potential gradients generally specified downward movement of water in the winter and spring. In summer through early fall, the hydraulic gradients indicated predominately upward movement of water, such that water below this depth could still move upward to ET.

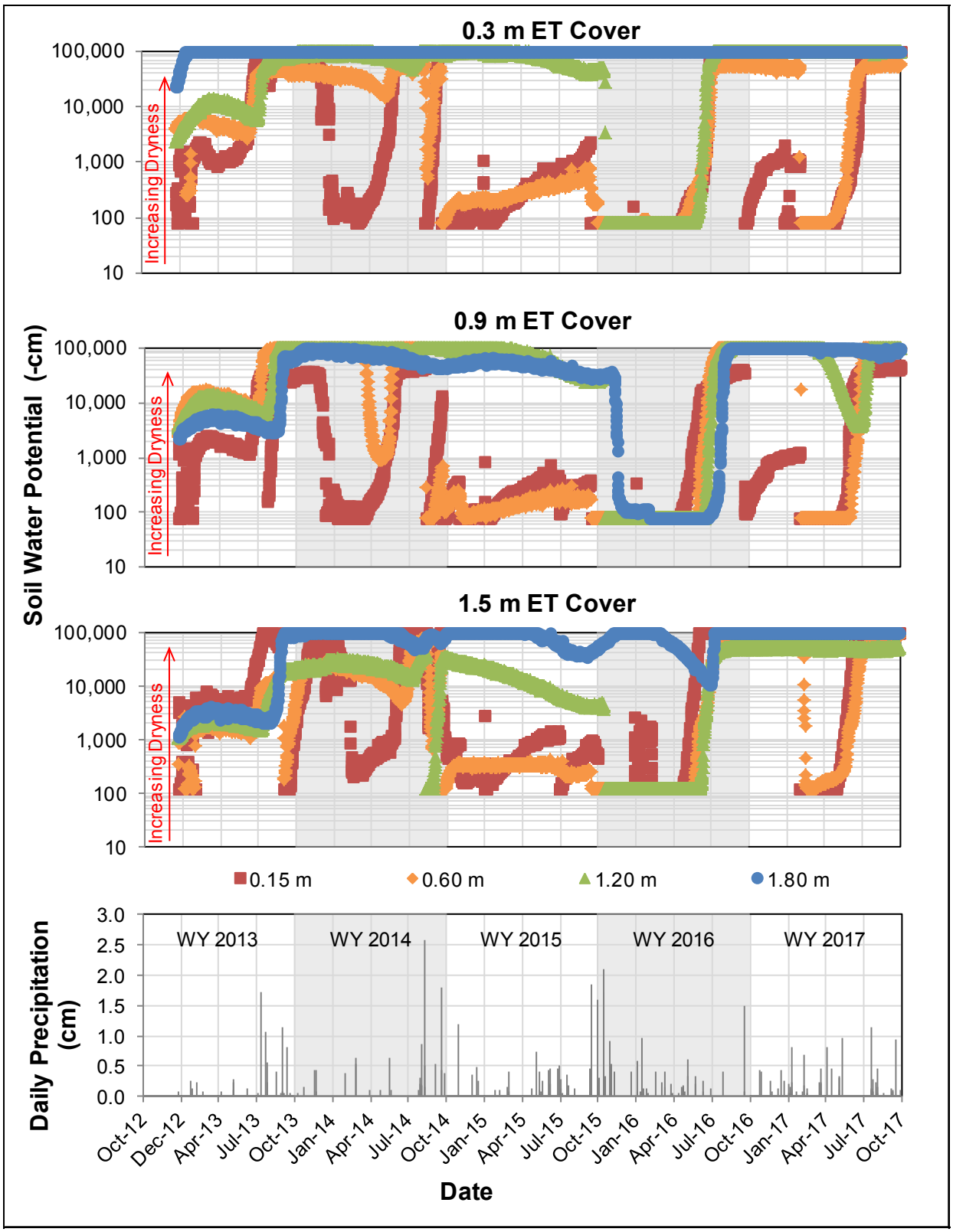


Figure 3: Test plot soil water potential

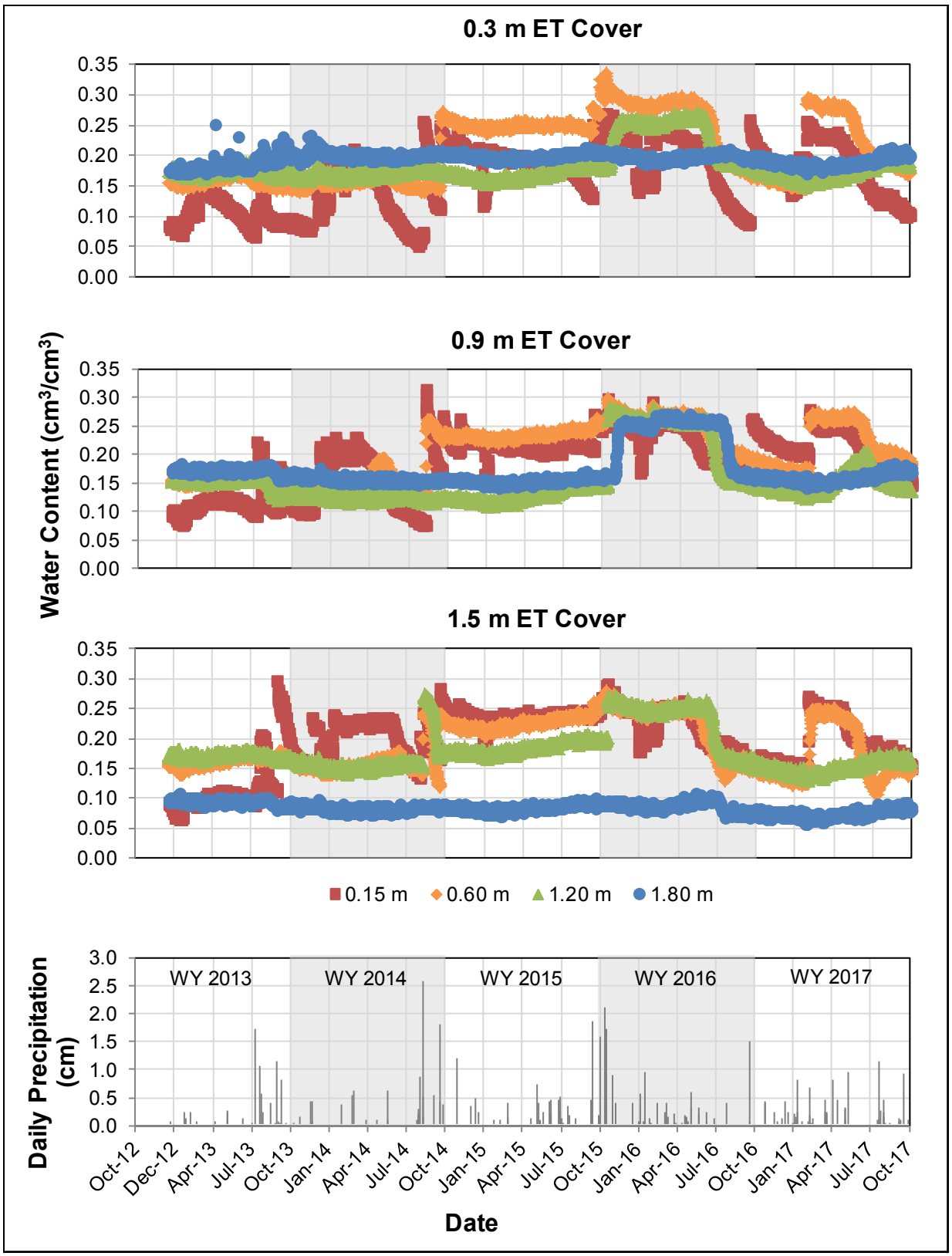


Figure 4: Test plot water content

Cover Material Water Storage

Cover material water storage is the total quantity of water that is in the cover. It is calculated by integrating the measured water content over the cover thickness with the following equation:

$$Water\ Storage = \int_0^L \theta(z,t)dz$$

where:

L is the cover thickness,

θ is the volumetric water content,

z is the depth of measurement, and

t is time.

Calculated cover material water storage over time, as averaged over the three sensor stations in each test plot, is shown in Figure 5.

Cover material water storage increases in response to winter and spring precipitation and declines with increased ET in summer and fall. Cover material water storage in the 0.9-m and 1.5-m cover material was greater in WY 2016 than other WYs due to greater precipitation in WY 2016. WY 2016 cover material water storage in the 0.30-m cover material was similar to WYs 2015 and 2017, indicating at least 0.30-m of cover is needed to store an average precipitation WY.

Material storage capacity is traditionally defined as the water content level below which water drainage becomes negligible (Hillel, 1980). By this definition, net percolation is negligible below the water content storage capacity. Storage capacity of the cover material was estimated from laboratory derived van Genuchten-Mualem model parameters (Table 1) and the van Genuchten-Mualem model (van Genuchten, 1980). Water storage capacity was assumed to be equal to the water content when the drainage flux from the cover material reaches a value of 1.0 x 10^{-7} cm/s or less (Meyer et al., 1997). This water content value (0.223 cm^3/cm^3) was then multiplied by the cover thickness, resulting in an estimated cover material field capacity of 6.8 cm, 20.4 cm, and 33.9 cm for the 0.30-, 0.90-, and 1.5-m cover, respectively.

At various times during WYs 2014 through 2017, the cover material water storage for the 0.3-m and 0.9-m covers exceeded the estimated storage capacity, indicating the additional water observed in excess of storage capacity percolated into the waste rock (Figure 5). Cover material storage for the 1.5-m cover exceeded the estimated cover material storage capacity near the end of WY 2014 and in WY 2016. Percolation of water into the waste rock during these time periods is supported by measured increased soil water potential and water content in the waste rock sensors (Figure 3, Figure 4). Water that percolates into the waste rock may report as net percolation flux or may be transported in the future to the surface via ET, depending on the depth of the zero-flux plane.

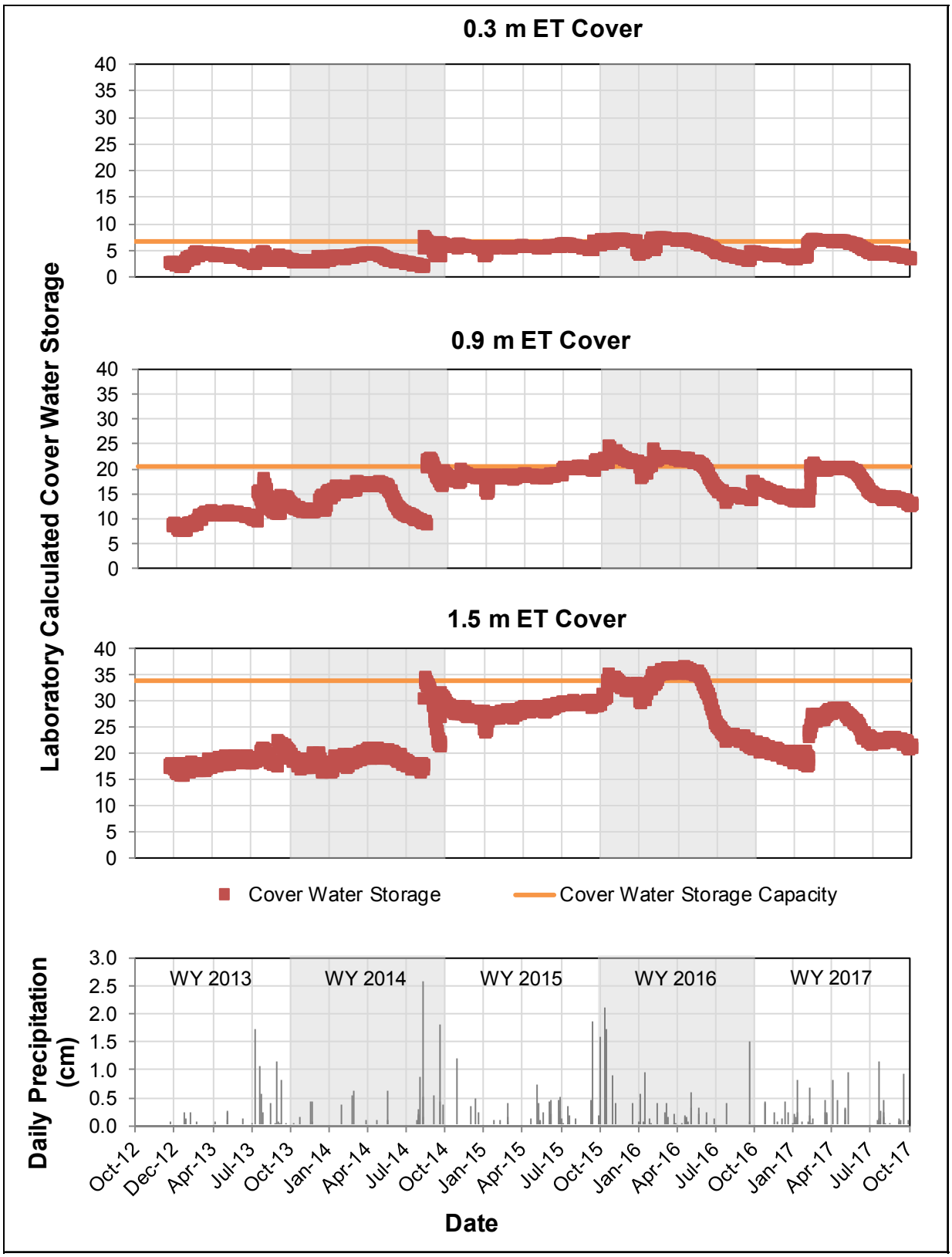


Figure 5: Cover water storage

Net Percolation Flux

Cumulative annual calculated net percolation flux values are presented in Table 3. Zero cumulative net percolation flux values were calculated for the 0.3- and 1.5-m covers for all WYs, indicating no downward movement of water at this depth during these time periods. Zero net percolation flux was also calculated for the 0.9 m cover except for WY 2016, where 0.68 cm (4.0% of precipitation) net flux reflected the wet conditions during the winter and spring to a depth of 1.8 m bgs. The average annual calculated net percolation flux for WYs 2013 through 2017 is 0.13 cm (0.8% of precipitation) for the 0.9-m cover and 0.00 cm for the 0.3- and 1.5-m covers.

Table 3: Calculated net percolation flux

Test plot	WY 2013 Flux		WY 2014 Flux		WY 2015 Flux		WY 2016 Flux		WY 2017 Flux		WY 2013 – 2017 Average flux	
	Total (cm)	% of Precip	Total (cm)	% of Precip	Total (cm)	% of Precip	Total (cm)	% of Precip	Total (cm)	% of Precip	Total (cm)	% of Precip
0.3-m Cover	0.00	0.0%	0.00	0.0%	0.00	0.0%	0.00	0.0%	0.00	0.0%	0.00	0.0%
0.9-m Cover	0.00	0.0%	0.00	0.0%	0.00	0.0%	0.68	4.0%	0.00	0.0%	0.13	0.8%
1.5-m Cover	0.00	0.0%	0.00	0.0%	0.00	0.0%	0.00	0.0%	0.00	0.0%	0.00	0.0%

Measured cumulative annual net percolation flux is presented in Table 4 for each cover test plot. With the exception of the 0.9-m cover, all monitoring stations measured 0.00 cm of WY cumulative flux in WYs 2013 through 2017. Measured cumulative flux at the 0.9-m cover was 0.14 cm (0.8% of precipitation) in WY 2016 and 0.00 cm for all other WYs. Average annual measured net percolation flux for WYs 2013 through 2017 was 0.03 cm (0.2% of precipitation) for the 0.9-m cover and 0.00 cm for the 0.3- and 1.5-m test plots.

Table 4: Water flux meter-measured flux

Test plot	WY 2013 Flux		WY 2014 Flux		WY 2015 Flux		WY 2016 Flux		WY 2017 Flux		WY 2013 – 2017 Average flux	
	Total (cm)	% of Precip	Total (cm)	% of Precip	Total (cm)	% of Precip	Total (cm)	% of Precip	Total (cm)	% of Precip	Total (cm)	% of Precip
0.3-m Cover	0.00	0.0%	0.00	0.0%	0.00	0.0%	0.00	0.0%	0.00	0.0%	0.00	0.0%
0.9-m Cover	0.00	0.0%	0.00	0.0%	0.00	0.0%	0.14	0.8%	0.00	0.0%	0.03	0.2%
1.5-m Cover	0.00	0.0%	0.00	0.0%	0.00	0.0%	0.00	0.0%	0.00	0.0%	0.00	0.0%

Average annual measured net percolation flux values at the 0.9-m cover was less than the calculated net percolation flux using soil water potential data (0.03 cm versus 0.13 cm). The discrepancy between measured and calculated net flux may be due to the base of the WFM being approximately 0.60 m deeper than the deepest soil water potential sensor (Figure 2). These data indicate that water percolating to 1.8 m bgs may still be removed from the soil profile by ET as indicated by the measured upward gradients between 1.2 m and 1.8 m bgs and rapid drying measured at the 1.8 m sensors (Figure 3, Figure 4). Thus, the calculated net percolation flux may serve as an upper estimate of net percolation while measured net percolation flux may be more representative of deeper net percolation.

As noted previously, the observed deeper wetting and net percolation flux in the 0.9-m cover test plot is most likely associated with surface depressions and ponding at the monitoring stations. An irregular surface and ponding in surface depressions can be expected in future reclamation at Round Mountain. Thus, the observed net percolation in the 0.9-m cover also can be expected to occur in the 0.3-m and 1.5-m cover systems; the sensor stations in these cover test plots happen to not be located in depressions.

Net percolation flux values for all locations represent poor vegetation conditions primarily consisting of invasive annuals. The establishment of native vegetation, particularly deeper rooting shrub type vegetation, can be expected to decrease the amount of net percolation flux during average and wet precipitation years.

Conclusion

During the slightly above average precipitation WY 2016, wetting was observed to a maximum depth of 1.2 m at the 0.3 m and 1.5 m ET cover system test plots. The deepest wetting (1.8 m) was observed in the 0.9 m ET cover system test plot due to focused run-on at the location of the monitoring stations. At all test plots, drying of the soil profile occurred in late spring and early summer in response to decreased precipitation and increased ET. The average annual calculated and measured net percolation flux over the monitoring period was zero for the 0.3 and 1.5 m ET cover systems and 0.8% and 0.2% of precipitation for the 0.9 m cover system. ET depths appeared to be at least 1.8 m bgs; consequently, the measured net percolation flux (0.2% of precipitation) for the 0.9 m cover system is most likely representative. The establishment of native vegetation, particularly deeper rooting shrub type vegetation, is expected to decrease the amount of net percolation. Results to date indicate no difference in the effectiveness of 0.3 m, 0.9 m, and 1.5 m ET cover system thicknesses in minimizing net percolation of precipitation into underlying waste rock.

Acknowledgements

We thank the staff and management at RMGC for their support of this project and for permitting the presentation of this work.

References

Allen, R.G., Pereira, L.S., Raes, D. and Smith, M. 1998. Crop evaporation – Guidelines for computing crop water requirements, Food and Agriculture Organization of the United Nations *Irrigation and Drainage Paper* 56, Rome, Italy.

Hillel, D. 1980. *Applications of Soil Physics*. San Diego: Academic Press.

Meyer, P.D., Rockhold, M.L. and Gee, G.W. 1997. *Uncertainty Analyses of Infiltration and Subsurface Flow and Transport for SDMP Sites,* NUREG/CR-6565, PNNL-11705, US Nuclear Regulatory Commission, Washington, DC.

Mualem, Y. 1976. A new model for predicting the hydraulic conductivity of unsaturated porous media, *Water Resour. Res.* 12: 513–522.

van Genuchten, M. Th. 1980. A closed form equation for predicting the hydraulic conductivity of unsaturated soils, *Soil Sci. Soc. Am. J.* 44: 892–898.

Wooding, R.A. 1968. Steady infiltration from a shallow circular pond, *Water Resour. Res.* 4: 1259–1273.

Proceedings of Mine Water Solutions 2018
June 12–15, 2018, Vancouver, Canada
Published by the University of British Columbia, 2018

The Role of Speciation for Selenium Treatment and Compliance with Site-Specific Aquatic Life Criteria

Ben Wozniak, Brooks Applied Labs, USA
Russ Gerads, Brooks Applied Labs, USA

Abstract

It is well known that for many elements, static water quality guidelines can be over- or under-protective for aquatic life. A variety of site-specific factors may either inhibit or enhance the uptake and bioaccumulation of an element into aquatic organisms like algae, invertebrates, and fish. Regulators have recognized this issue for decades, promulgating guidance for the generation of site-specific contaminant limits and, especially in the case of selenium, tissue-based criteria that may be adopted by states or provinces. The Aquatic Life Criterion for Selenium released by the USEPA in 2016 recommends adoption of a multi-component standard for regulatory management of water quality, including limits on selenium concentrations in water, whole fish, fish muscle, and fish eggs or ovaries. While similar regulations in Canada remain under development, provinces like British Columbia have established tissue-specific guidelines for selenium. These criteria can add a high degree of complexity to controlling selenium discharge for companies involved in mining activities, particularly if measured tissue concentrations indicate that impairment is occurring. In such cases, investigations into the cause and potential corrective actions (treatment) are typically necessary.

The mobility, treatability, and extent to which selenium is bioaccumulated in aquatic organisms are directly impacted by the molecular forms of selenium in solution. In chemistry terms, the different molecular forms an element can be present as is referred to as "species." Selenite and selenate (collectively referred to as inorganic selenium) are the most abundant, naturally-occurring soluble selenium species in most aquatic environments. Mining activities may release these species into wastewaters and, if left untreated, receiving waters. While conventional physical/chemical treatments are effective for selenite removal, biological treatment has been identified as the preferred treatment method for selenate by the USEPA. Such treatment systems can, depending on the operating conditions, induce formation of organic selenium species that bioaccumulate at levels significantly greater than those of the initial inorganic selenium species. Proper selection and maintenance of the treatment technology are therefore facilitated by speciation analysis, and in turn increase the likelihood that site-specific selenium

criteria will be met. Furthermore, speciation analysis can elucidate the viability of applied preparatory and analytical methods for the measurement of total selenium.

Introduction

Selenium (Se) is a naturally-occurring element that is chemically similar to sulphur. While it is essential for most organisms, due in part to its role in antioxidant enzymes, it also has a variety of toxic effects if present at elevated concentrations (Tinggi, 2003). The range between deficiency and excess has been estimated to be as small as one order of magnitude (WHO, 1996; USEPA, 2016), meaning that understanding and controlling exposure is critical to prevent deleterious effects.

Selenium's presence in the environment is due to both natural processes and anthropogenic activities. Natural weathering of selenium-rich minerals can mobilize this element, but human activities such as mining, coal combustion, oil refining, and agriculture are also significant contributors. Among mining activities, those involving coal, sulphide minerals, phosphates, iron ore, and uranium are most commonly associated with selenium releases. Whether through oxidation of naturally-exposed rock or overburden and tailings produced from mining operations, selenium trapped in these materials can be released to soil, sediment, and water. There it can be bioaccumulated by autotrophs (e.g., plants and algae), which in turn are consumed by heterotrophs (e.g., zooplankton, insects, fish, birds, and humans). As the selenium is transported through the food chain, molecular transformations can occur which can increase the percentage of organic selenium species. The result is that selenium is biomagnified up the food chain, potentially to toxic levels.

A variety of factors are known to impact the uptake, toxicity, and biomagnification of selenium. While natural waters typically contain selenium as the inorganic species selenite (SeO_3^{2-}) and selenate (SeO_4^{2-}), primary producers have been shown to metabolize these into organic selenium species such as selenomethionine and dimethylselenide (Umysová et al., 2009; LeBlanc and Wallschläger, 2016; Neuman et al., 2003). Some organic selenium species have been shown to bioaccumulate more rapidly (Besser et al., 1993) and exhibit toxicity at lower concentrations (Kiffney and Knight, 1990) than inorganic species of selenium.

Besides the critical role of speciation, other factors have also been shown to influence selenium bioaccumulation. The presence of other ions in the water may affect selenium uptake by an organism. Sulphate, for example, has been shown to be antagonistic to selenate absorption in algae (Williams et al., 1994) while nitrite can interfere with selenite uptake in *Stenotrophomonas maltophilia* (Antonioli et al., 2007). The rates at which different organisms (either within the same or different trophic level) accumulate selenium and the structure of the local food chain also make it challenging to directly correlate Se concentrations in the water column to toxic effects in biota.

In recognition of the numerous factors affecting the transfer of selenium from water to higher tropic levels, scientists and regulators have recommended that site-specific selenium criteria be used to protect aquatic life. In 2016 the USEPA published guidelines calling for a multi-component criterion for protection of aquatic life from selenium toxicity (USEPA, 2016), summarized in Table 1. Separate selenium limits are provided for fish tissue and water matrices; however, when data for multiple matrices is available, fish eggs/ovaries are given precedence over whole fish/fish muscle, which in turn supersede those from the water column. This order of precedence was established because fish, and especially their developing embryos, are generally the most sensitive to selenium in freshwater systems.

Table 1: USEPA recommended freshwater ambient chronic water quality criterion for selenium

Fish tissue	Water column
15.1 mg/kg dw egg/ovary	1.5 µg/L monthly average for lentic systems
8.5 mg/kg dw whole body	3.1 µg/L monthly average for lotic systems
11.3 mg/kg dw muscle	Intermittent exposure equation for short-term exposures

dw = dry weight

Similar guidelines in Canada are still under development, although British Columbia has proposed guidelines for selenium that include tissue, water column, sediment, and invertebrate components which are summarized in Table 2 (Beatty and Russo, 2014). Both the USEPA and British Columbia guidelines are not legally-binding regulations, but rather serve to assist states and provinces in developing their own water quality regulations affecting specific industries or point sources.

Table 2: British Columbia water quality guidelines for selenium for protection of aquatic life

Fish tissue	Other matrices
11 mg/kg dw egg/ovary	2.0 µg/L monthly average in water column
4 mg/kg dw whole body	2 mg/kg in sediment (alert concentration)
4 mg/kg dw muscle (interim)	4 mg/kg in invertebrate tissue (interim)

While selenium concentrations of fish eggs or ovaries are given primacy in aquatic life guidelines, several issues limit their utility for routine monitoring purposes. The cost of fish collection, as well as its impact to potentially-sensitive populations, will affect the frequency at which it can be performed. Moreover, since it may take months or years for selenium concentrations in fish tissues to reach equilibrium after there are significant new inputs or reductions to a system (USEPA, 2016), there are circumstances where fish tissue concentrations may not adequately reflect the long-term impacts to the aquatic ecosystem. For these and other reasons, water sampling will remain an essential component of any selenium monitoring plan. As will be presented herein, speciation analysis of the chemical forms of

selenium in these waters is key for evaluating their treatability and bioavailability. The accuracy of standard methods applied for total selenium quantitation, which are used to determine compliance with site-specific selenium limits, will also be shown to be directly impacted by selenium speciation.

The Role of Speciation for Selenium Treatability and Bioavailability Assessments

Selenite and selenate are the most common forms of selenium present in mining wastewaters. Numerous treatment options are available for selenite, but conventional options like iron co-precipitation are ineffective for selenate. Several reviews have identified biological treatment as one of the best options for selenate removal, in part because it is cost-effective and has been proven in full-scale installations (Sobolewski, 2005; Sandy and DiSante, 2010). Therefore, it is prudent for industries needing to implement selenium treatment and collaborative service providers to characterize waste streams via speciation analysis before and during bench- or pilot-scale studies.

Systems for biological treatment of selenium-laden waters take many forms, but anaerobic bioreactors are one of the most common iterations. In most of these systems, specially-selected heterotrophic bacteria use selenium as a terminal electron acceptor during the oxidation of a carbon source (either present in the wastewater or intentionally added prior to treatment), resulting in the reduction of selenite and selenate to elemental selenium (Se^0). This elemental selenium may then be removed from the effluent via filtration or it can be temporarily retained in the reactor (to be eventually removed by backflushing during a maintenance cycle). Well-maintained and optimized bioreactors have been shown to treat mining and other wastewaters containing mg/L concentrations of selenium down to single-digit µg/L levels.

Depending on the bacterial strains involved, the chemical environment, and the availability of nutrients, other less-desirable selenium species may be formed by bioreactor systems. Figure 1 shows a chromatogram of an effluent from a bioreactor used to treat a wastewater initially containing only selenite and selenate. Of particular note are the appreciable concentrations of the reduced selenium species, selenosulphate and selenocyanate (SeCN), as well as the organic selenium species that are present. Brooks Applied Labs has also quantified significant concentrations of the volatile selenium species dimethylselenide (DMSe) and dimethyldiselenide (DMDSe), as well as their degradation products dimethylselenoxide and methylseleninic acid, in effluents from other bioreactor systems. While the toxicity of all these species have not been fully characterized, it has been shown that the bioavailability of certain species like selenomethionine can be several orders of magnitude higher than those of inorganic selenium (Besser et al., 1993).

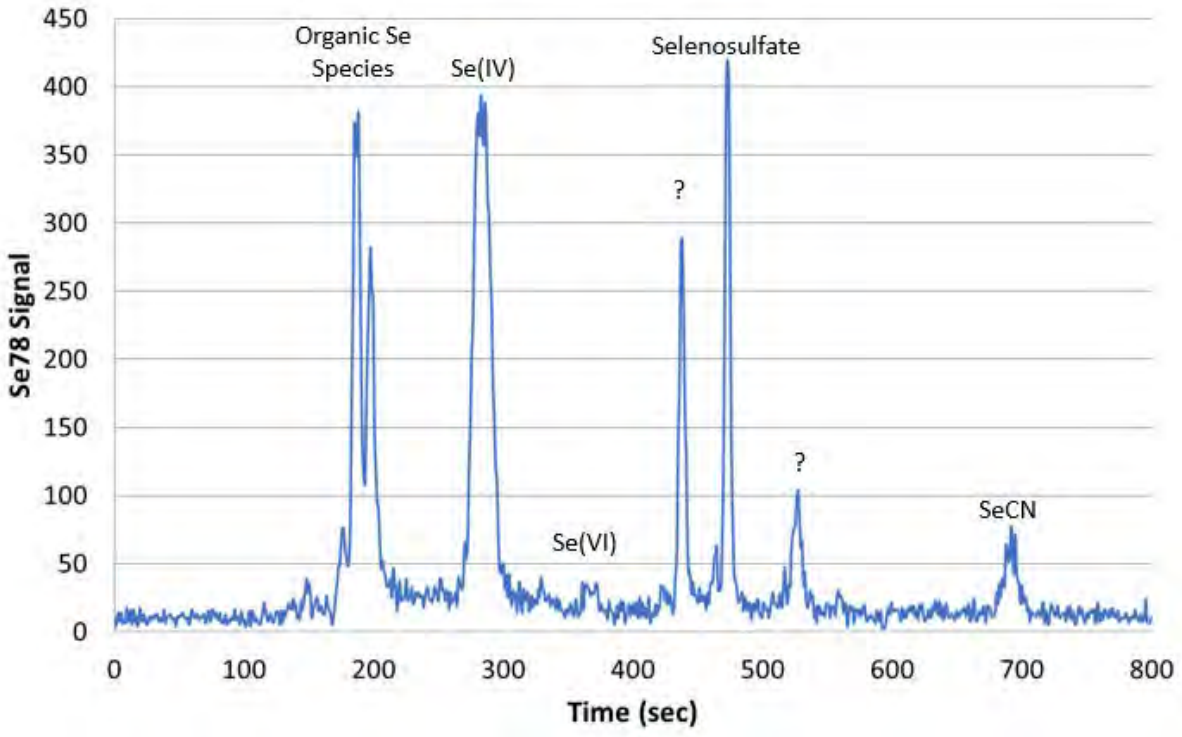


Figure 1: Selenium speciation in a bioreactor effluent via HPLC-ICP-MS

Since the goal of the treatment process is to reduce the uptake of selenium in the aquatic environment, conversion of inorganic selenium into forms that are significantly more bioavailable must be avoided. Otherwise, there is the potential that the treatment process itself will enhance the biomagnification of selenium, as has been reported by others (. et al., 2003). Methods that can quantify low levels of organic selenium species in the aquatic environment are also required due to the high bioavailability of these forms. Figure 2 shows an example of one such method, high-performance liquid chromatography inductively coupled plasma collision reaction cell mass spectrometry (HPLC-ICP-CRC-MS), which can reliably quantitate down to 5 mg/L of selenomethionine in waters.

Selenium speciation analysis is essential for not only selecting an appropriate treatment system but also monitoring its performance, thereby increasing the probability that it serves the goals of mitigating selenium ecotoxicity and corporate liability. Based on experience working with various treatment providers, the potential significance of the presence of certain selenium species in bioreactor effluents is summarized in Table 3. Routinely monitoring the quality of the effluent using speciation analyses (in addition to standard parameters such as pH and ORP) allows system operators to make timely adjustments to maintain optimal reactor performance.

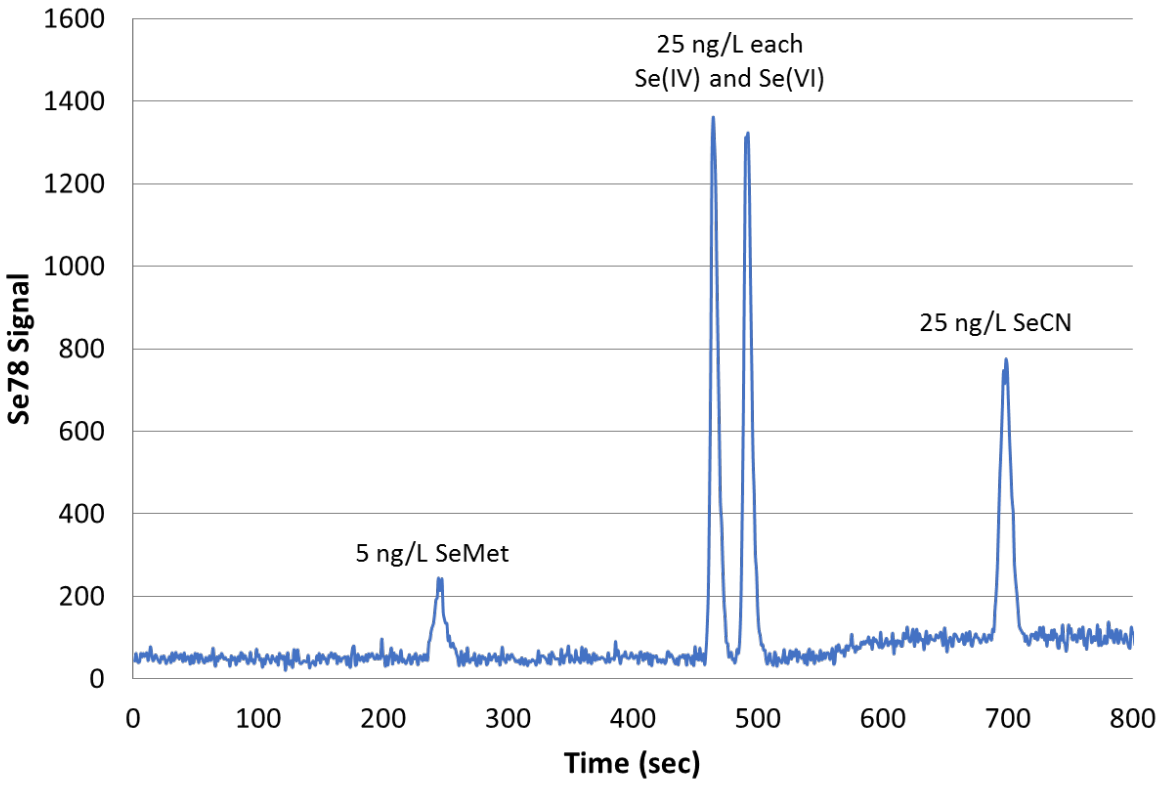


Figure 2: Separation of selenomethionine (SeMet), selenite, selenate, and selenocyanate by HPLC-ICP-CRC-MS

Table 3: Indicator species in bioreactor effluents

Selenium species	Potential indication
Selenocyanate	Overfeeding; Toxic reactor conditions (cell death)
Selenosulphate	Excess Se(0) buildup; ORP too low (sulphate reduction)
Elemental Se	Ionic strength too high; Improper Se(0) retention mechanism
Volatile Se (DMSe, DMDSe)	Improper bacteria strain; Improper degassing of system
Seleno-amino acids	Improper bacterial strain
Initial Se species	Bacteria colony has not equilibrated; Flow too high; Underfeeding; Concentration of other contaminants too high (toxic)

The Role of Speciation on the Accuracy of Selenium Measurements

It is critical that industries generating waste streams obtain accurate total and dissolved selenium data to monitor the efficacy of their treatment processes and compliance with discharge limits. The methods most commonly employed for selenium quantitation today use inductively coupled plasma mass spectrometry (e.g., USEPA methods 1638, 200.8, and 6020). Most were first promulgated over a decade ago and

developed primarily for ambient waters. Few methods specifically address the unique and varied selenium species that can be present in environmental samples and their associated chemical reactions (although it is noteworthy that USEPA methods 7740, 7741, and 7742 do specifically state that special sample containers may be required if samples contain volatile Se species).

These standard methods for quantitation of selenium and other trace elements generally recommend collection of samples into polymeric bottles (e.g., high density polyethylene or HDPE). Fractions for both total recoverable (unfiltered) and dissolved (0.45µm filtered) elements are preserved in their original bottles to a pH less than 2 with nitric acid. Further digestion of the samples is only strictly required for the total recoverable fractions, unless precipitates form in the dissolved fractions after filtration and acidification. Digestion most commonly involves removing an aliquot of the sample from the original, preserved sample container and then heating it with nitric and hydrochloric acids on a hot plate apparatus.

The Impact of Volatile Selenium Species

Selenium in samples containing only selenite and selenate may be adequately quantified by standard methods, but inaccurate results can be obtained for complex matrices containing more unique species. When samples contain volatile selenium species, for example, incomplete digestion may result in significantly high-biased data. Table 4 lists the results for an influent sample containing primarily inorganic selenium species and its associated effluent sample in which volatile selenium species were detected. The total recoverable selenium fraction for each sample was digested while the dissolved selenium fractions were initially not digested, in accordance with most promulgated methods. Good agreement between the two fractions was obtained for the influent sample, demonstrating that all the selenium was soluble before treatment. However, the undigested dissolved Se result for the effluent sample (185µg/L) is not only about 7 times greater than the associated total recoverable Se result (27.5µg/L), but also greater than the initial influent concentration (155µg/L dissolved). While it is often assumed that the chemical form of an element has no impact on the accuracy of ICP-MS measurements, volatile compounds are known to have enhanced mass transport in commonly used sample introduction systems (Juresa et al., 2006); the consequence is that small quantities of volatile compounds are measured as high concentrations relative to the non-volatile species used for the instrument calibration. As can be seen in the example listed in Table 4, this issue was resolved by digesting the dissolved selenium fraction identically to the total recoverable fraction. The applied digestion (involving heating with nitric acid) was sufficient to convert the volatile selenium species to non-volatile forms that had the same instrument response relative to the calibration standards.

Table 4: The effect of digestion on a sample containing volatile Se species

Sample Type	Total Rec. Se	Diss. Se (undigested)	Diss. Se (digested)
Influent	153	155	–
Effluent	27.5	185	22.1

All results in µg/L

The Impact of Reduced Selenium Species and Elemental Selenium

Promulgated methods for selenium analysis can also generate significantly biased total or dissolved selenium data if the samples contain reduced selenium species like selenocyanate and selenosulphate. These species are produced via reaction of elemental selenium with cyanide or sulphite, respectively, and have been detected in bioreactor effluents as noted above and as reported in other studies (e.g., LeBlanc and Wallschläger, 2016). These species can degrade back into colloidal, red elemental selenium during standard sample preservation (acidification to a pH < 2). This red elemental selenium is known to adsorb onto the surface of HDPE bottles commonly used for sample collection, as shown in Figure 3. Since most standard methods require removing an aliquot of the preserved sample from the original container for further digestion in a new container, any selenium adsorbed to the container will not be accounted for and therefore result in a low bias in the measured selenium concentrations.



Figure 3: Adsorption of red elemental Se on HDPE (left); Untreated bottle (right) shown for comparison

Another way this loss of reduced selenium species from solution can manifest itself is through temporally-variable total selenium concentrations. Figure 4 is a chromatogram for selenium speciation

analysis performed on a bioreactor sample that was identified to contain a significant amount of selenosulphate and selenocyanate. When this sample was preserved to pH < 2 in its original container and then an aliquot digested on a hot block apparatus a few days later, the selenium concentration was determined to be 32.0 µg/L. Most promulgated methods for total selenium quantitation allow for a holding time of up to 6 months for acid-preserved samples. When this acid-preserved sample fraction was re-digested and re-analyzed less than 8 weeks later, it was observed that the selenium concentration had decreased by 49% to 16.4 µg/L. The precipitation and loss of selenosulphate and selenocyanate from solution did not occur immediately upon preservation for this specific sample, but instead occurred over the course of a few weeks.

This process can occur over a matter of minutes to months, depending on the individual sample characteristics and oxidative capacity of the added preservative. Because treatment system operators and regulatory agencies must have confidence that the measured effluent concentrations are accurate, promulgated methods cannot be blindly applied to complex matrices like bioreactor effluents. More appropriate sample containers that do not strongly adsorb elemental selenium (e.g., borosilicate glass) and more rigorous preservation methods have both proved successful for generating accurate and consistent selenium data for these types of samples.

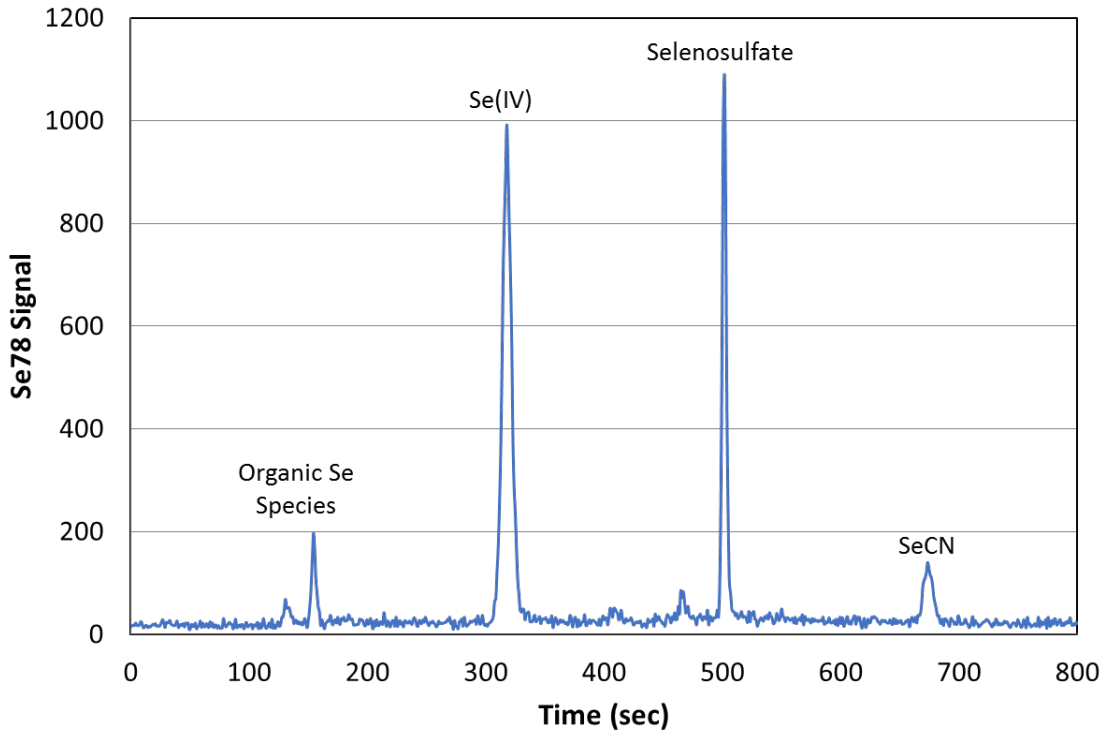


Figure 4: Selenium speciation of a bioreactor effluent exhibiting temporally-variable dissolved Se results

Conclusion

The molecular forms of selenium present in solution directly impact bioaccumulation and biomagnification factors, as well as the probability that a given treatment will reduce both the loading and toxicity of selenium to the aquatic environment. Information regarding the bioaccumulation and biomagnification of selenium species is limited to a handful of molecules, necessitating additional research for volatile species and their degradation products. Regardless, compliance with site-specific aquatic life criteria for selenium, whether expressed in the form of fish tissue or water column concentrations, can be achieved more rapidly and cost-effectively by including selenium speciation analysis as part of a routine monitoring program.

Quantifying the molecular forms of selenium present in a sample and understanding how their unique chemistry can impact methods for total selenium determination is crucial. Ensuring the availability of accurate data for application to decision-making processes is of the utmost importance for the sake of both the environment and the bottom line for the relevant corporations. While modern instrumentation has decreased the occurrence of analytical issues (e.g., polyatomic interferences) that can bias data, less emphasis has been placed on how the molecular forms of an element affect proper sample collection, preservation, and digestion procedures. A holistic approach that considers the impact of all these variables on the resulting data is required.

Acknowledgements

The authors wish to thank the anonymous clients who helped support these investigations, as well as the more than fifty scientists at Brooks Applied Labs who make performing this work possible.

References

Amweg, E.L., Stuart, D.L. and Weston, D.P. 2003. Comparative bioavailability of selenium to aquatic organisms after biological treatment of agricultural drainage water, *Aquat Toxicol*. 63(1):13–25.

Antonioli, P., Lampis, S., Chesini, I., Vallini, G., Rinalducci, S., Zolla, L. and Righetti, P.G. 2007. *Stenotrophomonas maltophilia* SelTE02, a new bacterial strain suitable for bioremediation of selenite-contaminated environmental matrices, *Appl. Environ. Microbial*. 73 (21): 6854–6863.

Beatty, J.M. and Russo, G.A. 2014. *Ambient Water Quality Guidelines for Selenium Technical Report Update*, British Columbia Ministry of Environment.

Besser, J.M., Canfield, T.J. and La Point, T.W. 1993. Bioaccumulation of organic and inorganic selenium in a laboratory food chain, *Environ Toxicol and Chem*. 12(1): 57–72.

Juresa, D., Kuehnelt, D. and Francesconi, K.A. 2006. Consequences of vapor enhancement on selenium speciation analysis by HPLC/ICPMS, *Anal. Chem.* 8(24): 8569–8574.

Kiffney, P. and Knight, A. 1990. The toxicity and bioaccumulation of selenate, selenite and seleno-L-methionine in the cyanobacteriumAnabaena flos-aquae, *A Arch Environ Contam Toxicol.* 19(4): 488–494.

LeBlanc, K.L. and Wallschläger, D. 2016. Production and release of selenomethionine and related organic selenium species by microorganisms in natural and industrial waters, *Environ Sci Technol.* 50(12): 6164–6171.

Neuman, P.M., De Souza, M.P., Pickering, I.J. and Terry, N. 2003. Rapid microalgal metabolism of selenate to volatile dimethylselenide, *Plant, Cell & Environment*, 26 (6): 897–905.

Riedel, G.F., Ferrier, D.P. and Sanders, J.G. 1991. Uptake of selenium by freshwater phytoplankton, *Water Air Soil Pollut.* 57(1): 23–30.

Sandy, T. and DiSante, C. 2010. *Review of Available Technologies for the Removal of Selenium from Water*, North American Metals Council.

Sobolewski, A. 2005. *Evaluation of Treatment Options to Reduce Water-Borne Selenium at Coal Mines in West-Central Alberta*, Alberta: Alberta Environment.

Tinggi, Ujang. 2003. Essentiality and toxicity of selenium and its status in Australia: A review, *Toxicology Letters*, 137(1–2): 103–110.

USEPA. 2016. Aquatic life ambient water quality criterion for selenium – Freshwater. EPA 822-R-16-006.

Umysová, D., Vítová, M., Doušková, I., Bišová, K., Hlavová, M., Čížková, M., Machát, J., Doucha, J. and Zachleder, V. 2009. Bioaccumulation and toxicity of selenium compounds in the green alga Scenedesmus quadricauda, *BMC Plant Biol*. 9(58).

Williams, M.J., Ogle, R.S., Knight, A.W. and Burau, R.G. 1994. Effects of sulfate on selenate uptake and toxicity in the green alga Selenastrum capricornutum, *Arch Environ Contam Toxicol*. 27(4): 449–453.

WHO. 1996. Trace elements in human nutrition and health, Geneva: World Health Organization.

Chapter 2:
Operational Water Management



Proceedings of Mine Water Solutions 2018
June 12–15, 2018, Vancouver, Canada
Published by the University of British Columbia, 2018

Is Water the Best Option? How to Evaluate which Fugitive Dust Management Practice is Right for Your Site

Jeff Ladderud, Freeport-McMoRan, USA

Abstract

Throughout the mining industry, fugitive dust emissions may present various health and safety challenges, such as limited visibility and/or respiratory problems, and are therefore the subject of regulation at the local, State, and Federal levels. The use of water trucks has been a go-to method for controlling fugitive dust emissions on unpaved roadways and other source areas such as tailings facilities. However, as water becomes an increasingly scarce resource, is it always the best option? Several families of topical dust suppressants are commercially available, including resins, polymers, lignosulfonates, salts, and asphalt emulsions. There are also non-chemical management practices available, including mulching, capping, and the implementation of administrative controls such as speed limits. Navigating the available options presents a challenge for mine-site decision makers.

This paper reviews several dust management strategies for light duty and haul roads, and tailings beaches. Drawing upon the author's experiences, it outlines a framework for evaluating the effectiveness and costs of alternative dust-management strategies. These include stakeholder discussions, laboratory tests for compatibility of any chemical dust suppressants with metal extraction processes and the environment, various field experimental design and evaluation techniques, and financial considerations. It is important to include as many voices as possible at stakeholder discussions. Dust management decisions affect many departments within any mining operation, and all need to buy in for a practice to be successful. It is imperative that any new suppressants used on site not adversely affect metal recovery or the environment (primarily air and water quality). Flotation and SX/EW compatibility testing on a laboratory scale look at metal recovery impacts, while flux chamber and leaching procedures detect possible air or water pollution from dust suppressants. Field trials of dust suppressants are an important step in evaluating their overall performance within a given operation. However, the careful design of such trials is important to account for the many confounding variables present. The quantitative and qualitative metrics that can be used to judge product performance are discussed. Finally, it is important to recognize that dust management requires striking a balance between life cycle expenditures and regulatory

compliance. Therefore, an accounting of direct and indirect dust management costs using water compared to other strategies will ultimately dictate whether an alternate management practice is worth pursuing.

Introduction

A blustery day or severe storm events on a mine site can spell headache for environmental managers and equipment operators alike. As the wind whips across the landscape, it has the potential to entrain fugitive particles from roadways, tailings beaches, and other disturbed areas, creating a cloud of dust that can pose health and safety challenges to miners and mining operations. There are also state and federal regulations governing the control of fugitive dust. For decades, water has been a reliable, albeit short-lasting tool deployed to mitigate such dust cloud events. Given the historic availability of water, its familiarity, and its low short-term cost, it is not difficult to understand how water has become ubiquitous in the realm of dust management. However, as water becomes an increasingly scarce or expensive (such as the case when desalinated sea water is used at a mine site) resource, opportunities exist to supplement with other dust management products and strategies.

A multitude of vendors and products have sprouted in response to these opportunities. But, with options ranging from using a water truck to apply magnesium chloride on a light-vehicle roadway to an aerial application of the latest and greatest polymer on an inactive tailings beach, how is one to discern the optimal management plan for their site? Faced with these opportunities and questions, Freeport-McMoRan has developed a framework for evaluating the effectiveness and costs of alternative dust-management strategies. These include stakeholder discussions, laboratory tests for compatibility of any chemical dust suppressants with metal extraction processes and the environment, various field experimental design and evaluation techniques, and financial considerations.

Step 1: Identify Areas to Manage

"For every vehicle traveling one mile of unpaved roadway once a day, every day for a year, one ton of dust is deposited along a 1,000-foot corridor centered on the road." (USDA Forest Service, 1983)

As this remarkable statistic shows, roadways can be a major source of fugitive dust emissions. Yet roadways are not the only cause of airborne particles at a mine site. A successful fugitive dust management plan begins with identifying all areas that may benefit from dust suppression measures. These may include haul roads, light vehicle roads, tailings beaches and dams, conveyor transfer points, and other disturbed areas such as lay-down yards. The conditions surrounding a dust management area will dictate which products may be effective there as well as how said products can be applied and evaluated. Each type of area presents its own suite of logistical and safety considerations. For example, the center of a tailings beach may be inaccessible to most application equipment due to soft ground and a

haul road may not be accessible at times due to haul truck traffic. Monitoring techniques at a lay-down yard will likely differ from those used on a light-vehicle road.

Step 2: Select a Product

Product selection for any given field evaluation or management plan is often founded in familiarity with a given vendor or product line. There are many dust suppressant vendors, and most offer a range of products engineered for a variety of applications. Product types broadly include water, hygroscopic salts, lignosulphonates, petroleum resins, polymer emulsions, and tar- and bitumen-emulsion products (Thompson and Visser, 2007). Inviting vendors to recommend a product after describing the condition at the site in question can generate a slate of potentially-effective products. There are also multiple published tables that recommend specific suppressant types for specific applications (e.g., Washington State Department of Ecology, 1996; Bolander and Yamada, 1999). Knowing what style of suppressant (e.g., petroleum resin, polymer, etc.) or control (e.g., crimp mulching, lower speed limits) is best suited to a site's operational and climatic conditions can assist in narrowing down a field of candidates. Cost will also inevitably come into play. Products are offered at a variety of price points, which are further influenced by shipping costs and application rates. Sometimes vendors will offer discounted or free product on a trial basis. It is important to establish the temporal goals of an evaluation project such that the amount of product applied is commensurate with the lifespan required of it. Under-application can lead to premature product degradation and unsatisfactory levels of fugitive dust from a treated area while over-application drains resources in terms of financial and operational impacts, including potential impacts to process as well as surface and ground waters.

Evaluating multiple products within a single trial offers the possibility of a direct comparison in performance between competing suppressants that would not otherwise be possible due to ever-changing ambient conditions. However, this direct comparison only applies insomuch as the evaluation plots are sufficiently close together geographically as to be subject to the same set of climatic and usage conditions. In some instances there may not be enough area available to test multiple products. If this happens, then it is preferable to trial a single product than to shrink the evaluation plot size to fit multiple products.

Step 3: Dust Suppressant Field Evaluation

Stakeholders

Field evaluations of dust suppressants are more successful when all associated parties have bought into the project. It is therefore crucial to engage all stakeholders and achieve a consensus prior to any field

activities. The list of stakeholders for any given project can vary but may include: Environmental, Mine Operations, Metallurgy, Site Services, Health and Safety, Security, Mill Manager, TSF Engineer of Record, Security, and product vendors.

Pre-test

Prior to field testing, all suppressants should be subject to a comprehensive laboratory evaluation to ensure that they will have no deleterious impact on site hydrometallurgical processes or the environment. This evaluation typically includes a flotation compatibility test to assure that the products will not negatively affect metal recovery, as well as batch and flux-chamber tests to check for potential water and air quality impacts. Laboratory testing of a product's suppression performance may be conducted as well, and there is a body of literature describing these tests (e.g., Grau, 1993; Copeland et al., 2008). However, it is the author's experience that results from such testing do not translate well into expected observations from a field evaluation. This is likely due to the many uncontrolled variables in a field setting. Therefore, well designed field trials provide the best predictor of product performance. However, results may differ from a full-scale usage scenario.

Process Compatibility

Process compatibility testing (at copper and molybdenum mines) involves adding dust suppressants at various dosages to a simulated flotation circuit that includes relevant site ore and flotation reagents. Changes in the recovery of the target product in the rougher concentrate are analyzed using ICP-MS. It also may include dosing the suppressant into a simulated SX/EW process and comparing extraction and strip efficiencies to a baseline case. Typically, suppressant reagents are added at varying doses ranging from 0.1 grams reagent per ton of ore up to 10 grams reagent per ton of ore. More research is needed to establish what concentration of suppressant is environmentally relevant for use in these compatibility tests. This concentration may vary depending upon site and product usage conditions and sites may opt to evaluate process compatibility at multiple suppressant concentrations in order to acquire a more refined understanding of how the suppressant impacts the process stream.

Environmental Compatibility

Environmental compatibility evaluations may include bottle roll batch tests and flux chamber tests. The former is designed to provide a conservative understanding of the potential suppressant-derived COC (constituents of concern) related impacts to ground waters while the latter offers a representative idea as to suppressant-based VOC emissions.

Bottle roll batch tests are used to assess potential water quality impacts by adding a dust suppressant, DI water, and earthen substrate (e.g., tailings, roadway material) to a bottle and rolling for 24

hours. Water samples decanted from the bottles are then submitted for VOC and SVOC analyses via EPA methods 8260 and 8270, respectively. If the suppressant being tested has an inorganic ion component (e.g. magnesium chloride) then that may be analyzed for as well. Bottle roll batch tests to assess potential air quality impacts follow the same procedure; but instead of submitting water samples, air samples from the headspace of the bottle are submitted for VOC and SVOC analyses using EPA method TO-17. Coordination with the analytical lab is important to ensure the integrity and relevance of sample data.

If product toxicity is of concern, a study in the style of Steevens et al. (2007) may provide information to understand potential human and environmental health risks.

Field Test

There are multiple articles that describe field evaluations of dust suppressants on roadways (e.g., Langdon, 1979; Sanders and Addo, 1993; Watson, 1996; Gillies et al., 2005; Qi et al., 2013). This paper follows in their footsteps and offers the following considerations and tools for a field evaluation at a mine site.

Layout of Test Plots

Creating a layout in which each plot is subject to, as much as is possible, an identical set of ambient conditions is optimum. In practice, this means ensuring that each plot experiences the same potential for blow-on dust and that all plots have the same wind, precipitation and drainage patterns. For roadways it is important that plots experience similar traffic loads and have the same grade and particle distribution. Plus it is optimal, but not necessarily critical, that all plots are the same size.

For tailings beach and dam evaluations, the recommended plot size is no smaller than 350 feet × 350 feet. For roadways, the recommended plots are no shorter than 1,000 linear feet, and that the entire width of the roadway is treated. In practice, trafficked portions of the roadway may receive a different product application rate than does the central crown or lateral berms. Plots should be contiguous to each other. Dust suppressant trials on tailings storage facilities must be mindful of any restrictions in place by the Engineer of Record regarding what products may be used, and if there is a required set-back from the dam crest during testing. These restrictions are in place to protect the geotechnical integrity of the TSF by maintaining full infiltration of water through the structure.

Infiltration

Any product applied to a tailings beach must not inhibit infiltration of water through the tailings, as doing so might compromise the stability of the engineered facility should the suppressant becomes layered amidst tailings. To this end, an infiltration test can be conducted on the crust of any product applied to a tailings beach or dam. This can be accomplished with a double-ring infiltrometer (Figure 1).



Figure 1: A double-ring infiltrometer is used to assess the infiltration rates of a suppressant-treated tailings beach surface. Shown here is an infiltration test being performed on a mature crust of the material being testing (dyed green for observational data collection)

Big Springs Number Eight (BSNE) Samplers

Arguably, the single most important aspect of a dust suppressant is how well it reduces fugitive dust emissions. There are several qualitative and quantitative methods available to evaluate the performance of a dust suppressant such as opacity readings, passive stationary dust collectors, and active vacuum-type dust collectors. Previous dust evaluations by the author have relied primarily on stationary-mounted, freely rotating Big Springs Number Eight (BSNE) dust samplers to assess the efficacy of applied dust suppressants in a field setting. BSNEs have been used in the agriculture for many years (Fryrear, 1986). This study also used BSNEs, making note of past lessons learned to improve the accuracy and reliability of the collected data.

BSNE samplers are designed to capture wind-dispersed sand and dust particles, providing a comparable measurement of dust emissions between plots (Mendez et al., 2011). Each sampling station consisted of one triple BSNE dust sampler and two regular BSNE samplers mounted on a 5-ft metal pole. The triple sampler contains three sampling ports and is mounted onto the pole with openings at approximately 5, 10, and 20 cm above the ground, where the majority of soil movement occurs. Two

regular BSNE samplers, each containing a single sampling port, are mounted with their openings at 50 and 100 cm above the ground (Fryrear and Saleh, 1993). This arrangement allows for the quantification of air-borne material at multiple heights above the eroding surface. The mass of captured solids is divided by the cross-sectional area of each device's sampling port and sampling interval and serves as the basis for obtaining a time-averaged estimate of sediment moving across the experimental plots. In instances where the sampler contained standing water, no sample is collected; but rather the sampler is emptied onto the ground and cleaned. In theory, a wet sample could be collected, dried and measured. However, experience suggests that the errors associated with this process may undermine the validity of the resulting data. Rain guard attachments can be added to the BSNE samplers to prevent water from ponding in the samplers. Experience suggests these to be approximately 85% effective in keeping samples dry.

BSNE samplers should be positioned within an evaluation plot in such a manner as to minimize the collection of blow-on dust (i.e., dust that did not originate from the evaluation plot). It is possible to lock the BSNEs from rotating, and this may help mitigate blow-on dust collection. However, it also may bias the sample collection because the BSNEs are designed to work facing directly into the wind. Similarly, placing two BSNEs close together can affect their ability to face upwind due to the creation of eddies.

Routine sampling and maintenance is important. Frequent sampling provides a higher-resolution data set, and allows for maintenance of the samplers. Sampling intervals need to be sufficiently long as to allow measurable amounts of particles to be collected in the BSNEs. Sampling is accomplished by opening the BSNE sampler and brushing the sediment into a sample container. When sampling it is important to tread lightly on the evaluation plot as to not break up the dust suppressant and use a designated ingress and egress route.

Dust Trailer

For roadway dust suppressant trials, a small utility trailer equipped with four BSNE samplers can be used to actively sample traffic-generated dust on the test plots (Figure 3). The trailer is pulled behind a pickup truck at a consistent speed (normally the permissible operating speed of the roadway being tested). Special consideration should be given to safety when collecting samples in this manner—especially when the trial is on a haul road. Experience suggests that the trailer must travel at least 4,000 feet to collect a minimum amount of measurable dust. This can be done by using multiple passes through any single evaluation plot. The dust collected in the BSNEs is used to calculate a mass flux (kg/m^2) value similar to that calculated from the stationary BSNEs. This value is then normalized to the total distance traveled by the trailer while collecting the sample.



Figure 2: BSNE sampling station showing the triple sampler near the ground, with openings at approximately 5, 10, and 20 cm height, and two single samplers placed at 50 and 100 cm above ground level. The samplers are allowed to rotate 360° unless site conditions require constraining them to specific directions



Figure 3: Small utility trailer equipped with four BSNEs to actively monitor vehicle-generated fugitive dust

Active Samplers

A number of active samplers such as that used by Sanders and Addo (1993), Kuhns et al. (2001), Thenoux et al. (2007), Kavouras et al. (2009) and Witt et al. (2012) are commercially available at various price points. The author has no first-hand experience with these and they are not discussed further in this paper.

Weather Station

It is beneficial to have a weather station collecting data in the vicinity of the evaluation plots. Often a site's weather station is not located close to the plots and therefore a new weather station will need to be installed in the plot area. The weather station should collect, at a minimum, data on wind speed, wind direction, and precipitation and log them on hourly intervals. Temperature and solar radiation measurements may also be collected. As with the BSNEs, routine inspections of the weather station and data logger are important so that any maintenance issues that may arise can be quickly remedied.

Time-lapse Camera Footage

PlotWatcher Pro time-lapse video cameras (Day 6 Outdoors, Columbus, GA) can be utilized to monitor the plots (Figure 4). These cameras take a photo at a programmed time interval (e.g., 30 seconds) during daylight hours, and then the footage from each day is condensed into a short time-lapse video. This video can offer information as to where the dust originates that is collected in the BSNE samplers. In conjunction with the weather station data, the videos may also be used to identify climatic conditions that lead to dust generation. The cameras are mounted on large, metal tripods, similar to that used for mounting the weather station.

EPA Method 9 and Other Visual Techniques

Often times, site Environmental personnel are trained to take EPA Method 9 opacity readings. Using Method 9, a qualified individual can quantify opacity by "taking opacity readings of plumes at 15-second intervals and averaging 24 consecutive readings (6 minutes)" (Randolph and Foster, 1993). Applicability of this method is therefore contingent upon having a qualified individual available and having a dust event that lasts for several minutes. A qualitative measurement of a dust event can be made under less stringent conditions using EPA Method 22.

It is likely impractical to assign personnel to make visual readings of dust events with sufficient regularity as to produce a meaningful and robust data set that can be used to compare competing dust suppressants. More plausible, however, is incorporating a modified Method 9 procedure to road evaluations in conjunction with the BSNE dust trailer. This would ensure that the opacity reader is on the scene at the moments of maximum dust generation. Based on the author's review of PlotWatcher video footage, dust events on tailings beaches and other non-road areas are much more sporadic than those

generated by vehicle traffic. Casual visual observations of the plots by site personnel may be considered as anecdotal evidence in a field evaluation.



Figure 4: A PlotWatcher Pro time-lapse camera takes a photo of the evaluation plot at designated time periods during daylight hours. These photos are combined to produce a video clip that is stored on a removable SD card

Another visual technique that may be useful in some instances is the EPA Visible Crust Test Method. In this method, one or more steel balls are dropped from a height of 12 inches onto a treated surface. A visual inspection is made as to whether or not the ball broke the crust. This is repeated several times. The challenge with this test is capturing the crustal heterogeneities that are often present in an evaluation plot, given that the method only samples a very small area of crust. The test is also, to a large extent, subjective, relying on the administrator's judgement as to whether the crust "held" under any particular ball drop.

Cost Evaluation

A dust suppressant may prove very effective in a field evaluation; yet it must also be affordable if a site is to adopt it as a best management practice. For this reason, a cost evaluation must be performed if the switch to a new dust suppressant is to be justified. Often a vendor is willing to make a first pass at this cost evaluation if the site shares certain financial details (e.g., operator costs, equipment maintenance costs, etc.) with them. The vendor has an agenda of demonstrating that their product will save the site money, so results from a vendor should be audited and/or paired with an independent cost evaluation completed by the site.

Major components of a product economic model generally include the life cycle cost of the product (including shipping and storage), the cost of water truck operators, the cost of equipment tires (vendors claim that water decreases tire lifespan as compared to some chemical dust suppressants), and the cost of road grading and maintenance. Compounding these is the frequency with which a product needs to be reapplied. Other elements are more difficult to quantify but may still be worth consideration. These include future water treatment costs (e.g., if magnesium chloride is adding chloride to the site that will need to be treated upon closure), an improved social license to operate due to fewer dust emission events, improved operator health and safety due to fewer dust emissions, and improved water conservation and stewardship. Certain models exist that may aid in the quantification of these costs (e.g., Liebenberg-Enslin, 2014).

Conclusion

A successful field evaluation of one or more dust suppressant strategies requires extensive planning and stakeholder coordination. The focus throughout the trial should be on isolating signal from noise in any data collected. In other words, are suppressant effects (or lack thereof) derived from the area under evaluation, or from somewhere else? Equally important is to keep sight of the bigger picture: will this dust-suppressant strategy decrease environmental and social liabilities at the site at a price that is affordable? Does this strategy negatively impact any site process or stakeholder in such a manner that it cannot be considered for use on site?

There are times when water may be the best option for dust management at all or part of a site. However, as this resource becomes increasingly scarce or expensive, it is in a site's best social and economic interests to evaluate other options. The methods discussed in this paper provide a framework for such an evaluation.

References

Bolander, P. and Yamada, A. 1999. *Dust Palliative Selection and Application Guide,* 9977 1207-SDTDC. San Dimas, CA: US Department of Agriculture, Forest Service, San Dimas Technology and Development Center. Retrieved from: https://trid.trb.org/view/713799.

Copeland, C.R., Eisele, T.C., Chesney, D.J. and Kawatra, S.K. 2008. Factors influencing dust suppressant effectiveness, *Minerals and Metallurgical Processing,* 25(4). Retrieved from: https://www.osti.gov/scitech/biblio/21222468.

Fryrear, D.W. 1986. A field dust sampler, *Journal of Soil and Water Conservation,* 41(2): 117–20.

Fryrear, D.W. and Saleh, A. 1993. Field wind erosion: vertical distribution, *Soil Science,* 155(4): 294–300.

Gillies, J.A., Etyemezian, V., Kuhns, H., Nikolic, D. and Gillette, D.A. 2005. Effect of vehicle characteristics on unpaved road dust emissions, *Atmospheric Environment,* 39(13): 2341–47. Retrieved from: https://doi.org/10.1016/j.atmosenv.2004.05.064.

Goossens, D. and Buck, B.J. 2012. Can BSNE (Big Spring Number Eight) samplers be used to measure PM10, respirable dust, PM2.5 and PM1.0? *Aeolian Research,* 5 (August): 43–49. Retrieved from: https://doi.org/10.1016/j.aeolia.2012.03.002.

Grau, R.H. 1993. Evaluation of methods for controlling dust. WES/TR/GL-93-25. Army Engineer Waterways Experiment Station Vicksburg Ms Geotechnical Lab. Retrieved from: http://www.dtic.mil/docs/citations/ADA270527.

Kavouras, Ilias G., Etyemezian, V., Nikolich, G., Gillies, J., Sweeney, M., Young, M. and Shafer, D. 2009. A new technique for characterizing the efficacy of fugitive dust suppressants, *Journal of the Air and Waste Management Association,* 59(5): 603–12. Retrieved from: https://doi.org/10.3155/1047-3289.59.5.603.

Kuhns, H., Etyemezian, V., Landwehr, D., MacDougall, C., Pitchford, M. and Green, M. 2001. Testing re-entrained aerosol kinetic emissions from roads: A new approach to infer silt loading on roadways, *Atmospheric Environment,* 35(16): 2815–25. Retrieved from: https://doi.org/10.1016/S1352-2310(01)00079-6.

Langdon, B.B. 1979. *An Evaluation of Dust Abatement Materials Used in Region 6*. Transportation Research Institute, Oregon State University.

Liebenberg-Enslin, H. 2014. A functional dependence analysis of wind erosion modelling system parameters to determine a practical approach for wind erosion assessments. PhD Thesis. Johannesburg.

Mendez, M.J., Funk, R. and Buschiazzo, D.E. 2011. Field wind erosion measurements with Big Spring Number Eight (BSNE) and Modified Wilson and Cook (MWAC) samplers, *Geomorphology,* 129(1–2): 43–48. Retrieved from: https://doi.org/10.1016/j.geomorph.2011.01.011.

Qi, J., Nadhir, A. and Knutsson, S. 2013. Measurement of dust emission from a road construction using exposure-profiling method, *Natural Science,* 05(12): 1255–63. Retrieved from: https://doi.org/10.4236/ns.2013.512153.

Randolph, K. and Foster, K. 1993. *Visible Emissions Field Manual EPA Methods 9 and 22.* US Environmental Protection Agency.

Sanders, T.G., and Addo, J.Q. 1993. Effectiveness and environmental impact of road dust suppressants, December. Retrieved from: https://trid.trb.org/view/448612.

Steevens, J., Suedel, B., Gibson, A., Kennedy, A., Blackburn, W., Splichal, D. and Pierce, J.T. 2007. *Environmental Evaluation of Dust Stabilizer Products.* ERDC/EL-TR-07-13. Engineer Research and Development Center, Vicksburg MS Environmental Lab. Retrieved from: http://www.dtic.mil/docs/citations/ADA471771.

Thenoux, G., Bellolio, J. and Halles, F. 2007. Development of a methodology for measurement of vehicle dust generation on unpaved roads, Transportation Research Record: Journal of the Transportation Research Board 1989 (January): 299–304. Retrieved from: https://doi.org/10.3141/1989-35.

Thompson, A.T. and Visser, R.J. 2007. Selection, performance and economic valuation of dust palliatives on surface mine haul roads, *Journal of the Southern African Institute of Mining and Metallurgy,* 107(7): 435–50.

USDA Forest Service. 1983. *What the Forest Service Does.*

Washington State Department of Ecology. 1996. *Techniques for Dust Prevention and Suppression*: 96-433.

Watson, J.G. 1996. Effectiveness Demonstration of Fugitive Dust Control Methods for Public Unpaved Roads and Unpaved Shoulders on Paved Roads. *DRI Document No*, 685–5200.

Witt, E.C., Wronkiewicz, D.J. and Shi, H. 2012. Preliminary assessment of an economical fugitive road dust sampler for the collection of bulk samples for geochemical analysis, *Journal of Environment Quality* 42 (1): 21. Retrieved from: https://doi.org/10.2134/jeq2012.0158.

Proceedings of Mine Water Solutions 2018
June 12–15, 2018, Vancouver, Canada
Published by the University of British Columbia, 2018

Dust Mitigation Using a Water Conservation Program

Steven R. Clark, EnviroTech Services Inc., USA

Abstract

When it comes to controlling dust at your operation, whether a mine, a batch plant or ancillary area, what are the options? We know watering alone is not the answer, but at the same time, we have an obligation to keep dust from flying to ensure a safe environment and keep our skies clear of pollution, for both regulatory requirements and our neighbours. Employing a water conservation program instead of looking to buy the first dust control product off the shelf is a first step to controlling dust and conserving water.

Application calibration and methodology development at mining sites (Cripple Creek Victor Gold, Spence BHP Chile, and New Caledonia Nickel) provided test results that led to the successful development and implementation of a water conservation program. With ease of access to a haul road for dust meter measurements, a water conservation case study in Larimer County Colorado provided quantitative results. This study is a collaboration of data collection and methodology refinement. Deployed in arid, semi-arid, and humid climates, the program resulted in water savings of between 50 and 70 %, as compared to dust mitigation by only water.

Introduction

Of all the natural resources being taxed by the needs of the modern world, perhaps the most important is water, as the demand for it continually expands. As water becomes scarcer, and increasingly important, new technologies are needed to find innovative ways to preserve this precious resource. In Chile, for example, the mining industry is investing billions of dollars to build desalination plants and pipelines; bringing ocean water as far as 200 km inland to meet their demand and maintain operations. It is a full-blown crisis for that nation, and a top priority for their government and economy. It has been reported that world water consumption will increase by 40% in the next 10 years, representing nearly exponential growth. In the USA, as more and more communities continue to be built, the drain on the current water infrastructure is increasing. For 25% of people and operations that rely on water from aquifers, this source is being consumed at a rate that will create significant problems meeting the demand in as few as two generations (HBS Alumni Bulletin, 2005).

A Proactive Approach to Dust Control

When it comes to controlling dust at your operation, whether a landfill, a transfer station, a haul road, or another ancillary area, what are the options? We know watering is not the answer, but at the same time, we need to prevent dust from flying to ensure a safe environment and keep our skies clear of pollution, for both regulatory requirements and neighbours. Creating a Dust Mitigation Program instead of looking to buy the first dust control product off the shelf is a first step to conserving water and, at the same time, maintaining the operational demands and environmental standards for a given site.

The program concept is straightforward enough. However, the process of effectively constructing and executing a program is quite involved. When undertaking a program, managers need to work with their team and their partners/vendors in analyzing the following elements:

1. *Site expectations:* It is important to understand how to balance your internal standards with your regulatory requirements, as well as how to keep your neighbours satisfied.
2. *Site aggregate:* Variations in native soil, such as clay content or gravel levels, greatly affect the approach that will yield the highest results.
3. *Climate:* Relative humidity and seasonal variations are critical to achieving predictable results through product choice, application frequency, and timing.
4. *Daily traffic:* The type and frequency of traffic is an essential variable for site management.
5. *Environmental responsibilities:* If you have additional, specifically defined responsibilities, the approach to your site may vary.
6. *Budget:* While efficiency is the goal of any program, some sites will have more stringent restrictions than others.
7. *Current usage rates:* Document and understand where you are starting from, both with water, supporting products, and maintenance, so that effective measurement of results is possible.

An effective evaluation may reveal immediate gains available to the project. In many instances, however, a manager may need to familiarize themselves on other products available to understand performance and application requirements. A product that has a more efficient application rate and responds to recharge efforts may be more expensive at first pass. Understanding a longer-term use of the product, as well as factoring how water resources can be saved, may reveal that it is effective, or that when applied, the cost is lower than a commodity. For this reason, it is also important that partners and vendors working on the project use sound science that can be quantified and demonstrated to the manager. It is not enough to accept claims made in marketing materials, or to reference a single project that may only have a few similarities to the one being worked on. The effort needs to be collaborative so

that the partner has a comprehensive understanding of your specific project, and can then make informed recommendations on how a program can be constructed. These background materials and preparation efforts will not only help determine the optimal approach, but create supporting documentation for decision makers. As water grows scarcer, increasingly sophisticated ways of measuring cost and usage will be required, and designing a program is an excellent step in this direction. A sound Program considers the long-term result of reducing resources use and creating a dust-free environment based on all variables, while maximizing budgetary efficiency.

Proof of Concept – Mines as Partners

When developing a program utilizing one of our products, the goal was to show that the program could work in a variety of climates: arid, semi-arid, and humid. The three locations chosen to cover these climates were the Atacama Desert, Chile (arid copper mine), Colorado, USA (semi-arid gold mine), and New Caledonia (humid nickel mine).

Being relatively close to the manufacturing facility, Cripple Creek Victor Mine collaborated on initial application rates ESI applicator truck and maintenance applications CCV water truck (Figure 1).



Figure 1: Application truck initial application, and water truck with maintenance application

The actual application rate from CCV water truck was calibrated using three fixed volume containers. The truck passed over the containers while watering, and the rate was measured at 0.15 gal/yd^2 (Figure 2).



Figure 2: Sample collected to calibrate water truck and dry lane left to test traction

It was determined that two passes of the water truck would be needed to meet a 0.3 gal/yd^2 application. When applying the initial application, a narrow dry area of the road was used to test the traction of a fully loaded haul truck (Figure 2).

A ramp brake test was conducted at a BHP mine in Chile. The test conducted with an empty CAT 793F haul truck compared water vs. product at the end of a 10% grade ramp section (Figure 3). The final braking distances and testing parameters are proprietary to the BHP, but the final stopping differences between water and product was ten meters with the truck requiring more distance on water than on product. The friction of the braking area was not affected by product application.



Figure 3: Ramp brake test in Chile

The last mine test was in New Caledonia on haul roads and access roads. The dust levels were so high that even the front gate security guards were required to wear respirators and eye protection at all times (Figure 4). This figure depicts the dust before, and at one week after the application, with no additional

treatments. The dust that was generated after one week remained heavy and would fall back to the road. Fugitive dust on the facility was eliminated with the treatment and following maintenance applications.



Figure 4: Dust before and after one week

Starting a Program

If your facility needs a Dust Mitigation Program, your first step is to research companies capable of bringing you the expertise needed to make the proper assessments. These programs are relatively new in many areas, so be prepared to ask the questions that will give you confidence in the partner you select. Most notably, your prospective partners should have a comprehensive understanding of the previous list and include each of those factors as you begin assessing your possibilities. Preserving our water supply goes beyond the needs of a specific project. It is a priority for all. When you implement a Dust Mitigation Program, you are contributing to the public good.

Dust Mitigation Case Study

Larimer County Landfill sits on the border of the Ft. Collins, Colorado, city limits. With the desire to be a good custodian of the city's resources and improve efficiency, the director of the landfill was seeking methods to reduce water use and control dust generated on the landfill roads. Water was the only method of dust control and the water being consumed was provided directly from Ft. Collins Utilities. After meeting with EnviroTech Services, the director made the decision to try an innovative method of dust control. EnviroTech's Dust Mitigation Program is a maintenance program that uses a humectant product, X-Hesion Pro (XPro)2. The general concept of the program is to use this unique product as an element that gets introduced to the site roads in such a way that it actually becomes part of the road base, as well

as an added element of the water being applied. The effect, as was demonstrated in this case, is that water usage is reduced by enhancing the effectiveness of water each subsequent time it is applied.

The assistant director of the landfill was directly involved in the program plan. He supervised the initial application, has been available during dust meter readings, and added the appropriate amount of XPro to the water truck when needed. The involvement of the landfill's management was critical so that multiple factors could be monitored and adjusted. For instance, knowing when to add product to the water truck is similar to changing the oil in your car. If the weather conditions are hot and windy, the frequency of adding XPro will be increased (much like driving a thousand miles per week will increase the frequency of your car's oil changes). The opposite is true if the weather is cool and wet; less water and product are needed. As with any topically applied product, rain will affect this program. A light rain is good and rejuvenates the existing XPro in the road. Heavy rainfall can wash most products from an unpaved road, but we have seen XPro continue to have dust-reducing effects after a three-inch rainfall. All these elements require someone in charge of the site paying attention so that conditions can be properly monitored. While not every site or manager will have access to dust meters or other advanced testing measures, visual inspection and tracking can still be relatively effective.

Equally important to the hands-on management of a program, of course, is selecting the product that will complement the water itself. As a humectant, XPro "likes" to hold onto water. When incorporated into the surface of the road, XPro causes loose material to become heavier. The dust created by traffic does not plume as much; it quickly drops back to the road. A key to controlling dust is understanding your road and the different dust levels produced on them. Active involvement by onsite personnel saves on equipment maintenance, fuel, and time.



Figure 4: Aerial view of the site's roads

Location

The initial application occurred at the Larimer County Landfill, as seen in Figure 4. The image from 2012 is used as a reference. The red line is the road to the dumpsite, and the blue line is the road for the scraper.

After meeting with the assistant director, the scope of the area to be treated was established. Road sections included:

- Haul Road (red) 32' × 5,280' (~18,773 yd^2)
- Scraper Road (blue) 32' × 2,640' (~9,386 yd^2)
- Variable width of roads, but averaged 32'
- Road distance was measured by driving, since Google maps no longer represent present roads
- Road base is native aggregate with some asphalt millings on the first half mile of haul road
- Expected traffic profile: ADT (variable/unknown amount heavy of traffic)
- Platform: **not treated**

Initial Application

The initial application was completed using EnviroTech's applicator truck. For the first treatment, a quick build-up of the humectant product was needed, so ESI applied a 50% mixture of water and X-Hesion Pro. The larger dose of XPro greatly decreased the water evaporation, and made future applications by Larimer County Landfill's water trucks less frequent.

The Program and Water Truck Applications

After the initial application (Figure 5), the road was maintained with water applications and water with XPro applications.



Figure 5: Detail of spray bar

With two days between the initial application and the beginning of the next week, it was anticipated that a light water would be needed. This water lasted noticeably longer than a regular water application (Figure 6).



Figure 6: Treated haul road

Temperature and humidity are relevant to the frequency of the application of product. At the beginning of this program a 10% application early in the morning for the first week was recommended. The 10% XPro/Water solution was mixed at the fill station of the Landfill (Figure 7).



Figure 7: Mixing water and product directly into the tank

At the initial application and for the first few product/water mixes, a representative from ESI laboratory was present to ensure quality control. After the first week, a schedule of a 10% application every week was recommended during hot summer days (Figure 8).



Figure 8: Water truck applying a 10% XPro solution

Application – August 16, 2014, 5:00 p.m.

After the dilution, the main haul road was treated at a specified application rate at a width of 14 feet. Each lane was treated completely from the end of the pavement to the platform where the refuse is deposited. It was decided that the area near the platform would not be treated due to the heavy traffic and the rapidly changing location of the deposit area.

The First Two Weeks: August 17–31, 2014

The earthmover changed areas on the property and was no longer using the treated scraper road. Notice the dust generated by the scraper on the untreated road (Figure 9) and the lack of dust on the treated road (Figure 10).



Figure 9: Scraper on untreated road – dust plume, August 25, 2014

Over the weeks of August 17 to August 31 on the treated sections, water was only applied once per day, down from six times per day, and XPro was used only twice during the 14-day period.



Figure 10: Truck on treated section – no dust plume, August 25, 2014

The Third Week: September 1 – 6, 2014

During the site visit on September 2, the water truck was out on the property watering untreated roads. The main haul road was not watered in two days and showed signs of very little dust (Figures 11 and 12). With the success of the program during the first three weeks, expanding the program onto other roads of the property was discussed. The water truck would be mixed with 20% to 30% XPro, and begin the process of building up the humectant material in the previously untreated roads.



Figure 11: Almost no dust without a water treatment



Figure 12: Right lane has road material from other areas of landfill

Quantitative Dust Data

While the assessment of a program's effectiveness can be largely ascertained through visual observation, as demonstrated above, it is ideal to use measuring equipment to further confirm and quantify results. Figures 13 to 17 show a sampling of charts generated from the data collected at the landfill. The data confirms the visual observation from the site.

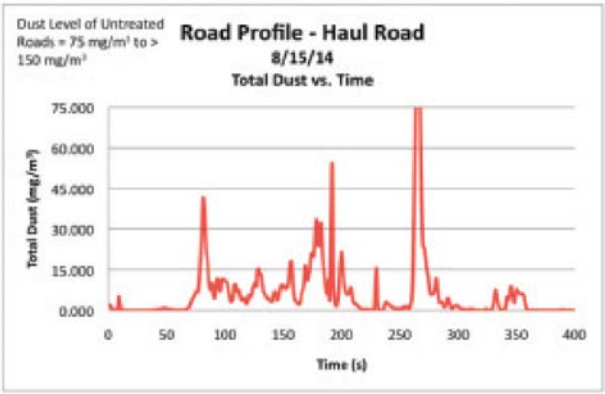


Figure 13: Haul road one day prior to the application

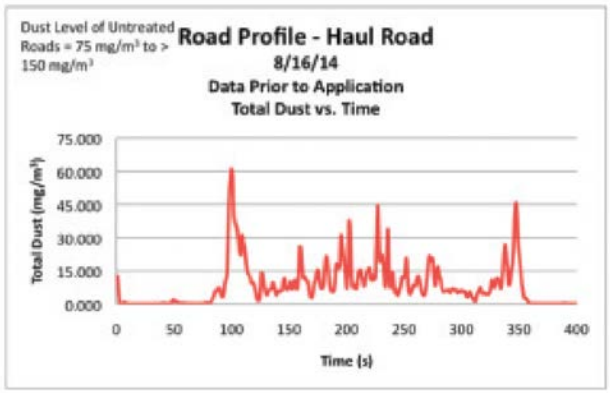


Figure 14: Haul road minutes prior to the initial application

Roads were watered earlier in the day, prior to measuring the dust levels. It is important to remember that dust is becoming visible above the measurement of 10 mg/m^3. This road is very dusty at the day's end.

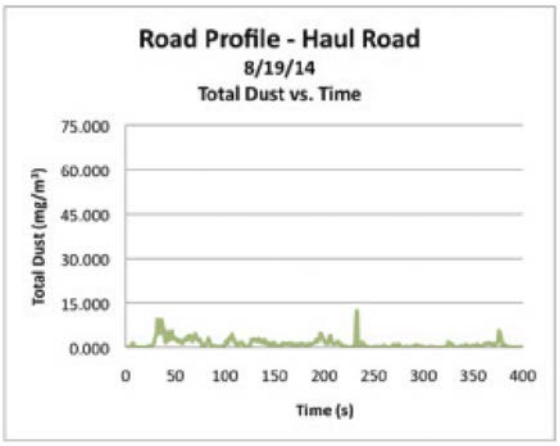


Figure 15: Haul road three days after application

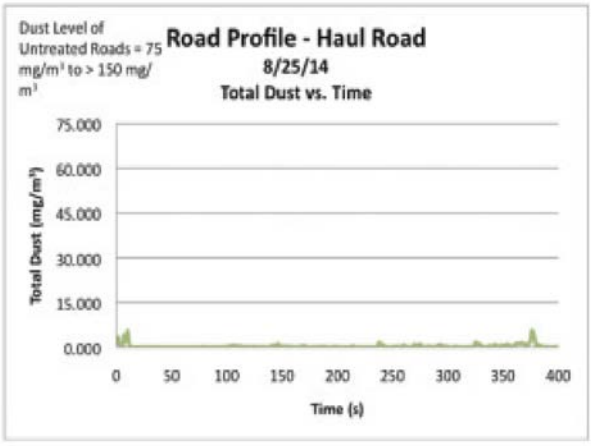


Figure 16: Haul road nine days after the application and two 10% adds to the water truck

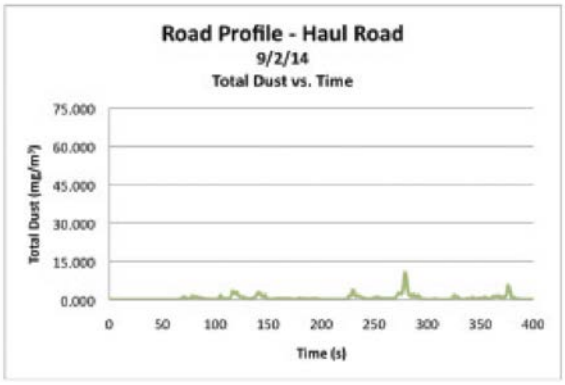


Figure 17: This measurement was taken in the early morning, prior to watering the roads

Conclusions

Collaborating with mines in different climates provided proof of concept. This led to dust mitigation program proposals being accepted at landfills, aggregate mines, and sand pits. Clearly, both visual and quantified data confirm that the program was very effective at reducing dust at the Larimer County Landfill. We know that prior to the application of X-Hesion Pro, four to six truckloads of water were being used a day. After the application, one to two truckloads of water were used. So, there was a savings of water, equipment usage, and personnel time ranging from 50 to 80 percent within the first month.

The Savings Scenario

The Larimer County Landfill operates six days a week. We have monitored water use and, since the program was implemented, have seen as little as one water truckload applied to control the facility's dust. From a conservative perspective, the water truck driver would have four free hours per day to be used on other landfill projects. That is like gaining one part-time trained employee without additional expense. It is difficult to document this savings and increased productivity, but its impact will be felt. After the initial application, the average amount of product being used at the landfill per week is equal to about one application (~350 gallons). Knowing that prior to the X-Hesion Pro application, six truckloads of water per day was reduced to two truckloads applied, the savings to the landfill would be:

21,000 gallons (Historical, six truckloads)
7,000 gallons (Present, two truckloads)
× 6 days a week of dust control
= 84,000 fewer gallons of water a week

Operating 52 weeks per year under this scenario, the landfill could see a water savings of more than 4 million gallons of water per year. The Program at the Larimer County Landfill was a very compelling example of an involved and proactive site partnering with a supplier familiar with managing site variables and creating real, measurable value for the end user. This is an example of how to approach a program of your own.

References

HBS Alumni Bulletin. 2005. Is water the new oil?, *Water Ltd.* 81(3). Retrieved from https://hbswk.hbs.edu/archive/turning-on-the-tap-is-water-the-next-oil

Bibliography

USDA (United States Department of Agriculture). 2018. Biopreferred product. Retrieved from https://biopreferred.gov/BioPreferred/faces/catalog/Catalog.xhtml

Proceedings of Mine Water Solutions 2018
June 12–15, 2018, Vancouver, Canada
Published by the University of British Columbia, 2018

Estimating the Wetting Time for Mine Waste Rock Piles

Mark Steinepreis, Stantec Consulting Ltd., Canada

Abstract

Waste rock pile seepage effluent is typically of low quality, and the timing of infiltration breakthrough has potential implications to site-wide water balances and costs associated with water management infrastructure such as effluent treatment plants. Flow through waste rock piles consists of surface runoff and infiltration into the body of the pile, and estimating the resulting flow beneath the pile is a challenging component of site-wide water balances. Runoff coefficients are often used to estimate the percentage precipitation that will be surficial and sub-surficial flow; however, waste rock piles will typically go through a period of "wetting-up" prior to breakthrough across the basal area of the pile. This wetting-up process typically takes many years, and occurs as infiltration is initially stored within the pore space of the material. Steady state flow will occur once the infiltration and the unsaturated hydraulic conductivity profile of the material reach an equilibrium.

As water balances are required during feasibility and environmental assessment phases, site-specific data are sometimes not available. Unsaturated flow modeling is required to estimate the "wetting-up" times, and input parameters include soil moisture characteristic curves and unsaturated hydraulic conductivity functions. Material models have been estimated by others for waste rock piles, and the variability of both has been observed, even within the same site. This paper presents a method of estimating the wetting time of a waste rock pile using 2-dimensional unsaturated flow analyses for a feasibility study for a prospective gold-producing mine in Manitoba, Canada, with limited available material properties.

This work indicates that 2-dimensional analyses are useful to estimate the timeframe for pile wetting up; however, early models will need to be confirmed using site-specific unsaturated hydraulic conductivity parameters for the waste rock. These models can be obtained from particle size distribution data, when available. Photographic procedures for estimating particle size distribution of waste rock have recently been proposed, and may be useful where laboratory testing is not available or not practical.

Introduction

The feasibility study is a critical step of a mining project that provides the engineering and economic

appraisal of the commercial viability for the project. Among the many components of assessing the capital and sustaining cost of a new mining project, developing the water balance for the project early on is becoming the norm due to the scarcity of water supply and the importance of managing the environmental impacts to existing surface and groundwater resources. However; site-specific data is usually limited at the feasibility stage, particularly for the future large volume of waste rock and overburden that is generated during the life cycle of the mine. This paper presents a method using a 2-dimensional unsaturated flow analyses to estimate the wetting time of waste rock piles based on published material parameter models, as an alternative to using other assumptions such as runoff coefficients to estimate flows.

Water flow through waste rock piles is a major source of metals and sulphate to the hydrosphere (Molson et al., 2005), and is an important component of the site-wide water balance. Predicting water flow through a pile is difficult due to the heterogeneous nature of waste rock. The hydrogeological properties of the waste rock are affected by the rock type, blasting patterns, and method of placement (Amos et al., 2015). These challenges complicate the pursuit of standard procedures that could apply to all mining operations.

Waste rock pile flow simulations have been performed for this study due to a project requirement to produce a mine wide water balance for a prospective gold-producing mine in northern Manitoba, Canada. The study was carried out during the feasibility stage and predates the availability of waste rock material on site for characterization. Simulations have therefore been performed using published hydrogeological properties of waste rock from other gold-producing operations in North America.

Site Description

The host rock for mineralization at the mine is a metallotect consisting of picritic flows, iron formation and felsic volcanic rocks. Regionally, principal rock types include rhyolite, overlain by andesite and sedimentary rocks, and an upper unit of basaltic rocks.

Average minimum monthly temperature for this area of Northern Manitoba during 1981 to 2010 was –29°C for January, and the average maximum was 22°C for June. The mean annual air temperature is –3.2°C, and the average monthly temperature is normally above freezing from May to September. The annual total precipitation for the region is 478 mm, with 33% occurring as snow and 66% as rain.

Hydrogeological Properties of Waste Rock

Waste rock typically comprises the entire spectrum of grain sizes, from clay to boulder size (Amos et al., 2015). However, the particle size distribution (PSD) of waste rock can differ markedly between different sites and even within the same site. The hydrogeological properties of the material are affected by the

PSD, and it is generally accepted that the two main pathways for water flow within a waste rock pile are gravity driven flow through large pore space (macropores) and capillary driven flow through matrix materials that are present around and between cobbles and boulders (Smith and Beckie, 2003; Nichol et al., 2005). Matrix material is the fraction that is less than 5 mm in size, as larger particles demonstrate little capillarity (Fretz et al., 2011).

A literature search was carried out to obtain the properties of waste rock for similar operations. The University of Waterloo in Ontario, Canada, has carried out numerous studies on the hydrogeology properties of the waste rock piles at the Diavik Diamond Mine and the Detour Gold Mine. Soil water content curves (SWCC) were developed for the matrix (<4.75 mm) fraction of waste rock samples from a historical pile at Detour (Cash, 2014). In lieu of site-specific data, these SWCCs have been assumed to be applicable to the matrix of the waste material for the Northern Manitoba mine. The projects are both located in northern Canada and are gold-producing operations; however, it cannot be known at this time whether the waste rock will have similar characteristics.

Waste rock is typically placed dry, and the bulk of the pile remains unsaturated in the long term (Mine Environment Neutral Drainage, 1995). Flow within unsaturated waste rock has been described as counter-intuitive (Swanson, 1999), in that flow through the matrix may be dominant over macropore flow under normal climactic conditions. Macropore flow may dominate after intense rainfall events (Herasymuik et al., 2006).

Macropore flow would typically be rapid, and therefore be of a better quality than matrix flow, due to the reduced contact time with the waste particles (Neuner et al., 2013). It would add conservativism with respect to the water quality component of the water balance model to assume that a proportion of total flow is matrix flow; however, an allowance for some macropore flow is also pertinent to include conservativism in basal seepage flows that may need to be managed downstream and may increase dewatering volumes from the pit.

The dry waste rock will have storage capacity, and a period of matrix wetting up will occur before there is breakthrough of flow into the subsurface from the base of the pile. The wetting front is defined as the horizontal plane at which there is an increase in water content over placement content (Trinchero et al., 2011). Another front occurs when the hydraulic conductivity and the infiltration rate reach an equilibrium, which will travel slower than the wetting front. This front is referred to here as the *equilibrium front*. Pile wetting is complete when the equilibrium front reaches the base of the pile, and infiltration at the crest is equal to basal outflow.

The mean SWCC curve from the upper porosity range (>0.3) of matrix samples in Cash (2014) were selected for simulation. The unsaturated hydraulic conductivity curve was calculated from the input SWCC using SEEP/W®, part of the Geostudio suite of software, which uses van Genuchten (1980)

theory for this purpose. Figure 1 presents the mean SWCC curves and the calculated unsaturated hydraulic curve that were input for the waste rock in the simulations.

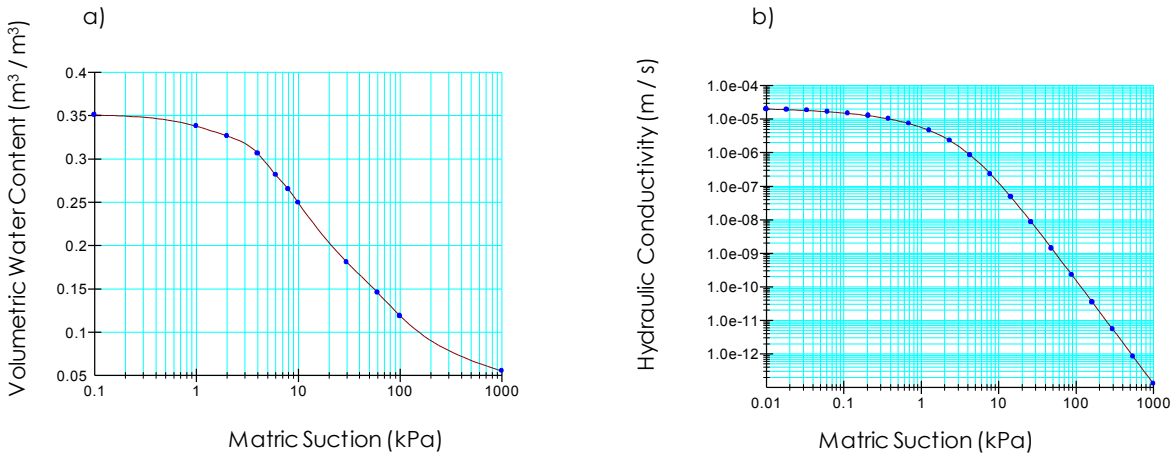


Figure 1: a) Soil water content curve (Cash, 2014) and b) unsaturated hydraulic conductivity curve used for the simulated waste rock pile

Numerical Modelling

For the purpose of simulation and based on the mine plan, it has been assumed that the pile will be constructed in 12 m lifts, and that each lift will take 2 years to construct. The entire lift height was "placed" instantaneously, and wetting of that lift progressed until the following lift was placed (instantaneously) on top. In lieu of site-specific information, it was assumed that 50% of the net precipitation travels through the pile rapidly through macropore flow, and that the remainder is available to wet up the matrix.

Simulations were performed on a 2-dimensional column of waste rock using SEEP/W®. Flow out the sides was not allowed, and a free draining condition was included at the base of the model. Waste rock is typically placed dry, below 0.06 m^3/m^3 (Mine Environment Neutral Drainage, 1995), and the initial condition (placement moisture content) within the model was assigned accordingly.

The flow boundary condition on the crest of the geometry was net annual average precipitation, minus (–) evaporation, and the 50% proportion that is assume to flow rapidly through the macropores. Separate analyses were performed in VADOSE/W, also part of the Geostudio suite of software, to estimate evaporation losses. Available data from the Government of Canada have been used as model inputs. As a result of the analyses, average annual evaporation was determined to be approximately 30% of the estimated precipitation.

Figures 2 and 3 represent the SEEP/W® outputs for the progression of the wetting and equilibrium fronts over the 6 years of deposition and an additional 20 years thereof; the equilibrium front is indicated

by the VMC = 0.16 contour. The wetting front progressed 4.0 m by the end of the 2 years for the first lift, and the equilibrium front progressed 2.2 m (Figure 2a). The progression of this wetting front was halted by the action of placing the second lift, and the pore water spread out vertically upwards and downwards due to capillary action (Figure 2b).

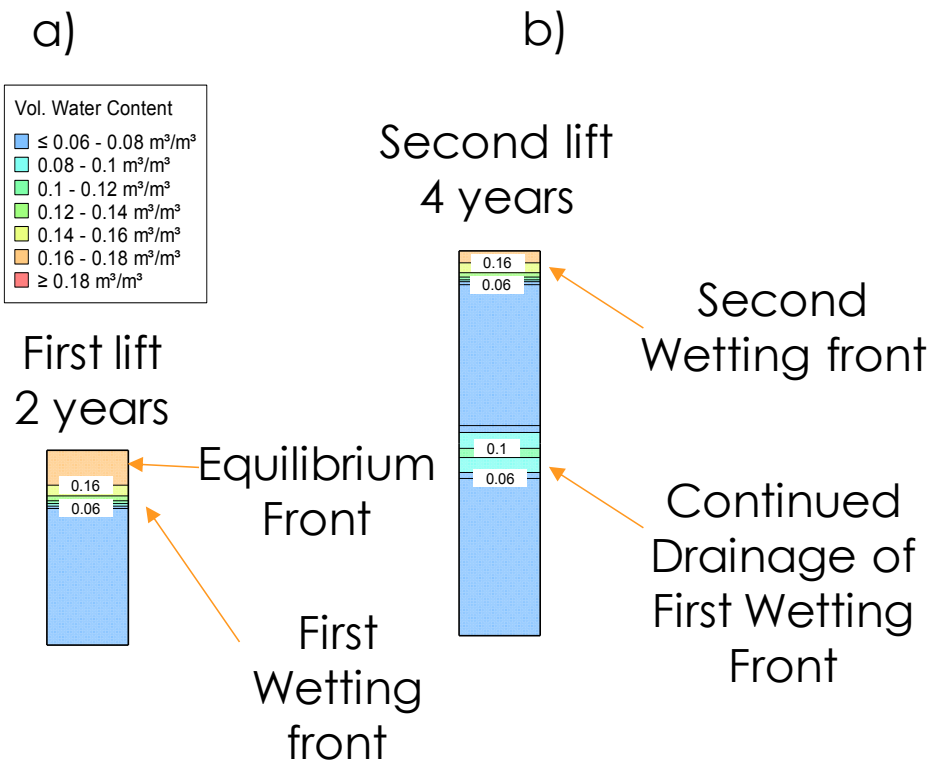


Figure 2: Progression of the wetting front in the simulated waste rock after a) 2 years, just prior to placement of the second lift and b) 4 years, just prior to placement of the third lift

The wetting fronts eventually converge with those from earlier lifts (Figure 3a), and the speed of progression at this time increases due to the locally higher moisture content (and therefore higher hydraulic conductivity), than the placement value. Full wetting up of the modelled column of waste rock matrix required 26 years (Figure 3b). A flush of metals and sulphate could be expected to enter the subsurface at this time. For comparison, it took more than a year for water to daylight into the sample collection system in a Diavik test waste rock plot at a depth of 1.7 m (Neuner et al., 2013). The timeframe of years is therefore plausible.

It is recognized that the lack of site-specific data to use as model inputs is a limitation to the simulations described in this paper. Results are sensitive to blasting and deposition technique, pile geometry, and climate

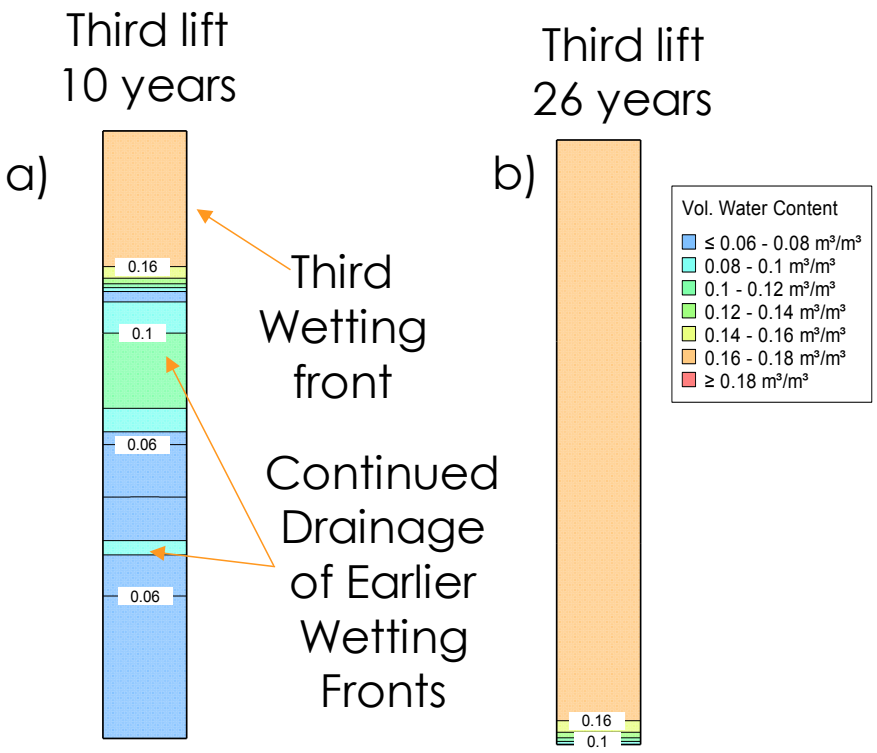


Figure 3: Progression of the wetting front in the simulated waste rock after a) 10 years, 4 years after placement of the third lift b) 26 years, at completion of wetting

Discussion

The simulations discussed in this paper were carried out as part of a mine water balance study at the feasibility (early) stage of the project. Site-specific data for the hydrogeological properties of the waste rock was not yet available at the time, and properties were assumed from literature values.

The results of the simulations indicate that it may take approximately 25 years to wet-up the matrix of the waste rock pile under the modelled conditions. Flow into the subsurface may occur sooner due to macropore flow; however, the quality is expected to be better than the water that seeps from the matrix. The simulated wet-up time is longer than the anticipated mine life by 20 years, indicating that routine water quality monitoring during operations may not encounter conditions that occur well after operations have ceased. The potential for later effects on groundwater and surface water will have implications in mine closure planning.

A clear companion to the current study is in the comparison of the estimated wetting front propagation times to performance in the field. The first step would be to obtain site-specific SWCC and unsaturated-k curves for the matrix within the waste rock, and modifying the predictive simulations as necessary. Installation of lysimeters and the use of test plots are recommended. Ongoing monitoring of

wells around the pile and the mine site as a whole may provide insight as to whether breakthrough of the equilibrium front has occurred.

It would also be pertinent to consider SWCC and unsat-k curves for the waste rock as a whole, such as considered by Martin et al. (2004), and compare simulation results to performance in the field. SWCC and unsaturated hydraulic conductivity curves for the waste rock will have to be prepared from particle size distribution data using van Genuchten (1980) or Fredlund and Xing (1994) fitting procedures. Techniques using photography have recently been proposed to estimate the particle size distribution of waste rock materials through the studies at Detour (Cash, 2014).

Conclusions

Simulations for the wetting up period of a column of waste rock were performed. The following conclusions are noted.

- Flow of precipitous water through waste rock piles is an important component on mine site water balances, yet no universal procedure for simulating and predicting the flows currently exists.
- Flow may be matrix or macropore dominated; however, an allowance for both sources of flow is pertinent depending on the desired nature of conservatism in the model.
- A slug of metals and sulphate would be expected when the matrix material has completely wetted up. The timing of this event is important for considerations such as the requirements for closure planning.
- The predicted time for breakthrough of matrix flow through the base of the specific pile evaluated has been predicted to be after 26 years, or approximately 20 years after cessation of operations.
- Macropore flow may enter the subsurface earlier; however, the quality of this water is expected to be better than the matrix flow due to a shorter contact time.
- Additional study is required to match simulations to field based observations.

Acknowledgements

The author would like to acknowledge the support of Aileen Cash for permission to display the results of her thesis work.

References

Amos, R.T., Blowes, D.W., Bailey, B.L., Sego, D.C., Smith, L. and Ritchie, A.I.M. 2015. Waste-rock hydrogeology and geochemistry, *Applied Geochemistry,* 57: 140–156.

Cash, A. 2014. Structural and hydrologic characterization of two historic waste rock piles. M.Sc. thesis, Department of Civil and Environmental Engineering, University of Alberta, Edmonton, Alberta.

Fredlund, D. and Xing, A. 1994. Equations for the soil-water characteristic curve, *Canadian Geotechnical Journal,* 31: 521–532.

Fretz, N., Momeyer, S., Neuner, M., Smith, L., Blowes, D., Sego, D. and Amos, R. 2011. Diavik waste rock project: Unsaturated water flow. In *Proceedings Tailings and Mine Waste*, Vancouver, Canada, 6–9 November, 2011.

Geoslope International Ltd. 2017. SEEP/W, Version 8.16.2.14053. Computer software. Calgary, Alberta, Canada.

Herasymuik, G., Azam, S., Wilson, G.W., Barbour, L.S. and Nichol, C. 2006. *Hydrogeological Characterization of an Unsaturated Waste Rock Dump. Sea to Sky Geotechnique.* Vancouver, Canada: CGC.

Martin, V., Aubertin, M., Bussière, B. and Chapuis, R.P. 2004. Evaluation of Unsaturated Flow in Mine Waste Rock. 57th Canadian Geotechnical Conference and the 5th joint CGS-IAH Conference, Canadian Geotechnical Society, 24–27 October 2004, Quebec City.

Mine Environment Neutral Drainage (MEND). 1995. Hydrogeology of waste rock dumps: MEND Associate Project PA-1. Retrieved from http://mend-nedem.org/wp-content/uploads/2013/01/1.Associate-Project-PA-1.pdf

Molson, J., Fala, O., Aubertin, M. and Bussière, B. 2005. Numerical simulations of pyrite oxidation and acid mine drainage in unsaturated waste rock piles, *Journal of Contaminant Hydrology,* 78(4): 343–371.

Neuner, M., Smith, L., Blowes, D.W., Sego, D.C., Smith, L.J.D., Fretz, N. and Gupton, M. 2013. The Diavik Waste Rock Project: Water flow through mine waste rock in a permafrost terrain, *Applied Geochemistry,* 36: 222–233.

Nichol, C., Smith, L., and Beckie, R. 2005. Field-scale experiments of unsaturated flow and solute transport in a heterogeneous porous medium, *Water Resources Research,* 41(W05018).

Smith, L. and Beckie, R. 2003. Hydrologic and geochemical transport processes in mine waste rock. In J.L. Jambor, D.W. Blowes and A.I.M Ritchie (eds), *Environmental Aspects of Mine Waste*: 51–72. Vancouver, BC: Mineralogical Association of Canada.

Swanson D.A. and O'Kane, M. 1999. Application of unsaturated zone hydrology at waste rock facilities: design of soil covers and prediction of seepage, *Proceedings America Society of Mining and Reclamation*, 1999: 517–526.

Trinchero, P., Beckie, R., Sanchez-Vila, X. and Nichol, C. 2011. Assessing preferential flow through an unsaturated waste rock pile using spectral analysis, *Water Resources Research,* 47, W07532, doi:10.1029/2010WR010163.

van Genuchten, M. Th. 1980. A closed-form equation for predicting the hydraulic conductivity of unsaturated soils, *Soil Science Society of America Journal,* 44: 892–898.

Proceedings of Mine Water Solutions 2018
June 12–15, 2018, Vancouver, Canada
Published by the University of British Columbia, 2018

3D Deposition and Water Balance Modelling with Muk3D and GoldSim

Carlo Cooper, MineBridge Software Inc., Canada
Jaco Grobler, Consultant, Chile
Miguel Palape Reyes, MineBridge Software S/A, Chile

Abstract

GoldSim is a widely used simulation package that is frequently used in the modelling of water balances for mine sites and Tailings Storage Facilities (TSF). One limitation of GoldSim is that TSFs can only be represented as 2D structures using the available GoldSim modelling tools.

Currently, water balance models of the TSF pond assume a constant tailings storage shape, notably a conical shape or the stage-area-volume curve of the last survey. They can also be comprised of a set of stage-storage curves for the pond and tailings that are based on deterministic modelling. This is then applied to a long duration model. The result is that elevations and volumes predicted by the TSF model may not be accurate, and they may not always be relied on as a realistic prediction.

Muk3D is a 3D modelling tool that simulates the filling of TSF's based on the geometric representation of tailings behaviour. As tailings surfaces are formed within the model, the interaction with the pond and the underlying topography is simulated, leading to more realistic deposition surfaces that can better predict TSF behaviour than 2D models. Muk3D does not include a water balance component in its modelling toolkit, and so has always relied on the user entering relevant data about the behaviour of the pond when developing tailings plans.

This paper discusses how GoldSim and Muk3D have been integrated allowing for 3D tailings deposition to be incorporated into an existing water balance model. The difference in results between the 2D models for a TSF used in GoldSim and the same models run using a 3D deposition model are explored, and advantages and limitations of this approach are discussed.

Introduction

No mine has a neutral water balance over its life. Understanding which case a mine falls into at a given point in its life, and how it impacts the operation, is done with a Site Wide Water Balance (SWWB). This is a numerical model that is aimed at understanding the net inflows and outflows of water into the entire

mine site, and determining either the deficit (and make-up water required) or the surplus (and volume of water that must be released). Depending on the location, the costs for make-up water or water treatment can be significant. Mines that have a water deficit need to introduce fresh water to the operation (river, groundwater, ocean). Mines that have a water surplus need to either store it or release (and potentially treat) it.

The water balance needs to incorporate all water sources and sinks on the site, as well as capturing how water is moving between different elements of the site. These elements include the mine, the waste dumps, the process plant, the TSF, and any water storage structures.

For the TSF, the water balance serves several important functions. A principle goal is to predict the volume of water that will need to be stored in the TSF over its life. This volume affects the pond elevations, the beach formation, and the rate of rise of the perimeter dykes, and ultimately can influence the constructability and geotechnical stability of the dams.

Representing a TSF in a water balance can be challenging. The primary tools that are used for building water balances are not very good at simulating 3D structures, and instead the TSF's are represented as very simple 2D models. These 2D models are not good at capturing the behaviour of the TSF, and so some of the information generated from such models cannot always be taken to be a reliable prediction.

This paper will demonstrate why these 2D models are not an adequate representation and propose an alternative that incorporates 3D modelling of the TSF using Muk3D.

Tools for Developing Water Balances

Regardless of the tool used to create the water balance model, the aims are the same. On a macro scale, the water inflows and outflows from the mine site are considered. Global inflows comprise two main components – water that enters the system that we have no control over (e.g. rainfall, snowmelt, dewatering) and water that can be controlled (make-up water pumped from the river, ground water, ocean, or other source). Global outflows are losses that are uncontrolled (seepage, evaporation) and those that can be controlled (release, treat, and release).

Two common tools used to develop water balances are Microsoft Excel and GoldSim. Excel is a widely used tool given its accessibility and ubiquitous use throughout the engineering world. The other tool that is commonly used is GoldSim software (version 12), developed by the GoldSim Technology Group LLC. GoldSim is a probabilistic simulation and modelling software package that has been extensively used for the development of graphically-oriented models with developed logic for networks, including pit lake water balances.

The model operates at a daily time step and is used to predict the TSF pond water level and volume. The volumes of these ponds are driven by rainfall, evaporation, and TSF deposition. A model is created by connecting basic elements that perform logical or mathematical functions and ultimately allow for the simulation of a complex process. Once a model has been built, probability distributions can be assigned to input data, allowing for stochastic modelling to be undertaken. Instead of providing a deterministic result, stochastic modelling provides a range of output values that can then be used to understand probabilistic outcomes, including the most likely/worst outcomes.

Simulating TSFs in GoldSim

GoldSim models are constructed by connecting processing elements that perform basic calculations, an example of which is shown in Figure 1. TSFs are generally represented as a reservoir, which is a modelling element that keeps track of inflows and outflows of solids and water. Lookup tables are then used to take the volumes in the reservoir (tailings and water) and predict elevations (pond and beach), and pond surface areas.

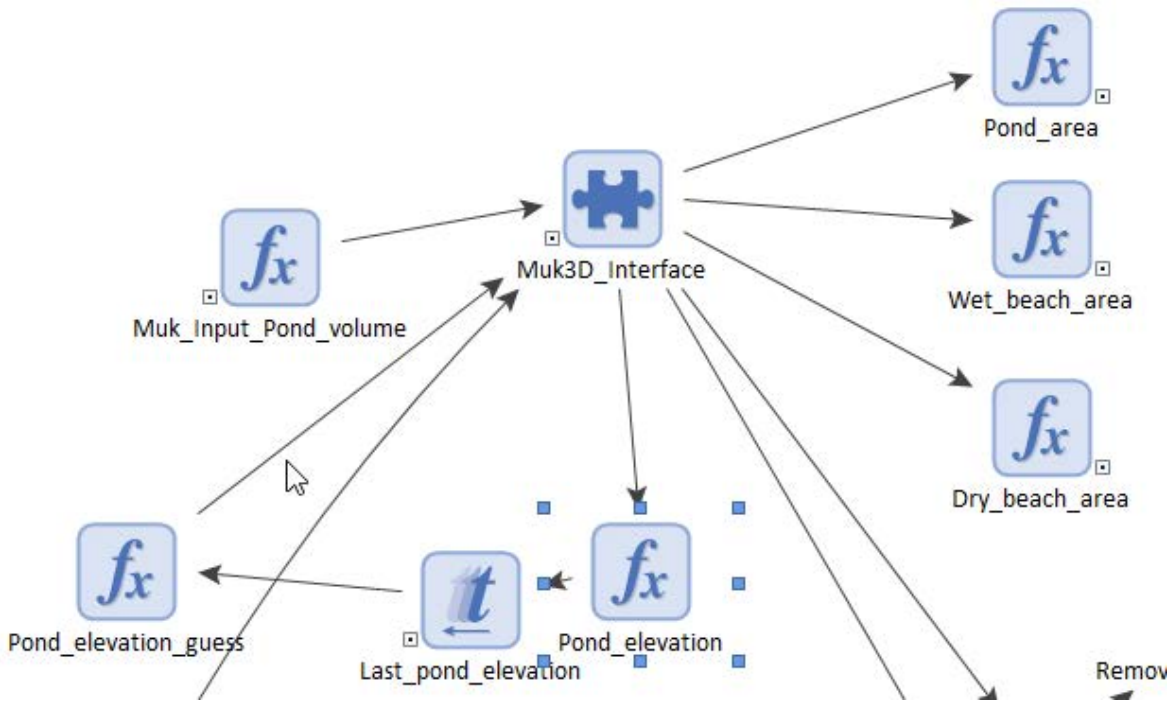


Figure 1: GoldSim elements connect to create a model

The main challenge with simulating a TSF accurately in GoldSim is that it is virtually impossible to model the 3D shape of a 3D phenomenon in 2D, and model how this evolves over time, for all but the simplest configurations. (The 2D model inherent assumption in the absence of 3D information.) As

tailings are poured into a TSF, the geometry of the TSF changes as the beaches are formed. The way the beaches build up is influenced by the pond elevations. The pond elevation depends on the beach formation and how much tailings are deposited below vs. above water, among other things. Thus, trying to model this over time and in 2-dimensions with storage curves and lookup tables is not a simple task.

The TSF geometry affects the pond area, which in turn affects the pond volume through augmentation in areal evaporation, rainfall, and runoff. If the evolution of the TSF geometry cannot be modelled accurately, then outputs from the water balance model that depend on pond and beach elevations, pond depths, and pond areas must be validated against 3-dimensional modelling to assess their accuracy.

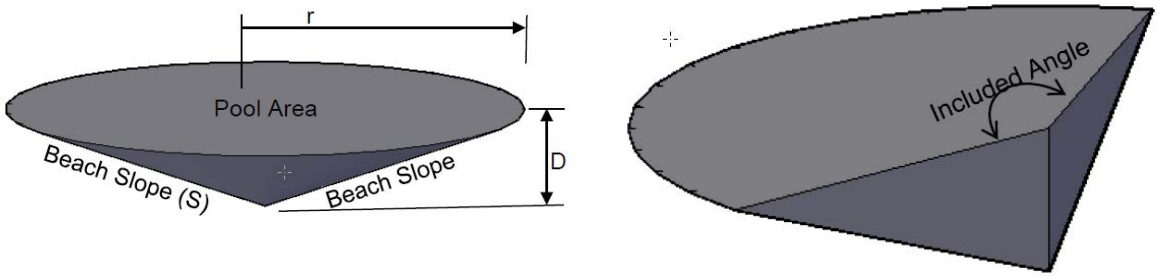
There have been some approaches that people have tried to improve the simulation of a TSF using the elements that are available in GoldSim. Hoekstra (2017) discusses three methods that simulate the TSF as an inverted cone (one considers the pond to be a cone, while one of the others is a wedged version of the cone), and the use of 2D lookup tables that attempt to add a time component into the lookup process.

The approaches discussed in this paper are for the modelling of "conventional" TSFs that have beached tailings with water going to a pond. This could cover cross-valley, ring dykes, or in-pit disposal systems. This approach would not be suitable in its current form for paste and thickened tailings deposits (e.g., down-valley discharge or central thickened discharge).

It is also important to note that these simplified modelling approaches neglect to account for the 3D shape of the tailings beach. The GoldSim-only model cannot properly account for the change in beach slope at the pond elevation, and instead assumes that the beach is uniform above and below water. This is seen as a significant limitation to modelling TSFs in a realistic way. This is the limitation the integration of a 3D deposition model is aimed at fixing.

Inverted Cone Approach

This method of modelling the TSF involves treating it as an inverted cone that is gradually filled up. Figure 2 shows schematics of the two conical models. A uniform beach slope above and below water is assumed. By using basic geometric calculations, it is possible to predict depths, areas, and pond elevations, based on the volume of the tailings in the beach, and the volume of water in the pond. The inverted cone would be applied to the situation where the pond is centralized in the TSF, while the wedged inverted cone is more applicable to cases where the dam is against a dam. This is combined with the fill-elevation curves for the empty TSF, the assumed beach slope, and area-volume lookup tables.



(a) Inverted cone (b) Wedged inverted cone

Figure 2: Schematics showing the cone models

The immediate problem with this model is that it relies on a uniform beach slope, which is generally not the case in operating TSFs. Thus, elevations, depths, and areas from this approach will not be accurate. The other problem is the assumption that the pond is conical/circular. Again, most TSFs do not have a pond configuration that mimics this. For example, in square paddocks, the pond might be better represented as an inverted pyramid.

Storage Elevation Curves (Tabular Method)

Storage curves are developed for different phases of the TSF life. Hoekstra (2017) and Donnelly (2017) have shown how interpolation between these curves can be done, and believe that it offers a more robust approach to modelling the TSF geometry over time. The idea behind this approach is that the storage elevation curves for the pond evolve over time to reflect the filling of the TSF. During calculations, intermediate storage elevation curves for the pond are interpolated based on the deposited volume of tailings, and these are used for predicting tailings and pond elevations, and pond areas.

Since the method uses storage elevation curves generated from 3D modelling, it has the advantage that the deposition could be done using realistic beach slopes above and below water. This would be fine for doing purely deterministic analysis (e.g., the pond has specific volumes over time, perhaps dictated by operational requirements); however once the inputs that would be used to generate the storage curves (different deposition configuration, different pond volumes, different beach slopes) are added, the pre-generated storage elevation curves become invalidated and the model may no longer predict elevations accurately.

Other Options

Coding a 3D TSF deposition module using the script element in GoldSim may be possible, but it is difficult and requires knowledge and experience in TSF deposition model development and coding in GoldSim. However, using the basic GoldSim calculation elements, there are few other options for

creating accurate 3D models for the TSF over time. The models discussed above might give acceptable answers for simple TSF configurations, or might be adequate in water balance models where the 3D behaviour of the TSF does not have a significant impact on the system (e.g., for site-wide water balances where the TSF makes up a small component of the overall system).

GoldSim does provide an element that allows interaction with Dynamic Link Libraries (DLLs). This is code that is compiled and allows for execution of numerical calculations outside of GoldSim. The use of this is explored in the following sections.

Modelling TSF with Muk3D

Muk3D is a 3D CAD tool that is specialized for the design and modelling of TSFs. It is a geometric model that allows tailings beaches to be created using assumed beach slope profiles.

One of the limitations of Muk3D is that it does not have a water balance model built into it, and so as a designer is running through a deposition plan they need to manually extract relevant data from the mass and water balance model (target pond volumes, deposited volume of tailings) to incorporate into the 3D model. Results of the deposition modelling (beach elevations, pond elevations and areas, beach areas, and storage elevation curves for the resulting basin, for example) are then entered back into the water balance model to improve the accuracy of subsequent calculations.

Comparison of GoldSim Pond Models with Muk3D Predictions

To compare some of the GoldSim based TSF models with Muk3D, a model from the GoldSim library was used (GoldSim, 2017b). This is a model prepared for a GoldSim web-based seminar that compares the conical, conical with wedge, and tabular approaches. The comparison with Muk3D was done by exporting tailings and pond volumes to a CSV and using this to drive an automated Muk3D model to deposit the target tailings volume with the target pond volume.

Circular Ring Dyke

The first scenario being considered is one that most closely resembles the conical shaped TSF pond models: a circular ring dyke with a centrally located pond. In this hypothetical example, the ring dyke is located on slightly sloping ground, so for at least some of its early life there will not be full perimeter discharge, which would simulate the wedged cone scenario. Once tailings have been built up enough, it becomes the inverted cone model. Figure 3 shows the basic configuration for the facility.

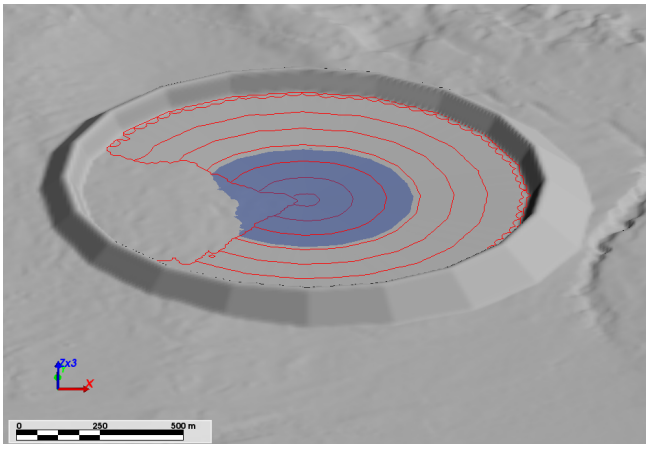
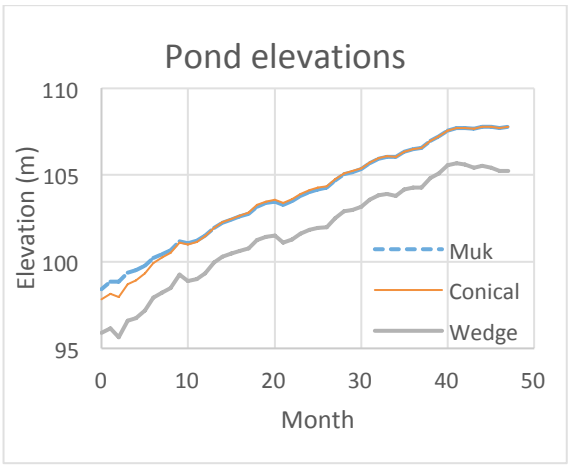


Figure 3: Basic configuration of the circular ring dyke model

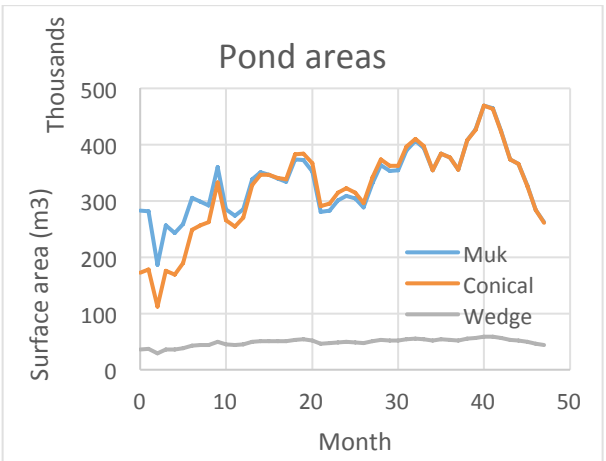
For this model, the same production volume of tailings and volume of pond water were applied to the GoldSim conical models and the Muk3D model. The GoldSim models were simulated daily, while the Muk3D model was run for the end of every month, for a 4-year period (48 runs). This was done out of practicality, since each Muk3D model takes between 20 seconds and 120 seconds to run.

In the Muk3D model, the tailings are assumed to have a uniform density and a uniform beach slope above and below water (1%). Muk3D was run to goal seek the beach elevation and pond elevation for the incremental volume of tailings and the end of month volume of water, respectively.

The predicted pond elevations and areas for the 3 models are shown in Figure 4.



(a) Pond elevations



(b) Pond areas

Figure 4: Results for conical modelling runs

We can see that in this scenario, the conical model closely matches the Muk3D pond elevation predictions. Once the model gets past Month 35, the Muk3D and conical elevation predictions are almost identical (the average difference between month 35 and month 48 is 1.6 mm). At month 35 the deposition

starts to approximate the cone being used, as illustrated in Figure 5. In earlier time steps, the basin geometry is not conical due to outcrops of original ground, and so the conical approximation is not a great model. The conical wedge model did a poor job of predicting pond elevation in this case. While it tracked the relative changes well, it was consistently off by around 2 m.

Comparison of pond areas shows similar agreement between the Muk3D and conical models, while the wedge model failed to give a reasonable approximation, as shown in Figure 4(b).

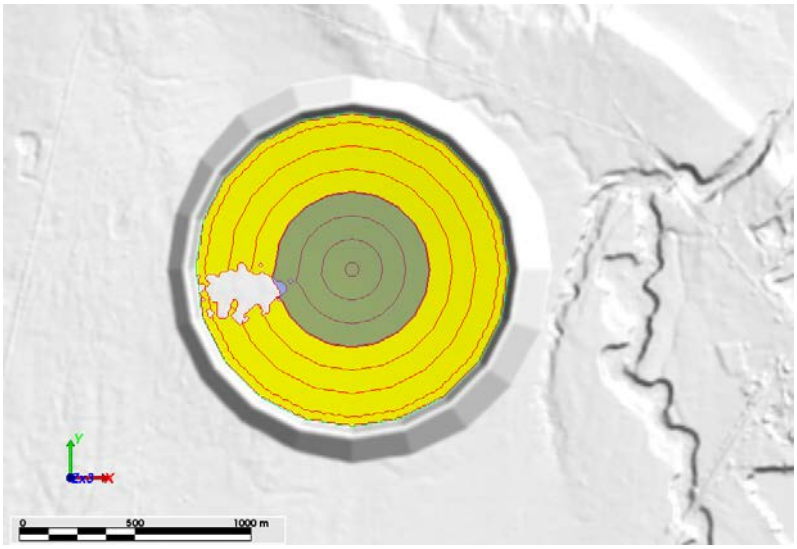
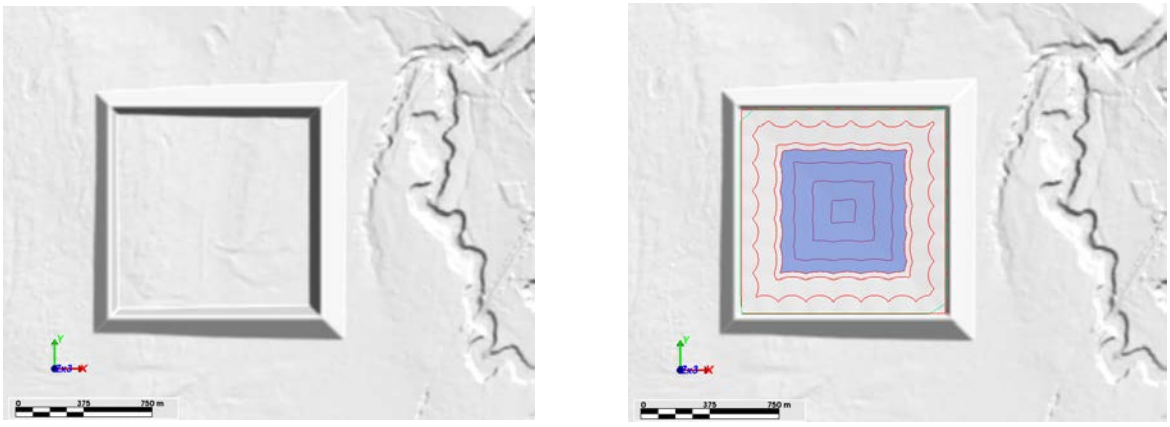


Figure 5: TSFF at month 35

Square Ring Dyke

To test the conical TSF models for a different dam geometry, a square ring dyke was created and filled with tailings and water, using the same assumptions for the conical model discussed above. The configuration is shown in Figure 6.



(a) Empty TSF (b) Full TSF

Figure 6: Square ring dyke model empty and with some tailings deposited

A comparison with the tabular approach was also undertaken for this configuration. Storage-elevation-area curve data was generated for five points in the life of the structure (no tailings, and tailings at four different elevations).

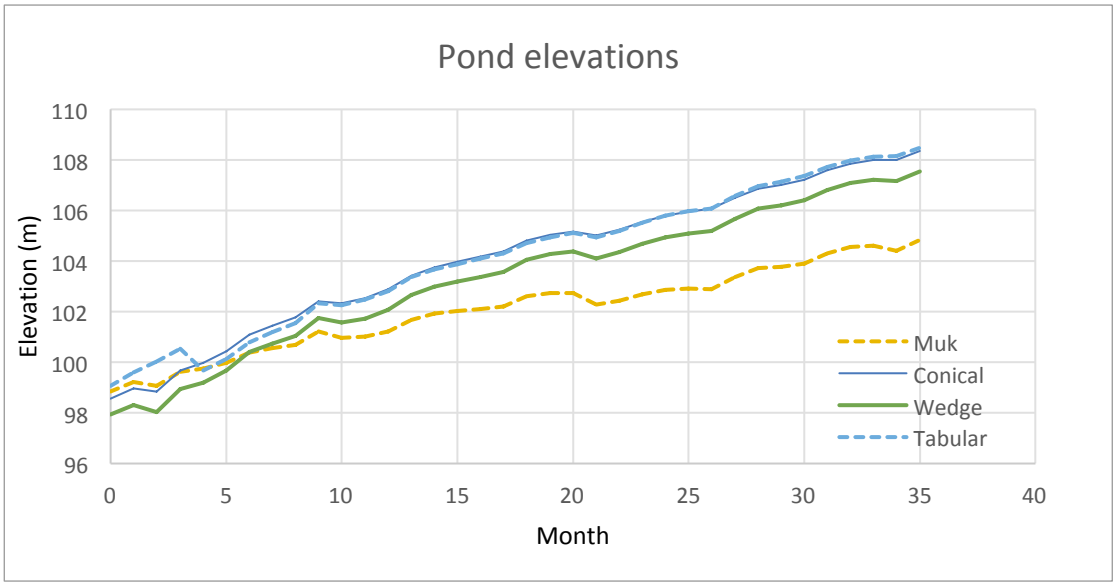


Figure 7: Pond elevation predictions for a square ring dyke

The results presented in Figure 7 show that the conical model does not accurately track the elevations, compared to the 3D deposition modelling. The tabular method results were very close to those of the conical model.

If the conical model was adapted to an inverted pyramid, then it is possible that it would provide a better prediction of pond elevations, especially once a full inverted pyramid shape is formed by the beaches (i.e. the tailings deposit is high enough that all original ground has been inundated). For an equivalent dimensioned pyramid vs. a cone (where diameter of the cone is equal to the side length of a pyramid), the cone has 78% of the volume of the pyramid. The smaller volume means that higher elevations will be reported for the conical model of a given volume of tailings and water.

Issues with Simplified Models of TSFs and Ponds

All the examples that have been considered here use a uniform beach slope, regardless of whether the beach is above or below water. In practice, it is probable that the beaches will have different slopes above and below water. For operating TSFs, where beach profiles can be measured, it is likely that the beach slopes are non-linear. This adds a further level of complication to modelling. At a high level, these simplified models of ponds may be adequate for Site Wide Water Balances (where the overall flows of water are considered more important than predictions of elevations from the TSF); however, for the TSF planning work they are inadequate.

Models that are more focused on the behaviour of the TSF, where designers are trying to understand the behaviour of the structure in the short and long term, require a more detailed model. This is where the ability to model a pond in a more rigorous way using Muk3D provides an advantage.

While some of the shortcomings of the conical TSF models could be overcome using the method of interpolating storage Elevation curves, it must be remembered that these input curves are only applicable for a single operating scenario. If there is more or less water, more or less tailings, different beach slopes, different densities, etc., the storage elevation curves for a facility will change. The beaches will form a different shape, and so these inputs would change. From the point of running these simulations in GoldSim it negates the ability of GoldSim to run a range of scenarios, and have the model react appropriately to each of these runs.

Integration of Muk3D deposition models within GoldSim

In the examples shown above, the Muk3D modelling was done by exporting the tailings and pond volumes to a CSV and running the deposition models using a macro written to read the inputs from the CSV. GoldSim provides no direct program integration outside of Microsoft Excel, and some database formats, as a mechanism for reading and writing data. It does however have an element that allows linking to a Dynamic Link Library (DLL).

Using example DLL code published by GoldSim (2017b) that allowed for Python code to be executed (Python is also used by Muk3D for scripting), a custom DLL was developed that allowed GoldSim to send data to Muk3D, wait while Muk3D does some processing, and then receive results back. Currently Muk3D can accept any number of variables from GoldSim if they are either Scalar or Vector data types. Muk3D can return scalars and 1D lookup tables, currently.

When Muk3D receives information from GoldSim, it needs to know what to do with it. A script is written in Muk3D that performs a set of actions and returns the required data to GoldSim.

A Simple Example

A simple implementation of Muk3D/GoldSim linkage was done using the following configuration:

- Square ring dyke, as illustrated in Figure 7.
- The pond is driven by a target volume. In practice it would come from a water balance volume, but in this example, it comes from a Random Walk element, the same as in the GoldSim models run for comparing methods.
- Tailings volume comes from the mass balance model. In this example the tailings are being deposited at 8,000 m^3 of deposited tailings per day.
- The Muk3D model is run using a 28-day time step.

The GoldSim model used was after Hoekstra (2017), which was modified to include the Muk3D deposition as a module within GoldSim. This model is not a water balance but an illustrative example that has deterministic pond water and tailings volumes.

Setup within Muk3D

To set up a GoldSim link in Muk3D, the interface (GoldSim inputs and outputs) need to be defined. Python code was written to tell Muk3D what to do when data from GoldSim is received. In this case, it tells Muk3D to deposit a volume of tailings (GoldSim input) from some pre-specified locations, with a target pond volume. Muk3D will solve for beach elevation and pond elevation. Data returned from the model is:

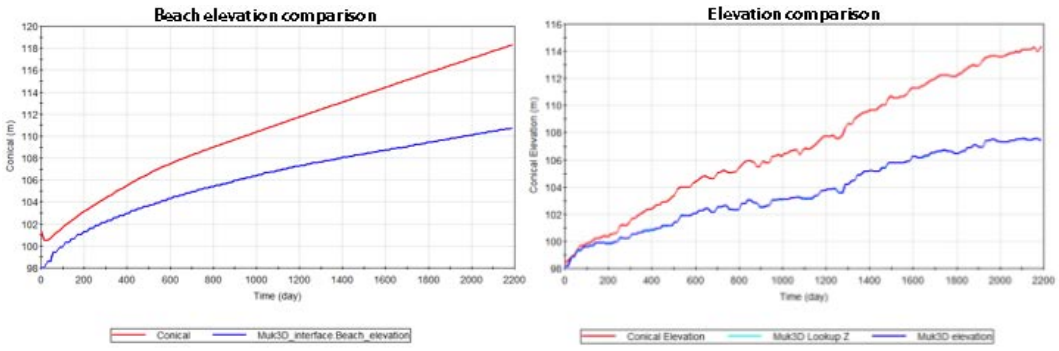
- Pond elevation;
- Beach elevation (maximum beach elevation);
- Pond depth;
- Storage elevation curve for the new pond (above the tailings surface).

Setup in GoldSim

Within GoldSim, the link to Muk3D is done by using a DLL element that links to the Muk3D DLL file, and defines a set of inputs and outputs. The inputs are the values that Muk3D needs to do "something" with. The outputs get fed back into the GoldSim model. The storage curve for the new basin geometry that was generated at the end of each Muk3D deposition run was used as the input to a 1D Lookup Table element in GoldSim, and the Muk3D pond elevations were checked by looking up the pond volume.

Results

The model was run for a 6-year period, with Muk3D deposition runs every 28 days. A summary of results for beach and pond elevations is shown in the graphs in Figure 8.



(a) Beach elevations (b) Pond elevations

Figure 8: Elevation predictions for conical and Muk3D model from GoldSim

The results are consistent with the examples shown in previous sections, which is to be expected. The difference is that these values were generated by GoldSim directly interacting with Muk3D. The pond elevations calculated from the volume-elevation curve returned from each Muk3D run are barely discernible on the graphs as they are coincident with the Muk3D elevations.

Limitations

Running a 3D deposition model does take a lot longer to get a result than using the simplified approaches covered in this paper, and so it is not feasible to do a daily simulation, over a long time period, incorporating the 3D deposition model. Muk3D uses a goal seeking approach to determine what a tailings surface looks like when it must deposit a given volume of tailings and hold a pond with a given volume of water.

To consider the shorter-term behaviour of the TSF would require additional logic in how tailings are deposited in the TSF. This example is pouring tailings around the entire perimeter, but when looking at very short time frames, that is not how the TSF is operated.

Future Work

Now that a reliable interface between Muk3D and GoldSim has been developed, the goal is to further test this linkage on more complicated projects. The examples used in this paper are trivial and do not reflect the range of operating philosophies, distribution systems, pond management strategies, or tailings profiles that would be encountered in practice.

The big opportunity that this modelling approach offers is the ability to run stochastic models, varying key parameters in the tailings deposition/water balance models, and starting to understand the impact that uncertainty has on the predicted behaviour of the TSF. Instead of running a single option, the opportunity to run a model with varying inputs (water volumes, tailings volumes, beach slopes, tailings densities, etc.) is possible. This provides the opportunity to better understand how a TSF reacts to different scenarios, or modelling inputs.

Conclusions

While GoldSim is a great tool for modelling TSF water balances, it lacks the ability to represent the evolution of 3D structures accurately. The application for the model and the type of structures being modelled may affect the results significantly.

Muk3D is a good tool for simulating TSFs, but it lacks the water balance component. By integrating the two pieces of software, the limitations that are imposed by each of them can be overcome and thus allows for more representative modelling of a TSF.

References

Donnelly, J. 2017. Dynamic simulation of a tailing storage facility. Retrieved from: https://support.goldsim.com/hc/en-us/articles/217994417-Dynamic-Simulation-of-a-Tailing-Storage-Facility. Accessed December 23, 2017.

GoldSim. 2017. Python DLL. Retrieved from: https://support.goldsim.com/hc/en-us/articles/215887887-Python-DLL. Last accessed December 2017.

GoldSim. 2017b. GoldSim Version 12. GoldSim Technology Group. Retrieved from: http://www.goldsim.com.

Hoekstra, D. 2017. Dynamically representing stage-storage-area relationships for tailings storage facilities. Retrieved from: https://support.goldsim.com/hc/en-us/articles/115009534607-June-Dynamically-Representing-Stage-Storage-Area-Relationships-for-Tailings-Storage-Facilities (Accessed December 3, 2017)

Proceedings of Mine Water Solutions 2018
June 12–15, 2018, Vancouver, Canada
Published by the University of British Columbia, 2018

Challenges in Containing Geochemical Risk at the Faro Mine Complex, Yukon

Dustin K. Rainey, Government of Yukon, Canada

Abstract

Beginning in 1969, three decades of open pit mining and milling of pyritic sulphides at the abandoned Faro lead-zinc-silver mine produced long-term geochemical risk in the form of 55 million tonnes of acid-generating tailings that are retained in a valley-fill impoundment. Geochemical risk from the tailings manifests not only as acid rock drainage that could progressively degrade receiving water quality over the course of years and decades, but also as low-probability, high-consequence events such as a flood-induced dam breach that would release geochemically reactive mine waste to the downstream environment. The Intermediate Dam, which is 650 m long and 32 m high, is the main geotechnical that ensures tailings and contact water do not migrate off site. Construction began in 1981, with the most recent raise completed in 1991, leaving a spillway that does not have the ability to pass a moderate or major flood without potentially overtopping and failing the dam. A project initiated in 2013 to design and implement an upgrade to the emergency spillway was unsuccessful because of insufficient integration between design and operations. The proposed spillway design eliminated critical storage capacity for contact water, increasing the likelihood of short-term environmental non-compliance.

Introduction

The Faro Mine Complex is located in subarctic Yukon, Canada, at 62°N latitude, with the tailings impoundment situated in the bottom of Rose Creek Valley (Figure 1). The tailings are therefore subject to seasonal weather extremes and freshet, whereby rapidly melting snowpack from a mountainous 200 km^2 catchment area introduces significant hydraulic risk to the impoundment. The tailings are highly pyritic and acid-generating, increasing the potential for leaching of metals such as zinc, lead, copper, iron, manganese, and cadmium. Their toxic nature was confirmed in 1975, when tailings were released to Rose Creek due to failure of a now decommissioned dam. In some areas of the floodplain where picking up small volumes of spilled tailings was considered infeasible, it took over 5 years for vegetation kill zones to develop. More than 40 years post-spill, little ecological regeneration is evident. Due to this long-term potential for downstream receiving environment degradation as a result of tailings loss, the Intermediate

Dam is the highest risk geotechnical structure at the Faro Mine Complex. A requirement for future site remediation is that the dam must be able to withstand a Probable Maximum Flood (PMF) event.

The Faro Mine Complex is in a state of care and maintenance while the remediation plan is being developed. To provide interim protection and risk reduction for the tailings impoundment until such time as a PMF design solution can be implemented, in 2013 the Faro Mine Remediation Project commissioned the design of an Intermediate Dam spillway upgrade to allow it to pass a 1-in-500-year return period flood event.

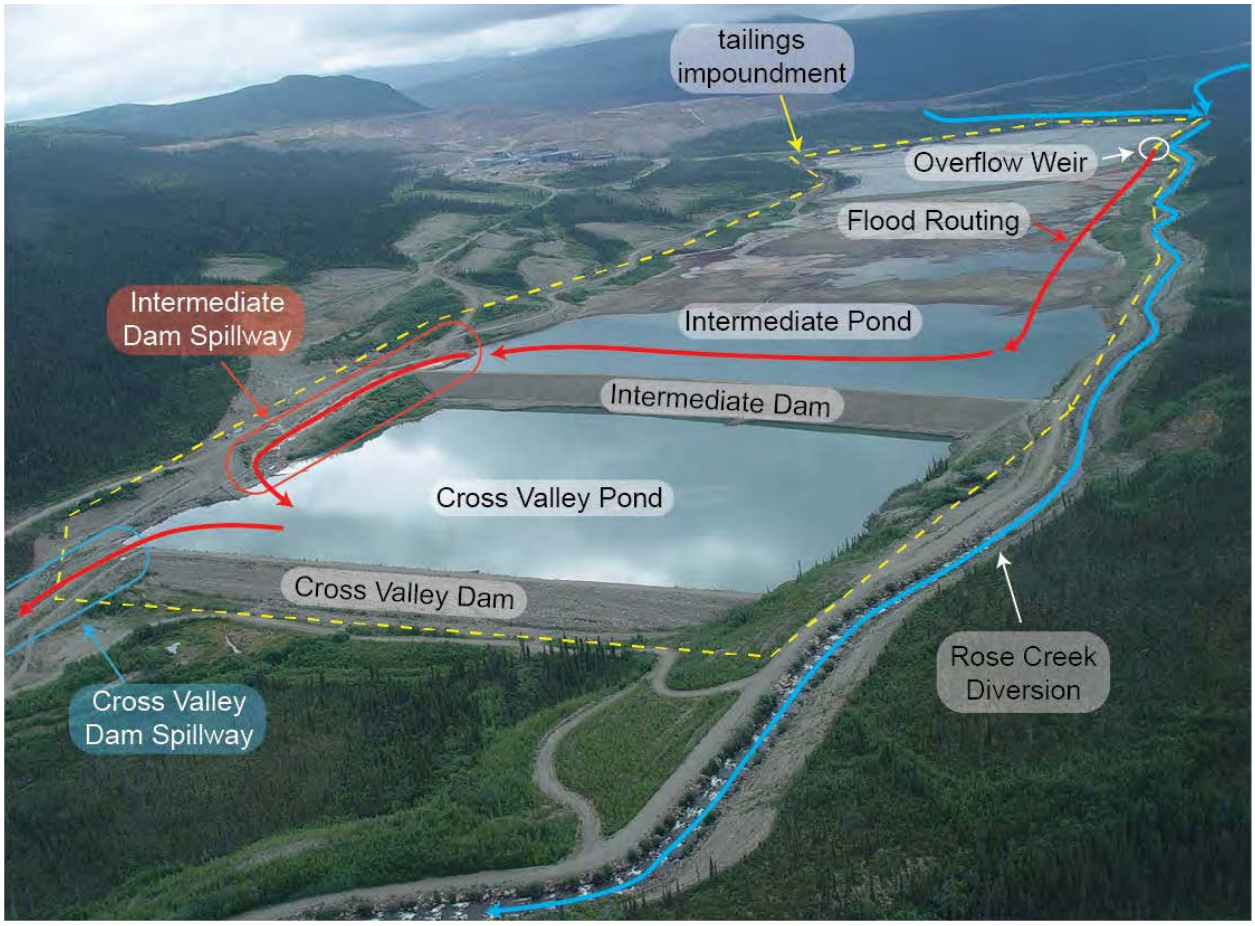


Figure 1: Overview of the tailings impoundment in the Rose Creek Valley, looking southeast

Flood Routing and Consequences

The Intermediate Dam is mainly protected by the 4.7 km-long Rose Creek Diversion (Figure 1). This diversion routes fresh water flows around the impoundment, and was originally designed to convey a 1-in-50-year return period flood event (estimated at 79 m^3/s). It was later modified to convey flows of 140 m^3/s, which is greater than the 1-in-500-year return period flood event. Un-engineered modifications and years of differential settlement of the dyke have created some sections of the diversion that were

estimated to have conveyance for less than a 1-in-50-year return period flood event. Therefore, blockage of the Rose Creek Diversion by any mechanism (e.g. backslope failure, icing) or flood flows exceeding the design capacity has the potential to cause non-contact water to enter the tailings impoundment. Not only would this contaminate non-contact water from the diversion, but excessive flows would overwhelm the Intermediate Dam emergency spillway capacity of 32 m^3/s, and potentially cause the dam to fail.

The most likely location where flood flows would enter the tailings impoundment is at an earthen overflow weir constructed at a low point in the dyke 800 m downstream of the start of the diversion (Figure 1). Flows in excess of the diversion capacity would enter the tailings impoundment through the overflow weir and report to the Intermediate Pond, which is an acidic, metal-contaminated body of water retained by the Intermediate Dam. The pond behind the dam might provide some flood attenuation capacity prior to flows entering the spillway; however, a flood event of this magnitude is most likely to happen in spring or early summer, when extra pond storage capacity is limited because of ongoing winter inflow. In order to create adequate storage capacity for winter inputs to the pond, summer pumping is used to partially dewater the pond and direct the water to a treatment plant prior to discharge to the environment. The pond has a total capacity of 1.47 million m^3, and is typically 60% to 80% full in spring, when pumping is initiated. Installed summer pumping capacity of 126 L/s is insufficient to allow for rapid dewatering of the pond in the event of flood inflows.

Under normal site operating conditions, water in Rose Creek bypasses the tailings impoundment where contact water in the Intermediate Pond is prevented from flowing down the emergency spillway by way of summer pumping (Table 1, “minor” flood event). In the case of a “moderate” flood event (Table 1), in which Rose Creek water is able to flow into the impoundment, any water potentially leaving the Intermediate Pond via the emergency spillway would enter the Cross Valley Pond, which is retained by the Cross Valley Dam (Figure 1). The Cross Valley Pond was historically used as a polishing pond for effluent from a lime-neutralization water treatment process in order to settle residual suspended solids. Treated and polished water was then syphoned out of the Cross Valley Pond from an upper compliant layer and discharged to the receiving environment. If the storage capacity of the Cross Valley Pond were exceeded, water would enter the receiving environment by flowing down the Cross Valley Dam emergency spillway, which has an estimated conveyance capacity between 200 and 300 m^3/s (compared to 32 m^3/s for the Intermediate Dam spillway).

It is important to highlight that the Intermediate Pond and Cross Valley Pond continually receive surface and ground water inputs year-round, meaning that water levels in the ponds must be actively managed to prevent water from leaving the ponds via the spillways. If acid rock drainage from the Intermediate Pond flowed down the spillway into Cross Valley Pond, significant water management and water treatment challenges would ensue because installed pumping and treatment capacity would not be

sufficient to prevent a non-compliant discharge, and therefore the ability to maintain environmental compliance would be compromised. Since completion of the Rose Creek Diversion construction in 1981, there have not been any "moderate" flood events that directed water from Rose Creek into the tailings impoundment. A "major" flood event (outlined in Table 3) is the worst-case scenario involving dam failure, and would release a significant volume of tailings. The purpose of the interim spillway upgrade project was to reduce the likelihood of a "moderate" flood event (up to a 1-in-500-year return period) to cause dam failure, until such time as PMF protection could be established. This was deemed a reasonable level of flood protection for a 10 to 15 year period, which was how long it was predicted that it would take until the PMF spillway would be constructed.

Table 1: Consequences of various flood scenarios

Flood event	Event description	Potential consequences with respect to tailings release
Minor	Flood flows are less than the design capacity of the Rose Creek Diversion, therefore no creek water enters the tailings impoundment.	None.
Moderate	Flood flows exceed the design capacity of the Rose Creek Diversion, **or** any failure of the diversion that causes creek water to flow into the tailings impoundment, **but** the capacity of the Intermediate Dam spillway is not exceeded.	Additional contaminated water to pump and treat from Intermediate and Cross Valley Ponds. Uncontrolled discharge of non-compliant water to the receiving environment through the spillways, but little to no loss of tailings.
Major	Flood flows exceed the design capacity of the Rose Creek Diversion, **or** any failure of the diversion that causes creek water to flow into the tailings impoundment, **and** flows exceed the capacity of the Intermediate Dam spillway, causing dam failure.	Loss of several million tonnes of sulphidic, heavy-metal contaminated, acid-generating tailings to the Rose Creek valley over a distance of multiple kilometres, resulting in severe, long-term impairment of aquatic and riparian habitats.

Spillway Upgrade Design Approach

The Intermediate Dam emergency spillway is currently sized to pass flows up to 32 m^3/s, which is a large storm event for the approximately 5 km^2 catchment area for the tailings impoundment. However, it was not designed to convey flows derived from the Rose Creek Diversion catchment, which at 200 km^2 is 40 times larger than the tailings impoundment catchment (Figure 2). In order to prevent overtopping and potential failure of the Intermediate Dam, it was determined that the spillway would need to be upgraded so that it could convey flood flows not only from the local impoundment catchment area, but also from the broader regional catchment area. The remediation plan will include configuring the tailings impoundment to pass a PMF event (estimated at ~ 700 m^3/s). However, various project constraints in 2013 made it infeasible to design and construct a PMF spillway on an expedited schedule. In order to aid in rapid implementation and risk reduction, an interim approach was adopted to design and construct an

upgrade to the existing Intermediate Dam spillway. The proposed upgrade would increase the spillway capacity from 32 m^3/s to 115 m^3/s, which was the estimated flow rate for a 1-in-500-year return period flood event for the Rose Creek Diversion overflow weir. The weir is the most likely location where the Rose Creek water would spill over into the tailings impoundment (Figure 1).

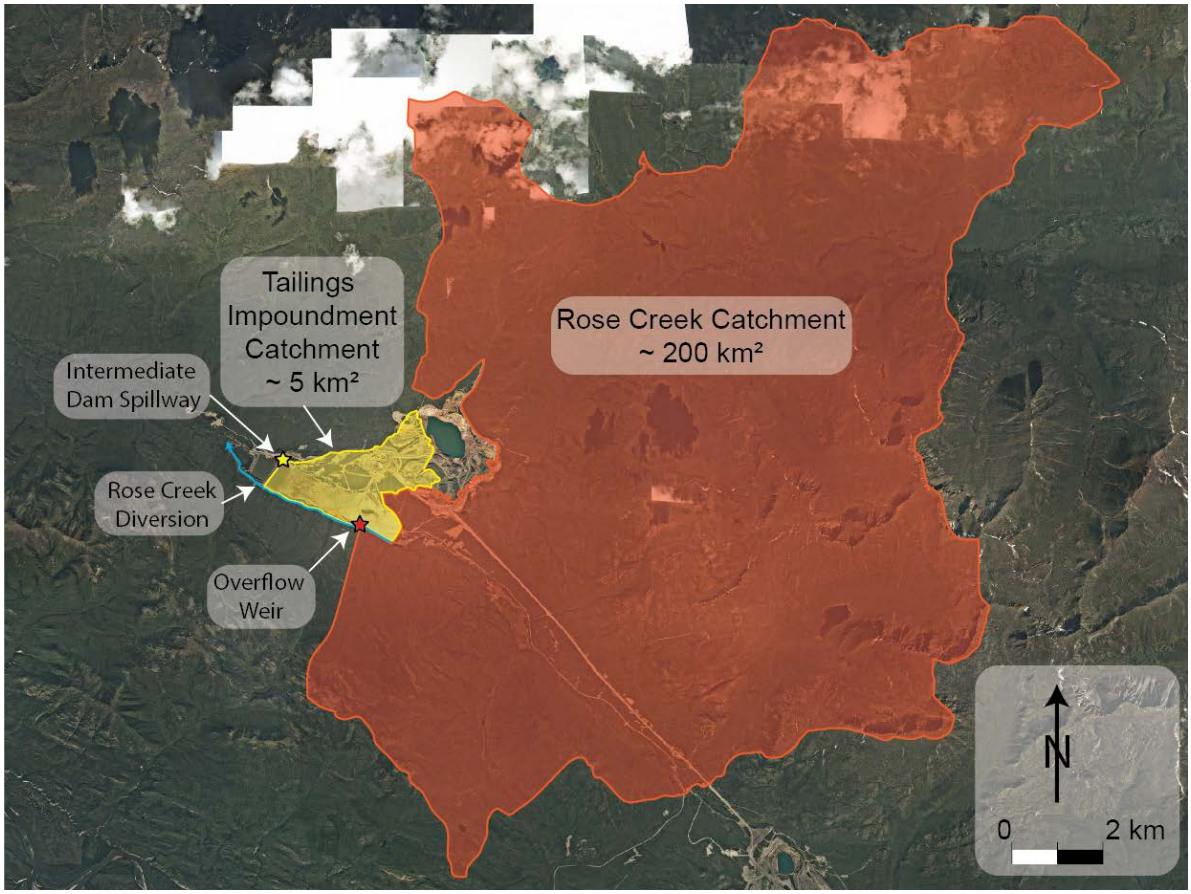


Figure 2: Comparison of catchment area size for the tailings impoundment (yellow) versus the catchment area for flows reporting to the Rose Creek Diversion overflow weir (red)

Consideration was given to expanding the capacity of the Rose Creek Diversion by raising the diversion dyke above design grade. The dyke also serves as an access road for vehicles and equipment, so any dyke raise would need to maintain adequate road access. Unfortunately, achieving the proper raise height would have excessively narrowed the road width, which could only be remedied by widening the dyke out onto the tailings. This would have involved intensive foundation investigations and potential tailings relocation in order to construct a stable structure, resulting in significant schedule delays and cost increases. If all of these Rose Creek Diversion dyke upgrades were implemented, the potential for blockage of the diversion would still have been present. An upgraded Intermediate Dam spillway would therefore be required to mitigate against the potential for diversion failure or blockage by any mechanism.

The proposed spillway upgrade design consisted mainly of raising the Intermediate Dam crest by approximately 1 m, and enlarging the existing rip-rap lined, earthen spillway by deepening it 1.2 m and marginally widening it, then installing gabion baskets and rip rap for erosion protection. The elevation of the current spillway invert at the intake is at an elevation of 1,047.7 m, and the pond bottom elevation is estimated at 1,037.7 m, which provides approximately 1.47 million m^3 of storage capacity. Lowering the spillway invert elevation from 1,047.7 m to 1,046.5 m (1.2 m net lowering) would cause a 30% loss in available storage capacity, and would invariably require maintaining the Intermediate Pond at lower water elevations than have historically been attained on a regular basis (Figure 3). Intermediate Pond storage capacity loss would have been exacerbated during construction of the spillway upgrade because of the requirement to over-excavate the base of the spillway at the intake down to an elevation of 1,045.0 m before placing fill and gabions to achieve the final intake design grade elevation of 1,046.5 m (Figure 3). Thus, during the proposed summer construction season, Intermediate Pond storage capacity would temporarily be reduced by 60%. Proposed construction scheduling would also have required the Intermediate Pond to be below an elevation of 1,045.0 m by the end of June 2016, when historical Intermediate Pond water elevation data indicate that such low water levels had never been attained that early in the season, and could not be attained without a complete upgrade of the pumping and conveyance systems.

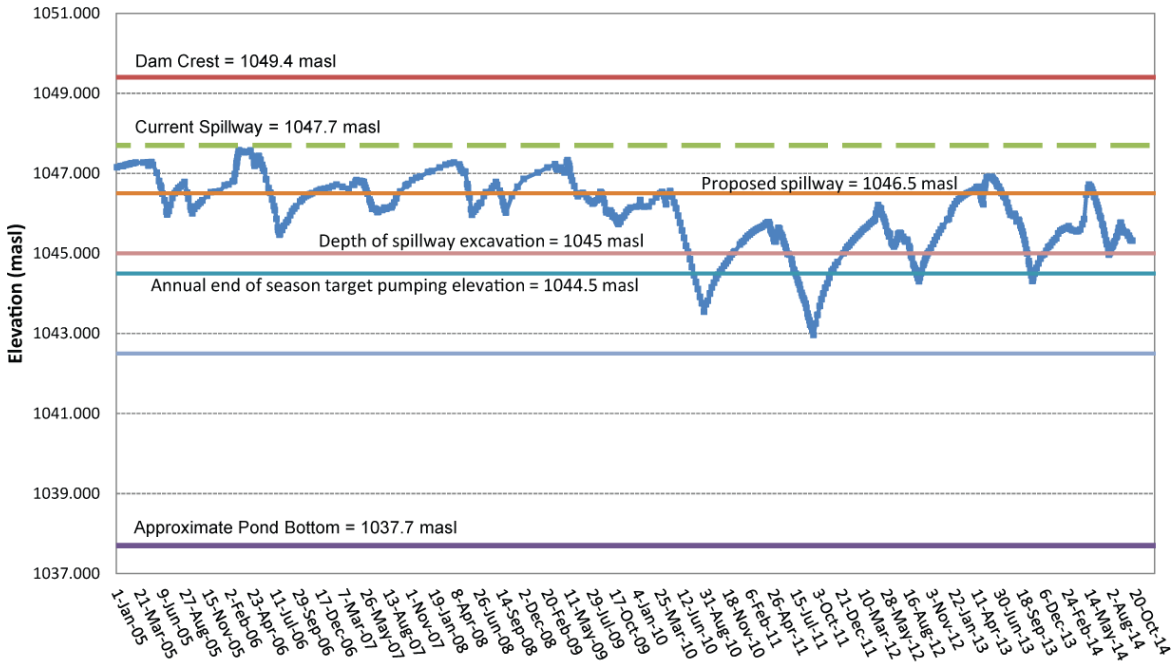


Figure 3: Intermediate Pond water elevations 2005 to 2014. Included are pertinent elevations related to annual water management targets and changes that would result from implementation of the proposed Intermediate Dam interim spillway design

Water Management Implications of Spillway Upgrade

The main ongoing challenge at the Faro Mine Complex is water management, due to the requirement to treat and discharge in excess of 6 million m^3 of mine-impacted water per year in order to maintain adequate storage capacity in the various pits and ponds. A key component of contaminated water management is seasonal (summer) dewatering and lime-neutralization treatment of acidic and/or metal-contaminated water from various reservoirs. This creates ample storage capacity in water containment areas to safely manage natural inputs of atmospheric precipitation, snowmelt, run-off, and ground water, therefore reducing the likelihood of discharging contact water to the receiving environment.

Annually, effective water management is most crucial during freshet and occasional extreme precipitation events. It is imperative that excess storage capacity also be maintained to protect against low-probability, large-magnitude floods and other geohazards that may only occur on a decadal scale or longer. By reducing the Intermediate Pond storage capacity by 30%, the proposed emergency spillway upgrade design increased the annual risk of exceeding the Intermediate Pond storage capacity, which could have resulted in acidic, zinc-laden water flowing down the spillway. Fortunately, the Intermediate Dam spillway does not discharge to the receiving environment, but terminates in the Cross Valley Pond (Figure 1). Allowing acid rock drainage from the Intermediate Pond to enter the Cross Valley Pond through the spillway would have presented significant challenges to site water management and maintaining environmental compliance.

Once the issues with Intermediate Pond storage capacity and excessive construction dewatering requirements were identified, potential water management mitigations were proposed. One solution would have involved upgrading the 126 L/s barge-mounted Intermediate Pond pumping system to a higher capacity shore-mounted system. However, upgrading the pumping system would also have required replacing ~5 km of high-pressure HDPE pipeline (100+ m of elevation gain), replacing a booster station, and upgrading electrical power distribution infrastructure. The highly acidic Intermediate Pond water also requires all pump components to be stainless steel, with considerable additional cost and fabrication lead times compared to standard pumps. Adding the pumping and conveyance mitigations to the spillway upgrade project would likely have increased project cost by more than 50% and added more than a year to the design and construction schedule.

An alternate solution was to re-design the spillway intake to maintain the same invert elevation, thereby preserving the original Intermediate Pond storage capacity. Key constraints to this approach were the inability to easily raise the dam or significantly expand the spillway laterally. Raising the dam crest more than 1 m cannot be accomplished just by adding material to the crest; it also requires adding material to the downstream face using a centreline construction method. Depending on the required height of the raise, it could also be necessary to significantly raise the Rose Creek Diversion dyke. It would be

difficult to expand the spillway laterally because construction would impinge on a key access road, electrical infrastructure, treatment effluent discharge piping, and a protected bird nesting habitat. Ensuring functional hydraulics of the intake structure at the existing invert elevation would also have required appreciable design effort, and may have required physical modelling to prove the concept. Construction costs for this option were also anticipated to be considerably higher than the initial estimate due to the anticipated inclusion of concrete to form the intake structure, as opposed to the earthen materials specified for the initial spillway upgrade design.

Project Outcome

The purpose of initiating a design to allow the Intermediate Dam emergency spillway to be upgraded to be able to safely pass a 1-in-500-year return period flood event, was to provide interim protection for the dam for a period of 10 to 15 years, until such time as the PMF solution could be implemented. Loss of Intermediate Pond storage capacity could have been resolved with additional cost and effort; however, the funder (Government of Canada) was concerned about escalating costs, ongoing delays, and increasing complexity for a temporary structure that would eventually need to be replaced. In response, a trade-off study was commissioned that mainly assessed cost, implementation schedule, and risk reduction (of dam failure) for two construction scenarios. The first scenario consisted of interim spillway construction followed by PMF spillway construction 10 years later as part of remediation plan implementation. The second scenario involved immediate construction of a PMF spillway in advance of site-wide remediation. The study assumed that PMF spillway construction could be completed in 2 years, and concluded that interim spillway construction was poor value for the level of flood protection received, particularly when most of the interim spillway construction works would need to be dismantled for PMF spillway construction. Following the study, the funder cancelled the interim spillway upgrade project with the intention of proceeding with a PMF design. Project governance challenges combined with unforeseen technical challenges prevented advancement of the PMF spillway design project. This resulted in the ongoing retention of risks associated with a hydraulically-induced geotechnical failure that could release large volumes of acid-generating, metal-contaminated tailings.

In order to provide some level of risk mitigation associated with flood events in the Rose Creek Diversion, minor upgrade works and additional channel capacity assessments were undertaken. Minor upgrade works consisted of vegetation clearing from the Rose Creek Diversion channel and planning for fill placement to bring settled sections of the dyke back to design grade. A physical survey and channel capacity assessment of the Rose Creek Diversion determined that the channel bottom was at a lower elevation than previously calculated from LIDAR data. Thus, the assessment determined that the Rose Creek Diversion could accommodate larger flows than previously calculated, and that protection against a

1-in-500-year return period flood event could be attained by completing the minor dyke raise earthworks. At present, the PMF design solution for the tailings impoundment is being advanced for inclusion in a remediation project proposal that is anticipated to be submitted for environmental assessment in 2018.

Ensuring geotechnical stability of high-risk structures like the Intermediate Dam reduces the likelihood of geochemical risk manifesting from low-probability, high-consequence flood events. Implementing the interim spillway would have reduced geotechnical risk, but at the expense of increasing the likelihood of geochemical risk realization. Ultimately, a permanent 30% reduction in Intermediate Pond storage capacity proved to be the fatal flaw that stopped the interim spillway upgrade project from proceeding. The storage capacity loss would have had a detrimental impact on operational water management in terms of achieving annual dewatering targets, and would have increased the likelihood of acid rock drainage discharge from the Intermediate Pond to the Cross Valley Pond via the spillway.

Unfortunately, geochemical conditions at the site have continued to degrade to the point where an acid rock drainage ground water plume originating from the tailings has started to migrate down the valley in the alluvial aquifer beneath the tailings impoundment. During construction of the Cross Valley and Intermediate Dams, a borrow source was developed in the base of the Cross Valley Pond footprint. This excavation extends into the alluvial aquifer, providing a direct connection for the contaminant plume to enter the Cross Valley Pond. The pond is now heavily contaminated with iron, manganese, zinc, and sulphate, and must be managed as a contact water pond (i.e. pump and treat prior to discharge). In less than five years after cancellation of the interim spillway upgrade project, the risk (acid rock drainage flowing down the spillway) that caused the cancellation was realized through an alternate process of ground water discharging to the Cross Valley Pond, clearly illustrating the types of challenges encountered when attempting to contain long-term geochemical risk at an abandoned mine site.

Conclusion

This case study highlights how geotechnical, operational, and geochemical disciplines must all be considered when long-term, active management of geochemically reactive mine waste is required. A technical solution that satisfies geotechnical considerations may not be compatible with the ideal geochemical approach, and either of those proposed solutions might not be readily implementable in operational situations where water management cannot be suspended for significant durations of time because non-compliant discharges could result. A key lesson learned is to ensure that understanding of operational water management practices is properly integrated into engineering designs early in the planning process, particularly for brownfield mine sites where effective ongoing water management is required in order to maintain environmental compliance.

Proceedings of Mine Water Solutions 2018
June 12–15, 2018, Vancouver, Canada
Published by the University of British Columbia, 2018

Total Water Management: Canada's Contribution to Sustainable Mine Development

Jon Fennell, Integrated Sustainability Consultants Ltd., Canada

Abstract

As a major player in the global mining sector, Canada recognizes the importance of proper management of water for successful mine development. As such, implementing effective diversion, capture, extraction, storage, and disposal strategies has been an integral part of the project design strategy. This typically involves elaborate and costly water management approaches comprising master drainage plans, dewatering and disposal wells, treatment facilities, storage ponds, and related conveyance infrastructure. Unfortunately, some of these approaches have fallen short of protecting the surrounding environment, with stresses being placed on surface water, groundwater, and related aquatic and terrestrial systems.

The challenges relating to safe management of water in the mining sector have been featured in many articles in the popular press. To address these challenges, prudent water management strategies integrating science, engineering, policy, and stakeholder concerns are needed to ensure acceptable outcomes. This requires an understanding of the spatial and temporal aspects of vulnerabilities and sensitivities relating to mining activities, and the development of forward-looking strategies to mitigate risks. Additionally, identification of meaningful opportunities to reduce water, waste, and energy footprints, accommodate climate change, and realize beneficial use scenarios is required to achieve the goal of sustainable mine development.

Total Water Management (TWM) is an emerging paradigm in the project delivery process where integration of corporate goals, assessment processes, planning methods, and technology selection is used to achieve net positive effects on the economic, social, and environmental aspects of today's and tomorrow's mines. This holistic approach requires an understanding of critical knowledge gaps at the site level, connectivity of water systems and their dynamics, risk exposures, mitigation strategies, and the design of performance monitoring systems to ensure regulatory compliance, maintain corporate image, and achieve successful mine closure (while avoiding or at least minimizing unintended consequences). This paper highlights the TWM process and provides examples of how it has been successfully applied in Canada and abroad.

Introduction

The mining sector is one of the major economic drivers of our global economy. Many countries around the world, like Canada, possess large deposits of minerals and metals, coal, and other products like oil sand and aggregate that are extracted to support economic growth. However, one of the major challenges for safe and profitable mine development is the management of water, both within the mine workings and across the broader mine development footprint. Site drainage and mine dewatering are two activities that often require the management of large quantities of water, which is sometimes released back into the environment. Some of this water may be of good quality, while other waters may have been compromised by certain constituents released during the extraction and processing phases (e.g. arsenic, selenium, nitrate). Having a full appreciation for the sources of mine-related constituents, how they may be mobilized, the associated hydrologic and hydrogeological aspects facilitating that occurrence, and the risks associated with each unique location is critical to the success of sustainable mine development.

So, what is sustainable mine development (SMD), and is it achievable? These are the questions being asked by many stakeholder groups and members of the public following reports of mine water releases, tailing dam breaches, lack of successful reclamation efforts, and the lasting impacts to the environment, both here in Canada and abroad. In the context of this paper, SMD may be described as follows:

> "The safe and economical development of mined natural resources where social benefit is maximized by mitigating risks to the physical and chemical environment in an anticipatory, proactive, and forward-looking manner."

Traditional approaches to water management have often segregated the various sciences, engineering disciplines, and management approaches relating to hydrology, hydrogeology, ecology, climatology, etc., resulting in missed opportunities for risk avoidance and impact mitigation. Therefore, a comprehensive and holistic approach to site-wide water management, taking into consideration the connectivity of physical and chemical systems and the related temporal dimension of land disturbance activities, is needed to achieve the goal of SMD.

Methodology

To adequately address water management challenges in the mining sector, water needs to be treated as one resource (i.e. Total Water Management). This means that surface water aspects cannot be disconnected from groundwater aspects, or the influences that climate has on these resources, because they are all intimately linked. Therefore, changes in one will tend to result in impacts to the others. Total Water Management (TWM) is a concept where the application of tailored, integrated, and practical

approaches to science, engineering, and policy are used to enhance front-end project designs and execution phases and ensure positive economic outcomes that respect social and environmental values placed on our watersheds. Central to the TWM concept is proactive risk analysis and impact management through the identification of key driving forces, and the development of strategies to facilitate efficient effects management through innovative process refinements. Also embodied in the philosophy of TWM is the concept of water security, that is, the management of mine waters to ensure successful mine development while protecting the surrounding environment and downstream users, both from a physical and chemical standpoint.

The success of an integrated approach like TWM is predicated on full knowledge of the local hydrologic system and its dynamics, the vulnerabilities and sensitivities of associated receptors, and an understanding of spatial and temporal risk exposure (at an appropriate scale), backed up with effective management and performance monitoring systems. Figure 1 provides an example of the process flow associated with TWM.

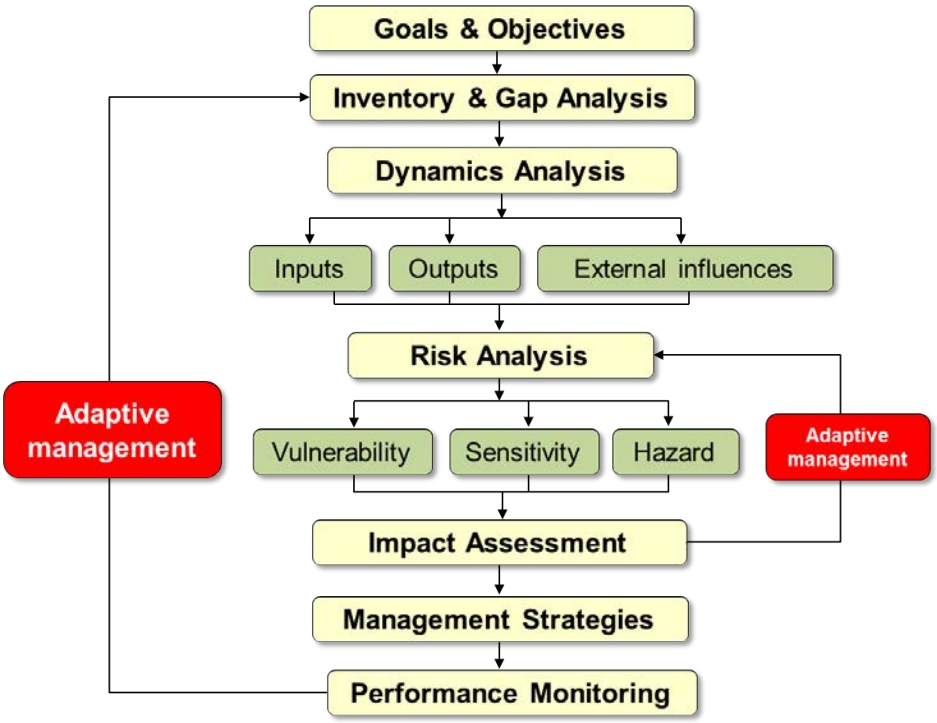


Figure 1: A systematic process of TWM to support SMD

The initial stage of the process involves the setting of realistic, achievable, and pragmatic goals and objectives to ensure a balance between economic, social and environmental needs and expectations. In the end, setting goals that negate the financial success of mining activities, and the related spin-off benefits, runs counter to the goal of providing goods and services to the consumer market. As such, this is probably

the most important phase in the TWM process, because it will set the stage for success in the other components.

Next, an inventory, or the "what do I have, and what do I need?", is required to provide the necessary point of reference and identification of gaps to focus efforts and resources in subsequent stages of the process. Often, critical gaps exist in data and information that hamper one, or all, of the desired goals and objectives. Conflicting regulations relating to air, land, and biodiversity may also interfere with desired outcomes for water; therefore, identifying these early on the process is key.

Following completion of a comprehensive inventory and gap analysis, assessing the influences that landscape alteration and climate variability may have on project success is key to placing any mine development and its potential impacts to the surrounding environment into a proper context. Natural systems are subject to variability, which can work against efforts to manage and rehabilitate them if need be. Understanding this variability, both in space and time, and knowing how a mine development may influence this variability is critical to achieving the goals and objectives established at the outset of the TWM process. This is where analogous case studies, bench-scale testing (e.g. net acid generation; humidity cell tests), model simulations, and strategically-designed baseline and monitoring programs can benefit the process greatly with full consideration of the need for statistical power and framing of uncertainty.

Risk analysis is also a central component, as unmitigated risks can have considerable influence on project success. Completion of a comprehensive risk review and tracking process (via risk register), taking into consideration the hazards associated with mining activities and the vulnerabilities and sensitivities of surrounding environments, is therefore critical. Competing interests can often play a role in this stage of the process, which can significantly influence the outcome of later stages. Uncontrollable risks, like climate variability and change, or developing social trends and policies, need to be acknowledged upfront and factored in. For example, in many cases water balance assessments are predicated on average flow conditions, which fail to accommodate the effects of seasonal, inter-decadal, or decadal variability. In many parts of the world, runoff characteristics are anything but average with conditions shifting from one extreme to another. Climate cycles such as the El Niño Southern Oscillation (ENSO) or Pacific Decadal Oscillation (PDO) play a key role in this regard. If neglected in project designs, these cyclical events can lead to significant management challenges and place strains on mitigation systems, resulting in costly measures to reconcile. When fully considered, these risks do become manageable if the right level of precaution is exercised.

Knowing how water management risks manifest themselves in space and time, and the associated uncertainties in modelled projections and forecasts, is important when conceptualizing, designing, building, and operating projects that extend well into the future. The implications related to water control,

storage, and treatment systems that do not have sufficient flexibility to accommodate changes in future conditions can be significant. A "no-regrets" approach to project design needs to be considered when planning for extremes (i.e., "plan for the worst, and hope for the best"). This includes a recognition that there are "known knowns" and known unknowns", which will result in some trade-offs. As well, some acceptance of the uncertainty around these aspects is needed, which requires proper framing and communication. In the end, the cost of under-designing a structure or control system may far outweigh the incremental cost of over-designing when the full life-cycle costs are considered. Breaching of the levees along the Mississippi River during hurricane Katrina, as well as the 2010 tailings dam failure near Kolontár, Hungary that resulted in deaths and environmental damage caused by the toxic red sludge flow, are prime examples of the catastrophic effects of under-designing. The Obed Coal Mine and the Mount Polley tailings pond failures here in Canada are more recent examples.

And then there are the so-called "unknown unknowns" that can result in unintended consequences. Put another way, this is the failure of imagination when assessing risks and their potential implications. A good example is the Elk Valley of south-east British Columbia, where metallurgical coal is being mined. Weathering of the mine tailings has led to releases of selenium to nearby water courses, which has been a focus of study and mitigation over the last decade. Although leaching of trace elements, like selenium, from mine waste is a well-documented impact for certain mining operations, the release of other more innocuous substances typically receives less attention. Yet, these innocuous substances can have equally deleterious effects. In the Elk Valley case, calcium was identified as one of the culprits, with elevated concentrations leaching from the mine waste piles into the nearby streams. Precipitation of carbonate minerals and cementation of the river substrate has subsequently led to impaired aquatic habitat and functioning of the hyporheic zone at some locations. This was an unintended consequence, but one that is still occurring nonetheless. Another example is the treatment and release of brackish wastewater in SE Queensland Australia in relation to coal seam gas development. Treated by reverse osmosis, the resulting water released back into the environment was devoid of calcium and magnesium. At the time this was not considered an issue; however, its incompatibility with the natural environment led to both calcium and magnesium being removed from the sediments and receiving waters in order to achieve chemical equilibrium. This inadvertently robbed aquatic organisms of necessary elements to build protective shells, and as such survive. This was certainly an unintended and very unfortunate outcome.

Needless to say, the risk analysis portion of any mine development is probably the most important aspect of achieving SMD. Interactive decision theory and the use of sophisticated modelling approaches can be, and have been, instrumental in exploring potential system weaknesses and identifying factors that may warn of an impending problem (e.g. precipitation trends indicating earlier, more intense, runoffs that may have negative implications for existing water management systems). However, the adage that "all

models are wrong, but some are useful" needs to apply, given that simulating complex systems with any degree of accuracy pre-supposes a comprehensive understanding of the systems involved, their connectivity, and their individual and collective dynamics. And then there are the impacts associated with cumulative effects, which mitigation strategies need to accommodate in advance to ensure success of risk management processes. However, this aspect can be overlooked.

Mitigation of unacceptable risks and impacts can be achieved by linking knowledge and expertise from various disciplines in a strategic manner to influence project design and accommodate the usually much-needed flexibility. This can be achieved by employing an adaptive style of management backed by robust modelling, performance monitoring, and response processes. Relevant aspects of the TWM process (as they relate to mine water management) include:

Opportunity Identification

- Review of existing management systems and identification of opportunities to reduce water use, incorporate offset supply sources, provide water to others, reduce energy and waste footprints, and avoid potential impacts.
- Identification of approaches or technologies, by a team of scientists, engineers and decision-makers, that increases process efficiencies, maintains profit margins, and enhances corporate profile.

Economic and Risk Evaluation

- Rigorous review of economic, environmental, and social costs of project decisions, management approaches, and technologies identified for integration.
- Identification of system dynamics/stresses, related risks to project success, and pre-emptive mitigation strategies (i.e., anticipatory engineering).

Technology Identification and Selection

- Identification of existing or new technologies, followed by ranking and weighting considering: i) technical viability, ii) ease of integration, iii) scalability, iv) economics (CAPEX and OPEX), v) environmental aspects, vi) regulatory considerations, vii) stakeholder acceptability, etc.
- Selection of the most sustainable management or design technology (guided by full life-cycle costs analysis) and incorporation into the front-end engineering design or retrofits.
- Identification of technology integration opportunities, leveraging of existing technology in a more efficient manner (i.e., optimization), or providing for design flexibility to accommodate future needs.

Implementation

- Development of a working strategy to integrate a new approach or technology into the design or process flow stream.
- Systematic execution and communication of progress to management and the project delivery team.

Performance Assessment

- Development and implementation of robust management systems, with adequate and sustained funding, to ensure intended goals of the approach or technology selection are being met.
- Effective and meaningful communication of results to internal management, regulators, and stakeholders to ensure alignment with goals, desired outcomes, and values.

Refinement through Adaptive Management

- Timely modification of the approach or technology implemented based on refined forecasts, trends in monitoring data, operating experience, and developing knowledge.
- Speedy assessment of emerging technologies and beneficial management practices to ensure intended sustainability goals are achieved.

And finally, after all of the risk analysis, impact assessment, and execution of management strategies, deployment of a robust system of performance monitoring at critical locations is required to ensure goals are met. For mines, this will typically include surface water and sediment monitoring stations, both in baseline locations and in proximity to known or potential source areas of contaminants. This may also include groundwater-monitoring stations to assess the movement of mine-related constituents through the subsurface towards, and into, connected water bodies or wetlands. This second component is sometimes given less attention compared to the easily accessible surface water systems. However, the groundwater vector is arguably the more important aspect, as it is not as obvious and treatable with the same level of success as surface water; moreover, it can provide a lasting pathway for contaminant movement despite all well-intentioned management efforts.

Any monitoring that is done must also be executed using a meaningful system of evaluation and reporting. Such systems need to be predicated on useful and understandable statistics to detect deviations or change from known or established conditions and trends, backed-up with useful visuals and graphics.

The application of a TWM approach at the initial stages, or front-end, of a project will provide the most benefit by allowing flexibility to be built-in. However, opportunities will likely exist within existing projects to achieve profitable solutions to water management challenges. The basis of such an approach is predicated on early identification of opportunities for improved efficiency, and the implementation of integrated technologies and approaches support reduce, re-use, re-cycle and replace strategies in a way

that respects project economics and minimizes the associated footprints (e.g., volume of water used or managed versus volume of output or waste generated). This is the essence of an adaptive management style, which provides the ability to move forward in an environment of "unknown unknowns." But again, timely detection of change outside natural or normal conditions is paramount.

Ultimately, to achieve the goals of integrated water management and SMD, an informed project delivery process, assisted by a pragmatic governance system, is required to facilitate the application of practical and economical solutions to mine water management challenges.

Important Considerations

Often, challenges to water management are addressed using a fragmented approach in which hydrologists, groundwater scientists, aquatic ecologists, design and process engineers, economists and social scientists work in isolation. The result can be lost opportunity for implementation of novel approaches and technologies that will achieve profitable sustainability. One example would be the provision of treated mine water to a local community to alleviate cumulative stress placed on nearby water supplies. Injection of treated water back into a stresses aquifer system is another. In order to recognize beneficial opportunities in the TWM process, aspects relating to each major component of the water management cycle must be incorporated into the project planning and execution phases. Some important considerations for surface water, groundwater, and their successful management include:

Surface Water

- Catchment analysis (high versus low yielding basins; sensitive stream orders).
- Runoff characteristics (peak flow, low flow, timing, and magnitude).
- Natural baseline water quality (with a focus on identifying natural contaminants and their associated spatial and temporal variability).
- Aquatic ecology, fisheries, and terrestrial species (sensitive versus threatened).
- Sources of risk or impact, pathways for propagation, and the receptors potentially affected (ecological and human).
- Assimilative capacity of the receiving environment, and related thresholds to ensure protection of that environment.
- Implications of climate variability and climate change on hydrological system function.

Groundwater

- Local hydrogeology and connectedness of groundwater systems (i.e. pathways for movement).
- Recharge characteristics.

- Natural baseline water quality (with a focus on identifying natural contaminants and their associated spatial and temporal variability).
- Groundwater contributions to surface water systems, including the importance.
- Transport and fate characteristics of various inorganic and organic contaminants in the subsurface.
- Implications of climate change and variability on the viability of groundwater systems.

Integrated Management

- Mine water interception (including tailings pond seepage) and site drainage control.
- Mine water re-use to offset water supply demands.
- Surface or subsurface disposal (flow augmentation, artificial recharge).
- Cumulative effects identification, assessment, and mitigation.
- Implementation of active and passive treatment (chemical systems, engineered wetlands).
- Habitat enhancement or replacement.
- Provision of water to external entities (beneficial use and substitution strategies).

Within the considerations provided above, several opportunities exist for scientists, engineers, and policy-makers to collaborate with stakeholders and interested parties on effective solutions tailored to a particular project or a cumulative effect challenge. This includes the use of existing, or new, technology that will translate to mine profitability and social license to practice, while preserving or enhancing human well-being and ecosystem integrity (i.e., the essence of SMD).

Discussion

The TWM approach has been employed in Canada and abroad to address water-related challenges in the resource extraction sector. The following are two examples of how it has been applied to large-scale industrial developments, spanning large geographical areas, in order to frame the associated risks, assess the potential impacts, and implement management strategies to ensure sustainable development goals.

Canadian Oil Sands

Canada's oil sands are one of the largest reserves of hydrocarbons in the world. At 1.7 trillion barrels (initial volume in place), and 170 billion barrels recoverable (using current technology), they exist as an important international energy supply. Currently, production is around 2.4 million barrels per day, and is projected to reach even higher number in the coming decades. The rate of development in the Athabasca region of northern Alberta has raised concerns that the surface mining and thermal in-situ oil extraction processes may potentially affect regional and local groundwater quality and quantity in this arguably

sensitive part of the province. To assist with managing water resources in this important economic region of Canada, frameworks have been developed to align with the goals of the Land-Use Framework (GoA, 2008) and Water for Life Strategy (AENV, 2003). Three general goals were identified through a facilitated process involving representatives from government, industry, academia, and consulting, which are:

- Management of water quantity to meet the needs of all users (including the environment).
- Preservation of water quality for the benefit of all users (including the environment).
- Maintenance of the hydraulic integrity of regional flow systems (including critical inter-connections).

Baseline assessments of the area's water resources were conducted, followed by the selection of characteristic physical and chemical indicators to assess and track changes and identify cause-and-effect relationships between human activities and natural water systems. Monitoring currently includes weekly stream flows in the Athabasca River (AENV/DFO, 2007), surface water quality, sediment quality and ecological integrity, groundwater level fluctuations in key aquifers influenced by mine dewatering, and monitoring for chemical constituents related to mining and waste disposal operations (AENV, 2011). Triggers for investigation and management actions have been derived from an assessment of available river flow data, hydrogeological information, and surface water and groundwater quality data. With respect to groundwater, approximately 1,500 well records and over 132,000 data records were assessed to define the range of natural variability for the area. Data is routinely assessed using statistical tests, such as Shewhart control charting (Lucas, 1982) and the Mann-Kendall test for trend (Mann, 1945; Kendall, 1975).

Terrain conductivity mapping on the river, and vulnerability mapping combined with future development projections, has been used to identify areas at higher risk to cumulative mine dewatering and tailing pond seepage. This is shown in Figure 2, along with the current and future surface water and groundwater monitoring stations.

A systematic process for investigating anomalous events was subsequently developed to differentiate between natural and human-related influences. This process includes the following sequential steps:

- Verification of detection;
- Preliminary assessment and source identification (natural versus industrial);
- Risk assessment (source-pathway-receptor and vulnerability-sensitivity-hazard analysis);
- Modification of the activity, or activities, responsible (if required); and
- Event closure, including post-closure monitoring.

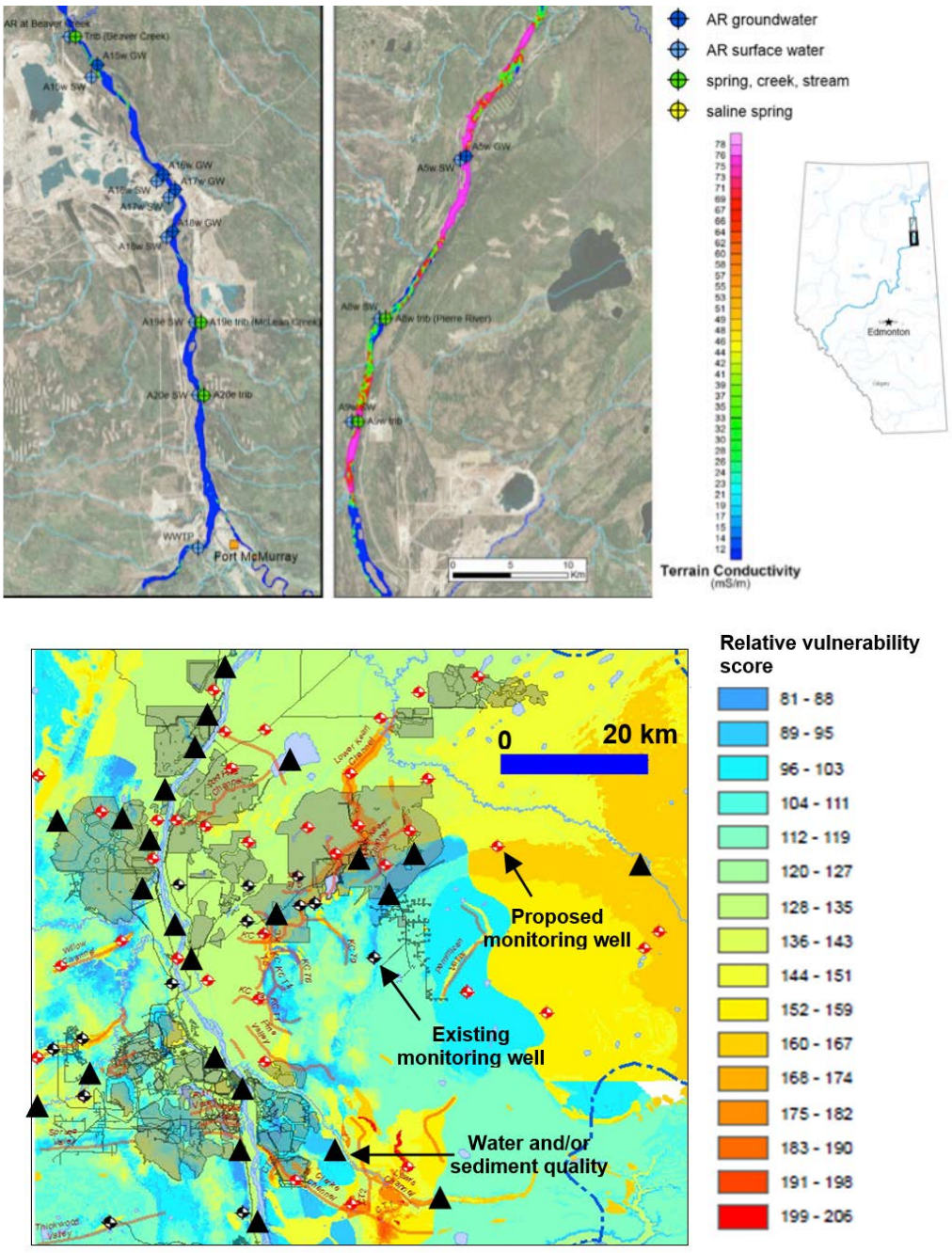


Figure 2: Terrain conductivity mapping of Athabasca River with sampling locations, and risk mapping showing existing and proposed monitoring
(Note: grey shaded areas represent footprints of existing and proposed oil sands mines)

If an event is determined to be related to natural causes, or within acceptable constraints to maintain the stated goals of the management process, the findings are incorporated into the regional understanding and associated triggers and limits are revised accordingly. Some of the management strategies, either government-initiated or self-imposed, that have been put in place include:

- Scaled-reduction in withdrawal from the Athabasca River to maintain ecosystem flows.
- Water recycle efficiency of 90% or better for thermal in-situ recovery operations.
- Regional-scale cumulative effects modelling to validate and refine monitoring and facilitate simulation of future development risks and climate change scenarios.
- Trade-off analysis relating to key indicators (e.g., a target species or social value) to determine optimal oil production trajectories (i.e., rapid versus slow).
- Reduction in mine tailings footprints through trailing of consolidation and drying techniques;
- Reclamation initiatives including engineered wetlands and end pit lake piloting.
- Investigation of natural versus industrial input and relative loading to area receptors.

Bitumen production from the Canadian oil sands continues to increase each year, with seven large-scale open-pit mines in operation and numerous thermal in-situ projects underway. The TWM approach has thus far provided a better understanding and appreciation of the natural setting and facilitated the development of monitoring and research activities to identify, attribute, and minimize impacts. Equally, the approach has resulted in a positive economic outcome by providing sustained employment and royalties that support the provincial economy.

SE Queensland, Australia

Coal seam gas (CSG) is becoming a significant resource for Queensland's shifting energy portfolio. The process involves the drilling of wells into deeply-buried coal seams, followed by the removal of large volumes of groundwater to reduce the hydrostatic pressure in deeply buried coal measures and facilitate the release of trapped methane. Concerns have arisen regarding the large number of proposed wells (>30,000), the magnitude of groundwater level drawdowns (up to 700 m or more in certain coal intervals), and potential effects to aquifers supporting local residents, industries, and groundwater-dependent ecosystems.

To properly frame the risks and potential impacts to local and regional groundwater resources, a TWM approach, similar to the Canadian oil sands example, was employed by the Queensland government. The approach was predicated on a review of current land and water use trends, development of water production forecasts, assessment of cumulative development effects, risk mapping based on the multi-criteria analysis approach, and a full assessment of baseline groundwater conditions. Sophisticated modelling was used to project long-term drawdown effects from CSG development and other activities, and the results were integrated into the development of a robust water-monitoring network and data analytics scheme to detect changes outside of the range of natural variability. Adaptive management strategies were also developed to address risks and potential impacts from CSG development, taking into

account the vulnerability and sensitivity of defined receptors (DERM, 2010a; 2010b). This was later mapped to facilitate development of regional monitoring. Figure 3 shows an example of the risk mapping output.

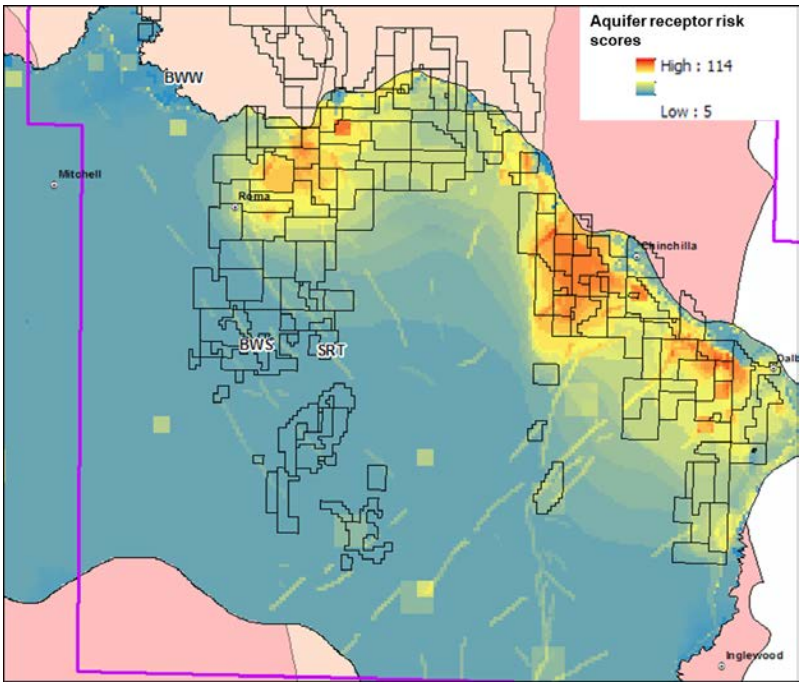


Figure 3: Example of multi-attribute point-scoring (MAPS™) risk mapping to support regional monitoring in the Surat Basin, SE Queensland

This systematic approach to cumulative effects assessment and mitigation has been instrumental in providing a structured, scientifically based process to support management decisions and align industry, government, and stakeholders with agreed-upon sustainable development commitments. The following are some of the management activities put into place:

- Elimination of evaporation ponds to dispose of produced water.
- Assessment of economical salt recovery and associated waste reduction.
- Lining of ponds to reduce the risk of brine leakage and soil salinization.
- Water substitution strategies for agriculture, aquaculture, and municipal sectors (i.e. beneficial use strategies).
- Placing high importance on injection of treated water back into high-risk, high-use aquifers.

The CSG sector in Queensland has benefited from this holistic approach to water management. As such, the TWM philosophy continues to support the sustainable development of natural resources to the economic benefit of the Australian economy.

Conclusion

To achieve the goal of integrated water resource management, a new paradigm of how we provide holistic solutions to water (and environmental effects) management needs to be embraced by industry and regulators. This will require institutional capacity and leadership among water professionals and governing agencies entrusted with sustainable management of this vital resource. By reinforcing integration of the sciences, engineering, and policy and using a systems-based approach, smart and economical delivery of sustainable outcomes will be ensured. TWM is the type of concept needed to achieve this goal, and one that will serve our society through the benefits realized. This approach has proven helpful in managing water challenges in two large Commonwealth countries, and hopefully will stimulate the move towards a more holistic, anticipatory, participatory, and sustainable way of mining here in Canada and abroad.

References

Alberta Environment (AENV). 2003. Water for life: Alberta's strategy for sustainability. Retrieved from: http://environment.gov.ab.ca/info/library/6190.pdf.

Alberta Environment (AENV). 2011. *Groundwater Management Framework, Northern Athabasca Oil Sands Region. Part 1: Technical Framework*.

Alberta Environment (AENV) and Department of Fisheries and Oceans (DFO). 2007. Instream flow needs and water management system for the Lower Athabasca River. Retrieved from: http://environment.alberta.ca/01231.html.

Department of Environment and Resource Management (DERM). 2010a. Coal seam gas water management policy. Retrieved from: http://www.sixdegrees.org.au/sites/sixdegrees.org.au/files/water-management-policy-1.pdf.

Department of Environment and Resource Management (DERM). 2010b. Preparing an environmental management plan for coal seam gas activities. Retrieved from: http://www.derm.qld.gov.au/environmental_management/land/documents/csg-environmental-management-plan.pdf.

Government of Alberta (GoA). 2008. Land-use framework. Retrieved from: http://www.edmonton.ca/environmental/documents/Alberta_Land_Use_Framework.pdf.

Kendall, M.G. 1975. Rank Correlation Method, 4th edition. London: Charles Gridden.

Lucas, J.M. 1982. Combined Shewhart-CUSUM quality control schemes, *J. Quality Technol.,* 14: 51–59.

Mann, H.B. 1945. Nonparametric tests against trend*, Econometrica,* 13: 245–259.

Proceedings of Mine Water Solutions 2018
June 12–15, 2018, Vancouver, Canada
Published by the University of British Columbia, 2018

Multi-Parameter Time-Lapse Dam Seepage Investigation

Tomas C. Goode, Stantec, USA
Rachael Peavler, Stantec, USA
Hhan Olsen, Stantec, USA

Abstract

The Dam Seepage Investigation and Conceptual-Level Mitigation Design Project was a mine water seepage investigation on a small collection reservoir and dam. It utilized multiple lines of evidence during a baseline and rising head test to increase levels behind the dam to determine seepage pathways. A baseline sweep of measurements (groundwater elevations, water quality sampling, electrical resistivity surveys) was completed prior to starting the rising head testing. The monitoring sites consisted of multiple well locations and electrical survey lines downstream of the dam as well as along both abutments and the up-gradient of the reservoir. The rising-head test consisted of a series of six distinct step changes to the reservoir level occurring over a time frame of approximately one month. The step changes ranged from 0.5 m rise (at the beginning of the test) to 1.5 m for the last step. Water levels and water quality were monitored at the wells continuously during testing, and weekly electrical resistivity surveys were completed.

Results of the testing included changes in water levels and water quality at downstream wells over time that mimicked changes in reservoir elevations. Time-lapse changes observed in subsurface resistivity (resulting from changes in water level as well as fluid conductivity) highlighted the spatial extents of the seepage beneath and around the dam. Two primary mechanisms were subsequently identified as controlling the overall flow of groundwater in the vicinity of the dam. 1) Dam Bypass: Some impacted groundwater migrates downstream of the dam along fracture pathways that are not in communication with the reservoir. 2) Direct Seepage: The cause of seepage is not related to a distinct defect or weakness in the dam structure. Instead, seepage from the reservoir is occurring along multiple flow paths. Seepage migrated around the right abutment, beyond the extent of the grout curtain, as well as through the central and possibly right upper portions of the grout curtain. Additional seepage pathways were identified beneath the grout curtain. Based on the findings from the seepage investigation, installation of pumping containment systems both upstream and downstream of the dam was recommended. The system consists

of three downstream and four upstream pumping wells and six monitoring wells. These wells will reduce groundwater flow bypassing the dam, and capture seepage coming directly from the reservoir. The spatial extent of the seepage from around the dam, as identified by the geophysics, guided the ultimate placement of the seepage collection wells.

Introduction

The Dam Seepage Investigation and Conceptual-Level Mitigation Design Project was completed in response to regulatory findings that indicated low pH and high sulphate water was present in a shallow piezometer located downstream of the dam. The mine proactively began investigations both downstream and upstream of the dam in late 2016 and early 2017 shortly following the regulatory finding to determine the causes of the poor water quality. The project included a seepage investigation phase and a conceptual-level design phase for seepage mitigation. The objectives of the seepage investigation included:

- Review previous studies.
- Improve the monitoring network immediately downstream of the dam and upstream of the sump.
- Evaluate existing conditions, including a Condition Assessment of the dam.
- Evaluate the timing and extent of potential seepage bypassing the dam.
- Assess aquifer properties and groundwater pumping potential.
- Identify likely seepage pathways.

Objectives of the conceptual-level design phase included the following:

- Develop and analyze alternatives for seepage mitigation measures.
- Select the most appropriate alternative for the seepage mitigation measures and develop a Conceptual-Level Design.

The seepage investigation first included baseline data collection, followed by a controlled rising-head test in the sump behind the dam. Baseline conditions were documented prior to conducting the rising-head test. The use of a time-lapse geophysical survey using electrical resistivity was used to identify regions impacted by hydrologic changes associated with dam seepage. Through the use of time-lapse resistivity surveys in the vicinity of the dam, locations with changes in moisture content occurring as a result of water-level rise within the sump behind the Dam were identified. Furthermore, the sump water-level rise acted as a stepped “rising-head” test so that hydraulic head changes at monitoring points downstream of the Dam can be measured during specific stages of reservoir filling; these data provided an additional line of evidence regarding the presence of seepage and assessing seepage pathways.

Methods

Water-Level Monitoring

Water levels in wells were collected using a combination of automated electronic pressure transducers and a manual electronic water-level sounder. The pressure transducers measured head above the transducer, while the water-level sounders measured depth to water below a set measuring point. In both cases, the water-level data were converted to a water-level elevation using the surveyed elevation of the top of the well casing. In cases where both methods were used at the same well, manual water-level sounder measurements were used to validate the pressure transducer data. Water levels in the sump were assessed visually using a staff gauge.

Water-Quality Sampling

Water-quality samples were collected from select groundwater monitoring locations, the sump, and the make-up water planned for use in the rising-head test. Water-quality analyses included field parameters (electrical conductivity and pH), bicarbonate, carbonate, chloride, sulphate, and dissolved and total metals.

Rising-Head Test Procedure

The initial starting sump water level was maintained at approximately 2,522.5 m amsl prior to 17 October 2016. Six distinct step increases were performed throughout the month-long test until the sump reached its maximum level of 2,527 m amsl on 17 November 2016. River water was conveyed to the sump and used as make-up water for each step. Process water continued to flow into the sump throughout the rising-head test at an approximate rate of 1.5 L/s. A sump pump was used to maintain the sump at its designated step level to within approximately +/- 0.1 m. to maintain the sump at its designated step level to within approximately +/- 0.1 m.

Geophysical Survey

Electrical resistivity survey data was collected along six geophysical profile lines, as shown in Figure 1. Five surveys (L1 through L5), totalling approximately 920 linear m, were conducted roughly parallel and perpendicular to the groundwater flow path surrounding the dam. These five were conducted prior to the rising-head test. The region of interest for the electrical geophysical survey is from land surface to a depth of approximately 30 m. This is the region that was determined to have the greatest potential for changes in moisture content over time. A sixth survey (L6) of 400 linear m was later conducted upstream of the ponded water, perpendicular to the groundwater flow path. The electrode locations were spaced at 4 m distances.

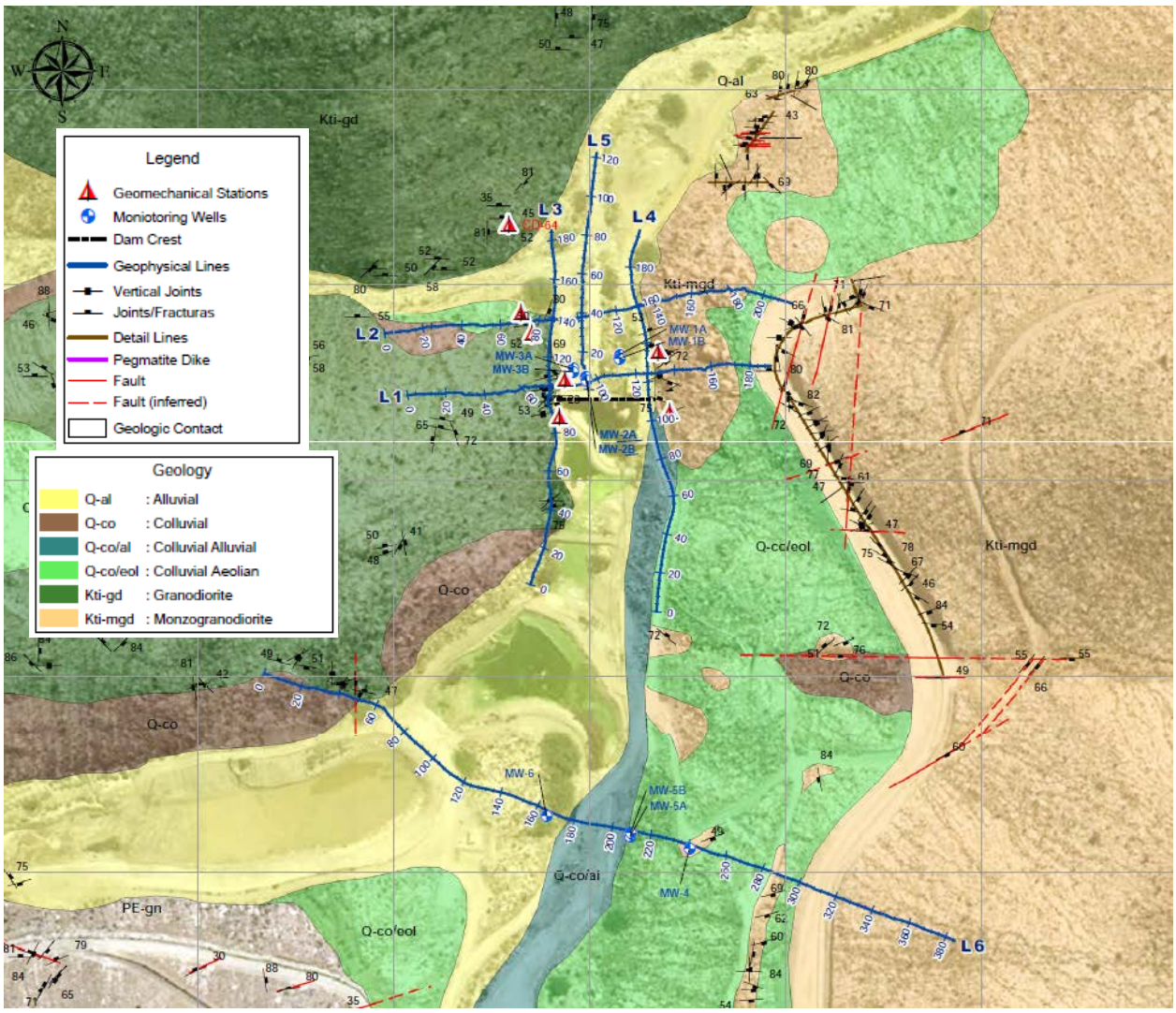


Figure 1: Select monitoring well and resistivity survey line locations

A baseline survey was completed before starting the rising-head test to establish the static subsurface resistivity upon which the time-lapse resistivity changes were based. Each survey line was modeled to produce a subsurface resistivity cross section, for a total of five baseline survey cross sections. At four different water-level increments in the rising-head test (at the end of approximately every ten days), the geophysical contractor conducted time-lapse electrical resistivity survey events. The survey events were completed in the same fashion as the baseline survey using the same electrodes in the same locations.

Unlike a static survey, the time-lapse survey is gathering information on a dynamic system. The subsurface groundwater conditions are actually changing during the time that the data is being collected. Consequently, this introduces an error into the measurements because it takes so long to collect all of the measurements. If all of the measurements are collected in the same way, and collected in the same order

each time, much of this error is reduced. Otherwise, errors in measurements are more easily confused with changes in water content. Adherence to repeating the same process for each time-lapse survey was essential for survey efficiency

Each survey line from the time-lapse survey events was modeled to produce a subsurface resistivity cross section in a similar fashion as the baseline survey. The baseline resistivity results were used as the initial resistivity configuration for each of the time-lapse inversions (i.e. the time-lapse models are regularized using the inversion results from the baseline resistivity survey models). Because the final resistivity values from the time-lapse and baseline surveys appear very similar, cross sections of the time-lapse surveys were produced to show the percentage change (+/–) from the baseline condition.

Electrical measurements during the surveys were made using a pole-dipole technique, where electrical current was injected into a single electrode (pole) while at the same time, the electrical voltage was measured between two other electrodes (dipole). Voltage was then converted into an apparent resistivity based on the specific geometry between the injected current pole and the voltage measuring dipole. These measurements were subsequently modeled to obtain the physical distribution of the various resistivity values of subsurface materials beneath the survey lines. The inversion software used by our geophysics subcontractor is DCIP2D, developed by University of British Columbia Geophysical Inversion Facility. Subsequent data review was conducted using RES2DINVx64 (Geotomo Software) for inversion by an independent QA/QC reviewer for quality of data collected in the field.

Water Level Response

Baseline water levels were used to generate an inferred baseline potentiometric surface map. The head contours show that downstream of the dam there are higher heads along the eastern portion of the valley and that groundwater flow is directed in a north-northwest direction until the drainage confluence. At this point, groundwater flow is directed northeast along the main drainage. This suggests one of the following three things:

1. there is a greater hydraulic connection between the areas upstream of the dam and the central to eastern portion of the valley downstream of the dam;
2. subsurface fractures or joints preferentially direct groundwater flow in a northwest direction; or
3. a combination of 1) and 2).

Of note are the relatively steep horizontal hydraulic gradients up and downstream of the dam (approximately 0.1 m/m) relative to the more gradual horizontal hydraulic gradients below the drainage confluence. The vertical hydraulic gradients as measured on 17 October 2016 show an upward gradient at MW-03 (0.0049 m/m), an equal vertical head gradient at MW-02 (0 m/m), and a very slight downward

gradient at MW-01 (within the margin of measurement error). The vertical hydraulic gradient was also calculated at the upstream shallow and deep well pair MW-05A/B. Vertical hydraulic gradients at this location are slightly downward (0.0092 m/m), indicating that some degree of groundwater may not be discharging to the sump as previously expected and may be instead flowing beneath or around the sump.

The combined rising-head test hydrograph data for sump water level and groundwater monitoring locations in close proximity to the Dam (including MW-01A/B, MW-02A/B, and MW-03A/B) are shown in Figure 2. All of the near monitored locations began to respond to the rising-head test during the first sump increase to 2,523 m amsl (as opposed to a distinct, delayed increase in downstream groundwater levels during a specific rising-head step level). This indicates that the cause of seepage is not related to a distinct defect or weakness in the dam above the 2,525.5 m amsl elevation.

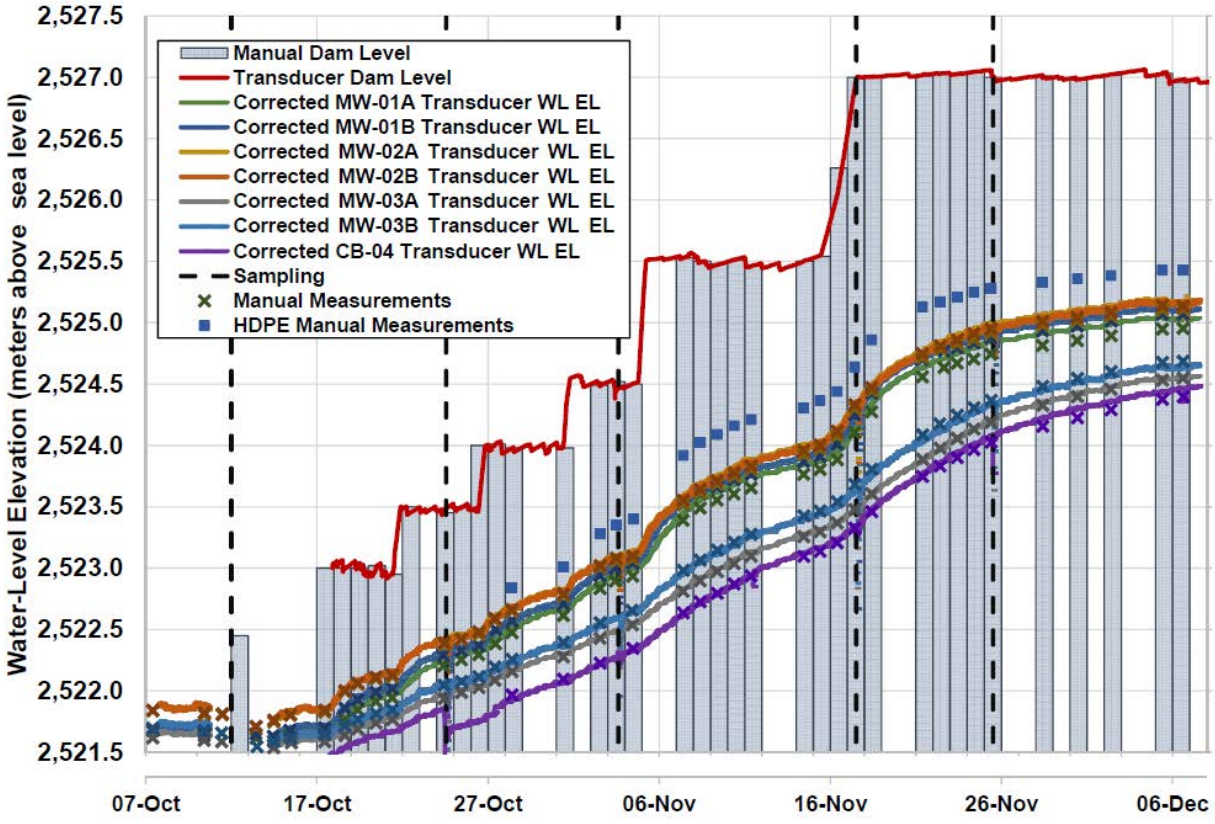


Figure 2: Combined rising-head test hydrograph data for sump water level and groundwater monitoring locations

Groundwater levels did not increase uniformly across the valley. Of the three well pairs, MW-01A/B increased the most between 17 October and 6 December 2016 (average of 3.38 m) and MW-02A/B increased on average only 0.05 m less than MW-01A/B (average of 3.33 m). MW-03A/B increased the least, an average of 0.42 m less than MW-01A/B (average of 2.97 m).

When comparing the shallow and deep well completions, the rate and total magnitude of increase are greater at the deeper wells on the right and left abutments (MW-01B and MW-03B), but are greater at the shallow well in the center (MW-02A). This indicates that the mechanisms affecting groundwater flow characteristics and/or seepage are different on the abutments than the center of the valley. The greatest increase is seen at the deeper, right well (MW-01B) suggesting that underflow beneath and/ or around the right side of the dam is occurring. During the rising-head test, the vertical gradient at MW-01A/B changed from a slight downward gradient to an upward gradient. A similar mechanism, although to a lesser degree, appears to be affecting the left portion of the valley. In the center, the water-level increase appears to be due to migration from the abutments more than underflow. If seepage near MW-02A/B is occurring, it is affecting the shallow completion (top of well screen 4.2 m bgs) roughly equal to the deep completion (top of well screen 14.2 m bgs).

Water Quality Response

Time series of key water-quality indicators sulphate, copper, electrical conductivity, and pH were evaluated with respect to the effects of the rising-head test are discussed for these four indicators.

Sulphate concentrations in the sump fluctuated between 2,500 and 4,997 mg/L during the rising-head test. In comparison, the baseline sulphate concentrations at MW-01A and MW-01B were significantly greater at 16,887 and 12,494 mg/L, respectively. In contrast, baseline concentrations at MW-02A/B and MW-03A/B were less or very similar to the sulphate concentrations in the sump during the rising-head test (between 2,031 and 3,460 mg/L). The concentrations at MW-01A consistently decreased during the rising-head test (16,887 to 14,761 mg/L) suggesting mixing of the local PLS-impacted groundwater. A possible trend due to effects from the rising-head test can also be seen at MW-02A and MW-03A, with concentrations increasing from 3,460 to 4,206 mg/L and 2,031 to 2,174 mg/L, respectively.

Dissolved copper concentrations in the sump fluctuated between 23 and 64 mg/L during the rising-head test, while the baseline dissolved copper concentrations at MW-01A and MW-01B were significantly greater at 202 and 92 mg/L, respectively. Similar to sulphate, baseline concentrations of dissolved copper at MW-02A/B and MW-03A/B were significantly less than the concentrations in the sump during the rising head test (between 0.035 and 8.591 mg/L). The concentrations at MW-01A and MW-01B decreased during the rising-head test (202 to 186 mg/L and 92 to 59 mg/L) suggesting mixing of the local PLS-impacted groundwater. A possible trend due to effects from the rising-head test can also be seen at MW-02A and MW-03A, with concentrations increasing from 8 to 21 mg/L and 0.035 to 0.104 mg/L, respectively.

Electrical conductivity in the sump fluctuated between 3,730 and 6,930 µS/cm during the rising-head test. In comparison, the baseline electrical conductivity at MW-01A and MW-01B was significantly greater at 15,570 and 14,590 µS/cm, respectively. In contrast, baseline electrical conductivity at MW-02A/B and MW-03A/B was in the same range as that observed in the sump during the rising-head test (between 4,110 and 5,640 µS/cm). Electrical conductivity at MW-01B decreased during the rising-head test (14,590 to 13,770 µS/cm) suggesting mixing of the local PLS-impacted groundwater. A possible trend due to effects from the rising-head test can also be seen at MW-02A and MW-03A, with concentrations increasing from 3,460 to 4,206 µS/cm and 4,110 to 4,400 µS/cm, respectively.

The sump pH fluctuated between 3.52 and 4.21 during the rising-head test. In comparison, the baseline pH at MW-01A/B. In contrast, baseline pH at MW-02A/B and MW-03A/B was greater than the pH observed in the sump during the rising-head test (between 5.27 and 6.95). At MW-01B, pH increased during the rising-head test (4.68 to 5.16) suggesting mixing of the local PLS-impacted groundwater. A possible trend due to effects from the rising-head test can also be seen at MW-02A, with pH decreasing from 5.27 to 4.63. This decrease is possibly related to the flushing of poorer quality water from the right abutment toward the valley center and left abutment.

Geophysical Response

Baseline Surveys

The electrical resistivity values presented in the cross sectional images developed from baseline geophysical investigation represent a composite of different lithological and hydrologic characteristics. Specifically, subsurface electrical resistivity is a function of water quality (particularly dissolved constituents), saturation, and porosity. In general, those areas of the subsurface with greater moisture content and/or increased dissolved solids (TDS) tend to have low resistivity. When saturated, increased porosity also tends to lower subsurface resistivity (resulting from increased water content). The presence of clay with its high porosity, exhibits this characteristic well. With the number of potential variables influencing the presence of low resistivity zones in the subsurface, it is important to utilize as much supporting information as possible when drawing inferences from the resistivity values presented in these figures. The results of the baseline geophysical surveys for L1 to L5 are presented in Figure 3.

L1 is located immediately downstream of the Dam and runs perpendicular to the axis of the canyon. The L1 cross section displayed in Figure 3 indicates predominantly high resistivity values, approximately 500 to 1,000 ohm-m and higher, along much of the cross section, particularly along the granodiorite and monzo-granodiorite upland areas. However, a low resistivity zone extends across the lowland area of the cross section. This low resistivity zone appears to have a focal point of approximately 10 ohm-m in the area along the right abutment, roughly beneath the alignment of L4. This low resistivity zone is shown in

greater detail along with the geologic cross section in Figure 4. Given the historical observation of groundwater with high TDS in monitoring wells, this low resistivity is believed to represent a concentration of high TDS water at this location. With the gradual increase in resistivity towards the center of the canyon, this may indicate a source of poor quality water moving along the right abutment, which is flowing into, and becoming diluted as it comes into contact with, native groundwater in other areas.

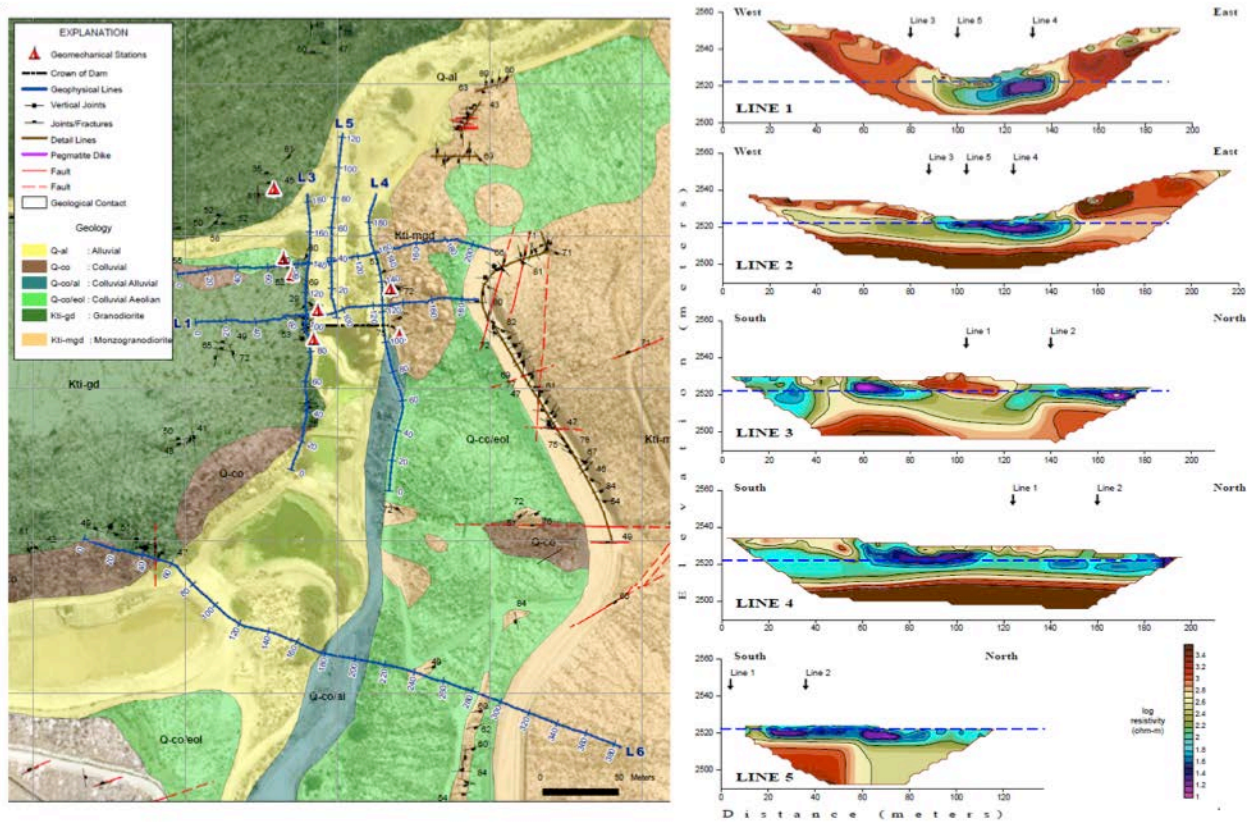


Figure 3: Baseline geophysical survey results for the 5 lines used for time-lapse surveys

The L2 cross section displayed in Figure 3 indicates high resistivity values, approximately 1,000 to 2,500-ohm-m and higher, below an elevation of 2,515 m amsl. This likely represents the base of the alluvial aquifer and the transition to consolidated granodiorite and monzo-granodiorite. Above this unit, the resistivity horizon with 500 to 1,000-ohm-m is likely representative of saturated alluvial sediments and highly fractured bedrock units. The low resistivity unit in the central to right-central portion of the canyon, with a focal point of approximately 10 ohm-m, is likely representative of high TDS water moving from the up-gradient into the area. The nature of the lower resistivity zone, skewed somewhat along the right side of the canyon, fits with the up-gradient observation in L1 showing a low resistivity zone along the right abutment.

The L3 cross section displayed in Figure 3 indicates a high resistivity value, approximately 1,000 to 2,500-ohm-m, below an elevation of 2,510 m amsl. This likely represents the transition into more consolidated granodiorite. Above this unit, the relatively horizontal zone with resistivity ranging from 100 to 500-ohm-m is likely representative of fractured and saturated bedrock units. The relatively low resistivity of this unit may be indicative of generally higher TDS water present in the rock unit. Those zones with resistivity values extending down to 10 ohm-m are likely pockets of high TDS water extending outwards from the Dam. The low resistivity zone observed to the north of the L2, correlates well with the low resistivity in the alluvium observed in L2; indicative of high TDS water in the alluvium down gradient of the Dam.

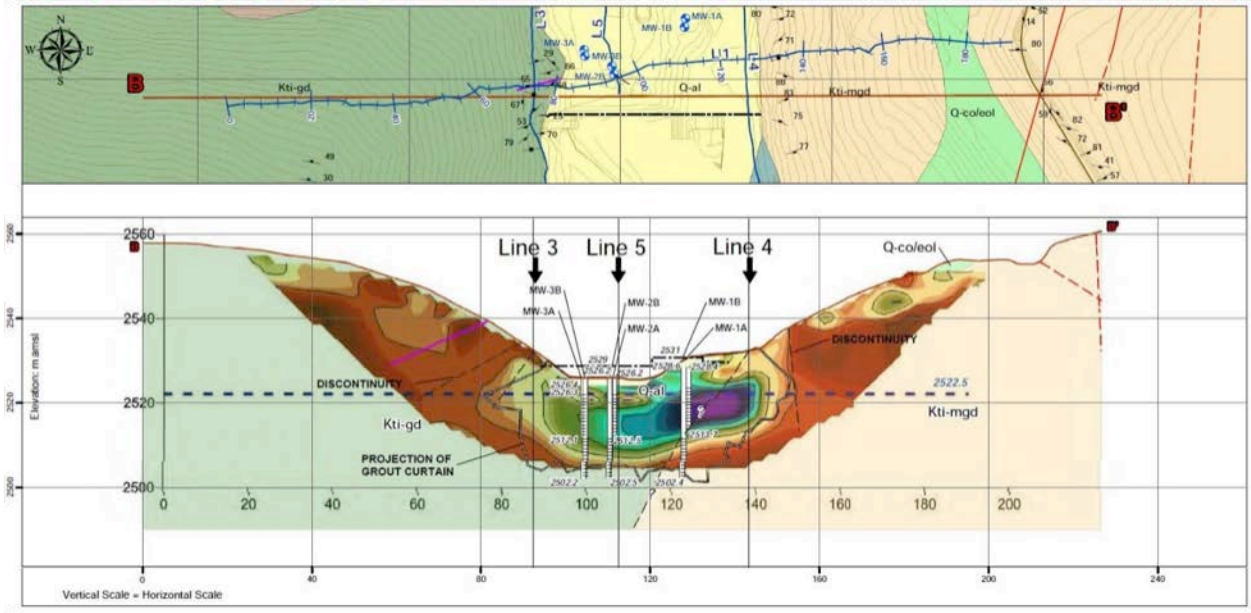


Figure 4: Detailed geophysical resistivity results along with geologic cross-section for L1

The L4 cross section displayed in Figure 3 indicates a high resistivity value, approximately 1,000 to 2,500-ohm-m, below an elevation of 2,515 m amsl. This likely represents the transition into more consolidated monzo-granodiorite. Above this unit, the relatively horizontal zone with resistivity ranging from 10 to 100-ohm-m is likely representative of saturated and highly fractured bedrock units. The low resistivity of this unit is indicative of high TDS water present in the rock unit, with potentially higher and lower TDS zones, as well as potentially higher porosity zones. The continuity of the low resistivity zone may be indicative of a relatively continuous flow pathway for the high TDS water moving through the right abutment. In turn, this correlates with the presence of the lower resistivity observed in both L1 and L2 in the vicinity of the right abutment.

The L5 cross section displayed in Figure 3 indicates a similar high resistivity feature at depth, approximately 1,000 to 2,500- ohm-m, below an elevation of 2,515 m amsl. However, this high resistivity

feature abruptly ends approximately 20 m north of the L2 alignment. This may be indicative of a sharp erosional feature in the bedrock unit or possibly a fault at this location. Above this unit, the relatively horizontal zone with resistivity ranging from 10 to 100-ohm-m is likely representative of alluvial sediments saturated with high TDS water. This also correlates with the presence of the lower resistivities observed in the alluvial sediments present in both L1 and L2 cross sections.

Time-Lapse Geophysical Response

The time-lapse evaluation of the subsurface resistivity included the re-survey of survey lines L1 through L5. A total of three repeat surveys were completed for the five survey lines, each approximately two weeks apart, with the final survey conducted approximately 1.5 months after the baseline. The greatest change in resistivity values was observed between the final resistivity survey and the baseline surveys. As a result (with one exception at L1), only the changes in resistivity from baseline to the final surveys (phase 4 surveys) are presented as cross sections. The change in resistivity was calculated for each cross section, and is displayed as percentage change rather than the absolute value of the change. This method of data evaluation emphasizes the spatial characteristics of the change in order to identify potential locations where seepage may be bypassing the dam.

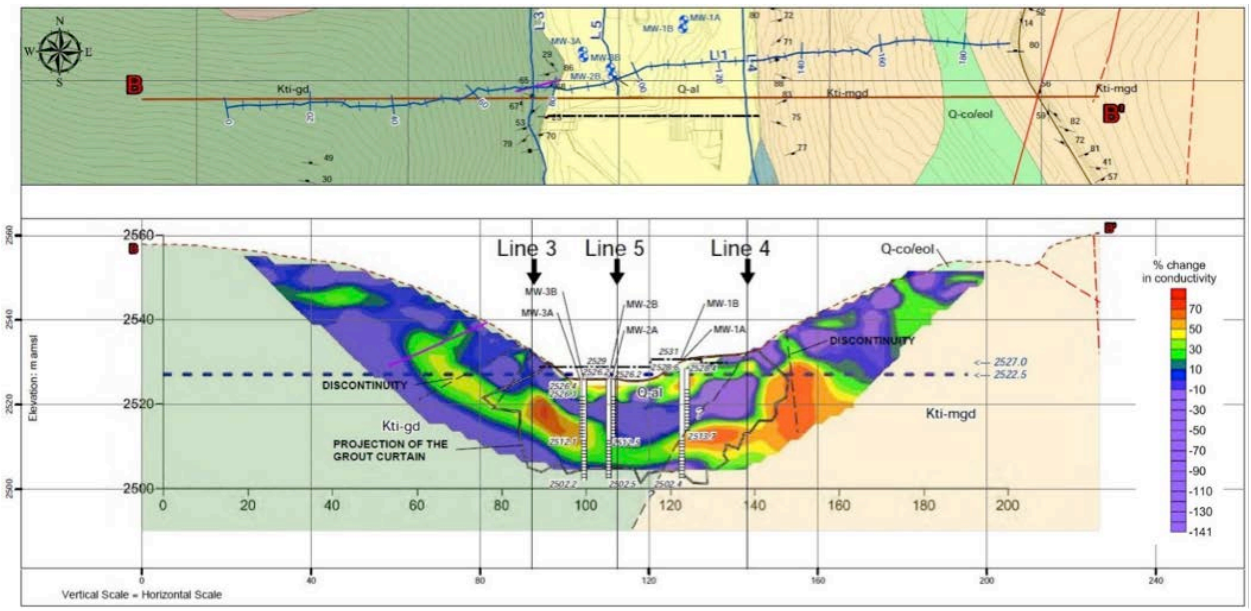


Figure 5: Percentage change in resistivity at L1

Figure 5 displays changes in electrical resistivity as percent change from the baseline resistivity survey to the final rising-head test survey at L1. The green to red colors indicate an increase in conductivity (decrease in resistivity). In areas near and above the water table, this may be an indication of change in moisture content – essentially an increase in the water table. However, much of the change

observed in the L1 cross section appears to be below the water table, which would indicate almost exclusively an increase in TDS. The most expanded region with increasing conductivity is along the right abutment, in the vicinity of a mapped geologic contact.

While the addition of relatively low TDS river water to the reservoir could potentially result in reduced conductivity (hence less green to red colors in Figure 5, it is likely that there were residual dissolved solids that were mobilized down gradient with the increase in water levels. This fits a conceptual model of the reservoir water pushing the concentration of high TDS water radially outwards, with dilution in the center and increased concentrations along its periphery.

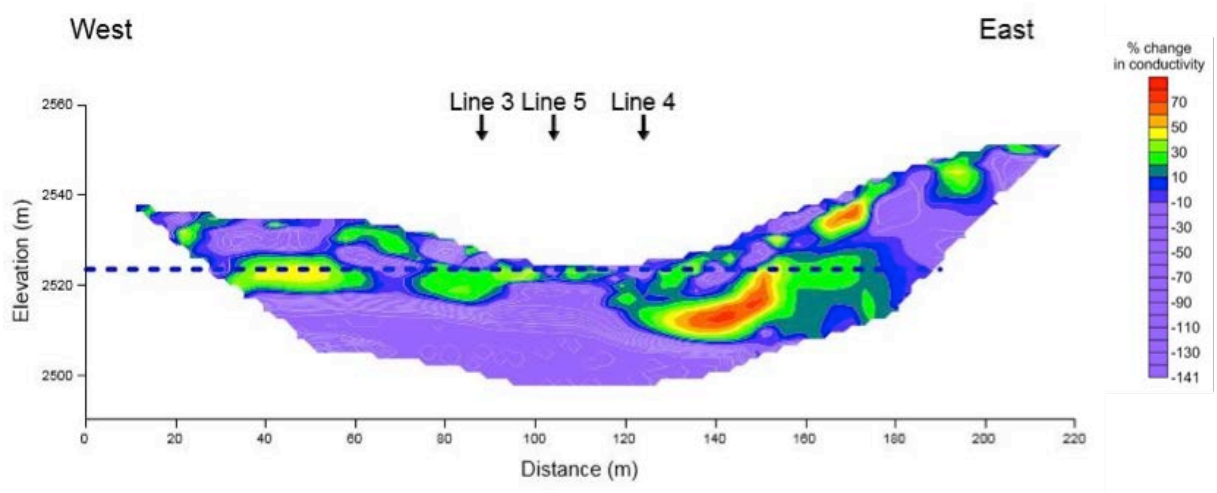


Figure 6: Percentage change in resistivity at L2

Changes in conductivity at L2 are displayed in Figure 6. A horizon of increased conductivity is observed across the elevation of approximately 2,520 m amsl. This is likely an indication of increasing water levels in the aquifer, showing a region of increased water content. The relatively moderate percentage of increase (less than 50 percent) may reflect this type of conductivity increase. However, the increased conductivity along the right side of the cross section (particularly the increase below the water table) is likely a function of migrating high TDS water. The high TDS water is forced outwards by the increasing water levels in the dam and the resultant increase in water levels in the aquifer.

Changes in conductivity observed at L3, as displayed in Figure 7, appear to behave similar to L2. Most of the increases in subsurface conductivity are observed below the water table in close proximity to existing high conductivity (low resistivity) zones. Increasing heads in the reservoir appear to have forced some water out and downwards into the left abutment. Moderate conductivity increases appear near the water table in the alluvium down gradient of the dam, while greater increases in conductivity are observed below the water table.

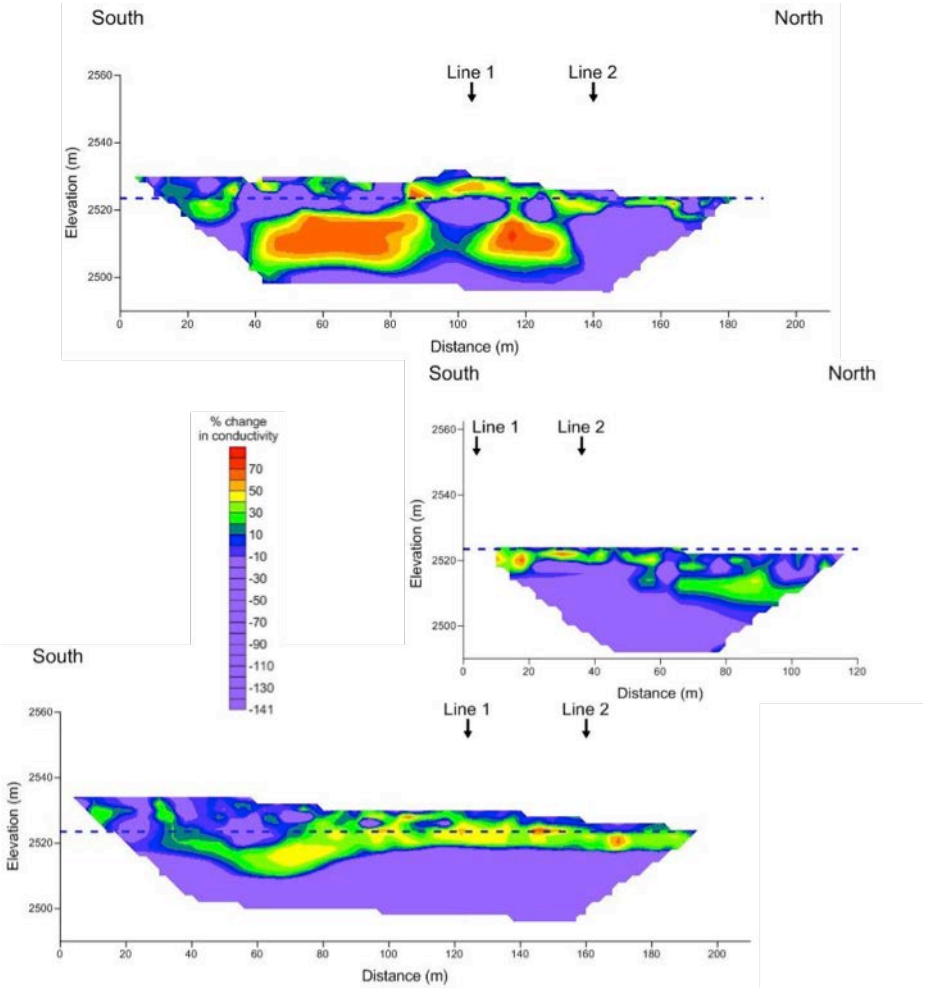


Figure 7: Percentage change in resistivity, from top to bottom; L3, L5, and L4

Changes in conductivity observed at L4, as displayed in Figure 7, show an almost continuous horizon of increased conductivity. Most of the increased conductivity is observed below, but in close proximity to the water table. This suggests that within this region of the subsurface there is a relatively continuous pathway for the migration of high TDS water. It is also important to note that the changes in conductivity through the horizon are very small. This modest percentage increase across the area is likely a function of the already high conductivity water present in that horizon.

Conductivity changes observed at L5, as displayed in Figure 7, are moderate. On the southern half of the line, the conductivity changes appear similar to those observed along L4, possibly a function of the already high conductivity water within the alluvium. Most of the changes also appear to be in close proximity to the water table, where only small changes would be expected as a result of increased moisture content. On the northern half of the survey line, small conductivity changes were observed well below the water table. These are likely the result of high TDS migrating down gradient. However, the

percentage increase in conductivity is relatively low, indicating that this water may be becoming more dilute by mixing with native groundwater.

Conclusions

A seepage investigation was completed both downstream and upstream of the Dam in late 2016 and early 2017 in response to regulatory findings that indicated low pH and high sulphate water was present in a shallow piezometer located downstream of the dam. The mine proactively began investigations shortly following the regulatory finding to determine the causes of the poor water quality. The investigations included:

- Drilling of six new wells downstream and four new wells upstream of the dam.
- Detailed geologic mapping in the vicinity of the dam.
- Rising-head test in the sump to add hydraulic stress to the groundwater system.
- Time-lapse geophysical resistivity surveys.
- Sampling for groundwater chemistry including isotopes that were used as tracers.

Evaluation of the investigation data provided clear indications that there are multiple components causing seepage beyond the dam. These include loss of very small but continuous volumes of water from the sump, and a groundwater flow component from upstream that is sourcing PLS-impacted groundwater through the right abutment to the downstream location. The combination of seepage from the dam and PLS-impacted groundwater bypass is causing groundwater downstream of the dam to have low pH and elevated sulphate, even though the previous grouting campaign in 2007 greatly reduced this source of contamination. The results of the investigation also provided valuable information pertaining to a geologic contact between the left abutment granodiorite and right abutment monzo-granodiorite. The granodiorite on the left side of the dam is strong, and has less weathering with a slight fracture tabular form and interlocking joints presenting a pseudo-stratification. On the right side of the dam, the rock is characterized as rounded with more weathering in the joints and is weaker. The contact between the granodiorite and monzo-granodiorite is thought to create a preferential pathway to groundwater flow.

The extent of impacted groundwater downstream of the dam is localized as pH levels rebound to natural levels within several hundred meters downstream, indicating that the system has good neutralization capacity. However, for on-going operations, an enhanced seepage containment system will be necessary.

Chapter 3:
Regulatory and Social Challenges



Proceedings of Mine Water Solutions 2018
June 12–15, 2018, Vancouver, Canada
Published by the University of British Columbia, 2018

Performance Review of a Passive Treatment System for Fe, As, and Mn at the Empire Mine State Historic Park

Neal Gallagher, Golder Associates Inc., USA
Daniel Millsap, California Department of Parks and Recreation, USA
Steve Lofholm, Golder Associates Inc., USA
Tom Rutkowski, Golder Associates Inc., USA

Abstract

Empire Mine, located in Grass Valley, California, USA, was one of the richest hard rock gold mines in California. Over its 106-year life, the mine produced nearly 5.6 million ounces of gold before it closed in 1956. The mine property is operated by the California Department of Parks and Recreation as Empire Mine State Historic Park and contains 367 miles of now flooded underground workings. While the mine was active, the Magenta Drain Tunnel (portal) was used to dewater the underground workings. Following the mine's closure, mining influenced water (MIW) continues to discharge from the portal. Flow rate from the portal varies seasonally and contains arsenic, iron, and manganese in excess of Federal and State primary and secondary drinking water standards. National Pollutant Discharge Elimination System (NPDES) permit limits for arsenic, iron, and manganese from the portal flow are 10, 300, and 50 micrograms per liter (µg/L) respectively. A full-scale passive treatment system (PTS), which has been in operation since November 2011, was designed and constructed to treat MIW from the portal to meet the NPDES permit limits. The PTS consists of a 0.5 acre settling pond, followed by a 1-acre aerobic wetland, and a 1.2-acre horizontal-flow manganese removal bed (MRB). PTS flowrate varies seasonally, and has averaged 155 gallons per minute (gpm) with a peak of 1,200 gpm. Metal removal results in the system have improved over time since start-up, corresponding with maturation of the PTS. Since February 2013, the PTS has provided effective removal of permitted metals to trace levels. During this time arsenic, iron, and manganese in PTS influent averaged 75 µg/L, 5,492 µg/L, and 2,385 µg/L, respectively. PTS effluent averaged 3 µg/L, 34 µg/L, and 11 µg/L, respectively. In addition to metals removal, flow through the PTS has also provided the benefit of increased pH, increased dissolved oxygen, and reduced turbidity. Site background information and a review of PTS performance with respect to arsenic, iron, and manganese is presented.

Introduction

Empire Mine, located in Grass Valley, California, USA, was one of the richest hard rock gold mines in California. Over its 106-year life, the mine produced nearly 5.6 million ounces of gold before it closed in 1956. The 856-acre mine property is operated by the California Department of Parks and Recreation as Empire Mine State Historic Park and contains 367 miles of now flooded underground workings. While the mine was active, the Magenta Drain Tunnel (portal) was used to dewater the underground workings. Following the mine's closure, mining influenced water (MIW) continues to discharge from the portal. Flow rate from the portal varies seasonally and contains elevated concentrations of arsenic, iron, and manganese. The discharge permit limits for arsenic, iron, and manganese from the portal flow are 10, 300, and 50 µg/L, respectively. The arsenic limit is equal to the EPA Primary Drinking Water Standard. The iron and manganese limits are equal to the EPA Secondary Drinking Water Standard.

A full-scale passive treatment system (PTS) has been in operation since November 2011 to treat MIW from the portal to meet the discharge permit requirements. The PTS consists of a 0.5 acre settling pond (SP), followed by a 1-acre aerobic wetland (W1), and a 1.2-acre horizontal-flow manganese removal bed (MRB and/or W2). The bulk of iron and arsenic are removed in the settling pond through precipitation and co-precipitation mechanisms, respectively. Polishing of iron and arsenic precipitates occurs early in the aerobic wetland flow path. The primary manganese removal mechanism is oxidation and precipitation of manganese dioxide. Manganese removal occurs in the latter portions of the aerobic wetland and through the manganese removal bed. The PTS influent design basis is provided in Table 1. Detailed results are presented for flow, iron, arsenic, and manganese. However, all parameters have consistently achieved permit conditions since operation began.

Table 1: Influent design basis

Parameter/criteria	Measured value	Discharge permit limits
Maximum design flow, gpm	1,200	–
Average design flow, gpm	230	–
pH, s.u.	7	>6.5, <8.5
Dissolved oxygen, mg/L	–	>7 mg/L, >85% saturation
Turbidity, NTU	96	5 NTU
Maximum influent iron concentration, µg/L	25,000	300, annual average
Maximum influent arsenic concentration, µg/L	301	10, monthly average
Maximum influent manganese concentration, µg/L	4,900	50, annual average

A site overview is provided in Figure 1. A conceptual model of the site including the water treatment system is provided in Figure 2. Figures 3, 4, and 5 show the settling pond outfall, aerobic wetland, and MRB, respectively.

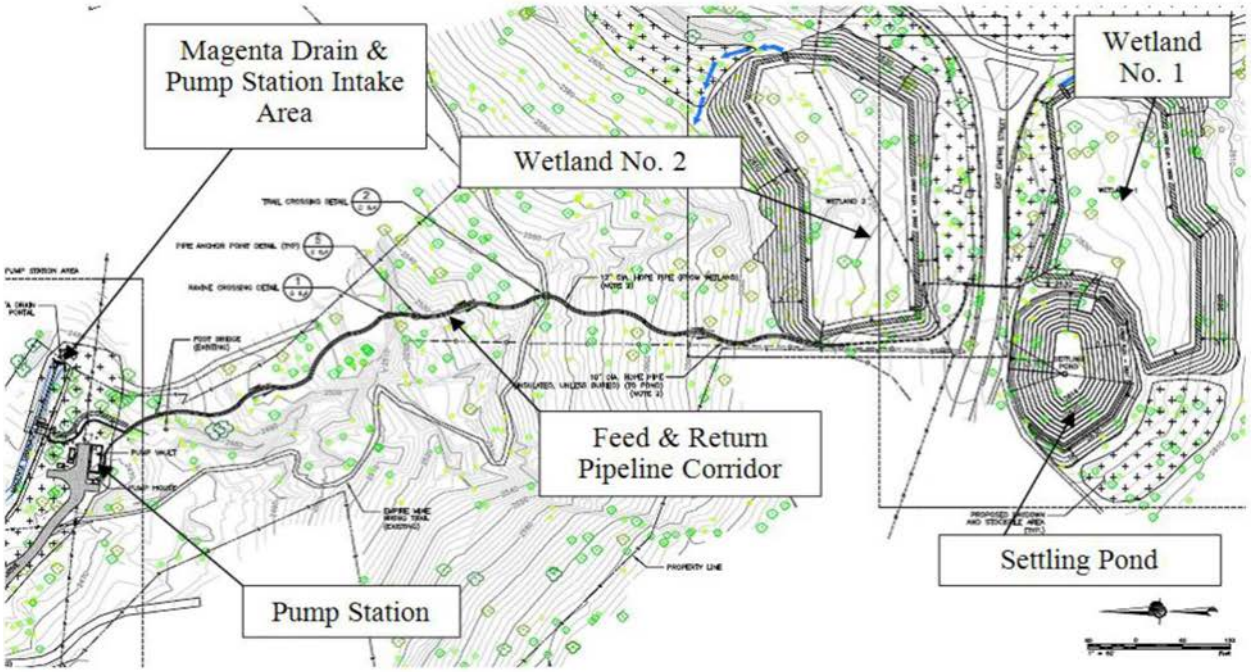


Figure 1: Magenta Drain passive treatment system site overview

Flow rates

The PTS experiences highly variable flow rates due to source water coming from mine working, which provide some attenuation of runoff from precipitation events; the regional climate, which is characterized by a winter wet season; a long, dry period from late spring through fall; and drought conditions which occurred from 2011 through 2016. Effluent flow rates are provided in Figure 6. The drought ended in winter of 2016/2017, and flow rates at the treatment system increased to a maximum flow of 1,200 gpm in February 2017 (this flow was an instantaneous measurement, not shown in Figure 6).

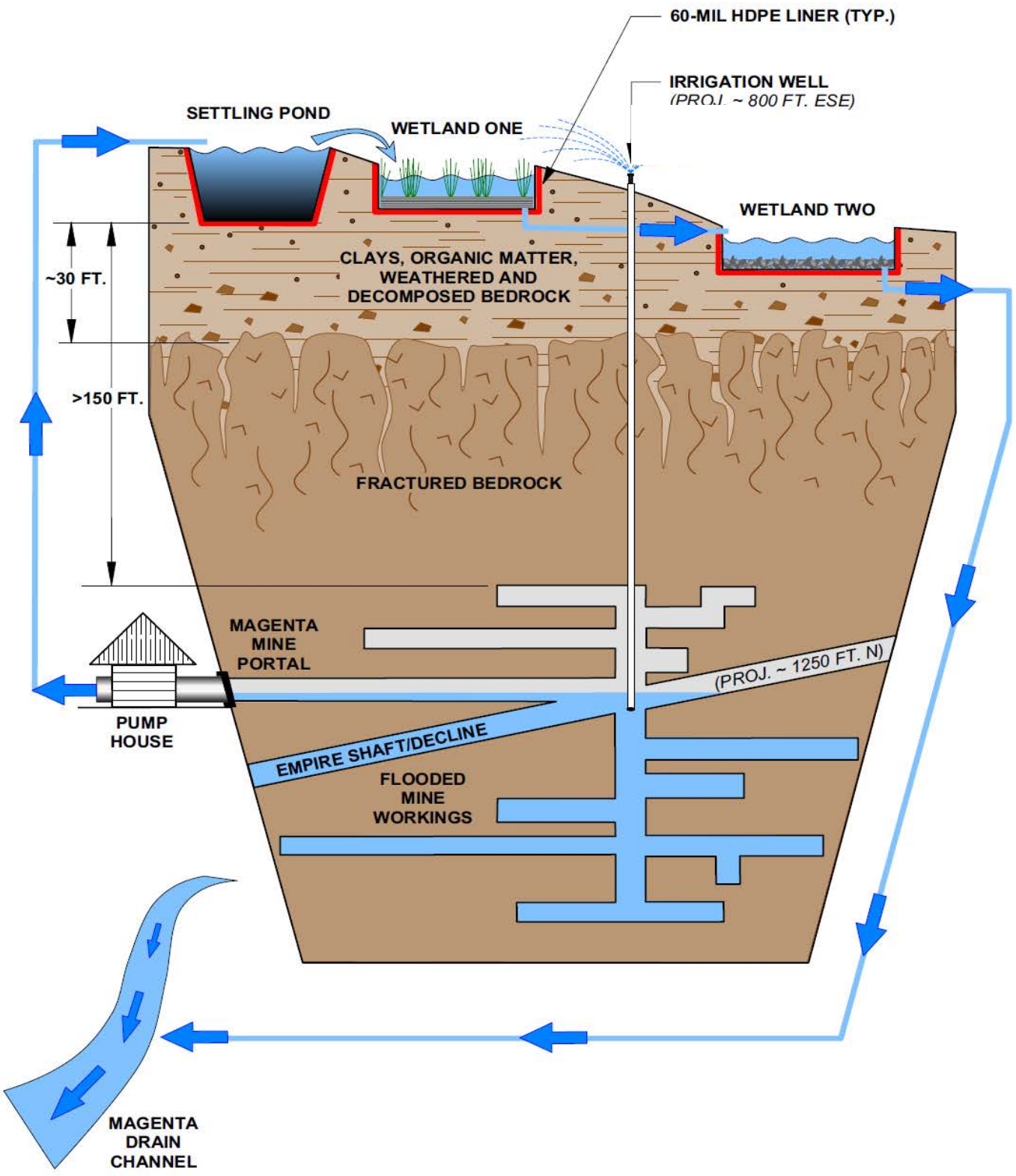


Figure 2: Conceptual site model



Figure 3: Settling pond outfall



Figure 4: Aerobic wetland



Figure 5: Manganese Removal Bed (MRB)

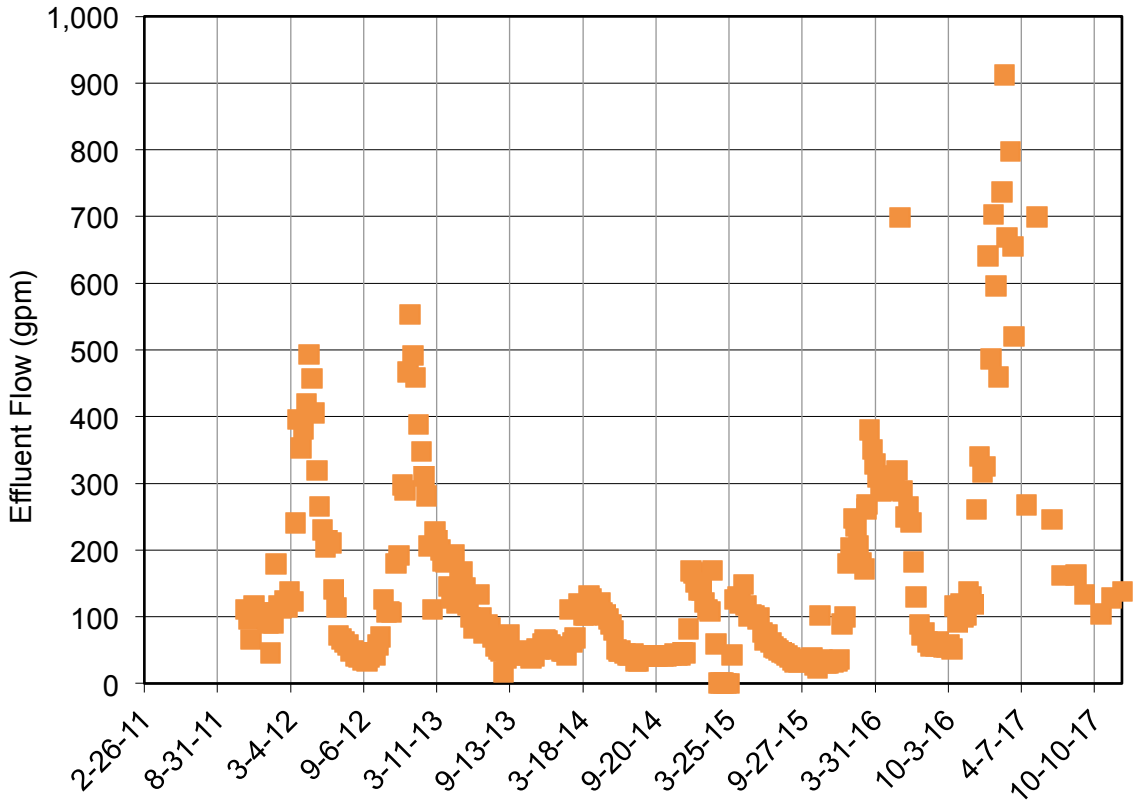


Figure 6: Discharge flow rate

Performance Results

The performance results presented focus on arsenic, iron, and manganese.

Arsenic

Arsenic concentrations throughout the system are provided in Figure 7 for the period from November 2011 to November 2017. Effluent arsenic concentrations have been consistently below the stringent discharge standard of 10 ug/L since April 2012. Higher concentrations prior to this date are attributed to the start-up period, during which the PTS became established and was maturing. The primary arsenic removal mechanism is attributed to co-precipitation with iron. The ratio of iron to arsenic in the influent is approximately 77:1. Iron to arsenic ratios for effective arsenic removal via iron co-precipitation are typically water specific. Arsenic removal via co-precipitation with iron is most effective when arsenic is in the form of arsenate (Bowell, 2003). The bulk of the arsenic removal occurs in the settling pond and aerobic wetland, closely mirroring iron removal.

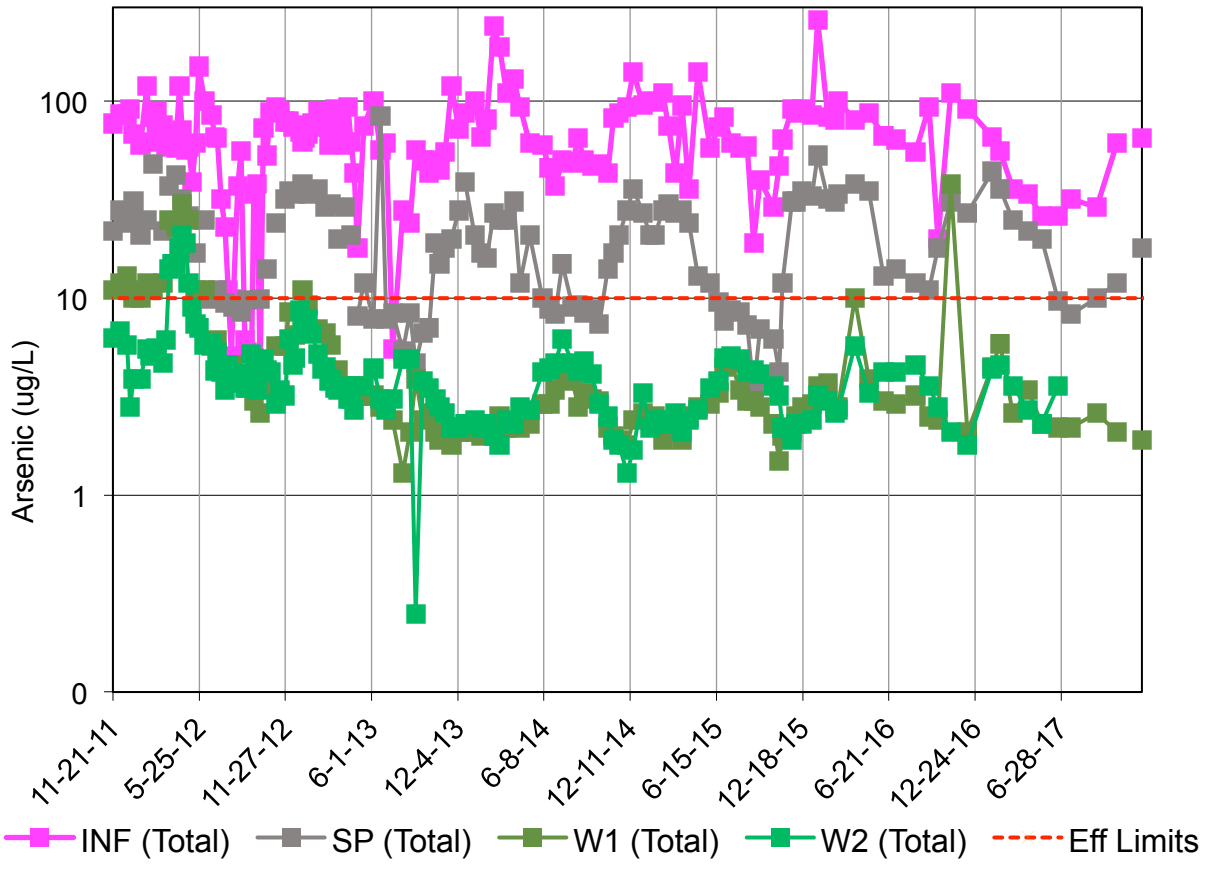


Figure 7: Arsenic performance

Iron

Effluent iron has been below the discharge limit consistently since April 2012. Iron concentrations throughout the system are provided in Figure 8. Iron removal occurs via oxidation and precipitation of ferric iron hydroxide. Both of these processes occur in the settling pond and aerobic wetland. Removal in the aerobic wetland also occurs via filtration as the water flows through dense vegetation. Iron removal rates in the wetland average 0.2 gram per square meter per day ($g/m^2/day$) and have a maximum of 1.9 $g/m^2/day$, which is well below the published rate of 10 $g/m^2/day$ (Kadlec and Wallace, 2009).

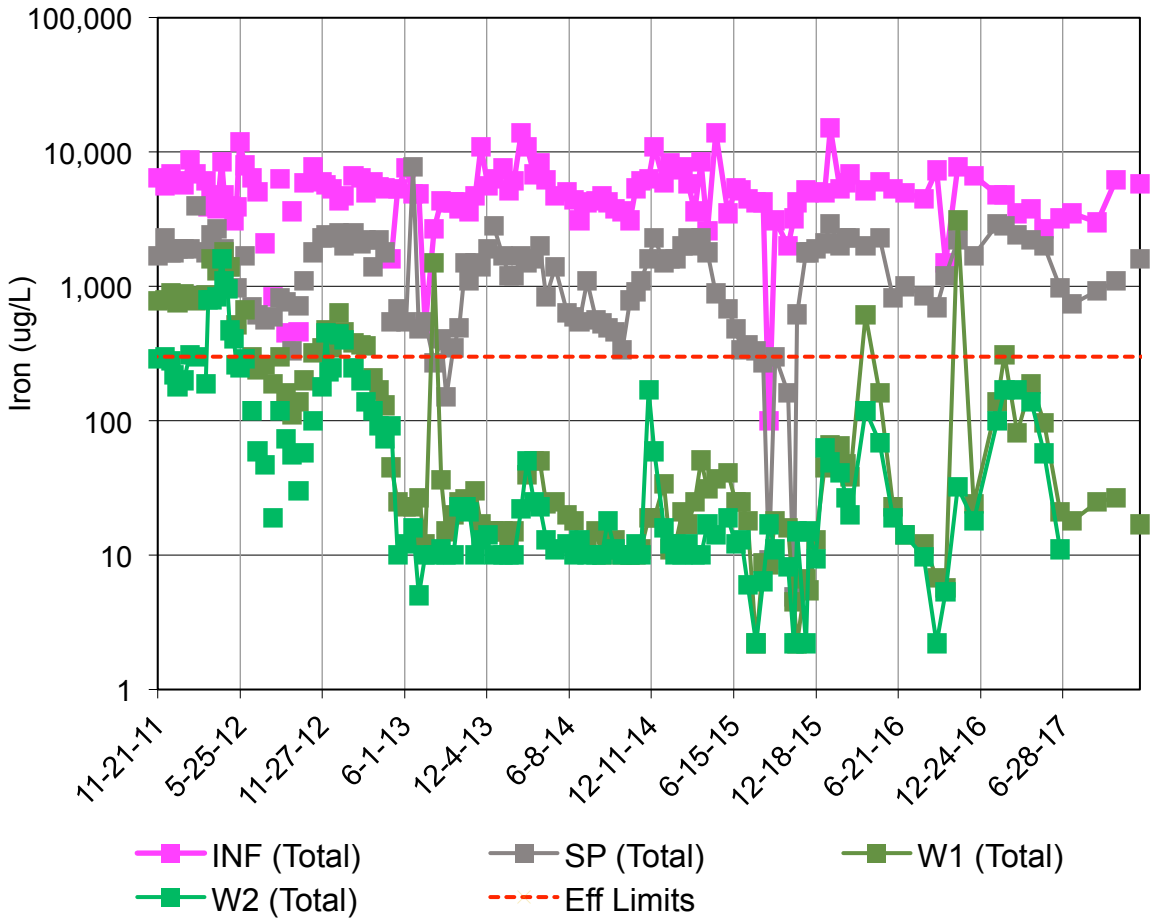


Figure 8: Iron performance

Manganese

Effluent manganese has consistently achieved the discharge permit limit of 50 ug/L in the post-start-up period. Manganese concentrations throughout the system are presented in Figure 9. A few effluent values have exceeded the permit limit in 2016 and 2017, but the annual average values have been in compliance with the permit limit. The primary manganese removal mechanism is oxidation and precipitation of

manganese dioxide. This system is notable for achieving very stringent effluent limits for manganese. Unlike iron and arsenic, little manganese removal occurs in the settling pond, and the majority of the removal occurs in the aerobic wetland. The system design did not assume that significant removal of manganese would occur in the aerobic wetland. However, because of the loading rates, removal in the aerobic wetland is typically sufficient to meet the permit limit. As a result, the influent to the manganese removal bed is typically very low, below 50 ug/L. Effluent from the manganese removal bed has been less than 1 ug/L, and is typically below detection.

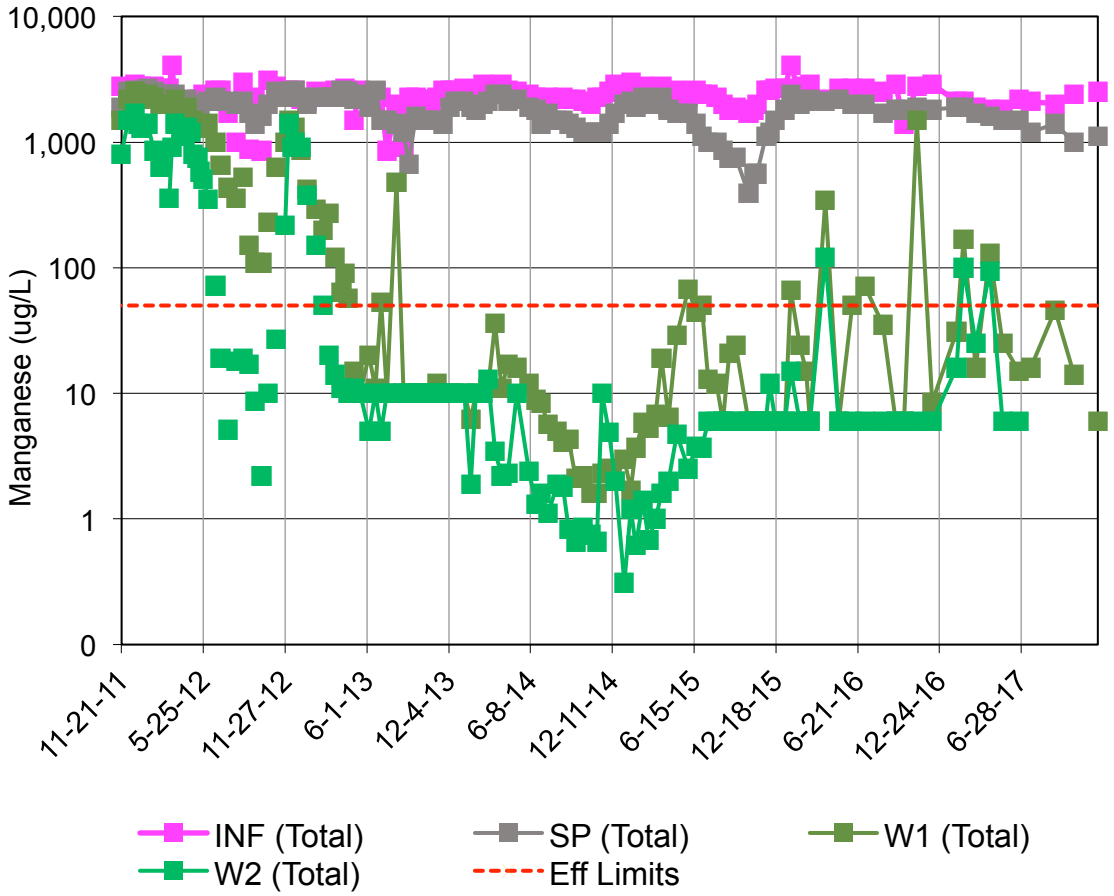


Figure 9: Manganese performance

In both aerobic wetlands and manganese removal beds, manganese removal occurs via the reaction presented in Equation 1.

$$Mn^{2+} + 0.5O_2 + H_2O = MnO_2 + 2H^+ (1) \qquad \text{Equation 1}$$

Published zero order removal rates for manganese in aerobic wetlands range from 0.5 to 1.0 g/m^2/d (Hedin et al., 1994). The average and maximum removal rates observed for the aerobic wetland are 0.32

and 1.97 g/m^2/d, respectively, comparable to the published ranges. In manganese removal beds, Mn removal is catalyzed by bacteria and Mn oxide surfaces, supported by constant pH and oxygen saturation. Figure 10 provides a visual of the dark precipitate coating on the limestone rock within the MRB, likely containing manganese oxide precipitate.



Figure 10: Precipitate coating in manganese removal bed

The rate of Mn removal from solution can be expressed as shown in Equation 2 (Means and Rose, 2005).

$$d[Mn]/dt = k\,[Mn][MnO_2]\ (2) \qquad \text{Equation 2}$$

Where:

[Mn] is the concentration of Mn in solution

[MnO_2] is the surface area of Mn oxide (including the effect of bacteria)

k is a rate constant and t is time

A first order removal equation has been empirically developed for manganese removal beds, as presented in Equation (3).

$$2.3 \text{ Log } (C/C_0) = -k_1ST \quad (3) \qquad \text{Equation 3}$$

Where:

C is effluent

C_0 is initial concentration

k_1 is a rate constant

S is the size fraction of limestone rock

T is retention time

A study of multiple removal systems in the Eastern US provided a k_1 value of 0.0004 m/hr ($10^{-3.35}$ m/hr) (Means and Rose, 2005). Measured first order rate constants (k_1) and temperature for the MRB, based on total Mn removal, are shown in Figure 11**.** The measured rate constant (k_1) ranged from near zero when the influent manganese was very low, up to 0.009 m/hr ($10^{-2.04}$ m/hr). Correlation of rate constant with temperature is observed during the initial operational period, through spring 2014. This correlation is not as strong after spring 2014, attributed to the impacts on rate constant calculations from MRB influent and effluent values typically measured near or below the analytical detection limit during this time.

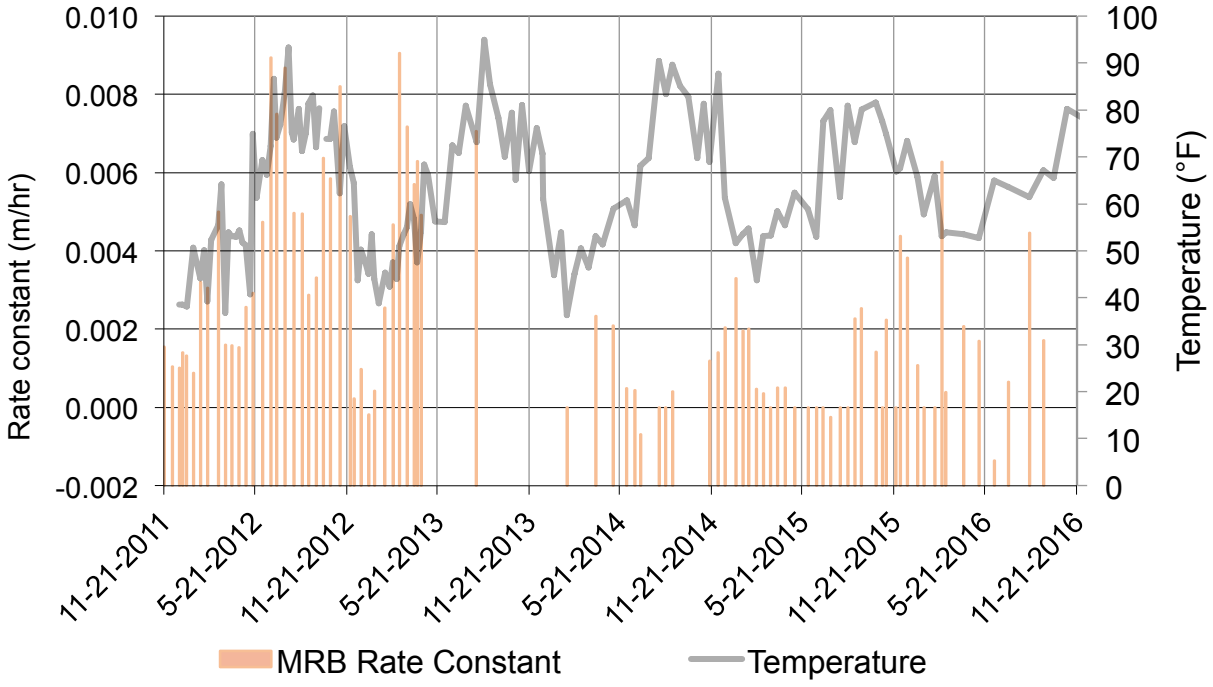


Figure 11: Temperature and manganese removal rate constant

Conclusion

The Magenta Drain Passive treatment system includes a settling pond, aerobic wetland, and manganese removal bed, and is effective at meeting the primary drinking water standard of 10 ug/L for arsenic and secondary drinking water standards of 300 ug/L for iron and 50 ug/L for manganese. The system has been effectively operating for more than six years since start-up in 2011, through very low flow periods associated with experienced drought conditions, as well as through high flow conditions during the post-drought 2016/2017 winter wet season. Zero and first order removal rates for iron and manganese are comparable to literature values in some instances, and lower than the literature values due to low influent loading in other instances. The low loading rates are reflective of the highly variable flow rate, which causes periods of low metal loading to treatment processes during low flow conditions and a conservative design that was necessitated by the very low discharge standards. This system is notable as an example of effective passive treatment to achieve the stringent primary drinking water standard limit for arsenic, and secondary drinking water standards for manganese and iron of 50 and 300 ug/L, respectively.

References

Bowell, R. 2003. The influence of speciation in the removal of arsenic from mine waters, *Land Contamination & Reclamation* 11(2): 231–238.

Hedin, R.S., Nairn, R.W. and Kleinmann, R.L.P. 1994. *Passive treatment of coal mine drainage.* US Bureau of Mines, Information Circular 9389, 35 pp.

Kadlec, R.H. and Wallace, S. 2009. *Treatment Wetlands,* Second Edition. CRC Press.

Means B. and Rose, A.W. 2005. Rate of manganese removal in limestone bed systems, *Proceedings of the National Meeting of the American Society of Mining and Reclamation,* Breckenridge, CO, June 19–23, 2005. Lexington, KY: ASMR.

Chapter 4:
Water as a Valued Asset



Proceedings of Mine Water Solutions 2018
June 12–15, 2018, Vancouver, Canada
Published by the University of British Columbia, 2018

New Tailings Encapsulation Methods Could Pave the Way toward Safe Long-Term Stacking of Filtered Tailings

Donald J. Lake, Terra CO2 Technologies Ltd., Canada
Lee A. Groat, The University of British Columbia, Canada

Abstract

Mine tailings are often stored underwater behind earthen dams; this is effective in the short term, but failure of these structures typically causes significant environmental damage. Dry stacking of filtered tailings is a promising alternative to traditional slurry tailings storage facilities, but limited mostly to very arid locations. A widely applicable fail-safe solution is needed. Siderite ($FeCO_3$) encapsulation of tailings is one such alternative that may prevent filtered tailings from contaminating water in a broader range of climates by buffering alkalinity and preventing oxidation of the tailings. To evaluate the preliminary feasibility of carbonate coating tailings, we synthesized siderite coatings (~10 μm) at room temperature using a novel system. We coated glass rods (100–200 μm) and assessed the stability of siderite coating material. As an indicator of water quality, we analyzed iron content and pH of leachate from siderite immersed in sulphuric acid solutions (pH 2–4) for 300 days. This paper presents our findings and further research that will be required to evaluate this technique.

We were able to coat glass rods with siderite, which is a first step towards coating complex mineral surfaces. We found that the leachate from aqueous storage of siderite had moderate pH and extremely low total iron concentrations when the starting pH was 2.5 or greater and the water:rock ratio was 37.5. In both acidic aqueous and air storage, the siderite oxidized to goethite and ferrihydrite within a period of 300 days. In conclusion, siderite is a promising coating material that merits further investigation. Future studies will need to consider the impact on coating integrity of anoxic storage and siderite conversion to ferrihydrite with oxic storage. During the transition of siderite to ferrihydrite there is potential for significant cation adsorption, which may have implications for improving water quality, but it is not yet known whether cation adsorption affects the maturation of ferrihydrite to more stable iron oxide phases that we consider likely to be suitable for long-term tailings encapsulation.

Introduction

Dry stacking of filtered tailings has been praised as a potential panacea for long-term tailings storage, especially in light of recent high-profile tailings dam failures. Unfortunately, dry-stacking techniques have shortfalls that limit their practical application for long-term tailings storage at many sites worldwide (Davies 2011). These failings include unwanted oxidation and leaching of potentially reactive tailings elements, which is a risk factor in dry-stacking operations due to availability of humidity and oxygen in the environment. Additionally, dry-stacked tailings can be mechanically unstable and vulnerable to erosional forces (e.g., wind). From the perspective of cost and preventing oxidation, underwater storage and sealed impoundments have traditionally been preferred solutions for tailings storage. However, despite potential cost advantages, dams also pose the risk of catastrophic breaches (e.g., Mt. Polley, Canada). Even ignoring the potential for human error in tailings dam construction, it is difficult to assure the required perpetual maintenance and treatment of such a facility – considering maintenance continuity must be assured through changes in government and generations of engineers, enduring longer than most financial and government institutions have been stable.

There has been significant pressure from the international community to improve upon the imperfect safety record of tailings dams (UNEP and GRID-Alenda, 2017). Fortunately, filtered tailings can address many of the safety concerns, though there is still room for improvement. To potentially provide a viable low-maintenance alternative to existing mine closure options, we synthesized siderite to encapsulate tailings and measured the effect of the coating material on water quality. This paper describes the feasibility of coating simulated tailings particles with a thin layer of siderite in an aqueous reactor. We tested the effect of siderite on water quality in a range of acidic oxidizing environments, and we speculate on the potential for cementing coated particles to form a cap on existing tailings storage facilities.

Materials and Methods

Synthesizing Siderite ($FeCO_3$) Coatings

Siderite coatings were synthesized and aged for 24 hours on glass substrates in an aqueous reactor at low temperature. Reagents were simulated iron sulphide acid rock drainage (ARD) prepared with laboratory-grade 0.1 M $FeSO_4$ and H_2SO_4 (pH 3) to provide divalent iron and sodium bicarbonate ($NaHCO_3$) as a pH-modifier and source of aqueous CO_2 for the synthesis of siderite. We used an aqueous reactor under CO_2 atmosphere and microcontroller-programmed peristaltic dosing to maintain synthesis conditions. With the goal of producing bicarbonate "on site" from CO_2 (ideally sourced from the atmosphere or flue gas), we used a novel electrochemical means of converting CO_2 to bicarbonate (Figure 1; Lake et al., 2017a), allowing siderite precipitation directly from the simulated tailings effluent. Figure 1 shows

several key components of the experimental system. The goal of the electrochemical approach is to produce relatively cheap alkalinity and reduce shipping of reagents to remote sites, although conventional purchased reagents (i.e., alkali salts with anions O^{2-}, OH^{-}, CO_3^{2-}, and HCO_3^{-}) are easily substituted when an electrochemical solution is impractical.

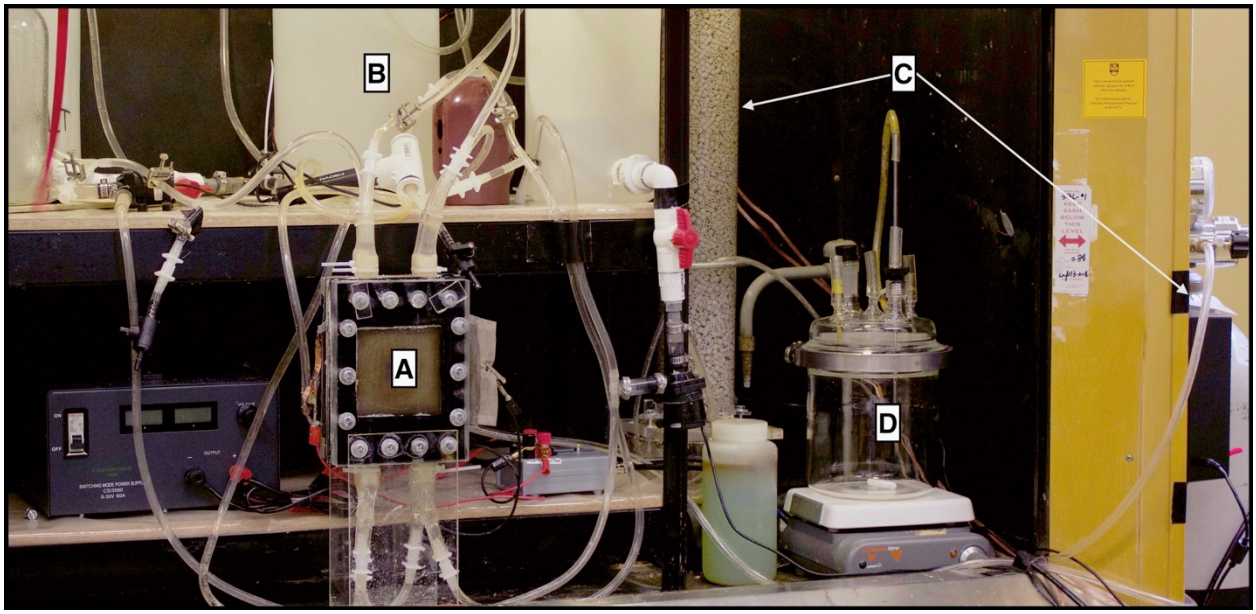


Figure 1: Electrochemical system producing alkalinity for the synthesis of siderite.
A is an electrolytic cell, B indicates storage tanks holding electrolyte, acid/bicarbonate, and simulated ARD, C points to a CO_2 tank and absorption column in line with the electrochemical cell, and D is the reaction vessel

The siderite coatings were precipitated on glass rods placed in the reactor. Glass was chosen as a substrate because it has a relatively high surface energy that simulates very approximately the surface properties of wetted or modified tailings mineral surfaces. For these preliminary experiments, a glass substrate was also used to control for any unwanted chemical interaction in the aqueous reactor that could be introduced with complex tailings minerals. Naturally these potential interactions must be explored in future work.

Siderite Stability and Impact on Water Quality

To analyze the effect our siderite coating material would have on water quality in a simulated tailings environment, we subjected the powder (1–40 µm particle size) to concentrations of H_2SO_4 with pH 2–4. The H_2SO_4 was prepared by mixing laboratory-grade sulphuric acid with distilled water (in equilibrium with air). No effort was made to prevent oxidation over the 300-day experiment in order to simulate near-surface acidic oxidizing conditions that could occur in tailings storage. Synthesized $FeCO_3$ (0.4 g) was added to five 15 mL vials of H_2SO_4 at starting acidities of pH 2 through 4 (0.5 increments). Starting pH

and temperature were measured before adding $FeCO_3$; after 300 days the same measurements were made, in both cases with a calibrated Barnant 30 pH meter. The samples were sealed, kept in the dark at ~20 °C, and agitated thoroughly for several seconds each month.

We measured the total iron concentration in the decanted water samples after 300 days with a Varian 725-ES ICP-OES instrument after passing the sample through a 1 μm filter. The samples were not acidified. Ten standards (in the range 0.781–200 ppm) and a blank were prepared with a $FeSO_4$–H_2SO_4 matrix at pH 3, which was chosen as an intermediate pH.

Coating Mineral Identification and Observation

For identification of the coating mineral before and after 300 days exposure to acidic oxidizing conditions, we collected X-ray powder-diffraction data over a range of 3 to 80° 2θ (scanning step of 0.048 2θ) with Cu*K*α radiation (35 kV and 40 mA) using a Bruker D8 Focus Bragg-Brentano diffractometer equipped with a graphite monochromator. Samples were first homogenized under ethanol with an agate mortar.

We inspected cross-sections of coatings (one week after synthesis) with a Philips XL30 scanning electron microscope (SEM) at the University of British Columbia at 15 kV beam voltage. The siderite-coated glass rods were set in epoxy pucks and sectioned. We ground and polished the samples instead of examining a fresh broken surface in order to qualitatively examine how the coatings might mechanically fail under abrasion (note the chipped and fractured edges of the glass rod in Figure 2).

Results

Coatings

The siderite coatings are 10–20 μm in thickness and adhered to the glass rod substrate that was suspended in the reactor; the left side of Figure 2A was the underside in the reactor and Figure 2B shows the coating in detail. Figures 2C and 2D are roughly the same field of view: surface roughness is illustrated using SE imaging (Figure 2C) and BSE imaging discerns the $FeCO_3$ coating as bright white against the lower mean atomic number glass substrate (Figures 2A, 2B, and 2D). There are abundant cracks in the coating; most cracks abruptly change direction before reaching the inner glass rod (Figure 2B), leaving a largely undisturbed carbonate film ~1 μm thick. The cracks traverse microsphere boundaries indicating that adherence between siderite microspheres is at least as strong as the microspheres themselves (e.g., Figure 2C). The origin of the cracks in the coating is not conclusively known, but is probably due to abrasion during grinding and polishing, or dehydration of remnant hydrous phases in the carbonate microspheres.

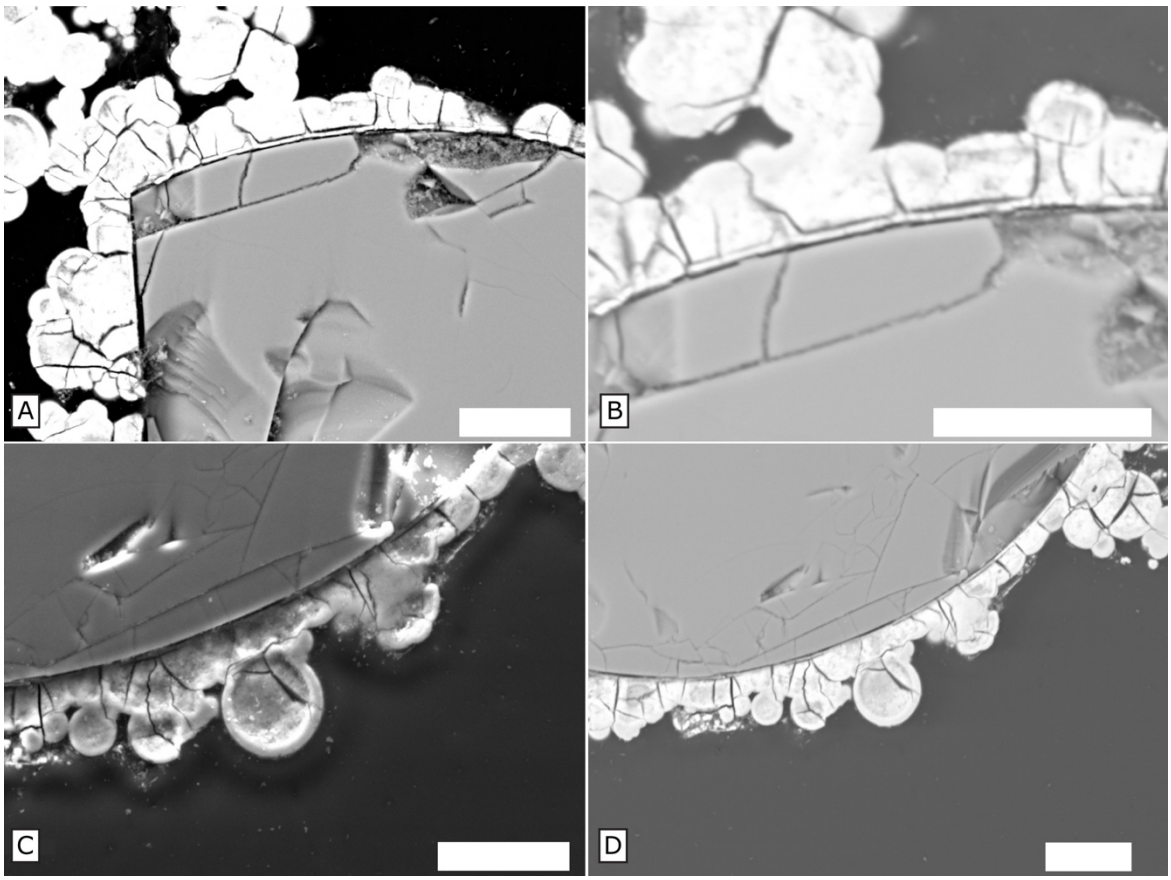


Figure 2: SEM images of siderite on glass substrate (20 µm scale bar)

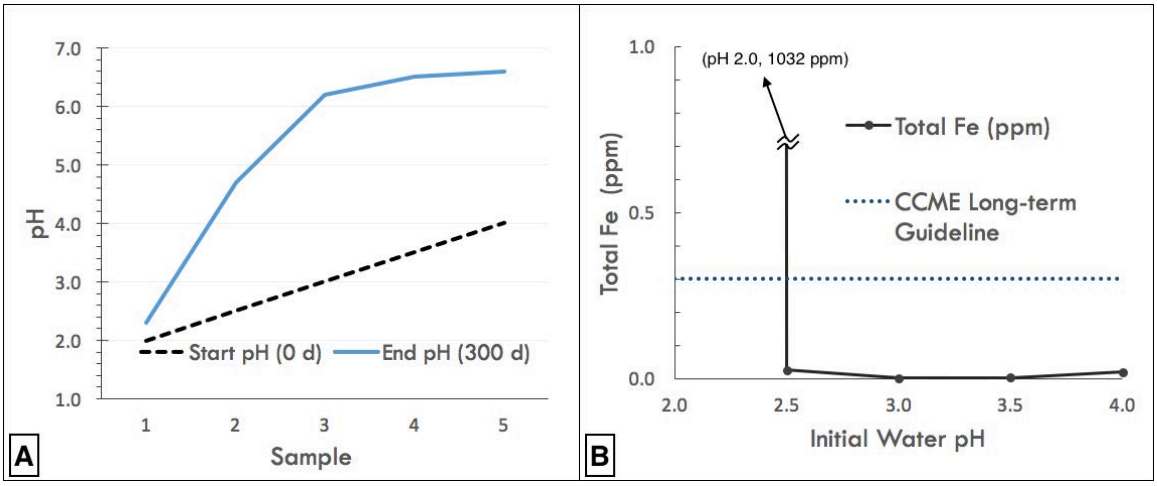


Figure 3: Siderite increases water pH and resists leaching iron

Siderite Impact on Water pH and Total Iron

Siderite powder (1–40 µm) raised the pH of waters containing sulphuric acid (Table 1, Figure 3A), and <0.02 ppm total iron was detected when the starting pH was 2.5 and greater (with a water-rock ratio of 37.5 for all samples, Figure 3B). The pH 3 and 3.5 samples have pH > 6 and very low iron concentrations

with error on the same magnitude as the measured value (Table 1). The pH 2 sample was only barely buffered by the carbonate material and had a final pH of ~2.3, and iron was measured at over 1,000 ppm for this sample. Clearly, the carbonate pH buffer can be overcome and iron can be expected to dissolve under high enough H_3O^+ concentration and/or large enough water:rock ratio.

Table 1: Water quality after siderite immersion in acidic oxidizing conditions

Sample	Start pH	End pH – 300 d	Fe (ppm) – 300 d	2σ (ppm)
1	2.0	2.3	1032.5	1.612
2	2.5	4.7	0.027	0.004
3	3.0	6.2	0.002	0.003
4	3.5	6.5	0.003	0.005
5	4.0	6.6	0.020	0.005

Change in Mineralogy

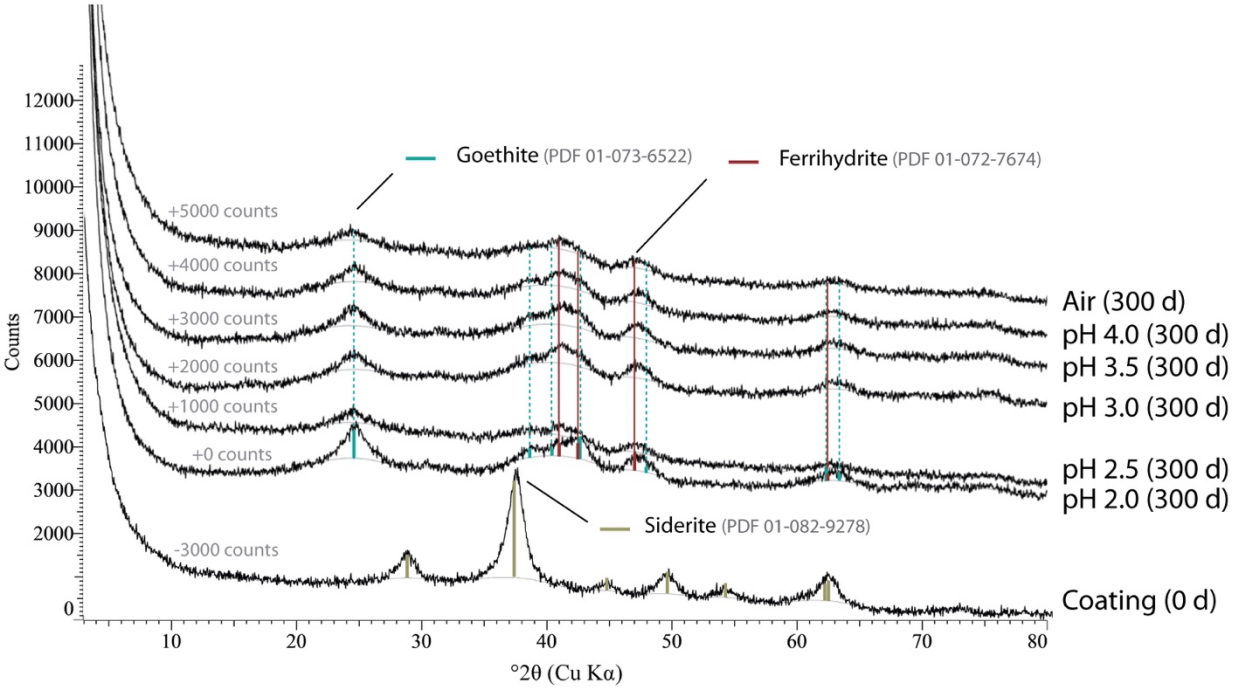


Figure 4: Siderite converts to a mixture of iron oxides over time

After 300 days, the siderite powder was completely converted to a mixture of goethite and ferrihydrite. Samples stored in sulphuric acid solutions with pH in the range 2–4 and a control sample stored in air have almost identical X-ray diffractograms (Figure 4). All samples show poorly defined broad peaks for goethite and intermediate compositions between 2-line and 6-line ferrihydrite (Schwertmann and Cornell,

2007), whereas the starting material was dominantly siderite (Figure 4, "Coating"). The low crystallinity suggested by the broad peaks is interpreted to be a combined function of small crystallite size as well as disordered structure. The pH 2.5 sample has systematically lower counts than other samples from $2\theta>30°$, which may be due to a less crystalline sample (as above), which is potentially a sample preparation effect (e.g., finer grinding).

Discussion

Carbonate Coating Considerations

Although we used an electrochemical system for bicarbonate production in this experiment, practical applications may easily substitute this process with purchased reagents. A minimum of one-hour aging the synthetic siderite precursor is required to produce stable siderite microspheres (Montes-Hernandez and François, 2016; Lake et al., 2017b), and aging for up to 24 hours or more seems to promote recrystallization along boundaries of siderite microspheres. Future work should attempt to coat more realistic tailings materials, such as gangue pyritic tailings rejected from flotation of ore minerals.

Siderite Impact on Water Quality

In samples with starting pH 2.5–4, total aqueous iron (< 1 μ filtered) was at least an order of magnitude lower than the Canadian Council of Ministers of the Environment (CCME) guidelines for long-term protection of aquatic life (0.3 ppm, CCREM, 1987). Water pH increased dramatically after 300 days for most samples, and this likely promoted oxygenation of ferrous iron (Singer and Stumm, 1968). The exception, a water sample that started at pH 2, only rose to pH 2.3 after 300 days and contained ~1033 ppm iron, with a noticeably yellow colour.

Effect of Siderite Transformation on Coating Effectiveness

Does it matter for tailings encapsulation that siderite is likely to transition to an oxide phase over time? Further experiments will definitively answer this question, but for now we may review several known factors that should be considered.

As long as pH is maintained over years to decades, ferrihydrite is known to age to more stable forms such as hematite or goethite, and this may provide heavy metal adsorption capacity in the interim (Schwertmann and Cornell, 2007). It is unknown whether cation adsorption interferes with ferrihydrite maturation. In any case, oxidation and oxide maturation should both be slow, depending on where and how the tailings are stored. Our initial siderite storage experiment was most representative of the oxic surface environment exposed tailings, whereas the depths of a storage facility are more likely to be

relatively anoxic. Over longer time-scales siderite may oxidize and mature to a stable rind, as in the similar natural analog of iron concretions in sandstone (e.g., Loope et al., 2010).

Potential advantages of the siderite to iron oxide transition are:

1. the interim pH buffering capacity of carbonate,
2. the presumed enormous capacity for metal (e.g., arsenic) and colloid adsorption by the initial ferrihydrite formation (Edwards and Benjamin, 1989, Schwertmann and Cornell, 2007); and
3. the likelihood that ferrihydrite will mature to a more stable iron oxide phase (Schwertmann and Cornell, 2007).

Based on this initial success, we are investigating whether the siderite to iron oxide transition is of any consequence to the coating integrity for coated tailings in realistic weathering scenarios.

Carbonate Cap Concept

If carbonate coatings on "high-risk" potentially acid generating (PAG) tailings prove to be successful, it should be possible to promote crystallization between coated particle surfaces and thereby "pave" over some existing tailings storage facilities with aggregates of coated particles to reduce water and oxygen infiltration. We speculate that such a cap could provide a cost-effective and long-lasting geological alternative to competing geomembrane materials such as high-density polyethylene (HDPE). As in the case of a geomembrane barrier, reclamation would also require a soil cover for revegetation. Preliminary testing of the carbonate cap hypothesis is ongoing.

Conclusion

We have synthesized siderite in an aqueous process and shown that it is a promising coating material for encapsulation of mine waste. We found that siderite has several advantageous properties, including a pH-buffering effect and the tendency to convert to goethite and ferrihydrite – phases with typically strong metal adsorption capacity and excellent stability in moderate pH waters. Over time ferrihydrite should mature to goethite or hematite, depending on the effect of cation adsorption on this process. Before siderite encapsulation of tailings can be proven for industrial use, future work must determine whether siderite and its eventual oxidation products can passivate a wide range of reactive mine tailings minerals over 100+ year time-scales and have a positive impact on water quality.

References

Canadian Council of Resource and Environment Ministers (CCREM). 1987. Canadian Water Quality Guidelines. Prepared by the Task Force on Water Quality Guidelines, Ottawa.

Davies, M. 2011. Filtered dry stacked tailings – the fundamentals, *Proceedings Tailings and Mine Waste,* Vancouver, Canada: 1–9.

Edwards, M. and Benjamin, M. 1989. Adsorptive filtration using coated sand: a new approach for treatment of metal-bearing wastes, *Research Journal of the Water Pollution Control Federation,* 61(9): 1523–533.

Lake, D.J., Groat, L.A., Carne, A. and Eaton, W.D. 2017a. Methods and systems using electrochemical cells for processing metal sulfate compounds from mine waste and sequestering CO_2. US Patent 9,695,050, issued July 4, 2017.

Lake, D.J., Groat, L.A., Gyenge, E., Carne, A. and Ritchie, J. 2017b. Siderite synthesis from iron-bearing acidic solutions combined with flue gases from combustion of fossil fuels. Poster presented at the GAC-MAC Annual Meeting, Kingston, ON, Canada, June 2017.

Loope, D., Kettler, R. and Weber, K. 2010. Follow the water: Connecting a CO_2 reservoir and bleached sandstone to iron-rich concretions in the Navajo Sandstone of south-central Utah, USA, *Geology* 38(11): 999–1002.

Montes-Hernandez, G. and François, R. 2016. Time-resolved in Situ Raman spectroscopy of the nucleation and growth of siderite, magnesite, and calcite and their precursors, *Crystal Growth & Design,* 16(12): 7218–7230.

Schwertmann, U. and Cornell, R. 2007. Ferrihydrite, in *Iron Oxides in the Laboratory: Preparation and Characterization:* 103–112. Weinheim: Wiley-VCH Verlag GmbH.

Singer, P. and Stumm, W. 1968. Kinetics of oxygenation of ferrous iron, in oxygenation of ferrous iron: The rate-determining step in the formation of acidic mine drainage. Federal Water Pollution Control Administration United States Department of the Interior via Harvard University, Cambridge, Mass: 1–36.

United Nations Environment Programme (UNEP) and GRID-Arendal. 2017. C. Roche, K. Thygesen and E. Baker (eds.) *Mine Tailings Storage: Safety is No Accident*, *a UNEP Rapid Response Assessment*. Retrieved from: http://www.grida.no/publications/383

Proceedings of Mine Water Solutions 2018
June 12–15, 2018, Vancouver, Canada
Published by the University of British Columbia, 2018

Follow the Money (and the Water) – The Goldcorp Water Valuation Toolbox

Brendan O'Brien, Goldcorp Inc., USA

Abstract

Goldcorp's CEO has challenged the company to make significant strides in water reduction over the next 10 years with an aspirational goal referred to as "Towards Zero Water." A central question that arises when beginning to plan and prioritize water reduction efforts in pursuit of this goal is, "What is the cost of water?" However, the mining industry does not have any standard methods for addressing this topic, and the costs of water management activities do not often fall neatly into their own accounting cost centers.

To address this challenge, Goldcorp has developed a spreadsheet model – the "Water Valuation Toolbox" – to standardize the compilation and presentation of operational costs and planned sustaining capital projects related to water management. This paper describes the development of the model and its subsequent use to create a company-wide set of water costs for the 2016 calendar year.

The project team worked through an iterative process involving both site-based and corporate stakeholders to gain insight into the data available and desired application of the results. Definitions and methodologies were then developed to capture and document a mine site's actual operational and planned future sustaining capital expenditures on water. This material comprised the basis of the Water Valuation Toolbox spreadsheet, which addresses the following aspects: definition of the scope and detail of cost (what specifically do we mean by "cost"?); methodology for defining and organizing a site's water activities (what "water" are we talking about?); methodology for combining future sustaining capital costs with current operating costs; tools for compiling and presenting these costs; and metrics for basic data analysis.

The completed spreadsheet model has provided Goldcorp with a useful tool to standardize, compile, and compare water costs across its operating portfolio. The application and population of the model for each operating site has yielded a valuable database of detailed costs to be used as a resource for the company to ensure that water management costs are considered in financial models when analyzing business scenarios. Ultimately, the Water Valuation Toolbox has allowed Goldcorp to answer the driving question of "What is the cost of water?" and will contribute to intelligent discussions and better business decisions.

Introduction

Goldcorp's CEO has challenged the company to make significant strides in water reduction over the next 10 years with an aspirational goal called "Towards Zero Water." A central question that arose when beginning to plan and prioritize water reduction efforts in pursuit of this goal was, "What does water cost at Goldcorp?" However, the mining industry does not have any standard methods for addressing this topic. Additionally, while the costs for water management activities are already accounted for within overall operating budgets, they do not often fall neatly into their own accounting cost centers.

To address this challenge, Goldcorp initiated the Cost of Water project and ultimately developed a spreadsheet model – the Water Valuation Toolbox (WVT) – to standardize the compilation and presentation of annual operational costs and planned sustaining capital projects related to water supply and management. This paper summarizes the development of the WVT and its use to create a company-wide set of water costs for the 2016 calendar year.

Project Overview

Drivers

The key factors driving the Cost of Water project were the company's needs to:

- Evaluate and prioritize projects that could reduce water consumption.
- Explore the feasibility of an internal water tax.
- Make cost data available to mine sites to help drive water use efficiency and cost optimization.

Objectives

In order to respond to the above drivers, the Cost of Water project was organized around the following objectives:

- Water cost methodology – develop definitions and methods that will allow the company to compile robust and well-defined costs for water supply and management at operating mine sites.
- Water cost tool – develop a tool for the standardized compilation and reporting of water costs.
- Current water costs – develop a company-wide set of current water costs.

Criteria

The following high-level criteria were identified early on and used to guide the project.

- Pursue the "true cost" of water, not simply the fees paid to access or appropriate water sources.

- The results should be inclusive of all costs involved in obtaining, moving, treating, and managing the water. Additionally, the results should convey an understanding of future sustaining capital requirements, rather than strictly focusing on the operation of existing infrastructure.
- Site-specific results should be developed for each operating mine site, with results structured in a way that allows "apples to apples" comparisons between sites and the compilation of meaningful company-wide averages.
- Cost results should, where possible, represent a full year of operations during the 2016 calendar year.

Methodology

Development of the definitions, methods, and tools was a highly iterative process involving the combined efforts of corporate staff, consultants, and site sustainability and accounting personnel. In general the process involved the following tasks:

- Consultation with corporate personnel from various departments to explore fundamental questions such as: "What is the central question?", "What are the key drivers and objectives?", and "What do we want to do with the resulting information?"
- Consultation with sites to address questions related to logistics and buy-in: "What information is available?", "How is it organized?", and "How do we ensure the WVT results are useful?"
- Work by the project team to develop concepts, terminology, and processes that utilized the insights gathered from consultation. In general, the resulting work was focused on addressing two central challenges which emerged from the consultation process:
    - Define an appropriate scope and level of detail for the term "cost" (i.e., what specifically do we mean by the word "cost" in the phrase "cost of water?")
    - Develop a methodology for organizing a site's various operational activities involving water (i.e., what "water" are we talking about when we refer to the "cost of water?")
- Iterative development and testing of the spreadsheet tool to implement the cost of water definitions and methods and allow their application in a consistent way across the company.
- Stakeholder review and feedback – corporate sustainability team, project steering committee, and site staff and general managers.

Results

Water Cost Terminology

As mentioned above, in order for the project team to develop a standardized tool for capturing and processing costs, it was first necessary to conceive and define the terminology for describing water activities and costs. It is these terms and their hierarchy that provide the vocabulary for and structure of the developed water costs. The key terms created in support of the WVT are summarized in the list below and their relationships are demonstrated in Figure 1.

	Activity Category	Supply	Supply	Operate	Operate	Discharge	Discharge
	Activity Name	Wellfield 1	Wellfield 2	Tailings reclaim to process	Mine dewatering 500 level	Sector 1 ETP	Sector 2 ETP
	Activity Type	Supply Wells	Supply Wells	TSF Reclaim	Dewatering – UG M	Effluent Treatment	Effluent Treatment
Cost Category	Cost Type	Annual Cost	Annual Cost	Annual Cost	Annual Cost	Annual Cost	Annual Cost
Operating - Direct Costs	Consultants/Contractors						
	Maintenance						
	Labor						
	Materials						
	Consumibles						
	Fuel						
	Power						
	Total Direct	$0	$0	$0	$0	$0	$0
Operating - Indirect Costs	Site Costs						
	Fees						
	Total Indirect	$0	$0	$0	$0	$0	$0
Sustaining Capital	current project 1						
	current project 2						
	Total Sustaining	$0	$0	$0	$0	$0	$0
	Activity total	$0	$0	$0	$0	$0	$0

Figure 1: Cost terminology and relationships

Activity terms:

- Water Activity – a site action involving obtaining, moving, treating, or managing water.
- Activity Name – each water activity at a site is given a unique name. The name should be a descriptive one that reflects the conventions and terminology typically used on site.
- Activity Type – the WVT defines a standardized list of generic water management actions falling within the scope of the project. Each of the in-scope water activities identified at a site is matched to one of the items in the Activity Type list. Mapping site actions and terminology to one of a fixed set of generalized terms allows "apples to apples" comparisons and consolidations of cost results.
- Activity Category – the standardized list of Activity Types is divided into three broad areas of organizational/water balance focus (Supply, Operate, and Discharge).

Cost terms:

- Cost Center – an ID number used in site accounting software to track expenditures related to a given water activity or activities. To gather raw data for the WVT, site accounting software was queried to report expenditures during the period of interest for the cost center numbers associated with the site's water activities.
- Cost Type – the WVT defines a standardized list of cost types that describe the generic type of expenditure. Cost types loosely map to the field "Cost Element" which often appears in SAP exports.
- Cost Category – three broad categories used to group together cost types based on how they might be used in a site budget or financial model (operating-direct, operating-indirect, and sustaining capital).

Cost Methodology

The principle task for this objective was to develop definitions and methods that would satisfy the project brief. The main areas addressed and their key outcomes are summarized below.

1. Definition and scope of "cost" within "cost of water":

- Cost means the total expenditure attributable to a water activity.
- Expenditures include any current (operational or capital) or future capital spending falling into three broad categories – Operating-Direct Costs, Operating-Indirect Costs, and Sustaining Capital.
- Operating costs include both direct costs (e.g., labour, consumables, and power) and indirect costs (e.g., site costs, fees, and taxes).
- Sustaining capital includes both current spending (expenditures during the reporting period tagged as capital) and the estimated cost of future sustaining capital projects.
- A future sustaining capital project refers to capital spending related to maintaining the site's ability to continue performing a given water activity in support of the current life of mine plan.
- Future sustaining capital projects for inclusion in the WVT should include any that the site is aware of that has a high likelihood of being required during the current life of mine.
- All operating expenditures attributable to a water activity should be included in order to represent the "true cost". In other words, expenditures must include not only the fees to obtain the water, but all subsequent spending on moving, treating, or otherwise managing it.
- Costs are forward looking. Past capital and operating expenditures on an activity (sunk costs) are not estimated or considered.

2. Method for compiling water activity costs:

- A cost is compiled for each in-scope water activity identified at a site.
- Exported expenditures from SAP, over the relevant time period and pertaining to a given activity, are tallied to calculate sub-totals by cost types (Consultants/Contractors, Maintenance, Labour, Materials, Consumables, Fuel, Power, Site Costs, Fees, Sustaining Capital).
- The total cost of a water activity is calculated by summing together the cost type sub-totals.
- Any capital expenditures for an activity during the reporting period should be recorded in the "sustaining capital" category. These costs may be included or excluded from the final summary of total and unit costs depending on the nature of the expenditures and what the user considers most appropriate.
- Estimated future sustaining capital project costs are compiled separately from the reporting period expenditures. Each project requires an estimate of the following: total cost in today's dollars, approximate average daily water throughput (m^3/day), and approximate useful life (limited to the current life of mine if appropriate). These characteristics are used to calculate an average \$/m^3 cost over the life of the project.
- Per direction from Goldcorp finance personnel, the current unit cost of a water activity may be summed directly with the estimated average unit costs for corresponding projects. No discounting or additional processing of the future sustaining capital project's unit cost is required in order to perform this.

3. Definition and scope of "water" within "cost of water":

- A "water activity" refers to an action related to obtaining, moving, treating, or otherwise managing water at a site.
- The activities to be considered when populating a site's WVT should include the full range of a site's water activities, including anything required to supply water, dewater mining operations, convey water, treat water, and discharge water.
- When considering the supply of water to various on-site users, only the activities related to the provision of water are included, not those related to the act of utilizing the water. For example, if a site uses water from a well for dust control or producing concrete, only the act of operating the well and pumping the water to the water truck fill point or to the concrete plant would be considered. The act of running water trucks to apply the water or the act of making concrete is outside the scope of this project.

4. Method for identifying and characterizing water activities:

- A site's current water infrastructure and life of mine plan should be assessed to identify all current and high likelihood future water activities.
- A list of all a site's water activities should be compiled (excluding the use of water as described above). Then each item is matched to one of the standardized Activity Types to facilitate consolidation and comparisons between sites.
- A corresponding volume of water must be estimated for each water activity for the reporting period. The volume should represent the cumulative flow during the year through that specific location or process.
- Sequential activities will each count the cumulative volume through that specific step. The result is a volume applicable to each point of expenditure, which in some instances means "double counting" the same water. This is appropriate and necessary and the volumes reported for activities should not be confused as portraying the mass balance of the site.

Water Valuation Toolbox

An Excel spreadsheet model was created to implement the cost methodology described above. The model consists of a series of interconnected tabs residing in a single Excel file and organized as follows:

- There are three sets of color-coded tabs organized by function – input worksheets, results tabs, and supporting information
- The tabs work together to facilitate three main uses (or "tools in the toolbox") – data capture, costs summary, and cost insights.

The WVT was created as a blank template to be copied and populated with data for a single site. In this way it can serve as a standardized tool bringing consistency to the compilation, reporting, and analysis of costs across the difference sites.

2016 Water Costs

Six WVT files were developed from the template, one for each of Goldcorp's operating sites. These files were populated with site-specific activities and associated cost data to produce total and unit cost results for each Activity Type present at that site. A company-wide summary of these primary results is included as Figure 2. An example of the full output from the WVT is included as Figures 3 to 6.

Activity Category	Activity Type	Mine 1	Mine 2	Mine 3	Mine 4	Mine 5	Mine 6	Operationally Controlled Sites Total		
		Cost ($USD)	Cost ($USD)	Cost ($USD)	Cost ($USD)	Cost ($USD)	Cost ($USD)	Volume (m3)	Cost ($USD)	Unit Cost ($/m3)
Supply	Lake Intake	$96,121	$163,907	$191,783				2,114,097	$451,811	$0.21
	Supply Wells	$17,824			$98,093	$1,697,910	$6,831,875	18,257,607	$8,645,701	$0.47
	Municipal Water		$188,450					83,498	$188,450	$2.26
	Third Party Supply			$68,462				55,723	$68,462	$1.23
	Bottled Water			$20,222				34	$20,222	$601.84
	Total - Supply	$113,945	$352,357	$280,467	$98,093	$1,697,910	$6,831,875	20,510,959	$9,374,646	$0.46
Operate	Dewatering – UG Mine	$447,174	$1,683,518	$2,840,986	$3,282,085	$2,833,910		11,329,122	$11,087,673	$0.98
	Dewatering – Open Pit	$0					$3,525,164	7,770,000	$3,525,164	$0.45
	Dewatering – UG Recycling	$209,468						289,099	$209,468	$0.72
	TSF Reclaim	$113,598	$50,107	$466,845	$103,016	$852,660	$2,570,084	68,489,273	$4,156,311	$0.06
	TSF Thickener	$229,374						1,337,885	$229,374	$0.17
	Seepage Management	$86,446	$2,239	$19,338			$5,367,147	3,316,186	$5,475,170	$1.65
	Potable Treatment	$31,947		$57,445	$201,147	$788,509	$0	443,458	$1,079,048	$2.43
	Sewage Treatment	$224,611	$60,074	$36,434	$189,357		$1,785,271	279,701	$2,295,747	$8.21
	Stormwater Management	$50,789	$28,955		$350,400			1,256,222	$430,144	$0.34
	Pond Network			$34,943	$61,363			9,940,912	$96,306	$0.01
	Conveyance			$16,586		$220,368		104,635	$236,954	$2.26
	Fire Water System			$132,443				6,000	$132,443	$22.07
	Total - Operate	$1,393,407	$1,824,892	$3,605,020	$4,187,368	$4,695,447	$13,247,666	104,562,493	$28,953,801	$0.28
Discharge	Cyanide Detox	$89,970	$1,980,782	$0	$7,487,651			4,326,966	$9,558,403	$2.21
	Effluent Treatment		$959,273	$349,280	$3,705,907			7,241,553	$5,014,459	$0.69
	Secondary Treatment	$44,094	$1,985	$0				3,592,630	$46,080	$0.01
	Discharge	$92,969		$47,144				5,375,298	$140,113	$0.03
	Municipal Sewage		$105,553					7,807	$105,553	$13.52
	Compliance Monitoring	$619,187	$393,309	$87,222	$1,040,250	$844,132		14,444,776	$2,984,101	$0.21
	Total - Discharge**	$846,220	$3,440,903	$483,645	$12,233,808	$844,132	$0	20,544,254	$17,848,708	$0.87
Total Volume of Water Handled (m3)**		12,071,313	9,816,832	26,077,134	8,586,882	1,902,267	87,163,278		145,617,706	
Total Cost of Water Activities ($USD)		$2,353,573	$5,618,152	$4,369,133	$16,519,269	$7,237,490	$20,079,541		$56,177,156	

**Excludes the volume for Compliance Monitoring

Figure 2: Cost results by activity type

Activity Category	Activity Type	Current Year Cost and Volume		
		Volume (m3)	Cost ($USD)	Unit Cost ($/m3)
Supply	Lake Intake	1,276,851	$163,907	$0.13
	Municipal Water	83,498	$188,450	$2.26
	Total - Supply	1,360,349	$352,357	$0.26*
Operate	Dewatering – UG Mine	1,389,154	$1,683,518	$1.21
	Sewage Treatment	22,483	$60,074	$2.67
	TSF Reclaim	851,455	$50,107	$0.06
	Stormwater Management	1,024,842	$28,955	$0.03
	Seepage Management	281,050	$2,239	$0.01
	Total - Operate	3,568,984	$1,824,892	$0.51*
Discharge	Effluent Treatment	2,683,300	$959,273	$0.36
	Municipal Sewage	7,807	$105,553	$13.52
	Cyanide Detox	667,365	$1,980,782	$2.97
	Compliance Monitoring	3,149,229	$393,309	$0.12
	Secondary Treatment	1,529,027	$1,985	$0.00
	Total - Discharge**	4,887,499	$3,440,903	$0.70*
Total Volume of Water Handled (m3)**		**9,816,832**		
Total Cost of Water Activities ($USD)		**$5,618,152**		

* Volume-weighted average
**Excludes the volume for Compliance Monitoring

Figure 3: WVT output – water cost and volume summary

Activity Category	Activity Type	FSC Volume (m3)	FSC Cost ($USD)	FSC Unit Cost ($/m3)	Current Yr Unit Cost ($/m3)	Current Yr + FSC ($/m3)	FSC / Current
Supply	Lake Intake	6,928,245	$217,549	$0.03*	$0.13	$0.16	24%
	Municipal Water	0	$0	$0.00*	$2.26	$2.26	0%
	Total - Supply	6,928,245	$217,549	$0.03*	$0.26*	$0.29*	12%
Operate	Dewatering – UG Mine	32,200,770	$725,163	$0.02*	$1.21	$1.23	2%
	Sewage Treatment	337,245	$72,516	$0.22*	$2.67	$2.89	8%
	TSF Reclaim	17,029,100	$1,450,326	$0.09*	$0.06	$0.14	145%
	Stormwater Management	0	$0	$0.00*	$0.03	$0.03	0%
	Seepage Management	8,048,250	$11,892,676	$1.48*	$0.01	$1.49	18552%
	Total - Operate	57,615,365	$14,140,682	$0.25*	$0.51*	$0.76*	48%
Discharge	Effluent Treatment	11,161,035	$362,582	$0.03*	$0.36	$0.39	9%
	Municipal Sewage	117,105	$181,291	$1.55*	$13.52	$15.07	11%
	Cyanide Detox	0	$0	$0.00*	$2.97	$2.97	0%
	Compliance Monitoring	0	$0	$0.00*	$0.12	$0.12	0%
	Secondary Treatment	0	$0	$0.00*	$0.00	$0.00	0%
	Total - Discharge**	11,278,140	$543,872	$0.05*	$0.70*	$0.75*	7%
Total Cost of Identified FSC Projects			**$14,902,103**				

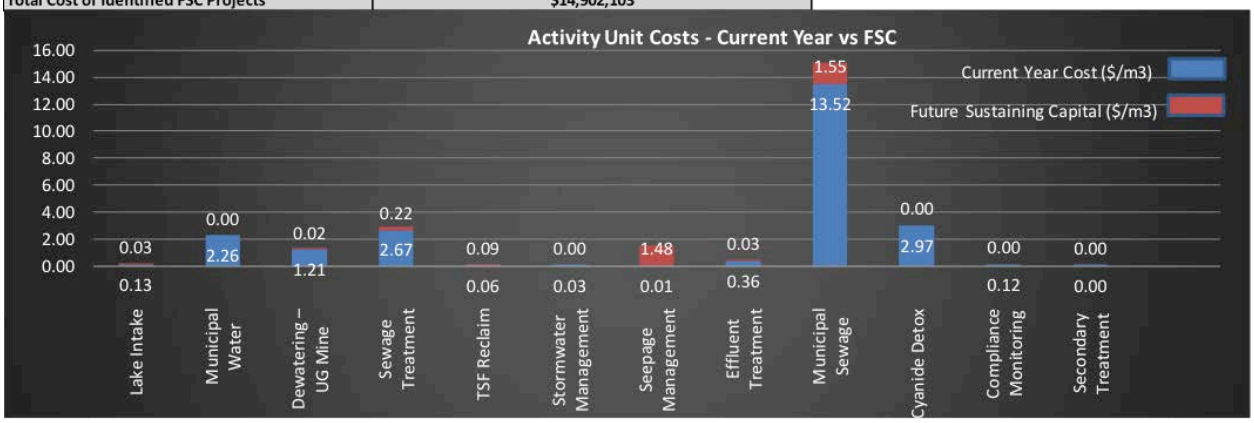
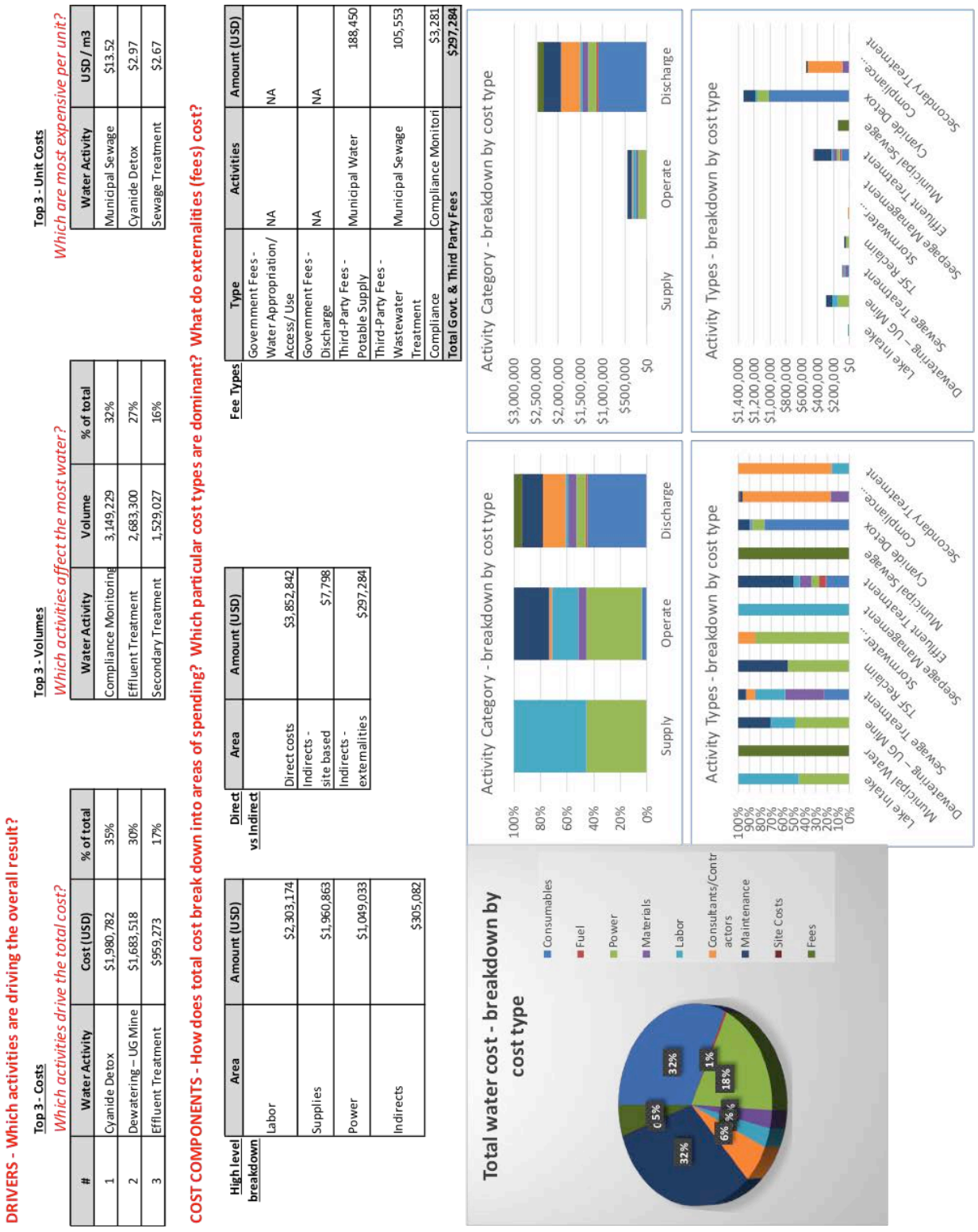


Figure 4: WVT output – future sustaining capital cost



#	Water Activity	Cost (USD)	% of total
1	Cyanide Detox	$1,980,782	35%
2	Dewatering – UG Mine	$1,683,518	30%
3	Effluent Treatment	$959,273	17%

Water Activity	Volume	% of total
Compliance Monitoring	3,149,229	32%
Effluent Treatment	2,683,300	27%
Secondary Treatment	1,529,027	16%

Water Activity	USD / m3
Municipal Sewage	$13.52
Cyanide Detox	$2.97
Sewage Treatment	$2.67

High level breakdown	Area	Amount (USD)	Direct vs Indirect	Area	Amount (USD)
Labor		$2,303,174		Direct costs	$3,852,842
Supplies		$1,960,863		Indirects - site based	$7,798
Power		$1,049,033		Indirects - externalities	$297,284
Indirects		$305,082			

Fee Types	Type	Activities	Amount (USD)
	Government Fees - Water Appropriation/ Access/ Use	NA	NA
	Government Fees - Discharge	NA	NA
	Third-Party Fees - Potable Supply	Municipal Water	188,450
	Third-Party Fees - Wastewater Treatment	Municipal Sewage	105,553
	Compliance	Compliance Monitori	$3,281
	Total Govt. & Third Party Fees		**$297,284**

Figure 5: WVT output – drivers and cost components

OTHER PERSPECTIVES

What part does water management play in driving overall production costs?
How much effort do we expend on water compared to rock?

Water Cost as a Portion of Production Cost:

Item	USD / tonne
Total Cost of Water / Gold Produced	$17.34
AISC (per ounce)	$872

Water Cost as % of AISC
2%

Water Cost Relative to Milling Cost:

Item	USD / tonne
Total Cost of Water / Tonnes of Ore Milled	$8.70
Milling cost per tonne	$46.00

Water Cost / Milling Cost
0.19

Water Mgmt Effort Relative to Mining:

Item	Value	Notes
Tonnes of water handled to produce an ounce of gold (tonne/oz.)	30.3	Total Volume of Water Handled / Gold produced
Tonnes of material milled to produce an ounce of gold (tonne/oz)	2.0	Tonnes of ore milled / Gold produced
Water to ore ratio	15.2	Water Handled (tonne/oz) / Material Milled (tonne/oz)

What is the total cost of water (i.e., "true cost") of water supply vs. the fee only cost ("purchase price")? What is the further cost to manage and discharge wate
What value is supported by water supplied to the site?

"True Cost" of Water:

	Item	Value	Notes
	Total vol of "supply" + dewatering (m3)	2,666,005	Excluding municipal supply and bottled water
	Total "supply" + dewatering fees ($)	$0	"
	Total cost of "supply" + dewatering ($)	$1,847,424	"
Purchase Price	Water supply 'purchase price' ($/m3)	$0.00	Fees per m3 of supply
True Cost - supply	Water supply 'true cost' ($/m3)	$0.69	Total cost per m3 of supply
True Cost - mgmt	Unit cost of water mgmt and disch. ($/m3)	$0.62	Vol wtd avg of "operate" + "discharge"

"Value":

Item	Value
Oz of gold equivalent per m3 "supply" + dewatering (oz/m3)	0.12
Revenue per m3 of "supply" (USD/m3)	$146

Figure 6: WVT output – cost and value perspectives

Additional Summaries and Metrics

A range of other metrics was developed to complement the basic unit cost results. These items attempt to provide insight into the "true cost" of site water activities, as well as providing a gauge of the effort expended on (and value derived from) water management. The themes covered are summarized below, and full details are shown in the example WVT output in Figures 4 to 6.

- Drivers and cost components – activities and cost types driving the overall total.
- Future sustaining capital costs – current year versus future spending.
- Other perspectives – relative effort expended on water and "true cost" vs. "purchase price" of water.

Conclusion

What does our water cost?

The fundamental question driving this project was a simple one: "What does our water cost?" On the surface, the answer is also very simple – a collection of total and unit costs for different activity types. However, responding to this simple question with simple answers was not an easy process. It required addressing the following challenges:

- Answering a multitude of questions to determine the appropriate scope.
- Developing a unique vocabulary and structure to support calculations.
- A complex process of fitting each site's water activities into the WVT mould.
- A significant amount of work to manually pre-process the raw data from SAP exports.

A further challenge was figuring out how to develop a practical and standardized process for implementing the methodology that had been developed. The execution of the project was lengthy and iterative, but has produced useful results that have been well received by both corporate and site personnel. In addition, the definitions and methods needed to give us the vocabulary and structure are now complete and available for future use and refinement.

Summary results for all six of Goldcorp's operationally controlled sites are included in Figure 2. An example of the detailed results produced with the WVT for each site is shown in Figures 3 to 6. At this time, the following is envisioned for the application of the WVT and cost results:

- Sites and projects will be expected to use the unit costs developed here as inputs in project planning, studies, financial models, and business planning wherever appropriate.
- Sites may, at their discretion, choose to update and maintain their toolbox to keep current water costs at their disposal.

- Benchmarking and collaborative sharing of costs will be pursued with other companies in the mining sector.
- At this time, Goldcorp has chosen not to implement an internal water tax. It was decided that the awareness of water activity costs provided by the execution of the Cost of Water project provided sufficient near term incentive for operational improvements.

It should be noted again that Goldcorp's costs for water supply and management, while they are not typically itemized or tracked separately in operating budgets (similar to the rest of the mining sector), are already accounted for within reported production costs.

What is the "True Cost" of Water?

The objectives and criteria outlined for this project suggest a deeper, more strategic layer to the desired outcome. Specifically, the phrase "true cost" was used, indicating the desire to develop a holistic view of the cost of managing water. A more conventional view would only look at water cost as either the unit price paid in fees to take the water or, at most, the price to access and then pump water to supply a site. The name chosen for the spreadsheet tool utilizes the words "valuation" and "toolbox" – indicating an attempt to describe water's value to our operations and doing more than just calculating unit cost results. The following are a number of observations that coalesced over the course of the project as we strove for insight into the cost and value of water.

- The cost of water is not a single thing and is not driven by water supply.
    - What makes up the "cost of water"? It almost goes without saying that the "cost of water" for a site is incomplete if one focuses only on water supply. However, after cataloguing the water activities and volumes observed across Goldcorp, it is clear that both the breadth (the number of activities) and depth (the water volume handled) of water activities fall into the operate and discharge categories. Furthermore, from the cost results it is clear that the overall cost of using water at a site is not driven by water supply activities. On average, water supply accounted for only 17% of the total cost.
    - What is the impact of bringing water on site? The cost of supply is not just the robust cost to supply the site. All the water brought onto site must be managed (and in some cases treated and discharged), and those activities have significant costs. Any water brought into the system is likely to incur the additional costs of those activities.
- The true cost of water activities must include all cost types and future sustaining capital.
    - What makes up the cost of water supply? Similar to the above, the fees or taxes paid to supply water to a site (the "purchase price") represent only a fraction of the total cost to

execute those activities. At Goldcorp's Canadian sites, the purchase price is less than 1% of the total cost of water supply. At the Latin American sites (which are in semi-arid environments), it still only represents one-third of the total.

  - What cost types drive site costs? Two things are usually top of mind when envisioning components of water cost: the purchase price, and the cost of pumping (i.e., power costs). On average across the company, these represent only 12% and 17% of the total cost respectively. Thus, 71% of the total cost is incurred through labour and supplies.
  - What is the picture when we look beyond the present? When future sustaining capital projects are included in the cost, they represent a significant portion of the total – ranging between 8% and 86%. Three sites have values over 70%. Focusing only on present infrastructure is very incomplete.

- Every site is unique, and there are only broad similarities between sites residing in similar climates.
  - Are there patterns in activity costs? Sites in similar climate zones have only rough similarities in their mix of supply vs. operate vs. discharge cost totals. At the activity type level, unit costs can have very wide variations across sites.
  - Is there a way to compress water costs to a single unifying value across the sites? – Many efforts were made to mine the completed data set for such a value, but none was found. This exercise was instructive, however, in revealing that each site's unique needs and characteristics drive very different outcomes. Makeup water requirements, mine depth (i.e., dewatering needs), water treatment requirements, and economic climate appear to be the primary factors at play.

Acknowledgements

Briana Gunn and Joe Donnelly were both involved during the initial stages of the project and made valuable contributions. Lisa Wade offered tremendous support and guidance in her roles as project champion and steering committee chair. Additionally, the project as a whole would not have been possible without significant support from the mine site personnel who took the lead in data collection and assisting us to develop site-specific version of the WVT: Francisco Hernandez, Agustin Alurralde, Ashley Moncrief, Doris Achircano, Jean-Félix Lepage, and Stephanie Thibeault. To everyone involved in bringing this project to fruition, I offer my sincere appreciation.

Proceedings of Mine Water Solutions 2018
June 12–15, 2018, Vancouver, Canada
Published by the University of British Columbia, 2018

A New Approach to Mitigation Banking

Eric McCleary, Stantec Consulting Services Inc., USA

Abstract

The use of a mitigation bank for ecosystem restoration is being developed as a pilot demonstration project in Western Pennsylvania to restore streams impacted by mine drainage and acid precipitation. Mine drainage and acid precipitation are problematic throughout Appalachia. In Pennsylvania alone, over 5,000 miles of streams have been impacted by these types of pollution. Mine/acid drainage affects ecosystem health typically by having a reduced pH with elevated acidity and metal levels (principally iron and aluminum). The task of restoring streams affected by mine/acid drainage is daunting, especially with reduced state and federal funding sources. The idea of employing mitigation banks, sponsored by private entities (i.e. industry, developers, etc.), to ecologically offset these types of pollution, as "out of kind" mitigation, has yet to be implemented through the federal mitigation banking program developed by the United States Army Corps of Engineers.

Lyons Run, in Westmoreland County, PA, along with various other streams in the north-central portion of Pennsylvania, are the pilot sites for this unique approach to mitigation banking. Installation of strategically placed and relatively low-cost passive limestone treatment units, designed to increase alkalinity and remove metals (where applicable), is the core of this restoration effort. Water quality trading, based on both measurable water quality improvement and carbon increases, provides ecological lift that can be objectively measured and traded to offset various environmental impacts. This approach is receiving support from the State of Pennsylvania, federal agencies, and private parties. The use of private funding to establish mitigation banks (as ecosystem banks) to offset unavoidable ecological impacts, accomplished through existing state and federal permitting programs, is attractive to all parties involved. These programs can produce significant environmental benefits, notably wild brook trout (*Salvelinus fontinalis*) recovery. This presentation introduces the concept, explores the development of the pilot project, covers the concerns of the state and federal agencies, presents the current status of the project (anticipated implementation being summer of 2018), and examines how it could be utilized throughout North America as an ecosystem restoration tool.

Introduction

Abandoned mine drainage (AMD) is one of the largest sources of stream degradation, with approximately 4,000 miles of waterways affected, as established by DEP's most recent stream assessment program (PADEP – Pennsylvania Department of Environmental Protection, 2014). Additionally, another 1,000 miles of waterways have been degraded by acid deposition (acid rain) in Pennsylvania. The impact of acid precipitation on Pennsylvania streams is likely greater than reported, as many of the streams affected have not been assessed in recent years, and the PADEP is relying on historical assessments, many of which occurred prior to or concurrent with acid deposition. The effects that these two sources of pollution have on aquatic environments are chemical, biological, and physical in nature. The primary effects are lower pH values (natural rain has a pH of 5.6–5.7), higher than normal acidities, and higher dissolved/precipitate metals, all of which negatively affect the aquatic environment. This acidic impairment can range from reducing populations of aquatic organisms in effected streams to completely decimating some streams of aquatic life.

Historical land uses have taken a toll on the landscape, diminishing the presence of aquatic biota within these streams. The degradation of surface waters via deposition and/or mine drainage is associated with high acidity, low pH, and elevated metal concentrations. Areas impacted by these forms of acid pollution typically lack sufficient alkalinity to buffer the low pH and/or high acidity and metals contamination, creating stream environments that are unsuitable for the growth and development of aquatic biota. Aluminum toxicity specifically has been identified as the major cause of brook trout (*Salvelinus fontinalis)* population decline in Appalachia (Lovich and Lovich, 1996; Dewalle et al., 1982; Sharpe et al., 1987; Webb et al., 1989). Efforts to curtail the decline of native aquatic biota have been undertaken in recent decades and have focused on increasing alkalinity though lime dosing, limestone sands, and limestone-based treatment systems. The increase in alkalinity and pH has the concomitant effect of decreasing aluminum concentrations, while increasing the acid neutralizing capacity (ANC) of the receiving streams. These chosen pilot projects are intended to document successful recovery, increase public awareness, and supply a vehicle for the successful reestablishment of aquatic resources through documentation of ecological lift and subsequent water quality trading.

Specifically, the efforts presented in this paper are focused on two separate geographical areas in Pennsylvania – one affected by abandoned mine drainage (Lyons Run) and one affected by acid precipitation (Middle Fork). The approach is the same in both cases: reduce the effects of acid waters on the receiving streams, provide objective data that supports the improvements or ecological lift, and generate environmental credits to compensate for unavoidable impacts associated with human development nearby.

Lyons Run (see Figure 1) is a stream that is approximately three and one-half miles long, located on public and private lands within Penn Township and the Municipality of Murrysville, located in Westmoreland County in south-western Pennsylvania, USA. This stream is severely polluted with abandoned mine drainage emanating primarily from three headwater source points that have been historically document by the United States Corps of Army Engineers (USACE, 1998). The acid mine drainage pollution resulted from previous deep mine coal extraction activities associated with mining of the Lyons Run Mine. The parties involved on this project are the Lyons Run Watershed Association, PADEP, and several consultants. The Lyons Run drainage currently impacts the receiving stream (Turtle Creek), which is a trout stock fishery. Amelioration of these AMD discharges would not only recover portions of Lyons Run, but would stabilize episodic acid slugs (from the Lyons Run AMD discharges) that negatively impact the larger Turtle Creek fisheries.

The Middle Fork (see Figure 2) is a stream that is approximately four and one-half miles long, located on public lands (Pennsylvania State Game lands) within Jones Township, Elk County, Pennsylvania, USA. This stream has been impacted by acid deposition that has reduced the population of native brook trout within the stream. Streams throughout much of this geographical area (north central Pennsylvania) have been negatively impacted in this way. The partners associated with this project are the Pennsylvania Game Commission, as the landowner, and a local natural gas company that is currently exploring this area for natural gas. It is an ideal pilot project for demonstration of wild brook trout recovery.

Methodology

Passive treatment systems are proposed with both systems, and were the chosen technology based on overall operation and maintenance costs, as well as effectiveness relative to the desired goals. The two areas do differ in the specific types of passive treatment selected, primarily due to the differing nature of the acid pollution at each site and the effectiveness of each type of treatment relative to that specific type of pollution.

On Lyons Run, one large passive treatment system that collects all three sources of AMD has been designed to offset the effects of the AMD responsible for the degradation of Lyons Run and its receiving stream, Turtle Creek. The specific type of system proposed for the Lyons Run site is a modified Successive Alkalinity Producing System (SAPS) that is developed for the extremely low pH, high acidity, and high metal concentrations found in the three main AMD discharges impacting Lyons Run. SAPS systems (see Figure 3) are typically designed with a piping (flushing) system buried in a bed of limestone at least 1 m in depth covered with a relatively thin layer (less than 0.3 m) of a locally available organic material (in this case mushroom compost) which is inundated with a minimum of 1 m of freestanding

water. Metals that precipitate in the limestone layer (aluminum and some iron) can be flushed via the piping system. This flushing sustains the treatment derived from the limestone dissolution for longer periods of time before maintenance is required. This system will require upwards of 1,800 metric tons of limestone and an area of approximately 0.8 hectares for installation.

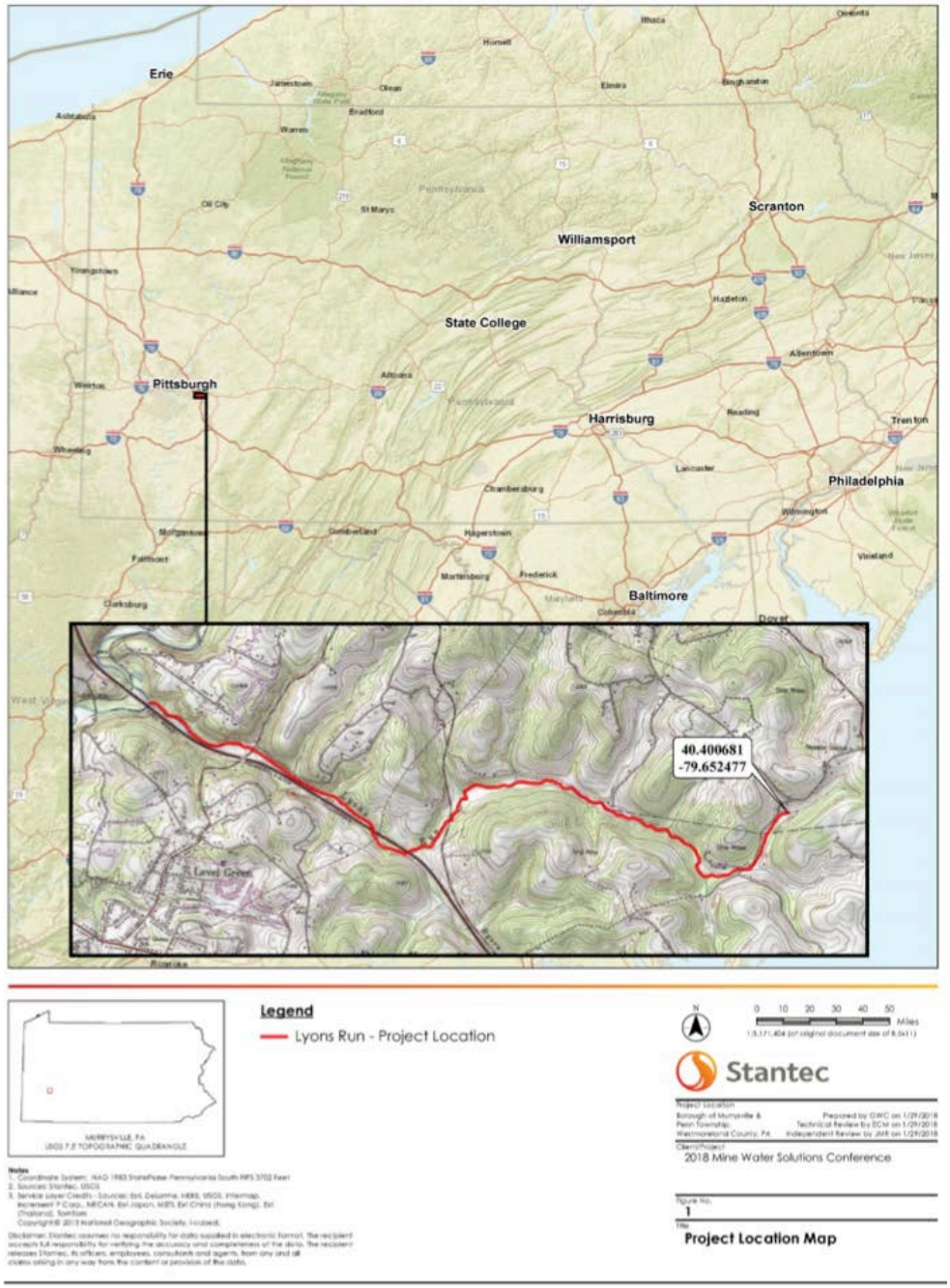


Figure 1: Lyons Run project location



Figure 2: Middle Fork project location

For the Middle Fork, six limestone anoxic drains (see Figure 4) are proposed with installation at the headwaters of Middle Fork (tributary to the Clarion River) to increase alkalinity in the headwaters. This will re-establish brook trout in the Middle Fork, which has been affected by acid precipitation and resulting aluminum dissolution. These limestone units (no larger than 90 metric tons) will be constructed at the groundwater sources prior to groundwater expression to the surface of the Middle Fork. The treatment units are approximately 10 m by 7 m in size and must be installed below ground level. It is felt that, with relatively minimal effort, significant environmental lift to the local aquatic environment can be

achieved. There is also a significant opportunity to transfer this approach to other local regions, remediating hundreds of miles of effected streams within this geographical region.

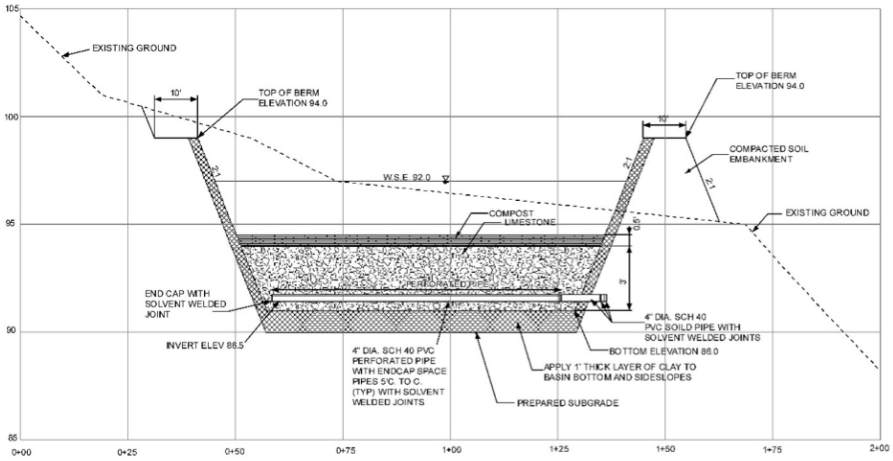


Figure 3: Lyons Run anoxic limestone drain

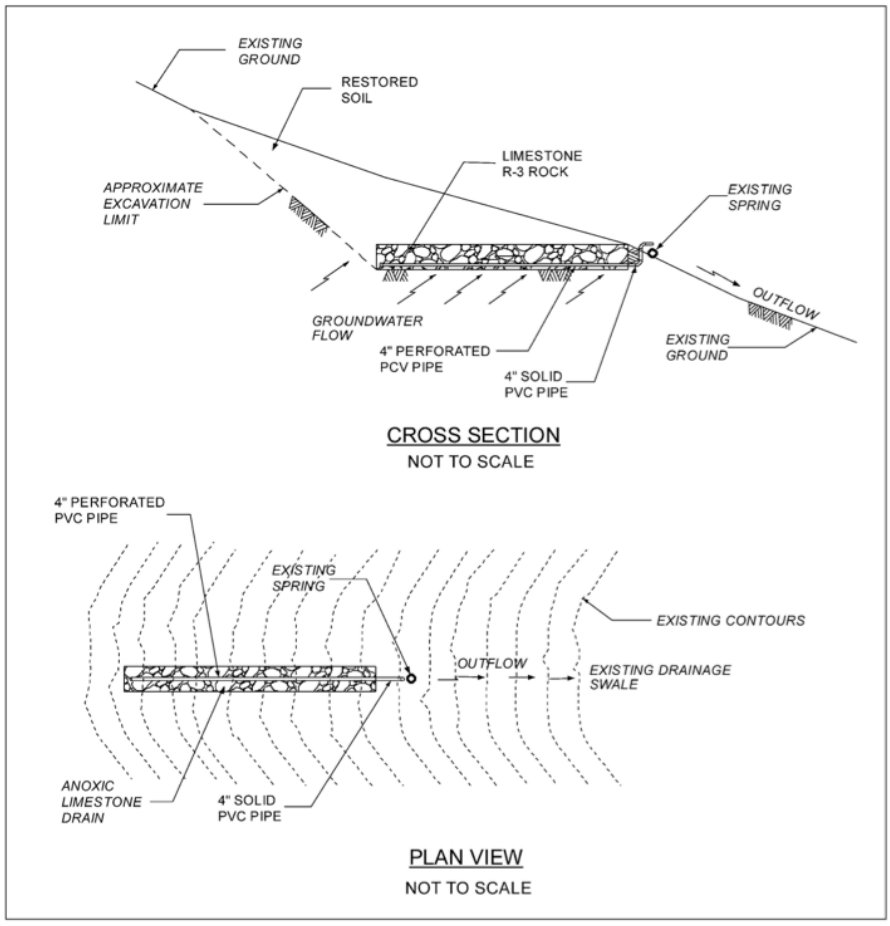


Figure 4: Middle Fork anoxic limestone drain

The water that is treated within both treatment systems will discharge to the receiving streams (Lyons Run and the Middle Fork) with elevated pH, lowered acidities, and lowered metal values. This type of treatment will result in the recovery of these streams, allowing for the return of aquatic biota (in the case of Lyons Run) or increases in biomass associated with macroinvertebrates and fish (in the case of the Middle Fork).

Results/Discussion

Since these are pilot projects in the final stages of implementation, with expected completion later this summer (2018), direct results with these systems are not currently available. However, discussion based on PADEP's consideration of AMD treatment, for use as aquatic resource compensation credit, can be developed as mitigation banking credits.

The data provided by bioassessments in these streams would allow for an objective evaluation of ecological lift based on a recently developed ecological functional lift protocol (310-2107-001 Pennsylvania Function Based Compensation Protocol – PADEP). This evaluation would lead to aquatic compensation based on measurable improvement that can provide for a form of water quality trading/mitigation banking. One of the key benefits of this type of approach is that it allows for "out-of-kind" compensation associated with impacts to the environment caused by human encroachments on a variety of aquatic resources.

Basically, the way this approach would work is the impaired resource would be assessed, and this assessment would then be compared against a non-impaired resource in the same geographical region. The difference between the impaired and non-impaired resources would be the ecological lift that could occur by the treatment method employed. The actual ecological lift would be the measured lift (based on aquatic assessments) of the impaired waters after treatment. This would be the basis of any credits available for offsetting other environmental impacts.

Based on the PADEP's Compensation Function Credit Calculation (Table 1), the resource can be assessed pre-mitigation and post-mitigation to determine functional lift of the aquatic resource for crediting purposes (see Tables 2 and 2a). Table 2 and Table 2a present hypothetical summary worksheets for two streams as an example of credit valuation.

The area proposed to be improved through implementation of the project must be established. This may entail identifying multiple reaches along a stream's path based upon similar water quality conditions, biological condition, or other measures of condition that are in common. The goal is to establish reaches that are likely to have similar functional lift for assisting in determining the differential and calculating credit generation. The area is determined by measuring the flow path of the stream and multiplying that value by the average width of the stream reach. Care should be taken to establish the average width by

measuring several riffle sections along the reach and averaging their values. The width is measured from the edges of the channel that would correspond to the bank full depth or ordinary high-water mark.

Table 1: Compensation Functional Credit Equation (PADEP)

FCG = AP x RV x CV x CIdiff	
FCG =	Functional Credit Gain
A_P =	Area of Project for each applicable function group (in acres, 0.00)
R_V =	Resource Value
C_V =	Compensation Value
CI_{diff} =	Condition Index Differential Value (0.00) (this is the difference between the existing condition and the projected/achieved condition post project implementation for each applicable function group)

The resource value is determined by using the AMD Set-Aside program draft guidelines for reviewing a Restoration Plan's worth. Deviation from the guidelines may be necessary in developing the final protocol for AMD projects and crediting; however, the utilization of most of the elements would provide consistency between program efforts related to AMD abatement. Should plan elements be removed from evaluation, the scoring break points would be adjusted accordingly. This value is a predetermined value.

As another measure of ensuring program consistency, the Compensation Value was linked to the AMD Set-Aside program's efforts to focus on those areas with sound watershed restoration planning and to those waters with the most need as evidenced by a Total Maximum Daily Load (TMDL). The location of a project within either an approved Hydrologic Unit Plan or a Qualified Hydrologic Unit Plan and the existence of a TMDL for AMD will achieve the highest Compensation Value. In addition to planning and TMDLs, the type of treatment system, risk rating, and cost benefit ratios were incorporated to distinguish projects not meeting the top categories and reward those with less risk or high cost:benefit ratios. These measures provide meaningful input for distinguishing Compensation Value levels, and are critical components to successful planning and implementation of high value projects. This value is also a predetermined value.

Establishing the functional lift provided by a project entails several steps, which are necessary to the calculation of credits and to ensure their appropriateness. The credit potential evaluation process depicted below would be completed for each reach identified in order to establish whether the potential to generate credit exists. The results are then used to determine which method is implemented to establish the value of the credits.

The stream reaches and the corresponding conditions must be established for the project, which may include water quality and other data demonstrating reaches that are affected by AMD or acid precipitation. The reaches would be separated into those attaining water quality standards and those that are not, for credit evaluation purposes. The Instream Comprehensive Evaluation (ICE) macroinvertebrate Index of Biological Integrity (IBI) has been selected as the best measure of ecological lift for AMD/acid runoff projects for this process. Traditional water quality data, while demonstrating non-attainment, will not necessarily provide the best demonstration of functional lift as needed for this process. In some cases, existing macroinvertebrate data may be available; however, data may need to be collected. Existing and collected data must fall within the ICE guidelines for collection methods and time of year. Utilization of the macroinvertebrate IBI for distinct reaches addresses issues related to existing physical conditions and natural attenuation as pollution moves downstream, as well as how it effects credit generation potentials. Hot spot areas may be identified and evaluated as separate and distinct reach areas.

Table 2: Aquatic Resource Condition Differential Worksheet X

Proposed AMD Treatment Condition Differential Calculation (Draft Version 1.0)

Project Name: Project Example Condition Measure: PA DEP Macroinvertebrate IBI

Function Group	Reach	Existing Resource Condition Value (C_{EXIST})	Reference Resource Condition Value	Potential Maximum Differential Value ($C_{MAXDIFF}$)	Observed Resource Condition Value (C_{IMROV})	Achieved Condition Differential Value (C_{DIFF})	Percent Differential Achieved
Riverine: RS	1	0.75	0.81	0.06	0.79	0.04	N/A
	2	0.22	0.79	0.57	0.74	0.52	0.91
	3	0.12	0.73	0.61	0.70	0.58	0.95

The values previously established are then placed into the equation and the results are calculated to determine the total credits generated for each identified reach. An example is provided in Worksheet Y in Table 2a. There are certain conditions that, when present, either limit the potential for generating credits, or that require a change in the manner in which the condition differential value is calculated. Specifically, if a stream reach is already attaining water quality standards (such as an IBI score > 0.63) then the actual IBI difference between the pre- and post-project IBI scores is utilized in the formula instead of the percent differential achieved, as described in the previous section.

Table 2a: Aquatic Resource Function Credit Worksheet Y

Proposed AMD Treatment Compensation Valuation (Draft Version 1.0)

Project Name: Project Example Site Identifier:

Function Group	Reach	Area of Project (A_P in 0.00 acres)	Compensation Value Factor (C_V)	Resource Value Factor (R_V)	Percent Differential Achieved	Compensation Value (credits 0.00)
Riverine: RS	1	3.22	2.5	2.5	0.04	N/A
	2	2.18	2.5	2.5	0.91	12.40
	3	0.16	2.5	2.5	0.95	0.95

Conclusion

Projects that offset environmental impacts (in this case aquatic resource impacts), while concomitantly restoring damaged ecosystems, are a developing frontier. This approach brings together industry and the environment in a symbiotic relationship that is beneficial to all parties. The funding source for these projects is not dependent on state or federal stakeholders to operate, and this allows for greater restoration opportunities as a result.

It is expected that providing ecological lift to damaged aquatic ecosystems is a viable mitigation approach that will be in more demand in the future. In consideration of the literature that has been reviewed as part of the function-based aquatic resource compensation technical guidance development; and the extensive discussions with various DEP personnel and other conservation organizations; the extent of the AMD pollution/acid deposition (within Pennsylvania alone) and the process and factors outlined provide a reasonable approach for moving this approach forward. The framework developed with these projects is sufficient to engage other state and federal stakeholders concerning the potential ability of these projects to provide both state and federal mitigation credits under the Pennsylvania Chapter 105 and United States Section 404 programs. In addition, this type of process may have the potential to extend beyond compensatory mitigation to other water quality pollutant problems and AMD/acid runoff treatment efforts.

References

Dewalle, D., Sharpe, W.E., Dinicola, R.S. and Kimmel, W.G. 1982. Causes of acidification of four streams on Laurel Hill in southwestern Pennsylvania, *J. Environ. Qual.* 13: 619–631.

Lovich, J.E. and Lovich, R.E. 1996. Decline of native brook trout *(Salvelinus fontinalis)* populations along the upper west branch of the Susquehanna River: Canaries outside the coal mine, *J. Pennsylvania Acad. Sci.* 70: 55–60.

PADEP – Pennsylvania Department of Environmental Protection. 2014. *Consideration of AMD Treatment for Use as Aquatic Resource Compensation Credit.* Harrisburg, PA: PADEP.

Sharpe, W.E., Leibfried, V.G., Kimmel, W.G., and DeWalle, D.R. 1987. The relationship of water quality and fish occurrence to soils and geology in an area of high hydrogen and sulfate ion deposition, *Water Res. Bull.* 23: 37–46.

USACE – US Army Corps of Engineers. 1998. 905(b) *Reconnaissance Study of Lyons Run Watershed; Turtle Creek Watershed Ecosystem Restoration of Acid Mine Discharge*. Pittsburgh, PA: USACE.

Webb, J.R., Cosby, B.J., Galloway, J.N. and Hornberger, G.M. 1989. Acidification of native brook trout streams in Virginia, *Water Resour. Res.* 25: 1367–1377.

Proceedings of Mine Water Solutions 2018
June 12–15, 2018, Vancouver, Canada
Published by the University of British Columbia, 2018

Mine Water: A Resource for the Circular Economy in South African Mining Communities

Dheepak Maharajh, Mintek, South Africa
Tamsyn Grewar, Mintek, South Africa
John Neale, Mintek, South Africa
Michelle van Rooyen, Mintek, South Africa

Abstract

South Africa is one of the thirty driest countries in the world and among the most water wasteful. The agricultural sector in South Africa uses ~70% of the country's total water resources, and the average South African uses 60% more water than the average global citizen; additionally, our waste water treatment plants are not all efficiently operational. Although the mining sector only uses 3 to 5% of the water resources, these situations increase pressure on the mining sector to deal with mine water pollution as the mine water contaminates ~37 billion litres of fresh water. The mines are also required to develop innovative ways to create jobs while stimulating economic growth in the mining communities. The mining industry in South Africa is still a major contributor to the economy, and any changes to mine sustainability will have dire impacts on the regional and national poverty levels. These are among the major reasons why a sustainable solution for the future of mining is required. A future that allows for a seamless movement of labour from mining into other industries when mines are spent or mechanization is required. The technology proposed in this paper is still a conceptual integration of technologies, and the target is to demonstrate the integrated system during the course of 2018 to 2019.

Using mine water as a resource has shown potential to create energy, jobs, food, and clean water through an integrated system. The rationale behind the concept is to generate various products by adopting a cradle-to-cradle approach, where the waste from one process technology is the raw material for the next. There are various potential technologies proposed for integration, and Mintek is involved in some of these at various stages of development. The concepts include biological sulphate reduction, SAVMIN®, algal bioenergy, biogas technologies, concentrated solar power and agriculture. The system delivers energy, fuels, food, and jobs while remaining environmentally responsible. The products produced in the system have available markets in the mines and communities. The electricity and food generated will be routed to the community, while the biofuels produced will be supplied to the mines to

partially meet their average fuel demand of ~70 ML/annum/mine. The concept will also enable mining companies to mitigate their environmental responsibility by generating a positive NPV through the various interventions. The concept is designed for the mining sector but can be adapted to deliver resources to rural or remote communities.

Introduction

South Africa is a water-scarce country, rated among the thirty driest countries in the world, and is currently experiencing its worst drought since 1904. The government expects water demand to outstrip supply as early as 2025 (Zhuwakinyu, 2017). In 2016/17, Level 2 water restrictions were put in place in Gauteng, and Level 6 restrictions were implemented in Cape Town from January 2018. Eight out of the nine provinces within South Africa, with the exception of Gauteng, were declared drought disaster areas. The mining sector is currently experiencing increasing pressure because of the pollution of water resources, and to provide insights into sustainable mine closure and job creation (Baxter, 2016). Using mine impacted water as a resource for the circular economy has the potential to provide re-use options to generate energy, food, and positive environmental benefits (Wolkersdorfer and Busisiwe, 2017).

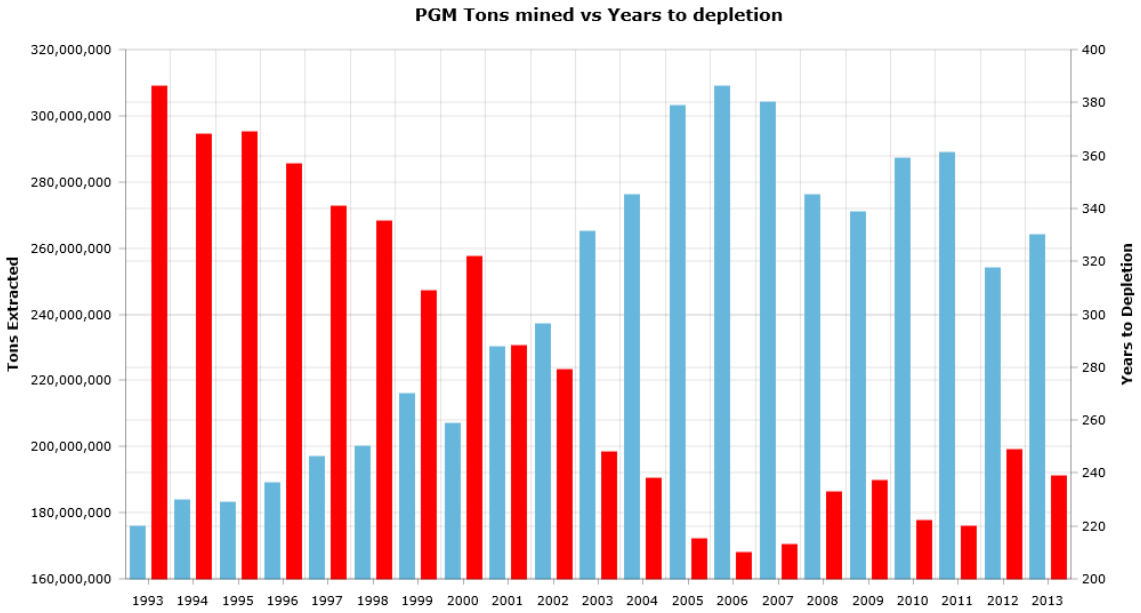


Figure 1: Lifespan of South African gold mines (Maynard, 2017)

The South African agricultural sector uses ~70% of water resources and the mining sector only 3 to 5%. However, mine impacted water has the potential to further contaminate clean fresh water resources. In the US the contamination of fresh water by mine water is estimated to be in excess of 60 billion litres per annum (Sumi and Gestring, 2013). In addition to agriculture and mining, another problem

compounding South Africa's water scarcity issues is the nonchalant attitude of average South Africans to water conservation. South Africans' average water consumption of 280 L/pp/d is almost 60% more than that of the global average (175 L/per person/d) (van Zyl et al., 2007). Around 40% of this allocation is utilized for watering lawns and gardens (Zhuwakinyu, 2017). The city of Cape Town has been identified as the one of the first cities in the world that will run out of water.

In addition to the water scarcity and pollution issues that plague the mining sector, there are critical concerns about the diminishing natural resources remaining to be mined. The estimated life span of mined resources in South African ranges from ~20 years for gold to ~200 years for platinum. This scenario is accompanied by the reduced extraction of the resources from the ground, which has resulted in job cuts (Maynard, 2017). For the mining sector to extend the lifespan of the mines, there is a critical need to increase mechanization at mines (Baxter, 2016). Although this could significantly increase the mine lifespan as mechanization allows deeper mining of resources, there is an increased risk of further job cuts. The South African labour force is very volatile, and the industry has been plagued with severe and often violent labour unrest over the last 5 to 10 years.

The South African economy is still very reliant on the mining sector, and changes to the mine outputs and labour force could have far reaching consequences. Figure 2 demonstrates a prediction of the impact on poverty levels of weakening mining in the Limpopo province. This puts mines in a catch-22 position, where non-mechanization reduces mine lifespans and subsequently jobs, while mechanization will increase the mine lifespan but still result in job cuts. However, this does create an opportunity for the mining sector to implement innovative solutions that foster sustainable development in mining communities.

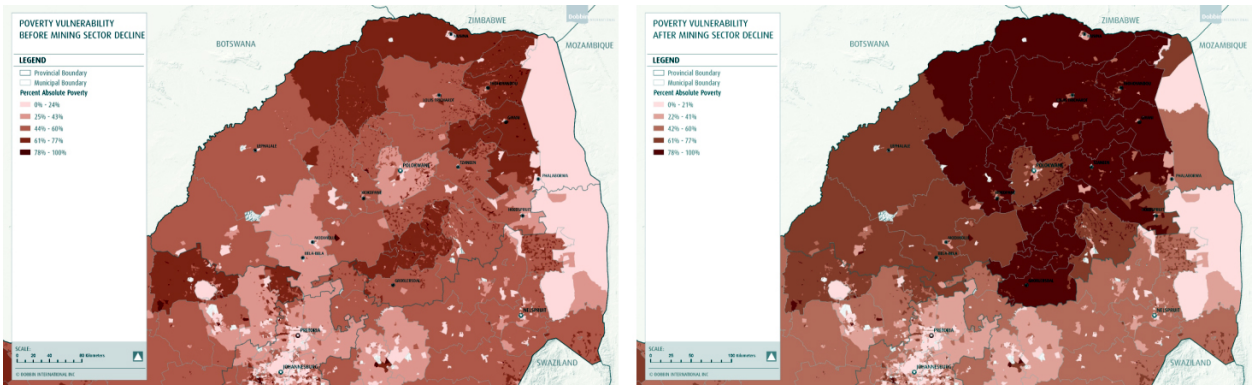


Figure 2: Current and predicted poverty with weakening mining sector in Limpopo, South Africa (Dobbin International, 2016)

Some of the key challenges facing the mining sector can be summarized as follows (Baxter, 2016):

- To reduce the utilization of key resources such as energy and water.
- To reduce the environmental impacts of the operations and of waste production;
- To ensure sustainable mine closure.
- To create new employment to make way for mechanization.

To address these challenges, Mintek has created a conceptual, integrated system that can create jobs, new products, and energy while ensuring sustainable mine water reuse. The system is built on a "cradle–to-cradle," minimal waste approach and employs various technologies to generate energy, food, fuel, and clean water.

This paper presents an overview and description of the conceptual process to enable mine impacted water to be used as a resource in the mining sector circular economy. The paper describes the technical components that enable the delivery of various products and services and how these technologies integrate in a symbiotic relationship to facilitate a highly efficient system.

Approach

The concept considers various technological processes at different Technology Readiness Levels (TRL) and integrates these into a systematic offering. Each process or technology offers links to one or more other process steps. The concept aims to deliver a system that utilizes the waste or by-products from one process as an input into another. Figure 3 provides an illustration of the conceptual, integrated flowsheet.

The paper presents an overview of conceptual linkages with scientific background supporting the integration of technologies and the generation of envisaged products.

Discussion

The proposed system includes technologies developed at Mintek, as well as proposed technologies available in the public domain at various TR levels. The overall aim of the proposed system is to utilize mine water as a resource to generate clean water, jobs, food, and energy. The subsequent sections will present a high-level indication of performance of some technologies and scientific justifications of the inclusion of other technologies.

Mine water treatment using Biological Sulphate Reduction (BSR)

The BSR process essentially constitutes the starting point of the integrated system after neutralization. The mine water is neutralized using limestone to a pH of 5 to 7. The neutralized water contains high levels of sulphates, as well as metals and other compounds (Table 1).

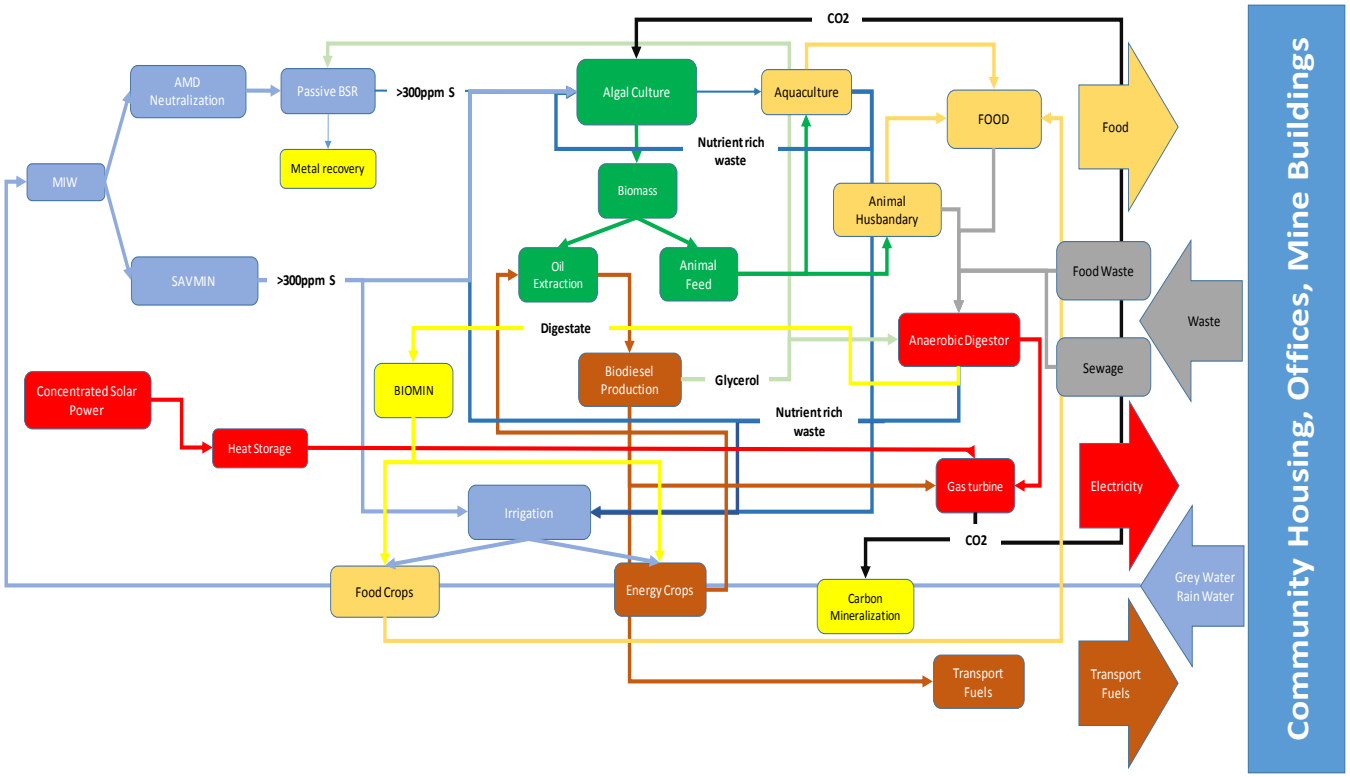


Figure 3: Conceptual, integrated model utilizing mine water for sustainable development

The laboratory-scale BSR system was designed as a down-flow system and was fabricated with a series of plastic columns, as demonstrated in Figure 5. The columns were packed with 20% m.m^{-1} hay, 20% m.m^{-1} cow manure, 20% m.m^{-1} wood shavings and 40% m.m^{-1} wood chips. These compounds provided a source of carbon as well as the inoculum of sulphate-reducing bacteria from the cow manure.

The system was tested over a period of 486 days and demonstrated >97% removal of sulphate from 3340 mg.L^{-1} in the feed solution to 90 mg.L^{-1} with a concomitant increase in S^{2-} concentration in the third column to 200 mg.L^{-1}. This increase in the S^{2-} is thought to b due to the sulphur speciation associated with biological sulphate reduction (Maree and Strydom, 1978). The BSR process is a sulphate dissimilatory process, which results in the sulphur compounds being transferred from one species to another rather than utilized biologically for protein synthesis, as is the case in an assimilatory process (Peck, 1967). The Mintek BSR technology is currently being piloted at a coal mine in South Africa (Figure 5).

Table 1: BSR Laboratory demonstration results summary

Element/ compound	Feed (mg/L)	Column 1 (mg/L)	Column 2 (mg/L)	Column 3 (mg/L)
SO_4^{2-}	3340	140	130	90
S^{2-}	9	802	360	200
NH_4^+	5	709	858	697
Be	<0.02	<0.02	<0.02	<0.02
HCO_3^-	106	7802	7676	7260
Na	258	195	209	241
Mg	537	514	447	399
Al	4.7	3.7	3.0	2.2
Si	5.2	23	27	29
PO_4^{3-}	<0.01	<0.01	0.1	0.1
Cl	<0.01	0.35	0.34	0.34
K	172	456	531	548
Ca	587	475	544	400
Cr	0.07	0.09	0.18	0.33
Mn	36	2.0	3.4	2.5
Fe	0.49	1.16	0.95	1.56
Co	0.06	<0.02	<0.02	<0.02
Ni	0.07	0.09	0.06	0.16
Cu	<0.02	0.03	0.04	0.02
Zn	<0.02	0.02	0.02	0.02
As, Mo, Ag, Cd	<0.02	<0.02	<0.02	<0.02
Pb	<0.02	0.1	<0.02	<0.02
Alkalinity	87	6395	6292	5951
pH level	6.93	6.97	7.20	7.23

The treated water after the BSR process still requires further downstream processing to allow for discharge, or can be re-purposed for other activities. The exiting water still contains high concentrations of NH_4^+ and HCO_3^- and moderate levels of PO_4^{3-}, which provide an excellent source of nutrients in agriculture or algal culture (Andersen, 2005). Both algal culture and agriculture require fertilizers, and the nutrients present in the treated water can provide irrigation quality water or a source of culture medium for algae. The subsequent agriculture and algal culture has the potential to create food, energy, and cleaner water (Naidoo et al., 2013).

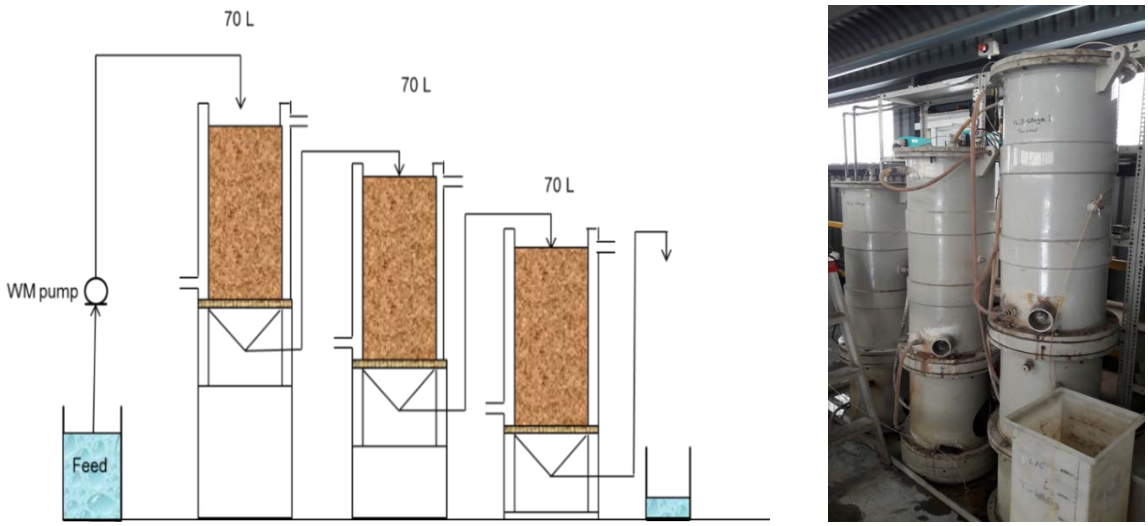


Figure 4: a) Laboratory-scale BSR system design 4b) Laboratory scale BSR model system



Figure 5: BSR pilot scale demonstration system

SAVMIN®

SAVMIN® is a process Mintek has developed over the last 20 years. In 1998, Mintek patented the SAVMIN® process. The main aspect that makes the process attractive for the treatment of AMD is that it allows for the removal of sulphates to concentrations of less than 200 mg/L (van Rooyen, 2016) by means of ettringite precipitation. The SAVMIN® process also includes the regeneration and recycling of a key reagent, aluminum hydroxide, thereby limiting the need for fresh reagent addition. Electrical power consumption is also limited because the process operates at ambient temperature and pressure.

Pilot tests were conducted at gold mines in South Africa. Recently, further developments on the SAVMIN® process have been made in partnership with Veolia Water Solutions and Technologies, a leader in water and wastewater treatment technologies. The original design of the SAVMIN® process consisted of five stages, which was improved by eliminating two reactors and two thickeners from the process (Figure 6). Additionally, extensive development was performed around the reagent regeneration process step, resulting in an impressive reduction in the operating cost of the process.

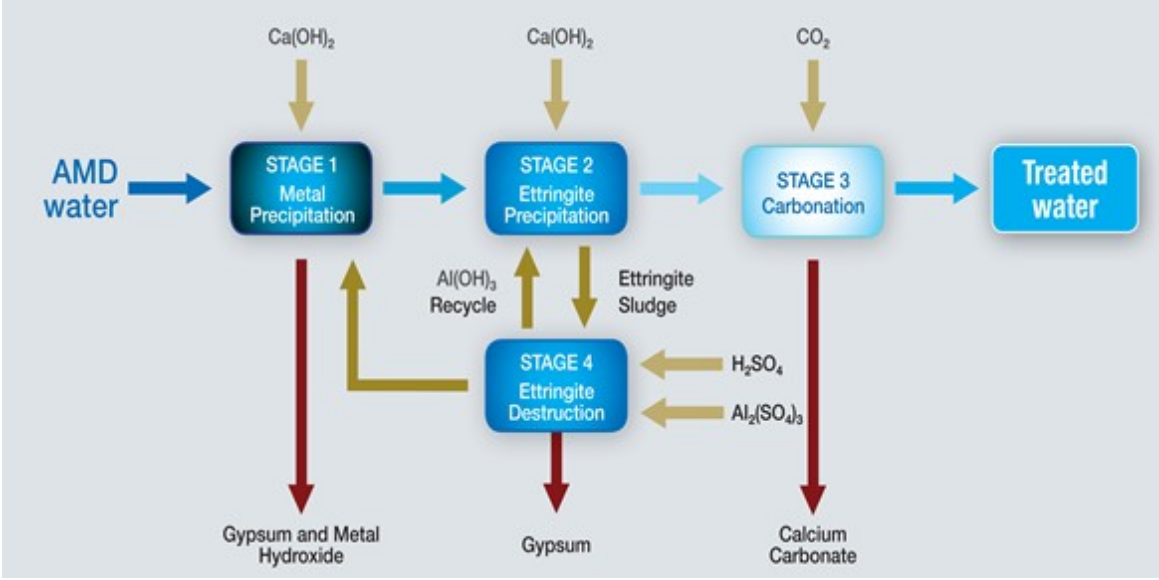


Figure 6: Current SAVMIN® Process Flowsheet

SAVMIN® has the ability to generate potable quality water with >92% sulphate removal (van Rooyen, 2017). The operating costs of the SAVMIN® technology have been successfully reduced by ~75% (Figure 7), which makes the technology a financially competitive option for potable water generation. The cost of treating acid mine water with a sulphate concentration of ~ 2g.L^{-1} has been reduced.

Algal Aquaculture and Agriculture

Algae has long been known to have applications in water treatment, production of energy, food, and many more (Naidoo et al., 2013; Moodley et al., 2015). Algae are capable of mopping up residual waste nutrients like phosphates, nitrogen, and sulphates, while accumulating heavy metals through bio-sorption or chelation (Zeraatkar et al., 2016). Algae are also well known to produce up to 70% of their dry weight as oil, and can also produce high value compounds for application in pharmaceuticals and nutraceuticals (Moodley et al., 2015). Algae are microscopic plants and therefore have the same nutrient requirements as plants. This makes algae an ideal inclusion within the proposed system as they can utilize the water

treated by the BSR process that still contains NH_4^+ and HCO_3^- and moderate levels of PO_4^{3-} as a nutrient source. This allows the water from the BSR process to feed into an algal system that utilizes the nutrients to generate lipids for energy, biomass for food or feed; the resultant water will be free of NH_4^+, HCO_3^- and PO_4^{3-} (Li et al., 2011).

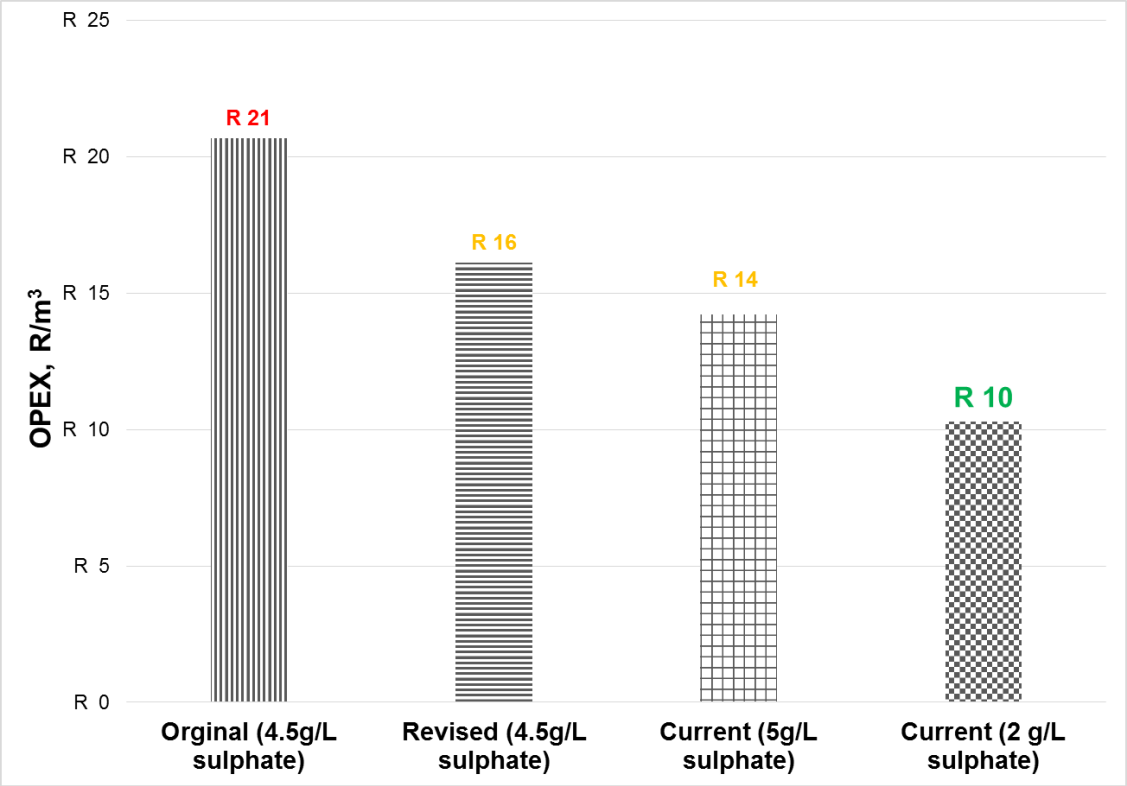


Figure 7: Evolution of SAVMIN® OPEX

This water can now feed into an aquaculture system to sustain the production of fish protein. The fish in the system can be fed the algal biomass from the preceding algal culture system. Fish consume the algae and produce waste nutrients like nitrates, phosphates, ammonia, etc., which in turn "pollute" the water that can be redirected back to the algal culture ponds or diverted to agriculture as irrigation water. The crops grown on the waste water can be bioenergy or food crops.

The products from the algal and aquaculture systems will be algal biomass, fish, and polluted water that provide a resource for agriculture. The algal biomass will be used to extract oil for the production of biofuels (Figure 8) while the waste biomass will be formulated into animal feed and fed back to the fish or other animal stocks. The products from agriculture will be food and energy.

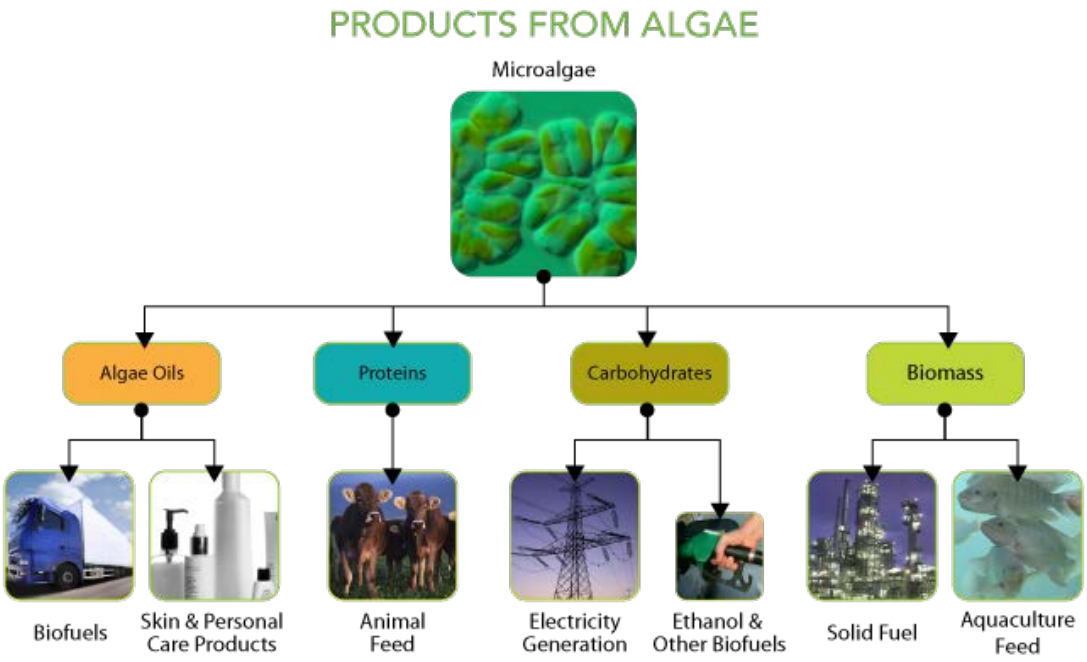


Figure 8: Products from algae
(http://www.atafood.com/Innovative-Microalgae-Products)

Livestock Farming and Anaerobic Digestion

The biomass generated from the algal system, as well as waste from aquaculture and agriculture, can be used to formulate animal feeds and used to farm sheep, beef, chicken, etc. These animals produce significant amounts of waste that generally pose an environmental risk due to the potential of creating eutrophication in rivers (Hill et al., 2005). However this waste material, together with food waste and sewage from the communities, can be collected and fed into an anaerobic digester for the production of biogas (Zhang et al., 2014) (see Figure 9). The biogas can then be used to power a gas turbine for electricity production.

Concentrating Solar Power (CSP)

CSP emerged in 1973; however, there have been references to similar principals as far back as 212 BC (Baharoon et al., 2015). CSP is available in four optical types: parabolic trough, dish sterling, concentrating linear Fresnel reflector, and solar power tower (Boerema et al., 2013). All these types work on the principal of collecting the sunlight over a large area and concentrating it to a central point. This facilitates an increase in temperature to up to 1,000 degrees Celsius, which heats up molten salt, which in turn generates electricity via a steam turbine (Law et al., 2014).

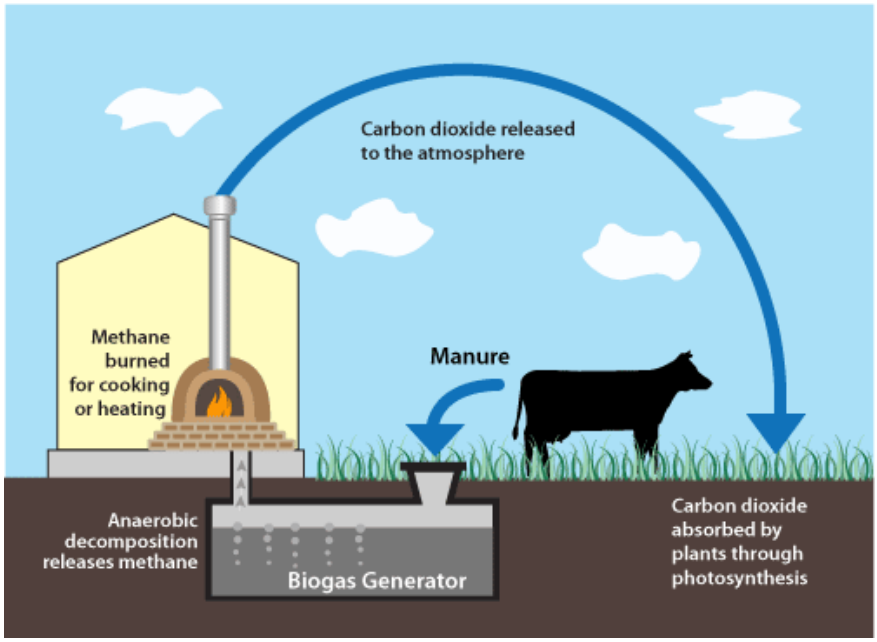


Figure 9: Biogas generation from animal waste
(http://agroindustriindonesia.blogspot.co.za)

Within the proposed system, CSP has the potential to generate power or treat water using solar thermal desalination technology (Gastli et al., 2010). Solar thermal desalination (STD) is a technology in which solar energy is used to evaporate water and then distil it to deliver clean drinkable water. STD has been long considered infeasible due to both capital and operating costs. However in a system like the proposed one (see Figure 3), where the waste heat from power generation is used for the treatment of mine water, the process could prove extremely feasible and could result in the production of potable water.

Conclusion

The system presented and discussed adopts a minimal to zero waste principal, in which by-products and waste materials are never discarded, but rather re-used as a resource in another process. This symbiotic system allows for the generation of food, energy, and clean water, while preserving the environment and preventing mine water pollution.

References

Andersen, R.A. 2005. *Algal Culturing Techniques*, 1st Edition. New York: Academic Press.

Baharoon, D.A., Rahman, H.A., Omar, W.Z.W. and Fadhl, S.O. 2015. Historical development of concentrating solar power technologies to generate clean electricity efficiently – a review, *Renewable and Sustainable Energy Reviews,* 41: 993–1027.

Baxter, R. 2016. *Mining in South Africa: The Challenges and the Opportunities*. Chamber of Mines, South Africa.

Boerema, N. Morrison, G., Taylor, R. and Rosengarten, G. 2013. High temperature solar thermal central-receiver billboard design, *Solar Energy,* 97: 356–368.

Dobbin International. 2016. Long-term sustainable economic and social development Limpopo Province. Presentation to Anglo American. Retrieved from: https://www.emaze.com/@AZFWRCTL/Presentation-Name

Gastli, A., Charabi, Y. and Zekri, S. 2010. GIS-based assessment of combined CSP electric power and seawater desalination plant for Duqum-Oman, *Renewable and Sustainable Energy Reviews,* 14(2): 821–827.

Hill, D.D., Owens, W.E. and Tchoounwou, P.B. 2005. Impact of animal waste application on runoff water quality in field experimental plots, *Int J Environ Res Public Health,* 2(2): 314–321.

Law, E.W., Prasad, A.A., Kay, M. and Taylor, R.A. 2014. Direct normal irradiance forecasting and its application to concentrated solar thermal output forecasting – a review, *Solar Energy,* 108: 287–307.

Li,Y., Chen, Y., Chen, P., Min, M., Zhou, M., Martinez, B., Zhu, J. and Ruan, R. 2011. Characterization of a microalga Chlorella sp. well adapted to highly concentrated municipal wastewater for nutrient removal and biodiesel production, *Bioresource technology,* 102(8): 5138–5144.

Maree, J.P. and Strydom, W.F. 1978. Biological sulphate removal from industrial effluent in an upflow packed bed reactor, *Water Research,* 21(2): 141–146.

Maynard, J. 2017. What's left of South Africa's natural resources. Retrieved from: https://www.southafricanmi.com/blog-18feb2017.html

Moodley, M., Bok, C., Chetty, D. and Maharajh, D. 2015. *Micro-algae: The Rise of Next Generation Biofuels,* edited by Alvise Perosa, Guido Bordignon, Giampietro Ravagnan, Sergey Zinoviev, 47–54. Venezia: Edizioni Ca' Foscari.

Naidoo, T., Zulu, N., Maharajh, D. and Lalloo, R. 2013. *Value Added Products from Microalgae,* edited by Faizal Bux, 137–159. Boca Raton: Taylor and Francis.

Peck, H.D. Jr. 1967. Enzymatic basis for assimilatory and dissimilatory sulfate reduction, *J. Bacteriol.,* 82(6): 933–939.

Sumi, L. and Gestring, B. 2013. *Polluting the future: How mining companies are contaminating our nation's waters in perpetuity.* Retrieved from www.earthworksaction.org

van Rooyen, M. 2017. Evolution of the SAVMINTM process for treatment of AMD, *Proceedings of SAIMM/MMMA Water 2017 Conference*, 10–11 July 2017, Emperor's Palace, Johannesburg, South Africa.

van Zyl, H.J., van Zyl, J.E., Geustyn, L., Ilemobade, A. and Buckle, J.S. 2007. *Water Consumption Levels in Selected South African Cities.* Retrieved from: http://www.wrc.org.za/Pages/DisplayItem.aspx?ItemID=3826&FromURL=%2FPages%2FAllKH.aspx%3F

Wolkersdorfer, C. and Busisiwe, Q. 2003. Passive mine water treatment with a full-scale, containerized vertical flow reactor at the abandoned Metsämonttu mine site, Finland, in *IMWA, Mine Water and Circular Economy.* Lappeenranta, Finland.

Zeraatkar, A.K., Ahmadzadeh, H., Talebi, A.F., Moheimani, N.R. and McHenry, M.P. 2016. Potential use of algae for heavy metal bioremediation, a critical review, *J Environ Manage,* 181: 817–831.

Zhang, C., Su, H., Baeyens, J. and Tan, T. 2014. Reviewing the anaerobic digestion of food waste for biogas production, *Renewable and Sustainable Energy Reviews,* 38: 383–392.

Zhuwakinyu, M. 2017. Water 2017: Review of South Africa's water sector. Retrieved from: http://www.creamermedia.co.za/article/water-2017-a-review-of-south-africas-water-sector-pdf-report-2017-08-25

Proceedings of Mine Water Solutions 2018
June 12–15, 2018, Vancouver, Canada
Published by the University of British Columbia, 2018

"Don't Make Waves:" Desalinated Water and the Social Licence to Operate in the Atacama Region, Chile

Cecilia Campero, The University of British Columbia, Canada, Chile

Abstract

Desalination is assumed to be important in overcoming physical resource limits, resolving water scarcity, and satisfying water demands for productive activities. In Chile the mining industry is leading the drive toward the construction of new desalination plants, followed by water supply companies that are focused on human consumption. This expanding process is confronting governance challenges due to the multiple interests around desalinated water and the impacts of the process (e.g. ecological, economic, and social).

The Atacama Region of Chile is home to major mining industries. It is located in the arid to extremely arid northern part of the country, where water is a contested resource with the farming community and indigenous people, affecting its availability even for human consumption. This context presents a challenge for local development and for the structure of governance, which is competing between territorial scales and the power to affect decision making. Drawing from company sustainability reports and environmental impact assessments, I examine three mining companies in the Atacama Region that are incorporating desalinated water into their water strategy, and facing both governance challenges and new interest from local communities. I also describe what the companies are doing to affect the acceptance of their project's Social Licence to Operate (SLO).

The broader intellectual objective of the article is, first, to explore desalinated water governance and the different interests pursued by actors. Second, the article considers how desalinated water is strategically articulated through the mining industry's social licence to operate. Finally, the article presents how companies are responding to new societal interest in desalinated water projects. Analysis of these processes evokes questions about the complex governance of desalination, revealing different interests and concerns, and also reveals the strategies used by both mining companies and social groups to achieve their goals.

Introduction

In water-scarce regions, such as Spain, Israel, and the Middle East, desalination is promoted as a means to increase water supply (Swyngedouw, 2013; Lee, 2016). With particular geographical characteristics, the

Chilean experience is also part of the expansion of desalination technologies. The northern and central regions of the country are water-scarce environments, and basins supplying water to mining companies in the north have an annual precipitation of less than 100 mm per year (Vicuña and Lagos, 2010).

During the last decade, numerous strategies have been growing to support desalination in Chile. Examples include the National Strategy of Water Resources 2012–2025 (DGA, 2013), in which desalination was presented not only as a way to confront scarcity, but also to stabilize the water source, addressing the variations of natural resources and climate change. Aligned with this is the National Plan Against Drought 2015 (Gobierno de Chile, 2015), which proposes the construction of desalination plants in four regions; and the National Policy of Water Resources 2015, which promotes the construction of desalination plants in water-scarce cities, making potable water for rural areas a priority. It also suggests the construction of "water pipelines" (*carreteras hídricas*) to convey water from different places in the country. This potential means to increase the water supply in Chile is augmented by a further means to improve the water supply, especially in relation to mining activities. The Chilean Congress started a discussion regarding the regulation of desalinated seawater for use in mining projects, so as to compel mines which consume over 150 litres of water per second to incorporate desalinated seawater into their operations.

A parallel strategy to encourage mining companies to incorporate desalinated seawater into their operations is emerging at the local level with communities. Local communities are increasingly demanding the use of desalinated seawater for mining operations. During 2015, Pelambres Mining Company had to promise to the Salamanca community the construction of a desalinated water plant in order to alleviate the conflict (La Nacion, March 11, 2015). "Where you dry, you pay" *(Por donde secas, pagas)* is one of the phrases heard in desalination demands (Cuenca, 2015). Examples like these show how community strategies are moving from demanding a reduction of fresh water consumption, to pressuring for the incorporation of desalinated water for use in mining operations.

Initiatives encouraging desalinated water use are confronted by governance challenges due to the multiple interests around water and the impacts of the process (e.g. ecological, economic, and social) (Swyngedouw, 2013). The objective of this paper is to highlight both the governance challenges and the new interest from local communities, and also to describe what companies are doing to affect the acceptance of the project Social Licence to Operate (SLO).

While an increasing amount of research literature is focusing on ocean water, the main focus is on aquaculture and fishing industries, and little is known about desalination in general, and in relation to mining industries in particular. In this article, I connect desalination practices with SLO in the mining sector. This Chilean case study will be presented in order to identify the importance of changes in the

demands of local groups regarding desalinated water, and to show how Chile is becoming the first country where desalinated water will be mandatory for use within the mining industry.

Methodology

This paper draws on research findings from three mining projects in the Atacama Region of Chile: Caserones, Candelaria, and Mantoverde. Each of these projects has incorporated desalinated water into their water strategy. The status and ownership of all current projects are summarized in Table 1. The data presented in this paper is based on company sustainability reports and environmental impact assessments. Environmental impact assessments are used in order to obtain data about new societal demands regarding mining operations and desalination projects. Sustainability reports are used to guide the perspective of mining companies on societal demands and their solutions for overcoming them. Finally, public sector documents and NGO reports are used in order to triangulate data.

Issues raised by the selected data sources were grouped according to the driving force–pressure–state–impact–response (DPSIR) model. This model has been successfully used by Borja et al. (2006) in water governance frameworks. The choice of the DPSIR model facilitates the identification of the challenges at different stages of desalinated water governance.

Table 1: Mining companies under study

Project	Firms	Headquarters	Desalination status	Desalination water rate	*Cost of new capacity (millions USD)
Caserones Mining Project	SCM Minera Lumina Cooper Chile/ Pan Pacific Copper Co., Ltd. (77,37%) and Mitsui & Co., Ltd (22,63%).	Japan	**Acquiring desalinated water since 2010	150 L/sec.	33
La Candelaria Mining Project	Lundin Mining	Canada	Functioning since 2013	300 L/sec.	270
Mantoverde	Anglo American Norte S.A.	United Kingdom	Functioning since 2014	120 L/sec.	62

*Investment includes plant and pumping system.

**To achieve environmental approval, the company made a commitment to acquire desalinated water, which they are purchasing from Cerro Negro Norte (iron mine). The investment amount corresponds to Cerro Negro Norte.

Governance in Desalinated Seawater

Desalination technology confronts not only economic, environmental, and technical challenges, but also a social challenge. Critical studies on desalination have mainly focused on the sustainability of the process,

with emphasis on the environment (e.g., CO_2 emission and brine disposal), the economic (e.g., energy consumption) and the social aspects (from the perspective of public consumption, e.g., lack of public trust and inequalities) (Dolnicar and Schäfer, 2009; Fragkou and McEvoy, 2016). Less attention has been paid to the governance challenges. The term governance implies all the manners, institutions, organizations, and scales by which social relations are expressed in the territory through formal and informal decisions (Bridge and Perreault, 2009). Swyngedouw (2013) has considered how desalination in Spain is inciting new conflicts due to the network of interests behind this technological expansion, e.g. environmental, legal rights over the seas, and the high cost of the process. A study prepared by the Organization for Economic Co-operation and Development (OECD, 2017) has identified governance issues in Chile related to trade-offs among water users (e.g. fisheries), unclear legal frameworks, and a lack of land-use planning strategy for coastlines.

The primary focus of the literature on desalination governance is on projects which are increasing the supply of water for public consumption, while the mining industries involved in desalination have received little focus and remain poorly defined. Nonetheless, mining operations using seawater or saline water are increasing around the world. Philippe et al. (2010) identified nine mining operations experimenting with this technology: one in Indonesia, two each in Australia and Canada, and four in Chile. Nowadays, these numbers have increased significantly, not only in operations, but also involving new countries, such as the Cerro Lindo mine, Justa mine, and Shougang Iron in Peru, and Trekkopje uranium mine in Namibia (ICMM, 2012; Emery, 2017). In Chile, as of 2017, seventeen desalination plants were approved for construction, and the government is planning approvals for another fourteen through the year 2024 (COCHILCO, 2015).

Desalination in mining projects is revealing not only governance challenges as part of the permit processes, but also is opening parallel governance issues due to the high energy cost. In addition, a new dimension of interests is emerging behind this technology. Local communities are intervening as actors, who, aside from being concerned with the environmental impacts generated by large-scale desalination plants and trade-offs across water users, are pressuring for allocation of desalinated seawater for nature and urban centers. Examples like these are introducing new demands from local communities in order to accept projects with potential impacts in their territories.

These social expectations, extended as well to new mining projects approvals, have been named in the literature as the Social Licence to Operate (SLO). They are emerging as a step forward from just the legal requirements in giving acceptance to mining interventions (Joyce and Thomson, 1999; Thomson and Boutilier, 2011; Moffat, 2016). Although the future legal requirement in Chile would compel mines that consume over 150 litres of water per second to incorporate desalinated seawater into their operations,

there are as yet no legal requirements concerning the allocation of desalinated seawater beyond mining use.

From Fresh Water to Desalinated Seawater

The Copiapó and Huasco rivers are the main sources of potable water in the Atacama Region. Both are in critical condition, and four communities with drought status (of nine in total) have been impacted (Copiapó, Tierra Amarilla, Caldera and Chañaral) (SISS, 2016). According to the Chilean Copper Commission-, (2007) four large mining companies are extracting water from both rivers (Candelaria, Caserones, Sociedad Punta del Cobre and Pascua Lama). The amount of freshwater used, and the projections of use by sector, are presented in Table 2.

Table 2: Water use by sector, Atacama Region (COCHILCO, 2007)

	2007		2017		2032 (projected)	
	Flow by use (m^3/s)	%	Flow by use (m^3/s)	%	Flow by use (m^3/s)	%
Agriculture	12,033	72.9 %	12,688	61.8%	12,688	52.1%
Drinking water	0,718	4.3 %	1,147	5.6%	1,290	5.3%
Industries	0,518	3.1 %	1,029	5.0%	2,822	11.6%
Mining	1649	10.0 %	4,183	20.4%	6,057	24.9%
Others	1592	9.6 %	1,473	7.2%	1,474	6.1%
	15,274	**100,0%**	**20,520**	**100%**	**24,331**	**100%**

Consequently, seawater desalination is a central strategy in the effort to supplement water sources for both industries and potable water supply. While the majority of desalination plants are used by the mining sector, there are three dedicated to potable water production (DGA, 2016). Since 2013, water used in copper mining has been increasingly obtained from ocean water; however, underground water remains the primary source, and the consumption of this source was reduced between 2014–2015 by only 6.1%. The same was evident for the aboveground water, which was reduced by 25.1% (see Table 3).

In supplementing water for mining industries, desalination processes have to overcome governance challenges as part of the permit process (including new expectations from local communities) and confront a parallel governance structure that appears as part of the high energy cost inherent in desalination. This means that, due to the high energy consumption, mining companies have to bargain

with new actors in a non-regulated process, in order to ensure a diversion of water resources (desalinated water by fresh water).

Table 3: Water extraction in copper mining in the Atacama Region (based on COCHILCO, 2015)

	Water extraction	Unit	2012	2013	2014	2015	Var. 2014–2015
Atacama	Aboveground water	L/sec	701	541	545	408	–25.1%
	Underground water	L/sec	747	759	750	704	–6.1%
	Acquired from others	L/sec	175	154	155	56	–63.9%
	Seawater	Lts/sec	0	248	433	508	17.2%
Chile	Aboveground water	L/sec	5,867	5,942	5,908	5,577	–5.6%
	Underground water	L/sec	5,749	6,200	6,302	6,430	2.0%
	Acquired from others	L/sec	763	577	742	1,064	43.5%
	Seawater	L/sec	978	1,287	1,707	2,275	33.3%

Desalinated Seawater in the Mining Industry: Governance and New Interests

When proposed desalination projects begin, their Environmental Impact Assessment (EIA), according to the Environmental Law (19.300), each public-sector representative must give their approval of, or comments on, the evaluated projects, which results in a Sectorial Environmental Approval (PAS) that grants the final RCA (Environmental Qualification Resolution). This permit process is not exclusive to desalination projects, but is applied to any kind of project that presents risks to human health, or has the potential to impact the quality or quantity of renewable natural resources.

In the permitting process for desalination projects, interests covered with major attention by public-sector representatives were brine disposal and the impacts on the marine ecosystem. Other issues with less consideration were energy consumption, landscape, acoustic/light pollution, waste spill, (post) closure mitigations, biodiversity, and climate change (Table 4).

Other important expectations were raised by municipal actors, over and abov the EIA's concerns. Municipalities were the main actors demanding desalinated water sharing before giving a green light to projects. For example, in the Candelaria project approval, the Municipality of Caldera demanded 50 L/sec for human consumption, while the requirement of the Municipality of Copiapó was to allocate water to nature at 30 L/sec (Copiapó River) (SEIAa, 2011). In the EIA of the Mantoverde mine, the municipality of Chañaral expressed its main concerns as brine disposal and changes along the coastline (SEIAb, 2011).

As part of the Caserones mining project approval (Lumina Cooper), desalinated water was required by the Municipality of Tierra Amarilla and SEREMI of Health in order to supply water to the industry, but also for the replenishment of natural sources. In the RCA the company committed to providing desalinated water for irrigation (SEIA, 2010). Other requirements included the construction of parks and green areas, and the construction of a viewpoint illuminated by solar energy for local communities to watch the plant's operational process.

In addition to the multiple interests pertaining to the EIA, a parallel governance structure addresses the high energy consumption required by the process. There are often high costs, but in the Chilean case these are increased due to the energy required to pump desalinated water from the coast to the mining operations, which are often located at high altitudes (around 3,000 masl) (Cisternas and Gálvez, 2018). This is relevant because energy is another scarce resource. The high costs involved in pumping water to mining operations increased between 2 and 4 US$ /m^3 (COCHILCO, 2007).

Some alternatives or responses to the high energy cost, involved fresh water rights agreements between potable water supply companies (located at high altitude) and mining companies (Table 4). Such agreements imply trading desalinated water with community centres close to the coast in exchange for fresh water rights for mining operations (COCHILCO, 2007). This approach, denominated as SWAP (opposite to the Source Water Assessment and Protection promoted by EPA in EEUU), was borrowed from the economic and financial term, referring to exchanges of water supplies (González, 2011). The project was formally discussed in the "public-private encounter for sustainable use of water resource in the Copiapó Valley" in Atacama. The encounter was led by representatives from the mining sector, the Ministerial Regional Secretariat (SEREMI) Agriculture, the Association of Agricultural Producers and Exporters (APECO), and the Canal Supervisory Commission of the Copiapó River (JVRC) (COCHILCO, 2007). It is worth mentioning that this alternative has not been exempt from disapproval, bringing new actors and scales into the debate and expanding the governance structure e.g. Sustainable Chile (Larrain and Poo, 2010), Press Research Center Chile (FMC, n.d.) and Coordinator for Water Defence and Life (Godoy, n.d.).Company responses to governance challenges are revealing a process that includes diverse effects and new emerging interests as factors in desalination approvals, some of which are explored in the next section.

Table 4: Governance in desalination according to actors' interests and level of intervention (based on Barau and Hosani, 2015)[1] (See appendix to this chapter for a guide to acronyms)

Component	Challenges	Sectors involved		
		Local/municipal	Regional	National
Driving forces	-Water scarcity -Regulation -Local communities' demands			
Pressures	-High energy consumption -Marine ecosystem -Trade -offs across water users -Brine disposal -Landscape -Biodiversity -Acoustic-light pollution -Climate change -Waste spill -Urban growth -Archaeology -Coastline -Pipelines and risks in case of breaks -Desalination sharing	Maritime gob M. Chañaral M. Caldera M. Copiapó M. Tierra Amarilla M. Caldera	SERNAPESCA NGO SUBPESCA SERNATUR Health Service SEREMI Health SAG CONADI DOH DGA GORE CONAF SEREMI Agriculture SEC SERPLAC	Evaluation Environmental Service (SEA)
State	-Mining industry is leading, followed by water supply companies -Incoherent land-use planning strategy for coastlines -Unclear legal frameworks -Cost of desalination		NGO	OECD/Chilean government COCHILCO
Impact	-Endangering of marine ecosystem -Brine disposal	Fisheries groups Maritime gob M. Chañaral Health Service SUBPESCA	NGO GORE	
Response	-Desalinated water -Desalinated water sharing -SWAPS	Potable water supply companies Mining companies APECO JVRC M. Copiapó M. Tierra Amarilla M. Caldera	SEREMI Agriculture SEREMI Health GORE NGO	COCHILCO

Companies' Responses: Earning the Acceptance of the Projects

Mining companies, through the incorporation of desalinated water into their water strategy, are covering a market not included in the State's strategy: water for extractive industries, agriculture, and for their

[1] Note: There are other governmental actors involved, which were not mentioned due to their complete approvals of projects (Ministry of Mining and entities related). For a detailed list of acronyms please refer to the appendix at the end of this chapter.

neighbours (Figure 1). The Caserones operation is not using desalinated water in its mining project, but is giving compensation for its fresh water use by allocating desalinated water to other users. In their sustainability reports this is expressed as follows: "to offset new water usage by the mine, the company also provides desalinated seawater for downstream irrigation use" (JX Nippon Mining & Metals Corporation, 2015; JX Nippon Mining & Metals Corporation, 2016). Water distribution includes 50 L/sec for human consumption to Caldera commune and 100 L/sec to the Mal Paso Channel (Tierra Amarilla community) to benefit agriculture and irrigators (Lumina Copper, 2008). Caserones has direct links with social groups at the municipal level (APECO and JVRC), due to both its water transfers for irrigation uses, and its water management improvement program for the Copiapó River, which was implemented with GORE collaboration.

The Mantoverde operation, in its sustainability report, declares that its desalination plant currently meets only the mine's needs, but emphasizes its reduction of water consumption in the Copiapó valley (Anglo American, 2014). Like Mantoverde, desalinated water is not shared by Candelaria with its neighbouring communities; however, the company has launched a Fishermen Development Fund to alleviate trade-offs across water users. "This fund offers local fishermen resources to develop individual or collective projects in the four main areas of housing, health, education, and economic development" (Lundin, 2017). The company also included in their RCA a commitment to construct parks, green areas, and a viewpoint for local communities to watch the plant's operation processes. Both companies, as part of the governance challenges, are framing their sustainability reports in order to include information about plant ocean discharges and marine ecosystems. While Candelaria provides data about the quantity and quality of their discharges, more information is required for Mantoverde's operation.

The advent of desalination, and subsequent energy cost, has broadened the already complex governance terrain in which desalination projects are involved, at the same time allowing collaboration between the actors that goes beyond the EEIA. Essentially, the question that remains open is how to resolve the social challenges inherent in desalination projects.

Conclusion

Despite helping to increase the water supply and provide a solution to water scarcity, desalinated seawater finds itself in a complex governance terrain due to the heterogeneous network of actors involved. This governance terrain is embedded at different levels and fuses diverse interests (Feitelson and Rosenthal, 2012). In addition to the governance inherent in the permitting process during the EIA, mining companies are involved in a parallel governance due to the high energy cost required in the process.

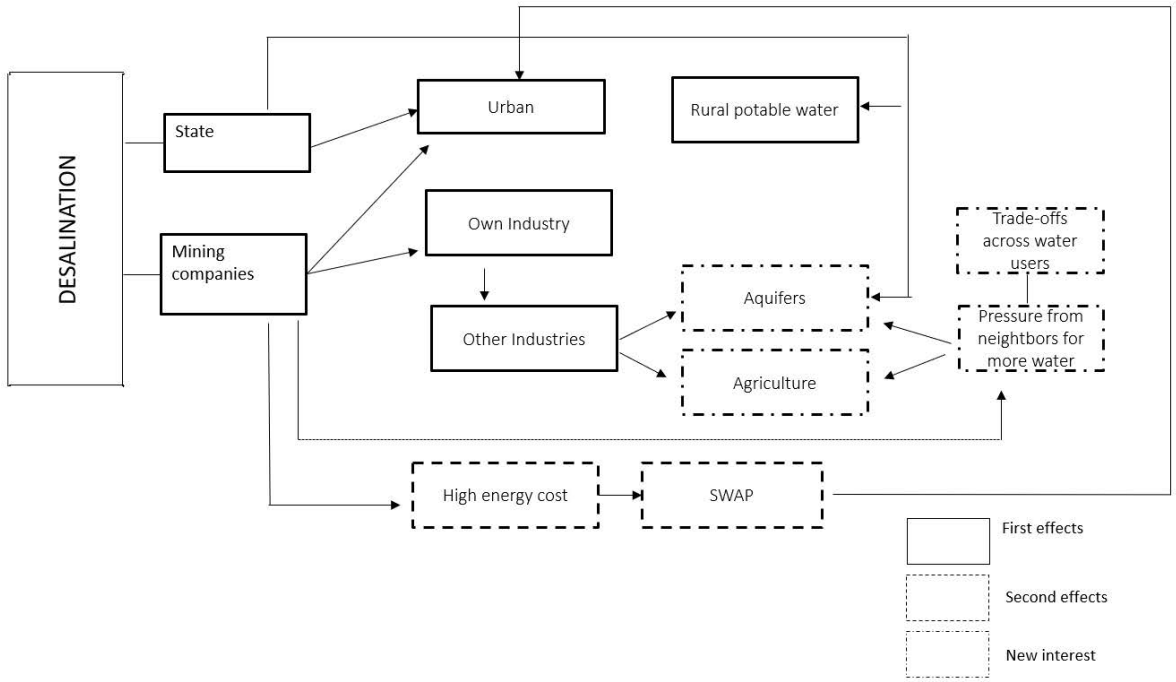


Figure 1: Mining industry responses to desalinated seawater uses by comparison with the State (based on Feitelson and Rosenthal, 2012)

In both governance arrangements, desalinated seawater allocations, either to watershed sustainability or for human consumption, are identified. During the EIA, mainly municipal authorities, connected with only one regional authority (SEREMI of Health), have required desalinated seawater sharing in order to give their approval to mining operations (SLO). Mining companies, in order to enhance their legitimacy, have included communities' expectations in different ways. Commitments to support local development initiatives have included, besides the sharing of desalinated water, the construction of a vantage point for local communities to observe the desalination process. Additionally, a new mode of reporting sustainability is being incorporated, covering plant ocean discharges and marine ecosystems.

During desalination plants' operational stage, water allocations are also identified, in order to reduce the associated energy costs. In this alternative, water supply companies, mining companies, local representatives from the agriculture sector, and one regional authority (Seremi of Agriculture) are involved. Notably, energy consumption was not at the core of the EIA's concerns from public authorities.

The multiple and often contradictory social networks involved in the desalination industry are reconfiguring the spatiality of water, with potential effects in the distribution and acquisition of processed water, something which should be explored with major attention.

Acknowledgements

The author thanks CONICYT for their funding through Becas Chile 74180023.

References

Anglo American. 2015. Sustainability report 2015. Driving change, defining our future.

Anglo American. 2014. Sustainable development report 2014. Focus: Effective partnership.

Barau, A. and Hosani, N. 2015. Prospects of environmental governance in addressing sustainability challenges of seawater desalination industry in the Arabian Gulf, *Environmental science and policy:* 145–154.

Borja, A., Galparsoro, I., Solaun, O., Muxika, I., Tello, E., Uriarte, A., et al. 2006. The European Water Framework Directive and the DPSIR, a methodological approach to assess the risk of failing to achieve good ecological status, *Estuarine, Coastal and Shelf Science,* 66: 1–2, 84–96.

Bridge, G. and Perreault, T. 2009. Environmental governance, in N. Castree, D. Demeritt, D. Liverman, and B. Rhoads (eds), *A Companion to Environmental Geography,* 475–497. Malden, Oxford: Blackwell Publishing Ltd.

Cisternas, A. and Gálvez, E. 2018. The use of seawater in mining, *Mineral Processing and Extractive Metallurgy Review* 39(1): 18–33.

COCHILCO. 2015. Consumo de agua en la minería del cobre al 2015. Santiago: Ministerio de Minería, Gobierno de Chile.

COCHILCO. 2007. Gestion del recurso hidrico y la mineria en Chile: diagnostico para mesa publico-privada nacional. Santiago: Ministerio de Minería, Gobierno de Chile.

Cuenca, L. 2015. Caserones: Por donde secas, pagas. From OLCA. Retrieved from: http://olca.cl/articulo/nota.php?id=105203

DGA. 2016. Atlas del Agua, Chile 2016. Santiago: Ministerio de Obras Publicas.

Dolnicar, S. and Schäfer, A. 2009. Desalinated versus recycled water: public perceptions and profiles of the accepters, *Environ. Manag.,* 90: 888–900.

Emery, A. 2017, December 6. Peru building Lima's first desalination plant, from BNamericas. Retrieved from: https://www.bnamericas.com/en/news/waterandwaste/peru-building-limas-first-desalination-plant1

Feitelson, E. and Rosenthal, G. 2012. Desalination, space and power: The ramifications of Israel's changing water geography, *Geoforum,* 43: 272–284.

Fragkou, M. and McEvoy, J. 2016. Trust matters: Why augmenting water supplies via desalination may not overcome perceptual water scarcity, *Desalination,* 397: 1–8.

González, J. 2011, April 25. Water SWAP o intercambio comercial de fuentes de abastecimiento de agua, from Sustentabilidad, desarrollo y evolucion. Retrieved from: http://sde-sesga.blogspot.ca/2011/04/water-swap-o-intercambiio-comercial-de.html

ICMM. 2012. Water management in mining: A selection of case studies.

Joyce, S., and Thomson, I. 1999. Earning a social licence to operate: Social acceptability and resource development in Latin America, *Mining Journal* 11: 441–443.

JX Nippon Mining and Metals Corporation. 2015. Sustainability report 2015.

JX Nippon Mining and Metals Corporation. 2016. Sustainability report 2016.

La Nacion. 2015, March 11. Gobierno logra destrabar conflicto entre vecinos de Salamanca y Pelambres. La Nacion.

Lee, M. 2016. Privatization of water desalination: the need to balance governmental and corporate control in California, *The Global Business Law Review,* 23: 1–28.

Lumina Copper. 2008, 9 26. Descripcion. Agua. Retrieved 2017 from: http://www.caserones.cl/articulo_imprimir.php?idnoticia=34

Lundin Mining. 2015. 2015 Sustainability report.

Lundin Mining. 2016. 2016 Sustainability report.

Moffat, K., Lacey, J., Zhang, A. and Leipold, S. 2016. The social licence to operate: a critical review, *Forestry,* 89: 477–488.

Newman, M. E. 2003. The structure and function of complex networks, *SIAM Review,* 45(2): 167–256.

OECD. 2017. Gaps and Governance Standards of Public Infrastructure in Chile. Public Governance Directorate.

Philippe, R., Dixon, R. and Dal Pozzo, S. 2010. Seawater supply options for the mining industry, *WIM2010 Proceedings of the Second International Congress on Water Management in the Mining Industry:* 13–20. Santiago, Chile.

SEIA. 2010, 1 13. Ficha del Proyecto:Proyecto Caserones. Retrieved 2017 from: Sistema de Evaluación de Impacto Ambiental: http://seia.sea.gob.cl/expediente/ficha/fichaPrincipal.php?modo=fichaandid_expediente=3281058

SEIAa. 2011, 6 24. Ficha del Proyecto: Planta Desalinizadora Minera Candelaria. Retrieved 2017 from: Sistema de Evaluación de Impacto Ambiental: http://seia.sea.gob.cl/expediente/expedientesEvaluacion.php?modo=fichaandid_expediente=4790049

SEIAb. 2011, 5 13. Ficha del Proyecto: Abastecimiento de Agua Desalada Mantoverde. Retrieved 2017 from: Sistema de Evaluación de Impacto Ambiental: http://seia.sea.gob.cl/expediente/expedientesEvaluacion.php?modo=fichaandid_expediente=4604731

SISS. 2016. Informe de gestión del Sector Sanitario. Gobierno de Chile.

Swyngedouw, E. 2013. Into the sea: Desalination as hydro-social fix in Spain, *Annals of the Association of American Geographers* 103(2): 261–270.

Thomson, I. and Boutilier, R. 2011. Modelling and measuring the social license to operate: Fruits of a dialogue between theory and practice.

Vicuna, S. and Lagos, G. 2010. Relación entre Agua, Energía y Cambio Climático: Estudio de alto nivel sobre el impacto económico del cambio climático en la industria minera de Argentina, Chile, Colombia y Perú. Santiago: Centro de Cambio Global UC.

Appendix

Abbreviations used in Table 4: Actors involved in the desalination projects approvals, and acronyms

Municipal	Regional	National	International
Agricultural Producers and Exporters (APECO)	Regional Government (GORE)	Environmental Superintendence	Organisation for Economic Co-operation and Development-OECD
Canal Supervisory Commission of the Copiapó River (JVRC)	National Corporation for Indigenous Development (CONADI)	Chilean Copper Commission (COCHILCO)	
Maritime government	General Water Directorate (DGA)		
Municipality of Chanaral	Hydraulic Works Directorate (DOH)		
Municipality of Caldera	Forestry National Corporation (CONAF)		
Municipality of Tierra Amarilla	Agricultural and Livestock Service (SAG)		
	Health service		
	NGO		
	Sub secretary of Fisheries (SUBPESCA)		
	National Service of Fisheries and aquaculture (SERNAPESCA)		
	National Service of Tourism (SERNATUR)		
	SEREMI (Ministerial Regional Secretariat) Health		
	SEREMI Agriculture		
	Superintendence of Electricity (SEC)		

Proceedings of Mine Water Solutions 2018
June 12–15, 2018, Vancouver, Canada
Published by the University of British Columbia, 2018

From Water Management to Water Stewardship in Mining Regions

Nadja Kunz, The University of British Columbia, Canada

Abstract

Expansion of the mining industry is increasingly constrained by a lack of water, too much water, or social opposition over water-related risks. A lack of water is a global concern with roughly two thirds of the world's largest mines now located in countries experiencing high water scarcity. This can create conflict with surrounding water users and constrain industry access to water. Too much water can prove equally costly for mining firms; for example, the 2010 flooding events in Australia's Bowen Basin led to billion-dollar production losses for the coal-mining sector. The floods also prompted regulatory changes due to concerns about the ecological impacts caused by the discharge of contaminated mine water. Gaining a comprehensive understanding of water issues in mining is challenging because the tasks that use water are interconnected and interdependent. This complexity is magnified at the catchment scale because the water system becomes more closely coupled to the climate and the stakeholders who use, impact, and/or regulate water are more diverse.

This paper provides a high-level overview of key water challenges facing the global mining sector and proposes an organizing framework to distinguish between research needs at two levels: Mine Water Management (within the company fence) and Mine Water Stewardship (beyond the company fence). The former focuses on addressing operational water risks at the mine site level, such as water reservoir optimization and understanding the impacts of water quality changes on flotation effectiveness. The latter explores opportunities to create regional synergies and networks in water provision for mining regions, including working with diverse stakeholders to address water supply and quality issues. It is argued that interdisciplinary thinking is needed at both levels, giving due consideration to both technical and social issues, and that this will be increasingly essential for successful mining companies of the future.

Introduction

Water has emerged as a top strategic business risk facing the global mining sector, and the mismanagement of water can result in significant financial consequences. In Australia, for example, the coal-mining sector faced billion-dollar production losses due to flooding events in 2011 (Devine, 2011),

while other regions have faced water shortages during drought conditions (Stegink et al., 2003). There is also growing community concern about the mining sector's impact on surface and groundwater systems, which has compromised projects globally. For example, statistics from the International Finance Corporation reveal that in the 17 years between 2000 and 2017, 58% of complaints about IFC investments in the mining sector included water issues (IFC and ICMM, 2017). In Canada, the recent rejection of the Taseko Mines New Prosperity project, primarily due to concerns from First Nation leaders about environmental impacts on Fish Lake, demonstrates how ongoing tensions can constrain mining development (Veiga and Tucker, 2015).

In 2007, the Centre for Sustainable Resource Processing (CSRP) in Australia published a report reviewing key trends in water management within the field of resource processing (Côte et al., 2007). As part of this work, a five-level hierarchical framework was developed to delineate research needs based on the building blocks of minerals processing operations, ranging from unit operations at the lowest level to linked networks of sites at the highest level. Through workshops with industry participants, research priorities were identified for each level of conceptual hierarchical framework (Table 1).

Looking back on the research priorities identified by industry experts in 2007 (Côte et al., 2007, and see summary in Table 1), there have been significant advances to addressing these issues by both research and practice. Governments and industry associations, often supported by academic research, have produced many guidance documents to improve water accounting and reporting and to facilitate identification and mitigation of key water risks. For example, the Australian Government published a leading practice handbook in 2008 that outlined drivers for the sector to address water risks, provided tools for risk management, and offered guidance on developing a mine site water balance and account (Department of Resources Energy and Tourism, 2008). Likewise, in 2006 to 2007, South Africa's Department of Water Affairs and Forestry published a series of 15 best practice guidelines covering topics including water resources protection, waste management, and integrated water resources management (Munnik and Pulles, 2009).

In recent years, voluntary disclosure standards by industry associations have improved the consistency in water reporting across national jurisdictions and internationally. For example, the Minerals Council of Australia (MCA) (2014), in conjunction with the Sustainable Minerals Institute of the University of Queensland, published a Water Accounting Framework (WAF) to address a widespread lack of consistency in water reporting across the sector. The Input-Output model and associated water quality descriptors were subsequently endorsed by MCA member companies. The widespread adoption of this framework has contributed to improved disclosure of water use in mining regions. For example, mines operating in the Upper Hunter Valley are now reporting their combined water use data on an annual basis to facilitate informed discussions with local communities (NSW Mining, 2013).

Table 1: Selected research priorities identified by Cote et al. (2007) through workshops with industry practitioners

Level of the hierarchical framework	Examples of research priorities identified at each level
Unit operation (Level 1)	• To gain the most benefit from the proposed conceptual model, a generic description of a unit process is needed that ensures the major sustainability and operational issues are dealt with effectively. • Conduct a data survey to quantify water, energy, and reagent fluxes entering and leaving unit operations. This information would enable completion of the framework at the technical level. Such a tool would assist all parties to better understand the implications of proposed water management initiatives.
The processing plant (Level 2)	• Develop a tool or information database for quantifying the differences in water, reagents and energy uses between one set of linked unit operations and another, enabling the estimation of overall system performance in terms of expected output, (e.g. mineral recovery or commodity purity level), operating and maintenance impacts on profitability and contribution towards sustainability objectives.
Site-level (Level 3)	• Guidelines are needed that can assist sites in developing a "good practice" water balance. • Compare the issues associated with managing water from a site vs. regional level. Develop guidelines for the effective management of water resources. Such a project would involve comparing the costs and benefits associated with central vs. remote water planning/action teams. • Research is needed into how to improve the level of transparency within a site, i.e. for management to ensure widespread understanding about the issues that impact various components of the system.
Operation as a unit (Level 4)	• It is often not recognized that the complexity of sustainable development may require new methods and skills in community engagement. There is a priority need to understand the differences in community engagement under a site-by-site legal compliance approach and an integrated sustainability approach. • A more effective method to regulate water use needs to be developed.
Linked sites (Level 5)	• Better modeling tools should be developed to demonstrate a wider range of potential synergies (and their benefits) to complement the current documentation of existing case studies. • Investigation of options for cost and risk sharing that will make synergies more attractive by overcoming too narrow a view of how profitable linkages can be implemented.

Recently, the International Council on Mining and Metals (ICMM) (2017) published a minimum disclosure standard for water reporting to which members will be required to comply from November 2018. This initiative is a significant step towards improved consistency in reporting mine water use data, which has historically been a barrier for benchmarking performance across sites and collating mine water use data at regional scales. In addition to improving water reporting, there has been considerable academic research to optimize water use and management with respect to water quality and quantity.

For example, experimental research has shown how salinity changes due to increased water recycling can impact product quality (Liu et al., 2011), while systems models have been developed to optimize water storage dams to minimize the risks of too much or too little water at the mine site level (Kunz and Moran, 2016).

In this paper, it is argued that while advances in the technical aspects of managing water issues will remain an important area of research for the mining field, there is a commensurate need to improve

understanding of how mine water use impacts stakeholders beyond the company fence. The paper begins by tracing the evolution of mine water management and stewardship in the academic literature. This is followed by a detailed case study at a mining site which finds that while employees show strong involvement in addressing technical water issues arising at the level of individual unit operations and tasks, there is a notable lack of involvement in contributing to water activities at higher levels of the system. It is concluded that there is a growing need for research on Mine Water Stewardship, and a framework is proposed for guiding future research that adopts a broadened view of mine water systems.

Review of Literature – the Evolving Dialogue towards Mine Water Stewardship

The past several decades have seen a significant increase in research on mine water issues globally (Figure 1). This rise has been particularly prominent from 2006 onwards, when there was an 80% increase in research outputs relative to the yearly publication average during the prior 1987 to 2005 period.

In contrast, research on water stewardship and governance in mining regions has only emerged over the past decade. Although publications on these topics have expanded rapidly since 2011 (Figure 2), they remain only a fraction of the overall publications in this field. This finding suggests that while significant progress has been made in addressing some of the research priorities identified by Cote et al. (2007), there has been less advancement on addressing the research needs at higher levels of the hierarchical framework.

Involvement in Water Issues at a Case Study Mine

To triangulate the findings from the preceding literature review, this section presents the results from a detailed case study at a mining site to investigate the extent to which employees are addressing water issues across different levels of the mine site water system. The case study mine is located in a sub-tropical climate and has high environmental value being located in close proximity to a Ramsar[1] wetland. The surrounding community comprises of a high representation of indigenous groups, and 25% of the mine site's workforce is indigenous. At the time of the study, the mine was undergoing a planned transition from open cut to underground mining (which introduces uncertainty into the future water balance and will involve a change in management structure). In this expansion, a major concern among local communities related to the potential impacts of the project on surrounding groundwater resources including local springs with high cultural value. Further details regarding the attributes of the site can be found in Kunz (2013).

[1] The Ramsar Convention is an international treaty that provides a framework for the conservation and wise use of wetlands and their resources. Ramsar sites represent wetlands that have been recognized as having international importance and conservation value (Ramsar, 2018).

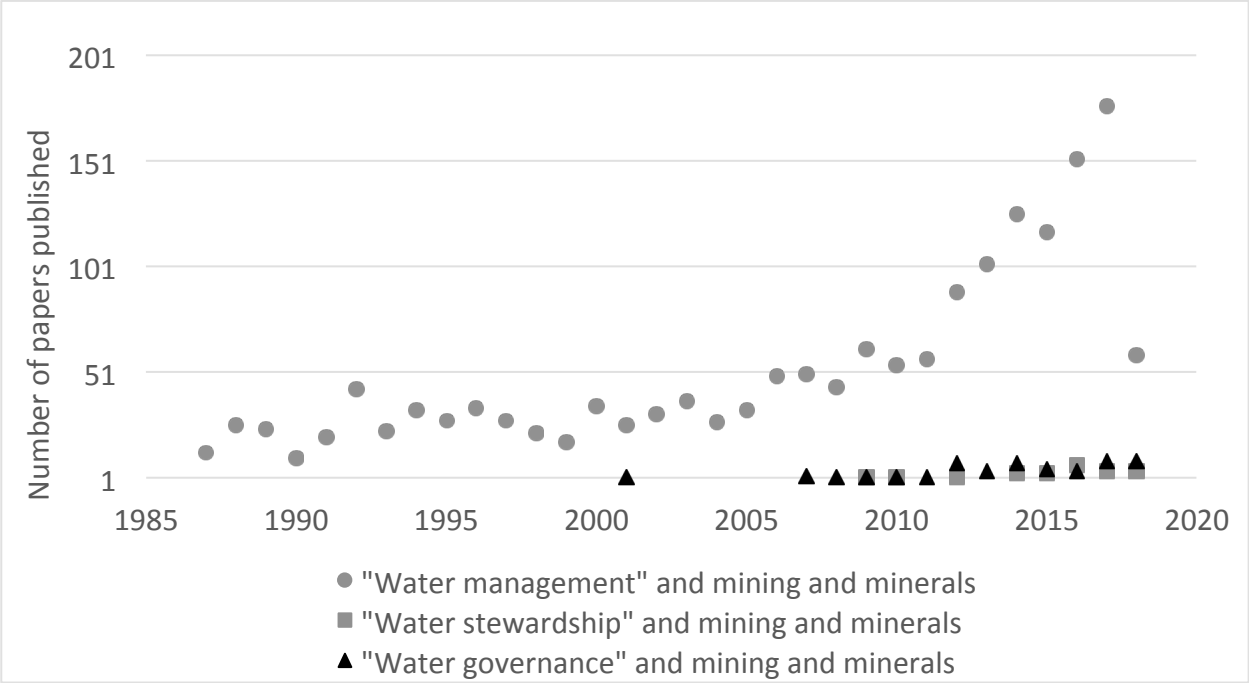


Figure 1: Number of papers published between 1987 and 2018 using the shown search terms. Literature search completed using the Elsevier ScienceDirect database

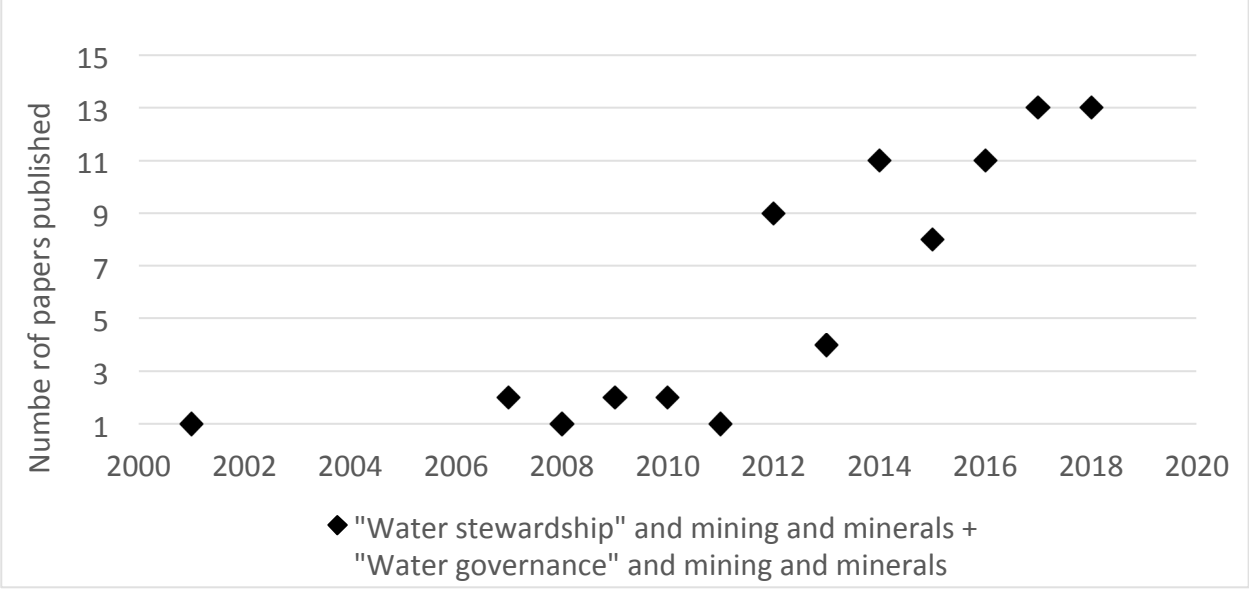


Figure 2: Papers published between 2000 and 2018 on water stewardship and governance within mining and minerals. Literature search completed using the Elsevier ScienceDirect database using the search terms indicated

As reported by Kunz (2013), an online survey was completed with the employees at this mine site to assess engagement in 12 water-related activities that previous site visits had identified as being important

for water management and stewardship. These activities were intentionally chosen to range in type from tactical to strategic, and were categorized across four levels of the water system: (1) unit operations, (2) mining tasks, (3) overall mine site, and (4) mining regions (*note:* the original framework of Cote et al. (2007) was condensed to four levels rather than five). Of the 425 employees at the mine site, 145 employees completed the survey, representing an overall response rate of 34%. The response rate across departments ranged from 27% (Mining and Mobile Maintenance) to 74% (Health, Safety and Environment). There was a higher response rate among the professional workforce, which included managers and engineers (63%) compared with employees working in the shift panels (25%).

As shown in Figure 3, survey results reveal that employees report more active engagement in activities at lower levels of the hierarchical framework, and considerably less engagement in activities at the highest system level.

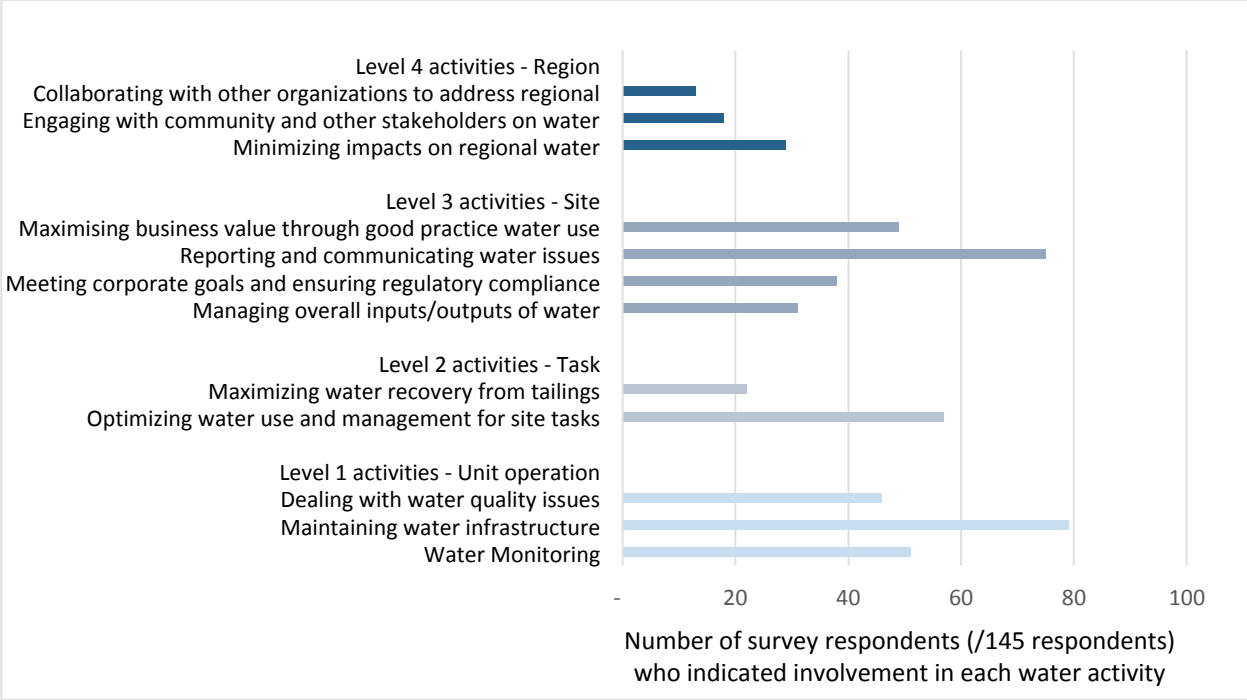


Figure 3: Reported involvement in different water-related activities at a case-study mining site. There was least involvement in water activities at the highest level of the hierarchical framework

Discussion

The findings from this paper point to a need for increased attention on addressing mine water issues beyond the company fence. In January 2017, ICMM members committed to a Position Statement on Water Stewardship that requires members to: (1) apply strong and transparent water governance, (2) manage water at operations effectively, and (3) collaborate to achieve responsible and sustainable water use. A striking element of this commitment is that it requires ICMM members to contribute as active

partners in addressing water issues at the catchment scale. This is a significant shift from the past, when it was generally accepted that the mining sector's role in broad issues of water allocation should involve negotiating with governments to secure access to water.

Already, there are examples of mining companies collaborating with other stakeholders including communities, governments, industry and civil society, to address shared water risks. The IFC and ICMM (2017) recently published a report that traces through global examples of collective action across Mongolia, Peru, South Africa, Canada and Australia. Mining companies have contributed as active water stewards through monitoring regional quality and quantity, increasing the disclosure of water data, and providing shared water and sanitation infrastructure to local communities. However there are currently relatively few of such examples. The pressure on companies to contribute to water stewardship at the catchment scale is likely to grow ever greater due to factors such as increased complexity of water challenges, the need to manage cumulative impacts, and the rise in community-company conflicts (Fraser, 2018).

The mining sector's aspirations towards water stewardship represent a positive step towards greater accountability by mining companies in resolving the complex water challenges affecting society. However, it also raises questions about the legitimacy of private sector involvement in water governance, a task that should ideally the responsibility of nation states (Kunz, 2016). A major challenge for future research will therefore involve investigating which organizational forms would maximize the legitimacy of private sector efforts towards catchment-based water management.

In addition to improved performance at the mine site level, effective water management and stewardship can also offer an entry point for companies to contribute towards broader sustainable development aspirations. To further progress this agenda, water issues and responses should be mapped to the framework of Moran and Kunz (2016) which distinguished mining sector sustainability aspirations at two scales: *Operating Sustainably* (which focuses on how mining activities are undertaken), and *Sustainable Development* (in terms of how the value generated from mining is distributed across society and over time). These two scales map directly to company responses to managing water issues "within" vs. "beyond" the mining fence (Figure 4).

Water is also a core component of the global sustainability agenda. In 2015, member states of the United Nations committed to 17 Sustainable Development Goals (SDGs) to address global environmental, social and economic imbalances. The mining sector is acknowledged as playing a crucial role in implementing the SDGs because of its global reach, power and impact (CCSI et al., 2016). Several of the SDGs relate to water, most principally SDG6 focussed on *Clean Water and Sanitation – Ensure availability and sustainable management of water and sanitation for all.* Effective water management

(within the fence) and water stewardship (beyond the fence) are directly relevant for meeting mining sector aspirations towards the SDGs (Figure 4).

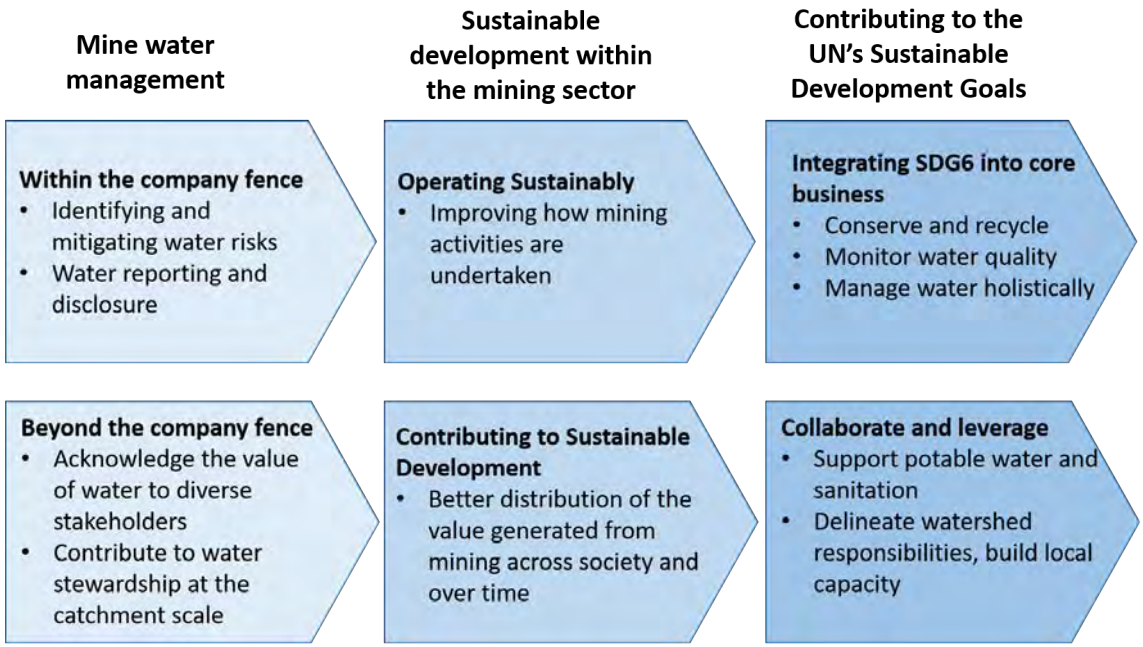


Figure 4: Mine water management can be delineated at two scales (column 1), which maps to the framework by Moran and Kunz (2016) (column 2), and the UN's SDGs (column 3)

Conclusion

In recent decades, there has been significant effort by academia, governments, investors, civil society, and industry to improve water management by the global mining sector. However, there remain community concerns about mining's impact on water, suggesting an ongoing need for attention to this topic. Future research should consider opportunities to improve the identification and mitigation of water risks at the mine site level, while also progressing the water stewardship agenda beyond the company fence. These efforts are important for improving the mining sector's contribution to sustainable development and ultimately for implementing the United Nation's Sustainable Development Goals.

Acknowledgements

The author would like to thank the case study site and the parent company at which some of this research was completed for participating in the project and for supporting the travel expenses during field research.

References

Côte, C., Kunz, N., Smith, K. and Moran, C.J. 2007. *Water Issues and Sustainable Resource Processing,* January: 1–53.

Department of Resources Energy and Tourism. 2008. *Water Management – Leading Practice Sustainable Development Program for the Mining Industry.* Canberra: Commonwealth of Australia. Retrieved from: http://www.ret.gov.au/resources/documents/lpsdp/lpsdp-waterhandbook.pdf.

Devine, J. 2011. *High Costs of Floods Confirmed.* Brisbane: Queensland Resources Council. Retrieved from: https://www.qrc.org.au/01_cms/details.asp?ID=2835.

Fraser, J. 2018. *Mining Companies and Communities: Collaborative Approaches to Reduce Social Risk and Advance Sustainable Development. Resources Policy.* doi:https://doi.org/10.1016/j.resourpol.2018.02.003.

ICMM. 2017. *A Practical Guide to Consistent Water Reporting.*

IFC and ICMM. 2017. *Water in the Mining Sector: Shared Water, Shared Responsibility, Shared Approach.*

Kunz, N.C. 2013. *Sustainable Water Management by Coupling Human and Engineered Systems,* Centre for Water in the Minerals Industry, Sustainable Minerals Institute. St Lucia: The University of Queensland.

Kunz, N.C. 2016. Catchment-based water management in the mining industry: Challenges and solutions, *The Extractive Industries and Society,* 3(4): 972–77. doi:https://doi.org/10.1016/j.exis.2016.10.012.

Kunz, N.C. and Moran, C.J. 2016. The utility of a systems approach for managing strategic water risks at a mine site level, *Water Resources and Industry,* 13: 1–6. doi://doi.org/10.1016/j.wri.2016.02.001.

Liu, W., Moran, C.J. and Vink, S. 2011. Quantitative risk-based approach for improving water quality management in mining, *Environmental Science & Technology,* 45(17): 7459. Retrieved from: http://www.ncbi.nlm.nih.gov/pubmed/21797262.

Minerals Council of Australia. 2014. *Water Accounting Framework for the Australian Minerals Industry*. Retrieved from: http://www.minerals.org.au/leading_practice/water_accounting_framework_for_the_ australian_minerals_industry/.

Munnik, R. and Pulles, W. 2009. *The Implementation of the Recently Developed Best Practice Guidelines for Water Resource Protection in the South African Mining Industry,* International Mine Water Conference, Pretoria, South Africa: Cilla Taylor Conferences. Retrieved from: https://www.imwa.info/docs/ imwa_2009/IMWA2009_Munnik.pdf.

NSW Mining. 2013. *Minerals Council of Australia Water Accounting Framework.* Retrieved from: http://www.nswmining.com.au/dialogue/latest-projects/water/minerals-council-of-australia-water-accounting-fra.

Ramsar. 2018. *Designating Ramsar Sites.* Retrieved from: https://www.ramsar.org/sites-countries/designating-ramsar-sites.

Stegink, H.D.J., Lane, J., Barker, D.J. and Pei, B. 2003. Water usage reductions at Queensland Alumina, in *Water in Mining 2003:* 293–99. Brisbane.

Veiga, M.M. and Tucker, C. 2015. Sustainability and public engagement in mining: The role of engineers, *Journal of Earth Science and Engineering,* 280–88. doi:10.17265/2159-581X/2015.05.002.

Chapter 5:
Water Management in Extreme Climates



Proceedings of Mine Water Solutions 2018
June 12–15, 2018, Vancouver, Canada
Published by the University of British Columbia, 2018

Current PMP Estimation and Meteorological Parameter Development for Mining Facilities in Data Limited Regions

Bill Kappel, Applied Weather Associates, USA

Abstract

Applied Weather Associates (AWA) has completed hundreds of Probable Maximum Precipitation (PMP) and other meteorological studies since the mid-1990s. The majority of the work was completed for the dam and nuclear communities in regions where data are plentiful and often included a long period of record.

Recently, AWA has completed PMP and other meteorological analyses for several mining facilities in many varied regions across the world. Several of these mine sites have been located in regions of extreme topography with very limited data coverage. This has presented unique challenges in the development of storm data, storm adjustments, spatial and temporal patterns of rainfall accumulations, and PMP development. This presentation will discuss the general PMP development background, lessons learned from the many years of PMP work that have been applied to the mining community, and how this process is completed for the mine locations where data are limited and terrain is often very complex. It will also discuss the major challenges encountered, and the solutions that were utilized to overcome the challenges.

Introduction

Applied Weather Associates (AWA) recently completed Probable Maximum Precipitation (PMP) and meteorological analyses in locations with limited data and extreme topographic settings. These included a large mine in Papua, Indonesia and a large mine in north-central Peru. AWA utilizes a storm-based approach to derive PMP (Mukhopadhyay and Kappel, 2016; World Meteorological Organization, 2009) and other meteorological parameters such as Annual Exceedance Probabilities (AEP) of PMP and Depth-Duration-Frequency (DDF) curves. Previous site-specific and regional PMP projects completed by AWA provide examples of PMP studies that explicitly consider the topography and meteorological characteristics of historic extreme precipitation over climatologically similar regions (Figure 1). These

PMP studies have received extensive review and the results have been used in computing the PMF for the watersheds and regions covered. In addition, several of these studies included the development of regional Precipitation Frequency (PF) climatologies (e.g. Kappel et al., 2014; Kappel et al., 2016). This study follows the same procedures used in those studies to determine PMP values for each location and to develop the PF database.

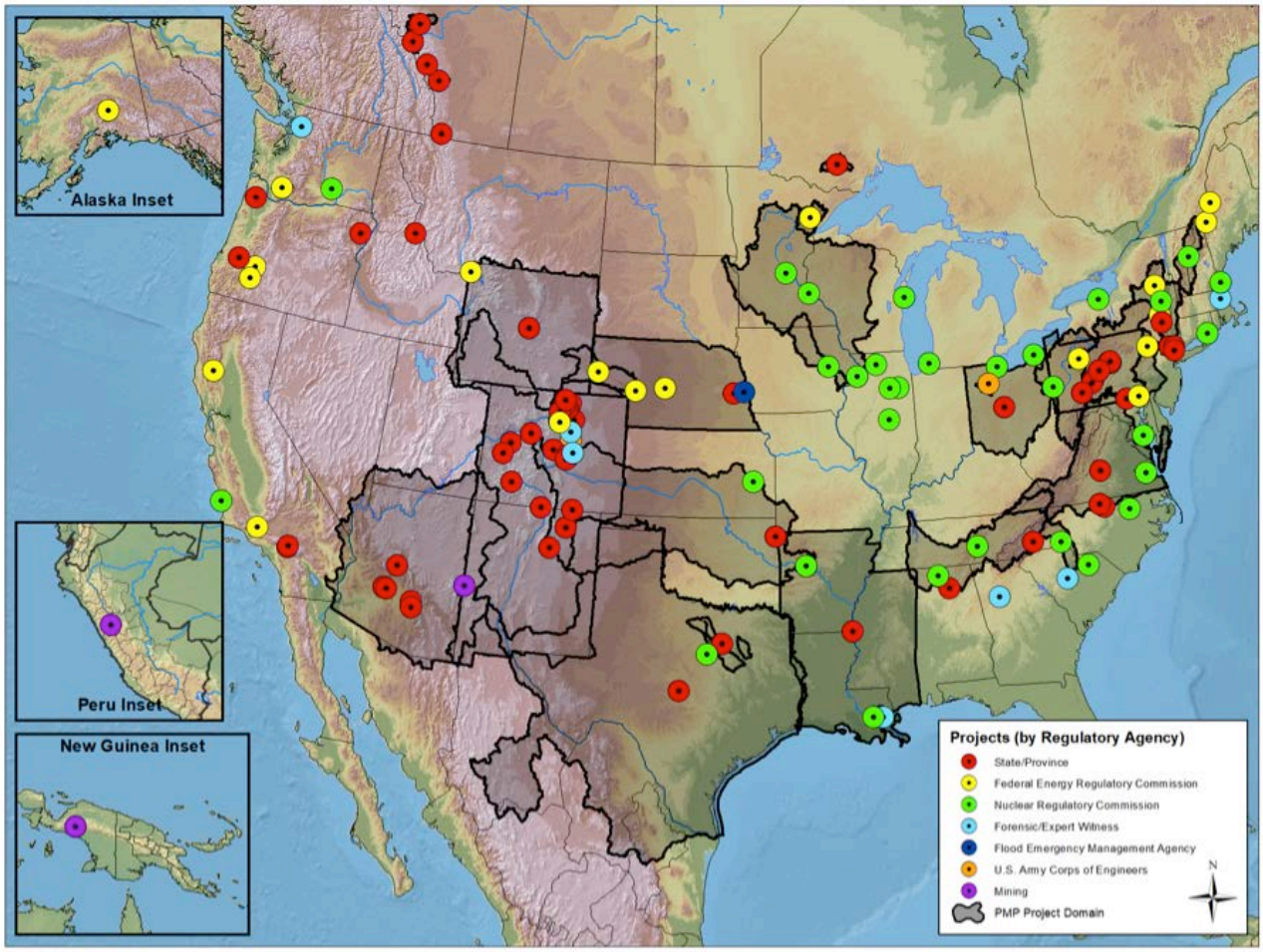


Figure 1: AWA project locations

The Indonesian mine is located just south of the equator (Figure 2), yet because of the topographic setting, the site can receive snow at the top of the basin at the same time that heavy monsoon rainfall is occurring at lower elevations. The region includes tropical glacial regions above the mine site to the tropical rainforest and ocean interface (Mealey, 1996). Terrain plays a key role in defining the PMP storm type and PF development, the magnitude of rainfall accumulations, and their associated spatial and temporal distributions. These factors were explicitly accounted for during the PMP and PF development processes.

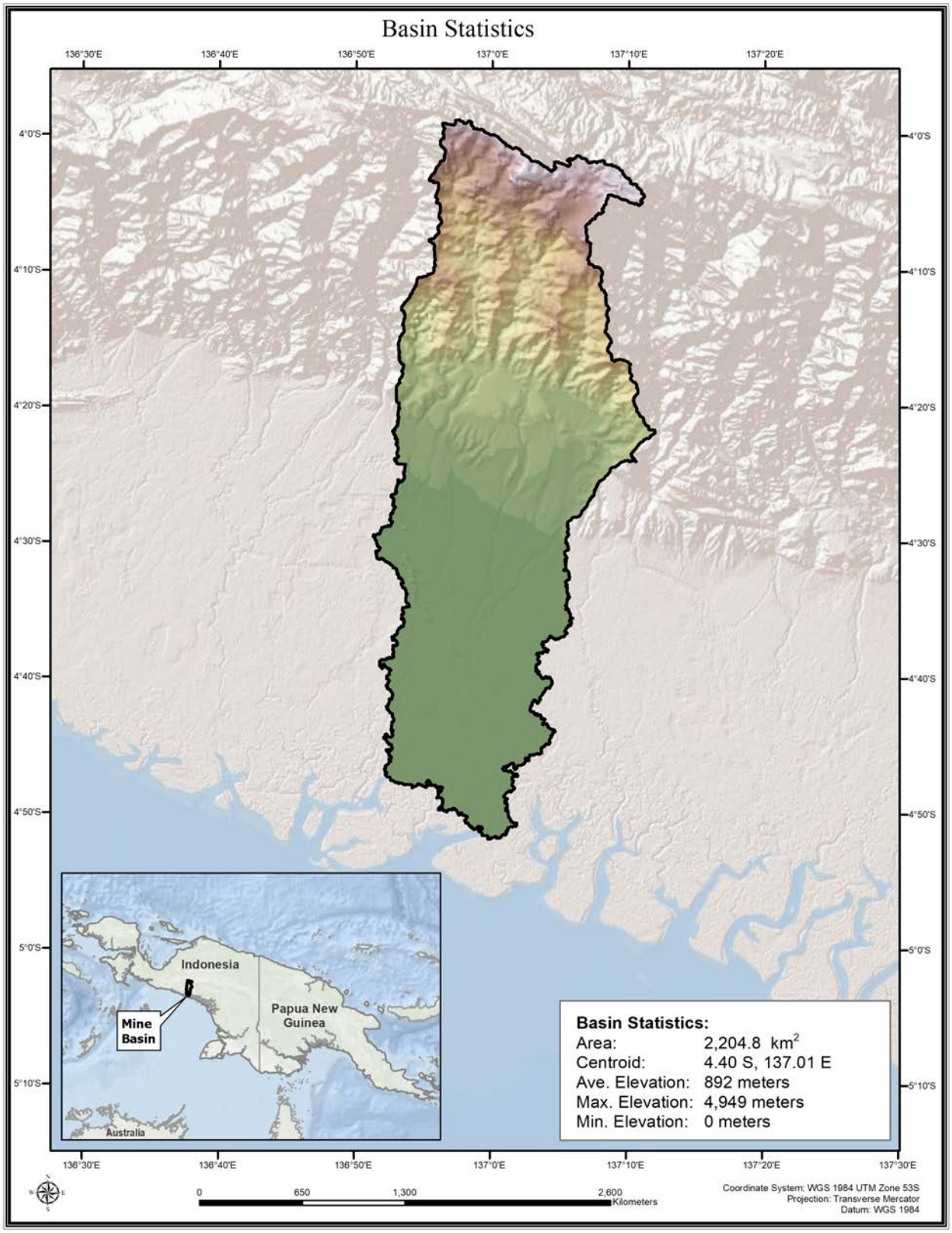


Figure 2: Indonesian basin location, topography, and regional setting

The mine in Peru is located in a mountainous region near the headwaters of the Marañón River at elevations ranging from 3,900 meters to 4,850 meters (Figure 3). These high elevations play a significant role in precipitation development and hence PMP values. In addition, the basin is located in a transition region between the humid upper Amazon basin to the east and the dry coastal regions to the west. Finally, significant topographical barriers exist both to the immediate west and east of the basin, limiting moisture availability. These factors were explicitly accounted for during the PMP and PF development process.

PMP Development Process

The storm-based approached used in these studies requires analyzing explicit precipitation data that represent PMP-type precipitation events that have or could occur over the location of interest. Therefore, AWA performs extensive data mining and analysis to identify the storm type(s), region of similar meteorology and topography, and individual extreme precipitation events. AWA's Storm Precipitation Analysis System (SPAS) is used to analyze all storms. SPAS produces hourly gridded precipitation data, as well as Depth-Area-Duration (DAD), mass curves (hyetographs), total storm isohyetal images, AEP maps, and several other standard outputs. In addition, AWA derives climatological data sets that are used to adjust individual storms. These include development of 100-year recurrence interval dew point climatologies, sea surface temperature climatologies, and 100-year recurrence interval precipitation frequency estimates.

Indonesia Data Mining

A search domain of 94°E, 10°N, 10°S and 165°E was determined to be a similar region of meteorological, climatological, and topographic characteristics where all storms within this domain could be considered transpositionable to the location. Hundreds of rainfall events that occurred in this region were investigated to identify potential events for final analysis, as well as to gain insight into the PMP storm types that are important (Figure 4).

The storm search was conducted by comparing the magnitude and frequency of the individual storm events by duration. Several storm durations were used and investigated: 1-hour, 6-hour, 24-hour, 72-hour, and 120-hour. The 100-year values derived from the PF analysis were utilized as an initial cut-off for identifying potential PMP-type storm events that required further evaluation. For the 120-hour duration, higher total depth thresholds were used. The surface station storm search resulted in several thousand-storm events being identified. In general, storms included in the long list all exceed the 100-year return frequency value for specified durations at the station location or are associated with known extreme floods. The resulting long storm list was extensively quality controlled to ensure that only the highest

storm rainfall values for each event were selected. Storms were then grouped by storm location and duration for further analysis.

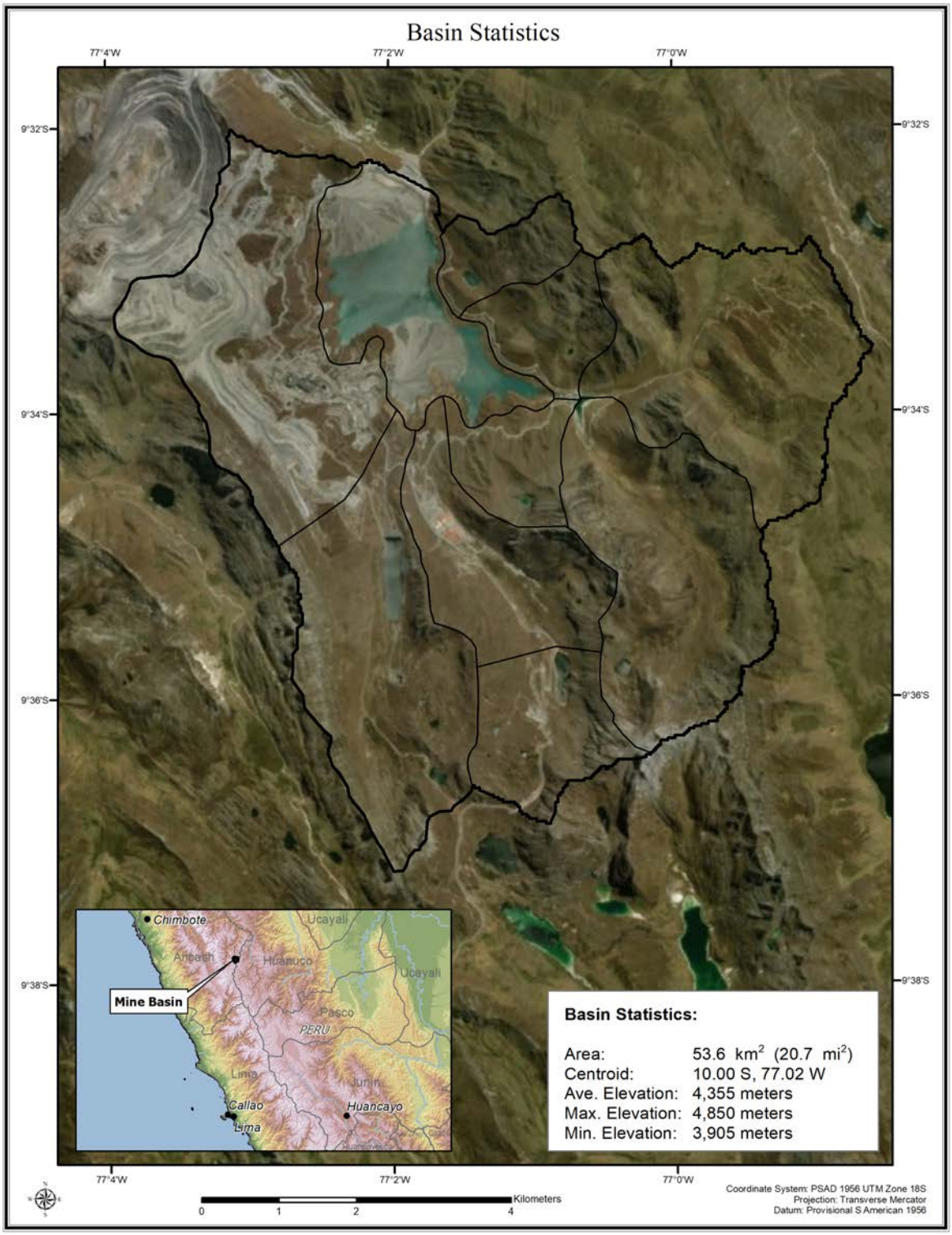


Figure 3: Peru basin location, topography, and regional setting

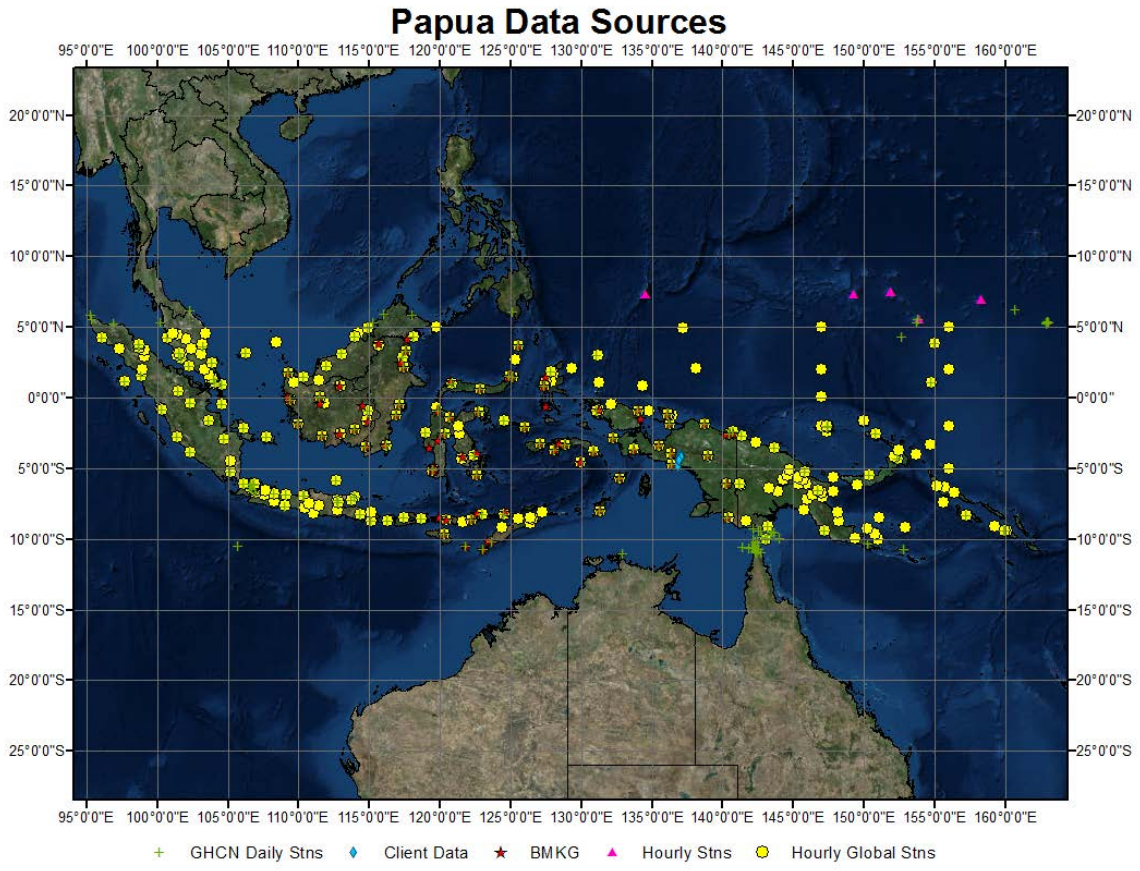


Figure 4: Storm search domain and stations types used

Ground-based observational data is sparse in this region. Therefore, other observational data were incorporated to capture extreme events that may not have been observed at a recording location. APHRODITE (Asian Precipitation – Highly-Resolved Observational Data Integration Towards Evaluation) daily data were investigated from 1985 to 2007 and TRMM (Tropical Rainfall Measuring Mission) satellite data were analyzed from 2008 to 2016 to flag any daily pixels over 124 mm. APRHODITE data search resulted in 90 storms being identified, and the TRMM data resulted in 84 storms being identified. These storms constituted the intermediate storm list against which further investigations were completed. These day/multi-day composites of precipitation storm centers were validated with surface station data from AWA's database.

Consideration was given to each storm's transpositionability to the basin and each storm's relative magnitude compared to other similar storms on the list. Figure 5 shows the locations of storms used for PMP development and data analysis. Each of these storms was extensively evaluated to determine which storms were needed for final SPAS analysis and PMP development. Storms were evaluated for transpositionability to the basin, and if so, whether another storm of similar storm type is significantly larger. Durations were also considered to ensure that several storms important for various durations were

included. The short list was finalized after all evaluations and included 15 distinct storm centers. These covered a wide region geographically, and included storms ranging from short duration intense rainfalls to long duration rainfall with several bursts of rainfall during a several day period.

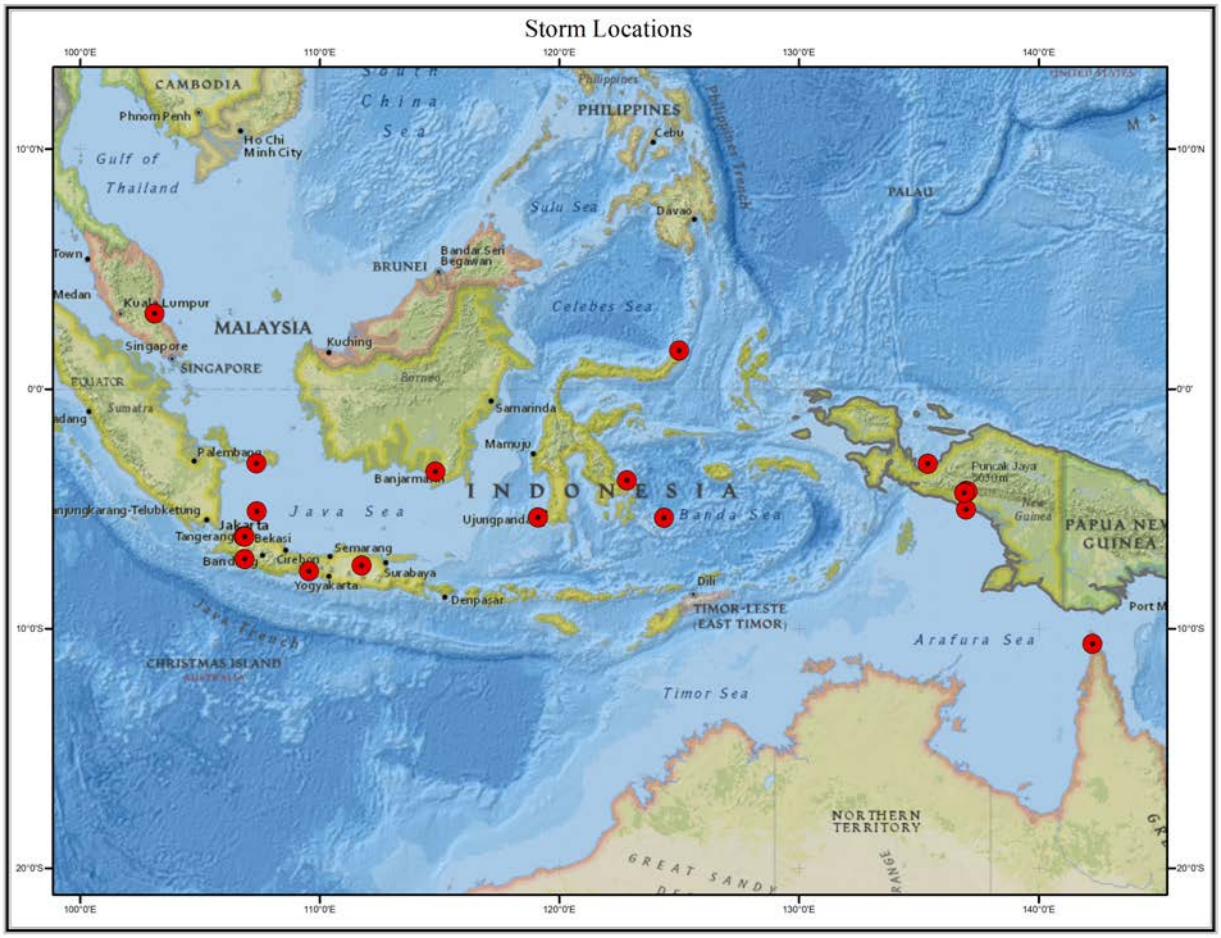


Figure 5: Short storm list locations used for PMP development

Peru Data Mining

A storm search domain covering the Altiplano and interior high elevations regions of Peru, from approximately 8°S to 16°S and 69°W to 78°W, was determined to be similar to the basin in regards to meteorological and topographical environments (Figure 6). This region was determined to be an appropriate transposition region where storms that occur in this domain could have occurred over the basin. The storm search domain utilized the important characteristics related to precipitation development over the basin. This included regions that represent the same transition zone between moisture inflow from the east/northeast (upper Amazon basin) and the west/southwest from the Pacific Ocean and regions that are influenced by similar topography.

Specific interactions of topography and moisture availability were considered and evaluated against surrounding regions. This included evaluating rainfall accumulation data provided by the client to determine the specific wet season period for the basin and comparing that to similar rainfall climatologies in other areas considered. This demonstrated that areas further south towards the Altiplano of southern Peru have a shorter wet season, signifying a different meteorological pattern than occurs over the basin. Therefore, rainfall patterns and individual storm events south of 16°S are not the same as would occur over the basin and are therefore not transpositionable.

In addition, elevation differences were explicitly considered. This is because the high elevation of the basin, generally between 3,500 m and 5,000 m, results in unique weather patterns and storm development characteristics in the basin. The high elevation of the basin means there is less total atmospheric column moisture to work with as the lower 3,500 m of the atmosphere, where most of the moisture and instability are located, are not available for storm development. This results in significantly lower amounts of total moisture availability and hence much lower total precipitation accumulations. Because of these elevation considerations, no storms were used which occurred in regions less than 2,500 m in elevation.

The storm search was conducted by comparing the magnitude of individual storm events by duration and location. Several storm durations were used and investigated: 1-hour, 6-hour, 24-hour, and 72-hour. The 100-year values, derived as part of this analysis, were used to quantify initial levels to investigate. These were utilized as an initial cut-off for identifying potential PMP-type storm events that required further evaluation. Several hundred storm events were identified. These storm events constituted the long list of storms to be further investigated and from which to derive the final list of storms used for PMP development. Remote sensing data were also used to supplement individual station data. CHRS satellite data were analyzed to flag any daily pixels that represented extreme precipitation accumulations from the long list. Station data and CHRS data were taken into consideration when the final short storm list was created and when a SPAS analysis was performed on the storm.

Consideration was given to each storm's transpositionability to the basin and each storm's relative magnitude compared to other similar storms on the list by location and duration. Figure 7 (on the next page) provides the final storm short list. Durations were also considered to ensure that several storms important for various durations were included. The short list was finalized after all evaluations and included 10 unique storm events. These covered a wide region geographically within the overall storm search domain and included storms ranging from short duration rainfalls to long duration rainfalls covering several days.

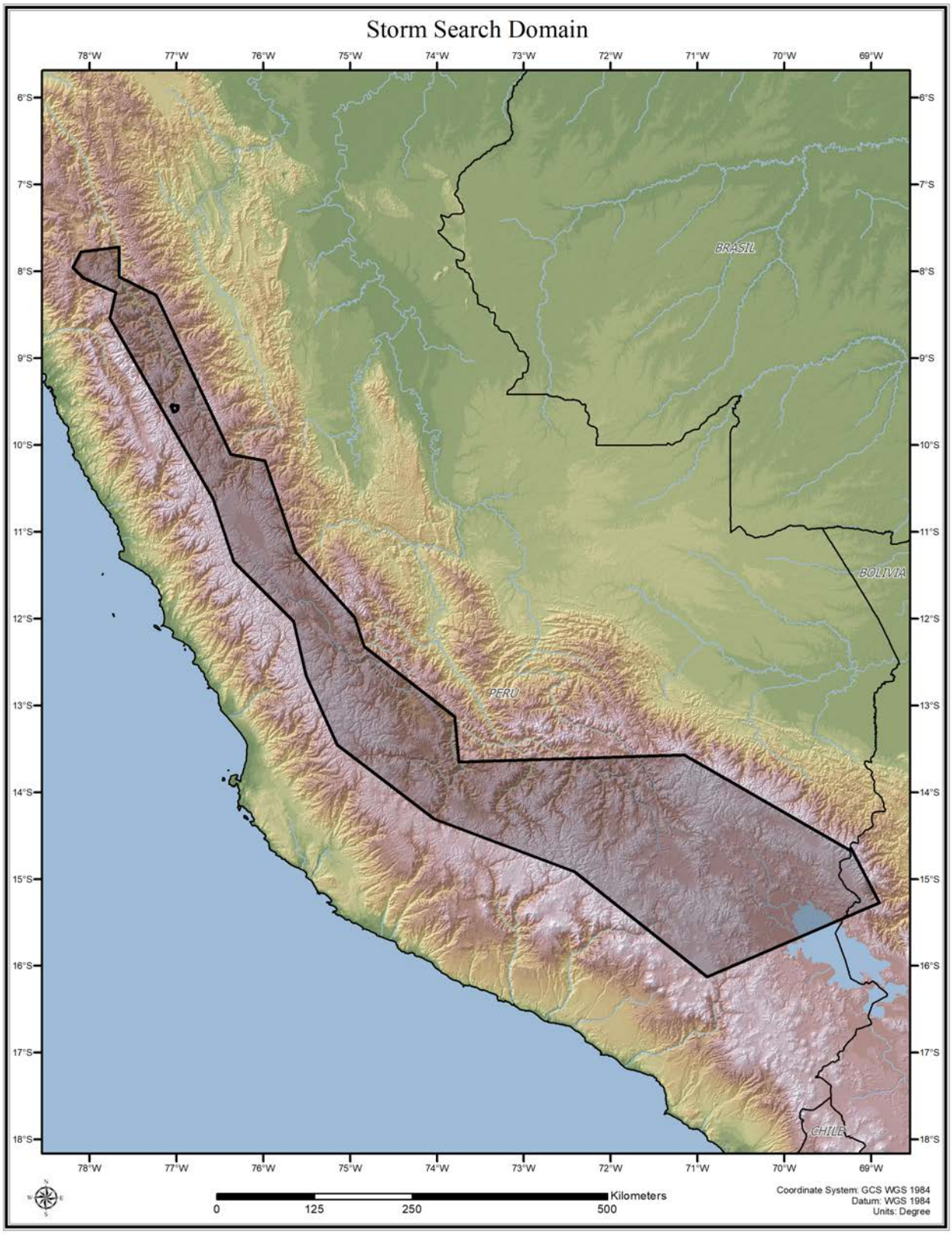


Figure 6: Storm search domain used for PMP development in Peru

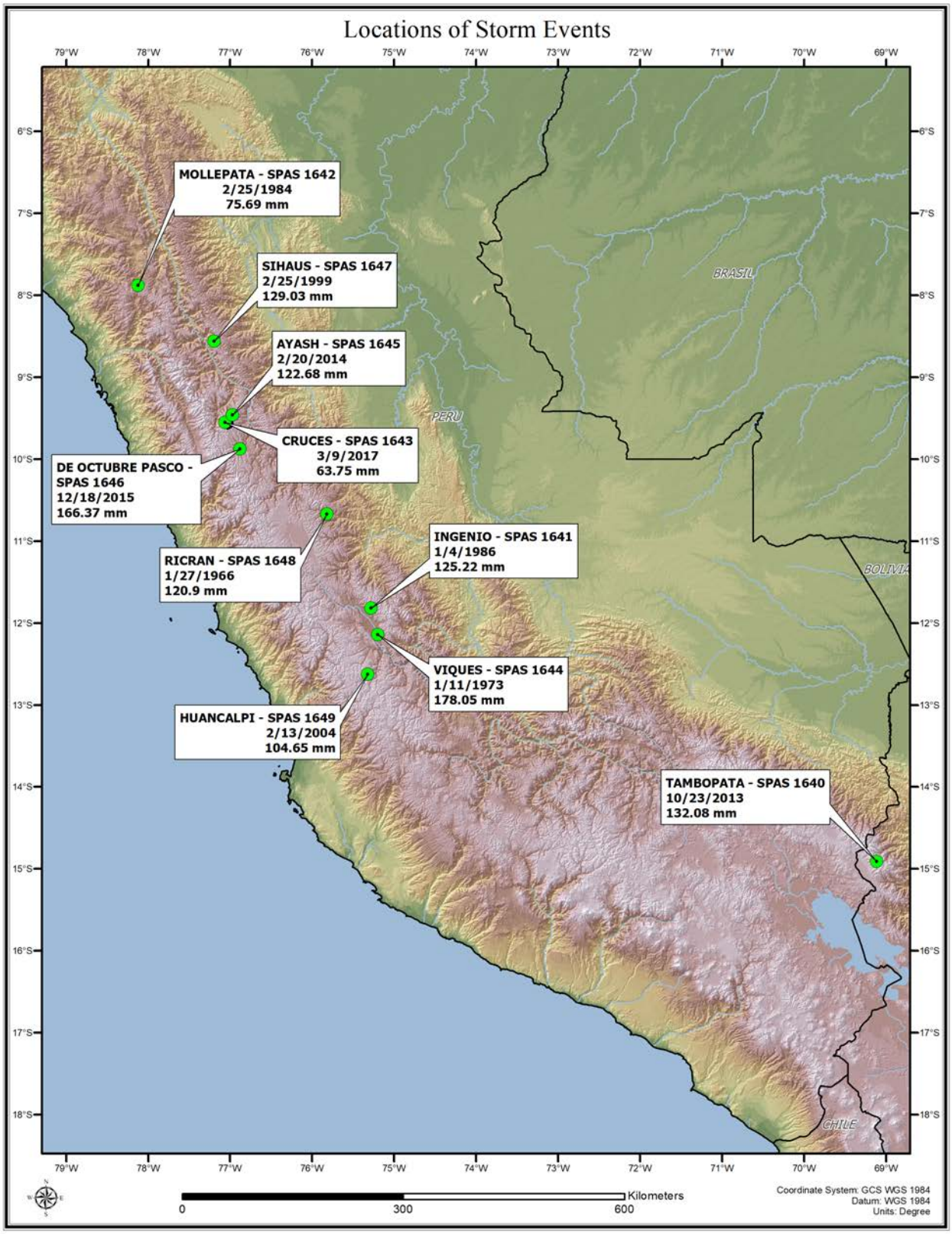


Figure 7: Storm list used for PMP development in Peru

Conclusion

AWA utilized the storm-based approach to development PMP values and other meteorological data for two unique mine locations, one in Papua, Indonesia and the other in the high mountains of north-central Peru. AWA utilized data furnished by the client/mining companies, local governmental entities, internal AWA database, and remote sensing observation to develop the information needed to calculate the results. PMP results and AEP of seasonal precipitation accumulations were developed. Each of these studies demonstrated that development of highly accurate and scientifically defensible PMP and other meteorological data are possible even in the most remote locations in the world. This is achieved through coordination and communication with the mine operations personnel, in combination with AWA experience and knowledge.

References

Kappel, W.D., Hultstrand, D.M., Muhlestein, G.A., Steinhilber, K., McGlone, D., Parzybok, T.W. and Tomlinson, E.M. 2014. Statewide Probable Maximum Precipitation (PMP) study for Wyoming.

Kappel, W.D., Hultstrand, D.M., Muhlestein, G.A., Steinhilber, K. and McGlone, D. 2016. Site-specific probable maximum precipitation and regional precipitation frequency analysis for the Grasberg Mine Basin and surrounding regions, Papua, New Guinea. Prepared for P.T. Freeport Indonesia and Freeport-McMoRan.

Kappel, W.D., Hultstrand, D.M., Rodel, J., Muhlestein, G.A., Steinhilber, K. and McGlone, D. 2017. Site-specific probable maximum precipitation and regional precipitation frequency analysis for the Antamina Mine Basin, Peru. Prepared for Compania Minera Antamina.

Mealey, G.A. 1996. *Grasberg: Mining the richest and most remote deposit of copper and gold in the world, in the mountains of Irian Jaya, Indonesia,* 1st edition. New Orleans, LA: Freeport-McMoRan Copper and Gold Inc.

Mukhopadhyay, B. and Kappel, W.D. 2016. Probable Maximum Precipitation, in V.P. Singh (ed.) *Handbook of Applied Hydrology,* 2nd Edition, McGraw-Hill Education.

World Meteorological Organization. 2009. *Manual for Estimation of Probable Maximum Precipitation,* No. 1045, WMO, Geneva.

Proceedings of Mine Water Solutions 2018
June 12–15, 2018, Vancouver, Canada
Published by the University of British Columbia, 2018

Hurricane Harvey Rainfall: Did It Exceed PMP, and What are the Implications?

Bill Kappel, Applied Weather Associates, USA

Abstract

Rainfall resulting from Hurricane Harvey reached historic levels over the coastal regions of Texas and Louisiana during the last week of August 2017. Although extreme rainfall from this type of landfalling tropical system is not uncommon in the region, Harvey was unique in that it persisted over the same general location for several days, producing volumes of rainfall not previously observed in the United States and most of the world. Harvey caused devastating flooding and severe stress to infrastructure in the region. Coincidentally, Applied Weather Associates (AWA) had recently completed an updated, state-wide Probable Maximum Precipitation (PMP) study for Texas. This storm proved to be a real-time test of the adequacy of those values. AWA calculates PMP following a storm-based approach. This same approach was used in the Hydrometeorological Reports developed by the National Weather Service and is recommended by the World Meteorological Organization and Canadian Dam Safety. Therefore, inclusion of all PMP-type storms is critically important to ensuring that appropriate PMP values are produced. This paper will discuss the analysis of the Harvey rainfall using the Storm Precipitation Analysis System (SPAS) program used to analyze all storms during AWA PMP development, compare the results of the Harvey rainfall analysis against previous similar storms, and provide comparisons of the Harvey rainfall against previous and current PMP depths. The implications of the storm on previous and future PMP estimates, dam safety design, and infrastructure vulnerable to extreme flooding will be discussed.

Introduction

Rainfall from Hurricane Harvey resulted in some of the greatest rainfall accumulation ever recorded in the United States. Rainfall accumulations were most extreme at large area sizes (greater than 5,000 mi^2) and long durations (greater than 24 hours). However, even at smaller area sizes and shorter durations, the storm still produced record-setting rainfall. This was extremely unusual, and points to the fact that the storm was truly a Probable Maximum Precipitation (PMP) event.

PMP is "theoretically, the greatest depth of precipitation for a given duration that is physically possible over a given storm area at a particular geographical location at a certain time of the year"

(WMO, 2009). Therefore, PMP represents a theoretical upper limit of the greatest amount of rainfall that can accumulate, and the analysis of the Harvey rainfall confirms that it reached that level.

The extreme rainfall caused devastating flooding, with the hardest hit region extending from the Houston metropolitan region through southwestern Louisiana. Fortunately, no high hazard structures failed during the vent. Coincidentally, Applied Weather Associates (AWA) had recently completed a statewide PMP study for Texas, updating the previous PMP values provided in HMR 51. Of course, this meant that the timing of the Harvey rainfall was perfect for testing and comparing the newly developed values.

The Background to Hurricane Harvey

Texas is home to some of the most extreme rainfall events ever observed in the USA, and in some cases the world. Favoured locations in the state include the Balcones Escarpment and immediate coastal regions from Corpus Christi through Beaumont-Port Arthur and southern Louisiana (Figures 1 and 2). These regions are favoured because of topographic interactions with moisture flowing in from the Gulf of Mexico around the Balcones Escarpment and hurricane landfall interaction with coastal terrain. Along the coastal sections during hurricane season, atmospheric steering current are very weak. This often results in slow movement of the landfalling tropical systems in this region, allowing heavy rain to accumulate over the same general region.

Given these favoured conditions, another major rainfall event was expected in the general region, and unfortunately will happen again. Within recent history, similar storms have happened in this area previously (e.g. Hearne 1899, Beulah 1967, Alvin 1979, Allison 2001) and will happen again. So, what made Harvey different? Harvey was unique as it was fueled by near record Gulf of Mexico sea surface temperatures that provided exceptional amounts of moisture for several days; it remained over the same general area for several days; and it was close enough to the coast to allow extremely moist air to continue to feed into the storm, while the storm was able to retain its warm-core tropical characteristics.

Several excellent analyses and discussions of the meteorological environment associated with Harvey's formation, track, and dissipation, as well as resulting flooding impacts, have been completed. The focus of this paper is on the rainfall accumulation of the storm and how it compares to PMP and extreme storm analyses. The reader is referred to the following resources for more information on the synoptic meteorological environment associated with the storm.

- https://www.nhc.noaa.gov/data/tcr/AL092017_Harvey.pdf
- https://www.weather.gov/hgx/hurricaneharvey
- https://weather.com/storms/hurricane/news/tropical-storm-harvey-forecast-texas-louisiana-arkansas
- American Water Resources Association-Impact (January 2018)

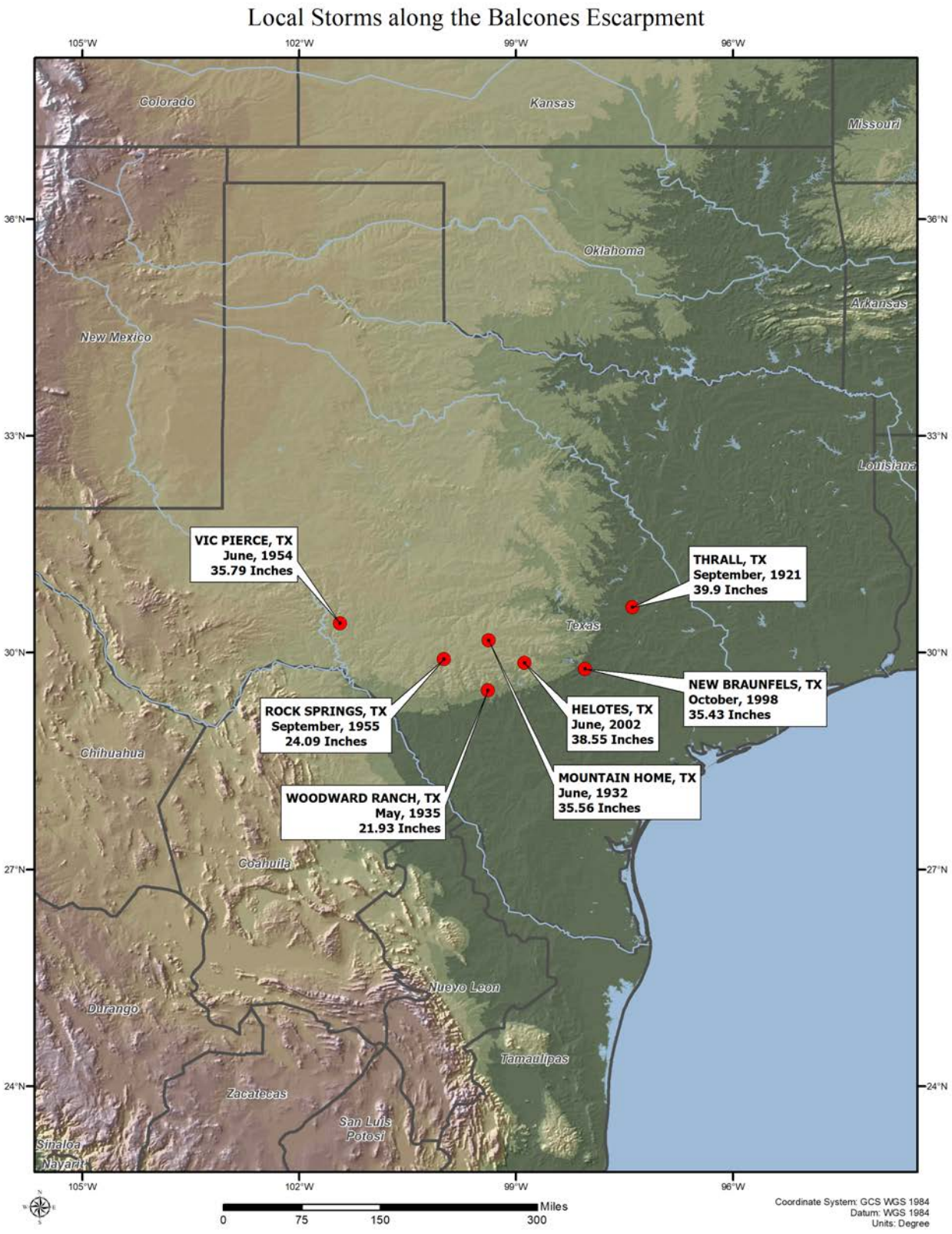


Figure 1: Storm locations effected by the Balcones Escarpment

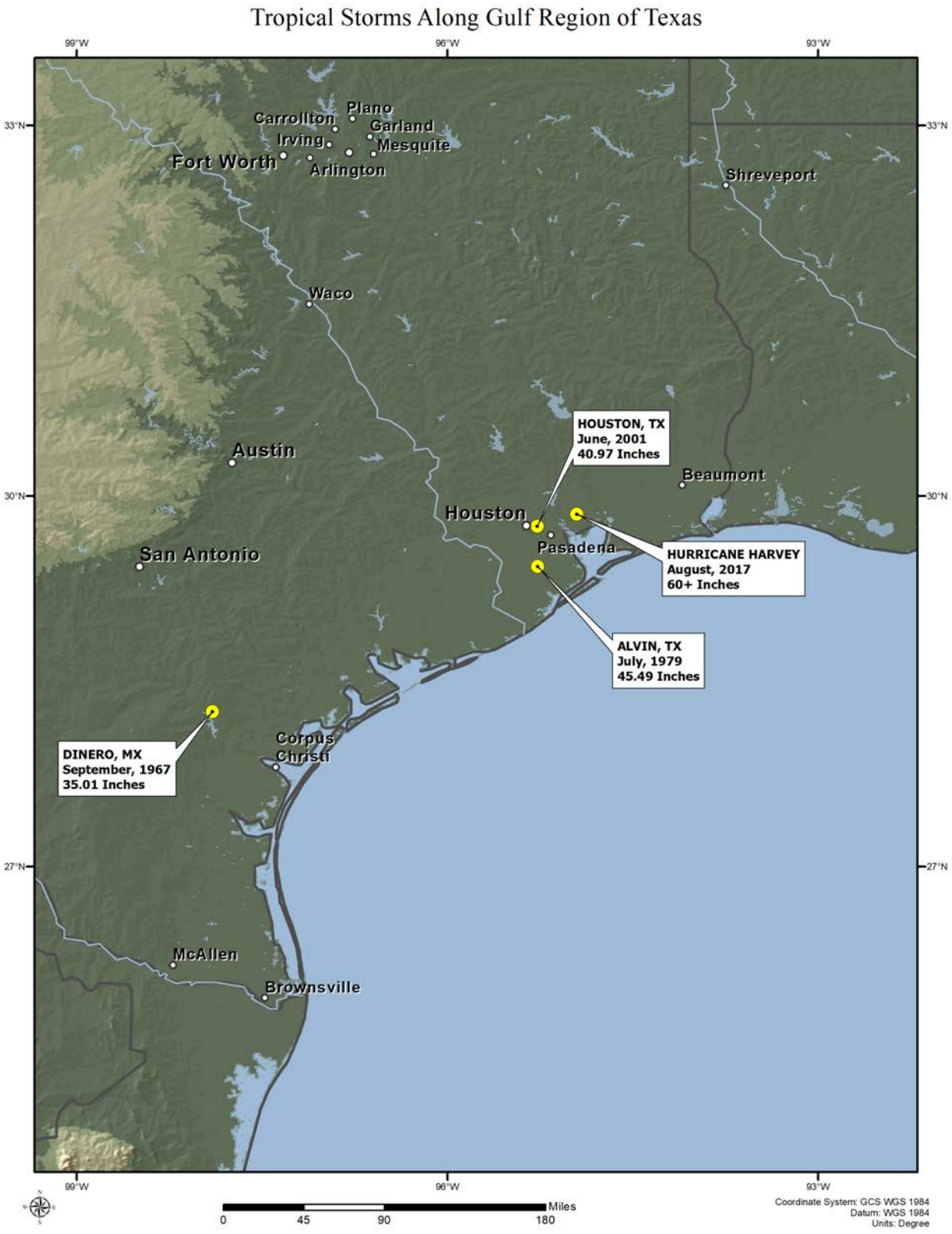


Figure 2: Storm locations along the Texas Gulf Coast similar to Harvey

SPAS Rainfall Analysis

AWA has completed more than 700 rainfall analyses since 2002 using our Storm Precipitation Analysis System (SPAS) (Figure 3). Results of these analyses have been primarily used as inputs for PMP development, model calibration, model validation, and forensic investigations. The SPAS process has been extensively reviewed and accepted for use in these types of analyses (NRC, 2017). SPAS produces several standard outputs, including hourly gridded rainfall data, total storm isohyetal maps, depth-area-duration information, annual exceedance probability maps, and mass curve accumulations. SPAS analyses were completed for all storms used during the Texas PMP study (Figure 4) and therefore provided a consistent and reliable data set from which to make comparisons of the forecast rainfall from Harvey, Harvey rainfall as it was occurring, and comparisons from the post-analysis investigations. The SPAS database was critical in understanding the severity of the potential rainfall from the storm before it occurred, and for communicating how this might compare to the recently updated PMP values, as well as understanding the hardest hit regions.

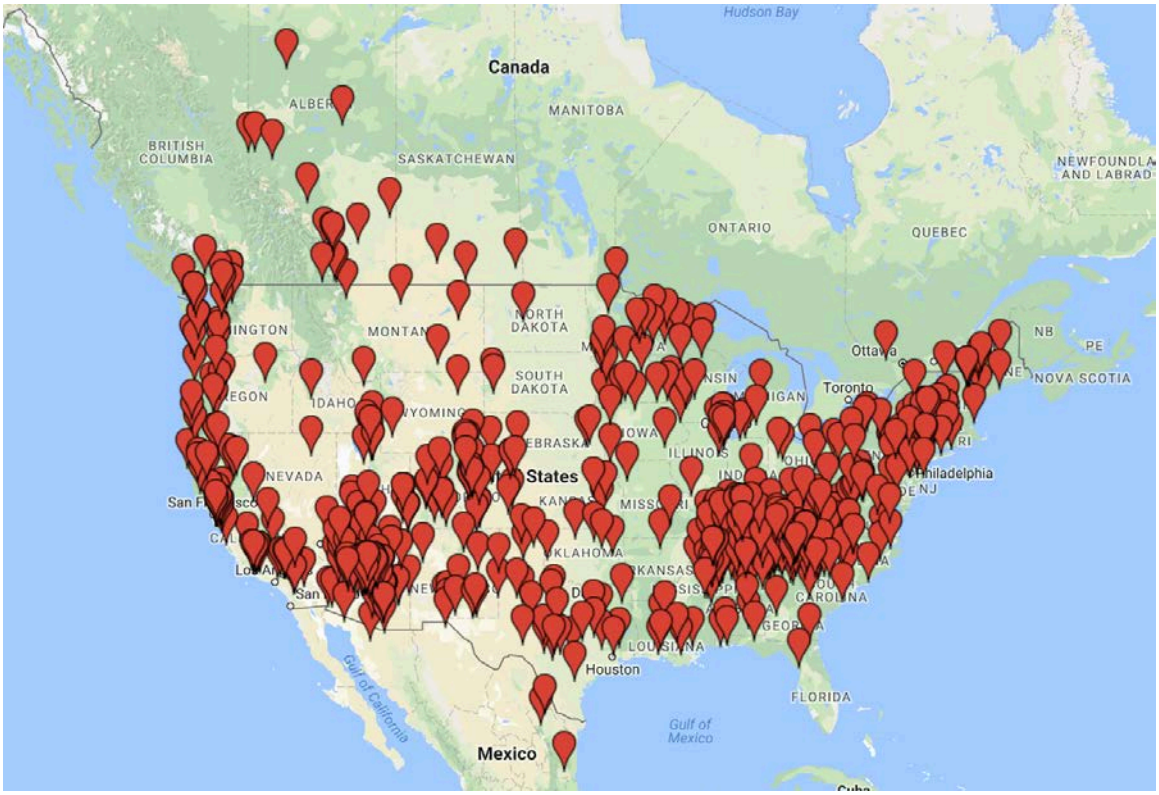


Figure 3: SPAS Storm locations analyzed in the United States and Canada

Forecast rainfall amounts were showing the potential for extreme rainfall as much as a week before landfall, as shown in Figure 5 (McMahan, 2017). AWA recognized the possibility of extreme rainfall and

how it could affect the dam safety community. This was especially relevant in the context that AWA had just completed the development of the state PMP values for Texas (Kappel et al., 2016).

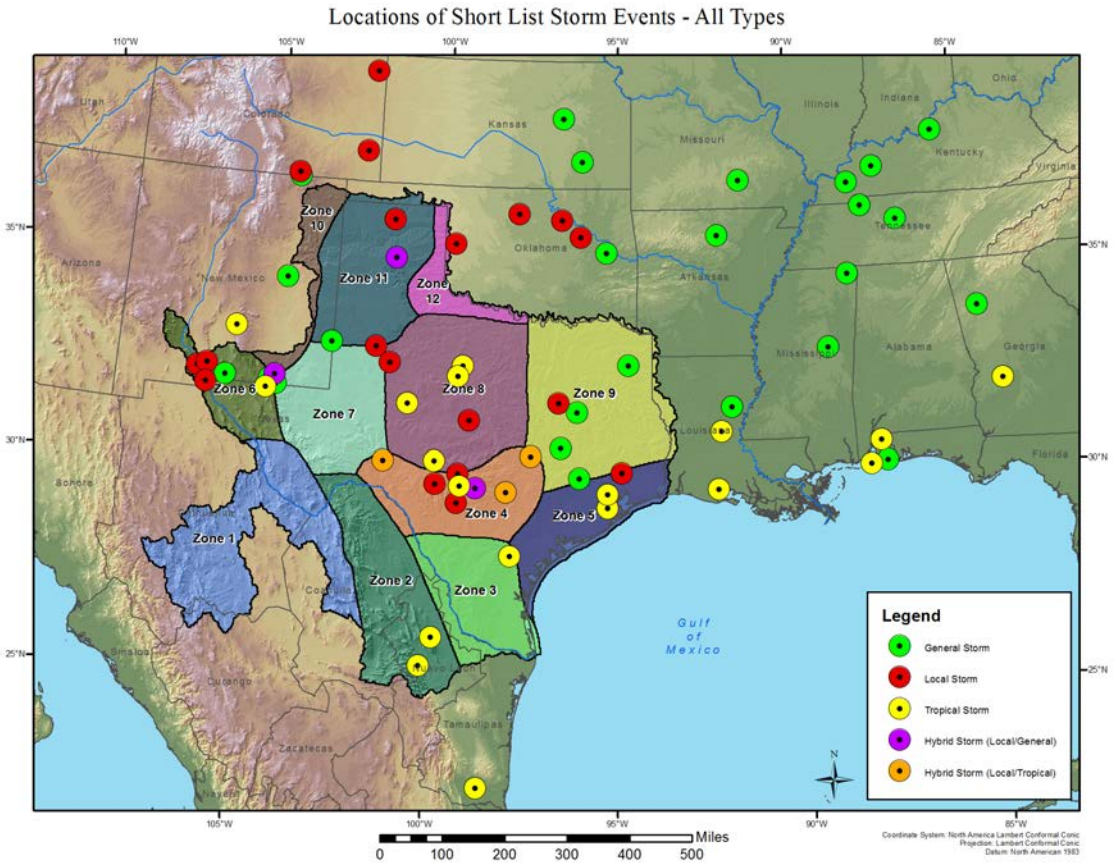


Figure 4: Storm locations used to calculate PMP in Texas

AWA was in contact with the Texas Commission of Environmental Quality (TCEQ) head of dam safety before the storm began to affect the region to help with situation awareness. While the storm was occurring, AWA continued communications with TCEQ and others involved in monitoring and analyzing the rainfall (e.g. Dr. Nielson-Gammon Texas state climatologist and professor at Texas A&M University). AWA immediately began an analysis of the rainfall using the SPAS program, and worked with Dr. Nielson-Gammon to develop various comparisons of the Harvey rainfall versus previous similar events, in order to put the rainfall accumulations in perspective.

The comparisons demonstrated that the Harvey rainfall far exceeded any other observed event, especially for durations greater than 24 hours and area sizes greater than 5,000-square miles, not only in Texas but also in the United States (Figure 6). Figure 7 provides the total storm accumulation pattern resulting from Harvey. Table 1 provides the results of the SPAS rainfall analysis as a depth-area-duration table. This provides a 3-dimensional look at the rainfall accumulation, both spatially and temporally.

Unprecedented amounts of rainfall occurred, with over 60 inches at the storm center during the 5-day period. Even more amazing was the volume of rainfall, with over 20 inches spread over more than 20,000-square miles during the 5-day period. This would be equivalent to more than 25 times the average daily flow through the Mississippi River (Nielson-Gammon, 2017).

The rainfall accumulation pattern followed a similar footprint as seen in other similar previous storms in the region (Figure 8). The heaviest rainfall was centered just inland from the coast, where coastal convergence process maximized the rainfall production. Also noteworthy was the accumulation pattern through time, with the heavy rainfall occurring over long time periods covering several days. The extreme rainfall, which occurred over several days, resulted in daily rainfall records that were set at the Houston Intercontinental Airport official observation site (KIAH). At this location, Harvey produced the greatest daily amount on August 27, and the fifth greatest daily amount on August 26 (Figure 9).

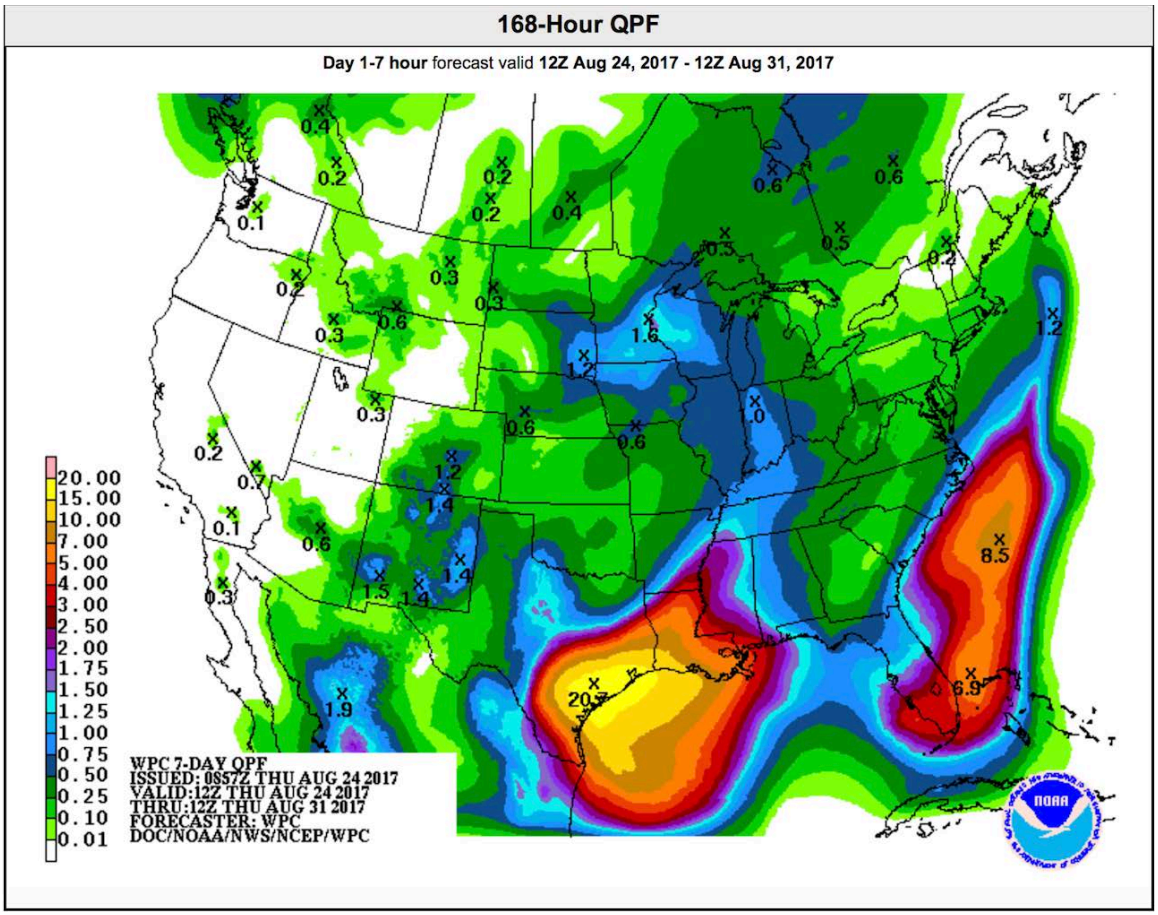


Figure 5: Quantitative Precipitation Forecast from the Weather Prediction Center for the period August 24, 2017 through August 31, 2017

Comparison to Previous Storms

As discussed previously, the storm location and overall pattern were similar to previous tropical rainfall events in the region. In June 2001, Hurricane Allison produced devastating flooding in the Houston region, with over 40 inches of rainfall occurring in 24 hours. This storm spatial coverage was similar to Harvey (Figure 10). However, the rainfall from Allison only lasted a little over a day. This resulted in total storm rainfall amounts and volumes that were much smaller than Harvey (Table 2). Previous to Allison was Alvin in 1979. Again, this tropical system produced extreme rainfall over the Houston area, with more than 40 inches in 24 hours in some locations (Table 3). Each of these storms was similar regarding storm type and location, but the total rainfall amounts and spatial coverage were limited by overall duration.

Duration: 48 h				**Duration: 72 h**				**Duration: 120 h**			
Area: 1000 sq mi				**Area: 1000 sq mi**				**Area: 1000 sq mi**			
Event	Average (in)	Amount (mrd)	% over previous record	Event	Average (in)	Amount (mrd)	% over previous record	Event	Average (in)	Amount (mrd)	% over previous record
LA Aug 1940	29.53	1.3	-0.6%	Harvey 2017	37.56	1.7	16%	Harvey 2017	43.29	2.1	33%
Harvey 2017	29.36	1.3	Harvey rel to HMR 51	LA Aug 1940	32.51	1.5	Harvey rel to HMR 51	LA Aug 1940	32.64	1.5	
TX Jun 1899	27.63	1.3	-22%	TX Jun 1899	31.10	1.4	-9%	TX Jun 1899	31.91	1.5	
Danny 1997	25.69	1.2	Harvey rel to AWA zone	Danny 1997	27.10	1.2	Harvey rel to AWA zone	Claudette 1979	27.78	1.3	
Claudette 1979	23.97	1.1	-17%	Alice 1954	26.93	1.2	-9%	Beulah 1967	27.20	1.2	
Area: 5000 sq mi				**Area: 5000 sq mi**				**Area: 5000 sq mi**			
Event	Average (in)	Amount (mrd)	% over previous record	Event	Average (in)	Amount (mrd)	% over previous record	Event	Average (in)	Amount (mrd)	% over previous record
Harvey 2017	23.54	5.5	11%	Harvey 2017	29.40	7.1	22%	Harvey 2017	36.34	9.0	42%
LA Aug 1940	21.15	4.8	Harvey rel to HMR 51	TX Jun 1899	24.19	5.5	Harvey rel to HMR 51	TX Jun 1899	25.60	5.8	
TX Jun 1899	20.01	4.5	-12%	LA Aug 1940	23.63	5.4	-4%	LA Aug 1940	23.93	5.4	
TX Oct 1994	18.60	4.2	Harvey rel to AWA zone	Beulah 1967	20.70	4.7	Harvey rel to AWA zone	Beulah 1967	22.40	5.1	
Georges 1998	18.33	4.2	-11%	TX Oct 1994	20.15	4.6	-1%	TX Oct 1994	20.86	4.7	
Area: 10000 sq mi				**Area: 10000 sq mi**				**Area: 10000 sq mi**			
Event	Average (in)	Amount (mrd)	% over previous record	Event	Average (in)	Amount (mrd)	% over previous record	Event	Average (in)	Amount (mrd)	% over previous record
Harvey 2017	20.81	9.7	25%	Harvey 2017	25.35	12.2	27%	Harvey 2017	31.84	15.7	49%
Georges 1998	16.62	7.5	Harvey rel to HMR 51	TX Jun 1899	19.97	9.1	Harvey rel to HMR 51	TX Jun 1899	21.39	9.7	
LA Aug 1940	16.16	7.3	-8%	Beulah 1967	18.50	8.4	-4%	Beulah 1967	20.50	9.3	
TX Jun 1899	16.02	7.3	Harvey rel to AWA zone	LA Aug 1940	17.94	8.1	Harvey rel to AWA zone	LA Aug 1940	18.37	8.3	
TX Oct 1994	16.00	7.3	-5%	TX Oct 1994	17.45	7.9	5%	TX Oct 1994	18.06	8.2	
Area: 20000 sq mi				**Area: 20000 sq mi**				**Area: 20000 sq mi**			
Event	Average (in)	Amount (mrd)	% over previous record	Event	Average (in)	Amount (mrd)	% over previous record	Event	Average (in)	Amount (mrd)	% over previous record
Harvey 2017	17.04	16.0	17%	Harvey 2017	21.03	19.7	29%	Harvey 2017	26.68	25.6	43%
Georges 1998	14.58	13.2	Harvey rel to HMR 51	Beulah 1967	16.30	14.8	Harvey rel to HMR 51	Beulah 1967	18.70	17.0	
Beulah 1967	13.00	11.8	-5%	TX Jun 1899	15.29	13.9	-4%	TX Jun 1899	17.02	15.4	
TX Oct 1994	12.46	11.3	Harvey rel to AWA zone	Georges 1998	14.58	13.2	Harvey rel to AWA zone	Georges 1998	15.71	14.3	
Floyd 1999	12.05	10.9	-5%	TX Oct 1994	13.92	12.6	13%	NC Sep 2010	14.83	13.4	

Figure 6: Comparison of the Hurricane Harvey rainfall against similar previous storms and the average daily volume of water flowing through the Mississippi River

Maximization of Hurricane Harvey

Most important for TCEQ and the dam safety community in general was whether Harvey exceeded PP estimates. This is because high hazard structures are designed for the Probable Maximum Flood (PMF). The PMF is a direct result of the PMP, therefore if PMP design values were exceeded there is a possibility that high hazard structures could be compromised.

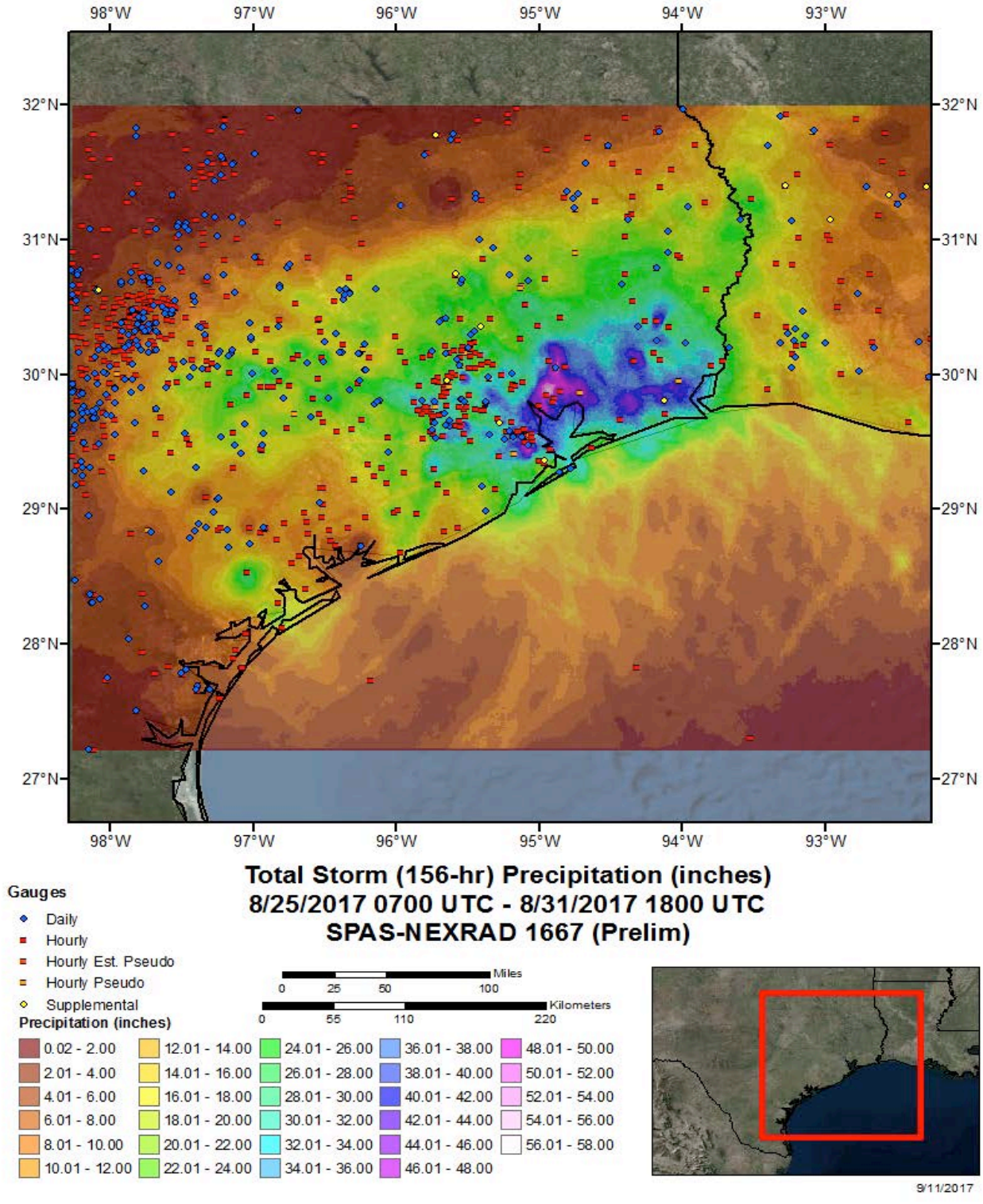


Figure 7: Hurricane Harvey SPAS 1667 total storm isohyetal

Table 1: Hurricane Harvey SPAS 1667 depth-area-duration table

SPAS Storm 1667 - August 25 (0700 UTC) - August 31 (1800 UTC), 2017 MAXIMUM AVERAGE DEPTH OF PRECIPITATION (INCHES)										
Area (mi^2)	Duration (hours)									
	1	6	12	18	24	36	48	72	96	Total
0.4	5.45	19.32	23.34	28.33	32.17	35.54	40.47	49.86	55.41	56.47
1.0	5.38	19.19	23.16	28.11	31.91	35.30	40.21	49.47	54.92	55.99
10.0	5.17	18.87	22.54	27.52	31.25	34.67	39.57	47.98	53.26	54.29
25.0	5.06	18.65	21.88	26.64	30.50	33.34	38.40	46.71	51.85	52.90
50.0	4.91	18.26	21.30	25.82	30.01	31.74	37.32	45.28	50.29	51.44
100.0	4.74	17.65	20.51	24.95	29.33	31.14	36.28	44.00	48.66	49.83
150.0	4.59	17.13	19.88	24.35	28.71	30.51	35.50	43.17	47.64	48.82
200.0	4.45	16.67	19.35	23.76	28.09	29.95	34.88	42.51	46.91	48.11
300.0	4.18	15.90	18.47	22.87	26.99	28.97	33.71	41.56	45.71	46.96
400.0	3.93	15.22	17.75	22.16	26.17	28.17	32.76	40.74	44.88	46.12
500.0	3.71	14.62	17.17	21.47	25.53	27.52	32.01	40.11	44.13	45.48
1000.0	2.99	12.21	15.20	19.09	22.68	25.11	29.36	37.56	41.67	43.29
2000.0	2.36	9.46	12.85	16.31	19.66	22.69	26.80	34.39	39.13	40.94
3500.0	1.85	7.58	11.03	14.23	17.41	20.76	24.79	31.35	36.49	38.41
5000.0	1.57	6.58	9.99	12.96	15.99	19.44	23.54	29.40	34.51	36.34
7500.0	1.29	5.58	8.83	11.66	14.39	17.97	21.90	26.99	31.83	33.88
10000.0	1.12	4.94	8.06	10.59	13.30	16.86	20.81	25.35	29.89	31.84
15000.0	0.89	4.17	6.95	9.24	11.55	15.18	18.66	22.84	26.83	28.93
20000.0	0.71	3.64	6.10	8.14	10.38	13.77	17.04	21.03	24.75	26.68
35000.0	0.52	2.71	4.65	6.27	7.83	10.67	13.40	17.10	20.12	22.11
50000.0	0.39	2.11	3.60	4.93	6.27	8.83	11.06	14.24	16.69	18.79
75000.0	0.29	1.53	2.69	3.68	4.62	6.61	8.37	11.33	13.32	15.06
100000.0	0.22	1.21	2.20	3.00	3.75	5.30	6.71	9.08	10.71	12.11
120162.0	0.18	1.05	1.91	2.59	3.22	4.59	5.83	7.88	9.31	10.53

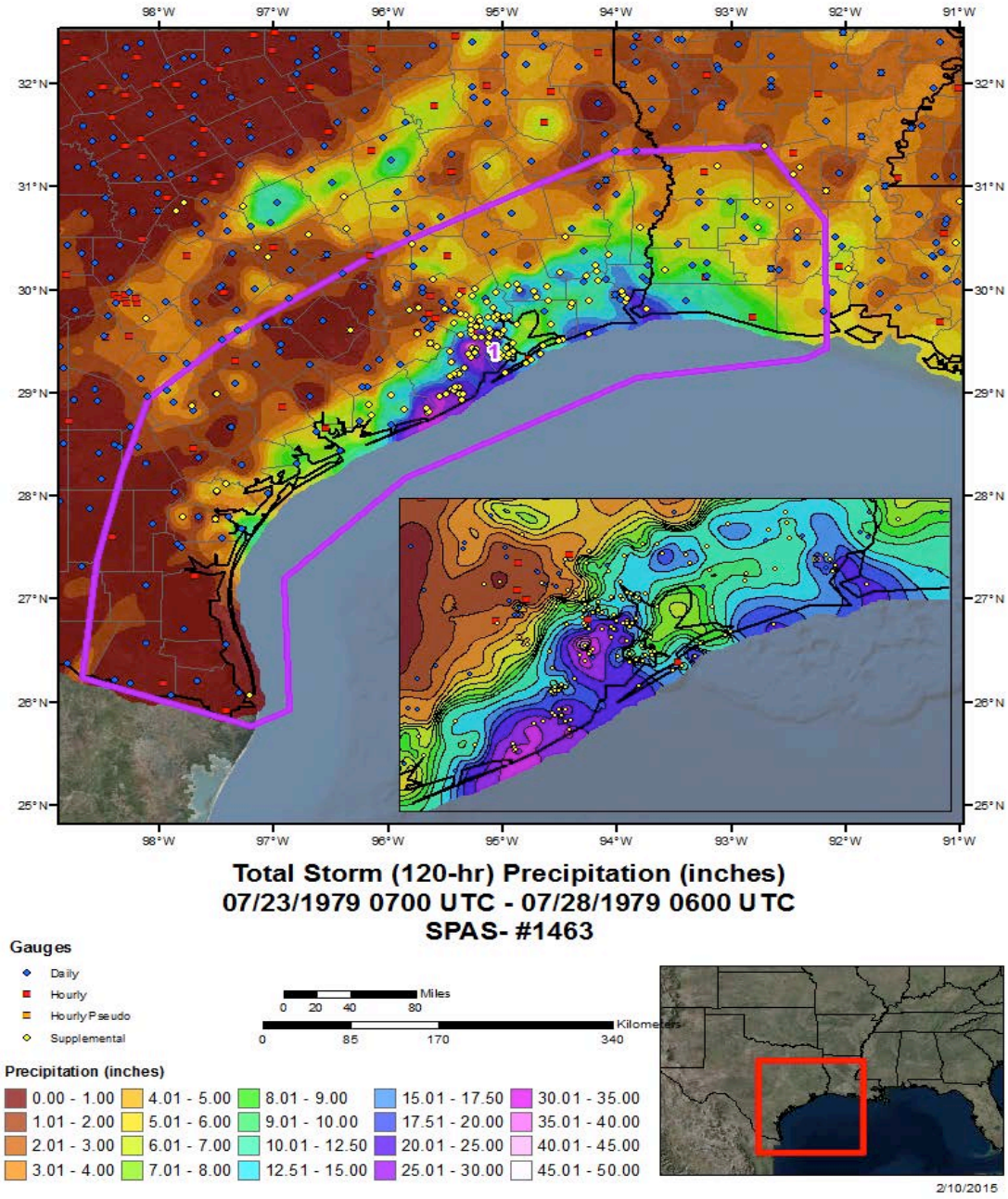


Figure 8: Alvin, SPAS 1463 July 1979 total storm isohyetal

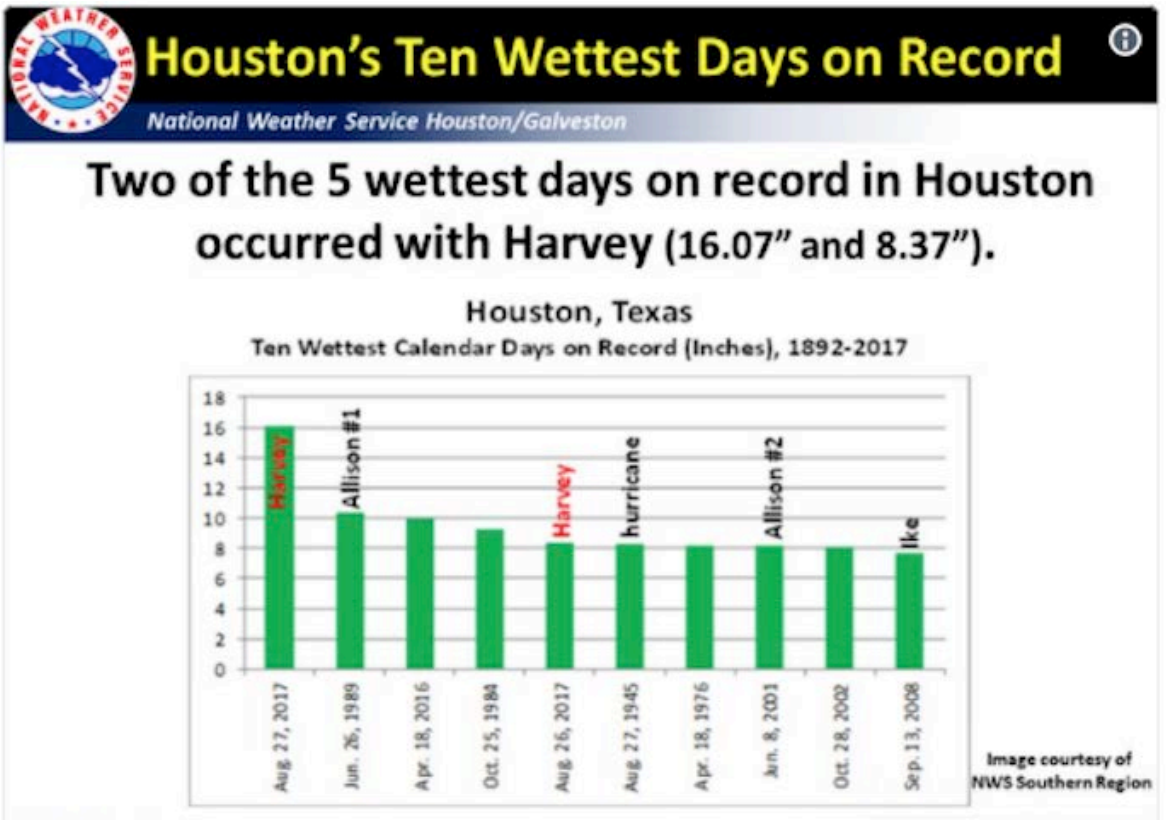


Figure 9: Daily rainfall records at the Houston official observation site (KIAH)

Remember that PMP is developed by analyzing actual storm events, then maximizing those storms, transpositioning those storms to your locations of interest, and combining the results to produce worst-case scenarios. AWA had already done this with numerous storms as part of the Texas state-wide PMP study (see Figure 4) and therefore had a readily available data set to compare to the Harvey values. As soon as the preliminary SPAS analysis of Harvey was completed, AWA began the in-place maximization process. Not surprisingly, Harvey was nearly at the maximum amount of moisture that the atmosphere could provide, with a resulting in place maximization factor of only 1.02. Figure 11 and Table 4 provide the in-place maximization factor analysis results. This shows that the storm could only have been 2% larger than observed had the maximum amount of atmospheric moisture been available to the storm versus what was observed. This is about as small of an increase as is possible, and out of all the hundreds of storms AWA has maximized over the years only a few have achieved this. These would include the world-record rainfall associated with the Smethport, PA July 1942 storm and the Hale, CO May 1935 storm. Each of these storms is very important for setting levels of PMP where they occurred.

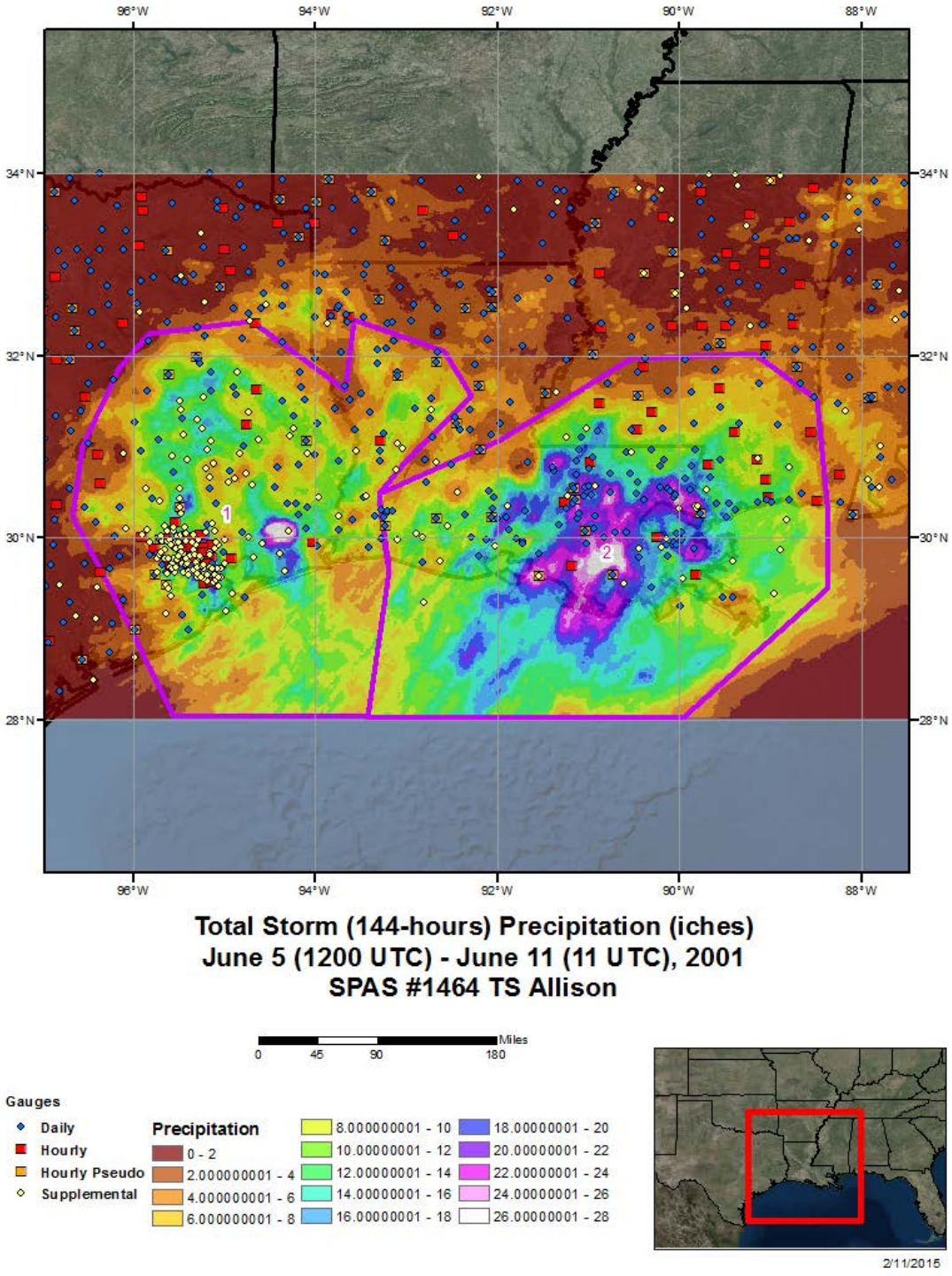


Figure 10: Allison, SPAS 1464 June 2001 total storm isohyetal

Table 2: Allison, SPAS 1464 June 2001 depth-area-duration table

Storm 1464 Zone 1 - June 5 (1200 UTC) - June 11 (1100 UTC), 2001													
MAXIMUM AVERAGE DEPTH OF PRECIPITATION (INCHES)													
	Duration (hours)												
areasqmi	1	3	6	12	18	24	36	48	72	96	120	144	Total
0.4	6.28	14.09	20.98	29.17	29.39	29.41	29.53	29.71	29.89	40.56	40.74	40.97	29.53
1	6.25	14.04	20.92	29.06	29.29	29.32	29.42	29.61	29.77	40.42	40.61	40.82	29.42
10	5.74	13.31	19.95	27.88	27.99	28.01	28.27	28.27	28.52	38.35	38.61	39.15	28.27
25	5.40	12.14	18.05	26.73	27.10	27.13	27.16	27.30	27.69	36.99	37.20	37.68	27.16
50	5.26	11.36	16.04	24.27	25.21	25.25	25.30	25.48	26.23	35.42	35.79	35.92	25.30
100	5.07	10.32	13.61	20.46	20.59	20.63	20.64	22.57	24.69	31.77	32.87	33.10	20.64
150	4.88	8.64	13.06	19.42	19.68	19.75	19.81	20.33	24.23	29.38	31.06	31.81	19.81
200	4.68	8.52	12.39	17.42	17.53	17.53	17.81	19.02	23.85	27.91	30.03	30.61	17.81
300	4.32	7.86	11.57	16.44	16.67	16.67	16.69	17.84	22.75	25.49	28.83	29.05	16.69
400	4.04	7.19	10.70	15.46	15.80	15.86	15.95	16.57	21.71	24.68	27.79	27.99	15.95
500	3.79	7.12	9.54	14.15	15.08	15.12	15.24	15.31	20.48	24.12	26.73	26.94	15.24
1,000	2.73	5.71	7.70	12.12	12.31	12.38	12.41	14.15	18.18	21.11	23.91	24.15	12.41
2,000	2.08	3.92	6.06	9.63	9.80	9.80	9.91	11.98	14.03	15.84	17.45	20.85	9.91
5,000	1.61	2.70	4.24	5.65	5.87	7.74	8.56	9.37	11.81	15.57	15.90	17.88	8.56
10,000	0.51	1.46	2.47	4.77	5.57	5.61	6.85	8.21	10.50	12.41	12.79	15.29	6.85
20,000	0.38	0.92	1.40	2.73	3.48	4.40	5.59	6.58	8.81	10.59	12.07	13.01	5.59
50,000	0.24	0.51	0.95	1.56	2.14	2.59	3.25	4.40	5.93	7.64	9.11	9.24	3.25
54,778	0.23	0.50	0.90	1.54	2.10	2.43	3.16	4.39	5.82	7.62	8.59	8.70	3.16

Table 3: Alvin, SPAS 1463 July 1979 depth-area-duration table

Storm 1463 Zone 1 - July 23 (0700 UTC) - July 28 (0600 UTC), 1979												
MAXIMUM AVERAGE DEPTH OF PRECIPITATION (INCHES)												
	Duration (hours)											
areasqmi	1	3	6	12	18	24	36	48	72	96	120	Total
0.4	6.46	13.79	20.52	32.51	39.79	43.08	45.46	45.47	45.48	45.49	45.49	45.49
1	6.45	13.75	20.47	32.37	39.61	42.88	45.24	45.24	45.27	45.28	45.28	45.28
10	6.26	13.36	19.88	30.47	36.90	40.15	42.25	42.31	42.39	42.39	42.44	42.44
25	6.09	12.97	19.41	27.97	33.82	35.34	37.29	37.61	37.61	38.37	38.54	38.54
50	5.89	12.75	18.87	25.26	31.40	32.67	34.06	34.06	34.06	35.59	35.78	35.78
100	5.60	12.24	18.06	23.89	28.14	30.20	31.27	31.30	31.57	32.81	35.23	35.23
150	5.40	11.82	17.46	22.77	27.53	28.61	28.61	29.89	30.69	30.71	34.68	34.68
200	5.22	11.44	16.92	21.72	26.10	27.27	27.80	27.85	30.01	30.41	34.13	34.13
300	4.89	10.70	15.85	20.55	24.89	25.60	26.56	26.99	29.39	30.26	33.03	33.03
400	4.58	9.99	14.65	18.73	22.62	22.62	22.62	26.21	28.92	30.12	31.94	31.94
500	4.28	9.38	13.53	17.75	21.71	22.08	22.41	25.41	28.48	29.97	30.84	30.84
1,000	3.52	7.61	9.64	14.52	17.83	20.48	21.95	23.89	26.35	27.69	27.85	27.85
2,000	2.48	5.87	8.09	11.33	13.74	16.14	19.00	19.18	22.03	24.35	24.51	24.51
5,000	1.71	2.65	5.10	7.63	9.24	12.10	14.33	15.27	15.40	19.07	19.16	19.16
10,000	0.51	1.33	2.22	5.06	7.06	8.95	10.55	10.69	11.55	14.87	14.95	14.95
20,000	0.30	0.77	1.61	2.31	2.82	4.82	4.82	5.62	9.71	10.62	10.81	10.81
50,000	0.24	0.51	0.87	1.54	2.08	2.56	3.60	4.29	4.74	5.72	5.77	5.77
54,778	0.24	0.50	0.82	1.51	2.04	2.55	3.47	3.98	4.72	5.10	5.15	5.15

Comparison to PMP values

Once Harvey was maximized, AWA was able to complete direct comparisons to the recently completed Texas state-wide PMP, as well as previous HMR 51 PMP values. The results of these comparisons showed that Harvey was significantly larger than the previous tropical storm PMP values in the region (Figure 12). However, Harvey did not exceed the overall PMP values for the region when all storm types were considered – with two minor exceptions. At 96 hours 20,000-square miles and 120 hours 20,000-square miles Harvey was 0.6% greater and 4.4% greater respectively (Table 5). Unfortunately, HMR 51 PMP values only extend to 72 hours, so similar comparisons to those values were not possible. This also demonstrates one of the problems with HMR 51 in that it does not provide PMP values at all required area sizes and durations for regions of the country where storms last longer than 72 hours, like the Texas coastal region.

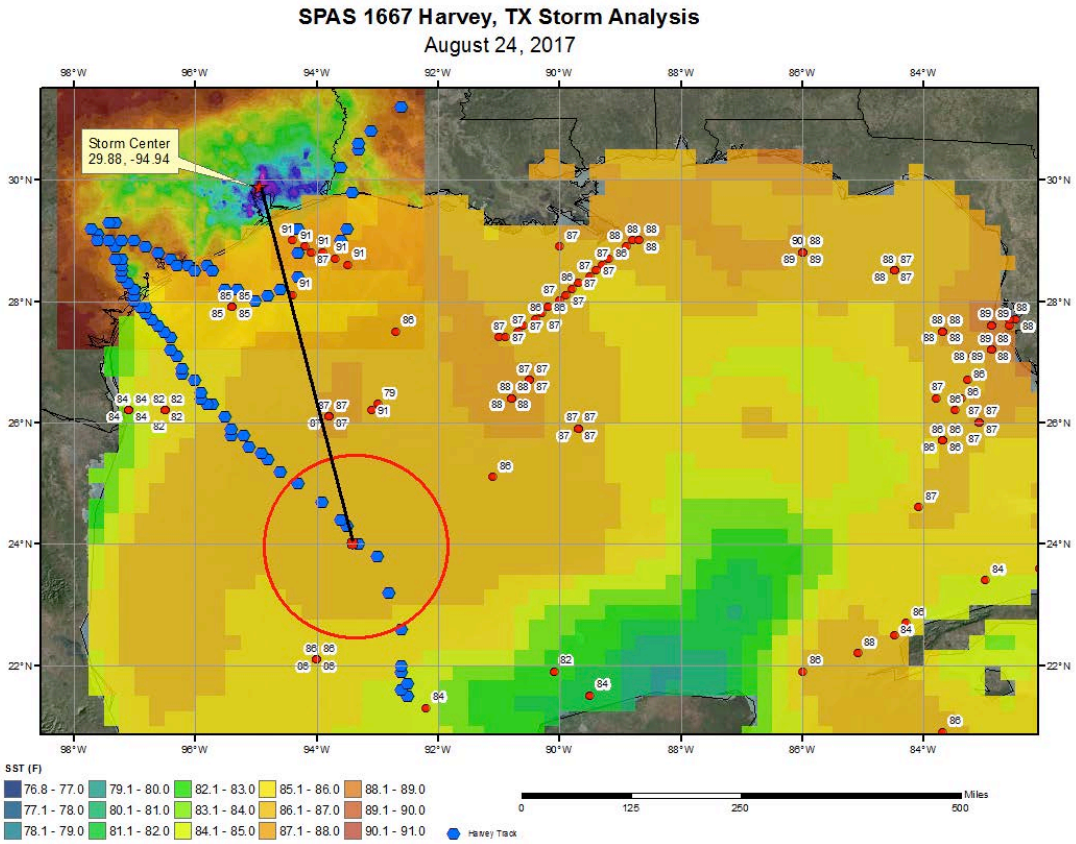


Figure 11: Hurricane Harvey in-place maximization

Table 4: Hurricane Harvey in-place maximization calculation spread sheet

Storm Name:	**SPAS 1667 - Hurricane Harvey**		**Storm Adjustment for Grid Points XX**					
Storm Date:	**August 24-29, 2017**							
AWA Analysis Date:	**9/11/17**							
Temporal Transposition Date	**15-Aug**							
	Lat	**Long**						
Storm Center Location	**29.88 N**	**94.94 W**	**Moisture Inflow Direction**	**SSE @ 415**	miles			
Storm Rep SST Location	**24.0 N**	**93.4 W**	**Basin Average Elevation**	**NA**	feet			
Transposition SST Location	**NA**	**NA**	**Storm Center Elevation**	**40**	feet			
Basin Location	*	*	**Storm Analysis Duration**	**24**	hours			
			Effective Barrier Height	**NA**	feet			
The storm representative SST is	**86.5 F**	with total precipitable water above sea level of				**4.77**	inches.	
The in-place maximum SST is	**87.0 F**	with total precipitable water above sea level of				**4.86**	inches.	
The transpositioned maximum SST is	**NA**	with total precipitable water above sea level of				**#VALUE!**	inches.	
The in-place storm elevation is	**40**	feet which subtracts	**0.02**	inches of precipitable water at		**86.5 F**		
The in-place storm elevation is	**40**	feet which subtracts	**0.02**	inches of precipitable water at		**87.0 F**		
The transposition storm elevation at	**NA**	feet which subtracts	**#VALUE!**	inches of precipitable water at		**NA**		
The moisture inflow barrier height is	**NA**	feet which subtracts	**#VALUE!**	inches of precipitable water at		**NA**		
The in-place maximization factor is	**1.02**							
The transposition factor is	**#VALUE!**							
The elevation/barrier adjustment factor is	**#VALUE!**							
The total adjustment factor is	**#VALUE!**							

Notes: Storm representative SST value was based on 24 hour SST values on August 23-25, 2017.

Not surprisingly, the storm far exceeded the NOAA Atlas 14 precipitation frequency values, with a large region experiencing greater than a 1,000-year recurrence interval (Figure 13). Preliminary investigations demonstrate that the storm was likely somewhere between a 10^{-5} and 10^{-6} recurrence interval.

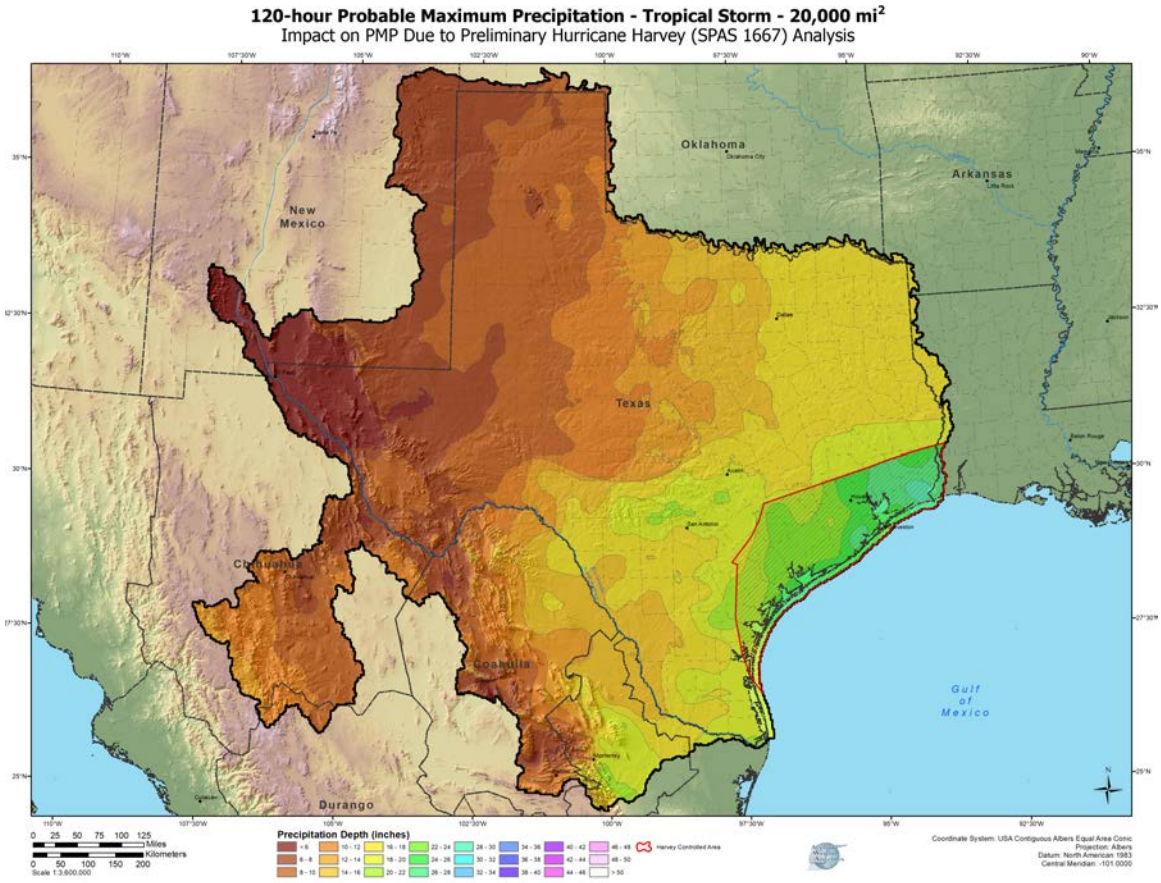


Figure 12: Region where tropical storm PMP values increased after Hurricane Harvey

Table 5: Comparison of PMP to maximized Harvey rainfall

	Average Tropical PMP (post-Harvey)	Average Tropical PMP (pre-Harvey)	Average % Increase	Average General PMP (pre-Harvey)	Average % Increase over General PMP	Average HMR 51 PMP	Average % Increase from HMR 51
5,000-sqmi 48-hour	-	-	-	-	No Increase	-	No Increase
5,000-sqmi 72-hour	29.2"	27.4"	6.6%	36.0"	No Increase	31.1"	No Increase
5,000-sqmi 96-hour	30.7"	N/A	-	N/A	-	N/A	No Increase
5,000-sqmi 120-hour	32.3"	N/A	-	N/A	-	N/A	No Increase
10,000-sqmi 48-hour	21.6"	21.1"	2.5%	25.0"	No Increase	22.9"	No Increase
10,000-sqmi 72-hour	25.0"	23.4"	7.1%	29.6"	No Increase	26.8"	No Increase
10,000-sqmi 96-hour	26.6"	23.6"	12.5%	28.2"	No Increase	N/A	No Increase
10,000-sqmi 120-hour	28.3"	23.8"	18.9%	28.4"	No Increase	N/A	No Increase
20,000-sqmi 48-hour	17.1"	16.2"	5.4%	20.5"	No Increase	22.8"	No Increase
20,000-sqmi 72-hour	20.4"	18.4"	10.9%	22.3"	No Increase	26.8"	No Increase
20,000-sqmi 96-hour	23.2"	20.6"	12.8%	23.1"	**0.6%**	N/A	No Increase
20,000-sqmi 120-hour	23.8"	20.8"	14.8%	22.8"	**4.4%**	N/A	No Increase

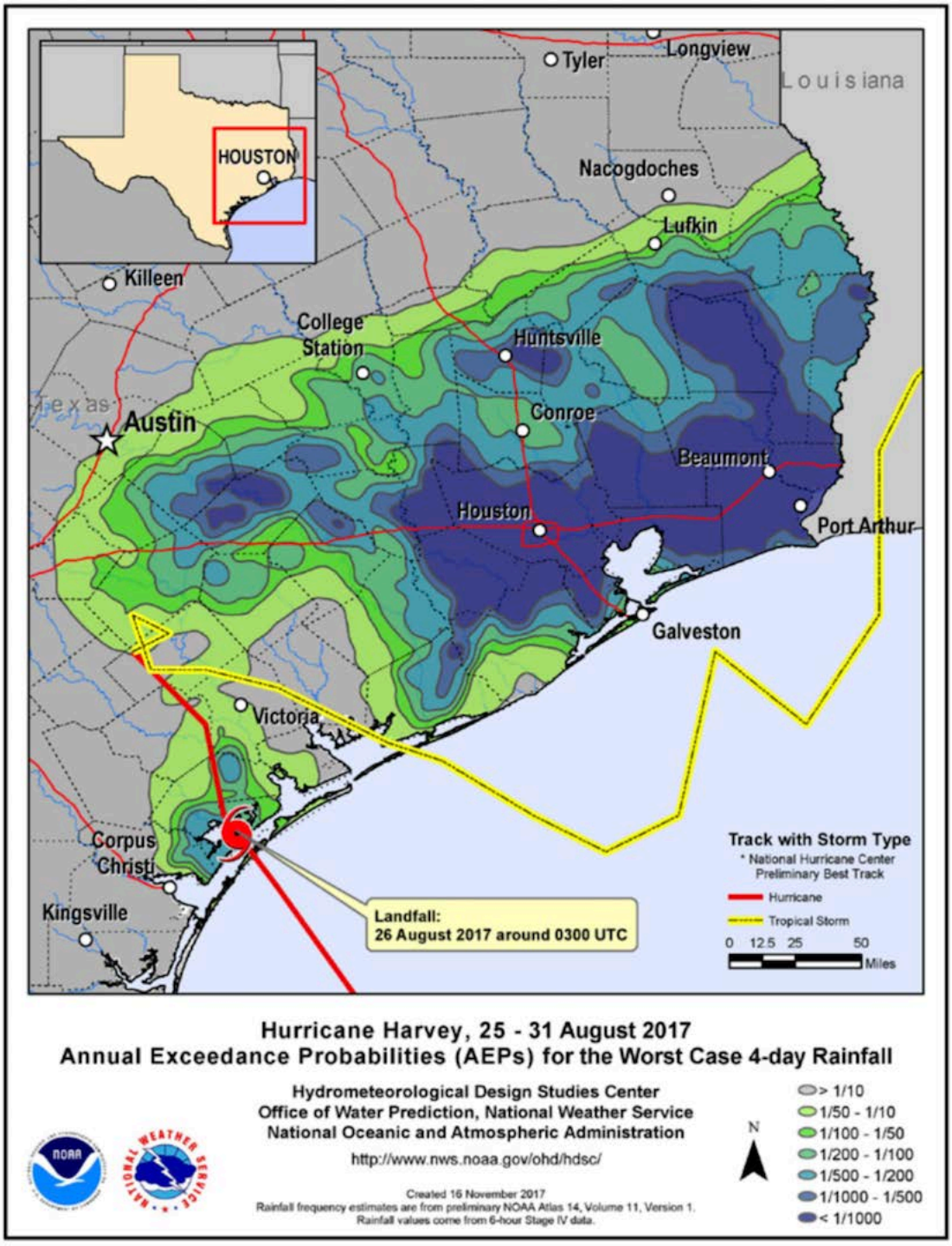


Figure 13: Annual Exceedance Probability of the Hurricane Harvey rainfall compared to NOAA Atlas 14 values

Conclusion

Harvey was a real-world example of a PMP-rainfall event and demonstrated that PMP can happen. One

very important outcome for the dam safety community is that even with Harvey producing PMP level rainfall, no high hazard dam failed in Texas or Louisiana. This is likely the result of good dam safety practices and design, as well as luck. Therefore, it is extremely important that the dam safety community follows standard practice in design of structures, monitoring of structures, and applying the most up-to-date science and data. Harvey also demonstrates the need to continually update the storm database and PMP estimates as new storms occur and the understanding of extreme rainfall mechanisms increases. A program should be in place that allows for updating of these databases and PMP values in real-time as events occur.

TCEQ dam safety, the National Weather Service, members of the academic community, and private consultants should all be commended for their monitoring, communication, and responses prior to, during, and after Harvey occurred. This type of coordination and communication should become the standard for other state dam safety and Federal dam safety offices, because these types of events will occur again.

References

Kappel, W.D., Hultstrand, D.M., Muhlestein, G.A., Steinhilber, K., McGlone, D., Parzybok, T.W. and Lawrence, B. 2016. Statewide Probable Maximum Precipitation for Texas. Prepared for the Texas Commission of Environmental Quality.

McMahan. 2017. Personal communication, August 2017.

Nielson-Gammon, Dr. 2017. Personal communication, September 2017.

Nuclear Regulatory Commission (NRC). 2017. Commercial Grade Dedication and Audit of SPAS, ENERCON Appendix B Program.

World Meteorological Organization (WMO). 2009. *Manual for Estimation of Probable Maximum Precipitation,* No. 1045, WMO, Geneva, 259 pp.

Proceedings of Mine Water Solutions 2018
June 12–15, 2018, Vancouver, Canada
Published by the University of British Columbia, 2018

Richmond Hill Mine Heap Leach Pad Soil Cover System Evaluation

Guosheng Zhan, Barrick Gold of North America, Inc., USA
Daniel Lattin, Barrick Gold of North America, Inc., USA
Jason Keller, GeoSystems Analysis, Inc., USA
Michael Milczarek, GeoSystems Analysis, Inc., USA

Abstract

LAC Minerals operated the Richmond Hill mine located in the northern Black Hills from 1988 to 1993 using conventional heap leach technology. Following active mining, LAC Minerals began reclamation actions in 1994.

The mine facilities were located in an area of relatively rugged terrain. Annual and daily temperature variations can be extreme. Annual precipitation and potential evapotranspiration average about 0.73 and 0.90 m (29 and 36 inches) per year, respectively.

The Richmond Hill Mine heap leach pads (HLPs 1 and 2, and HLP 3) were reclaimed in 1996 using a three-layer evapotranspiration (ET) cover designed to limit meteorological infiltration through the facilities.

HLP seepage outflow rates have been measured on an approximately weekly basis from December 1996 to present. Large seasonal and wet/dry outflow cycles have been observed. Several years after the cover system installation, increased HLP drainage rates were observed, which could be due to increased permeability of the compacted layer in response to pedogenic processes such as wetting/drying, freeze/thaw, and root development.

The estimated net infiltration rate through the multilayer cover system during the monitoring period is about 34% of precipitation, which is well within the range of observations from other studies. To evaluate the cover system efficiency, a monthly time-step, spreadsheet-based, parsimonious water balance model was created. The model considers close inter-relation between precipitation, ET, and cover net infiltration on a monthly scale, and continuous feedback of water movement in the soil-plant-atmosphere continuum. The model accurately reproduces the recorded seepage rates for the monitoring period after pedogenic processes ceased.

The revegetated and reclaimed Richmond Hill Mine heap leach pads have been monitored for a relatively long-term period. Results from 20 years of cover system monitoring provide a general review of ET cover system performance for closure of other comparable facilities, and offer guidance for ET cover system requirements in other areas with similar climate.

Introduction

LAC Minerals operated the approximately 162 hectare (400 acre) Richmond Hill mine located in the northern Black Hills, four miles (6.4 km) northwest of Lead, South Dakota. Active mining of the mine occurred from 1988 to 1993 using conventional heap leach technology. Ore was crushed to ¾" minus and placed on the leach pads in twenty-foot lifts. Following active mining, LAC Minerals began reclamation actions in 1994.

The mine facilities were located at an elevation between 1,676 and 1,829 m (5,500 and 6,000 feet) above sea level in an area of relatively rugged terrain.

The Richmond Hill Mine heap leach pads (HLPs 1 and 2 and HLP 3) were reclaimed in 1996. Reclamation consisted of grading to 2.5:1 (H:V) slope and a multi-layer evapotranspiration (ET) cover designed to limit meteorological infiltration through the facilities (Figure 1). The ET cover design consisted of, from bottom up:

1. 0.3 m (1 foot) of compacted spent ore amended with bentonite (amended soil liner) with a minimum of 7% bentonite by dry weight;
2. 1.2 m (4 foot) of thermal barrier / drainage layer material; and
3. 0.15 m (0.5 foot) of stockpiled topsoil.

To control subsurface drainage from the drainage layer, the amended soil liner was extended past the geomembrane liner that exists below the HLP and a minimum 0.30 m (1.0 foot) deep drainage trench was cut into the original ground surface to collect any subsurface water flow from above the top of the amended soil liner (Figure 2). The drainage collection trenches are sloped to drain to perimeter drainage channels. To control surface water drainage, a series of drainage benches are constructed within the HLP, which are graded to route water towards perimeter drainage channels.

The ET cover surfaces were reclaimed with a grass seed mix and deep rooting vegetation (i.e. trees and shrubs) are prevented from establishing on the ET cover.

HLP 1 and 2 and HLP 3 ET cover areas are nearly identical at about 10.5 hectares (26 acres) each. Of this area, approximately 20% of the HLP 1 and 2 surface and 42% of the HLP 3 surface has a shallow grade (i.e. less than 5% slope).

Recorded leachate outflow overtime from the HLP 1 and 2 and HLP 3 ET are nearly identical with combined flow of 13 million gallons per year, or 1.56 l/s (25 gpm). Water treatment at the Richmond Hill Leach Pad sites consists of two main treatments: a biological plant and a reverse osmosis (RO) plant.



Figure 1: Richmond Hill mine leach pad 1 and 2 and leach pad 3

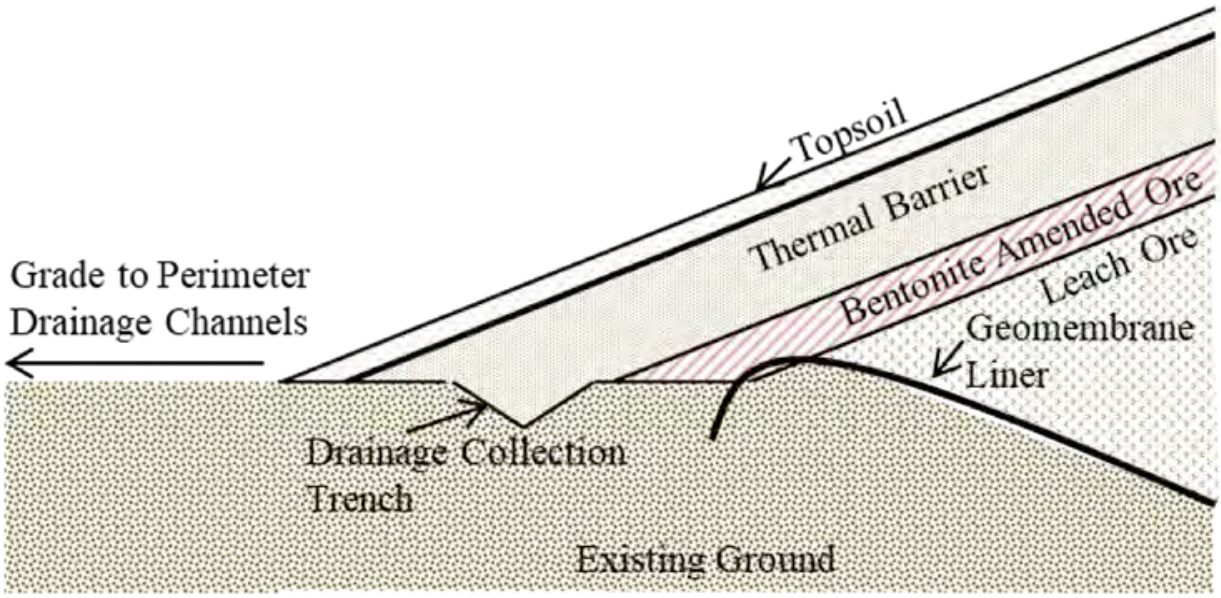


Figure 2: Evapotranspiration cover and drainage collection trench

Climate

Precipitation has been measured at the Richmond Hill Mine weather station with a heated rain gauge. Recorded annual precipitation ranges from 0.30 to 1.12 m (12 to 44 inches), with an average of about 0.73 m (29 inches). Average monthly precipitation ranges from a low of 26.42 mm (1.04 inches) in December to a high of 119.90 mm (4.72 inches) in June. Snowpack accumulates during the months of December, January, February and March, when most precipitation falls as snow. Snowpack melts during the months of April, May and June.

Potential evapotranspiration (PET) was not directly measured. It was estimated from temperature data using the Hargreaves equation (Hargreaves and Samani, 1985). Estimated annual PET ranges from 0.84 to 1.02 m (33 to 40 inches), with an average of about 0.90 m (36 inches). Average monthly PET ranges from a low of 15.24 mm (0.60 inches) in December to a high of 163.32 mm (6.43 inches) in July.

Average monthly temperatures range from a low of –5°C (23°F) in January to a high of 20°C (68°F) in July, with an average over the year of 7°C (44°F).

As indicated on Figure 3, the majority of precipitation falls in the April to June time frame, coincident with the snowmelt period, before significant evapotranspiration occurs at the site. The climate pattern at the mine causes a significant proportion of the precipitation to infiltrate into the cover system during periods of low evapotranspiration and subsequently percolate into the leach pads.

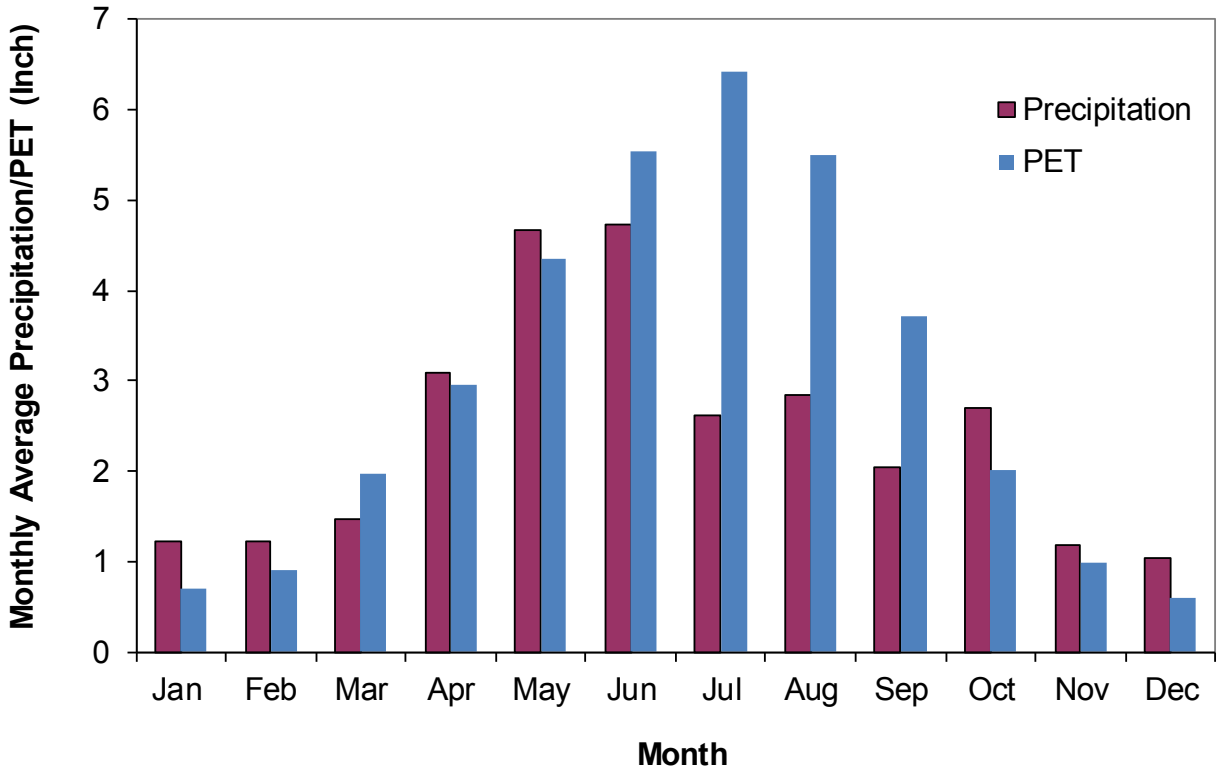


Figure 3: Average monthly precipitation and PET at Richmond Hill mine

HLP Outflow Rates

HLP seepage outflow rates have been measured by Richmond Hill mine on an approximate weekly basis from 1997 to the present. Seepage outflow is measured from manual readings of the water level in V-notch weirs installed at the HLP 1 and 2 sump and the HLP 3 effluent pipe. Outflow rates over time are presented on Figure 4, in addition to water year (WY = October 1 through September 30) cumulative precipitation measured at the Richmond Hill weather station. Increased seepage outflow is generally observed during spring freshet and in response to large precipitation events. Minimum seepage outflow is typically measured in late fall and winter. The average WY seepage outflow and precipitation for the 19 WY measurement record is presented in Table 1. The average annual HLP seepage outflow over this period was 32.1% of precipitation for HLP 1 and 2 and 31.3% of precipitation for HLP 3.

Less than 25% of precipitation reported as seepage outflow during the initial three years after the installation of the cover systems, even though WYs 1998 and 1999 were the wettest year on record (1.02 and 1.12 m, or 40.29 and 44.04 inches). The HLP average annual outflow rates are presented in Table 2.

The effective net percolation rates, calculated as the seepage outflow divided by the HLP surface area, are presented versus time in Table 3. The minimum effective net percolation rate is assumed to approximate the base flow from the HLPs. It should be noted that because seepage outflows are measured

on an approximately weekly basis, it is possible that peak seepage outflow and maximum effective net percolation rates may be greater than measured.

The increase in estimated net percolation over time may be an indication that the amended soil liner K_{sat} has increased over time. A number of studies have observed an increase in clay cover system K_{sat} and a decrease in water holding capacity due to the formation of larger pores in response to pedogenic processes such as wetting/drying, freeze/thaw, and root development (Albright et al., 2010; Benson et al., 2011; Orellana et al., 2010). Both Benson et al. (2011) and Orellana et al. (2010) observed the largest K_{sat} increases were observed for compacted clay covers with K_{sat} increases after construction. The study by Benson et al. (2011) observed that the number of compacted clay covers failing to achieve their design K_{sat} increased sharply at compacted clay thicknesses less than 1.0 m. Benson et al. (2011) also reported that the long-term K_{sat} value for clay liners studied generally fell within the range of 7.5×10^{-6} cm/sec to 6.0×10^{-4} cm/sec, regardless of cover type. The estimated maximum effective flux rate of 6.1×10^{-6} cm/sec (Table 3) is similar to this range of values.

Table 1: Water year precipitation and seepage outflow as percent of precipitation (WY 1998 to WY 2016)

	Precipitation (in)	Pad 1 and 2 (%)	Pad 3 (%)
1998	40.29	23	22
1999	44.04	22	20
2000	34.84	25	25
2001	18.50	38	42
2002	17.69	25	26
2003	21.60	29	28
2004	12.12	44	37
2005	20.83	27	29
2006	32.58	30	31
2007	28.30	34	32
2008	33.13	39	34
2009	29.28	39	37
2010	30.99	43	41
2011	32.52	40	38
2012	20.38	31	31
2013	34.19	23	24
2014	33.08	41	42
2015	39.19	33	33
2016	22.13	35	37
Average All	**28.72**	**32**	**31**
Average 1998 – 2000	**39.72**	**23**	**22**
Average 2001 – 2005	**18.15**	**32**	**32**
Average 2006 – 2016	**30.52**	**35**	**34**

Table 2: Measured heap leach pad average annual seepage outflow rate (gpm)

Water Year	HLP 1 and 2	HLP 3
1998–2000	13.7	13.0
2001–2005	8.2	8.3
2006–2016	15.3	15.0
All	13.2	12.9

Table 3: Heap leach pad measured effective net percolation flux rates

Water Year	Effective net percolation flux rate (cm/sec)					
	Average		Maximum		Minimum	
	HLP 1 and 2	HLP 3	HLP 1 and 2	HLP 3	HLP 1 and 2	HLP 3
1998-2000	8.2E–07	7.7E-07	6.0E-06	3.8E-06	2.9E-07	3.0E-07
2001-2005	4.9E-07	5.0E-07	2.7E-06	3.1E-06	2.2E-07	2.5E-07
2006-2016	9.2E-07	9.0E-07	5.6E-06	6.1E-06	2.6E-07	2.9E-07
All	7.9E-07	7.7E-07	6.0E-06	6.1E-06	2.2E-07	2.5E-07

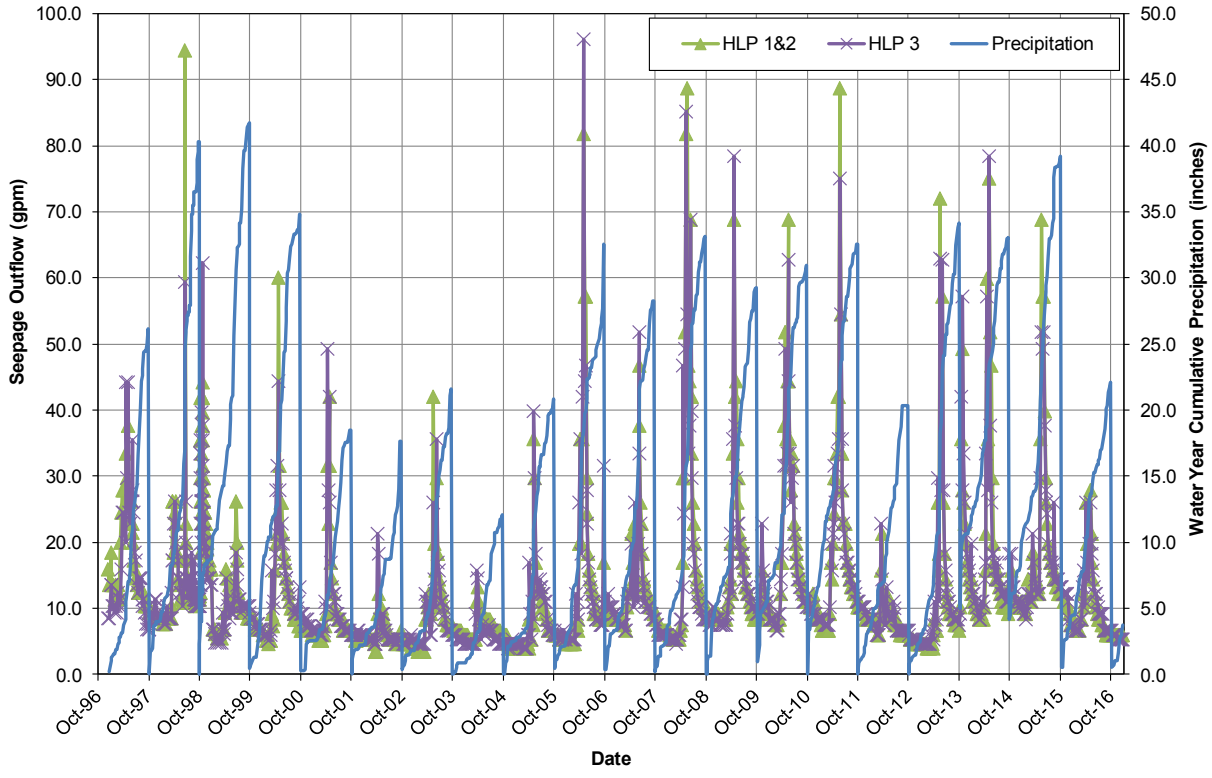


Figure 4: Measured heap leach pad seepage outflow and water year cumulative precipitation

Water Balance Model

HLP calibrated water balance models were developed using the site precipitation data and calculated PET. The calibrated models are able to predict future leach pad seepage outflow rates under normal or extreme climate conditions.

The HLP water balance model was implemented in Microsoft Excel using monthly time steps for HLP inflows and outflows. The HLP water balance is based on the Vandewiele et al. (1992) model, described by:

$$S_t = S_{t-1} + P_t - R_t - Q_t \quad \text{Equation 1}$$

Where t is time (month), S is soil-water storage, P is monthly snowmelt/rainfall, R is monthly actual evapotranspiration (AET) and subsurface runoff, and Q is monthly HLP seepage outflow.

R is calculated as:

$$R_t = min\left[E_t \times \left(1 - a_1^{\frac{W_t}{E_t}}\right), W_t\right] \quad \text{Equation 2}$$

Where E is PET, a_1 is a positive parameter, and W is water available for evapotranspiration and subsurface runoff, calculated as:

$$W_t = P_t + S_{t-1} \quad \text{Equation 3}$$

Q is divided into slow seepage (i.e. baseflow) and fast seepage by:

$$Q_{slow} = \left[a_2 \times (S_{t-1})^{b1}\right] \quad \text{Equation 4}$$

$$Q_{fast} = \left[a_3 \times S_{t-1} \times \left(P_t - E_t \times \left(1 - exp\left(-\frac{P_t}{E_t}\right)\right)\right)\right] \quad \text{Equation 5}$$

Where a_2, a_3, and b_1 are positive parameters.

Water balance model applied precipitation and PET are presented in Figure 5.

Model parameters a_1, a_2, a_3, and b_1 were calibrated to measured seepage data from January 2001 through December 2016 for HLP 1 and 2 and HLP 3 as a joint objective function, resulting in one set of calibrated parameters for both HLPs. Additionally, the calibration incorporated a precipitation timing correction factor to account for winter snow and spring freshet. The calibration was restricted to January 2001 and later data so as not to include early-post construction HLP conditions. Calibrated model parameters are provided in Table 4.

Model predicted and measured seepage outflow is presented on Figures 6 and 7 for HLP 1 and 2 and HLP 3, respectively. The model accurately represents base flow and increased seepage outflow events.

Differences between model predicted and measured seepage could be partially due to the seepage outflow measurements being on a weekly basis, which were used to generate monthly average flows. The model predicted seepage outflow from HLP 1 and 2 and HLP 3 during the simulated period (January 2001 through December 2016) was 34% of precipitation, corresponding to measured seepage outflow for HLP 1 and 2 of 35% of precipitation and for HLP 3 of 34% of precipitation for the same period. The remaining 66% of precipitation is predicted to be lost to evapotranspiration or subsurface runoff.

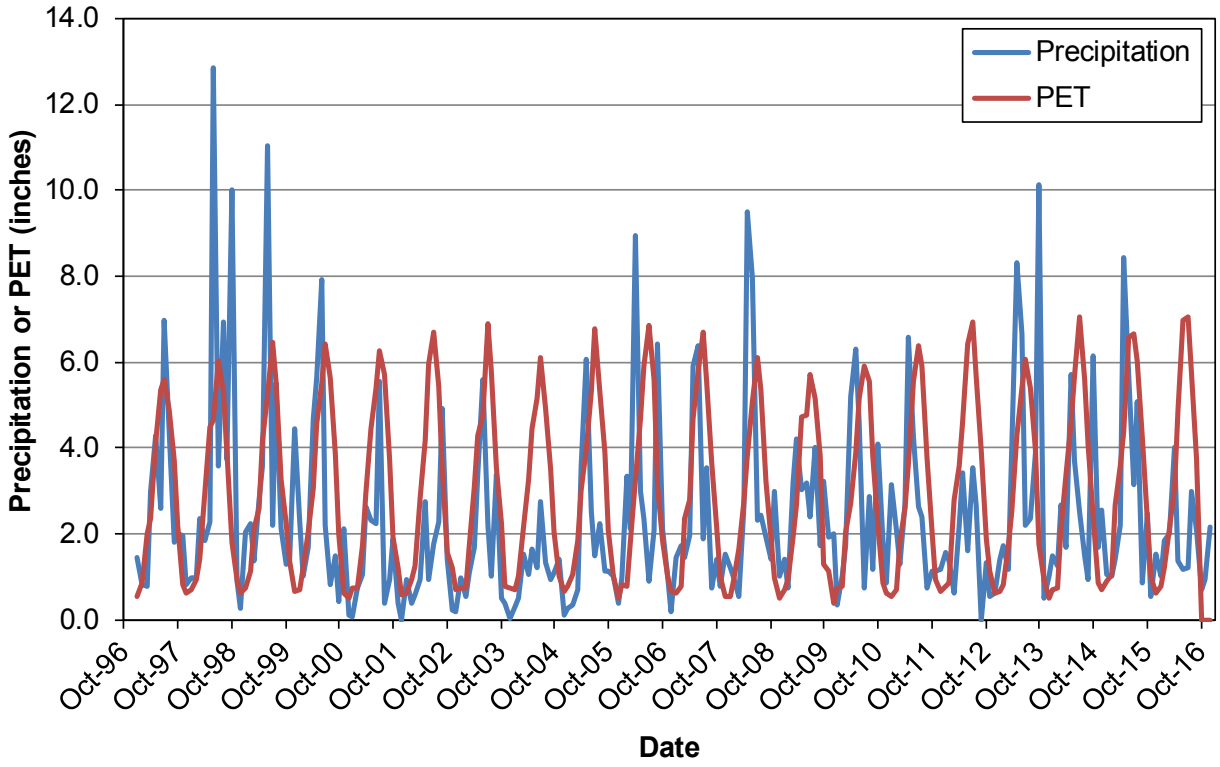


Figure 5: Water balance model monthly applied precipitation and potential evapotranspiration

Table 4: Heap leach pad water balance model calibrated parameters

Parameter	Calibrated value
a_1	0.70
a_2	0.10
a_3	0.0032
b_1	1

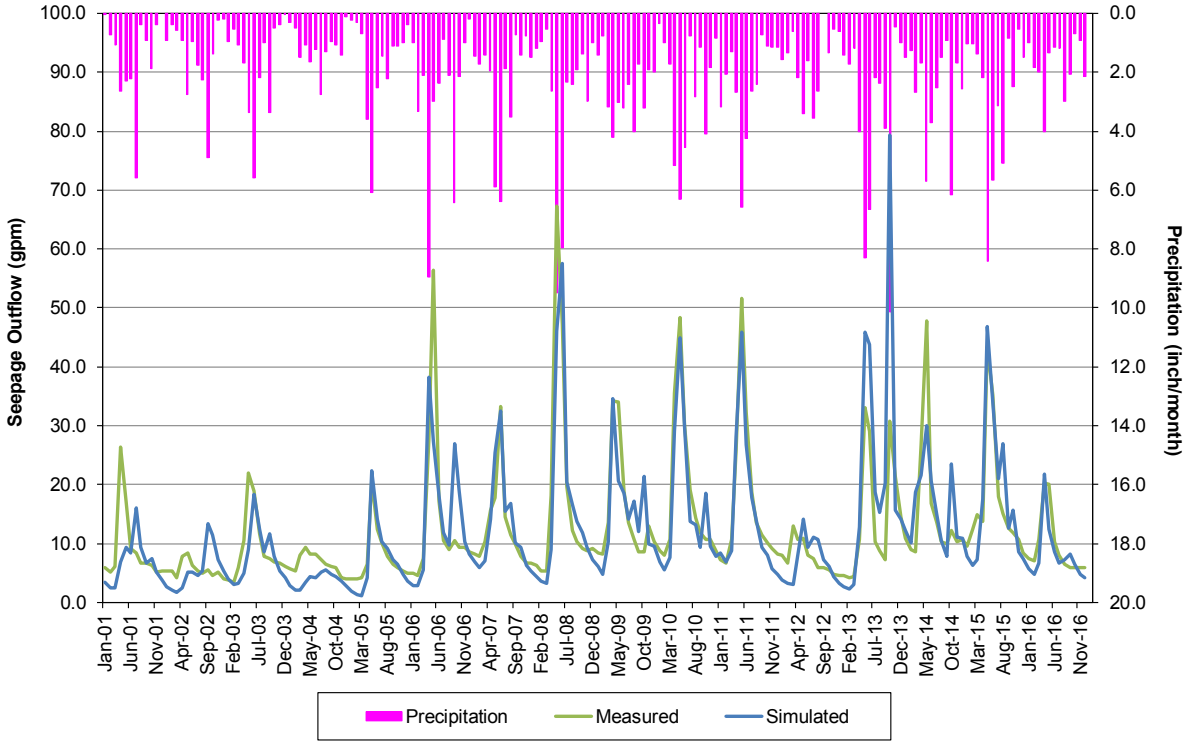


Figure 6: Monthly measured and modelled seepage outflow for heap leach pad 1 and 2

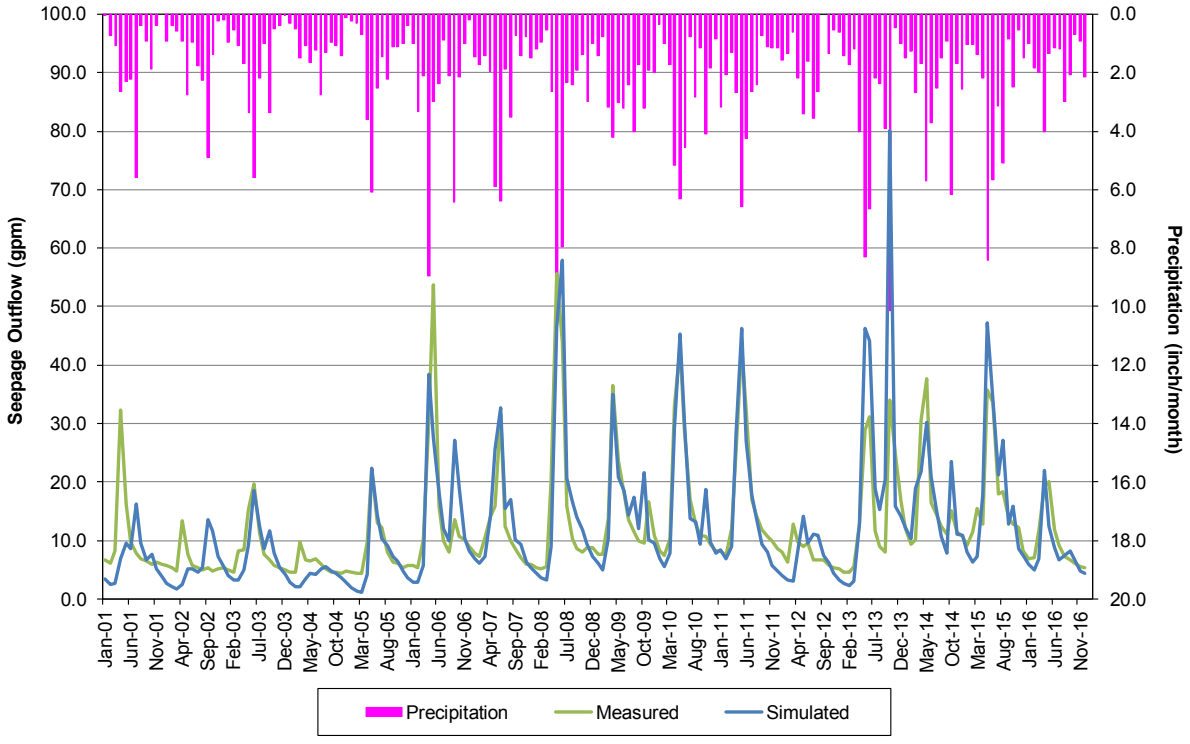


Figure 7: Monthly measured and modelled seepage outflow for heap leach pad 3

Discussion

It appears that the K_{sat} of the amended soil liner increased in the early time between 1996–2000 in response to pedogenic processes. Post-construction changes in soil structure consist of decreasing density and the formation of larger pores which may be formed by biological process such as ingress of plant roots and burrowing of worms and insects. Volume changes caused by wet-dry cycling and frost action also reduce the bulk density of soils and can result in formation of larger pores and a broader pore size distribution. An increase in hydraulic properties is anticipated in response to these changes in soil structure.

Richmond Hill mine is located at a relative wet area with a precipitation to potential evapotranspiration (P/PET) ratio of 0.80. Based on the actual data and calibrated model results, we estimate that 66% of precipitation is lost to ET or subsurface runoff and 34% becomes net percolation, which results in seepage outflow from the pads.

Apiwantragoon et al. (2015) presented a comprehensive review of the field-scale performance of landfill ET covers at 12 sites across the United States. Test sections were constructed at these sites with large (10 × 20 m, 33 × 66 feet) drainage lysimeters for continuous and direct monitoring of the ET covers over a period of 3 to 6 years. The 12 test sites in eight states represent a broad range of geography, climates, soils, and vegetation communities. Based on the P/PET ratio, one site is arid, seven are semiarid, two are subhumid, and two are humid following definitions in UNESCO (1979). The diversity in climates is evident in the range of average annual precipitation (0.12 to 1.26 m, 4.72 to 49.61 inches) and the range in P/PET (0.06 to1.10). The study concluded that net percolation is very sensitive to annual P/PET ratio and when P/PET ratio is greater than 0.2, the net percolation is generally high.

Figure 8 is adapted from Apiwantragoon et al. (2015) and shows their data (named as ACAP) and other available field data measurements. When the P/PET ratio is 0.80, such as Richmond Hill mine, the expected net percolation is in the range of 60 – 350 mm (2.36 – 13.78 inches) per year (redline on Figure 8). The simulated and measured Richmond Hill's net percolation of 248 mm (730 mm × 34%) (9.76 inch) per year is well within this range (green dot on Figure 8).

Conclusions

The revegetated and reclaimed Richmond Hill mine heap leach pads have been monitored for 20 years.
A review of the monitoring data indicates that K_{sat} of the amended soil liner most likely increased in the early time between 1996–2000 in response to pedogenic processes. Based on the analyses in this study, it took about four years for pedogenic processes in the Richmond Hill cover system to stabilize. It is evident that observed HLP seepage outflow rates could be well simulated by a model from 2001 to now.

HLP 1 and 2 and HLP 3 have nearly identical areas about 10.5 hectares (26 acres), but have 20% and 40% flat area (< 5% slope), respectively. The observed HLP seepages from these two cells are nearly identical, indicating that flat areas do not make a difference for the Richmond Hill HLP cover system efficiencies.

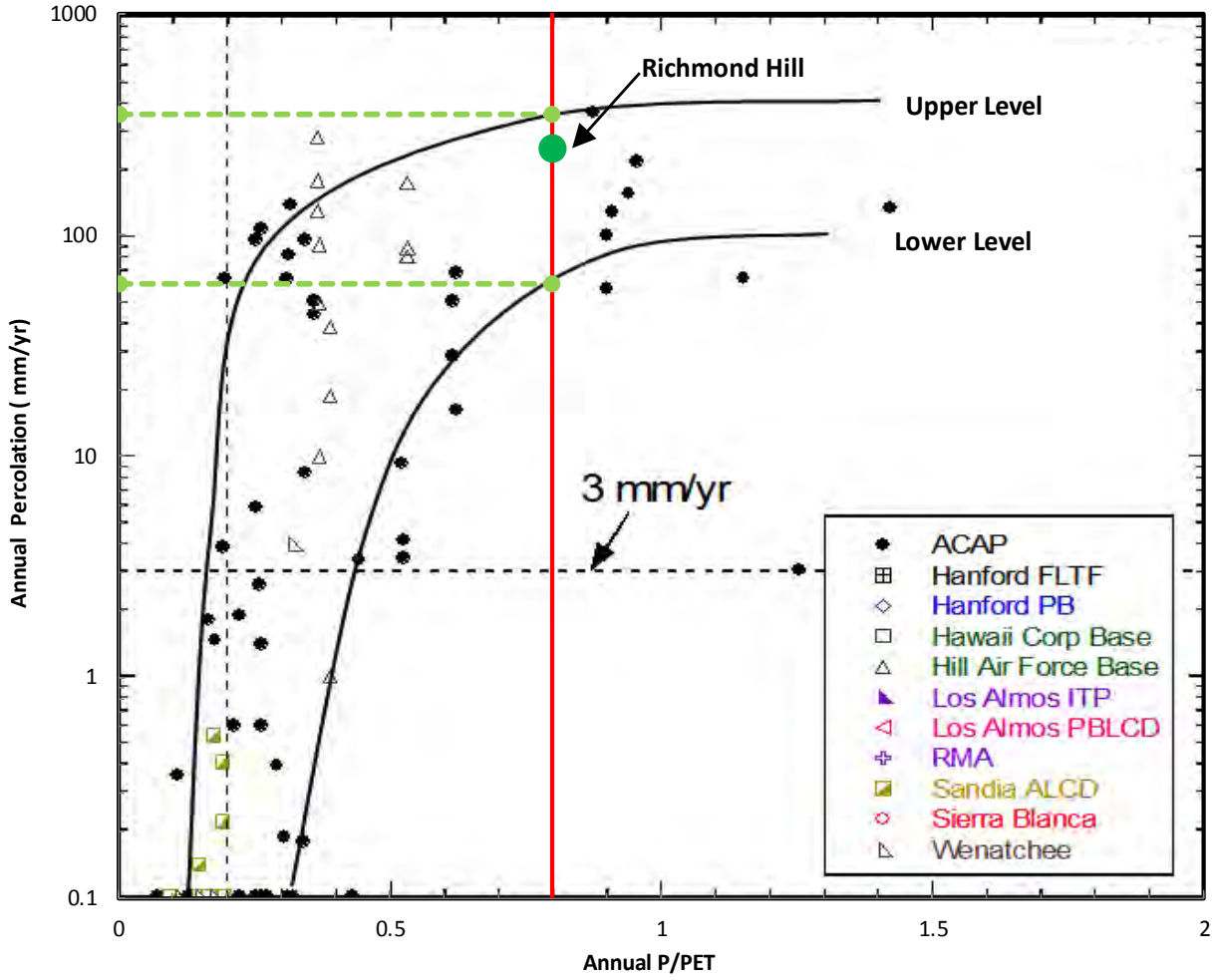


Figure 8: Annual percolation as a function of ratio of annual P/PET from Richmond cover, ACAP covers and other studies (adapted from Apiwantragoon et al., 2015)

Net percolation rates at HLP 1 and 2 and HLP 3 were accurately simulated by a monthly water balance model. Simulated percolation rates are about 34% of precipitation. High percolation rates are due to the high P/PET ratio of 0.80 at the site. Expecting an ET cover to eliminate or effectively limit meteoric infiltration at a high P/PET site (>0.2) is not realistic regardless of soil type, cover thickness and cover configuration. At subhumid and humid sites, an ET cover system can reduce, but not eliminate, net percolation. Thus, the cover system at Richmond Hill HLP is considered to be functional and has met the design objective.

Results from 20 years of cover system monitoring at Richmond Hill mine provide a general review of ET cover system performance for closure of other comparable facilities, and offer guidance for ET cover system requirements in other areas with similar climate.

Acknowledgements

This paper was generated from the Richmond Hill mine reclamation program. Thanks to the Richmond Hill staff for long-term data collection. Special thanks to Barrick Gold Corporation for granting permission to publish this technical summary.

References

Albright, W.H., Benson, C.H., and Waugh, W.J. 2010. *Water Balance Covers for Waste Containment: Principles and Practice*. Reston, VA: ASCE Press.

Apiwantragoon, P., Benson, C.H. and Albright, W.H. 2015. Field hydrology of water balance covers for waste containment, *J. Geotech. and Geoenvironmental Eng*. 141(2): 04014101-1-20. DOI: 10.1061/(ASCE)GT.1943-5606.0001195

Benson, C.H., Sawangsuriya, A., Trzebiatowski, B. and Albright, W.H. 2007. Pedogenic effects on the hydraulic properties of water balance cover soils, *J. Geotech. and Geoenvironmental Eng*. 133(4): 349–359.

Benson, C.H., Albright, W.H., Fratta, D.O., Tinjum, J.M., Kucukkira, E., Lee, S.H., Scalia, J., Schilicht, P.D. and Wang, X. 2011. Engineered cover for waste containment: Changes in engineering properties and implications for long-term performance assessment. Nuclear Regulatory Commission Report NUREG/CR-7028.

Hargreaves, G.H. and Samani, Z.A. 1985. Reference crop evapotranspiration from temperature, *Applied Engineering in Agriculture*, 1(2): 96–99.

Orellana, R., Ludwick, W., Zhan G., Baumann, W., Milczarek, M., Rice, R.C., Yao, T.M. and Keller, J. 2010. Final results of the cover system test panel trials at the Pierina Mine, in A. Fourie, M. Tibbet and J. Wiertz (eds) *Proceeding of the Fifth International Conference on Mine Closure*, November 23–26, 2010, Viña del Mar, Chile.

UNESCO. 1979. *Map of the world distribution of arid regions*. MAB Technical Note No. 7. Paris.

Vandewiele, G.L., Xu, C.Y. and Win, N.J. 1992. Methodology of comparative study of monthly water balance models in Belgium, China and Burma, *Journal of Hydrology,* 134: 315–347.

Proceedings of Mine Water Solutions 2018
June 12–15, 2018, Vancouver, Canada
Published by the University of British Columbia, 2018

Investigation of Feed Water Treatment Options in an Arid Area

Mohsen Barkh, SGS Canada Inc., Canada

Abstract

A water treatment option was required to provide feed water for a mine in an arid area in Africa. The required feed water needs to have a quality of 200 mg/L or less of chloride with a flow rate of 1,200 m^3/hr. Constraints existed not only with respect to the available source of raw water, but also in terms of the available alternatives for the ultimate disposal of waste streams.

The two technically and economically viable options, Ion Exchange (IX) and Reverse Osmosis (RO), were compared. Two types of source water, brackish water RO (BWRO) and sea water RO (SWRO), were selected and investigated. The waste disposal alternative with the least environmental issues is the Zero Liquid Discharge (ZLD) arrangement. Different variations of ZLD, including an evaporator, crystallizer, and solar evaporation pond were investigated. The evaporator of choice is a vertical falling film mechanical vapour compression type. Vertical falling film evaporators have a very good reputation in industrial areas. Mechanical vapour compression was selected as the source of energy for evaporation because steam was not available at the site. To determine if the solar evaporation was a viable system, the evaporation rate in the area was estimated and the precipitation records were obtained. A decision matrix was developed to quantify the advantages and disadvantages of the different options. A partial ZLD system (that is, a Low Liquid Discharge system) including an evaporator and crystallizer was adopted for the design.

Introduction

In many metallurgical processes, water acts as both reaction and transport media; therefore, quality and quantity of the available water on site has a significant effect on the feasibility of the overall process. In arid areas, providing a water source with the required quantity is crucial, but, in many cases, the available water has such a poor quality that it cannot be used for metallurgical processing without initial treatment. The high cost of feed water treatment along with the quantity limitations, reinforces the application of a system to minimize water loss from the waste system. Due to the complexity of the situation, considering all different parameters for selecting the best available option requires a full engineering study.

To minimize loss of water, a zero liquid discharge (ZLD) system could be used. ZLD is a general term referring to a series of unit operations that produces solid waste from brine. The ZLD system for brine could be a combination of membrane, evaporation, crystallizer, and dryer. In arid areas, ZLD is used to recover water from the waste; however, the high cost of the recovery process significantly impacts the feasibility of the system. This study is a detailed investigation and analysis in an arid area that supports the fact that using ZLD to maximize recovered water is not a viable option.

Description of the Situation

The subject of this study is a mine located in an arid area in Africa that processes minerals through a wide range of low pH metallurgical processes such as ion exchange, solvent extraction, and precipitation. The total water consumption of the process is about 2,000 m^3/ hr, which requires 1,200 m^3/hr of fresh water plus 800 m^3/hr recycled water. The metallurgical process design was completed based on the quality of available water produced by a desalination facility located 50 km away from the mine. According to the design document, the maximum acceptable concentration of chloride in the process water was 250 mg/L.

The main objective of the desalination facility was to produce potable water with acceptable quality, according to the local regulations, for the nearby city. Since the desalination facility had unused capacity, it was agreed to sell a certain volume of the treated water surplus to the mine and other potential buyers. According to the local regulation, a high concentration of chloride is not an issue for drinking water, and the desalination facility, in part due to these less stringent regulations, is producing treated water with an average chloride concentration above 650 mg/L. The excessive chloride concentration combined with the low operating pH of the metallurgical process accelerates corrosion to the point that pipes and equipment need to be replaced frequently. This frequent equipment replacement increases the operating expense of the mine beyond the acceptable range.

It was therefore requested by mine management to investigate different feed water treatment options to produce water with acceptable chloride concentrations, prevent corrosion, and reduce operating costs.

This article reviews the mine's possible technology options along with financial challenges which affected the decision-making process.

Water Sources

Although desalinated water from the existing treatment facility was available, the mine management decided to investigate two other available water sources in the area. The available water sources were seawater from the South Atlantic Ocean and groundwater from the mine's surrounding area. Table 1 shows the typical quality of water from the city reservoir and underground sources. The average TDS of the Atlantic Ocean water for this study was assumed to be 39,000 mg/L.

Table 1: Raw water qualities

Item	Measure	City reservoir water (typical)	Underground water (typical)
pH	#	6.0–9.0	7.5
TDS	mg/L	1,000	13,083
Conductivity	mS/m	150	647
Turbidity	NTU	1.0	0.2
Sodium, Na+	mg/L	400	802
Calcium, Ca2+	mg/L	150	405
Magnesium, Mg2+	mg/L	70	91
Potassium, K+	mg/L	200	37
Chloride, Cl–	mg/L	600	1774
Nitrate, NO3–	mg/L N	10	3.4
Sulphate, SO42–	mg/L	200	591
Fluoride, F–	mg/L	1.5	0.2

Technology Selection

Since the main objective of the water treatment was to remove chloride ions only, technologies with the ability to selectively remove ions should be considered first. These technologies are basically precipitation methods and selective ion exchange systems (Metcalf and Eddy, 2013). Although it is not very wise to remove all ions when it is necessary to remove only one ion, some bulk ion removal technologies could be used for water with relatively low TDS. In this case, due to the relatively low TDS of the feed water, and the lack of a well-established commercialized method for removing chloride only, some multiple element removal methods were considered.

The main commercialized bulk ion removal technologies are Ion Exchange (IX), Reverse Osmosis (RO), and Evaporation (Kurniawan et al., 2006). In this case, evaporation was immediately eliminated due to power limitations and lack of steam on site. Therefore, only ion exchange and reverse osmosis were considered for the trade-off study.

In general ion exchange technology is not a good option for treating water with high TDS (Pinto et al., 2015). Due to the high TDS of both seawater and groundwater, the only potentially feasible

technology for water from these sources would be RO technology. As a result, it was decided to review reverse osmosis for all three different water types and limit the ion exchange option to the water from the desalination facility only.

In this study four different design options were considered to produce feed water with the desired quantity and quality for the mine:

- Option 1: RO fed by seawater
- Option 2: RO fed by groundwater
- Option 3: RO fed by surplus from the desalination plant
- Option 4: IX fed by surplus from the desalination plant followed by a small RO unit to recover water from the spent regeneration solution.

Table 2 presents a summary of the above-mentioned options.

Option Methods

Reverse Osmosis (RO) and Seawater

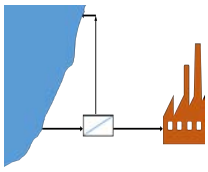
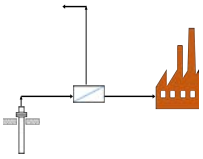
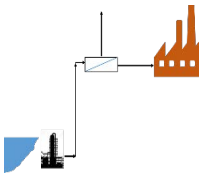
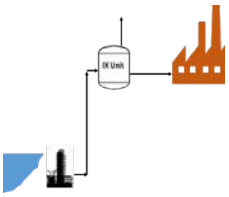
With the selection of seawater as the feed, it was necessary to use a special high pressure seawater membrane, which typically has a recovery of only 50%. The low efficiency of the membrane required high inflow water to meet the target water quantity. The excessive feed flow rate increased the size and energy consumption of the required feed pumps. The designed treatment facility required 432 pressure vessels with 8 elements per pressure vessel.

Due to the high feed volume, the number of required cartridge filters, the volume of injected acid, inhibitor, and all other pre-treatment reagents were increased significantly. In addition, to reduce suspended solids in the seawater, the design included a clarifier unit and flocculent package for pre-treatment, which was a unique unit operation for this option only.

Reverse Osmosis (RO) and Groundwater

The groundwater, despite its high TDS concentration, could be classified as brackish water. Therefore, a less expensive type of membrane with a lower operating pressure was selected for this option. Unlike the seawater option, the groundwater source has low suspended solids and so no clarifier or flocculent pre-treatment was necessary for this method. In addition, due to the high efficiency of the membrane and the possibility of mixing the treated water with bypassed water, the feed flow rate was reduced to 1600 m^3/hr and the treatment unit configuration was changed to 6 elements per pressure vessel with a total of 207 pressure vessels.

Table 2: Summary of investigated options

Name	Option 1: RO fed by seawater	Option 2: RO fed by groundwater	Option 3: RO fed by surplus from desalination plant	Option 4: IX fed by surplus from desalination plant
Source water	South Atlantic Ocean	Ground water	City reservoir water	City reservoir water
TDS of source water	TDS: 39,000 mg/L (Published data)	TDS: 13,083 mg/L (Average of reports)	TDS: 1,000 mg/L	TDS: 1,000 mg/L
Schematic				
Target/Goal In terms of chloride content	241 mg/L (Providing water with Chloride content of 250 mg/L or less)	227 mg/L (Providing water with Chloride content of 250 mg/L or less)	246 mg/L (Providing water with Chloride content of 250 mg/L or less)	250 mg/L (Providing water with Chloride content of 250 mg/L or less)
Required feed water to treatment system	3,000 m^3/hr	1,600 m^3/hr	1,400 m^3/hr	1,260 m^3/hr
Provided water flow rate	1,203 m^3/hr	1,253 m^3/hr	1,161 m^3/hr	1,200 m^3/hr
Recovery (%)	40	78	83	95

To increase the efficiency of the treatment unit, a reject staging system was used. The reject staging system is an Ro membrane system with different type of membrane and potentially higher operating pressure which use the reject stream from the original system as feed to separate more clean from the rejected stream. Addition of the reject staging system, which converted almost 390 m^3/h of the rejected volume to the permeate, had a significant effect on overall efficiency of the treatment system and reject volume reduction. In this method, a clarifier and flocculent were not required in the pre-treatment train and reagent consumption was reduced by almost 50%. A disadvantage of this method was that due to the underground water quality, adding sodium hypochlorite and sodium bisulphate to the pre-treatment operation became necessary. The significant reduction of the feed pump's size and energy consumption were some of the main advantages of this option compared to the previous option.

Reverse Osmosis (RO) and Reservoir Water

The water from the city reservoir had the lowest TDS concentration of all available water sources; therefore, it was the best feed for the RO membrane. Due to the high quality of the water, a tangible portion of the feed water (almost 33% of the permeate) could be mixed directly with treated water without exceeding the target chloride concentration.

The significant bypass flow rate had positive effects on the size of the membrane's pumps and overall energy consumption of the system. The bypass volume also allowed a reduction of the number of pressure vessels to 143 as well as a 30% reduction in the pre-treatment reagents.

Due to the high quality of the reservoir water, injection packages for sodium bisulphate and sodium hypochlorite were eliminated. Similar to the underground water option, a reject staging system was designed for this method to reduce the volume of rejected water and increase overall efficiency of the treatment facility.

Ion Exchange (IX) and Reservoir Water

The ion exchange option was designed based on using strong base anion (SBA) resin to remove chloride and other existing anions. The reason for selecting a high capacity SBA resin was the unavailability of a chloride selective resin. SBA, besides adsorbing chloride, adsorbs all other anions such as sulphate and nitrate based on their affinity to the resin (Dow Liquid Separations, 2018). The ion exchange design was completed based on the total available anions and their concentration in the reservoir water, which led to some additional volume for resin requirement.

Four modular units were designed to provide the required treated water in parallel. Each unit consisted of three identical columns operated on a merry-go-round circuit in a 12-hour cycle.

The regeneration solution (up to 50%) was recycled in the process to reduce reagent consumption as well as the volume of the waste stream. Due to the availability of sodium hydroxide on site, the hydroxide cycle was selected for the regeneration process. A small RO unit was also designed to concentrate the rejected solution and minimize the loss of water in the waste system.

Preliminary Options Screening

After technical review of the different treatment options, a conceptual economic evaluation at +/– 30% accuracy was developed for each option to estimate capital and operating costs, based on the major equipment costs only. At this level, the cost of construction and feed water were not considered. Table 3 shows a summary of estimated costs per options.

At this point a ranking system was developed to provide simple comparison method. In this ranking system, the numbers in a row of data was scaled between 0 and 10 by allocating score 10 to the highest

value in the row and score 0 to the lowest value. Then a raw score was calculated as the difference between calculated score and maximum possible score (10).

Table 3: Cost estimate summary

	RO and seawater	RO and groundwater	RO and reservoir water	IX and reservoir water
CAPEX				
CAPEX (CAD$)	18,560,233	12,842,217	8,134,745	8,893,492
Ranged Capital cost (out of 10)	10.0	4.5	0.0	0.7
Raw score	0.0	5.5	10.0	9.3
OPEX				
OPEX (CAD$/yr)	7,807,474	1,753,317	1,222,344	484,129
Ranged Operating cost (out of 10)	10.0	1.7	1.0	0.0
Raw score	0.0	8.3	9.0	10.0
ANNUAL TOTAL COST				
Interest (%/yr)	6.0	6.0	6.0	6.0
Plant life (yr)	25	25	25	25
Amortization factor	0.08	0.08	0.08	0.08
C (CAD$/yr)	9,259,380	2,757,922	1,858,698	1,179,838
Ranged total cost (out of 10)	10.0	2.0	0.8	0.0
Raw score	0.0	8.0	9.2	10.0
PRODUCT COST				
Product capacity (m^3/hr)	1,200.0	1,200.0	1,200.0	1,201.0
Product cost (CAD$/$m^3$)	0.88	0.26	0.18	0.11

Besides the economic factors, the mine management needed to make their final decision based on practical factors such as the availability of required electricity, skilled workers, and real estate as well as the complexity of the technology, constructability, and other site-specific factors.

The final decision in this case was supported by generating a decision-making matrix to cover all involved factors and their effect (weight) on the decision-making process. In the weight allocation system, the factors with poor effect had the lowest weight (0) and the most effective factor weight was indicated by number 10. Table 4 shows the developed decision-making matrix for the options

Table 1: Decision-making matrix

			RO and seawater		RO and groundwater		RO and reservoir water		IX and reservoir water	
"WANTS" – Desirable criteria		Weight	Raw score	Weighted score	Raw score	Weighted score	Raw score	Weighted score	Raw score	Weighted score
1	Complexity	5	3	15	5	25	5	25	7	35
2	Space constraints	5	3	15	5	25	5	25	4	20
3	Reliability	6	5	30	5	30	5	30	5	30
4	Constructability	5	5	25	5	25	5	25	5	25
5	Operability	8	4	32	5	40	5	40	6	48
6	Maintainability	8	5	40	5	40	5	40	6	48
7	Modularity	6	5	30	7	42	7	42	4	24
8	Project schedule	5	5	25	5	25	5	25	5	25
9	Waste stream management	5	3	15	4	20	5	25	5	25
10	Maturity of the technology	8	5	40	5	40	5	40	7	56
11	Staff safety measures	9	4	36	5	45	5	45	4	36
12	Skilled operators	8	4	32	5	40	5	40	8	64
13	Electricity requirement	7	5	35	5	35	5	35	7	49
14	Chemical requirement	7	4	28	5	35	5	35	3	21
15	Construction duration	5	3	15	6	30	6	30	5	25
16	Capital cost	5	0	0	5.5	27	10.0	50	9.3	46
17	Operating cost	5	0	0	8.3	41	9.0	45	10.0	50
Total weighted score:			**Option 1:**	**413**	**Option 2:**	**566**	**Option 3:**	**597**	**Option 4:**	**627**

The calculated total weighted scores in the decision-making matrix supported the idea that using RO for seawater and ground water were the least favourable options. On the other hand, the decision-making matrix indicated both ion exchange and reverse osmosis as viable options with water from the city reservoir. Based on the total weighted score from the decision-making matrix, ion exchange technology

with feed water from the city reservoir and sending rejected volume to the tailings pond was the best available option.

However, due to recycling of water from the metallurgical process tailings pond, the mine management decided to review different waste management alternatives to prevent potential changes in the quality of the water from the tailings pond.

The available waste management options in the area were ocean disposal, evaporation ponds, and a Zero Liquid Discharge (ZLD) system such as a combination of evaporation and crystallizer. The final stage of the process selection was completed by reviewing available waste disposal alternatives for both ion exchange and reverse osmosis technologies for treating water provided by the desalination facility.

Waste Management Alternatives

Ocean Disposal

It was assumed that the required environmental permissions would be granted to the mine without any limitation or additional levy. In addition, no special discharge facility in the certain depth of the ocean that required additional engineering design and construction effort was necessary. Also, it was assumed that the rejected water from both systems could be discharged to the ocean without additional processing. The major costs of ocean disposal were assumed to be the procurement of a discharge pump and construction of a pump station and waste transfer line from the mine site to the ocean. The ocean disposal alternative generally could be an attractive alternative when environmental regulations are not highly restricted.

Evaporation Pond Disposal

Solar (evaporation) ponds are another alternative of an ultimate disposal system that could be used in this environment. Generally, an evaporation pond is not an economically viable alternative if the net evaporation rate in the area is less than 500 mm per year (Nakoa et al., 2016). This “break-even point” could be modified based on actual site situations such as the existence of a natural pond area that eliminates excavation costs or strict environmental regulations. This alternative generally is not appropriate for humid coastal areas.

It was assumed that the required environmental permissions would be granted to the mine without any limitation or additional levy. The required surface area of the pond was calculated based on temperature profile, annual precipitation, and other available local meteorological information. The construction and lining of the pond was considered as the major capital cost, and the cost of pumping rejected water to the pond as the only tangible operating cost. Similar to the ocean disposal alternative, it was assumed that the rejected water from both systems could be discharged to the evaporation pond without additional processing.

Zero Liquid Discharge (ZLD) Disposal

The other ultimate disposal alternative is zero liquid discharge (Nakoa et al., 2016; Das, 2005). ZLD does not refer to a specific arrangement, but rather to a chain of selected units to convert the liquid waste stream to a solid or semi-solid waste stream. The proposed ZLD arrangement was a combination of evaporator and crystallizer. Since generating waste in the form of semi-solid (slush) was acceptable to the mine, the dryer (which is a very expensive unit) was eliminated from the proposed ZLD arrangements. The evaporator and crystallizer both could concentrate liquid streams. In theory, an evaporator should concentrate a stream up to the crystallization point but no single crystal should be generated (Treybal, 1955). In practice, however, the brine stream of an evaporator might contain up to 300 ppm crystals in the form of suspended solids. Evaporators are not designed to handle liquid streams containing crystals or slurries. It is a crystallizer that could concentrate the feed stream into a slurry with 20% (wt./wt.) or more crystal content (Treybal, 1955).

Table 2: Applicable range of TDS for ZLD technologies

Evaporator	25,000 <TDS < 300,000 mg
Crystallizer	TDS > 300,000 mg

Table 5 shows the operating TDS ranges for both an evaporator and a crystallizer. The main structure of the water treatment processes in options 3 and 4 must be verified to ensure the waste stream out of the treatment units were in the proper TDS range to meet the required feed quality for the evaporators. The preliminary review of the generated waste from the RO system indicated that the waste stream was not concentrated enough to be fed to the evaporator directly. To fulfill the feed requirement for the evaporator, a third stage RO unit was added to the previous 2-stage RO system for city reservoir water.

Evaporators and crystallizers are very expensive equipment, and an effort was made to minimize their feed flow rate. In this study, both units were chosen to be a “mixed salt” type with vertical falling film in the evaporation area. The evaporators and crystallizer chosen were limited to a mechanical vapour compression (MVC) type due to lack of steam on site.

For the ion exchange option, due to the existence of the small RO system on the waste stream in the original design, the generated waste stream (without additional unit) was suitable for direct feeding to the evaporator.

Disposal system

Table 6 summarizes the design basis of the two selected treatment options associated with three disposal alternatives considered in this study. It is important to mention that the use of the third stage of reverse

osmosis in the ZLD (evaporator and crystallizer) alternative had a direct effect on the waste stream flow rate.

Table 3: Design basis for reservoir water and proposed waste management alternatives

Disposal option	RO and reservoir water	IX and reservoir water
With: Ocean disposal	Required feed water: 1,300 m^3/hr Recovery: 92% Treated water: 1,200 m^3/hr Waste flow rate: 100 m^3/hr	Required feed water: 1,245 m^3/hr Recovery: 96% Treated water: 1,200 m^3/hr Waste flow rate: 45 m^3/hr
With: Evaporator + Crystallizer (ZLD)	Required feed water: 1,220 m^3/hr Recovery: 98% Treated water: 1,200 m^3/hr Waste flow rate: 20 m^3/hr	Required feed water: 1,203 m^3/hr Recovery: 99% Treated water: 1,200 m^3/hr Waste flow rate: 45 m^3/hr
With: Evaporation pond	Required feed water: 1,300 m^3/hr Recovery: 92% Treated water: 1,200 m^3/hr Waste flow rate: 100 m^3/hr	Required feed water: 1,245 m^3/hr Recovery: 96% Treated water: 1,200 m^3/hr Waste flow rate: 45 m^3/hr

Table 7 presents the calculated capital cost and operating cost of each treatment options plus proposed waste management alternative.

Table 4: Capex and Opex of treatment options and waste management alternatives

Disposal Option	Option 3 (RO)	Option 4 (IX)
With: Ocean disposal	CAPEX: 15,743,393 CAD OPEX: 1,053,663 CAD/yr	CAPEX: 12,406,650 CAD OPEX: 7,775,487 CAD/yr
With: Evaporator + Crystallizer	CAPEX: 21,785,029 CAD OPEX: 2,092,468 CAD/yr	CAPEX: 15,966,340 CAD OPEX: 8,016,405 CAD/yr
With: Evaporation pond	CAPEX: 29,632,070 CAD OPEX: 804,850 CAD/yr	CAPEX: 11,666,011 CAD OPEX: 7,707,232 CAD/yr

As shown in Table 7, the operating cost of the ZLD (evaporator and crystallizer) was the highest operating cost for both ion exchange and reverse osmosis treatment options. In general, the ion exchange technology was less sensitive than the RO technology to the variations of waste management alternatives. The main reason for the sensitivity of RO technology to the waste management alternative was the volume of generated waste by this technology. In the ZLD option, which had a low volume of waste, the capital and operating costs of the third stage membrane eliminated the potential advantage of the low waste flow rate. According to Table 7, both capital and operating costs of ion exchange options were lower than capital and operating costs of the RO options with the similar waste management alternatives.

The technical review also showed that the required feed water was varied by selecting different treatment options and waste management alternatives. Therefore, it was decided to apply the principles of net present value calculation to consider the effect of the volume of purchased feed water on the actual cost of treated water for different options.

The cost of produced water in Table 8 was calculated based on CAD 4.4/m^3 as the current price of water at the mine site with high chloride concentration. Based on the updated technical and economic evaluation with different waste management alternatives, the decision-making matrix for the mine was updated. Table 9 shows the updated decision-making matrix.

Table 5: Cost estimate summary with alternative waste management options and cost of feed water

	RO and ocean disposal	RO and pond disposal	RO and Evap and Crys.	IX and ocean disposal	IX and pond disposal	IX and Evap and Crys.
CAPEX						
CAPEX(CAD)	15,743,394	29,632,070	21,785,030	12,406,650	11,666,011	15,966,340
Ranged capital cost (out of 10)	2.3	10.0	5.6	0.4	0.0	2.4
Raw score	7.7	0.0	4.4	9.6	10.0	7.6
OPEX						
OPEX (CAD/yr)	51,661,936	51,413,123	49,603,531	56,242,640	56,174,385	54,863,121
Ranged operating cost (out of 10)	3.1	2.7	0.0	10.0	9.9	7.9
Raw score	6.9	7.3	10.0	0.0	0.1	2.1
ANNUAL TOTAL COST						
Interest (%/yr)	6.0	6.0	6.0	6.0	6.0	6.0
Plant life (yr)	25	25	25	25	25	25
Amortization factor	0.08	0.08	0.08	0.08	0.08	0.08
C (CAD/yr)	52,893,490	53,731,142	51,307,702	57,213,172	57,086,979	56,112,115
Cash for buying treated water (CAD/yr)	506,082,720	506,082,720	474,939,168	484,671,528	484,671,528	468,321,163
NPV	5,793,279,336	5,782,571,325	5,415,431,909	5,464,352,410	5,465,965,578	5,269,415,076
Ranged total cost (out of 10)	2.7	4.1	0.0	10.0	9.8	8.1
Raw Score	7.3	5.9	10.0	0.0	0.2	1.9
PRODUCT COST						
Product capacity (m^3/hr)	1,300	1,300	1,220	1,245	1,245	1,203
Product cost (CAD/m^3)	4.6	4.7	4.8	5.2	5.2	5.3

Table 6: Updated decision-making matrix

		RO and ocean disposal		RO and pond disposal		RO and Evap&Crys		IX and ocean disposal		IX and pond disposal		IX and Evap&Crys	
"WANTS" – Desirable criteria	**Weight**	**Raw score**	**Weighted score**	**Raw score**	**Weighted score**	**Raw score**	**Weighted score**	**Raw score**	**Weighted score**	**Raw score**	**Weighted score**	**Raw score**	**Weighted score**
Complexity	5	5	25	5	25	2	10	7	35	7	35	4	20
Space constraints	5	5	25	5	25	2	10	4	20	4	20	1	5
Reliability	6	5	30	5	30	3	18	5	30	5	30	3	18
Constructability	5	5	25	5	25	5	25	4	20	4	20	4	20
Operability	8	5	40	5	40	3	24	3	24	3	24	1	8
Maintainability	8	5	40	5	40	3	24	6	48	6	48	4	32
Modularity	6	7	42	7	42	6	36	4	24	4	24	3	18
Project schedule	5	5	25	5	25	3	15	5	25	5	25	3	15
Waste stream management	5	5	25	8	40	10	50	5	25	8	40	10	50
Maturity of the technology	8	5	40	5	40	5	40	7	56	7	56	7	56
Staff safety measures	9	5	45	5	45	5	45	4	36	4	36	4	36
Skilled operators	8	8	64	8	64	6	48	8	64	8	64	6	48
Electricity requirement	7	5	35	5	35	2	14	7	49	7	49	4	28
Chemical requirement	7	5	35	5	35	4	28	3	21	3	21	2	14
Construction duration	5	6	30	6	30	5	25	5	25	5	25	4	20
Capital cost	8	7.9	63	0.9	7	4.8	39	9.5	76	9.9	79	7.7	62
Operating cost	8	7.1	57	7.4	60	9.9	79	0.9	7	1.0	8	2.8	22
Total weighted score:		**Option 3:**	**646**	**Option 2:**	**608**	**Option 2:**	**530**	**Option 3:**	**585**	**Option 4:**	**604**	**Option 3:**	**472**

As the decision-making matrix shows, the best choice was treating the city reservoir water with RO technology associated with ocean disposal. The high score of the ocean disposal alternative was earned due to two assumptions: no environmental restrictions for discharging waste stream to the ocean, and no ocean discharge system design. As expected, the lowest scores in the decision-making matrix were related to the ZLD (evaporator and crystallizer) waste management alternative due not only to the high capital and operating costs of the units, but also to the complexity of the operation and skilled worker requirements. The overall outcomes of the evaporation pond alternative for both treatment options were very similar and no actual advantage could be defined between different treatment options with the evaporation pond alternative.

Conclusion

The required capital and operating costs of using seawater was high enough to eliminate the advantage of the free availability of the seawater. The water from the city desalination facility, due to the low TDS concentration, was the best available option for both reverse osmosis and ion exchange technologies.

Treating water from the city reservoir by ion exchange technology was selected as the best available choice if the generated waste could be disposed to the existing tailings pond. If the mine management decided to protect the tailings pond water quality by managing the waste or treatment facility separately, treating water from the city reservoir by reverse osmosis associated with disposing the waste stream to the ocean would be the best choice.

The study proved that a combination of evaporator and crystallizer as zero liquid discharge would be the least attractive waste management option, due not only to their capital-intensive nature, but also to their unit operation complexity and related technical issues.

Acknowledgements

The author would like to thank Mr. Mohammad Toghraei for his generous contribution to this study and for sharing his vast knowledge and experience of designing membrane systems with the design team. This work could not be completed without continued support, reviews, and comments from Mr. Fabrizio Stefani, Senior Project Manager in SGS-Bateman Engineering; Mr. Daniel Millar, Senior Process Engineer; and Mr. Alan Drake, Manager of Process Engineering, Mining and Metals in Wood PLC. The author would like to especially thank Mrs. Parisa Zaini for her time and invaluable comments during the review of the first draft of this paper.

References

Das, T.K. 2005. *Innovative Methodology and Technologies for Process Pollution Prevention.* Hoboken: J. Wiley.

Dow Liquid Separations. 2018. DOWEX Ion Exchange Resins, Fundamentals of ion Exchange. Retrieved from: http://www.dow.com/liquidseps

Kurniawan, T.A., Chan, G.Y.S., Lo, W.H. and Babel, S. 2006. Physico-chemical treatment techniques for wastewater laden with heavy metals, *Chemical Engineering Journal,* 1–2 (118): 83–98.

Metcalf and Eddy, Inc., Tchobanoglous, G., Stensel, H.D., Tsuchihashi, R. and Burton, F. 2013. *Wastewater Engineering: Treatment and Resource Recovery*. New York: McGraw Hill.

Nakoa, K., Rahaoui, K., Date A. and Akbarzadeh, A. 2016. Sustainable Zero Liquid Discharge Desalination (SZLDD), *Solar Energy,* 1(135): 337–347.

Pinto P.X., Al-Abed, S., Balz, D., Butler, B., Landy, R. and Smith, S. 2015. Bench-scale and pilot-scale treatment technologies for the removal of total dissolved solids from coal mine water, *Mine Water and the Environment,* 1(35): 94–112.

Treybal, R.E. 1955. *Mass-Transfer Operations.* New York: McGraw-Hill Education.

Proceedings of Mine Water Solutions 2018
June 12–15, 2018, Vancouver, Canada
Published by the University of British Columbia, 2018

Application of SAGR Bioreactors for Ammonia Treatment in Mining Effluents

Michael Bratty, Golder Associates Ltd., Canada
Alessandro Di Biase, University of Manitoba, Canada
Victor Wei, University of Manitoba, Canada
Martin Hildebrand, Nexom, Canada
Jan A. Oleszkiewicz, University of Manitoba, Canada

Abstract

Ammonia treatment is a growing concern in the mining industry. Ammonia is commonly found in mining effluents as a by-product of cyanide degradation, and as a residual of blasting compounds. This paper explores the application of the Submerged Attached Growth Reactor (SAGR) in mining effluents, in particular in cold climates, exploring the fundamental principles and related experience from other sectors. The SAGR under construction at the subject site of this paper will be the first implementation of this technology in a mining context.

Introduction

Ammonia management is an increasing concern in the mining industry. Ammonia is a nutrient, and may promote algal growth in receiving waters, and lead to the loss of dissolved oxygen. Ammonia is also extremely toxic to aquatic life in the non-ionized form (free ammonia), so target concentrations in receiving water are low. For example, in Canada, the un-ionized ammonia concentration for the protection of freshwater aquatic life is only 0.019 mg/L (CCME, 2001).

Historically, many mines have relied on natural degradation for the management of ammonia; however, space limitations and new regulations are motivating changes to past practices. Natural degradation can take place through volatilization of ammonia at high pH, or through nitrification, or through uptake by aquatic plants, including microalgae. Researchers have noted that natural degradation of ammonia can be poor in gold mill tailings ponds, where metals and metal complexes can be present that are toxic to algae and other microorganisms, but polishing ponds, where metals are low, are important contributors to ammonia removal (Martel and Bocking, 2003).

In Canada, new Metal Mine Effluent Regulations (MMER) are currently in the first reading stage of the legislative process, and are anticipated to be enforced in 2021 (Canada Gazette, 2017). New regulations can mean stricter operational limits for metal mines for total ammonia nitrogen (TAN). As a result of decreasing reliance on natural degradation and increasing regulation, some mines are facing a need for new ammonia management strategies.

Recently, Golder Associates Ltd. carried out an evaluation of technologies that are applicable to treatment of ammonia-rich minewaters at an operating gold mine in the Canadian Shield. Ammonia is present in minewaters as a by-product of the use of blasting compounds, and as a residual of cyanidation, cyanide destruction, and hydrolysis of cyanate. Two water sources at the mine were considered:

- The supernatant of the tailings storage facility (TSF), containing up to 190 TAN (average 133 for 2012–2017) and up to 22 mg/L dissolved copper at pH 8-9 and temperatures between 1°C (winter) and 15°C (summer). The relatively high levels of dissolved Cu indicate the possible presence of complexing cyanide species. The TSF water also contained 20–30 mg/L cyanate, and 130 mg/L thiocyanate.
- A historic, flooded pit, with TAN levels of 30–60 mg/L and copper of 0.2 mg/L, and temperatures consistently 8°C at depth, and up to 15°C in surface waters in summer. The pit water contained only negligible levels of cyanate and thiocyanate.

At the subject site, the TAN target for effluent is 10 mg/L, but the effluent must also be non-acutely toxic, so a target of <1 mg/L TAN is also considered.

The evaluation included both established and emerging technologies, with a focus on suitability for treatment of cold waters. The evaluation included the following options: natural degradation, Moving Bed Bioreactor (MBBR), struvite formation through electrocoagulation, breakpoint chlorination, air stripping, ion exchange (with several sub-alternatives for brine handling), and the Submerged Attached Growth Reactor (SAGR). The evaluation considered two water sources: the tailing pond reclaim (TSF water), and a flooded pit. An existing MBBR has been operational for a number of years, but operational difficulties meant that additional treatment capacity was required. The existing MBBR has been treating water from underground, which contains relatively low levels of ammonia, and which has a warm temperature (15–25°C). Since the MBBR was a known technology for the mine owners, consideration was given to the benefits of expanding the system.

The main findings of the evaluation were:

- Natural degradation is the lowest cost option, but insufficient land area is available to construct new water holding ponds at the subject site at this time. Natural degradation is inhibited in the existing TSF, likely due to the presence of elevated copper, which is toxic to the algae and other

microorganisms that accelerate Natural Degradation. Consideration was given to a floating baffle system and pre-treatment process, within the TSF, to remove copper and encourage natural degradation. Such a system could seasonally reduce the load on other ammonia treatment systems.

- MBBR technology was the preferred option for warm waters (greater than 15°C), due to a small footprint, and familiarity of the technology to site staff. However for colder waters, the MBBR option was more costly, mainly due to the cost of heating the feed water.
- The electrocoagulation/struvite process had a relatively high capital cost for electrocells; the operating cost was dominated by the costs of power and added phosphorous.
- The SAGR technology was selected for construction due to lowest capital and operating cost for cold waters.

At the site used in the case study, the net present capital and operating costs (NPC) over the project lifespan are summarized in Table 1, based on treating an anticipated effluent volume of 2M m^3, made up of a combination of 50% pit water and 50% TSF water. The NPC are listed as a multiple of the NPC of the SAGR technology and are conducted at a level of detail sufficient to select among options. The operating cost of the MBBR includes an allowance to heat the feed water by 10°C, on average, using fuel oil in a submerged combustion process. Without heating expenditures, the operating cost of the MBBR and the SAGR were comparable. The two are comparable biological nitrification processes. Heating costs are expected to be one of the main differentiators between the MBBR and SAGR technologies in cold climates.

Table 1: Net present capital and operating cost factors for subject site

Technology	Net present cost factor
SAGR	1.0
MBBR	1.5
Struvite formation with electrocoagulation	2.6
Breakpoint chlorination	3.1
Ion exchange with electroreduction	6.2
Natural degradation with floating baffles	0.4

The tailing storage facility water (reclaim) at the subject site also contains thiocyanate. Thiocyanate is known to be degraded in nitrifying systems (Given and Meyer, 1998; Tanabene et al., 2018), and more work is planned to determine the kinetics of thiocyanate degradation in the SAGR technology. Thiocyanate degradation is believed to be a source of alkalinity for the nitrification reaction, reducing added inputs.

SAGR Technology

The submerged attached growth reactor was developed by Nexom (Winnipeg, Canada). Nexom was formerly known as Nelson Environmental, founded in 1997. Nexom has completed approximately forty installations of the SAGR in North America in municipal and industrial treatment applications. The subject site will be the first implementation of the SAGR in a mining context. The submerged attached growth reactor concept is illustrated in Figure 1. Key elements of this system as applied to the subject site are:

- Pre-treatment for metals and cyanide reduction (e.g. including weak acid dissociable WAD cyanide oxidation and trace metals removal).
- Rock bed fixed-film nitrifying bioreactor, supplemented with phosphorous and alkalinity to maintain bacterial growth (as per typical ratios required).
- Wood chip cover, to retain heat while allowing the release of blower off-gasses from the bed.
- Blower for aeration of bed to provide the oxygen needs for nitrification.
- A recycle pump, if necessary, diluting feed with effluent (not shown).
- The rock mass that forms the media provides not only surface area for attached growth, but also a thermal buffer to reduce temperature shocks to nitrifiers.
- Operations demonstrated to maintain nitrification at temperature as low as 1°C in municipal and industrial applications.

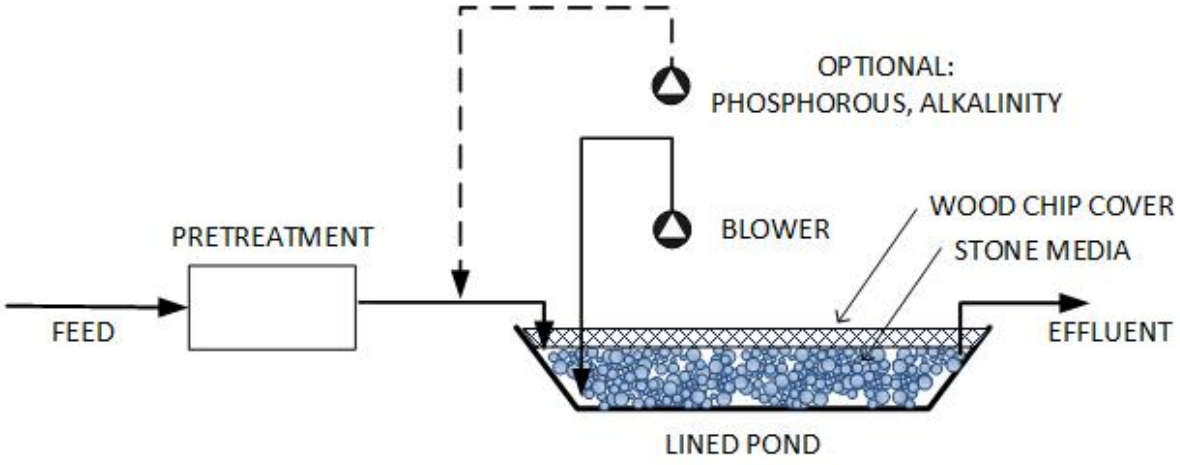


Figure 1: SAGR concept for mine water treatment

At the subject mine, an existing pond is being converted for use as a SAGR bed, with consequent cost savings. Figure 2 shows the mine water pond prior to conversion at the subject site. The project is under construction at the time of writing, and will be started up in June 2018 with an initial capacity of 5,300 m^3/d.



Figure 2: Converting an existing mine water pond to a SAGR

The SAGR uses the same biochemical nitrification process as the moving bed bioreactor (MBBR) technology, but in a semi-plug flow concept as opposed to a continuous stirred tank reactor (CSTR). The plug flow reactor concept can be modified for a SAGR by using a recycle pump, that is, by pumping effluent from the SAGR to an inlet pond or feed distributor structure. Due to the inherent nature of these systems, a plug flow reactor is less resistant to feed toxicity compared to a CSTR, but is better able to meet consistently lower effluent targets.

Cold Water Operation

A distinguishing feature of the SAGR, demonstrated in municipal tertiary treatment wastewater applications, is its capability in obtaining excellent and reliable performance at temperatures reported to be as low as 1°C, with minimal operator supervision. The submerged attached growth reactor is typically inoculated and established in the summer season with warm water. Attached growth nitrifying biomass is encouraged to grow on the media rock-bed. Then, as the water temperature drops in the fall season, the media bed acts as a thermal buffer to reduce the temperature shock. Lower temperatures reduce the activity of the nitrifying biomass, but the large media bed and large attached growth inventory of biomass continues to nitrify, albeit at a lower rate. Since the media bed is sized for the lower rates of nitrification, the SAGR continues to meet effluent ammonia targets even at low temperatures.

Pilot Testing

Objectives

The mine owner elected to conduct a pilot trial prior to implementation of the SAGR at the subject site. The pilot trail was carried out over more than 47 days, at a room temperature of 18–19°C (work is ongoing at the time of writing). The pilot trial was not intended to provide design data for operations; rather, the design basis for construction was developed from Nexom's database of projects at a variety of temperature conditions.

The goals of the pilot trail were divided into Phase 1 and Phase 2 as follows:

Phase 1

- Confirm the treatability of the two water sources, complete with pre-treatment for cyanide oxidation and copper removal.
- Produce effluent samples for toxicity testing.
- Elucidate the kinetics of cyanate hydrolysis in the aerated gravel bed with nitrifiers biofilm present.

Phase 2

- Measure change in performance at lower temperatures.
- Measure thiocyanate oxidation in the aerated gravel bed for the TSF water source.

Only Phase 1 is reported in this paper.

Materials and Methods

A series of six 1 m tall benchtop pilot-scale SAGR reactors were set up in the laboratory. The samples were shipped from the mine from three different sources:

1. tailings thickener overflow (representing the input water quality to the TSF);
2. tailings reclaim (representing the outflow from the TSF) and;
3. historic pit water source.

The samples were stored at room temperature in Nexom's warehouse. The reactors were filled with a pea gravel media and aerated with small air pumps. The columns were foil-covered to prevent the influence of UV degradation. Due to the presence of cyanide complexes in some of the feed samples, the off-gasses were collected in caustic-filled stripping columns. The pH of the feed was adjusted to 7.0, and phosphate was added at a rate of 2–3 mg/L as PO_4-P.

The columns were inoculated with a ratio of working volume (0.5 L) to seed volume of 0.4 with wasted activated sludge from the west end water pollution control centre (Winnipeg, Canada). The

hydraulic retention time (HRT) of these columns varied between 0.4 and 2.4 days, based on the void space of the media.

The feed and effluent samples were assayed for ammonia, nitrite, nitrate, and phosphorous every two to three days per week using flow injection analyser (FIA, Lachat QuikChem). Cyanate was indirectly determined by ammonia concentration analysis on FIA. The method was comprised of: sample acidification to below 2 pH, digestion at 95°C for 1 hour, and pH adjustment to 7. Difference between the sample digested and undigested was calculated being the cyanate concentration.

Results and Discussion

Influent Water Variability

The influent water quality for the Pit water and the TSF water samples is illustrated in Figures 3 and 4 respectively. The tailing storage facility water was represented by two samples, taken from different parts of the circuit, so a range of feed ammonia concentrations represents some of the variability in the water source.

The Pit water quality was represented by a single sample. The nitrite in the sample rose slightly over the course of the work, and the ammonia dropped, which indicates that some partial nitrification was occurring in the influent storage vessels. The tailing storage facility water did not show evidence of nitrification, which could be attributed to free ammonia and/or copper toxicity to nitrifiers in the barrels.

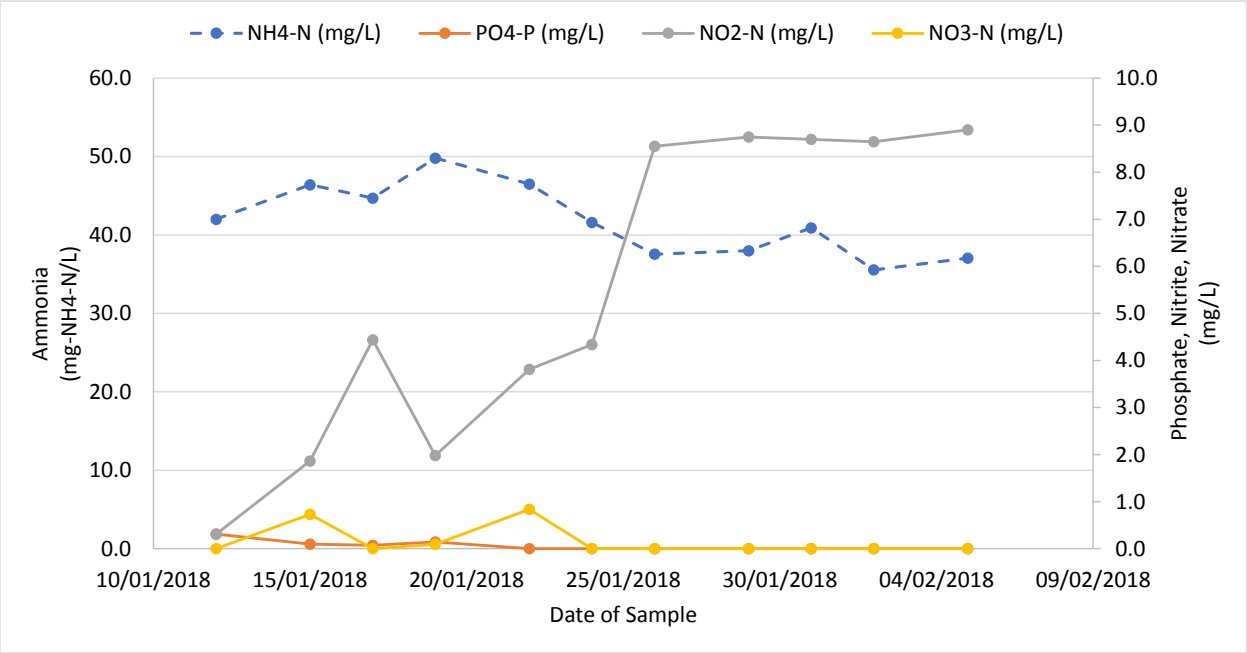


Figure 3: Influent trend for Pit water

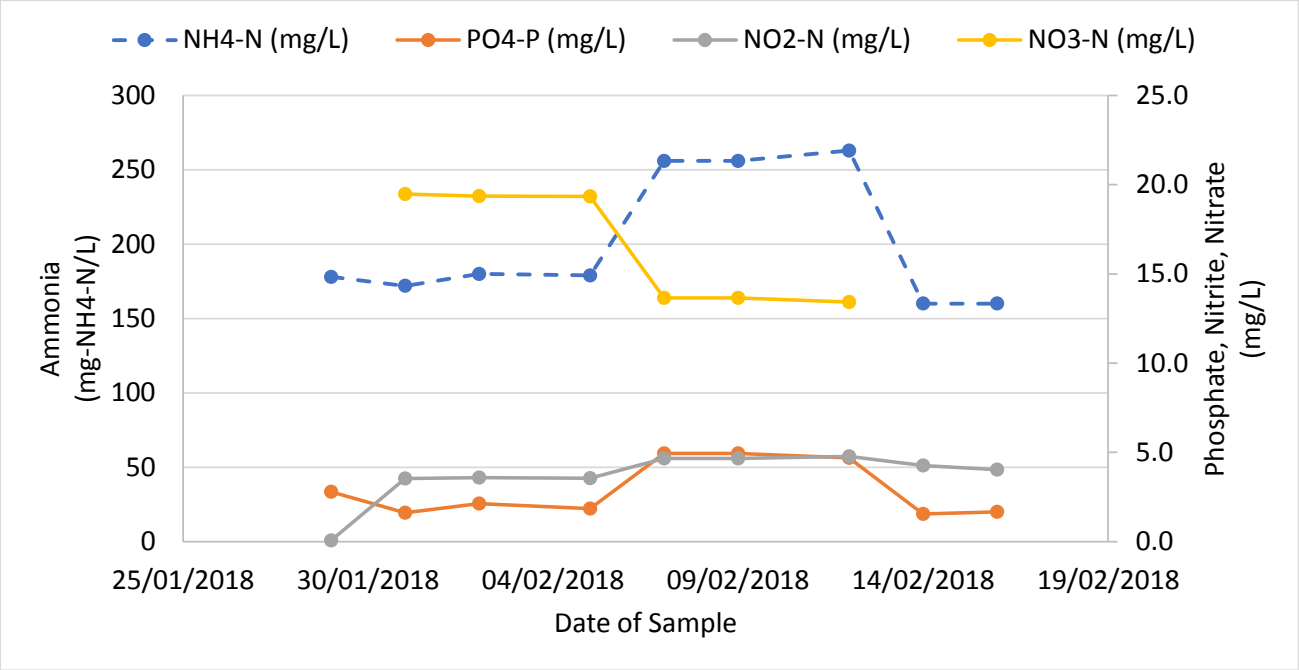


Figure 4: Influent trend for TSF sample

Effluent Quality

The effluent water quality for the Pit water and the TSF water samples is illustrated in Figures 5 and 6, respectively. The columns receiving Pit water showed a rapid onset of nitrification, so levels of ammonia and nitrite in the effluent were below target values within 5 days from start-up. The hydraulic retention time (HRT) of these columns varied between 0.4 and 0.7 days, without any measurable effect on the effluent ammonia or nitrite. Therefore, the columns were not operated at the limit of the potential performance at room temperature. Operations at cold temperature are ongoing and therefore no results are shown.

In the case of the TSF water, the columns were exposed to a series of conditions: initially the TSF water was fed without pre-treatment and without dilution. The ammonia levels were inhibitory to the nitrifying microorganisms, as was the copper level. The concentration of unionized ammonia was measured at a level that is associated with toxic effects on nitrifiers (Anthonisen et al., 1976). Subsequently, the TSF water was blended with the Pit water at a ratio of 1:1.4. After this change was made, the modified column showed rapid development of nitrification.

Effluent Quality – With Cyanate Spike

A test was carried out using a column that was initially acclimatized to the Pit water, then fed a combination of Pit water and cyanate. The hydraulic retention times varied between 1.1 and 2.4 days. Cyanate was spiked to the feed water at concentration of 15 mg-CNO-N/L as nitrogen. Cyanate will

spontaneously hydrolyze to ammonia and carbonate, as shown below in equation 1, and the rate of reaction is dependent on pH, temperature, and other factors.

$$CNO^- + 2H_2O \Rightarrow NH_3 + HCO_3^- \qquad \text{Equation 1}$$

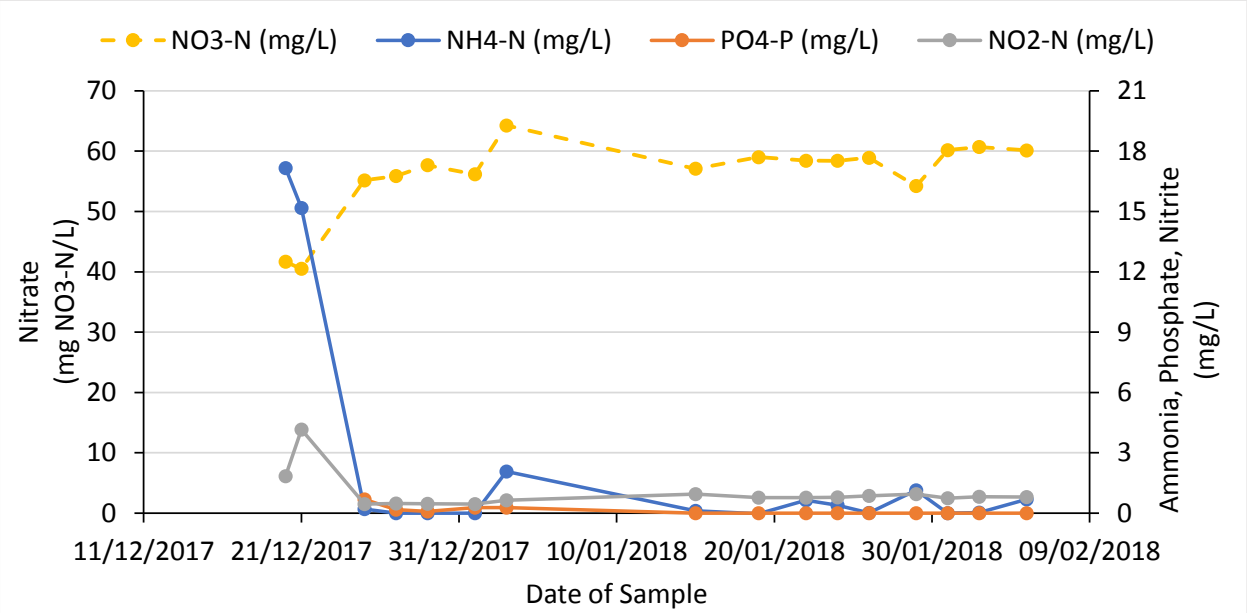


Figure 5: Effluent trend for Pit water

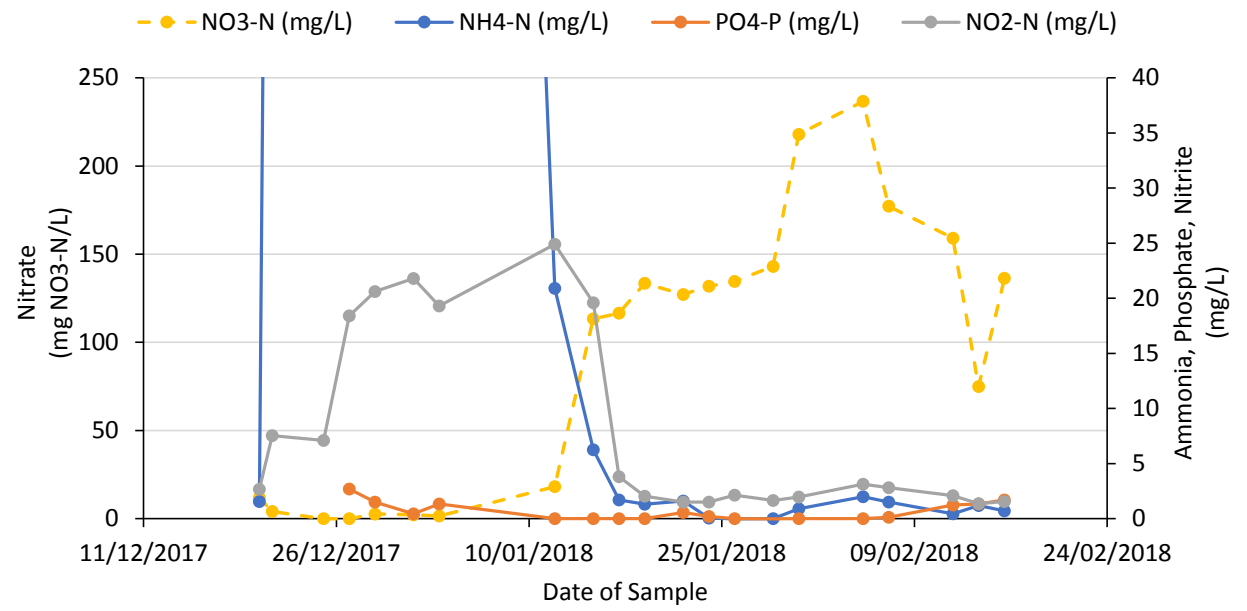


Figure 6: Effluent trend for TSF water

The goal of the cyanate spike test was to determine the fate of cyanate in the column at pH 7 within the time frame of typical HRT in SAGR beds. More work is planned as Phase 2 to refine the

understanding of cyanate behaviour. Reported rates of cyanate hydrolysis in the literature are highly variable, with abiotic degradation rates lower than biotic ones (Palatinszky et al., 2015). The results are illustrated in Figures 7 and 8. Figure 7 shows that after a period of acclimatization, the column adapted to the spike and was able to fully nitrify influent nitrogen and the nitrogen added as cyanate. Figure 8 illustrates the mass balance for inorganic nitrogen for both influent and effluent. Abiotic hydrolysis rates are expected to be significantly longer than the rates of cyanate removal inferred by Figure 8.

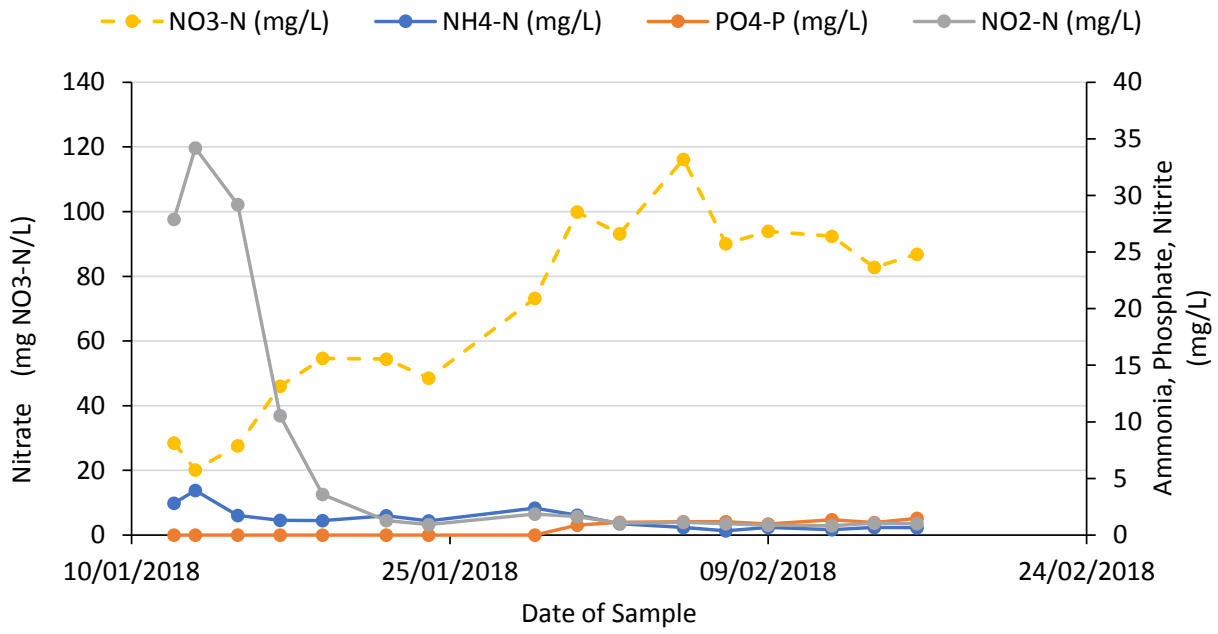


Figure 7: Effluent trend of Pit water with cyanate spike

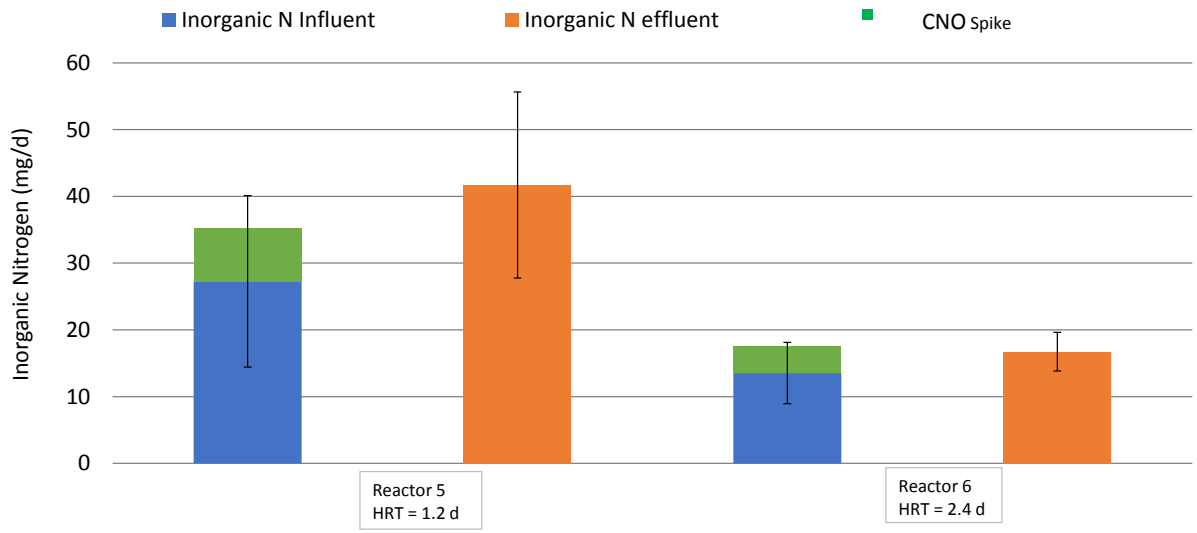


Figure 8: Nitrogen balance, with CNO spike

Conclusion

An alternatives analysis for new ammonia management systems was carried out at an active gold mine in the Canadian Shield. A range of seven options was considered, including both proven and emerging technologies. Natural degradation is a proven option for ammonia management at mine sites around the world, but space limitations, and potentially stricter effluent limits for total ammonia nitrogen, mean other options must be considered. The submerged attached growth reactor (SAGR) technology was selected for the subject site based on a wide range of experience in cold influent water in municipal and industrial applications. The SAGR uses the same biochemical nitrification process as the moving bed bioreactor (MBBR) technology, but in a semi-plug flow concept as opposed to a continuous stirred tank. The project is under construction at the time of writing, and will be started up in June 2018 at an initial capacity of 5,300 m^3/d. The SAGR was estimated to be 33% lower in cost compared to MBBR, a more conventional technology. The cost savings were mainly due to lower capital costs and the reported ability of the SAGR to operate reliably at influent water temperatures as low as 1°C, eliminating the need to heat the water. The submerged attached growth reactor is reported to operate well in cold water due to development of a large inventory of biomass on the media. Other ammonia management options were more expensive under the conditions of the subject site.

A bench-scale pilot plant was instigated to demonstrate the treatability of two water sources from the subject site: the tailings storage facility reclaim water, containing up to 190 mg/L TAN along with up to 22 mg/L dissolved copper, and the excess water in a historic open pit, containing up to 60 mg NH_4-N/L. The Pit water was rapidly nitrified with only five days start-up using inoculum from a municipal treatment system. The Pit water did not require pre-treatment. The tailing storage facility water showed evidence of toxicity to nitrifiers, and this is supported by observations of low rates of natural degradation of ammonia in the TSF water on the site. However, with management of unionized ammonia concentrations and pre-treatment of the influent water for copper removal, the TSF water was successfully treated with SAGR technology. Cyanate spiked to the columns was oxidized to nitrate within less than 1.2 days hydraulic retention time at pH 7 and at room temperature.

More work is planned to test the SAGR at lower temperatures, and to further elucidate the behaviour of cyanate. The tailing storage facility water at the subject site also contains thiocyanate. Thiocyanate can be degraded in nitrifying systems and more work is planned to determine the kinetics of thiocyanate degradation in the SAGR technology.

Acknowledgements

The authors gratefully acknowledge the support of the mining company that instigated this work and supported this paper, and all our colleagues and coworkers who have supported elements of this work, including: Marie-Pier Ross-Pilon of Golder Associates in Montreal, Marcus Yu of Golder Associates in Vancouver, and Maciej Kowalski at the University of Manitoba.

References

Anthonisen, A.C., Loehr, R.C., Prakasam, T.B. and Srinath, E.G. 1976. Inhibition of nitrification by ammonia and nitrous acid, *J Water Pollut Control Fed*. 48(5): 835–52.

Canada Gazette. 2017. Vol. 151, no. 19, May 13, 2017. Retrieved January 2018 from: http://www.gazette.gc.ca/rp-pr/p1/2017/2017-05-13/html/reg2-eng.html

CCME (Canadian Council of Ministers of the Environment). 2001. Guideline for the protection of aquatic life. Retrieved from: http://st-ts.ccme.ca/en/index.html?chems=5,6&chapters=1

Given, B. and Meyer, S. 1998. Biological treatment of tailings solution at the Nickel Plate Mine, *Proceedings of the 22nd Annual British Columbia, Mine Reclamation Symposium,* Penticton BC, Canada.

Martel, R.L. and Bocking, K.A. 2003. Water management and the use of natural degradation in a gold mine tailings management facility, *Sudbury 2003 Conference Presentation Mining and the Environment,* May 25, 2003.

Palatinszky, M., Herbold, C., Jehmlich, N., Pogoda, M., Han, P., von Bergen, M., Lagkouvardos, I., Karst, S.M., Galushko, A., Koch, H., Berry, D., Daims, H. and Wagner, M. 2015. Cyanate as an energy source for nitrifiers, *Nature*, 254(6).

Tanabene, R., Genty, T., Gonzales-Merchan, C., Bussiere, B., Potvin, R. and Neculita, C.M. 2018. Nitrification-denitrification of thiocyanate, ammonia, and nitrates in highly contaminated gold mine effluents using methanol as energy source, *J. Envir. Eng.* 144(5).

Proceedings of Mine Water Solutions 2018
June 12–15, 2018, Vancouver, Canada
Published by the University of British Columbia, 2018

Incorporating Climate Variability into Water Balance Modelling to Help Inform Water Management Design: The Pebble Mine Project

Alana Shewan, Knight Piésold Ltd., Canada
Jaime Cathcart, Knight Piésold Ltd., Canada

Abstract

Water plays a key role in the operation of mining projects, and it is essential that water management facilities be designed to manage the inflows and outflows required for proper operations, as well as accommodate any unpredictable runoff resulting from storms events. The amount of water available varies by year, season, and day, so how do you design for this? Establishing a predictive water balance model during the mine design stage is one of the most important considerations for minimizing water management problems during the operation and closure stages for a project. The water balance model needs to simulate mine operations under normal climate conditions and also under unusually wet and dry periods of varying durations. Key water management planning may be driven by the spring melt of a winter snowpack in cold regions, the variation in snowpack accumulation, and the timing of the freshet season.

The current industry standard for introducing climate variability into water balance modelling is to model monthly precipitation values as distributions, which are typically based on the mean and standard deviation values of historical monthly precipitation. The water balance model is then run for thousands of iterations using Monte Carlo simulation techniques to produce a large range of potential precipitation conditions and corresponding results. This procedure is effective, but it has a major shortcoming in that it simulates precipitation in every month as being completely independent of precipitation in any proceeding or following month. Areas that experience strong climate cycles resulting in extended dry or wet periods may not be correctly represented by this type of modelling.

This paper presents a case study for the proposed Pebble Mine project (Pebble) in Alaska and highlights the importance of a climate variable water balance model for informing the water management plan and design. The Pebble water balance model utilizes a 68-year monthly time-series of temperature and precipitation that was developed using a long-term regional dataset in combination with the extensive hydrometeorological dataset collected for Pebble. The time-series data were stepped through the model

incrementally by year for the planned life of the project, thereby preserving the inherently cyclical nature of the climate record including wet and dry cycles, while creating 68 unique sets of water balance results for each month of each year of the project. The results were used to develop a robust water management strategy that supplies sufficient water to maintain full mine operations, even during prolonged dry periods, and maintains downstream flow requirements for aquatic habitat and resources.

Introduction

The annual runoff pattern in south-central Alaska is dependent on both the annual precipitation pattern and seasonal temperature variations. It is typically represented as a bimodal hydrograph, with high flows during the spring and fall, and low flows during the winter and summer. The high flows in the spring are largely due to snowmelt, while those during the fall are largely due to rainstorms. The magnitude and timing of the spring freshet flows are driven by the accumulation of winter snowpack and the temperature variation of the spring season. Low flows are largely supplied by groundwater discharge, since surface water is largely trapped in snow and ice during the winter, and is scarce due to evaporation and low rainfall during the summer.

Long-term climate records have shown variability in temperatures, not only from year to year but also on multi-year and multi-decadal scales. The patterns of temperature variability are strongly correlated to oceanic temperatures and atmospheric settings in the Pacific Ocean, which most notably are the El Niño Southern Oscillation (ENSO) and the Pacific Decadal Oscillation (PDO) systems (Shulski and Mogil, 2009). Warm and cold phases of the ENSO cycle typically last for several months every two to four years (Papineau, 2001) while the PDO phases tend to shift on a multi-decadal scale (Wendler and Moore, 2012). In 1976 the PDO underwent a dramatic shift from a predominately negative phase to a predominantly positive phase. The climate post-PDO-shift resulted in warmer temperatures and increased precipitation compared to the climate before the PDO-shift (Hartmann and Wendler, 2005).

The air circulation over Alaska is driven by the ENSO and PDO systems, therefore, the climatic conditions at Pebble tend to be relatively wet and warm, or cold and dry, depending on the phases of these systems. The large variation in seasonal, yearly, multi-year, and multi-decadal climate and runoff patterns presents a challenge for water management planning. Accurately predicting climate trends and cycles is not possible (Wendler et al., 2017), but the large range of potential conditions can be modelled using historical data. A water balance model that captures the inherently cyclical nature of the historic climate record is a useful design tool for minimizing the potential for water management problem to occur during the operation and closure stages of a project.

Background: The Pebble Project

The proposed Pebble project is the world's largest known undeveloped copper and gold resource. It is located in southwest Alaska, approximately 200 miles (322 km) southwest of Anchorage and approximately 20 miles (30 km) west of the communities of Iliamna, Newhalen, and Nondalton (Figure 1). Pebble is proposed to be a conventional drill, blast, truck, and shovel operation with a mining rate of up to 90 million tons per year (82 million tonnes per year). The project has a proposed 20-year operating mine life with a total of 1.2 billion tons (1.1 billion tonnes) of material mined (PLP, 2017). The developed mine site will include an open pit, a tailings storage facility (TSF), a power plant, water treatment plants, milling/processing facilities, and supporting infrastructure (Figure 2). Plans for the design and operation of Pebble have focused on the avoidance and minimization of environmental impacts to waterbodies, wetlands, wildlife and aquatic habitat, and areas of cultural significances. The mine layout has been minimized by locating the majority of the site infrastructure in one watershed – that of the North Fork Koktuli River (NFK).



Source: (PLP 2017)

Figure 1: Pebble project location

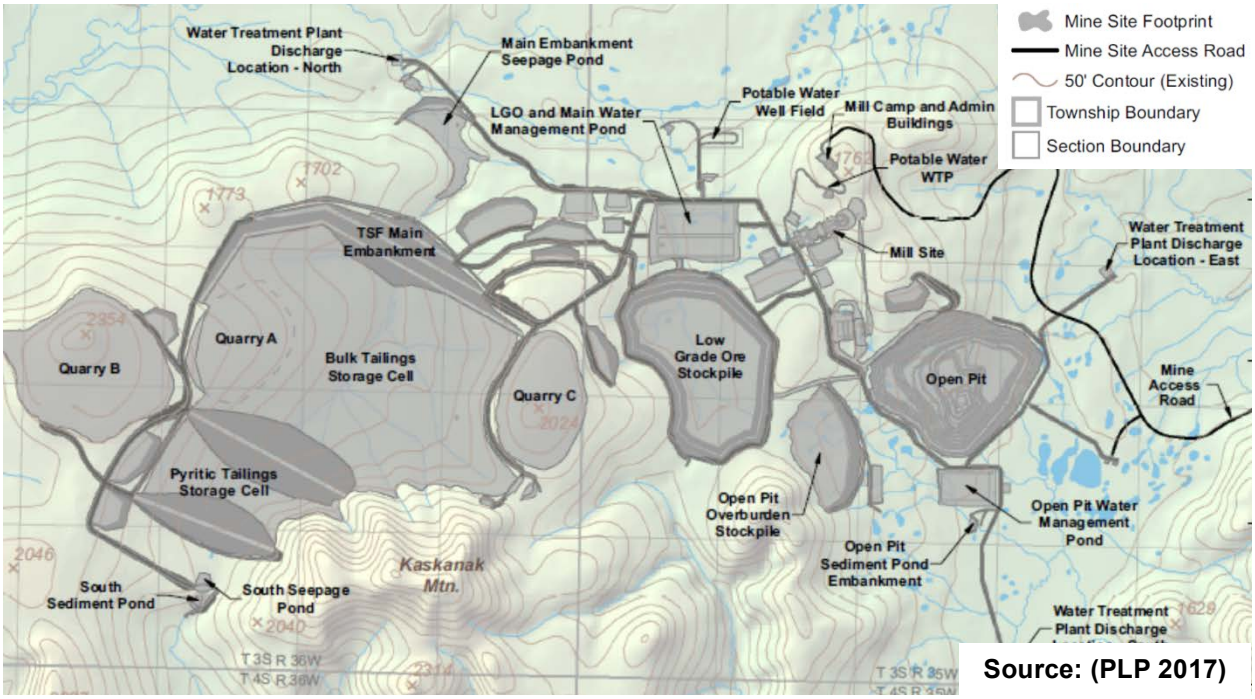


Figure 2: Mine site layout

Hydrometeorology at Pebble

The climate of Pebble is classified as maritime continental, with summer temperatures moderated by the open waters of the Bering Sea and Cook Inlet, and winter temperatures influenced by the presence of sea ice in Bristol Bay during the coldest months of the year (KP, 2012). Mean monthly temperatures range from about 55°F (13°C) in the summer to about 2°F (–17°C) in the winter (PLP, 2017). The Mean Annual Precipitation (MAP) in the NFK drainage is approximately 57 inches (1,450 mm) and in the South Fork Koktuli River (SFK) drainage is approximately 51 inches (1,300 mm). About one-third of this precipitation falls as snow (KP, 2012).

Climate Variability

Long-term temperature and precipitation estimates were developed for Pebble on the basis of 5 years of data collected in the mine area and 68 years of data collected by the US Weather Service at the nearby (~20 miles away) airport at Iliamna. Streamflows were collected at 26 stream gauging stations in the NFK, SFK and Upper Talarik (UT) watersheds, of which 3 are operated by the USGS; these watersheds are shown on Figure 3 (KP, 2012).

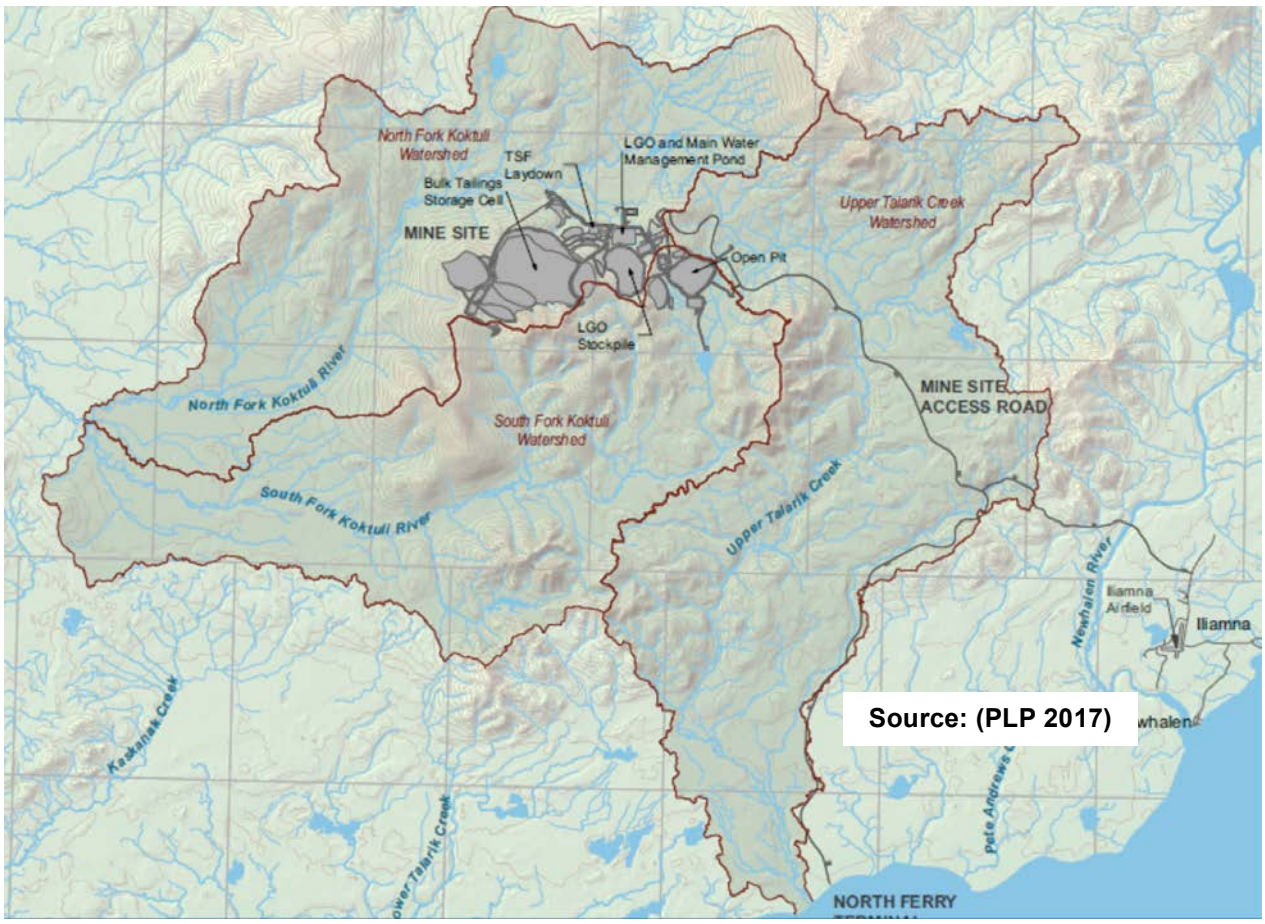


Figure 3: Pebble watersheds

Precipitation at Pebble is very difficult to accurately measure because of consistently strong wind conditions and the associated precipitation gauge under-catch. A watershed model, which was calibrated to the extensive stream flow and groundwater level dataset, was used as the primary basis for developing the precipitation estimates at Pebble (Cathcart and Smith, 2013).

The long-term annual average temperatures and annual total precipitation estimates for Pebble are shown in Figures 4 and 5, respectively. The average annual temperature is estimated to be 30°F (–1°C); however, the warmest annual average temperature is 35°F (2°C) in 1978, while the coldest annual average temperature is 24°F (–4°C) in 1956.

The average annual precipitation is estimated to be approximately 57 in. (1,300 mm), while the driest year on record, 1968, had a total precipitation of 33 in. (833 mm), and the wettest year, 1971, had a total precipitation of 98 in. (2,490 mm). Figures 6 and 7 demonstrate the year-to-year and multi-decadal climate variability that has been historically observed at Pebble.

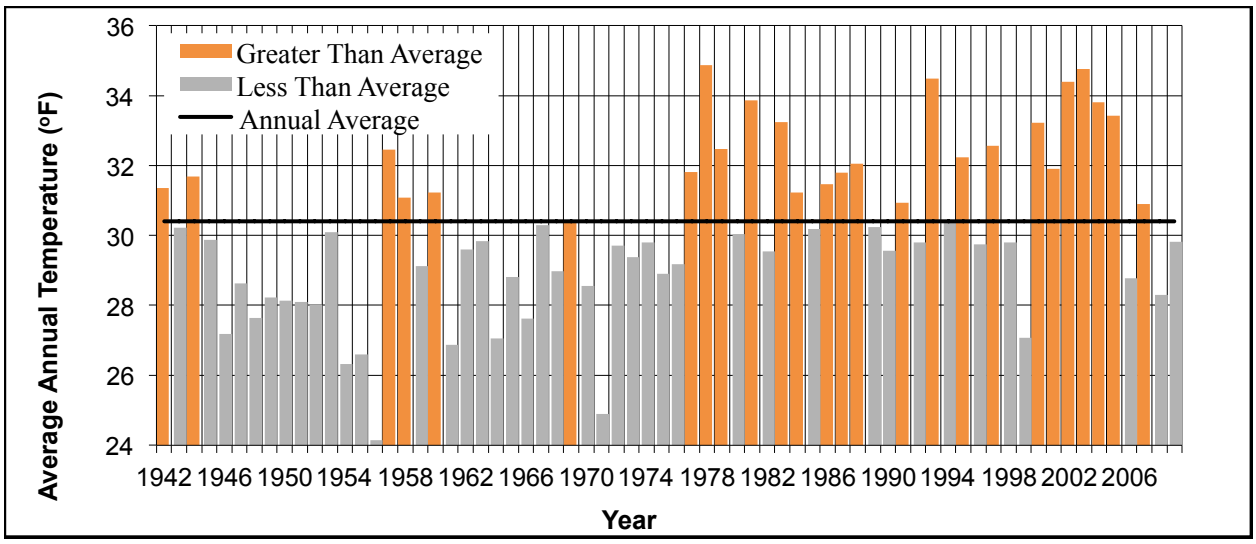


Figure 4: Long-term mean annual air temperature at Pebble

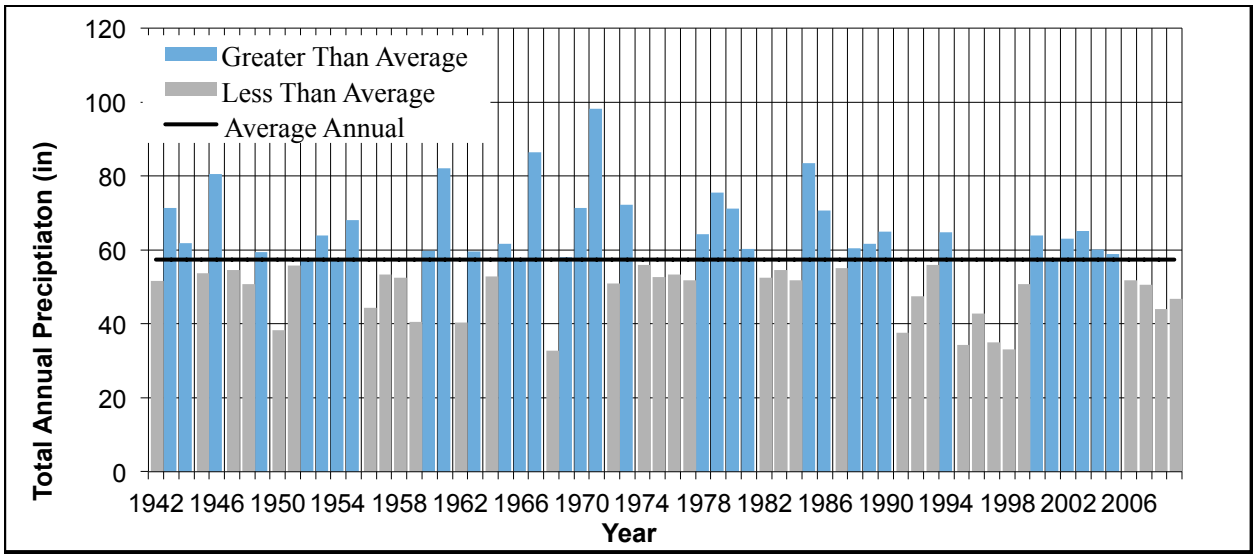


Figure 5: Long-term annual precipitation at Pebble

The long-term records also indicate the strong seasonal and month-to-month climate variability at Pebble. Figure 6 shows the patterns of monthly average air temperature and monthly total precipitation for the full data record, and Figure 7 shows the monthly runoff for each year of record in grey (as determined by the water balance model) and the long-term average runoff in blue. The annual hydrograph typically has peak runoff during the spring and fall and low runoff during the winter and summer. The first peak generally occurs in May, as a result of snowmelt, while the second peak occurs between August and October, as a result of rainfall events. Variations in temperatures, however, can sometimes produce peak freshet runoff in June as a result of colder and longer winters producing large snowpacks and/or the late onset of the spring melt period.

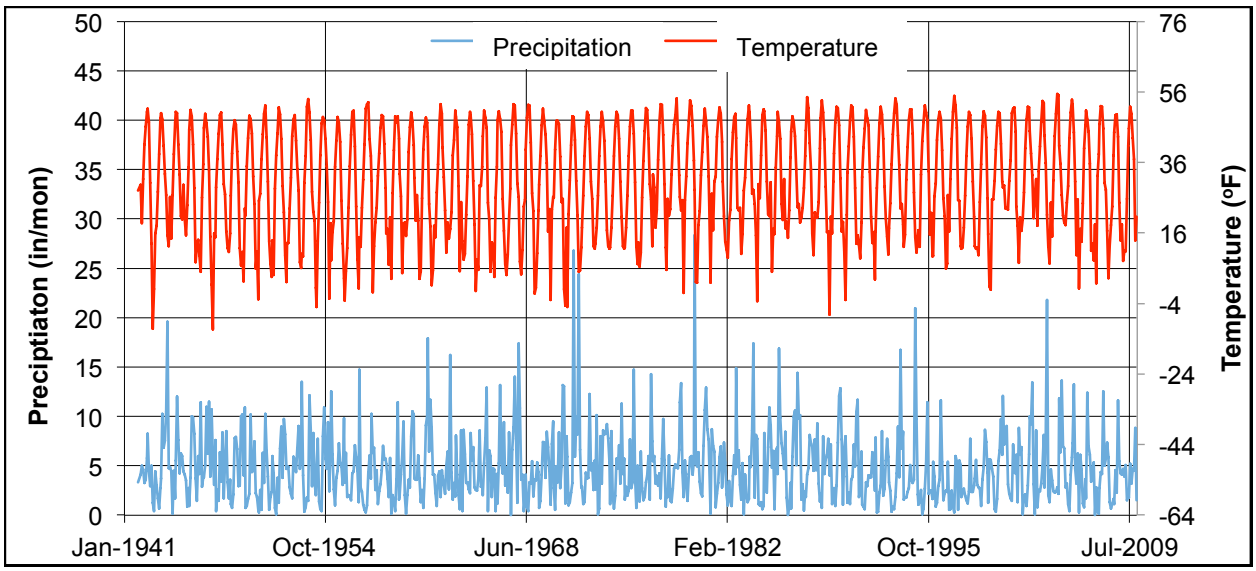


Figure 6: Long-term monthly average temperature and monthly total precipitation at Pebble

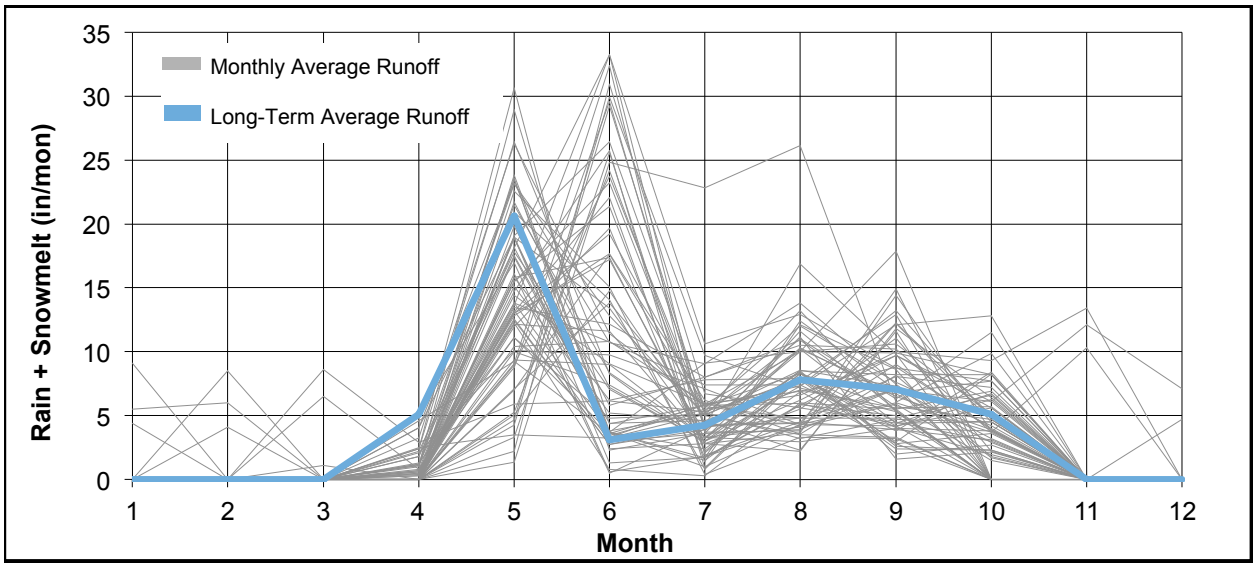


Figure 7: Long-term and average monthly rainfall and snowmelt at Pebble

Water Management Strategy and Water Balance Model

The main objective of the water management plan for Pebble is to manage water that originates within the project area in an environmentally responsible manner while providing an adequate water supply for mining operations. Primary design considerations are the need to capture and treat all contact water prior to its release to the environment, to operate the mine without requiring additional water from off-site sources, and to release water to sustain or enhance downstream aquatic resources. Development of the water management plan involved the consideration of these factors with the constraints of the project facility layout, process requirements, area topography, hydrometeorology, aquatic habitat/resources, and

regulatory discharge requirements, which ultimately led to the need for six water management ponds (WMP). The primary purposes for each are summarized in Table 1, and the locations of the ponds are shown on Figure 2.

Table 1: Description of water management ponds

Water management feature	Purpose
Open pit WMP (OP WMP)	Manage surface and groundwater from open pit dewatering prior to treatment at the water treatment plant (WTP)
Low Grade Ore WMP (LGO WMP)	Collect and manage runoff and seepage from the Low Grade Ore (LGO) stockpile. Surplus water from this pond will be directed to the Main WMP.
Main Embankment seepage collection pond	Collect and manage runoff and seepage from the Main TSF embankment. Surplus water from this pond will be directed to the Main WMP.
TSF (bulk tailings cells)	Storage of non-potential acid generating (NPAG) tailings solids and management of runoff from tailings beaches and quarries. Surplus water from this pond will be directed to the Main WMP.
TSF (pyritic tailings cell)	Storage of potential acid generating (PAG) tailings solids and to provide chemical stability of the solids (wet cover). Surplus water from this pond will be directed to the bulk tailings cell.
Main WMP	Storage and management of surface water runoff from the Mill site and surplus water from other water management facilities. Surplus water from this pond will be used as make-up water in the process and treated at the WTP.

All of these water management facilities will be designed to meet dam safety requirements and will have appropriate storm storage and freeboard allowances. The storm storage and freeboard requirements are based on estimates of extreme precipitation and/or runoff events, such as the 100-year, 24-hour precipitation event, or the Probable Maximum Flood (PMF) event. The runoff volumes associated with these events are considered over and above the maximum operating pond levels.

A water balance model was developed using the long-term monthly temperature and precipitation dataset established for Pebble. Modelling climate variability played a key role in dictating the range of operating pond volumes, pumping rates, and water treatment rates that will be required in order to facilitate normal operations of the project even under unusually wet and dry conditions of varying duration.

Water Balance Model

The water balance model is site-wide and considers all mine facilities including the TSF, open pit, process plant, LGO stockpile, and water management ponds. The model tracks the movement of water through the Pebble footprint area including runoff from the mine facilities, groundwater inflows, evaporation, water stored in facilities, and water lost to the tailings voids. The water balance is used to predict the full

range of possible flows in the mine site area and to estimate the water storage capacity requirements for the mine under normal, wet, and dry climatic conditions.

Climate variability was introduced into the Pebble water balance by utilizing the 68-year monthly time-series of temperature and precipitation, as discussed in previous sections. The time-series data were incrementally stepped by year within the model, for the planned life of the project, therefore persevering the inherent cyclical nature of the climate record. A schematic of how the shifting time-series is used in the model is shown on Figure 8. The model generated 68 unique sets of results of water flow and storage over the full life of the mine, and distributions were then fit to each set of 68 output values so that probabilities of occurrence could be determined. These results facilitated the development of a robust water management strategy that accounts for a full range of possible climate and runoff conditions. Adequate storage in each of the WMPs was determined so that excess water during extended wet periods can be captured and stored to maintain full mine operations during periods of extended dry periods, while maintaining adequate flow releases for aquatic resources both during wet and dry periods.

	Realization 1	Realization 2	Realization 3	Realization 4
Mine Life: Years 1 to 20	Year 1	Year 2	Year 3	Year 4
	Year 2	Year 3	Year 4	Year 5
	Year 3	Year 4	Year 5	Year 6
	. . .	. . .	. . .	. . .
	Year 19	Year 20	Year 21	Year 22
	Year 20	Year 21	Year 22	Year 23
	Year 21	Year 22	Year 23	Year 24
	. . . .	. . .	. . .	. . .
	Year 66	Year 67	Year 68	Year 1
	Year 67	Year 68	Year 1	Year 2
	Year 68	Year 1	Year 2	Year 3

Figure 4: Schematic of shifting time-series

Climate Variability Water Balance Model Results

The climate variability water balance model was used as a tool to help define the water management plan so that it can meet its main objectives as defined above. The Main WMP operation is used as an example to illustrate the results of the water balance model.

The priority for the Main WMP is to supply water to the process plant at all times. The logic in the model was set up such that enough water always remained in the pond to supply the process, even during prolonged dry periods. (Note that the longest period of below-average precipitation in the historic record is five years.) A secondary priority of the Main WMP is to regulate inflows so that surplus water can be

discharged at reasonably constant rates to the WTP for treatment and ultimate release to the downstream environments. This water is intended to maintain aquatic habitat and resources. The challenge was to determine the balance between storage in the WMP and the water treatment rates that would maintain a water supply to the process while providing adequate flows to the downstream aquatic habitat and resources. This was an iterative process, with pond volumes and treatment rates varied to meet the goals. Ultimately, variable treatment rates were required to meet the objectives. Flow rates to the WTP were reduced when pond volumes were approaching low levels and increased when pond volumes were approaching high levels. The low-level trigger was determined by evaluating the amount of water required in the pond to maintain water to the process under prolonged dry periods, while the upper trigger was determined to maintain enough free storage in the ponds to allow for the large inflow volumes during high runoff years, and particularly high snowmelt volumes.

The results from the water balance model for the Main WMP are provided on Figure 9. The pond volume results from all 68 model realizations are shown on Figure 9A. Two unique realizations were selected to demonstrate the flexibility of the water management plan to address the high variability climate at Pebble. Realization 1, shown on Figure 9B, represents the wettest 20-year sequence within the time-series data with an annual average precipitation of 64 in. (1,635 mm), an annual maximum of 98 in. (2,490 mm), and an annual minimum of 51 in. (1,295 mm). Realization 2, shown on Figure 9C, represents the driest 20-year sequence with an annual average precipitation of 51 in. (1,288 mm), an annual maximum of 65 in. (1,562 mm), and an annual minimum of 33 in. (838 mm).

The first year of precipitation under Realization 1 is very high, and consequently, there is a drastic increase in pond volume in Year 1 of operations. The maximum operating pond volume was determined assuming these conditions; therefore, the risk of miss-operation is minimalized. Spikes in the pond volume are seen on an annual basis for each year of operations under this realization, representing the effects of snowmelt in the spring and rainfall in the fall. The magnitudes of the spikes vary depending on the phases of the ENSO and PDO. The water management strategy effectively manages these events by drawing down the pond volume each year to provide sufficient capacity to captured the runoff from the spring snowmelt, and then again for the fall storms.

The first year of precipitation under realization 2 is much lower than in realization 1, and results in a much smaller starting pond volume. The minimum pond volumes for this realization are much lower, but the rules applied to the water treatment rates allow for adequate water volumes to be maintained in the pond to provide a constant feed to the process. The treated flows released to the downstream environments are lower in realization 2, but this was deemed acceptable since the flows in all the streams would also be low under natural non-mine conditions for these climatic conditions.

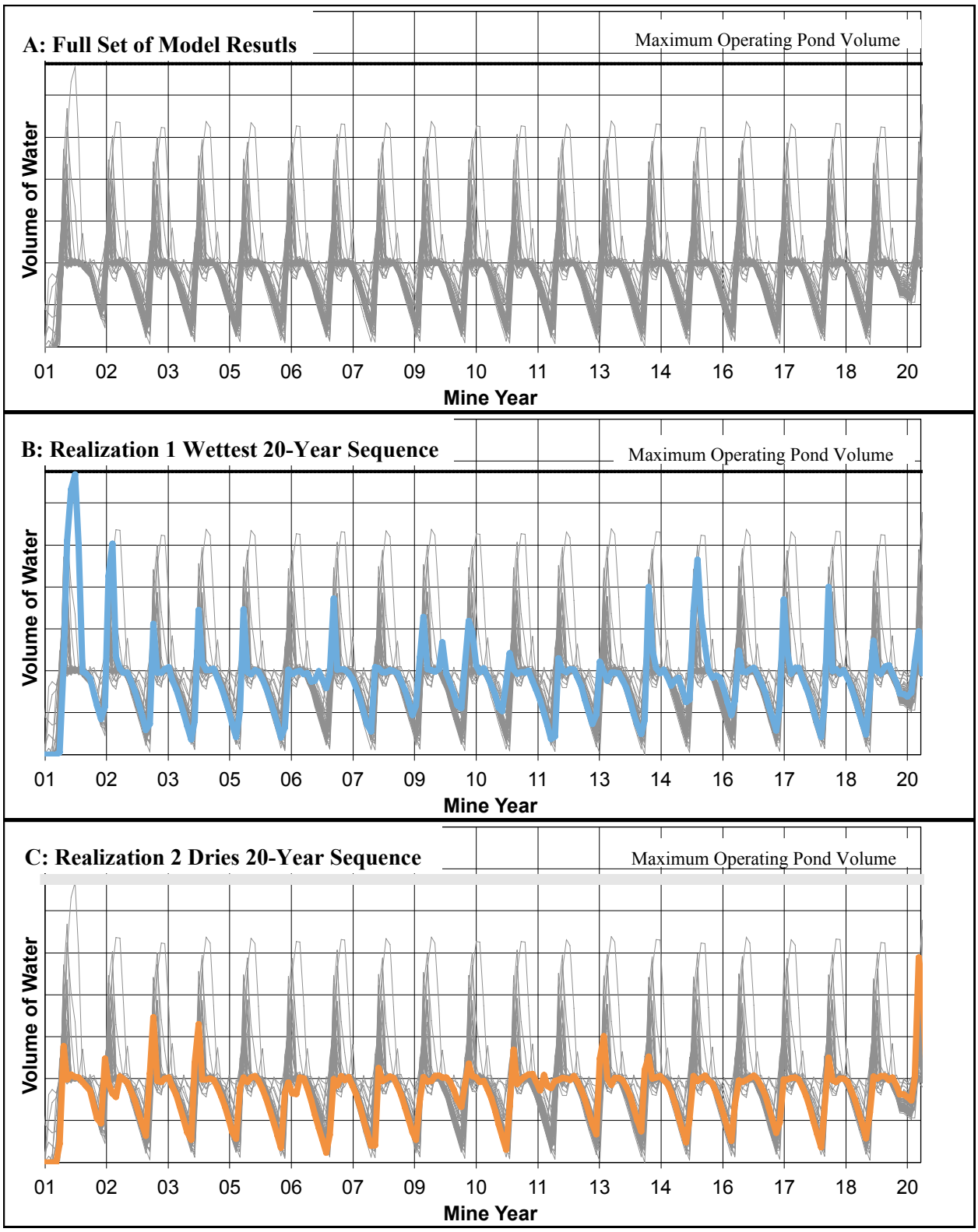


Figure 9: Range of predicted pond volumes for the main water management pond

Conclusion

The climate in south-central Alaska is highly variable with large monthly, seasonal, and annual ranges, and is dependent on the strong climate cycles, resulting in extended dry or wet periods. A water balance model was developed that utilizes 68 years of monthly temperature and precipitation data to address climate variability at Pebble, and its implications for water management strategies. The time-series data were incrementally stepped through in the model by year for the planned life of the project, thereby preserving the inherently cyclical nature of the climate record. Pebble's water management strategy was therefore evaluated under the full range of historic climate variability, regardless of it being a wet or dry phase. The results were a robust water management strategy that includes providing adequate storage in each of the water management ponds to supply sufficient water to maintain full mine operations, while maintaining downstream flow requirements for aquatic resources.

References

Cathcart, J. and Smith, R. 2013. The pebble project: Using streamflow to quantify precipitation in an extreme northern environment, *Proceedings of the First International Conference on Mine Water Solutions in Extreme Environments, Lima, Peru*. Vancouver, Canada: InfoMine, Inc.

Hartmann, B. and Wendler, G. 2005. Significance of the 1976 Pacific climate shift in the climatology of Alaska, *Journal of Climate,* 18: 4824–4839.

Knight Piésold Ltd. (KP). 2012. Pebble project hydrometeorology. Prepared for Pebble Limited Partnership. Ref. No. VA101-176/40-1.

Papineau, J. 2001. Wintertime temperature anomalies in Alaska correlated with ENSO and PDO, *International Journal of Climatology,* 21: 1577–1592.

Pebble Partnership (PLP). 2017. Pebble Project Department of the Army Application for Permit. Ref. No. POA-2017-271. December 2017.

Shulski, M. and Mogil, H.M. 2009. Alaska's climate and weather, *Weatherwise*, January–February 2009 issue.

Wendler, G. and Moore, B. 2012. The first decade of the new century: A cooling trend for most of Alaska, *The Open Atmospheric Science Journal*, 6: 111–116.

Wendler, G., Gordon, T. and Stuefer, M. 2017. On the precipitation and precipitation change in Alaska, *Atmosphere,* 8: 253.

Proceedings of Mine Water Solutions 2018
June 12–15, 2018, Vancouver, Canada
Published by the University of British Columbia, 2018

A Real Challenge in Mine Water Management in a High Precipitation Area: Grasberg Mine

Nanda Rinaldi, PT Freeport Indonesia, Indonesia
Iwan Setiawan, PT Freeport Indonesia, Indonesia
Vladimir Ugorets, SRK Consulting (US), Inc., USA
Göktuğ Evin, SRK Consulting (US), Inc., USA

Abstract

The Grasberg Mine is the world's largest gold mine, and is also one of the largest copper producers in the world. The mine poses a real challenge for hydrogeologists due to its size and complex hydrogeological setting, including structurally controlled groundwater flow. The mine sits in a mountainous area with rainfall of up to 5 m per year. The site geology features highly undulated sedimentary rocks and vertical intrusions hosting the mineralization. Karstification exists in the area and influences structural control of the groundwater flow path in the vicinity of the open pit and underground mines.

The applied mining method for the Grasberg intrusive complex (GIC) also complicates water management. The existing open pit is approximately 1.5 km deep and a block cave operation is under development approximately 400 m below the pit bottom. Block caving will propagate to the pit bottom eventually and will create a highly transmissive cave zone, which will connect drawpoints to the bottom of the open pit.

Near the GIC, the East-Ertsberg skarn system (EESS) has been mined since 1982 by systems of five vertical block caves (GBT1, GBT2, IOZ, DOZ, and DMLZ). The implemented dewatering systems for both the GIC and EESS areas, with a total flow of approximately 41,000 gallons per minute (gpm) or 2.6 m^3/s, allows lowered water levels in the vicinity of the open pit and underground mines by discharging groundwater via gravity by a system of upward drainholes drilled from the underground drifts.

To assist in the development of dewatering and mine water management strategies for the remaining life of mine, a comprehensive groundwater flow model was developed by using the finite-element *MINEDW* code and calibrated to the available flow and water level data collected over a 20-year period of active mining.

Hydrogeological Conditions

The Grasberg Mine is located in Papua, Indonesia in a mountainous area where a rainfall of up to 5 m per year is subject to El Niño's periodic occurrence. The site geology is extremely complex with highly undulated sedimentary rocks and vertical intrusions hosting the mineralization. Karstification exists in the area and influences structural control of the groundwater flow path in the vicinity of the open pit and underground mines.

Regional Hydrogeology

The regional geologic framework of the Grasberg minerals district consists of a series of folded and faulted carbonate and sandstone units that range from about 700 to 3,000 m in thickness. These formations have relatively low permeability unless karstified or fractured. The maximum thickness of the formations occurs along the Yellow Valley syncline near GIC, and to the north of the EESS as shown in Figure 1.

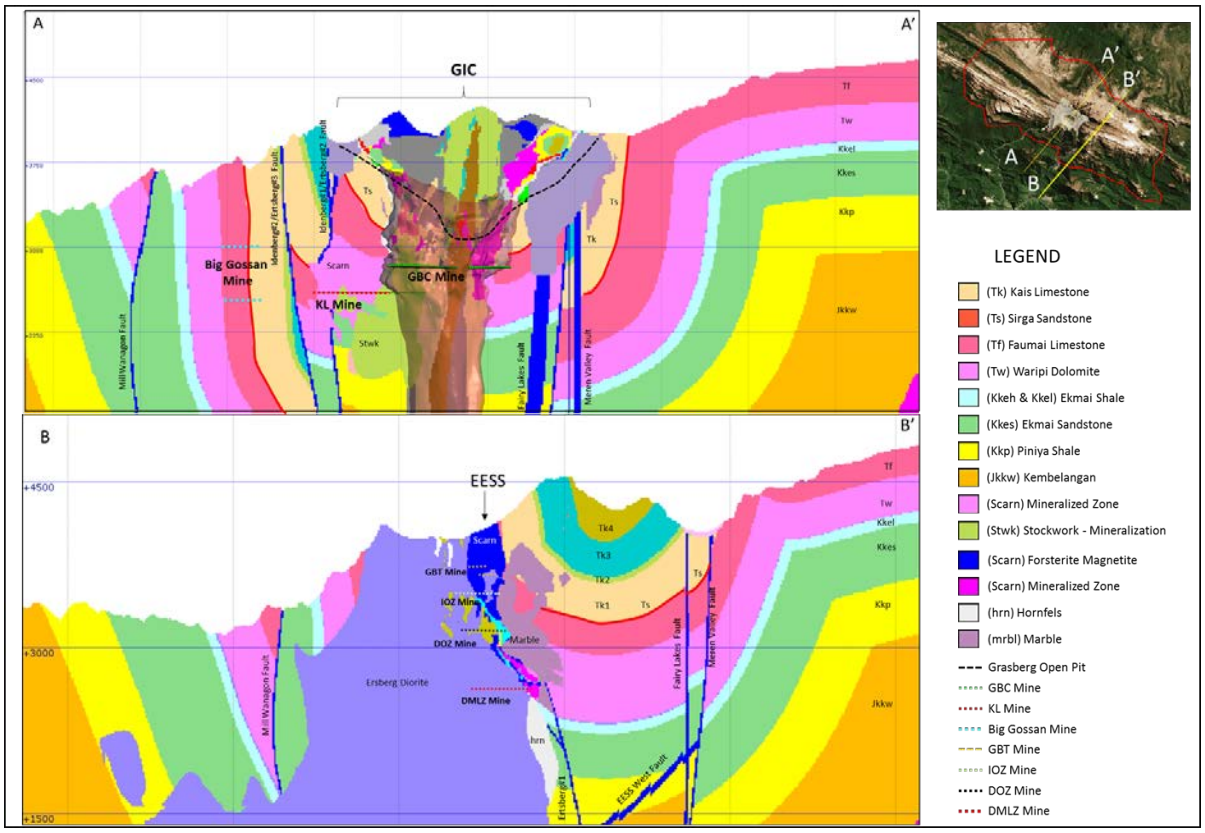


Figure 1: Geology of Grasberg and EESS mines shown with cross-sections

The Grasberg Mine complex is located at the intersection of two major structural systems: NW/SE-trending faults that are parallel to the axis of the Jayawijaya Mountains, and NE/SW-trending cross-faults, normal to the axis of the mountains. The Idenberg #1 and #2, Fairy Lakes, and Meren Valley and axial

faults and the Grasberg, Carstensz and New Zealand Pass cross faults are major water-bearing features in vicinity GIC and EESS.

Within the Grasberg area, the most important and permeable water-bearing units are: the Poker Chip Zone (currently mined out); the fractured upper part of the Kali intrusive; the Heavy Sulphide Zone (HSZ) contacts between the sedimentary units and the GIC; and Grasberg, Idenberg#1 and Carstensz faults.

The near-surface limestone units are often karstified to depths of 300 m below ground surface and significantly deeper along major structures. The karstic features in the limestone provide permeable conduits for groundwater flow as confirmed by a series of tracer tests. There are three major known karstic sinkholes/features: Carstenszweide (CST) with two sinkholes to the north of the GIC and Yellow Valley with one sinkhole to the north/northeast of the EESS.

The ore within the EESS occurs within a skarn that formed at the contact between the Ertsberg diorite intrusion and the primary limestone country rock. Mining of the DOZ started in late 2000 by block caving similar to the previous block caving in the overlying GBT I, GBT II and IOZ mines. The cave propagated to the surface in a portion of the eastern half of the DOZ mine and up to the IOZ cave in the western part of the DOZ and formed a combined GBT/IOZ/DOZ cave. Mining of the DMLZ started in 2015 by block caving at an elevation of 2,600 mamsl (meters above mean sea level) (or approximately 500 m below the DOZ level) and a combined GBT/IOZ/DOZ/DMLZ cave zone would be formed.

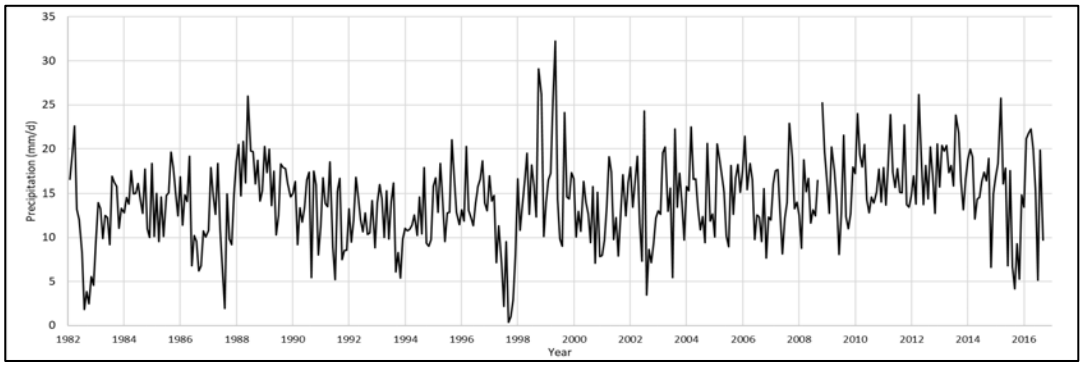
Within the EESS area, key preferential pathways of the groundwater are: diorite at an elevation above about 3,400 mamsl, West Fault Zone, and Guru, Ertsberg #1 and Cave faults. As the DOZ/DMLZ cave and crack limits expand through time into these units, they will contribute lateral residual passive inflow directly to the cave zone.

Groundwater Recharge and Discharge

Recharge of precipitation is a major stress to the groundwater system and varies significantly across the HSA (hydrogeological study area). Recharge of surface water into the groundwater system occurs predominantly through sinkholes in the karstic limestone or through areas with outcrops of more permeable intrusive rocks. Figure 2 shows the location of 19 rainfall stations installed within the HSA. Rainfall stations are located at elevations ranging from 3,100 to 4,544 mamsl in the Upper Wanagon to the west of the GIC (northwest of the proposed KL block cave). Data from the stations are available from 1995 through 2017. The rainfall data define the following two major areas with different precipitation rates (Figure 2):

- High elevation (15 stations) with average precipitation ranges from 9.1 to 10.9 mm/d (long-term average rate of 9.8 mm/d); and

- Southern slope (4 stations) with average precipitation ranges from 13.2 mm/d to 16.3 mm/d (long-term average rate of 15.0 mm/d). It is envisaged that the topographical divide at the southern part of the HSA acts as a boundary to the S-N trending winds. Therefore, precipitation condenses at the southern part of the divide.



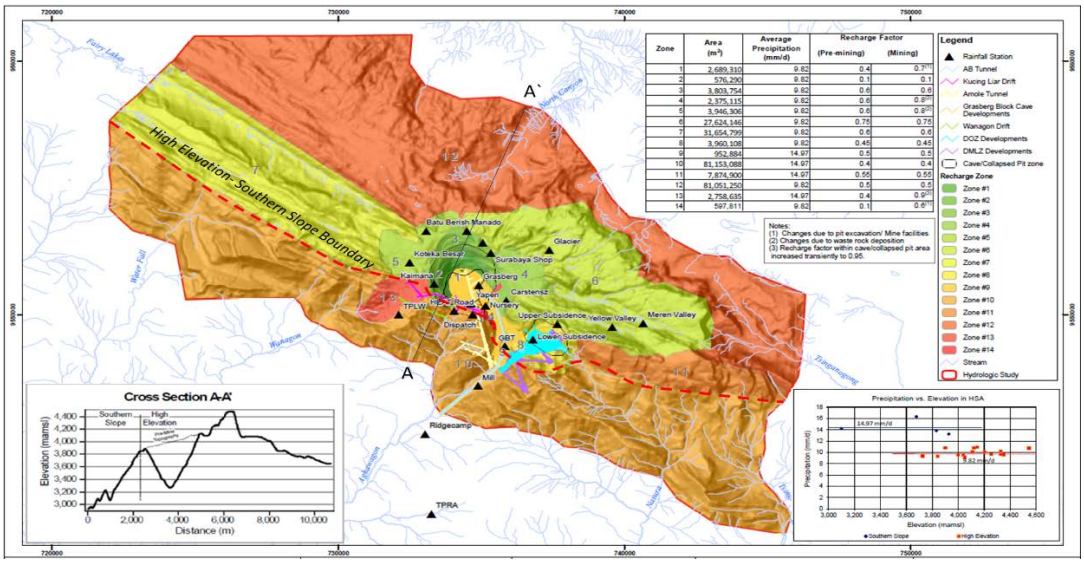


Figure 2: Location of rainfall stations, distribution f precipitation zones and recharge factors and historic precipitation data

Figure 2 shows historic monthly averaged precipitation rates for Mill station with the longest (from 1982) record indicates large variation in rainfall and the impact of strong El Nino events (in 1982, 1987, 1997, 2003, and 2015). The maximum measured monthly average precipitation is 32.3 mm/d (Mill, April 1999) and minimum measured monthly average precipitation is 0.08 mm/d (Yellow Valley, September 1997). The wettest conditions occur in December through April and relatively dry conditions occur in June through August.

As much as 75% of the precipitation is estimated to recharge the groundwater system in these closed alpine karst basins. Recharge in the non-karstified areas is estimated to range from 60% in areas underlain

by limestone to 10% to 45% in areas underlain by intrusive rocks as shown in Figure 2. This distribution is based on analyses of slope, presence of surface water outflow and hydraulic parameters. Recharge factor values were verified in the process of model calibration.

Groundwater in the HSA eventually discharges into one of nine major streams. However, both major and minor faults and related structures allow groundwater to flow beneath topographic divides, at least at the sub-basin level. Additionally, groundwater discharge occurs as springs along beds of low permeability rock. Most of these springs occur at an elevation of about 3,300 mamsl, probably at the base of the alpine karst system. These springs comprise the headwaters of most of the perennial streams.

Generally, the regional groundwater flows from the topographic highs at the watershed divide toward areas of lower elevation in the south or southeast. Intrusive complexes generally show low permeability, and tend to be hydraulic barriers to the groundwater flow generated by meteoric recharge in the Jayawijaya Mountains.

Groundwater Inflow Management

Figure 3a shows the locations of groundwater intersections by drifts and drillholes, and locations of flow measurement stations.

Groundwater flow in the GIC area discharges into the Amole drift with maximum measured flow up to 12,000 gpm from drainholes installed in the northern part of the drift (above X/C #17). During excavation of the open pit, significant inflow was not observed (the maximum observed inflow in the north-eastern segment of the pit did not exceed 1,500 gpm) due to efficient groundwater capturing from the Amole drift below.

Current groundwater inflow to the Grasberg Block Cave (GBC) development is about 4,000 gpm. The majority of inflow is observed along the contacts between the Karume and Kali intrusives and the carbonate rocks. A series of hydraulic tests from Amole piezometers to the GIC indicate that the GIC rocks generally are of low permeability except where fractures/structures exist.

The cave will break through to the bottom of the pit during mining of the GBC and the cave and crack zones will propagate into the walls of the Grasberg Pit. Due to its location below the Grasberg Pit, rainfall within this area infiltrates and enters the proposed GBC and KL (Kucing Liar) mines.

Groundwater flow in the DOZ mine discharges into MLA drift and partially through DOZ pipe. Total mine discharge (inflow to drillholes, drifts and draw points) was in the range of 10,000 to 12,000 gpm (MLA flow is up to 8,000 gpm) when measured from 2004 through 2013. Groundwater intersections have occurred starting in 2014 in DMLZ developments (water discharges into AB tunnel) with total flow of up to 10,000 gpm, resulting in decreased MLA flow from 8,000 to as low as 3,000 gpm. This decrease indicates a good hydraulic connection between the DOZ and DMLZ mines.

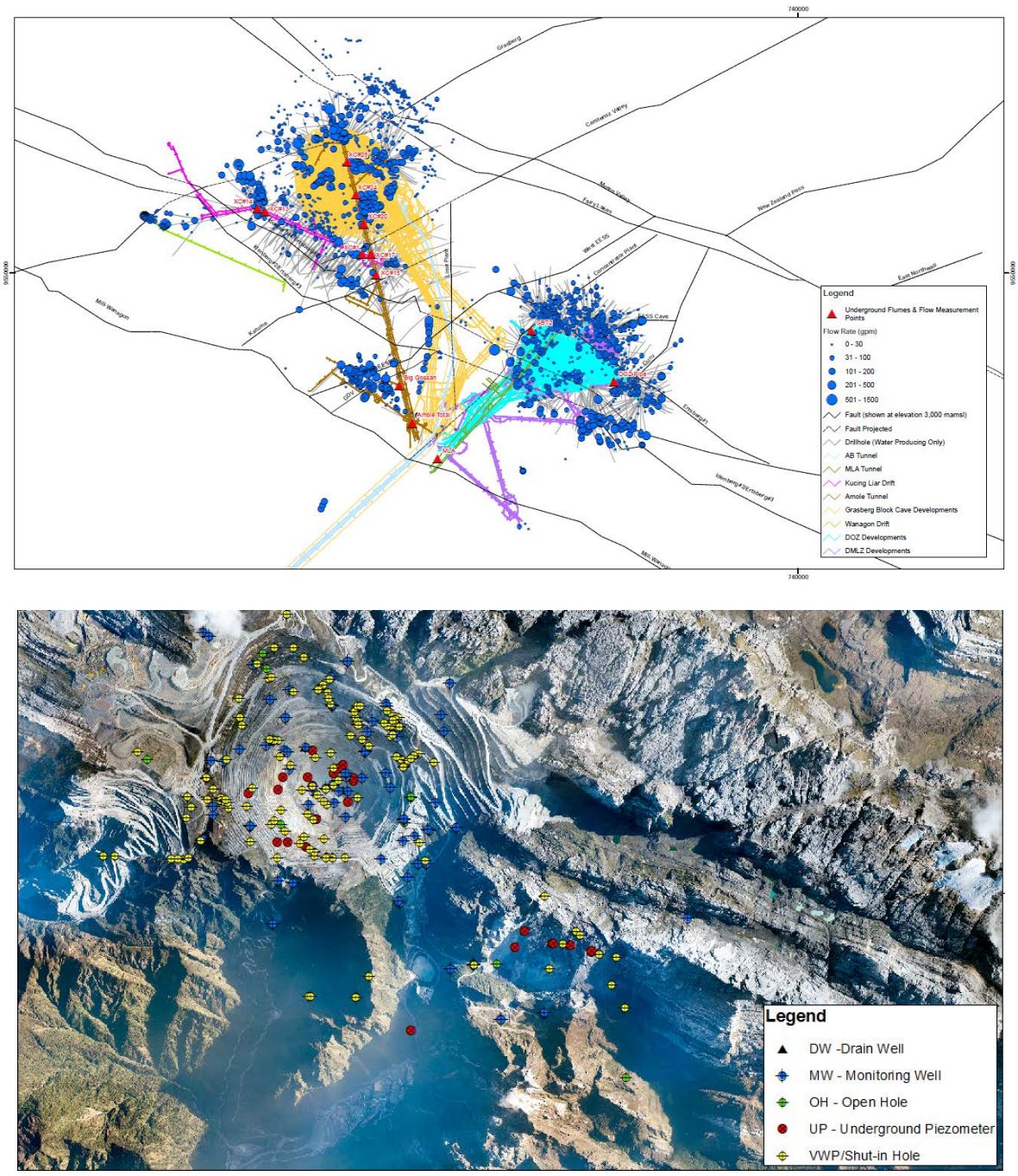


Figure 3: Location groundwater intersections by drainholes, flow measurement stations (a), and piezometers with water level measurements (b)

Groundwater Level Distribution

Figure 3b shows locations of monitoring wells with measured water levels.

Prior to mining and dewatering of the Grasberg Pit and based on anecdotal evidence, the groundwater levels in the GIC and surrounding limestone were about the same. As a result of drilling underground drainholes into the contact zones on both sides of the HSZ, water levels in the GIC and

contact zones have decreased significantly while the water levels in the surrounding limestone have been dropping at a much slower rate. Water level declines in the surrounding limestone have occurred only in areas near the HSZ contact or close to the dewatering drainholes. Piezometers in south, east and northeast limestone showed a small amount of drawdown, while those in the north and northwest of the HSZ remained high. The lack of drawdown is attributable to the ring of low permeability limestone/marble below the hinge point of the wineglass–shaped GIC.

Measured water levels in the underground piezometers installed within the lower part of the GIC stand at 2,855 to 3,108 mamsl (i.e., about 35 to 288 m above the GBC mining area). Most of these piezometers are artesian holes with measured water levels between 8 and 12 m above the Amole drifts. Although the pressure heads are above the Amole drift level, the flows are small, which confirms that the GIC rock is of low permeability and likely extends to the GBC level.

Measured water levels in the EESS area are limited and measured in the range from 3,440 to 3,150 mamsl (DOZ level) and from 3,1000 to 2,585 mamsl (DMLZ level) in underground piezometers within the north wall sedimentary rock. Water levels in the surface piezometers are measured within fractured diorite (from 3,808 to 3,426 mamsl) and about 3,700 mamsl in Yellow Valley syncline.

All water level measurements indicate a presence of downward hydraulic gradient due to groundwater intersections from underground developments and low permeability of the rock.

Description of Groundwater Flow Model

The numerical model was developed to predict groundwater inflows to existing and being constructed block cave mines. The model was constructed by using the *MINEDW* finite-element code, which is specially designed to model mine dewatering projects. Some key features of this code – collapsing grid to simulate open pit excavation, non-linear flow in the drains intersecting large groundwater flow in the permeable faults, modeling of permeable faults by additional linking nodes with additional transmissivity, changes hydraulic conductivity in time to simulate cave/crack line propagations – were specially designed to model groundwater flow in the vicinity of the Grasberg open pit and EESS block cave mines (Azrag et al., 1998; Ugorets, 2016).

The three-dimensional finite-element grid of the model contains 175,716 nodes and 328,797 elements in 17 numerical layers and encompasses an area of about 251 km^2 within nine surface water basins, covers in detail the existing and future mines and are shown in Figure 4.

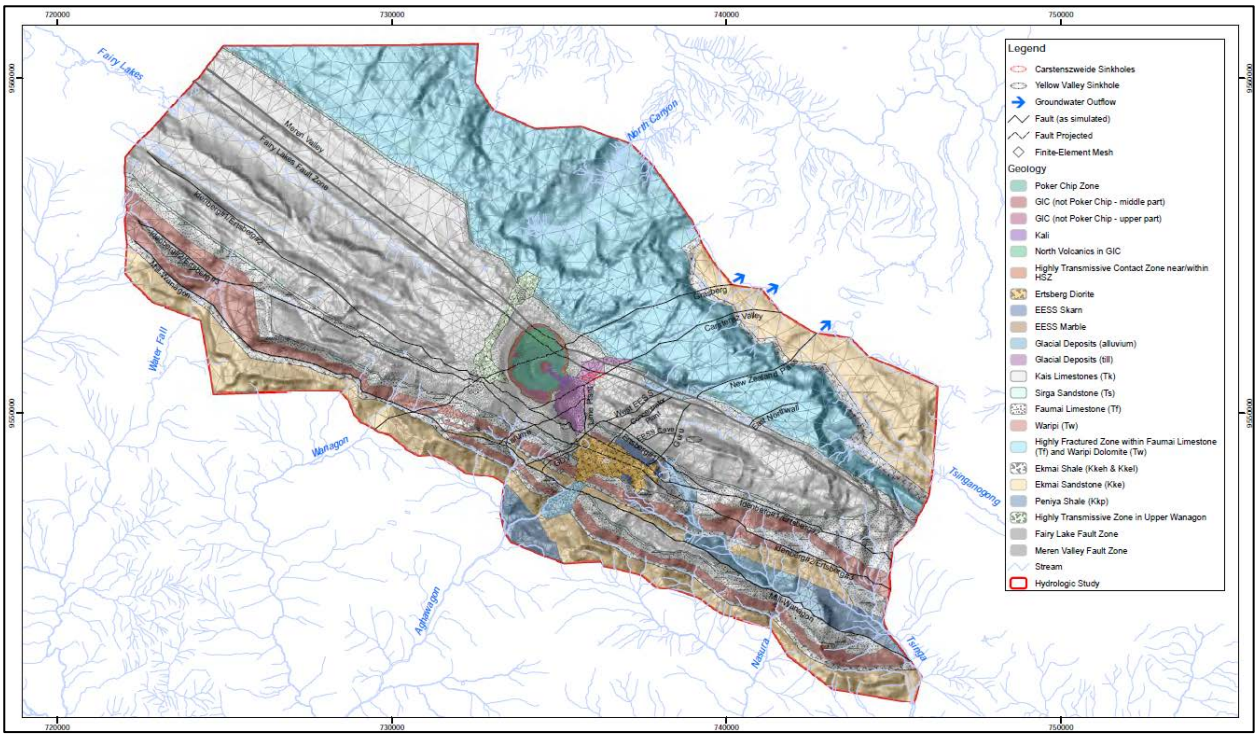


Figure 4: Plan view of finite-different mesh of model shown simulated geology in uppermost layer and faults

Simulation of Hydrogeology

Sixty-two hydrogeologic zones with various hydraulic parameters were incorporated into the model and simulated, generally decreasing hydraulic conductivity values with depth. Hydrogeologic zones in cross section A-A' through the Grasberg and KL areas are shown in Figure 10a before excavation of the open pit when the open pit will be fully excavated and when Grasberg and KL block caves will be completed. Hydrogeologic zones in cross section B-B', through the EESS area, are shown on Figure 10b a for pre-mining conditions and at the end of DMLZ block caving.

The hydraulic conductivity tensor has been rotated with respect to the model grid such that K_{xx} is oriented at an azimuth of 117^0 (or N63^0W), parallel to the trend of the Jayawijaya Mountains and the associated fold axes. Some of the hydrogeologic units (e.g., all intrusive and metamorphic rocks) simulated isotropic, but most of the sedimentary units have been made anisotropic with the general relationship $K_{yy} \geq K_{xx} \geq K_{zz}$. This anisotropy is used to represent the effects of the major joint system and small faults.

Simulation of Faults

The 17 major faults are incorporated into the model by linking two nodes with very high transmissivity between them. The horizontal traces of the nodes linked to represent the various faults are indicated in

Figure 4. The vertical traces of the nodes linked to represent the various faults are shown in the two cross sections of the model in Figures 5 and 6. There are 22,776 pairs of such linked nodes in the model. Two major regional faults to the north from GIC (Meren Valley and Fairy Lakes) were simulated by a system of narrow elements with high hydraulic conductivity and low storage parameters.

Simulation of Recharge from Precipitation

Recharge from precipitation is assigned by multiplying recharge factors by rainfall rates within two precipitation zones (both shown in Figure 2).

Monthly average data for each precipitation zone were obtained by averaging available data starting in 1995 from rain stations within each area. Prior to 1995, data from Mill station (available from 1982) were used to reproduce precipitation within these two zones by multiplying Mill precipitation records by coefficients of 0.691 and 1.004. These two coefficients represent the relationship between estimated average precipitations for these two zones to the Mill average rainfall value.

Long-term average precipitation data were used for pre-mining steady-state and predictive transient simulations. Monthly precipitation was used to apply recharge during transient calibration (from 1982 through 2016).

Simulation of Underground Workings and Groundwater Intersections

The underground workings and associated dewatering systems are presented in the model as drifts and drillholes. They are incorporated into the model by specific drain nodes with time-variable leakance factors depending on a difference between water level and an elevation of mine development (Azrag et al., 1998; Ugorets, 2016). Using this approach allows more realistic simulation of high water discharge by drainholes drilled into the transmissive faults.

Groundwater flow near discharge points in fractured and faulted rock is usually non-Darcian, and the standard groundwater flow equation breaks down in describing such flow (Dudgeon, 1985). To account for this non-Darcian flow, authors used the non-linear flow algorithm of *MINEDW* (HCI, 1993), which include both linear and non-linear coefficients from the Forchheimer equation.

All drainholes and parts of the drifts that have intercepted a significant amount of water (i.e., greater than about 50 gpm) are simulated in the model by drain nodes with head dependent leakance factors and considering non-Darcian flow. They are represented by a series of 3,876 model drain nodes.

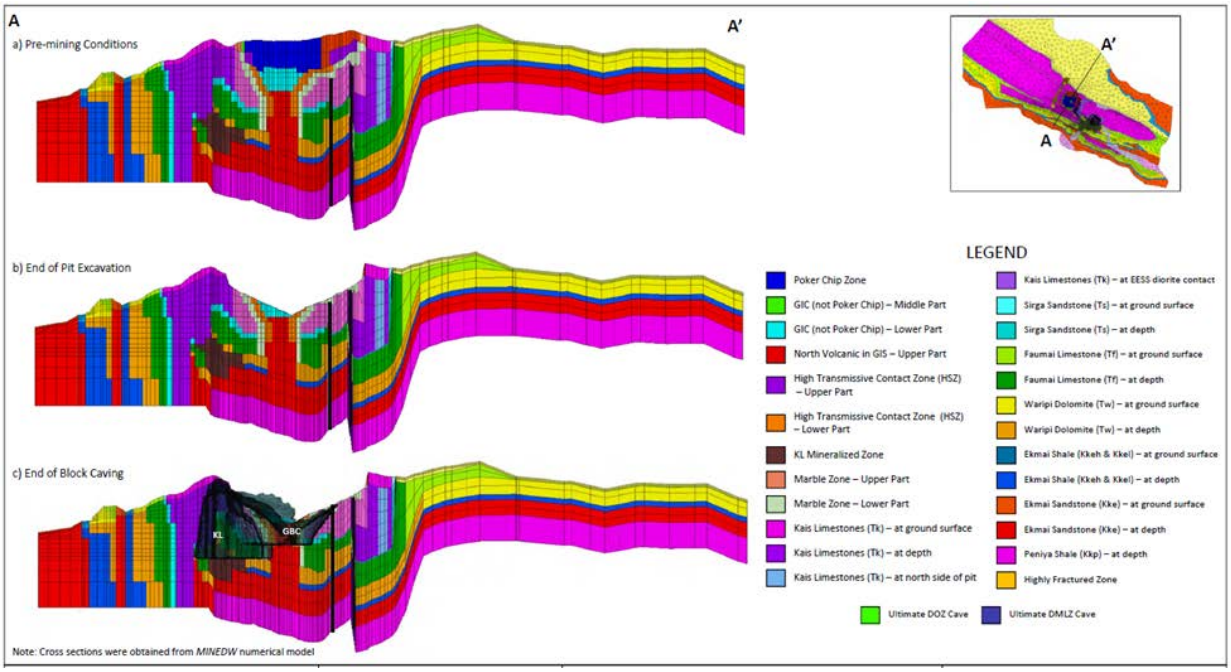


Figure 5: Model cross-section through Grasberg area

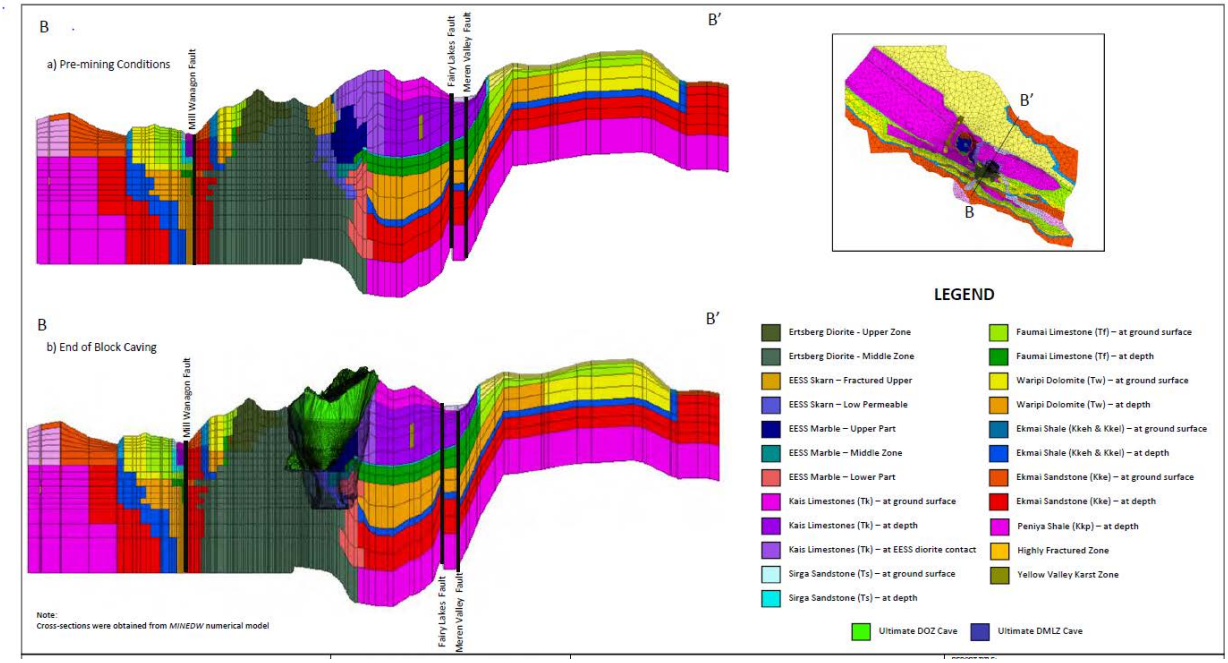


Figure 6: Model cross-section through EESS area

Simulation of Open Pit

The excavation of the Grasberg Pit is simulated by pit nodes with a collapsing grid inside the pit area. This was done by the changing of the elevations of the nodes at the top of the first layer within the pit area to the specified pit elevation. The hydraulic properties within the area of the collapsing grid are adjusted

to the appropriate values as the grid collapses, to simulate mining. Annually pit plans from 1996 to 2018 were incorporated into the model using linear monthly interpolation. The final elevation of the bottom of the Grasberg Pit was assumed to be 3,085 mamsl. The collapsed grid for the final Grasberg Pit is shown in the model cross section in Figure 5.

A zone of relaxation around the excavated open pit was simulated by automatically assigning elements below the pit nodes at the appropriate time. The hydraulic conductivity of this approximately 50 m wide zone is assumed to be 0.1 m/day.

Simulation of Block Caves

The EESS, GBC and KL block caves are simulated by:

- Assigning relatively large values of hydraulic conductivity to the cave and fractured zones (K=1 m/d and K=0.1 m/d, respectively), and
- Increasing the assigned recharge factor over the area where the cave limit is predicted to propagate to the ground surface from the original value in that area (which ranges from 0.1 – 0.75 to 0.95).

Historic and future propagations of the EESS cave and fractured zone limits (shown in Figures 6 and 7) observed and estimated by geotechnical models were incorporated into the model. Future propagations of GBC and KL BC were simulated similarly.

Although development of the cave and fractured zones will be essentially continuous in time, it is simulated in the model in different discrete stages.

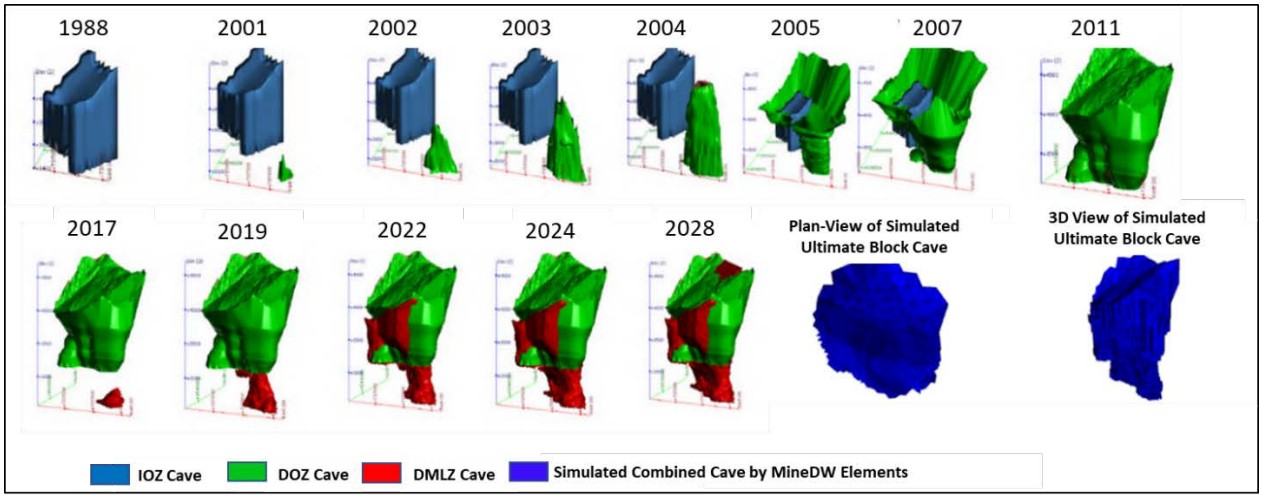


Figure 7: Simulated propagation of IOZ, DOZ, DMLZ cave zones in time

Model Calibration and Predictions

The model was calibrated to groundwater flows intersected by underground drainholes and measured water levels in time. As example, comparison of measured and calibrated total flows at the portals of dewatering drifts is shown in Figure 8. Calibrated model to transient conditions was used for predicting groundwater inflows to proposed block caves and total flows at the portal of dewatering drifts. Their results are shown in Figure 9.

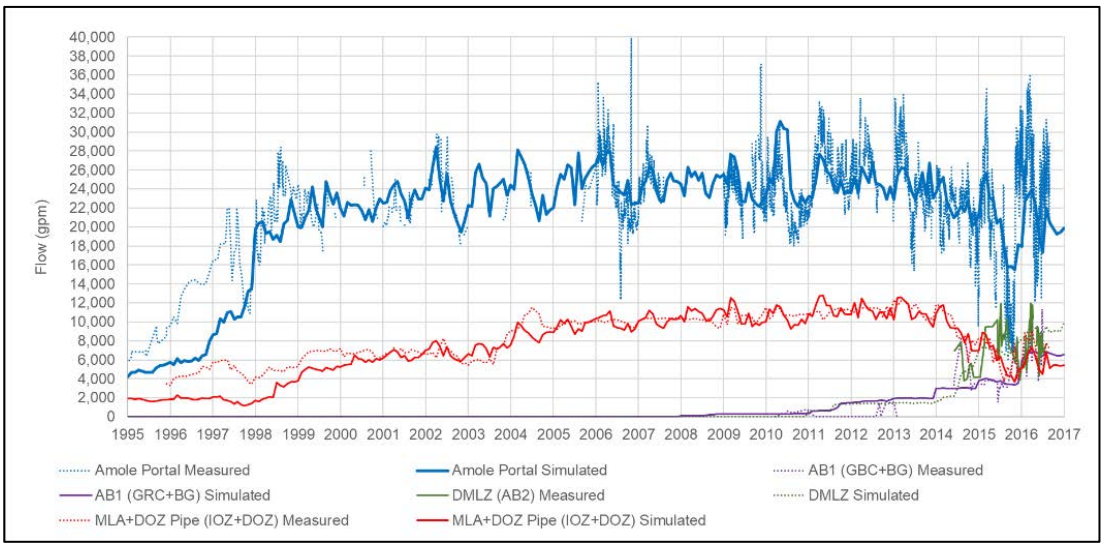


Figure 8: Results of model calibration to measured flows in dewatering drifts

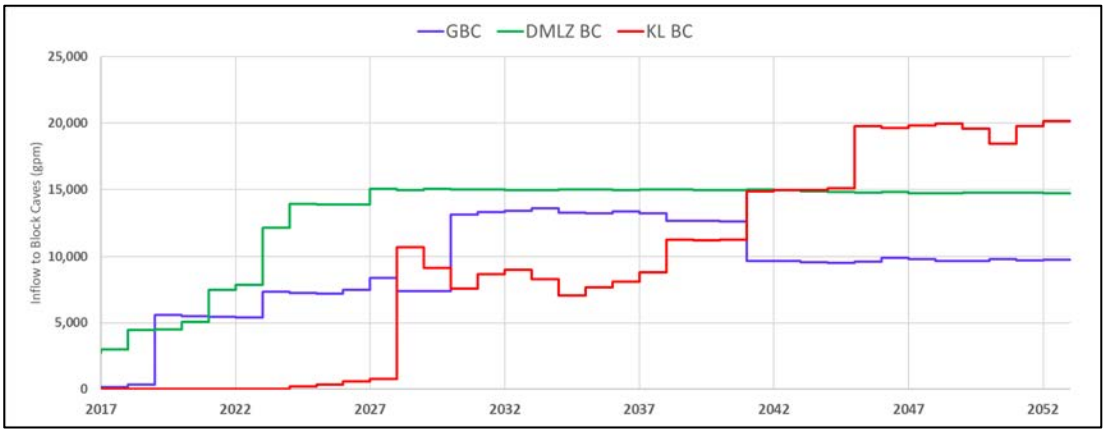


Figure 9: Predicted inflows to GBC, DMLZ, and KL Caves

Maximum predicted inflow to block caves simulated under long-term precipitation conditions and Base Case scenario of cave/crack zone propagation are:

- GBC – 12,800 gpm (or 0.8 m^3/s);
- DMLZ – 15,000 gpm (0.95 m^3/s);

- KL BC –20,000 gpm (or 1.26 m^3/s); and
- Total mine discharge to block caves and ancillary drifts –56,700 gpm (or 3.57 m^3/s).

Predictions of the water table at the end of mining indicate that these three block caves will locally create very steep "cone of depression" around the mines.

Conclusions

Challenges in mine water management in high precipitation areas of the Grasberg Mine posed by complex hydrogeological and mining settings were addressed during the comprehensive conceptualization and numerical modeling processes, including:

- Development of conceptual hydrogeological models of individual mine areas, including complex lithology and presence of transmissive structures with spatial contrasts (up to three orders of magnitude) in hydraulic conductivity distribution.
- Extremes in recharge rates from precipitation and their drastic variability in time and space.
- Presence of karstic zones (sinkholes) and highly permeable faults with non-linear flow conditions.
- Simulation groundwater discharge to drainholes and underground developments by drain nodes with head-dependent leakance factors and considering non-Darcian flow.
- Handling of large amounts of monitoring data (groundwater flows and water levels) with model calibration to more than 20 years transient mining conditions.
- Simulation of complex mining developments including the Grasberg Pit with dynamic changes in open pit elevation and propagation of ZOR around the pit, GBC block cave operation below ultimate Grasberg Pit, and five stages of cave and fractured zone propagations in the EESS (from GBT1, GBT2, IOZ, DOZ, and DMLZ block caves) required detailed handling of transient hydraulic parameters modification in space.
- Using specialized finite-element groundwater modeling *MINEDW* code allowed for the simulation of the items described below (this code was modified by developer several times during process of the modeling by author requests), and minimized numerical problems in the process of the transient simulations.

The results of the predictive numerical simulations and conducted sensitivity analysis indicate that the propagation of the cave zone and associated crack limit into the carbonate rock (and intrusive rock for EESS) is the most sensitive parameter with respect to predicted inflows to the block caves. Cave material and adjacent highly fractured rock propagates toward the ground surface and intersects the permeable shallow groundwater system. Inflow to the block caves also depends on transmissivity of the faults

intersecting the block cave and hydraulic conductivity of marble zones that limit groundwater inflow to the cave.

The numerical model predicts that the groundwater system at the end of mining will reach near-steady-state conditions and total flow in the AB, Amole, and MLA portals will remain at a rate of about 56,700 gpm during post-mining conditions.

References

Azrag, E.A., Atkinson, L.C. and Ugorets, V.I. 1998. Use of a finite element code to model complex mine water problems, in *Mine Water and Environmental Impacts*, Proceedings of the International Mine Water Association Symposia, Johannesburg, South Africa, Vol. 1: 31–41. Johannesburg: International Mine Water Association.

Dudgeon, C.R. 1985. Effect of non-Darcy flow and partial penetration on water levels near open-pit excavation, Hydrogeology in the service of man, *Memoires of the 18th Congress of the International Association of Hydrogeologists,* Cambridge, XVIII(4): 122–132.

HCI. 1993. MINEDW – a finite element program for three-dimensional simulation of mine dewatering, unpublished report. Hydrologic Consultants, Inc.

Itasca International Inc. 2016. *MINEDW 3.0 User Manual.*

Ugorets, V.I. 2016. Benefits of MINEDW code for mine dewatering projects in complex hydrogeological settings, in *Proceedings of 4th Itasca Symposium on Applied Numerical Modeling in Geomechanics,* March 7–9, 2016, Lima, Peru, pp. 509–518.

Proceedings of Mine Water Solutions 2018
June 12–15, 2018, Vancouver, Canada
Published by the University of British Columbia, 2018

Numerical Groundwater Flow and Thermal Transport Modelling in Cold Regions

Mundzir Basri, Stantec, Canada
Niloofar Firoozy, Stantec, Canada

Abstract

Groundwater inflow estimation to mine pits in cold regions is one of the many challenges in mine development projects. Pit groundwater inflow can be estimated using a numerical groundwater flow model that is developed for the mine site. Such groundwater flow modelling is commonly simulated under steady-state conditions. In northern cold regions, groundwater flow modelling approach for estimating pit inflow is difficult due to freezing of the pit wall during winter periods. Sub-zero air temperatures can freeze the pit wall, which in turn reduces the hydraulic conductivity of the pit wall to practically zero. The frozen ground with near zero hydraulic conductivity will prevent groundwater inflow into the mine pit.

The paper discusses application of a freezing and thawing module built in a three-dimensional groundwater flow and thermal transport FEFLOW model to predict groundwater inflow rates into the mine pit. A series of simulation runs, from simple, one-dimensional steady-state modelling to more complex three-dimensional, transient, variably saturated groundwater flow and thermal transport modelling with water-ice phase change was completed. The following four modelling scenarios were evaluated: steady-state saturated unconfined aquifer, transient saturated groundwater flow, transient variably saturated flow, and transient variably saturated flow and thermal transport with freezing-thawing module. The results of groundwater inflow simulations obtained from one excavation site in Winnipeg area and an open pit mine in Northern Manitoba are presented and discussed in this paper. Significant reduction in pit groundwater inflow estimation was observed for the open pit mine using frozen walls in comparison to the standard groundwater flow modelling approach.

Introduction

Open pit mine development has been increasing significantly in the last decade. Groundwater inflow estimation to mine pits is one of the main tasks in open pit mine development projects. The construction and operation of open pits could have significant impacts on the environment, such as altering the ambient groundwater system. Groundwater inflow to the open pit could affect the slope stability,

complicate pollution control, and consequently increase the mining cost. To reduce the groundwater inflows to the pits, dewatering plans that include cut-off walls, perimeter pumping wells, and piping system are designed and used by engineers. The optimal dewatering plan reduces groundwater inflow to excavation area and the impacts of project construction and operation on the surrounding environment, as well as minimizing the associated costs.

Groundwater inflows can be estimated using analytical or numerical modelling; however, numerical modelling is generally more accurate due to its capability in simulating discontinuous, non-homogeneous and anisotropic mediums, transient flow, and temperature impacts.

In the cold climate regions, when continuous or discontinuous permafrost exist and air temperatures vary considerably from well below freezing during winter to well above freezing during summer, groundwater inflow estimates using traditional analytical solutions and steady-state numerical groundwater flow approaches can be inaccurate. Generally, when the soil temperature drops below freezing, the water changes phase from liquid to solid within the soil formations. This frozen ground acts as a shield, which reduces the hydraulic conductivity of the soil to approximately zero and reduces the groundwater flow significantly. This natural phenomenon is a practical seasonal dewatering plan regardless of existence of continuous or discontinuous permafrost, which would reduce the mining operational costs in some cases. However, most mining projects are designed based on the steady-state models, which do not include the coupled impact of seasonally variable temperature and flow. Additionally, the standard groundwater flow modelling approach yields constant groundwater inflow to an open pit year-round. This standard approach fails to capture seasonal freezing-thawing process, which is a characteristic of groundwater flows in northern cold regions.

The objective of this paper is to evaluate the impact of freezing and thawing process in pit groundwater inflow estimation using a newly coupled groundwater flow and thermal transport model. The groundwater inflow estimates obtained from both modelling approaches, standard and coupled flow and transport, were based on flow and thermal properties as well as time varying air temperatures from actual mine site in Northern Manitoba. However, both models were not calibrated against observed groundwater inflows in the field. These results will be refined as soon as groundwater inflows measured in the field are available.

Methodology

Coupled groundwater flow and thermal transport models with freeze-thaw process were developed to assess the impact of sub-zero temperatures on groundwater inflow estimates. Air temperatures can change groundwater temperatures along the excavated walls of open pits, which in turn change the groundwater phase from fluid (liquid) to ice (solid) and vice versa. Traditionally, this water-ice phase change process is

not accounted for or coded in the groundwater flow and thermal transport modelling approach. Hydraulic conductivity at the overburden layer and along pit walls therefore remain the same throughout the simulation periods in traditional groundwater flow and thermal transport modelling approach.

Coupled groundwater flow and thermal transport models with a freeze-thaw process modelling approach accounting for seasonal variation of atmospheric temperatures could be used to provide a feedback between a change in groundwater temperature and a related change hydraulic conductivity.

FEFLOW-piFreeze (DHI Mike, 2016) was used to estimate groundwater inflow to an open mine pit in a cold region where temperatures fall enough to potentially freeze groundwater at the pit wall interface. To simulate the freezing and thawing process (water to ice and vice versa), the piFreeze module was introduced to the FEFLOW model (Diersch, 2014).

A series of modelling simulations was performed to compare the standard flow modelling results with those obtained from the coupled flow and thermal model. The coupled groundwater flow and thermal transport model with freeze-thaw process was assessed and tested for a simple one-dimensional model to confirm freeze-thaw effects on hydraulic conductivity changes in porous media using piFreeze. For this modelling scenario, groundwater inflow was not assessed and reported. Transient saturated groundwater model with and without freeze and thaw was assessed using a simple 3D model. This modelling simulation was then performed on an excavation site in Winnipeg, MB. The outcome of the simulation will not be presented in this paper but will be discussed in the Results section. Lastly, a complex 3D model based on an actual mine site in Northern Manitoba was used to compare the standard modelling approach with coupled groundwater flow and thermal transport approach for a transient variably saturated condition.

Modelling Scenarios

The first modelling scenario being evaluated in this paper is the Lunardini benchmark model (Jeffery et al., 2006). Lunardini is a three-zone model that is divided into three sections fully frozen, partially frozen, and thawed. A simple 1D model was defined in FEFLOW for coupled groundwater flow and thermal transport scenario. By commencing the simulation and accounting for expansion of the fully frozen parts, hydraulic conductivity dropped to almost zero. In the thawing process, the temperature increased to above zero and hydraulic conductivity went up to ambient condition for partially frozen and thawed sections. Therefore, the impact of coupled flow and thermal transfer modelling on hydraulic conductivity changes in porous media was confirmed using the Lunardini benchmark model.

The second modelling scenario is a simple excavation model (Figure 1) to allow further comparison of the standard method and the coupled method developed. This model was defined as a simple

rectangular excavation with 3 hydrostratigraphic units. The groundwater inflow to the excavated area was simulated using both standard and coupled methods and the results were compared.

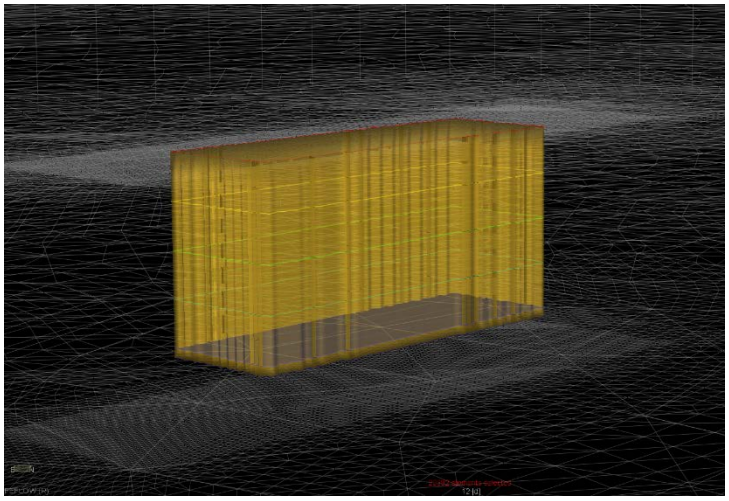


Figure 1: Excavation area with simplified boundary conditions

The variably saturated flow and thermal transport model was developed for a mine site located in the Northern Manitoba (Figure 2). This model represents a complex system with significant heterogeneity and an approximately 300 m depth open pit. Based on Environment of Canada (2013), historical climate data, the average temperature over 30 years showed subzero conditions for 6 months of the year at the mine site. Therefore, the groundwater inflow to the mine pit was expected to decrease significantly using coupled groundwater flow and thermal properties model due to approximately zero hydraulic conductivity within this period.

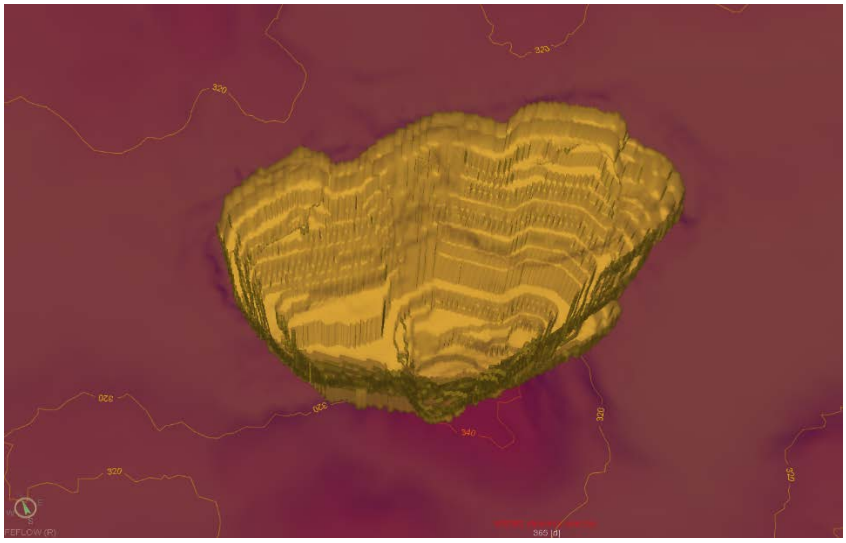


Figure 2: Open pit mine at Northern Manitoba

Results

The simulation results obtained from the standard and coupled flow modelling are presented in this section. The groundwater inflow to the excavation area and the open pit was predicted to decrease for the scenarios with freezing and thawing cycles. For the excavation model, the average inflow was reduced by 50% when the freezing and thawing was incorporated into the simulations (Table 1). The minimum seepage to the excavation area was $1x10^{-5}$ m^3/s, which occurred during the winter (freezing) period. The maximum seepage was also attributed to the thawing months during snow melt when large volumes of water were released to the surface of the pit and the model domain. The total inflow to the excavation shows the reduction of 50% over the simulation time. The total, minimum, and maximum inflows are the FEFLOW output, which were derived as inflow rates (m^3/s).

Table 1: Daily groundwater inflow into deep excavation

Time (month)	Temperature (°C)	Inflow – with freezing and thawing (m^3/s)	Inflow – without freezing and thawing impact (m^3/s)*
1	–23	0.00001	0.02402
2	–25	0.00066	0.00741
3	–15	0.00208	0.05976
4	–5	0.00199	0.02053
5	5	0.02311	0.01956
6	15	0.02015	0.02357
7	17	0.02310	0.02405
8	15	0.02215	0.02125
9	8	0.02108	0.01678
10	2	0.00239	0.02253
11	–15	0.00014	0.02548
12	–17	0.00004	0.01466
	Total	0.11388	0.27959
	Average	0.05587	0.17392
	Min	0.00001	0.00741
	Max	0.02311	0.05976

The pit groundwater inflow comparisons obtained from the standard groundwater flow model and coupled flow-thermal model with and without freeze-thaw cycles for a mine site in the Northern Manitoba is presented in Figure 3. The temperature was below zero from January to the end of March and then from November to the end of December. The estimated groundwater inflow to the mine pit is almost

zero during the freezing months. By increasing the temperature, the groundwater inflow to the pit increased as well. The total predicted inflow obtained from the steady-state standard groundwater flow simulation was 0.28 m^3/s. The transient variably saturated groundwater-flow model predicted 0.026 m^3/s for the total inflow. The predicted inflow obtained from the coupled transient variably saturated groundwater-flow and thermal transport predicted a maximum of 0.026 m^3/s and zero during sub-zero temperature periods over 6 months with the total average annual groundwater inflow of 0.0058 m^3/s.

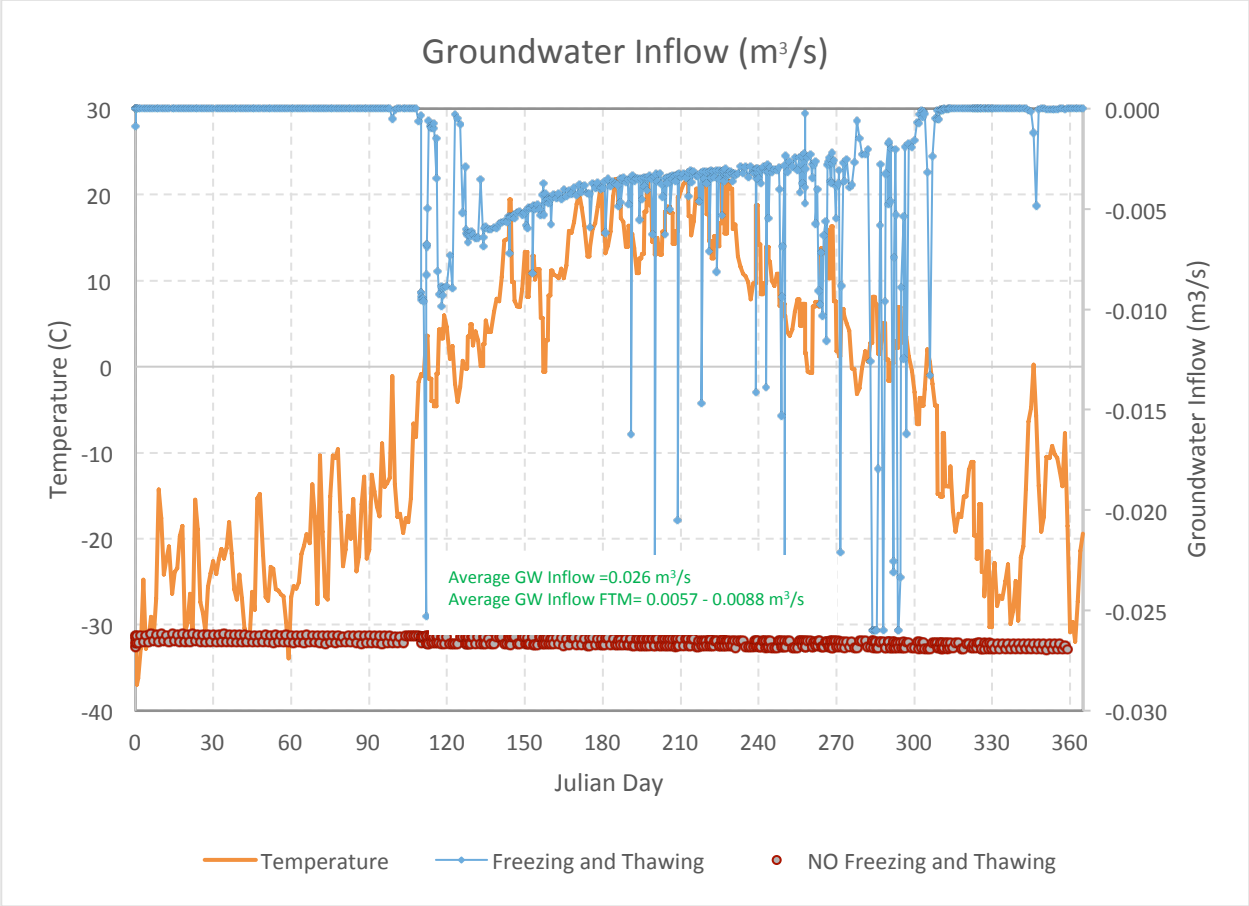


Figure 3: Groundwater inflow comparison using standard (no freezing and thawing) and coupled flow and thermal (with freezing and thawing) scenarios

Conclusion

In this paper the application of a freezing and thawing module in groundwater inflow estimation was assessed using four modelling scenarios. By incorporating changes in the thermal properties, groundwater inflow decreases significantly. Hydraulic conductivities of the areas exposed to air temperature reduced to approximately zero when the air temperature dropped to zero and below zero (during winter periods). The standard and coupled methods were assessed using a complex model designed for an actual mine site in Northern Manitoba. The simulation results using the coupled method showed that the total groundwater

inflow for one year of simulation was reduced to one-quarter of the total groundwater inflow derived from the traditional groundwater flow modelling approach.

The coupled groundwater flow and thermal properties approach is a more reliable representation of the inflow to excavations or ground opening in cold regions due to its ability to incorporate climate conditions into the modelling process.

References

DHI Mike. 2016. piFreeze – A Freeze/Thaw Plug-in for FEFLOW: User Guide.

Diersch, H.-J. 2014. *FEFLOW: Finite Element Modeling of Flow, Mass and Heat Transport in Porous and Fractured Media.* Berlin: Springer.

Bibliography

Government of Canada. 2015. Environment and natural resources, past weather and climate. Retrieved from http://climate.weather.gc.ca/historical_data/search_historic_data_e.html.

Jeffrey, C.M., Voss, C.I. and Siegel, D.I. 2007. Groundwater flow with energy transport and water-ice phase change: Numerical simulations, benchmarks, and application to freezing in peat bogs, *Advances in Water Resources,* 30(4): 966–983, ISSN 0309-1708, https://doi.org/10.1016/j.advwatres.2006.08.008.

Proceedings of Mine Water Solutions 2018
June 12–15, 2018, Vancouver, Canada
PUBLISHED BY THE UNIVERSITY OF BRITISH COLUMBIA, 2018

Enhanced Reclamation of the Giant Nickel Tailings Storage Facilities in British Columbia, Canada

Allison Brown, Barrick Gold Inc., Canada
Drummond "Dusty" Earley III, D3 Geochemistry LLC, USA

Abstract

The Giant Nickel Mine (Giant Nickel) is located approximately 10 km north of the community of Hope, British Columbia, Canada and comprises a closed underground copper and nickel mine, mill, and waste disposal facilities that were operated from 1959 to 1974. The Upper and Lower tailings storage facilities (TSFs) ceased operation in the mid-1970s and contain an estimated 4 to 5 million tonnes of mill tailings. A soil cover was placed on the tailings surface in 1995 and the site was revegetated with volunteer native plant species and deemed to be in a "passive closure" state requiring no active management and limited monitoring. Barrick Gold Corporation (Barrick) acquired the closed property in 2002 as part of a merger with Homestake Mining Company (Homestake).

In recent years following the Mount Polley tailings dam failure, the British Columbia Ministry of Energy, Mines and Petroleum Resources (BC MEMPR) has required all active and closed TSFs in the province be evaluated for compliance with current dam safety requirements. In response to this directive Barrick initiated a holistic evaluation of the Giant Nickel TSFs and is updating the site closure plan to reflect the company's overarching goal of creating a stable, non-polluting landform with a beneficial end use. This evaluation focuses on several unique but related aspects, including: dam safety; tailings and construction material geochemistry (e.g. metal leaching and acid rock drainage potential); water balance; predictive long-term water quality; and, contaminant flow paths.

Results from environmental monitoring, water quality modelling and geochemical characterization are also being used to design a passive water treatment feature to polish perennial seepage from the Upper TSF prior to release. This represents an important improvement on previous reclamation efforts, which considers input from regulators, community members and First Nations.

This project demonstrates that reclamation of older, closed mine sites can be enhanced, according to modern standards and best available technologies, to meet the social, environmental, and economic needs of the surrounding communities.

Introduction

Giant Nickel is located approximately 10 km north of the community of Hope, British Columbia, Canada (Figure 1) and comprises a closed underground copper and nickel mine, mill and waste disposal facilities that were operated from 1959 to 1974. The Upper and Lower TSFs ceased operation in the mid-1970s and contain an estimated 4 to 5 million tonnes of mill tailings. A soil cover was placed on the tailings surface in 1995 and the site was revegetated with volunteer native plant species (mostly alders, conifers and shrubs) and deemed to be in a "passive closure" state requiring no active management and limited monitoring. Barrick acquired the closed property in 2002 as part of a merger with Homestake.



Figure 1: Giant Nickel site location in British Columbia, Canada

The climate of the Giant Nickel site is classified as West Coast Marine/Alpine, which is characterized by relatively mild, wet winters and cool, moderately dry summers. The average annual precipitation is approximately 1,500 to 2,000 mm (Knight Piésold, 2016b) and the average annual lake evaporation is approximately 900 to 1,1000 mm (Summit Environmental Consultants, 2010). There is therefore an excess water balance for water bodies in this area and frequent runoff events, especially in the fall rainy season and spring freshet.

The TSFs were constructed in a north-south trending intermontane valley located adjacent to steep bluffs to the west as shown in Figure 2. The site drains to the east and south into Stulkawhits Creek, which is a primary tributary to the Fraser River. Runoff from the bluff reports to the heel of the Upper TSF and then flows southward down Bearsh. Creek to Stulkawhits Creek.



Figure 2: Giant Nickel TSF facilities and Bearsh. Creek

In early 2015, during Barrick's initial reconnaissance survey of the Giant Nickel TSFs and dams in response to BC MEMPR orders after the Mount Polley tailings dam failure, it was noted that two water ponds had developed on the TSFs: one on the Lower TSF and a much smaller pond on the Upper TSF in a low-lying area between two dykes. In 2015, water from the former Upper TSF pond was conveyed along a constructed channel called "Saskatoon Creek" to the Lower TSF pond as shown on Figure 3. The Lower TSF pond was drained that same year, but filled up again in 2016.

Water quality monitoring conducted along Saskatoon Creek and in the receiving environment indicates that contact and non-contact water in the area is generally of good quality. Some contact water samples collected in 2015 and 2016 (e.g. seeps and ponded water) showed slightly elevated iron, manganese, sulphate and trace metals concentrations, including aluminum, copper and selenium. Iron was the only constituent that consistently exceeded BC Water Quality Guidelines (BC WQGs) for freshwater aquatic life in perennial tailings seepage (Knight Piésold, 2017).

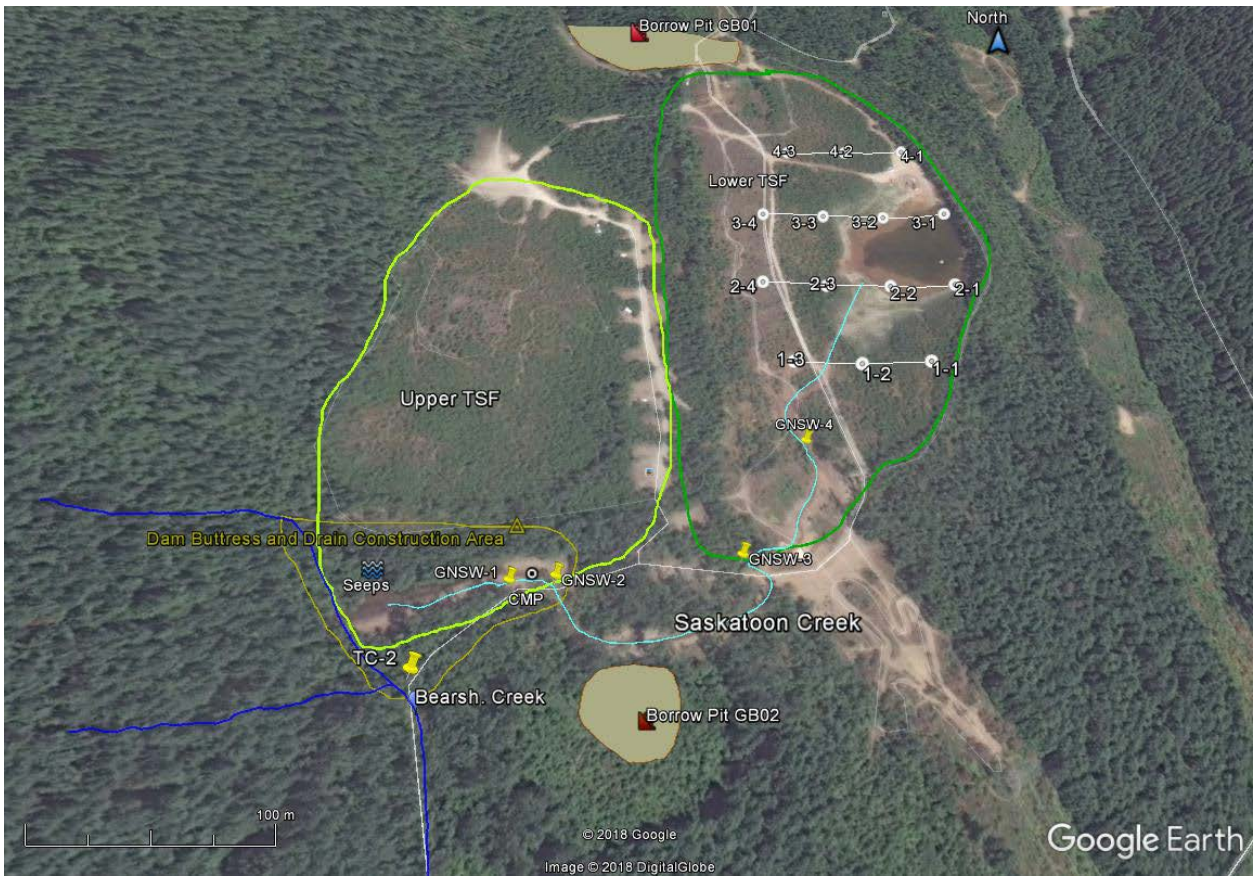


Figure 3: Giant Nickel TSF reclamation and study area

Closure and reclamation activities at Giant Nickel are governed by *Mines Act* Permit M-64, which was revised and re-issued by BC MEMPR in 2017. The Giant Nickel TSF site is leased Crown land with no designated land status and sparse population. Some land parcels along BC Nickel Mine road are under private ownership but are largely undeveloped. The site is situated directly within a transmission line corridor and adjacent to forested areas with logging operations. In addition, there is heavy off-road recreational vehicle traffic in the area.

The multiple land uses in this area present a unique challenge for establishing an end land use for the site. Engagement with relevant regulatory agencies, local community members and First Nations stakeholders led Barrick to initiate an evaluation of the Giant Nickel TSFs and update the closure plan to reflect the company's overarching goal to create a stable, non-polluting landform with a beneficial end use. While the main driver of the evaluation is related to dam safety and engineering, the studies include other related aspects, including tailings and construction material geochemistry (e.g. metal leaching and acid rock drainage potential [ML-ARD]); water balance; predictive long-term water quality; and, contaminant flow paths. This evaluation has given Barrick an opportunity to review the success of past

closure and reclamation practices while applying modern knowledge and methods to enhance site conditions.

As the project evolved from conceptual design through to detailed engineering and construction, Barrick, in partnership with a multi-disciplinary team of technical experts, endeavoured to use monitoring and site investigation results to understand the operational history, build on previous reclamation efforts and refine execution plans. As described in the following sections, three important elements of this work include: predictive water quality modelling, geochemical characterization, and water treatment design.

At the time of writing, Barrick was in the early stages of executing a significant project to regrade the Lower TSF and install dam buttresses, collection channels, diversion ditches and other water management features for both the Lower and Upper TSFs to minimize ponding on the facility and promote draindown of the tailings. The final land use and remediation plan for the site is under development in consultation with key stakeholders. Construction is anticipated to be complete by year-end 2018.

Predictive Water Quality Modelling

The Giant Nickel TSFs have a positive water balance and perennial seepage has existed along the south toe of the Upper TSF since the facilities ceased operation. A key component of the enhanced reclamation of the TSFs is construction of a passive water treatment feature to mitigate potential environmental impacts associated with discharging seepage from the Upper TSF to the environment.

To initiate design of this feature, parameters of interest were determined based on seepage water quality monitoring results. Parameters of interest were identified by comparing average water quality results to BC WQGs for freshwater aquatic life (BC MOE, 2017). A comparison of average surface water quality results from locations representing the Upper TSF drainage (GNSW-1), points along Saskatoon Creek (GNSW-2-, GNSW-3, GNSW-4), Bearsh. Creek (TC2) and Stulkawhits Creek (TC1) is presented in Figure 4. Where guideline values are pH-dependent, a value of 7.9 was used to represent the typical pH of potential receptors. Where guideline values are hardness-dependent, it was assumed that hardness of the receiving environment (Stulkawhits Creek) is 30 mg/L. Where an analytical result is reported as less than the detection limit, its value is assumed to be equal to half of the detection limit for calculation purposes. All metals results are presented as total concentrations.

Parameter	Freshwater Aquatic Life WQG	GNSW-1-U	GNSW-2-U	GNSW-3-U	GNSW-4-L	TC2	TC1
		Average Value 2015-2016 (mg/L)					
pH - *pH units*	6.5-9.0	7.0	7.0	7.3	7.7	7.4	7.5
Alkalinity (as total $CaCO_3$)	NL	ND	29	29	52	22	23
Ammonia (as N)	pH and temperature-dependent	0.04	0.10	0.07	0.04	0.01	0.009
Total Dissolved Solids (TDS)	NL	ND	495	469	433	74	54
Total Suspended Solids (TSS)	Change relative to background	ND	6	4	3	2	2
Aluminum (Al)	pH-dependent	0.028	0.035	0.047	0.044	0.084	0.102
Antimony (Sb)	NL	0.00005	0.00005	0.00005	0.00005	0.00005	0.00006
Arsenic (As)	NL	0.00010	0.00006	0.00006	0.00008	0.00007	0.00013
Barium (Ba)	NL	0.0323	0.0296	0.0321	0.0323	0.0160	0.0180
Beryllium (Be)	NL	0.0005	0.0005	0.0005	0.0007	0.0018	0.0015
Bismuth (Bi)	NL	0.00003	0.00003	0.00003	0.00003	0.1	0.1
Boron (B)	NL	0.005	0.007	0.005	0.006	0.005	0.005
Bromide (Br)	NL	0.025	0.025	0.025	0.025	0.025	0.025
Cadmium (Cd)	Hardness-dependent	0.00001	0.0010	0.0010	0.0012	0.0036	0.0029
Calcium (Ca)	NL	0.0002	0.0002	0.0002	0.0004	0.0003	0.0004
Chloride (Cl)	600	0.486	0.486	0.480	0.440	0.290	0.300
Chromium (Cr)	NL	0.0002	0.0010	0.0011	0.0014	0.0040	0.0030
Cobalt (Co)	0.11	0.0020	0.0027	0.0027	0.0022	0.0037	0.0030
Copper (Cu)	Hardness-dependent	0.0004	0.0003	0.0003	0.6855	0.0009	0.0016
Fluoride (F)	Hardness-dependent	0.04	0.03	0.03	0.03	0.06	0.06
Iron (Fe)	1	9.74	5.39	1.97	0.69	0.32	0.17
Lead (Pb)	Hardness-dependent	0.00003	0.00003	0.00003	0.00003	0.00003	0.00003
Lithium (Li)	NL	0.003	0.003	0.003	0.003	0.003	0.003
Magnesium (Mg)	NL	32.2	43.3	40.3	44.2	4.6	3.8
Manganese (Mn)	Hardness-dependent	0.736	0.650	0.582	0.419	0.065	0.019
Mercury (Hg)	NL	0.000003	0.000003	0.000003	0.00001	0.00002	0.00002
Molybdenum (Mo)	2	0.0003	0.0034	0.0034	0.0040	0.0108	0.0087
Nickel (Ni)	NL	0.0179	0.0188	0.0172	0.0140	0.020	0.025
Nitrate and Nitrite (as N)	Hardness-dependent	0.08	0.07	0.09	0.07	0.07	0.1
Phosphorus (P)	NL	0.03	0.006	0.008	0.01	0.005	0.004
Potassium (K)	NL	5	8	7	7	3	2
Selenium (Se)	NL	0.0002	0.0200	0.0201	0.0251	0.0715	0.057
Silver (Ag)	Hardness-dependent	0.00001	0.00100	0.00101	0.00125	0.0036	0.0029
Silicon (Si)	NL	11	11	10	8	6	4
Sodium (Na)	NL	2.18	2.78	2.66	2.60	1.70	1.20
Strontium (Sr) - *Bq/L*	NL	2	3	3	3	2	3
Sulphate (SO_4)	NL	130	182	168	182	18	12
Thallium (Tl)	NL	0.00005	0.02000	0.02004	0.02504	0.07100	0.05700
Tin (Sn)	NL	0.00005	0.00005	0.00005	0.00005	0.00005	0.00005
Titanium (Ti)	NL	0.005	0.005	0.005	0.005	0.005	0.006
Uranium (U)	NL	0.00001	0.00001	0.00001	0.00001	0.00001	0.00001
Vanadium (V)	NL	0.0003	0.0003	0.0003	0.0003	0.0003	0.0003
Zinc (Zn)	Hardness-dependent	0.002	0.003	0.002	0.003	0.002	0.002

Legend:
Exceeds freshwater aquatic life WQG

Notes:
1. All units are in mg/L unless otherwise noted in italics.
2. Guidelines are for total metals.
3. Limits are short-term maximums for single grab samples.
4. NL denotes no short-term maximum limit exists for single grab samples.
5. ND denotes no data.
6. Where laboratory results were below the Method Detection Limit (MDL), 50% of the MDL was used for calculating average values.

Figure 4: Average surface water quality of Upper TSF seepage (Barrick Gold Inc., 2017)

The primary constituent of concern for the Upper TSF seepage water is total iron. It is of interest to note that iron concentrations progressively decrease over the length of the current seepage collection channel, from GNSW-1 through GNSW-4 (Figure 5), which may indicate that water quality improvements can be achieved with adequate retention time.

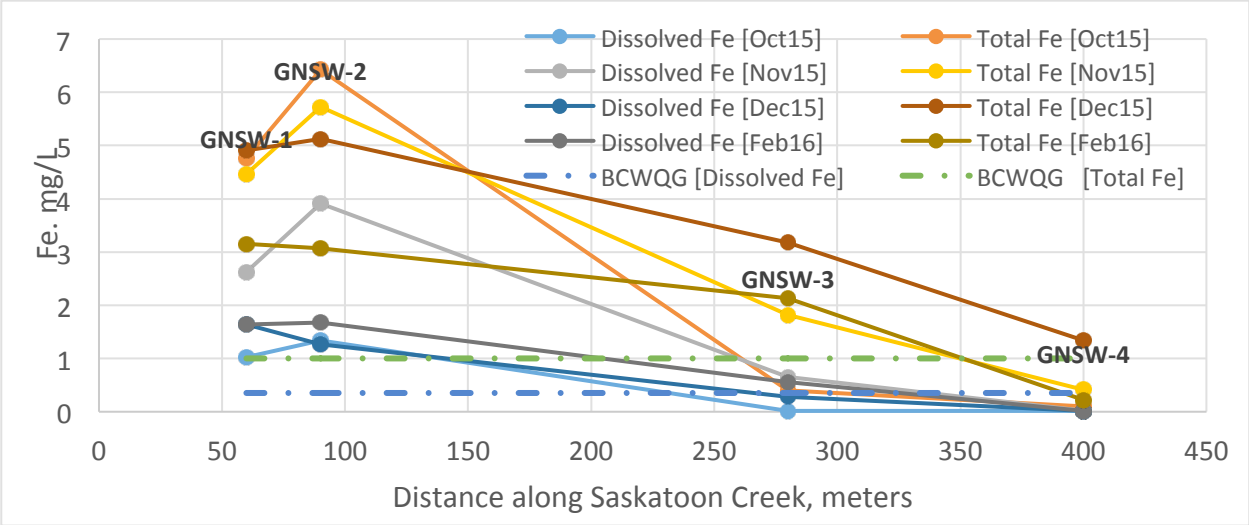


Figure 5: Saskatoon Creek iron concentrations compared to BC WQG

Geochemical computer modelling indicates that iron is oxidizing and precipitating at a predictable kinetic reaction rate such that iron concentrations meet BC WQGs for total and dissolved iron by the time the seepage water reaches GNSW-4, less than 500 m downstream of GNSW-1 (Figure 6). Computer simulations also show that passive treatment of iron is possible such that a discharge of treated seepage to the environment at Bearsh. Creek will meet BC WQGs given sufficient retention time and oxidation.

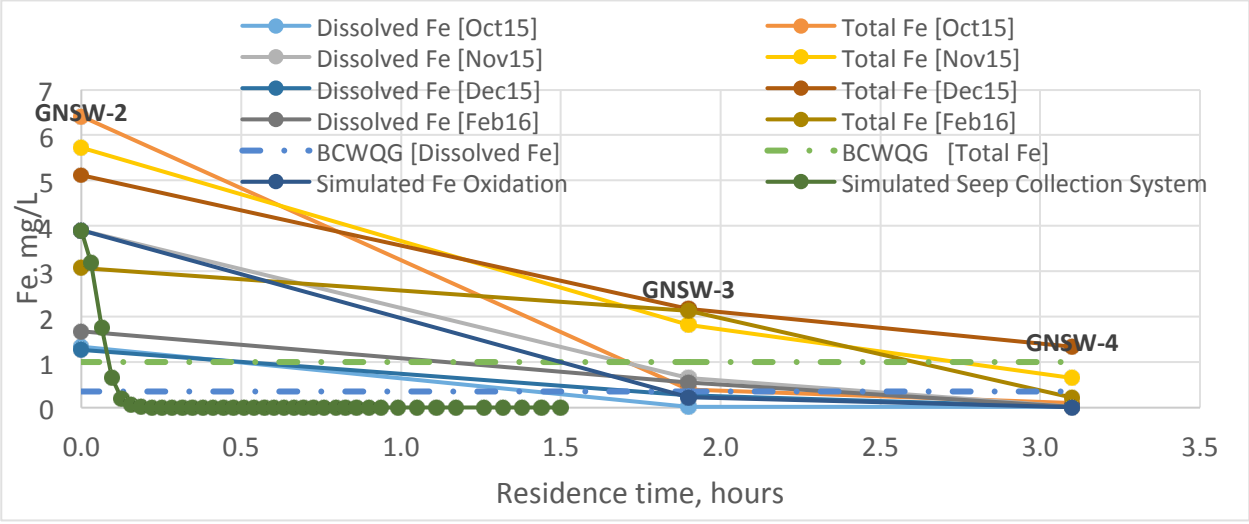


Figure 6: Saskatoon Creek actual and simulated iron concentrations versus time

Geochemical Characterization

Although there has been no evidence of acid generation or significant metal leaching observed on site to date, Barrick initiated geochemical characterization of construction materials and tailings to better understand the current and predicted future state of the site and adjust construction and mitigation plans as needed. Results of borrow material testing done in 2016 showed that construction source materials are non-acid generation and have little metal leaching potential (Knight Piésold, 2016a). However, as engineering design and permitting progressed for construction, it was identified that infilling the Lower TSF with coarse rock to eliminate water ponding on the surface could change the saturated and free-draining state that the TSF had been in for several decades.

In 2017 Barrick was asked by BC MEMPR to investigate potential impacts of the proposed works on long-term tailings geochemistry. Barrick undertook an extensive sampling and analysis program to address the following questions:

- What is the predicted post-construction pore water and seepage water quality?
- What impact could this changed water quality have on the receiving environment?
- What mitigation measures are required?
- What monitoring should be undertaken on the Lower TSF following construction to evaluate the new condition and potential environmental impacts?

Methodology

Tailings samples were collected from the Lower TSF by sonic drilling in October 2017. Drilling services were provided by Mud Bay Drilling from Surrey, BC using their Sonic ATV-2 rig (Figure 7). A 3.5-inch diameter sonic core barrel was used to collect continuous core samples of the tailings in 10 to 20-foot sampling intervals. Approximately 5 to 6 feet of core was extruded from the core barrel into thick plastic bags for handling. Water was not used in coring until bedrock was encountered beneath the tailings. Most of the sonic borings were drilled into moist to saturated tailings materials.



Figure 7: Sonic drilling rig operations for tailings sampling on the Lower TSF

Tailings samples were collected at different borehole locations and depths along 4 east-west traverses across the Lower TSF for geographic coverage with a spacing of approximately 50 m as shown on Figure 3. Continuous tailings samples were collected at approximately 1 to 5-foot intervals (0.3 to 1.5 m, original drilling units are feet below ground surface) depending upon core recovery and depth of the horizon. Tailings were logged and sampled by geologists and environmental professionals with requisite training requirements. The bagged core was placed in boxes and the bags were cut and peeled back for photographs, logging, and sample collection. Figure 8 and Figure 9 are representative field photographs of oxidized and unoxidized tailings cores, respectively.

Continuous, representative samples of the Lower TSF tailings were collected from each borehole. Tailings samples were taken from the oxidized zone near the ground surface and unoxidized tailings at progressively deeper depths below the surface up to a maximum depth of approximately 22.5 m below ground surface. Surface cover, construction fill and underlying native ground were not sampled. The sampling horizons were determined visually during logging. A titanium trowel was used to collect the sample by scoring a wedge-shaped groove along the entire length of each core interval, representing approximately a ⅛ to ¼ split. Approximately 0.5 to 4 kilograms of material were collected with each sample depending upon the length, density and moisture content of the retrieved core material.



Figure 8: Oxidized tailings core from the Lower TSF

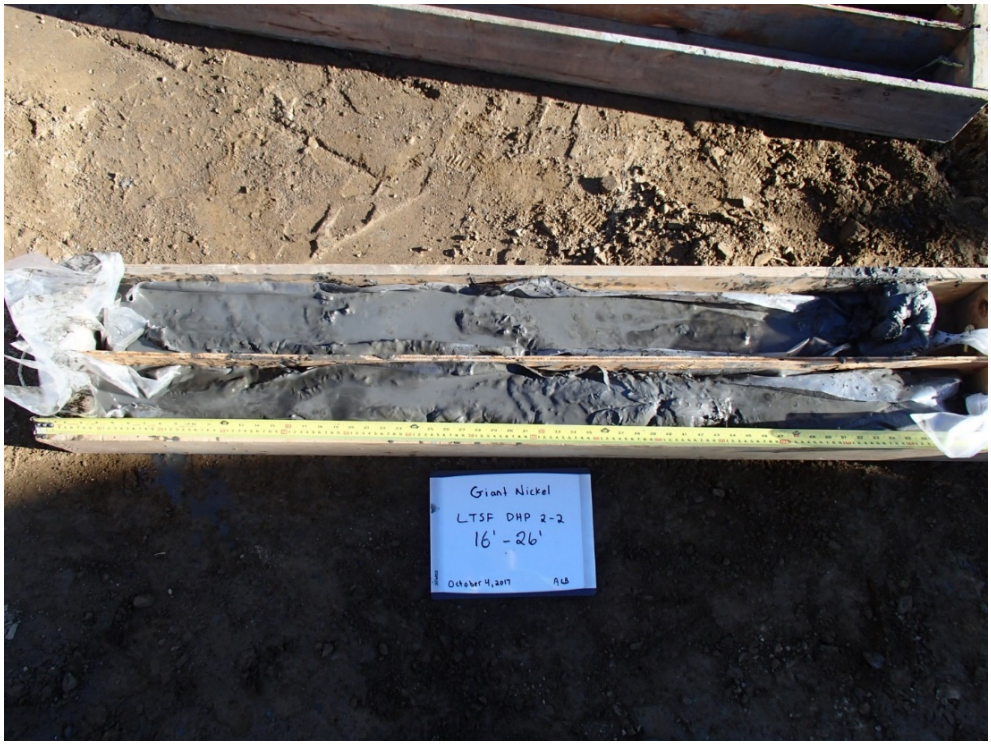


Figure 9: Unoxidized tailings core from the Lower TSF

The sample was collected in a heavy-duty plastic sampling bag, labelled, and sealed. The samples were then overpacked in 5-gallon plastic pails and sealed with Chain of Custody forms prior to shipment to Maxxam Laboratory located in Burnaby, BC for analysis. After the samples were collected, the core residues were discarded on site and the core hole was backfilled with 2 bags of bentonite at the base plus core residue and local fill material on top.

A total of 84 samples, not including duplicates, were collected for geochemical characterization. This equates to approximately 1 sample per 50,000 tonnes of tailing, which is a representative sampling ratio according to MEND guidelines (MEND, 2009). Acid base accounting and other geochemical analyses are also being conducted according to MEND (2009) guidelines.

Data and Discussion

Figure 10 provides strip log profiles of each sonic borehole. In each borehole the relatively thin oxidized tailings zone near the ground surface appeared to transition relatively sharply into the thicker deposits of unoxidized tails at greater depth based on visual criteria. The maximum thickness of the oxidized zone is approximately 2 m and the maximum thickness of the unoxidized tails is approximately 15 m.

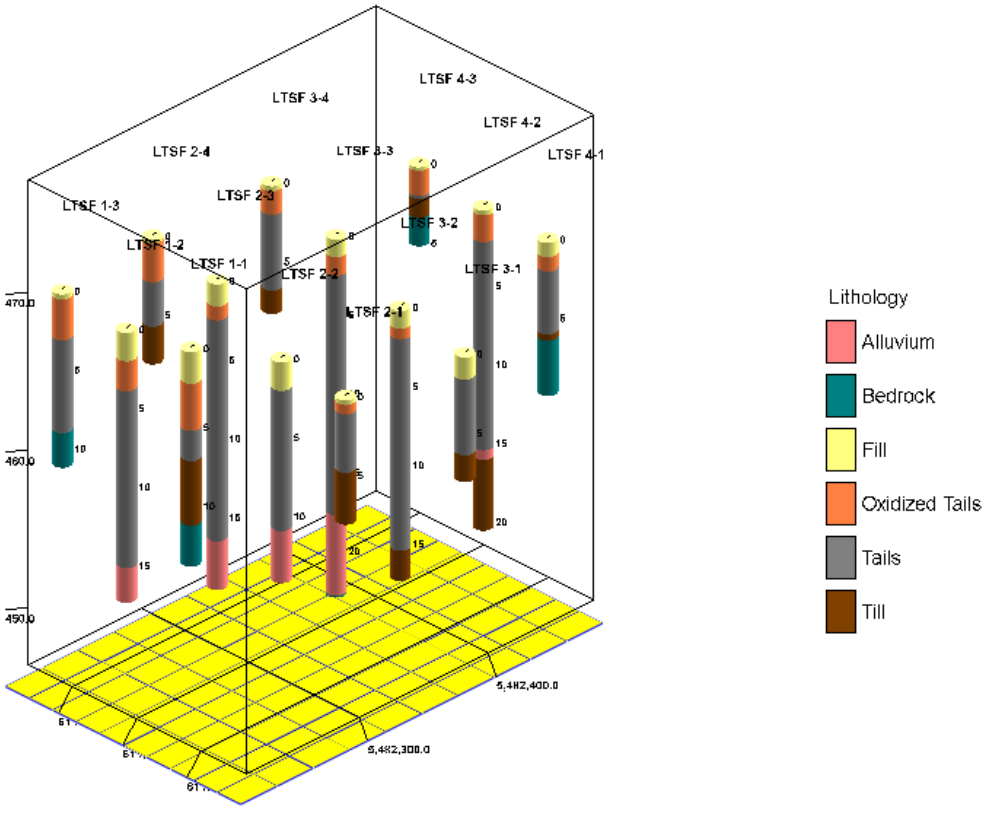


Figure 10: Lower TSF borehole logs (elevations, asl and depths, bgs in meters)

The primary indicator of oxidation is the orange to yellowish brown colour of the tailings, likely as a result oxidation of iron sulphide minerals to iron oxide minerals near the surface of the Lower TSF (Figure 8). The oxidized tailings also appeared to be coarser grained than the unoxidized tailings and was predominantly characterized as a fine sandy silt with lesser clay. The unoxidized tailings are dark grey and wetter than the oxidized tails as they contain more clay and the texture ranged from a sandy silt clay to silty clay. Loss of clay from the oxidized zone may have resulted during weathering and infiltration causing clays to be mobilized to deeper horizons in the Lower TSF. Thin hardpan and ferricrete layers were observed at the contact between oxidized and unoxidized tails in some boreholes indicating downward eluviation of clays and iron from the oxidized zone and illuviation in the unoxidized zone. Within the unoxidized zone lenses in some core intervals contained up to 5 % fine grained but visible sulphides and metal oxides.

The tailings were deposited directly on glacial till, alluvium and bedrock (chlorite mica schist). A thin zone of organic plant matter was encountered in several boreholes at the contact between the tailings and native ground. The alluvial deposits rest underneath the central and deepest part of the Lower TSF and may have been deposited in a pre-existing stream valley deposit. No groundwater was encountered below the tailings of the Lower TSF and the relatively permeable alluvium channel may facilitate drainage. However, the unoxidized tailings in the central and thickest region of the Lower TSF is saturated due to high rates of precipitation, ponding at the surface, and low permeability resulting from high silt and clay contents. The oxidized tailings are thinnest in this region possibly because of near surface saturation and low oxygen content.

The overall distribution of the Lower TSF tailings can be described as a relatively thick wedge of material deposited in a valley or depression located between the Upper TSF and the Lower TSF dams (Figure 10). The upper tailings are oxidized but seepage water is not acidic and has relatively low concentrations of leachable metals. The samples have been submitted for laboratory analyses to determine their full ML-ARD potential as the new reclamation configuration may change the overall water balance and drainage characteristics of the TSFs. Alluvial deposits at the base of the TSF may have been deposited by pre-existing streams or post glacial outwash on top of bedrock and till and appear to facilitate drainage of the tailings.

A final tailings geochemical assessment will be completed once results from laboratory testing are available.

Water Treatment Design

The current TSF reclamation plan includes construction of a passive water treatment feature to mitigate elevated total iron concentrations in seepage from the Upper TSF. A preliminary alternatives assessment

was undertaken by Barrick in 2016 to evaluate potential mitigation options. Following evaluation of water monitoring data and predictive water quality results, a preliminary treatment design was developed collaboratively by Barrick, D3 Geochemistry and Knight Piésold. At the time of writing the passive water treatment feature comprised the following elements:

- Collection and transmission of seepage by way of buried drainage channels to a collection basin.
- Aeration of water as it enters the collection basin over rough rock feature.
- Transmission of water along a meandering, rip-rap filled channel to a final discharge point.
- Retention time of 0.2 hours or more (D3 Geochemistry, 2017).
- Discharge of water that meets BC WQGs.

Additional refinements may be made to this plan once results of geochemical characterization and other site investigations are available.

Conclusion

In recent year owners of closed mines in British Columbia have been required to evaluate TSFs and demonstrate conformance with current dam safety requirements. This directive gave Barrick an opportunity to gain an improved understanding of operational practices and post-closure conditions at the closed Giant Nickel Mine near Hope, British Columbia; evaluate success of reclamation activities implemented by Homestake; and revise long-term closure plans in consideration of modern standards, regulatory requirements, and community expectations.

In 2017 Barrick initiated a construction project to improve geotechnical conditions and water management at the Giant Nickel TSF site. A multi-disciplinary team was established to provide input into conceptual and detailed designs for the project. The overarching objective of the project is to create a stable, non-polluting landform with a beneficial end use. To achieve the design goals, consideration was given to the following interrelated aspects: dam safety; tailings and construction material geochemistry (e.g. metal leaching and acid rock drainage potential); water balance; predictive long-term water quality; and contaminant flow paths.

Outcomes of site investigations, ongoing environmental monitoring, and new information gleaned through recent construction activities are being used to continually refine and improve mitigation strategies and designs. As an example, water quality data collected from perennial Upper TSF seepage and Saskatoon Creek along with data collected from waste rock and tailings geochemical assessments is being used to design a passive water treatment feature as part of the overall TSF reclamation construction. Implementation of a passive treatment feature will help Barrick improve environmental outcomes for the Giant Nickel site, comply with current regulatory requirements, and meet community expectations.

The work at Giant Nickel, although not yet complete, shows the benefit of having a multi-disciplinary team working collaboratively to progressively refine designs as new information becomes available. It also demonstrates that progressive reclamation concepts can also be applied to closed or legacy mines in an effort to apply new knowledge, standards, and practices to enhance environmental and social outcomes.

Acknowledgements

Many people have contributed their knowledge, skills, and experience to the Giant Nickel project over the years. Special thanks go to the current TSF reclamation project team, including representatives from Barrick, Knight Piésold, JDS Energy & Mining, D3 Geochemistry and Wiens & Tri-west Ventures Ltd.

References

Barrick Gold Inc. 2017. Tailings Storage Facility Embankment Stabilization Surface Water Monitoring Plan, Final – Rev 3.

British Columbia Ministry of Environment (BC MOE). 2017. British Columbia Approved Water Quality Guidelines: Aquatic Life, Wildlife & Agriculture, Summary Report.

D3 Geochemistry. 2017. Giant Nickel Upper TSF water quality review and prediction.

Knight Piésold. 2016a. Giant Nickel TSF 2016 Borrow Materials Reconnaissance Test Pit Program.

Knight Piésold. 2016b. Diversion of Bearsh Creek. Application for change approval for work in and about stream.

Knight Piésold. 2017. Waste Discharge Authorization Application Technical Assessment Report.

Mine Environment Neutral Drainage (MEND). 2009. Prediction Manual for Drainage Chemistry from Sulphidic Geologic Material, MEND Report 1.20.1.

Summit Environmental Consultants. 2010. Okanagan Water Supply and Demand Project: Phase 2 Summary Report.

Proceedings of Mine Water Solutions 2018
June 12–15, 2018, Vancouver, Canada
Published by the University of British Columbia, 2018

Implementing a Long-Term Closure Strategy for the Premier Gold Mine in Northwest British Columbia

Michael Dabiri, Klohn Crippen Berger, Canada
Charles Masala, Klohn Crippen Berger, Canada
Helena Lidhage, Boliden Limited, Sweden

Abstract

The Premier Gold Mine near Stewart, British Columbia, Canada, ceased mining operations in 1998. Since then, closure activities have included stabilization and revegetation of waste rock dumps, treatment of discharge from the underground mine, and upgrades to the Tailings Storage Facility (TSF). This paper focuses on the on-going implementation of a long-term water management strategy for the TSF and related components in a wet environment that receives an average of 2,200 mm of annual precipitation. Additional consideration is given to treatment of underground mine discharges and management of the resulting water treatment sludge.

Site-specific challenges include:

1. metal leaching and acid rock drainage (ML/ARD) from contemporary and historical mining activities on the site dating back to the 1920s, as well as potentially acid generating mine tailings and waste rock;
2. a wet environment subject to extreme storms and high peak flows; and
3. topographic and geologic constraints, including scarcity of construction materials and geohazard risks associated with steep, rocky terrain.

Sources of ML/ARD for the site were characterized through site-wide hydrologic and water quality modelling assessments. These were used to identify and quantify sources of chemical mass loading from historical and contemporary mining activities, and to assess the impact of proposed water management plans and external influences, such as upstream hydroelectric developments and climate change.

Measures that mitigate ML/ARD risks include:

1. design and implementation of a water cover and rockfill blanket to prevent oxidation and mobilization of tailings within the TSF;
2. reconstruction of water treatment sludge clarification ponds; and

3. on-going development of a long-term water treatment sludge management plan that accounts for the possibility of perpetual water treatment from underground workings.

Flood management measures include design and construction of a TSF closure spillway in bedrock, implementation of stabilizing measures on the TSF dam, and decommissioning the existing fuse plug spillway. These measures are designed to safely route peak design flows in excess of 500 m^3/s without compromising dam stability. Much of the site is characterized by high geohazard risks due to steep, rocky terrain and frequent rockfall.

The water management plan was designed to:

- eliminate reliance on diversion channels and access roads that are subject to risk of failure due to rockfall, and
- facilitate safe monitoring and sampling in key discharge areas. This includes construction of an upgraded TSF seepage monitoring system, allowing safe measurement and sampling of seepage, as well as scaling and ongoing monitoring of high-risk rock surfaces.

Geohazards, steep topography, and scarcity of suitable granular construction materials introduced additional challenges to the design and construction of water management infrastructure. However, the development and on-going implementation of water management solutions at the Premier Gold Mine has achieved the desired outcomes, by meeting challenges with suitable solutions.

Introduction

The Premier Gold Mine is 18 km north of Stewart, British Columbia, Canada, and 2.4 km northeast of the British Columbia-Alaska border, in an area commonly referred to as the "Golden Triangle" due to the abundance of high-grade gold deposits discovered in the region.

The history of mining activity near the Premier Gold Mine dates back to the 1860s, and the mine itself has been mined by various operators since 1918. Most recently, the mine was reopened by Westmin Resources in May of 1989. Mining ceased and the property was put into active care and maintenance in April of 1996. Milling of ore from the nearby Snip Mine, and other nearby operations, continued into the summer of 1996. Boliden acquired the Premier Gold Project from Westmin Resources in 1998 as part of a larger transaction.

To reduce the long-term risk and maintenance requirements of the closed facility, engineering design to improve the mine's long-term geotechnical, hydraulic, and environmental performance was implemented. During the planning and implementation process, which has been ongoing for several years, there have been many challenges requiring special mitigation measures. The most significant challenges to date can be summarized into three categories:

1. Water quality – metal leaching and acid rock drainage (ML/ARD).
2. Water management – peak flows and volumes, due to the wet climate.
3. Geotechnical – due to topographic and geologic constraints.

Each of these issues is discussed, with specific examples and their resolutions, through each of the key project planning and implementation stages. The purpose of this paper is to provide the reader with real-life examples of the challenges and resolutions to plan and implement a successful closure plan under these conditions.

Project Infrastructure and Setting

The Premier Gold Mine consists of six levels of underground workings and an open pit on the east banks of Cascade Creek, a tributary to the Salmon River. Key mine infrastructure includes

1. a tailings storage facility (TSF) located within the former Cascade Creek channel;
2. a seepage collection system downstream of the TSF dam;
3. a mine water treatment plant (MWTP) located near, and treating discharge from, the lowest mine portal (the 6-Level portal); and
4. two clarification ponds constructed in a series with upper and lower containment dams including a divider dam.

Tailings within the TSF are impounded by a 50 m-high, zoned earthfill dam. Cascade Creek is diverted around the TSF and into the former Leslie Creek channel using a deflection berm and rock-blasted channel (the Cascade Creek Diversion Channel, or CCDC). Feeding into upper Cascade Creek, a hydroelectric project was constructed in 2013 that impounds Long Lake, and discharges back into Cascade Creek downstream of the CCDC, but upstream of the MWTP discharge, via a pair of penstocks.

The mine is within the coastal mountain range of northwest British Columbia, and is subject to sharp variations in topographic relief (from approximately 200 m to 1,800 m elevation). Climate in the area is influenced by the Pacific Ocean and coastal mountains. As storm air masses from the Pacific Ocean move inland (west to east), they rise in response to the presence of coastal mountains, resulting in high levels of precipitation on the windward slopes. Temperatures are moderated by proximity to the Pacific Ocean, and result in higher proportions of precipitation falling as rainfall on the coast compared to inland areas of the province.

Planning for Closure

Closure Objectives

Closure objectives were established in order to meet regulatory and organizational criteria with respect to

geotechnical stability, water management, water quality, and to facilitate long-term monitoring of the facilities.

The primary objectives of the closure design were as follows:

1. Long-term geotechnical integrity of the tailings dam and other key infrastructure (i.e., TSF, MWTP).
2. Low maintenance management of the TSF (i.e., maintain TSF water cover and route PMF, construct a low maintenance closure spillway, and facilitate seepage monitoring).
3. Improvement or maintenance of existing, compliant discharge water quality from the TSF (i.e., demonstrate that water quality objectives will be achieved with uncontrolled spillway discharge) and underground mine (via the MWTP).

Plans for management of the TSF required demonstrating that the facility would meet water quality, geotechnical and hydraulic performance requirements over the long term with no operational, and minimal maintenance, requirements.

Decommissioning of the underground workings was not considered as part of the closure plan at this stage, as it presented significant technical challenges that were not addressed within the project timeline and might hinder the possibility of future exploration on the site. Notably, underground discharge from the 6-Level portal contains elevated levels of zinc, cadmium, and other metals, and is not suitable for discharge to the environment without treatment. Water quality may improve with flooding of the underground workings; however, the configuration of the underground workings is such that all underground water drains to the lowest portal (the 6-Level portal), and extensive fracturing within the open pit, collapsed underground workings near surface, and other undefined connections to the surface (unsealed and unmapped boreholes, portals, etc.) result in significant hydraulic connectivity between surface water and groundwater flows. While these factors substantially increase flows within the underground, and thus required treatment rates, these same factors make it challenging to take effective measures to promote flooding of the underground workings to control ML/ARD and outflows.

Analysis and Design

Hydrologic, water quality, and geotechnical analyses were performed to develop a closure plan that satisfied the specified objectives for stability, passive flood management, and water quality.

To develop a closure plan that satisfied water quality compliance criteria, an assessment of site water quality was performed to identify the main sources of chemical mass loadings. This involved development of a conceptual model that identified potential sources of chemical mass loading, and a review of historical documentation and water quality data to qualitatively rank these sources for geochemical risk. Risk factors were dependent on both the ML/ARD potential of the material (where

historical potentially acid generating (PAG) mine tailings ranked highly, while waste rock ranked relatively low, for example), as well as contaminant transport potential (where subaerially deposited historical tailings within creek beds ranked highly, but subaqeously deposited tailings within the TSF ranked very low based on historical supernatant water quality results). In all, the primary sources of chemical mass loadings on the site were generally from the underground workings, which produce comparatively high concentrations of dissolved cadmium, copper, and zinc, and the Premier Mine Area (historic subaerially deposited tailings and waste rock). The TSF was not found to be a significant source of chemical mass loadings. Although receiving environment water quality exceeds BC regulatory guidelines for cadmium, aquatic life studies have shown limited long-term impact to aquatic life resulting from mine discharges (Minnow [2012]; Stantec [2012, 2013]). On this basis, maintaining at least existing water quality is taken to be the design basis for closure.

Issues with hydrometric data collection due to steep terrain and creeks resulted in challenges in calibrating hydrologic models both for the purposes of water quality modelling and design flood analysis (see below). Though water quality and flow monitoring data are collected at regular intervals over an extensive network of locations, persistent issues included quality of flow data: steep terrain and challenging climate conditions make access for flow monitoring, especially during winter and freshet (key times) and accurate flow measurements very challenging. Continuous flow monitoring is very difficult in most locations. This was addressed by calibration of results against site data, where available, and regional studies. As data available for calibration was limited, conservative parameters were used to parametrize potential variability during extreme conditions (low-flow and high flows).

Based on the conceptual model, various closure options, as well as potential external influences, were examined using a chemical mass-balance approach in order to assess the relative impact that each had on downstream water quality. External influences examined included extreme dry events (200-year dry year), variations in climate parameters due to climate change, and implementation of a hydroelectric facility in the upstream watershed. Closure options evaluated for the TSF included decommissioning upstream diversions, and raising the TSF water level to promote saturation of tailings (this is also beneficial for flood routing, as discussed below). The impacts of decommissioning water treatment of underground discharge were also evaluated, but resulted in a significant degradation of receiving water quality, and decommissioning of water treatment was not evaluated further. The overall evaluation provided results showing that the proposed TSF closure measures resulted in minor changes to TSF discharge water quality under typical conditions, but significantly improved discharge water quality under extreme dry conditions, due to the water cover being maintained.

Based on the water quality modelling results, the selected TSF closure design included raising the operational water levels and increasing flows to the facility to maintain the water cover. Both of these

factors result in an increased flood management risk. To quantify the increased risk, a hydrologic assessment was performed to quantify the potential impact of the Inflow Design Flood (defined by Boliden as the PMF), conservatively assuming that the hydroelectric project at Long Lake (also designed for the PMF) would have no attenuating effects during the flood.

Including Long Lake, the TSF has an upstream catchment area of approximately 50 km^2, most of which is diverted via a large rock-cut channel (the CCDC). The CCDC was originally designed and constructed to handle the peak 1,000-year flood, but was subsequently assessed as having sufficient capacity to convey the PMF without freeboard. However, a geohazard review of the structure indicated a non-trivial risk of blockage of the channel due to ravelling of the slope, especially during extreme rainfall or snowmelt events. Various options for upgrading and partial diversion of the channel (e.g. fuse plugs) were examined, but it was ultimately thought that the risk of channel failure could not be sufficiently reduced. Therefore, the option to upgrade the TSF infrastructure to safely route the full PMF flood, with a peak flow of approximately 500 m^3/s, was selected. As the water quality modelling had emphasized the importance of maintaining water covers, lowering the spillway invert was not an option, so the routing capacity could only be increased by raising the dam or widening the spillway. A 60 m wide, rock cut spillway was designed to route the peak PMF flows, assuming failure of the CCDC.

The PMF flood wave entering the TSF was modelled using a two-dimensional hydraulic model in order to assess the height and velocity of the flood wave at various locations within the TSF, including the spillway approach and channel, and the TSF dam face. Based on these results, design elements were incorporated to prevent resuspension including a rockfill apron over tailings deposited upstream of the spillway, as well as riprap reinforcement and flattening of the TSF upstream dam face. By upgrading the TSF to allow for routing the design flood through the facility, the competing risks associated with the large flood volumes, ML/ARD, and diversion geology could be mitigated.

The closure plan requires ongoing, indefinite treatment of discharge from the underground mine. While the current treatment system produces discharge water quality results within permit limits, the relatively large volumes of hydroxide sludge produced in the process require relocation from the MWTP settling ponds for long-term storage and management. Historically, sludge has been deposited subaqueously in the TSF. However, the potential impact of this on pond water quality, and the future impacts the practice may continue to have as the pond storage capacity reduces over time, was not known. Geochemical testing of the sludge and water quality modelling was performed for a) existing practices (subaqueous sludge disposal within the TSF), b) external subaerial storage in a dry cell adjacent to the TSF, and c) external subaqueous storage in a small pond adjacent to the TSF. The results indicated that the existing practice had negligible short-term impact to TSF water quality, and it was recommended that the practice continue. .

Downstream of the TSF main dam, the frequent occurrences of rockfall from the valley slopes have resulted in unsafe conditions for seepage flow and water quality monitoring. As a result, collection of water quality samples and flow data has been discontinued. While collection of data further downstream is possible to confirm water quality compliance, lack of data specific to the seepage is problematic for monitoring of the facility, as well as water quality modelling. In order to mitigate this risk, a rockfall hazard assessment was performed using photogrammetry methods, in order to predict the likely mass, trajectory and extents of slope failure. Based on this assessment, a seepage monitoring system was designed to separate the monitoring area from zones of higher rockfall hazard. The new system includes backfilling of the existing monitoring pond with coarse rockfill along with providing a manhole-weir structure to monitor and collect seepage flows, and a catch-basin to contain rockfalls a safe distance from the monitoring point. The manhole was connected to the existing seepage monitoring pond dam low-level outlet pipes, and the entire structure was reshaped to form a geotechnically stable landform, with the objective of declassifying the seepage dam.

In the Premier Mine area, stability and flood routing assessments indicated that the MWTP settling pond dams did not meet required stability or flood routing criteria. Though limited design or construction information was available on the dams, document reviews and site investigation revealed that the dams were constructed upon the historical 1950s tailings facility, and appeared to be founded upon fine tailings, peats and other low-strength materials. In addition, these dams were oversteepened, likely to accommodate steep topography. The toes of the external dams are located close to the banks of Cascade Creek, which shows signs of erosion and bank migration. The ponds are used for settling fine particles from the treatment process, so reducing pond volume may reduce treatment effectiveness. In order to better understand the in-situ conditions affecting treatment pond dam stability, geotechnical site investigations were performed, including test pits and sonic coring, and piezometers were installed in all of the dams. This data was used to better understand dam fill and foundation conditions, monitor phreatic levels and calibrate stability models. Based on these results, concerns related to dam stability were confirmed, and various designs for dam remediation were considered. Design alternatives included HDPE liners and cut-off walls to reduce phreatic levels, in-situ restructuring of the dams, and complete dam reconstruction with updated zoning and foundation conditions. Ultimately, the Upper Dam design included completely removing the dam reconstructing it with flatter design slopes, rockfill shell and a low-permeability core. The impact of the reduced volume resulting from the flattened dam slopes on particle settling effectiveness was assessed and quantified, and mitigative measures (flocculants) were proposed should elevated TSS levels be identified. As the Divider Dam cannot be removed from service due to the requirement to have at least one pond in operations at all times, buttressing of the Dam was

proposed in stages. Design of the Lower Dam and downstream buttressing of the Divider Dam is currently underway.

Implementation of the Planned Closure Works

Construction of the designed works described above was completed in 2017. Specifically, the works included:

- Upgrading the TSF closure spillway to route the PMF.
- Upgrading the TSF upstream dam face to prevent damage from flood waves during the PMF.
- Decommissioning of the Emergency Spillway fuse plug.
- Construction of a revised TSF Seepage Monitoring system.
- Reconstruction of the MWTP Upper Pond dam, and upstream works on the MWTP Divider Dam (works within the Lower Pond, i.e. the Lower Dam and the Divider Dam downstream works, are scheduled for 2018).

The permitting and commissioning of these structures is a separate consideration and is not discussed here in detail. This section focuses on the issues encountered during construction of the works, and their resolutions. Construction activities in 2017 are summarized below, along with a selection of issues and their resolutions.

Construction of the closure spillway was conducted first, as it was to be used as the source of riprap and rockfill to the remaining work areas. Construction involved:

1. bedrock and overburden excavation to establish the 60 m-wide spillway design lines;
2. placement of riprap where bedrock was not encountered;
3. establishing a bedrock control sill; and
4. construction of a rockfill apron over tailings upstream of the spillway.

Poor rock quality was encountered in places during spillway excavation. In most areas, design grades were achieved by placing riprap from the excavation. However, to reinstate the spillway control sill in order to control the pond levels, a concrete overflow sill was required. In addition, Survey Monitoring Pins were placed on the downstream end of the spillway, where it drops off sharply towards Cascade Creek, in order to monitor degradation and erosion of rock once the spillway is commissioned.

Safety concerns were noted during placement of the rockfill spillway apron, and the construction was not completed. A review of the as-constructed condition showed the apron was sufficient to prevent significant tailings mobilization out of the spillway during events up to the 200-year flood, assuming the CCDC did not fail during the event.

Construction of the dam face riprap involved placing rockfill to flatten the upstream face of the dam to 2.5H:1V (from 1.5H:1V), and topping with a layer of riprap – keyed into the existing tailings beach – to prevent erosion. There were no significant technical issues encountered during this work.

The Emergency Spillway fuse plug was decommissioned by raising the structure to the dam crest elevation, and placing riprap on the upstream face. The downstream shell was flattened (as part of design) to account for a lack of suitable core materials on site.

Construction of the MWTP upper pond dams and spillways included (a) removal and reconstruction of the existing Upper Dam to meet stability criteria, (b) in-situ flattening of the Divider Dam, by filling to the upstream and trimming the downstream face, and (c) establishing an emergency spillway for the Upper Pond in bedrock. Similar to the TSF closure spillway, poor rock quality and limited availability of suitable high-fines core material required significant changes to the dam and spillway design during construction. In particular, construction delays resulted in placement of till core materials under wet Fall conditions, which resulted in saturation of the material. In order to accommodate the compromised material and achieve design objectives, a change in dam zoning was required to reduce the reliance of the dam on the strength of the material. Furthermore, additional foundation preparation was provided, to allow for the construction of a cut-off wall should the dam not perform as intended, due to higher core permeability.

During foundation preparation for the upstream Divider Dam construction, various pipes were unexpectedly encountered during dam and foundation excavation, some of which introduced significant inflows when exposed. . To prevent pressure build up, drain material was placed around the pipe outlet and coarse dam fill material zoned around it.

Conclusions

Though there were numerous issues with the construction activities associated with unexpected conditions encountered during excavations and the impacts of wet weather, the closure design meets the original objectives:

- **Closure management of the TSF** – An analysis shows that water cover would be maintained, and discharge water quality improved, by decommissioning the Fuse Plug and routing Indian Creek into the TSF. (This work is pending, once the TSF spillway discharge is permitted.) The spillway and upstream TSF dam face were upgraded so that the facility can safely route the PMF inflow, protecting the dam. Though the tailings apron will not prevent mobilization of tailings during the design flood, the constructed works are sufficient to prevent significant mobilization of tailings during spillway flows up to the 200-year return period inflow event (with the CCDC intact).

Infrastructure that allows safe measurement and collection of dam seepage facilitates ongoing monitoring of the performance of the facility.

- **Long-term geotechnical integrity of tailings dam and other key infrastructure (e.g., TSF, MWTP)** – The TSF was upgraded to safely route the PMF flood wave. Additionally, the MWTP Upper Pond dam was designed and reconstructed to meet required dam safety criteria, with the design modified to make use of available materials, and allowances for contingencies in case dam performance is not as intended. The MWTP Divider Dam was also designed to satisfy dam safety criteria, despite the challenges associated with it being constructed on top of the historic tailings pond, layers of organics, and open pipes. Construction of the Divider Dam downstream works, and the Lower Dam, is planned for 2019.
- **Improvement or maintenance of existing discharge water quality –** Water quality analysis indicates that the selected closure plan results in improved discharge water quality, and improved water quality downstream. This is achieved by maintaining tailings water cover, and continued treatment of underground discharge.

Acknowledgements

The authors would like to thank the many members of the Boliden and KCB project teams who worked diligently over a long period of time to overcome the technical challenges presented by this project, and allow it to become an example of responsible mine closure in British Columbia.

A special thought for Ben, a valuable member of the Premier team, who tragically passed away in a traffic accident on his way to the site in June, during the early stages of the 2017 construction work.

References

Minnow Environmental Inc. 2012. Aquatic effects monitoring program for the Premier Gold Project, March 2012.

Stantec Consulting Ltd. 2012. Third-party review of Boliden's "Premier Gold" Project of the work done for permit amendment with focus on the aquatic environment – Final.

Stantec Consulting Ltd. 2013. Aquatic effects monitoring program design, October 22, 2013.

Proceedings of Mine Water Solutions 2018
June 12–15, 2018, Vancouver, Canada
Published by the University of British Columbia, 2018

The Effect of Variability of Design Storms on the Galore Creek Project

Charles Masala, Klohn Crippen Berger, Canada
Andrew Thrift, Teck, Canada
Yapo Alle-Ando, Teck, Canada

Abstract

The Galore Creek project ("the Project") is in northwest British Columbia, Canada, within the territory of the Tahltan First Nation, an area characterized by significant spatial variability in precipitation. In this region, it is not uncommon for precipitation to vary more than 100% within a short distance. For the Galore Creek Watershed (Galore Watershed), which has a catchment area of approximately 140 km^2 and annual precipitation ranging from 1,300 mm to 2,500 mm, spatial variability of precipitation can have significant implications for water management design parameters. Therefore, the design storms on the site should consider, and incorporate, spatial variability of precipitation and resulting stream flow.

Spatial variability of precipitation at the Project is influenced by both regional and local factors. Regional factors are influenced by the Pacific Ocean and coastal mountains. The air masses from the Pacific Ocean bring precipitation to the coast. As storm air masses move inland, they are forced to rise due to the presence of coastal mountains along the windward slopes, resulting in widespread precipitation. This results in a regional trend of decreasing precipitation from southwest to northeast. On a local scale, precipitation is influenced by local topography and the orientation of the Galore Watershed.

This paper focuses on the variability of rainfall. The local spatial variability of rainfall was measured using tipping bucket rain gauges and project meteorological stations. For Galore Watershed, rainfall decreases along a southwest to northeast direction, like regional precipitation. Based on the assessment, two sets of design storms were identified and estimated for the Galore Creek Watershed, which could serve as inputs for estimating engineering design parameters for the project.

Introduction

The Galore Creek Project ("the Project") is in the remote coastal mountains of northwestern British Columbia, Canada, in a transition zone between the wetter coastal region and the drier interior. The Project is approximately 150 km northwest of the port of Stewart, as shown in Figure 1. This area is

characterized by significant spatial variability in precipitation and stream flow. Due to significant spatial variability, the Hydrological Atlas of Canada (Department of Fisheries and the Environment, 1978) identifies this area as susceptible to large discrepancies between inflow (precipitation) and outflow (runoff and evapotranspiration) in the standard watershed hydrological water balance model.

The Project is located within the Galore Creek Watershed (Galore Watershed), which has a catchment area of approximately 140 km^2. Annual precipitation in Galore Watershed ranges from 1,300 mm to 2,500 mm. This spatial variability of precipitation has significant implications for water management design parameters (design parameters), which can impact the project cost. Therefore, the design parameters on the site consider, and incorporate, spatial variability of precipitation.

Project Setting

Regional spatial variability of precipitation at Galore Creek is caused by proximity to the Pacific Ocean and the presence of coastal mountains. The air masses from the Pacific Ocean bring precipitation to the coast, particularly in the autumn and winter. As storm air masses move inland (west to east) from the coast, they rise in response to the presence of coastal mountains along the windward slopes, resulting in widespread precipitation. This results in wetter coastal areas and a drier interior, as shown in Figure 1. The annual precipitation isohyets near the Project range from 2,400 mm to 1,600 mm.

The Pacific Ocean also supplies a heat source, which moderates the temperatures along the coast compared to the inland area. Therefore, precipitation on the coast has a higher proportion of rainfall than snowfall, compared to inland. Coastal mountains have the effect of further reducing temperature inland, increasing the proportion of snowfall compared to the coast.

Within Galore Watershed, the spatial variability of precipitation is caused by variability in topography (elevation from valley bottom to alpine ranges from less than 300 m to more than 2,400 m), catchment size (140 km^2), and the orientation of the valleys relative to the regional precipitation trend (south to north). This paper focuses on the spatial variability of rainfall.

Measuring Local Rainfall Variability

Local spatial variability of rainfall in the Galore Watershed was measured using tipping bucket rain gauges (TBRG) and project meteorological stations. The locations of TBRGs used for measuring rainfall are presented in Figure 2.

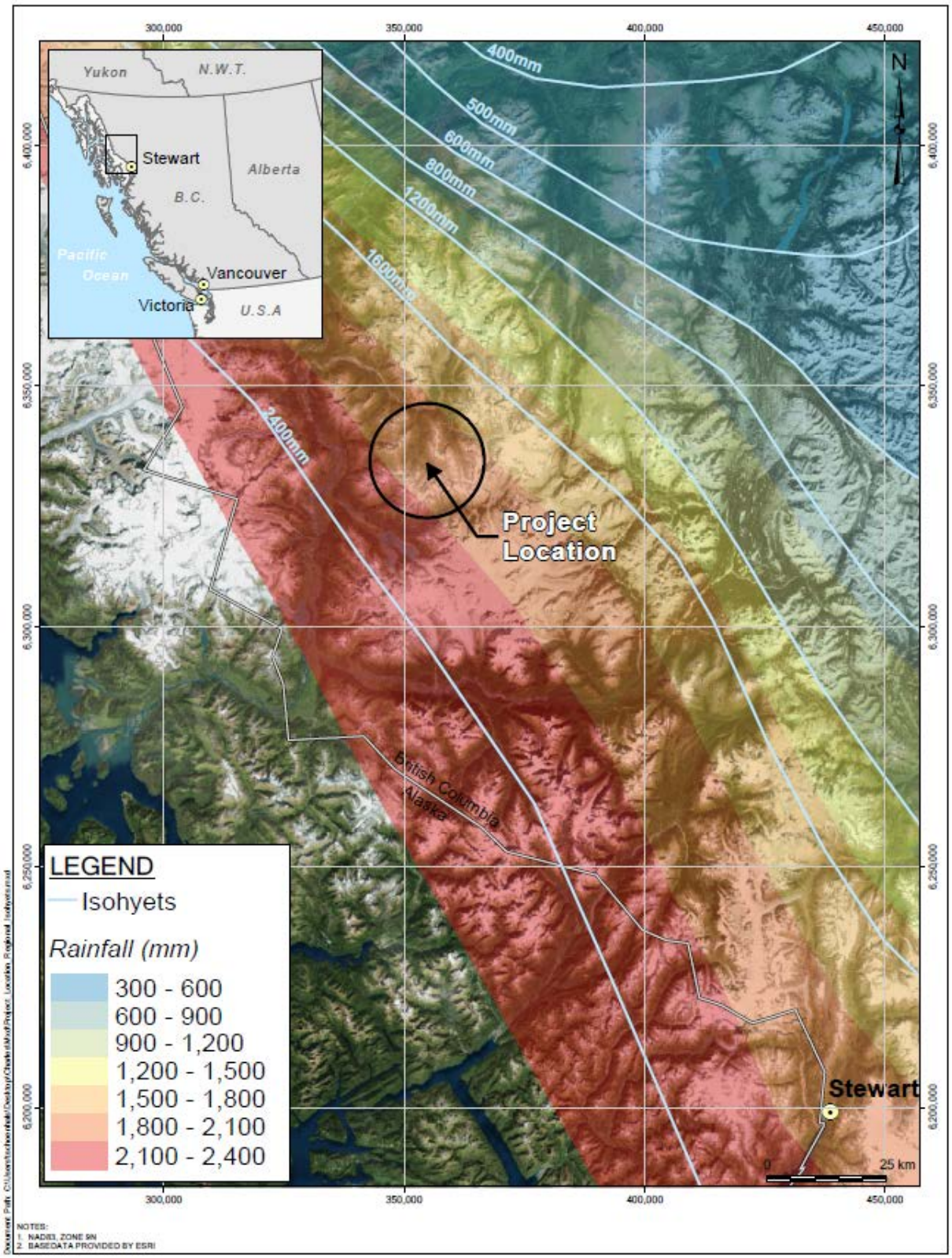


Figure 1: Project location and isohyets

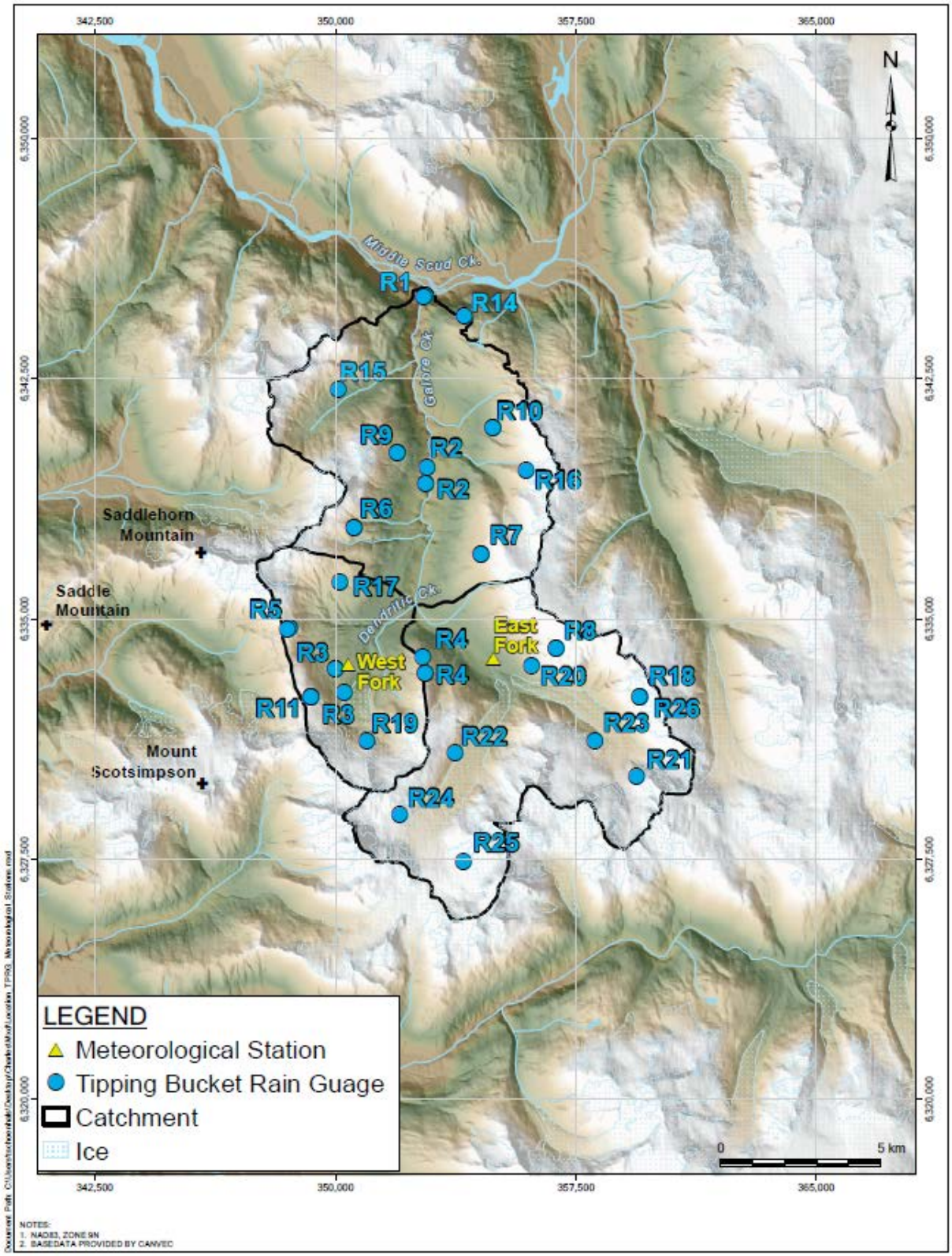


Figure 2: Location of tipping bucket rain gauges and meteorological stations

Tipping bucket rain gauge (TBRG)

A TBRG network was installed in Galore Watershed specifically to measure spatial variability (aerial and altitude) of rainfall. Since TBRGs measure only rainfall, they functioned only during the warmer months (typically from June to October).

The TBRG monitoring program at Galore Project evolved over the study period. Initially, only five TBRGs were installed on site in 2005, during which data was collected from August 23 to October 23. Due to significant variability of the results in the 2005 study, five TBRG were considered inadequate for measuring spatial variability over the watershed, and therefore the number of TBRGs was increased to 11 in 2012. The results of the 2012 monitoring campaign (from June 24 to September 23) indicated that even more TBRGs were required to get a better understanding of spatial variability of rainfall in the Galore Valley, especially considering the importance of water management for the project. Therefore, in 2013, a total of 25 TBRGs were installed on a grid, as shown in Figure 2. In 2013 data was collected from June 13 to September 29.

Meteorological Stations

There are two meteorological stations in the Galore Valley — East Fork Meteorological Station (EFMS) and West Fork Meteorological Station (WFMS). EFMS is the main weather station on site, and data records used for this study were from 2004 to 2013. EFMS was used as a reference station for assessing spatial variability of Galore Valley. There were only two years of data from the WFMS at the time of study (2012 and 2013); therefore WFMS was not used for this assessment.

Assessment of Spatial Variability

The spatial variability of TBRG data were assessed using total and peak rainfall over the period of record of each year. Total rainfall for each TBRG was calculated concurrently with data from EFMS, over the period of records for each year. Peak rainfall for each TBRG was also calculated concurrently with data from EFMS over the periods of record for each year. The peak rainfall was calculated as the average of the three largest peaks over the period of record for each year. The distribution of rainfall of Galore Valley was normalized by calculating a ratio of total rainfall at each TBRG location to total rainfall at EFMS. The normalized distribution of rainfall over the Galore Watershed is presented in Figure 3.

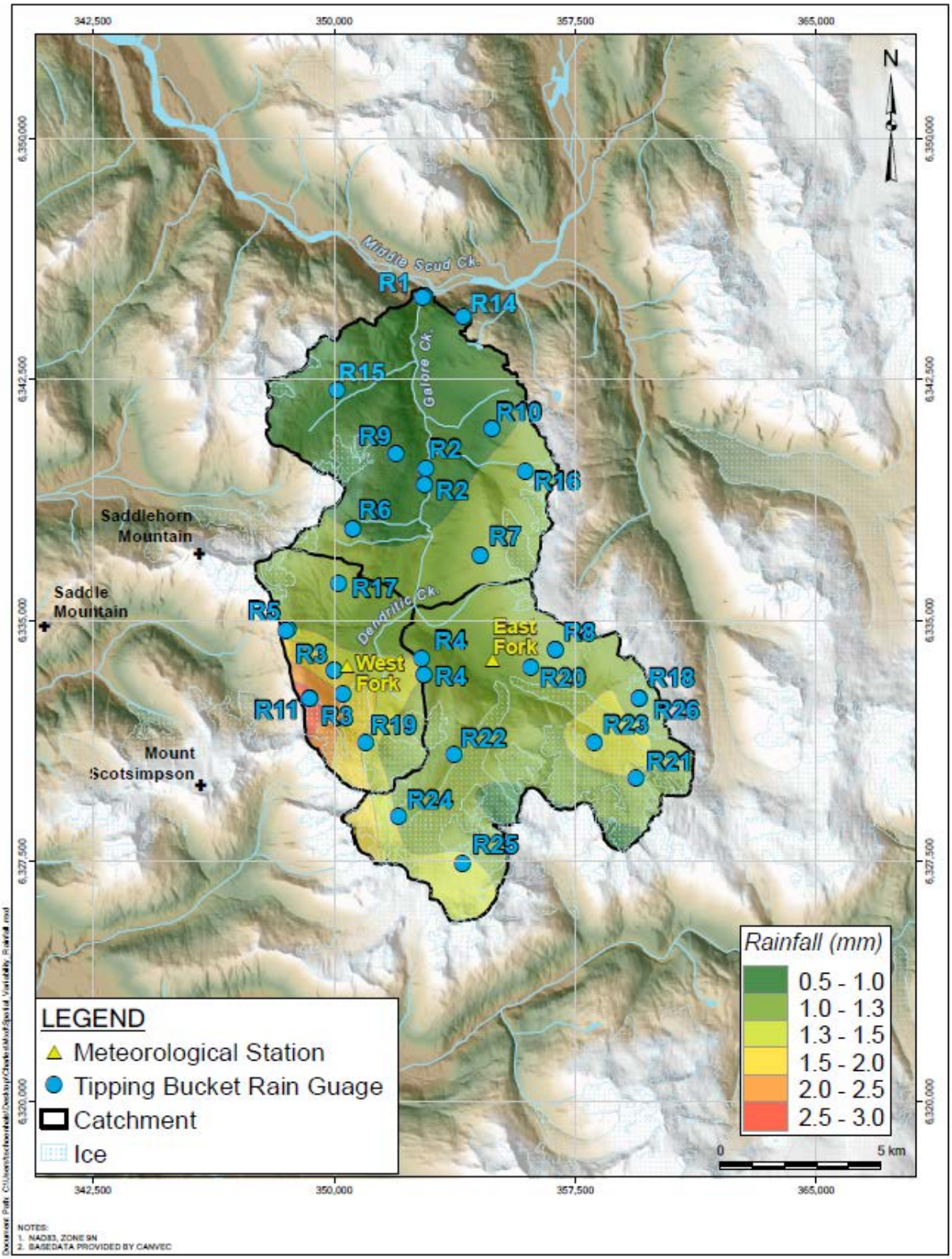


Figure 3: Spatial variability of rainfall over Galore Watershed

Evaluation of Design Storms

Long-term Data

Since Galore Creek had a short period of data (2004 to 2013) at the time of the study, a regional station was required for estimating design storms for the site. After a review of several regional stations, Stewart, BC was identified as the most suitable station for estimating long-term parameters for the Project site. Although Stewart is approximately 150 km from Galore Creek, it was selected based on the following reasons:

- It had the longest period of consistent data in the region (1910 to 2013).
- It had concurrent data with the Project site over the period of site monitoring (2004 to 2013).
- It had a good qualitative relationship with site peak storms. Major storms between the site and Stewart occur within a few days' lag and are similar in magnitude and peaks.
- It had the strongest correlation with EFMS precipitation data.

Correlation analysis was performed between EFMS and Stewart for periods of overlapping data between the two stations. Correlation analysis was performed for monthly precipitation (2004 to 2010). Monthly precipitation data showed reasonable correlation between the two stations (EFMS and Stewart) as shown in Figure 4.

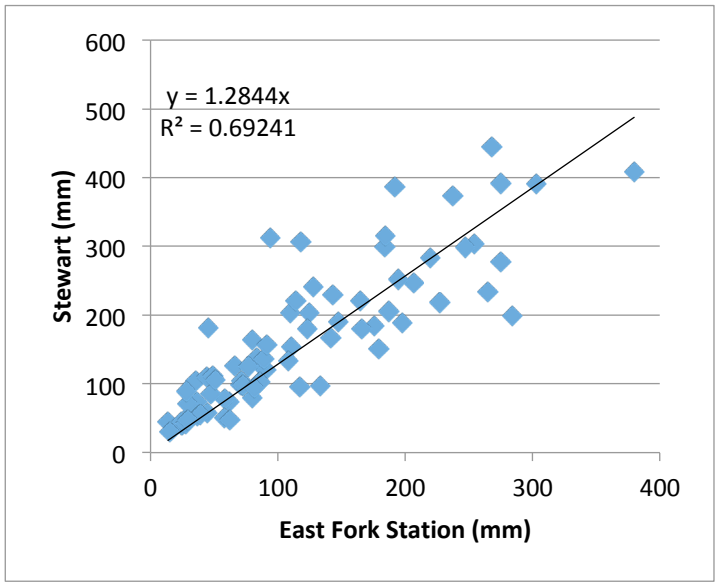


Figure 4: Monthly precipitation data correlation East Fork Meteorology Station and Stewart (2005 to 2011)

A qualitative correlation was also established between peak rainfall data of EFMS and Stewart by observing occurrence of peak storms. It was observed that almost half of the annual peaks from 2005 to 2011 at EFMS and Stewart occurred within one or two days of one another. This suggests that the peak

storms were caused by the same storm system, suggesting a correlation between the peak storms at the two stations.

Based on this analysis, it is assumed that precipitation received at EFMS station correlates to precipitation received at Stewart.

Statistical Tests of Long-Term Data

Statistical tests were performed on the Stewart station precipitation data, using Hyfran Plus (statistical program), to assess for statistical representativeness and strength of data over the period of record from 1910 to 2013, for annual extreme rainfall values. The following statistical analyses were conducted on the data:

- Stationarity test. The Kendall test was used to assess whether there was a trend in and annual peaks data. The result indicated that for annual peak, there is a 95% chance the values are stationary over the period of record.
- Homogeneity test. The Wilcoxon test was used to assess whether the data were homogenous on an annual basis. The data were divided into two subgroups: 1910 to 1950 and 1950 to 2013. The results indicated that for annual peaks, there is a 95% chance that the values are homogenous over the period of record.
- Independence test. The Wald-Wolfowitz test was used to assess independence of observations for annual peaks data. The result indicated that for annual peaks, there is a 95% chance that the values are independent over the period of record.

The summary of statistical test results is presented in Table 1.

Table 1: Stewart data, statistical representativeness

	Hypotheses		Results
Test	H_0	H_1	Annual Peak Rainfall
Test for Independence (Wald-Wolfowitz)	The observations are independent	Observations are dependent (autocorrelation of order 1)	We accept H_0 at a significance level of 5 %.
Test for Stationarity (Kendall)	No trend is apparent in the observations	There is a trend in the observations	We accept H_0 at a significance level of 5 %.
Test for Homogeneity (Wilcoxon) (1910 to 1950/1950 to 1915)	The averages of the two samples are similar	The averages of the two samples are different	We accept H_0 at a significance level of 5 %.

Note: These results indicate that there is a 95% significant level (chance) that the data meet each of the above tests. The 95% significant level is the generally acceptable level.

The results demonstrate that the rainfall dataset used over the period from 1910 to 2013 does not show any trending due to climate change, or any shift due to change in instrumentation. The data meets the criteria for applying parametric statistics methods (fitting to different distributions). This means that rainfall parameters developed from this dataset are representative of the period of record, and they are not changing with time.

Statistical Distribution of Stewart Data

The annual peak data at Stewart were fitted to several statistical distributions, and Gumbel distribution was selected as the most suitable based on how closely the sample parameters compare to the population parameters as shown in Table 3. The Kolmogorov-Smirnov goodness of fit test was also conducted, and the results demonstrated that the data meet Gumbel distribution.

Table 3: Annual peak rainfall – Gumbel distribution parameters

Statistic	Sample	Population
Sample size	96	infinite
Range	183	infinite
Mean (mm)	70	70
Variance (mm2)	678	678
Std. deviation (mm)	26	26
Coeff. of variation	0.37	0.37
Std. error	2.66	
Skewness	1.4	1.1
Excess Kurtosis	5.8	2.4

Transposition Factor between East Fork Meteorology Station and Stewart

A transposition factor between EFMS and Stewart was calculated as the ratio between the average of the peak storms at EFMS (56.8 mm) and Stewart (53.6 mm), over the concurrent period (2004 to 2011). A transposition factor of 1.06 was calculated. The calculated transposition factor was used to transfer the intensity duration frequency (IDF) curve for Stewart to the EFMS. The Stewart depth-duration-frequency (DDF) table was estimated based on Gumbel distribution for Stewart data from 1910 to 2013, and DDF by Environment Canada using data from 1978 to 2005.

Discussion of Results

Spatial distribution of precipitation over Galore Watershed was evaluated based on relative ratios of rainfall (total and peaks) to EFMS (ratios) over the periods of record, as presented in Figure 3. Evaluation of rainfall, using a grid introduced in 2013, provides a good basis for understanding the variability of

rainfall over Galore Watershed. It captures local areas in the watershed with higher rainfall, such as the West Fork sub-area. The grid also demonstrates consistency of measured rainfall between adjacent TBRGs, giving more confidence in parameters estimated. The grid provides a good basis for locating future additional meteorological stations in the watershed if required.

Table 4 presents a comparison of ratios of stations where data were collected in 2005, 2012 and 2013. The ratios for the three years of TBRG data collection are the same or very similar, demonstrating a consistency of relationship between the TBRGs and EFMS for the rainfall collected over the different periods.

Table 4: Transposition factors between East Fork Station and Galore Creek sub-areas

TBRG Station	2005	2012	2013
R1	0.9	0.7	0.7
R2	0.8	0.8	0.8
R3	2.0	1.5	1.5
R4	1.3	1.3	1.3
R5		1.3	1.3
R6		1.0	1.0
R7		1.3	1.3
R8		1.0	1.0
R9		0.7	0.7
R10		0.9	0.9
R11		2.8	2.8

As shown in Figure 3, the spatial variability of rainfall is generally consistent with the regional trend, where rainfall reduces in a northwest direction.

The assessment of spatial variability of rainfall shows the weakness in using single meteorological stations in a watershed like Galore Creek, where there is significant variability of rainfall. The ratios estimated for 2013 data range from 0.7 to 2.8, meaning rainfall in Galore Watershed varies from –30% to +280% of the rainfall recorded at EFMS. The average ratio for 2013 data is 1.17, meaning the average rainfall over Galore Watershed during the period of record was 17% higher than that estimated at EFMS.

Based on site hydrology and the results of spatial variability of rainfall, Galore Watershed was divided into three sub-areas, East Fork sub-area, West Fork sub-area and Lower sub-area as shown in Figure 3. The average of the ratios for each sub-area are presented in Table 5. The average ratios in Table 5 allow for transposition of EFMS parameters such as the DDF over the sub-area.

Table 5: Transposition factors between East Fork Station and Galore Creek sub-areas

Sub-area	East Fork	West Fork	Lower
Ratio	1.1	1.6	0.9

Although three sub-areas were assessed based on the ratios in Table 5, for design, two sets of values are proposed: West Fork sub-area and the rest of the watershed. The ratios for East Fork and Lower sub-areas are very similar, therefore a single transposition factor of 1.1 is adopted for this area. The design storms for the West Fork area and the rest of the watershed are presented in Tables 5 and 6.

Table 6: West Fork sub-areas and rest of watershed design storms (24 hrs)

Return period (years)	West Fork sub-area	Rest of Galore Watershed
2	116	79
5	149	102
10	171	117
25	199	136
50	219	150
100	240	164
200	260	177

The difference between the two sets of approximately 50% represents significant impact on the water management design in the two areas.

Conclusion

These are the main conclusions of this study:

- Characterizing spatial variability using a grid identified areas of higher rainfall and demonstrated consistency of rainfall between adjacent TBRGs, providing more confidence in estimating design parameters for the project.
- By evaluating spatial variability of the Galore Creek Watershed, two sets of design storm parameters were estimated for the wettest sub-catchment (West Fork) and the rest of the catchment.
- The relationship of rainfall between Galore Creek and Stewart (150 km away) was established by correlating monthly precipitation, as well as occurrence and magnitude of peak storms. It was demonstrated that most of the peak storms at Stewart Climate Stations and Galore Creek occur within one or two days of each other, indicating that they are likely caused by the same general

storms. This also demonstrates that in this region, most big storms are caused by general storms rather than local storms.

- The direction of spatial variability of precipitation at Galore Creek is consistent with the regional trend; that is, precipitation decreases in a northwest direction.

Acknowledgements

The authors would like to thank Galore Creek Mining Corporation for the opportunity to write this paper.

Reference

Department of Fisheries and the Environment. 1978. Plate 25. Water balance – derived precipitation and evapotranspiration, *Hydrological Atlas of Canada*, Atmospheric Environment Service.

Proceedings of Mine Water Solutions 2018
June 12–15, 2018, Vancouver, Canada
Published by the University of British Columbia, 2018

Hydrogeology of the Coffee Gold Project: Groundwater Interactions in an Area of Discontinuous Permafrost

Laura-Lee Findlater, Lorax Environmental Services Ltd., Canada
H. Jean Cho, Independent Consultant, Canada
David Flather, Lorax Environmental Services Ltd., Canada
Jennie Gjertsen, Goldcorp Inc., Canada
James Scott, Goldcorp Inc., Canada

Abstract

The Coffee Gold project is a proposed gold mine located in the White Gold District of west-central Yukon, approximately 130 km south of the City of Dawson. The project comprises a complex of four open pits positioned at the height of land in an area of discontinuous permafrost. Multiple hydrogeological and geotechnical programs have been undertaken at the site to characterize the groundwater and permafrost regimes to support estimation of operational water management and effects assessment in the receiving environment. The well-developed monitoring network includes 7 Westbay systems, 11 conventional monitoring wells, 12 thermistor/vibrating wire combination installations, plus standalone thermistor strings and vibrating wire piezometers. The data indicate permafrost thickness ranging from largely absent on south-facing slopes to over 160 m thick on north-facing slopes, with permafrost thickness decreasing with elevation. Groundwater levels in ridge areas, coincident with mine infrastructure, range from 220 m below ground surface to artesian conditions. Groundwater level hydrographs are observed to fluctuate by up to 30 m at some locations. Hydraulic conductivity data range over several orders of magnitude, typical of a fractured bedrock system. Mineralized structures and creek traces represent areas of enhanced hydraulic conductivity. The data from these programs and others have been used to develop a conceptual model of groundwater flow at the site. This conceptual model has informed the development of a steady-state groundwater model developed using MODFLOW-2005. The permafrost distribution was incorporated into the structuring of the groundwater model, which was calibrated to water levels and creek baseflows. The results of the groundwater model indicate that seepage losses from pit lakes to groundwater are modest (4 litres per second or less) during post-closure, with pit groundwater inflows influenced by runoff accumulation in nearby pits. Overall, impacts to baseflow in receiving drainages is small and within measurement accuracy.

Introduction

The Coffee Gold project is a proposed gold mine located in the White Gold District of west-central Yukon, approximately 130 km south of the City of Dawson and 330 km northwest of Whitehorse. The project was first explored by Kaminak Gold Corporation, which was acquired by Goldcorp Inc. in 2016. The project is located in the northern Dawson Range of the Yukon-Tanana terrane, forming a moderate plateau that escaped Pleistocene glaciation. The topography generally consists of rounded ridges with incised v-shaped valleys (Goldcorp, 2017). Elevations across the property range from 400 to 1,500 m above sea level, with the majority of the property above the tree line, and supporting short shrubby vegetation. The proposed mine complex is located along a ridgeline due south of the Yukon River (Figure 1). Surface drainage goes to tributaries of the Yukon River, the most notable of which include Coffee Creek, Latte Creek, Halfway Creek, and YT-24.

The study area is characterized by a cold, continental climate with an average annual temperature of –2.5°C, with monthly average air temperatures ranging from –19°C (December) to +13°C (July). Annual precipitation averages 370 mm/yr at 975 m elevation. Pronounced valley bottom temperature inversions occur during the winter months whereby ridgetop temperatures are up to 10°C higher than measurements recorded at valley bottom locations. These inversions result in a reversal of the normal lapse rate (decreasing temperature with increasing elevation) and are commonly caused by cold Arctic air masses pooling in the valley bottoms from late October to early March. The project is in an area classified as extensive discontinuous permafrost with low to medium ice content (National Resources Canada, 1995).

The planned layout of mine facilities is shown in Figure 2. Ore will be extracted from four pits, which include (maximum depth in parentheses) Supremo (140 m), Latte (150 m), Kona (90 m) and Double Double (100 m). The Supremo pit will be mined in 5 phases, with sub-pits referred to as SU1, SU2, SU3W, SU3N, SU4N, SU4S, SU5N and SU5S. Kona and Double Double pits will be completely backfilled with waste rock at closure, while other pits will be partially backfilled. The majority of remaining mine waste (300 Mt) will be housed in the permanent Alpha WRSF, located in the headwaters of Halfway Creek. The proposed 60 Mt heap leach facility (HLF) consists of a conventional, multi-lift, free-draining ridge-top leach pad.

Hydrogeological information has been collected at the Coffee Gold mine site since 2013, with major field programs undertaken in 2014 and 2015. The data from these field programs and others have been used to develop conceptual and numerical models of groundwater flow, which have been used to determine mine environmental effects in support of a Project Proposal submission to the Yukon Environmental and Socio-economic Assessment Board (YESAB) (Goldcorp, 2017).

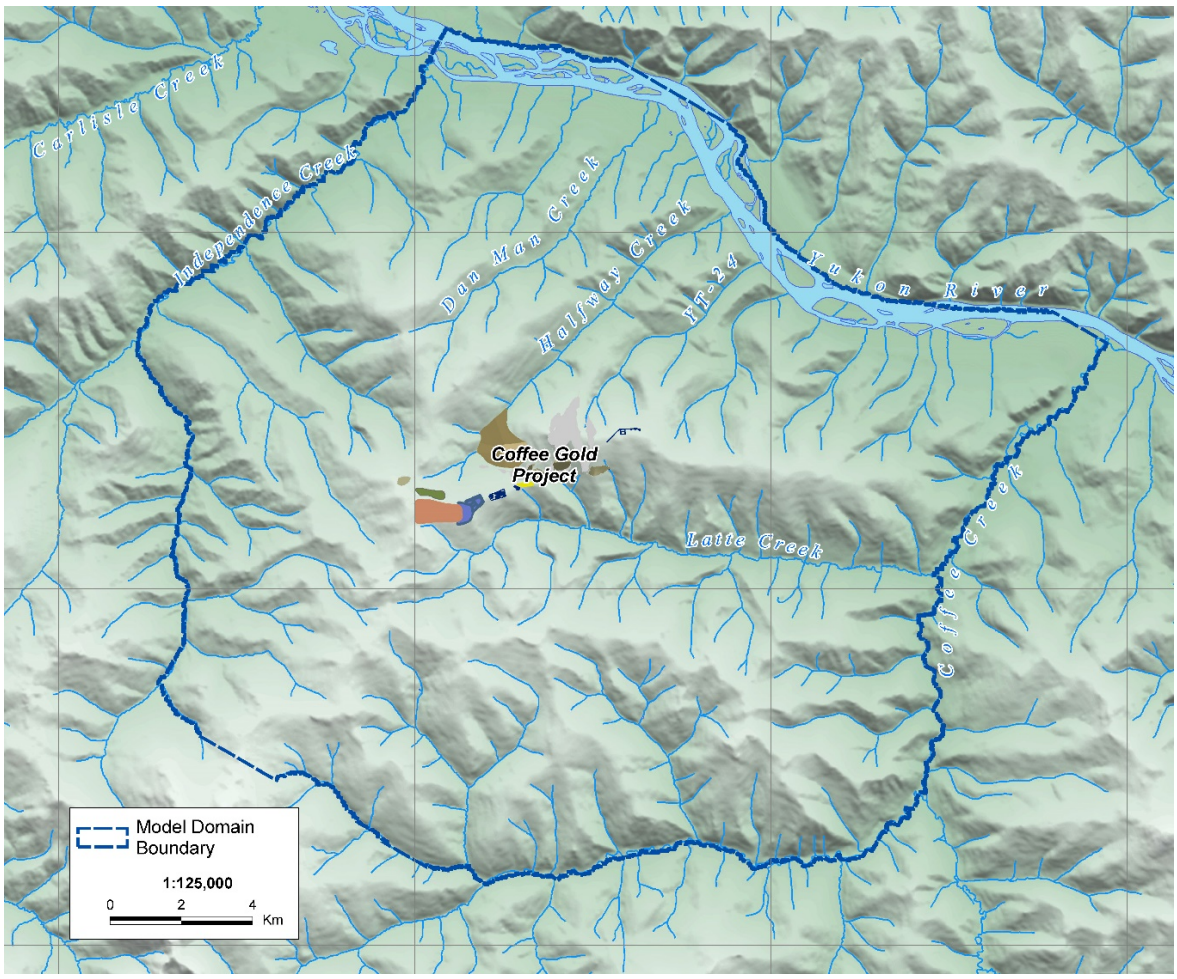


Figure 1: Project location and groundwater model domain

Field Programs

The first groundwater field program, spearheaded by Tetra Tech in 2013, installed single vibrating wire piezometers (VWPs) in four exploration drillholes in and around the deposit area with early data suggesting deep water levels – >100 m below ground surface (bgs) – on ridgetops. Within the broader exploration program, drillers had reported a single instance of recovering ice in core at depth (75 m bgs) in a north facing drillhole. The subsequent field program led by Lorax in 2014 sought to broaden the coverage of the monitoring network and enable sampling of groundwater quality through conventional monitoring wells. Five pairs of shallow (~150 m) and deep (~200 m) monitoring wells along with two multipoint thermistors, were installed using diamond-drilling methods in higher elevation areas. Packer testing was also undertaken. Significant challenges were experienced throughout the program on account of deep water levels, poor ground conditions and deeper-than-expected permafrost. Two nested borehole pairs on north facing slopes ice-jacked prior to collection of meaningful groundwater level and groundwater quality data.

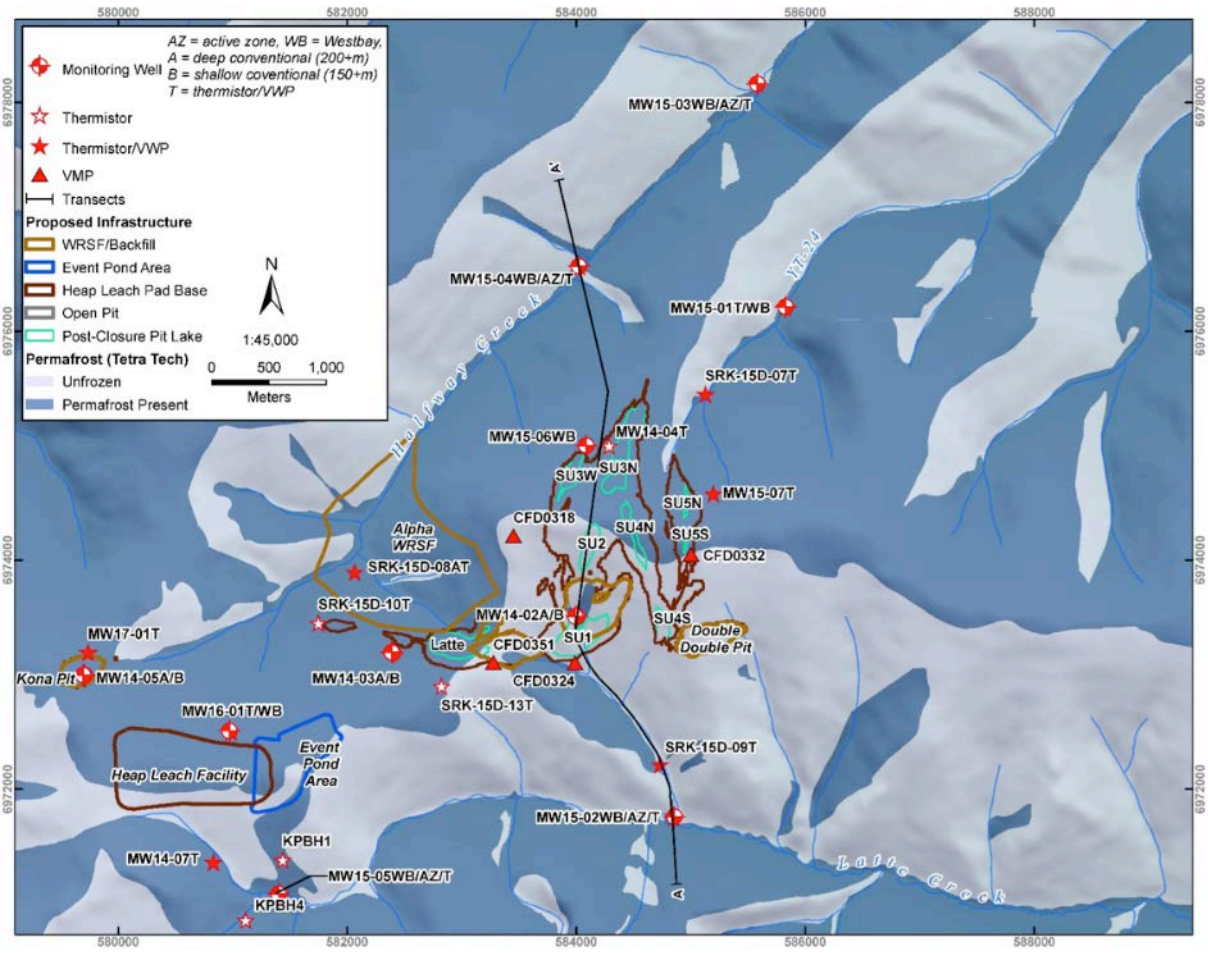


Figure 2: Arrangement of Coffee Gold mine facilities.
Shaded areas of permafrost are based on Tetra Tech (2016)

In light of the challenges faced in the 2014 field program and concerns over potential permafrost thickness, new drilling and installation methods were sought for the 2015 field program, which focussed primarily on lower elevation areas adjacent to creek channels. The new installation approach included advancing two reverse circulation drillholes from each pad – the first drillhole being equipped with a combination thermistor/VWP string, the second drillhole being equipped with a Westbay monitoring system to enable water quality sampling of sub-permafrost groundwater. To protect the Westbay casings from ice-jacking, sacrificial steel HQ rods were lowered just past the depth of permafrost and secured at surface, thereby blinding off frozen ground. The first drillhole slated for thermistor/VWP installation allowed for initial assessment of permafrost conditions for the Westbay system design with continuous readings of ground temperature and groundwater pressures thereafter. Packer testing and/or airlift recovery tests were performed on the thermistor/VWP drillholes.

The combination of VWP/thermistor string and Westbay installation nests proved to be a successful means of collecting reliable, high quality groundwater data. Similar instrument nests were installed at two

other locations in 2016 and 2017. In total, 7 Westbays, 11 conventional monitoring wells, 4 stand-alone VWPs and 17 deep (>20 m) thermistor strings (mostly combined with VWPs) have been installed across the mine site. The installations span elevations of ~560 masl to ~1250 masl on multiple slope aspects (Figure 2).

Data and Conceptual Model Development

Permafrost

Permafrost is of hydrogeological significance as it is considered to behave like an aquiclude or an aquitard and can confine sub-permafrost groundwater such that it exhibits artesian conditions (Woo, 2012). The drilling programs undertaken by Lorax determined the base of permafrost at multiple locations. An interpretation of broader permafrost occurrence, led by Tetra Tech, has been supplanted by multiple field and desktop studies on shallow ground conditions (Tetra Tech, 2016).

Overall, permafrost extends to greatest depths in ridge areas and appears to reduce in thickness towards areas of lower elevation; north-facing slopes tend to have thicker and more prevalent permafrost than south-facing slopes. The thickest permafrost (~165 m) is encountered near the north end of the proposed Supremo pit at MW14-04T. Permafrost in the project area is relatively warm (between 0 and -1.7°C) and is coolest on north facing slopes. A summary plot of estimated permafrost thickness versus elevation in shown in Figure 3. The finding of increased permafrost thickness with elevation was an important one as it countered a previously held conceptual model for the site which envisioned thicker permafrost in valley bottoms compared to ridge areas. The previous conceptual model had not benefitted from drilling and/or thermistor data.

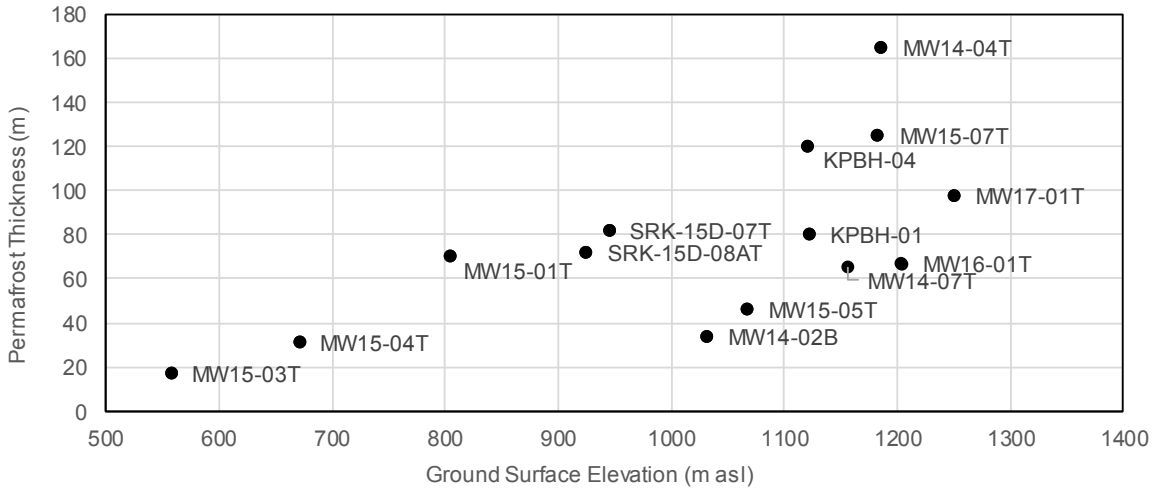


Figure 3: Permafrost depth versus ground surface elevation at Coffee Gold mine site

Hydraulic Testing Data

The project is underlain by a package of metamorphosed Paleozoic rocks of the Yukon-Tanana terrane that was intruded by a large granitic body in the Late Cretaceous. The main Coffee Gold mineralization is associated with an extensional deformation event that occurred during the Cretaceous which resulted in the formation of steep-to-vertical brittle fractures and normal faults cross-cutting all lithologies at Coffee (Berman et al., 2007).

Hydraulic testing at the Coffee project has been undertaken on multiple lithologies located within pit footprint areas and farther afield. Data are shown plotted versus depth in Figure 4. Based on the wide spread in values for the major rock units and combinations thereof, rock type does not appear to exert a large influence on hydraulic properties. Rather, structural features, which cross-cut all lithologies, impart the dominant control on hydraulic conductivity. The hydraulic conductivity (K) data are typical of a fractured bedrock system with values ranging over several orders of magnitude (<1E–10 m/s to >1E–06 m/s). A regression line though the data points indicates a broad trend of decreasing K with depth with the exception of a cluster of higher K values at over 200 m depth. Most of these elevated values at depth are attributed to a testing program led by SRK that specifically targeted geologic structures intersecting the proposed pits. SRK reported a narrow range (1E–07 m/s to 3E–06 m/s) of K values for the structures (SRK, 2015). Borehole testing near creek channels yielded K values averaging 1E–06 m/s, which is consistent with the results for pit structures and supports the inference that major creek traces (i.e. Latte Creek, Latte tributary, Halfway Creek, YT-24; see Figure 1) represent permeable fault structures.

Groundwater Water Levels

Water levels are relatively deep (from 130 m to over 220 m below ground surface) in ridge areas, but flowing artesian conditions are encountered at moderate to high elevations at two locations (MW16-01T, MW14–07T) in the south-western project area. The proposed Kona pit shell and the SU3W and SU5N/S sub-pits of the Supremo Pit complex lie above the pre-mine water table (Figure 2); while the remaining pits and sub-pits are advanced below the water table.

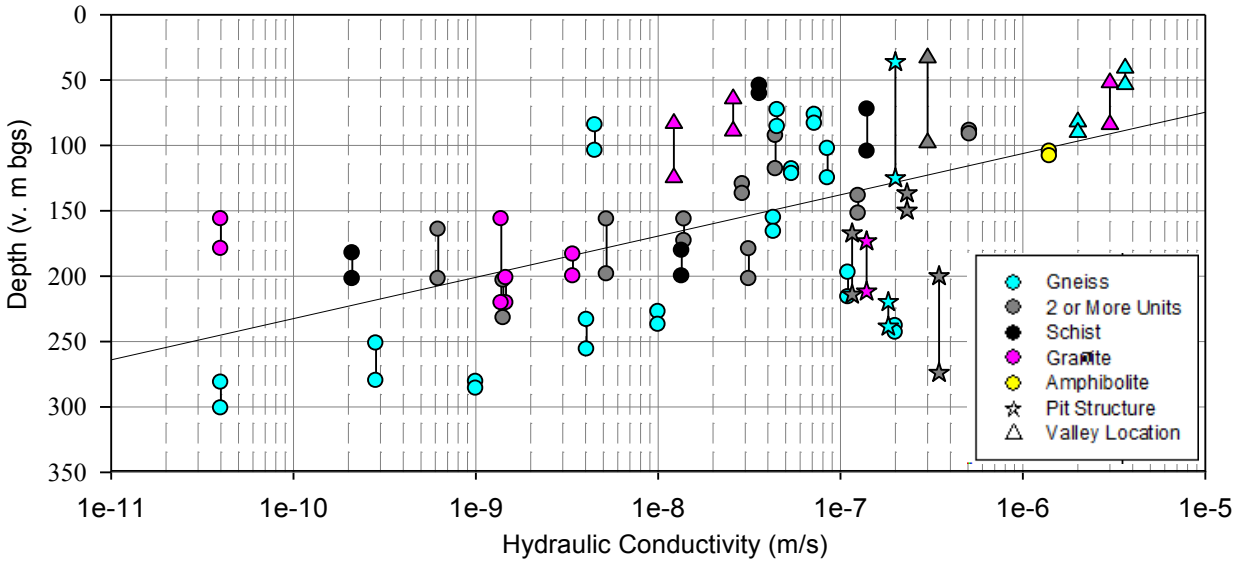


Figure 4: Hydraulic testing data versus depth

Water level hydrographs indicate variable response to seasonal recharge patterns, with fluctuations ranging from approximately <1 m to over 30 m. Fluctuations in the range of 0 m to 10 m are typical. The magnitude of seasonal fluctuations is not clearly correlated to well collar elevation, nor to the presence of permafrost. The largest seasonal shift (30 m) is observed at a vibrating wire piezometer (CFD-351) in a saddle area where permafrost is absent (Figure 2, Figure 5). At monitoring locations where permafrost depth is accurately known, groundwater pressures generally exceed the base of permafrost, demonstrating confined conditions. The notable exceptions are the slope draining the SU3W pit, where the water table at MW15-06WB is inferred to be at least 50 m below the base of permafrost, and the slope draining Kona Pit, where water levels are about 20 m below the base of permafrost at MW17-01T (Figure 6).

The continuous water level record indicates that the hydrographs at most wells are reasonably insensitive to individual rainfall events; rather, they follow a gradual seasonal increase that peaks anywhere between late summer and winter. Timing of peak groundwater levels is highly variable across the site. In 2016, the water level hydrograph at CFD-0351 peaked in late August, while the MW15-07T hydrograph peaked in mid-December (Figure 5). At MW15-04T, a reasonably shallow (<60 m) VWP in Halfway Creek, groundwater levels peaked in mid-May and mid-September in response to freshet and later, summer rainfall (Figure 5). Nested instrumentation reveals both upward and downward vertical hydraulic gradients in both upland and low-lying areas. In some instances, horizontal hydraulic gradients exceed topographic gradients, including the upper reaches of Latte Creek (MW14-07T/ MW15-05T) and along the Latte Creek tributary (MW14-02/CFD-0324; SRK15D-09/MW15-02T).

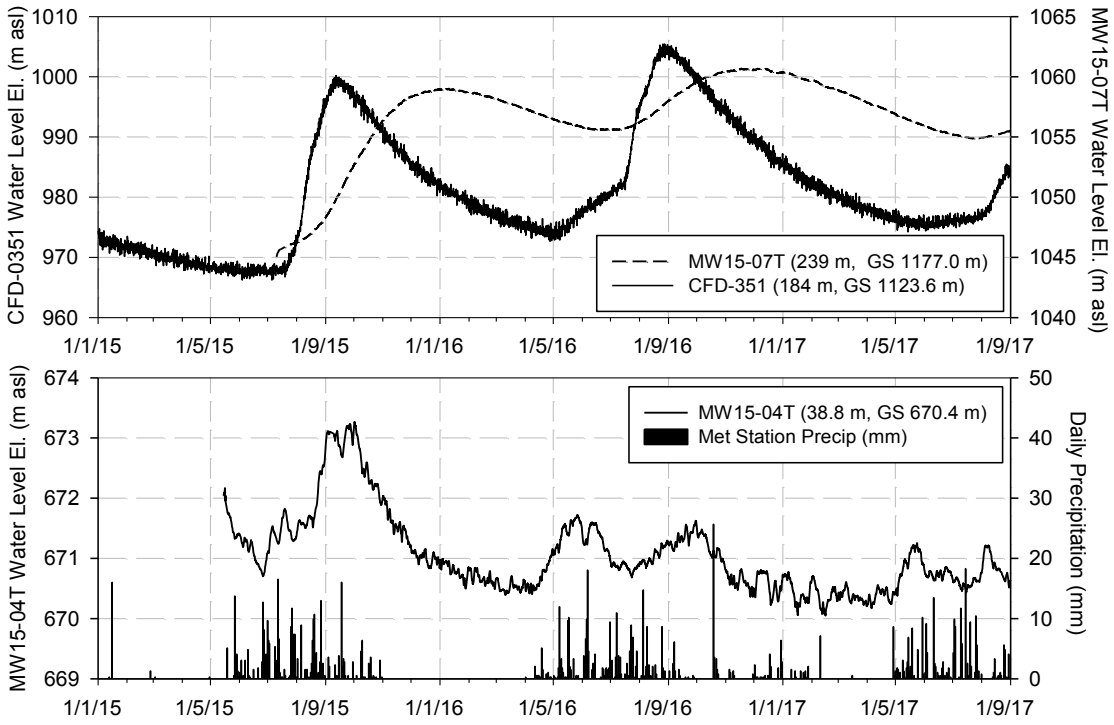


Figure 5: Water level hydrographs for selected monitoring locations at the Coffee project. Depth of sensor location and ground surface elevation at collar provided in parentheses. Instrument locations are shown in Figure 2

Conceptual Model

A conceptual hydrogeological cross section (Figure 6), has been prepared along section line A-A', which transects the Supremo Pit complex (Figure 2). The section shows baseline water levels, hydraulic conductivity measurements, borehole airlift yields (where applicable) and permafrost distribution. The permafrost distribution is based on a permafrost map prepared by Tetra Tech, with permafrost thickness inferred from field measurements and the elevation trend shown in Figure 3.

Artesian conditions are observed along the Latte tributary, while deeper water levels are found on the southwest slope draining towards Halfway Creek. The Coffee Creek fault under Latte Creek is a mapped fault while Halfway Creek is an inferred fault based on drilling results (fractured rock and high airlift yields). The proposed SU3 pit complex resides above the water table in permafrost while the SU1 pit terminates below the water table.

Groundwater Model

In order to predict project impacts on groundwater, a three-dimensional numerical groundwater model was developed using MODFLOW-2005 (Harbaugh, 2005). The numerical model incorporates project activities that may alter groundwater quantity, namely open pit development and placement of waste rock.

The model was run in steady state mode for baseline, end of operations and post-closure periods. Baseline model development, calibration and post-closure results are presented herein.

Baseline Model Development and Calibration

The model boundary extends from the Yukon River in the northeast to Independence Creek in the northwest (Figure 1). Coffee Creek forms the eastern and south-eastern boundary. The south-western edge of the model follows smaller tributaries to Independence Creek and Coffee Creek. Constant head boundary conditions were applied to major creeks along the perimeter of the model boundary, while drain conditions were applied to interior creeks. Recharge rates on non-frozen areas vary with topographic elevation, consistent with observed precipitation gradients. Recharge rates on non-frozen ground between elevations of 600 m to 1400 masl are equivalent to 15% mean annual precipitation (MAP). A nominal recharge rate of 5 mm/yr, or 1.1% of MAP, was applied to upland areas (>1,200 masl) underlain by permafrost while zero recharge was applied to frozen ground below this elevation.

Permafrost is inferred to be of very low hydraulic conductivity (Woo, 2012; Kane et al., 2013; Walrood et al., 2012) and is used to define the top layer of the model. Since permafrost is known to be discontinuous in the project area, a low hydraulic conductivity representing permafrost (6×10^{-10} m/s) was applied only to areas mapped as permafrost by Tetra Tech (2016) (dark blue areas in Figure 2). The thickness of the top layer was determined from an analysis of permafrost thickness informed by the thermistor data, as presented in Figure 3. In the near vicinity of the mine, thermistor data were contoured both manually and digitally to create the base of the permafrost layer. In farther afield areas, the thickness of permafrost is inferred based on elevation, using an average, linear relationship derived from the thermistor data (Figure 3). At the lowest elevations, a nominal groundwater model layer thickness of 5 m was maintained.

The model grid spacing is variable with cell width ranging from 12 to 70 m with tighter spacing used in areas of structural complexity and inferred faulting. The model domain is divided vertically into four layers. Hydraulic conductivity is variable over the model domain and varies with depth. Non-frozen bedrock shallower than 100 m below ground surface is assigned a higher hydraulic conductivity value than deeper bedrock, consistent with measured trends (Figure 4, Figure 7). Several high hydraulic conductivity features were implemented in areas of drilled structures, regional faults and along creek traces where hydrogeological testing indicated enhanced bedrock permeability.

The groundwater model was run in steady-state mode and was calibrated to creek baseflows and water levels measured at a low point on the groundwater hydrograph (circa June 2015). The baseflow targets were derived from measured basin yields which typically ranged from 0.4 to 0.9 L/s/km^2 for the winter period.

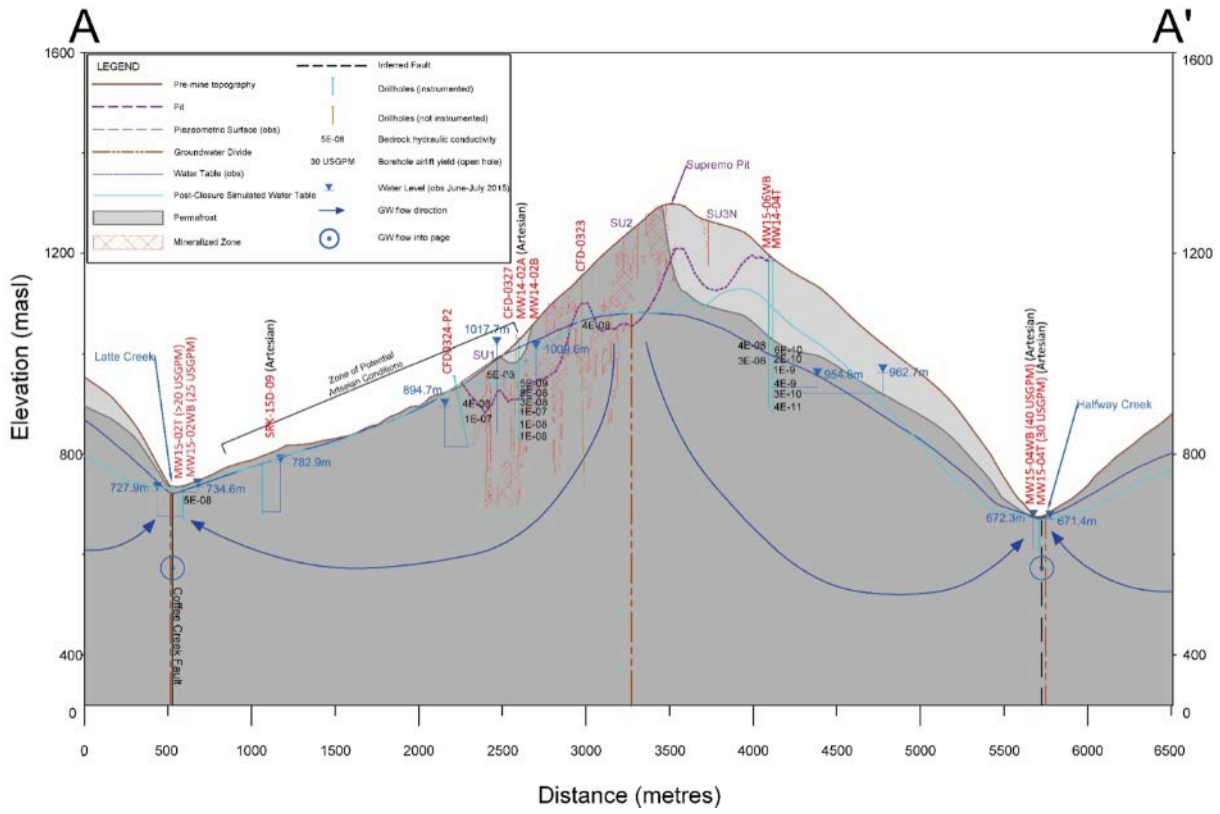


Figure 6: Hydrogeological cross section A-A

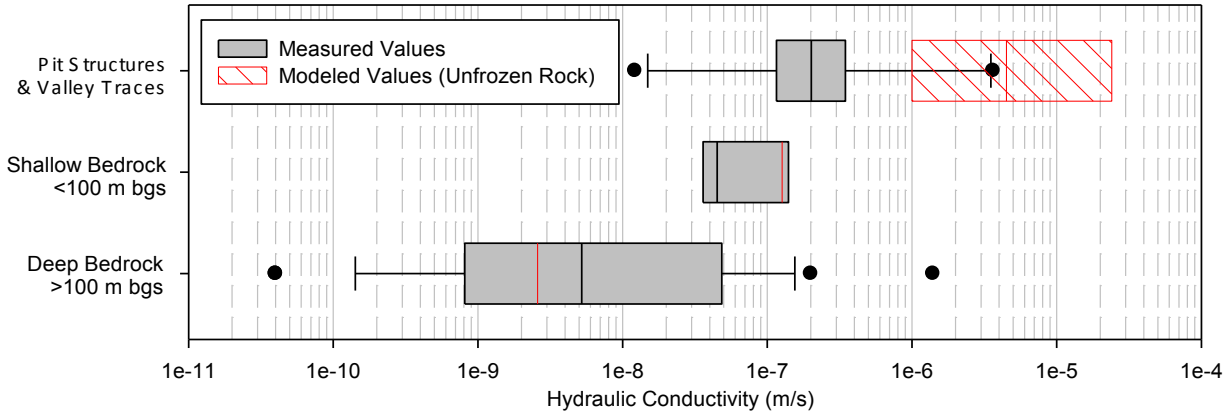


Figure 7: Box and whisker plots of calibrated and measured hydraulic conductivity values (m/s) for shallow and deep bedrock and permeable features

Recharge and hydraulic conductivity were varied to match calibration targets through a combination of manual and model-automated parameter optimization. Overall, the calibrated hydraulic conductivity values were found to be reasonably consistent with measured data, although the optimized value of hydraulic conductivity for mineralized structures were generally higher than measured in the field (Figure 7). As indicated in Figure 7, a single value of hydraulic conductivity was used for shallow and deep unfrozen bedrock; pit and valley structures were modeled using a range of values.

Baseflows simulated by the calibrated model fall within the ranges estimated from the winter flow data. Normalized root mean squared error (NRMSE) for the 42 water level targets used in the model is <1.2%, with a low absolute residual mean (5.5 m). Head residuals are not biased in one direction. The model is considered reasonably calibrated for these reasons and because it captures high and low hydraulic conductivity features without introducing unsubstantiated heterogeneity to achieve calibration targets.

Post-Closure Model

The baseline groundwater model was reconfigured to assess pit lake seepage losses and creek baseflows during post-closure. This was achieved through modification of recharge and flow boundary conditions to simulate placement of mine waste, the HLF and open pit development. Zero recharge was applied to the HLF footprint to account for a robust liner system. Zero recharge was also applied to the footprint area of the Alpha WRSF, where the steep topography, permafrost and rock drains are assumed to allow water to flow through the base of the waste rock pile and report to the sediment pond. Depending on permafrost presence and topography, recharge on mine waste backfilled into pits is anywhere from 0% to 35% of MAP.

Pit lakes are expected to form in all pit shells at closure due to groundwater inflows and meteoric inputs. Meteoric inputs cause pit lakes to form above the elevation that would otherwise be dictated by the water table alone. To arrive at reasonable post-closure pit lake elevations, an iterative exercise between the groundwater model and the GoldSim Water Balance Model (WBM) developed for the site was conducted to integrate groundwater flowpaths and pit leakage rates into the WBM. Leakage versus pit lake stage curves were determined for key pits using the groundwater model which were then coded into the WBM along with meteoric water inputs and other diversions. Ultimately, it was found that all pits will reach their spill point within three decades of cessation of mining.

The Post-Closure model was run in steady state with all pit lakes as constant heads at their spill point. Vertical through-taliks were assumed to form under pit lakes originally situated on permafrost. This was achieved by adjusting the K of the underlying permafrost upwards to that of unfrozen, shallow bedrock (Figure 7). Ultimate pit lake elevations and seepage losses for the Post-Closure are shown in Table 1, with the simulated post-closure water table shown in Figure 5.

Table 1: Summary of pit boundary conditions applied in the post-closure groundwater model

Pit	Pit advanced through permafrost (PF)	Max pit depth (m)	Pit bottom elevation (masl)	Pre-mine water table elevation (masl)	Pit Lake (constant head) elevation (masl)	Net groundwater flow to pit[1] (L/s)
SU1	PF absent	154	871	1,077	942	3.2
SU2	Yes	236	1,031	1,100	1,061	–0.7
Latte	Yes	150	950	1,025	998	–3.8
SU3W[2]	No	98	1,150	1,100	1,176	–0.3
SU3N	Yes	204	1,013	1,087	1,050	–0.6
SU4N	Yes	193	1,062	1,080	1,083	2.4
SU4S	PF absent	110	990	1,089	1,013	–0.8
SU5S[2]	No	103	1,151	1,091	1,165	–6.2
SU5N[2]	No	117	1,050	1,089	1,140	1.8
Double Double[3]	PF absent	100	991	1,030	R=35% MAP	–0.8
Kona[3]	No	90	1,162	1,162	R=0% MAP	0

Notes:

1. Negative value indicates seepage loss from pit to groundwater system.
2. Bedrock hydraulic conductivity underlying pit is converted from a permafrost value to a shallow bedrock value.
3. Pit completely backfilled with mine waste, recharge (R) as indicated.

Appreciable groundwater mounding (tens of meters) is observed in the vicinity of the Latte and Supremo pit complex, with exception to the southernmost Supremo Phase 1 (SU1) pit, where water levels are drawn down by ~20 m (Figure 6). The SU1 pit is advanced well below the pre-mining water table (Figure 5, Table 1).

Seepage losses from the pits are generally small (Table 1). Seepage losses from SU5S largely report to nearby pits (SU5N and SU4). Overall, combined seepage losses from the pits to Latte Creek (including Latte Tributary), Halfway Creek, and YT-24 are 4 L/s, 3 L/s and 0.5 L/s. Despite the underlying assumption of pit lake levels at their spill point and the formation of through-taliks under the pit lakes, seepage losses from the mine facilities are limited vertically by underlying low K deep bedrock and in some areas, laterally, by low K permafrost. The generally tight bedrock conditions also limit simulated changes to creek baseflows, despite the relatively large changes in groundwater levels in the mine footprint area (Table 1). Post-closure baseflows are generally within 5% of simulated baseline baseflows, except in Halfway Creek, where baseflow is expected to increase by ~10% near its confluence with the Yukon River.

Conclusion

A multiphase hydrogeological field program has been undertaken at the proposed Coffee Gold mine site. Challenges arising from greater-than-anticipated permafrost thickness prompted a switch from conventional monitoring wells to VWP/thermistor strings coupled with Westbay systems, allowing for continuous monitoring of ground temperature and groundwater pressures along with sampling of sub-permafrost groundwater. Overall, permafrost extends to greatest depths in ridge areas and appears to reduce in thickness towards areas of lower elevation; north-facing slopes tend to have thicker and more prevalent permafrost than south-facing slopes. The thickest and coldest permafrost (~165 m deep, –1.7^{o}C) is encountered near the north end of the proposed Supremo pit.

Hydraulic testing results indicate that structural features, and not rock type, impart the dominant control on hydraulic conductivity. Structures hosting mineralization reported a narrow range of K values (1E-07 m/s to 3E-06 m/s). Holes advanced near creek channels reported similar hydraulic conductivity values, supporting the inference that valley traces represent fault structures. Outside of structures, hydraulic conductivity is observed to decrease with depth.

Groundwater levels across the Coffee project are highly variable with respect to vertical and hydraulic gradients, depth to water level, and the timing and magnitude of hydrograph fluctuations. This variability speaks to the complexity of a groundwater system in an area of topographic relief influenced by faulting and discontinuous permafrost.

A steady state, three-dimensional MODFLOW groundwater model has been developed for the Coffee project that has been calibrated to water levels and measured baseflows. Calibrated hydraulic conductivity values generally fall within ranges of measured values, except for structures, which are simulated to be more permeable than mean measured values. Permafrost was modelled as a low hydraulic conductivity layer within the model domain. Recharge on unfrozen ground was assumed to be 15% of MAP, while recharge on frozen ground was assumed to be zero, except on high elevation areas where a nominal value was used.

A steady state simulation of post-closure conditions found that seepage losses from pits to nearby creeks were small (4 L/s or less) despite the underlying assumption of pit lake levels at their spill point and the formation of through-taliks under the pit lakes. Seepage losses from the mine facilities are limited vertically by underlying low hydraulic conductivity deep bedrock and, in some areas, laterally, by low conductivity permafrost. The generally tight bedrock conditions also limit simulated changes to creek baseflows, despite the relatively large changes in groundwater levels in the mine footprint area.

Acknowledgements

The author would like to gratefully acknowledge Kaminak Gold Corporation and Goldcorp for supporting these studies and allowing publication for the benefit of others. The author would also like to acknowledge the other consulting teams who have worked on this project, including and not limited to Tetra Tech and SRK, who have shared data and expertise, allowing a multi-discipline approach to the hydrogeological interpretation of this complex area.

References

Berman, R.G., Ryan, J.J., Gordey, S.P. and Villeneuve, M. 2007. Permian to Cretaceous polymetamorphic evolution of the Stewart River region, Yukon-Tanana terrane, Yukon, Canada: P-T evolution linked with in situ SHRIMP monazite geochronology, *Journal of Metamorphic Geology,* 25(7): 803–827.

Goldcorp Inc., 2017. Coffee Gold Mine Project Proposal for Executive Committee Screening Pursuant to the Yukon Environmental and Socio-economic Assessment Act. March 2017.

Harbaugh, A. 2005. MODFLOW-2005, the US Geological Survey modular ground-water model – the Ground-Water Flow Process: US Geological Survey Techniques and Methods 6-A16.

Kane, D.L., Yoshikawa, K. and McNamara, J.P. 2013. Regional groundwater flow in an area mapped as continuous permafrost, NE Alaska (USA), *Hydrogeology Journal,* 21(1): 41–52.

NRCan, 1995.Canada Permafrost Map MCR-4177. *National Atlas of Canada,* 5th edition. Retrieved from: http://ftp2.cits.rncan.gc.ca/pub/geott/atlas/archives/english/5thedition/environment/land/mcr4177.jpg

SRK Consulting, 2015. Hydrogeologic Investigations Report Coffee Project, Yukon, December 18, 2015.

Tetra Tech EBA. 2016. Coffee Gold Project: Environmental Baseline Report, Mine Site Study Area: Surficial Geology, Permafrost, and Terrain Stability, May 2, 2016.

Walvoord, M.A., Voss, C.I. and Wellman, T.P. 2012. Influence of permafrost distribution on groundwater flow in the context of climate-driven permafrost thaw: Example from Yukon Flats Basin, Alaska, United States, *Water Resour. Res. 48*(7): 17 pp.

Woo, M. 2012. *Permafrost Hydrology*. New York: Springer.

Proceedings of Mine Water Solutions 2018
June 12–15, 2018, Vancouver, Canada
Published by the University of British Columbia, 2018

Planning Climate Change Adaptation Practices in Watershed Ecosystems: What is the Mining Sector Developing?

Gabriel Castillo Devoto, The University of British Columbia, Canada

Abstract

Ore deposits are distributed in different locations of the earth's geography and are often located in remote, ecologically sensitive, and less-developed areas that include many indigenous lands and territories. Some of the world's major ore deposits are located in close proximity to principal mountain regions where watershed ecosystems develop, making it especially important to consider this aspect in relationship to mining projects and their land reclamation stage. All of the world's major rivers originate in mountains, and more than half of the world's mountain areas play a vital role in supplying water to downstream regions. Mining companies that are developing the ore deposits in these areas have a strategic challenge regarding how to contribute to understanding and managing mountain watershed ecosystems in a climate change scenario.

This paper finds that major mining companies adopt a static average of environment indicators and water balance during the design and planning. There is not a consistent evaluation of the future climate change impacts or predictive models that could help companies and regulators to establish a robust risk management plan. Ecosystem adaptation under changing climate conditions is currently not a priority in closure plans and climate change risk management, which in the long term could result in poor landscape reclamation with an extreme cost. This paper presents a review of different strategies that have been applied by the Top Ten mining companies (by market capitalization in the world) to manage the risk of climate change. A systematization process and a benchmarking framework using Trend Analysis are presented to summarize practices that mining companies are applying to manage and adapt to climate change risks along its direct impact area.

Introduction

The global agreement on climate change was reached at the 21st Conference of the Parties (COP21), in December 2015. This commitment revealed the increasing interest of governments over time with the

challenges of climate change. Country signatories acknowledge that:

> "climate change is a common concern of humankind and the Parties should, when taking action to address climate change, respect, promote and consider their respective obligations on human rights, the right to health, the rights of indigenous peoples, local communities, migrants, children, persons with disabilities and people in vulnerable situations and the right to development, as well as gender equality, empowerment of women and intergenerational equity" (UNFCCC, 2015).

This agreement brings new challenges and opportunities for society in planning, design, and cooperation through capacity building and technology transfer (Hermwille, 2016). Mining companies are not an exception, and indeed may make a significant contribution.

The purpose of COP21 is to constrain the increase in global average temperatures to well below 2˚C, and pursue efforts to achieve 1.5˚C above preindustrial levels; improve the ability to adapt to adverse climate change; and foster low carbon emissions development. The negotiated outcomes will influence national policies and energy technology choices for the coming decades. The additional costs that these policies could pose for businesses are still unclear (UNFCCC, 2015).

A changing climate presents physical risks to mining and metals operations, because these industries are often located in challenging geographies (ICMM, 2013) and manage climate sensitive resources (i.e. water and energy). Climatic conditions will disturb the stability and efficacy of infrastructure and equipment, environmental protection and site closure practices, and the accessibility of transportation routes (Nelson and Schuchard, 2011). It can be reasonably argued that the long-term success and prosperity of mining companies will depend on their ability to manage their climate change impacts with mitigation plans and to reduce the risk with adaptation programs (Pearce et al., 2011). As is highlighted by the International Council on Mining & Metals (ICMM), an extensive range of risks and opportunities for the mining and metals sector presents in a changing climate. In their report they mention that the main business impacts are direct physical risks to core operations, including the health and safety of employees, physical assets, processes, and operations and maintenance activities (ICMM, 2013). The document argues that effective risk management processes at both operational and corporate levels have incorporated the climate change considerations. Shareholders, investors, and insurers are beginning to contemplate the consequences of climate risk to long-term financial performance of the companies, and will pressure companies to minimize carbon liabilities and develop adaptation plans (Nelson and Schuchard, 2011). Indeed, in 2016 a group of mining companies received a request from a group of shareholders (Aiming for A coalition) in support of strategic climate resilience for 2035 and a comprehensive response to the challenges posed by climate change (Glencore, 2016).

There are still significant uncertainties about the magnitude, frequency and spatial occurrence of climate change (Institute of Environmental Management & Assessment, 2015). Odell highlights that the relationship between mining and climate change has received limited attention (Odell et al., 2017). Such uncertainties make it difficult to assess the impacts on actual mining operations or future projects around the word, but it is possible to contemplate a range of factors, based on the available literature.

Researchers argue that the mining sector is not giving enough attention to the adaptation plans in areas that have been disturbed by mining operations, and that the climate change risk in the watershed surrounding the mining activities requires more understanding. In order to develop this idea, a systematic review was conducted of the current publicly available data and self-reported information provided by the global top ten mining companies by market capitalization. The sources of information included corporate sustainability reports (2016/2017) and the CDP (formerly the Carbon Disclosure Project). The assessment used benchmark methodology to identify and understand the management context of climate change impacts and risks in the mining sector. Four criteria were used to assess the actual dynamic of the mining sector, represented in these companies, related to climate change management. The assessment criteria were used in an attempt to understand what mining companies are doing in relation of climate change; what the most important climate-related risks for mining companies are; what future impacts the companies mentioned might face in extreme weather scenarios; and lastly, how the mining companies are planning to adapt to climate change risk and impacts. The results will improve our understanding of the actual practices, and more importantly, the gap between current and best practices in the mining sector.

Methodology

Trend Analysis, an Initial Benchmarking Process

There are many definitions of benchmarking; as a performance measurement tool, the effectiveness of a benchmark depends on its practical value. According to the US National Research Council, benchmarking is the systematic process of measuring one's performance against recognized leaders for the purpose of determining best practices that lead to superior performance when adapted and utilized (National Research Council of the National Academies, 2005). Companies studying best practices have the greatest opportunity for gaining a strategic, operational, and financial advantage (Kelessidis, 2000).

Benchmarking exercises typically involve four levels of assessment (Parks et al., 2010): trend analysis; peer comparison; direct agency contact; and benchmarking networks. This paper applies a trend analysis exercise to address the following core research question: What kind of practices are mining companies applying to adapt to climate change risks? This question is explored through reviewing the most recent sustainability reports (2016/17) of the global top ten mining companies, to understand the

development trends regarding climate change risk management and adaptation. This research seeks to identify examples of "best practices" being employed by the companies, rather than measuring the best performance among them. A common set of measures related to climate change has been defined and integrated into a data collection system.

Trends in Best Practices Managing Climate Change Risk

This study reviews the top ten mining companies ranked in April 2017 by S&P (Table 1), a provider of worldwide financial and commodity markets analytics (S&P Global Market Intelligence, 2017). In this study, mining refers to companies involved in the extraction of a broad range of metals and minerals, including precious metals, base metals, industrial minerals, coal, and uranium.

The peer group selected for this study includes BHP Billiton Group, Rio Tinto, Glencore Plc, Vale SA, Coal India Ltd., PJSC Norilsk Nickel Co., Grupo México SAB (and Southern Cooper Corp.)[1], Anglo American Plc, Barrick Gold Corp and Freeport-McMoRan Inc.

Pearce et al. (2011) explain the high level of vulnerability of the mining industry to climate change, mostly because mining facilities were designed and built assuming a stable climate. The study recognizes climate-related hazards such as wildfires, floods, windstorm, water scarcity, and sea-level rise. More recent research conducted by Phillips (2016) shows the impacts of flooding on coastal operations in the event of sea level rise and increasing water scarcity in mining regions.

In the first section, we assess the actual corporate management approaches that these mining companies employ to manage the impacts of climate change. Table 2 indicates the objective for each parameter that was used to review the information provided in the latest sustainability report for each company (available until February 2018). At the same time, when available, we reviewed the climate change performance data and the risk management information reported by each company in the 2017 CDP.

In the second section, we assess the actual expected climate-related risks that each company reported for their operations. The research risk parameters are indicated in Table 3. These parameters were defined and adapted based on the literature review (Pearce et al., 2011; Ford et al., 2010; Odell et al., 2017; Bowyer et al., 2014; Nelson and Schuchard, 2011). Each parameter received one point (1) for each company that identified that risk in its latest sustainability report (available until February 2018). At the same time, when available, we reviewed the climate change performance data reported by each company in the 2017 CDP, assessing the climate-related risks reported.

[1] Southern Copper Corp. is a majority-owned, indirect subsidiary of Grupo Mexico SAB de CV ("Grupo Mexico), and both present the same Sustainability Reports. We rank Freeport-McMoRan Inc. as the 10th company.

Table 1: Top 25 metal and mining companies ranked by April 28 market cap
(Source: S&P Global Market Intelligence)

Ranking						Market cap change from (%)	
Current	End-March 2017	End-April 2016	Institution name	Trading symbol and exchange	Market cap (US$B)	End-March 2017	End-April 2016
1	1	1	BHP Billiton Group	BHP-ASX	89.10	(2.6)	11.9
2	2	2	Rio Tinto	RIO-LON	73.98	–1.0	17.4
3	3	3	Glencore Plc	GLEN-LON	56.55	0.3	64.8
4	4	5	Vale SA	VALE5-BSP	43.47	–8.4	60.2
5	6	6	Southern Cooper Corp.	SCCO-US	27.34	–1.4	19.1
6	5	4	Coal India Ltd.	533278-BOM	26.73	–4.6	–2.2
7	7	7	PJSC Norilsk Nickel Co.	GMKN-ME	24.10	–3.1	5.5
8	8	9	Grupo México SAB de Cv	GMEXICO.B-MEX	22.72	–2.3	14.2
9	10	14	Anglo American Plc	AAL-LON	20.11	–6.2	39.3
10	9	8	Barrick Gold Corp	ABX-US	19.49	–12.0	–13.6
11	11	11	Freeport-McMoRan Inc	FCX-US	18.43	–4.6	5.1
12	13	10	Newmont Mining Corp.	NEM-US	18.03	2.9	–2.8
13	12	20	Hindustan Zinc Ltd.	500188-BOM	17.67	–6.1	61.5
14	14	15	PJSC Polyus	PLZL-ME	14.74	–2.1	4.8
15	17	13	Potash Corp. of Sask.	POT-TSX	14.14	–1.2	–4.9
16	16	16	Fresnillo Plc	FRES-LON	13.84	–3.5	15.2
17	18	17	Agrium Inc.	AGU-TSX	12.95	–1.5	8.5
18	24	27	PJSC Alrosa	ALRS-ME	12.68	6.6	50.8
19	20	18	Saudi Arabian Mining Co.	1211-TSE	12.58	–1.3	10.5
20	15	28	Fortescue Metals Group Ltd.	FMG-ASX	12.37	–16.4	52.6
21	19	19	Newcrest Mining Ltd.	NCM-ASX	12.14	–6.8	9.4
22	26	16	Franco-Nevada Corp.	FNV-TSX	12.12	3.9	–3.0
23	25	34	Albemarle Corp.	ALB-US	12.06	3.1	62.4
24	21	37	Teck Resources Ltd.	TECK.B-TSX	11.97	–5.0	69.0
25	23	12	Goldcorp Inc.	GG-US	11.94	–4.3	–28.8

Data as of April 28, 2017. The company list was obtained from mining-focused companies included in the most recent Industry Monitor.

Table 2: What are mining companies doing about climate change risk management?

Parameter	Objective
a. Development of policies and corporate guidelines	Assess the actual establishment of specific policies or corporate guidelines related to climate change management
b. Highest management decision level of climate change	Assess who is responsible for making decisions for the strategy and direction of the company in regards to climate change management
c. Reporting of climate change data	Assess the mechanism the companies use for sharing and disclosing their climate change information
d. Mechanism for climate change risk identification	Assess the process established in each company for describing the risks and modeling future impacts

Table 3: What are the most important climate-related risks the companies mentioned could have?

Parameter	Objective
a. Temperature	Assess the recognized and reported risks that the companies could have, related to the changing climate. When the report reviewed showed this parameter as a direct risk for any of his operations, one point (1) was assigned to the parameter reported.
b. Heat waves	
c. Sea-level rise	
d. Precipitation	
e. Floods	
f. Storms	
g. Wind	
h. Drought	
i. Snow	
j. Fog	
k. Wildfires	

In the third section, we assess the actual expected impacts that each company reported for their operations, related to climate change risks. The research impact parameters are indicated in Table 4. These parameters were defined and adapted based on the literature review (Pearce et al., 2011; Ford et al., 2010; Odell et al., 2017; Bowyer et al., 2014; Nelson and Schuchard, 2011). Each parameter received one point (1) for each company that recognized a type of impact in the latest sustainability report (available until February 2018). At the same time, when available, we reviewed the climate change performance data reported by each company in the 2017 CDP, assessing the future impacts reported.

In the fourth section, we assess the actual plans for climate change adaptation that each company reported for their operations. The research adaptation plan parameters are indicated in Table 5. These parameters were defined and adapted based on the literature review (Pearce et al., 2011; Ford et al., 2010; Odell et al., 2017; Bowyer et al., 2014; Nelson and Schuchard, 2011). Each parameter received one point (1) for each company that recognized a kind of adaptation plan for climate change in the latest

sustainability report (available until February 2018). At the same time, when available, we reviewed the climate change performance data reported by each company in the 2017 CDP, assessing the adaptation plans reported.

Table 4: What are the future impacts the companies could experience in extreme weather scenarios?

Parameter	Objective
a. Infrastructure disturbance b. Supply chain routes c. Product delivery routes d. Workforce health e. Water access f. Productivity reduction g. Reputational damage h. Increment cost i. Policy and regulatory change j. Energy access	Assess the recognized and reported impacts by the companies, which could occur due to climate-related risks. When the report reviewed shows this parameter as a direct impact for any of his operations, one point (1) was assigned to the parameter reported.

Table 5: How are the mining companies planning to adapt to climate change risk and impacts?

Parameter	Objective
a. Risk scenario assessment b. Energy efficiency c. Research collaboration d. Stakeholder communication e. Staff training and education f. Emergency response plans g. Water management plans h. GHG emissions control i. Review of business strategy	Assess the actions developed and reported for adaptation to climate change by the mining companies. When the report reviewed showed this parameter as an adaptation action for any of its operations, one point (1) was assigned to the parameter reported.

Data and Discussion

What are Mining Companies Doing about Climate Change Risk Management?

Development of Policies and Corporate Guidelines

In June 2007 BHP established its first Climate Change Policy (BHP Billiton Limited, 2007), in which the company recognized the importance of addressing the risks associated with climate change. In 2015, BHP published its Climate Change: Portfolio Analysis report, which described the way this company approaches portfolio evaluation and scenario planning, including the implications of a transition to a lower emissions future (BHP Billiton, 2016).

In the case of Vale, the company has established management commitments, such as the Sustainability Policy, Global Mitigation, and Adaptation to Climate Change policy (Vale, 2017). Vale takes into account the management of ecosystem services related to energy, climate change, water, and community, aiming for a net positive impact.

Anglo American published its Climate Change Policy in 2011, expressing in this document its commitment to addressing the causes of climate change and to helping to protect Anglo American employees and assets, as well as local communities and the environment, against potential climate change impacts (Anglo American, 2016).

The mining companies operate in different regions worldwide, and most of them use the local environmental legal framework as the basis, and then apply their own guidelines and standards as a corporate mandate. As is presented in Table 6, only these three companies just mentioned have already defined a specific corporate policy for climate change management. Other companies are in the process of developing this specific policy and including their corporate commitments. All of the companies have climate considerations as part of their environmental programs.

Highest Management Decision Level of Climate Change

When evaluating the highest level of direct responsibility for climate change within each organization, this research aims to discern who is responsible for making decisions for the strategy and direction of the company in regard to climate change management. This helps to understand the level of criticism that each company could experience in regard to climate-change associated risks, given that we have limited knowledge about how organizations evaluate adaptive actions (Linnenluecke et al., 2013).

The BHP report mentioned that climate change is a priority governance and strategic issue for the BHP Board; however, it is the management level that has primary responsibility for responses to climate change. GHG reduction is considered in senior executive and leadership remuneration (BHP Billiton Limited, 2017a).

At Rio Tinto, climate change actions are debated at senior levels of management and by the Board Sustainability Committee. The executive committee approves the climate change position statement and the 2017 Climate Change Report (Rio Tinto – CDP Disclosure Insight Action, 2018).

The board of Glencore has established a committee with responsibility for sustainability, including climate change, namely the Board HSEC committee (Glencore, 2016).

At Anglo American, climate change is reviewed by the Group Technical Director of the Board. The Group Technical Director is supported by the Group head of safety and sustainable development, the head of environment, and the lead for energy and carbon effectiveness (Anglo American – CDP Disclosure Insight Action, 2018).

At Barrick, a Climate Change Committee has been established to improve the existing energy management plan and develop a comprehensive climate change strategy (Barrick – CDP Disclosure Insight, 2018). A Freeport-McMoRan report did not detail a specific management group working on climate change. The board is responsible for risk oversight, with reviews of certain areas being conducted by the relevant board committees that report to the full board. But there is not enough information to understand which level makes decisions about responses to climate change (FCX – CDP Disclosure Insight Action, 2018).

Other companies that were assessed did not mention a specific management group in charge of this issue in their sustainability reports.

Table 6: Actions taken by mining companies to manage climate change risk

Company	Policy development	Management decisions	Reporting	Risk identification
BHP Billiton Group	×	Board and managers	CDP TCFD	Corporate Risk Management
Rio Tinto	–	Board Sustainability Committee	CDP WRI WBCSD	–
Glencore Plc	–	Board HSEC Committee	CDP	On-site assessment
Vale SA	×	–	CDP WRI	Corporate Risk Management
Grupo México SAB de Cv	–	–	Registro Nacional de Emisiones	–
Coal India Ltd.	–	–	–	–
Norilsk Nickel Co.	–	–	–	Risk Management Policy
Anglo American Plc	×	Board Group Technical Director	CDP	ORM IDM
Barrick Gold Corp	–	Climate Change Committee	CDP CPLC	Scenario development
Freeport-McMoRan Inc.	–	–	CDP	Sustainable Development Risk Register

CDP: Carbon Disclosure Project
TCFD: Taskforce on Climate-related Financial Disclosures
WRI: World Resources Institute
CPLC: Carbon Pricing Leadership Coalition
ORM: Operational Risk Management
IDM: Investment Development Model

Reporting of Climate Change Data

The process of creating value in the industry implies information and knowledge sharing on climate change management, which will contribute to increased understanding of GHG emissions in the products' life cycle. Corporations and interested groups require a better image to understand the actions of the company in climate change related issues (Özsözgün and Emel, 2016), and the data collected will help in management decisions. A group of companies made a voluntary submission of climate change information to the CDP. These companies include BHP, Rio Tinto, Anglo American, Vale, Freeport-McMoRan, Glencore and Barrick.

In addition, BHP information is aligned with the Financial Stability Board's Taskforce on Climate-related Financial Disclosures (TCFD) (BHP Billiton Limited, 2017a). Rio Tinto reports a consolidated Group level using the GHG Protocol developed by World Resources Institute (WRI) and WBCSD (Rio Tinto, 2017). In the case of Vale, the company also maintained the GHG Protocol Program for its corporate inventory of GHG emissions (Vale, 2017). Grupo México mentioned that their GHG inventories are verified independently, and that the company has been taking this action since before this was mandatory (Grupo Mexico, 2017).

Anglo American reported to CDP for the first time in 2006. Since then, the company continues to participate in the global environmental disclosure system for business (Anglo American – CDP Disclosure Insight Action, 2018). In 2016, Barrick joined the Carbon Pricing Leadership Coalition (CPLC), led by the World Bank as Secretariat (Barrick Gold Corporation, 2017).

Mechanism for Climate Change Risk Identification

There is still uncertainty about the risk and impacts the ecosystem will experience with a changing climate. Therefore the data used, the modeling process, and the interpretation of the likelihood of this effects is a challenge (Yousefpour et al., 2012).

BHP has established an "Our Requirements for Risk Management" standard, with the framework for risk management relating to climate change and material risks around health, safety, environment, and community (BHP Billiton Limited, 2017b). Rio Tinto recognizes the significant risks for businesses and society that climate change will create; however, Rio Tinto considers that climate change also presents opportunities (Rio Tinto, 2017).

At Glencore, the board assesses and approves overall risks, supported by the HSEC committee. The sites are required to annually report climate change-related risks and opportunities (Glencore, 2016). Vale mentioned that the risks related to climate change are monitored and updated every year (Vale, 2017). Norilsk Nickel implemented a corporate risk management framework (CRMF) in 2016. And the company's Board of Directors adopted a Corporate Risk Management Policy (Nornickel, 2017).

Anglo American considers climate change and extreme weather events a material risk to their business in multiple ways. This approach has two key processes to manage climate-change risks: the Operational Risk Management (ORM) for operations, and the Investment Development Model (IDM) for projects. Barrick was working to set targets around climate change in 2017. As part of the target-setting exercise, the company is developing scenarios to identify initiatives to lower carbon emissions and targeted emissions (Barrick – CDP Disclosure Insight, 2018). Freeport-McMoRan has instituted a Sustainable Development Risk Register (SDRR). This tool enables the company to identify key risks and opportunities across the safety, environmental, social, economic, and value chain spectrums (including climate change related) (FCX – CDP Disclosure Insight Action, 2018).

What Are the Most Important Climate-Related Risk the Companies Could Have?

The review of the sustainability report remarks on different risks related to the climate that could affect operations. The principal three risks that could affect the mining companies are the variations in patterns of precipitation, storms, and droughts. These three add up to a total of 54% of the risk reported. The second highest risk was floods, which was allocated 13% of the risk consideration by companies. In Figure 1, it can be seen that temperature and sea-level rise are considered to be the third most risky group.

The physical effects of temperature increments could affect the performance of the workforce, and these could materially and adversely affect the financial performance of the assets (BHP Billiton Limited, 2017b). In some operations, the temperature increase could generate ice sheet melt, which could block accesses (Glencore – CDP Disclosure Insight Action, 2018).

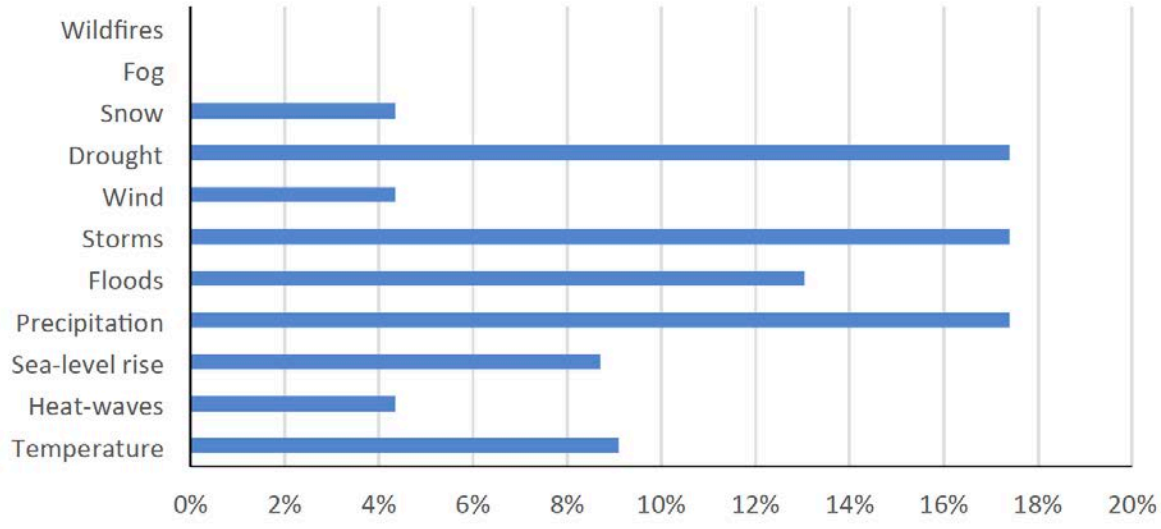


Figure 1: Percentage of risk reported by mining companies

Port facilities could be adversely affected by rising sea levels, with potential reduction or disruption in production capacity, which could adversely affect financial performance (BHP Billiton Limited, 2017a). Sea level rises could impact coastal operations on coastal stock piles and cause infrastructure damage (Rio Tinto, 2017). Shipping disruptions have the potential to interrupt product delivery and could impact on production rates if they occur for extended periods of time (Glencore, 2016). This would result in higher costs for usage of the ports, which in turn may raise the cost of goods (Barrick – CDP Disclosure Insight, 2018).

Rainfall change patterns could intensify water stress and impact the availability of water for operations (BHP Billiton Limited, 2017b). There is a high degree of uncertainty associated with rainfall, which will impact future risks (Rio Tinto – CDP Disclosure Insight Action, 2018). Other operations will require an upgrade to stormwater facilities as well as water storage facilities (Glencore – CDP Disclosure Insight Action, 2018).

For BHP, extreme floods and droughts could impact water management at their operations, potentially disrupting or reducing production capacity (BHP Billiton Limited, 2007). The Grupo Mexico has a program in place to protect their facilities against events such as damage to signalling systems and landslides (Grupo Mexico, 2017).

There is an increased likelihood of more intense and more frequent storm systems, including tornados, hurricanes and cyclones, which could impact production (BHP Billiton Limited, 2017b). For Rio Tinto, changes in the intensity and frequency of tropical cyclones have the potential to damage infrastructure and interrupt business operations (Rio Tinto, 2016).

Extreme droughts and floods may impact water management (BHP Billiton Limited, 2017b). In the case of Glencore, the company has developed a risk register to identify likelihood/consequences, mitigation controls, and action plans for droughts (Glencore, 2016). Norilsk Nickel noted that abnormal droughts would cause water shortages in storage reservoirs, with the possibility of the failure of power production by turbines (Nornickel, 2017)

What are the Future Impacts the Companies Could Experience in Extreme-Weather Scenarios?

There are two major concerns, as presented in Figure 2, about the future impacts of a changing climate with extreme scenarios. The first one is the change in regulations related to the GHG emissions reduction, as well as the carbon price potential policy. This modification could affect operational costs and investment returns; in consequence, this parameter is of concern to 18% of mining companies. The second concern is infrastructure damage caused by climate change. Tailings and dams are mentioned as infrastructures of concern, as initial designs did not consider the risks of climate change. A third concern is access to water, a resource that is required in the entire mining cycle.

Policy and Regulatory Change

BHP considers the absence of regulatory certainty about climate change in different countries to be a management challenge (BHP Billiton, 2016). Rio Tinto considers that as countries work to deliver their commitments, this may impact competitiveness (Rio Tinto, 2017).

Glencore engages with policy-makers throughout the public policy development process from design through to implementation and compliance (Glencore – CDP Disclosure Insight Action, 2018). Vale is monitoring and assessing the development of international policies for the management of risks, and the price of carbon in capital investment decisions (Vale, 2017).

Grupo Mexico considered regulatory changes as a principal risk, and is developing actions and projects to manage this risk to business opportunities (Grupo Mexico, 2017). For Anglo American, the financial implications of climate change will only become evident as countries develop and implement domestic policies. They are placing emphasis on implementing energy and emission savings (Anglo American, 2017).

Infrastructure Disturbance

Dam safety reviews are underway at all significant operated and non-operated BHP sites. Those reviews include considering how climate change might impact risk and design requirements. BHP created a centralized function for dams and tailings governance and risk management (BHP Billiton Limited, 2017b). One risk would be having to treat greater amounts of water in shorter time periods in the event of extreme precipitation (Glencore, 2017). Grupo Mexico has an improvement program in place to protect their facilities against landslides (Grupo Mexico, 2017). Norilsk Nickel is reviewing their buildings to control the risk of destruction to ensure safe operating conditions (Nornickel, 2017). Anglo American reported that changes in rainfall variability may cause operational disruptions due to floods and droughts, and may negatively affect land rehabilitation outcomes (Anglo American – CDP Disclosure Insight Action, 2018).

Supply Chain Routes

Access to infrastructure, such as rail, ports, power and water, is critical to mining. Public or privately-operated infrastructure may be inadequate, and the impact of climate change may increase competition (BHP Billiton Limited, 2017a). The supply of essential raw materials and energy to Rio Tinto operations is considered a risk (Rio Tinto, 2016). The Grupo Mexico is considering a growing risk for their transportation division (Grupo Mexico, 2017).

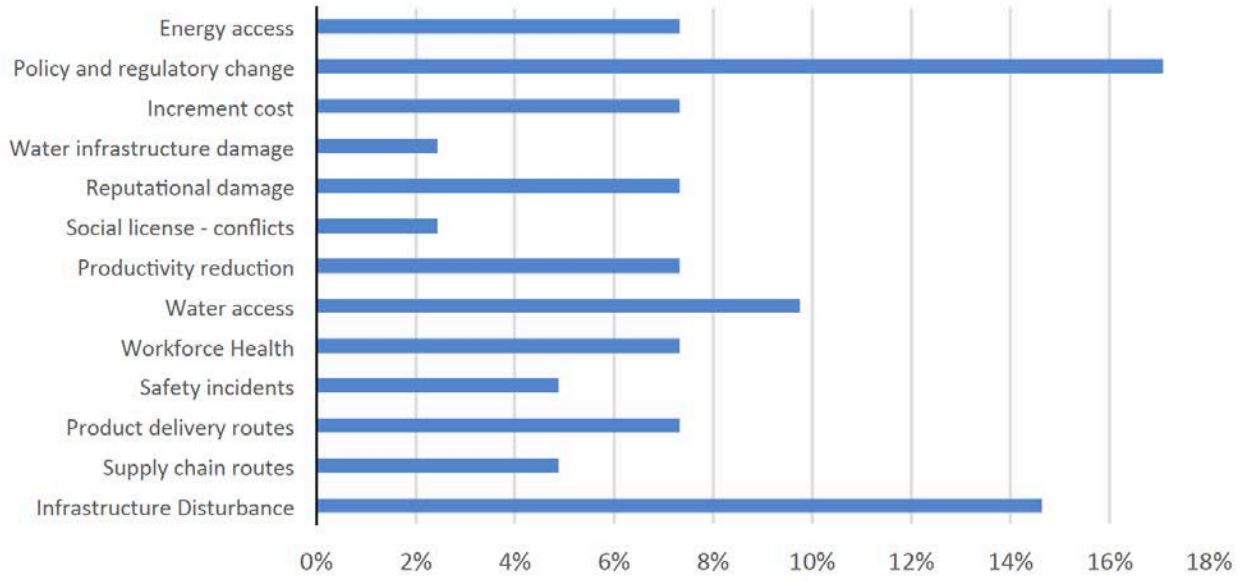


Figure 2: Percentage of future impacts in extreme-weather scenarios

Product Delivery Routes

BHP and Rio Tinto consider that the impacts of climate change could affect product transportation, the expansion of business, and the ability to operate efficiently (BHP Billiton Limited, 2017a; Rio Tinto, 2016). The same consideration is reported by Glencore (Glencore, 2016).

Workforce Health

Barrick highlighted that changing temperatures may result in the migration of some diseases (Barrick – CDP Disclosure Insight, 2018). This could result in health fears among communities, employees, and contractors.

Water Access

As BHP described, the impact of a changing climate may increase competition for restricted resources. Grupo Mexico reinforced their water management systems and improved water reuse in their production chain (Grupo Mexico, 2017). Glencore and Freeport-McMoRan utilized their annual scenario planning design adaptation plans for times of water shortage or extreme surplus (Glencore – CDP Disclosure Insight Action, 2018). Norilsk Nickel devloped a hydrological monitoring system to forecast water levels in rivers and water bodies in their operations, and to classify and analyze hydrological data (Nornickel, 2017).

Productivity Reduction

The companies considered that the different risks identified (tornados, changes in precipitation pattern,

rises in sea level, floods, droughts, etc.) could generate long periods of interruptions to internal roads resulting in loss of production, delay in new project,s and impacts on existing commodity markets (Glencore – CDP Disclosure Insight Action, 2018).

Reputational Damage

BHP considered potential exposure to increased court cases and unexpected environmental expenses as potential reputation risks if their performance and commitments are not successfully achieved (BHP Billiton, 2016). For Rio Tinto, a poor reputation could cause difficulty in accessing new mineral resources (Rio Tinto, 2017). A lack of good perception could impact the business and operations, said Glencore (Glencore, 2016).

Incremental Cost

Increases in the price of electricity due to carbon charges and conversion to more expensive low carbon alternative energy sources is reported by BHP (BHP Billiton, 2016). Associated costs may be payments to governments for GHG emissions (Barrick – CDP Disclosure Insight, 2018).

Energy Access

Natural disasters that affect the production or distribution of energy will intensify the competition for energy resources. For Freeport-McMoRan, regulations could increase the cost of electricity production and the cost of purchased power, but the magnitude of the impact is uncertain at this time (FCX – CDP Disclosure Insight Action, 2018).

How are the Mining Companies Planning to Adapt to Climate Change Risks and Impacts?

New adaptation approaches will be required to effectively manage climate change risks and impacts (Denton et al., 2015). In Figure 3, future collaborative climate change adaptations are listed, based on risk scenario assessment and research. The second adaptation action that companies are taking is to control GHG emissions, and to communicate this process with their stakeholders.

BHP is applying an internal price on carbon for their investment decisions (BHP Billiton, 2016). Each Rio Tinto operation uses a framework of risk analysis and management to identify and assess climate-related risk and determine appropriate risk management actions (Rio Tinto, 2017). Glencore has incorporated energy and carbon into their annual planning process, as well as any anticipated changes in regulations (Glencore – CDP Disclosure Insight Action, 2018).

Vale follows the main trends in mitigation and adaptation strategies and supports regulatory and economic instruments applicable to each country. Vale has been working on its adaptation strategy since 2010; the company recognizes that the physical impacts of climate change may affect not only its

business but also its workforce, communities, and the surrounding environment, and that good risk management minimizes these impacts (Vale, 2017).

Anglo American is working with experts on climate science to better understand and prioritize adaptation controls. Also, it is considering adaptation measures in a new project. Among the key adaptation measures, Anglo American considers catchment impacts, long-term water supply security, the community exposure, changes in mine and equipment design, and changes in hazard monitoring and emergency preparedness (Anglo American – CDP Disclosure Insight Action, 2018).

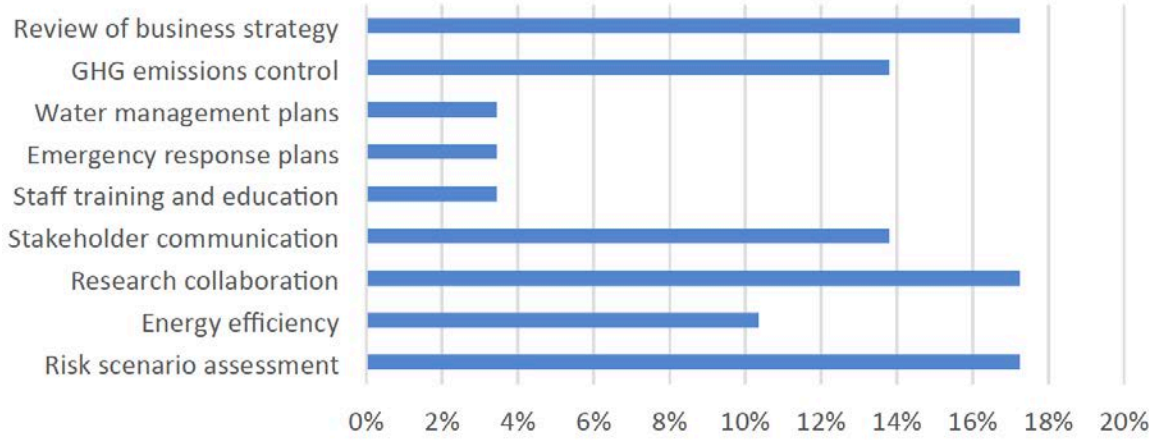


Figure 3: Future climate change adaptation actions

Energy Efficiency

For Rio Tinto, the use of new technology will be a key enabler for reducing energy usage and GHG emissions from operations (Rio Tinto – CDP Disclosure Insight Action, 2018). BHP evaluates the integration of renewable energy sources into their operations (BHP Billiton Limited, 2017b). Glencore believes there is a significant gap between the energy reality and the various carbon policy scenarios (Glencore, 2016).

Research Collaboration

BHP has interventions with different initiatives, as The Forests Bond, issued by the International Finance Corporation, is a signatory to the World Bank's "Putting a Price on Carbon" statement and a member of the World Bank's Carbon Pricing Leadership Coalition. BHP is also a member of the Energy Transitions Commission (BHP Billiton Limited, 2017b). Rio Tinto supports research into carbon capture and storage and low-emissions technologies for coal, by supporting the work of the Cooperative Research Centre for GHG Technology and the Australian Coal21 Fund (Rio Tinto – CDP Disclosure Insight Action, 2018).

Vale is committed to promoting the sustainability agenda with its suppliers through the *Programa Carbono na Cadeia de Valor* (in English, Carbon in the Value Chain Program), and supports the research

and development of new technologies to mitigate and evaluate the impacts of climate change (Vale – CDP Disclosure Insight Action, 2018). Anglo American has a platform for innovation, called FutureSmartTM Mining Open Forums. The Open Forums on Water, Processing, Mining and Energy have stimulated ideas that are progressing into tangible collaborative solutions (Anglo American – CDP Disclosure Insight Action, 2018).

Stakeholder Communication

BHP mentioned that it has contributed to numerous policy reviews throughout their global operating regions. They actively participated in the work of the Energy Transitions Commission (energy-transitions.org). BHP is a member of the Financial Stability Board's Taskforce on Climate-Related Financial Disclosures (TCFD), which develops voluntary, consistent, climate-related financial risk disclosures (BHP Billiton, 2016). Rio Tinto is a co-chair of the B20 taskforce on Energy, Climate and Resource Efficiency, which provides recommendations for action by G20 governments to address climate change (Rio Tinto – CDP Disclosure Insight Action, 2018).

Staff Training and Education

BHP promotes staff training and education to think differently about longer-term emissions reduction goals. These targets will be implemented with innovation and collaboration across BHP's functions and assets (BHP Billiton, 2016).

Emergency Response Plans

At Vale, contemplation of extreme scenarios to identify potential climate impacts on operations and local communities – from natural disasters, desertification, and floods, to changes in economic living conditions – can help strengthen approaches to adaptation and emergency response plans (Vale, 2017).

GHG Emissions Control

BHP's longer-term goal aims to achieve net-zero operational GHG emissions in the second half of this century. BHP identifies that a pathway to net-zero emission over coming decades will require long-term planning for the long-life assets in their portfolio, a deep understanding of the development pathway for low-emissions technology, and a firm commitment from their leadership (BHP Billiton Limited, 2017b).

Water Management Plans

In 2014 Rio Tinto replaced the group-wide freshwater use target with site-specific targets at more than 30 sites where water is a material risk. The targets address water supply, ecological impacts, or surplus water management issues (Rio Tinto, 2017). Glencore has established water usage reduction projects. They note

that potential upgrades to storm water facilities might be required, as well as water-storage facilities (Glencore, 2017). In order to estimate and monitor the forest carbon flow resulting from the change in land use, a database of environmental recovery and suppression activities was established, with georeferenced data accounted annually (Vale – CDP Disclosure Insight Action, 2018).

Review of Business Strategy

BHP expects that non-hydro renewables will gain market share in the power sector. Nevertheless, despite rapid growth in renewables and electric vehicles, the world will still require roughly four-fifths of its growing total energy needs to come from non-renewable sources in 2040 (BHP Billiton, 2016). Glencore plans to adopt a combination of both emission intensity targets and absolute emission reduction targets across their business (Glencore, 2017).

Vale is contemplating a departure from fossil fuels in the business model. It promotes a contribution to the debate with information and analyses to stimulate innovation for the challenges of climate change. Part of Vale's strategy will be to adopt a corporate policy with the government to handle climate change, and leverage efforts to speed up low-emission technologies (Vale, 2017).

In 2017, Anglo American's Board approved a climate-change-related indicator for executive financial remuneration. This responsibility has driven Anglo American to incorporate their response to climate change into their strategy, operational solutions and project design (Anglo American – CDP Disclosure Insight Action, 2018).

Results

Most of the mining companies recently established policies related to climate change management were motivated by global agreements and trends in the reduction of greenhouse gases. These global agreements were supported by the investors, who demand that the mining companies identify, disclose, and define plans to manage climate-related risks. Of the top ten companies assessed, eight of them have complied with the CDP, reporting their emissions measurement and control progress on a yearly basis. GHG reduction is considered a key performance metric for business, and some companies consider this performance in their senior executive and leadership remuneration.

The principal risks considered by the mining companies are related to water resources and the different stages of the water cycle. Either an increase or a decrease in the water balance for short periods in an extreme-weather scenario could be a risk for the different mining stages. Some regions may have more risk than others, and more assessment is required to understand specific potential risks.

The highest impact reported by the mining companies due to climate change is related to various countries' legal framework and global policies regarding carbon price and reduction of greenhouse gases.

This concern is focused on the cost associated with possible carbon taxes in different countries and at different levels. Furthermore, the impact of the infrastructure and buildings at each site will affect operations, results, and revenues in different regions and in different levels.

Also, physical changes due to changing of temperature patterns may result in the migration of some diseases, which could result in damage to the health of the employees, contractors, communities, and ecosystem. This could promote variations in health and safety protocols to prevent impacts.

Most of the interventions designed and planned have been focused in mitigation actions, such as the reduction of greenhouse gases emission and the control of fuel use; and the disclosure and reporting of emissions. However, there is no strong evidence that real adaptation plans have been designed, based on ecosystem solutions for climate change impacts.

This research, focusing on information from the sustainability reports and the CDP, provides a broad perspective of the companies' management related to climate change risk. Still needed is a more detailed assessment of site-specific contexts in regions that have higher risk of climate change impacts.

Conclusions

The mining companies recognized that climate change would impact the mining industry in all stages, and it is a risk that is highly relevant right now. The companies recognize that we still cannot be certain of the level of impacts and how they will affect the different regions in the long term. These challenges will require variations in business strategies, investment in new technologies, and more research. More than ten years ago, some companies started to assess risks and establish internal policies for managing GHG; other are just getting started. But it is essential to share the knowledge learned, promote best practices, and support the industry in transition to a low-carbon market.

Water is the most significant element that will continue play a crucial role in the mining industry, either as water for operations use, or as water as a natural element in the watershed. It is important to highlight that more than 67% of the risks reported are related to the water resource. Tailings and dams are mentioned as concerns because their initial design did not consider the risks of climate change. Therefore, we need a deep understanding and robust research of ecosystem adaptations and climate change impacts in watersheds where mining companies have operations.

Knowing the general risks and the impacts, the managements' next step should be planning actions to prevent and control these risks, despite the uncertainty of the changes. The mining sector is still in the process of reviewing and learning how to adapt to climate change impacts. Considering mining operations as part of the watershed will support the design of ecosystem-based adaptation plans that could reduce and control the risk of climate change, especially in the closure stage and reclamation areas.

References

Anglo American – CDP Disclosure Insight Action. 2018. Climate change 2017 information request Anglo American.

Anglo American. 2016. Climate change: Our plans, policies and progress.

Anglo American. 2017. Sustainability report 2016.

Barrick – CDP Disclosure Insight. 2018. Climate change 2017 Barrick Gold Corporation.

Barrick Gold Corporation. 2017. Annual report 2016. Public company report.

BHP Billiton 2017. Annual report 2017.

BHP Billiton Limited. 2007. BHP Billiton climate change policy. 2007.

BHP Billiton. 2016. Climate change: Portfolio analysis views after Paris, 20.

BHP Billiton. 2017. CDP 2017 climate change information request.

Bowyer, P., Bender, S. Rechid, D. and Schaller, M. 2014. Adapting to climate change: Methods and tools for climate risk management – CSC report 17:124.

Denton, F., Wilbanks, T.J., Abeysinghe, A.C., Burton, I., Gao, Q., Lemos, M.C., Masui, T. et al. 2015. Climate-resilient pathways: Adaptation, mitigation, and sustainable development. Climate change 2014 impacts, adaptation and vulnerability: Part A: Global and sectoral aspects, 1101–31. Retrieved from: https://doi.org/10.1017/CBO9781107415379.025.

FCX – CDP Disclosure Insight Action. 2018. Climate change 2017 report Freeport-McMoRan Inc.

Ford, J.D., Pearce, T., Prno, J., Duerden, F., Ford, L.B., Beaumier, M. and Smith, T. 2010. Perceptions of climate change risks in primary resource use industries: A survey of the Canadian mining sector, *Regional Environmental Change,* 10(1): 65–81. Retrieved from: https://doi.org/10.1007/s10113-009-0094-8.

Glencore – CDP Disclosure Insight Action. 2018. Climate change 2017 report, Glencore Plc.

Glencore. 2016. Climate change considerations for our business, 15. Retrieved from: www.glencore.com.

Glencore. 2017. Sustainability report 2016.

Grupo Mexico. 2017. Development with purpose, 2016 sustainable development report.

Hermwille, Lukas. 2016. Climate change as a transformation challenge, 19–22. Retrieved from: https://doi.org/10.14512/gaia.25.1.6.

ICMM. 2013. Adapting to a changing climate: Implications for the mining and metals industry, *Climate Change,* March: 62.

Institute of Environmental Management & Assessment. 2015. Climate change resilience and adaptation: IEMA guide, November.

Kelessidis, V. 2000. Benchmarking: Dissemination of innovation management and knowledge techniques. Report produced for the EC funded project, 0–32.

Linnenluecke, M.K., Griffiths, A. and Winn, M.I. 2013. Firm and industry adaptation to climate change: A review of climate adaptation studies in the business and management field, *Wiley Interdisciplinary Reviews: Climate Change* 4(5): 397–416. Retrieved from: https://doi.org/10.1002/wcc.214.

National Research Council of the National Academies. 2005. Measuring performance and benchmarking project management at the Department of Energy Management. Retrieved from: https://doi.org/10.17226/11344.

Nelson, J. and Schuchard, R. 2011. Adapting to climate change: A guide for the mining industry, *Business for Social Responsibility,* 10. Retrieved from: www.bsr.org/reports/BSR_Climate_Adaptation_Issue_Brief_Mining.pdf.

Nornickel. 2017. Corporate social responsibility report 2016. Retrieved from: https://www.nornickel.com/files/en/results/csr_reports/NN_CSO2016_ENG.pdf.

Odell, S.D., Bebbington, A. and Frey, K.E. 2017. Mining and climate change: A review and framework for analysis. The extractive industries and society. December. Elsevier: 0–1. Retrieved from: https://doi.org/10.1016/j.exis.2017.12.004.

Özsözgün, A. and Emel, E. 2016. Inseparable parts of sustainability: Business, climate change, and integrated reporting. Climate change and the 2030 corporate agenda for sustainable development 19:1. Retrieved from: https://doi.org/doi:10.1108/S2051-

Parks, J., Ryus, P., Coffel, K., Gan, A., Perk, V., Cherrington, L., Arndt, J. and Nakanishi, Y. 2010. A methodology for performance measurement and peer comparison in the public transportation industry. Retrieved from: https://doi.org/10.17226/14402.

Pearce, T.D., Ford, J.D., Prno, J., Duerden, F., Pittman, J., Beaumier, M., Berrang-Ford, L. and Smit, B. 2011. Climate change and mining in Canada, *Mitigation and Adaptation Strategies for Global Change,* 16 (3): 347–68. Retrieved from: https://doi.org/10.1007/s11027-010-9269-3.

Phillips, J. 2016. Climate change and surface mining: A review of environment-human interactions and their spatial dynamics, *Applied Geography,* 74. Elsevier Ltd: 95–108. Retrieved from: https://doi.org/10.1016/j.apgeog.2016.07.001.

Rio Tinto – CDP Disclosure Insight Action. 2018. Climate change 2017 report Rio Tinto.

Rio Tinto. 2016. Climate change report.

Rio Tinto. 2017. Partnering for progress, 2016 sustainable development report, Vol. 5. Retrieved from: http://search.ebscohost.com/login.aspx?direct=true&db=afh&AN=9409210832&site=ehost-live.

S&P Global Market Intelligence. 2017. Quarterly rankings of top companies remain stable. 2017. Retrieved from: https://marketintelligence.spglobal.com/our-thinking/ideas/quarterly-rankings-of-top-companies-remain-stable.

UNFCCC. 2015. Report of the Conference of the Parties on its twenty-first session, held in paris from 30 November to 13 December 2015. Addendum, Part Two: Action taken by the Conference of the Parties 1194 (January): 1–36. Retrieved from: http://unfccc.int/resource/docs/2015/cop21/eng/10a01.pdf.

Vale – CDP Disclosure Insight Action. 2018. Climate Change 2017 Vale.

Vale. 2017. 2016 Sustainability Report. Retrieved from: www.vale.com/rs2016.

Yousefpour, R., Jacobsen, J.B., Thorsen, B.J., Meilby, H., Hanewinkel, M. and Oehler, K. 2012. A review of decision-making approaches to handle uncertainty and risk in adaptive forest management under climate change, *Annals of Forest Science,* 69 (1): 1–15. Retrieved from: https://doi.org/10.1007/s13595-011-0153-4.

Chapter 6:
Water Treatment



Proceedings of Mine Water Solutions 2018
June 12–15, 2018, Vancouver, Canada
Published by the University of British Columbia, 2018

Removing Selenium from Very Low Concentration Mine Water

Mohsen Barkh, SGS Canada Inc., Canada

Abstract

Despite the availability of different selenium removal options, removing selenate (SeO_4^{2-}) from diluted mine water is an ongoing industrial challenge for many projects.

The ion exchange process is one of the most effective selenate removal methods that can concentrate selenate and other contaminants in a small reject volume. Waste management method and regeneration frequency are key parameters that determine the feasibility of selenium removal by ion exchange.

One of the best available options for managing selenium waste is returning the element to a stable state by chemical precipitation. In the proposed methodology, the concentration of selenium(VI) was increased through an ion exchange system and a high-concentration regeneration solution was precipitated at low pH using sodium hydrosulfite (sodium dithionite, $Na_2S_2O_4$) as a reducing reagent.

Introduction

Developing low cost and reliable technologies to remove selenium from water is a priority for many industry sectors in order to meet environmental standards and regulations.

Selenium is stable in aqueous solution as oxyanions of selenium(IV) and selenium(VI). The current regulations in Canada require a selenium concentration in discharge water of between 1–5 µg/L. Achieving selenium levels within this range in discharge water from mines is challenging given that:

- Removal is limited by minimum and maximum feasible ranges of design flows that can vary greatly over time.
- It exists in a variety of chemical forms.
- It is relatively dilute in concentration.
- Removal from water is confounded by the water matrix (temperature, pH, and other chemicals).
- Treatment generally results in a concentrated by-product or residual.
- Re-release from the residuals can occur (Sandy and Disante, 2010).

Most of the reported research with precipitation, co-precipitation, adsorption, ion exchange, reverse osmosis elimination, chemical reduction, and biological reduction of selenium ia applicable to the removal of selenium(IV) from waste water, but not very effective for selenium(VI) under moderate conditions (Nishimura et al., 2007).

Studies show that, although some anaerobic bacteria can reduce selenium(VI) to elemental selenium, the main disadvantage of the process is the long retention time requirement (Murphy, 1988). Nishimura et al. (2000) have identified barium selenate precipitation and reduction with ferrous hydroxide as promising candidates for removing selenium(VI) from neutral solutions. They also pointed out that barium selenate precipitation can be used for separating selenium(VI) from process liquors containing a large quantity of selenium(VI), but cannot remove selenium(VI) to a concentration lower than 100 mg/L and requires further removal operation of selenium(VI) for disposal to the environment (Nishimura et al., 2007).

While these physical, chemical, and biological treatment technologies have the potential to remove selenium, there are very few technologies that have successfully and/or consistently removed selenium in water to less than 5 µg/L at any scale (Sandy and Disante, 2010).

Ion exchange is one of the few technologies with good potential to achieve the dischargeable concentration consistently. The application of weak basic anion (WBA) resin for selenium species removal was investigated by Dzul Erosa (Dzul Erosa et al., 2009). Rajamohan reviewed strong acid cation (SAC) for selenium removal, but their main target was selenium(IV) (Rajamohan et al., 2016). Nishimura and his team focused their work on selenium(VI) and they used weak basic chelating resin for their work (Nishimura et al. 2007).

Since selenium(IV) could be removed with a wide variety of technologies, the focus of this work was on selenium(VI) only. Selenium(VI) concentrations ranging from 20 to 2,300 µg/L were selected as the feed solutions based on the current situation in different mines in British Columbia. The acceptable pH for discharge in British Columbia (and many other places) is between 6 to 8.5 µg/L, therefore, the experiment was designed to produce treated water within this range. The suggested process in this paper could be used as a final polishing/post-treatment process prior to discharging the mine water to the environment.

According to Nishimura, the predominant species of selenium(VI) in this range of pH is SeO_4^{2-}, which has a higher affinity to resin than sulphate and chloride ions ($SeO_4^{2-} > SO_4^{2-} >> Cl^-$) (Nishimura et al., 2007). All test solutions were generated by adding selenium(VI) to RO water to increase certainty of observations in the test work.

In many mining operations, a higher than dischargeable concentration of selenium is introduced to the process, wash, or waste water. In general, the concentration of selenium in wash water from coal

mines could be in the range of 50 to 2,000 µg/L. Although some treatment technologies such as biological treatment and reverse Osmosis can meet the required discharge water quality, those technologies could hardly offer a feasible treatment method for water with low selenium concentrations due to their high volume of generated waste or high retention time. In this work, several tests have been conducted on removing selenium from diluted solutions (2,000 µg/L or lower) using ion exchange technology.

Experimental

Description of the method

The test study was designed to cover four objectives: selecting the proper type of resin, evaluating the resin's ability to remove selenium from dilute (20 µg/L) solution, reviewing the regeneration process, and observing selenium precipitation from rejected solution. The mine's wastewater, the coal mine wash water in particular, had a neutral pH and temperature equivalent to ambient temperature. Due to the high volume of the wastewater, any attempt to change the pH or temperature of the water did not seem feasible. Therefore, the focus of the work in this research was removing selenium(VI) from water without pH adjustment or temperature modification. Also, the test work was designed in a way to eliminate the need for any post-treatment processes for both economical and technical reasons. The batch tests were designed to choose the most effective resin type for the treatment. The column tests with selected resin were run to evaluate resin performance with low and high concentrations of selenium in a continuous process. The collected selenium from resin in regenerated solution was then subjected to chemical precipitation to produce elemental selenium.

Batch Scoping Tests

The studies by Rajamohan on WBA and Nishimura on weak basic chelating resin revealed that these resins were not able to treat diluted selenium(VI) solutions and produce dischargeable water (Nishimura et al. 2007), (Rajamohan et al., 2016). To address this issue, the current work evaluated different types of resins and their performance on diluted solutions.

The main objective of the batch tests was selecting the resin with best performance for the next step (column test). To do this, three different types of resins, chloride form of a strong base anion (SBA), sodium form of a strong acid cation (SAC), and sodium form of a chelating resins, were selected.

A series of batch tests with different resin quantities was conducted to remove selenium from solutions at low concentration. The ability of the resins and the required selenium-to-resin ratio were evaluated. The tests were also run long enough to reach the full equilibrium state. A selenium(VI) solution with 1,000 µg/l concentration was chosen for the tests. For each type of resin, four batches of 100 mL of the solution were added to four 250 mL shake flasks. Then 1, 2.5, 5, and 10 g of the resin was

added to each flask, respectively. The flasks were shaken for 30 minutes, then samples were taken for ICP-MS analysis for dissolved metals. The analytical results were used to select the most suitable type of resin, estimate the maximum achievable selenium removal efficiency, as well as optimum selenium-to-resin ratio.

Column Test

The objectives of the column test were generating breakthrough curves, evaluating the regeneration process, and producing regeneration solution with a relatively high concentration of selenium. The regeneration solution from the column test would later be used for the sodium dithionite chemical precipitation test.

In total, three column tests were conducted: scoping, diluted solution, and a concentrated selenium test. All the tests included using 100 mL of SBA in a 1-inch diameter column followed by a regeneration process according to the UPCORE^{TM} procedure provided by Dow Chemical.

At the beginning, a scoping column test was run with 1,000 µg/L solution to ensure that the resin had the capacity of removing selenium(VI) to lower than discharge levels in a continuous process. The low concentration concern in the process was addressed by running a two-stage diluted solution column test. The test was started with a very low concentration of selenium (21.7 µg/l) that, after collecting a sufficient number of samples, was replaced by a solution with a high selenium concentration (681 µg/L). The purpose of the high concentration feed was not only to test the ability of the resin but also to accelerate the loading process and increase loading of selenium on the resin for the regeneration process. The third column test was the high selenium concentration (2,350 µg/L), which was run to confirm the results of previous tests and provide detailed information about the regeneration process.

Scoping Test

In this test, the feed solution was loaded from the top of the column at 160 (± 3%) mL/min and treated water was collected from the bottom of the column in a large container. After 90 minutes, the test was stopped, an overall sample of treated water from the container was collected and sent for dissolved metals analysis.

Diluted Solution Test

The satisfactory results from the scoping test were used to design column tests with diluted solution. The diluted solution test was designed to identify the potential issues with low selenium concentration in the feed solution. To run this test, a stock solution with 681 µg/L selenium was synthesized by adding selenium(VI) to RO water then 535 mL of the stock solution was diluted with 16 litres of RO water to generate diluted solution with 21.7 µg/L selenium. This diluted feed solution was loaded to the top of the

column at 255 mL/min for 40 minutes. Dissolved metals samples from the treated water container were collected every 10 minutes for dissolved metals analysis.

Once the diluted solution was exhausted, the feed water was replaced with the stock solution and the loading process was continued for another 110 minutes with the same flow rate. The treated water container was changed after switching to the stock solution to keep the two treated waters separate. During the loading of stock solution, dissolved metal samples from the treated water container were collected every 30 minutes.

When loading was completed, the resin was regenerated according to the UPCORE^{TM} procedure with 450 ml of 10% sodium chloride solution. The regeneration process was counter-current and both the regeneration and slow rinse flow rates were 102 mL/min. The regeneration solution and slow rinse water samples were sent for dissolved metal analysis.

Concentrated Solution and Regeneration Test

The third column test was conducted with 20 L of feed containing 2,350 μg/L of selenium in solution. The test procedure was similar to the second test (with a single feed), but the volume of regeneration solution in this test was 600 ml. The regeneration solution was collected in 100 mL cuts (batches) followed by two 100 mL cuts of the slow rinse water. Samples of regeneration and slow rinse cuts were then sent for dissolved metals analysis.

Chemical Precipitation Test

The objective of this test was to remove selenium from the regeneration solution using sodium dithionite as the precipitation reagent. The precipitation tests were conducted with two different selenium concentrations. The feed for first test was prepared by combining all regeneration solutions and slow rinse cuts. The feed for the second test was prepared by adding a sufficient amount of water to 20 mL of the first feed to achieve 1:50 dilution factor. Samples of both feeds were sent for dissolved metals analysis. The final volume of the first feed for the test work was 560 mL and the volume of the second feed was 960 mL.

The tests were conducted by adding a sufficient amount of 1 N sulphuric acid solution to each feed to reduce the pH of the solution to less than 2. Then 1.54 g of sodium dithionite was added to each solution and the solutions were mixed for three minutes before taking the first set of water samples. Then both reaction solutions were aged overnight and the second set of samples were collected the next day to evaluate the effect of ageing on selenium removal.

Results and Discussion

Feed Water Quality

All feed water and stoke solutions were prepared by adding standard solution of selenium (VI) solution to RO water. All diluted solutions were prepared by adding sufficient amount of RO water to stock solution to achieve desirable concentrations. Table 1 illustrates the analysis of the stock solution.

Table 1: Stock solution quality

Sample ID	17-01-18-16519-IXB-Feed		**Sample ID**	17-01-18-16519-IXB-Feed	
Analysis	**Units**		**Analysis**	**Units**	
Temperature Upon Recei	°C	14.0	Manganese (dissolved)	mg/L	0.0044
Hardness (dissolved)	mg/L as CaCO3	2.72	Molybdenum (dissolved)	mg/L	0.00047
Aluminum (dissolved)	mg/L	0.111	Nickel (dissolved)	mg/L	0.0005
Antimony (dissolved)	mg/L	< 0.0002	Phosphorus (dissolved)	mg/L	0.042
Arsenic (dissolved)	mg/L	< 0.0002	Potassium (dissolved)	mg/L	0.053
Barium (dissolved)	mg/L	0.0030	Selenium (dissolved)	mg/L	2.35
Beryllium (dissolved)	mg/L	0.000039	Silicon (dissolved)	mg/L	0.09
Bismuth (dissolved)	mg/L	< 0.000007	Silver (dissolved)	mg/L	< 0.00005
Boron (dissolved)	mg/L	0.015	Sodium (dissolved)	mg/L	0.69
Cadmium (dissolved)	mg/L	0.000017	Strontium (dissolved)	mg/L	0.00227
Calcium (dissolved)	mg/L	0.45	Sulfur (dissolved)	mg/L	1.5
Chromium (dissolved)	mg/L	0.00093	Thallium (dissolved)	mg/L	< 0.000005
Cobalt (dissolved)	mg/L	0.000163	Tin (dissolved)	mg/L	0.00028
Copper (dissolved)	mg/L	0.0027	Titanium (dissolved)	mg/L	0.0020
Iron (dissolved)	mg/L	0.058	Uranium (dissolved)	mg/L	0.000426
Lead (dissolved)	mg/L	0.00152	Vanadium (dissolved)	mg/L	0.00023
Lithium (dissolved)	mg/L	0.0048	Zinc (dissolved)	mg/L	0.006
Magnesium (dissolved)	mg/L	0.386	Zirconium (dissolved)	mg/L	< 0.002

Since the stock solution was prepared by using RO water, the concentration of all other ions in the solution was very low.

Batch Scoping Test / Resin Selection

The batch scoping tests revealed that the low concentration selenium(VI) solution had very little affinity to either strong acid cation (SAC) or chelating resins. Figure 1 shows the concentration of selenium in feed and treated water with SAC and chelating resins. As the graphs show, the concentration of selenium in treated water is almost the same as the concentration of selenium in the feed.

Figure 2 shows the concentration of selenium in the feed and treated water with different amounts (mass) of SBA resin. It is seen that the solution concentration of selenium decreased with increasing mass of resin up to almost 3g, at which point adding resin had no significant effect on selenium removal. The effect of the resin mass on selenium removal is observed in the adsorption curve. As the curve shows, after a certain point (3g in this test) increasing resin mass had no effect on the mass of adsorbed selenium.

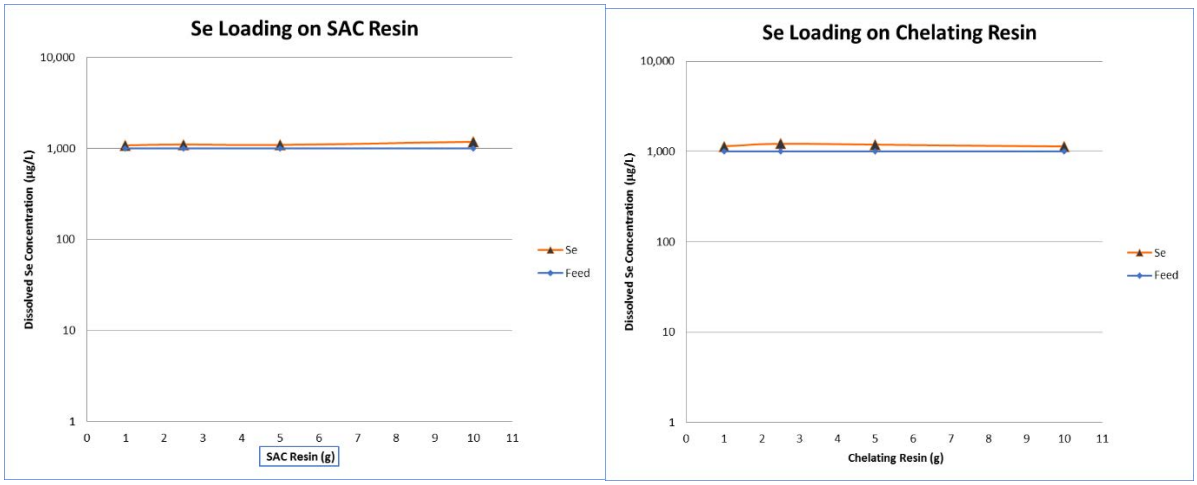


Figure 1: Loading curves for SAC and chelating resins

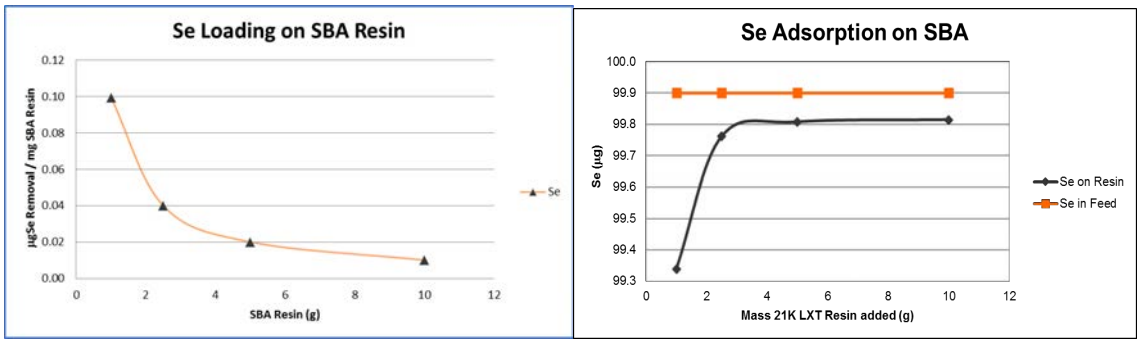


Figure 2: Loading and adsorption curves for SBA resin

The positive results from tests with SBA could be due to existence of SeO_4^{2-} as a predominant species of selenium(VI) at neutral pH. The selenium adsorption curve also confirmed that there is an optimum selenium-to-resin ratio that provides the maximum selenium removal by the minimum amount of resin. The information from loading and adsorption curves could be used to determine the minimum required resin for any feed water with similar water matrix to the test solution.

Column Scoping

The column-scoping test with SBA resin provided satisfactory results. The concentration of selenium in treated water after running 14.4 litres of the feed water with 1,000 µg/L of selenium was 0.2 µg/L. The calculated loading rate in this test was 0.144 g of selenium per every litre of the resin in absence of the competitive ions. This result was considered promising since only 100 mL of the resin was used for treating such a large volume of the water. However, the selenium concentration used in this test was higher than the commonly observed concentration of selenium in local mines. In addition, similar to other

studies with different types of resins (Rajamohan et al., 2016), the scoping test results could be limited to high concentrations only. Based on the author's previous experiences, regenerating of the resin after loading cyanide on SBA in different sets of work had also been problematic. The test with the diluted solution and elution process was designed to review those potential issues.

Diluted Solution Tests

Figure 3 illustrates the result of loading the ion exchange resin in a column with diluted solution. As the graph shows, the low initial concentration of the selenium in the feed had no significant effect on the SBA resin performance. The test completed with 10 L of feed solution proved the fact that a small amount of resin, 100mL in this case, could remove a sufficient amount of selenium to keep the overall concentration of selenium in the treated water below 5 µg/L. This could be a promising result with positive economical implications for removing selenium from diluted solutions.

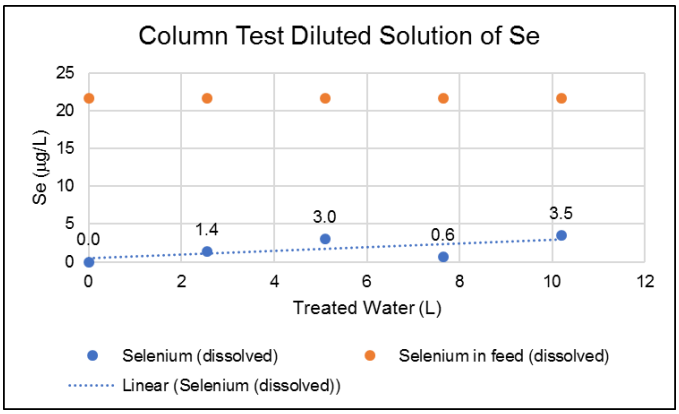


Figure 3: SBA resin loading with diluted solution

Figure 4 shows the results of loading the column with stock solution after finishing the diluted solution. The calculated deposit of the selenium on the resin at the beginning of the stock solution loading was 182 µg. The injected selenium to the column from stock solution in this test was more than 19,000 µg from 28 L of the feed. As Figure 4 shows, the sudden change in the concentration of selenium had no negative impact on the resin performance and the selenium concentration in the treated water was consistently below the discharge limit. This proves the capability of ion exchange technology to treat feed with fluctuating selenium concentrations.

Comparing the shape of the loading curve with a standard breakthrough curve revealed that SBA resin was far from the exhaustion and that loading could be continued for a long time. The longer loading period increases the gap between two subsequent regenerations and reduces overall frequency of regeneration. The low frequency for regeneration reduces both reagent consumption and operating costs of the treatment unit.

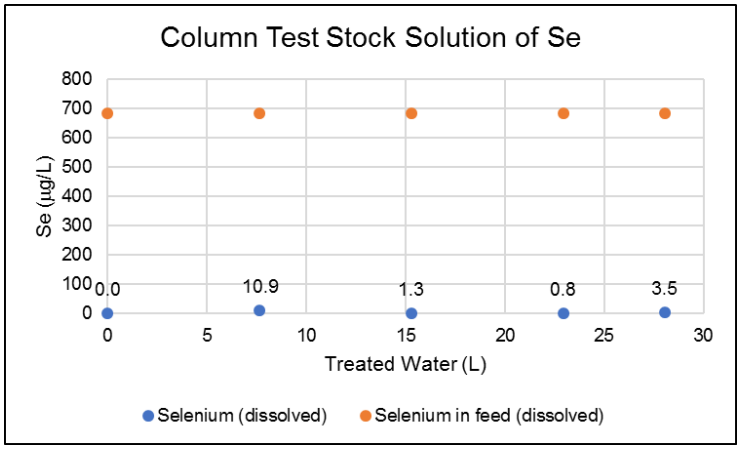


Figure 4: SBA resin loading with stock solution

Figure 5 illustrates the results of SBA resin loading with the concentrated solution. The feed concentration in this test was 2,350 µg/L and 100 mL of SBA resin reduced the selenium concentration in 20 L of treated water to below the discharge limit. The analytical results of this test and the observations from the stock solution test can be used to estimate the range of feed concentration for ion exchange treatment. The selenium concentration in this test was almost 100 times higher than the similar parameter in the diluted solution. However, the SBA resin presented a robust and consistent performance for both concentration levels.

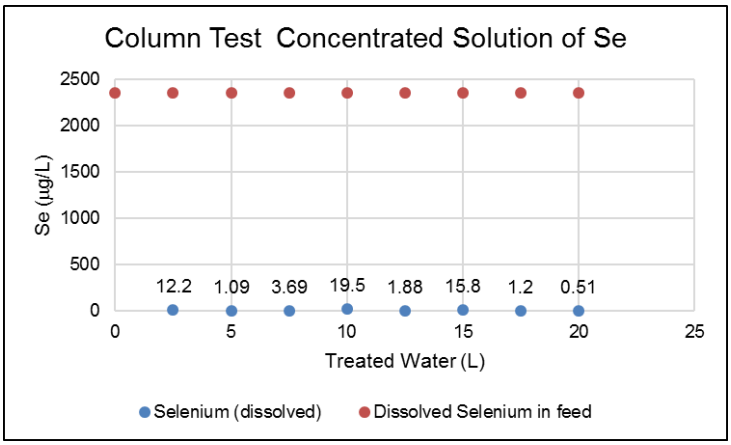


Figure 5: SBA resin loading with concentrated solution

Concentrated Solution

Figure 6 shows the results for removal efficiency of the SBA resin for the concentrated solution. The average removal efficiency (99.7%) is shown with a red dotted line. The figure shows no significant changes in the removal efficiency or resin performance when increasing volume of the treated water or

length of the treatment. It should be mentioned that the consistency in resin performance is a positive outcome and could be useful for industrial scale-up of the ion exchange system.

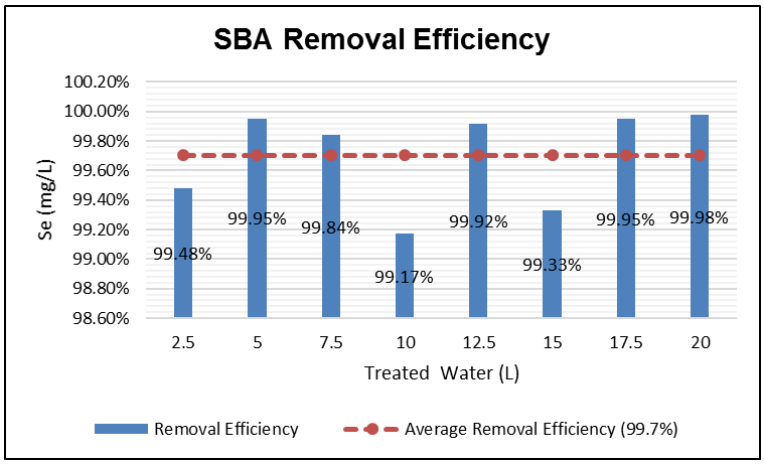


Figure 6: SBA removal efficiency for selenium

The results of concentrated and diluted solution tests together, confirmed the possibility of using lead-lag configuration in the industrial scale. In a lead-lag configuration, at the beginning of the cycle, the lead column removes a significant amount of the contaminant and diluted solution is sent to the lag column as feed. If concentration of the contaminant in the diluted solution becomes lower than leakage concentration of the resin, the water passes through the lag column without any change in the contaminant concentration. The diluted solution test confirmed that 21.7 µg/L was high enough for the SBA resin to adsorb selenium. Therefore, if the lead column were used to treat water to a low concentration of selenium, but higher than the discharge limit, the lag column could be used to reduce selenium concentration to below the discharge limit. The selenium concentration in effluent from the lead column could be very low and still this water could be used as feed for the lag column.

Regeneration Test

Figure 7 shows the SBA resin regeneration (elution) curve. The trend of this curve is similar to the general elution curve for ion exchange resin. Mass balance data shows that the regeneration process was highly efficient. Lack of exhaustion in the loading stage of the test could be one of the main reasons for this high efficiency. It is important to repeat the regeneration test with fully exhausted resin to ensure the obtained regeneration efficiency would be achievable in real unit operation.

As the curve shows, the first cut of collected sample from the column was mostly residual RO water from the previous stage of the process with low selenium concentration. The second and third cuts of the regeneration solution removed more than 85% of the selenium from the resin. The other cuts of

regeneration solution carried less than 15% of the contaminants. The non-uniform distribution of the contaminants in the regeneration solution is important for two practical reasons, as discussed below.

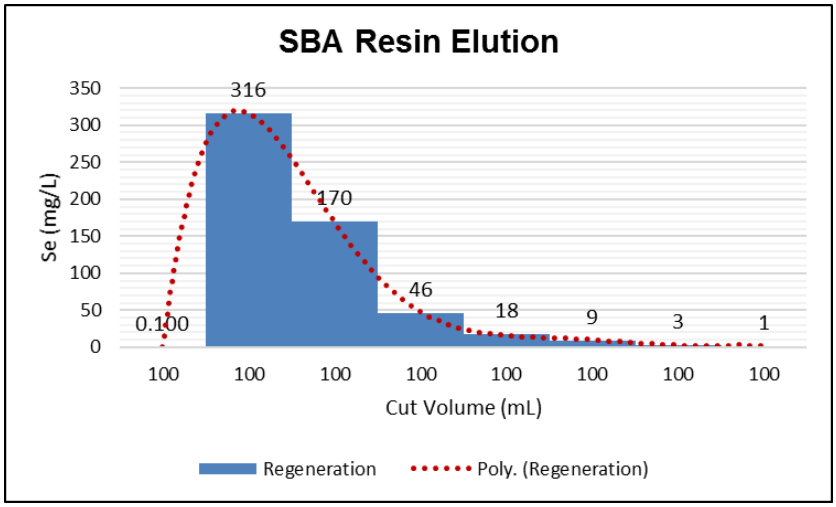


Figure 7: SBA regeneration (elution) curve

First, this uneven selenium distribution in the regeneration solution can be used to optimize selenium concentration in the waste management process where selenium concentration causes problems or puts limitations on the system. For example, when a collected regeneration solution from an ion exchange process was fed into a waste management process such as chemical precipitation to form solid selenium. In this case, the proper selection of the regeneration cuts (volume) could be used to provide desirable selenium concentration for the waste management process

Secondly, the low concentration of the selenium in the last portions of the regeneration solution could be recycled to the regeneration process. Choosing the recycled volume requires selenium distribution in the regeneration solution.

Chemical Precipitation test

Figure 8 shows the regeneration solution immediately after adding sodium dithionite (left) and the aged reaction solution after 18 hours (right). The instant colour change suggests a fast reaction between sodium dithionite and either selenium or chloride in the regeneration solution. The colour change after 18 hours suggested either continuation of the same reaction or deferring to a new reaction.

Unfortunately, neither instantaneous reaction after adding sodium dithionite nor the secondary reaction had a positive effect on selenium precipitation. The initial concentration of selenium in the regeneration solution, 78,800 µg/L, was reduced only to 58,100 µg/L immediately at the end of reaction time and then went up to 61,000 µg/L after 18 hours ageing. The selenium removal efficiency in this test was about 25%, which was not sufficient for selenium precipitation.

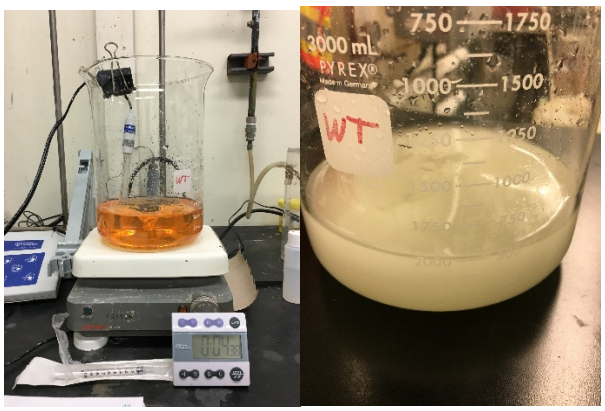


Figure 8: Concentrated regeneration solution precipitation by sodium dithionite

The same test was repeated for the diluted solution that is shown in Figure 9 (end of reaction time (left) and after 18 hours ageing (right). In diluted solution, no immediate reaction was observed after adding sodium dithionite, but some suspended solids appeared in the aged solution. Despite the different observations in the diluted solution from the previous test, the result was very similar. The initial concentration of selenium in the feed, 728 µg/L, was reduced to 646 µg/L at the end of the reaction time and stayed almost the same, 632 µg/L, after 18 hours. The overall removal efficiency of the diluted test was 11%, which showed a negative impact of low concentration on the precipitation process.

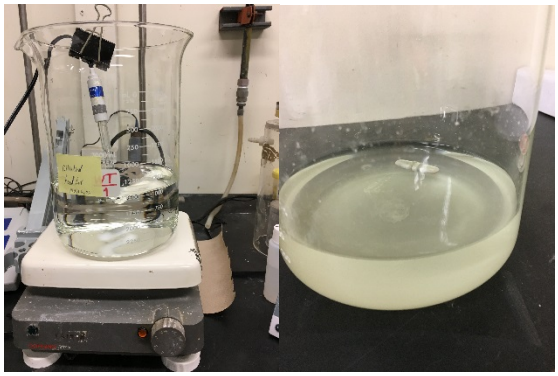


Figure 9: Diluted regeneration solution precipitation by sodium dithionite

Conclusion

The resin selection tests revealed that SBA resin was the only type of resin which could remove selenium from diluted solutions and was able to produce treated water with lower than discharge limit selenium concentrations. The scoping tests with small columns proved that the SBA resin performance was consistent and reliable in removing selenium to lower than discharge limit concentrations.

The column tests with diluted solution confirmed suitability of using SBA resin to remove selenium(VI) from very diluted solutions. It also revealed that changes in selenium concentration had no effect on the resin performance throughout the treatment process.

Using concentrated solutions in the last column test showed that SBA resin could be suitable for a wide range of selenium concentrations. The regeneration evaluation test highlighted the efficiency of the regeneration process to remove adsorbed selenium on the resin and preparing resin for the next treatment cycle. Finally, the non-uniform distribution of selenium in the regeneration solution suggested the possibility of recycling the regeneration solution and flexibility in waste management processes.

The selenium precipitation using sodium dithionate did not provide promising results and presents the need for more work on waste management of the process to achieve a feasible treatment option for removing low concentration of selenium from mine water.

Acknowledgements

The author would like to thank Link Ding and Ali Rashid for their generous contribution to this study and for conducting all related test work. This work could not be completed without continued support reviews and comments from Mrs. Dominique Lascelles, Manager – Metallurgy, SGS Vancouver. The author would like to especially thank Mrs. Parisa Zaini for her time and invaluable comments during the review of the first draft of this paper.

References

Dzul Erosa, M.S., Höll, W.H. and Horst, J. 2009. Sorption of selenium species onto weakly basic anion exchangers, *Reactive & Functional Polymers,* 8(69): 576–585.

Murphy, A.P. 1988. Removal of selenate from water by chemical reduction, *Ind. Eng. Chem. Res*., 1(27): 187–191.

Nishimura, T., Hashimoto, H. and Nakayama, M. 2007. Removal of selenium(VI) from aqueous solution with polyamine-type weakly basic ion exchange resin, *Separation Science and Technology,* 14(42): 3155–3167.

Rajamohan, N., Rajesh Kannan, R. and Rajasimman, M. 2016. Kinetic modeling and effect of process parameters on selenium removal using strong acid resin, *Engineering, Technology & Applied Science Research,* 4(6): 1045–1049.

Sandy, T. and Disante, C. 2010. *Review of available technologies for the removal of selenium from water.* North American Metals Council-Selenium Work Group.

Proceedings of Mine Water Solutions 2018
June 12–15, 2018, Vancouver, Canada
Published by the University of British Columbia, 2018

Synthetic Water Calibration for Water Quality Parameters and Water Treatment Program Validation

Lynda Smithard, McCue Engineering Contractors, Canada

Abstract

To support the Environmental Assessment (EA) of a new gold mine project in British Columbia, Canada, McCue Engineering Contractors completed the preliminary design of a mine water treatment plant (WTP) using a water profile modeled by others for the future open pit sump water. The water profile is complex and the treatment plan includes heavy metals removal by chemical precipitation. Plant effluent quality was initially predicted largely based on published theoretical heavy metal solubility data.

To address uncertainty with the treatment process and improve the inputs for the impact assessment model (by others), McCue created a synthetic water sample from field leachate samples and laboratory-grade salts to match the modeled plant inlet water profile. The synthetic water sample was used to validate the water treatment process at a bench scale and provide effluent quality data for impact assessment modeling. The bench-scale test program also provided valuable data that will be needed in the future to advance the design of the mine water treatment plant from preliminary to detailed.

Data from the bench-scale work reduced uncertainty as to what could be achieved with water treatment at the project site and what impact the treated water would have on the local environment. This was important in satisfying both the regulators reviewing the EA and the project stakeholders, including local First Nations.

The bench-scale test results and data from an ensuing full-scale treatment plant at another project site have also contributed to the body of knowledge for heavy metals precipitation treatment performance. For instance, previously, literature indicated that no or negligible removal could be achieved for copper. McCue's work has provided valuable data for copper that could benefit EA work at other mine sites globally.

McCue will present the synthetic sample method, bench-scale test program results, and how they related to the detailed design and performance of a full-scale metals precipitation plant that offered an economical treatment program for complex water containing high levels of salts in addition to heavy metals.

Introduction

The future gold mine project is located in northern British Columbia, Canada. An application for an Environmental Assessment Certificate/Environmental Impact Statement was submitted in December 2015 for this project, undergoing a coordinated environmental assessment under both the *British Columbia Environmental Assessment Act* and the *Canadian Environmental Assessment Act*. In October 2016, reviewers at BC Ministry of Energy and Mines (MEM) provided comments indicating that the information provided to date on the proposed water treatment systems at post-closure was insufficient to support the surface water quality effects assessment. In response to these comments, additional work was undertaken related to the closure and post-closure water management plans and associated surface water quality model results.

In that context, McCue evaluated the active water treatment options for dissolved metals in mine affected water during closure and post mine closure of the future open pit mining project. McCue had previously completed a preliminary WTP design in early summer 2016 for the open pit sump water for the mine operation. At that preliminary stage, McCue made several assumptions since a bench-scale test program to validate the chemical treatment process had yet to be completed. The preliminary design was completed with the intention of using a two-stage chemical treatment program combined with settling for the removal of dissolved and total metals, respectively. The metals precipitation process was to be validated by a bench-scale test program at a later time when a representative water sample could be collected and used in the test program.

However, to support the evaluation of closure and post-closure water treatment options, McCue was asked by the environmental consultant who would complete the water quality effects assessment, to prepare a synthetic site water sample and complete a bench-scale test program to validate the predicted Pit Sump WTP effluent quality presented in the preliminary design report, issued in July 2016 by McCue.

The Pit Sump WTP preliminary design and the bench-scale test program results that followed were incorporated into the evaluation of active treatment options for mine affected water in closure and post-closure to reduce uncertainty as to what level of water treatment could be achieved.

This document summarizes the Pit Sump WTP preliminary design, the synthetic water sample and bench test program results, as well as an overview of the results of a full-scale metals precipitation plant employing a similar water treatment process at large infrastructure project in Lower Mainland BC. This work fills in many data gaps in the theoretical end points for water treatment by metals precipitation. It further establishes practical end points, which have been demonstrated to be lower than the theoretical ones.

Regulatory Framework

Major projects in BC are assessed for potentially significant adverse environmental, social, economic, health and heritage effects by the Environmental Assessment Office (EAO). Descriptions of the BC Environmental Assessment Process and the Environmental Impact Assessment Process are provided in Appendix A. Applicable regulatory guidance for the design work is also summarized in Appendix A.

Stakeholder Involvement

During the environmental assessment, the EAO seeks input from Scientific Professionals, Indigenous groups, the public, local governments, and federal and provincial agencies to help ensure that no adverse effects are missed. Therefore, Ministries of Environment (MOE) and Energy & Mines (MEM) as well as First Nations are involved in the EA process.

Project Description

Project Overview

The mine project is located in northern BC and is the future site of an open pit gold mining operation. The objective of the Pit Sump WTP is to treat mine affected water collected from the pit sump and pit perimeter groundwater dewatering wells to a quality suitable for discharge to a fish-bearing creek. The intent is to operate the WTP for approximately seven months of the year from March through September each year of the mine operation.

Design Criteria – Inlet Water Quality

The Pit Sump WTP design focused on treatment of nine target (identified by others) dissolved metal parameters; the inlet values provided for those parameters are shown below in Table 1.

In addition, the preliminary design incorporated the following assumptions:

- The inlet pH is near neutral to slightly acidic: an inlet pH range between six and seven was assumed.
- The total suspended solids (TSS) of the homogenized inlet water stream was assumed to be approximately 300 mg/L TSS.

Table 1: WTP inlet water quality – target parameters

Parameter	95th Percentile
Dissolved aluminum	0.179
Dissolved antimony	0.027
Dissolved arsenic	0.035
Dissolved cadmium	0.00736
Dissolved chromium	0.0009
Dissolved cobalt	0.0072
Dissolved copper	0.00395
Dissolved manganese	3.22
Dissolved zinc	1.357

Note: All data expressed in mg/L

Design Criteria – Discharge Water Quality

The discharge targets provided to McCue are summarized in Table 2 below. Some of the parameters are hardness or pH dependent and accordingly the targets for these parameters have been indicated as a range.

Table 2: End of pipe water treatment discharge targets

Parameter	Guideline (mg/L)
Dissolved aluminum	0.1
Dissolved antimony	0.018
Dissolved arsenic	0.01
Dissolved cadmium	0.0000352–0.000254
Dissolved chromium	0.002
Dissolved cobalt	0.008
Dissolved copper	0.004
Dissolved manganese	1.4 – 1.6
Dissolved zinc	0.0150

Notes:

1. It is assumed the 30-day average hardness is less than 50 mg/L as $CaCO_3$
2. It is assumed the maximum temperature of the water in the creek is 15°C

Design Criteria – Flow Rate

The WTP design is based on a maximum flow rate of 285 litres per second (L/s).

Key Technical Issues

Key technical issues impacting the design of the WTP included:

- Representative water sample is not available for bench-scale test and design work. First, a water profile modeled by the consultant was used for the preliminary design, and then synthetic site water was prepared to validate that design.
- The mean temperature is below zero between November and March. Temperature is a key factor in the application and/or performance of some water treatment technologies.

Preliminary Treatment Process

The preliminary treatment process for the mine affected water consisted of a two-stage metals precipitation, coagulation, and flocculation chemical program followed by settling in ponds for solids removal. Following the second settling pond the water will be buffered (as necessary) to a suitable pH for discharge to the creek. The preliminary WTP process flow diagram is illustrated on Figure 1.

The preliminary chemical treatment program consisted of the following: pH adjustment and metal hydroxide precipitation; metal hydroxide precipitation or sulphide precipitation; coagulation; flocculation; and, pH neutralization.

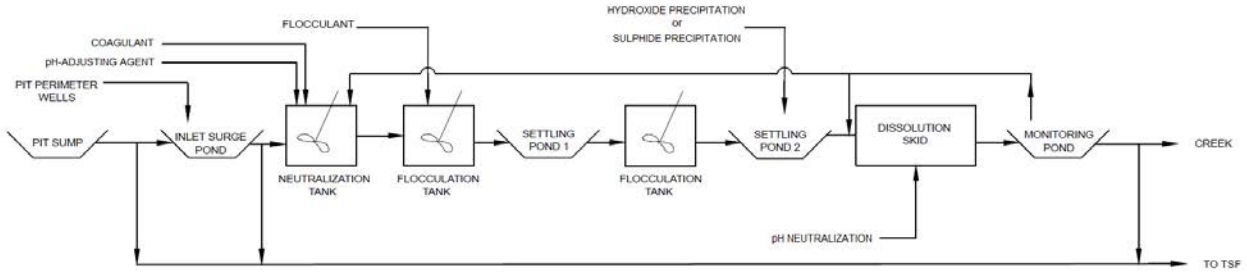


Figure 1: WTP preliminary design process flow diagram

Subsequent bench-scale tests helped determine whether the two-stage chemical treatment process should include hydroxide precipitation optimized at two target pH ranges or a hydroxide precipitation stage followed by sulphide precipitation (see "Bench Scale Test Program" Section).

Literature Findings on Metals Removal

Theoretical and Predicted End Points

A comparison between the theoretical and the predicted minimum effluent concentration attainable through the identified chemical program is presented in Table 3 below. The minimum predicted effluent concentration was based on the greater concentration of the theoretical percent removal and theoretical minimum effluent concentration from literature. This data is based on metal solubility data. Where this data was not available, the predicted minimum effluent concentrations were based on the results of a neutralization test previously completed for the project by others. Those results did not account for the

addition of a coagulant and were, therefore, conservative.

Table 3: Theoretical vs. predicted end points

	Single-stage hydroxide		Two-stage hydroxide		Two-stage hydroxide/sulphide	
	Minimum effluent concentration attainable					
Parameter	Theoretical (10.5 – 11.5)[1]	Predicted	Theoretical (8 – 9/10.5 – 11.5) [1]	Predicted	Theoretical (8 – 9) [1]	Predicted
Dissolved aluminum	–	0.103	0.05	0.1	0.05	0.05
Dissolved antimony	NR	NR	NR	NR	NR	NR
Dissolved arsenic	0.005	0.005	0.005	0.005	0.005	0.005
Dissolved cadmium	0.0005	0.0005	0.0005	0.0005	0.0005	0.0005
Dissolved chromium	NR	0.0007	NR	NR	NR	NR
Dissolved cobalt	–	0.0001	–	0.0001	–	0.0001
Dissolved copper	NR	NR	NR	NR	NR	NR
Dissolved manganese	–	0.0042	–	0.0042	0.01	0.01
Dissolved zinc	0.05	0.05	0.05	0.05	0.01	0.01

Notes:

1. All reported data expressed in mg/L
2. [1] pH set point for chemical precipitation reaction
3. "–" – information unavailable for the specified pH range
4. NR – No or negligible estimated removal
5. Theoretical values based on: BioteQ Environmental Technologies, 2015; Eckenfelder, 2000, 38–156; Ersoz, 2013; Scott, 1977; Peters et al.,1985: 165–196; Robinson and Sum, 1980; Xiao et al., 2008.

Limitations Based on Solubility

- Removal of metals from mixed metal wastes by hydroxide precipitation may not be effective since the minimum solubilities for different metals occur at different pH conditions. The pH required to precipitate most metals from water ranges from 6 to 9; aluminum generally forms aluminum hydroxide that precipitates at pH >5.0 but the aluminum can re-enter solution again at pH 9.0; manganese precipitation is variable due to its many oxidation states, but will generally precipitate at a pH of 9.0 to 9.5. Sometimes, however, a pH of 10.5 is necessary for complete removal of manganese (Skousen, 2014).
- Insoluble sulphide precipitation does not treat manganese, as manganese sulphide has a higher solubility than ferrous sulphide (Department of Army, US Army Corps of Engineers, 2001).

Data Gaps Specific to Contaminants of Concern

Regarding theoretical end points of chemical programs, no information was available for:

- Aluminum, cobalt and manganese, single-stage hydroxide process, at pH = 10.5 – 11.5

- Cobalt and manganese, two-stage hydroxide process, at pH = 8 – 9 / 10.5 – 11.5
- Cobalt, two-stage hydroxide/sulphide process, at pH = 8 – 9 / 10.5 – 11.5
- No or negligible estimated removal for antimony, chromium and copper for all three processes

Synthetic Water Sample

Four iterations of synthetic water samples were prepared by McCue to fit the Pit Sump WTP inlet water profile modeled and provided by the consultant as part of the prior submission to the BC EAO.

McCue received nine leachate water samples from the mine. The water samples were mixed together to make one homogenized sample (Raw Water) at McCue's Delta facility. Once homogenized, samples were collected for total metals, dissolved metals, TSS, anions and nutrients analyses.

Based on the Raw Water analytical results, McCue diluted the homogenized leachate water sample using deionized water at a ratio of 1:4. The concentrations of dissolved antimony, arsenic, barium, chromium and iron were then increased or spiked using laboratory-grade metal salts.

The values for target parameters from the predicted inlet WTP water profile, and lab analysis for Raw Water and the synthetic sample used for bench testing are summarized in Table 4 below.

Table 4: Target parameters in predicted, raw and synthetic inlet water

Parameter	Predicted maximum inlet (95th percentile)	Raw water	Synthetic inlet water
Dissolved aluminum	0.179	7.970	2.21
Dissolved antimony	0.027	0.008	0.304
Dissolved arsenic	0.035	0.004	0.00864
Dissolved cadmium	0.00736	0.12900	0.0291
Dissolved chromium	0.0009	< 0.0005	0.0017
Dissolved cobalt	0.0072	0.0375	0.0094
Dissolved copper	0.00395	0.14700	0.04
Dissolved manganese	3.22	6.10	1.37
Dissolved zinc	1.357	18.900	4.23

Note:
1. All reported data expressed in mg/L

Bench Scale Test Program

Objectives

The bench-scale test program had the following objectives:

- Support the selection of the successful chemical program: investigate the efficacy of single-stage hydroxide precipitation, two-stage hydroxide precipitation and two-stage hydroxide/sulphide precipitation process; each of them also incorporating a coagulant.
- Support the selection of a flocculant.
- Optimize hydraulic retention times for neutralization, coagulation, and flocculation.
- Verify the anticipated performance.
- Provide settling rate information to re-evaluate and optimize (i.e. minimize) the footprint of each settling pond.
- Characterize the sludge volume and quality at each step.

This documents focuses only on the first objective.

Methodology

Table 5 below shows the work completed to verify the metals precipitation process. The process verification was performed over a series of nine tests; three for each of the possible process configurations.

Table 5: Process verification/optimization summary

Process configuration	Stage	Test 1	Test 2	Test 3
Single-stage hydroxide precipitation + coagulant	–	Vary pH / Constant coagulant dosage	Constant pH / Vary coagulant dosage	Vary pH and coagulant dosage based on Test 1 and 2
Two-stage hydroxide precipitation + coagulant	1	Constant pH / Constant coagulant dosage	Constant pH / Vary coagulant dosage	Vary pH and coagulant dosage based on Test 1 and 2
	2	Constant pH / No coagulant added	Constant pH / Vary coagulant dosage	
Two-stage hydroxide and sulphide precipitation + coagulant	1	Constant pH / Constant coagulant dosage	Constant pH / Constant coagulant dosage	Validate best performing chemical program from Test 1 and 2
	2	Constant pH / Vary sulphide dosage	Vary pH / Constant sulphide dosage	

Decision Criteria

The performance of each metal precipitation process was evaluated by comparing the target dissolved metal concentrations in last-stage supernatant water samples of each test against the end of pipe treatment targets in Table 2.

Bench Testing Results

Table 6 and Table 7 below show the results corresponding to the best performing tests for each chemical program evaluated during the bench testing. The values for the Synthetic Inlet Water are also presented.

Table 6: Bench testing results – dissolved metal concentrations

Parameter	Synthetic inlet water	Single-stage hydroxide	Two-stage hydroxide	Two-stage hydroxide / sulphide	Flocculated[1] two-stage hydroxide / sulphide
Dissolved aluminum	2.21	0.104	0.0578	0.0161	**0.119**
Dissolved antimony	0.304	0.00344	0.00168	0.0078	0.0129
Dissolved arsenic	0.00864	0.00037	0.00032	0.00043	0.00046
Dissolved cadmium	0.0291	**0.000239**	<0.000005	<0.0000050	<0.0000050
Dissolved chromium	0.0017	<0.0001	<0.0001	<0.00010	<0.00010
Dissolved cobalt	0.0094	0.00032	<0.0001	0.00094	0.00021
Dissolved copper	0.04	<0.0002	<0.0002	<0.00020	0.00029
Dissolved manganese	1.37	0.288	0.00077	0.624	0.226
Dissolved zinc	4.23	0.0043	<0.001	<0.0010	0.000059

Notes:

1. [1] Pass/fail testing of several flocculants was performed on a qualitative basis, where "pass" was considered to be an instance where a visible flocculant formed. Afterwards, the short-listed flocculants, based on Pass/Fail and Settling velocity testing, were evaluated in terms of target dissolved metals concentrations
2. All reported data expressed in mg/L
3. Analytical results provided by an accredited third-party laboratory
4. "<" – Less than the reported detection limit
5. **bold** – indicates the reported concentration is over the end of pipe treatment target

Table 7: Bench testing results – removal percentage

Parameter	Single-stage hydroxide	Two-stage hydroxide	Two-stage hydroxide / sulphide	Flocculated two-stage hydroxide / sulphide
Dissolved aluminum	95.29%	97.38%	99.27%	94.62%
Dissolved antimony	98.87%	99.45%	97.43%	95.76%
Dissolved arsenic	95.72%	96.30%	95.02%	94.68%
Dissolved cadmium	99.18%	>99.98%	>99.98%	>99.98%
Dissolved chromium	>94.12%	>94.12%	>94.12%	>94.12%
Dissolved cobalt	96.60%	>98.94%	90.00%	97.77%
Dissolved copper	>99.50%	>99.50%	>99.50%	99.28%
Dissolved manganese	78.98%	99.94%	54.45%	83.50%
Dissolved zinc	99.90%	>99.98%	>99.98%	>99.99%

Some highlights from these results are:

- Sufficient removal of multiple parameters, such as cadmium and aluminum, at a single process pH is often unachievable due to the parameter-specific relationship between the optimal formation of hydroxides and pH.
- A single-stage hydroxide precipitation process would not provide sufficient treatment because of the process pH having to vary to achieve sufficient removal of all target parameters. However, this should be investigated further on each case, considering each raw water composition.
- Although the bench testing demonstrated that the treatment targets could be achieved with either a two-stage hydroxide precipitation process or a two-stage hydroxide/sulphide precipitation process, the advantage of the latter is that the process pH would remain within the allowable pH range for discharge to the environment, and therefore neutralization would not be required prior to discharge. Neutralization could be needed to lower the effluent pH for discharge to the creek after a two-stage hydroxide treatment process.

Comparison to Literature Findings

The bench testing results demonstrated better metal removal rates and lower dissolved metals concentrations than the preliminary predicted discharge concentrations provided by McCue in the preliminary design, which are summarized in the "Theoretical and Predicted End Points" Section of this document.

Stakeholder Acceptance

Data from the bench-scale work reduced uncertainty as to what could be achieved with water treatment at the project site and what impact the treated water would have on the local environment. This was important in satisfying both the regulators reviewing the EA and the project stakeholders, including local First Nations.

Scaling Up – Full-Scale WTP Case Study

Bench Scale Tests on Representative Water Samples

Bench tests were recently performed by McCue on metals contaminated water samples from a large infrastructure project currently under construction in the Port of Vancouver. The water discharge is required to meet both the Provincial and Federal Surface Water Quality standards for marine discharge. Strict standards, particularly for copper and zinc, the presence of salts (from seawater intrusion), and construction activities in the excavation have made the water treatment project technically challenging.

The bench-scale tests were modeled on the metals precipitation tests previously completed by McCue for the gold mine project.

Table 8 below compares the concentration of targeted parameters in inlet and treated water between previous bench tests with synthetic water and the current program on samples from the Port project.

Full-Scale WTP Performance

Following the bench-scale test program, McCue rapidly deployed a full-scale metals precipitation plant at the Port project site. The chemical precipitation program has consistently removed copper, zinc and other target metals from the construction water at a fraction of the cost of the other treatment methods considered by McCue's client. Typical results from the full-scale WTP operation are also provided in Table 8 for comparison. The results indicate better performance at a field scale than at a bench scale. Furthermore, the results prove that metals precipitation is a viable method for reducing heavy metals, including copper.

Table 8: Performance using representative water sample vs. synthetic water sample

Parameter	Synthetic inlet water	Flocculated two-stage precipitation	Port project inlet water (bench scale)	Port project bench scale	Port project inlet water (operation)	Port project treated water
Dissolved aluminum	2.21	0.119	<0.010	NM	0.0100	<0.0060
Dissolved antimony	0.304	0.0129	<0.0010	NM	<0.00060	<0.00060
Dissolved arsenic	0.00864	0.00046	<0.0010	NM	<0.00060	<0.00060
Dissolved cadmium	0.0291	<0.0000050	<0.000513	<0.000010	0.000248	<0.000030
Dissolved chromium	0.0017	<0.00010	<0.0010	NM	<0.00060	<0.00060
Dissolved cobalt	0.0094	0.00021	0.0087	0.00423	0.00504	0.00075
Dissolved copper	0.04	0.00029	0.0168	0.00149	0.0158	<0.00090
Dissolved manganese	1.37	0.226	4.730	3.650	2.93	0.146
Dissolved zinc	4.23	0.000059	2.410	0.00529	0.0271	<0.0090

Notes:

1. All reported data expressed in mg/L
2. Analytical results provided by a third-party laboratory
3. "<" – Less than the reported detection limit
4. "NM" – Not measured

Conclusion

The work presented in this document could have both a local and global impact by:

- Filling gaps in the literature on data for end points of chemical precipitation of aluminum, cobalt and manganese at specific pH – values that were recorded for the bench tests performed.
- Filling gaps in the literature on data for end points of chemical precipitation of antimony, chromium and copper, which were found to decrease in the bench tests performed.
- Revising theoretical end points of chemical precipitation programs and establishing practical end points, which have been demonstrated to be lower than the theoretical ones.
- Establishing a detailed procedure and methodology to test and compare chemical precipitation programs.

Filling in gaps in knowledge decreases uncertainty as to what level of water treatment and environmental protection can be achieved. Lowering uncertainty helps with gaining social (First Nations) and regulatory acceptance. Better data also helps advance engineering design work more efficiently. Combined, the work will lower both project risk and cost.

References

BioteQ Environmental Technologies. 2015. Metals Removal from Kemess Pit Water Laboratory Testing – Final Report.

Department of Army, US Army Corps of Engineers. 2001. Engineering and Design – Precipitation / Coagulation / Flocculation. *Manual No. 1110-1-4012*.

Eckenfelder, W.W., Jr. 2000. *Industrial Water Pollution Control*. New York: McGraw-Hill Series in Water Resources and Environmental Engineering.

Environmental Assessment Office. 2015. Environmental Assessment Office USER GUIDE – An Overview of Environmental Assessment in British Columbia.

Ersoz, M. 2013. *Best Practices Guide on Metals Removal by Treatment*. London: IWA Publishing.

Government of British Columbia. Environmental Mitigation Policy. Last modified May 13, 2014. Retrieved from: https://www2.gov.bc.ca/gov/content/environment/natural-resource-stewardship/policy-legislation/environmental-mitigation-policy

Government of British Columbia. The Environmental Assessment Process. Last modified March 14, 2018. Retrieved from: http://www.eao.gov.bc.ca/process.html

Ministry of Environment, Ecosystems Branch, Environmental Sustainability and Strategic Policy Division. 2014. Procedures for mitigating impacts on environmental values (environmental mitigation procedures). Version 1.0.

Peters, W. Roberts, Ku, Y. and Bhattacharyya, D. 1985. Evaluation of Recent Treatment Techniques for Removal of Heavy Metals from Industrial Wastewaters, *AICHE Symposium Series,* 81(243): 165–196.

Robinson, A.K. and Sum J.C. 1980. Sulfide Precipitation of Heavy Metals. *EPA-600/2-80-139.*

Scott, M.C. 1977. *Sulfex™- A New Process Technology for Removal of Heavy Metals from Waste Streams*.

Skousen, J. 2014. Overview of Acid Mine Drainage Treatment with Chemicals. Acid Mine Drainage, Rock Drainage, and Acid Sulfate Soils: Causes, Assessment, Prediction, Prevention, and Remediation. West Virginia University. 325-337. 10.1002/9781118749197.

Wang, L.K., Hung, Y. and Shammas, N.K. 2005. *Physicochemical Treatment Processes*, Vol. 3, Handbook of Environmental Engineering. New Jersey: Humana Press.

Xiao, F., Zhang, B. and Lee C. 2008. Effects of low temperature on aluminum (III) hydrolysis: Theoretical and experimental studies, *Journal of Environmental Sciences,* 20(8): 907–914.

Appendix A – Regulatory Framework

The preliminary design was completed in accordance with the following provincial regulatory guidance:

- Technical Guidance 1 of the Environmental Management Act – Environmental Impact Assessment and Technical Assessment Report (TG1), prepared by the British Columbia Ministry of the Environment (BC MOE).
- Technical Guidance 7 of the Environmental Management Act – Assessing the Design, Site, and Operation of Sediment Ponds Used in Mining (TG7), prepared by the BC MOE.

Environmental Assessment Process in BC

Major projects in British Columbia, Canada, are assessed for potentially significant adverse environmental, social, economic, health and heritage effects by the Environmental Assessment Office (EAO), as required by the *BC Environmental Assessment Act* (Government of British Columbia, 2017). The company building the project (the proponent) provides details on what they believe to be the potential adverse effects of the project, and how they mitigate those effects. Figure 2 illustrates the process.

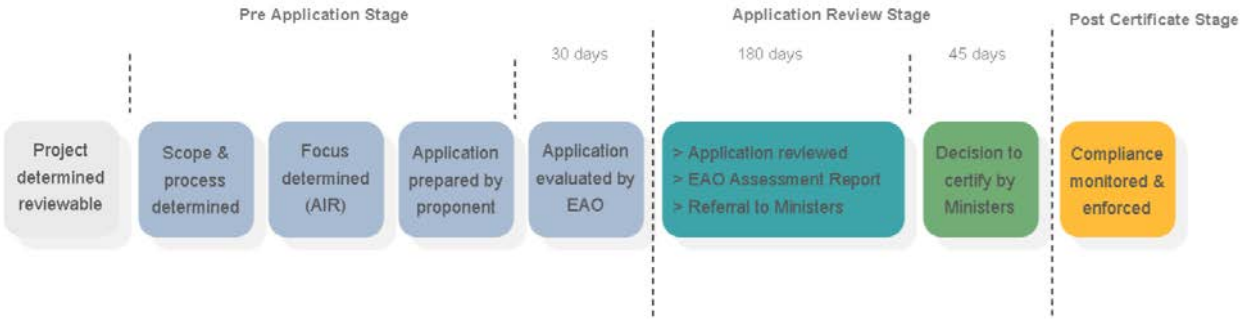


Figure 2: Environmental Assessment Process Chart (Environmental Assessment Office, 2015)

Environmental Impact Assessment Process in BC

An environmental impact assessment determines the nature and extent of environmental impacts from a proposed development and outlines what mitigation measures would be appropriate. This evidence is used to make informed and durable natural resource decisions (Government of British Columbia, 2014). The environmental impact assessment is included within the Environmental Mitigation Policy and supporting procedures; it is meant to be preceded by the "Identification of environmental values and components of concern" stage and to be followed by the "Consideration and application of mitigation".

Stakeholder Involvement

During the environmental assessment, the EAO seeks input from Scientific Professionals, Indigenous groups, the public, local governments, and federal and provincial agencies to help ensure that no adverse effects are missed. Therefore, Ministries of Environment (MOE) and Energy & Mines (MEM) as well as First Nations are involved in the EA process.

Proceedings of Mine Water Solutions 2018
June 12–15, 2018, Vancouver, Canada
Published by the University of British Columbia, 2018

Changing Effluent Regulations in Canada, Helping Mine Sites to Reach New Limits

Sean Miller, Maxxam Analytics International Corporation, Canada
Terry Obal, Maxxam Analytics International Corporation, Canada

Abstract

In 2018 Environment and Climate Change Canada (ECCC) is planning to release the final version of the Metal Mining Effluent Regulations (MMER). This will be the first extensive update to the MMER since they were conceived in 2002. The updated regulations have new or more restrictive limits for key contaminants of concern to many mining operations in Canada. These include un-ionized ammonia, arsenic, cyanide, lead, and others. As well, changes to evaluating the toxicity of effluents being discharged to saline waters are being considered.

Analytical laboratories play an important role in supporting mining activities in Canada. Laboratory test results are used to demonstrate and record regulatory compliance, and to make critical decisions during mine operation and mine closure. To adequately support mining operations and meet the regulatory requirements governing them, the need to measure metal concentrations in a variety of sample matrices at ultra-trace (sub-part per billion and in some instances, sub-part per trillion) levels continues to challenge the industry. With the new limits being proposed in the MMER updates, mine sites may need to include ultra-trace analytical capabilities in their monitoring programs.

New analytical technologies that support higher sensitivity (lower detection limits), increased data reliability, and lower costs, are available. The demand for ultra-trace level metal analyses has spawned new analytical technologies: ICP- mass spectrometry (ICP-MS); and ICP-tandem mass spectrometry (ICP-QQQ). A review of these technologies and their applications will help mine sites to choose what will work best for a specific site or monitoring program.

New challenges that could impact the compliance of regulatory monitoring programs are emerging, along with the demand for lower detection limits and new technologies. Contamination of samples and diligent protocols for sample handling and processing will be important to mine sites that are required to meet more stringent discharge limits.

Introduction

On May 13 2017, Environment and Climate Change Canada (ECCC) published the proposed amendments to the Metal Mining Effluent Regulations (MMER) in the Canada Gazette, Part I (ECCC, 2017). Following the 60-day consultation period, ECCC anticipated that the final amendments would be published in Canada Gazette, Part II, approximately 12 months later. This would suggest that as of July 2018, the amended regulations would be enacted and mines in Canada would begin the three-year transition period towards full implementation.

Changes to the MMER are aimed at strengthening effluent quality standards, improving the efficiency of environmental effects monitoring (EEM), and adding diamond mines to the regulations. Improving the national baseline mining effluent standards is also described by ECCC as bringing the benefit of aligning them with provincial and territorial standards where possible.

In particular, changes to effluent quality standards and some components of EEM rely on the ability of commercial analytical laboratories to deliver accurate and appropriate data to meet the needs of monitoring programs. Over the last few years, advancements in Inductively Coupled Plasma (ICP) technology have made it possible to measure environmental variables at lower detections limits, and to achieve these lower detection limits in more complex sample matrices.

Additional considerations around data quality and quality assurance are becoming increasingly important as monitoring programs begin to take advantage of lower detection limits at the analytical labs, in particular contamination. Whether from deposition, mishandling, material transfer, or carry over in the lab, the level of diligence required to deliver high quality data at ultra-trace detection limits is not something that should be underestimated during field collection or in the laboratory.

Regulatory Changes in the Mining Sector

These amendments represent the first update to the MMER since they were conceived in 2002. Starting in December 2012, a 10-year review was conducted including representatives from metal, diamond, and coal mines, as well as national associations, provinces, territories, indigenous organizations, environmental non-government organizations, and other federal departments. The review concluded in April 2015, at which point the drafting of the amendments continued, until they were published in the Canada Gazette Part I in May 2017.

The objectives of the proposed amendments to the Metal Mining Effluent Regulations are to reduce the risks of the negative effects of mines on fish and fish habitat, improve the efficiency of certain performance measurement and evaluation requirements, and provide regulatory clarity regarding releases of effluent to fish-frequented water bodies for diamond mines (ECCC, 2017). More specifically, the

proposed amendments would impose more stringent limits for arsenic, copper, cyanide, lead, nickel, and zinc, as well as introduce limits for un-ionized ammonia; they would require that mine effluent not be acutely lethal to *Daphnia magna* for mines to maintain their authority to deposit, while providing flexibility so that a first acute lethality failure would not result in a loss of the authority to deposit; they would allow for the use of a marine species to test for acute lethality when saline effluent is being released into a saline environment; and they would improve the efficiency of the EEM protocols, without compromising environmental protection. Examples of the EEM amendments include adding a fish tissue study for selenium, and the addition of chloride, chromium, cobalt, sulphate, thallium, uranium, phosphorus, and manganese to the suite of substances being monitored.

Table 1: Proposed effluent limits (ug/L) and traditional laboratory detection limits

Element	Current limit (monthly mean)	Proposed limit (existing mine)	Proposed limit (new mine)	MMER required MDL	Laboratory detection limit
Arsenic	500	300	100	2.5	0.1
Copper	300	no change	100	1	0.2
Cyanide	1000	500	500	5	1
Lead	200	100	80	5	0.2
Nickel	500	no change	250	12.5	1
Zinc	500	no change	400	10	5
Radium-226	0.37 Bq/L	no change	no change	0.01 Bq/L	0.005 Bq/L
TSS	15000	no change	no change	2000	500
Un-ionized ammonia	no limit	500	500	50	20

The majority of the amendments discussed above involve the support and services of a commercial analytical laboratory, including water chemistry and ecotoxicology capabilities. Effluent samples from mine sites are not always ideal samples from an analysis perspective. Interferences such as salinity, sulphates, pH, and TDS can sometimes require dilution of samples, resulting in raised detection limits above the regulatory standards. While it is important that mine sites collect their samples on schedule and report effluent concentration below the discharge limits described in the MMER, it is equally important for the laboratories to understand the nature of the samples and have the appropriate instruments to achieve the required detection limits. Schedule 3 of the proposed MMER amendments (ECCC, 2017) provides the minimum laboratory method limits (Table 1).

In order to stay current with innovations in analytical instrumentation, and be able to provide the highest level of data quality to mining clients in Canada, laboratories need to be investing in the latest ICP technology. This new generation of instrumentation has the ability to accommodate more complex samples while achieving lower detection limits, as discussed below.

At the sample reception counter within the analytical laboratory, it is now common practice for mining samples to be isolated from the traditional stream of environmental samples to avoid issues with contamination and carry over on the analytical instruments. Much cleaner laboratory protocols and facilities have become the norm in order to satisfy the quality assurance and quality control protocols specific to new instrumentation operating at ultra-trace concentrations. The result for the mine is better environmental data and ultimately higher confidence in their analytical laboratory partner. The ability to measure lower concentrations of the substances included in the MMER amendments provides greater definition of what may be happening in the water treatment system, and can result in proactive mitigation of deficiencies ahead of non-compliance with the discharge limits or challenges with toxicity testing.

Analytical Technologies to Meet Future Effluent Regulations in Mining

To meet the proposed effluent monitoring standards, laboratories are faced with three key analytical challenges:

- reaching required reporting (detection) limits;
- presence of interfering species; and
- complex sample matrices.

In order to achieve the analytical sensitivity required to produce reliable and defensible data at the levels of the new standards, contract analytical laboratories are challenged to provide increasingly lower limits of detection without compromising the integrity, validity and representativeness of the analytical results. To do so, suppliers of laboratory testing services must implement newer technologies to minimize data variability at trace (part-per-billion) and at times, ultra-trace levels (part-per-trillion) levels.

The presence of interfering species, as well as matrix effects due to complex sample matrices, are addressed by applying inductively coupled mass spectrometric (in particular, triple quadrupole) techniques in the laboratory.

Metals Analyses using Inductively Coupled Plasma (ICP) Mass Spectrometric (MS) Techniques

The determination of metals concentrations in environmental matrices (soil, water, air, and tissue) has evolved significantly over the last 30 years, to meet the changing needs of the marketplace. Historically, metals analyses were performed using atomic absorption (AA) spectrophotometry to measure part-per-million (ppm) and part-per billion (ppb) concentrations. As the need to detect lower concentrations of

specific metals has increased over the years, technology has evolved with the introduction of ICP optical emission spectrophotometry (ICP-OES) affording ppb and at times part-per-trillion (ppt) levels of detection. ICP-OES instruments are now commonplace in most analytical laboratories. The continued drive for higher sensitivity and data reliability at ultra-trace levels resulted in the development and implementation of ICP-mass spectrometric (ICP-MS) techniques and most recently ICP-triple quadrupole mass spectrometers (ICP-QQQ). Figure 1 illustrates the typical sensitivities achieved with each analytical method.

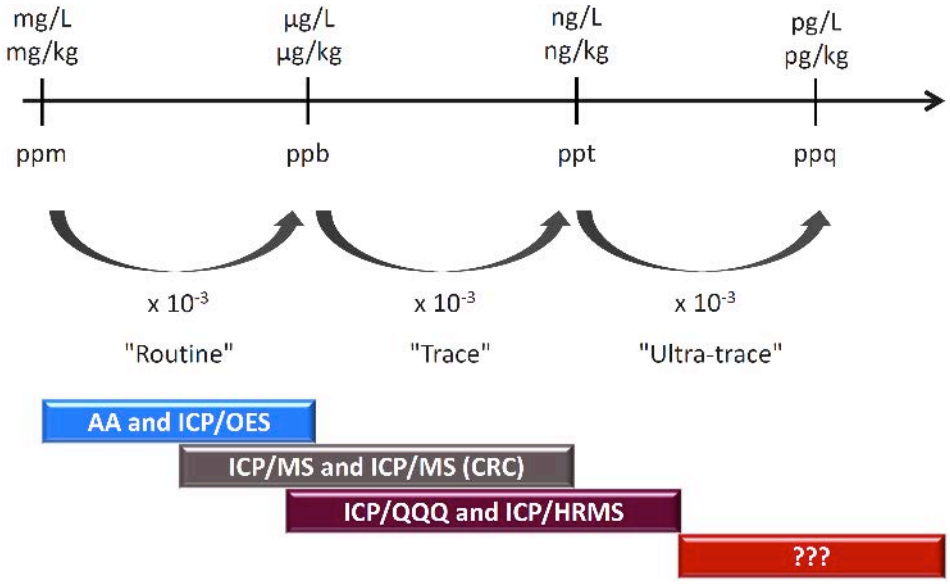


Figure 1: Achievable limits of detection for metals by various analytical technologies

The determination of metals using ICP-MS (single quadrupole and triple quadrupole; see Figure 2) techniques is a must to meet the proposed regulatory standards.

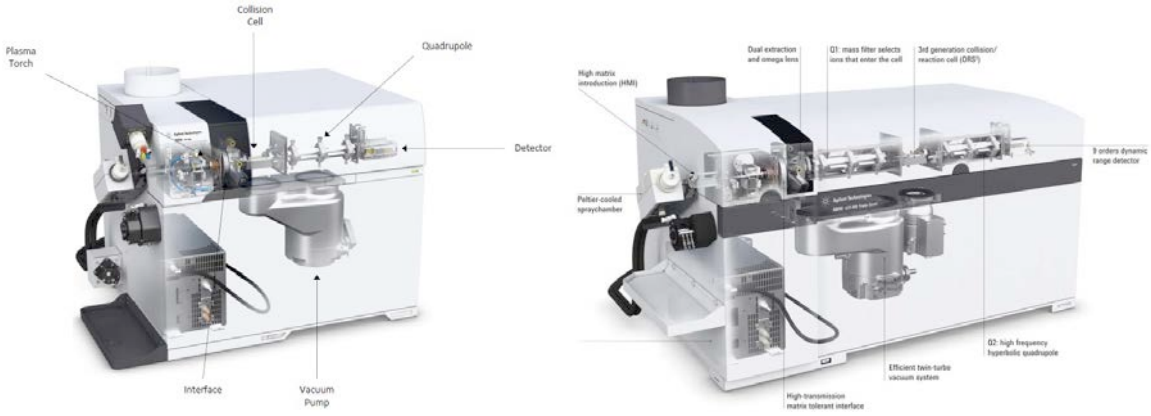


Figure 2: Schematic comparison of ICP-MS instrumentation – single quadrupole vs. triple quadrupole

Interfering Species, Complex Sample Matrices and Interpretation of "Non-detects"

Sample Processing ("Clean Room")

The elimination of background interferences and extraneous sources of contamination is critical to accurate measurement of metal concentrations in effluents at trace levels. This is an important consideration in the laboratory, as background concentrations of the metals of interest can be found virtually everywhere. To address the risk of false positive results due to background, "clean room" facilities and sample processing protocols are an absolute in the analytical sequence. Figure 3 shows a typical clean room configuration at an ultra-trace level metals laboratory.

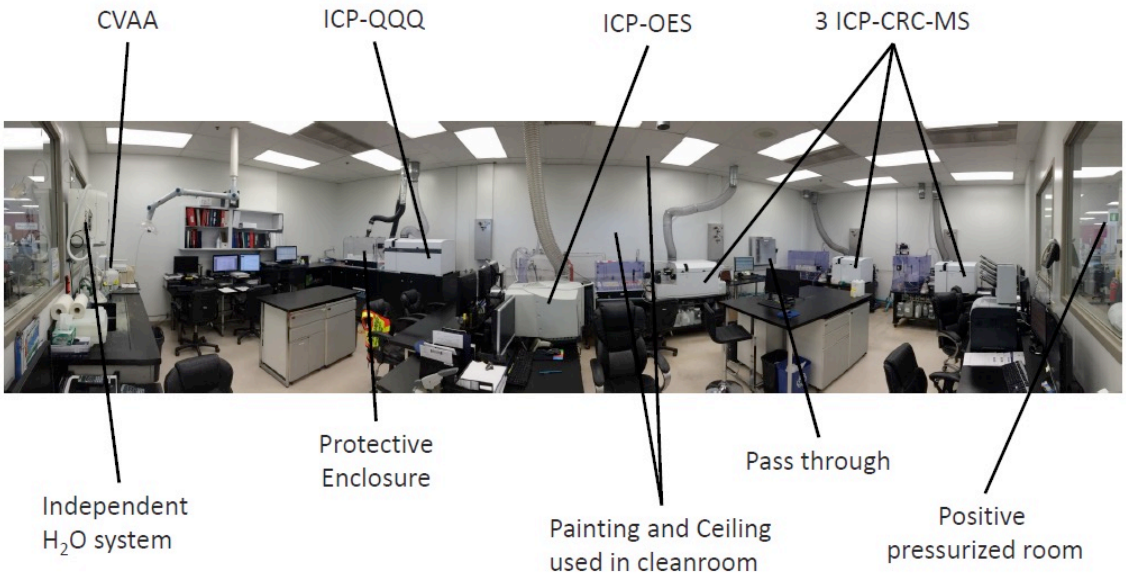


Figure 3: Ultra-trace level metals processing and analysis facility at Maxxam

Chemical Resolution

The presence of interfering species and matrix effects can have a significant impact on a laboratory's ability to achieve trace and ultra-trace level sensitivities. The typical approach to addressing these challenges is to dilute the sample and re-analyze. However, the method detection limits for non-detected parameters *must* be increased proportionately with the dilution factor, which in many cases raises the MDL higher than the proposed effluent standards. The lower detection limits achieved by ICP-MS and ICP-QQQ techniques overcome these challenges in some cases. Typical analytical sensitivity achievable using ICP-MS techniques are presented in Table 2. More importantly, through "chemical resolution" (vs. mass resolution) of the elements of concern, interfering species and matrix effects can be overcome without dilution. This is achieved by (see Figure 4 below):

- converting the interfering species into a new species;
- converting the analyte ion into a reaction product ion (mass-shift mode).

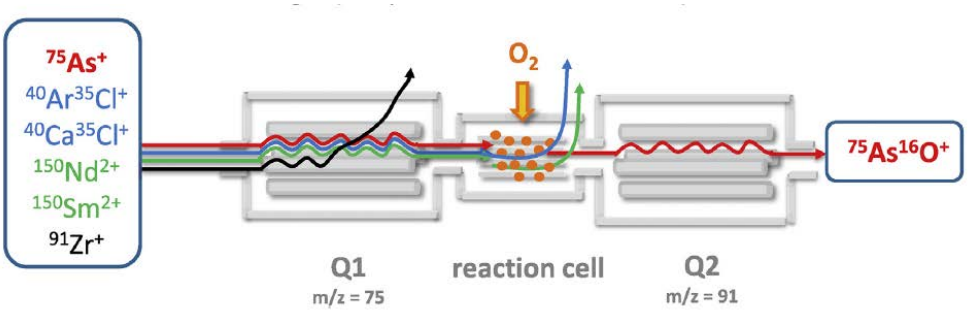


Figure 4: Chemical resolution of ^{75}As from interfering species having the same mass-to-charge (m/z) ratio

Table 2: Typical analytical reporting limits (ug/L) for metals by ICP-MS and ICP-QQQ

Element	ICP-MS	ICP-QQQ
Arsenic	0.1	0.02
Copper	0.2	0.05
Lead	0.2	0.006
Nickel	1	0.03
Zinc	5	0.2

Sampling Considerations

Background concentrations of the metals of concern, particularly at trace levels, are everywhere. As shown in Table 3, trace metals that can easily contaminate samples come from many potential sources.

The mitigation, if not elimination, of extraneous sources of contamination during the sample collection process is critical to the success of any environmental monitoring program. It is important that any field-sampling program include:

- Clean and proofed (if possible) field sampling equipment.
- Processes that minimize sample handling and manipulation from the time of sample collection to the analysis.
- A robust and rigorous field quality assurance program that monitors potential background contamination through the collection of "blind" field blanks.

To support the integrity of field sampling activities for ultra-trace metals analyses, Maxxam recommends specialized sampling kits that include controlled and traceable field sampling containers, filters and preservatives (see Figure 5).

Table 3: Potential sources of field contamination

Source	Potential contaminants
Sampling equipment: Gloves Sample bottles Sample vials Filtering supplies	Cupper (Cu), Zinc (Zn), Aluminum (Al)
Stack emissions Cigarette smoke	Arsenic (As), Cadmium (Cd), Lead (Pb) Mercury (Hg)
Personal care products, e.g.: Shampoos Perfumes	Aluminum (Al), Lead (Pb), Nickel (Ni) Selenium (Se)
Jewellery	Gold (Au), Silver (Ag), Tungsten (W)
Perspiration	Copper (Cu), Chromium (Cr), Iron (Fe) Magnesium (Mg), Sodium (Na), Zinc (Zn)



Figure 5: Field sampling kit for ultra-trace metal samples

Conclusion

The details around which of the proposed amendments to the MMER will be included, excluded, or modified prior to publication in the Canada Gazette Part II are uncertain as of June 2018. There has been extensive multi-stakeholder consultation up to the first publication and a substantial amount of feedback, both support and concern, during the 60-day consultation period. Whatever direction the new amendments take towards meeting lower detection limits, evaluating the toxicity of effluent on new species, or including additional resource sectors (such as diamonds and coal), your analytical laboratory partners are already proving out the science to support the success of mine site monitoring programs.

References

ECCC (Environment and Climate Change Canada). 2017. Regulations amending the metal mining effluent regulations, 151(19), May 13, 2017.

Proceedings of Mine Water Solutions 2018
June 12–15, 2018, Vancouver, Canada
Published by the University of British Columbia, 2018

Water Use, Quality and Treatment at Syncrude's Mineable Oil Sands Operation in Northern Alberta[1]

Warren Zubot, Syncrude Canada Ltd., Canada

Abstract

The oil sands industry, located in northern Alberta, Canada, makes a significant contribution to Canada's economy. In total, the deposits contain an estimated 1.7 trillion barrels of oil, of which 300 billion barrels are recoverable using current technology. Depending on the depth of the deposit, raw bitumen is produced either by in-situ well technology or mining. After mining, bitumen is recovered from the oil sand using a warm water extraction process, generating a tailings material composed of oil sands process water, sand, silt, clay and some unrecovered bitumen.

A key driver for Syncrude's long-term sustainability is improved environmental performance, which includes water management. Water is integral to both operational and environmental aspects of Syncrude's business, with short-term objectives to ensure adequate volumes of process water of sufficient quality are available for process needs. Longer-term objectives include maintaining acceptable water quality to maximize bitumen production, facilitating terrestrial and aquatic reclamation objectives, and demonstrating to our stakeholders prudent and responsible use of the available water resource.

To improve environmental performance, Syncrude has been developing a technology that uses an upgrading by-product, petroleum coke, to treat oil sands process water. Syncrude is constructing a prototype water treatment facility designed to treat oil sands process water (OSPW) to a quality to ensure it can be safely released to the environment in a manner that is protective of ecological and human health. The facility, scheduled for commissioning in the summer of 2018, will build upon a smaller scale pilot completed by Syncrude in 2012 at the Mildred Lake lease. The treatment process is a novel application of known treatment processes, and is based upon filtration of the water through a contained deposit of petroleum coke. However, unlike conventional sand filtration, the petroleum coke filtration media is composed of carbon. The 2012 program confirmed previous studies that showed petroleum coke – a by-product of SCL's Fluid Coking™ process – can be used as activated carbon (adsorption) to reduce concentrations of dissolved organic compounds present in OSPW. The results confirmed that the technology's treatment efficiency exceeded 80% for hydrocarbons components such as naphthenic acids

[1] This paper is only available as an abstract.

and polycyclic aromatic hydrocarbons and produced treated water that was acutely non-toxic based on a 96-h rainbow trout bioassay. Similar to the 2012 program, the 2018 program will involve the hydraulic deposition of a freshly produced slurry of OSPW and petroleum coke into a large earthen containment cell equipped with engineered underdrainage. This structure will be situated within the south-east quadrant of the Mildred Lake Settling Basin. The treatment is designed to reduce concentrations of suspended solids, free phase hydrocarbons, and dissolved organic compounds present in OSPW.

The intent of the field pilot study is to provide additional information to assess the water treatment process and validate at a prototype scale. The quality of the OSPW will be chemically monitored throughout the treatment. The final treated water produced will be evaluated using a triad approach that will include chemical testing, whole effluent toxicity testing, and standard chronic testing. Chronic toxicity testing will be conducted using commercial laboratories, and on-lease using a mobile test facility equipped with outdoor microcosms to evaluate biological effects in real-time.

Syncrude produces about 20 kg of product petroleum coke per barrel of synthetic crude oil produced and, based on the current state of knowledge, the technology has a commercialization potential to treat between about 8 and 12 Mm^3 of OSPW per year. This presentation will review Syncrude's water use and quality and discuss this novel water treatment process including key results of the 2012 field program and the 2018 program.

Proceedings of Mine Water Solutions 2018
June 12–15, 2018, Vancouver, Canada
Published by the University of British Columbia, 2018

Water Treatment for Mine Closure: A Bioremediation Pilot-Scale Study

Leonard Santisteban, Freeport-McMoRan, USA
Ilsu Lee, Freeport-McMoRan, USA
Shane Hansen, Freeport-McMoRan, USA
Erick Weiland, Freeport-McMoRan, USA
Dan Ramey, Freeport-McMoRan, USA

Abstract

Metal mines approaching the end of active operations must prepare for the potential long-term treatment of mining-influenced water (MIW). It is therefore imperative to identify options for cost-effective treatment technologies and strategies. For example, biologically-based passive remediation technologies are a proven, cost-effective option for treating mildly to moderately impacted waters at low- to moderate-flow rates. However, their applicability to highly impacted waters is less understood. The objective of this project was to conduct a pilot-scale test for optimizing the design criteria of sulphate-reducing biochemical reactors and treating wetlands for improving the quality of highly impacted MIW.

A pilot-scale bioremediation treatment system was constructed to treat MIW emerging from a historical mine facility located in the south-west USA. The acidic (pH ~3 s.u. and 8,500 mg/L acidity as $CaCO_3$) water contained elevated concentrations of aluminum (>900 mg/L), iron (>150 mg/L), copper (>900 mg/L), manganese (>500 mg/L), zinc (>300 mg/L), and sulphate (>16,000 mg/L), which was higher than what is typically treated using passive bioremediation. The treatment system consisted of three stages: pre-treatment, primary treatment, and post-treatment. The pre-treatment stage was designed to decrease iron and aluminum concentrations. The primary treatment stage consisted of a sulphate-reducing biochemical reactor (SRBR) to remove remaining metals and sulphate. The post-treatment wetlands were designed to remove manganese (Mn) and impart a final water quality polishing step. The treatment system was operated from July 2014 to November 2015.

Results indicated that metals and sulphate removal met treatment goals. Both calcium hydroxide [$Ca(OH)_2$] and limestone [$CaCO_3$] pre-treatment options effectively removed aluminum (>91%), iron (>99%), and copper (>72%), and significantly reduced the acidity and metal content of water to be treated by the SRBR. SRBRs removed iron, copper, uranium, cobalt, cadmium, and nickel below detection

limits, in addition to removing up to 65% of sulphate. Post-treatment wetlands removed 70% of Mn, with the majority of the remaining metals sequestered in the wetland sediments. The results indicated that SRBRs and treatment wetlands are a viable option for highly impacted waters characterized by elevated metal concentrations, significant metal acidity, and low pH. Our findings also corroborate the conclusions drawn by other practitioners indicating that treating this type of MIW requires a very large footprint. It is therefore worth noting that inclusion of either pre-treatment option resulted in a >67% reduction in SRBR size required compared to no pre-treatment. Regardless, bioremediation systems are a viable technology for the treatment of a wide range of water chemistry on mine sites approaching closure. Furthermore, this study indicates that managing long-term MIW liabilities using passive treatment technologies at a site is a feasible option

Introduction

Biological remediation (hereafter bioremediation) strategies are potentially cost-effective and relatively low maintenance technologies for treating mining-influenced waters (MIW), particularly for remote or closed mine sites. One such technology relies on biological sulphate reduction mediated by sulphate-reducing bacteria (SRB) to increase alkalinity and pH while producing sulphide anions. Aqueous metal ions are removed through precipitation as metal sulphides (Sheoran et al., 2010). Sulphate-reducing biochemical reactors (SRBRs) are effective for the treatment of MIWs (e.g., Sheoran et al., 2010). SRBRs, however, are less effective in treating certain MIW constituents, primarily manganese (Mn), and therefore additional bioremediation technologies must be incorporated within the treatment system. Constructed treatment wetlands remove Mn and residual MIW constituents (e.g., total suspended solids) through biotic and abiotic processes, such as precipitation and settling of hydroxide and carbonate minerals. Combined, these bioremediation technologies could potentially reduce long-term liabilities for the mining industry and be deployed and operated with relatively low construction, maintenance, and monitoring costs (e.g., Sheoran et al., 2010; Kadlec and Wallace, 2009). However, less known, is the effectiveness of passive bioremediation for MIWs with high metal loadings.

The objective of this project was to conduct a pilot-scale test for optimizing the design criteria of sulphate-reducing biochemical reactors and treating wetlands for improving the quality of highly impacted MIW. In this study, a pilot-scale bioremediation treatment system was constructed in the south-western United States to evaluate the treatment of MIW emerging from a copper leach facility and overburden stockpile. The study provided critical information for determining whether passive treatment is feasible and cost-effective for treatment of this type of water, as well as affording insight into potential design parameters of a full-scale system.

Methodology

The treatment system consisted of three stages: pre-treatment, primary treatment, and post-treatment. Each stage of the treatment system evaluated was designed to target specific subsets of constituents of concern (CoCs). A pre-treatment stage raised influent pH and targeted removal of aluminum (Al) and iron (Fe). A sulphate-reducing biochemical reactor (SRBR) primary treatment stage stabilized the pH of the treated MIW in the circumneutral range and converted sulphate into aqueous sulphide ions. The primary treatment stage reduced sulphate concentrations while removing copper (Cu), zinc (Zn), and other divalent metals via the biochemically-driven formation of metal sulphides. It also removes remaining aluminum and iron. The third and final treatment stage, treatment wetlands, targeted elevated Mn concentrations and biological oxygen demand (BOD) present in the SRBR effluent, add alkalinity to provide further buffering capacity to treatment system effluent, and remove other metals that may exit the SRBRs.

Chemistry of the influent MIW evaluated is shown in Table 1. The MIW was acidic (pH <3) and contained elevated amounts of Al (942 mg/L), Fe (161 mg/L), Cu (976 mg/L), Mn (552 mg/L), and Zn (383 mg/L). The initial operating condition (i.e., flow rate) of the bioremediation process was determined based on MIW chemistry, published literature on SRBRs, and results from other Freeport-McMoRan (FMI) pilot- and bench-scale SRBR and treatment wetland operations.

Table 1: Chemistry of MIW used in the treatability study.
Results based on samples collected December 2013

Parameter	Concentration	
	mg/L	mole/L
Aluminum	942	0.0349
Arsenic	<1.25	–
Cadmium	2.31	0.00002
Calcium	285	0.0071
Chromium	<0.300	–
Cobalt	5.37	0.0001
Copper	976	0.0154
Iron	161	0.0029
Lead	<0.375	–
Magnesium	641	0.0264
Manganese	552	0.0100
Nickel	1.65	0.00003
Potassium	<25	–
Sodium	70	0.0030
Zinc	383	0.0059
Chloride	<100	–
Fluoride	265	0.0139
Sulphate	16,400	0.1708
TDS	17,817	
pH	3.05	

Pre-Treatment Stage

The treatment system evaluated three discrete treatment stages: (1) pre-treatment using either limestone or calcium hydroxide; (2) primary treatment using a SRBR; and (3) post-treatment wetlands. The effectiveness of the two pre-treatment strategies evaluated was compared against a system with no pre-treatment. The limestone pre-treatment system utilized four 33-gal drums (LT–1 to –4) each packed with 15 gal of ~1 in. angular limestone. Limestone-treated water was then metered into two SRBRs, which are described in detail below. The second pre-treatment option evaluated active chemical treatment using $Ca(OH)_2$. Raw MIW was actively treated by mixing with powdered $Ca(OH)_2$ in a 30-gal drum for 8 hours, followed by at least a week of gravity settling. After complete settling of the chemical sludge, the supernatant, which contained minimal Al and Fe was drained into 30-gal drums (labelled as CT-1 and CT-2) and used as feed solution for two additional SRBRs. We also evaluated a no pre-treatment strategy by directing raw MIW directly into two final SRBRs.

Primary Treatment (SRBR) Stage

The primary treatment SRBRs were each constructed using a 90-gallon drum with influent, effluent, and gas emission ports. All six SRBRs contained 4 inches of limestone (ca. 1 in. size) at the bottom to retain natural organic substrates (NOS) in the reactor and to provide additional alkalinity to effluent. The organic substrate mixture of woodchips, sawdust, alfalfa hay, and walnut shells served as electron donors required to support biological sulphate reduction. Limestone chips were mixed in with the organic substrate mixture to provide additional alkalinity. SRBR-1 contained 40% (by weight) of limestone to evaluate the effect of an increased amount of limestone on metal removal, while SRBR–2 to –6 consisted of identical mixtures and 30% (by weight) of limestone (Table 2). The total height of the NOS mixture in each SRBR was 36 in.

Table 2: Composition of NOS in pilot-scale SRBRs for the three experimental treatments evaluated.

	SRBR–1		SRBR–2 to 6	
NOS materials	Wt. %	Wt. Kg	Wt. %	Wt. Kg
Alfalfa hay	9	10	10	11
Sawdust	8	9	10	11
Woodchips	17	19	20	21
Walnut shells	26	30	30	31
Limestone	40	46	30	31
Mixture	100	114	100	105

All organic mixtures (except SRBR-1) included a baseline of 30 wt. % walnut-shells and 20 wt. % woodchips. The walnut shells and wood chips served as a long-term electron source (ITRC, 2013) as well as providing structural support to maintain proper hydraulic conductivity. Alfalfa hay (9 to 10 wt. %) acted as a labile electron donor source. Sawdust (8 to 10 wt. %) was included as a short- and medium-term electron donor source. Limestone (30 wt. %) was added to neutralize the mineral acidity of MIW and the expected acidic fermentation products generated within the SRBRs.

The SRBRs were inoculated with a sulphate-reducing bacterial culture in the form of commercially available Earthgro steer manure (50 wt. %) and locally obtained cow manure (50 wt. %). The SRBRs were then filled with MIW and allowed to sit idle to incubate bacterial colonies for approximately four weeks. After the incubation period, SRBRs were operated continuously in down-flow mode for the duration of the test period. The water level in the SRBRs was maintained at 1–2 in. above the surface of the NOS mixture.

Post-Treatment Constructed Wetland

The final component of the treatment system was a free water surface wetland (i.e., constructed wetland [CW]) to polish SRBR effluent. Twelve (12) wetlands were constructed for this evaluation. CW-1 and CW-2 received combined SRBR-1 and SRBR-2 effluent, CW-3 and CW-4 received SRBR-3 effluent, CW-5 and CW-6 received SRBR-4 effluent, CW-7 and CW-8 received potable water (negative control), CW-9 and CW-10 received raw MIW (positive control), and CW-11 and CW-12 received SRBR-5 effluent. SRBR-6 did not report to any wetlands because it was a duplicate of SRBR-5. The sizing of constructed wetlands designed to treat MIW depends upon the loading rate of constituents to be removed (Kadlec and Wallace, 2009). The general rule-of-thumb for sizing a wetland to remove Mn is 1 – 2 $g/m^2/d$ (Hedin and Nairn, 1993). For this evaluation, a sizing criterion of 2 $g/m^2/d$ was selected. The treatment system was designed to receive a flow rate of 2 L/d (0.0004 gpm), with the potential to be increased during the study. Assuming a flow rate of 0.0004 gpm and the sizing rule of 2 $g/m^2/d$, the recommended total size of the CW to treat 600 mg Mn/L was calculated to be 0.65 m^2. Each pair of wetlands (each: 41 in. × 18 in. × 12 in.; 3.4 ft^2, 0.3 m^2) was operated in parallel.

The wetland substrate consisted of 10-inches of a mixture of manure compost, topsoil, construction sand, and limestone gravel. Three species of native wetland plants were selected for planting in the pilot-scale system: Southern cattail (*Typha domingensis*), Olney's threesquare (*Schoenoplectus olneyi*), and hardstem bulrush (*S. acutus*). Each wetland was planted with two cattails culms and four plugs of each species of *Schoenoplectus*. Prior to system start-up, samples of the wetland substrate and plant material were collected and analyzed to serve as a baseline with which to compare changes in geochemistry and plant metal uptake following the introduction of MIW.

Three metrics were used to assess the fate of Mn in plants living within SRBR-receiving wetlands: bioaccumulation factor, enrichment factor, and translocation factor. Bioconcentration factor (BCF) represents a plant's ability to accumulate metals from soil and is the ratio of Mn in the whole plant relative to its concentration in wetland sediments and is calculated as:

$$BCF = \frac{C_{plant}}{C_{sediment}}$$

where C_{plant} denotes the concentration of Mn in the entire plant and $C_{sediment}$ denotes the concentration of Mn in sediments. Enrichment factor (EF) represents the degree of accumulation of Mn in plant shoots (i.e., above-ground biomass) relative to its concentration in wetland sediments and is calculated as:

$$EF = \frac{C_{shoots}}{C_{sediment}}$$

where C_{shoots} denotes the concentration of Mn in plant shoots. Lastly, translocation factor (TF) was calculated to assess the relative transfer of Mn within the plant, from roots to shoots, and is calculated as:

$$TF = \frac{C_{shoots}}{C_{roots}}.$$

The treatment system was commissioned in July 2014, operated and routinely monitored through November 2015. Regular monitoring of the treatment system included equipment settings, flow rate measurements, field chemistry parameters (pH, oxidation-reduction potential, electrical conductivity, dissolved oxygen, and temperature), and analyzing metal concentrations (specifically Al, Fe, Cu, Zn, and Mn). Water samples were collected at each stage of the treatment system. In order to prepare dissolved samples, liquid samples were filtered with a 0.45 µm membrane, diluted, and acidified within 24 hours after sampling prior to being delivered to an analytical laboratory for metal and sulphate concentrations.

Results and Discussion

Results from this study indicated that a bioremediation treatment system comprised of a SRBR followed by a constructed wetland effectively reduced metals and sulphate concentrations in the MIW to meet site water quality objectives. Furthermore, the addition of a pre-treatment stage to the bioremediation system improves the overall effectiveness and reduces the size of SRBR required.

Pre-Treatment Stage

The calcium hydroxide [$Ca(OH)_2$] and limestone ($CaCO_3$) pre-treatment stages removed Al (97% and 91% removed, respectively), Fe (100% removed for both), and Cu (86% and 72% removed, respectively). Additionally, both pre-treatment stages raised the pH of the MIW to over 5 (s.u.) and increased alkalinity. Limestone and $Ca(OH)_2$ pre-treatment effectively removed Al and Fe from the MIW with an inferred

hydraulic retention time (HRT) of 9.5 days and by dosing 4.1 g of $Ca(OH)_2$ per 1 L of MIW, respectively. The removal of these metals significantly reduced aqueous metal acidity and total metal content of the water requiring treatment by the SRBR (Figure 2). d

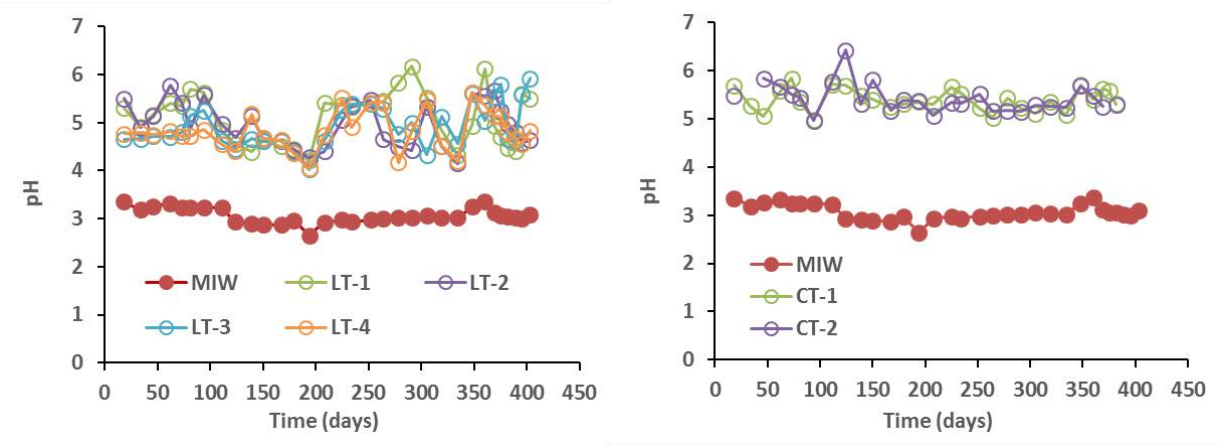


Figure 1: Change in pH following pre-treatment of MIW.
Influent pH (red) is shown relative to four limestone pre-treatment reactors (LT-1 to LT-4) and two Ca(OH)2 pre-treatment reactors (CT-1 and 2)

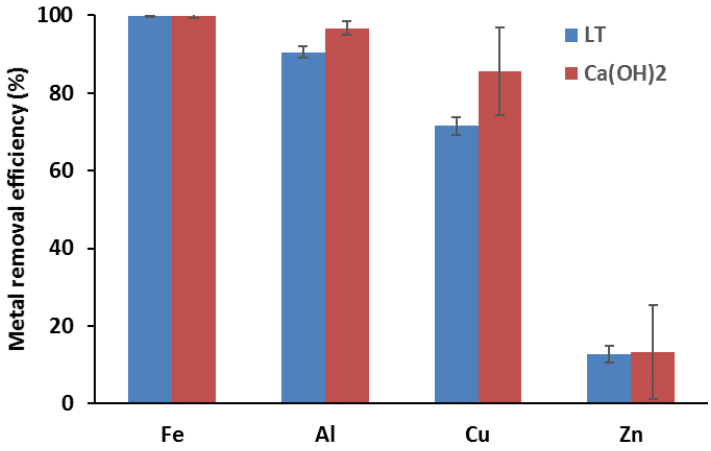


Figure 2: Metal removal efficiency (%) of iron (Fe), aluminum (Al), copper (Cu), and zinc (Zn) of limestone (LT) and Ca(OH)2 pre-treatment. Whiskers represent ±1 standard deviations

Primary Treatment (SRBR) Stage

Overall, the SRBRs produced sufficient alkalinity to increase the pH and alkalinity of the MIW. Sufficient biogenic sulphide was generated to remove aqueous metal ions [primarily Cu, Zn, Cd, cobalt (Co), nickel (Ni), and lead (Pb)] as insoluble metal sulphide precipitates. A performance metric utilized to evaluate SRBR effectiveness is the sulphate removal rate (SRR), which must be greater than the metal loading rate (MeLR). When the SRR is greater than or equal to the MeLR, metal removal is optimized within the SRBR. Additionally, the selection of flow rate, which depends on MIW chemistry, is critical for the

design of an effective SRBR system. SRBR flow rates used during this pilot-scale study are illustrated in Figure 3. The vertical shaded area of Figure 3 represents the time period, corresponding to the highest metal removal rate, determined for each treatment system. Metal and sulphate removal efficiencies of the individual SRBRs, relative to optimal flow rates, are presented in Table 3.

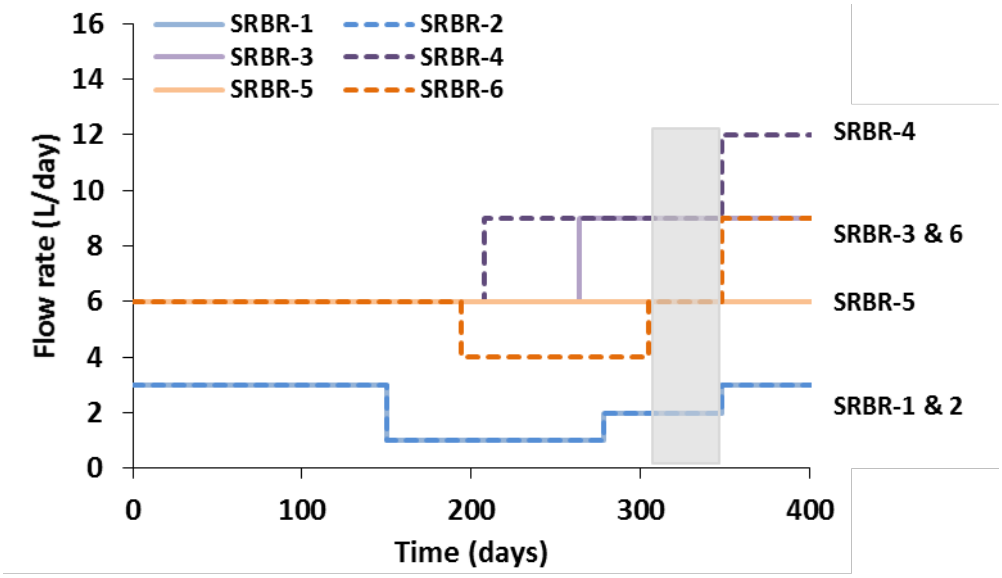


Figure 3: Operational flow rates for each of the SRBRs. Shaded area represents the operational time period when highest metal removal rates were observed.
The optimal flow rate as shown in this figure was used for calculating HRT, metal/sulphate removal efficiencies (Table 1), and the metal/sulphate removal rates (Table 2)

Table 3: Percentage removal of metals and sulphate at flow rate associated with the highest metal removal for each treatment strategy

	Flow rate (L/d)	HRT (d)	Al (%)	Fe (%)	Cu (%)	Mn (%)	Zn (%)	Sulphate (%)
SRBR-1	2	80	99	100	100	68	100	72
SRBR-2	2	80	99	96	100	19	100	68
SRBR-3	9	16	80	–	100	26	100	18
SRBR-4	9	17	79	–	100	34	100	30
SRBR-5	6	24	73	–	100	10	99	27
SRBR-6	6	26	55	–	100	0	100	28

% Removal = (Concentration In – Concentration Out) / Concentration In) × 100

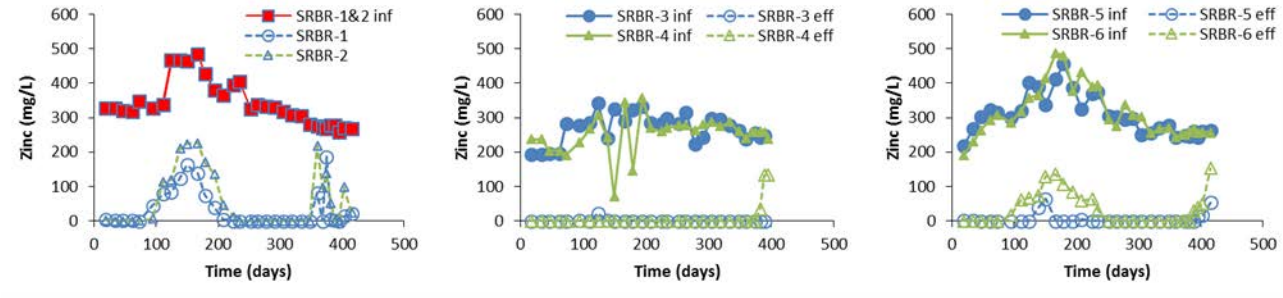


Figure 4: Zinc removal from MIW without pre-treatment (SRBR-1 and 2), Ca(OH)2-pretreated (SRBR-3 and 4), and limestone pre-treated MIWs (SRBR-5 and 6) by SRBRs.
Influent (inf) concentrations are plotted with solid lines and markers and SRBR effluent (eff) concentrations are plotted with dashed lines and open markers

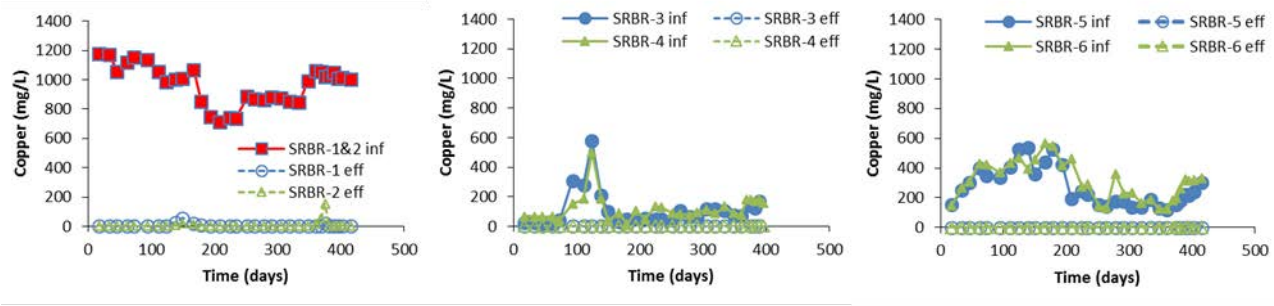


Figure 5: Copper removal from MIW without pre-treatment (SRBR-1 and 2), Ca(OH)2-pretreated (SRBR-3 and 4), and limestone pre-treated MIWs (SRBR-5 and 6) by SRBRs.
Influent (inf) concentrations are plotted with solid lines and markers and SRBR effluent (eff) concentrations are plotted with dashed lines and open markers

SRR, MeLR, and metal removal rate (MeRR) for each SRBR is presented in Table 4. MeLR and MeRR for each SRBR were calculated and reported here in three different ways: 1) including all metals; 2) excluding Mn because it is a non-target metal for removal; and, 3) excluding Mn, Al, and Fe because the latter two can be removed by simply adjusting pH. All SRRs were greater than the MeLRs, indicating that biological sulphate reduction was sufficient to remove target metals as metal sulphides. The differences between MeLR and MeRR were greatest when Mn was included in these calculations because Mn was not effectively removed by any SRBR.

Table 4: Metal loading and removal rates at optimal flow rates for each treatment strategy.

	Flow rate	HRT	All metals		Except Mn		Except Mn, Al, Fe		
			MeLR†	MeRR††	MeLR†	MeRR††	MeLR†	MeRR††	SRR†††
SRBR-1	2 L/d	80 d	1.04	0.99	0.91	0.91	0.33	0.33	1.87
SRBR-2	2 L/d	80 d	1.14	1.02	1.00	0.99	0.36	0.36	1.95
SRBR-3	9 L/d	16 d	1.30	0.86	0.58	0.57	0.50	0.50	1.55
SRBR-4	9 L/d	17 d	1.29	0.85	0.60	0.58	0.51	0.51	1.65
SRBR-5	6 L/d	24 d	1.25	0.74	0.69	0.65	0.53	0.53	1.03
SRBR-6	6 L/d	26 d	1.06	0.51	0.62	0.51	0.43	0.39	1.11

† MeLR: metal loading rate (mmol metal/Kg·d), which is a function of the influent metal concentrations, and the flow rate;
†† MeRR: metal removal rate (mmol metal/Kg·d) which is a function of the decrease in metal concentrations and the flow rate; and,
††† SRR: sulphate(SO42–) removal rate (mmol SO42–/Kg·d), which is a function of the decrease in sulphate concentrations and the flow rate

Findings for the primary treatment stage (SRBR) are summarized below:

- A SRBR substrate consisting of walnut shells (30 wt%), limestone (30 wt%), woodchips (20 wt%), alfalfa hay (10 wt%), sawdust (10 wt%), and 1 wt% of manure (inoculant), is an effective mixture.
- The optimal HRTs under the three treatment strategies evaluated were:
    - 80 days with no pre-treatment (SRBR-1 and SRBR-2);
    - 17 days with calcium hydroxide pre-treatment (SRBR-3 and SRBR-4); and,
    - 25 days with limestone pre-treatment (SRBR-5 and SRBR-6).
- Achievable SRRs and MeRR were:
    - SRR equalled 1.87–1.95 mole SO_4^{2-}/Kg/day and MeRR equalled 0.91–0.99 mmol/Kg/day when receiving MIW without pre-treatment;
    - SRR equalled 1.55–1.65 mole SO_4^{2-}/Kg/day and MeRR equalled 0.57–0.58 mmol/Kg/day for the SRBRs receiving $Ca(OH)_2$–pretreated MIW; and,
    - SRR equalled 1.03–1.11 mole SO_4^{2-}/Kg/day and MeRR equalled 0.51–0.65 mmol/Kg/day for the SRBRs receiving limestone-pretreated MIW.
- Cd, Co, Ni, and U were removed to below detection limits (<0.1 mg/L) by all SRBRs. It should be noted that Cd and Co concentrations were rarely reduced during the pre-treatment stage, suggesting that biogenic or chemical sulphide precipitation and/or co-precipitation processes are necessary to remove them. However, Ba (0.5 mg/L in MIW) was not efficiently removed by pre-treatment or the SRBRs (only 30–50% removal).

Post-Treatment Constructed Wetland

The performance of treatment wetlands varied with influent chemistry. In the absence of any prior treatment, the pH of raw MIW improved from a mean of 2.9 to 4.4 s.u. by the time it exited the wetlands. Following SRBR treatment, pH increased from a mean of 6.6 to 7.4 s.u. Oxidation-reduction potential (ORP) of SRBR-treated water improved from a mean of –406.6 to +49.1 mV in wetland effluent, as required to promote Mn oxidation and precipitation.

Overall, Mn was reduced by 71% as MIW passed through the treatment systems. The bulk of Mn removal (84%) occurred in the oxidation ponds and treatment wetlands, with the remaining Mn (16%) removed by SRBRs (Figure 6). Mn removal varied among wetlands in response to influent water chemistry (e.g., pH and presence of other metals) and Mn loading. Mn was reduced to <10 mg/L in the constructed wetlands that represented the most favourable environmental conditions and sizing for the loading rate. The calculated first-order removal rate for the best-performing constructed wetlands (0.010 m/d) was comparable to the median value reported by Tarutis et al. (1995) (0.011 m/d) (Table 5). However, Mn removal efficiency within several wetlands decreased when Mn loading exceeded the original design criteria, as evident in CW-11 and CW-12 (Figure 6 and Table 5).

Findings for the constructed wetland treatment stage are as follows:

- Analysis of metal accumulation in wetland sediments indicates that the constructed wetlands were effective at removing aqueous constituents beyond Mn (e.g., Al, Cd, Co, Cu, Fe, and Zn). The mechanism most likely responsible for the accumulation of these constituents is adsorption onto sediment surfaces, as well as precipitation of oxide and hydroxide minerals (Kadlec and Wallace 2009).
- As expected, Mn removal was lowest in constructed wetlands exhibiting low pH (median <4) or low ORP (median <–100 mV).
- The fate of Mn within wetland plants varied among species. *S. olneyi* and *T. domingensis* took up the greatest concentration of Mn from sediments and sequestered it in their biomass, as evidenced by BCF values of 3.4 and 2.6, respectively (Table 6). BCF values >>1 indicate a species' potential for remediation, in this case for Mn, via plant uptake and storage, with plants serving as another sink for Mn in addition to sediments. EF values similarly varied among species with *S. olneyi* and *T. domingensis* again showing the greatest concentration of Mn in shoots relative to sediments (EF = 3.2 and 3.4, respectively). This indicates that these two species are transferring the greatest concentrations of Mn into their above-ground biomass, where Mn is primarily being stored. *S. acutus* and *T. domingensis* exhibited greater Mn concentrations in shoots than roots (i.e., TF >1), whereas *S. olneyi* (TF = 0.9) exhibited nearly equal concentrations in above- and below-ground biomass.

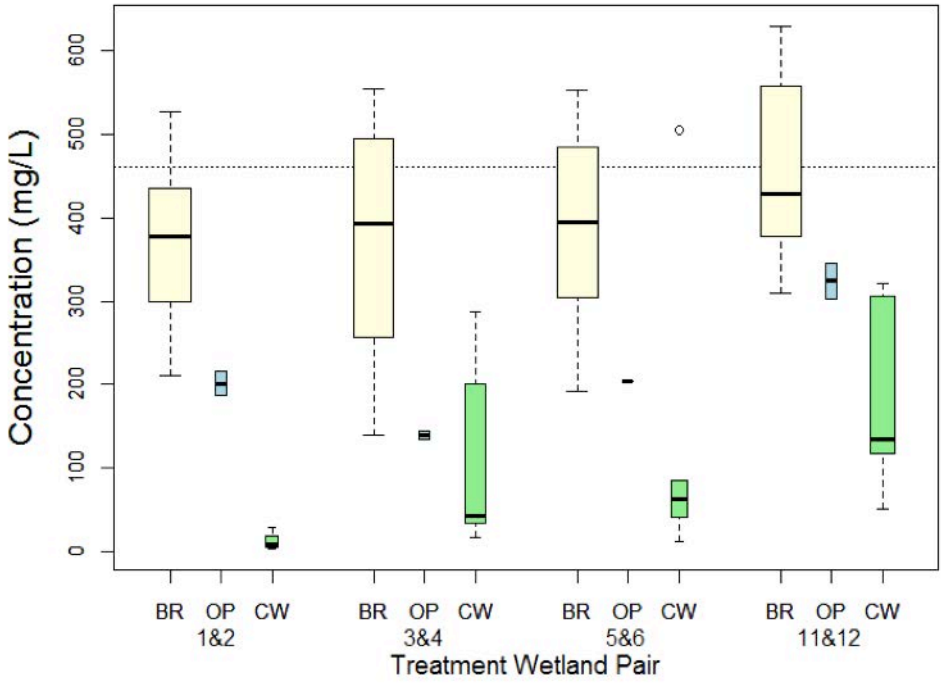


Figure 6: Boxplots summarizing dissolved Mn concentrations in effluent at each stage of the treatment system (excluding pre-treatment): BR = SRBR (yellow); OP = oxidation pond (blue); and CW = constructed wetland (green).
Dotted line represents median dissolved Mn (= 461 mg/L) in water to be treated. Range of Mn in influent was 378 to 720 mg/L. BR data is from Oct. 2014 to Nov. 2015; OP data is from Jul. to Aug. 2015; and CW data is from Jul. to Oct. 2015

Table 5: Summary statistics for treatment efficiency, area-adjusted removal, and first-order removal rate of dissolved Mn among constructed wetland pairs receiving SRBR-treated water

Wetland pair	Treatment efficiency (%)	Area-adjusted removal (g/m2·d)	First-order removal (m/d)
1 & 2	96%	0.62	0.010
3 & 4	70%	0.63	0.008
5 & 6	69%	0.91	0.008
11 & 12	59%	1.23	0.006
Median:	69%	0.63	0.008

Where: Treatment efficiency (%): $\left(\frac{C_{in}-C_{out}}{C_{in}}\right) \times 100$

Area-adjusted removal (g/m^2·d): $(C_{in} - C_{out})\frac{Q}{A}$

First-order (i.e., areal) removal (m/d): $\frac{Q}{A}\ln\left(\frac{C_{in}}{C_{out}}\right)$

- Overall, wetland plants performed well without exhibiting signs of toxicity to Mn when receiving SRBR-treated water, which is essential for phytoremediation to be effective. Variations observed in Mn uptake and transfer to above-ground biomass indicate that plant selection should be guided by treatment objectives and goals. Metal toxicity was, however, evident in plants within positive control wetlands (i.e., receiving un-treated MIW; CW-9 and CW-10), which further indicates the need for treatment of key MIW constituents such as Al, Fe, Cu, and Zn upstream of the wetlands.

Table 6: Bioconcentration (BCF), enrichment (EF), and translocation (TF) factors for the three wetland plant species evaluated

Species	BCF	EF	TF
Schoenoplectus acutus	1.2	1.3	1.2
Schoenoplectus olneyi	3.4	3.2	0.9
Typha domingensis	2.6	3.4	2.1

Conclusion

Recommended criteria for a full-scale passive bioremediation system designed to treat this highly impacted MIW are outlined below:

- Limestone pre-treatment effectively removed Al and Fe and raised pH with an HRT of 9.5 days. However, calcium hydroxide was observed to be more effective than limestone. $Ca(OH)_2$ has the ability to treat relatively higher flow rates than limestone and would avoid maintenance issues related to limestone armouring. However, $Ca(OH)_2$ pre-treatment is likely to require greater capital and operation expenses.
- MIW with highly elevated levels of sulphate and metal concentrations is best treated using the combination of $Ca(OH)_2$, an SRBR, and post-treatment wetland. This combination optimizes metal/sulphate removal and minimizes total treatment system size required.
- Treating MIW using an SRBR without pre-treatment is technically feasible. However, it will require sludge removal (Al and Fe precipitates) from the SRBR, which would need to be 3 to 4.5 times larger than a system implemented with pre-treatment.
- We recommend a SRBR substrate mixture consisting of walnut shells, limestone, woodchips, hay, sawdust, and a small amount of manure to treat highly impacted MIW. Pecan shells can be substituted for walnut shells, based on prior work by the authors, without reducing SRBR performance.
- Using the first-order removal rate and the results from the most effective pair of wetlands (i.e., CW-1 and –2; k = 0.010 m/d), a flow rate of 10 gpm, a starting Mn concentration of 460 mg/L, and a target effluent concentration of 10 mg/L, the recommended size for a full-scale treatment

wetland is 4.9 acres. Additionally, it is recommended that an oxic limestone bed be incorporated into the bioremediation treatment system just prior to the wetland to alleviate the Mn removal burden for the wetlands and allow for a smaller footprint.

This study evaluated passive bioremediation for MIW characterized by elevated metal concentrations having a calculated total acidity of ~8,500 mg/L as $CaCO_3$. This study effectively expands the application of passive bioremediation technology to highly impacted MIWs, and demonstrates that passive bioremediation should be included when evaluating options to treat this type of MIW. This technology has the potential for low installation and maintenance costs compared to active water treatment, and is particularly applicable to remediation of remote and/or closed mine site(s).

Acknowledgements

This work would not have been possible without the support of mine personnel and the hard work and dedication to the project exhibited by FMI laboratory technicians who contributed invaluable support with all aspects of fieldwork.

References

Hedin, R.S. and Nairn, R.W. 1993. Contaminant removal capabilities of wetlands constructed to treat coal mine drainage, in G.A. Moshiri (ed.), *Constructed Wetlands for Water Quality Improvement:* 187–195. Boca Raton, FL: Lewis Publ.

ITRC (Interstate Technology Regulatory Council). 2013. Biochemical reactors for mining-influenced water.

Kadlec, R.H. and Wallace, S.D. 2009. *Treatment Wetlands.* 2nd Ed. New York: CRC Press.

Sheoran, A.S., Sheoran, V. and Choudhary, R.P. 2010. Bioremediation of acid-rock drainage by sulphate-reducing prokaryotes: A review, *Minerals Engineering,* 23: 1073–1100.

Tarutis, W.J. Jr., Stark, L.R. and Williams, F.M. 1995. Sizing and performance estimation of coal mine drainage wetlands, *Ecological Engineering,* 12: 353–372.

Proceedings of Mine Water Solutions 2018
June 12–15, 2018, Vancouver, Canada
Published by the University of British Columbia, 2018

Biochemical Cyanide Treatment of Gold Mine Tailings Supernatant: Pilot and Demonstration Trials

James Harrington, Alexco Environmental Group, USA
Monique Simair, Contango Strategies Ltd., Canada
Justin Bourne, Lorax Environmental Services Ltd., Canada
Rachel Martz, Contango Strategies Ltd., Canada
Vanessa Friesen, Contango Strategies Ltd., Canada
Ben Ferris, Kumtor Gold Company, Kyrgyz Republic

Abstract

Two factors combine to make Kumtor's Tailings Management Facility (TMF) fairly unique: 1) the cyanide (CN) destruction circuit is located downstream of the TMF pond rather than in the mill; and, 2) water is not reclaimed from the TMF pond back to the mill due to the distance (~8 km) and elevation difference (~350 m). While the INCO SO_2/Air cyanide destruction process employed at the Effluent Treatment Plant (ETP) has been effective for 20 years, the ammonia produced by this process makes it challenging for Kumtor to comply with its Total Ammonia discharge criterion. To address this, the authors explored the viability of a biochemical cyanide treatment process referred to herein as the "cyanohydrin process". The primary benefit of the cyanohydrin process for Kumtor is that, unlike many other cyanide destruction methods, this process destroys cyanide without producing ammonia or nitrate. While Alexco has employed the cyanohydrin process at 15 heap leach sites, the authors are not aware of any full-scale application in tailings facilities. The cyanohydrin process occurs in two stages: first is the reaction of cyanide with aldehydes or ketones, where the carbon in the cyanide forms a covalent bond with the carbon in the aldehyde or ketone. The resulting cyanohydrin compound no longer measures as free, weak-acid dissociable (WAD), or total cyanide. The second reaction is cyanohydrin degradation by microbes that subsequently use the cyanohydrin for both a carbon and nitrogen source to support their growth. By incorporating nitrogen from cyanide into microbial biomass, formation of ammonia is prevented while still effectively degrading the cyanide. This is different from conventional biological cyanide destruction, which focuses on oxidative degradation of cyanide into ammonia.

Following preliminary test work, the authors set up a series of pilot-scale tests at the mine site in 200 L covered barrels and 1 m^3 Intermediate Bulk Container (IBC) totes exposed to the atmosphere in July 2017. The containers were filled with a mixture of tailings (fresh slurry from the pipeline with some

mature solids and water from the TMF as a microbial inoculum), and then dosed with varying amounts of glucose, fructose, and phosphorus; controls were also established. Over approximately 75 days of monitoring, barrels treated with amendments showed ~75% to ~90% removal of total cyanide (from ~60 mg/L to 14.5, and <5 mg/L), without the production of ammonia or nitrate. It is important to note that neither nitrite nor nitrate was formed, as these could represent degradation by-products of ammonia. Moreover, dissolved oxygen measurements through the trials confirmed that the systems remained in aerobic, oxidizing ranges, confirming that ammonia was not converting to nitrate and then elemental nitrogen gas.

For the purpose of this manuscript, a representative trial that gave approximately 75% removal is presented as a typical conservative case. Trends for total cyanide degradation were similar to those of CN-WAD; therefore, discussions of cyanide in this paper are made in the context of CN-T and understood to be reflective of CN-WAD and overall treatment of cyanide. Throughout this manuscript, cyanide or CN refer to total cyanide. Following the pilot-scale testing in barrels and IBC totes, the authors undertook a full-scale cyanohydrin test in August 2017, with fructose and phosphorus being mixed and dosed in the mill. All tailings produced in the mill during the 7.5-day test setup period (~170,000 m^3) were deposited into an "Isolated Pond" within the permitted footprint of the TMF. This setup period was followed by 30 days of monitoring prior to freezing of the pond surface. Data from the Isolated Pond displayed the same trends as the barrels, if not accelerated. Cyanide concentrations were reduced by approximately 39% (from 91 mg/L to 56 mg/L). Of equal significance, ammonia concentrations in the Isolated Pond are essentially unchanged despite the substantial cyanide destruction. On the strength of the results of these studies, Kumtor implemented the cyanohydrin process at full scale early in 2018. Performance will be evaluated later in the year.

Introduction

Kumtor gold mine is in the Issyk-Kul Region of Kyrgyzstan, located about 350 km southeast of the capital of Bishkek (Figure 1, Figure 2). The mine is situated at an elevation of approximately 4,000 metres above sea level (masl). Kumtor's Tailings Management Facility (TMF) is fairly unique for two reasons: 1) the cyanide (CN) destruction circuit is located downstream of the TMF pond rather than in the mill; and, 2) water is not reclaimed from the TMF pond back to the mill due to the distance (~8 km) and elevation difference (~350 m). The INCO SO_2/Air cyanide destruction process has been employed at the Effluent Treatment Plant (ETP) for 20 years. While this process is effective at cyanide destruction, the ammonia it produces makes it challenging for Kumtor to comply with its Total Ammonia discharge criterion.

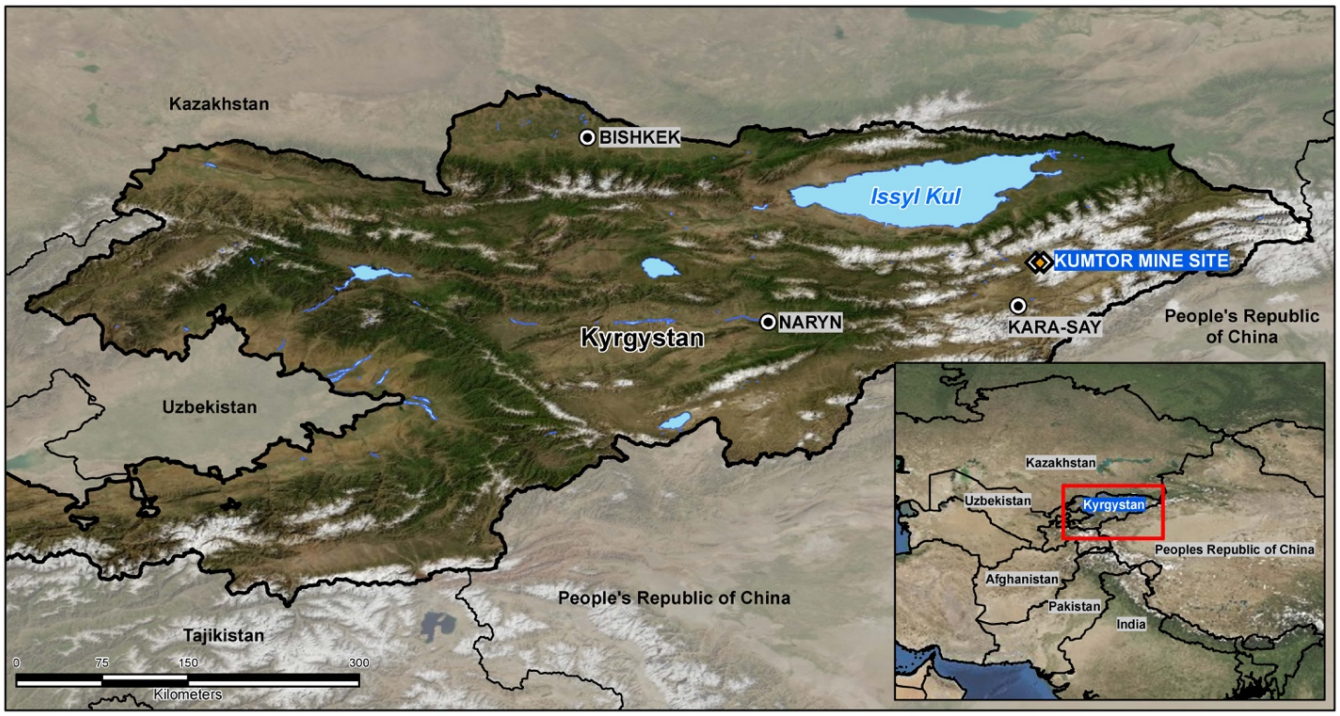


Figure 1: Kumtor site location map

Kumtor has explored multiple options for reducing ammonia discharge concentrations from the ETP. Consideration of direct ammonia treatment methods included conventional treatment (e.g., air/steam stripping, chlorination, ozonation, ion exchange), as well as passive and semi-passive constructed wetland treatment systems. These were all ruled out as technically infeasible or uneconomical, largely due to challenges relating to the high altitude, low temperature, and high flow rates. Reduction of cyanide and ammonia outputs from the mill have also been evaluated, but with limited success as the complex ore mineralogy often requires substantial amounts of cyanide to liberate the gold, and challenging blasting conditions limit the ability to control nitrogen residues entering the mill with the ore. It is worth noting that Kumtor has sourced a chemical alternative to sodium cyanide that bench-scale tests have indicated to be much more efficient at gold recovery with Kumtor's ore (thus leading to lower cyanide concentrations in the tailings discharge). This chemical is also slated for pilot testing at the mill in early 2018.

Cyanide degradation has the potential to create ammonia, in a ratio of as much as 53% ammonia as N produced per mg of CN. That is to say, 100 mg/L of cyanide could produce up to 53 mg/L of ammonia, if directly transformed, through processes such as the ETP's SO_2/Air oxidation process. Therefore, any amount less than this ratio of conversion indicates some other mechanisms at work, either consuming nitrogen so that it does not produce ammonia, or further conversion of ammonia to nitrate (through oxidation).

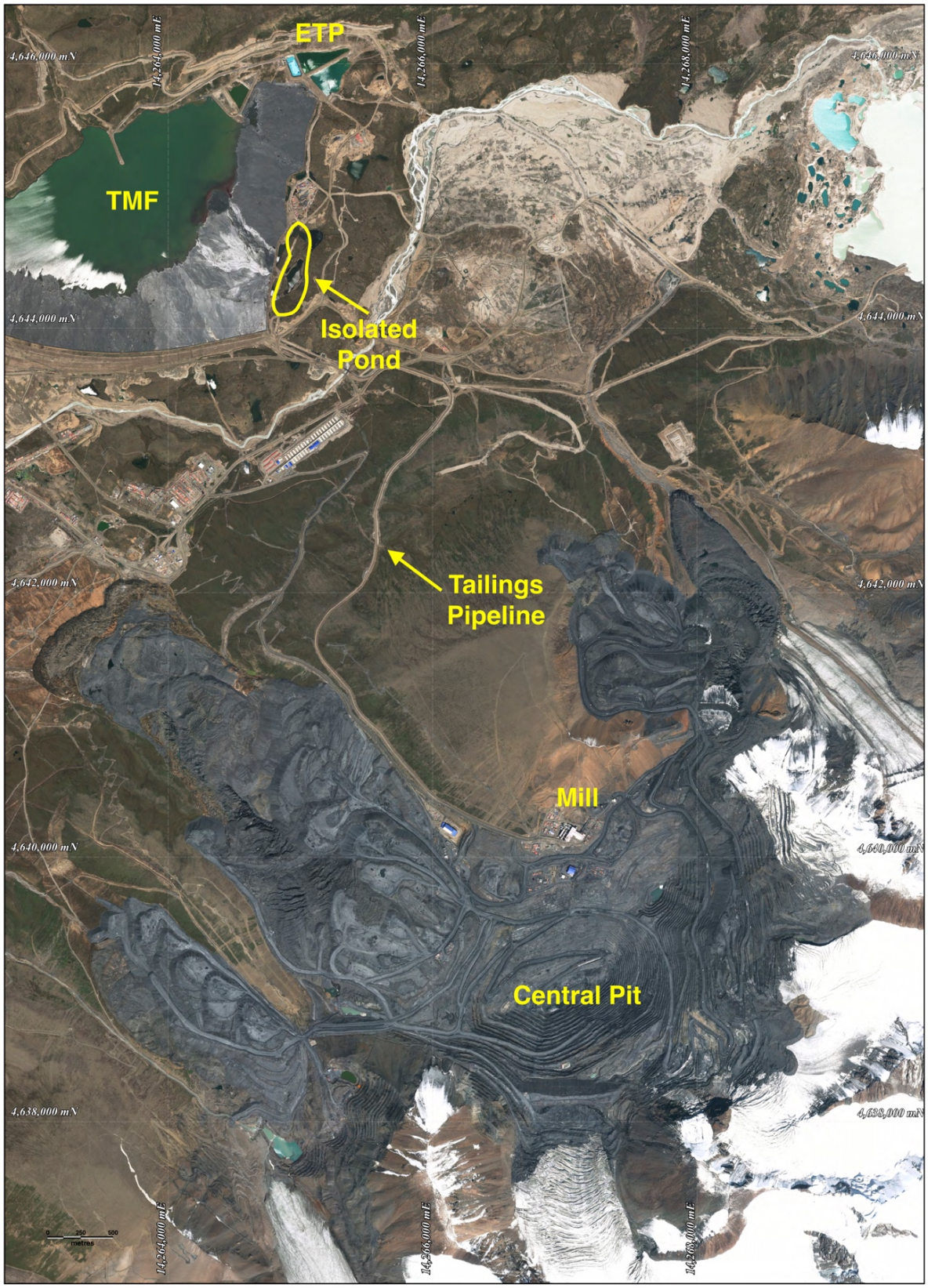


Figure 2: Kumtor site overview

This investigation began with a nitrogen balance of the TMF, whereby it became evident that there were existing processes occurring in the TMF pond that were acting as a nitrogen sink. While a majority of the influent cyanide was being removed within the pond, this was producing a concomitant increase in ammonia concentrations that was less than the stoichiometric ratio would predict. Further, nitrate and nitrite concentrations were decreasing within the pond, ruling them out as ammonia oxidation by-products. Total Kjeldahl Nitrogen (TKN) concentrations also generally decreased within the pond.

The apparent nitrogen sink in the TMF revealed by the rudimentary nitrogen balance described above led the investigators to believe that free carbon from residual mill reagents led to cyanide destruction in the pond through pathway(s) similar to the "cyanohydrin process" that was described in the literature as early as the 19th century (Kiliani, 1885) and used worldwide in chemical synthesis. The cyanohydrin process occurs in two stages: first is the reaction of cyanide with aldehydes or ketones, where the carbon in the cyanide forms a covalent bond with the carbon in the aldehyde or ketone (AEG, 2017a). The resulting cyanohydrin compound no longer measures as free, weak-acid dissociable (WAD) or total cyanide. The second reaction is cyanohydrin degradation by microbes that subsequently use the cyanohydrin for both a carbon and nitrogen source to support their growth. By incorporating nitrogen from cyanide into microbial biomass, formation of ammonia is prevented while still effectively degrading the cyanide (Figure 3). This is different from conventional biological cyanide destruction, which focuses on oxidative degradation of cyanide into ammonia.

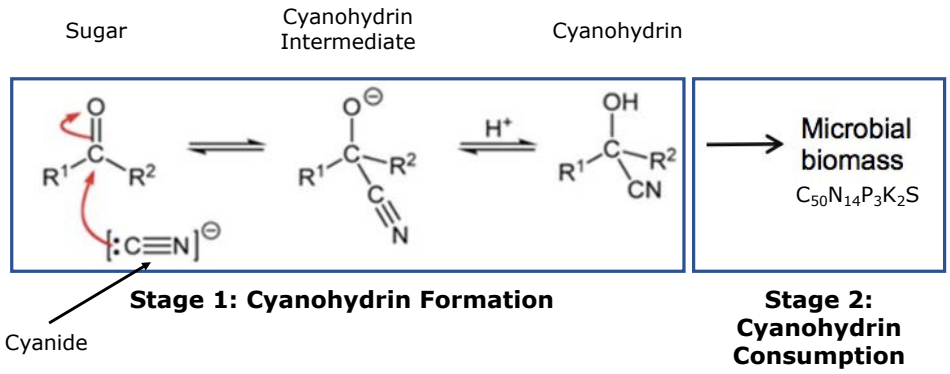


Figure 3: Cyanohydrin treatment process

From the promising insights gleaned from the TMF nitrogen balance, it was decided to evaluate the feasibility of employing the "cyanohydrin process" on an industrial scale at Kumtor with the goal of decreasing cyanide concentrations in tailings water (supernatant) while preventing the formation of ammonia or nitrate. The investigators have employed the cyanohydrin process at 15 heap leach sites, however the present implementation at Kumtor's tailings management facility is believed to be the first in the world of this magnitude.

Methodology

Pilot-Scale Test

The Cyanohydrin Barrel and Tote pilot trials (Phase 2) were assembled between July 4–10, 2017. These built on an initial preliminary set of tests (Phase 1) that informed dosing rates. For Phase 2, eight trials were set up inside a sea can using 200 L barrels filled with a slurry of tailings liquid and solids, each amended with different quantities of organic carbon (glucose or fructose) and phosphorous (Table 1). The dosing rates for these trials were based on the nitrogen balance described above. Two trials were set up outdoors in 1 m^3 totes filled with a slurry of tailings liquid and solids, each amended with different quantities of organic carbon and phosphorous (Table 1). Both the barrels and totes were monitored for treatment performance (destruction of cyanide and prevention of ammonia and nitrate formation) and a wide range of variables to allow for understanding performance and enabling optimizations. Monitoring included microbiological analyses on samples collected from select barrels on August 26, 2017, which is detailed by Contango (2018a). For sake of brevity in the manuscript, only three barrel and tote trials are presented. Full results are provided in Contango (2018a).

Earlier barrel trials noted little performance difference between glucose and fructose, therefore, less costly glucose was added to 5 trials while fructose was added to one trial for comparison and to provide a link between the two phases of barrel trials (AEG, 2017b). Phosphorous was added to barrels and totes using a diluted solution of phosphoric acid. Phosphorous was added to the starting mixture of all the barrels and totes, except for the control, which contained no amendments. Initial phosphorous was mixed into the tailings slurry with organic carbon (as appropriate to the trial objective) but resulted in no detectable phosphorous in the water; therefore, phosphorous was added a second time on July 25, 2017, following the same dosing concentrations as the initial dose but this time, added to the overlaying water column without mixing. In select trials, a third phosphorous addition was made in the same way as the second phosphorous addition to ensure its availability to microbes.

Full-Scale Test

The full-scale test was established in summer 2017 as an "Isolated Pond" using berms within and along the edge of the TMF (Figure 2, Figure 4). The discharge of the cyanohydrin-amended tailings to the bermed Isolated Pond area of the TMF occurred from August 25 to September 1, 2017, for a total of 7.5 days. Tailings were discharged into the Isolated Pond at a rate of approximately 1,000 m^3/hour, for a total of approximately 170,000 m^3 of amended tailings in the trial. The tailings were amended with a targeted fructose concentration of 250 mg/L and a phosphorous concentration of 1.35 mg/L as phosphate-P (Table 1). The amendments were mixed as batches in the mill and injected into the tailings line (AEG, 2017c). Over the course of the trial, approximately 30 tonnes of fructose and 270 kg of an 85% solution of

phosphoric acid were added to the tailings. The Isolated Pond was monitored for the same variables as the pilot-scale barrel and tote trials. Bacteria were identified genetically (by DNA sequencing) and quantified by growth assays. Details on the microbiological testing are provided in Contango (2018b). Two sampling locations, Isolated Pond-NW and Isolated Pond-NE, were used for water chemistry analysis to assess spatial variability within the pond. Sampling was conducted from August 30 to November 4, 2017. The two sampling locations had virtually identical results; therefore, the results presented in this paper are an average of the two locations. Due to formation of ice after approximately 30 days of monitoring, results for the Isolated Pond presented in this paper include only the first 31 days of data to avoid the confounding aspects of interpreting the ice-concentration effects.

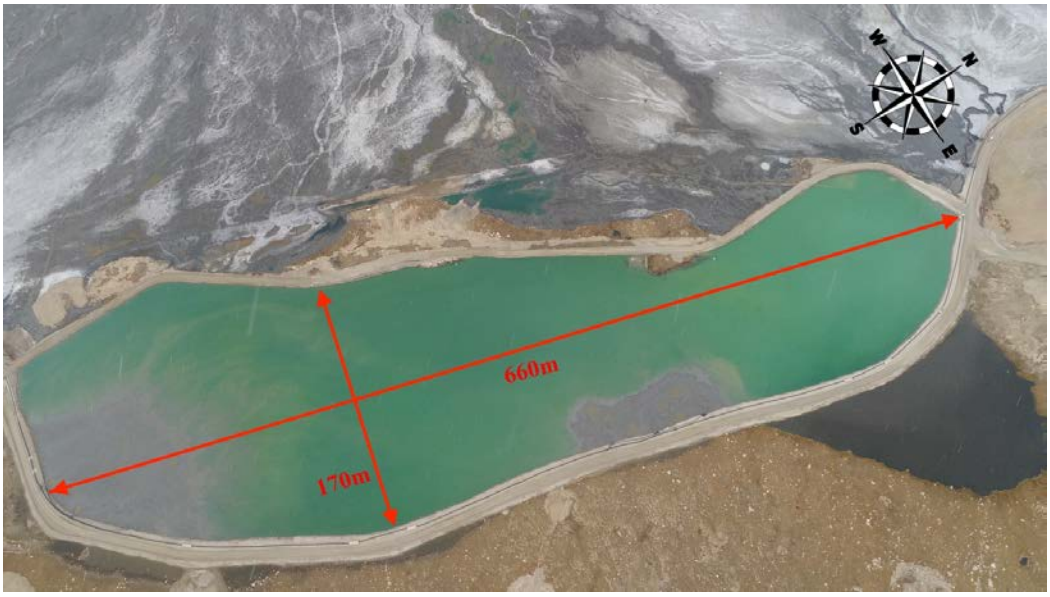


Figure 4: Overhead photo of Isolated Pond (taken 19 September 2017)

Table 1: Amendments used in pilot-scale and full-scale testing

Test Phase	Description	Test type	Organic carbon (mg/L)	Phosphoric acid (mg/L as P)	Dosing
Phase 2 Barrels/Totes	Open control with P only	Open IBC tote	–	0.8	Organic carbon added in 1 dose. Phosphoric acid added in 2 doses
	Sealed treatment fructose + P	Sealed barrel	484.7	0.2	
	Sealed control No amendments	Sealed barrel	–	–	–
Full-scale trial	Isolated pond	Open pond	250.0	1.35	Added in mill prior to discharge to Isolated Pond

Calculation of Theoretical Ammonia Discharge

As indicated above, Kumtor is not concerned with the efficiency of their existing INCO SO_2/Air cyanide destruction circuit, but rather with the ammonia produced as a by-product of this process. As the

destruction of cyanide by the cyanohydrin method does not result in a concomitant in ammonia within the TMF, it effectively decreases theoretical ammonia discharge potential of the ETP. For the purpose of this study, the theoretical ammonia discharge is defined as the sum of the potential ammonia that could be discharged from the ETP due to CN oxidation through the INCO SO_2/Air process and influent ammonia concentrations from the TMF pond to the ETP – Equation 1: Example of biological cyanide oxidation.

$$CN + \frac{1}{2}O_2 + H^+ + 2H_2O \rightarrow HCO_3 + NH_4 \qquad \text{Equation 1}$$

Data and discussion

Total Cyanide

Trends for CN-T degradation were similar to those of CN-WAD, therefore, discussions of cyanide in this paper are made in the context of total cyanide (herein referred to as CN) and understood to be reflective of CN-WAD and overall treatment of cyanide.

Full- and pilot-scale trials amended with organic carbon experienced a significant decrease in CN (Figure 5), without the production of measurable ammonia. Pilot-scale trials using similar dosings of different organic carbon sources (*i.e.* fructose or glucose) did not display notable differences in results. The trials amended with only phosphorous showed near complete removal of CN, however these trials experienced an increase in ammonia concentrations. This confirms the investigators' hypothesis that the addition of organic carbon (fructose or glucose) is necessary to prevent substantial formation of ammonia or nitrate during microbial degradation of CN. The control trial showed only minimal and very delayed decreases in CN concentration, affirming that amendment additions are necessary to stimulate microbial degradation of cyanide.

The pilot-scale trials were monitored for approximately 75 days until the supernatant water in the barrels and IBC totes was depleted to levels where it was no longer considered representative. At this final sampling event, CN was decreased by ~75% to ~90% (from ~60 mg/L to 14.5 and <5 mg/L in respective representative trials) in the organic carbon and phosphorous amended trial (no change in ammonia or nitrate concentrations), 98% (from 58 mg/L to 0.7 mg/L) in the phosphorous amended trial (albeit with a corresponding full conversion to ammonia, and some nitrate production), and 19% (from 66 mg/L to 54 mg/L) in the control trial (no change in ammonia or nitrate concentrations; Figure 5, Figure 6, Figure 7).

The full-scale Isolated Pond trial ran for approximately 30 days prior to the onset of freezing conditions. At this time, CN was decreased by 39% (from 91 mg/L to 56 mg/L) while ammonia concentration had no change beyond the range of method error of the assay (Figure 5, Figure 6, Figure 7). Additionally, there was no significant change in the nitrate concentration (which could indicate

conversion of cyanide through ammonia to nitrate). For comparison, after 30 days of treatment in the pilot-scale trial, CN was decreased by only 15% (from 62 mg/L to 52 mg/L) in the organic carbon and phosphorous amended trial (Figure 5, Figure 7). By a correlational projection it is reasonable to assume that after 75 days the full-scale trial would have attained similar or better treatment than the pilot-scale trial (*i.e.* >76% CN removal with no measurable ammonia production). Data from the pilot-scale trials also suggest that CN removal had not reached completion, further suggesting that concentrations would continue to decrease for some time. CN-Total with data normalized to start at 100% for comparison between pilot-scale and full-scale trials over days of treatment; data for the pilot-scale trial was averaged for the initial time point before normalizing.

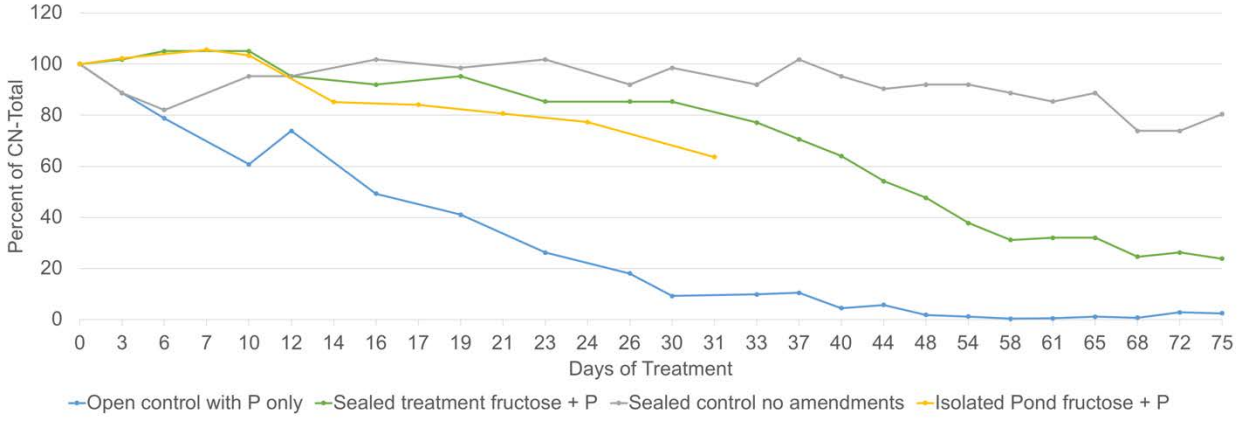


Figure 5: Percentage of CN-Total over time (normalized to initial concentration for each test)

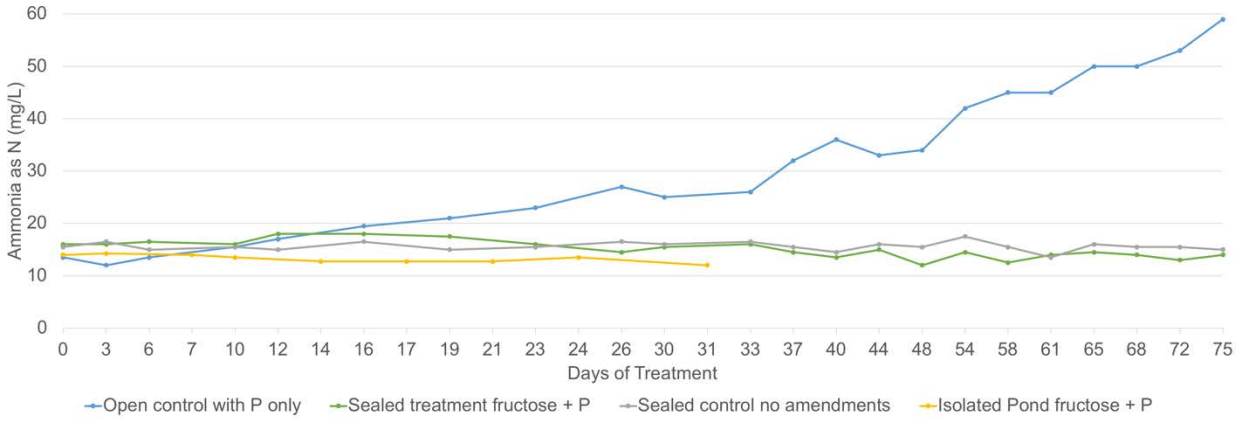


Figure 6: Change in ammonia as N over time

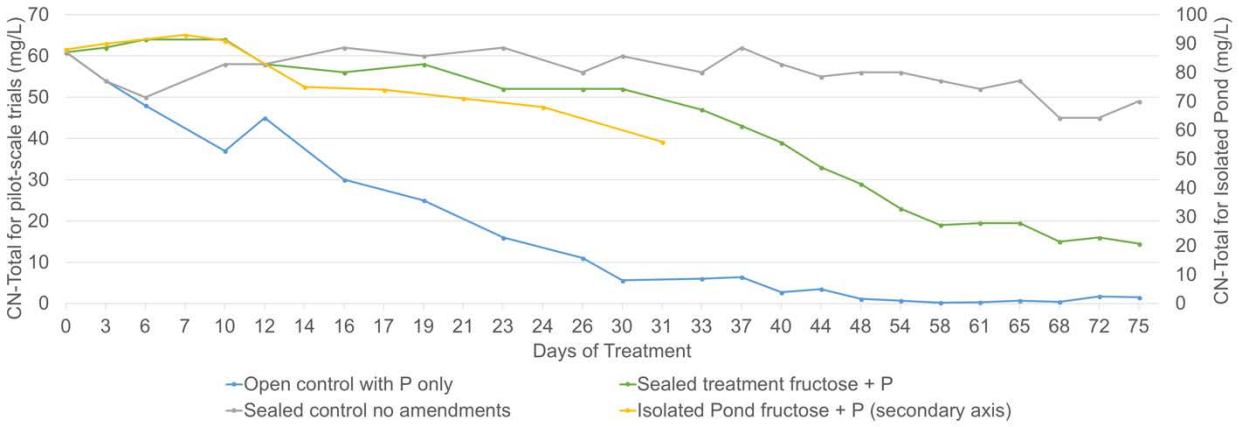


Figure 7: Decreasing cyanide concentration overtime

Ammonia

It should be recalled that the primary goal of this investigation was to decrease ammonia concentrations in the ETP discharge. While Kumtor has never had difficulty complying with discharge criteria for cyanide, this study focused on reducing concentrations of cyanide in the TMF to minimize the ammonia produced via cyanide destruction in the ETP. As the ETP process essentially completely oxidizes all cyanide to ammonia, this section discusses the "theoretical" ammonia concentrations that would result in the ETP discharge based on influent cyanide and ammonia loadings.

Pilot-scale trials amended with organic carbon (fructose) successfully brought and maintained the theoretical ETP ammonia discharge below the recent total ammonia discharge criterion of 23.48 mg/L after 68 days (Figure 7). It should be noted that while the ETP discharge criteria are re-calculated annually, the ammonia limit has remained constant at 23.48 mg/L from 2015 through 2017. Before freezing, the full-scale Isolated Pond followed the same decreasing trend of theoretical ETP ammonia as the pilot-scale trials amended with carbon and phosphorous. This decreasing trend of theoretical ETP ammonia suggests the full-scale Isolated Pond would reach the Total Ammonia discharge criterion of 23.48 mg/L within a similar time frame.

Conversely, trials that were not amended with organic carbon were not able to decrease the theoretical ETP ammonia discharge as any cyanide destruction resulted in direct formation of ammonia. The pilot-scale trial amended with phosphorous but not organic carbon showed increased concentrations of theoretical ETP ammonia discharge. Therefore, in the open control with P only trial, cyanide was transformed to ammonia and microbial uptake through the cyanohydrin process did not occur. During the course of the pilot-scale trial, the control barrel had no overall change in theoretical ETP ammonia discharge concentrations.

Ammonia was not produced in any of the trials that were amended with organic carbon and phosphorous, despite significant cyanide degradation, however, it was produced in the trial amended with

only phosphorous (Figure 6). This confirms that organic carbon additions are needed, as well as phosphorous additions, to support microbial growth and prevent ammonia formation.

Cyanide degradation has the potential to create ammonia, which can then be further oxidized to nitrate. To confirm that cyanide in the trials had not simply been converted to ammonia and then to nitrate, both parameters were analyzed in all samples. Nitrate was actually removed in trials amended with glucose or fructose, further suggesting that cyanide is being removed from the system with the nitrogen being bound in an inaccessible form (*e.g.* biomass) or transformed by denitrification to nitrogen gas and removed from the system entirely.

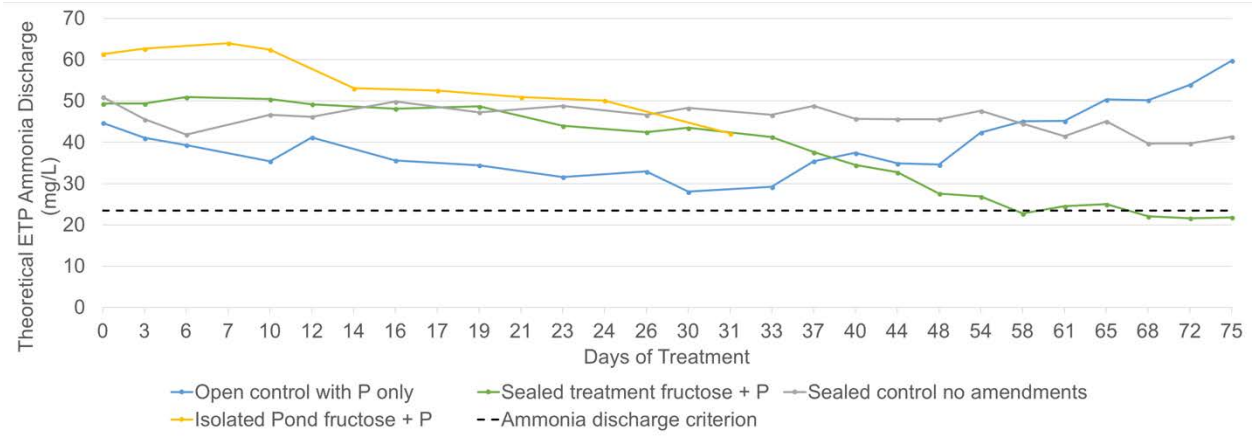


Figure 7: Theoretical ETP Ammonia Discharge (ammonia + ammonia potential from cyanide)

Results and Conclusion

The primary benefit of the cyanohydrin process from an ammonia compliance perspective at Kumtor is that, unlike most other cyanide destruction methods, this process destroys cyanide without producing ammonia.

The Cyanohydrin Barrel and Tote pilot trials (Phase 2) were monitored for approximately 75 days, during which the glucose and fructose dosed barrel resulted in a ~75% removal of cyanide (~60 mg/L down to 14.5 mg/L), without the production of ammonia or nitrate (Figure 5, Figure 6, Figure 7). It should be noted that concentration trends suggest that cyanide destruction had not yet reached completion in these trials. As such, further cyanide destruction would be expected if the tests had been continued longer. It should also be noted that additional phosphorous was observed to accelerate the cyanide degradation processes (supported by data in additional barrels and trials; Contango, 2018a), while additions of organic carbon, such as glucose or fructose, are needed to prevent ammonia formation resulting from cyanide destruction. The higher rate of cyanide transformation when amended with phosphorous only indicated that there is microbial capacity for cyanide degradation that is phosphorous limited, and that it is likely that cyanide transformation to ammonia, which is observed in the tailings

impoundment now, is at least partially microbially mediated. The slower transformation with added sugars suggests that microbes capable of utilizing the cyanohydrin pathway are not as prevalent, at least initially. The higher rates of cyanide removal observed later in the barrels and totes suggest that microbial growth is a factor. The initial incubation of these trials provides a phase where capable microbes are growing to an abundance that supports the cyanide transformation in the presence of sugars.

The full-scale Isolated Pond trial resulted in similar, if not accelerated trends of cyanide destruction without ammonia formation as was demonstrated by the pilot-scale trials performed earlier in the same year (Figure 5, Figure 6, Figure 7; Contango, 2018b). This may be due to the presence of microbial communities in the Isolated Pond area prior to testing, while no such colonies would have been established in the barrels or totes prior to the pilot test work. The Isolated Pond results are promising as the full-scale trial is most representative of the full-scale TMF Pond.

In the approximately 30-day monitoring period before ice formation, 35 mg/L (~39%) of the cyanide was removed from the Isolated Pond, and no significant increase of ammonia was measured. This suggests that, after treatment of the initial volume of water stored in the TMF, cyanide destruction via the cyanohydrin method could be effective at Kumtor. To this end, full-scale dosing of glucose and phosphorus to the tailings line were initiated by Kumtor in early 2018.

Acknowledgements

The authors would like to acknowledge the support of the staff and management at Kumtor Gold Company and Centerra Gold Inc. throughout the course of this study and the preparation of this manuscript.

References

AEG. 2017a. Cyanide treatment approach for Kumtor Mine – revised.

AEG. 2017b. Updated barrel test results and additional thoughts about phase II field trials for cyanide treatment in Kumtor tailings.

AEG. 2017c. Operating instruction procedure for mixing and dosing fructose solution into the tailings line.

Contango Strategies Ltd. 2018a. Technical memo – Cyanohydrin barrel and tote trials (phase 2). Document #002_0917_13C.

Contango Strategies Ltd. 2018b. Technical memo – Cyanohydrin isolated pond trials. Document #002_0917_15C.

Kiliani, H. 1885. Ueber das Cyanhydrin der Lavulose (About the cyanohydrin of levulose), *Chemische Berichte,* 18(2): 3066–3072.

Proceedings of Mine Water Solutions 2018
June 12–15, 2018, Vancouver, Canada
Published by the University of British Columbia, 2018

Alkaline Flush Technology: An In-Situ Treatment Method for Mining Impacted Alluvial Aquifers

Olufunsho Ogungbade, Freeport-McMoRan Inc., USA
Shane Hansen, Freeport-McMoRan Inc., USA

Abstract

Alkaline Flush (ALF) technology is a potential in situ remediation strategy for treatment of alluvial aquifers impacted by acid rock drainage (ARD) and historical mining activities. ALF involves introducing solutions with elevated alkalinity into alluvial aquifers to adjust groundwater and sediment pH, as well as modify the surface chemistry of sediments to limit the mobility of constituents of concern. Along with the reduction of acidity associated with groundwater and sediment, this technology may precipitate constituents of concern into stable mineral forms, significantly reducing their aqueous concentrations over both the short- and long-term. Application of ALF technology may provide "enhanced attenuation" and "resiliency." Enhanced attenuation is the acceleration in treatment time achieved with ALF compared to natural attenuation, whereas resiliency is the capacity of the remediated system to resist future impacts after ending ALF treatment.

ALF has been extensively tested in the laboratory on alluvial sediments impacted by acidic and metal-rich waters using laboratory-scale column and pilot-scale tank experiments. The experiments consisted of three stages: equilibration of the sediments with mining-influenced water (MIW); treatment with an alkali-enhanced water; followed by a MIW/circumneutral rinse. The equilibration stage re-equilibrated the impacted sediments to site conditions (both sediments and water were collected from the same site). The treatment stage evaluated the effectiveness of alkalis and circumneutral waters in treating impacted sediments. The rinse stage was performed to evaluate the response of the treated sediments when a source of impacted or non-impacted water is introduced into the system after it has been treated. This final stage quantifies the acid and metals buffering capacity imparted to the sediments during the treatment stage. Alkali reagents such as sodium sesquicarbonate, sodium hydroxide, and calcium hydroxide, and circumneutral ground waters with alkalinity (expressed as equivalents of $CaCO_3$) range of 130 to 240 mg/L were tested in these experiments.

Based on the column test results, the potential benefits of using ALF technology are 1) reduced remediation time required to reach remedial action objectives and 2) resiliency of the treated system to

resist re-acidification in the presence of MIW after treatment has been terminated. Laboratory results showed the effectiveness of ALF technology at neutralizing alluvial groundwater and sediment acidity, as well as reducing aqueous metal concentrations to levels below remedial action objectives. This technology offers an opportunity for remediation of alluvial aquifer systems that may provide time and cost savings over those associated with other potential remedial alternatives.

Introduction

Acid rock drainage (ARD) and historical mining activities have the potential to result in the release of acidic waters with elevated metal concentrations into waterways, thereby influencing alluvial aquifer sediments and groundwater. Several conventional remediation technologies (e.g. pump-and-treat) have been utilized to remediate impacted groundwater, but have required long periods of treatment time because they do not amend the impacted sediments, which are a major source of acidity and heavy metals. The impacted sediments act as a store of acidity and metals that could be released into groundwater that comes in contact as it migrates through the aquifer after other source(s) of metals and acidity (aqueous) may have been controlled. Furthermore, these conventional technologies tend to be very expensive and often require a long time to meet remedial action objectives (RAOs).

Alkaline Flush (ALF) technology is a potential alternative in situ remediation strategy for treatment of alluvial aquifers impacted by ARD and historical mining activities. ALF involves introducing solutions with elevated alkalinity, alkali solution or circumneutral water, into an alluvial aquifer to raise the pH of impacted groundwater and sediment, as well as modify the surface chemistry of sediments to limit mobility of constituents of concern (CoCs). Along with the reduction of acidity associated with groundwater and sediment, this technology may precipitate metals of concern into stable mineral forms, significantly reducing their aqueous concentrations over both the short- and long-term. This technology offers an opportunity for remediation of alluvial aquifer systems that may provide cost savings over those associated with other potential remedial alternatives.

This paper describes a laboratory-scale column experiment performed to evaluate the efficacy of ALF to remediate previously impacted alluvial sediments and groundwater. Three alkalis, sodium sesquicarbonate (Sesqui), sodium hydroxide, and calcium hydroxide, plus four circumneutral waters from readily available sources were utilized in this experiment. The circumneutral waters had natural alkalinity range of 130 to 240 mg/L. The column test was designed and conducted to achieve the following objectives:

- Evaluate the potential of ALF using circumneutral waters and alkalis that may be implemented in the future to reduce long-term groundwater impacts and requirement for long-term water treatment.

- Characterize the geochemical processes that ALF exploit in reducing the sediment acidity and aqueous metal concentrations under treatment with different alkalis and circumneutral waters, both short-term and long-term.
- Determine the changes in mineralogy and chemistry of treated sediments, especially the mineralogy of sequestration for metals with elevated concentrations in the aqueous and solid phases of the alluvial system.

Increases in aqueous pH and reduction of aqueous metal concentrations to levels below the RAOs observed in the column effluent were used to monitor the rate and achievement for sediment acidity neutralization and metals sequestration, respectively. The results of this laboratory-scale test may be used to establish design parameters for a pilot-scale study to further evaluate ALF under field conditions.

Methodology

The column test consisted of fifteen columns that were 6 inches in diameter by 5 feet long and constructed of polyvinyl chloride (PVC) pipes (Figure 1). The columns were packed with between 45.8 to 47.9 kg of impacted < 3/8-inch sediments of average pH 4.15 and sediment acidity of approximately 1,100 mg/kg measured at pH 7.0 (Tables 1 and 2). The sediment acidity was measured using a method developed for sediment based on standard methods for measuring aqueous acidity. This method calls for titrating a 1:1 sediment-water suspension with an alkali solution to a set pH, which usually requires 45 to 120 minutes. The column pore volume (PV), which is the volume within the column not occupied by sediments, ranged from 10.2 to 11.1 litres. The column was designed to have solutions introduced from the bottom to maintain a saturated flow condition throughout the columns. A 4-inch thick, clean sand layer was installed on top of a coarse filter pad to provide structural support for the sediment column above and for improved distribution of flow throughout the column. The coarse filter pad, placed in the column's bottom cap, was installed to hold the sand layer in place and prevent flow down into the solution influent tube. The column effluent was collected at the top of the column from tubing that passed through a flow cell that had a pH probe inserted into it to measure and record the effluent pH every 30 minutes. The tubing from the flow cell was connected to a 2-gallon bucket placed on the column stand to collect all effluent exiting from the column. The feed solutions were delivered in 5-gallon buckets (for circumneutral waters) or 15-gallon barrels (for alkali solutions). Tubing from the feed bucket (or barrel) was connected to a peristaltic pump which had tubing connected to the inlet (bottom) of the columns.

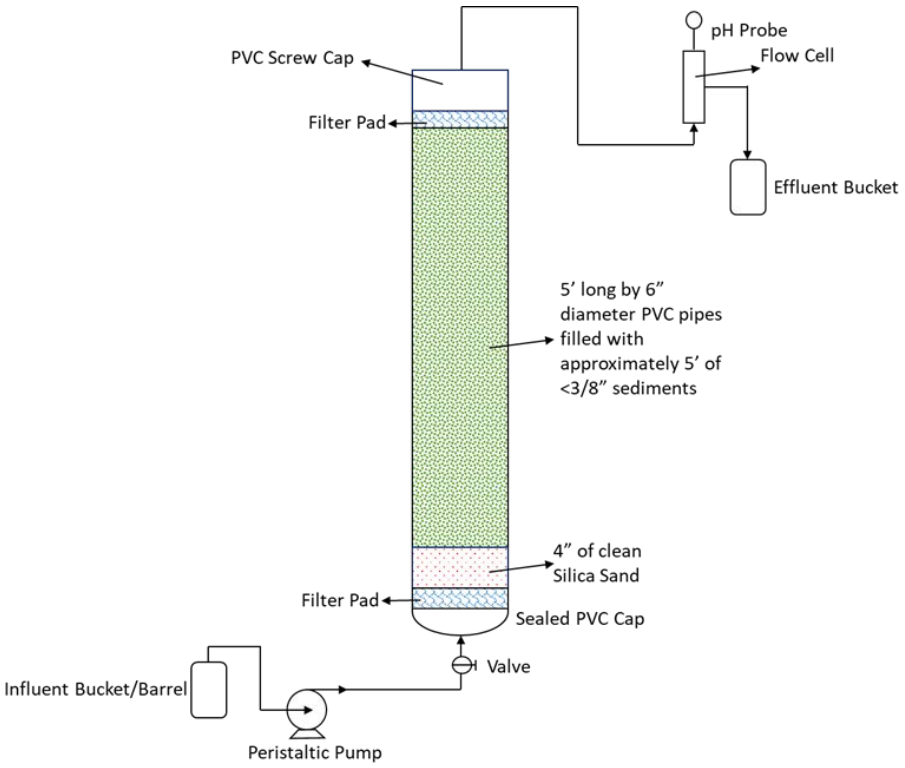


Figure 1: Schematic diagram of column setup (not to scale)

Table 1: Chemical composition (in mg/kg) of impacted sediments used in column testing

Analyte	Concentration
Aluminum	59,800
Arsenic	<5.0
Barium	0.08
Calcium	23,400
Cadmium	<0.5
Cobalt	34.6
Chromium	121.9
Copper	300
Iron	65,900
Potassium	21,300
Magnesium	5,400
Manganese	1,600
Molybdenum	<10.0
Sodium	12,500
Nickel	12.6
Lead	162.6
Selenium	<2.0
Zinc	300

Table 2: Column sediments mineralogy data reported in weight percent (wt%)

Mineral	Concentration
Quartz	26.07
Plagioclase	21.44
K-Feldspar	16.63
Garnet	3.17
Gypsum	1.50
Magnetite	2.24
Hematite	1.36
Goethite	1.45
Apatite	0.39
Fe(OH)/FeO*	4.11
Calcite	< 0.01
Aluminum sulphate	< 0.01
Alunite	< 0.01
Jarosite	0.08
Pyrite	< 0.01
Phosphates	< 0.01
Sulphates/sulphides	< 0.01

* Consists of iron oxides/hydroxides containing varying levels of: Al, Ca, Cu, Mn, Pb, S, Si, and Zn

Experimental Design

The column test consisted of fifteen columns designed to study the following scenarios:

- No treatment action taken (1 column).
- ALF treatment using circumneutral waters (4 columns) from natural and readily available sources.
- ALF treatment using alkalis, followed by dissection for solid-phase characterization (3 columns).
- ALF treatment using alkalis, followed by rinsing with impacted (no-source control) or non-impacted (source control scenario) groundwater (7 columns).

The no-action scenario was evaluated by flushing the impacted sediments in the column with impacted groundwater (W-A; Table 3) collected from the same impacted area as the sediments. This scenario represents a control for the column test. One set of four columns was used to evaluate ALF treatment using circumneutral waters (W-B to E). This set of columns, except the column treated with the circumneutral water containing the highest alkalinity (W-E), was dissected after treatment for solid-phase

characterization. This column was rinsed with impacted groundwater (W-A) after treatment to evaluate the no-source control scenario. For the purposes of this paper, source control is defined as the 'complete' physical and chemical stabilization of all point and non-point sources of contamination (i.e., only groundwater free of impacts from mining activities will flow through the system after treatment).

A total of 10 columns were designed to study the ALF treatment using alkalis. These sets of columns were either dissected immediately after treatment, rinsed with impacted groundwater (no source control scenario), or rinsed with non-impacted groundwater (source control scenario). The columns designed to receive ALF treatment using alkalis were grouped into three sets based on the alkalis used during the treatment stage. Four of the 10 columns were treated with Sesqui ($Na_2CO_3 \cdot NaHCO_3 \cdot 2H_2O$), of which three columns were treated with a low concentration of Sesqui (low Sesqui) and one column was treated with high concentration of Sesqui (high Sesqui). A second set of three columns was treated with sodium hydroxide (NaOH). The final three columns were treated with calcium hydroxide ($Ca(OH)_2$). The alkali-based columns, except the high Sesqui column, were designed to receive the same target alkalinity of 1,350 mg/L as $CaCO_3$ during treatment. The high Sesqui column was designed to receive a target alkalinity of 6,640 mg/L as $CaCO_3$ during treatment. The average concentrations of major constituents in the influent treatment solutions are shown in Table 3.

Table 3: Average concentrations of major constituents in treatment solutions

Waters/RAO	Source	pH (s.u.)	Acidity (mg/L as $CaCO_3$)	Alkalinity (mg/L as $CaCO_3$)	Sulphate (mg/L)	Al (mg/L)	Cu (mg/L)
RAO	n/a	6-9	NA	NA	600	5	1
Water A (W-A)	Groundwater	3.95	180	NA	2,100	27	2.1
Water B (W-B)	Groundwater	7.89	NA	130	1,300	BDL	0.014
Water C (W-C)	Groundwater	8.1	NA	230	170	BDL	0.007
Water D (W-D)	Mine shaft	7.81	NA	240	680	BDL	0.008
Water E (W-E)	WTTP effluent	8.04	NA	240	190	BDL	0.013
Low Sesqui	Alkali solution	10.1	NA	1,350	NA	NA	NA
High Sesqui	Alkali solution	10.0	NA	6,610	NA	NA	NA
NaOH	Alkali solution	12.3	NA	1,320	NA	NA	NA
$Ca(OH)_2$	Alkali solution	12.3	NA	1,080	NA	NA	NA

Notes: n/a = not applicable, WWTP = wastewater treatment plant,
BDL = below detection limit; numbers in bold exceed the groundwater RAO

One column from each set of the three columns treated with the same alkali was dissected immediately after treatment to characterize the changes in sediment chemistry. A second column in the

alkali-based treatment set was rinsed with circumneutral groundwater (W-B) after the treatment stage was completed to test the source control scenario. The third column in the alkali treatment set was rinsed with impacted groundwater (W-A) after the treatment stage was completed to test the no-source control scenario. The single alkali-based column treated with high Sesqui was rinsed with W-B after the treatment stage was completed to test the source control scenario.

To ensure the same baseline starting point for all columns tested, all columns were flushed with acidic groundwater (W-A) in the first stage of the test, referred to as the acid equilibration stage after filling the columns with sediments. Based on the mass of sediments in each column and amount of water required to saturate the columns, the average porosity of sediments in the columns was estimated to be 36% (or 10.7 litres in each column). The columns were then subjected to two or three experimental stages depending on the scenario being tested. The treatment stage was terminated when the effluent pH from the columns was at or near pH 7. Upon termination of the treatment stage, one circumneutral water-based and three alkali-based were rinsed with acidic groundwater (no-source control scenario) and four alkali-based columns were rinsed with circumneutral groundwater (source control scenario).

Column influent and effluent samples were analyzed for acidity, alkalinity, pH, electrical conductivity (EC), anions (chloride, fluoride, nitrite/nitrate and sulphate), total dissolved solids (TDS); and, metals and trace elements (Al, As, Ba, Cd, Co, Cr, Cu, Fe, Mn, Mo, Ni, Pb, Se, and Zn) for both total and dissolved aqueous concentrations. The aqueous results were evaluated with respect to potential RAOs. Sediment samples were tested for short-term acidity, mineralogy, and elemental constituents before and after column testing.

Results and Discussion

The aqueous results were evaluated using four metrics: treatment solution demand (TSD) to reach the target pH and/or a site RAO; observed enhanced attenuation; capacity of the aqueous/sediment system to resist re-acidification; and, excess alkalinity demand (EAD). TSD, expressed in terms of pore volumes (PVs), is the number of PVs of treatment solution required to achieve the RAO of a specific CoC or pH within the aqueous phase of the alluvial groundwater system. Enhanced attenuation is the degree of accelerated remediation, expressed in terms of an acceleration factor, achieved in the observed treatment solution demand when using alkali relative to an approach based on circumneutral or a no-action scenario. Resiliency of the system is defined as the capacity of the remediated system, both aqueous and sediments, to resist re-acidification as a result of the buffering capacity imparted to the sediments and aqueous phases during treatment. For the purposes of this paper, EAD is defined as the amount of excess alkalinity added to the acidic sediments in order to increase the column effluent pH to 7.0 compared to the amount of

alkalinity required to reach this same pH based on the measured sediment acidity from bench-scale sediment titration experiments.

Column Test Aqueous Results

Treatment solution demand required to meet RAOs.

The aqueous results were evaluated with respect to the number of PVs of alkali solution or circumneutral water required to achieve the RAOs for pH, metal concentrations (Al, Cu, and Mn), trace elements (Cd and Co), sulphate, and TDS (Table 4).

Table 4: Treatment solution demand (PVs) required to achieve major RAOs

Parameters	RAO	RAO Units	W-B	W-C	W-D	W-E	Low Sesqui	High Sesqui	NaOH	$Ca(OH)_2$
pH of 6	6–9	su	104	60	59	60	14	4.1	11	47
Al	5	mg/L	32	12	18	12	12	3.8	10	8.5
Cd	0.01	mg/L	7.2	6.5	6.6	6.8	7.0	4.3	6.5	5.3
Co	0.05	mg/L	9.2	8.5	9.6	8.3	12	5.6	11	47
Cu	1	mg/L	27	11	15	12	11	4.1	10	8.2
Mn	0.2	mg/L	73	49	37	64	13	5.6	11	52
TDS	1	g/L	NR	13	NR	16	14*	NR	NR	9.8
Sulphate	600	mg/L	NR	14	NR	15	14	NR	NR	11

* TDS RAO was only achieved in one low Sesqui-based column; NR = RAO not reached

Enhanced Attenuation

The enhanced attenuation results show that the alkali-based treatment (ALF) significantly reduced the time required to meet RAOs for pH, major metals (Al, Cu and Mn), and trace elements (Cd and Co), relative to circumneutral water W-B, which had the lowest treatment alkalinity (Table 5). Table 5 compares the reduced pore volumes required to meet a RAO relative to water from W-B. Overall, high Sesqui treatment provided the greatest observed enhancement in treatment solution demand required to meet RAOs for aqueous pH, major metals (Al and Cu), and trace elements (Cd and Co). Only low Sesqui, calcium hydroxide, and W-C provided enhanced attenuation for TDS and sulphate.

Table 5: Enhanced attenuation relative to circumneutral water W-B

Enhancement in PVs to reach RAO relative to circumneutral water W-B for[1]:	W-C	W-D	W-E	Low Sesqui	High Sesqui	NaOH	$Ca(OH)_2$
pH of 6	44	45	45	90	100	93	57
Al	21	14	20	20	28	21	23
Cd	0.8	0.6	0.4	0.3	2.9	0.8	1.9
Co	0.8	–0.4	0.9	–2.8	3.7	–1.6	–37
Cu	16	12	16	15	22	16	18
Mn	22	35	8.0	58	NA	NA	NA
TDS	3.0	NA	NA	1.5	NA	NA	5.7
Sulphate	2.0	NA	NA	1.1	NA	NA	4.2

Notes: [1]Enhanced attenuation for TDS and sulphate was calculated relative to circumneutral water E (W-E) because TDS and sulphate RAOs were not achieved with W-B; a negative number denotes that there was no enhancement in treatment solution demand; NA = not applicable

Resiliency of Treated System

Both alkali- and circumneutral water-based treatments imparted buffering capacity to the sediments within the treated columns, termed resiliency of the treated system for the purposes of this paper ("6). Therefore, the sediments rinsed with acidic, metal-rich groundwater (W-A) after these treatments were able to resist re-acidification and maintain the sequestration of CoCs to varying degrees. Columns treated with circumneutral water E and the alkalis were the only treatment options evaluated for resiliency.

Table 6: Resiliency for different treatment options

Resiliency (in PVs required) to exceed RAO for:	W-E	Low Sesqui	NaOH	$Ca(OH)_2$
pH of 6	40+	38	3.7	7.1
Al	40+	67+	57	45+
Cd	40+	67+	32	45+
Co	33	30	23	45+
Cu	40+	67+	59	45+
Mn	3.6	9.0	2.6	5.6
TDS	2.6	NA	NA	5.6
Sulphate	2.6	0.8	NA	5.6

Note: "+" indicates that the RAO had not been exceeded at the termination of the acidic rinse stage

Excess Alkalinity Demand

Alkalinity, in excess of the short-term sediment acidity determined by titration, was retained in all of the alkali and circumneutral water-based columns during the treatment stage (Table 7). The amount of

alkalinity retained in the columns ranged from 2.7 (W-B) to 3.7 (W-D) times the short-term sediment acidity determined for the circumneutral water-based columns, and from 2.7 (sodium hydroxide treatment) to 11 (calcium hydroxide treatment) times the short-term sediment acidity determined for the alkali-based columns. From an operational perspective, the excess alkalinity retained in the columns means that more alkali and circumneutral water will be required during treatment than is required to neutralize the measured sediment acidity, which will in turn potentially increase treatment duration and cost. However, the excess alkalinity retained in these columns is a beneficial result of the alkaline-based treatment approaches and is likely to provide buffering against potential re-acidification from future sources of aqueous and sediment acidity within the alluvial groundwater system.

Table 7: Excess alkalinity retained in columns

Treatment option	Net alkalinity utilized (mg $CaCO_3$/kg sediment)	Excess alkalinity demand*
W-B	3,400	2.7
W-C	3,890	3.2
W-D	4,440	3.7
W-E	3,590	2.9
Low Sesqui	4,220–4,770	3.4–3.8
High Sesqui	8,150	6.6
Sodium hydroxide	3,200–3,770	2.7–3.1
Calcium hydroxide	10,600–13,100	8.6–11

* Excess Alkalinity Demand = Net alkalinity utilized for treatment divided by short-term sediment acidity

Post-Treatment Sediment Characterization Results

Sediment characterization after column testing was performed to evaluate the sediment pH, residual sediment acidity and alkalinity in the treated sediments, and how treatment affected the chemical and mineralogical composition of the treated sediments. The sediments in the columns were partitioned into three equal sections, bottom (influent end), middle and top (effluent end), for post-treatment sediment characterization.

Residual Sediment Acidity/Alkalinity

Both alkali- and circumneutral water-based treatments were effective at increasing sediment pH, neutralizing the measured short-term sediment acidity and imparting alkalinity to the sediments (Figures 2 and 3). Overall, the post-treatment results indicated that the circumneutral waters and low Sesqui are the most effective at distributing alkalinity throughout the entirety of the sediments during treatment.

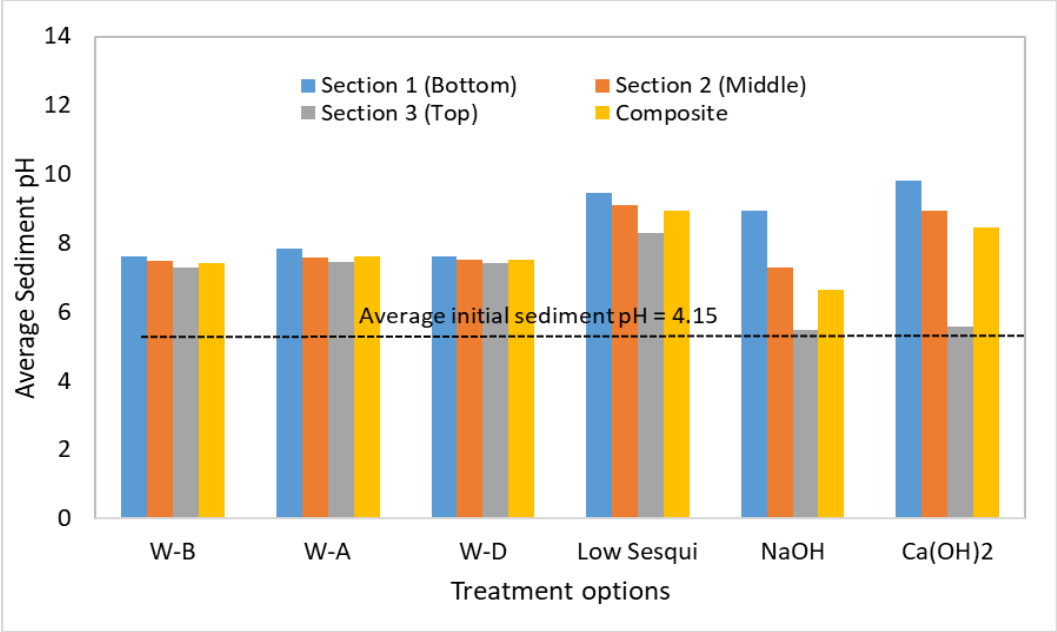


Figure 1: Post-treatment sediment pH

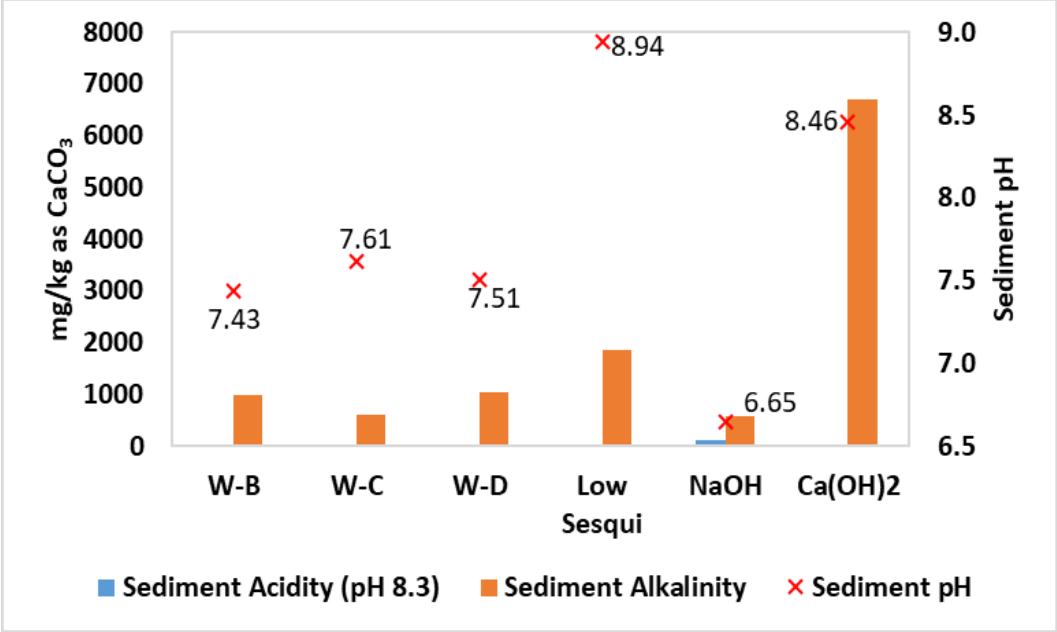


Figure 2: Post-treatment residual sediment acidity, sediment alkalinity, and sediment pH

Elemental Constituents

The only considerable differences in average elemental constituents in the treated sediment samples compared to pre-test samples was increase in the base cations of the alkalis used: Na in the Sesqui and sodium hydroxide treatment columns, and Ca in the calcium hydroxide treatment column. Increases were also observed in iron concentrations along with decreases in sulphur and phosphorus concentrations.

Changes in Mineralogy

The various mineralogical analysis methods used have a limitation in detecting minerals that are amorphous and/or present at low concentrations; however, on average, calcite was reported at trace levels in all the columns except the column treated with W-E, which was reported as zero. The highest calcite concentration was reported for the calcium hydroxide columns, which is consistent with mass balance calculations and residual sediment alkalinity measured for the calcium hydroxide treated sediments. Other important minerals, such as gypsum, iron oxide/hydroxide, jarosite, and cation exchange capacity (CEC), appear to have undergone transformation as a result of ALF treatments (Table 8).

Table 8: Percentage change in mineral concentrations in post-treatment sediments compared to pre-test sediments

Treatment option	Gypsum	FeO/FeOH	Jarosite	CEC
W-B	–100%	14%	532%	24%
W-C	–100%	3%	1056%	9%
W-D	–100%	10%	987%	28%
Low Sesqui	–100%	12%	47%	34%
Sodium hydroxide	–100%	12%	92%	25%
Calcium hydroxide	–100%	–27%	512%	37%

Note: A negative number denotes a decrease

Conclusion

The column test results demonstrated the ability of the ALF technology to neutralize sediment acidity as well as reduce aqueous metal, sulphate, and TDS concentrations to levels below the groundwater RAOs. These results also show dissimilarities in the geochemical dynamics for the different alkalis that are likely to have important implications for applicability, design, and operation of any future pilot-scale study or implementation of this treatment technology. The high Sesqui treatment option achieved the aqueous pH and major metals RAOs sooner than the other alkali- and circumneutral water-based treatment options. This is likely due to the higher concentration of alkalinity supplied to the column over a shorter timeframe. However, sulphate and TDS RAOs were not achieved with high Sesqui treatment. The column test results also suggest that achieving the sulphate and TDS RAOs may not be likely using sodium hydroxide. The sulphate and TDS were achieved with two of the circumneutral waters that had sulphate and TDS concentrations below the RAOs. The RAOs for aqueous pH and evaluated metals were achieved with all circumneutral water-based columns.

A comparison of the observed resiliencies computed for the different treatment options suggests that ALF imparted buffering capacity to the sediments, allowing the sediments to resist re-acidification and minimize dissolution of sequestered metals to varying degrees. The circumneutral water containing the

highest concentration of alkalinity, W-E, provided beneficial resiliency against a decrease in aqueous pH upon introducing low pH impacted water following treatment, while sodium hydroxide provided the least benefit. For the metals evaluated, manganese was the first metal to exceed its RAO upon re-introducing low pH impacted water following treatment. Both alkali- and circumneutral water-based treatments imparted sufficient resiliency in the sediments to maintain aluminum and copper sequestration. Only W-E and calcium hydroxide treatment provided significant resiliency against increases in sulphate and TDS concentrations upon introducing low pH impacted water following treatment.

The metrics developed (treatment time, enhanced attenuation, and resiliency) are performance parameters that may be used to evaluate and compare different alkalis and circumneutral waters. Other aspects related to alkali treatment of an alluvial system like the cost of alkali, undesired mineral precipitation during mixing or at the injection point, transportation hazards, etc., may pose challenges during the field implementation and must be taken into account in the selection of an alkali- and/or circumneutral water for field testing and/or full-scale implementation.

Proceedings of Mine Water Solutions 2018
June 12–15, 2018, Vancouver, Canada
Published by the University of British Columbia, 2018

The Development of a New Peat-Based Weak Anion Exchange Material that Removes Sulphate from Acidic Water

Liudmyla Kildyshova, University of Minnesota Duluth, USA
Rami Hallak, American Peat Technology LLC, USA
Igor V. Kolomitsyn, University of Minnesota Duluth, USA

Abstract

Peat is a slowly renewable resource. Because of its limited availability, it is essential to add value to products that are produced from peat. Recently, we reported the development of three peat products for the removal of dissolved heavy metals: APTsorb II^{TM}, APTsorb III^{TM}, and APTsorb II*Na^{TM}, with Cd^{2+} breakthrough capacities of 13 mg/g, 16 mg/g, and 22 mg/g respectively. This research describes the development of a new peat-based weak anion exchange material that effectively removes sulphate and other anions from very acidic waters. For instance, such water can be found as a result of oxidation of pyritic materials producing acid mine drainage. The new material (APTsorbNH2) is created using the Duff reaction under modified conditions. We demonstrated that a reaction of a prepared surface of peat granules with hexamethylenetetramine formed amine groups, instead of the expected aldehyde groups. Moreover, a reaction of the prepared peat surface with an adduct of alkyl aldehyde and alkyl amine formed amine groups as well. Thus, a reaction of peat granules with an adduct of acetic aldehyde and methylamine in water at 120^{o}C for 17 hours resulted in an increase of nitrogen concentration from 3.1% to 5.28%. A reaction of peat granules with hexamethylenetetramine in water at 120^{o}C for 17 hours resulted in increase of nitrogen concentration from 3.1% to 7.12%. The new material has a measured total anion exchange capacity between 60 to 80 mEq/100 g using both batch and column methods. The weak anion exchange properties were demonstrated in column experiments by loading the new material with a 0.1N solution of H_2SO_4 in water and successfully regenerating with a 0.1N solution of NaOH in water. It is believed that a lignin fraction of peat is responsible for a successful reaction of hexamethylenetetramine or an adduct of alkyl aldehyde and alkyl amine with the peat surface. A reaction mechanism and a new technique for measuring anion exchange capacity, as well as performance data using synthetic water, is presented in this paper.

Introduction

Peat is a natural product formed largely from the inhibited decomposition of plant materials (Morita, 1980). Deposits of the partially decomposed plant materials form in shallow bogs, occurring most abundantly in cool temperate regions of the northern hemisphere. The conditions which favour the formation of peat are absence of air through water saturation, humidity, acidity, and nutrient-poor environments which reduce microbial activity. It is a slowly renewable natural resource for which there are many uses, particularly in horticulture. Recently, we reported the development of a number of new peat granular products (Kolomitsyn at al., 2017; US Patent # 9,649,620, US Patent # 9,561,489; Kolomitsyn at al., 2016) that are designed to remove heavy metals from mine and storm waters. These peat products utilize the natural ability of peat to sorb metal ions by the following mechanisms: ion-exchange, complexation, chemisorption, surface adsorption, and adsorption-complexation (Brow at al., 2000). Our group also demonstrated that a peat lignin, in contrast to a wood lignin, exhibits a strong ion-exchange and complexation properties (Goncharov at al., 2017). For instance, Eger at al. (2016) used peat granules to successfully remove dissolved and particulate copper from mine water drainage. That system was installed at the Soudan Underground Mine State Park in Minnesota and successfully treated mine water with flow rates of 50–80 gal/min. However, there is no report outlining peat as an anion exchange material. The goal of this research is to develop a new peat-based material with introduced anion exchange properties that can be used as a weak anion exchanger for mine water treatment.

Synthesis of Peat Based Weak Anion Exchange Material (APTsorbNH2)

Materials

All commercial reagents were ACS reagent grade and were used without further purification. Peat granules (bioAPT) were provided by American Peat Technology LLC and are commercially available. All experiments were carried out using thermally treated granules, called APTsorb150, which were produced by thermally treating bioAPT peat granules according to the procedure reported in Kolomitsyn at al. (2017, US Patent Application # 15/611,175).

Methodology

Measurement of the Concentration of SO_4^{2-} anion Using Ion Chromatograph (IC)

IC analysis was performed using a Metrohm 881 Compact IC Pro, which was equipped with a pump, injector, eluent degasser, MSM, MCS, IC conductivity detector, column, and 858 professional sample processor. The following analytical conditions were used to measure the concentration of sulphate anion: Column: Metrosep A Supp 5–150/4.0, Metrohm ion analysis; guard column: Metrosep RP2 guard/3.6;

mobile phase: 3.2 mM Na_2CO_3/1.0 mM $NaHCO_3$ in type I DI water; flow rate: 0.7 mL/min; column temperature: 35 ºC; injection volume: 20 µL.

Hydrolysis of Thermally Treated Peat Granules with a Solution of Na_2CO_3

400 ml of 1M solution of Na_2CO_3 was added to 20 g of thermally-treated peat granules (APTsorb150) and refluxed for 20 hrs. The granules were filtered, washed with deionized water and dried at 105^{o}C for 24 hours to give 16.36 g (81.8%) of hydrolyzed peat granules.

Hydrolysis of Thermally Treated Peat Granules with a Solution of Na_2CO_3 and HCl

A 2.5 L amount of 1M solution of Na_2CO_3 was added to 500 g of thermally treated peat granules and refluxed for 22 hrs. The pH of the reaction mixture changed from 11.6 to 9.5 after hydrolysis was completed. The granules were filtered and washed with deionized water. A 2.5 L amount of a 1M solution of HCl in water was then added to the wet granules and refluxed for 3 hrs. The granules were filtered and washed with deionized water until there was no Cl^- anion present. The presence of Cl^- anion was measured by testing the filtrate with $AgNO_3$. The granules were then dried at 105^{o}C for 24 hrs. From the starting weight of 500 g of thermally treated peat granules, 342 g (68.4%) of the hydrolyzed intermediate product was obtained. The resulting granules were analyzed for total nitrogen.

Reaction Of Thermally Treated, Hydrolyzed Peat Granules with an adduct of Methyl Amine and Acetic Aldehyde

40 ml of H_2O was added into 43.3 ml (38.8 g) of a 40% solution of methylamine (CH_3NH_2). A solution of 30 ml water and 28.2 ml (22 g) of acetic aldehyde (CH_3CHO) was carefully added drop wise to the resulting water solution of CH_3NH_2 at 0^{o}C, and then DI water was added up to 200 ml. 20 g of thermally treated and hydrolyzed intermediate peat granules from the procedure described above were wetted with water for 12 hours at room temperature. The media was filtered, and a 40 ml solution of CH_3NH_2 (100 mmol)/CH_3CHO (100 mmol) was added. The reaction mixture was kept at 120^{o}C in an autoclave reactor for 17 hrs. The granules were filtered, washed with water until there was no color leaching, and dried at 105^{o}C for 24 hr. The resulting granules were analyzed for total nitrogen. The results are shown in Table 1. The same procedures were used to create multiple products where the total nitrogen and total anion exchange capacity were measured.

Reaction of Thermally Treated, Hydrolyzed Peat Granules with Hexamethylenetetramine

20 g of thermally treated and hydrolyzed peat granules were wetted with DI water for 12 hours. The water was decanted and a solution of the hexamethylenetetramine (5 g, 35.7 mmol) in 20 ml water was added. The reaction mixture was kept at 120^{o}C in an autoclave reactor for 17 hrs. The granules were filtered,

washed with water until there was no color leaching, and dried at 105°C for 24 hr. The granules were analyzed for total nitrogen and total anion exchange capacity. The data are presented in Table 1.

Measuring the Anion Exchange Capacity of Peat Based Weak Anion Exchanger Material (APTsorbNH2) by Equilibrium Method

50 ml of 10,000 ppm (102 mM) solution of H_2SO_4 in Type I DI was added to 0.5 g of modified peat granules and rotated by rotator for 1 hour at room temperature at 30 rpm. Peat granules were centrifuged at 4,000 rpm for 15 minuts and the solution was decanted. The remaining solution was transferred from the tube by pipet. 50 ml of 0.5 N solution of NaOH in water was added to the peat granules and was rotated by rotator for 3 hours at 30 rpm. The solution was filtered, the granules were washed with DI water 3 times (3 × 5 ml), and all washings were combined. The total volume was adjusted to 100 ml by adding a Type I DI water to combined washings. One milliliter of the resulting water solution was diluted to 100 ml by type I DI water, filtered through 0.45 µm syringe filter (PTFE membrane), and the concentration of SO_4^{2-} was measured by ion chromatography technique. The total number of NH_2 groups (anion exchange capacity) was calculated by following formula:

$$NH_2\ \left(\frac{mEq}{100\ g}\right) = \frac{C\ SO_4^{2-} ppm \times 1000}{48}$$

All data are presented in Table 1.

Measuring the Anion Exchange Capacity of Peat Based Weak Anion Exchanger Material (APTsorbNH2) by Column Method

The total anion exchange capacity of APTsorbNH2 weak anion exchange media produced by the HMTA-reacted peat granules was determined by bench-scale columns using 0.1N solution of H_2SO_4 in water at a flow rate 5 ml/min (0.1 m/hr, 3.28 BV/hr). The 50 g of APTsorbNH2 media (combined product from lines 4 and 5, Table 1) was pre-wetted in Type I deionized water for a minimum of 3 hours. The column (62 mm ID × 50 mm H) was loaded from the top, first with a plastic screen to retain the media inside the column, then with a layer of HCl-washed Red Flint filter gravel (granular size 3–5 mm), and then with the pre-wetted APTsorbNH2 media. A second plastic screen was placed on top of the APTsorbNH2 media, and a second layer of filter gravel was spread on the top of the screen. The influent flow was controlled by a peristaltic pump, and all flows were bottom fed to produce an upward flow. A minimum of 10 bed volumes of Type I deionized water were pumped through the column prior to the testing solution.

Run 1

A solution of 0.1N of H_2SO_4 in water was introduced into the column. The solutions were at room temperature. Each empty bed volume of effluent samples was collected and titrated using a 0.1N solution

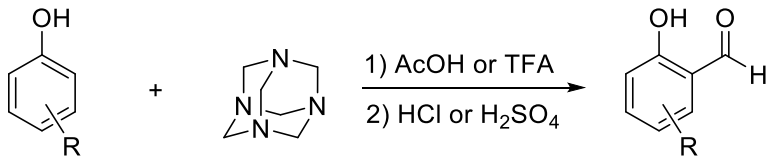
of sodium hydroxide in water and phenolphthalein as an indicator. Influent was delivered into the column until the concentration of H_2SO_4 in the influent was equal to the concentration in the effluent. The influent solution was changed to a 0.1N solution of NaOH and the column was regenerated until no SO_4^{2-} ions were found in the effluent ($Ba(NO_3)_2$ test). The plot of adsorbed H_2SO_4 concentration versus empty bed volume was constructed (Figure 1). A total anion exchange capacity was calculated from the graph when the concentration of H_2SO_4 in the effluent was equal to the concentration in the influent. All NaOH washings were combined and analyzed for SO_4^{2-} using ionic chromatography technique and the total amount of SO_4^{2-} retained by the APTsorbNH2 media was calculated to confirm the total anion exchange capacity calculated from the graph. The column was carefully opened and a small sample of APTsorbNH2 media was taken for total nitrogen.

Run 2

The media from Run 1 was washed with DI water in the column until a stable pH of 7.5 was observed. A solution of 0.1N of H_2SO_4 in water was introduced into the column. The solutions were at room temperature. Each empty bed volume of effluent samples was collected and titrated using a 0.1N solution of sodium hydroxide in water and phenolphthalein as an indicator. Influent was delivered into the column using peristatic pump until the concentration of H_2SO_4 in the influent was equal to the concentration in the effluent. Influent was changed to a 0.1N solution of NaOH and the column was regenerated until no SO_4^{2-} ions were found in the effluent. All calculations were carried out as described in Run 1. A sample of the APTsorbNH2 media was taken for total nitrogen. Results are presented in Table 1 and Figure 1.

Results and Discussion

The Duff reaction (Scheme 1) has been widely used for introduction of aldehyde group to phenols (Duff and Bills, 1934; Grimblat at al., 2016). The Duff formylation involves the treatment of a phenol with hexamethylenetetramine (HMTA) in acidic media, followed by hydrolysis, in order to afford the desired aldehyde (Scheme 1). Ogata at al. (1968) suggested that a reaction of phenols with HMTA proceeds with formation of intermediate amines before hydrolysis to aldehyde. Moreover, amines were obtained as reaction products in some instances (Masurier at. al., 2008).



Scheme 1: The Duff reaction

Peat does not naturally have any anion exchange capacity, and by itself exhibits a nitrogen content of only 2.57% (line 1, Table 1). Chemically, peats are largely organic material, which contain hemicelluses, celluloses, lignin, humic and fulvic acids. Lignin, humic and fulvic acids are naturally occurring phenol-containing polymers. Indeed, when a natural reed-sedge peat was subjected to the reaction with HMTA it resulted in an introduction of weak anion exchange properties (line 2, Table 1). Nitrogen concentration in the resulting product increased from 2.57% to 6.29%, indicating that a reaction occurred with an attachment of nitrogen to the peat surface. The new material also exhibited a respectable anion exchange capacity of 73.3 mmol/100 g, which was measured by a newly developed equilibrium method. These data suggest that it is possible to develop a peat-based anion exchange material using peat as a natural polymer and modified Duff reaction conditions to introduce nitrogen in the form of an amine group. Unfortunately, the resulting product was not stable at pH 8.5 and higher due to the presence of hydrolyzable humic and fulvic acids fraction in the natural peat material.

Table 1: Reaction of peat and peat granules with hexamethylenetetramine (HMTA) and with a mixture of acetic aldehyde and methyl amine

Lines	Peat material	Pre-treatment	Chemical reagents	N (%)	Anion exchange capacity (N, mEq/100 g)	
					Equilibrium method	Column method
1	Reed-sedge peat			2.57		
2	Reed-sedge peat		HMTA	6.29	73.4	
3	APTsorb150	1. Na_2CO_3 2. HCl		3.1	5.0	
4	APTsorb150	1. Na_2CO_3 2. HCl	HMTA	7.12	58.3	84
5	APTsorb150	1. Na_2CO_3 2. HCl	HMTA	7.16	57.6	84
6	APTsorb150	1. Na_2CO_3 2. HCl	CH_3CHO/CH_3NH_2	5.18	55.7	
7	APTsorb150	1. Na_2CO_3 2. HCl	CH_3CHO/CH_3NH_2	5.31	58.4	
8	APTsorb150	1. Na_2CO_3 2. HCl	CH_3CHO/CH_3NH_2	5.44	63.0	

The hydrolysis of peat under pH above 8.0 conditions, which leads to destruction of peat structure, is fully recognized and widely reported in literature (Fuchsman, 1980). The natural peat instability at higher pH inspired the development of a new treatment procedure to stabilize the peat structure. It was

achieved through peat granulation followed by thermal treatment to create a peat granular product, called APTsorb150 (Kolomitsyn at al. US Patent Application # 15/611,175, 2017). When APTsorb150, after pre-treatment with Na_2CO_3 and HCl, was subjected to the reaction with HMTA, it resulted in an increase of nitrogen concentration from 3.1% to 7.12% and 7.16% for two different runs. The total weak anion exchange capacity was measured by an equilibrium method giving 58.3 mEq/100 g and 57.6 mEq/100 g for two different samples. An increase in nitrogen concentration and subsequent attachment of H_2SO_4 to the surface of the peat granules during an equilibrium test suggests that the introduced nitrogen is, in fact, amine nitrogen that exhibits anion exchange properties. Therefore, under the modified Duff reaction conditions, a lignin portion of the peat is reacting with HMTA introducing new anion exchange properties as outlined in Scheme 2.

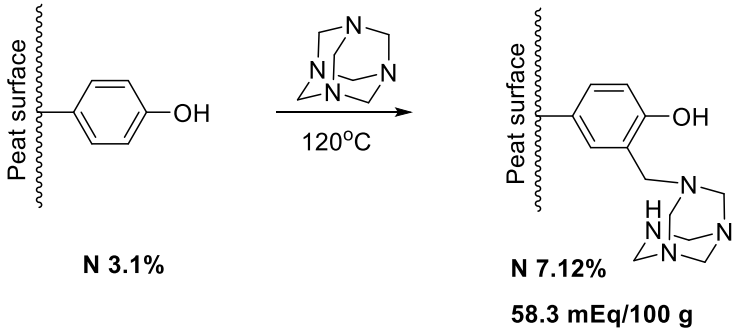
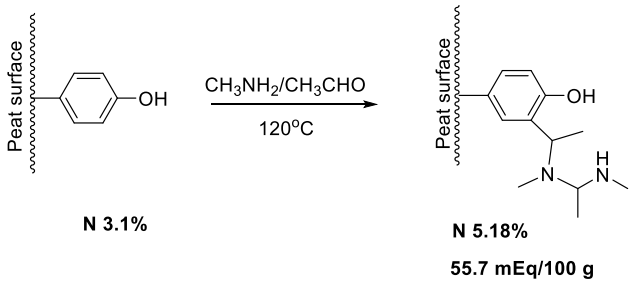


Figure 2: Possible structure of amine group after reaction of thermally treated, hydrolyzed with Na_2CO_3 and HCl peat granules with hexamethylenetetramine (HMTA)

HMTA is formed in nearly quantitative yield from condensation of ammonia and formaldehyde at pH=8–10 (Blažzević at al., 1979). Consequently, the reaction of aliphatic or aromatic aldehydes with primary amines, called the Schiff reaction, can create an adduct that will react with a lignin portion of peat in the same fashion as we observed for HMTA. Indeed, when APTsorb150 after pre-treatment with Na_2CO_3 and HCl was subjected to the reaction with an adduct of CH_3CHO and CH_3NH_2 under 120°C and 235 kPa pressure, the resulting material exhibited an increase of nitrogen concentration from 3.1% to 5.18%, 5.31, and 5.44% in 3 different runs (lines 6, 7, 8, Table 1). The new material also exhibited a respectable anion exchange capacity of 55.7 mEq/100 g, 58.4 mEq/100 g, and 63.0 mEq/100 g, respectively. Therefore, under modified Duff reaction conditions a lignin portion of peat also reacts with an adduct of CH_3CHO and CH_3NH_2 introducing new anion exchange properties, as outlined in Scheme 3.



Scheme 3: Possible structure of amine group after reaction of thermally treated, hydrolyzed with Na_2CO_3 and HCl peat granules with an adduct of CH_3CHO and CH_3NH_2

Effect of Pre-Treatment of Peat Granules with Na_2CO_3 and HCl

Natural peat is susceptible to a hydrolysis reaction at pH 8.0 and higher. The hydrolysis releases humic acids into the solution, and therefore colours the water. It also leads to destruction of the peat structure (Fuchsman, 1980). The stability problem was resolved by peat granulation and thermal treatment (Kolomitsyn at al. US Patent Application # 15/611,175, 2017) that led to the development of APTsorb150 peat granules. These granules are stable without losing structural integrity despite being refluxed with a 1M solution of Na_2CO_3 for 8 hours at pH=10.2. During this treatment, the peat granules lost only 18.2% of their original mass. When Na_2CO_3 pre-treated granules were subjected to the reaction with HMTA, it resulted in an increased nitrogen concentration from 2.79% to 5.5% (lines 2 and 5, Table 2). This increase, however, is lower compared to the nitrogen concentration (6.51%) after reaction of untreated ATPsorb150 peat granules with HMTA. Moreover, when Na_2CO_3 pre-treated APTsorb150 granules were treated with a solution of HCl, and then subjected to the reaction with HMTA, the nitrogen concentration increased from 2.93% to 7.1% (lines 3and 6, Table 2). These data suggest that after pre-treatment with Na_2CO_3 to remove residual humic acids, the surface of peat granules requires additional pre-treatment with HCl to increase the concentration of nitrogen in the final product.

Table 2: Effect of APTsorb150 peat granules surface pre-treatment with a solution of Na_2CO_3 and HCl on the reaction with hexamethylenetetramine (HMTA)

Lines	Pre-treatment	Reagent	N, %
1	No treatment		3.1
2	1. Na2CO3		2.79
3	1. Na2CO3 2. HCl		2.93
4	No treatment	HMTA	6.51
5	Na2CO3	HMTA	5.50
6	Na2CO3/HCl	HMTA	7.10

Measuring the Weak Anion Exchange Nature of APTsorbNH2 by Column Method

The total anion exchange capacity of APTsorbNH2 and the weak anion exchange nature of the introduced amine groups on the surface of peat granules were demonstrated through bench-scale column testing using 0.1N solution of H_2SO_4 in water (Table 3 and Figure 1). Several batches of APTsorbNH2 weak anion exchange media were produced by the HMTA method. As can be seen from the Run 1 results depicted in Figure 1, the APTsorbNH2 granules for bed volumes 1–6 removed virtually all of the H_2SO_4 acid that was introduced into the column. Starting with bed volume 7, breakthrough was reached, an indication that the anion exchange sites on the peat APTsorbNH2 granules started to fill up with the SO_4^{2-} anions; a portion of the acid introduced into the column remained in the aqueous solution and exited the column. At about bed volume 19, the concentration of the effluent plateaued at around 0.082 N, showing that all of the anion exchange sites on the peat granules had filled up with the SO_4^{2-}anions. The 0.1N solution of NaOH was used to regenerate the APTsorbNH2 granules in the column and then granules were washed with DI water until the effluent reached a neutral pH.

The Run 2 results are depicted in Figure 1. After washing APTsorbNH2 granules from the Run 1 experiment with DI water, a 0.1N solution of H_2SO_4 was introduced into the column. The breakthrough for the APTsorbNH2 granules was reached at around bed volume 5, and the performance of the weak anion exchange media plateaued around bed volume 17 at an effluent concentration of 0.09 mEq/100 g. The curves for the Run 1 and Run 2 samples are very similar; demonstrating that the performance by the APTsorbNH2 granule media was repeatable after the media was regenerated using 0.1N NaOH solution.

These data suggest that nitrogen introduced to peat granules under modified Duff reaction conditions exhibited amine like properties. The resulting new peat granular material, APTsorbNH2, is behaving like a weak anion exchanger, and the properties are retained even after media regeneration.

Table 3: Results of column experiments

Runs	Flow rate, ml/ min	$m_{granules}$, g	ID, mm	Bed depth, mm	Empty bed volume (ml)	Flow rate, BV/hr	Flow velocity, m/hr	N of peat, %	Total anion exchange capacity
									mEq/100 g
1	5	50	62	31	92.3	3.28	0.10	6.47	84
	Regeneration with a solution of 0.1N NaOH in water								
2	5	50	62	31	92.3	3.28	0.10	6.37	56
	Regeneration with a solution of 0.1N NaOH in water								

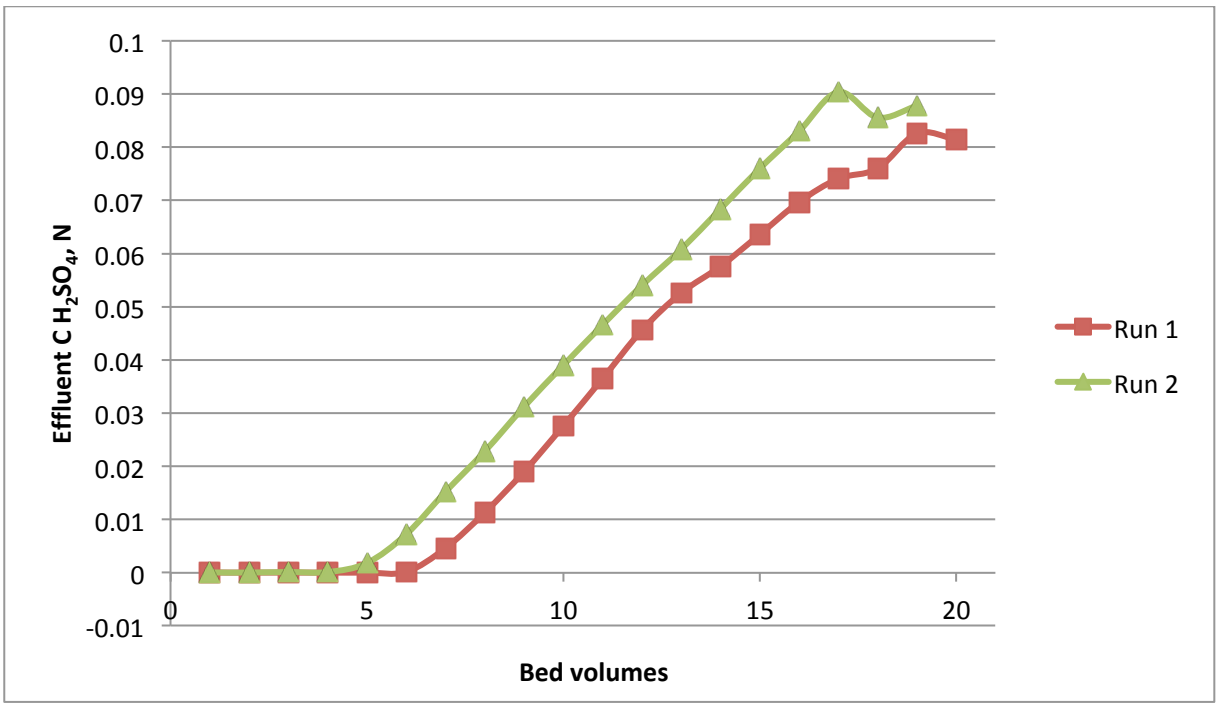


Figure 1: Column data of sorption of H_2SO_4 on a peat based weak anion exchanger APTSorbNH2

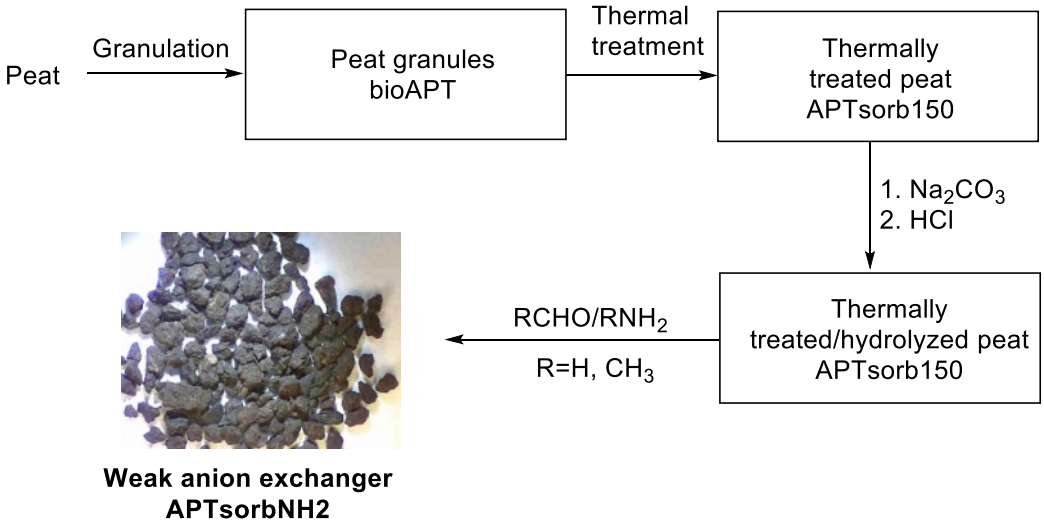


Figure 2: General scheme to produce a peat based weak anion exchanger APTSorbNH2

Conclusion

In conclusion, for the first time we have demonstrated that the reaction of a granulated and thermally treated peat (APTsorb150) with HMTA or with an adduct product of CH_3CHO and CH_3NH_2 proceeds

with an attachment of amine nitrogen on the surface of peat granules introducing weak anion exchange properties to peat. The weak anion exchange nature and a total anion exchange capacity was measured by two independent procedures, namely equilibrium and column methods. The pre-treatment with Na_2CO_3 followed by HCl of APTsorb150 is required to remove residual humic acids and to prepare the peat surface for further reaction. A reaction of pre-treated peat granules with HMTA led to the formation of a new peat granular material, APTsorbNH2, with anion exchange capacity of 58.3 mEq/100 g and 84 mEq/100g, depending on the measurement protocol.

The chemical steps that are required to produce APTsorbNH2 granules are depicted in Figure 2. First, reed-sedge peat was granulated to produce the bioAPT peat product. Second, the bioAPT peat product was thermally treated to produce APTsorb150 peat granules. APTsorb150 was then chemically treated with a solution of Na_2CO_3, followed by a solution of HCl. Finally, the pre-treated granules were subjected to the reaction with HMTA or with an adduct product of CH_3CHO and CH_3NH_2 under modified Duff reaction conditions to produce a new peat-based weak anion exchange material, APTsorbNH2.

Acknowledgements

The authors gratefully acknowledge the continuous support of American Peat Technology LLC, Minnesota, which allowed us to accomplish this work.

References

Blažzević, N., Kolba, D., Belin, B., Šunjić, V. and Kajfež, F. 1979. Hexamethylenetetramine, a versatile reagent in organic synthesis, *Synthesis,* 3: 161–76.

Brown, P.A., Gill, S.A. and Allen, S.J. 2000. Metal removal from wastewater using peat, *Water Research* 34(16): 3907–16.

Duff, J.C. and Bills, E.J. 1934. Reactions between hexamethylenetetramine and phenolic compounds. II. Formation of phenolic aldehydes. Distinctive behavior of p-nitrophenol*, J. Chem. Soc.* 1305–8.

Eger, P., Jones, P. and Green, D. 2016. Solving mine drainage water issues with peat-based sorption media, *Mining Engineering* 68(2): 38–43.

Fuchsman, C.H. 1980. *Peat. Industrial Chemistry and Technology*. New York: Academic Press.

Goncharov, V., Hannah Leopold, H., Kildyshova, L. and Kolomitsyn, I.V. 2017. Toward development of a new generation of peat granular products for waste water remediation: Reaction mechanism of peat surface with heavy metals cations. Poster presented at 253rd ACS National Meeting, San Francisco, California, April 2–6, 2017.

Grimblat, N., Sarotti, A.M., Kaufman, T.S. and Simonetti, S.O. 2016. A theoretical study of the Duff reaction: Insights into its selectivity, *Organic & Biomolecular Chemistry,* 14(44): 10496–10501.

Kolomitsyn, I.V., Jones, P.W. and Green, D.A. 2016. Particulate sorption medium prepared from partially decomposed organic matter for selective sorption between competing metal ions in aqueous solutions. US Patent Application # 15/052,403, filed on Feb 24, 2016.

Kolomitsyn, I.V., Jones, P.W. and Green, D.A. 2017. Particulate sorption medium prepared from partially decomposed organic matter. US Patent # 9,649,620, May 16, 2017.

Kolomitsyn, I.V., Jones, P.W. and Green, D.A. 2017. Particulate sorption medium prepared from partially decomposed organic matter. US Patent # 9,561,489, February 7, 2017.

Kolomitsyn, I.V., Kildyshova, L. and Green, D.A. 2017. Weak anion exchange particulate medium prepared from phenol-containing organic matter from anions contained in aqueous solutions. US Patent Application # 15/611,175, June 1, 2017.

Masurier, N., Moreau, E., Lartigue, C., Gaumet, V., Chezal, J.-M., Heitz, A., Teulade, J.-C., and Chavignon, O. 2008. New opportunities with the Duff reaction, *The Journal of Organic Chemistry* 73(15): 5989–92.

Morita, H. 1980. Peat and its organic chemistry*, Journal of Chemical Education,* 57(10): 695–6.

Ogata, Y., Kawasaki, A. and Sugiura, F. 1968. Kinetics and mechanism of the Duff reaction, *Tetrahedron* 24(14): 5001–10.

Proceedings of Mine Water Solutions 2018
June 12–15, 2018, Vancouver, Canada
Published by the University of British Columbia, 2018

Lime Treatment: Advantages of a Proven Technology and Competing Alternatives

Kristina Minchow, Golder Associates Inc., USA
Bridgette Hendricks, Golder Associates Inc., USA
Ryan Schipper, Golder Associates Inc., USA

Abstract

Precipitation of metal hydroxides using lime has traditionally been one of the most common treatment technologies used at mines sites for treatment of mining-impacted water. While lime treatment continues to have a place in the water treatment arsenal for mining applications, evaluation and implementation of other technologies is on the rise. These alternative technologies include treatment processes that are proven in other applications but are "innovative" and "emerging" technologies for mine water treatment. Alternative technologies include membrane treatment, sulphide precipitation, electrocoagulation, and passive treatment, are increasingly being evaluated and implemented at mining sites. This paper compares lime treatment to alternative technologies for mine water treatment and presents a summary of indicator factors that can be used when considering alternative technologies. The drivers for lime treatment alternatives include regulatory changes to meet lower limits, limits on constituents not previously regulated, cost and operational factors, and technology improvements.

Even though lime remains a viable process compared to alternative technologies, and may provide an advantage over alternative technologies on a gross removal and cost basis, lower regulatory limits require evaluation of technologies that have not historically been considered or required for mining impacted waters. This paper presents the continued advantage of lime treatment for mining-impacted waters, such as: simplicity, chemical cost, and system flexibility. Where lime treatment alone used to be sufficient as a single-treatment approach, it is now often paired with additional treatment steps to accommodate lower regulatory limits. Increasingly stringent discharge limits may also result in treatment requirements for relatively clean sources of water that have historically not required treatment. This paper touches on the need for additional treatment steps in less constituent-heavy water as an area where alternatives to lime treatment can be evaluated. The impacts of lime treatment versus other technologies on secondary waste, safety, and other operational factors are included in the discussion.

Introduction

Sources of mining impacted water (MIW) that may require treatment typically include non-contact dewatering water, contact water, excess tailings water, seeps, and other similar sources. Lime treatment for metals removal has been one of the more commonly implemented water treatment technologies and continues to be an important component of MIW treatment. The selection of technologies required to produce a compliant effluent is dependent on the specifics of the project, the water quality, and the discharge limits. This paper targets general conditions when lime treatment is typically the most cost effective technology, when additional treatment steps are required, and some innovative technologies that are being evaluated and/or installed to replace or complement lime treatment.

Key components of a typical lime treatment system include the following:

- Reaction tank is a well-mixed aerated tank with typical reaction time from ten minutes to two hours. Lime is added to increase the pH with most metals precipitating in the range of 8.5 to 10.5.
- Solids separation process such as a conventional clarifier, settling pond, inclined plate clarifier, tube settler, ballasted clarifier, and similar. Polymers are typically added to promote settling.
- Polishing filtration may or may not be included.
- Effluent pH adjustment to neutralize pH to required range for discharge.
- Sludge management systems.
- Chemical feed systems.

Dissolved metals precipitate in the reaction tank when the hydroxide ions in the hydrated (slaked) lime combine with metal ions. Then solids separation steps remove the precipitated metals from the treated water. Calcium concentrations increase as a result of the lime addition. Calcium sulphate and/or calcium carbonate will also precipitate if present above their solubility limits.

The components above are part of a typical low-density sludge (LDS) system; high-density sludge (HDS) systems are discussed in later sections but generally make use of the same equipment as well as additional reaction and mixing tanks.

Benefits of Lime Treatment in Mining Applications

Lime treatment has a long history of application at mining sites for treatment of metal and sulphate impacted water. The primary benefits of metal hydroxide precipitation over other treatment processes and the use of lime over other chemical agents for treatment of MIW include the following:

- Availability – lime is readily available in several areas where mining occurs and is typically transported in bulk to operating mines for other purposes.

- Cost - lime is a fairly low cost water treatment chemical relative to other alternatives. The water treatment usage requirements for lime on an annual or daily basis are typically much less than required for other purposes at the mine, such as in froth flotation in copper, nickel and zinc production and for maintaining pH in a cyanide leach circuit for gold/silver recovery. As a result of its wide use, mining companies can typically negotiate favourable pricing.
- Effectiveness – hydroxide precipitation is effective for the precipitation of many metals, sulphate, and carbonate in MIW. Strict surface water metal discharge limits can often be achieved with just chemical reaction and solids removal (clarification). Polishing filtration may be required. Oxidation and iron (naturally occurring or supplemental) can improve the removal of target metals.
- Flexibility – lime treatment systems can handle changes in flow and concentration, and be operated intermittently unlike many other treatment processes (membranes, biological processes, IX, etc.).
- Secondary waste form – the sludge produced from precipitation is often easier to manage at active mine sites than liquid waste (brine). Lime sludge generally dewaters more effectively than sludge from caustic treatment, producing less dewatered sludge for disposal.
- Equipment – the equipment required for a lime treatment system is similar to other equipment used at operating mine sites (pumps, tanks, mixers, and clarifiers).
- Safety – lime slurry requires less special handling, storage and safety protocols than concentrated sodium hydroxide.
- Proven and effective with a long track record of operating and meeting surface water discharge limits at mine sites throughout the world.
- Treatability testing can be accomplished effectively through jar testing and settling testing. Scale up from bench test data is not uncommon.

While the situation at non-operating mine sites (historic, undergoing reclamation, closed, and similar) may not present as many advantages as operating mine sites for implementing lime treatment, the technology is often still cost effective for many of the reasons listed above.

In particular, when the MIW has a high metals load, high dissolved iron content and high dissolved sulphate with a requirement for sulphate removal, lime treatment provides cost effective bulk contaminant removal. See Table 1 for the results of lime addition to various pH set points in acid mine drainage water with high sulphate and metals concentrations. The concentrations presented in the table are representative of residual parameter concentrations following lime addition and solids removal. In this common example, lime treatment provides reductions in the concentrations of metals as well as TDS and sulphate.

Table 1: Lime treatment of acid mine drainage

Parameter	Raw water	pH 8	pH 9	pH 10	pH 11
	mg/L	mg/L	mg/L	mg/L	mg/L
TDS	27,687	7,570	2,766	2,454	2,426
Fluoride	52	6	4	7	<1
Sulphate	18,500	5,390	1,840	1,610	1,610
Aluminum	1,100	0.10	1.4	16	1.04
Cobalt	13	0.023	0.009	0.0084	0.038
Copper	878	0.13	0.10	0.11	0.13
Iron	1100	<0.07	<0.07	<0.07	<0.07
Lead	0.34	<0.073	<0.073	<0.073	<0.073
Magnesium	1,300	890	56	0.91	0.55
Manganese	210	17	0.21	<0.005	0.0066
Nickel	3.6	0.037	<0.03	<0.03	<0.03
Silica	140	0.91	0.35	0.12	0.89
Strontium	1.5	0.66	0.68	0.64	1.0
Zinc	69	0.11	<0.03	<0.03	<0.03

Alternative Technologies to Lime Treatment

In many cases, MIW lime treatment still represents the most cost-effective treatment process for mine water; however, alternative technologies may be a more appropriate option depending on the site conditions and mine-life stage, water chemistry, and discharge limits. In general alternative technologies can be more favourable than lime treatment at sites where:

- The site is in reclamation, lime is not available and the sites may be remote with no or poorly maintained roads. Often power is not available at these sites either.
- The cost for lime sludge disposal is high and/or trucking offsite is required.
- A relatively low flow (less than 10 to 20 m^3/hr) requires treatment that increases the unit operational cost for a lime system. The operational labour may be similar to a much larger system.
- Where constituents are present and regulated that are not effectively treated by lime addition including selenium, boron, nitrogen species (ammonia, nitrate, nitrite), chloride, sodium, potassium, TDS, and sulphate (to levels lower than approximately 1,800 mg/L)

Lime treatment may be used in combination with alternative technologies to provide pre-treatment or residuals (brine) treatment for bulk metals removal and then a more specialized process is used to reduce contaminants not well treated by lime. Technologies often evaluated and increasingly

implemented at mine sites are summarized below. Lime treatment is included in the Precipitation Technologies section below for completeness and contrast to other precipitation technologies. The technologies discussed below include processes that are considered a replacement to lime treatment and also in addition to lime treatment.

Precipitation Technologies

Precipitation technologies, including lime treatment, provide removal of dissolved species from MIW through a change in pH. The precipitation step changes the form of the target species from soluble to particulate and is followed by a solid liquid separation step. Typical solids removal steps include clarification, dissolved air flotation, ballasted clarification, microfiltration or ultrafiltration, and other types of conventional filtration.

In hydroxide precipitation the alkali chemical provides hydroxide ions that combine with the metal cations in the water to form insoluble metal hydroxides. Hydrated lime, $Ca(OH)_2$, also adds calcium that may precipitate sulphate and/or carbonate present in the water to form additional precipitated solids (either calcium sulphate or calcium carbonate). Most metals in MIW precipitate at elevated pH values, commonly in the range of 8.5 to 10.5. Other typical alkali chemicals include limestone, sodium hydroxide, and magnesium hydroxide. Most are more expensive than lime and are not as commonly used at mine sites. These other alkali chemicals may be used to minimize sludge if sulphate or carbonate are present above saturation limits and do not require removal, if the alternative chemicals have a price advantage, or if they have a treatment advantage. For instance, boron has been shown to precipitate/co-precipitate with magnesium at pH values near 10.5. Hydroxide precipitation efficiency is improved by co-precipitation with iron (either naturally occurring or added to the reaction tank) and by oxidation.

Sulphide precipitation differs from hydroxide precipitation in that it is more specific for precipitation of cationic heavy metals, does not affect pH, is not as dependent upon pH for effective metals treatment, and generates a smaller volume of sludge (metal-sulphide solids) relative to hydroxide precipitation. Constituents such as sulphate, manganese, and alkalinity will not be removed by sulphide precipitation. Metals may be economically recovered from the sulphide precipitate in some cases, defraying the treatment costs. Reagents include iron sulphide, sodium hydrosulfide, sodium sulphide, calcium sulphide, organo-sulfide (trade name TMT®), and biologically produced sulphide. Sulphide precipitation can often achieve lower residual metals levels than hydroxide precipitation; however, the reagents are more expensive and there is the potential for sulphide gas formation and release if the pH is not monitored and maintained at target levels. Sulphide precipitation was selected over lime precipitation and installed at the Wellington-Oro mine site near the ski town of Breckenridge, Colorado in 2008 for the selective removal of cadmium and zinc. The plant is located near tourist destinations and operated by the

town's municipal operators. The system operates between 12 and 34 m3/hr (spring runoff flow) and removes cadmium from 0.059 mg/L to less than the discharge limit of 0.004 mg/L and zinc from 123 mg/L to less than 0.225 mg/L.

Electrocoagulation

The electrocoagulation (EC) process involves passing an electrical current through water disrupting the ionic charges of dissolved species. Precipitation and co-precipitation of dissolved species result due to several mechanisms. One of the primary mechanisms is coagulation by iron or aluminum (depending on the electrode metal type) cations released from the corrosion of the electrode blades at the anode. Since chemicals are not added, there are no supplemental ions added to the water due to treatment chemicals. The EC unit replaces the reaction tank and chemical feed systems used in conventional precipitation, however, downstream solids separation is still required. EC has been used extensively in the treatment of metal finishing wastewater, shipyard runoff water and food processing wastewater.

Typically the capital equipment cost for EC is higher than chemical precipitation for most MIW treatment cases, however, standard models and designs are becoming more common. EC operating costs may be lower than chemical precipitation for labour, sludge disposal, and chemicals. Electrode blades require replacement and cost can be a factor in operating cost depending on local availability of metal material for electrode replacement Electrical power demand is likely higher and varies inversely with the ionic strength of the water being treated.

EC can generally remove most metals encountered at mine sites, although limited success with antimony and boron has been reported, and it is not effective at low pH so EC is not a candidate for acid mine drainage. Selenium removal to less than 0.005 mg/L has been achieved in bench tests, however, the sludge production is very high and longer reaction times required increasing the EC equipment cost.

Biological Treatment

For treatment of MIW, biological systems may be effective for cyanide, ammonia, nitrate, some metals, and phosphorus. Various configurations of biological systems are commercially developed and have been used on MIW treatment. Biological systems can operate aerobically, anaerobically or anoxically depending on the target contaminants, space available, water matrix and other factors. At mine sites, biological treatment has been used for removal of metals, nitrogen species and cyanide. The Homestake Mine in Lead South Dakota used a rotating biological contactor (RBC) fixed film biosystem to treat cyanide, ammonia and metals in MIW sources. Biological treatment of selenium is one of the commercially proven methods to treat selenium in water. Challenges associated with implementing biological treatment at mine sites include: the often cold water temperatures; the requirement for supplementation of nutrients (often carbon is required and phosphorus); polishing treatment; the negative

impact of higher TDS (above 15,000 mg/L) and bio-toxic metals such as copper; the space required; and the limited flexibility with regard to flow and contaminant load.

Passive Treatment

Passive treatment has a proven track record in the treatment of mining wastewater. Passive configurations that are considered proven include wetlands, anaerobic biochemical reactors (BCRs), and aeration channels with settling basins. Passive configurations that are emerging include alternatives to limestone for alkalinity addition (kiln dust, steel slag, ViroMine™, Ecotite™) specialty media for adsorption or ion exchange (peat, Ecotite™) and variations of the proven passive configurations. The appropriate selection of a passive process or processes is driven primarily by water quality and flow rate, against the site-specific availability of open area. Treatability testing is required for implementation of passive treatment with both bench-scale and pilot scale testing recommended. The testing can take several weeks to several months.

While passive treatment has been proven effective in treatment of MIW with systems in operation more than twenty years, innovations and improvements are constantly being made. Winter operations on cold water can reduce treatment efficiency and spring runoff or other high flows can be difficult to manage and so implementation should be considered on a case-by-case basis but the technology has a place in mining water treatment, particularly at closed mine sites.

One of the more commonly implemented passive treatment systems for acid mine drainage is the BCR. The BCR is often followed by an aeration channel, aeration pond, or wetland to polish and oxygenate the water prior to discharge. The BCR is also one of the few established technologies for selenium treatment at mine sites.

Reverse Osmosis

RO treatment is a high-pressure filtration process that utilizes a series of semipermeable membranes to reject most dissolved ions in a concentrated brine stream producing a high quality effluent (permeate) stream. The brine is typically in the range of 25 to 50 percent of the influent, but can be lower depending on influent water chemistry and level of pre-treatment. Pre-treatment may be required to remove organic compounds, fouling compounds, scaling compounds, or suspended solids. Antiscalant addition and pH adjustment are typically included with an RO system. MIW sources may require pre-treatment to reduce aluminum, iron, manganese, and silica concentrations. A typical RO system will be skid mounted and include the membranes, high-pressure feed pump, a pre-treatment cartridge filter, and membrane-cleaning skid.

Regulation of TDS, sulphate, chloride, sodium, and other difficult to treat, highly soluble parameters makes RO one of the few process equipment choices. Brine management is key to the successful

implementation of an RO system. In cases where the TDS load is predominately sulphate, an RO system can be used to concentrate sulphate in the brine stream. Lime treatment of the brine reduces the sulphate and allows blending of all, or a portion of the treated brine with the permeate prior to discharge, thus minimizing or eliminating the brine.

Nanofiltration (NF) is also used in some innovative MIW treatment applications. The NF concentrates primarily divalent species (metals and sulphate) while allowing most of the monovalent ions to pass through the membrane to the NF permeate. The NF brine can be recycled, as the divalent species are concentrated, and managed by a lime precipitation process that eliminates the brine stream.

Selective Media – Ion exchange, adsorptive media, titanium media, iron based media, activated alumina, etc.

Ion exchange/adsorptive media has been used in a variety of applications for removal of trace levels of metals and other contaminants and, in some applications, removal of higher concentrations of target species. The equipment consists of simple column systems loaded with the resin or media. MIW is pumped through the columns at a rate that provides the appropriate contact time. When the resin or media is loaded with contaminants, it is either replaced or regenerated. The volume of secondary waste generated by these column systems is typically less than 10% of the forward flow and less than RO brine. At mine sites, these types of systems are used as a polishing process after a bulk metals removal step or used when the MIW is a fairly low TDS and fairly clean water. Several products have been deployed as innovative solutions for metals removal from MIW, or are in development, for treatment of key parameters such as mercury, selenium, boron, and arsenic.

Evaporation

Evaporation technologies concentrate the soluble constituents in wastewater by removing the water as a vapour, where it may or may not be condensed. Both passive and active types of evaporation could be used to manage MIW and, in particular, high TDS MIW or concentrated liquid residuals from other treatment processes. Equipment such as a mechanical vapour recompression (MVR) evaporator can be used as part of an active treatment train or more passive systems such as pond evaporation could be used. The MVR evaporator produces a high quality liquid condensate that is virtually contaminant free but must be discharged or managed, while MVR brine will contain virtually the entire contaminant load in a volume of 1 to 10 percent relative to influent flow. Thermal evaporator systems without steam condensers are typically less capital cost than MVR systems, however, have much higher energy costs and do not produce a liquid distillate stream. Passive or semi-passive evaporation include solar evaporation ponds, and enhancements such as sprayers. Water is not recovered from the passive and semi-passive processes and the residue must be removed in intermittent campaigns. Evaporation can serve as the primary

treatment system for contaminated water or more commonly for management of secondary waste streams from other water treatment processes such as RO brine.

Innovations in Lime Treatment

One of the upgrades to the LDS process that is being implemented more often is the HDS process that reduces the volume of sludge for disposal.

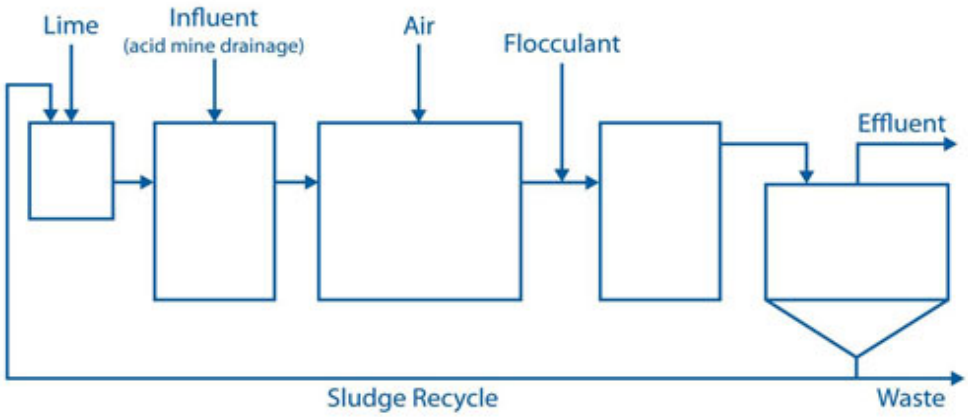


Figure 1: Lime HDS system

Other variations or enhancements to traditional lime treatment include sludge recycle back to the reaction tank rather than the lime mix tank, ettringite precipitation, combination of lime and caustic to minimize sludge, addition of barium for sulphate precipitation, and use of a microfilter or ultrafilter for solid liquid separation. Typical drivers for implementing these strategies and limitations include:

- Sludge recycle – provides surface area for precipitate formation and enhances the settleability of precipitate in cases where the solids generated are low. Also useful when high levels of calcium sulphate precipitation are expected to reduce scaling on equipment.
- Ettringite precipitation – achieves low residual sulphate concentrations; however, this requires careful metering of chemical feeds and tight pH control. The effectiveness is impacted by the overall ionic strength of the water. Limited full-scale implementation.
- Lime and sodium hydroxide combination – adding a target dose of lime and then polishing to a target pH value with sodium hydroxide can be used to get the benefits of both chemicals. Less sludge is produced than with a fully lime system, but with improved dewatering performance. Barium – barium precipitates sulphate very effectively and to very low residual levels. The downside of the process is the high cost of the barium. Could be effective for short-term treatment projects, low flows or targeted removal requirements.

- Microfiltration – microfiltration is replacing conventional clarification in some applications and being used to polish clarifier overflow in other applications where high quality effluent is required for discharge or as a feed to another process such as an RO.

Mine Water Treatment Applications – Colorado

To illustrate how widely lime treatment is used, Table 2 presents a snapshot of treatment plant for AMD in an area of Colorado, called the mineral belt, characterized by extensive mining activity. Along and near the heavily travelled interstate corridor are the remnants of historic mines and several operating (or soon to be in closure) mines. Many of these sites have active MIW treatment facilities that are based around lime treatment. The table also shows the cases where lime treatment has evolved to the currently implemented technology and two cases where an alternate to lime is currently in use. All information presented in Table 2 was obtained from public documents presented in the references acknowledged at the end of this paper.

Table 2: Overview of installed treatment systems in Colorado's mineral belt region

Plant name	Mine status	Treatment sstem	Installed
Argo Tunnel	Historic mine drainage – State of Colorado	NaOH	1998
		Lime	2005
		Lime HDS	2013
North Clear Creek	Historic mine drainage – State of Colorado	Lime HDS	2017
Climax Molybdenum	In operation	Lime Ponds	1983
		Lime Treatment Plant	2014
Henderson Urad	Closure announced	Lime Treatment Plant	1997
Eagle Mine	Closed	Lime	1990
LMDT	Historic mine under Bureau of Reclamation	NaOH	1992
Wellington ORO	Closed – Town of Breckenridge and Summit County	Sulphide Precipitation	2008
Summitville	Closed – EPA	Lime emergency action	mid 1990's
	Closed – State of Colorado	Lime HDS	2011
Keystone	Care/Maintenance	Lime with DAF	
Confidential Mine	Closed	Passive BCR and Wetlands	2016
Gold King Emergency Response	Closed	Lime	2016

As demonstrated above, lime treatment remains a viable and competitive treatment approach. The most recently constructed lime treatment plants (North Clear Creek, Climax, and Summitville) are all treating higher flows (115 to 350 m^3/hr) and higher metals loads.

Case Studies

Case Study: Closed Mine Site (Colorado)

Alternative and innovative treatment technologies were evaluated for treatment of MIW as part of a historic mine clean-up project. Water in the underground workings of the mine causes seeps from several adits and impacts ground water in the surrounding area. These sources of MIW are collected with seepage from a former tailing disposal area and are treated in a common active treatment plant. This plant, which has been operating for 20+ years, uses oxidation and lime addition to precipitate metals and settle them in a conventional clarifier. Treated water is discharged to surface water. Waste sludge is currently disposed of on-site, however the capacity for disposal is limited and expected to run-out. The blended influent water can be characterized as a typical acid mine drainage water with low pH, high iron, sulphate and other metals.

Evaluation of a new water treatment process was completed with a key objective of decreasing the waste for disposal that may need to be hauled off-site in the future. Minimize the overall operational costs of a new plant was also part of the evaluation criteria. Technologies included in the treatment evaluation were: lime HDS, sulphide precipitation, passive treatment (several configurations), in-mine treatment, and electrocoagulation.

In-mine treatment and electrocoagulation were determined to be not well suited to the site constraints and water quality. Passive treatment, with options including aerobic wetlands, manganese removal beds, and biochemical reactors were ruled out based on the total land area required, which exceeded 8 hectares for treatment of less than 70 m^3/hr.

Sulphide and lime precipitation were tested to determine sludge production and chemical dosing for development of a life cycle cost comparison. The final cost evaluation matrix is presented in Table 3.

Two important drivers to the operational cost were the chemical consumption and sludge disposal. Sulphide precipitation required considerable chemical input in order to precipitate the high levels of influent manganese. Despite the increased chemical usage, the volume of sludge produced from the sulphide precipitation treatment was less than 0.9 tonnes per day, compared to almost 3.5 tonnes from lime treatment.

Table 3: Cost comparison for sulphide precipitation and lime HDS treatment

Alternative	CAPEX/Year(s) incurred ($millions)	WTP chemical plus sludge disposal cost ($/year)	OPEX/Year(s) incurred ($/year)	Life cycle cost ($millions)
Alternative 1: Sulphide precipitation	$5.43/ 0	$217,000	$560,000/ 1–25	$16.44
Alternative 2: Lime HDS	$8.06/ 0	$200,000	$590,000/ 1–25	$19.66

Case Study: Closed Mine Site (Western US)

A low volume acid mine drainage seep from historic mine workings had historically been captured and pumped back to the mine workings. As levels rose in the workings, one treatment campaign was undertaken to reduce the volume of MIW in the mine pool. The campaign was a several week operation of a mobile RO system that discharged the permeate water and returned the brine to the mine pool. As the levels in the mine pool again rose to critical levels, alternatives were evaluated including bench-scale passive treatment testing and active treatment that would include RO treatment with discharge of permeate and brine returned to the mine pool after lime treatment. Bench testing of active treatment included both RO testing and lime testing. The results of the treatability studies were used to develop economics for active, passive and semi passive treatment options. The economics showed that the active treatment could be accomplished in three months at a cost of approximately $2,200,000 while the passive treatment would require 23 months and cost approximately $800,000. Once the mine pool was drained down, the passive option could then be used long-term to treat the seep rather than continue to return water to the mine pool and treat in a campaign style. The passive treatment system has been operational since 2009.

Since the start of operations, the passive treatment system has successfully drained down the mine pool and continues to successfully treat the seep water. The seep water is a typical AMD water with pH as low as 2.1 and many dissolved metals concentrations in the 100+ mg/L range. During the first 9 years of operation, the passive treatment system has removed approximately 95% of the combined iron, zinc, aluminum, copper, and cadmium. After bulk metal removal, a constructed wetland downstream provides complete evapotranspiration of the treated water.

This system has been successful and was preferable to a lime treatment system due to a number of site specific factors including:

- The unattended historic site is in a remote area that is not easily accessible for ongoing treatment operations and lime deliveries (ample area was also available for passive treatment at the site).

- The site does not have line power and generators would be required to operate active treatment components.
- The climate of the site allows for year round operation of the wetland that provides complete evapotranspiration.
- The seep flow is less than 3 m^3/hr, which is more amenable to passive treatment technologies.

The site factors for this project were key to the selection and favourable economics of the passive treatment system. Every site is different and it is important to evaluate those differences and how they impact the various treatment technologies.

Case Study: Active Mine Site (South America)

A gold mine in South America was evaluated for upgrades to their water treatment facility, which manages excess tailings water. The treatment process currently includes pH adjustment with caustic and an added ferric coagulant but does not achieve proposed treatment objectives for several metals, including copper. Since this is an operating mine, lime is used in large quantities in the mill and solids are managed via recirculation to the tailing storage facility.

Bench testing was performed on-site to compare the use of caustic to lime for precipitation of metals. All bench testing was carried out with set points reflective of the existing infrastructure including reaction times, chemical additions, and aeration capacity. The results of the tests are shown in Table 4.

Table 4: Bench-scale treatability testing results

Parameter	Raw water	Caustic addition (pH 10)	Lime addition (pH 10)
	mg/L	mg/L	mg/L
Aluminum	0.129	0.045	0.047
Cobalt	0.11	0.10	0.11
Copper	0.0396	0.0129	<0.0005
Iron	0.057	0.019	0.017
Lead	0.0121	0.0035	0.0023

Overall, the use of lime was advantageous for removal of metals to low levels and enhanced the solids settling. The lime treatment tests produced larger volumes of sludge, but this does not have a negative impact since the sludge is disposed of on-site. In addition to greater metals removal, the cost of lime is significantly cheaper than that of caustic and will reduce the operating cost of the treatment facility while using the existing equipment. The key driver was achieving a residual copper of less than 0.005 mg/L and this level was achieved with the lime.

Case Study: Active Mine (Europe)

As part of the pre-feasibility evaluation for a developing mine site in southern Europe, an alternative assessment was performed to look at treatment of the projected MIW. The water was different than typical acid mine drainage water with near neutral pH, but elevated metals concentrations. The treatment limits were very stringent and required removal of many different constituents to very low levels. Several constituents including lead, aluminum and zinc were evaluated for treatment using lime precipitation, while other metals such as molybdenum and arsenic required precipitation with iron addition at a low pH. Alternative technologies were also evaluated in addition to these chemical precipitation processes for the removal of selenium.

In this case, the stringent treatment limits drove a need for multiple processes in addition to lime treatment. Since the selenium treatment process was a significant driver to cost, it was recommended that a more complete water quality characterization be performed to confirm the need for alternative treatment technologies.

Conclusion

Precipitation of metal hydroxides using lime will continue to be an important tool in treatment of MIW. While evaluation and implementation of other technologies is on the rise, the benefits of lime treatment continue to have a place in the water treatment arsenal for mining applications. The drivers for implementation of alternatives to lime treatment or supplemental processes include regulatory changes to meet lower limits, limits on constituents not previously regulated, cost and operational factors, and technology improvements. These drivers may impact the placement of lime in the water treatment system as a pre-treatment process to a membrane system, a biological selenium treatment system, or other targeted treatment processes. In addition, lime treatment may play a role as a residuals management process such as a brine treatment process rather than as the main treatment step at an MIW treatment plant. It is apparent that in most cases for treatment of MIW, implementation of emerging technologies will be in addition to lime treatment rather than as a replacement. The implementation of alternative technologies to lime treatment is very site dependent but can provide great benefits should the opportunity arise.

References

Colorado Department of Public Health and Environment. 2018. Eagle Mine site summary. Retrieved January 2018 from: https://www.colorado.gov/pacific/cdphe/eagle-mine-site-summary

Colorado Department of Public Health and Environment. 2018b. Summitville Mine. Retrieved January 2018 from: https://www.colorado.gov/pacific/cdphe/summitville-mine

ITRC. 2010. Mining Waste Treatment Technology Selection Case Study: Wellington-Oro Water Treatment Plant, Summit County, Colorado. Retrieved January 2018 from: https://www.itrcweb.org/miningwaste-guidance/cs67_wellington_oro.htm

ITRC. 2010b. Mining Waste Treatment Technology Selection. Argo Tunnel Site, Clear Creek, Colorado. Accessed January 2018. https://www.itrcweb.org/miningwaste-guidance/cs41_argo_tunnel.htm

Martinek, M. 2014. Climax water treatment plant is open for business, *Leadville Herald*, August 14, 2014. Retrieved January 2018 from: http://www.leadvilleherald.com/news/article_2aa322b2-232c-11e4-b610-001a4bcf6878.html.

US Bureau of Reclamation (BOR). 2016. Leadville Mine Drainage Tunnel Treatment Plant (LMDT) Fact Sheet. Loveland, CO. Retrieved from: https://19january2017snapshot.epa.gov/sites/production/files/2016-12/documents/co-0021717-leadville-mdt-final-sob-2016.pdf

Proceedings of Mine Water Solutions 2018
June 12–15, 2018, Vancouver, Canada
Published by the University of British Columbia, 2018

Electrocoagulation for the Removal of Silica in Reverse Osmosis Rejects from Acidic Rock Drainage Water Treatment

Zhong Xie, National Research Council of Canada, Canada
Marco Gomez Orzatti, National Research Council of Canada, Canada
Saviz Mortazavi, Natural Resources Canada, Canada
Eben Dy, National Research Council of Canada, Canada
Wei Qu, National Research Council of Canada, Canada

Abstract

Conventional chemical processes, such as lime treatment, are often used for treatment of acidic rock drainage (ARD) streams. In certain cases, further treatment by a membrane separation, e.g. reverse osmosis (RO) or nanofiltration (NF), is necessary. Although high levels of water recovery can be achieved with NF/RO, a high salinity concentrate stream remains to be managed and/or treated.

During the NF and RO process, ions in the concentrate stream become increasingly concentrated. NF/RO concentrates from the treatment of ARD water contain high levels of various impurities, depending on the geochemistry of the waste rock and the treatment processes applied. Presence of cross-linked fine colloidal particles, especially silica, at certain levels in NF/RO concentrate streams can cause membrane fouling, which is a significant operational and water management challenge.

Electrocoagulation (EC) is a mature technology for many types of industrial wastewater treatments. The technology can remove metal ions, colloidal suspensions, fine particles, and soluble inorganic pollutants from aqueous solutions by introducing highly charged polymeric metal hydroxide species. In this paper, EC is explored as a treatment option for concentrated ARD water, with a focus on silica removal. Fe metal plates were employed as sacrificial electrodes. The experiments systematically investigated the influence of pH, dissolved oxygen (DO), current density (CD), and duration on the formation of green rusts (GRs) and silica removal. Batch tests have proved the concept that EC is a viable approach for silica removal from 80% RO reject water. Silica can be reduced from ~14 ppm down to ~3.0 ppm under 25 mA/cm^2 current density for 60 minutes, or 12.5 mA/cm^2 for 120 minutes. This level of silica removal can alleviate the membrane fouling during subsequent NF/RO treatment. The DO level in solution has an important influence on pH and water chemistry. It also governs ferrous or ferric or

ferrous/ferric mixed GR generation, and impacts the removal of silica in RO rejects from ARD water treatment. EC with ferrous green rust formation under the lowest DO level is best for silica removal.

Introduction

Acidic rock drainage (ARD) is recognized as a typical issue for many gold and copper mines. A common practice currently is to discharge to a designated pond for further process or reuse. This discharge is one major source of mine effluents. An effective management of discharge is very important to the mining industry, especially under tightening environment regulations.

To achieve green mining practice and to reduce the environmental footprint, increasing water recycling is crucial as it will minimize effluent discharge to ponds. Presently, the RO/UF/MF/NF (Reverse Osmosis/Ultra-Filtration/Micro-Filtration/Nano-Filtration) technologies are popular treatment choices, and can be adapted to mine sites. But membrane fouling has been a problematic issue, causing filtration and separation system failures and thus leading to additional operational costs. Therefore, consideration should be given not only to membrane material improvement, but also to other technologies that can serve as a pre-/post-treatment step to meet water quality specifications. Electrocoagulation (EC) technology is considered to be one such promising complementary technology for increasing overall effectiveness when integrated with membrane filtration technologies.

EC is a mature technology for treating many types of industrial wastewater (Dai et al., 2015; Mendoza et al., 2014; Mohammad et al., 2004; Moussa et al., 2017; Zeppenfeld, 2011). During EC, water splits in the cathode and releases hydroxyl ions (OH^-) to the solution. In the anode, a sacrifice metal, like Fe or Al plates, oxidizes into ions under applied direct current (DC). The dissolved metal ions hydrolyze or react with OH^- and generate various highly charged polymeric metal hydroxide species, such as polymeric Al $(OH)_n^{3-n}$. The polymeric ions serve as coagulants and can capture metal ions, colloidal suspensions, fine particles, and soluble inorganic pollutants from the wastewater.

Silica exists in significant amounts in many types of wastewater; it is particularly problematic for water treatment processes using membrane separation technologies due to scale formation and membrane fouling (Den and Wang, 2008). Water chemistry becomes complicated with the presence of silica. Depending on the concentration, solution pH and other components present, various forms of silica, such as monosilicic (<100 ppm), polysilicic (>100 ppm), colloidal and sol gel, exist in solution. Although only monosilicic species exist in ARD water, we speculate that silica could be the major contributor to membrane clogging when cross-linked with sub-micron particles and their clusters in RO rejects. An in-situ coagulation through an electrochemical process is expected to be an effective way to remove silica and fine particles. This paper shares the results regarding the effectiveness of a proposed EC process for the removal of silica in concentrated RO rejects from ARD water treatment.

Experiments

Water Chemistry of ARD Concentrates

Water samples were provided by NRCan CANmet Mining from its ARD pilot plant RO rejects. An 80% concentrated drainage was tested. The analysis of water samples was carried out by a commercial laboratory (CARO Analytical Services, Richmond, British Columbia, Canada). This analysis is summarized in Table 1.

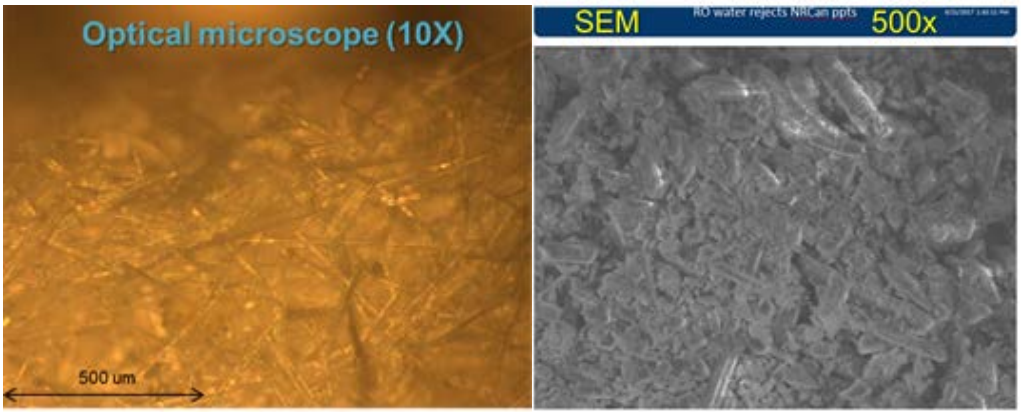
Table1: Water chemistry of 80% RO rejects

Element	Concentration	Other properties
Al	18,900 ug/L	pH = 5~6
B	<500 ug/L	
Co	1,750 ug/L	ORP = 250 mV
Cu	5,200 ug/L	
Fe	650 ug/L	
Mn	21,300 ug/L	DO: ~50%
Si	14,500 ug/L	
Zn	3,320 ug/L	Conductivity: 23~24 ms/cm
Ca	437 mg/L	
Mg	651 mg/L	TDS: 11~12

Other than magnesium (Mg), calcium (Ca), manganese (Mn) and aluminum (Al), a high content of silica of 14.5 ppm was found in the concentrate.

Analysis of Filtration Residue

The solid phase residue in as-received water samples were analyzed using an optical microscope and SEM after filtration with a 0.45 um filter paper.



(a) (b)

Figure 1: Optical (a) and SEM (b) morphologies of 80% RO reject residue filtered with 0.45 um paper

As seen in Figure 1, fine sticky particles aggregated and needle shape residues were found in residues. These residues might be responsible for the NF/RO membrane fouling.

EC Experimental Set Up

An illustration and setup of electrocoagulation (EC) are shown in Figure 2.

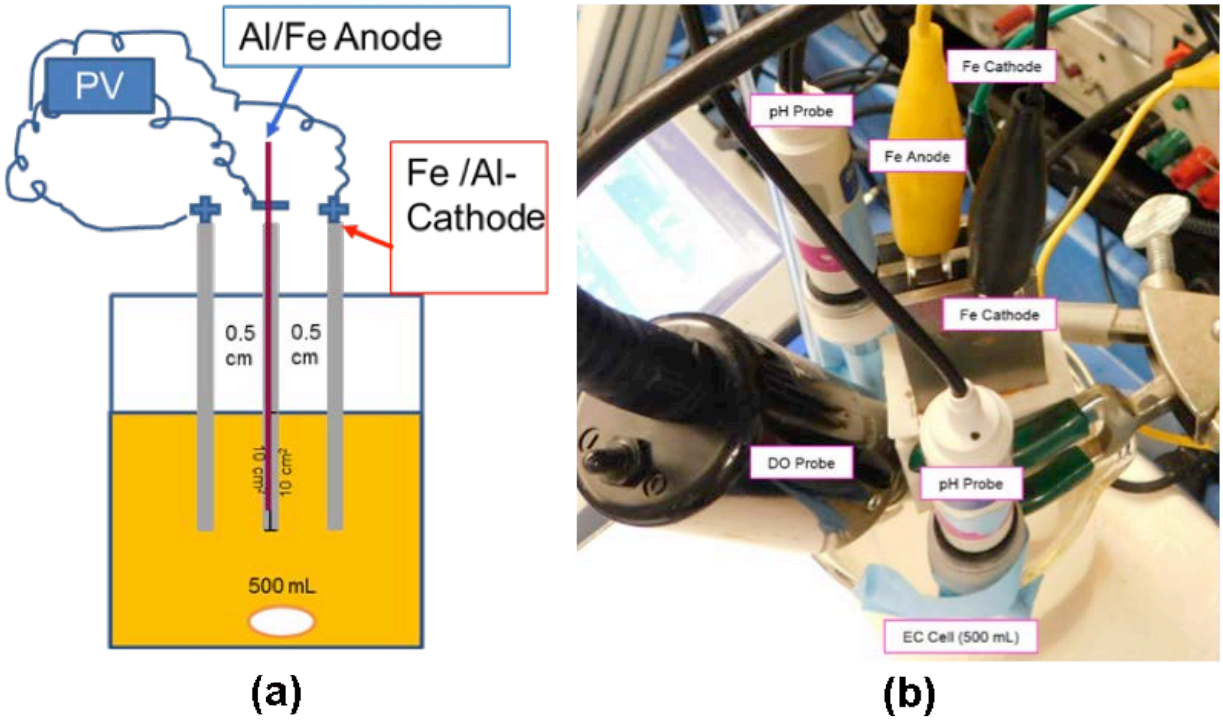


Figure 2: Batch EC testing device: (a) illustration; and (b) actual EC unit

Three regular iron plates were placed in parallel in a 500 cc beaker. The middle plate was used as the anode, and two side plates served as sacrifice cathodes. The exposed surface area was 5 cm × 2 cm for each electrode. The anode-cathode distance was set at 0.5 cm. Two pH probes were immersed in the solution to monitor pH variations. A dissolved oxygen (DO) meter was used to monitor the DO level during EC. A nitrogen or air purging frit was employed to control the DO level and, as such, the ratio of ferrous to ferric iron. The DC electricity provided was precisely controlled through a potentiostat, EG&G Model 263A.

Elemental analyses of the solutions were conducted with a PerkinElmer PinAAcle 900F atomic adsorption spectrometer (AAS) calibrated versus certified standard solutions. The test methods were validated versus the 80% reject analyzed by a commercial laboratory.

EC Green Rusts Formation Fundamentals

The Fe electrode-based EC is a green rust formation and conversion process (Moreno et al., 2009). Unlike typical green rust (GR) technologies, where the green rusts are generated by introducing chemicals, the GRs in EC are created through an electrochemical process under DC. The in-situ generated GRs are highly active and are capable of capturing various pollutants at different efficiencies.

On the cathode, the following reaction occurs:

$$H^+ + 2\ e^- = H_2\,(g) \text{ or } \quad E^o = 0.0$$

$$H_2O + 4\ e^- = H_2 + OH^-$$

With proton reduction, OH^- is released, and the solution pH increases subsequently. The final pH achieved is 9 or 10 with Fe electrodes, even if the initial pH was acidic.

On the anode, Fe predominantly oxidizes to Fe^{2+} and dissolves into aqueous solution through the reaction:

$$Fe = Fe^{2+} + 2\ e^- \qquad E^o = 0.45$$

In an acidic media, Fe^{2+} cations are oxidized slowly in the presence of DO:

$$Fe^{2+} + O_2 + 2\ H_2O \rightarrow Fe^{3+} + 4\ OH^-$$

In a neutral or alkaline media, Fe^{2+} is immediately transformed into ferrous hydroxide followed by a quick oxidation reaction with DO to form iron (III) hydroxide:

$$Fe^{2+} + 2\ OH^- \rightarrow Fe(OH)_2$$

$$4\ Fe(OH)_2 + O_2 + 2\ H_2O \rightarrow 4\ Fe(OH)_3$$

The hydrolysis and conversion of ferrous or ferric iron during EC can generate different types of so-called GR products: greenish $Fe(OH)_2$; reddish $Fe(OH)_3$; and intermediate by-products, a mixture of reddish or brownish Fe(II)/Fe(III) with the formula $[Fe(II)^{(6-x)}Fe(III)^{x}(OH)_{12}]^{x+}[(A)_{x/n}\cdot yH_2O]^{x-}$. They are highly active double-layer hydroxides (DLH) and are able to capture various impurities present in drainages.

Figure 3 shows the structure of DLH green rust and its principle of pollutant capture. Through creating different conditions, GRs with different ratio of Fe^{2+}/Fe^{3+} can be produced.

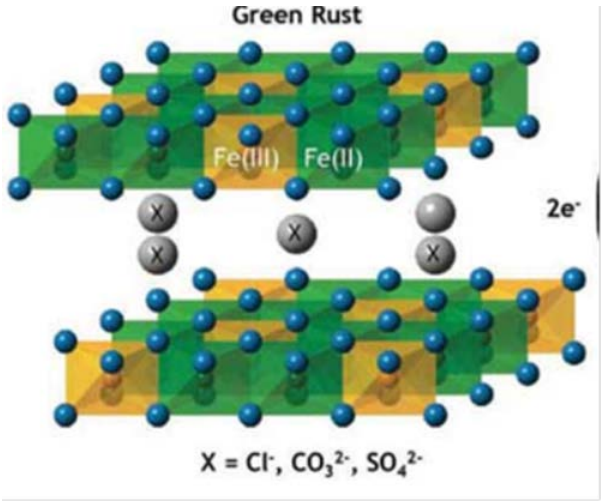


Figure 3: Double Layer Hydroxide (DLH) structure of green rust and pollutant capture

GRs are formed under circumneutral to alkaline conditions in suboxic environments. One of the factors often used to visually determine the success of pollutant removal with EC using Fe electrodes is the formation of dark green flocs (Moreno et al., 2009). There are different routes for the formation of green rusts. Figure 4 shows the possible routes of GR generation in the Eh-pH diagram of an aqueous Fe system.

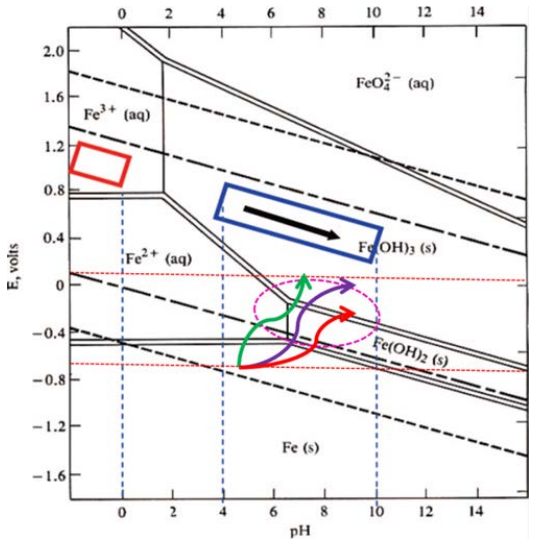


Figure 4: Eh-pH diagram of Fe-H_2O system with possible routes (green, red and pink) for GR formation. Modified from Moreno et al., 2009

In ARD RO rejects, the pH behaves quite differently. Complex reactions can happen in ARD water samples depending on reduction-oxidation potential (ORP), DO, pH as well as other buffering ions. The objective of our study was to identify the conditions, such as pH, DO, current density, and EC duration

that are favourable for the right GR formation. The dark green color was used as a visual indicator, and AAS elemental analysis was employed to verify the removal of silica in water samples.

Experimental Results

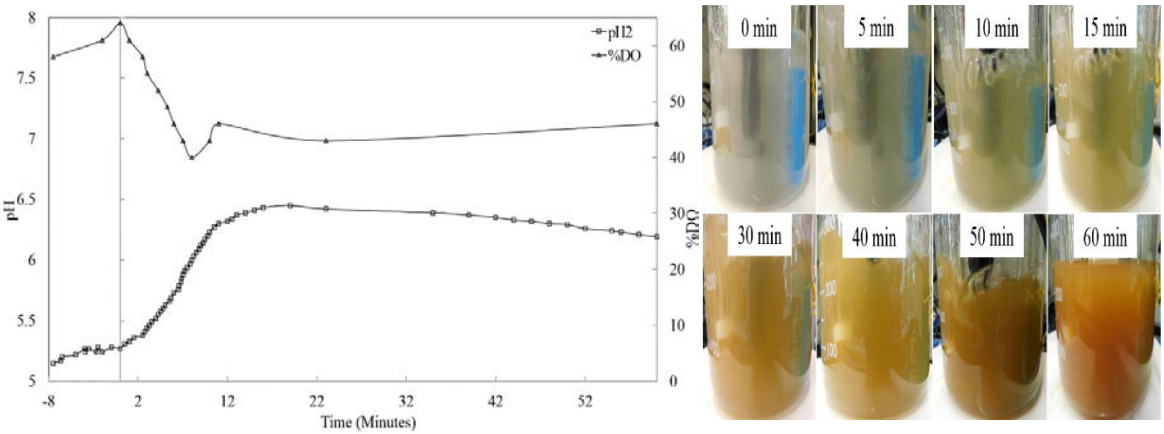
Dependence of pH, Green Rust Formation, Silica Removal on DO Level

It is uncertain what kind of Fe^{2+}/Fe^{3+} GR is ideal for silica removal. Three different cases are designed for different GR generation.

Case1: Ferric Green Rust Formation under Air Purging (High Level DO)

When air/O_2 is present, Fe^{2+} generated from EC will be oxidized into ferric Fe^{3+}, forming sparingly soluble $Fe(OH)_3$ precipitates. Figure 5 (a) shows the pH and DO variation during an EC process. Figure 5(b) records the flocs colour change during EC operation.

Under a high DO level, the green ferrous rusts are converted into brown red ferric rust, with reddish or brown precipitates observed during EC operation. The hydrolysis of ferric ion releases OH^- and suppresses the pH increase. After about 10 minutes, the pH stabilized around 6.2 to 6.4. The Si concentration in the filtrates was about 6 ppm after EC under 12.5 mA /cm^2 current density for 60 minutes. Although ferric GR has very low solubility, the silica removal is not effective. Therefore, it is not preferred to produce ferric rust during an EC process for the removal of silica.

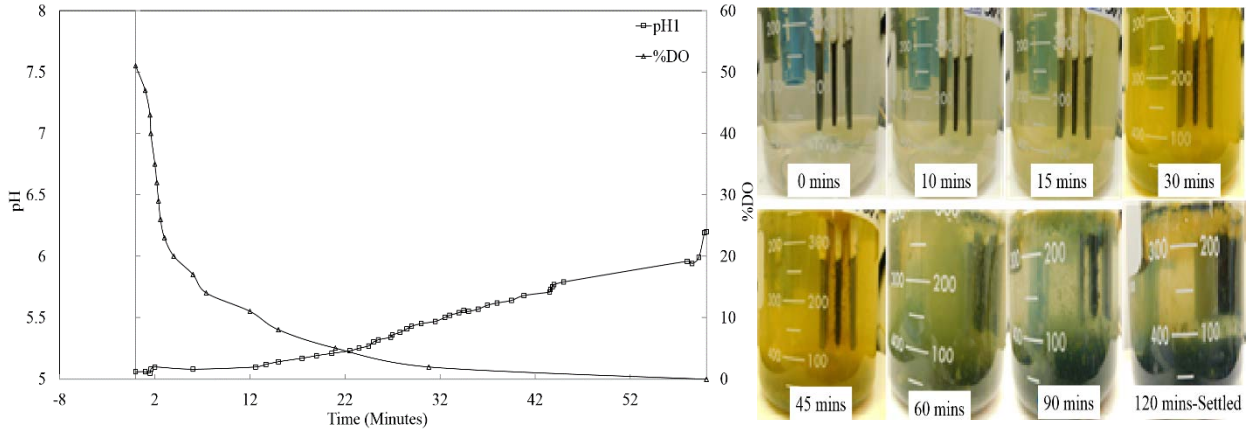


(a) (b)

Figure 5: (a) pH and DO change when air is applied during 1 hour EC and (b) colour changes as EC progresses. Testing conditions: room temperature, current density 12.5 mA/cm²

Case 2: Mixed Ferrous and Ferric Green Rust Formation under Moderate DO Level

It is believed that green rust with a formula of $[Fe(II)^{(6-x)}Fe(III)^{x}(OH)_{12}]^{x+}[(A)_{x/n}\cdot yH_2O]^{x-}$ at a certain ratio of Fe^{2+}/Fe^{3+} could be the optimal coagulant for the removal of certain pollutants. These experiments were designed to study the effects of mixed Fe^{3+} and Fe^{2+} generated during EC operation on silica removal. Figure 6 (a) shows the pH and DO variation during the EC process. DO level in the initial water sample was maintained at about 50%. As EC progressed, the DO level reduced gradually, and pH increased slowly, ending at a pH of about 6.0. Figure 6(b) shows the color change of precipitates from reddish into green. The ferrous ions generated from EC are converted into ferric ions during the first 45 minutes due to the presence of O_2 in solution. With the DO level reduced, ferrous green rust became predominant in the remaining period. The final outcome was a certain mixture of Fe^{3+} and Fe^{2+} green rust, with Fe^{2+} green rust as the predominant product.



(a) (b)

Figure 6: pH and % DO levels (a) and colour change (b) during a 60-minute EC with initial DO of about 50%. Testing conditions: room temperature, current density 6.25 mA/cm²

AAS analysis of silica concentration did not see a substantial change or reduction when compared with Case 1 of ferric green rust generation. The low pH profile might have contributed to the low silica capture. Whether the level of DO is maintained at 50% during electrocoagulation (case 1) or allowed to decrease (case 2), it does not seem to have a dramatic influence on silica removal.

Case 3: Ferrous Green Rust Formation with EC under N_2 Purging (Anoxic)

With prior N_2 purging before starting EC, the DO was precluded from the sample solution. Under such conditions, the EC product will be ferrous GRs predominant. Figure 7 (a) shows the pH change and DO level.

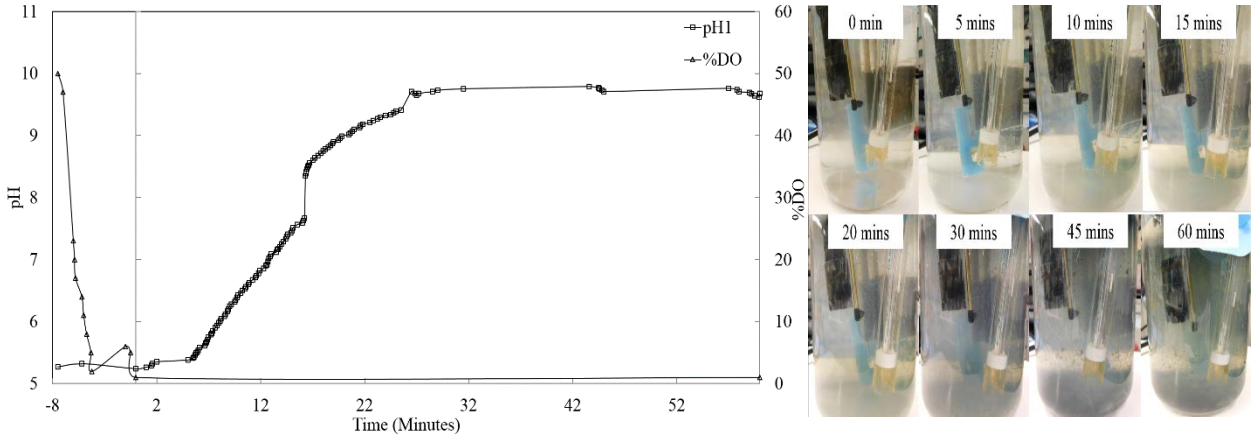


Figure 7: pH and % DO levels during 60 minutes EC when N_2 is previously applied to reduce DO to zero (a). Colour change with EC progressing (b).
Testing condition: room temperature, current density 25 mA/cm²

As can be seen from Figure 7 (a), with prior N_2 purging, the DO level dropped to less than 1% in about 8 minutes and remained flat during the entire EC operation. The local pH increased gradually and was stable at about pH 10 after roughly 30 minutes. The color of the precipitates during EC operation is presented in Figure 7(b). Light to dark blue/white ferrous GRs are observed throughout the EC process.

pH is a key parameter of water chemistry. When pH reaches 10, theoretically almost all metal ions will be precipitated, as in lime treatment processes and captured by coagulants. Also, the cathodic generated OH^- neutralizes the proton in acidic ARD water. Elevating the pH value is a foundation of EC effectiveness. Therefore, it can be concluded that maintaining a negligible DO level at the beginning of and during electrocoagulation is favourable for higher silica removal in comparison to cases 1 and 2, as pH increased to 10.

Figure 8 shows a comparison of silica concentration in the liquid and solid phases at two different DO levels. The AAS analysis was conducted immediately after liquid/solid separation using a centrifuge. As can be seen from Figure 8, silica removal is efficient with a silica concentration of 3.3 ppm when ferrous green rust formed (case 3). In contrast to case 1, where ferric green rust formed under a high DO level, EC can only reduce the silica concentration from an initial 13 ppm down to 8.7 ppm after 60 minutes. The precipitate analyses confirmed a mass balance of silica in filtrate and residue. This echoes our observation of pH and color change during the EC process. It is crucial to create conditions favourable for ferrous green rust formation than ferric green rust. Thus, the level of DO before electrocoagulation seems to have a dramatic influence on silica removal.

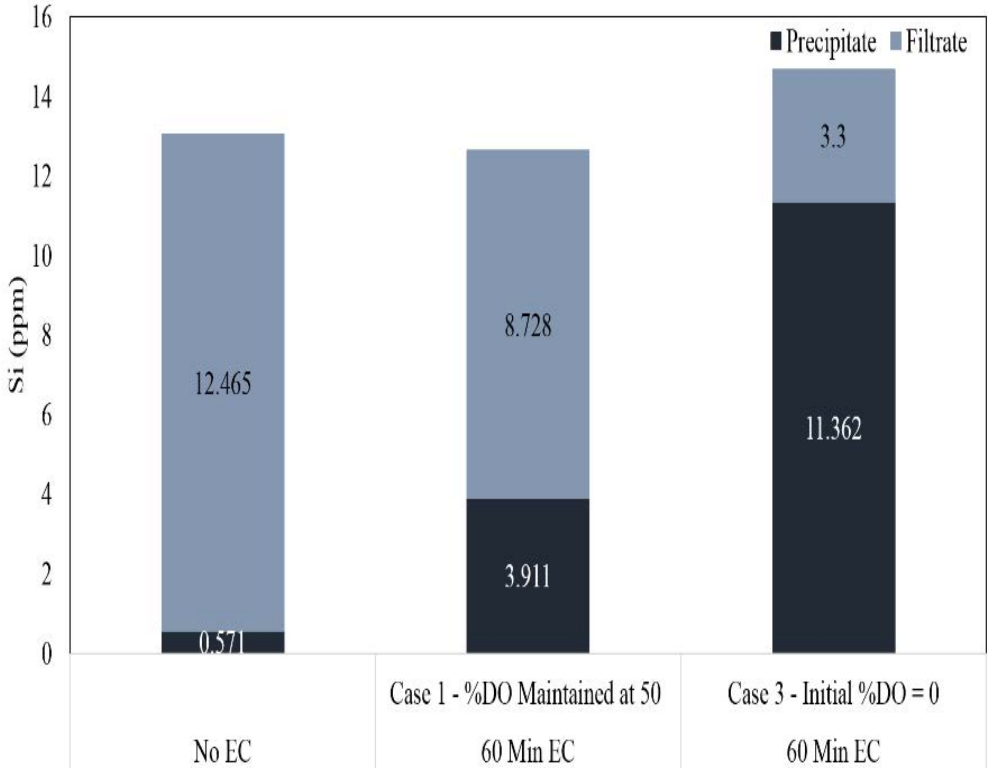
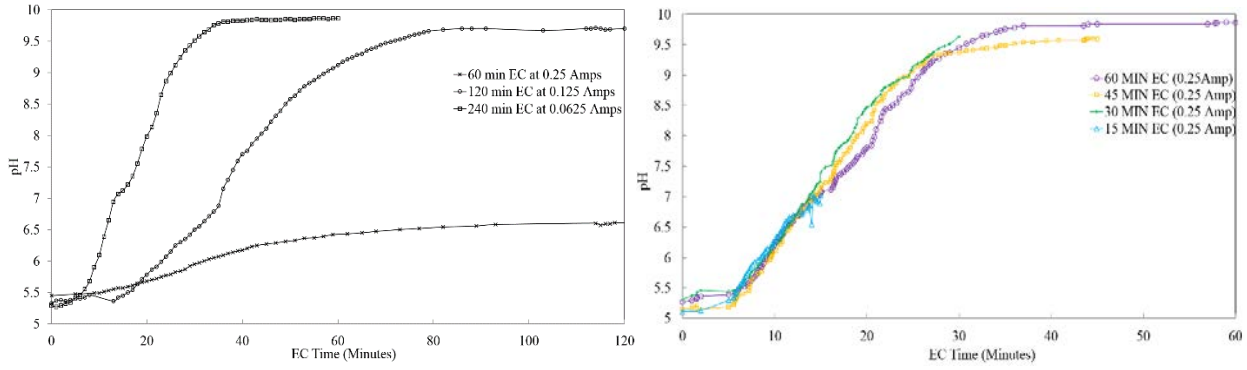


Figure 8: Si concentration in filtrate and precipitate after 1 hour EC at 0.25 Amps, DO=50% and DO=0%

Dependence on Current Density and Duration

While we identified the critical factors for silica removal, DO and pH, a further optimization on current density and duration was performed. Figure 9 (a) and (b) shows the dependence of pH on current density and EC duration respectively.



(a) (b)

Figure 9: Dependence of pH on EC current density (a) and duration (b)

As can be seen from Figure 9 (a), current density plays a crucial role in manipulating the pH of a solution. Under low current density, the pH remained acidic. When current density increased, the pH

changed rapidly. At 25 mA/cm^2 current density, the pH increased linearly with EC duration, levelling off after 30 minutes. High pH ensures the impurities can be captured into precipitates effectively.

Current density also plays a major role in silica capture from the ARD reject concentrates. From Figure 10, the silica removal efficiency increased when the current density was increased from 6.25 mA/cm^2 to 25mA/cm^2. Higher current density will benefit pH increase, as shown in Figure 9, and silica removal rate. The optimal silica removal conditions are found to be 25mA/cm^2, 60 minutes or 12.5 mA/cm^2 120 minutes with the ferrous GR predominant EC process.

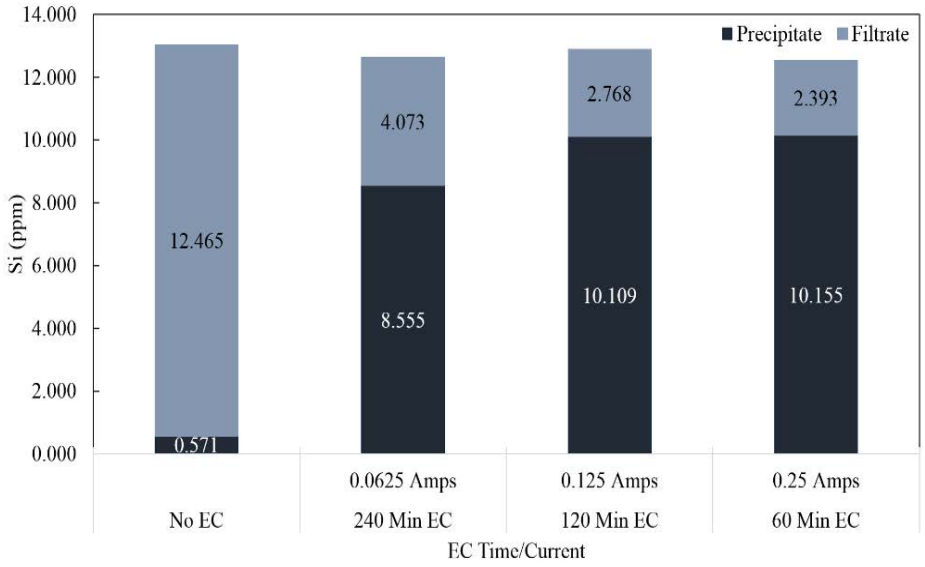
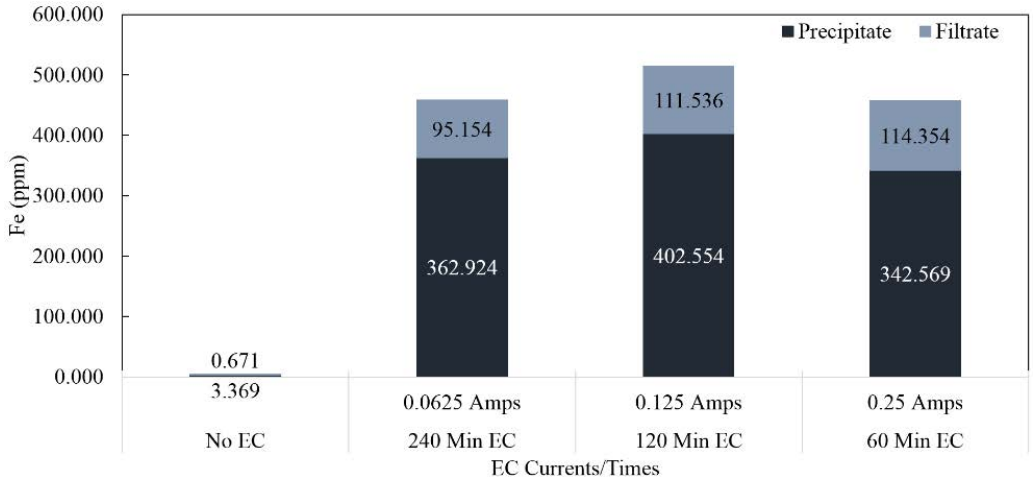


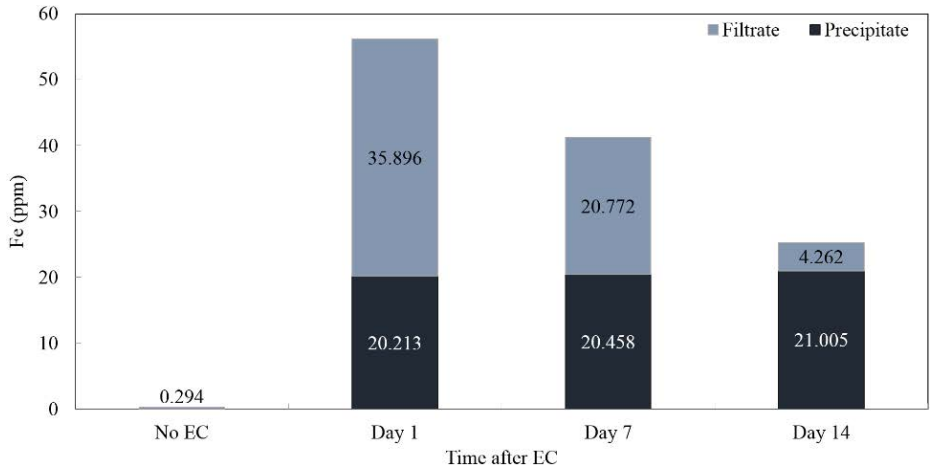
Figure 10: Dependence of silica removal on EC current density

Fe Removal for Discharge Post EC Retention

From silica removal testing (cases 1 to 3), we can see that ferric green rust is not the preferred product for silica removal. Therefore, EC was controlled to create Fe^{2+} predominant conditions. Figure 11 (a) shows the Fe^{2+} level after EC under different current densities. Roughly 100 ppm Fe^{2+} remained in solution. An additional step is required to convert high soluble Fe^{2+} to sparingly soluble Fe^{3+} in order to meet the discharge criteria after EC treatment. This could be done either through air purging or prolonged retention time to convert ferrous into ferric precipitates after liquid-solid (silica) separation. Figure 11 (b) shows change in Fe concentration during post-EC retention period. After 14 days, the Fe concentration decreased to less than 5 ppm. Continuous aging or purging with air can further contribute to bringing the Fe level to discharge limits.



(a)



(b)

Figure 11: Fe concentration after EC under different current densities (a) and Fe concentration change during post retention period (b)

Conclusion

Our laboratory tests proved that EC is a viable approach for removing silica in RO rejects from an ARD water treatment plant. Silica can be reduced from ~14 ppm down to ~3.5 ppm under the following conditions: removal of dissolved O_2 followed by EC with Fe plates at 25mA/cm^2 current density for 60 minute or 12.5 mA/cm^2 for 120 minutes. The removal of silica could effectively prevent membrane fouling.

The DO level in solution has a significant influence on the pH, governs ferrous, ferric or mixed ferrous/ferric GR generation, and impacts the removal of specific pollutants (silica in this case). From our observations, it can be concluded that EC with ferrous green rust formation under the lowest DO level is best for silica removal.

In view of the complex water chemistry of concentrated ARD water, further studies are required to explore the optimal conditions to capture other pollutants using EC. In addition, studies are also required to validate EC's effectiveness in the treating of RO rejects from ARD water treatment plants.

Acknowledgments

The authors wish to thank NRCan CANmet for providing water samples for testing and the NRC Environmental Advancement in Mining (EAM) Program for financial support.

References

Dai, X., Xu, Y. and Dong, B. 2015. Effect of the silica-rich, oilfield-produced water with different degrees of softening on characteristics of scales in steam-injection boiler, *Desalination,* 361: 38–45.

Den, W. and Wang, C.J. 2008. Removal of silica from brackish water by electrocoagulation pre-treatment to prevent fouling of reverse osmosis membranes, *Separation and Purification Technology,* 59: 318–325.

Mendoza, V., Emmanuel, I., Martín-Domínguez, A., Pérez-Castrejón, S., Santiago, G. and Lucila, S. 2014. Electrocoagulation to remove silica from cooling towers water, *Tecnología y Ciencias del Agua,* 3: 41–50.

Mohammad, Y.A., Mollaha, P.M. and Jewel, A.G. 2004. Fundamentals, present and future perspectives of electrocoagulation, *Journal of Hazardous Materials,* B114: 199–210.

Moreno, H.A.C., Cocke, D.L., Gomes, J.A.G., Morkovsky, P., Parga, J.R., Peterson, E. and Garcia, C. 2009. Electrochemical reactions for electrocoagulation using iron electrodes, *Ind. Eng. Chem. Res.* 48: 2275–2282.

Moussa, D.T., El-Naas, M.H., Nasser, M. and Al-Marri, M.J. 2017. A comprehensive review of electrocoagulation for water treatment: Potentials and challenges, *Journal of Environmental Management,* 186: 24–41.

Zeppenfeld, K. 2011. Electrochemical removal of calcium and magnesium ions from aqueous solutions, *Desalination,* 277: 99–105.

Proceedings of Mine Water Solutions 2018
June 12–15, 2018, Vancouver, Canada
Published by the University of British Columbia, 2018

A New Zero Water Intake Technology for Chemical Treatment of Mining Tailings

Colin Klein, SNF, Canada
Morgan Tizzotti, SNF, France
Kirk Thomas, SNF, USA
Trong Dang-Vu, SNF, Canada

Abstract

Treatment of mine tailings commonly utilizes polymer flocculants and/or coagulants to enhance solid-liquid separation. The preparation of these polymer solutions requires a significant volume of water, which, depending on the application, is recovered very slowly, or may not be recovered at all due to evaporative losses. In addition, low quality (high fine solids content) water can potentially have a detrimental effect on polymer performance due to, for example, polymer being consumed by the fines in the water.

As a solution to this challenge, SNF has developed a new tailings treatment process that rapidly recovers a high volume of water from treated tailings. This process uses a combination of flocculants with different properties added in sequence to enhance the dewatering performance as compared to a single flocculant treatment. The test results conducted on oil sands mature fine tailings have shown that initial (immediate) net water release was positive. This means that within a very short period of time, the volume of water released from the treated tailings is higher than the volume of water used in the flocculant solution to treat the tailings. Furthermore, the quality of the water released was high, with little to no fine solids, and its reuse for preparing new polymer solutions had no negative impact on polymer performance. Water chemistry has also been found to be unaffected by this process. This potentially allows water to be recycled an unlimited number of times without affecting flocculant performance. As a result, high quality water is readily available to be recycled for preparation of more polymer solution. This new zero water intake approach effectively eliminates the need for water from other sources to be used for the polymer make-down, offering significant reductions in water consumption and capex and opex related to pipeline and water pumping energy.

Finally, the environmental impact of the polymers used in the new zero water intake technology, particularly cationic polymer, is also discussed.

Introduction

The oil sands deposits in northern Alberta, Canada, constitute one of the world's largest oil reserves. Currently, a significant portion of this bitumen is extracted using the Clark Hot Water Extraction process. (Masliyah et al., 2004). This process uses significant amounts of water, consuming approximately three barrels of water for each barrel of bitumen produced (Kasperski and Mikula, 2011). This requires oil sands facilities to draw large quantities of fresh water from the Athabasca River, which could potentially affect the aquatic ecosystem, particularly during low winter flows (Allen, 2008). The mineral portion of the oil sands ore contains sand as well as fine clays, which are separated from the bitumen and are discharged from the process as tailings slurry. Coarse sand tailings settle quickly and form beaches, but fine tailings separate and run into the pond, forming a slurry. These fines gradually settle to form a material know as Mature Fine Tailings (MFT) or Fluid Fine Tailings (FFT). A significant portion of the water used for extraction of bitumen remains trapped in the MFT due to its extremely slow consolidation. As a result, the resulting volume of tailings (coarse and fine) is 1.4 times larger than the original volume of oil sand ore (Kasperski and Mikula, 2011; Camp, 1977). This results in significant accumulation of fine tailings at oil sands mining operations. A number of processes have been developed to treat these tailings so that tailings volumes can be reduced and tailings ponds can be reclaimed. These processes include beach drying, centrifugation, and blending coarse and fine tailings streams into a non-segregating mixture (COSIA, 2017). The majority of tailings treatment processes in oil sands utilize synthetic polymer flocculants to allow water to be more easily separated from the MFT or other tailings.

A number of studies have determined that treatment performance using a single flocculant can be improved by the application of two flocculants/coagulants in sequence. Yuan and Shaw (2007) investigated the effect of adding anionic flocculant and cationic coagulant in different sequences to oil sands tailings. They determined that the best performance was achieved by treating with flocculant first, then coagulant, and then another smaller addition of flocculant. Tizzotti et al. (2014) proposed a simpler dual treatment, replacing cationic coagulant with cationic flocculant, and demonstrated the advantages of cationic flocculant over coagulant. Vedoy et al. (2016) also found that MFT treatment could be improved with the application of two polymers in sequence. Studies have also been conducted that demonstrate the effectiveness of dual polymer treatment on thickener applications (Dang-Vu et al., 2014). In addition, Dang-Vu et al. (2016) developed a novel MFT deposition process in which flocculated MFT is deposited and then capped with coarse tailings. Dual polymer treatment was found to be the most effective treatment for this application as well.

Depending on the application, polymer treatment can require a significant amount of water for polymer solution preparation. Furthermore, this water may be recovered very slowly, or may not be recovered at all due to evaporative losses. In addition, low quality (high fine solids content) and chemistry

change of the water can potentially have a detrimental effect on polymer performance. Therefore, it would be advantageous if water could be recovered very rapidly and with high quality from treated tailings so that it could be reused for polymer make-down. Dual polymer treatment has shown potential for this application. SNF has investigated the feasibility of this concept.

Materials and Methods

Mature fine tailings (MFT) samples were obtained from three different oil sands operators. The properties of the MFT samples are shown in Table 1. These properties were determined in SNF's laboratory located in Edmonton, Alberta. The composition was measured using Dean Stark extraction. The sand content was measured by wet sieving with a 45 µm-opening sieve. The clay content was determined from methylene blue index. Anionic flocculant with medium charge density and medium molecular weight and cationic flocculant with high charge density and high molecular weight were used. Flocculant solutions (anionic and cationic) were prepared at a concentration of 0.4% in process water, unless otherwise stated. These solutions were prepared daily for each test conducted to limit the effects of polymer solution aging. The water chemistry was measured by a third party laboratory (Maxxam Analytics).

Table 1: MFT properties

Sample	Solids [wt%]	Water [wt%]	Bitumen [wt%]	Sand (–45 µm) content [wt%]	Clay content [wt%]
MFT 1	28.0	70.2	1.5	98.1	100
MFT 2	24.0	71.7	0.6	99.3	100
MFT 3	42.0	56.1	1.8	76.0	52.5

Gravity Drainage Tests

MFT samples were homogenized and 200 g aliquots were subsampled for flocculation tests. These aliquots were mixed with selected dosages of polymer solution until the desired flocculated structure was formed; then, the flocculated MFT was deposited on a 1 mm mesh screen and the amount of release water collected was measured over time. For dual polymer tests, the selected dosage of anionic polymer was added first, followed by mixing, and then the cationic polymer was added and mixed until the desired floc structure was obtained.

Benchtop Centrifugation Tests

Flocculation was conducted in the same way as for gravity drainage tests. Flocculated samples were placed in 500 mL centrifuge tubes and centrifuged using a Thermo Scientific Heraeus Megafuge 16 at 900

×g for 5 minutes. After centrifugation, the amount of centrate water was measured to determine tailings volume reduction.

Large-Scale Dewatering Tests Using Dynamic Flocculation Apparatus

Larger-scale tests were conducted using SNF's in-line dynamic flocculation apparatus. A diagram of this apparatus is shown in Figure 1. The MFT flow rate was approximately 850 g/min. Polymer flow rate corresponding to the selected dosage was injected and the speed of the dynamic mixers, SNF's Flomix®, was adjusted accordingly. Samples were collected at the discharge and deposited on 1 mm mesh screens. Dewatering was measured in the same way as for the gravity drainage tests.

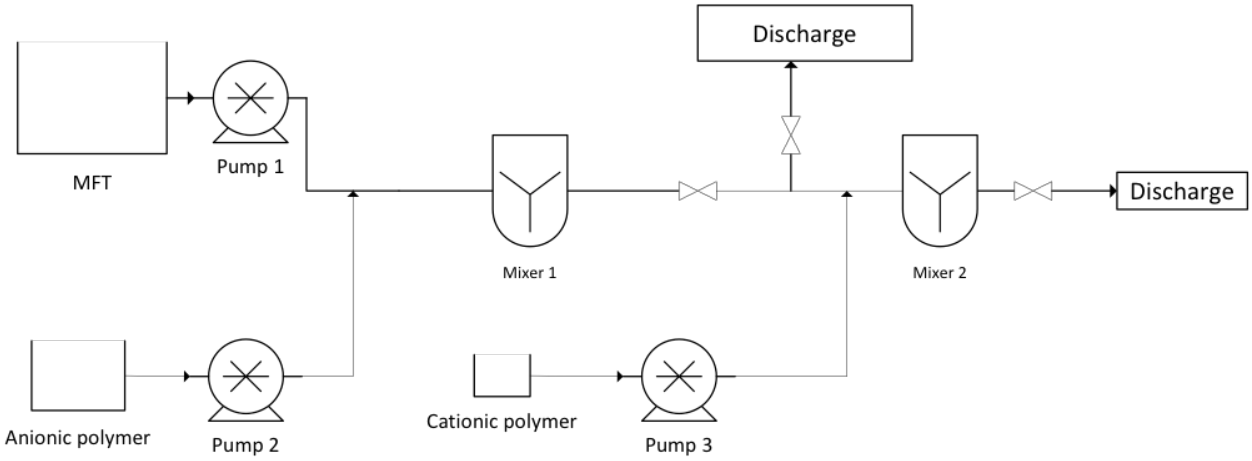


Figure 1: In-line flocculation unit

Results and Discussion

Figure 2 shows the effect of dual polymer treatment on the volume reduction of MFT 1 by gravity drainage.

For this MFT, single polymer treatment caused a practically negligible change in total tailings volume after 1 hour of dewatering, while dual polymer treatment significantly increased volume reduction over the same period. These results demonstrate the potential for dual polymer treatment to increase the dewatering rate of MFT. Figure 3 shows the corresponding solids content of the release water produced from the dewatering tests.

These results show that dual polymer treatment greatly improved the quality of tailings release water, reducing the amount of fine solids that would be recycled into the process. These results are in agreement with the findings of Zhu et al. (2017), who also observed an improvement in dewatering performance using dual polymer flocculation as compared to single polymer flocculation. In addition,

Yuan and Shaw (2007) also observed a significant improvement in release water clarity using sequential additions of anionic polymer followed by cationic polymer.

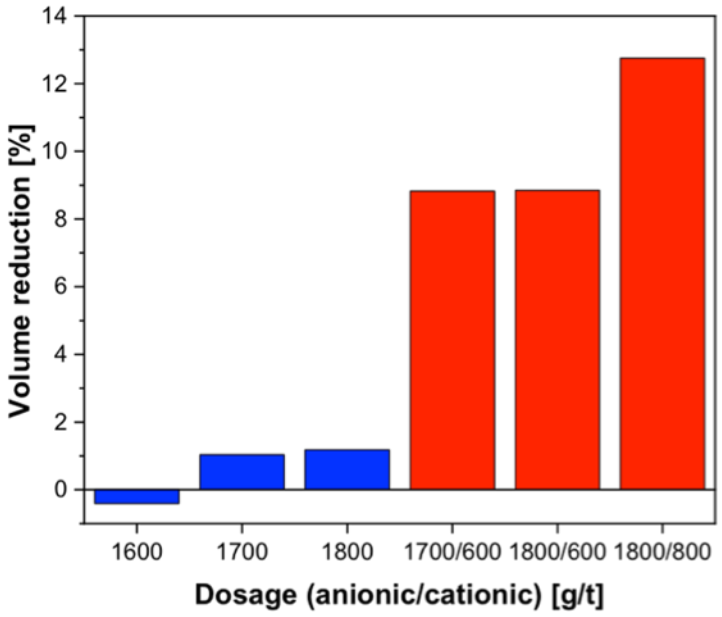


Figure 2: Effect of dual polymer treatment on MFT dewatering

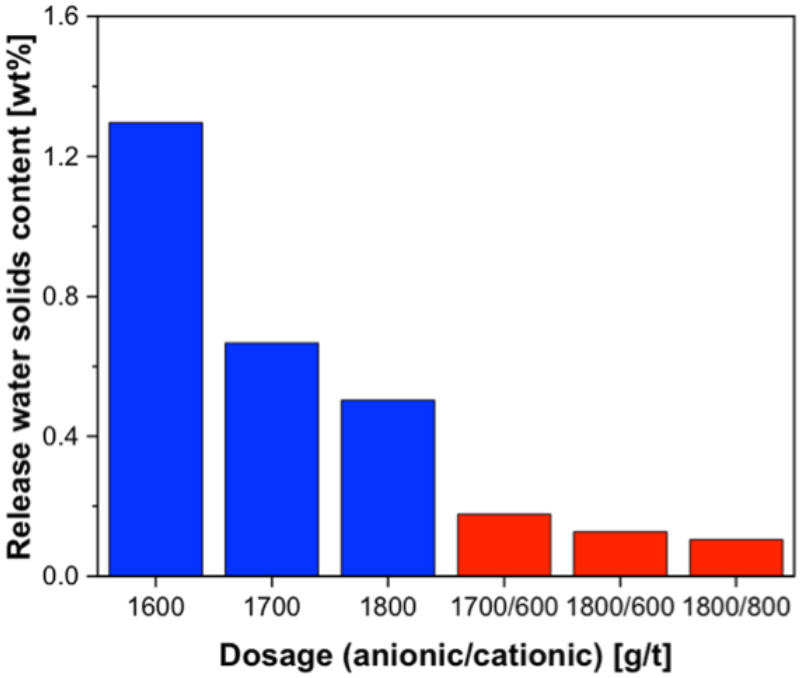


Figure 3: Effect of dual polymer treatment on MFT release water solids content

Figure 4 shows the visual difference between dual polymer and single polymer treated MFT. Dual polymer treatment results in a more compact, "grainy" floc structure, which allows for more rapid water

release than single polymer treatment. Because of this, dual treatment leads to drier cake; while with single polymer treatment, a significant volume of water still remained on the top of the cake. Figure 5 shows images of release water samples from dual polymer treated MFT and single polymer treated MFT. The total suspended solids (TSS) concentration of the release water from single polymer treatment was 0.06%, while for the dual polymer treated sample the TSS was 0.01%. This demonstrated that dual polymer treatment produces water with much higher quality (lower suspended solids) than single polymer treatment.



Figure 4: Dual polymer treated MFT (left image) and single polymer treated MFT (right image)



Figure 5: Release water samples from dual polymer treated MFT (left) and single polymer treated MFT (right)

Based on the results obtained using MFT 1 with gravity drainage, additional tests were conducted using mechanical dewatering (centrifugation) using MFT 2 to determine if this process could also improve water recovery for mechanical dewatering applications. Figure 6 shows the results of bench top centrifugation tests with dual polymer treatment compared to single polymer treatment. Dual polymer treated MFT had approximately 10 % higher volume reduction. Furthermore, the water quality was also improved for this application using dual polymer, as shown in Figure 7. The centrate of dual polymer treated MFT was very clear, while that from the single polymer treated MFT had a noticeable amount of suspended fine solids even after centrifugation. This demonstrates that dual polymer treatment can increase water recovery for mechanical separation methods as well as for gravity drainage. Similar results were obtained for filtration of MFT by Côté et al. (2013). They found that dual polymer treatment improved filtration performance due to greater fines capture of dual polymer leading to less fouling of the filter cloths.

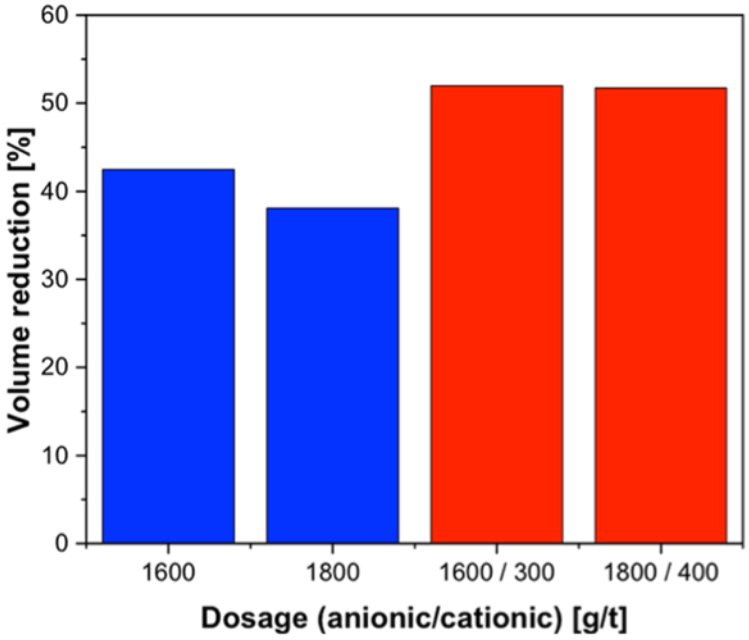


Figure 6: Effect of dual polymer treatment on centrifugation of MFT

The effect of dual polymer treatment on water chemistry and corresponding polymer solution performance was investigated, and the obtained results are presented in Table 2 and Figure 8. It has been observed that process water chemistry can have a significant effect on flocculation of tailings, particularly pH, as well as calcium and magnesium concentrations (Sworska et al., 2000). Comparison of the water chemistry of process water used for initial polymer make-down, and water chemistry of MFT water and of the resulting release water from treated MFT, shows insignificant variation in ion concentrations (Table 2).



Figure 7: Centrate from dual polymer treatment (left) and centrate from single polymer treatment (right)

Figure 8 compares the average volume reduction of MFT treated with polymers prepared in process water to treatment with polymer prepared in release water from previous tests. These tests were conducted three times and the average and standard deviation were determined. The average volume reduction using polymer prepared in process water was 22.7%, while with recycled water it was 18.9%. As shown in Figure 8, these results are within error, demonstrating that using recycling water recovered directly from treated MFT has no negative effect on flocculant performance.

These results demonstrate that by using dual polymer treatment, net water release (the amount of water recovered minus the amount of water added as polymer solution) will be positive after a short period of time, meaning that the amount of water recovered will be equal to, or greater than, the amount of water used for polymer make-down. Furthermore, the higher quality (lower solids content) of release water produced will prevent the accumulation of fines in recycled water. Finally, results show no significant impact on flocculant performance with the use of recycled water for polymer solution make-down. These results demonstrate SNF's new Zero Water Intake Technology (ZWIT) utilizing SNF's flocculants, where water recovered is recycled directly for polymer make-down. This technology eliminates overall water consumption for tailings treatment. The ZWIT required additional cost for a cationic flocculant and its injection system; however, it reduces operating and capital costs by eliminating pumping water from other parts of the plant for polymer make-down, including pumps, pipeline, energy, manpower and maintenance.

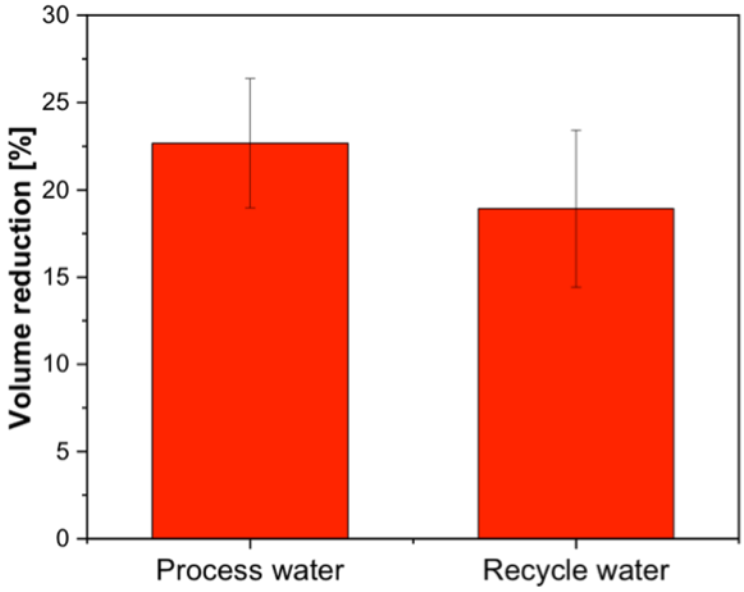


Figure 8: Effect of recycled release water on flocculation performance

Table 2: Water chemistry of process water and release water

Ion	Concentration (mg/L)		
	Process water	**MFT water**	**Release water**
Na	792.0	690.0	853.0
K	12.0	11.1	13.0
Ca	7.9	9.8	11.6
Mg	6.8	6.4	7.6
Cl–	766.3	603.5	733.7
HCO3–	790.0	960.0	830.0
SO42–	226.3	67.6	146.5
CO32–	43.0	51.0	55.0
pH	8.7	8.8	8.7

In addition to the process improvement, SNF's proposed ZWIT has minimal environmental impact. It is well known that anionic polyacrylamide flocculants (used in this study) have very low toxicity to aquatic organisms. Adverse effects seen in laboratory tests occur at concentrations greater than 100 mg/L, and are most likely due to the increase in viscosity of the test medium. In general, cationic flocculants (proposed in the ZWIT) have been found to be toxic to aquatic organisms (mainly fish and crustaceans) at concentrations of 5 to 10 ppm. However, in practice, cationic flocculants are quickly and irreversibly

adsorbed by suspended solids, removing them from the water phase (Blystone, 2017). Furthermore, cationic flocculants, as opposed to cationic coagulants such as polydadmac, hydrolyze quickly in water with pH greater than 6, losing their cationic functionality (Blystone, 2017). Note that oil sands tailings have a pH around 8. Therefore, flocculant usage does not present a long-term risk for plant or animal life under normal operating conditions, because any concentration discharged to the natural environment will be lower than the adverse effect concentration (Blystone, 2017).

Conclusions

The conclusions of this work can be summarized as follows:

- Dual polymer treatment significantly increases water release from treated MFT as compared to single polymer treatment.
- Release water from dual polymer treatment has significantly lower solids content than single polymer treatment.
- The benefits of dual polymer treatment also apply to mechanical dewatering methods, such as centrifugation.
- Release water chemistry is not significantly affected by dual polymer treatment.
- Recycling release water from dual polymer treatment to prepare polymer solution does not significantly impact subsequent flocculation performance.
- These results demonstrate the viability of a Zero Water Intake process for polymer make-down in tailings treatment.

References

Allen, E.W. 2008. Process water treatment in Canada's oil sands industry: I. Target pollutants and treatment objectives, *Journal of Environmental Engineering and Science,* 7(2): 123–138.

Blystone, S.L. Environmental aspects of polyelectrolytes. *Paper presented at the 2017 Regional CMP Conference*, October, 2017, Fort McMurray, Alberta, Canada.

Camp, F.W. 1977. Processing Athabasca tar sands – tailings disposal, *Canadian Journal of Chemical Engineering* 55(5): 581–591.

COSIA. 2017. Tailings projects. Retrieved January 15, 2018, from: http://www.cosia.ca/initiatives/ tailings/tailings-projects

Côté, C., Sibbel, K., Heffel R., Cafferata, K., Chengara, A., Duttlinger, W. and Knauer, J. 2013. Mature fine tailings treatment using inline flocculation and filtration, in N. Beier and V. Giang (eds), *Proceedings of Tailings and Mine Waste 2013*, Banff Alberta Canada: University of Alberta, Oil Sands Tailings Research Facility: 203–212.

Dang-Vu, T., Salehi, R. and Ramey, S. 2014. Oil sands mature fine tailing spiking for thickener application, in D. Sego, G. Wilson and N. Beier (eds.), *Proceedings of the Fourth International Oil Sands Tailings Conference*, Lake Louise Alberta Canada: University of Alberta, Dept. of Civil and Environmental Engineering: 467–470.

Dang-Vu, T., Keele, H., Lacoste-Bouchet, P., Salehi, R., Najafi, A., Klein, C., Nelson, A. and Ramey, S. 2016. In-situ deposition of treated tailings, in D. Sego, G. Wilson and N. Beier (eds), *Proceedings of the Fifth International Oil Sands Tailings Conference*, Lake Louise Alberta Canada: University of Alberta, Dept. of Civil and Environmental Engineering: 69–73.

Kasperski, K.L. and Mikula, R.J. 2011. Waste streams of mined oil sands: Characteristics and remediation, *Elements* 7: 387–392.

Masliyah, J., Zhou, Z., Xu, Z., Czarnecki, J. and Hamza, H. 2004. Understanding water-based bitumen extraction from Athabasca Oil Sands, *Canadian Journal of Chemical Engineering,* 82(4): 628–654.

Sworska, A., Laskowski, J.S. and Cymerman, G. 2000. Flocculation of the syncrude fine tailings, Part I: Effect of pH, polymer dosage and Mg2+ and Ca2+ cations, *International Journal of Mineral Processing,* 60(2): 143–152.

Vedoy, D., Botha, L. and Soares, J. 2016. Filtering mature fine tailings flocculated with single and dual anionic/cationic polymers, in S. Barrera and R. Jewell (eds), *Proceedings of the 19th International Seminar on Paste and Thickened Tailings,* Santiago, Chile, Paste 2016: 1–12.

Tizzotti, M., Frederic, P. and Dang-Vu, T. 2014. Dual polymeric flocculants treatment for the dewatering of whole oil sands tailings, *Proceedings of the World Heavy Oil Congress 2014*, New Orleans, Louisiana, USA, WHO14: 233–239.

Yuan, X.S. and Shaw, W. 2007. Novel processes for treatment of syncrude fine transition and marine ore tailings, *Canadian Metallurgical Quarterly*, 46(3): 265–272.

Zhu, Y., Tan X. and Liu, Q. 2017. Dual polymer flocculants for mature fine tailings dewatering*, Canadian Journal of Chemical Engineering,* 95(1): 3–10.

Bibliography

Dennis, M.E. 2007. Polyelectrolyte use in the oil sands industry: Safety aspect and environmental benefits, in R.E. Randall (ed.) *Proceedings of the Eighteenth World Dredging Congress* (WODCON XVIII), Lake Buena Vista, Florida, USA: 8C-3, 1415.

Proceedings of Mine Water Solutions 2018
June 12–15, 2018, Vancouver, Canada
Published by the University of British Columbia, 2018

Containerized Water Treatment for Remote Mine Sites

Veneil Sundar, BQE Water, Vancouver, Canada
Brent Baker, BQE Water, Vancouver, Canada
Alain Consigny, BQE Water, Vancouver, Canada

Abstract

Although lime treatment remains the most common treatment method for mine impacted waters, there are instances where it is neither a good fit from a technical performance perspective, nor is it the most cost-effective solution. Depending on site-specific requirements, the shortcomings of lime treatment can be any one of the following: difficulty to achieve ultralow discharge limits for certain metals and metalloids; inability to be deployed in a modular/containerized fashion; or the high cost of managing waste sludge.

This paper describes the water treatment that was implemented at the Silvertip Mine located in a remote area of northern British Columbia (BC), Canada. Although lime treatment was originally envisaged, the site water quality and discharge requirements, combined with constraints in footprint and overall capital cost, led to the adoption of sulphide precipitation as the treatment process of choice. Sulphide precipitation is known to be a highly effective tool for achieving ultralow discharge limits in mining effluents, and offers the possibility of a containerized mine water treatment design that:

- Minimizes capital costs and the need for skilled labour trades at remote project sites.
- Reduces water treatment plant footprint.
- Reduces the quantity of residue produced during treatment and enables possible value recovery.

The Silvertip project was able to take advantage of all of these benefits. The treatment process underwent regulatory reviews and performance demonstration, which was required because the application at Silvertip was the first sulphide precipitation treatment system to be applied in BC. The success of Silvertip removes the need for pilot demonstrations for future projects where sulphide treatment may be considered. To help reduce project risks and costs, BQE Water accepted full responsibility for water in the project, from the initial evaluation of treatment options and bench-scale testing, through permitting, to the full-scale implementation.

Introduction

The Silvertip project is an underground silver-lead-zinc mine located in a remote area of northern British Columbia (BC), Canada, approximately 16 km south of the Yukon border and 90 km southwest of the small community of Watson Lake. Several companies have been involved in the exploration and development of the property since the late 1950s, resulting in the construction of significant site infrastructure, including 26 km of access roads and 2.7 km of underground workings. In June 2015, JDS Silver received a Mines Act permit to resume mine operation. The water treatment process forming the basis of the JDS Silver permit application was HDS lime neutralization. However, due to low discharge limits for zinc and cadmium, which represent the two metals of concern in this project, HDS lime would result in a large plant footprint and large quantities of waste sludge being produced. This led JDS Silver to investigate possible alternate treatment systems, with BQE Water contracted to assist.



Figure 1: Silvertip Mine site

Water Treatment Requirements at Silvertip

There were two distinct phases for the project:

1. dewatering of existing underground workings; and
2. treatment of excess mine impacted water during the mine and mill operation.

During the initial underground dewatering phase, the ponds that would form part of the overall site water management system, including the 20,000 m^3 main collection pond (MCP) and 5,000 m^3 main

polishing pond (MPP), were still under construction. Consequently, underground water was pumped directly to the WTP for treatment prior to direct discharge into Silvertip Creek, as shown in Figure 2.

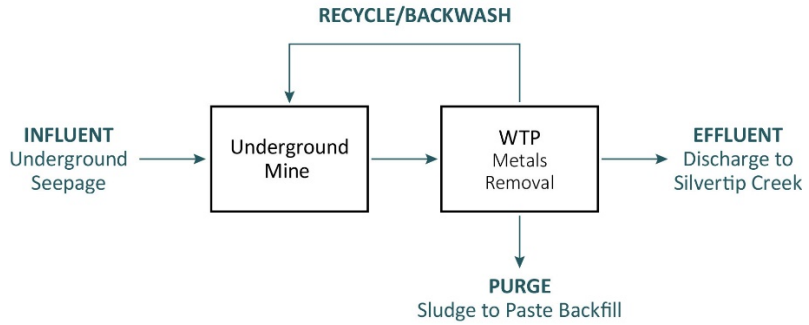


Figure 2: WTP block flow for underground dewatering phase

During the mine and mill operation phase, site water including underground seepage, dry-stack tailings seepage, mill process water, and run-off from various sources were collected in the MCP. As presented in Figure 3, the WTP is used to actively manage MCP levels by treating excess water to the applicable discharge limits prior to discharge into Silvertip Creek. The main function of the MPP located downstream of the WTP is to minimize the risk of non-compliance by introducing a delay between sampling of the WTP for discharge and release of treated water into the environment. This delay allows for sufficient time for an analytical laboratory located in the Lower Mainland near Vancouver to carry out assays and report.

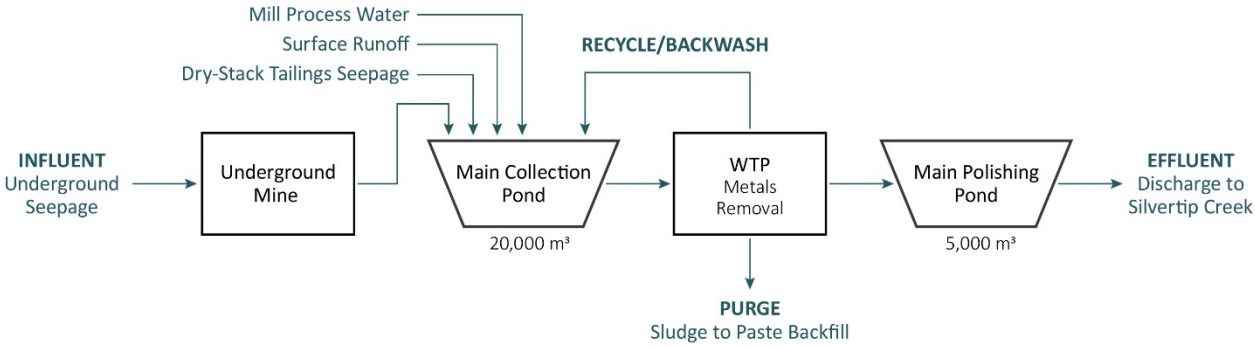


Figure 3: WTP block flow for the mine and mill operation phase

Table 1 summarizes the water quality data used to design the WTP for both phases of the project. Assay results were available to determine underground water quality. The water quality in the MCP during mine and mill operation was predicted by Lorax Environmental Services based on the water balance and geochemical modelling.

Table 1: WTP feed water quality

WTP Parameter	Units	Underground water assay	Main collection pond (mean)	Permit discharge requirement
Flow	m^3/day	720	2,640	1,752 Yearly avge 3,000 Daily max
pH	–	7.0	7.6	6.5–9.0
TSS	mg/L	27.8	–	30.0
As	mg/L	0.008	0.016	0.024
Cd	mg/L	0.020	0.041	0.0018
Co	mg/L	0.002	0.061	0.02
Cu	mg/L	0.001	0.033	0.03
Pb	mg/L	0.004	0.031	0.046
Hg	mg/L	–	0.002	0.000067
Zn	mg/L	3.700	4.170	0.500

The two main constituents of concern at Silvertip are zinc and cadmium but other constituents, including copper, cobalt and arsenic, were also flagged as potential concerns once the mine and mill are in production. Also noteworthy is that the sulphate concentration in both the underground and MCP water are either below or at gypsum saturation, which is typically between 1,500 and 2,000 mg/L, depending on the water composition and temperature. This is significant as the sulphate concentration has a bearing on the operation of the HDS lime neutralization process and the production of waste sludge.

Evaluation of Treatment Methods

Although there are many treatment processes that could theoretically be considered for the water flow and quality shown in Table 1, there are principally only two processes that are practical and that have been applied on a large scale to treat similar mining wastewater streams. These are HDS lime neutralization and sulphide precipitation. Originally, HDS lime neutralization was proposed as the treatment method of choice and included in the project permit application. However, the high cost of implementing HDS lime at a remote site such as Silvertip, combined with the uncertainty of achieving the target end-of-pipe limits for some of the metals, led JDS Silver to engage BQE Water to help re-evaluate the treatment approach for the project. The key process features and advantages and disadvantages of HDS lime and sulphide precipitation are discussed below, with specific focus on the process implementation at Silvertip.

HDS Lime Neutralization

HDS lime neutralization removes metals in the form of metal hydroxides, while relying on the generation of crystalline gypsum to improve both the settling properties of the waste sludge solids and the water

quality of the final effluent (Aubé and Lee, 2015). The function of crystalline gypsum is three-fold:

1. promote particle growth and faster settling, which reduces the size of the solid-liquid separation equipment;
2. entrain fine amorphous metal hydroxides in the crystalline gypsum solids to produce lower residual total metals in the final effluent; and
3. minimize equipment scaling.

In terms of operational flexibility, the HDS process has only one degree of freedom, which is the pH set point in the metal precipitation reactors. The following reaction summarizes the chemistry for precipitating metal hydroxides and gypsum, where Me represents divalent metals such as cadmium or zinc but the reaction can easily be modified to include trivalent metals such as aluminum and ferric iron:

$$2H_2O_{(l)} + MeSO_{4(aq)} + Ca(OH)_{2(s)} \rightarrow Me(OH)_{2(s)} + CaSO_4.2H_2O_{(s)}$$

The extent of metal removal achievable by HDS lime neutralization is driven by the metal hydroxides solubility, which is a strong function of solution pH. While some metals can be removed to very low levels at pH < 9, others require a much higher pH (Aubé and Zinck, 2003). Most metals exhibit a minimum solubility at a particular pH that is unique to each metal, resulting in increases in the residual metal concentration in solution when the pH is either lower or higher than optimum. At Silvertip, the original design contemplated operating the HDS lime plant at pH > 9.5, and possibly as high as 11, to achieve all applicable target discharge limits. Since the operating pH was to be higher than the maximum allowable pH for discharge, the original design included an effluent acidification stage using carbon dioxide (CO_2) injected into the HDS effluent to bring the final pH to below 9.

Side effects of the operation at high pH and subsequent CO_2 addition to re-acidify the final effluent are an increase in waste sludge production and a risk of increased TSS in the effluent due to partial removal of calcium through calcium carbonate precipitation. The original HDS design used several large reactors in series with the option to aerate to ensure high lime utilization and conversion of ferrous iron to ferric iron. Most importantly, the fact that sulphate concentrations in the plant feed were either below or at gypsum saturation meant that a very small amount of gypsum would form in the plant. Since the HDS process relies on the production of crystalline gypsum to operate properly, there would likely be a very significant risk of poor HDS process performance at Silvertip unless the solid-liquid separation equipment was oversized to counter low solids production compared to conventional HDS. Clearly, this would have a negative impact on both capital cost and plant footprint.

From this analysis, we can summarize the key advantages and disadvantages of HDS lime for the application at Silvertip as follows:

Advantages

- The process is well known and accepted by the industry and regulatory agencies in BC.

Disadvantages

- The process is not likely to operate as conventional HDS due to low sulphate and metal loading in plant feed.
- Need to operate at high pH and then acidify the effluent.
- Due to large plant footprint (and cost), cannot be designed as a containerized system.

Sulphide Precipitation

Sulphide precipitation removes metals from water in the form of metal sulphide solids. Unlike lime precipitation, sulphide precipitation systems offer two degrees of freedom in the process including pH and Eh set points in the metal precipitation reactor (Kratochvil et al., 2015). Sulphide is a much stronger ligand than hydroxide for most metals, and this means the majority of metal sulphides exhibit solubilities that are many orders of magnitude lower than those of the corresponding metal hydroxides. Consequently, sulphide precipitation can achieve much lower concentrations of dissolved metals in treated effluent and often without the need for pH adjustment, as is the case for the Silvertip water.

Different forms and sources of sulphide are available, including NaHS, Na_2S and TMT. Regardless of the type and source, the kinetic reaction between sulphide and metals in solution is fast. This eliminates the need for long retention times, unlike HDS systems, to ensure high reagent utilization.

With sulphide precipitation, no gypsum is produced which reduces the amount of waste sludge. In contrast to HDS sludge solids, metal sulphides can be blended with metal concentrates produced at the site; recovering value from metals contained in the wastewater, assuming it is of interest to mines with highly polluted streams containing significant mass load of metals (Ashe et al., 2008). At Silvertip, this is not the case as the sludge solids would be blended into the underground paste backfill material. The following reaction shows the example of the removal of divalent metals using sodium sulphide (Na_2S).

$$MeSO_{4(aq)} + Na2S_{(aq)} \rightarrow MeS_{(s)} + Na_2SO_{4(aq)}$$

The three aspects of sulphide precipitation that are sometimes cited as disadvantages are:

1. the formation of very small, almost colloidal, particulates of metal sulphide that are difficult to separate from solution;
2. the lack of familiarity of the mining industry and regulators with these systems; and,
3. the health and safety risks related to potential hydrogen sulphide formation.

While the risk of colloids formation is real, BQE Water has developed engineering designs minimizing this risk and has constructed 16 large-scale metal precipitation plants treating mine wastewater at projects around the world. The tools used to prevent the formation of colloids focus on controlling the levels of solution supersaturation with respect to metal sulphides, which are highly insoluble and form rapidly and irreversibly. Additionally, the process is proven at mine sites in extreme wet and cold environments in Northern Canada (Consigny et al., 2015). That said, none of the company's sulphide precipitation plants have been built in British Columbia, which meant extra scrutiny would be applied to the water treatment at Silvertip if the ChemSulphide® process was to be applied there. Given the high solubility of hydrogen sulphide gas, the health and safety risk is quite low for applications like Silvertip where low sulphide doses are required to remove trace metals.

The key advantages and disadvantages of sulphide precipitation application at Silvertip can be summarized as follows:

Advantages

- Well proven process
- Operate at neutral pH
- Eliminate the need for effluent acidification using CO_2
- Reduce the production of waste sludge
- Instant reaction, eliminate the need for large precipitation reactors
- Process can be designed to fit in standard sea containers
- Small plant footprint

Disadvantages

- Lack of familiarity with the process among British Columbia regulators
- Introduction of new reagent at the mine site

Treatment Process Selection and Permitting Implications

Table 2 provides a summary of the comparison between HDS lime and sulphide precipitation salient to selecting the most appropriate water treatment for the Silvertip project.

Table 2: Comparison between HDS lime and sulphide precipitation

HDS lime neutralization	Sulphide precipitation
Lime reactor with aeration, long HRT	Use of in-line reactors
Large clarifier	Solid-liquid separation in a sea container
Need for effluent acidification via CO_2 addition to meet discharge pH limit	No need to change the pH (eliminate re-acidification stage)
Sludge production of up to 1.35 kg/m^3 of water treated	Sludge production < 0.1 kg/m^3 (mostly TSS coming from underground)

Based on the comparison presented in the table above and preliminary assessment of cost, schedule, and logistical benefits of the ChemSulphide® process, JDS selected sulphide precipitation as the treatment process of choice for the Silvertip project.

The position of the BC Ministry of Energy and Mines (BC MEM), the agency responsible for approving permits for mining projects in the province, is that a pilot demonstration is required for any water treatment process that has not yet been implemented at a BC mine site. This meant that despite the fact that BQE Water could provide operating data from multiple reference sites using ChemSulphide® for mine water treatment elsewhere in the world, JDS Silver would not receive a permit until ChemSulphide® was demonstrated on the Silvertip water.

Although bench-scale testing was conducted as part of the initial treatment selection process, a pilot demonstration was required. Based on experience from previous projects, both BQE Water and JDS Silver had a high level of confidence in applying ChemSulphide® at Silvertip. This confidence, coupled with the aggressive project schedule, led JDS Silver to make the decision to proceed and build the ChemSulphide® treatment plant without a pilot demonstration. Instead, the plan was to commission the plant and use the first two weeks of plant operation as the demonstration on which Silvertip would receive their permit.

ChemSulphide® Plant Description

Each ChemSulphide® plant is unique, and this section aims to provide a closer look into the overall process that was implemented at Silvertip, as well as highlight some of the readily available equipment that was used to meet the water treatment objectives on site.

Process Overview

The Silvertip WTP block flow diagram is presented in Figure 4.

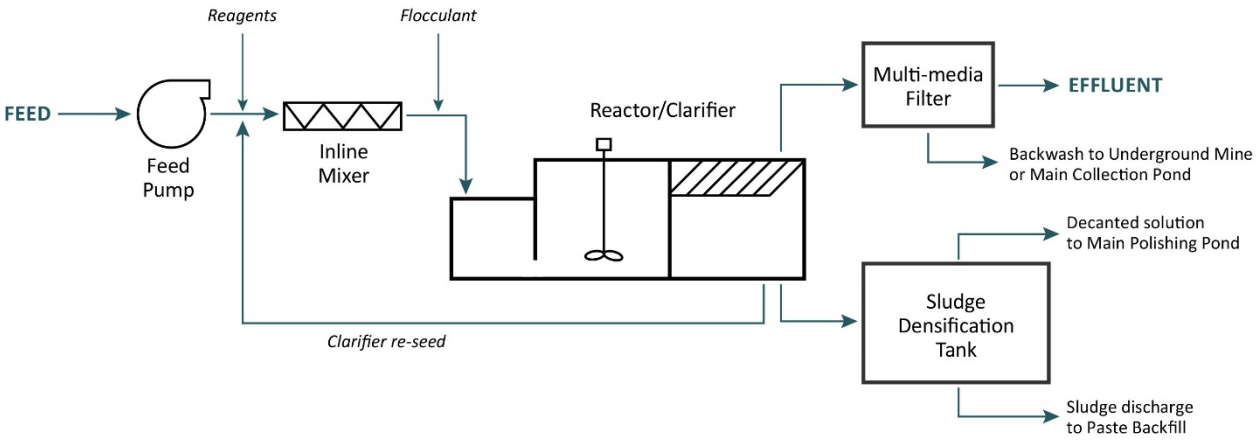


Figure 4: WTP block flow diagram

The overall process contains six discrete steps, which are described in Table 3.

Table 3: Water treatment stages at Silvertip

Step	Name	Description
1	pH Adjustment	Sulphide precipitation reaction produces acid. Sodium hydroxide is injected upstream in inline mixers to ensure the final effluent pH is within permitted limits.
2	Reaction	Sulphide reagents are injected upstream in inline mixers to react with dissolved metals in the impacted waters to yield metal sulphide solids and acid.
3	Flocculation	Flocculant is injected in a modified frac-tank clarifier. Gentle agitation in the mix chamber facilitates particle agglomeration and increases particle size to improve settling.
4	Clarification	Flocculated solution flows through a lamella plate, which reduces the superficial velocity of the flocs to separate them from the treated water.
5	Filtration	Clarifier supernatant is polished in multimedia filters to remove fine particulates before it is discharged to Silvertip Creek via the MPP.
6	Densification	Sludge is periodically purged to a holding tank, where additional residence time allows for further compaction. Thickened sludge is sent to the paste backfill plant for disposal.

Plant Overview

The modular WTP was designed to house all equipment in three 40' L × 11.5' W × 9.5' H extra-wide shipping containers and one 53' L × 8.5'W × 10.5' H frac-tank. The high rise rate of solids and low solids generation rate allow for smaller equipment, making containerization feasible. The unmodified shipping containers and frac-tanks were readily available from local vendors. Most of the lead time required to deliver these units was a result of customization to ensure proper accessibility and compatibility with the process.

As shown in Figure 5, the containerization of the plant allows for easy placement onsite, with minimal civil work. Another benefit of containerization is the ability to double stack containers to reduce

footprint and eliminate pumps by taking advantage of gravity flow; two of the containers depicted in Figure 5 were double-stacked for this very reason.



Figure 5: Silvertip WTP

Project Execution

Table 4 shows key milestones for the Silvertip project. The plant was operating and discharging to the environment within five months of the final design being issued, meeting the compressed project schedule laid out by the client.

Table 4: Key milestones for the Silvertip project

Milestone	Date
Contract awarded to BQE Water for WTP design	December 1, 2015
Process Engineering Design issued for construction	February 3, 2016
Equipment delivered at site	April 24, 2016
Water treatment plant operating and discharging to Silvertip Creek	May 14, 2016

Containerization

All components of the WTP, with exception of the motor control centre (MCC), were fabricated and installed in the Lower Mainland near Vancouver, British Columbia. Shipping containers pre-modified with doors, penetrations, insulation, lighting and HVAC were shipped to a local fabricator for process equipment, piping and electrical installation. BQE Water was able to oversee construction and make frequent site visits to the local fabrication shop to advise on design, which is a major advantage that is typically not available when a plant is constructed onsite in remote areas.

Another advantage of local fabrication was the ability to partially commission the WTP once the containers were fully packaged. Traditionally, inputs/outputs (IO) from process equipment and instrumentation are terminated to IO cards in a central control cabinet that houses the programmable automation controller (PAC). This method would require substantial inter-container wiring, which is contrary to the overall strategy of the project. Alternatively, the use of remote drops allows IO from process equipment and instrumentation to be terminated to IO cards in each container; onsite, each remote drop is connected via a single Ethernet cable to the central control cabinet housing the PAC. Partial commissioning of the WTP involved testing the PAC/HMI programs and confirming the input/output terminations to each remote drop. This commissioning step was conducted by BQE Water at the fabricators facility, allowing changes to be made easily in a controlled construction environment, which significantly reduced costs and disbursements.

The fully packaged containers were shipped to site after partial commissioning. Minimal site infrastructure was required to install the WTP at site, including:

1. Preparation of a level, crushed gravel pad for the WTP foundation.
2. Placement of the shipping containers.
3. Installation of the MCC into one of the fully packed shipping containers (a used MCC already at the mine was repurposed for the WTP).
4. Distribution of power from the MCC to the process equipment.
5. Installation of inter-container and battery limit piping.

The shipping container slated for housing the MCC was fast-tracked and shipped to site first to save time on the project schedule, allowing site construction activities to occur in parallel with local fabrication.

Operation

The underground dewatering phase began immediately after successful WTP commissioning and start up. Reagents were dosed into the system with effluent recycling back to the underground mine. Effluent was discharged into Silvertip Creek after three consecutive hourly assays met the discharge water quality targets. Figures 6 and 7 summarize the zinc and cadmium assays during WTP start up and underground dewatering, respectively. In Figure 6, the influent zinc concentration decreased over the first few days as a result of effluent recycle to the underground mine; the plant was treating and retreating water in a loop. The influent zinc concentration increased shortly after the effluent was directed to Silvertip Creek.

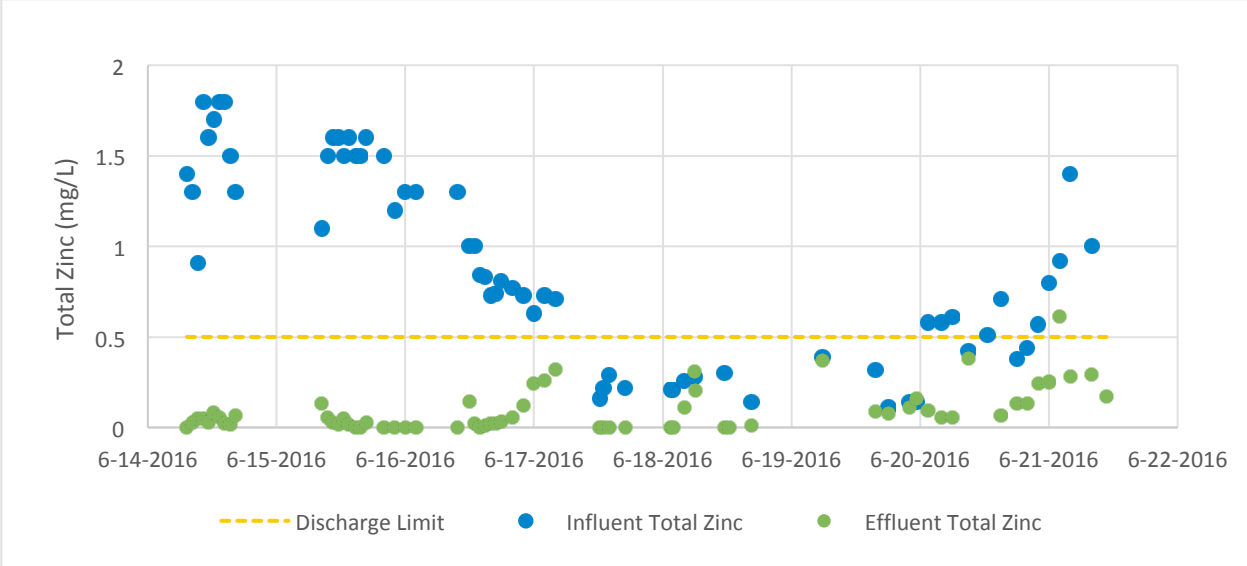


Figure 6: Hourly zinc assays following plant start-up

Figure 7 shows the effluent concentration for cadmium and zinc were well below the permit limit. Effluent assays were below targets for discharge permit, and other non-permitted elements met BC WQG.

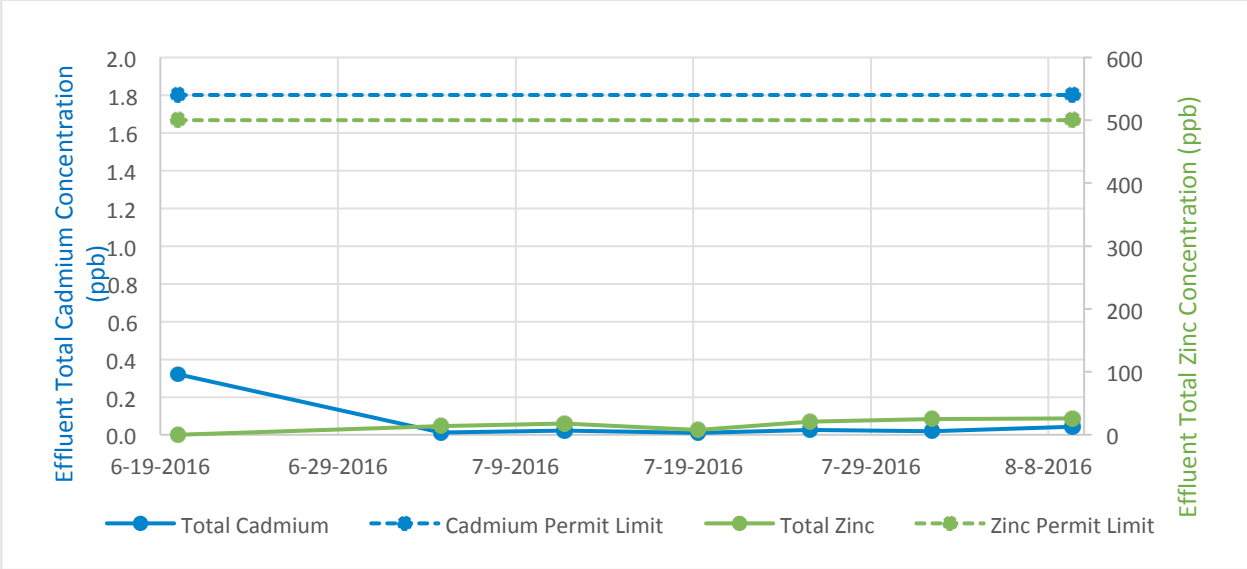


Figure 7: Weekly environmental discharge zinc and cadmium assays

Figure 8 illustrates the dewatering rate of the underground mine following start up on June 14, 2016. Initially, the average design treatment rate for the underground dewatering phase was 30 m^3/hr (or 720 m^3/day, 22,320 m^3/month). The bottlenecks limiting the overall treatment rate of the WTP during the mine-dewatering phase were:

1. Downtime associated with physically moving the dewatering pump deeper into the tunnels.
2. Lost hydraulic capacity from moving the pump deeper into the tunnels.

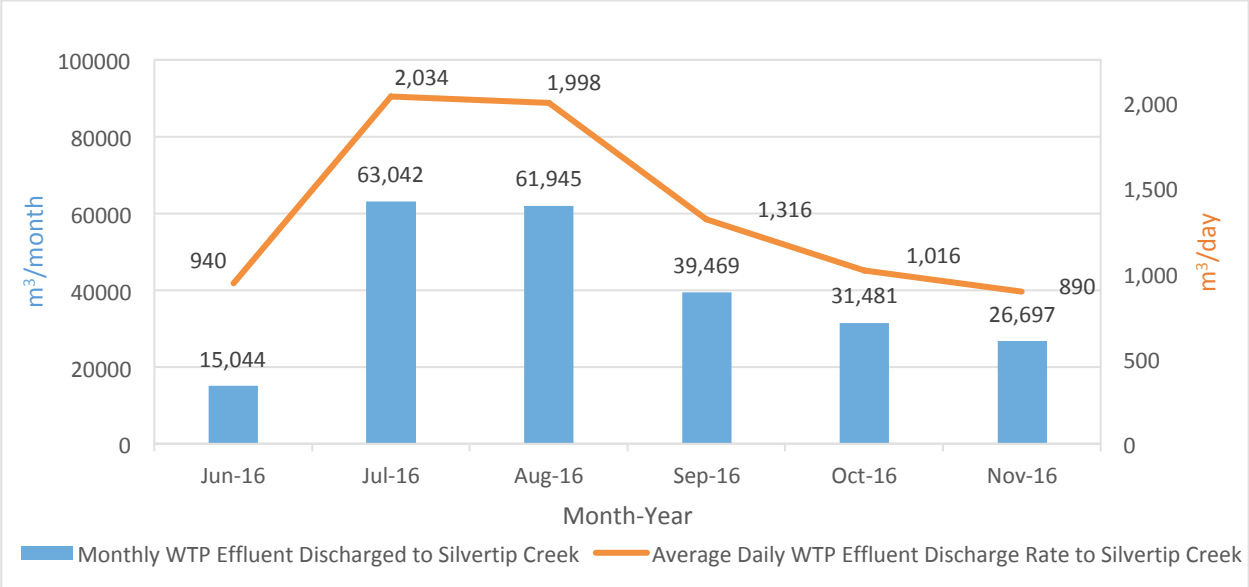


Figure 8: Dewatering rate of the underground mine

The treatment rate was initially high and decreased over time as a result of moving the pump deeper into the tunnels. The WTP transitioned to treating MCP water in Q4 2016, following the completion of the underground dewatering phase.

Capital Costs

Traditional cost factor analysis, where multiplication factors of 4 or greater are applied to the base equipment cost, does not provide accurate estimates for containerized plants. The integration of highly packaged equipment reduces the total amount of labour required to deliver the plant. In this case, highly packaged refers to systems that are structurally mounted to a frame and have some degree of process piping and electrical/instrument wiring already in place. These units only require power and inlet/outlet piping connections to be made prior to being ready for operation. Loose shipped equipment, on the other hand, requires substantially more work to incorporate into the shipping containers. Table 5 categorizes loose shipped and highly packaged equipment installed in the Silvertip WTP.

Table 5: Loose and highly packaged equipment in the Silvertip WTP

Equipment	Loose shipped	Highly packaged
Air compressor	×	
Tanks/Pumps/Agitators	×	
Flocculant makeup		×
Frac-tank clarifier		×
Lamella plate pack		×
Multimedia filter		×

Table 6 summarizes the installed cost factor for the containerized Silvertip WTP. A key component to the lower installed cost factor is the element of offsite construction. With an overall effort to reduce costs, this approach offsets the high labour rates of remote sites with lower labour rates in urban areas. Further, this eliminates the high cost associated with transporting and housing skilled labour for plant construction. The end result is a project where over 95% of the costs are incurred offsite, with the remaining costs a result of integrating the containerized WTP on site.

Table 6: Silvertip WTP cost factor analysis

Direct costs	$ CDN
Final WTP cost	1,700,000
Equipment cost subtotal	580,000
Installed cost factor	2.9

Conclusion

Sulphide precipitation is a very effective tool for achieving ultralow discharge limits in mining effluents, and due to its specific qualities of fast reaction time and high solids settling rates offers the possibility of a containerized mine water treatment design which:

- Minimizes capital costs and the need for skilled trades labour at remote sites projects.
- Reduces water treatment plant footprint.
- Reduces the quantity of residue produced during treatment and enables possible value recovery.

The Silvertip project was able to take advantage of all these benefits while paving the way for future ChemSulphide® process applications in British Columbia. The operational success at Silvertip removes the need for pilot demonstrations that would otherwise be required for treatment processes not yet implemented in the province. The reason that the Silvertip project was able to maximize the value generated by the ChemSulphide® process was because BQE Water was invited to participate in the project in the early stages of planning, before any major decisions about water treatment were made. As

an expert with a broad range of water treatment experience and technical capabilities, BQE Water helped reduce project risks and costs by accepting full responsibility for water in the project from the initial evaluation and bench-scale testing, through permitting, to the full-scale implementation.

References

Aubé, B. and Lee, D. 2015. The High Density Sludge (HDS) process and sulphate control, *Proceedings from the 10th International Conference on Acid Rock Drainage*, Santiago, Chile.

Aubé, B. and Zinck, J. 2003. Lime treatment of Acid Mine Drainage in Canada, *Proceedings of the Brazil-Canada Seminar on Mine Rehabilitation*, Florianópolis, Brazil.

Ashe, N., McLean, I., Nodwell, M. and Claridge, T. 2008. Review of operations of the BioSulphide® Process Plant at the Copper Queen Mine, Bisbee, Arizona, *Proceedings of International Symposium on Hydrometallurgy*, Phoenix, USA.

Consigny, A., Kratochvil, D. and Cote, J.C. 2015. Commercial scale novel approaches to water treatment at remote sites in extreme cold climates, *Proceedings of Mine Water Solutions in Extreme Environments*, Vancouver, Canada.

Kratochvil, D., Ye, S. and Lopez, O. 2015. Commercial case studies of life cycle cost reduction of ARD treatment with sulphide precipitation, *Proceedings of the 10th International Conference on Acid Rock Drainage*; Santiago, Chile.

Proceedings of Mine Water Solutions 2018
June 12–15, 2018, Vancouver, Canada
Published by the University of British Columbia, 2018

Mixing Zone Assessment for Mine Effluent Discharges in Receiving Waters: Challenges and Solutions through Best Practices

Mijanur R. Chowdhury, Minnow Environmental Inc., Canada
Cheryl Wiramanaden, Minnow Environmental Inc., Canada
Pierre Stecko, Minnow Environmental Inc., Canada
Kevin Martens, Minnow Environmental Inc., Canada

Abstract

The assessment of a mixing zone is an important component of the aquatic impact assessment of effluent discharges from different water management facilities (e.g., tailings ponds, sedimentation ponds, pit lakes) of proposed, existing, and legacy mines into receiving waters. A mixing zone is an area adjoining the discharge point where the water quality objectives for one or more parameters, based on chronic exposure, may be exceeded locally. Mixing zone assessment for a discharge entails the evaluation of its physical extent, and biological and chemical influence of the discharges in the zone. Different regulatory agencies provide standard technical guidance for conducting a mixing zone assessment by devising a field program and/or using modelling tools. However, there are key challenges associated with the practical application of the technical guidance using either approach (i.e., a field program or modelling); these challenges can be successfully navigated through the use of best practices.

This study describes several case studies of mixing zone assessments for different types of mine effluent discharges that include two types of discharge configurations (e.g., shore-line discharge through a channel and a multi-port diffuser), two receiving water types (lakes and rivers), and different chemical compositions of the effluent. Standard effluent plume delineation techniques, such as field tracer study (adding a tracer or using a tracer that is already present in effluent) and mixing zone models were applied in these studies. An analysis of the challenges and possible best practices to implement these studies in different mine sites are also presented. Further, research on the development of new modelling tools that will streamline the mixing zone assessment is identified.

Introduction

Sustainable discharge of mine water (effluent) from any proposed, existing, or legacy mine site with a positive water balance is a critical element of its water management plan. Such a discharge may occur from various water management facilities (e.g., tailings ponds, sedimentation ponds, pit lakes) of a mine site through different types of outlet structures, such as single-port pipelines, multi-port diffusers, or a channel. The receiving water environment can be in the form of a stream, river, lake, reservoir, or coastal water. Depending on the discharge configurations and receiving water flow characteristics, many of these effluent discharges do not mix instantaneously with the receiving water, resulting in mixing zones adjacent to the discharge outlet structure. A mixing zone is thus the portion of the receiving water body where the effluent concentration is progressively diluted by the receiving water until, at some distance from the discharge point, the applicable water quality objective (WQO) are satisfied for all parameters. It is considered a place where effluent is diluted with the receiving water, but the dilution is not viewed as treatment (USEPA, 1995). In this zone, criterion continuous concentrations (CCC), or WQO based on chronic exposure, are allowed to exceed without compromising chemical and biological integrity of the receiving environment. There are few states in the USA that allow the exceedance of criterion maximum concentrations (CMC), or WQO based on acute exposure, in the zone of initial dilution (IDZ, a small zone inside the mixing zone) for certain specific discharges. However, the majority of regulatory agencies in the US and Canada only allow the exceedance of CCC criteria (or a chronic WQO; Figure 1).

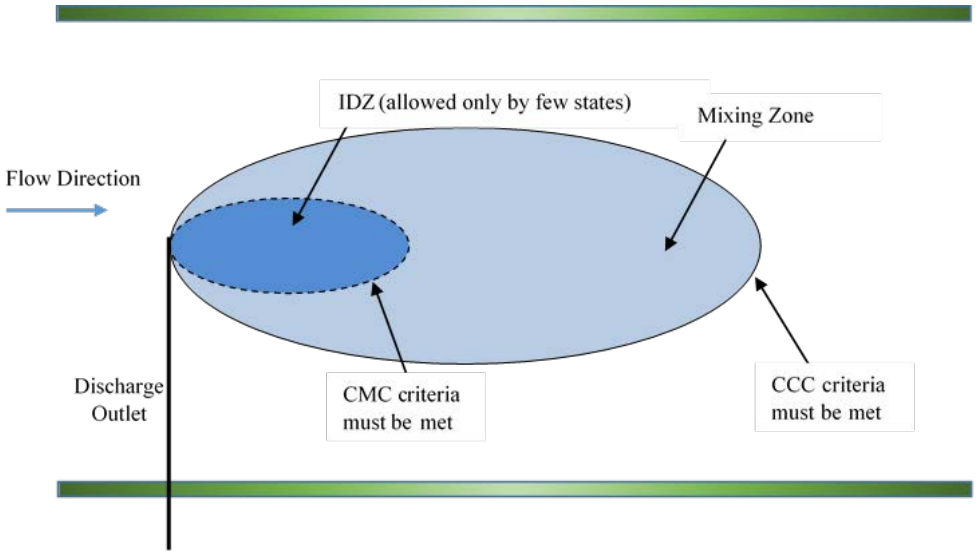


Figure 1: Illustration of a mixing zone (IDZ: zone of initial dilution, CCC: criterion continuous concentration, CMC: criterion maximum concentration)

A mixing zone assessment includes the evaluation of the physical extent of the effluent plume, and the biological and chemical influence of the discharge on the receiving environment. Standard technical

guidance to conduct the assessment is available from the relevant regulatory agencies in the USA (e.g., USEPA, 1995; USEPA, 1996) and Canada (e.g., Environment Canada, 2003; MDDEP, 2007). This study outlines the challenges and possible best practices to practically implement the technical guidance based on a number mixing zone studies that were recently undertaken for selected mining operations in Canada.

The major part of a mixing zone assessment is the evaluation of the physical extent of the zone, and concentration gradient of the effluent (percent effluent) inside the zone. The size of the mixing zone is dependent on the physical mixing processes of the effluent into the receiving water which generally occur into two distinct phases (Chowdhury and Testik, 2014): near-field and far-field mixing processes. In the near-field region (NFR), the discharged effluent experiences strong initial mixing, and the discharge conditions (e.g., discharge rates, angle, depth, and concentration) are the parameters that are most likely to have a major impact on effluent dilution. Far-field is where effluent mixing is more dominated or controlled by ambient water characteristics processes such as current, turbulence, and wave action.

The physical extent of the mixing zone is often evaluated through field work and/or modelling. Field work involves tracking the dispersion of effluent using a tracer that is either naturally present in the effluent or added for the duration of the test. Rhodamine WT, a fluorescent dye with low potential for toxicity or adverse effects in the aquatic environment, is the most preferred added tracer. An advantage of using tracers already present in the effluent is that they have an established equilibrium in the receiving environment (Environment Canada, 2003). Most mine effluents contain a variety of constituents that could potentially be used, such as sodium, chloride, magnesium, and conductivity, as they are generally considered to be conservative mixers. Several mixing zone assessment computer models, such as Visual PLUME (USEPA, 2003) and Cornell Mixing Zone Expert System (CORMIX; Doneker and Jirka, 2007) are available for this purpose. CORMIX is the only model that is frequently updated with new capabilities, and can be applied for a wide range of discharge environments. As such, it is widely used and a universally accepted model for mixing zone assessment. The CORMIX predicted effluent dilution and corresponding effluent parameter concentrations are considered to be accurate within +/– 50% based on extensive comparison with field and laboratory data (Doneker and Jirka, 2007). The required inputs for the CORMIX model included discharge characteristics (e.g., discharge flow rates, angle, discharge channel depth and width, and effluent density), receiving water characteristics (water density, mean depth, velocity, and Manning's parameter), and wind conditions (speed and direction). The CORMIX predicted effluent plume behaviour is dependent on the careful selection of these input parameters. It is best practice to evaluate the physical extent of the mixing zone using a combination of data from field studies and from modelling. A field tracing study can be conducted for given discharge and receiving water conditions, the results of which can be used to validate the model results. The validated model can then be used to evaluate the mixing zone for varying discharge and receiving water conditions. However,

conducting both field and modelling is not possible in all cases for various reasons (e.g., time constraints, associated costs). For a proposed mine, modelling is the only option as discharge is typically not yet occurring, and would not be until the commencement of mine operations.

The mixing zone assessment also includes an evaluation of changes in receiving water chemistry and biology due to the discharge. The discharged effluent should not be acutely toxic to aquatic life. The standard protocol for effluent toxicity testing is the WET (whole effluent toxicity test) in which samples of effluent are introduced to test organisms. The test analyzes the effluent sample on the basis of the number of test organism deaths after a specific exposure time period (CCME, 2016). The mixing zone assessment should also evaluate if a sufficient zone of passage is preserved for fish or other organisms to migrate through or around the mixing zone. However, there is no consensus on how to define avoidance thresholds for mixing zones (IDEQ, 2000). The standard practice is based on research on the avoidance behaviour of native fish to chemical parameters (typically metals) in the mixing zone. Risk of adverse bioaccumulative effects should also be evaluated if the effluent contains bioaccumulative compounds (e.g., mercury and selenium). Bioaccumulative effects are typically assessed using the tissue residues of native periphyton, benthic macroinvertebrates, and fish that are collected from upstream and downstream of the discharge (IDEQ, 2000).

This study describes the mixing zone assessments that were recently conducted for effluent discharges from a number of mine sites in different parts of Canada:

- Mixing zone assessment for existing effluent discharges from two closed mines located in north-east, ON into two large lakes (Figure 2 and 3): both mines discharge excess water from their respective tailings basins via a channel (shore-line discharge) into two large lakes (Lake 1 and Lake 2). Prior to discharge into the lake, the effluent is treated to meet the discharge criteria in their respective effluent treatment plants (ETP). These studies were conducted for two different purposes; however the objective of delineating the mixing zone remained the same.
- Mixing zone assessment for an existing effluent discharge from an operating mine site located in British Columbia through a multi-port diffuser into a large flowing river (Figure 4): the discharge occurs from the mine tailings pond through a 5.4 m long, 10-port diffuser that extends 130 m into the middle of a large flowing river in BC, and approximately longitudinally in the river with the ports pointing downstream in a line oriented nearly parallel with the river flow.



Figure 2: Shore-line discharge through a meandering channel into a large lake (Lake 1). Delineated effluent plume is also shown.
(Details of the effluent plume are provided in the later sections)

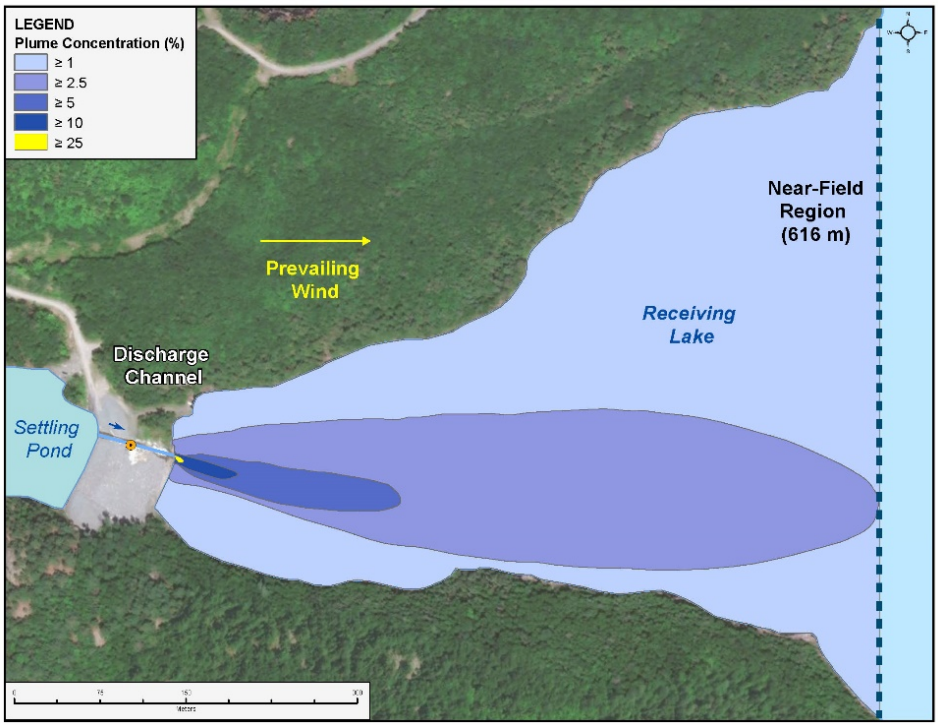


Figure 3: Shore-line discharge through a steep channel into a large lake (Lake 2). Delineated effluent plume is also shown (details of the effluent plume are provided in the later sections)

The above studies at different mine sites rendered a unique opportunity to analyze the implementation of the mixing zone assessment in diverse situations, for example discharge from different mine sites, through different configurations (channel and a multiport diffuser), into two types of receiving environment (rivers and lakes). This manuscript provides a description of the methods used for these studies, followed by results and conclusions.

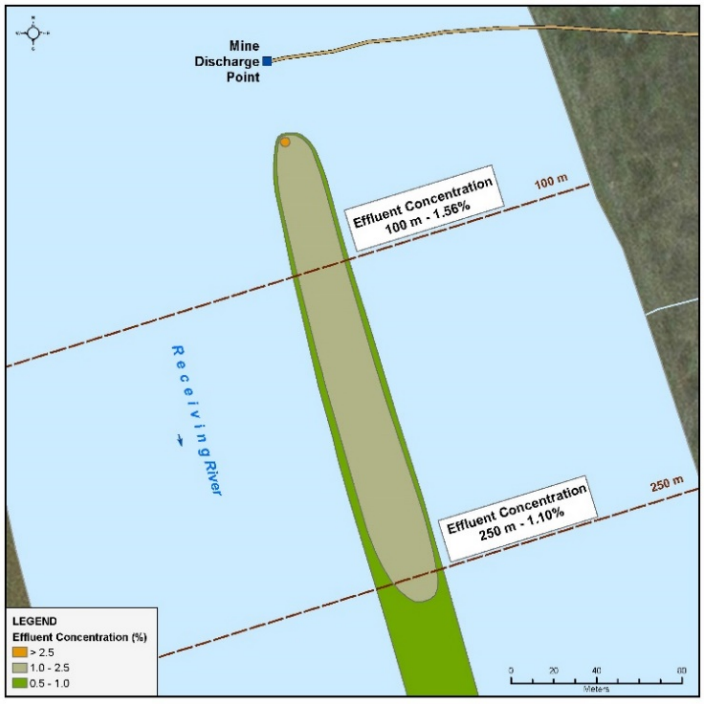


Figure 4: Discharge through a diffuser into a large flowing river. Delineated effluent plume is also shown (details of the effluent plume are provided in the later sections)

Methodology

Methods for the Shore-line Discharge into Lake 1

The mixing zone assessment study for the discharge into NE Ontario Lake 1 involved both field work and modelling. First, a dye tracing field study was conducted to delineate the mixing zone for a constant discharge rate of treated effluent. Then, the mixing zone was assessed for treated and untreated effluent under various effluent discharge and receiving water conditions using CORMIX modelling.

The methodology of the dye study involved continuous Rhodamine WT dye injection at the effluent discharge location, and the measurement of the dye concentration at different downstream locations of the effluent creek, and in the localized receiving lake water. During the dye injection period, treated effluent discharge was controlled to a flow of 120 L/s and the dye is injected at a rate of 75 mL/min following the technical guidance (Environment Canada, 2003).

The observed effluent plume behaviour in the dye tracing field study was first used to validate the CORMIX model prediction for the discharge. CORMIX3, the CORMIX sub-model for a surface channel discharge system, was used to determine the extent of the effluent plume to various dilution factors (i.e., 50%, 25%, 10%, 5%, 2%, and 1%) for the discharge during the dye study. Once validated, the model was used to delineate the plume for treated and untreated effluent for various discharge and receiving water conditions. The most dominant input parameters that influence the effluent plume behaviour in the CORMIX3 simulations were effluent discharge rates, effluent and receiving water density, and receiving water flow condition, which were determined through field program or based on monitoring data. The current discharge rates for treated effluents were supplied by the mines, while the possible future discharge rates were obtained from a separate water balance study. The density difference between effluent and receiving water dictates whether the effluent will be a floating or sinking plume. The densities of the effluent and the receiving water are a function of temperature and solid concentrations (dissolved and suspended). Total suspended solid (TSS) concentration was considered to have nominal effect on the density of the effluent and receiving water as their TSS concentration were observed to be very low. The density of effluent and receiving water was determined, using the estimated total dissolved solids (TDS) concentrations and a representative temperature, for the respective seasons during the discharge period (i.e., spring, summer, and fall). As no direct measurements of TDS concentrations were available, they were estimated from measured specific conductance, using the standard relationship between specific conductance and TDS (APHA 1999). The specific conductance and temperature of effluent and receiving water were measured by deploying temperature loggers (U22-001, HOBO) and conductivity loggers (HOBO U24 Conductivity Logger) in the effluent creek and the receiving water. During the three discharge seasons, the calculated effluent density was lower than the calculated density of the receiving lake surface water. As such, it is expected that the effluent plume would float on the water surface during the three discharge seasons.

Lake circulation and surface water current patterns were recorded using drogues equipped with global positioning system (GPS) tracking units. Temporal and vertical variations of water current (speed and direction) were also measured using an upward looking RDI 1200 kHz, 4-beam Workhorse Sentinel ADCP (acoustic Doppler current Profiler) (RD Instruments, 1996). While the drogue study provided Lagrangian surface water velocity and direction (i.e., at different spatial positions) as the drogues moved, ADCP provided Eulerian velocity (i.e., at a fixed point). The observed path of the drogues indicated a general unidirectional surface water current pattern driven by the prevailing wind in the localized receiving lake water. The dominant unidirectional surface current and the absence of any distinctive circulation pattern were probably due to the limited fetch in this area, as the area is sheltered by an island and a peninsula to the west of the effluent creek outlet. Based on the drogue study and analysis of ADCP

data, the surface water current was determined to be about 1% of the wind speed which is consistent with the well-established principle that lake surface water velocity is generally 1 to 3% of wind speed (Wetzel, 2001). A statistical analysis of long-term hourly meteorological data showed that the local wind direction is predominantly from the west and northwest directions, and the average of mean hourly wind speed was in the range of 2.5 to 3.1 m/s. As such, the water current was taken as 2.5 cm/s for CORMIX modelling of average receiving water condition.

The discharge depth and average depth of the lake was determined from the lake bathymetry. A typical Manning's Coefficient for lakes, a measure of the roughness of the lakebed, was used (0.015). This value is commonly used in modelling similar lake environments.

Methods for the Shore-line Discharge into Lake 2

The scope of the Lake 2 mixing zone assessment study was to estimate the metal concentrations in the NFR of Lake 2 using an appropriate modelling technique. As no field program was undertaken, the modelling input parameters were determined based on appropriate assumptions. Also different from the Lake 1 study was that the discharge occurs year round, while the discharge in Lake 1 only occurred in open-water season (spring, fall, and summer). As such, the complexity associated with the effluent plume behaviour in ice-covered receiving environments needed to be included.

A mixing zone assessment was conducted using CORMIX3, and the effluent buoyancy in the open water season was estimated following the similar procedure of Lake 1 study, i.e. based on the density difference between the effluent and the receiving lake water which was estimated based on temperature and specific conductance. As no monitoring data for the receiving water temperature were available, it was assumed to be 1^{o}C less than the effluent temperature for the three open water seasons (spring, summer, and fall). This assumption was based on the observation in Lake 1 study, and the fact that the average effluent temperatures were more than 0°C in winter, while the receiving lake was frozen, suggesting that effluent temperature is generally higher than the receiving lake water. During the three open water seasons, the calculated effluent density was lower than the calculated density of the receiving lake water. A different approach was undertaken to estimate the effluent buoyancy in the winter, as the lake is generally ice-covered in the winter, and the CORMIX model does not have the capability to simulate the ice-covered scenario. In an ice-covered lake, the water temperature just below the ice-cover is expected to be just over 0°C, and increases with depth to a final water temperature of maximum density (4°C; Bengtsson, 2012). As the warm effluent flows into the receiving lake, the ice cover was assumed to melt uniformly over the depth of the ice-cover due to heat carried by the warmer effluent. The effluent plume is then expected to sink (due to its higher density than the water density just below the ice-cover) to a depth where the receiving water density becomes equal to the effluent density. The depth was

assumed to be 2 m under ice (i.e., 3 m including 1 m of ice). At this depth, the effluent plume was assumed to spread predominately horizontally like the surface water plume during the open water season.

The average depth of the lake was assumed to be 6 m for the open water season, which is consistent with bathymetry near the discharge location. It was assumed that the ice-cover thickness would be 1 m in winter. As described, the effluent plume is expected to first melt the ice at the surface, and then sink to a depth where the receiving water density becomes equal to the effluent density. The depth was assumed to be 2 m under ice (i.e., 3 m including 1 m of ice). Therefore, the winter season was represented by decreasing the total lake depth in the CORMIX3 model by 3 m.

Similar to Lake 1 study, the water velocity of Lake 2 surface water during the open water season was assumed to be equal to 1% of the prevailing wind speed. During the winter, the receiving Lake 2 water velocity at 3 m depth was assumed to be near stagnant (0.5 cm/s). The maximum water velocity of an ice-covered lake is typically in the range of 1 to 3 cm/s due to convective circulation and wind-driven tilting of ice-cover (Bengtsson, 2012). As such, the assumed 0.5 cm/s water velocity was a conservative assumption.

Methods for the Discharge through a Diffuser into a Large River

Mixing zone assessment for the discharge was conducted using a conductivity-based plume delineation technique (i.e., an existing tracer). The conductivity-based plume delineation was conducted using a YSI EXO-series sonde (YSI Inc., Yellow Springs, Ohio), which is equipped with a Geographic Positioning System (GPS) and has data logging capabilities. Specific conductance measurements were logged at 0.5-second intervals as transects were completed through the effluent mixing zone, with the sonde held approximately 0.5 m below the surface. Effluent specific conductance data for the same day were provided by the mine for determining relative dilution within the river. Specific conductance measurements from upstream of the discharge were used to identify background conditions. Average river discharge was obtained from the Water Survey of Canada. Based on the specific conductance data, effluent concentrations at each logged location within the mixing zone were calculated using the following equation:

$$\% \text{ Effluent Concentration} = \frac{SC_{measured} - SC_{reference}}{SC_{effluent} - SC_{reference}} \qquad \text{Equation 1}$$

Where:

$SC_{measured}$, $SC_{reference}$, and $SC_{effluent}$ are specific conductance at the measured location, upstream location (i.e., background), and of discharged effluent respectively.

A titration of effluent in receiving environment water was completed using samples collected to determine an appropriate correction factor to apply to specific conductance measurements. This was

completed as measurements do not exactly reflect the actual concentration in the river, and applying a correction factor results in a more accurate in-situ effluent concentration. The actual dilution of specific conductance within the river was calculated using the percent effluent measured followed by correction using the equation derived from the laboratory titration results.

Results

Assessment for the Lake 1 Study

The dye study was used to delineate the treated effluent plume as well as to validate the CORMIX model. As the effluent travels through a long meandering channel (referred to as effluent creek, Figure 2), the effluent was observed diluted to 50% effluent at the mouth of the creek. The plume was dispersed in the east and southeast direction driven by wind during the delineation period, and the effluent discharge created a shore-line attached plume. The CORMIX predictions for the plume extent were determined in the receiving lake environment, and were in good agreement with the dye study observations. Note that the discharge through the channel into Lake 1 is complex as the channel protrudes about 10 m into lake and has an oblong discharge configuration. CORMIX3 model has not been validated with such discharge configuration. As such, the close agreement is encouraging.

Simulations were performed with the validated model for the other scenarios with 100% effluent plume at the outlet of effluent creek, which was conservative based on the dye study. The effluent was predicted to be positively buoyant and to remain at the water surface throughout the dispersing periods because the effluent density was less than that of the receiving water. Due to wind-driven vertical mixing, the effluent plume penetrated to a maximum 1.5 m from the water surface.

The prevailing wind speed and the effluent discharge flow rates were the two dominant factors that played a key role on the dilution of discharged effluent. Under prevailing wind conditions (i.e., with wind speed of 2.5 m/s from the west and northwest direction) the predicted effluent plumes were shore-line attached, which agreed with the observations in the dye study. Under these conditions, the effluent plume is predicted to be diluted to 1% within a 1.5 km longitudinal extent, provided that the effluent discharge rate does not exceed 0.2 m^3/s (200 L/s; Figure 2). When the effluent discharge rate increased to 0.3 m^3/s (300 L/s), the effluent was predicted to be diluted to 1% in about 2.5 km. When the effluent discharge rate exceeds 0.4 m^3/s, the effluent plume was not expected to be diluted to 1% within the available longitudinal extent of the receiving environment in the east and southeast direction (i.e., within 3.8 km, which is the distance between the effluent creek and the receiving lake outlet). When the effluent discharge rate is 0.5 m^3/s and 0.8 m^3/s, the maximum dilution factors within the receiving lake were predicted to be 5% and 10% respectively.

Assessment for the Lake 2 Study

CORMIX mixing zone modelling delineated the predicted effluent plume in Lake 2 for effluent from the TMA under maximum and average discharge rates, seasonal receiving water, and various wind conditions. The effect of seasonal effluent and receiving water temperature changes on effluent dilution in Lake 2, the receiving lake, were evaluated by running simulations representing four seasonal input conditions. For the three open-water seasons, the predicted effluent was positively buoyant and remained at the water surface throughout the dispersing periods because the effluent density was less than that of the receiving water (Figure 3). Wind-driven vertical mixing was predicted to cause the effluent plume to penetrate to a maximum 3.5 m from the water surface. The effluent dilution in the winter is approximately half that of the open water seasons, as the ambient water velocity was assumed to be much lower (0.5 cm/s) compared to open water season (e.g., 2.5 cm/s under average wind conditions).

The prevailing wind speed and the effluent discharge flow rates were the two dominant factors that played a key role on the dilution of discharged effluent. For example, under prevailing wind conditions (i.e., with wind speed of 2.5 m/s from the west and northwest direction), the effluent plume in the summer was predicted to be diluted to 3.3% and 2.5% at the edge of the NFR under maximum and average discharge rates extending 1,107 m and 617 m into the lake respectively.

Assessment for the BC River Study

Laboratory titrations of effluent against the receiving river reference water confirmed that calculated effluent concentration (% effluent) using Equation (1) based on field measurements of specific conductance overestimate the actual effluent concentrations within the mixing zone by approximately 33% (Figure 5). A correction equation was derived using the titration results for effluent concentrations up to 7% effluent (the approximate in-situ range), which is:

$$\text{actual \% effluent} = 0.6637 * \text{calculated \% effluent} \qquad \text{Equation 2}$$

The potential reason for the non-conservative behaviour of conductivity documented by the titration results was identified. In an ideal solution (e.g., a solution of ions at infinite dilution), conductivity (or specific conductance, which is a temperature-normalized measure of conductivity) is directly proportional to the concentration of ions (electrolytes). As the concentration of electrolytes increases, interactions between ions start to occur (e.g., the formation of ion pairs; Morel, 1983); this has the effect of retarding conductivity (Smedley, 1980) such that conductivity is no longer directly proportional to ion concentration (Atkins, 1994). When two waters mix (e.g., a concentrated effluent solution into a more

dilute freshwater receiving environment as is the case with the discharge of mine effluent into the river), although the concentrations of ions in the concentrated solution become proportionately diluted, conductivity may not.

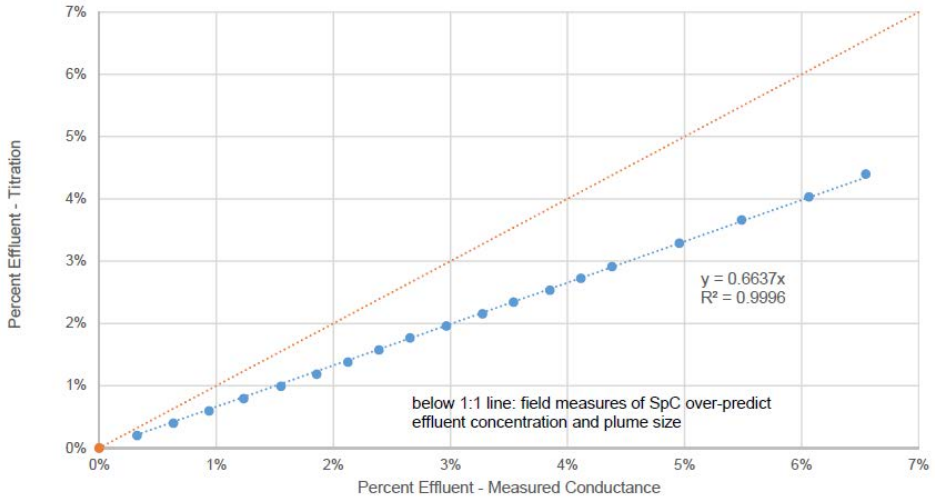


Figure 5: Results of effluent – receiving river water laboratory titrations relative to a 1:1 dilution (orange line)

Based on the calculation of percent effluent using specific conductance followed by correction for non-conservation measurement, it was determined that 1% effluent plume (100:1 dilution) was detectable 263 meters downstream (Figure 4). At 100m from discharge, measured effluent concentration was 1.6% (66:1 dilution), while the effluent concentration at 250 m was 1.1% (91:1 dilution). The maximum recorded effluent concentration during the delineation was 3.1% (32:1 dilution) measured 38 m from the discharge.

Conclusions

This paper presented the results of mixing zone assessments for three different types of mine effluent discharges from two closed and one operating mine sites. A comprehensive study that includes both modelling and field works was undertaken to evaluate the mixing zone for the discharge through a meandering channel into Lake 1. The study showed that the CORMIX3 model with validation through the field study can simulate the effluent plume from a protruding channel discharge with complex oblong discharge configuration. A CORMIX modelling study was conducted to evaluate the mixing zone from a steep channel discharge into Lake 2. As no field program was undertaken in this study, model input parameters were selected with appropriate assumptions that demonstrate the challenges to conduct a modelling study without validation through a field study. This study also shows the limitation of current available models to simulate the discharge in ice-covered receiving water. While the field program for Lake 1 mixing zone assessment involved tracking the effluent dispersion with an added tracer, the

assessment for the discharge through the diffuser into the river involved field study with existing tracer (specific conductivity). The latter study demonstrates the necessity for conducting a laboratory titration when specific conductivity-based plume delineation technique is implemented.

These mixing zone studies showed that there is a need for an improved modelling tool to assess the physical mixing zone size for a wide range of situations, especially in an ice-covered receiving environment. The current available mixing model (e.g., CORMIX) only provides the dilution or percent effluent, based on which the concentrations of chemical parameters are estimated. As such, the possible metal specific transport-transformation is not often taken into account for mixing zone assessment. A mixing zone model which can simulate both aspects (physical dispersion and chemical transformation) would streamline the mixing zone assessment greatly, and perhaps will allay the fear of some organizations (e.g., C-SAW, 2003) about the negative consequence of mixing zone approval by regulators.

Acknowledgements

We would like to thank the mines that have contributed to this work.

References

APHA (American Public Health Association). 1999. *Standard Methods for the Examination of Water and Wastewater*. Washington, DC: APHA.

Atkins, P.W. 1994. *Physical Chemistry*. Oxford: Oxford University Press, UK.

Bengtsson, L. 2012. Ice covered lakes, in L. Bengtsson, R.W. Herschy and R.W. Fairbridge (eds.) *Encyclopedia of Lakes and Reservoirs:* 357–360, New York: Springer-Verlag.

C-SAW (Campaign to Safeguard America's Water). 2003. T*he mixing zone manual – how to stop the dilution-solution*. Campaign to Safeguard America's Water, Alaska.

CCME (Canadian Council of Ministers of the Environment). 2016. *Water Quality Guideline for the Protection of Aquatic Life*. Canadian Council of Ministers of the Environment.

Chowdhury, M.R. and Testik, F.Y. 2014. A review of gravity currents formed by submerged single-port discharges in inland and coastal waters, *Environmental Fluid Mechanics* 14(2): 265–293.

Doneker, R.L. and Jirka, G.H.. 2007. *User's Manual for CORMIX: A Hydrodynamic Mixing Zone Model and Decision Support System for Pollutant Discharges into Surface Waters*. US Environmental Protection Agency, Technical Report EPA-823-K-07-001.

Environment Canada. 2003. *Revised technical guidance on how to conduct effluent plume delineation*. National Environmental Effects Monitoring Office. Gatineau, Quebec.

Environment Canada. 2012. *Metal Mining Technical Guidance for Environmental Effects Monitoring*. ISBN 978-1-100-20496-3.

Government of Canada. 2012. *Consolidated Metal Mining Effluent Regulations (MMER)*. SOR/2002-222. Current to December, 2016.

IDEQ (Idaho Department of Environmental Quality). 2000. *Evaluation of Proposed New Point Source Discharges to a Special Resource Water and Mixing Zone Determinations*: Thompson Creek Mine Facility, Upper Salmon River Subbasin, Idaho.

Ministère du Développement durable, de l'Environnement et des Parcs (MDDEP). 2007. *Calculation and interpretation of effluent discharge objectives for contaminants in the aquatic environment, 2nd Edition, Quebec*. Ministère du Développement durable, del'Environnement et des Parcs, Direction du suivi de l'état de l'environnement.

Morel, F.M.M. 1983. *Principles of Aquatic Chemistry*. Toronto: John Wiley and Sons, Toronto, Canada.

RD Instruments. 1996. *Acoustic Doppler Current Profiler: Principles of operation a practical primer*. San Diego, California. Available at http://rdinstruments.com/

Smedley, S.I. 1980. *The interpretation of ionic conductivity in liquids*. New York: Plenum Press.

USEPA. 1995. *EPA Region VIII Mixing Zones and Dilution Policy*. Denver, CO: US Environmental Protection Agency, Region 8, Water Management Division.

USEPA. 1996. *Memorandum: EPA Guidance on Application of State Mixing Zone Policies in EPA-Issued NPDES Permits*. US Environmental Protection Agency. Memo from Robert Perciasepe to Water Program Directors, dated August 6, 1996.

USEPA. 2003. *Dilution Models for Effluent Discharges*, 4th Edition (Visual Plumes). EPA/600/R-03/025. Athens, Georgia: US Environmental Protection Agency, Ecosystems Research Division.

Wetzel, R.G. 2001. *Limnology: Lake and river ecosystems*. San Diego, California: Academic Press.

Proceedings of Mine Water Solutions 2018
June 12–15, 2018, Vancouver, Canada
Published by the University of British Columbia, 2018

In-Situ Treatment of Arsenic in a Pit Lake – A Case History

Adam Whitman, Meridian Beartrack Company, USA
Tom Patterson, SLR International, USA

Abstract

Treatment and discharge is a fairly common element of mine water management plans. During closure and the post-closure period, it is preferable to eliminate or minimize treatment requirements. The former Royal Mountain King (RMK) Mine in California, USA, in closure since 1994, requires long-term active water management. The water management plan includes storage of mine water in a pit lake with seasonal release of pit lake water under a discharge permit. The constituents of concern are Total Dissolved Solids (TDS) and arsenic. To manage TDS, water is discharged using an automated system that precisely proportions the discharge flow to the flow of the receiving stream, so that receiving water standards are met. Arsenic can largely be managed in the same way, but because of pit lake concentrations and effluent limits, it controls how much water can be discharged. Therefore, reducing pit lake arsenic concentrations is necessary to maximize water released from the pit each year.

An in-situ treatment process for the pit lake was developed and has been in use since 2011. The treatment process is based on mixing a solution of ferrous sulphate into the pit lake. Treatment has been effective in reducing the arsenic concentration from 120 µg/L to less than 50 µg/L, which is approximately the concentration where TDS controls the discharge. Since 2011, there have been several refinements and improvements to the process, and some challenges to overcome. This paper describes the water management and treatment processes, and identifies some of the more noteworthy refinements and solutions to challenges that we have experienced. In particular, this paper provides a discussion of the influence of pit lake stratification and arsenic speciation on the performance of treatment.

Introduction

Treatment and discharge is a common element of many mine water management plans. During closure and the post-closure period, it is preferable to eliminate or minimize treatment requirements.

Mining was completed at the former Royal Mountain King (RMK) Mine near Copperopolis, California, USA, in 1994. Closure and reclamation was initiated and continues to the present day. Due to

residual ground and surface water quality issues unique to the region, seepage and leachate from several closed mine waste management units is collected and stored in one of the former open pits of the mine (Skyrocket Pit Lake; see Figure 1) and is discharged seasonally along with excess water that naturally flows into the pit lake. The excess water in the pit is discharged to a nearby stream (Little Johns Creek) during high flows, and the flow of the discharge is proportional to the flow in the stream, so that water quality in the stream is protected. Figure 1 illustrates a schematic of the water management system for the closed mine.

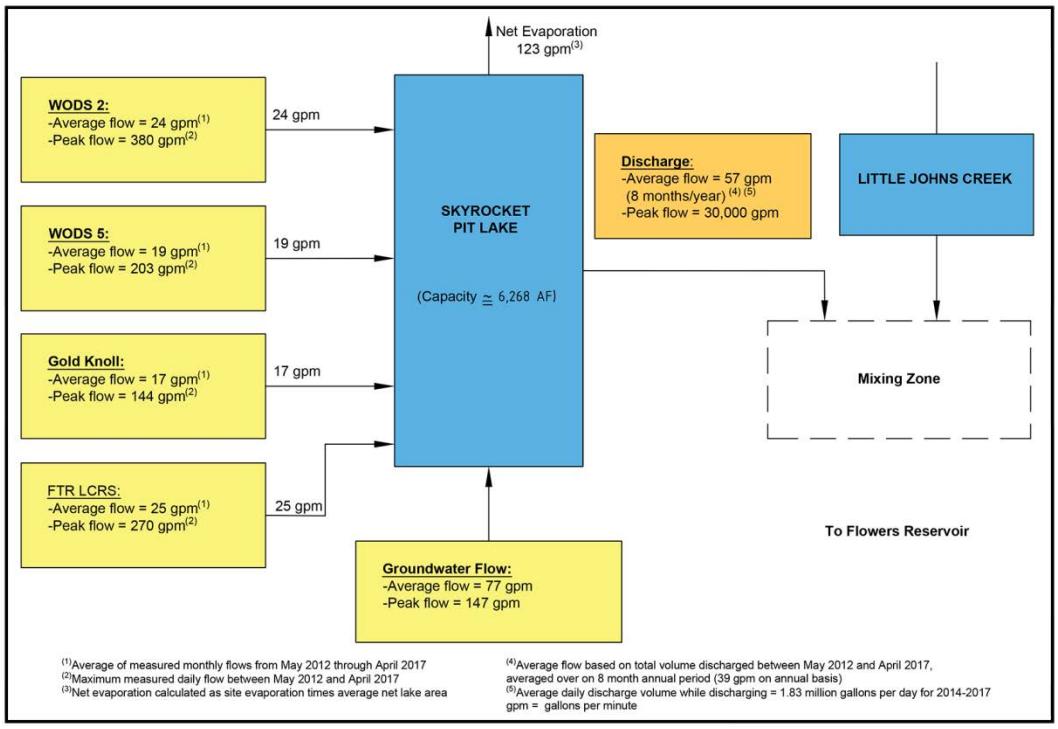


Figure 1: Water management schematic

The water is discharged from the pit lake under a National Pollutant Discharge Elimination System (NPDES) permit. Discharge limits for arsenic primarily control the allowable rate of discharge.

The primary sources of arsenic in the pit lake are groundwater inflows and possibly oxidation of sulphide minerals in the pit walls. Therefore, control of arsenic by treating or otherwise managing the seepage and leachate water being transferred to the pit lake would be ineffective. Because the mine is in closure and passive, low maintenance management of the site is preferred, and in-situ batch treatment of arsenic in the pit lake was evaluated.

In the summer of 2010, Meridian Beartrack Company implemented a pilot study to test an in-situ arsenic removal process for Skyrocket Pit Lake. The process selected for pilot testing was in-situ treatment by addition of ferrous sulphate solution after Vogels and Johnson (1998). The ferrous ions

oxidize to ferric ions in the pit lake, and the ferric ions react with arsenate to form an insoluble salt. The insoluble salt and dissolved arsenic are co-precipitated with ferric hydroxyoxides formed by excess of ferric ion in the pit lake water. The pilot test was successful and allowed development of a full-scale process that was implemented in 2011, and has been in use periodically to the time of writing this paper.

This paper describes the treatment process, and identifies some of the more noteworthy refinements and solutions to challenges that have been experienced.

Site Conditions

Skyrocket Pit Lake is approximately 55 acres in area and approximately 350 feet deep. The volume of the pit lake is approximately 5,700 acre feet (1.86 billion gallons). Vertical profiling of electrical conductivity (EC), temperature, and dissolved oxygen indicates that there is a shallow seasonal thermocline and a pycnocline that was assumed to be permanent at a depth of approximately 185 feet (Figure 2). Below the pycnocline, conditions are anoxic, and the EC and arsenic concentrations are higher.

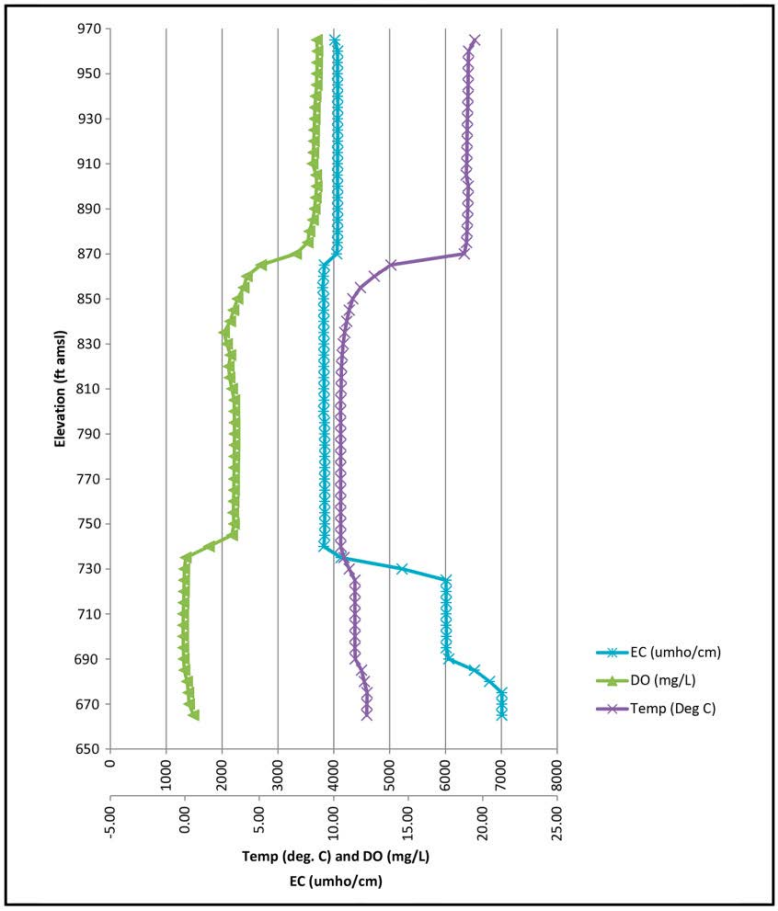


Figure 2: October 2009 depth profiles

Little Johns Creek is an ephemeral drainage, except in the area immediately in the vicinity of the pit and downstream for approximately one mile, where it is perennial. Flows in Little Johns Creek in the vicinity of the RMK mine vary from near zero during the late summer and fall, to daily averages over 165 cubic feet per second (75,000 gallons per minute; 4,670 litres per second) during extreme flood flows.

Treatment Testing

Bench-scale testing performed by MBC showed that ferrous sulphate could be effective in reducing dissolved arsenic levels. The bench-scale testing indicated that approximately 10 mg/L of ferrous sulphate reduces the arsenic concentration in pit lake water to near non-detect levels.

The bench test results were used to develop a pilot test of in-situ treatment of the pit lake. The pilot test program occurred over a period from August 8, 2010 to February 6, 2012. The pilot test successfully demonstrated that arsenic could be removed from the pit lake water, and data from the pilot test were used to develop a full-scale system.

Description of the Treatment Process

Figure 3 shows the layout of the treatment system equipment and Figure 4 shows the process flow diagram.

The system consists of an 8" HDPE intake pipe laid on the ground surface. The intake pipe is connected to the suction side of a 1,800 gpm capacity diesel-powered pump. An 8" HDPE discharge line is connected to the discharge side of the pump, and is equipped with an in-line magnetic flow meter. The discharge line extends approximately 50 feet into the pit lake (i.e., away from the shoreline), and the end of the discharge line is capped with an 8" × 4" reducer to increase the velocity of the discharge into the pit lake to promote rapid mixing of pit water with the reagent.

A 500 gallon mixing/day tank is used to mix and store the reagent feed solution. The reagent solution is conveyed from the day tank into the discharge line with a metering pump at a flow rate of 2 gpm.

A 10% reagent feed solution is prepared each day using 420 gallons of pit lake water and 7 bags (50 lbs. each) of ferrous sulphate heptahydrate ($FeSO4 \cdot 7H2O$). The pH of the reagent water is adjusted below 4.5 with hydrochloric acid prior to adding the ferrous sulphate to slow the oxidation in the mix tank.

After mixing, the concentration of iron in the discharge line going into the pit lake is approximately 20 mg/L. Assuming a 10-fold dilution in the occurring at the pipe outlet in the pit lake, the concentration of iron in the reaction zone is estimated to be on the order of 2 mg/L. This concentration is one-fifth of the 10 mg/L dose demonstrated in the bench tests to be 100% effective at removing arsenic. This lower dose is based on observed performance and in consideration of keeping reagent usage to a minimum.

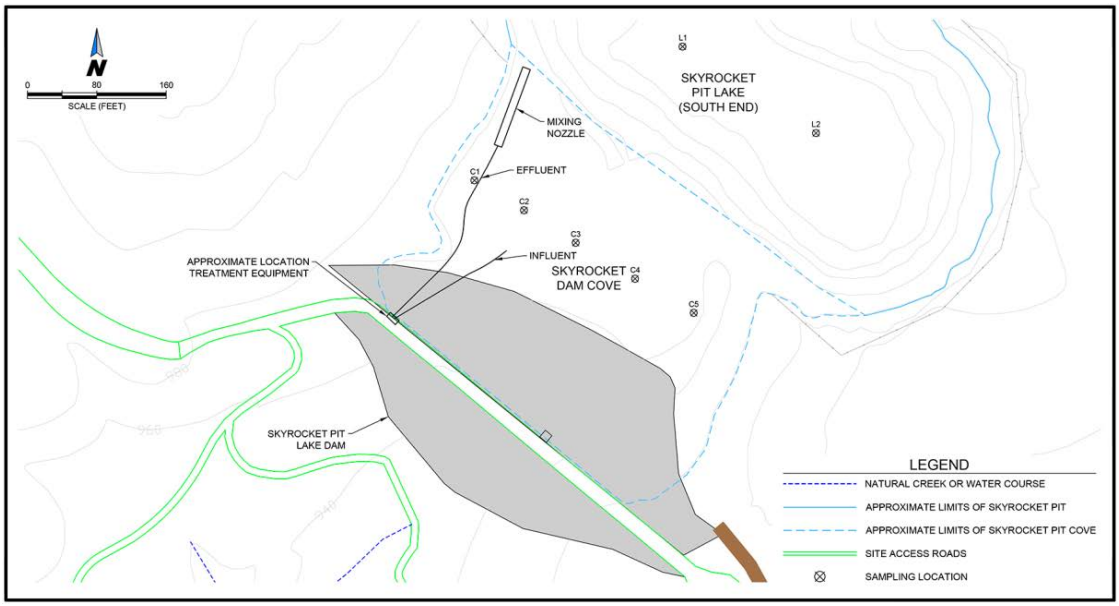


Figure 3: SRP equipment layout and sampling locations

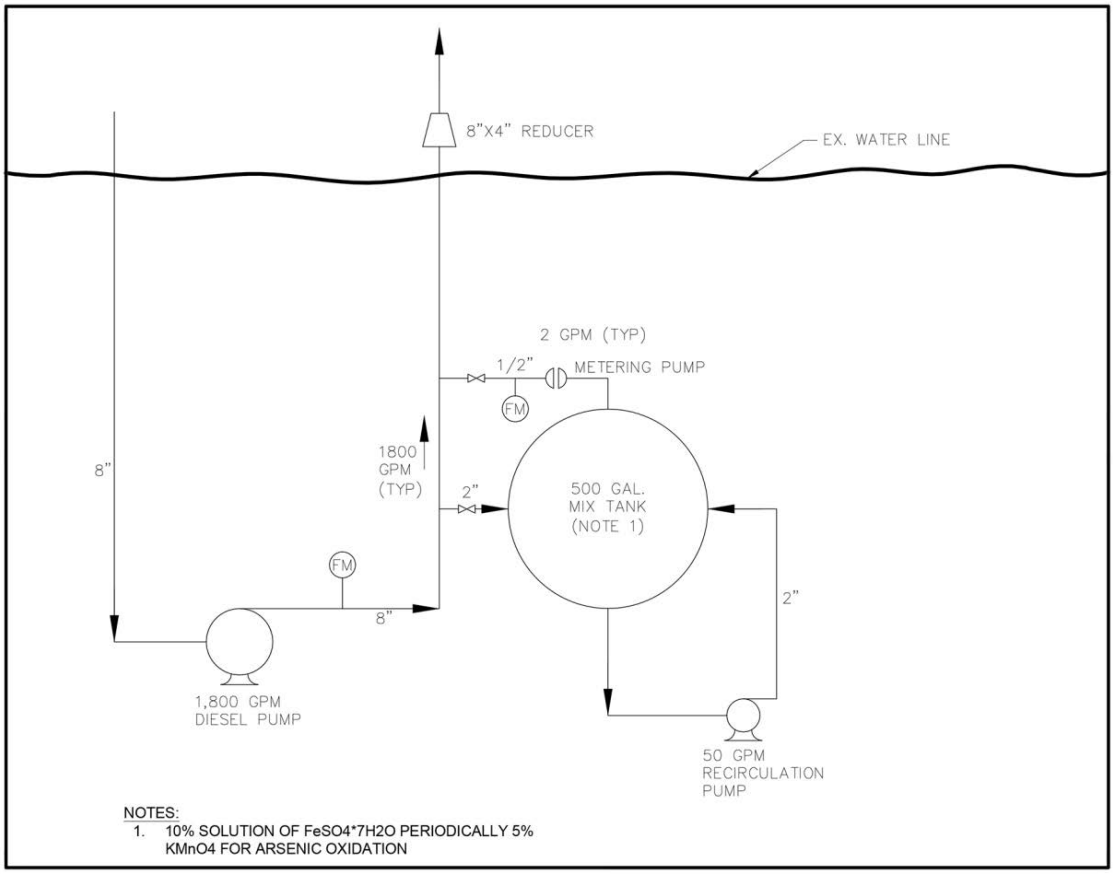


Figure 4: SPL treatment system process diagram

Operations

Water can be discharged from Skyrocket Pit Lake to Little Johns Creek only when conditions in the creek allow. This includes a high flow (greater than 1,000 gpm) and low TDS (less than about 200 mg/L). These conditions only occur during the wet season (i.e., November through April or May). The treatment system is operated for a few weeks to a couple of months prior to this discharge season. Typically, the treatment system is operated 3 to 5 days per week, with the equipment operating 7 hours per day. Two batches (i.e., 2 × 420 gallons) of the reagent feed solution is prepared for each day of operation. However, there have been occasions where a more rapid decrease in arsenic was required, and on these occasions, three batches are prepared each day and the system is run 10 hours per day.

Monitoring

The treatment performance is monitored very closely because the arsenic concentration controls the discharge rate. Water quality samples are collected at set stations in the pit lake one to three times per week during and after operation of the treatment system.

The sampling locations are shown in Figure 3. There are 5 locations (C1 through C5) within the cove where the treatment system is located and near the outlet for the discharge and two additional lake samples located to the northeast (L1 and L2). Near-surface (5 foot) and deeper samples (15 feet deep in the cove and 25 feet in the lake) are collected. Not all locations are tested during each sampling event. In addition to the routine monitoring samples, some special samples were also collected to refine the treatment system or better understand how the system works, and these include sampling locations at the end of the discharge line and vertical profile sampling.

Total (i.e., unfiltered samples) arsenic and iron concentrations are measured at each location. However, dissolved (i.e., filtered samples) arsenic and iron concentrations as well as arsenic speciation (As^{3+} and As^{5+}) have been measured. For the samples of opportunity, a larger suite of analyses have occasionally been performed (i.e., cations and anions, additional metals, nutrients, pH, etc.).

In addition to these water quality samples, system parameters, such as flow rates, reagent consumption, pressures, are monitored. Daily field reports are prepared documenting the number of hours the pumping system was operated, along with flow rates for the 10% ferrous sulphate solution and the inlet water.

Discussion

Sampling results for any particular day indicate that the arsenic and iron concentrations are remarkably similar at all the sampling stations. The relative percent difference between maximum and minimum measured arsenic concentrations among samples on a single day is typically less than 5%. This indicates

that the surface layer of the pit lake is rapidly mixed relative to the amount of time required to remove arsenic.

Iron levels at the monitoring locations are low; typically less than 0.3 mg/L. This is much lower than the target concentration for the treatment zone (i.e., 2 mg/L). This is also a result of mixing; presumably, most of the reaction occurs in the vicinity of the discharge nozzle and then the high iron water rapidly disperses in the surface of the pit lake.

Figure 5 shows the average arsenic concentrations at the monitoring locations versus time for the past three years. In addition, Figure 5 shows the days when treatment was occurring and the daily mass of ferrous sulphate added to the pit lake.

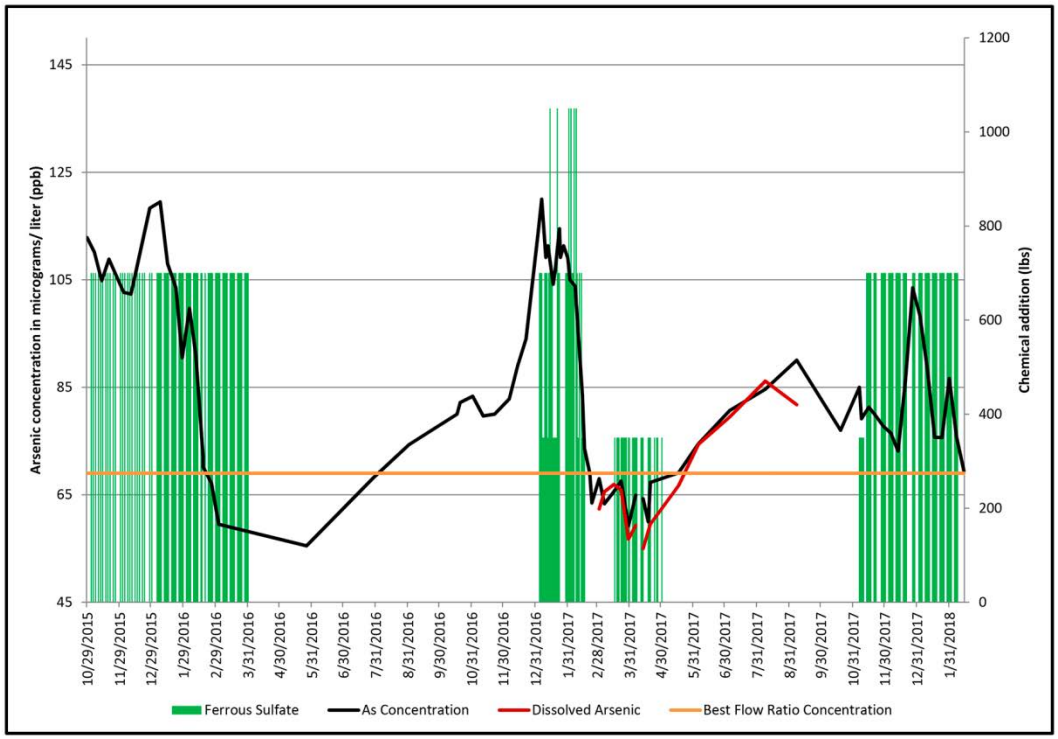


Figure 5: Pit lake arsenic concentrations vs. time

As shown in Figure 5, the concentration of arsenic in Skyrocket Pit Lake decreases from the starting range of 105 to 115 µg/L to an ending range of 55 to 75 µg/L. Once treatment is initiated, the concentration typically drops slowly at first and then very rapidly. Usually, three to four weeks of treatment are necessary to drop the concentration by 50 µg/L. After cessation of treatment, the concentration stays low for a few months and then gradually begins to rise. There are also rapid rises in concentration that typically occur during December.

The rapid rise in concentration during December is attributed to overturning of the pit lake. The seepage and leachate water that is transferred into the surface of the pit has an overall higher average TDS

concentration than the pit lake. During summer and fall, while there is a seasonal thermocline, the water column is statically stable. When the surface layer cools, the higher TDS water at the surface becomes denser than the deeper water causing and unstable condition.

To verify that the rapid arsenic concentration increase was caused by overturning of the pit lake, temperature and EC probes were suspended at 4 depths in the water column with data loggers storing parameter values twice per day. The temperature and EC data for late 2017 are presented in Figures 6 and 7, respectively. The EC (proportional to TDS) is initially higher in the shallowest probe compared to the other depths, and gradually decreased during November and early December. The temperature in the shallowest probe was also decreasing during this period. During mid-December 2017, the temperature and conductivity in the three deeper probes rapidly changed indicating a turnover event; the EC and temperature were relatively uniform throughout the shallowest three depths after the turnover. This is coincident with the rapid change in arsenic concentration which occurred between December 13 and December 27, 2017 (Figure 5). This confirms that the rapid increase in arsenic concentration that typically occurs in December is related to overturning of the pit lake.

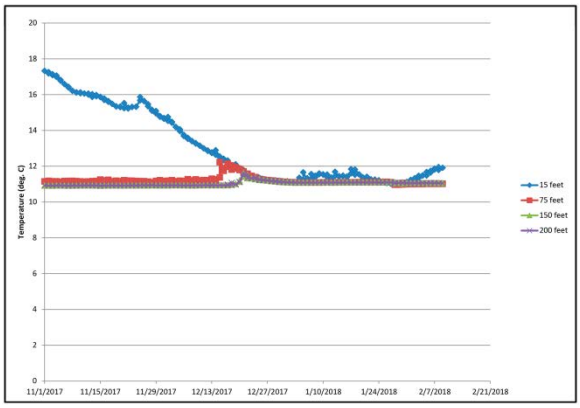


Figure 6: Temperature data loggers

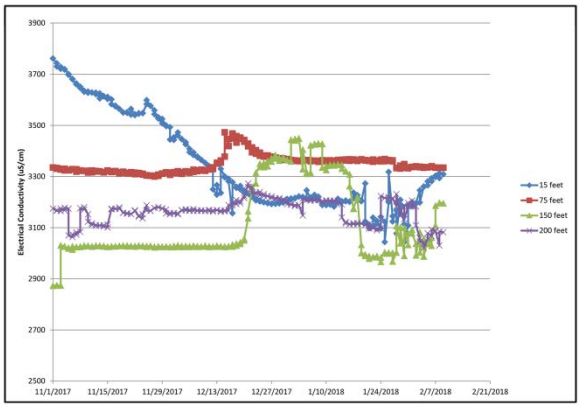


Figure 7: Electrical conductivity data loggers

The results of the vertical profile evaluations were used to establish criteria for initiating treatment of the pit lake. If the arsenic concentration of the pit lake is greater than the effluent limit minus the potential increase in concentration due to turnover, then treatment must be initiated. For example, the lake turnover typically causes an increase in arsenic concentration on the order of 25 to 40 µg/L in the surface layer (Figure 5). The maximum effluent concentration allowed by the NPDES permit is 94 µg/L. Therefore, if the pit lake is treated down to a concentration less than 54 µg/L (i.e., 94–40 µg/L) prior to December, then it is less likely that turnover of the lake will restrict discharges to the creek.

The gradual rise in arsenic concentration that occurs outside of the treatment and discharge periods is attributed to the flow of groundwater into the pit lake, oxidation of arsenopyrite in the pit walls, and/or diffusion of arsenic from below the pycnocline. The changes have been analyzed through water and mass

balance modelling, and any number of these three mechanisms could be active. Because little can be done to reduce these natural sources, little effort has been expended on doing so.

The slow initial drop in concentration during treatment is troublesome because it can restrict discharges if a heavy rain occurs early in the treatment period. Possible causes that were considered and investigated are speciation of the arsenic and settling rate of the precipitate. Arsenic speciation is a possible cause because the reduced form of dissolved arsenic (arsenite) is not removed sufficiently by precipitation with iron. Arsenic will naturally oxidize in oxidizing conditions, but the kinetics are relatively slow and may require a few weeks in the surface of a pit lake. Also, the strongly reducing conditions at the bottom of the pit lake could cause reduced arsenic in the lower layer of the lake, which would be mixed up during a turnover event.

Water samples from four depths in the pit lake (50, 100, 200, and 300 feet deep) were collected on October 19, 2017 (i.e., before turnover of the pit lake) and analyzed for arsenic species (As^{3+} and As^{5+}) to determine if reduced arsenic in the pit lake was affecting the treatment rate. The results indicated that the samples from the upper three depths were >99% As^{5+}; the sample from 300 feet had 95% As^{5+}. Based on the overwhelming abundance of As^{5+}, it is unlikely that the presence and slow oxidation of reduced arsenic is the cause of the slow initial rate of arsenic removal.

The rate of particle settling is currently believed to be the most likely cause of the slow initial removal rate for arsenic. During bench testing, small amounts of iron hydroxyoxide precipitate were observed but only for the highest doses of ferrous sulphate tested. Further, the dose that is used in the pit lake is over an order of magnitude lower than the highest bench test doses.

The reaction chemistry at the low iron dosages may be causing a very fine-grained particulate or possibly colloids that do not settle well. It may take a couple of weeks for particles to coagulate sufficiently to settle from the water column. Alternatively, we speculate that the removal may also be dependent on biological processes which could be stimulated by the addition of iron, and it may require a prolonged period of time for biomass that helps to remove the iron to develop and then settle out of the water column.

Dissolved versus total arsenic measurements were performed beginning of March 2017 to help evaluate how the arsenic removal rate is influenced by settling of particulates. Dissolved arsenic is operationally defined as that fraction which passes through a 0.45 μm filter during sample collection prior to preservation. As shown in Figure 5, the arsenic treatment had already begun to work before the dissolved and total measurements began, but treatment had been suspended for a period of approximately one month prior to starting these measurements.

During the period of treatment in March 2017, the treatment operations were one batch per day three days per week to maintain a low concentration of arsenic (i.e., the treatment process was operated at a

reduced rate). As shown in Figure 5, there was a rapid initial drop at the beginning of treatment in both total and dissolved arsenic by approximately 10 µg/L. This was followed by a period of total arsenic being up to 10 µg/L higher than dissolved arsenic, indicating about 15% particulate-phase arsenic, but the concentrations of both dissolved and total were increasing. Approximately 1 week after the cessation of treatment, dissolved and total arsenic were approximately equal (i.e., 100% dissolved).

The increase in arsenic concentration during the period of treatment is attributed to a much higher inflow of groundwater during this period. Groundwater levels were very high in the vicinity of the site at the end of this rainy season, and the increased gradient drove groundwater into the pit at a higher rate.

The dissolved vs. total arsenic measurements do not clearly represent a slow settling rate controlling the initially slow decrease in total arsenic. If this were the case, the dissolved arsenic concentration would drop faster than total. Then, the total would drop to levels closer to dissolved as precipitate settling occurred. This was not observed, as shown in Figure 5. However, the increased influx of arsenic with groundwater and the reduced rate of treatment during the study period are factors that complicate interpretation. Further study is necessary.

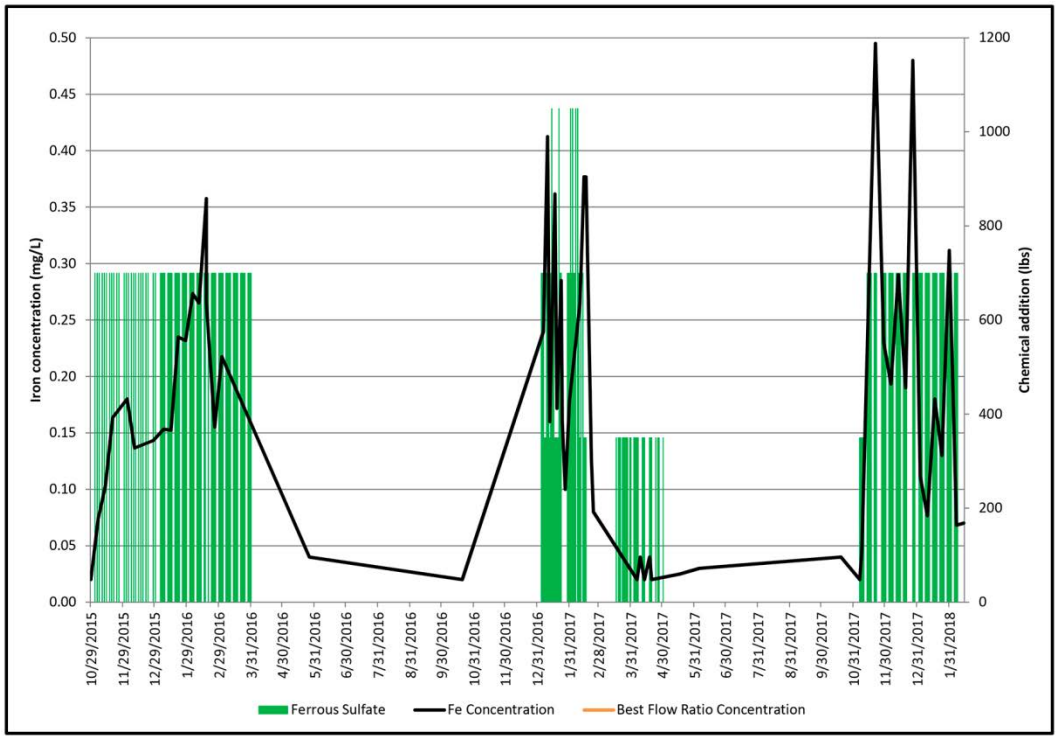


Figure 8: Pit lake iron concentrations vs. time

Figure 8 shows the average iron concentrations versus time in the pit lake. The iron concentration during treatment is very low, usually less than 0.5 mg/L. As noted above, this is substantially less than the target concentration of 2 mg/L in the treatment zone at the end of the pipe and this is attributed primarily

to rapid dispersion in the surface layer of the lake. The concentration is clearly affected by the addition of the ferrous sulphate, as one would expect. Also, the concentration is very "spiky", which suggests that the rate of removal may vary in response to environmental conditions. For example, windy versus calm conditions may cause different degrees of turbulence, which in turn prohibits or promotes settling. This may be further evaluated in the future to investigate the slow initial rate of arsenic removal.

Mass Balance Considerations

The monitoring data were used to evaluate the mass balance of arsenic in the pit lake. The initial (pre-treatment) amount of arsenic in the upper layer (i.e., above the pycnocline) is about 1,400 pounds. After treatment when the concentration is less than 65 µg/L, the mass of arsenic is approximately 870 lbs. This suggests that approximately 530 pounds of arsenic are precipitated in the pit lake by treatment. This arsenic settles to the bottom of the pit lake where it either becomes part of the sediments or gets re-dissolved in the anoxic zone. During the period since treatment was initiated (i.e., beginning in 2010), the range of arsenic concentrations has not changed significantly even though additional arsenic is introduced into the pit lake with the inflow of groundwater. While this period of time is probably too short to make any conclusions about the final fate of arsenic in the pit lake, it appears that the arsenic that is removed by treatment is more likely permanently sequestered into the sediments at the bottom of the pit lake. With the strongly reducing conditions at the bottom of the pit lake, it is possible that other reactions occur, such as formation of metal sulphides such as pyrite or arsenopyrite, that more strongly lock the arsenic in a solid phase.

Two samples were collected near the bottom of the pit lake on January 4, 2011 (after the first season of treatment), at locations NE75 and C215. These samples were very cloudy indicating high solids content (the sampler was on the bottom of the pit lake and likely pulled in solids that had settled on the bottom). The analytical results from these samples were used to estimate a ratio of arsenic to iron in the particulate and to estimate the amount of arsenic removed per pound of ferrous sulphate applied. The results for NE75 indicated an arsenic to iron ratio of 3.5%; for sample C215 the ratio is 3.0%

There were 28,000 pounds of ferrous sulphate heptahydrate applied during the period preceding collection of the samples. Ferrous sulphate heptahydrate is 20% iron, so assuming an arsenic to iron ratio of 3.25% during the period of treatment results in:

Amount of arsenic removed = 28,000 lbs. × 20% × 3.25% = 182 lbs.

The above analysis is based on data from earlier in the implementation of treatment. There have been some refinements to the process methods and equipment to improve the efficiency of treatment, but the amount of iron added in an event where the concentration drops by half is roughly the same. The amount of arsenic calculated to be removed during 2017 is based on the change in concentration above

(i.e., 530 lbs.) and is the same order of magnitude as the amount calculated based on the 2011 measurements (i.e., 182 lbs.), so the difference may not be significant. However, the difference may be an indication of an improvement to treatment efficiency due to the refinements to the treatment process and methods.

Conclusions

The results presented herein indicate that the relatively simple in-situ treatment process with ferrous sulphate successfully reduces the arsenic concentration in Skyrocket Pit Lake water. In-situ treatment has been used to reduce the initial concentrations by nearly 50% from 120 µg/L to less than 65 µg/L. This reduction in arsenic concentration provides a factor of safety for the success of the water management systems at the mine, which are dependent on seasonal discharge to Little Johns Creek.

The primary sources of arsenic in the pit lake are inflows of naturally-occurring arsenic in groundwater at the site and possibly oxidation of arsenic minerals in the pit walls. There is currently no method available to control these sources, so treatment will likely be necessary in the long term.

Skyrocket Pit Lake is seasonally stratified, and the turnover typically occurs early in the discharge season and causes a rapid increase in the arsenic concentration. Limnologic study of the pit lake verifies that the seasonal overturning is the cause of observed changes in arsenic, and offers opportunities to address the change through planning (i.e., treat to a target concentration well below the maximum allowable effluent concentration, so that the overturn does not interfere with the discharge). Also, as it appears that the static instability in the pit lake is partly due to transfer of seepage and leachate from other mining waste units that is high in TDS, there may be an opportunity to lower the outlets of the transfer pipes to a deeper layer of the pit to reduce the density of the surface layer and reduce the potential for overturning.

Further, process monitoring is planned to evaluate if a slow initial reduction in arsenic concentration can be eliminated. While it is most likely that this treatment consequence must be addressed through planning, it is possible that flocculants and coagulants could be effective.

Long-term monitoring will indicate if the arsenic is permanently sequestered to the bottom sediments and if re-mineralization occurs, but data collected to the time of writing this paper supports that precipitated arsenic remains in the sediments at the bottom of the pit lake.

References

Vogels, C.M. and Johnson, M.D. 1998. Arsenic remediation in drinking waters using ferrate and ferrous iron, Technical completion report acct no. 01-4-23922, June. New Mexico Water Resources Research Institute.

Chapter 7:
Miscellaneous



Proceedings of Mine Water Solutions 2018
June 12–15, 2018, Vancouver, Canada
Published by the University of British Columbia, 2018

Seawater Intrusion at Abandoned Coal Mines in the Labin Region, Croatia

Mladen Kuhta, Croatian Geological Survey, Croatia
Željka Brkić, Croatian Geological Survey, Croatia

Abstract

Underground coal mines in the Labin Paleogene basin on the Istrian peninsula in Croatia ceased operation in 1988 after more than two centuries of mining. Throughout the next three years, most of the mines were flooded. The total volume of exploitation fields and stable underground corridors that had been flooded by groundwater was estimated at 12 million cubic metres. Given that the mine works had drained the surrounding karst aquifer, it was assumed that stored waters and underground recharge could be used for public water supply or for industrial purposes. To confirm this assumption, comprehensive hydrogeological research was conducted, including quantifying the geometry and volume of flooded underground works, identifying hydrogeological characteristics of the rock units, and exploring the water hydrochemistry and dynamics. Ultimately, despite favourable hydrogeological conditions and large drainage capacity, it was determined that the hydrochemical characteristics of the mine waters rendered the water unsuitable for most uses. One of the highlighted problems was the excessive chloride content. Since the mines are located in permeable carbonate rocks and their deepest parts are only 1 km from the coastline, seawater intrusion was a common occurrence at the time of exploitation. Data from this period show that the drainage water in the deepest parts of the mine consisted of 25 to 85% seawater.

Although several available shafts have been investigated, the results obtained in the Labin shaft are representative of the entire mining system due to its drainage function and intensive groundwater dynamics. During low water conditions at the top of the water column (up to a depth of 60–70 m), fresh water with a chloride content of <250 mg/L prevails. The chloride content significantly increases with depth. At a depth of –200 m, it ranges from 1,350 to 2,010 mg/L, while at the bottom of the shaft at a depth of –350 m, the content ranges between 1,810 and 2,380 mg/L. During high water conditions, overflow from the shaft appears. The content of chlorides in the overflow water ranges from 194 up to 1,200 mg/L.

Introduction

The very first data about mining in the area of the Labin Paleogene basin on the east side of the Istrian Peninsula date back to the year 1420, and the data are about the extraction of coal and resin surface outcrops. Underground coal mining started in 1755. Until 1924, all excavations were conducted above the groundwater table in several so-called "old pits". Investigations have shown that the thickest coal layers are located on the eastern edge of the syncline structure and, following the bedding, gradually sink to greater depths. Because of this finding, three new pits (shaft mines) were opened: Raša, Labin, and Ripenda, in which coal was extracted from below groundwater levels. The pits are well interconnected at several levels. Following the spread of the coal layers, pits were developed from the southwest towards the northeast, and in this direction, the depth of mining increased. Thus, Raša mining was conducted up to approximately 300 m in depth, Labin mining was up to 400 m, and Ripenda mining was conducted at up to almost 500 m in depth.

The golden age of mining began just before World War II. A record production of 1.2 million tons was achieved in 1942, when mining in the "new pits" had already reached a depth of –250 m below sea level. Despite strong financial support from the former Yugoslavian government, the next decades were marked by a gradual decline in production, followed by a large increase in the operational costs of mining and drainage in works that reached depths of approximately –500 m below sea level. After the cessation of mining activity in 1988, large parts of the abandoned underground works were flooded.

The total volume of exploitation fields and stable underground corridors flooded by groundwater was estimated at 12 million cubic metres (Kuhta, 2004). Given that the mining works had drained the surrounding karst aquifer, it was assumed that stored waters and underground recharge could be used for public water supply or for industrial purposes. To confirm this assumption, comprehensive hydrogeological research has been initiated, including quantifying the geometry and volume of flooded underground works, identifying the hydrogeological characteristics of the rock units, as well as exploring the water hydrochemistry and dynamics. Ultimately however, despite the favourable hydrogeological conditions and large drainage capacity, it was determined that the hydrochemical characteristics of the mine waters limit their potential uses. One of the highlighted problems was the excessive chloride content. Since the coal mines are located near the sea, some parts are less than 1 km from the coast, and the extraction in the karst environment occurred well below sea level; salt water intrusions were a common occurrence during the exploitation. It was assumed that the seawater intrusions would stop after the mines were flooded with fresh groundwater. However, even during the first investigations (Rubinić et al., 1993, 1995), was shown that the chloride content in the groundwater exceeded the Maximum Allowable Concentration (MAC) for drinking water. Since this could significantly reduce the utility of these waters, the chloride content has been specifically studied during this project.

Study Area

The site being investigated is located in the Dinaric karst area that covers the southern half of Croatia (Figure 1). Coal mines in the Labin area are formed within the Istrian Tertiary syncline, which stretches across the northern part of the peninsula for about 90 km. Although coal deposits occur in other parts of the syncline, exploitable quantities were determined only in the area of Labin and the nearby Pićan basin. The geology of the Labin area, as well as the position of the mines, is shown in Figure 1.

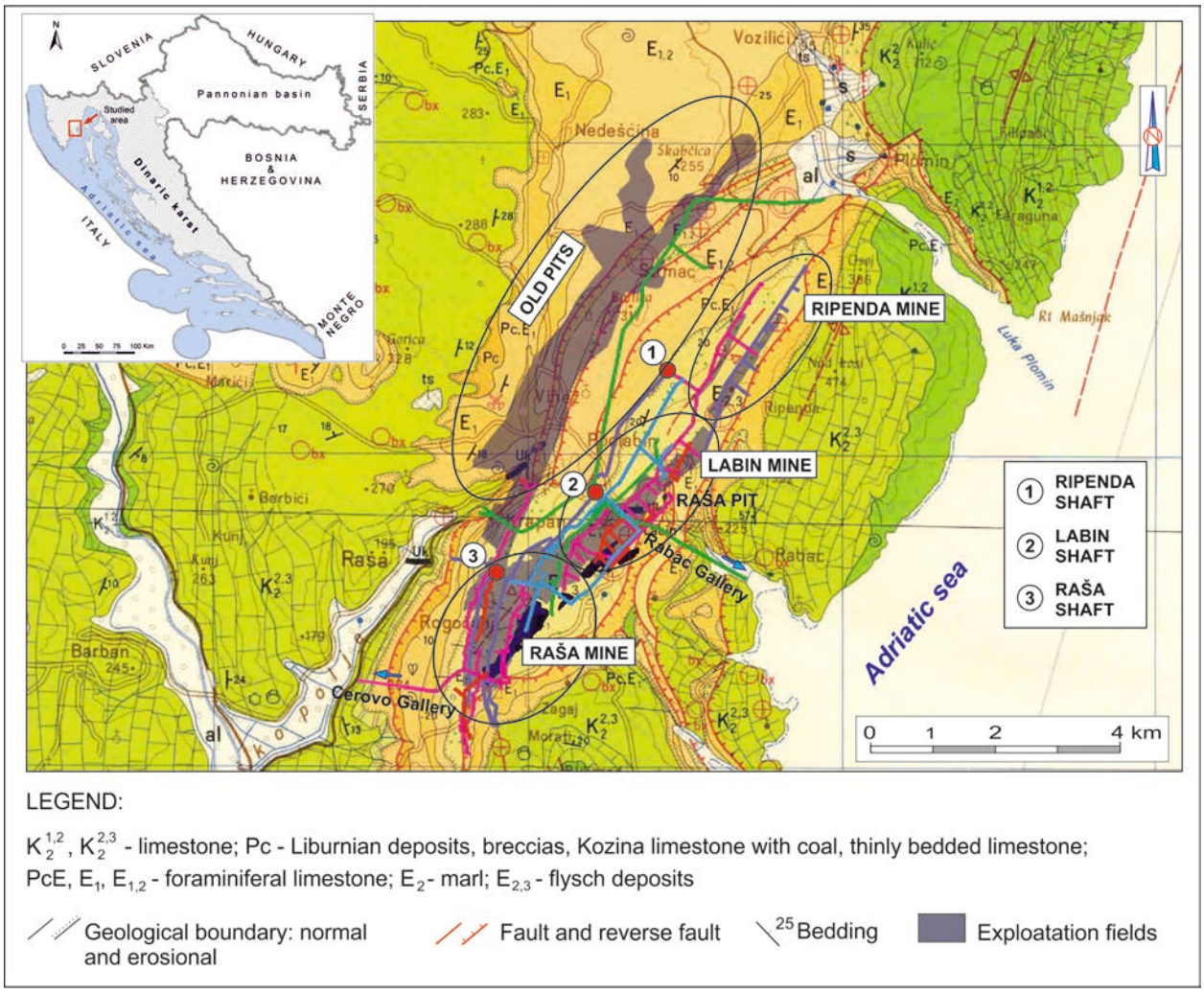


Figure 1: Geological map of the Labin coal mines area (geology after: Šikić et al., 1969)

The basement of the coal layers is made up of carbonate deposits of the Upper Cretaceous, predominantly represented by different types of limestone (Šikić et al., 1969; Šikić and Polšak, 1973). Deposition during the Paleogene was mainly controlled by intense syn-sedimentary tectonic deformation of the former carbonate platform area. After the emersion period during the transition between the Cretaceous and the Tertiary periods, the first Paleogene sediments were deposited within several isolated

fresh water basins on the karstified Cretaceous basement. The first lithostratigraphic unit was Liburnian deposits of Paleocene (Pc). The series begins with breccias, on which (or directly on Cretaceous deposits) follow the so-called Kozina limestone, which is brown to dark grey, dense and homogeneous, predominantly bituminous limestone with varied freshwater and brackish fauna and flora. Within this limestone, there are numerous layers of coal, ranging from several centimetres to over 3 m thick. This coal falls into the category of bituminous coal, with a heat content of 25–31 MJ/kg, and is characterized by its high (8–10%) sulphur content of organic origin. In the upper part of the Liburnian sediments, there is thinly bedded light to dark grey limestone, which comprises the transition to the upcoming marine sedimentation conditions. The total thickness of the Liburnian deposits is from 100 to 150 m, and the thickness of the Kozina layers with coal ranges from 80 to 120 m.

The conditions of carbonate sedimentation continued through the Upper Paleocene and lasted until the Middle Eocene. During this period, 100 to 180 m thick foraminiferal limestone series (Pc,E) were deposited. After the deposition of foraminiferal limestone, the orogenic deepening of the sedimentation environment occurred, and deposition of clastic deposits gradually prevailed. First, the marls of the Middle Eocene (E_2) were deposited, followed by deposition of flysch deposits ($E_{2,3}$), which also consist mainly of marls but frequently change to various types of limestone, sand, breccia and conglomerate.

Thereafter, due to the strong north-east-south-west-oriented regional tectonic stress, thrust-related deformations occurred, reaching a maximum in the Oligocene/Miocene, when the complex tectonic structure of the Dinaric region was formed (Korbar, 2009). The Istrian Tertiary syncline was uplifted, and its northeast wing was reversely faulted and thrusted, resulting in its modern shape.

Large areas of carbonate rocks, formed by intensive tectonic disturbance and dynamic endogen processes, result in very deep and irregular karstification and complex hydrogeology. The vast thickness of the carbonate deposits allows for the development of deep karst aquifers. In such circumstances, any mining below the groundwater table results in the activation of lateral inflows. Given the great mining depth and the long duration of exploitation, i.e., the intensive drainage of groundwater, it can be assumed that a wide depression cone was formed around the mains; this cone influenced the hydrogeology of the wider area. Furthermore, the proximity of the karst aquifer to the sea allowed salt water intrusions. This phenomenon was particularly pronounced in the development works on the eastern side of the mines.

With the cessation of mining and the flooding of the open underground spaces, the process of restoring natural hydrogeological norms followed, but this process will not be completely realized. First, there are numerous artificial underground channels in the aquifer that connect parts of the system that, in natural conditions, would likely be separate. In addition, the drainage galleries Rabac (connected to the Labin shaft; 10.53 masl; Figure 1) and Cerovo (connected to the Raša shaft; 10.81 masl; Figure 1) drain

the aquifer during the high-water states, which changes the natural discharge conditions and reduces aquifer storage.

Methodology

To show the concentration and dynamics of the chloride content in the mine's drainage waters at the time of coal extraction, privately archived data from mine geologist Mr. Mirko Tomašić were used. The amount of chloride in the groundwater at the Labin shaft and in the drainage gallery of Rabac in the period soon after flooding, i.e., from 1992 to 1994, was processed on the basis of data from Rubinić et al. (1993, 1995). The majority of the data was collected during a hydrogeological investigation conducted by the Croatian Geological Survey, 2003 (Kuhta, 2004). During these explorations, the groundwater of the entire mining system was examined. The major observation points were the main shafts Labin, Raša, and Ripenda. The results obtained are quite similar; as a representative, the situation on the Labin shaft is described. The Labin shaft is 573 m deep (Figure 5). Its entrance is at an altitude of 218 masl, but is currently closed with a concrete plate. The only possible access to the shaft today leads through a 2.6 km long drainage gallery from Rabac. The gallery is connected to the shaft at the altitude of 10.53 masl. The submerged part of the shaft is approximately 360 m deep (depending on the groundwater level). In the sunken section, a few mining horizons (levels) are connected to the shaft at the depths of –140, –242, –303 and –352 metres. Through the first three horizons, direct communication is possible with the Labin mine, as well as with the Raša and Ripenda mines. Direct communication is not possible through the lowest horizon, since the water gate on that horizon was closed before the flooding.



Figure 2: Groundwater level logger (a) and sampling in the Labin shaft (b)

The groundwater level in the shaft was measured every 6 hours using a WL 15 (Global Water, USA) logger (Figure 2a) from April 2003 to January 2004. The operation of the device was calibrated periodically with manual measurements taken with a Water Level Meter. Data on the daily precipitation in the Labin area were obtained from the State Meteorological and Hydrological Service.

Groundwater samples (Figure 2b) were collected using a bailer every 50 m to a depth of –340 m. This sampling was carried out on four occasions, during various hydrological conditions. At the same time, field measurements of water temperature and electrolytic conductivity were performed using KLL-MPS-D3 multiparameter probes (SEBA Hydrometrie, Germany). The measurements were performed every 10 m to a depth of –190 m. Chemical analyses of the samples, including the chloride content (Cl–), were performed in the laboratory of the Public Health Institute of the Istrian County in Pula.

Results

The content of chlorides in mining groundwater varies depending on the hydrological conditions in the wider area. The groundwater dynamics were processed on the basis of the groundwater level (GWL) measurements from the Labin shaft.

Groundwater Dynamics

The Labin shaft has a very important role in the groundwater dynamics within the study area. At an altitude of 10.53 masl, the shaft is connected to the 2.6 km-long Rabac gallery that ends at the seashore. In low water conditions, the GWL is below the height of the overflow (Figure 3). In high water conditions, i.e., when GWL reaches a 10.53 masl, the groundwater drains directly into the sea through the Rabac gallery. It should be noted that the Rabac gallery is directly connected to the "old pits", which are situated over the groundwater table, and therefore, the gallery drains percolating waters from that area as well.

The daily precipitation recorded by the Labin weather station and the results of the GWL measurements are highly correlated (Figure 3). The reaction of the GWL to precipitation is very fast and confirms the highly karstic characteristics of the aquifer. The lowest GWL of 6.85 masl on the Labin shaft was reached at the end of the dry season at the end of September 2003. The extreme amount of precipitation that fell on the 29th of September 2003 caused a sudden rise in groundwater levels of almost 4 m, and the discharge was activated. The overflow practically did not stop until the end of the observation period. The highest levels of groundwater were recorded after heavy precipitation on 31st December, 2003, when a total of 97 mm of rain fell. On the same day, the groundwater level reached 11.38 masl. The difference between the minimum and maximum recorded GWL was only 4.53 m. According to Rubinić et al. (1995), the highest recorded GWL in the observation period from 1992 to

1994 was 13 masl. It can be assumed that it would have been significantly higher if there were no drainage possibility through the Rabac gallery and Cerovo gallery on the other side of the system.

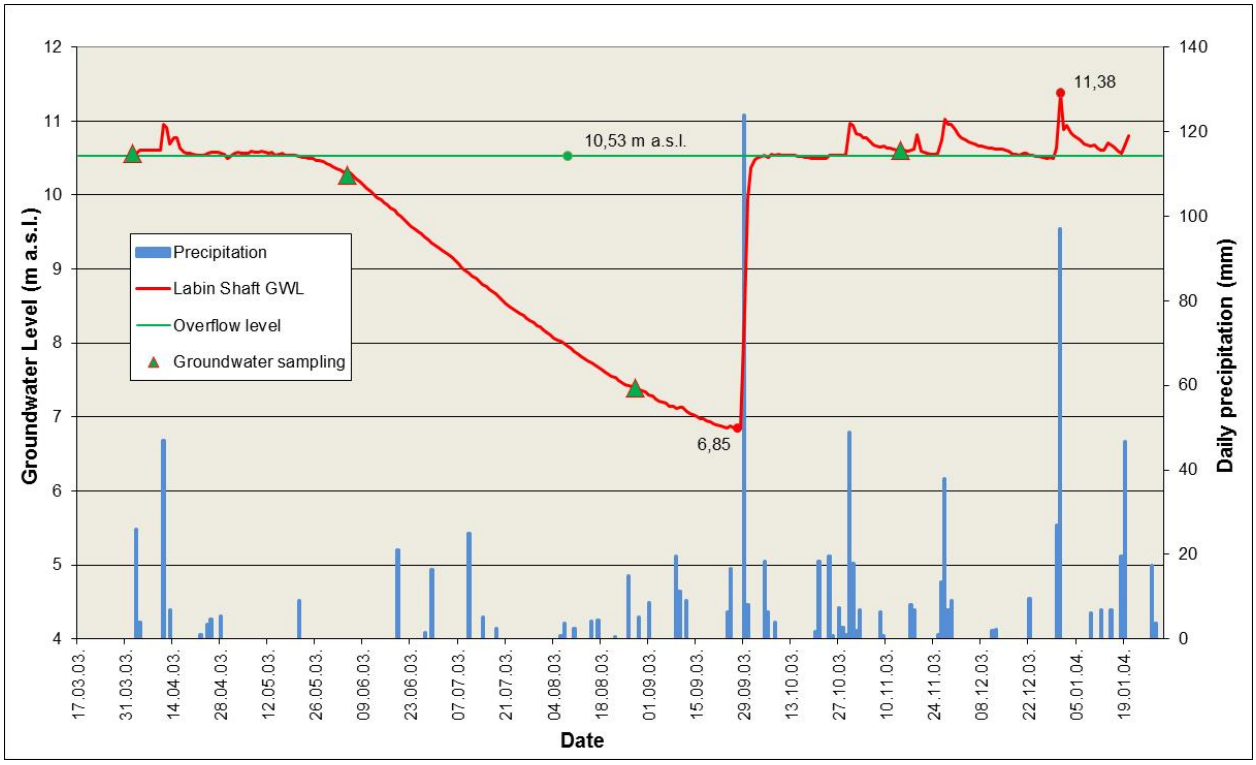


Figure 3: Groundwater level (GWL) on the Labin shaft compared with daily precipitation

During dry periods, there is no outflow at the exit of the Rabac gallery. At higher water conditions, it usually ranges from tens to several hundreds of L/s (Figure 4a). However, in extreme situations the discharge can reach over 10 m^3/s (Figure 4b).



Figure 4: Discharge on the exit of the Rabac drainage gallery during "normal" high water conditions (a) and in an extreme situation on October 1993 (b)

Chloride Content Variations

During the extraction period, smaller or larger amounts of seawater were regularly recorded on the eastern outermost corridors, from the Raša mine through Labin to Ripende. In 1934, an accidental breakthrough of seawater occurred on the XIV horizon (–140 m) in the southern part of the Raša mine ("Cavern" area), which was a particularly serious problem. Most of the mine was first flooded with fresh groundwater and mud, which was followed by an intrusion of clear seawater. The area was closed and isolated, but further coal extraction was abandoned in that part of the mine.

With the exception of this event, it can generally be concluded that the amount of seawater has increased with exploitation depth, that is, from the south towards the north. The most prominent occurrences of seawater were recorded at the XIV (–140 m) level in the Raša mine, the XX (– 340 m) and XXIV (–450 m) levels in the Labin mine, as well as at the XXIV and XXV (–440 and –480 m) levels in the Ripenda mine. The content of chloride in the drainage waters of Ripenda was reconstructed on the basis of data collected during 1984/85 (private archive data of Mr. Tomašić). Observation points were located in the deepest corridors (–450 to –480 m), which are from 850 to 1,350 m away from the seashore. The total chloride content was very high. In the more heavily loaded sectors, it usually ranged from 6,000 to 12,000 mg/L, which means that the percentage of seawater in the drainage was between 25 and 50%. At maximum salinity (approximately 16,000 mg/L Cl), it reached 70%. The variations in chloride content were very poorly correlated with the levels of precipitation.

The impact of seawater intrusions was observed during the first research efforts immediately after the flooding of the mines (Rubinić et al., 1993, 1995). The results of sampling carried out along the depth of the water column in the Labin shaft showed that during low water conditions and in the shallow depths, the chloride content was approximately 100 mg/L, but at greater depths, they were significantly higher. For example, at a depth of –140 m, they reached up to 1,000 mg/L, and at a depth of –350 m, they reached above 3,000 mg/L. In periods of high groundwater, samples were taken at the exit of the Rabac gallery. According to the results, the chloride content was also high in these cases and frequently ranged from 300 to 600 mg/L, with a maximum recorded value of 1,200 mg/L. It is important to recall that in such conditions, the drainage water of the Rabac gallery also contains an unknown quantity of fresh water that has drained in from the "old pits" situated above the groundwater table.

The salinity measurement of the main waters during investigations from 2003–2004 was carried out during four field tours that aimed to capture different hydrological conditions (Figure 3). The temperature, electrolytic conductivity and chloride concentration data in relation to the location in the water column within the Labin shaft are shown in Figure 5.

The measurements indicate that in low water periods (no overflow from the shaft), the surface layer of fresh water reached depths of about 60–70 m. Below this depth, chloride content was found to be

constantly higher than the MAC for drinking water (250 mg Cl^-/L), and was found to increase with depth. The most significant changes occurred at depths below –140 m, i.e., after the connection of the XIV level to the shaft. At a depth of –140 m, chloride content ranged from 380–550 mg/L. The changes were particularly pronounced between –180 and –190 m, where the XVI level is connected. At this point, the chloride content rapidly increased, and ranged from 1,350 to 2,010 mg/L. Chloride content continued to increase as depth increased, but these changes were not as pronounced. At –240 m, the chloride content ranged from 1,470 to 2,210 mg/L, and near the bottom of the shaft, at –340 m, it ranged from 1,810 to 2,380 mg/L. Chloride content changes in the area of the XIV and XVI levels were followed by a sudden rise in water temperature.

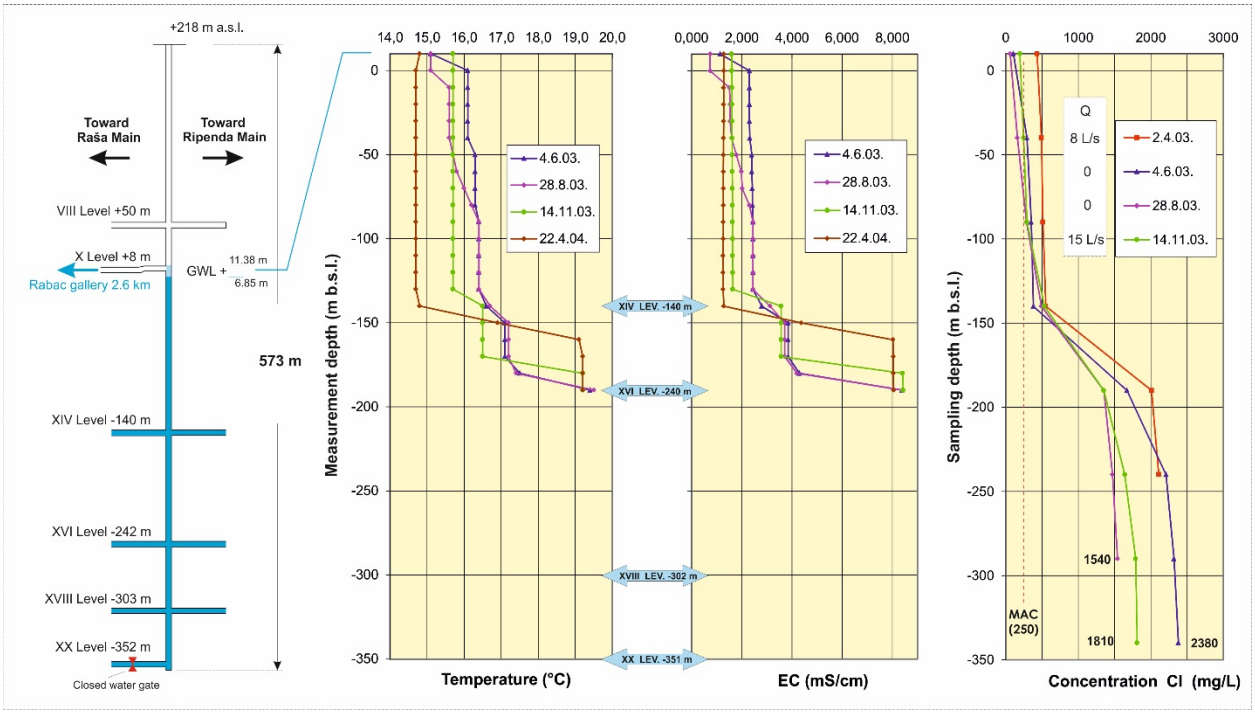


Figure 5: Water temperature, EC and Cl^- concentration in Labin shaft

During high water periods, i.e., instances of outflow from the shaft to the Rabac drainage gallery, the chloride content was determined on two occasions (Figure 3). At the time of the first sampling (2nd April 2003), the chloride content was 430 mg/L. Sampling was carried out immediately after the start of outflow (approximately 8 L/s). The second sampling (14th November 2003) was performed after a longer outflow period (approximately 15 L/s), and the chloride content was significantly less (only 194 mg/L).

Discussion

During the full development of the main underground corridors, an annual average of approximately 520 L/s of groundwater, with a varying share of seawater, was pumped from the mines to enable coal

exploitation. In the period before the final abandonment, due to the closure of several levels in the Raša and Labin pits, annual average groundwater pumping had decreased to 350 L/s. The final immersion of the mines began in March 1988, and was completed by the overflow of main water from the Labin shaft to the Rabac drainage gallery in May 1991 (which lasted three years and two months). Based on these data and the estimated volume of the flooded space, an average recharge of 102 L/s was calculated. Initial recharge was likely to be equal to pumping immediately before the flooding, i.e., approximately 350 L/s. Later, with the water table rise and by the reduction of the hydraulic gradients, the recharge decreased and was considerably less than the calculated average of 102 L/s.

During flooding, the mining areas were primarily filled with fresh groundwater, but they were also partly filled with seawater. Since the coal mines are situated in a coastal karst area, with some parts of the mines being less than 1 km from the coastline, and with the exploitation taking place far below sea level, the salt water intrusions were expected. When considering the possibility of using mining waters, it is particularly important to discuss the seawater penetration mechanism and the expected variations in the future. In this respect, it should be noted that the highest seawater recharge was at the initial stage of flooding, and it has decreased with the reduction of the hydraulic gradient. The total amount of seawater intrusion cannot be quantified.

After the mines were flooded, the balance between fresh and seawater was established. The balance is partly defined by natural conditions but, at the same time, significantly affected by the fact that the maximum groundwater levels are limited due to the positioning of the artificially formed drains, i.e., by discharge through the Rabac and Cerovo drainage galleries.

Although some deviations in anisotropic karst environments have been observed, variations in chloride concentrations in mining waters can be generally interpreted according to the well-known Gyben-Herzberg relationship. At low water conditions, the groundwater level in the Labin shaft drops to approximately 6 masl, which means that the expected depth of the sea and freshwater interface should be approximately –240 m. Under such conditions, deeper parts of the mine are exposed to the seawater intrusion. Since the groundwater state is low to moderate for most of the year, significant amounts of seawater are able to intrude deep into the mainland. Due to the possibility of draining through the Rabac and Cerovo galleries, the maximum groundwater levels are limited during the high-water conditions. As mentioned, the highest recorded levels in the Labin shaft reached approximately 13 masl (Rubinić et al., 1995). In such conditions, the interface zone should be depressed at a depth of approximately –420 m; i.e., only the deepest parts of the mines (Ripenda pit) are exposed to the intrusion of seawater. Given the karst characteristics of the aquifers, the groundwater level rise following precipitation events is very fast. Because of this outcome, there is not enough time for the gradual extrusion of the salty water, which enters the system during longer low water periods. The trapped part of the seawater rises up to the natural

cavities and mining corridors above the interface zone and ultimately drains through the Labin shaft and the Rabac drainage gallery.

The studies noted that the highest concentrations of chloride are present in the initial phase of overflow. With sustained high water conditions, the chloride content stabilizes and then gradually decreases. When such conditions cease, the chloride content gradually decreases, and in the upper part of the aquifer, a lens of completely fresh water is formed. It is interesting to note that even after the long dry period recorded in 2003 (Figure 3), its depth did not exceed 60–70 m. It is evident that the anthropogenic changes in the aquifer have had a significant effect on the processes of mixing fresh and seawater, and have caused significant deviation from the Gyben-Herzberg relation. This finding is also confirmed by the sudden changes in the physico-chemical characteristics of the groundwater in the area of the particular mining horizons (Figure 5).

Conclusion

Despite the favourable hydrogeological conditions, and with the remarkable drainage potential of more than 76 km of the mining works, the established hydrochemical characteristics of mine water have been shown to be a limiting factor for their use. One of the highlighted problems is the excessive chloride content due to seawater intrusions. It is significant that with changes in the dynamic conditions of the aquifer, the high chloride content rises from the deeper parts of the system and spills over into the overflow water. It can be assumed that a similar process would occur in the case of dynamic changes induced by water pumping. Because of this assumption, the mine water is not rated as a potential source of potable groundwater. It should be mentioned that in addition to chlorides, excessive levels of other minerals such as iron, manganese, and sulphate were measured in deeper parts, and further limit the utilization of groundwater from the abandoned Labin coal mines.

References

Baturić, J. 1962. *Problem Kaverne u Raši* (The problem of the cavern in the mine of Raša, in Croatian), *Krš Jugoslavije* 3: 107–131.

Korbar, T. 2009. Orogenic evaluation of the External Dinarides in the NE Adriatic region: A model constrained by tectonostratigraphy of Upper Cretaceous to Paleogene carbonates, *Earth-Science Reviews* 96(4): 296–312.

Kuhta, M. 2004. *Istražni radovi u svrhu ocjene vodnog potencijala napuštenih ugljenokopa Labinštine* (Investigations for the purpose of assessing the water potential of abandoned coal mines in Labin area, in Croatian), professional report, in Croatian. Institut za geološka istraživanja, Zagreb.

Rubinić, J., Tomašić, M. and Kukuljan, I. 1995. *Vodni potencijal jamskih prostora Labinštine* (Water potential of Labin mains, in Croatian), *Proceedings of the 1st Croatian Geological Congress, 2*, Opatija: 519–522.

Rubinić, J., Tomašić, M., Dobrović, D. and Kukuljan, I. 1993. *Istraživanje vodnog potencijala jamskih prostora napuštenih ugljenokopa s područja Labinštine, preliminarni rezultati* (Exploration of the water potential of the abandoned coal mains of Labin, preliminary results, in Croatian), professional report, in Croatian. JVP za slivno područje istarskih slivova, Labin.

Šikić, D. and Polšak, A. 1973. *Osnovna geološka karta SFRJ 1:100.000, Tumač za list Labin L33–101* (Basic geological map of SFRJ, scale 1:1000.000, guidebook of sheet Labin, in Croatian). Institut za geološka istraživanja, Zagreb, Savezni geološki institut, Beograd.Šikić, D., Polšak, A. and Magaš, N. 1969. *Osnovna geološka karta SFRJ 1:100.000, List Labin L33–101* (Basic geological map of SFRJ, scale 1:1000.000, Sheet Labin, in Croatian). Institut za geološka istraživanja, Zagreb (1958–1967), Savezni geološki zavod, Beograd.

Chapter 8:
Author Index



Author Index

Alle-Ando, Yapo 519
Baker, Brent 703
Balfour, John 123
Banerjee, Monisha 181
Barkh, Mohsen 433, 569
Basri, Mundzir 487
Bourne, Justin 623
Bratty, Michael 449
Brkić, Željka 747
Brooker, Murray 153
Brown, Allison 495
Campero, Cecilia 363
Cathcart, Jaime 461
Cho, H. Jean 531
Chowdhury, Mijanur R. 719
Clark, Steven R. 223
Consigny, Alain 703
Cooper, Carlo 245
Dabiri, Michael 509
Dang-Vu, Trong 691
Devoto, Gabriel Castillo 545
Di Biase, Alessandro 449
Dy, Eben 677
Earley, Drummond “Dusty” III 495
Evin, Göktuğ 473
Fennell, Jon 269
Ferguson, Paul 139
Ferris, Ben 623
Findlater, Laura-Lee 123, 531

Firoozy, Niloofar 487
Flather, David 531
Fraser, Michelle 51
Friesen, Vanessa 623
Gale, Tyler 93
Gallagher, Neal 299
Gautrey, Simon 163
Gerads, Russ 195
Gjertsen, Jennie 531
Goode, Tomas C. 283
Grewar, Tamsyn 349
Groat, Lee A. 313
Grobler, Jaco 245
Hallak, Rami 649
Hansen, Shane 609, 635
Harrington, James 623
Heisler, Dallas 45
Hendricks, Bridgette 661
Hildebrand, Martin 449
Jim, Chris 181
Kappel, Bill 389, 401
Keller, Jason 181, 419
Kildyshova, Liudmyla 649
Kinghan, Peter 3
Klein, Colin 691
Kolomitsyn, Igor V. 649
Kuhta, Mladen 747
Kunz, Nadja 377
Ladderud, Jeff 209
Lake, Donald J. 313
Lattin, Daniel 419
Lee, Ilsu 609
Lidhage, Helena 509
Lines, Stephen 51

Lofholm, Steve 299
Maharajh, Dheepak 349
Martens, Kevin 719
Martz, Rachel 623
Masala, Charles 509, 519
Mattson, Bruce 123
Mayer, John Markus 77
McCleary, Eric 337
Milczarek, Michael 153, 181, 419
Miller, Sean 597
Millsap, Daniel 299
Minchow, Kristina 661
Mortazavi, Saviz 677
Neale, John 349
O'Brien, Brendan 323
Obal, Terry 597
Ogungbade, Olufunsho 635
Oleszkiewicz, Jan A. 449
Olsen, Hhan 283
Orzatti, Marco Gomez 677
Patterson, Tom 733
Peacock, Edward 153
Peavler, Rachael 283
Pereira, Cristian 31
Pesonen, Nicole 109, 139
Qu, Wei 677
Raghav, Madhumitha 15
Rainey, Dustin K. 259
Ramey, Dan 609
Reidel, Frits 153
Reyes, Miguel Palape 245
Rinaldi, Nanda 473
Robinson, Jamie 3
Russell, Kathleen 123

Rutkowski, Tom....299
Rzepecki, Piotr....93
Saavedra, Victor Muñoz....65
Santisteban, Leonard....609
Schipper, Ryan....661
Scott, James....531
Self, Clay....181
Sencza, Walter....51
Setiawan, Iwan....473
Shewan, Alana....461
Simair, Monique....623
Smith, Sheldon....51
Smithard, Lynda....583
Stecko, Pierre....719
Steinepreis, Mark....237
Sundar, Veneil....703
Thomas, Andy....109
Thomas, Kirk....691
Thrift, Andrew....519
Tizzotti, Morgan....691
Trapp, Alexander....139
Trubilowicz, Joel W.....65
Ugorets, Vladimir....31, 473
van Rooyen, Michelle....349
Weber, Daniel....153
Wei, Victor....449
Weiland, Erick....15, 609
Wels, Christoph....109, 139
Whitman, Adam....733
Wiramanaden, Cheryl....719
Wozniak, Ben....195
Wytrykush, Carla....45
Xie, Zhong....677
Yao, Tzung-mow....153

Zhan, Guosheng.....419
Zubot, Warren.....607